Patai Series:
The Chemistry of Functional Groups
Series Editor: Zvi Rappoport

Volume Editors: Zvi Rappoport and Ilan Marek

The Chemistry of Organozinc Compounds

R-Zn

Patai Series online:
http://www.interscience.wiley.com

WILEY

An Interscience® Publication

The chemistry of **organozinc compounds**

Part 1

Edited by

ZVI RAPPOPORT

The Hebrew University, Jerusalem

and

ILAN MAREK

Technion-Israel Institute of Technology, Haifa

2006

John Wiley & Sons, Ltd

An Interscience® Publication

The chemistry of
organozinc compounds

Patai Series: The Chemistry of Functional Groups

A series of advanced treatises founded by Professor Saul Patai and under the general editorship of Professor Zvi Rappoport

The **Patai Series** publishes comprehensive reviews on all aspects of specific functional groups. Each volume contains outstanding surveys on theoretical and computational aspects, NMR, MS, other spectroscopic methods and analytical chemistry, structural aspects, thermochemistry, photochemistry, synthetic approaches and strategies, synthetic uses and applications in chemical and pharmaceutical industries, biological, biochemical and environmental aspects.
To date, over 110 volumes have been published in the series.

Recently Published Titles

The chemistry of the Cyclopropyl Group (Volume 2)
The chemistry of the Hydrazo, Azo and Azoxy Groups (Volume 2, 2 parts)
The chemistry of Double-Bonded Functional Groups (Volume 3, 2 parts)
The chemistry of Organophosphorus Compounds (Volume 4)
The chemistry of Halides, Pseudo-Halides and Azides (Volume 2, 2 parts)
The chemistry of the Amino, Nitro and Nitroso Groups (2 volumes, 2 parts)
The chemistry of Dienes and Polyenes (2 volumes)
The chemistry of Organic Derivatives of Gold and Silver
The chemistry of Organic Silicon Compounds (2 volumes, 4 parts)
The chemistry of Organic Germanium, Tin and Lead Compounds (Volume 2, 2 parts)
The chemistry of Phenols (2 parts)
The chemistry of Organolithium Compounds (2 volumes, 3 parts)
The chemistry of Cyclobutanes (2 parts)
The chemistry of Peroxides (Volume 2, 2 parts)
The chemistry of Organozinc Compounds (2 parts)

Forthcoming Titles

The chemistry of Anilines
The chemistry of Organomagnesium Compounds

The Patai Series Online

Starting in 2003 the **Patai Series** is available in electronic format on Wiley InterScience. All new titles will be published as online books and a growing list of older titles will be added every year. It is the ultimate goal that all titles published in the **Patai Series** will be available in electronic format.
For more information see under **Online Books** on:

www.interscience.wiley.com

The chemistry of **organozinc compounds**

Part 1

Edited by

ZVI RAPPOPORT

The Hebrew University, Jerusalem

and

ILAN MAREK

Technion-Israel Institute of Technology, Haifa

2006

John Wiley & Sons, Ltd

An Interscience® Publication

John Wiley & Sons Ltd, The Atrium, Southern Gate, Chichester,
West Sussex PO19 8SQ, England

Telephone (+44) 1243 779777

Email (for orders and customer service enquiries): cs-books@wiley.co.uk
Visit our Home Page on www.wiley.com

Other Wiley Editorial Offices

John Wiley & Sons Inc., 111 River Street, Hoboken, NJ 07030, USA

Jossey-Bass, 989 Market Street, San Francisco, CA 94103-1741, USA

Wiley-VCH Verlag GmbH, Boschstr. 12, D-69469 Weinheim, Germany

John Wiley & Sons Australia Ltd, 42 McDougall Street, Milton, Queensland 4064, Australia

John Wiley & Sons (Asia) Pte Ltd, 2 Clementi Loop #02-01, Jin Xing Distripark, Singapore 129809

John Wiley & Sons Canada Ltd, 6045 Freemont Blvd, Mississauga, Ontario, L5R 4J3, Canada

Wiley also publishes its books in a variety of electronic formats. Some content that appears in print may not be available in electronic books.

Library of Congress Cataloging-in-Publication Data:

The chemistry of organic compounds / edited by Zvi Rappoport, Ilan Marek.
p. cm.—(Chemistry of functional groups)
Includes bibliographical references and index.
ISBN-13: 978-0-470-09337-5(Cloth : alk. paper)
ISBN-10: 0-470-09337-4(cloth : alk. paper)
1. Organozinc compounds. I. Rappoport, Zvi. II. Marek, Ilan.
QD412.Z6C54 2006
547′.05661—dc22
2006018005

British Library Cataloguing in Publication Data

A catalogue record for this book is available from the British Library

ISBN-13: 978-0-470-09337-5
ISBN-10: 0-470-09337-4

Typeset in 9/10pt Times by Laserwords Private Limited, Chennai, India
Printed and bound in Great Britain by Biddles Ltd, King's Lynn, Norfolk
This book is printed on acid-free paper responsibly manufactured from sustainable forestry in which at least two trees are planted for each one used for paper production.

Dedicated to

Jean F. Normant

and to

Uzi and **Micki**

Contributing authors

Varinder K. Aggarwal	School of Chemistry, University of Bristol, Cantock's Close, Bristol, BS8 1TS, United Kingdom. Fax: +44 117 929 8611; e-mail: v.aggarwal@bristol.ac.uk
Jaap Boersma	Debye Institute, Organic Chemistry and Catalysis, Utrecht University, Padualaan 8, 3584 CH Utrecht, The Netherlands. Fax: +31 30 252 3615; e-mail: J.Boersma@chem.au.nl
Olivier Buriez	Ecole Normale Supérieure, Département de Chimie, UMR CNRS-ENS-UPMC 8640 "PASTEUR", 24 rue Lhomond, Paris Cedex 05 F-75231, France. Fax: +33 14 432 3325; e-mail: olivier.buriez@ens.fr
Donald J. Burton	Department of Chemistry, University of Iowa, Iowa City, IA 52242, USA. Fax: +1 319 335 1270; e-mail: donald-burton@uiowa.edu
André B. Charette	Department of Chemistry, Université de Montréal, P.O. Box 6128, Station Downtown, Montréal, Québec, Canada H3C 3J7. Fax: +1 514 343 5900; e-mail: andre.charette@umontreal.ca
Timothy Clark	Computer Chemistry Center, University of Erlangen-Nürnberg, Nägelsbachstr. 25, D-91052 Erlangen, Germany. Fax: +49 9131 852 6565; e-mail: clark@chemie.uni-erlangen.de
Athanassios G. Coutsolelos	Chemistry Department, Laboratory of Bioinorganic Chemistry, University of Crete, PO Box 2208, GR-71003 Heraklion, Crete, Greece. Fax: +30 281 054 5054; e-mail: coutsole@chemistry.uoc.gr
Charles R. Davis	Sigma-Aldrich, 6000 N. Teutonia Avenue, Milwaukee, WI 53209, USA. Fax: +1 414 298 4224; e-mail: cdavis1@sial.com
Rudi van Eldik	Institute for Inorganic Chemistry, University of Erlangen-Nürnberg, Egerlandstr. 1, D-91058 Erlangen, Germany. Fax: +49 9131 852 7387; e-mail: vaneldik@chemie.uni-erlangen.de
Liu-Zhu Gong	Department of Chemistry, Ludwig-Maximilians-Universität München, Butenandtstr. 5-13, D-81377 München, Germany. Fax: +49 8921 807 7680; e-mail: gonglz@ciou.au.cn

Corinne Gosmini	C.N.R.S. UMR 7582, Laboratoire d'Electrochimie Catalyse et Synthése Organique, Université Paris XII, 2-8 rue H. Dunant, F-94320 Thiais, France. Fax: +33 14 978 1148; e-mail: gosmini@glvt-cnrs.fr
Albert Guijarro	Departamento de Química Orgánica, and Instituto de Síntesis Orgánica (ISO), Universidad de Alicante, Ap. 99, E-03080, Alicante, Spain. Fax: +34 96 590 3549; e-mail: aguijarro@ua.es
Toshiro Harada	Department of Chemistry and Materials Technology, Kyoto Institute of Technology, Matsugasaki, Sakyo-ku, Kyoto 606-8585, Japan. Fax: +81 75 724 7580; e-mail: harada@chem.kit.ac.jp
Qian Hu	Herbert C. Brown Laboratories of Chemistry, Purdue University, 560 Oval Drive, West Lafayette, Indiana 47907-2084, USA. Fax: +1 765 496 3380; e-mail: qhu@purdue.edu
Zhihong Huang	Herbert C. Brown Laboratories of Chemistry, Purdue University, 560 Oval Drive, West Lafayette, Indiana 47907-2084, USA. Fax: +1 765 496 3380; e-mail: huang70@purdue.edu
Johann T. B. H. Jastrzebski	Debye Institute, Organic Chemistry and Catalysis, Utrecht University, Padualaan 8, 3584 CH Utrecht, The Netherlands. Fax: +31 30 252 3615; e-mail: j.jastrzebski@chem.uu.nl
Tsuneomi Kawasaki	Department of Applied Chemistry, Faculty of Science, Tokyo University of Science, Kagurazaka, Shinjuku-ku, Tokyo 162-8601, Japan. Fax: +81 33 235 2214; e-mail: tkawa@rs.kagu.tus.ac.jp
Florian F. Kneisel	Department of Chemistry, Ludwig-Maximilians-Universität München, Butenandtstr. 5-13, D-81377 München, Germany. Fax: +49 8921 807 7680; e-mail: knochel@cup.uni-muenchen.de
Paul Knochel	Department of Chemistry, Ludwig-Maximilians-Universität München, Butenandtstr. 5-13, D-81377 München, Germany. Fax: +49 8921 807 7680; e-mail: paul.knochel@cup.uni-muenchen.de
Gerard van Koten	Debye Institute, Organic Chemistry and Catalysis, Utrecht University, Padualaan 8, 3584 CH Utrecht, The Netherlands. Fax: +31 30 252 3615; e-mail: g.vankoten@chem.uu.nl
Helena Leuser	Department of Chemistry, Ludwig-Maximilians-Universität München, Butenandtstr. 5-13, D-81377 München, Germany. Fax: +49 8921 807 7680; e-mail: knochel@cup.uni-muenchen.de
Joel F. Liebman	Department of Chemistry and Biochemistry, University of Maryland, Baltimore County, 1000 Hilltop Circle, Baltimore, MD 21250, USA. Fax: +1 410 455 2608; e-mail: jliebman@umbc.edu

Marco Lombardo	Department of Chemistry "G. Ciamician", University of Bologna, via Selmi 2, I-40126 Bologna, Italy. Fax: +39 051 209 9456; e-mail: marco.lombardo@unibo.it
Edwige Lorthiois	Novartis Pharma AG, Novartis Institutes for Biomedical Research, Protease Platform WKL-122-3-27, Klybeckstrasse 144, CH-4002 Basel, Switzerland. Fax: +41 61 696 1163; e-mail: edwige.lorthiois@novartis.com
James A. Marshall	Department of Chemistry, University of Virginia, PO Box 400319, Charlottesville, VA 22904, USA. Fax: +1 434 924 7993; e-mail: jam5x@virginia.edu
Seijiro Matsubara	Department of Material Chemistry, Graduate School of Engineering, Kyoto University, Kyoudai-katsura, Nishikyo, Kyoto 606-8501, Japan. Fax: +81 75 383 2438; e-mail: matsubar@orgrxn.mbox.media.kyoto-u.ac.jp
Christophe Meyer	Laboratoire de Chimie Organique, associé au CNRS, ESPCI, 10 rue Vauquelin, F-75231, Paris Cedex 05, France. Fax: +33 14 079 4660; e-mail: christophe.meyer@espci.fr
Ei-ichi Negishi	Herbert C. Brown Laboratories of Chemistry, Purdue University, 560 Oval Drive, West Lafayette, Indiana 47907-2084, USA. Fax: +1 765 496 3380; e-mail: negishi@purdue.edu
Sergiu P. Palii	Department of Chemistry, University of Florida, P.O. Box 117200, Gainesville, FL 32611-7200, USA. Fax: +1 352 392 0872; e-mail: palii@ufl.edu
Jacques Périchon	C.N.R.S. UMR 7582, Laboratoire d'Electrochimie Catalyse et Synthése Organique, Université Paris XII, 2-8 rue H. Dunant, F-94320 Thiais, France. Fax: +33 14 978 1148; e-mail: perichon@glvt-cnrs.fr
Sylvie Perrone	Department of Chemistry, Ludwig-Maximilians-Universität München, Butenandtstr. 5-13, D-81377 München, Germany. Fax: +49 8921 807 7680; e-mail: sylvie.perrone@cup.uni-muenchen.de
Itaru Sato	Department of Chemistry, School of Science and Technology, Kwansei Gakuin University, Sanda, Hyogo 669–1337, Japan. Fax: +81 79 565 9077; e-mail: isato@ksc.kwansei.ac.jp
Gudrun Schürer	Computer Chemistry Center, University of Erlangen-Nürnberg, Nägelsbachstr. 25, D-91052 Erlangen, Germany. Fax: +49 9131 852 6565; e-mail: Gudrun.Schuerer@chemie.uni-erlangen.de
Mathias O. Senge	School of Chemistry, Trinity College Dublin, Dublin 2, Ireland. Fax: +353 1 896 8536; e-mail: sengem@tcd.ie
Natalia N. Sergeeva	School of Chemistry, Trinity College Dublin, Dublin 2, Ireland. Fax: +353 1 896 8536; e-mail: sergeevn@tcd.ie
Suzanne W. Slayden	Department of Chemistry, George Mason University, 4400 University Drive, Fairfax, VA 22030-4444, USA. Fax: +1 703 993 1055; e-mail: sslayden@gmu.edu

Kenso Soai — Department of Applied Chemistry, Faculty of Science, Tokyo University of Science, Kagurazaka, Shinjuku-ku, Tokyo 162-8601, Japan. Fax: +81 33 235 2214; e-mail: soai@rs.kagu.tus.ac.jp

Knut Sommer — Bayer MaterialScience AG, Business Unit Polyurethanes, Process Research Isocyanates, Building R79, D-47812 Krefeld, Germany. Fax: +49 215 188 3228; e-mail: Knut.Sommer@bayermaterialscience.com

Georgios A. Spyroulias — Department of Pharmacy, University of Patras, Panepistimioupoli—Rion, GR-26504 Patras, Greece. Fax: +30 261 096 9950; e-mail: gspyroul@upatras.gr

Claudio Trombini — Department of Chemistry "G. Ciamician", University of Bologna, via Selmi 2, I-40126 Bologna, Italy. Fax: +39 051 209 9456; e-mail: claudio.trombini@unibo.it

Guangwei Wang — Herbert C. Brown Laboratories of Chemistry, Purdue University, 560 Oval Drive, West Lafayette, Indiana 47907-2084, USA. Fax: +1 765 496 3380; e-mail: wang47@purdue.edu

Ning Yin — Herbert C. Brown Laboratories of Chemistry, Purdue University, 560 Oval Drive, West Lafayette, Indiana 47907-2084, USA. Fax: +1 765 496 3380; e-mail: nyin@purdue.edu

Dmitri V. Zagorevskii — Department of Chemistry and Chemical Biology, Rensselaer Polytechnic Institute, 209C Cogswell Laboratories, 110 8th Str., Troy, NY 12180, USA. Fax: +1 518 276 4887; e-mail: zagord@rpi.edu

Foreword

The present volume is another one in 'The Chemisty of Functional Groups' series, which deals with organometallic derivatives. Closely related to it are the two recent volumes (3 parts) on *The Chemistry of Organolithium Compounds* (Zvi Rappoport and Ilan Marek, Eds., 2003 and 2005). Although almost ignored for more than 100 years since the initial discovery by Frankland, organozinc compounds are today among the most useful classes of organometallic reagents used in organic and organometallic syntheses. Considering the remarkable renaissance in organozinc chemistry in the last 15 years, we felt that the time had come for a comprehensive volume, which will emphasize the new developments in the Chemistry of Organozinc Compounds.

The two parts of the present volume contain 19 chapters written by experts from 12 countries. They include chapters dealing with structural chemistry, thermochemistry, and mass spectrometry of organozinc compounds, with ^{67}Zn NMR as a probe, with mechanisms of reactions of zinc enzymes, and with the rearrangements of and the dynamic behaviour of organozinc derivatives. Several chapters are devoted to special classes of organozinc compounds such as allenylzinc reagents, 1,1-bimetallated species, organozincate compounds, fluorinated organozinc reagents and the chemistry of organozinc enolates, and an extensive chapter deals with functionalized organozinc compounds. Reactions carried by organozinc reagents such as cyclopropanation, coupling reactions, carbozincation and enantioselective additions are covered in other chapters. Generation of organozinc compounds by electrochemistry and their reactions, as well as the photochemical transformations of the special group of zinc porphyrins and phthalocyanines are discussed in other chapters. We gratefully acknowledge the contributions of all the authors of these chapters.

The literature coverage is mostly up to and sometimes including 2005.

We will be grateful to readers who draw our attention to any mistakes in the present volume, or to omissions and new topics, which deserve to be included in a future volume on organozinc compounds.

Jerusalem and Haifa
May 2006

Zvi Rappoport
Ilan Marek

The Chemistry of Functional Groups Preface to the series

The series 'The Chemistry of Functional Groups' was originally planned to cover in each volume all aspects of the chemistry of one of the important functional groups in organic chemistry. The emphasis is laid on the preparation, properties and reactions of the functional group treated and on the effects which it exerts both in the immediate vicinity of the group in question and in the whole molecule.

A voluntary restriction on the treatment of the various functional groups in these volumes is that material included in easily and generally available secondary or tertiary sources, such as Chemical Reviews, Quarterly Reviews, Organic Reactions, various 'Advances' and 'Progress' series and in textbooks (i.e. in books which are usually found in the chemical libraries of most universities and research institutes), should not, as a rule, be repeated in detail, unless it is necessary for the balanced treatment of the topic. Therefore each of the authors is asked not to give an encyclopaedic coverage of his subject, but to concentrate on the most important recent developments and mainly on material that has not been adequately covered by reviews or other secondary sources by the time of writing of the chapter, and to address himself to a reader who is assumed to be at a fairly advanced postgraduate level.

It is realized that no plan can be devised for a volume that would give a complete coverage of the field with no overlap between chapters, while at the same time preserving the readability of the text. The Editors set themselves the goal of attaining reasonable coverage with moderate overlap, with a minimum of cross-references between the chapters. In this manner, sufficient freedom is given to the authors to produce readable quasi-monographic chapters.

The general plan of each volume includes the following main sections:

(a) An introductory chapter deals with the general and theoretical aspects of the group.

(b) Chapters discuss the characterization and characteristics of the functional groups, i.e. qualitative and quantitative methods of determination including chemical and physical methods, MS, UV, IR, NMR, ESR and PES — as well as activating and directive effects exerted by the group, and its basicity, acidity and complex-forming ability.

(c) One or more chapters deal with the formation of the functional group in question, either from other groups already present in the molecule or by introducing the new group directly or indirectly. This is usually followed by a description of the synthetic uses of the group, including its reactions, transformations and rearrangements.

(d) Additional chapters deal with special topics such as electrochemistry, photochemistry, radiation chemistry, thermochemistry, syntheses and uses of isotopically labeled compounds, as well as with biochemistry, pharmacology and toxicology. Whenever applicable, unique chapters relevant only to single functional groups are also included (e.g. 'Polyethers', 'Tetraaminoethylenes' or 'Siloxanes').

This plan entails that the breadth, depth and thought-provoking nature of each chapter will differ with the views and inclinations of the authors and the presentation will necessarily be somewhat uneven. Moreover, a serious problem is caused by authors who deliver their manuscript late or not at all. In order to overcome this problem at least to some extent, some volumes may be published without giving consideration to the originally planned logical order of the chapters.

Since the beginning of the Series in 1964, two main developments have occurred. The first of these is the publication of supplementary volumes which contain material relating to several kindred functional groups (Supplements A, B, C, D, E, F and S). The second ramification is the publication of a series of 'Updates', which contain in each volume selected and related chapters, reprinted in the original form in which they were published, together with an extensive updating of the subjects, if possible, by the authors of the original chapters. Unfortunately, the publication of the 'Updates' has been discontinued for economic reasons.

Advice or criticism regarding the plan and execution of this series will be welcomed by the Editors.

The publication of this series would never have been started, let alone continued, without the support of many persons in Israel and overseas, including colleagues, friends and family. The efficient and patient co-operation of staff-members of the Publisher also rendered us invaluable aid. Our sincere thanks are due to all of them.

The Hebrew University
Jerusalem, Israel

SAUL PATAI
ZVI RAPPOPORT

Sadly, Saul Patai who founded 'The Chemistry of Functional Groups' series died in 1998, just after we started to work on the 100th volume of the series. As a long-term collaborator and co-editor of many volumes of the series, I undertook the editorship and I plan to continue editing the series along the same lines that served for the preceeding volumes. I hope that the continuing series will be a living memorial to its founder.

The Hebrew University
Jerusalem, Israel
May 2000

ZVI RAPPOPORT

Contents

List of abbreviations used

Ac	acetyl (MeCO)
acac	acetylacetone
Ad	adamantyl
AIBN	azoisobutyronitrile
Alk	alkyl
All	allyl
An	anisyl
Ar	aryl
Bn	benzyl
Bu	butyl (C_4H_9)
Bz	benzoyl (C_6H_5CO)
CD	circular dichroism
CI	chemical ionization
CIDNP	chemically induced dynamic nuclear polarization
CNDO	complete neglect of differential overlap
Cp	η^5-cyclopentadienyl
Cp*	η^5-pentamethylcyclopentadienyl
DABCO	1,4-diazabicyclo[2.2.2]octane
DBN	1,5-diazabicyclo[4.3.0]non-5-ene
DBU	1,8-diazabicyclo[5.4.0]undec-7-ene
DIBAH	diisobutylaluminium hydride
DME	1,2-dimethoxyethane
DMF	*N*,*N*-dimethylformamide
DMSO	dimethyl sulphoxide
ee	enantiomeric excess
EI	electron impact
ESCA	electron spectroscopy for chemical analysis
ESR	electron spin resonance
Et	ethyl
eV	electron volt
Fc	ferrocenyl
FD	field desorption

FI	field ionization
FT	Fourier transform
Fu	furyl(OC_4H_3)
GLC	gas liquid chromatography
Hex	hexyl(C_6H_{13})
c-Hex	cyclohexyl(*c*-C_6H_{11})
HMPA	hexamethylphosphortriamide
HOMO	highest occupied molecular orbital
HPLC	high performance liquid chromatography
i-	iso
ICR	ion cyclotron resonance
Ip	ionization potential
IR	infrared
LAH	lithium aluminium hydride
LCAO	linear combination of atomic orbitals
LDA	lithium diisopropylamide
LUMO	lowest unoccupied molecular orbital
M	metal
M	parent molecule
MCPBA	*m*-chloroperbenzoic acid
Me	methyl
MNDO	modified neglect of diatomic overlap
MS	mass spectrum
n	normal
Naph	naphthyl
NBS	*N*-bromosuccinimide
NCS	*N*-chlorosuccinimide
NMR	nuclear magnetic resonance
Pen	pentyl(C_5H_{11})
Ph	phenyl
Pip	piperidyl($C_5H_{10}N$)
ppm	parts per million
Pr	propyl (C_3H_7)
PTC	phase transfer catalysis or phase transfer conditions
Py, Pyr	pyridyl (C_5H_4N)
R	any radical
RT	room temperature
s-	secondary
SET	single electron transfer
SOMO	singly occupied molecular orbital

t-	tertiary
TCNE	tetracyanoethylene
TFA	trifluoroacetic acid
THF	tetrahydrofuran
Thi	thienyl(SC_4H_3)
TLC	thin layer chromatography
TMEDA	tetramethylethylene diamine
TMS	trimethylsilyl or tetramethylsilane
Tol	tolyl(MeC_6H_4)
Tos or Ts	tosyl(*p*-toluenesulphonyl)
Trityl	triphenylmethyl(Ph_3C)
Xyl	xylyl($Me_2C_6H_3$)

In addition, entries in the 'List of Radical Names' in *IUPAC Nomenclature of Organic Chemistry*, 1979 Edition, Pergamon Press, Oxford, 1979, p. 305–322, will also be used in their unabbreviated forms, both in the text and in formulae instead of explicitly drawn structures.

CHAPTER 1

The reaction mechanisms of zinc enzymes

GUDRUN SCHÜRER and TIMOTHY CLARK

Computer Chemistry Center, University of Erlangen-Nürnberg, Nägelsbachstr. 25, D-91052 Erlangen, Germany
Fax: +49 9131 852 6565; e-mail: clark@chemie.uni-erlangen.de

and

RUDI VAN ELDIK

Institute for Inorganic Chemistry, University of Erlangen-Nürnberg, Egerlandstr. 1, D-91058 Erlangen, Germany
Fax: +49 9131 852 7387; e-mail: vaneldik@chemie.uni-erlangen.de

The chemistry of organozinc compounds
Edited by Z. Rappoport and I. Marek

I. INTRODUCTION

Zinc is an essential trace element. More than 300 enzymes that require zinc ions for activity are known. Most catalyze hydrolysis reactions, but zinc-containing representatives of all enzyme classes are known[1], such as, for instance, alcohol dehydrogenase (an oxidoreductase), farnesyl-/geranyl transferase (a transferase), β-lactamase (a hydrolase), carbonic anhydrase (a lyase) and phosphomannose isomerase.

The function of zinc ions may be either catalytic or structural. Enzymes with a co-catalytic center of two or even three zinc ions in close proximity are also known. In a new type of zinc-binding site, the protein interface, zinc ions are fixed at the interface of two proteins with the aid of amino acid residues. The ligand residues are usually His, Asp, Glu or Cys, which interact via nitrogen, oxygen or sulfur donors with the metal ion. In catalytic binding sites, His coordination dominates and an additional reactive water molecule is bound.

Missing or disfunctional zinc enzymes may have severe pathological effects (for details of the physiological impact of zinc see, e.g., References 2–4). Therefore, understanding their modes of action, especially their reaction mechanisms, is essential. Much work has been devoted to this topic, both experimental and theoretical. Among other experimental techniques, X-ray structural studies of inhibitor-complexes and kinetic measurements have played important roles and a range of computational methods from force fields to density functional or *ab initio* methods has been used to gain insight into the microscopic details of reactions in the active sites of zinc enzymes.

This review will give a subjective account of mechanistic studies on some representative zinc enzymes comprising the enzyme classes I–IV (oxidoreductases, transferases, hydrolases and lyases). It does not claim to be comprehensive, as a comprehensive review would be far too extensive for this work. Lowther and Matthews[5] have reviewed the metalloaminopeptidases and Noodleman and coworkers[6] have reviewed calculational studies on metalloenzymes. We apologize in advance for any omissions and point to previous reviews on this and related subjects to be found, e.g., in References 7–11.

II. STRUCTURAL ASPECTS

A number of important structural aspects of zinc complexes as found in enzymes are introduced in this section to serve as background information for the subsequent sections. Aquated Zn(II) ions exist as octahedral $[Zn(H_2O)_6]^{2+}$ complexes in aqueous solution. The coordinated water molecules are loosely bound to the Zn^{2+} metal center and exchange rapidly with water molecules in the second coordination sphere (see Figure 1) with a rate constant of *ca* 10^7 s^{-1} at 25 °C extrapolated from complex-formation rate constants of Zn^{2+} ions with a series of nucleophiles[12]. The mechanism of the water exchange reaction on Zn(II) was studied theoretically, from which it was concluded that the reaction follows a dissociative mechanism as outlined in Figure 2[13].

The Zn^{2+} ion interacts favorably with N-, O- and S-donor ligands and shows a strong preference for tetrahedral over octahedral coordination in enzymes. In the case of model complexes, Zn^{2+} can form four-, five- and six-coordinate complexes, dictated by the

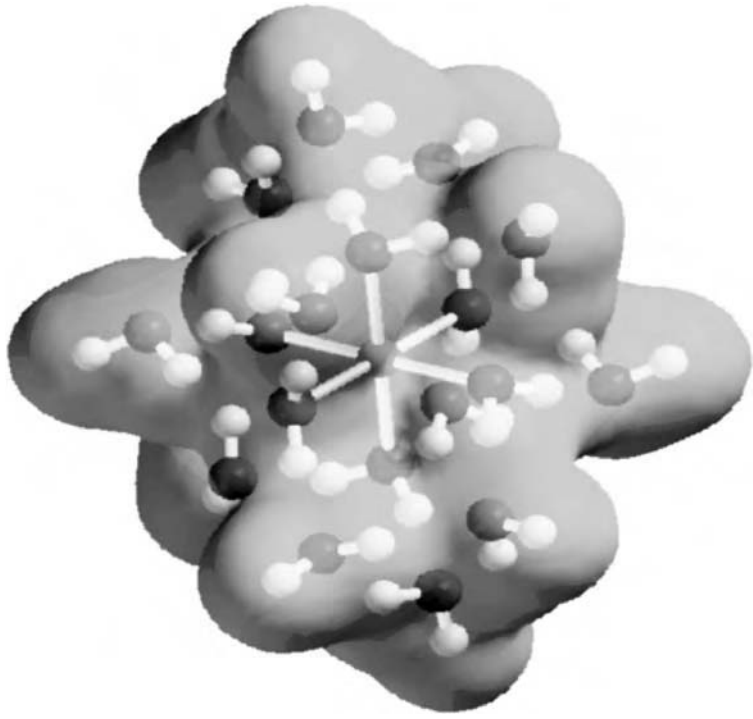

FIGURE 1. Schematic presentation of the Zn(II) ion surrounded by six water molecules in the first coordination sphere and 12 molecules in the second coordination sphere

ligand size, structure and charge. The coordination geometry varies from tetrahedral to trigonal pyramidal, tetragonal pyramidal, trigonal bipyramidal and octahedral on increasing the coordination number from four to six. Coordination chemists have synthesized many model Zn(II) complexes to mimic the biological role of Zn(II) enzymes and their reaction mechanisms[9, 14, 15]. In these systems the Zn(II) ion is usually four-coordinate with a tetrahedral structure of the general form $Zn^{II}(XYZ)(H_2O)$, where X, Y and Z are usually His, Glu, Asp or Cys. In addition, there are a variety of zinc enzymes with polynuclear active sites as shown in Figure 3. Numerous groups have modeled the catalytic cycle of zinc enzymes successfully using well-selected synthetic model complexes[9].

Another important structural aspect in terms of the reaction mechanisms of zinc enzymes concerns the coordination mode of water and carboxylates, which can bind in a monodentate or bidentate fashion to the Zn(II) center, as shown in Figure 4.

This is also especially true for the binding of carbonate and hydrogen carbonate, which can both act as monodentate and bidentate ligands. For quite some time it was not possible to isolate stable hydrogen carbonate metal complexes since these tend to undergo rapid loss of CO_2. However, more recently such complexes have been isolated and well characterized. It has also been shown that, depending on the nature of the spectator ligands,

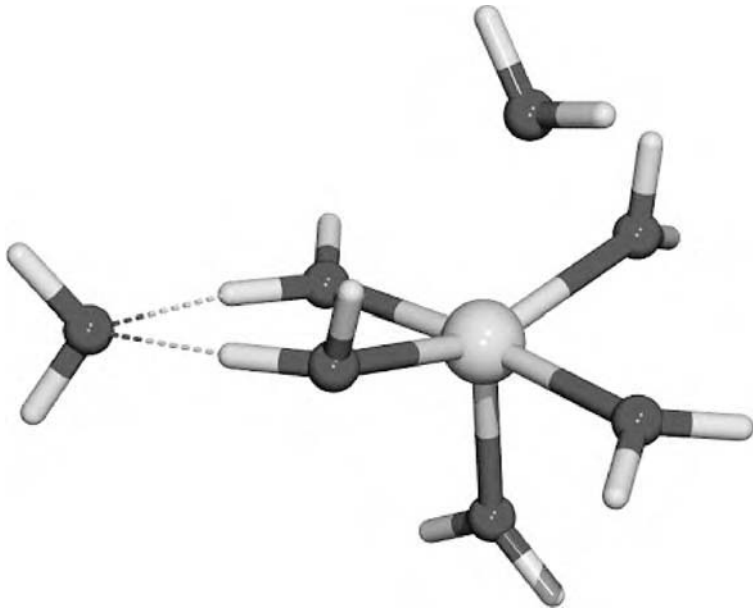

FIGURE 2. Transition state structure for water exchange on $[Zn(H_2O)_6]^{2+}$ demonstrating the dissociation of an axially coordinated water molecule induced by an entering water molecule from the second coordination sphere

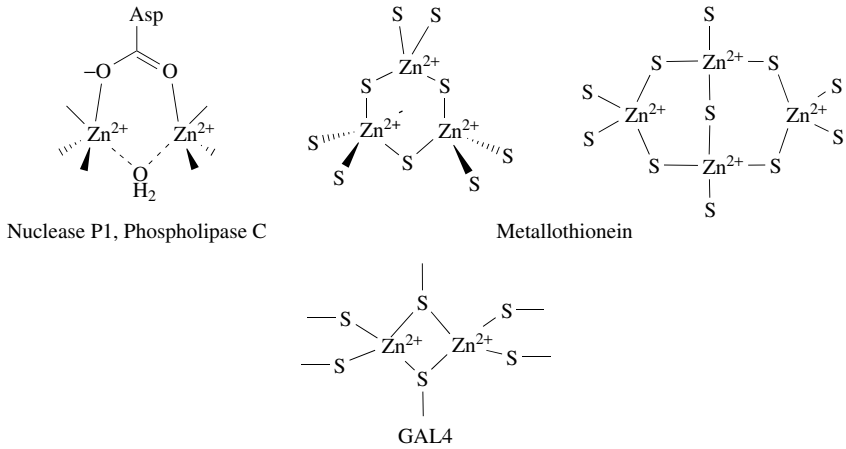

FIGURE 3. Polynuclear zinc sites in enzymes and proteins. Adapted with permission from Reference 9. Copyright (2004) ACS

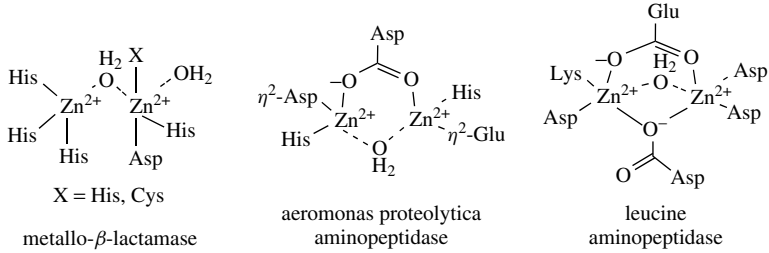

FIGURE 4. Active sites of some dinuclear zinc enzymes. Adapted with permission from Reference 9. Copyright (2004) ACS

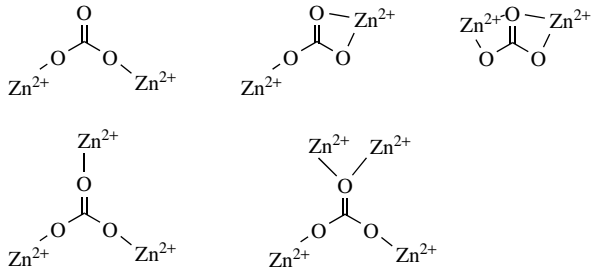

FIGURE 5. Coordination mode of the bridging carbonate ligand in multinuclear zinc complexes. Adapted with permission from Reference 9. Copyright (2004) ACS

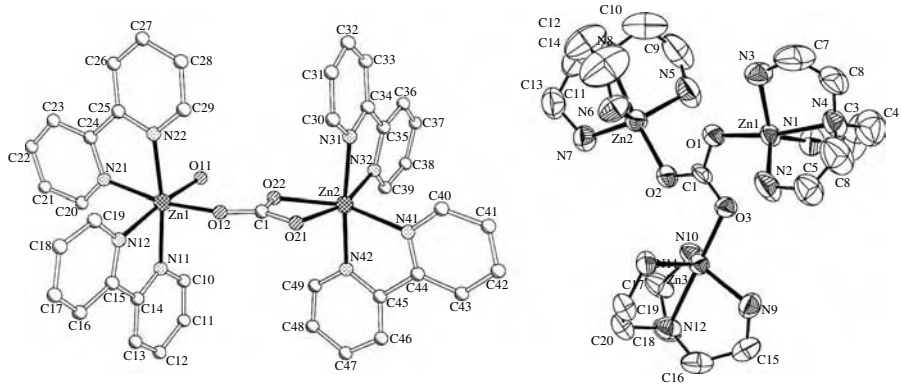

FIGURE 6. Crystal structures of $\{[Zn(bpy)_2]_2(\mu\text{-}CO_3)\}^{2+}$ and $\{[Zn(tren)]_3(\mu_3\text{-}CO_3)\}^{4+}$. Adapted with permission from References 16 and 17 from the Royal Society of Chemistry. Copyright (2001) RSC

carbonate can bind to Zn(II) not only in a monodentate or bidentate fashion but also simultaneously to two and three Zn(II) centers as shown schematically in Figure 5[9, 16–18]. A few typical structures are shown in Figure 6.

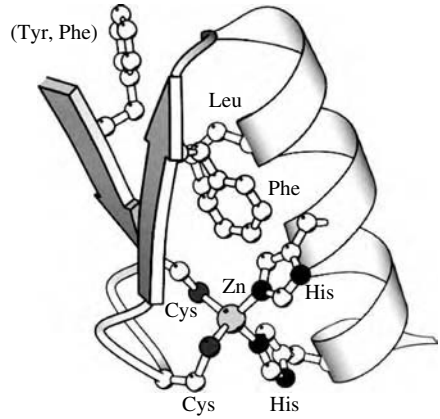

FIGURE 7. Structure of a zinc-finger domain. Reprinted with permission from Reference 19. Copyright 2004 American Chemical Society

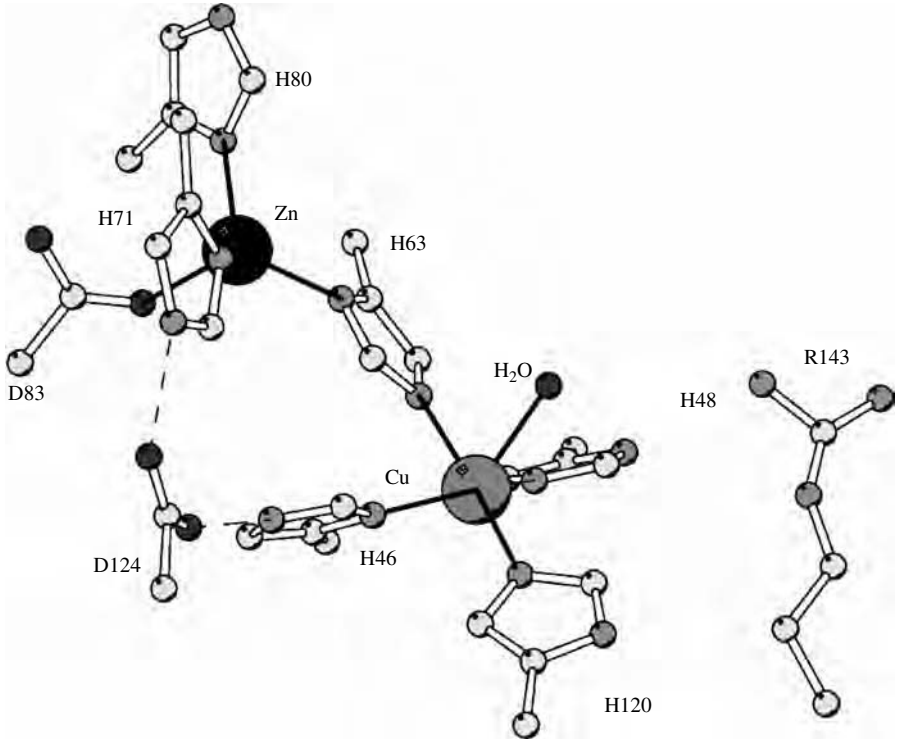

FIGURE 8. Molecular structure of Cu,Zn-SOD. Reprinted from Reference 20. Copyright 2004, with permission from Elsevier

Another area in which Zn(II) complexes play an important role concerns the recognition of Cys_2His_2 zinc-finger protein domains, which exhibit a characteristic tetrahedral structure as shown in Figure 7. More than 4000 such domains are present in over 700 proteins[19].

Finally, Zn^{2+} also plays an important role in Cu,Zn-SOD (copper–zinc superoxide dismutase) for which the structure is shown in Figure 8[20]. Although it is well-known that Zn(II) is not involved in electron-transfer chemistry, it is generally believed that the essential role of Zn(II) ion in SODs is to accelerate both the oxidation and reduction of superoxide by controlling the redox potential of the Cu(II) ion and superoxide ion in the catalytic cycle[21].

III. GENERAL REACTION MECHANISMS

Zinc enzymes usually catalyze a closely related class of reactions that all involve the addition of a nucleophile (usually OH^-) to a positively charged carbon-center (usually a carbonyl carbon atom). By far the most prevalent mechanism is of the general base type, in which a general base uses the electron-withdrawing effect of zinc coordination to deprotonate what would otherwise be a weak acid, such as water or ethanol. The zinc-coordinated nucleophile can then attack the electrophilic center. Note that Zn(II)–OH, for instance, is a far weaker nucleophile than OH^- and that the catalytic effect arises from the generation of the nucleophile in far higher local concentration than would be available in solution at that specific pH and not from an activation of the nucleophile. Bertini and coworkers have investigated the influence of zinc-binding on the pK_a values and nucleophilicity of hydroxo-containing species[22]. Generally, the electrophile is not coordinated to the zinc before the nucleophile attacks, but only as the tetrahedral intermediate is generated (see Figure 9).

The suggestion that the electrophile is activated by coordination to the zinc ion is prevalent in the experimental literature but usually does not find support in theoretical investigations. The binuclear zinc enzymes can be an exception because one zinc center can coordinate the electrophile while the other is used to generate the nucleophile. A question often raised for binuclear zinc enzymes is whether the nucleophile (usually OH^-) is bridged or coordinates to only one of the zinc atoms. This question is often made more difficult by the fact that bridging hydroxides are often found in X-ray structures

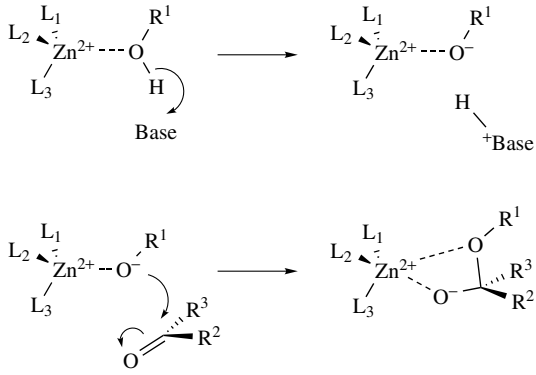

FIGURE 9. General reaction mechanism of zinc enzymes. L_1-L_3 represent any amino acid residues coordinated to the zinc

but are not necessarily present in the active form of the enzyme in solution. Bridging hydroxides are often suggested to be the nucleophile in experimental work, although a hydroxide coordinated to two zinc centers is an inherently weaker nucleophile than one coordinated to a single zinc center. Usually, theoretical studies suggest that a non-bridging nucleophile is the active species, although there are exceptions. These points will be discussed below.

IV. A NUMBER OF ENZYMES

A. Class I: Oxidoreductases

Although zinc itself is not redox-active, some class I enzymes containing zinc in their active sites are known. The most prominent are probably alcohol dehydrogenase and copper–zinc superoxide dismutase (Cu,Zn-SOD). All have in common that the redox-active agent is another transition-metal ion (copper in Cu,Zn-SOD) or a cofactor such as nicotinamide adenine dinucleotide (NAD^+/NADH). The Zn(II) ion affects the redox reaction only in an indirect manner, but is nevertheless essential and cannot be regarded simply as a structural factor.

However, the redox activity of sulfur ligands in zinc sites, known as the zinc redox switch[23,24], is also important and constitutes a basic motif for controlling protein function in redox biology. The Zn–S interaction offers specific mechanisms for enzyme catalysis, establishes the reactivity of zinc sites that were hitherto believed to play only a structural role, allows zinc to be tightly bound and yet available and, importantly, generates redox-active coordination environments for the redox-inert zinc ion. These activities are critically involved in the regulation of protein structure and function and in mobility, transfer, redistribution and sensing of cellular zinc, as is becoming evident from the continuing exploration of the protein metallothionein and other proteins involved in cellular zinc homeostasis[23]. One example is the zinc/sulfur cluster in metallothionein, which acts as a remarkable biochemical device that controls the concentration of readily available zinc inside the cell[25].

Moreover, zinc is also known for its antioxidant properties. These appear to be independent of zinc metalloenzyme activity, but are based on protecting sulfhydryl groups or antagonizing redox-active transition metals that cause the site-specific formation of free radicals[26].

1. Alcohol dehydrogenase

Alcohol dehydrogenases (ADH; EC 1.1.1.1), for which several X-ray structures are available[27–35], catalyze the biological oxidation of primary and secondary alcohols via the formal transfer of a hydride anion to the oxidized form of nicotinamide adenine dinucleotide (NAD^+), coupled with the release of a proton. Liver alcohol dehydrogenase (LADH) consists of two similar subunits, each of which contains two zinc sites, but only one site within each subunit is catalytically active. The catalytic zinc is coordinated in a distorted tetrahedral manner to a histidine residue, two cysteine residues and a water molecule. The remaining zinc is coordinated tetrahedrally to four cysteine residues and plays only a structural role[9].

The essential features of the catalytic cycle (see Figure 10) involve the binding of NAD^+, the displacement of the water molecule by alcohol, the deprotonation of the coordinated alcohol to give a zinc alkoxide intermediate, the hydride transfer from the alkoxide to NAD^+ to give a zinc-bound aldehyde, the displacement of the aldehyde by water and the release of NADH. The principal role of the zinc in the dehydrogenation reaction is, therefore, to promote deprotonation of the alcohol and thereby enhance hydride transfer

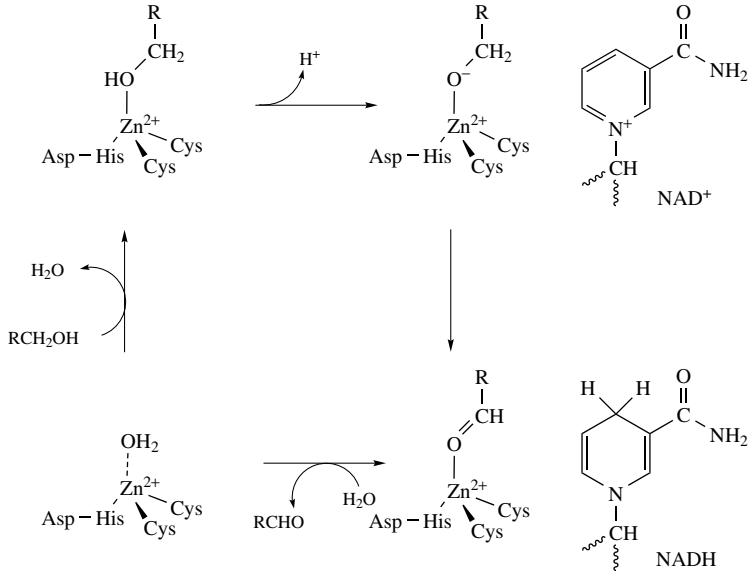

FIGURE 10. Essential features of the mechanism of action of liver alcohol dehydrogenase. Adapted with permission from Reference 9. Copyright (2004) ACS

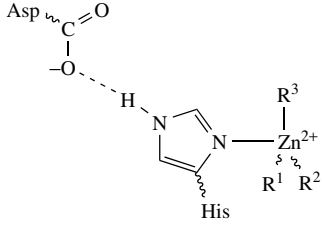

FIGURE 11. Asp-His-Zn triad present in many zinc enzymes, e.g. in LADH

from the incipient alkoxide species. Conversely, the role of the zinc in the reverse reaction (hydrogenation) is to enhance the electrophilicity of the carbonyl carbon atom[9,36–38].

The active site of LADH contains an Asp-His-Zn triad (see Figure 11). This pattern is quite common in zinc-enzymes. The aspartate affects the structure, electronic properties and energetics of the active site and thus the catalytic activity. Indeed, Asp49 is conserved in all mammalian ADHs[39].

2. Superoxide dismutase

The enzyme copper, zinc superoxide dismutase[20,40] (Cu,Zn-SOD, EC 1.15.1.1) catalyzes the disproportionation of superoxide anion to dioxygen and hydrogen peroxide (equations 1 and 2). Crystallographic data can be found in References 41–46. This antioxidant enzyme is present in the cytosol and mitochondrial intermembrane space of eukaryotic cells and in the periplasmic space of bacterial cells as a homodimer of 32 kDa. Each monomer binds one copper and one zinc ion. The reaction mechanism involves the

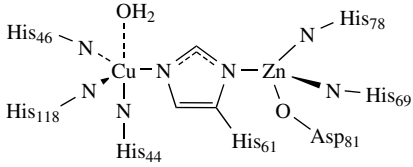

FIGURE 12. The active site of Cu,Zn SOD. Adapted with permission from Reference 50. Copyright (2003) Wiley & Sons

sequential reduction and reoxidation of Cu(II), for which both reactions are relatively pH-independent[47,48]. Mutants of Cu,Zn-SOD gain some properties that are associated with the development of amyotrophic lateral sclerosis (ALS), a progressive degenerative disease of motor neurons[49].

$$\mathrm{ECu(II)} + \mathrm{O_2}^{\bullet -} \longrightarrow \mathrm{ECu(I)} + \mathrm{O_2} \quad (1)$$

$$\mathrm{ECu(I)} + \mathrm{O_2}^{\bullet -} + 2\mathrm{H}^+ \longrightarrow \mathrm{ECu(II)} + \mathrm{H_2O_2} \quad (2)$$

In the metal-binding site (Figure 12) the Cu(II) ion is coordinated by four histidines in a distorted square-planar coordination sphere and by a fifth axial water ligand, while the tetrahedral zinc ion is coordinated by three histidines, one of which is deprotonated and bridges to the copper, and by a carboxylate group[50].

The zinc ion is currently thought to have only a structural function in the active site of Cu,Zn-SOD. However, the Zn(II) center has been suggested to be essential in order to accelerate the highly endergonic electron transfer from the Cu(I) center to $O_2^{\bullet -}$, which is bound to Zn(II)[51]. Studies of the disproportionation of a semiquinone radical anion ($Q^{\bullet -}$) with an imidazole-bridged dinuclear Cu−Zn compound as a model system show that Zn(II) facilitates the reduction of $Q^{\bullet -}$ by coordination. Moreover, it also facilitates the oxidation step by shifting the redox potential of the Cu(II) center[51]. A thorough theoretical investigation of the mechanism has been performed recently by Pelmenschikov and Siegbahn[52].

B. Class II: Transferases

Zinc has been identified as a cofactor in a growing number of proteins that utilize thiols as nucleophiles, including proteins that catalyze the transfer of methyl groups to thiols. The latter category includes the Ada protein involved in the response of *E. coli* to DNA alkylation, cobalamin-independent and -dependent methionine synthases, enzymes involved in the formation of methylcoenzyme M in methanogenesis and the prenyl transferases farnesyl-protein transferase (PFTase) and geranylgeranyl-protein transferase (PGGTase). Because the pK_a values for the formation of thiolates from thiols are lower than the corresponding values for alcohols and for water, thiols were generally considered not to require coordination to Lewis acids. However, enzyme-bound zinc plays an important role for the activation of thiols for nucleophilic attack[53].

1. Prenyl transferases

The prenyl transferases[54] are a class of enzymes that is involved in post-translational modification of membrane-associated proteins. These enzymes catalyze the transfer of a farnesyl (FTase, EC 2.5.1.58, for structural information see References 55–65) or geranylgeranyl group (GGTase I, EC 2.5.1.59; GGTase II, EC 2.5.1.60, for structural information

see References 66–70) to a C-terminal cysteine residue contained in a C-terminal tetrapeptide signal sequence, frequently referred to as a CAAX motif, where C is cysteine, A any aliphatic amino acid and X a prenylation specificity residue[71].

Protein prenylation is an ubiquitous post-translational modification since virtually all small monomeric guanosine triphosphate (GTP) binding proteins, the β-subunits from heterotrimeric G-proteins and many other proteins are so modified. The fact that many prenylated proteins are involved in signaling processes has generated considerable interest. In particular, the observation that Ras proteins (a family of the G-proteins) are farnesylated and that the inhibition of prenylation of oncogenic Ras variants halts the growth of certain types of cancer has sparked an explosion of work in this area. Inhibitors of FTase and GGTase I are being explored as possible anticancer agents[65].

The reaction is shown in Figure 13. The zinc ion in the active site of PFTase is coordinated by a histidine, a cysteine and most likely a bidentate aspartate in its resting state.

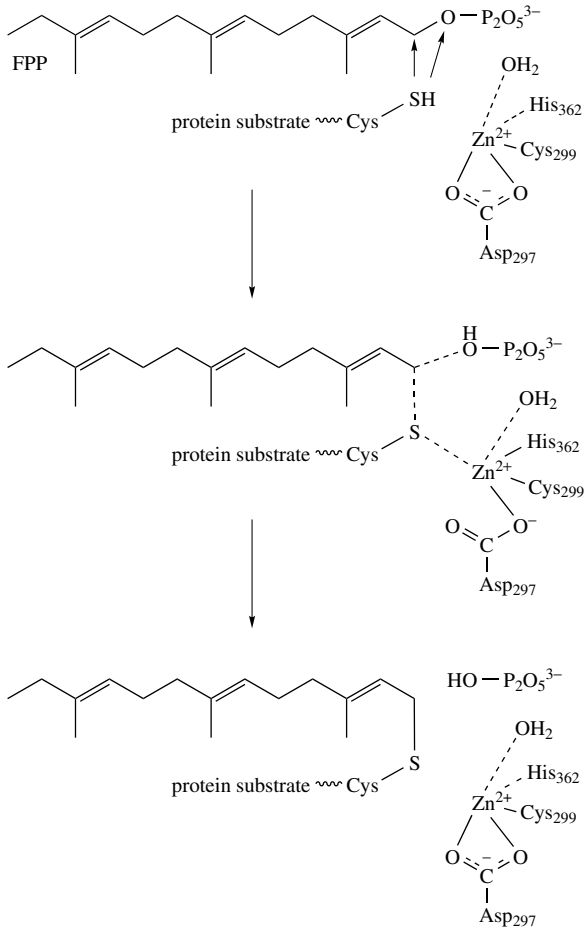

FIGURE 13. The reaction catalyzed by FTase. Adapted with permission from Reference 65. Copyright (2003) ACS

A fourth low-Z ligand, for example from the water that is seen in many crystal structures, does not make a detectable contribution to the EXAFS spectrum and is thus presumably at a longer distance from the zinc. Upon peptide binding, one low-Z ligand, most likely one of the aspartate oxygens, is displaced by the peptide cysteine thiol. After transfer of the C1 of farnesylpyrophosphate to the peptide thiolate to form the thioether product, the zinc returns to ZnS(N/O)3 ligation, indicating that the Zn–S thioether interaction is extremely weak, with the thioether having been most likely displaced by the second oxygen from the carboxylate. Structural changes such as these, with alternation of the carboxylate from monodentate to bidentate, a leitmotif in zinc-enzyme mechanisms, would provide an effective mechanism to increase the nucleophilicity of the peptide thiolate during the farnesyl transfer reaction. Conversion of the carboxylate to bidentate ligation in the transition state could shift electron density onto the peptide cysteine, thus increasing the nucleophilicity of the zinc-thiolate and facilitating catalysis of farnesylation[72]. For further information see, e.g., References 71,73–87.

C. Class III: Hydrolases

The zinc hydrolase superfamily is a group of divergently related proteins, predominantly enzymes, which includes aminopeptidases, carboxypeptidases and non-peptidase enzymes such as deacetylases. Some use a single zinc atom in catalysis (monozinc) while others use two or even three zinc atoms (co-catalytic). The common structural scaffold of the superfamily consists of an eight-stranded β-sheet flanked by six α-helices. Although in some cases the active sites of the divergent member of the superfamily are homologous, no overall conservation exists[88]. Catalysis in this enzyme group is believed to operate via a general-base mechanism (see Figure 9). The nucleophilic water molecule is deprotonated by the carboxylate residue of Asp or Glu or, in the case of bovine lens leucyl aminopeptidase, by a neutral Lys. The nucleophilic attack on a peptide bond leads to a *gem*-diolate intermediate that decomposes to build the reaction products. The hydrolysis of phospholipase C works in an analogous manner. However, alkaline phosphatase shows a phosphoseryl intermediate with a covalent bond between the enzyme and the substrate.

1. Aminopeptidase

Aminopeptidases (AP, EC 3.4.11.1) are exopeptidases that remove the N-terminal amino acid from proteins. They require active sites with *two* zinc centers to achieve the cleavage. The active site of *Aeromonas proteolytica* aminopeptidase (AAP, structural information is given in References 89–94) is located in a loop region near the edge of the binding pocket. It consists of two Zn^{2+} ions, each coordinated with a histidine and an aspartate or a glutamate. Additionally, an aspartate and a water molecule or hydroxide ion bridge the two metal ions. These have equivalent structural environments, suggesting a symmetrical role in catalysis. Both Zn^{2+} ions have approximately tetrahedral coordination polyhedra if the weak interaction to the second oxygen atoms of the carboxylate ligands is neglected. The coordination stereochemistry for all Zn^{2+}-ligand interactions (*syn* and in-plane for carboxylate and head-on for histidine) is in agreement with observed zinc binding preferences[95]. An additional glutamate residue (Glu151) is located near the active site, in structural analogy to the metallo-peptidases thermolysin and carboxypeptidase A. It has been suggested to play the role of a general base in the catalytic reaction. This residue is hydrogen bonded to the bridging water/hydroxide[91].

A catalytic mechanism (Figure 14) was proposed on the basis of kinetic, spectroscopic and crystallographic data[90,96–100]. The substrate peptide binds to Zn_2 with its N-terminal amino group and to Zn_1 with the carbonyl oxygen of the scissile peptide bond. Additionally, the N-terminus interacts with Asp179. Upon substrate binding, the bridging water

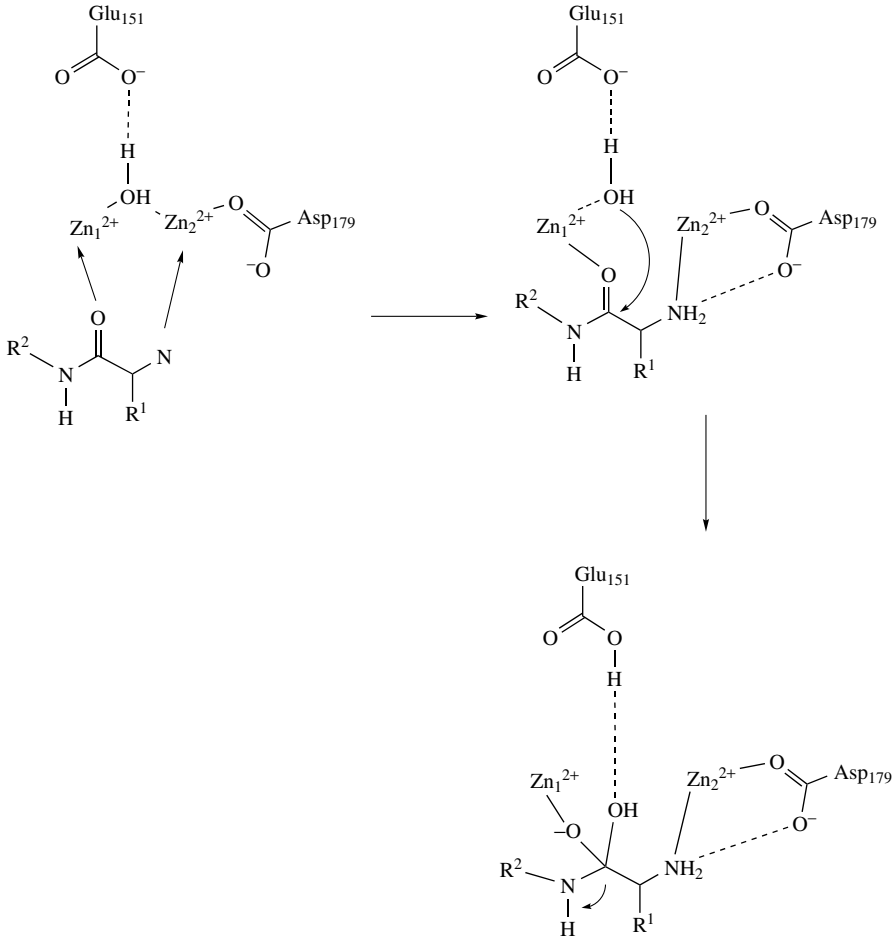

FIGURE 14. Reaction mechanism of AAP proposed by Stamper and coworkers. Adapted from References 90 and 102. Copyright (2001) and (2004) ACS

molecule loses its coordination to Zn_2 and becomes terminally bound to Zn_1. The bond cleavage is assisted by a hydrogen bond from Asp99 to Nδ1 of the Zn_2 ligand His97 (for clarity, this is not shown in Figure 14). Such carboxylate-histidine-metal triads (see Figure 11) can be found in several zinc-containing enzymes[101]. A hydrogen bond between the terminal water molecule and Glu151 allows deprotonation of the former to give a hydroxide ion as nucleophile. The nucleophilic attack results in the tetrahedral intermediate, which is coordinated to Zn_1. The neutral Glu151 may act as a proton donor for the peptide nitrogen. The rate-limiting step is probably the C−N bond cleavage step, that is, the product formation[90]. QM/MM calculations confirm this proposal to a high degree[102]. However, they show that the substrate carbonyl oxygen is not coordinated to Zn_1 in the intermediate structures, but only to Zn_2 by its N-terminus. The coordination of

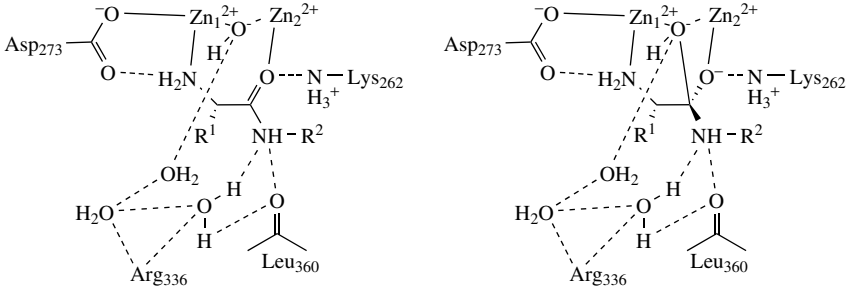

FIGURE 15. Reaction mechanism of BlLAP as proposed by Sträter and Lipscomb. Adapted from References 103 and 110. Copyright (1995) and (2002) ACS

the carbonyl oxygen to Zn_1 occurs at first when the nucleophilic attack of the Zn_1-bound hydroxide ion takes place.

In spite of the different active site residues, the reaction mechanism of the *bovine lens* leucyl aminopeptidase (blLAP) follows a similar path (Figure 15). Based on the X-ray structures of the free enzyme and the enzyme-inhibitor complexes[103–109], it was suggested that the substrate carbonyl oxygen is coordinated to Zn_1 (Zn_{488} in References 103–109) and a bridging hydroxide ion acts as the nucleophilic agent. In the resulting negatively charged tetrahedral intermediate, the protonated oxygen of the *gem*-diolate group is coordinated as a bridging ligand between the two metal ions and the second, unprotonated oxygen is additionally bound to Zn_1. After the cleavage of the peptide bond, the peptide nitrogen is protonated by a water molecule. The function of Lys262 is to stabilize the substrate carbonyl carbon in the reactant structure and the unprotonated *gem*-diolate oxygen in the tetrahedral intermediate. Moreover, Lys262 probably has the function to act as a proton shuttle. The incoming water molecule is deprotonated to form the nucleophilic species and later the proton is transferred to the nitrogen of the scissile peptide bond to facilitate the decomposition of the tetrahedral intermediate[110]. Furthermore, the coordination pattern of the tetrahedral intermediate as was suggested by Sträter and coworkers[103, 104] could not be confirmed by QM/MM calculations, but consists of a *gem*-diolate group only coordinated to Zn_1 via its unprotonated oxygen[110].

BlLAP was investigated intensively by Weston and coworkers using DFT methods[111, 112]. They found that two water channels lead to the active site, a larger one for the substrate and a smaller one for water. Thus, the enzyme is capable of regenerating the nucleophilic species continuously[112].

2. Carboxypeptidase

Carboxypeptidase A[113] (CPA, EC 3.4.17.1) is a proteolytic enzyme that cleaves C-terminal amino acid residues with hydrophobic side chains selectively. Several X-ray structures are available[114–122]. The active site of CPA consists of a hydrophobic pocket (primary substrate recognition site) that is primarily responsible for the substrate specificity, a guanidinium moiety of Arg145 that forms hydrogen bonds to the carboxylate of the substrate, and Glu270, whose carboxylate plays a critical role, functioning either as a nucleophile to attack the scissile carboxamide carbonyl carbon of the substrate or as a base to activate the zinc-bound water molecule, which in turn attacks the scissile peptide bond[123]. However, semiempirical calculations had shown that the direct attack of

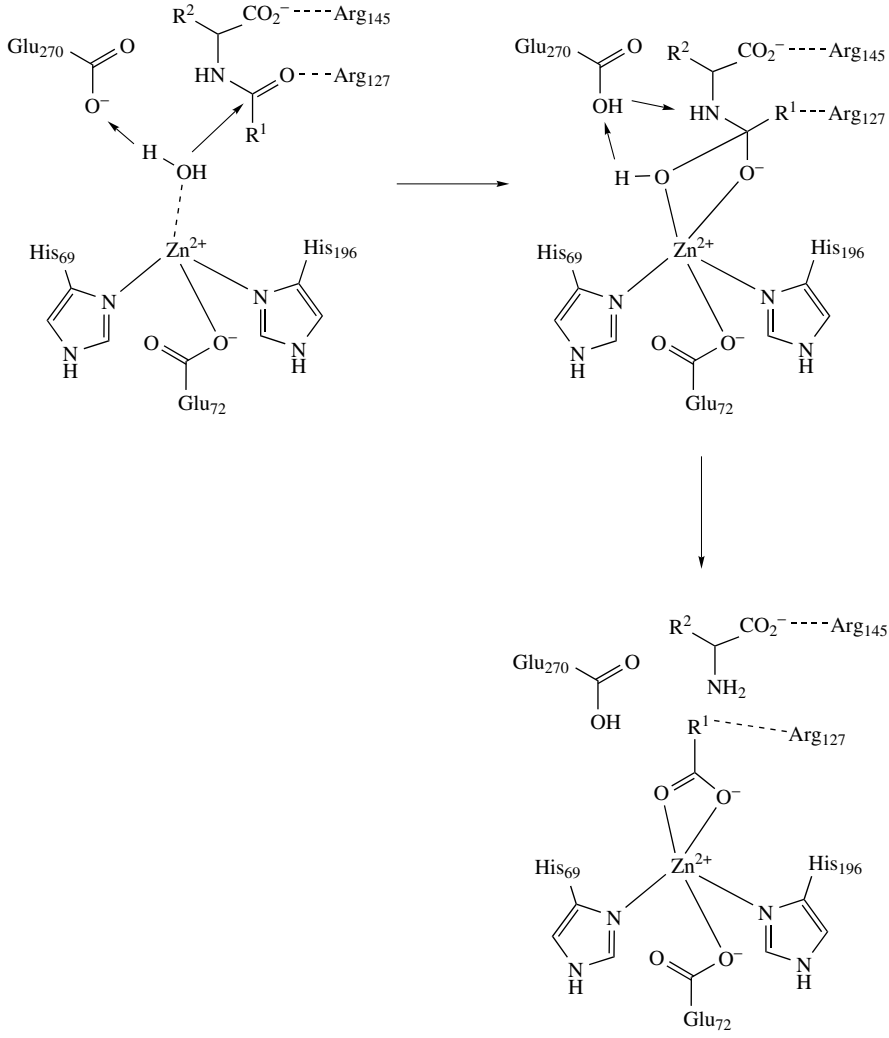

FIGURE 16. Reaction mechanism of carboxypeptidase A. Adapted with permission from Reference 126. Copyright (2002) Wiley & Sons

Glu270 resulting in an anhydride intermediate is much less favorable than the attack of a deprotonated water molecule[124]. The active-site zinc ion is coordinated to the backbone amino acid residues of His69, Glu72, His196 and a molecule of water. Upon binding a substrate to the enzyme, the scissile amide carbonyl oxygen has been suggested to coordinate to the zinc ion, whereby the carbonyl carbon becomes an electrophilic center (Figure 16). However, earlier semiempirical molecular orbital (AM1) calculations on a model system[125] had suggested that the substrate is not coordinated to the zinc in the transition state for the addition, but that the catalysis results from the deprotonation

of the zinc-coordinated water by Glu270. These conclusions were supported by further semiempirical[126,127] and molecular-dynamics (MD) calculations[127]. For further reading see, e.g., References 128–130.

3. Thermolysin

Thermolysin (EC 3.4.24.27, for crystallographic data see References 131–138), a classical hydrolase, is, along with Carboxypeptidase A, one of the two oldtimers of mechanistic zinc-enzyme chemistry[139]. These enzymes are closely related to each other, though thermolysin is an endopeptidase. Their active sites (see Figure 17) bear a close resemblance, with the zinc centers of each being bound to the protein by a combination of one glutamate (Glu166 in the case of thermolysin) and two histidine residues (His142 and His146), a ligand combination that is common to many other metallopeptidases. The glutamate residue of each enzyme is capable of binding in both unidentate and bidentate manners. The remaining binding site is occupied by a solvent water or the enzyme substrate[9].

Thermolysin was one of the first enzymes to be investigated using QM/MM techniques. Rivail and coworkers[140,141] studied the hydrolysis of a model peptide substrate (formamide) by thermolysin. Two mechanisms were considered, one involving only one water molecule and the other involving two water molecules. The QM region was described by the AM1 Hamiltonian and included the zinc atom, the three amino acid ligands, the formamide and one or two water molecules. The rest of the system, including the remainder of the enzyme and the crystallographic water molecules, was described using the AMBER force field. The comparison between the two hydrolysis reactions shows that the mechanism assisted by an ancillary water (Figure 17) is favored. The fact is explained by the better nucleophilicity of the oxygen atom in the water dimer and a less constrained transition state. The zinc atom of the catalytic center acts as a Lewis acid and the ligands as an electron reservoir. Further information can be found in References 142–150.

4. β-Lactamase

There are four classes (A, B, C and D) of β-lactamases, of which the most recent to be discovered, the so-called metallo-β-lactamases (or class B β-lactamases, EC 3.5.2.6), are dinuclear zinc enzymes. The molecular structures of several metallo-β-lactamases have been determined[151–162] and while the intimate details may vary, there are several common features. Interestingly, while the various metallo-β-lactamases contain two zinc centers, the *Bacillus cereus* β-lactamase activity is still observed in a monozinc form[163–165]. Crystallographic data[155,156,166] show that the first zinc ion (Zn_1) is tetrahedrally coordinated by three histidine residues and a water molecule. The second zinc ion (Zn_2) is coordinated by the carboxylate group of an aspartate, the methylthiolate group of a cysteine, the imidazole ring of a histidine, the Zn_1-bound water molecule and a second water molecule. The resulting coordination environment for Zn_2 is close to a trigonal bipyramidal arrangement. It is commonly assumed that the Zn_1-bound water is present in its deprotonated form at neutral pH in the *B. cereus* active site and, therefore, could readily attack the β-lactam carbonyl[167].

The role of the second zinc is uncertain. It has been postulated that coordination via the nitrogen serves to (i) position the substrate for nucleophilic attack, (ii) polarize further the N−C(O) bond and (iii) stabilize the negative charge on the nitrogen leaving group[168]. The mode of action of the binuclear enzyme is shown in Figure 18.

Calculations pertaining to the mechanism of action of metallo-β-lactamases have been performed for the mono-zinc β-lactamase of *Bacillus cereus*[169,170] as well as on the binuclear β-lactamase of *Bacteroides fragilis*[171]. Molecular-dynamics and quantum-mechanical

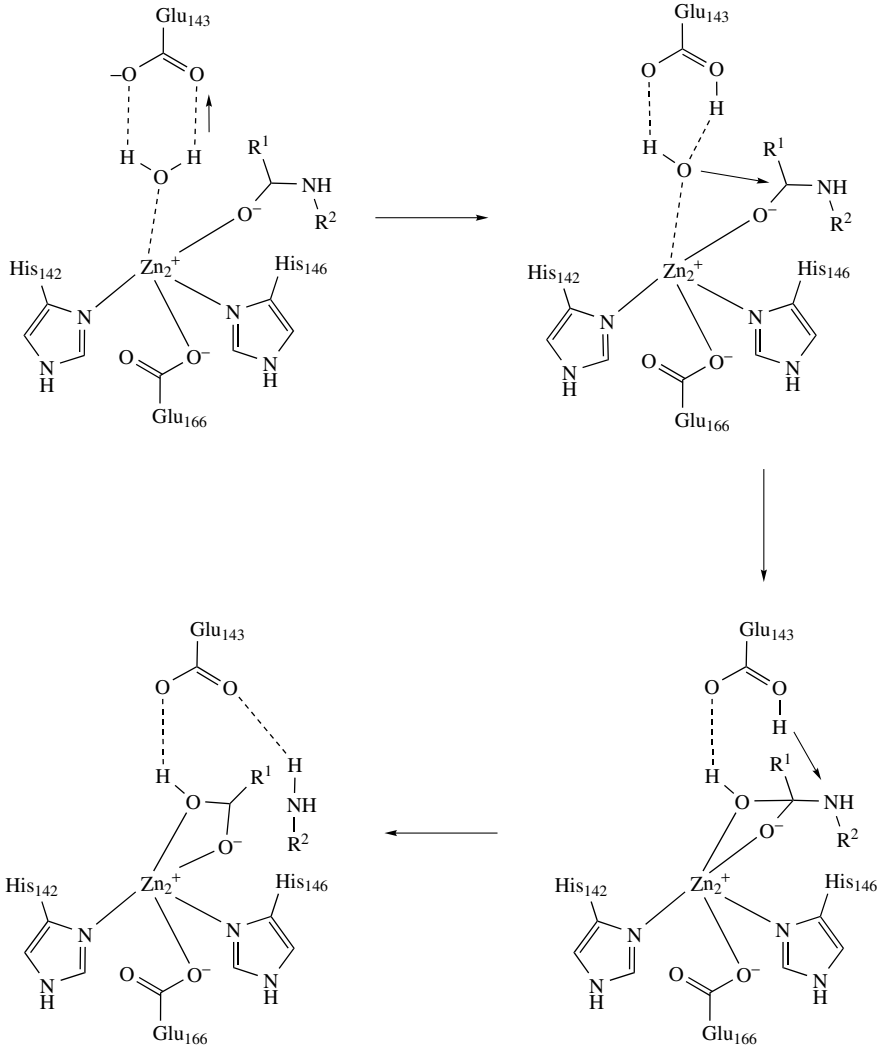

FIGURE 17. Favored reaction mechanism of thermolysin. Adapted with permission from References 9 and 140. Copyright (2003) and (1998) ACS

calculations have suggested that there is a dynamic equilibrium between bridging and nonbridging hydroxide structures[171], similarly to the situation found for bovine lens leucyl aminopeptidase[110], and have investigated the relative stabilities of OH^- and H_2O ligands on zinc. Studies on model systems[9] indicate that the bridging hydroxide is not very reactive because (i) the bridging hydroxide and the coordinated substrate do not align properly to facilitate nucleophilic attack and (ii) the nucleophilicity of the hydroxide is diminished because it coordinates to two zinc centers. The mechanism has been proposed to involve coordination of the β-lactam carboxylate group to one of the zinc centers,

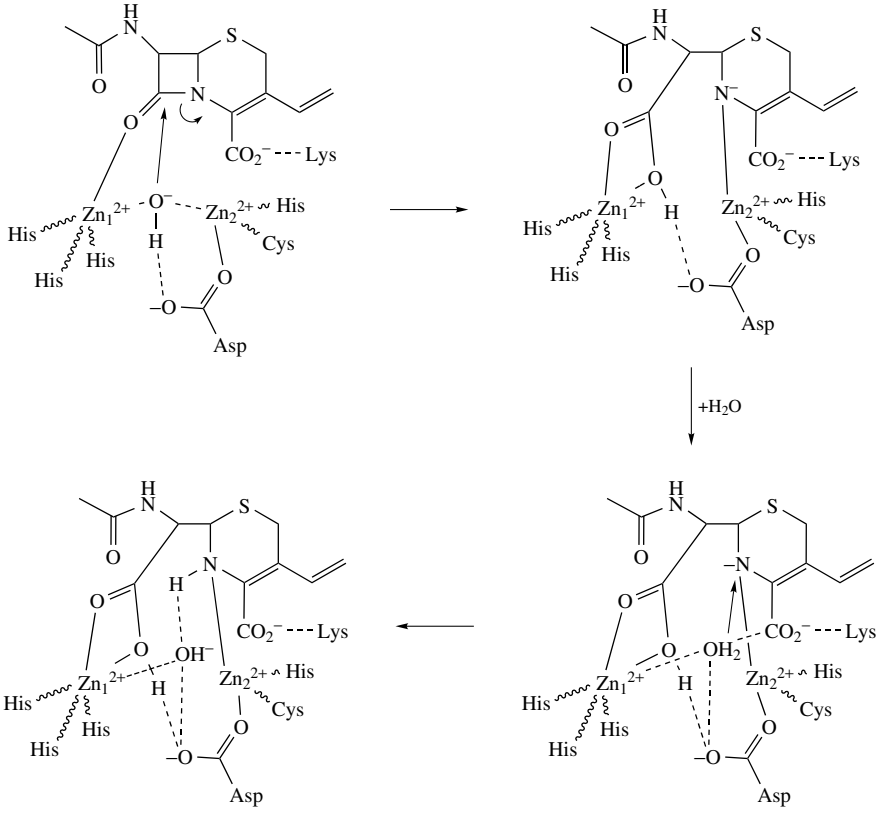

FIGURE 18. Reaction mechanism of the *Bacteroides fragilis* β-lactamase. Adapted with permission from Reference 168. Copyright (1999) ACS

followed by rate-limiting nucleophilic attack by the bridging hydroxide at the coordinated substrate[172–174]. However, since mononuclear complexes have comparable activities, it is evident that the second zinc center is not a requirement for catalytic activity. In fact, it is worth noting that the Zn^{2+}-catalyzed methanolysis of nitrocefin has been reported to occur via two mechanisms, one of which involves a single zinc center and the other two zinc centers[175]. For further reading see References 154,158,168,176–188.

5. Alkaline phosphatase

Alkaline phosphatase (ALP; EC 3.1.3.1, for crystallographic data see References 189–201) cleaves phosphate from phosphate monoesters in a non-specific manner under alkaline conditions[193,195]. It contains two Zn^{2+} and one Mg^{2+} ion in its active site. The latter is connected to Zn_2 by Asp51 and is proposed to enhance enzymatic activity. The perturbation of the active site topology by the exchange of Asp51 by a glutamate residue leads to a drastically reduced activity and the loss of Zn_2[202]. The first stage of the catalytic reaction involves the monophosphate $[ROPO_3]^{2-}$ η^2-coordinated to the two zinc centers, accompanied by dissociation of the Zn_1-bound water molecule; the two oxygen

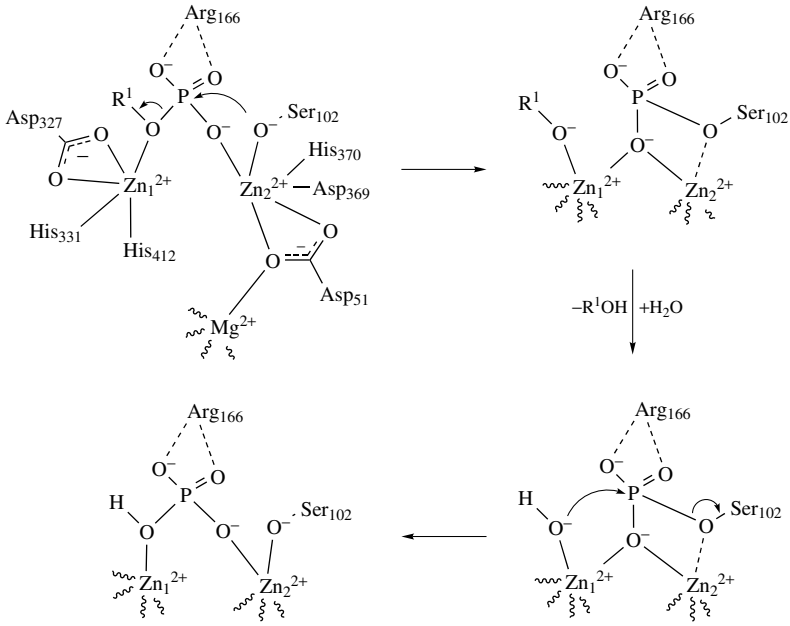

FIGURE 19. Reaction mechanism of alkaline phosphatase. For clarity, the complete active site is shown only in the first structure. Adapted with permission from Reference 10. Copyright (2005) ACS

atoms of $[ROPO_3]^{2-}$, which do not coordinate to the zinc centers, interact with Arg106 via two hydrogen bonds. The phosphorus of the coordinated phosphate ligand is attacked by the deprotonated Ser102 residue in a S_N2 manner, thereby cleaving the P−OR bond and forming a phophoseryl intermediate. The phosphate group is now coordinated only to Zn_2. In this regard, the two zinc centers play several roles. First, one of them activates the P−OR bond towards cleavage by coordinating the −OR group. Second, coordination of the Ser-OH group to the other facilitates the deprotonation that generates the incipient Ser-O^- nucleophile. Once formed, the zinc alkoxide group is hydrolyzed to release ROH and generate a zinc-hydroxide species. Subsequent nucleophilic attack of the hydroxide ligand on the phosphoenzyme intermediate cleaves the phosphorus-Ser102 bond, thereby forming a bridging phosphate $[HOPO_3]^{2-}$ complex. Displacement of $[HOPO_3]^{2-}$ by water completes the catalytic cycle. The catalytic mechanism is shown in Figure 19[10, 203]. This two-step sequence results in overall retention of configuration, a result in accord with the experimental observations[9]. For further information see References 204–210.

6. Phospholipase C

Phospholipase C (PLC, EC 3.1.4.3) catalyzes the hydrolysis of the phosphodiester bond in phospholipids. It releases the second messenger molecule diacylglycerin (DAG) important in the signal transduction cascade and a phosphorylated headgroup[10]. The active site of the enzyme contains three Zn^{2+} ions with two of them in close proximity. Only few crystal structures are solved until now[211–213].

A consistent catalytic mechanism of phospholipase C from *Bacillus cereus* based on molecular mechanics calculations was reported by da Graça Thrige and coworkers[214]. The

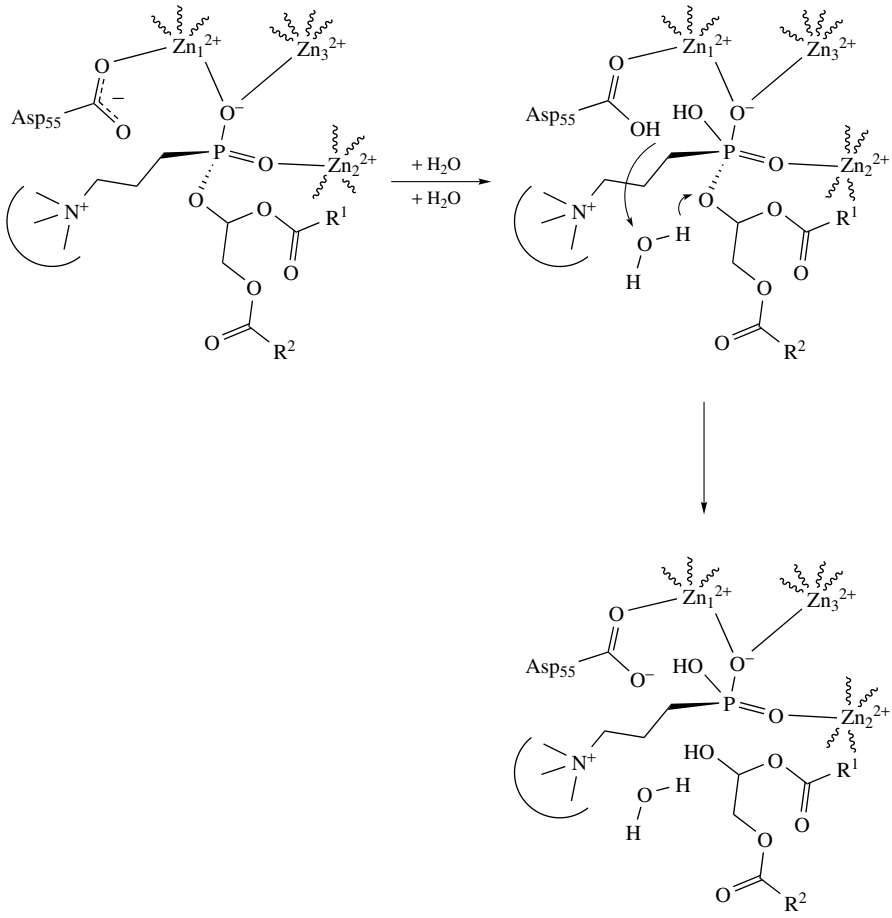

FIGURE 20. Reaction mechanism of phospholipase C. Adapted with permission from Reference 214. Copyright (1997) Wiley & Sons

mechanism involves a nucleophilic water molecule activated by an acidic residue (Asp55) that performs the nucleophilic attack on the phosphorus atom in the substrate, leading to a trigonal bipyramidal penta-coordinate intermediate (and structurally similar transition state). The subsequent collapse of the intermediate leads to the reaction products and regeneration of the enzyme. In this second step a second water molecule is used as a proton shuttle between Asp55 and the oxygen anion of diacylglycerin. The mechanism is shown in Figure 20. Further investigations about the catalytic cycle are given in Reference 215.

D. Class IV: Lyases

1. Carbonic anhydrase

Carbonic anhydrase (CA, EC 4.2.1.1), the first enzyme recognized to contain zinc[216–218], is ubiquitous. It occurs in animals, plants and bacteria. The essential physiological function

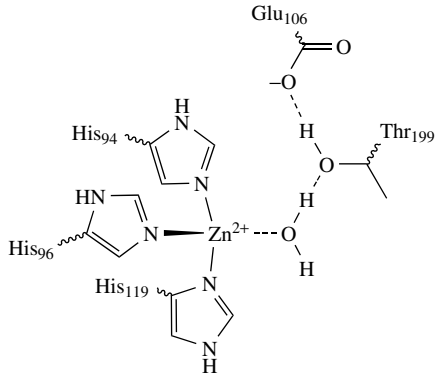

FIGURE 21. Active site of carbonic anhydrase. Adapted with permission from Reference 9. Copyright (2004) ACS

of the enzyme is to catalyze the reversible hydration of carbon dioxide and it thus plays an important role in respiration, transporting CO_2 between metabolizing tissues and the lungs, and intracellular CO_2/HCO_3^- equilibration. In addition to its physiological function, carbonic anhydrase also catalyzes non-physiological reactions such as hydration of aldehydes and esters. Numerous X-ray structures are available, e.g., in References 219–238.

In the CA-isoform II, zinc is coordinated to the nitrogen atoms of His94(N_3), His96(N_3), His119(N_1) and the oxygen atom of an $OH(OH_2)$ group to form an approximately tetrahedral complex at the bottom of a 15 Å deep cavity. The Zn−OH is incorporated into a hydrogen bond network that includes Thr199 and Glul06 (Figure 21). The mechanism of action for the hydration of CO_2 comprises the following steps: (i) deprotonation of the coordinated water with a pK_a of about 7 (via a His64 shuttle)[239] to give the active zinc hydroxide derivative $[(His)_3Zn{-}OH]^+$, (ii) nucleophilic attack of the zinc-bound hydroxide on the carbon dioxide substrate to give a hydrogen carbonate intermediate $[(His)_3Zn{-}OCO_2H]^+$ and (iii) displacement of the hydrogen carbonate anion by H_2O to complete the catalytic cycle. For (ii) two mechanisms have been proposed, namely the 'Lipscomb'[240] and 'Lindskog'[241] mechanisms, which are distinguished according to how the initial Zn−OH−CO_2 adduct is converted to the Zn−OCO_2H intermediate hydrogen carbonate complex. In the Lipscomb mechanism, an intramolecular proton transfer is suggested to occur from the coordinated hydroxo ligand to the CO_2 bound oxygen atom. In the Lindskog mechanism, Zn−OH bond cleavage occurs to induce an intramolecular isomerization to form the carboxylate bound hydrogen carbonate complex (Figure 22). The mechanism of the reverse dehydration of hydrogen carbonate to CO_2 and OH^- involves the rapid displacement of the coordinated water molecule by hydrogen carbonate in a ligand substitution reaction, followed by the reverse of (ii) to form the Zn−OH−CO_2 complex which subsequently releases CO_2.

A unique aspect of the catalytic activity of CA is the fact that the hydroxo form of the enzyme catalyzes the hydration of CO_2 through the direct binding of CO_2 to the hydroxo ligand, whereas the aqua form of the enzyme catalyzes the dehydration of hydrogen carbonate through a ligand substitution process. This difference in mechanism is nicely demonstrated by the overall volume profile shown in Figure 23, which was constructed on the basis of the effect of pressure on the catalytic hydration and dehydration processes[242]. Both these catalytic processes show characteristic pH dependencies that center around the pK_a value of the coordinated water molecule. Many model Zn(II) and

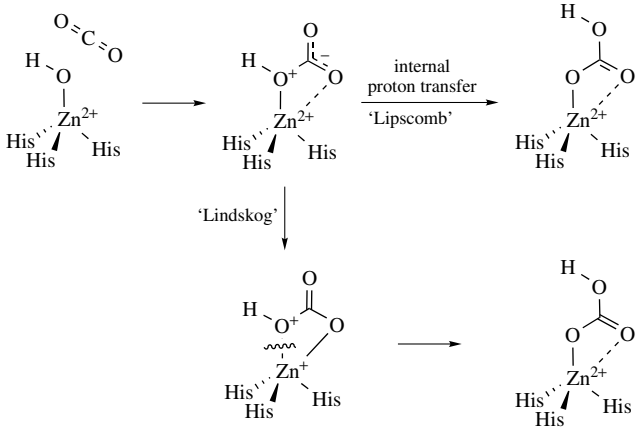

FIGURE 22. Schematic representation of the Lipscomb and Lindskog mechanisms. Adapted with permission from Reference 9. Copyright (2004) ACS

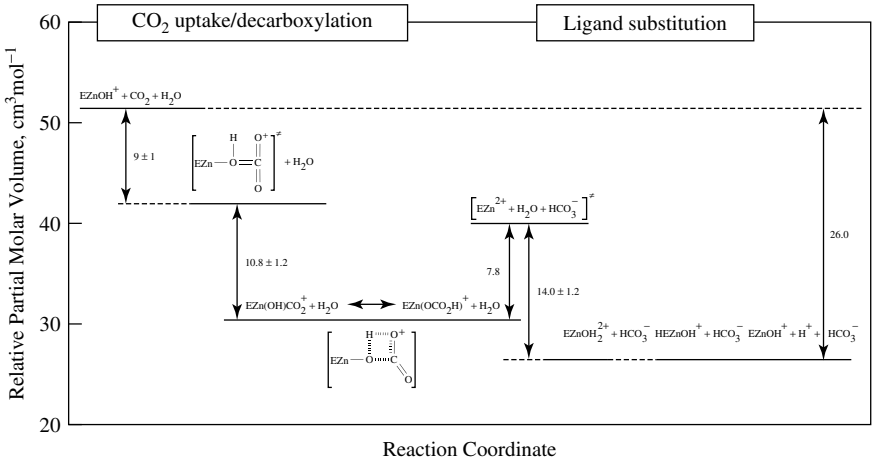

FIGURE 23. Overall volume profile for the CA catalyzed hydration of CO_2 and dehydration of HCO_3^-. Adapted from Reference 242. Copyright (1996) Academic Press Elsevier

Cu(II) complexes have been synthesized and studied to mimic the catalytic activity of CA[243–247]. Mechanistic studies have assisted to reveal the details of the hydration and dehydration mechanism and the catalytic activity of the model complexes[248–251].

CA has been the subject of numerous theoretical studies, most of which have centered on differentiating between the Lipscomb and Lindskog mechanisms or on the proton-transfer step. Early studies[252] concentrated on substrate binding and simple models for the active site[253], but soon mechanistic studies on model active sites were being published[239, 254–268]. It was suggested quite early[269] that active-site water molecules may change the mechanism significantly and studies have been published on metal-substituted CAs[270] and on the influence of sulfur in the substrate[271, 272].

V. ACKNOWLEDGMENT

The authors gratefully acknowledge financial support from the Deutsche Forschungsgemeinschaft through SFB 583 on Redox-Active Metal Complexes.

VI. REFERENCES

1. B. L. Vallee and K. H. Falchuk, *Physiol. Rev.*, **73**, 79 (1993).
2. B. L. Vallee, in *Zinc Enzymes* (Eds. I. Bertini and H. B. Gray), Birkhäuser, Boston, 1986, pp. 1–15.
3. M. Hambidge, R. J. Cousins and R. B. Costello, *J. Nutr.*, **130**, 1341S (2000).
4. W. Maret, *BioMetals*, **14**, 187 (2001).
5. W. T. Lowther and B. W. Matthews, *Chem. Rev.*, **102**, 4581 (2002).
6. L. Noodleman, T. Lovell, W.-G. Han, J. Li and F. Himo, *Chem. Rev.*, **104**, 459 (2004).
7. J. E. Coleman, *Curr. Opin. Chem. Biol.*, **2**, 222 (1998).
8. W. N. Lipscomb and N. Sträter, *Chem. Rev.*, **96**, 2375 (1996).
9. G. Parkin, *Chem. Rev.*, **104**, 699 (2004).
10. J. Weston, *Chem. Rev.*, **105**, 2151 (2005).
11. D. E. Wilcox, *Chem. Rev.*, **96**, 2435 (1996).
12. F. A. Dunand, L. Helm and A. E. Merbach, *Adv. Inorg. Chem.*, **54**, 1 (2003).
13. M. Hartmann, T. Clark and R. van Eldik, *J. Mol. Model.*, **2**, 354 (1996).
14. E. Kimura, *Curr. Opin. Chem. Biol.*, **4**, 207 (2000).
15. S. Aoki, *Chem. Rev.*, **104**, 769 (2004).
16. Z.-W. Mao, G. Liehr and R. van Eldik, *J. Chem. Soc., Dalton Trans.*, 1593 (2001).
17. Z.-W. Mao, G. Liehr, F. W. Heinemann and R. van Eldik, *J. Chem. Soc., Dalton Trans.*, 3652 (2001).
18. H. Erras-Hanauer, Z.-W. Mao, G. Liehr, T. Clark and R. van Eldik, *Eur. J. Inorg. Chem.*, 1562 (2003).
19. D. Jantz, B. T. Amann, G. J. Gatto, Jr and J. M. Berg, *Chem. Rev.*, **104**, 789 (2004).
20. A.-F. Miller, *Curr. Opin. Chem. Biol.*, **8**, 162 (2004).
21. S. Fukuzumi, *Pure Appl. Chem.*, **75**, 577 (2003).
22. I. Bertini, C. Luchinat, M. Rosi, A. Sgamellotti and F. Tarantelli, *Inorg. Chem.*, **29**, 1460 (1990).
23. W. Maret, *Biochemistry*, **43**, 3301 (2004).
24. A. M. Neculai, D. Neculai, C. Griesinger, J. A. Vorholt and S. Becker, *J. Biol. Chem.*, **280**, 2826 (2005).
25. W. Maret, *J. Nutr.*, **130**, 1455S (2000).
26. S. R. Powell, *J. Nutr.*, **130**, 1447S (2000).
27. H. Li, W. H. Hallows, J. S. Punzi, K. W. Pankiewicz, K. A. Watanabe and B. M. Goldstein, *Biochemistry*, **33**, 11734 (1994).
28. J. Benach, S. Atrian, R. Gonzalez-Duarte and R. Ladenstein, *J. Mol. Biol.*, **282**, 383 (1998).
29. J. Benach, S. Atrian, R. Gonzalez-Duarte and R. Ladenstein, *J. Mol. Biol.*, **289**, 335 (1999).
30. H. Cho, S. Ramaswamy and B. V. Plapp, *Biochemistry*, **36**, 382 (1997).
31. S. Ramaswamy, M. El Ahmad, O. Danielsson, H. Jornvall and H. Eklund, *Protein Sci.*, **5**, 663 (1996).
32. S. Ramaswamy, M. Scholze and B. V. Plapp, *Biochemistry*, **36**, 3522 (1997).
33. M. S. Niederhut, B. J. Gibbons, S. Perez-Miller and T. D. Hurley, *Protein Sci.*, **10**, 697 (2001).
34. B. J. Gibbons and T. D. Hurley, *Biochemistry*, **43**, 12555 (2004).
35. T. H. Venkataramaiah and B. V. Plapp, *J. Biol. Chem.*, **278**, 36699 (2003).
36. U. Ryde, *Int. J. Quantum Chem.*, **52**, 1229 (1994).
37. U. Ryde, *J. Comput.-Aided Mol. Des.*, **10**, 153 (1996).
38. U. Ryde, *Biophys. J.*, **77**, 2777 (1999).
39. F. L. Gervasio, V. Schettino, S. Mangani, M. Krack, P. Carloni and M. Parrinello, *J. Phys. Chem. B*, **107**, 6886 (2003).
40. A. Desideri and M. Falconi, *Biochem. Soc. Trans.*, **31**, 1322 (2003).
41. L. Banci, I. Bertini, F. Cramaro, R. Del Conte and M. S. Viezzoli, *Eur. J. Biochem.*, **269**, 1905 (2002).

42. L. Banci, I. Bertini, F. Cramaro, R. Del Conte and M. S. Viezzoli, *Biochemistry*, **42**, 9543 (2003).
43. P. Cioni, A. Pesce, B. Morozzo Della Rocca, S. Castelli, M. Falconi, L. Parrilli, M. Bolognesi, G. Strambini and A. Desideri, *J. Mol. Biol.*, **326**, 1351 (2003).
44. M. A. Hough and S. S. Hasnain, *J. Mol. Biol.*, **287**, 579 (1999).
45. R. W. Strange, S. Antonyuk, M. A. Hough, P. Doucette, J. Rodriguez, P. J. Hart, L. J. Hayward, J. S. Valentine and S. S. Hasnain, *J. Mol. Biol.*, **328**, 877 (2003).
46. R. W. Strange, S. V. Antonyuk, M. A. Hough, P. A. Doucette, J. S. Valentine and S. S. Hasnain, *J. Mol. Biol.*, **356**, 1152 (2006).
47. J. Hirose, M. Minakami, K. Settu, K. Tsukahara, J. Ueda and T. Ozawa, *Arch. Biochem. Biophys.*, **383**, 246 (2000).
48. B. Alvarez, V. Demicheli, R. Durán, M. Trujillo, C. Cerveñansky, B. A. Freeman and R. Radi, *Free Radical Biol. Med.*, **37**, 813 (2004).
49. J. S. Valentine and P. J. Hart, *Proc. Natl. Acad. Sci. U.S.A.*, **100**, 3617 (2003).
50. C. Belle and J.-L. Pierre, *Eur. J. Inorg. Chem.*, 4137 (2003).
51. H. Ohtsu and S. Fukuzumi, *Angew. Chem., Int. Ed. Engl.*, **39**, 4537 (2000).
52. V. Pelmenschikov and P. E. M. Siegbahn, *Inorg. Chem.*, **44**, 3311 (2005).
53. R. G. Matthews and C. W. Goulding, *Curr. Opin. Chem. Biol.*, **1**, 332 (1997).
54. P. J. Casey and M. C. Seabra, *J. Biol. Chem.*, **271**, 5289 (1996).
55. H. W. Park, S. R. Boduluri, J. F. Moomaw, P. J. Casey and L. S. Beese, *Science*, **275**, 1800 (1997).
56. S. B. Long, P. J. Casey and L. S. Beese, *Biochemistry*, **37**, 9612 (1998).
57. S. B. Long, P. J. Casey and L. S. Beese, *Nature*, **419**, 645 (2002).
58. P. Dunten, U. Kammlott, R. Crowther, D. Weber, R. Palermo and J. Birktoft, *Biochemistry*, **37**, 13042 (1998).
59. S. B. Long, P. J. Hancock, A. M. Kral, H. W. Hellinga and L. S. Beese, *Proc. Natl. Acad. Sci. U.S.A.*, **98**, 12948 (2001).
60. T. S. Reid and L. S. Beese, *Biochemistry*, **43**, 6877 (2004).
61. C. L. Strickland, W. T. Windsor, R. Syto, L. Wang, R. Bond, Z. Wu, J. Schwartz, H. V. Le, L. S. Beese and P. C. Weber, *Biochemistry*, **37**, 16601 (1998).
62. I. M. Bell, S. N. Gallicchio, M. Abrams, L. S. Beese, D. C. Beshore, H. Bhimnathwala, M. J. Bogusky, C. A. Buser, J. C. Culberson, J. Davide, M. Ellis-Hutchings, C. Fernandes, J. B. Gibbs, S. L. Graham, K. A. Hamilton, G. D. Hartman, D. C. Heimbrook, C. F. Homnick, H. E. Huber, J. R. Huff, K. Kassahun, K. S. Koblan, N. E. Kohl, R. B. Lobell, J. Lynch, J. J. R. Robinson, A. D. Rodrigues, J. S. Taylor, E. S. Walsh, T. M. Williams and C. B. Zartman, *J. Med. Chem.*, **45**, 2388 (2002).
63. S. J. DeSolms, T. M. Ciccarone, S. C. MacTough, A. W. Shaw, C. A. Buser, M. Ellis-Hutchings, C. Fernandes, K. A. Hamilton, H. E. Huber, N. E. Kohl, R. B. Lobell, R. G. Robinson, N. N. Tsou, E. S. Walsh, S. L. Graham, L. S. Beese and J. S. Taylor, *J. Med. Chem.*, **46**, 2973 (2003).
64. S. L. Gwaltney, II, S. J. O'Connor, L. T. Nelson, G. M. Sullivan, H. Imade, W. Wang, L. Hasvold, Q. Li, J. Cohen, W. Z. Gu, S. K. Tahir, J. Bauch, K. Marsh, S. C. Ng, D. J. Frost, H. Zhang, S. Muchmore, C. G. Jakob, V. Stoll, C. Hutchins, S. H. Rosenberg and H. L. Sham, *Bioorg. Med. Chem. Lett.*, **13**, 1359 (2003).
65. T. C. Turek-Etienne, C. L. Strickland and M. D. Distefano, *Biochemistry*, **42**, 3716 (2003).
66. J. S. Taylor, T. S. Reid, K. L. Terry, P. J. Casey and L. S. Beese, *EMBO J.*, **22**, 5963 (2003).
67. T. S. Reid, K. L. Terry, P. J. Casey and L. S. Beese, *J. Mol. Biol.*, **343**, 417 (2004).
68. H. Zhang, M. C. Seabra and J. Deisenhofer, *Structure Fold. Des.*, **8**, 241 (2000).
69. O. Pylypenko, A. Rak, R. Reents, A. Niculae, V. Sidorovitch, M. D. Cioaca, E. Bessolitsyna, N. H. Thomä, H. Waldmann, I. Schlichting, R. S. Goody and K. Alexandrov, *Mol. Cell*, **11**, 483 (2003).
70. A. Rak, A. Niculae, A. Kalinin, N. H. Thomä, V. Sidorovitch, R. S. Goody and K. Alexandrov, *Protein Expression Purif.*, **25**, 23 (2002).
71. A. K. Saha and D. W. End, *Bioorg. Med. Chem. Lett.*, **15**, 1713 (2005).
72. D. A. Tobin, J. S. Pickett, H. L. Hartman, C. A. Fierke and J. E. Penner-Hahn, *J. Am. Chem. Soc.*, **125**, 9962 (2003).
73. P. B. Cassidy and C. D. Poulter, *J. Am. Chem. Soc.*, **118**, 8761 (1996).
74. V. A. Clausen, R. L. Edelstein and M. D. Distefano, *Biochemistry*, **40**, 3920 (2001).

75. J. M. Dolence and C. D. Poulter, *Proc. Natl. Acad. Sci. U.S.A.*, **92**, 5008 (1995).
76. B. Dursina, N. H. Thomä, V. Sidorovitch, A. Niculae, A. Iakovenko, A. Rak, S. Albert, A.-C. Ceacareanu, R. Kölling, C. Herrmann, R. S. Goody and K. Alexandrov, *Biochemistry*, **41**, 6805 (2002).
77. H.-W. Fu, J. F. Moomaw, C. R. Moomaw and P. J. Casey, *J. Biol. Chem.*, **271**, 28541 (1996).
78. H. L. Hartman, K. E. Bowers and C. A. Fierke, *J. Biol. Chem.*, **279**, 30546 (2004).
79. C.-C. Huang, P. J. Casey and C. A. Fierke, *J. Biol. Chem.*, **272**, 20 (1997).
80. H. Kim and C.-H. Yang, *Eur. J. Biochem.*, **265**, 105 (1999).
81. S. C. MacTough, S. J. DeSolms, A. W. Shaw, M. T. Abrams, T. M. Ciccarone, J. P. Davide, K. A. Hamilton, J. H. Hutchinson, K. S. Koblan, N. E. Kohl, R. B. Lobell, R. G. Robinson and S. L. Graham, *Bioorg. Med. Chem. Lett.*, **11**, 1257 (2001).
82. R. Millet, J. Domarkas, R. Houssin, P. Gilleron, J.-F. Goossens, P. Chavatte, C. Logé, N. Pommery, J. Pommery and J.-P. Hénichart, *J. Med. Chem.*, **47**, 6812 (2004).
83. F. Minutolo, M. Antonello, S. Barontini, S. Bertini, L. Betti, R. Danesi, G. Gervasi, G. Giannaccini, C. Papi, G. Placanica, S. Rapposelli and M. Macchia, *Il Farmaco*, **59**, 887 (2004).
84. F. Minutolo, V. Asso, S. Bertini, L. Betti, G. Gervasi, E. Ghilardi, G. Giannaccini, G. Placanica, G. Prota, S. Rapposelli and M. Macchia, *Il Farmaco*, **59**, 857 (2004).
85. F. G. Njoroge, B. Vibulbhan, P. Pinto, C. Strickland, P. I. Kirschmeier, W. R. Bishop and V. Girijavallabhan, *Bioorg. Med. Chem. Lett.*, **14**, 5877 (2004).
86. J. Pan and S.-C. J. Yeung, *Cancer Res.*, **65**, 9109 (2005).
87. S. F. Sousa, P. A. Fernandes and M. J. Ramos, *Biophys. J.*, **88**, 483 (2005).
88. M. A. Wouters and A. Husain, *J. Mol. Biol.*, **314**, 1191 (2001).
89. C. C. DePaola, B. Bennett, R. C. Holz, D. Ringe and G. Petsko, *Biochemistry*, **38**, 9048 (1999).
90. C. Stamper, B. Bennett, T. Edwards, R. C. Holz, D. Ringe and G. Petsko, *Biochemistry*, **40**, 7035 (2001).
91. B. Chevrier, H. D'Orchymont, C. Schalk, C. Tarnus and D. Moras, *Eur. J. Biochem.*, **237**, 393 (1996).
92. W. T. Desmarais, D. L. Bienvenue, K. L. Bzymek, R. C. Holz, G. A. Petsko and D. Ringe, *Structure*, **10**, 1063 (2002).
93. C. C. Stamper, D. L. Bienvenue, B. Bennett, D. Ringe, G. A. Petsko and R. C. Holz, *Biochemistry*, **43**, 9620 (2004).
94. K. P. Bzymek, A. Moulin, S. I. Swierczek, D. Ringe, G. A. Petsko, B. Bennett and R. C. Holz, *Biochemistry*, **44**, 12030 (2005).
95. D. W. Christianson, *Adv. Protein Chem.*, **42**, 281 (1991).
96. B. Bennett and R. C. Holz, *J. Am. Chem. Soc.*, **119**, 1923 (1997).
97. B. Bennett and R. C. Holz, *Biochemistry*, **36**, 9837 (1997).
98. B. Bennett and R. C. Holz, *J. Am. Chem. Soc.*, **120**, 12139 (1998).
99. G. Chen, T. Edwards, V. M. D'Souza and R. C. Holz, *Biochemistry*, **36**, 4278 (1997).
100. R. C. Holz, B. Bennett, G. Chen and L. J. Ming, *J. Am. Chem. Soc.*, **120**, 6369 (1998).
101. D. W. Christianson and R. S. Alexander, *J. Am. Chem. Soc.*, **111**, 6412 (1989).
102. G. Schürer, H. Lanig and T. Clark, *Biochemistry*, **43**, 5414 (2004).
103. N. Sträter and W. N. Lipscomb, *Biochemistry*, **34**, 9200 (1995).
104. N. Sträter and W. N. Lipscomb, *Biochemistry*, **34**, 14792 (1995).
105. S. K. Burley, P. R. David, R. M. Sweet, A. Taylor and W. N. Lipscomb, *J. Mol. Biol.*, **224**, 113 (1992).
106. H. Kim, S. K. Burley and W. N. Lipscomb, *J. Mol. Biol.*, **230**, 722 (1993).
107. H. Kim and W. N. Lipscomb, *Proc. Natl. Acad. Sci. U.S.A.*, **90**, 5006 (1993).
108. H. Kim and W. N. Lipscomb, *Biochemistry*, **32**, 8465 (1993).
109. H. Kim and W. N. Lipscomb, *Adv. Enzymol. Relat. Areas Mol. Biol.*, **68**, 153 (1994).
110. G. Schürer, A. H. C. Horn, P. Gedeck and T. Clark, *J. Phys. Chem. B*, **106**, 8815 (2002).
111. S. Erhardt and J. Weston, *Chembiochem*, **3**, 101 (2002).
112. S. Erhardt, E. Jaime and J. Weston, *J. Am. Chem. Soc.*, **127**, 3654 (2005).
113. D. W. Christianson and W. N. Lipscomb, *Acc. Chem. Res.*, **22**, 62 (1989).
114. I. Garcia-Saez, D. Reverter, J. Vendrell, F. X. Aviles and M. Coll, *EMBO J.*, **16**, 6906 (1997).
115. I. Massova, P. Martin, S. deMel, Y. Tanaka, B. Edwards and S. Mobashery, *J. Am. Chem. Soc.*, **118**, 12479 (1996).

116. J. T. Bukrinsky, M. J. Bjerrum and A. Kadziola, *Biochemistry*, **37**, 16555 (1998).
117. F. Jensen, T. Bukrinsky, J. Bjerrum and S. Larsen, *J. Biol. Inorg. Chem.*, **7**, 490 (2002).
118. D. M. van Aalten, C. R. Chong and L. Joshua-Tor, *Biochemistry*, **39**, 10082 (2000).
119. J. H. Cho, D. H. Kim, S. J. Chung, N.-C. Ha, B.-H. Oh and K. Y. Choi, *Bioorg. Med. Chem.*, **10**, 2015 (2002).
120. J. D. Park, D. H. Kim, S. J. Kim, J. R. Woo and S. E. Ryu, *J. Med. Chem.*, **45**, 5295 (2002).
121. A. Kilshtain-Vardi, M. Glick, H. M. Greenblatt, A. Goldblum and G. Shoham, *Acta Crystallogr., Sect. D*, **59**, 323 (2003).
122. H. M. Greenblatt, H. Feinberg, P. A. Tucker and G. Shoham, *Acta Crystallogr., Sect. D*, **54**, 289 (1998).
123. K. J. Lee and D. H. Kim, *Bioorg. Med. Chem.*, **6**, 1613 (1998).
124. A. Vardi-Kilshtain, G. Shoham and A. Goldblum, *Mol. Phys.*, **101**, 2715 (2003).
125. A. Alex and T. Clark, *J. Comput. Chem.*, **13**, 704 (1992).
126. A. Kilshtain-Vardi, G. Shoham and A. Goldblum, *Int. J. Quantum Chem.*, **88**, 87 (2002).
127. S. Álvarez-Santos, Á. González-Lafont, J. M. Lluch, B. Oliva and F. X. Avilés, *New J. Chem.*, 319 (1998).
128. R. Breslow and D. L. Wernick, *Proc. Natl. Acad. Sci. U.S.A.*, **74**, 1303 (1977).
129. J. B. Cross, T. Vreven, S. O. Meroueh, S. Mobashery and H. B. Schlegel, *J. Phys. Chem. B*, **109**, 4761 (2005).
130. W. L. Mock and H. Cheng, *Biochemistry*, **39**, 13945 (2000).
131. J. F. Gaucher, M. Selkti, T. Prange and A. Tomas, *Acta Crystallogr., Sect. D*, **58**, 2198 (2002).
132. M. Senda, T. Senda, T. Ogi and S. Kidokoro, *Acta Crystallogr., Sect. A*, **58**, C278 (2002).
133. A. C. Hausrath and B. W. Matthews, *Acta Crystallogr., Sect. D*, **58**, 1002 (2002).
134. M. Selkti, A. Tomas, J. F. Gaucher, T. Prange, M. C. Fournie-Zaluski, H. Chen and B. P. Roques, *Acta Crystallogr., Sect. D*, **59**, 1200 (2003).
135. J. F. Gaucher, M. Selkti, G. Tiraboschi, T. Prange, B. P. Roques, A. Tomas and M. C. Fournie-Zaluski, *Biochemistry*, **38**, 12569 (1999).
136. D. R. Holland, P. L. Barclay, J. C. Danilewicz, B. W. Matthews and K. James, *Biochemistry*, **33**, 51 (1994).
137. A. C. English, S. H. Done, L. S. D. Caves, C. R. Groom and C. D. Hubbard, *Proteins: Struct., Funct., Genet.*, **37**, 628 (1999).
138. D. H. Juers, J. Kim, B. W. Matthews and S. M. Sieburth, *Biochemistry*, **44**, 16524 (2005).
139. D. W. Christianson and W. N. Lipscomb, *J. Am. Chem. Soc.*, **110**, 5560 (1988).
140. S. Antonczak, G. Monard, M. F. Ruiz-Lopez and J.-L. Rivail, *J. Am. Chem. Soc.*, **120**, 8825 (1998).
141. S. Antonczak, G. Monard, M. Ruiz-López and J.-L. Rivail, *J. Mol. Model.*, **6**, 527 (2000).
142. M. C. Izquierdo and R. L. Stein, *J. Am. Chem. Soc.*, **112**, 6054 (1990).
143. M. Izquierdo-Martin and R. L. Stein, *J. Am. Chem. Soc.*, **114**, 325 (1992).
144. B. W. Matthews, *Acc. Chem. Res.*, **21**, 333 (1988).
145. M. Mejri, E. Pauthe, V. Larreta-Garde and M. Mathlouthi, *Enzyme Microb. Technol.*, **23**, 392 (1998).
146. K. M. Merz, Jr and P. A. Kollman, *J. Am. Chem. Soc.*, **111**, 5649 (1989).
147. M. K. Pangburn and K. A. Walsh, *Biochemistry*, **14**, 4050 (1975).
148. V. Pelmenschikov, M. R. Blomberg and P. E. Siegbahn, *J. Biol. Inorg. Chem.*, **7**, 284 (2002).
149. T. Takeuchi, A. Böttcher, C. M. Quezada, T. J. Meade and H. B. Gray, *Bioorg. Med. Chem.*, **7**, 815 (1999).
150. Z. R. Wasserman and C. N. Hodge, *Proteins: Struct., Funct., Genet.*, **24**, 227 (1996).
151. N. O. Concha, B. A. Rasmussen, K. Bush and O. Herzberg, *Structure*, **4**, 823 (1996).
152. N. O. Concha, B. A. Rasmussen, K. Bush and O. Herzberg, *Protein Sci.*, **6**, 2671 (1997).
153. P. M. Fitzgerald, J. K. Wu and J. H. Toney, *Biochemistry*, **37**, 6791 (1998).
154. J. H. Toney, P. M. Fitzgerald, N. Grover-Sharma, S. H. Olson, W. J. May, J. G. Sundelof, D. E. Vanderwall, K. A. Cleary, S. K. Grant, J. K. Wu, J. W. Kozarich, D. L. Pompliano and G. G. Hammond, *Chem. Biol.*, **5**, 185 (1998).
155. A. Carfi, S. Pares, E. Duee, M. Galleni, C. Duez, J. M. Frère and O. Dideberg, *EMBO J.*, **14**, 4914 (1995).
156. A. Carfi, E. Duee, R. Paul-Soto, M. Galleni, J. M. Frère and O. Dideberg, *Acta Crystallogr., Sect. D*, **54**, 45 (1998).

157. N. O. Concha, C. A. Janson, P. Rowling, S. Pearson, C. A. Cheever, B. P. Clarke, C. Lewis, M. Galleni, J. M. Frere, D. J. Payne, J. H. Bateson and S. S. Abdel-Meguid, *Biochemistry*, **39**, 4288 (2000).
158. D. J. Payne, J. A. Hueso-Rodriguez, H. Boyd, N. O. Concha, C. A. Janson, M. Gilpin, J. H. Bateson, C. Chever, N. L. Niconovich, S. Pearson, S. Rittenhouse, D. Tew, E. Diez, P. Perez, J. de la Fuente, M. Rees and A. Rivera-Sagredo, *Antimicrob. Agents Chemother.*, **46**, 1880 (2002).
159. I. Garcia-Saez, J. Hopkins, C. Papamicael, N. Franceschini, G. Amicosante, G. M. Rossolini, M. Galleni, J. M. Frere and O. Dideberg, *J. Biol. Chem.*, **278**, 23868 (2003).
160. J. H. Ullah, T. R. Walsh, I. A. Taylor, D. C. Emery, C. S. Verma, S. J. Gamblin and J. Spencer, *J. Mol. Biol.*, **284**, 125 (1998).
161. H. Kurosaki, Y. Yamaguchi, T. Higashi, K. Soga, S. Matsueda, H. Yumoto, S. Misumi, Y. Yamagata, Y. Arakawa and M. Goto, *Angew. Chem., Int. Ed.*, **44**, 3861 (2005).
162. J. Spencer, J. Read, R. B. Sessions, S. Howell, G. M. Blackburn and S. J. Gamblin, *J. Am. Chem. Soc.*, **127**, 14439 (2005).
163. R. Bicknell and S. G. Waley, *Biochemistry*, **24**, 6876 (1985).
164. E. G. Orellano, J. E. Girardini, J. A. Cricco, E. A. Ceccarelli and A. J. Vila, *Biochemistry*, **37**, 10173 (1998).
165. R. Paul-Soto, M. Zeppezauer, H. W. Adolph, M. Galleni, J. M. Frère, A. Carfi, O. Dideberg, J. Wouters, L. Hemmingsen and R. Bauer, *Biochemistry*, **38**, 16500 (1999).
166. S. M. Fabiane, M. K. Sohi, T. Wan, D. J. Payne, J. H. Bateson, T. Mitchell and B. J. Sutton, *Biochemistry*, **37**, 12404 (1998).
167. M. I. Page, *Chem. Commun.*, 1609 (1998).
168. Z. Wang, W. Fast and S. J. Benkovic, *Biochemistry*, **38**, 10013 (1999).
169. D. Suárez and K. M. Merz, Jr, *J. Am. Chem. Soc.*, **123**, 3759 (2001).
170. N. Díaz, D. Suárez and K. M. Merz, Jr, *J. Am. Chem. Soc.*, **123**, 9867 (2001).
171. D. Suárez, N. Díaz and K. M. Merz, Jr, *J. Comput. Chem.*, **23**, 1587 (2002).
172. N. V. Kaminskaia, C. He and S. J. Lippard, *Inorg. Chem.*, **39**, 3365 (2000).
173. N. V. Kaminskaia, B. Spingler and S. J. Lippard, *J. Am. Chem. Soc.*, **122**, 6411 (2000).
174. N. V. Kaminskaia, B. Spingler and S. J. Lippard, *J. Am. Chem. Soc.*, **123**, 6555 (2001).
175. P. J. Montoya-Pelaez and R. S. Brown, *Inorg. Chem.*, **41**, 309 (2002).
176. J. Antony, N. Gresh, L. Olsen, L. Hemmingsen, C. J. Schofield and R. Bauer, *J. Comput. Chem.*, **23**, 1281 (2002).
177. H. Boerzel, M. Koeckert, W. Bu, B. Spingler and S. J. Lippard, *Inorg. Chem.*, **42**, 1604 (2003).
178. S. Bounaga, A. P. Laws, M. Galleni and M. I. Page, *Biochem. J.*, **331**, 703 (1998).
179. J. Y. Cha, A. Ishiwata and S. Mobashery, *J. Biol. Chem.*, **279**, 14917 (2004).
180. G. L. Estiú, R. M. Rasia, J. A. Cricco, A. J. Vila and M. C. Zerner, *Int. J. Quantum Chem.*, **88**, 118 (2002).
181. J. J. A. Huntley, S. D. B. Scrofani, M. J. Osborne, P. E. Wright and H. J. Dyson, *Biochemistry*, **39**, 13356 (2000).
182. M. Krauss, N. Gresh and J. Antony, *J. Phys. Chem. B*, **107**, 1215 (2003).
183. H. Park, E. N. Brothers and K. M. Merz, Jr, *J. Am. Chem. Soc.*, **127**, 4232 (2005).
184. R. M. Rasia and A. J. Vila, *Biochemistry*, **41**, 1853 (2002).
185. C. De Seny, C. Prosperi-Meys, C. Bebrone, M. I. Rossolini, G. M. Page, P. Noel, J. M. Frère and M. Galleni, *Biochem. J.*, **363**, 687 (2002).
186. J. H. Toney, G. G. Hammond, P. M. D. Fitzgerald, N. Sharma, J. M. Balkovec, G. P. Rouen, S. H. Olson, M. L. Hammond, M. L. Greenlee and Y.-D. Gao, *J. Biol. Chem.*, **276**, 31913 (2001).
187. J. H. Toney, J. K. Wu, K. M. Overbye, C. M. Thompson and D. L. Pompliano, *Protein Expression Purif.*, **9**, 355 (1997).
188. Z. Wang, W. Fast, A. M. Valentine and S. J. Benkovic, *Curr. Opin. Chem. Biol.*, **3**, 614 (1999).
189. L. Ma and E. R. Kantrowitz, *Biochemistry*, **35**, 2394 (1996).
190. L. Ma, T. T. Tibbitts and E. R. Kantrowitz, *Protein Sci.*, **4**, 1498 (1995).
191. J. E. Murphy, T. T. Tibbitts and E. R. Kantrowitz, *J. Mol. Biol.*, **253**, 604 (1995).
192. J. E. Murphy, B. Stec, L. Ma and E. R. Kantrowitz, *Nat. Struct. Biol.*, **4**, 618 (1997).
193. K. M. Holtz, B. Stec and E. R. Kantrowitz, *J. Biol. Chem.*, **274**, 8351 (1999).

194. B. Stec, M. J. Hehir, C. Brennan, M. Nolte and E. R. Kantrowitz, *J. Mol. Biol.*, **277**, 647 (1998).
195. B. Stec, K. M. Holtz and E. R. Kantrowitz, *J. Mol. Biol.*, **299**, 1303 (2000).
196. M. H. Le Du, T. Stigbrand, M. J. Taussigi, A. Ménez and E. A. Stura, *J. Biol. Chem.*, **276**, 9158 (2001).
197. M. H. Le Du, C. Lamoure, B. H. Muller, O. V. Bulgakov, E. Lajeunesse, A. Ménez and J. C. Boulain, *J. Mol. Biol.*, **316**, 941 (2002).
198. M. M. E. de Backer, S. McSweeney, P. F. Lindley and E. Hough, *Acta Crystallogr., Sect. D*, **60**, 1555 (2004).
199. T. T. Tibbitts, J. E. Murphy and E. R. Kantrowitz, *J. Mol. Biol.*, **257**, 700 (1996).
200. J. Wang, K. A. Stieglitz and E. R. Kantrowitz, *Biochemistry*, **44**, 8378 (2005).
201. P. Llinas, E. A. Stura, A. Ménez, Z. Kiss, T. Stigbrand, J. L. Millan and M. H. Le Du, *J. Mol. Biol.*, **350**, 441 (2005).
202. C. L. Wojciechowski and E. R. Kantrowitz, *Biochim. Biophys. Acta*, **1649**, 68 (2003).
203. J. E. Coleman, *Annu. Rev. Biophys. Biomol. Struct.*, **21**, 441 (1992).
204. H.-C. Hung and G.-G. Chang, *Protein Sci.*, **10**, 34 (2001).
205. M. J. Jedrzejas and P. Setlow, *Chem. Rev.*, **101**, 607 (2001).
206. E. E. Kim and H. W. Wyckoff, *J. Mol. Biol.*, **218**, 449 (1990).
207. T. Klabunde, N. Sträter, R. Fröhlich, H. Witzel and B. Krebs, *J. Mol. Biol.*, **259**, 737 (1996).
208. T. Koike and E. Kimura, *J. Am. Chem. Soc.*, **113**, 8935 (1991).
209. N. Sträter, B. Jasper, M. Scholte, B. Krebs, A. P. Duff, D. B. Langley, R. Han, B. A. Averill, H. C. Freeman and J. M. Guss, *J. Mol. Biol.*, **351**, 233 (2005).
210. C. L. Wojciechowski and E. R. Kantrowitz, *J. Biol. Chem.*, **277**, 50476 (2002).
211. N. M. Antikainen, A. F. Monzingo, C. L. Franklin, J. D. Robertus and S. F. Martin, *Arch. Biochem. Biophys.*, **417**, 81 (2003).
212. E. Hough, L. K. Hansen, B. Birknes, K. Jynge, S. Hansen, A. Hordvik, C. Little, E. Dodson and Z. Derewenda, *Nature*, **338**, 357 (1989).
213. S. Hansen and E. Hough, *J. Mol. Biol.*, **234**, 179 (1993).
214. D. da Graça Thrige, J. R. B. Buur and F. S. Jørgensen, *Biopolymers*, **42**, 319 (1997).
215. S. F. Martin and P. J. Hergenrother, *Biochemistry*, **38**, 4403 (1999).
216. N. U. Meldrum and F. J. W. Roughton, *Nature (London)*, **131**, 874 (1933).
217. N. U. Meldrum and F. J. W. Roughton, *J. Physiol.*, **80**, 113 (1933).
218. D. Keilin and T. Mann, *Biochem. J.*, **34**, 1163 (1940).
219. P. A. Boriack, D. W. Christianson, J. Kingery-Wood and G. M. Whitesides, *J. Med. Chem.*, **38**, 2286 (1995).
220. S. K. Nair, D. Elbaum and D. W. Christianson, *J. Biol. Chem.*, **271**, 1003 (1996).
221. C. A. Lesburg, C. Huang, D. W. Christianson and C. A. Fierke, *Biochemistry*, **36**, 15780 (1997).
222. L. R. Scolnick, A. M. Clements, J. Liao, L. Crenshaw, M. Hellberg, J. May, T. R. Dean and D. W. Christianson, *J. Am. Chem. Soc.*, **119**, 850 (1997).
223. F. Briganti, S. Mangani, P. Orioli, A. Scozzafava, G. Vernaglione and C. T. Supuran, *Biochemistry*, **36**, 10384 (1997).
224. P. A. Boriack-Sjodin, S. Zeitlin, H. H. Chen, L. Crenshaw, S. Gross, A. Dantanarayana, P. Delgado, J. A. May, T. Dean and D. W. Christianson, *Protein Sci.*, **7**, 2483 (1998).
225. R. Recacha, M. J. Costanzo, B. E. Maryanoff and D. Chattopadhyay, *Biochem. J.*, **361**, 437 (2002).
226. D. Duda, C. Tu, M. Qian, P. Laipis, M. Agbandje-McKenna, D. N. Silverman and R. McKenna, *Biochemistry*, **40**, 1741 (2001).
227. C.-Y. Kim, J. S. Chang, J. B. Doyon, T. T. Baird, Jr, C. A. Fierke, A. Jain and D. W. Christianson, *J. Am. Chem. Soc.*, **122**, 12125 (2000).
228. C. Y. Kim, P. P. Chandra, A. Jain and D. W. Christianson, *J. Am. Chem. Soc.*, **123**, 9620 (2001).
229. J. D. Cox, J. A. Hunt, K. M. Compher, C. A. Fierke and D. W. Christianson, *Biochemistry*, **39**, 13687 (2000).
230. C. Y. Kim, D. A. Whittington, J. S. Chang, J. Liao, J. A. May and D. W. Christianson, *J. Med. Chem.*, **45**, 888 (2002).
231. D. M. Duda, L. Govindasamy, M. Agbandje-McKenna, C. K. Tu, D. N. Silverman and R. McKenna, *Acta Crystallogr., Sect. D*, **59**, 93 (2003).

232. R. Saito, T. Sato, A. Ikai and N. Tanaka, *Acta Crystallogr., Sect. D*, **60**, 792 (2004).
233. Z. Fisher, J. A. Hernandez Prada, C. K. Tu, D. Duda, C. Yoshioka, H. An, L. Govindasamy, D. N. Silverman and R. McKenna, *Biochemistry*, **44**, 1097 (2005).
234. M. D. Lloyd, R. L. Pederick, R. Natesh, L. W. L. Woo, A. Purohit, M. J. Reed, K. R. Acharya and B. V. L. Potter, *Biochem. J.*, **385**, 715 (2005).
235. D. Bhatt, C. Tu, S. Z. Fisher, J. A. Hernandez Prada, R. McKenna and D. N. Silverman, *Proteins*, **61**, 239 (2005).
236. D. M. Duda, C. Tu, S. Z. Fisher, H. An, C. Yoshioka, L. Govindasamy, P. J. Laipis, M. Agbandje-McKenna, D. N. Silverman and R. McKenna, *Biochemistry*, **44**, 10046 (2005).
237. V. Menchise, G. De Simone, V. Alterio, A. Di Fiore, C. Pedone, A. Scozzafava and C. T. Supuran, *J. Med. Chem.*, **48**, 5721 (2005).
238. M. Budayova-Spano, S. Z. Fisher, M. T. Dauvergne, M. Agbandje-McKenna, D. N. Silverman, D. A. A. Myles and R. M. McKenna, *Acta Crystallogr., Sect. F*, **62**, 6 (2006).
239. D. Lu and G. A. Voth, *J. Am. Chem. Soc.*, **120**, 4006 (1998).
240. J.-Y. Liang and W. N. Lipscomb, *Biochemistry*, **27**, 8676 (1988).
241. S. Lindskog, in *Zinc Enzymes* (Ed. T. G. Spiro), Wiley, New York, 1983, pp. 78–121.
242. X. Zhang, C. D. Hubbard and R. van Eldik, *J. Phys. Chem.*, **100**, 9161 (1996).
243. D. A. Palmer and R. van Eldik, *Chem. Rev.*, **83**, 651 (1983).
244. A. N. Acharya, A. Das and A. C. Dash, *Adv. Inorg. Chem.*, **55**, 128 (2004).
245. Z.-W. Mao, G. Liehr and R. van Eldik, *J. Am. Chem. Soc.*, **122**, 4839 (2000).
246. A. Peter and H. Vahrenkamp, *Z. Anorg. Allg. Chem.*, **631**, 2347 (2005).
247. F. Gross and H. Vahrenkamp, *Inorg. Chem.*, **44**, 3321 (2005).
248. X. Zhang, R. van Eldik, T. Koike and E. Kimura, *Inorg. Chem.*, **32**, 5749 (1993).
249. X. Zhang and R. van Eldik, *Inorg. Chem.*, **34**, 5606 (1995).
250. Y.-J. Sun, L. Z. Zang, P. Cheng, H.-K. Lin, S.-P. Yan, W. Sun, D.-Z. Liao, Z.-H. Jiang and P.-W. Shen, *Inorg. Chem.*, **42**, 508 (2003).
251. R. van Eldik, *Inorg. Chem.*, **43**, 2756 (2004).
252. A. Sawaryn and W. A. Sokalski, *Int. J. Quantum Chem.*, **16**, 293 (1979).
253. A. Pullman and D. Demoulin, *Int. J. Quantum Chem.*, **16**, 641 (1979).
254. J. Lipinski and A. Sawaryn, *Studia Biophys.*, **84**, 89 (1981).
255. C. M. Cook, K. Haydock, R. H. Lee and L. C. Allen, *J. Phys. Chem.*, **88**, 4875 (1984).
256. K. M. Merz, Jr, R. Hoffmann and M. G. S. Dewar, *J. Am. Chem. Soc.*, **111**, 5636 (1989).
257. M. Hartmann, T. Clark and R. van Eldik, *J. Mol. Model.*, **2**, 358 (1996).
258. M. Krauss and D. R. Garmer, *J. Am. Chem. Soc.*, **113**, 6426 (1991).
259. M. Solà, A. Lledós, M. Duran and J. Bertán, *J. Am. Chem. Soc.*, **114**, 869 (1992).
260. J. Åqvist and A. Warshel, *J. Mol. Biol.*, **224**, 7 (1992).
261. J. Åqvist, M. Fothergill and A. Warshel, *J. Am. Chem. Soc.*, **115**, 631 (1993).
262. M. C. Menziani and P. G. De Benedetti, *Struct. Chem.*, **3**, 215 (1992).
263. Y. J. Zheng and K. M. Merz, Jr, *J. Am. Chem. Soc.*, **114**, 10498 (1992).
264. A. Warshel and J. K. Hwang, *Faraday Discuss.*, **93** (*Structure and Activity of Enzymes*), 225 (1992).
265. D. N. Chin and G. M. Whiteside, *J. Am. Chem. Soc.*, **117**, 6153 (1995).
266. A. N. Isaev, *J. Mol. Struct. (THEOCHEM)*, **582**, 195 (2002).
267. A. Bottoni, C. Z. Lanza, G. P. Miscione and D. Spinelli, *J. Am. Chem. Soc.*, **126**, 1542 (2004).
268. H. Chen, S. Li and Y. Jiang, *J. Phys. Chem. A*, **107**, 4652 (2003).
269. M. Hartmann, K. M. Merz, Jr, R. van Eldik and T. Clark, *J. Mol. Model.*, **4**, 355 (1998).
270. M. Solà, J. Mestres, M. Duran and R. Carbó, *J. Chem. Inf. Comput. Sci.*, **34**, 1047 (1994).
271. S. Sinnecker, M. Bräuer, W. Koch and E. Anders, *Inorg. Chem.*, **40**, 1006 (2001).
272. S. Schenk, J. Kesselmeier and E. Anders, *Chem. Eur. J.*, **10**, 3091 (2004).

CHAPTER **2**

Structural organozinc chemistry

JOHANN T. B. H. JASTRZEBSKI, JAAP BOERSMA
and GERARD VAN KOTEN

Debye Institute, Organic Chemistry and Catalysis, Utrecht University, Padualaan 8, 3584 CH Utrecht, The Netherlands
Fax: +31 30 252 3615; e-mail: g.vankoten@chem.uu.nl

The chemistry of organozinc compounds
Edited by Z. Rappoport and I. Marek

I. INTRODUCTION

Organozinc compounds are the first organometallic compounds ever made. Already in 1852, Edward Frankland prepared diethylzinc by heating ethyl iodide with zinc metal in a Carius tube[1]. Diethylzinc appeared to be a volatile colourless liquid that inflames spontaneously upon exposure to air. Until the invention of the Grignard reagents around 1900 organozinc compounds were used extensively as alkylating agents in organic synthesis.

Until fairly recently, little was known of the structures and properties of the organozinc compounds occurring as intermediates in various reactions. Interestingly, the complex-forming ability of organozinc compounds had already been recognized very early. In 1858, Wanklyn reported the formation of the ionic sodium triethylzinc complex[2]. One year later, Frankland observed that the formation of dimethylzinc from methyl iodide and zinc was accelerated by the addition of dimethyl ether or diethyl ether. It appeared that separation of the dimethylzinc from the ether was impossible, but it lasted until 1962 when it was established that dimethylzinc and dimethyl ether form a 1:1 complex in solution, which is appreciably dissociated in the vapour phase[3].

Most of the structures of organozinc compounds have been determined by X-ray crystallography, but, in view of the fact that many of these compounds are liquids, also Gas-phase Electron Diffraction of some volatile organozinc compounds as well as solution studies have been used. The latter category involves molecular weight measurements, microwave titrations, dipole moment determinations and complexation reactions. ^{57}Zn NMR spectroscopy has not played an important role since only one naturally occurring isotope of zinc possesses a nuclear magnetic moment, i.e. ^{67}Zn with a natural abundance of 4.11% and a nuclear spin of 5/2. Because of its low receptivity and its quadrupole moment, ^{67}Zn has received very little attention[4] and in only a few cases have resonances of zinc ions in aqueous solutions been observed.

In the February 2005 version of the CSD database[5], 349 structures containing one or more direct zinc–carbon interactions have been found (excluding structures containing the Zn–CN structural motif). Together with the gas-phase data, this means that at that date a total of 354 molecular structures had been determined. Of these structures a large majority (225) deals with compounds in which 4-coordinate zinc is present.

With its electron configuration $3d^{10}4s^2$, its normal valency is 2^+ and the symmetrical, full, low-lying 3d shell of the Zn^{2+} ion does not cause ligand–field effects in coordination complexes. Its coordination behaviour is therefore relatively simple in that it basically forms trigonal planar or tetrahedral complexes with electron-donating ligands. Some examples of organozinc compounds containing formally Zn^+ (organozinc cations) and Zn^- (organozincates) are known.

In a typical organozinc compound of the type R_2Zn, the zinc–carbon bonds occupy two equivalent sp-hybridized molecular orbitals, resulting in a linear coordination. The dipole moment of symmetric diorganozinc compounds in non-polar solvents is therefore zero, as indeed was observed for Me_2Zn in cyclohexane solution[6]. In this situation, the valency shell of the zinc atom has only two pairs of bonding electrons, but four empty low-energy orbitals available for bonding. As a consequence, two further coordinate bonds with ligands containing non-bonding electrons may form. Zinc is fairly electropositive with a Pauling electronegativity of 1.6 and diorganozinc compounds therefore contain covalent but rather polar zinc–carbon bonds. This bond polarity is responsible for the ease with which such compounds form coordination complexes. In the absence of electron donors, diorganozinc compounds containing saturated alkyl or aryl groups, with a few exceptions, occur as monomers. Apparently, the zinc in these compounds is unable to attain coordination saturation through the formation of aggregates via alkyl or aryl bridges by electron-deficient multi-centre bonds, which is the common structural motif in,

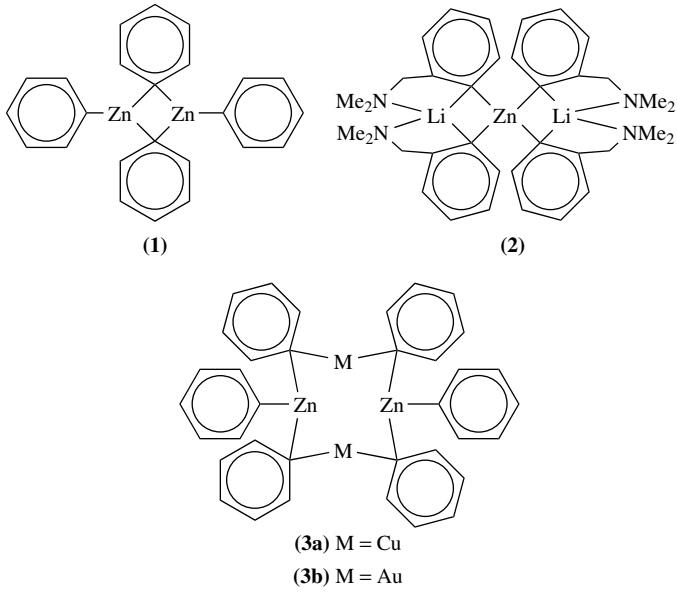

FIGURE 1. Some examples of observed (**1** and **2**) and proposed (**3**) structures of organozinc compounds containing a bridging aryl group

e.g., structural organocopper[7] and organolithium[8] chemistry. The relatively small electron deficiency of zinc together with the relative large size of the zinc atom are thought to be responsible for this lack of additional coordination. In a few cases structures having bridging alkyl or aryl groups between two zinc atoms, e.g. **1**[9], or zinc and a metal like lithium, e.g. **2**[10], copper **3a** or gold, e.g. **3b**[11], or aluminium have been observed, or have been proposed in a few cases (Figure 1). Moreover, the exchange of alkyl groups between various alkyl metal compounds and alkyl zinc compounds in solution has been attributed to the formation of transient species in which bridging alkyl groups are present[12–14].

If one of the organic groups in a diorganozinc compound is replaced by an electronegative monoanionic grouping like a halogen atom or an alkoxy-, aryloxy- or organoamido group, but also by an alkynyl group, both the acceptor character of the zinc and the donor character of the zinc-bound electronegative group are enhanced. As a consequence, such compounds always form aggregates via multi-centre bonding of the electronegative substituent with various zinc centres.

The self-association and/or complex formation of organozinc compounds involves considerable rehybridization of the zinc valence orbitals. When only one coordinate bond is formed, the zinc atom becomes sp^2-hybridized and the resulting complex is planar or nearly so with bond angles around the zinc of about 120°. The zinc centre then still has one unoccupied valence orbital and remains coordinatively unsaturated. Three-coordinate zinc, however, is relatively rare and only occurs when steric crowding around the zinc prevents the approach of a fourth ligand.

In general, both vacant valence orbitals of the zinc centre are used and consequently the bonding situation of zinc becomes close to sp^3-hybridization reflected by a tetrahedral coordination geometry of the zinc centre.

As the 3d shell of zinc is completely filled it cannot function as a dative bond acceptor (Lewis acid). Also, the high ionization potential of the 3d electrons makes it very unlikely that they can be used in dative π-bonding (Lewis base) with electron-accepting ligands. However, the latter possibility cannot be excluded completely in some complexes of diorganozinc compounds with planar *N*-heterocyclic ligands. Although coordination numbers five and six are well-known for both monoorganozinc and inorganic zinc compounds, in diorganozinc compounds this five- or six-coordination is seen only in a few special instances.

From a structural point of view, three classes of organozinc compounds can be distinguished according to the number of carbon atoms directly bound to zinc. These classes are: (i) ionic organozinc compounds in which the number of directly zinc-bound carbon atoms (three or four) exceeds the valence number of zinc, the so-called organozincates; (ii) the diorganozinc compounds and their coordination complexes, which can be divided into subclasses depending on various types of coordinating ligands; and (iii) heteroleptic RZnX compounds in which X is an electronegative substituent like a halogen atom or a monoanionic group bound to zinc via an electronegative atom like oxygen or nitrogen. Depending on the nature of X, also the latter class of compounds may be further divided into subclasses. In the following sub-sections the structural aspects of these classes of compounds will be discussed.

II. ORGANOZINCATES

A. Introduction

Organometallic compounds that exhibit Lewis acidity on the metal centre are susceptible towards nucleophilic attack by alkali metal compounds, thus forming the so-called 'ate compounds' in which the Lewis acidic metal is often coordinatively saturated. Already in 1858 Wanklyn reported the formation of a crystalline compound formulated as $[Et_3Zn]Na$ which he obtained from the reaction of diethylzinc with metallic sodium (equation 1)[2, 15, 16].

$$3\ Et_2Zn + 2\ Na \longrightarrow Zn + 2[Et_3Zn]Na \qquad (1)$$

Compounds of the types $[R_4Zn]M_2$ and $[R_3Zn]M$ can be prepared from the reaction of a strongly electropositive metal with the diorganozinc compound or directly from the reaction of the parent compounds R_2Zn with RM[10–22]. In the first type of compounds the anionic zincate fragment has a formal negative charge of minus two and in the second type of compounds of minus one. In particular, conductivity measurements[23, 24] provided information on the products formed by dissolution of alkali metal alkyls in zinc alkyls.

In the early days the organozincates and organozinc compounds were regarded as academic curiosities whose structural characterization was particularly hampered by their extreme sensitivity towards oxygen and moisture. This phenomenon had already been recognized by Frankland and has plagued chemists ever since[25].

When it was recognized that 'ate' compounds often have enhanced reactivity and selectivity profiles compared to their parent organometallic compounds[26, 27], systematic studies of synthetic applications and structural features of organozincates started. Nowadays, organozincates and other organozinc reagents are valuable synthetic tools in organic chemistry which have had comparable impact in organic synthesis as the corresponding organocopper and -cuprate reagents[28]. Recent developments in the synthetic and structural chemistry of zincates have been nicely reviewed[29, 30].

Some examples of the synthetic usefulness of zincate reagents in organic synthesis are: stereoselective alkylation reactions of cyclic ketones[31], conjugate-addition reactions

to α,β-unsaturated carbonyl compounds[32], ring-opening reactions of epoxides[33] and the oxovanadium-induced ligand coupling of aryltrimethylzincates (equation 2)[34].

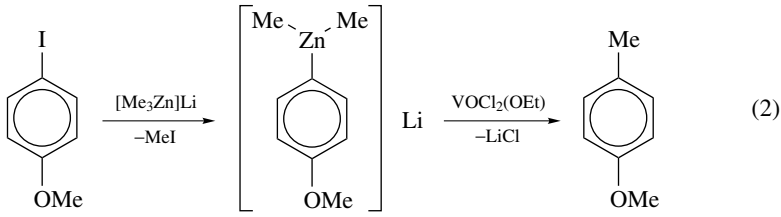

(2)

Computational studies have extensively contributed to the better understanding of the mechanistic aspects of reactions with organozincates[35–37].

In early days structural investigations on organozincates were limited to physicochemical measurements. For example, the calcium, strontium and barium tetraethylzincates were studied by ^{1}H NMR and UV spectroscopy and by cryoscopic molecular-weight determinations[38]. These solution studies provided limited information, contrary to the more recently combined NMR and Raman spectroscopic and EXAFS studies on 'highly coordinated' heteroleptic organozincates $[Me_3ZnR]Li_2$ (R = CN or SCN). These suggested the presence of a R–Zn bond and a Zn-centred dianion[35,39,40].

X-ray structural investigations on organozincates provided very detailed information about the structure of these species in the solid state. It has now been well-established that two types of organozincates exist, i.e. 'highly coordinated' zincates containing a $[R_4Zn]^{2-}$ dianionic fragment in which the zinc atom is tetrahedrally coordinated, and zincates containing a $[R_3Zn]^-$ monoanionic fragment in which the zinc atom has a trigonal coordination geometry. Depending on the particular zincate involved and or the presence of additional solvent donor molecules, the zincates may exist as real anionic and cationic fragments in the crystal lattice. Most probably they exist in (polar) solvents either as solvent separated ion pairs, or as contact ion pairs in which the anionic and cationic fragments are integral parts of a neutral aggregate.

B. Tetraorganozincates $[R_4Zn]M_2$

The zincates $[Me_4Zn]Li_2$ (**4**) and $[(HC{\equiv}C)_4Zn]K_2$ (**5**) are the first examples of which the structures in the solid state were unambiguously established by X-ray crystallographic techniques. Compound **4** was prepared by mixing Me_2Zn and MeLi in a one-to-two molar ratio in diethyl ether. After removal of the solvent **4** was obtained as a white pyrophoric microcrystalline powder. Its structure was determined from the X-ray powder data[41]. At first sight the structure seems to consist of $[Me_4Zn]^{2-}$ dianionic units located at the special position 0, 0, 0 and two lithium cations at 0, 0, 0.5 and 0, 0.5, 0.25 in space group $I\bar{4}$ (Figure 2). The four methyl groups of the Me_4Zn unit are arranged in an almost perfect tetrahedral arrangement [C–Zn–C bond angles 105(2) and 111(2)°]. The observed Zn–C bond distance of 2.07(15) Å is slightly elongated, compared to that in linear Me_2Zn (1.930(2) Å in the gas phase (from gas-phase electron diffraction studies)[42]. Each of the methyl groups also has interactions with the two lithium atoms, C–Li(1) 2.52 and C–Li(2) 2.84(4) Å, rendering each lithium atom pseudo-tetrahedrally surrounded by four carbon atoms. Such secondary interactions are not uncommon for lithium, and have also been observed in the solid state structures of unsolvated Me_4Li_4[43] and Et_4Li_4[44].

$[(HC{\equiv}C)_4Zn]K_2$ (**5**) was prepared from potassium acetylide and $Zn(NH_3)_2(SCN)_2$ in liquid ammonia. Its structure in the solid state was obtained from X-ray powder data[45].

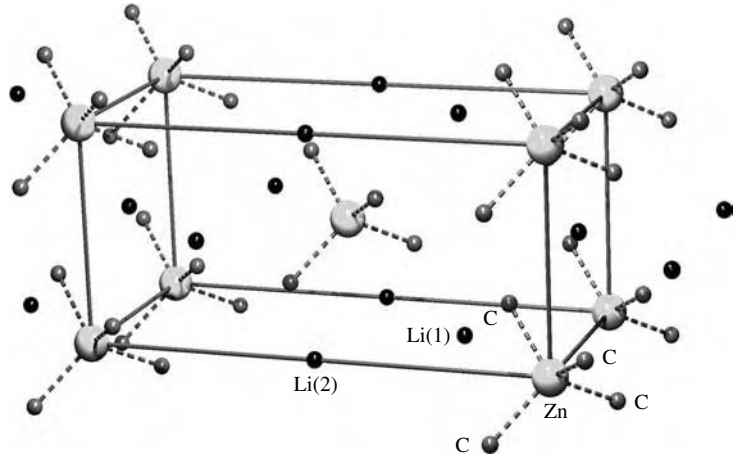

FIGURE 2. Unit cell contents of **4** in the space group $I\overline{4}$

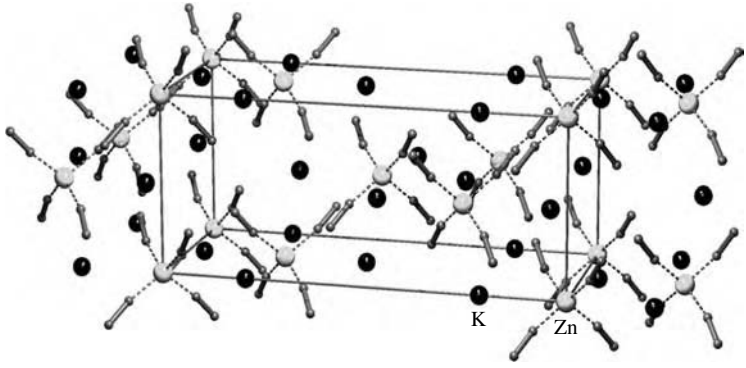

FIGURE 3. Unit cell contents of **5** in the space group $I4_1/a$

The zinc atoms are located at the special position 0, 0, 0 and the potassium atoms at 0, 0, z in the tetragonal space group $I4_1/a$ (Figure 3). The four acetylide groups are arranged in a tetrahedral fashion around the zinc atom, with a Zn−C bonding distance of 2.0(1) Å and bond angles of C−Zn−C of 105(5) and 112(5)°. The Zn−C(1)−C(2) bond angle of 175(5)° is close to the ideal value of 180°. The C(1)−C(2) bond length of 1.4 (2) Å of the acetylenic moiety is elongated compared to the C−C bond length in normal organic acetylene compounds. This elongation has been explained by back donation from zinc to the acetylene substituent via a $d_\pi - p_\pi$ interaction. The relatively close proximity of the potassium cations to three neighbouring acetylenic moieties (3.1 to 3.5 Å) points to an electrostatic interaction of these cations with the π-system of the acetylene.

Single crystals of the bis-ammonia adduct of **5**, $[(HC{\equiv}C)_4Zn]K_2(NH_3)_2$ (**6**), were obtained by crystallization from liquid ammonia at 195 K and special equipment was used to isolate the crystals at low temperature.[46] The solid state structure of **6** was determined by single-crystal X-ray crystallography (Figure 4)[47]. Its solid state structure, a

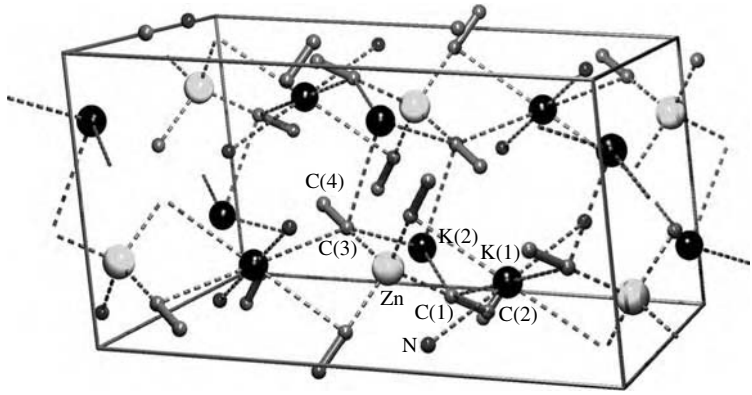

FIGURE 4. Unit cell contents of **6**; atoms outside the cell are omitted for clarity

coordination polymer, shows similarities with that of **5**. Also in this case, the zinc atom is tetrahedrally coordinated by four σ-bonded acetylene groups. The C−Zn−C bond angles are in the range of 105.8(1) to 116.9(2)°, indicating that the tetrahedral coordination geometry at zinc is more distorted than that observed in **5**, which is explained by the presence of ammonia molecules in the second coordination sphere of zinc. K(1) is octahedrally coordinated by four HC≡C units in a side-on bonding mode [bonding distances range from 2.997(3) to 3.276(3) Å], and two ammonia molecules in *trans*-position with bond distances K(1)−N of 2.952(4) Å. K(2) is octahedrally coordinated by six HC≡C units in a side-on bonding mode with similar bonding distances as observed for K(1).

The tetraorganozincate $[(PhC{\equiv}C)_4Zn]Li_2(TMEDA)_2$ (**7**) was prepared according to equation 3.

$$\{[(Me_3Si)_2]_2N\}_2Zn + 4PhC{\equiv}CLi \xrightarrow[TMEDA]{\text{toluene/THF}} \underset{(\mathbf{7})}{[(PhC{\equiv}C)_4Zn]Li_2(TMEDA)_2} + 2[(Me_3Si)_2]_2NLi \quad (3)$$

The structure of **7** in the solid state was determined from a single-crystal X-ray crystallographic study[48]. The overall structural geometry comprises a pseudo-tetrahedral $[(PhC{\equiv}C)_4Zn]^{2-}$ dianion with average Zn−C bond distances of 2.05 Å and two Li(TMEDA) cations each bonded via π-acetylide interactions to two acetylide groups (Figure 5). The pairwise symmetrical bonding of the acetylide groups with each of the Li(TMEDA) cations induces a considerable distortion from an ideal tetrahedral geometry at zinc. The C−Zn−C bond angles vary from 102.9(5) to 115.4(10)°. However, these interactions do not induce a major distortion in the linearity of the σ-bonding of the acetylenic groups to zinc (average Zn−C≡C bond angle 175°).

The synthesis and structural characterization of a series of spirocyclic organozincates containing two five- or six-membered metallacycles in which zinc is the central spiro atom, is shown in Scheme 1. Compound **8a** was prepared via an elegant one-pot synthesis, starting from 1,5-dichloropentane, $ZnCl_2$ and a lithium/sodium alloy (1% sodium) in diethyl ether as a solvent (equation 4 in Scheme 1).[49] Subsequent treatment of a solution of **8a** with TMEDA afforded the corresponding TMEDA complex **8b** of which the structure in the solid state was unambiguously established by an X-ray crystal structure determination.

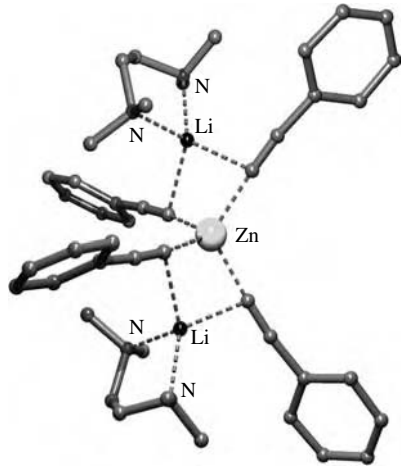

FIGURE 5. Molecular geometry of **7** in the solid state

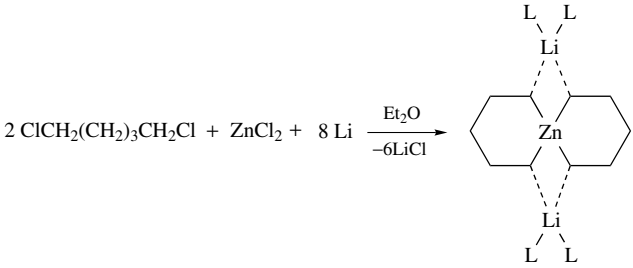

(4)

(8a) L = Et_2O
(8b) L_2 = TMEDA

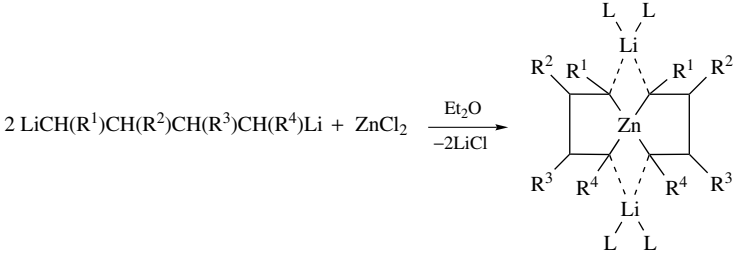

(5)

(9a) $R^1 = R^2 = R^3 = R^4 = H$; L = Et_2O
(9b) $R^1 = R^2 = R^3 = R^4 = H$; L_2 = TMEDA
(9c) R^1 = Me; $R^2 = R^3 = R^4 = H$; L_2 = TMEDA
(9d) $R^1 = R^4$ = Me; $R^2 = R^3 = H$; L_2 = TMEDA
(9e) R^2 = Me; $R^1 = R^3 = R^4 = H$; L_2 = TMEDA
(9f) $R^2 = R^3$ = Me; $R^1 = R^4 = H$; L_2 = TMEDA

SCHEME 1

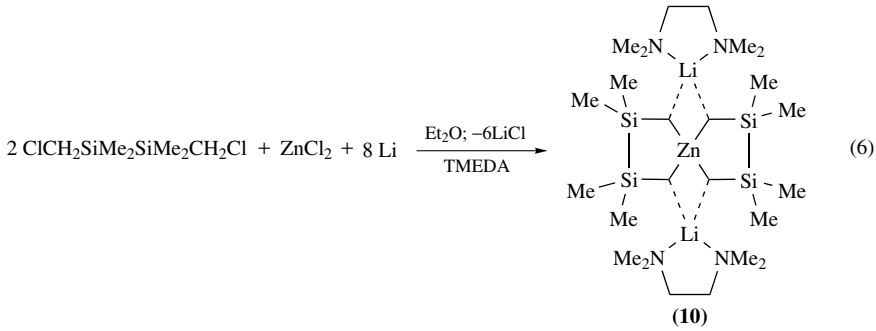

SCHEME 1. (*continued*)

These spirocyclic zincates, each containing two five-membered metallacycles having methyl substituents at the various positions of the five-membered ring, were prepared from the corresponding 1,4-dilithio compounds and $ZnCl_2$ in diethyl ether. Some examples are shown in equation 5 in Scheme 1[50]. Similar compounds with other donor molecules at lithium, like DME, Pr_2O and dioxane, were reported in the same paper. The structural features of the zincates in solution were studied by ^1H, ^{13}C and DEPT NMR spectroscopic techniques. It was concluded that they most likely exist in apolar solvents like benzene as discrete aggregated species having a $ZnLi_2$-core stoichiometry, but that they occur in polar solvents like THF as solvent separated ion pairs. Furthermore, it was shown that the compounds having chiral centres in the five-membered ring, i.e. **9c–f**, exist in solution as complicated mixtures of stereoisomers. The spirocyclic zincate (**10**) was prepared via a similar one-pot reaction as **8a** in the presence of TMEDA (equation 6 in Scheme 1)[51].

The structures in the solid state of zincates **8b**, **9b** and **10** which have many similarities were unambiguously established by X-ray crystallography (Figure 6). Relevant structural features, bond distances and angles are given in Table 1.

The spirocyclic structures of **8b**, **9b** and **10** consist of two zincacyclopentane (**8b** and **10**) or two zincacyclohexane (**9b**) rings, having the zinc atom in common. Each of the lithium atoms is bonded to the α-carbon atoms of the two metallacycles, while a tetrahedral coordination geometry at lithium is reached by bidentate N−Li coordination

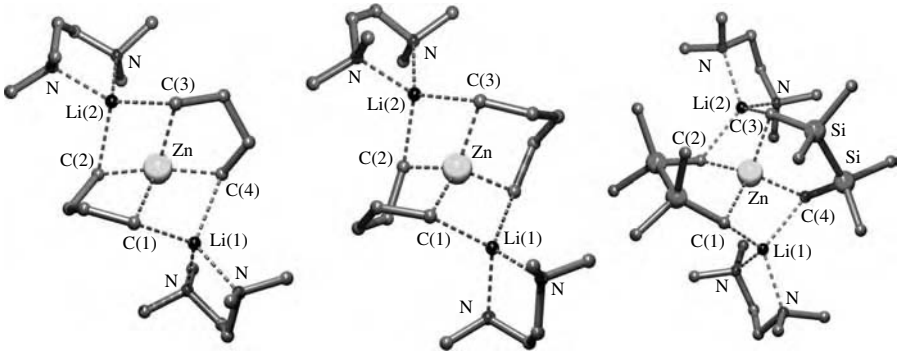

FIGURE 6. Molecular geometries of **8b**, **9b** and **10** in the solid state

TABLE 1. Relevant bond distances and angles in **8b**, **9b** and **10**

Bond distances (Å)	**8b**	**9b**	**10**
Zn−C(1)	2.133(4)	2.115(4)	2.139(2)
Zn−C(2)	2.122(5)	2.109(4)	2.205(2)
Zn−C(3)	2.127(5)	2.119(4)	2.139(2)
Zn−C(4)	2.127(4)	2.129(4)	2.205(2)
C(1)−Li(1)	2.282(7)	2.312(8)	2.347(5)
C(2)−Li(2)	2.257(8)	2.279(8)	2.255(4)
C(3)−Li(2)	2.299(8)	2.302(8)	2.347(5)
C(4)−Li(1)	2.232(9)	2.316(8)	2.225(4)
N−Li (average)	2.130(8)	2.124(8)	2.170(5)
Bond angles (°)			
C(1)−Zn−C(2)	101.1(2)	90.5(2)	98.90(9)
C(1)−Zn−C(3)	106.4(2)	122.8(2)	123.96(13)
C(1)−Zn−C(4)	119.2(2)	119.5(2)	108.18(9)
C(2)−Zn−C(3)	118.6(2)	119.1(2)	108.18(9)
C(2)−Zn−C(4)	110.1(2)	117.9(2)	120.43(12)
C(3)−Zn−C(4)	102.4(2)	90.0(2)	98.90(9)

of the TMEDA molecule. The bridge bonding of the α-carbon atoms to zinc and lithium represents an example of electron-deficient two-electron three-centre type of bonding. These bridged bonds between lithium and zinc are slightly asymmetric, as is indicated by the different bonding distances between zinc and carbon, and lithium and carbon, respectively (Table 1). As expected, the bond distances between zinc and the four α-carbon atoms in these zincates are slightly elongated compared to the zinc−carbon bond distance in linear neutral dialkylzinc compounds. The observed α-carbon−lithium bond distances (Table 1) are in the same range as those found in alkyllithium compounds[43,44]. The observed C−Zn−C bond angles deviate considerably from the ideal tetrahedral value (Table 1) as a result of the acute angles in the five-membered metallacycles. However, in **9b** the angle between the planes defined by C(1), C(2) and Zn and C(3), C(4) and Zn amounts to 89.2(1)°, a value close to the ideal value of 90° for tetrahedra. In **8b** this value is 81.8°, indicating a more distorted situation at zinc compared to that in **9b**.

The tetraorganozincate **11**, obtained from the 2:1 reaction of 2-{[(dimethylamino) methyl]phenyl}lithium[52] with bis{2-[(dimethylamino)methyl]phenyl]}zinc[53] (equation 7), represents the only example of a highly coordinated tetraorganozincate in which an aryl organic group is bound to zinc.

The structure of **11** in the solid state (Figure 7) was established by an X-ray crystal structure determination[10]. The four aryl groups are η^1-bonded to the central zinc atom with bonding distances ranging from 2.124(4) to 2.152(3) Å. The $C_{ipso}-Zn-C_{ipso}$ bond angles range from 106.51(15) to 111.26(15)°, indicating a slightly distorted tetrahedral coordination geometry at zinc. The aryl groups are pairwise bridge-bonded between zinc and lithium atoms in an asymmetric manner, as is indicated by the difference in bonding distance between C_{ipso} and zinc and C_{ipso} and lithium (C−Li 2.234 Å mean value). The rather acute angles [mean value 120.4(3)°] between the $C_{para}-C_{ipso}$ and the $C_{ipso}-Li$ vectors compared to the angle of the corresponding vectors with the $C_{ipso}-Zn$ bond [mean value 167.3(3)°] suggest that there is considerable π-interaction of C_{ipso} with lithium. Such an asymmetric bonding mode of an aryl group between lithium and other metals has been observed before in cuprates[7,54] and aurates[55]. Finally, each lithium atom

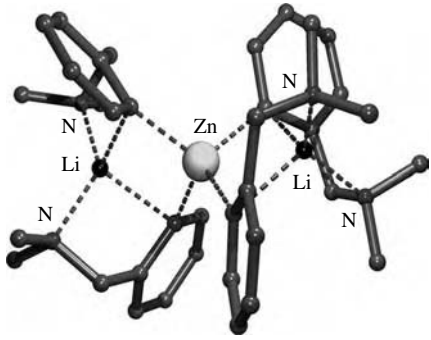

FIGURE 7. Molecular geometry of **11** in the solid state

is tetrahedrally coordinated by intramolecular N−Li coordination with the two *ortho*-dimethylaminomethyl substituents.

1/2 $[2\text{-}Me_2NCH_2C_6H_4Li]_4$ + $(2\text{-}Me_2NCH_2C_6H_4)_2Zn$

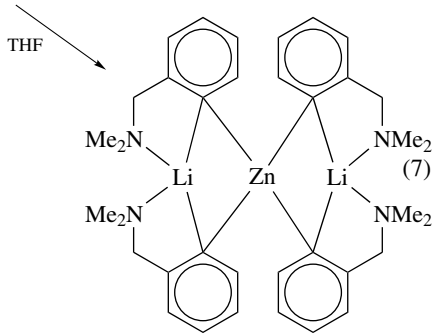

(7)

(11)

C. Homoleptic Triorganozincates $[R_3Zn]M$

Reaction of $(Me_3SiCH_2)_2Zn$ with an alkali (K) or alkali earth metal (Ba, Sr or Ca) in a suitable solvent affords the corresponding triorganozincates **12–16** (Scheme 2).

The structures in the solid state of these compounds, **12**[56], **13–15**[57] and **16**[58], have been established by X-ray crystal structure determinations. In all cases the anionic part, i.e. the $[(Me_3SiCH_2)_3Zn]^-$ anion, has comparable structural features (Table 2). The anionic part of **12** is shown as a representative example (Figure 8).

As expected, the observed Zn−C bond distances (Table 1) are slightly elongated compared to the bond length found in linear dialkylzinc compounds [e.g. the Zn−C bond distances in $(Me_3Si)_2CH-Zn-C(SiMe_3)_3$ are 1.946(4) and 1.971(3) Å, respectively][59]. Although the various C−Zn−C bond angles differ from the ideal value of 120° for a perfect trigonal geometry, the sum of these bond angles (Table 2) for all compounds is 360° within experimental error, indicating a perfectly planar arrangement at the zinc

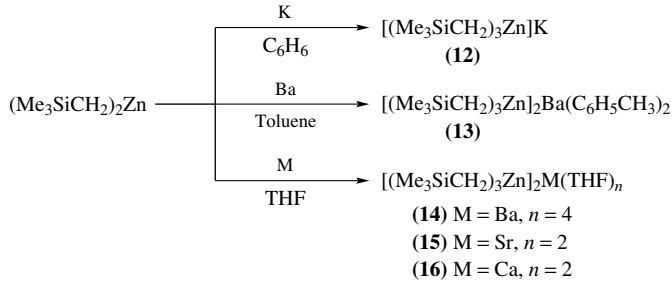

SCHEME 2

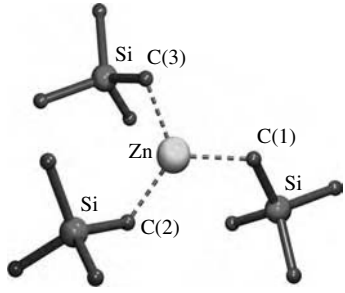

FIGURE 8. Molecular geometry of the $[(Me_3SiCH_2)_3Zn]$ anion in **12**

TABLE 2. Structural features of the $[(Me_3SiCH_2)_3Zn]^-$ anion in compounds **12–16**

Bond distances (Å)	**12**	**13**	**14**	**15**	**16**
Zn−C(1)	2.043(3)	2.080(5)	2.125(2)	2.076(7)	1.996(2)
Zn−C(2)	2.026(3)	2.012(5)	2.013(8)	2.019(6)	2.081(2)
Zn−C(3)	2.086(4)	2.072(4)	2.066(7)	2.095(7)	2.080(2)
C·····X [a]	3.15–3.27	3.03–3.06	3.06–3.23	2.81–2.86	2.66–2.72
Bond angles (°)					
C(1)−Zn−C(2)	123.0(1)	119.6(2)	120.5(3)	120.1(3)	119.6(1)
C(1)−Zn−C(3)	113.0(1)	119.8(2)	116.1(3)	114.4(3)	114.79(9)
C(2)−Zn−C(3)	123.7(1)	120.6(2)	123.3(3)	125.4(3)	125.6(1)
Σ [b]	359.7	360.0	359.9	359.9	360.0

[a] Closest contacts between C(1) and C(3) and the alkali or alkali earth metal cation X.
[b] Sum of the C−Zn−C bond angles.

atom. That the C(1)−Zn−C(3) bond angles are significantly smaller than 120° is not unexpected because these carbon atoms have (long-range) interactions with the cations in the crystal lattice.

Although the structural features of the anionic part of all compounds **12–16** are comparable, these structures are entirely different with respect to the cationic parts and relative positions of cations and anions within the unit cell. In the crystal lattice of **12** each potassium atom has long-range interactions with seven carbon atoms. In **13** and **14** each barium atom has an interaction with two carbon atoms [C(1) and C(3)] of two adjacent

$[(Me_3SiCH_2)_3Zn]^-$ anions, in **13** two additional toluene molecules and in **14** four additional THF molecules have interactions with barium, rendering this atom eight-coordinate. Similarly, in the crystal lattice of **15** and **16** the strontium and calcium atoms interact with two $[(Me_3SiCH_2)_3Zn]^-$ anions, while a pseudo-octahedral coordination geometry at these atoms is reached by coordination of two THF molecules which are in *cis*-position.

In an approach similar to the synthesis of **12**, the neopentyl derivatives $[(Me_3CCH_2)_3Zn]K(C_6H_6)$ (**17**) and $[(Me_3CCH_2)_3Zn]Na$ (**18**) have been prepared from the reaction of $(Me_3CCH_2)_2Zn$ and potassium and sodium, respectively. Also, the structures of these compounds were crystallographically determined and are closely related to the structures of the (trimethylsilyl)methyl zincates described above[56].

Mixing a diorganozinc compound with an organometallic reagent in an appropriate solvent is another approach to the synthesis of triorganozincates (Scheme 3).

$$[(Me_3Si)_2CH]_2Zn + (Me_3Si)_2CHLi \xrightarrow[1\text{ eq. TMEDA}]{Et_2O} \underset{\textbf{(19)}}{\{[(Me_3Si)_2CH]_3Zn\}Li(Et_2O)_2TMEDA} \quad (8a)$$

$$2\,(PhCH_2)_2Zn + (PhCH_2)_2Mg(THF)_2 \xrightarrow{THF} \underset{\textbf{(20)}}{2\,[(PhCH_2)_3Zn]_2Mg(THF)_6} \quad (8b)$$

SCHEME 3

Reaction of $[(Me_3Si)_2CH]_2Zn$ with $(Me_3Si)_2CHLi$ in a 1:1 molar ratio in the presence of one equivalent of TMEDA in diethyl ether as a solvent affords zincate **19** as the only product[60] (equation 8a in Scheme 3). It should be noted that when this reaction is carried out in the absence of TMEDA the zincate $[(Me_3Si)_2CH]_3ZnLi(Et_2O)_4$ is obtained, while the presence of excess TMEDA results in the formation of $[(Me_3Si)_2CH]_3ZnLi(TMEDA)_2$.

When dibenzylzinc and dibenzylmagnesium are mixed in a 2:1 molar ratio in THF as a solvent, a rapid disproportionation reaction occurs (equation 8b) resulting in the formation of tris(benzylzincate) (**20**)[61]. It is notable that the reversed reaction is also possible, i.e. addition of excess TMEDA to a THF solution of **20** results in the immediate formation of $(PhCH_2)_2Zn(TMEDA)$ and $(PhCH_2)_2Mg(TMEDA)$ in quantitative yield. This observation indicates that the actual structures of zincates present in solution are influenced by the type of solvent and by the presence and nature of additional donor molecules.

The structures in the solid state of both **19** and **20** have been established by X-ray crystal structure determinations. For both compounds the unit cell contains well distinguishable triorganozinc anions and corresponding cations, $[Li(OEt_2)_2(TMEDA)]^+$ for **19** and $[Mg(THF)_6]^{2+}$ for **20**. The molecular geometries of the triorganozinc anions, $[\{(Me_3Si)_2CH\}_3Zn]^-$ for **19** and $[(PhCH_2)_3Zn]^-$ for **20**, are shown (Figure 9).

The solid state structure of **19** comprises the packing of eight discrete $[\{(Me_3Si)_2CH\}_3Zn]^-$ anionic units and eight $[Li(OEt_2)_2(TMEDA)]^+$ cationic units in an orthorhombic unit cell. The coordination geometry of zinc in the anions is almost perfectly trigonal planar; within experimental error the Zn−C bonding distances are equal [2.089(9) Å mean value]. Also, the C−Zn−C bond angles are all close to the ideal value of 120° [120.4(4), 119.6(4) and 118.7(4)°, respectively]. The lithium cations are each bidentate coordinated by one TMEDA molecule and two additional monodentate coordinated diethyl ether molecules.

An X-ray crystal structure determination of the $[t\text{-}Bu_3Zn]^-$ anion present in **21**[62] has an almost perfect trigonal planar arrangement [Zn−C bond distances 2.080(7), 2.059(7) and 2.057(8) Å; C−Zn−C angles 118.1(2), 120.7(3) and 120.6(3)°]. Compound **21** was prepared by reacting 1,3,4,6,7,8-hexahydro-2*H*-pyrimido[1,2]pyrimidine, Me_2Zn and *t*-BuLi (equation 9). It is notable that the methyl groups initially bound to zinc all become

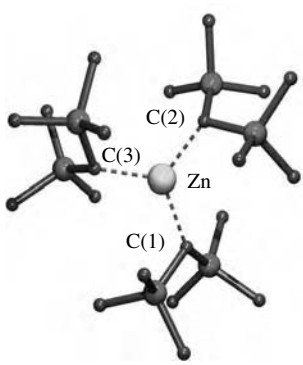

(19)

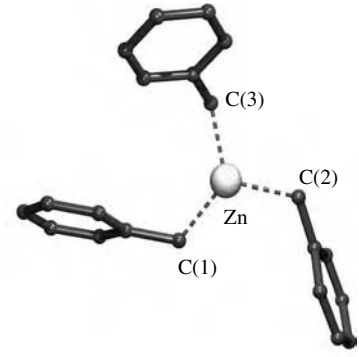

(20)

FIGURE 9. Molecular geometries of the triorganozincate anions of **19** and **20**

replaced by *t*-butyl groups during the reaction. Also, the cationic part, i.e. $Li_8(H)(hpp)_6$, has interesting structural features, but it is beyond the scope of this chapter to discuss this aspect in detail.

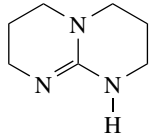

hppH

$$+\ Me_2Zn \xrightarrow{1.5\ \text{eq}\ t\text{-BuLi}} [t\text{-}Bu_3Zn]Li_8(H)(hpp)_6 \quad \textbf{(21)} \qquad (9)$$

Reaction of zincate $[(Me_3Si)_2N]_3ZnNa(12\text{-crown-}4)_2$, which exists in solution as solvent-separated ion pairs, with phenylacetylene results in the quantitative substitution of the anionic $[(Me_3Si)_2N]^-$ groups by $[PhC{\equiv}C]^-$ groups to give zincate **22** (equation 10)[63].

$$[\{(Me_3Si)_2N\}_3Zn]Na(12\text{-crown-}4)_2 + 3\ PhC{\equiv}CH \xrightarrow[-3(Me_3Si)_2NH]{DME} [(PhC{\equiv}C)_3Zn]Na(12\text{-crown-}4) \quad (\textbf{22}) \qquad (10)$$

Recrystallization of **22** from THF afforded a crystalline material, suitable for an X-ray crystal structure determination. Surprisingly, the asymmetric unit contains two different zincate anions, one having a planar trigonal geometry with almost equal Zn(2)−C bond distances (1.967 Å, mean value), the sum of the bond angles at Zn(2) being 360.0°. The other $(PhC{\equiv}C)_3Zn$ anion is associated with one THF molecule, rendering the zinc atom four-coordinate (Figure 10). In this latter anion the Zn−C distances are slightly elongated [Zn(1)−C 2.003 Å, mean value] compared to the first one. The relatively long Zn−O coordination bond [2.244(5) Å] and the sum of the C−Zn(1)−C bond angles of 356.1° indicate that Zn(1) has rather a tetrahedral than a planar trigonal pyramidal geometry, with the coordinating oxygen atom residing at the apical position.

As described in the previous section, reaction of two equivalents of 2-[(dimethylamino) methyl]phenyllithium with bis(2-[(dimethylamino)methyl]phenyl)zinc affords the highly

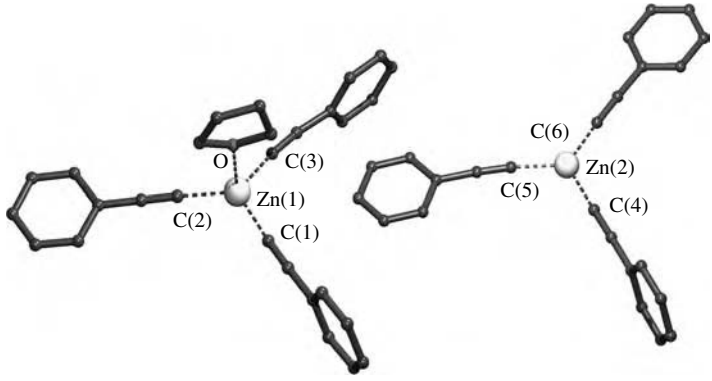

FIGURE 10. Molecular geometries of the $[(PhC{\equiv}C)_3Zn(THF)]^-$ and $[(PhC{\equiv}C)_3Zn]^-$ anions as present in the asymmetric unit of **22**

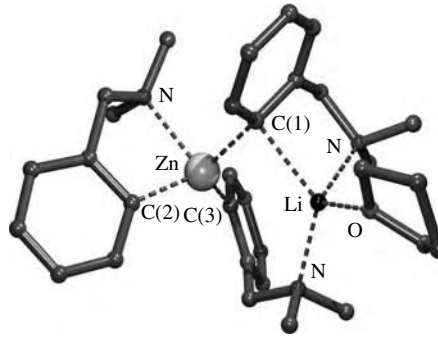

FIGURE 11. Molecular geometry of **23** in the solid state

coordinated tetraorganozincate $[(2\text{-}Me_2NCH_2C_6H_4)_4Zn]Li_2$. When the same reaction is carried out with 1:1 zinc-to-lithium stoichiometry, triorganozincate $[(2\text{-}Me_2NCH_2C_6H_4)_3Zn]Li(THF)$ (**23**) was obtained, whose structure in the solid state was established by an X-ray crystal structure determination[10]. Compound **23** does not comprise (solvent) separated ions, but both in the solid state and in solution this compound exists as a neutral species. The molecular geometry of **23** in the solid state (Figure 11) reveals a distorted tetrahedral coordination geometry at zinc as a result of the bonding of three C_{ipso} atoms of the three aryl groups [Zn−C(1) 2.082(2), Zn−C(2) 2.038(2) and Zn−C(3) 2.026(2) Å] and one intramolecularly coordinating Me_2N group. One of the aryl groups is η^1,μ^2-bridge-bonded via C_{ipso} between zinc and lithium in a rather asymmetric way, which is reflected in the different bond distances between zinc and C_{ipso} (2.082 Å) and lithium and C_{ipso} (2.414 Å) as well as the different C(4)···C(1)−Zn and C(4)···C(1)−Li bond angles of 159.66 and 117.96°. A distorted tetrahedral coordination geometry at lithium is reached by additional intramolecular coordination of two Me_2N substituents and a THF molecule. Molecular weight determinations (by cryoscopy in benzene) and ^1H and ^{13}C NMR studies revealed that this structure in the solid state is most likely retained in solution.

Preliminary ^1H and ^{13}C NMR studies pointed to the existence of heterozincates $[(Me_2NCH_2C_6H_4)_2(n\text{-}Bu)Zn]Li$ or $[(Me_2NCH_2C_6H_4)(n\text{-}Bu)_2Zn]Li$ in equilibrium with **23**

in solutions containing $(Me_2NCH_2C_6H_4)_2Zn$ and *n*-BuLi in 1:1 molar ratio. The presence of such heterozincates was furthermore corroborated by the observation of the exclusive formation of an 1,4-addition product, obtained from reaction of these heterozincates with 2-cyclohexenone (equation 11). The additional formation of the 1,2-aryl-addition product is not unexpected, because in a separate experiment it was demonstrated that reaction of **23** with 2-cyclohexenone affords this 1,2-adduct exclusively.

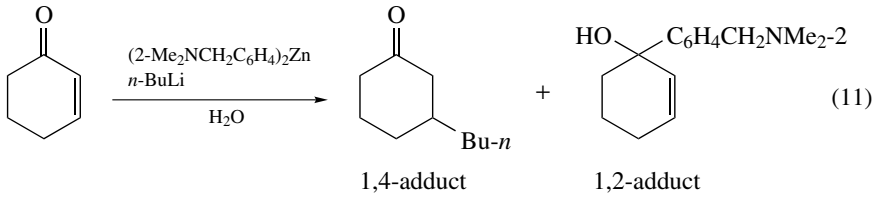

(11)

The structures of three triarylzincates, $[(Ph_3Zn)_2]$ $Mg_2Br_3(THF)_6$ (**24**), $[Mes_3Zn]MgBr(THF)_5$ (**25**) and $[(2,4,6\text{-}i\text{-}Pr_3C_6H_2)_3Zn]Li(TMEDA)_2$ (**26**), have been established in the solid state by X-ray crystal structure determinations. The first two compounds were prepared from the reaction of $[ZnBr(NPMe_3)]_4$ with excess of the corresponding Grignard reagent[64], while the latter compound was isolated as a side product from the reaction of zinc halide containing $VCl_2(TMEDA)_2$ with 2,4,6-*i*-$Pr_3C_6H_2Li$[65]. The molecular geometry of the respective triarylzincate anions are shown in Figure 12. All three compounds have in common that in the solid state they exist as solvent separated ion pairs. The coordination geometry at zinc in all three anions is almost perfectly planar trigonal. To release steric interference between the *ortho*-substituents in **25** and **26**, the aryl groups in these compounds are tilted with respect to the trigonal plane in a propeller-like conformation. The presence of a complex counter cation $[Mg_2Br_3(THF)_6]^+$ in the solid state of **24**, in which the three bromine atoms bridge between two magnesium atoms while in **25** the counter cation is a simple $\{MgBr(THF)_5]^+$ cation, is notable. In the solid state structure of **26** the asymmetric unit contains, in addition to the $[Li(TMEDA)_2]^+$ cation, an additional neutral $Li_2Cl_2(TMEDA)_2$ molecule.

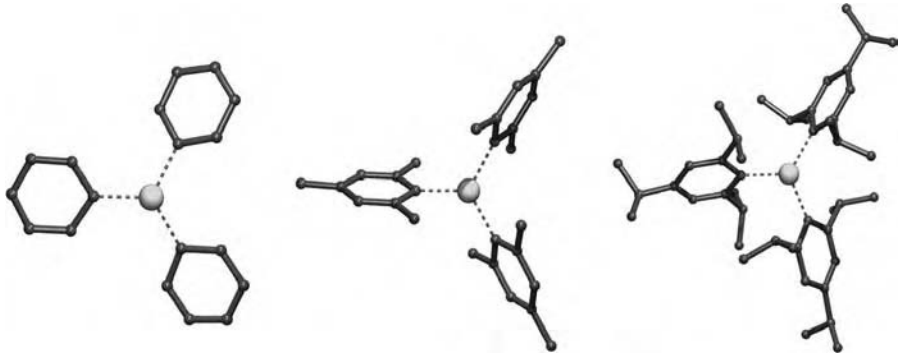

(24) **(25)** **(26)**

FIGURE 12. Molecular geometry of the triarylzincate anions as present in **24**, **25** and **26**

D. Heteroleptic Triorganozincates [$R_2R'Zn$]M

So far, only organozincates have been considered in which the three or four organic groups bound to zinc are identical (homoleptic zincates). It is well established that heteroleptic organozinc compounds undergo the so-called Schlenk equilibrium (equation 12). This is also true for heteroleptic zincates (equation 13). In this case, the equilibria are even more complicated, due to the possible formation of a variety of homo- and heteroleptic species.

$$R_2Zn + R'_2Zn \rightleftarrows 2\ RR'Zn \tag{12}$$

$$[R_3Zn]^- + [R'_3Zn]^- \rightleftarrows [RR'_2Zn]^- + [R_2R'Zn]^- \tag{13}$$

Such equilibria are driven by thermodynamics and therefore a selective synthetic route towards one of these species and isolation of such heteroleptic zincates in pure form is often very difficult or impossible. Only if one of the species has a sufficiently enhanced thermodynamic stability compared to the others in the equilibrium is its isolation as a pure compound possible. This is often the case when the various groups bound to zinc have a sufficiently different electronegativity, for example when one of the groups is bound to zinc via a heteroatom, or when the steric requirements of the groups bound to zinc are rather different. Sometimes it is possible to isolate one of the species present in the Schlenk equilibrium as a solid material, for example when one of the species preferentially crystallizes from solution.

The heteroleptic zincate [$(Me_3SiCH_2)_2PhZn$]K (**27**) was isolated as a side product from a benzene solution of the homoleptic zincate [$(Me_3SiCH_2)_3Zn$]K due to reaction of this zincate with the benzene solvent (equation 14)[56].

$$[(Me_3SiCH_2)_3Zn]K \xrightarrow[-Me_4Si]{C_6H_6} \underset{(\mathbf{27})}{[(Me_3SiCH_2)_2PhZn]K} \tag{14}$$

The asymmetric unit of **27** is located near a crystallographic inversion centre, resulting in a dimeric molecular geometry (Figure 13), involving asymmetric bridging of the Me_3SiCH_2 group between zinc and potassium [Zn−C(1) 2.06(1), K−C(1) 3.10(1) Å]. The potassium atom is η^6-bonded with the symmetry-related σ-zinc-aryl group [C−K distances range from 3.10(1) to 3.65(1) Å]. It should be noted that the potassium also has (long-range) interactions with an aryl group of a neighbour dimeric unit. The sum of the C−Zn−C bond angles around zinc is 360°, which is in line with a planar trigonal coordination geometry at zinc.

According to the procedures shown in Scheme 4, three triorganozincates (**28–30**) containing the benzylic Ph(Me_3Si)CH group have been prepared[66]. Both in the solid state and in solution these compounds exist as solvent-separated ion pairs, the counter cation being Li(TMEDA)$_2$. Two of these, the heteroleptic ones [{Ph(Me_3Si)CH}Me_2Zn]Li(TMEDA)$_2$ (**28**) and [{Ph(Me_3Si)CH}$_2$MeZn]Li(TMEDA)$_2$ (**29**), have been structurally characterized by X-ray crystallography.

The molecular geometries of the triorganozincate anions as present in **28** and **29** are shown in Figure 14. The sum of the Zn−C bond angles around zinc in **28** and **29** is close to 360° (359.9 and 359.6°, respectively), indicating a slightly distorted trigonal planar coordination geometry at zinc. The differences in Zn−C bond distances between the benzylic carbon atom [2.113(4) Å] and the two methyl carbon atoms [2.005(5) and 2.011(5) Å] is notable. The elongation of the benzyl carbon-to-zinc distance indicates that a major part of the negative charge is located on the benzylic carbon atom. In a

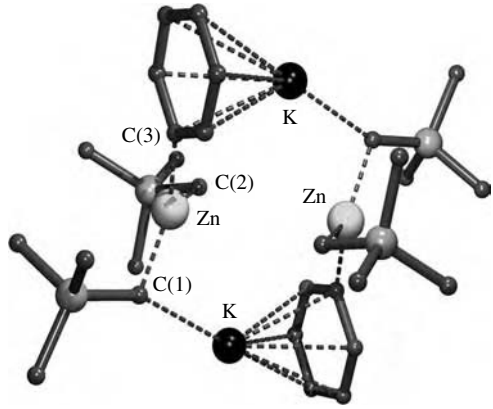

FIGURE 13. Molecular geometry of the dimeric units as present in the solid state structure of **27**

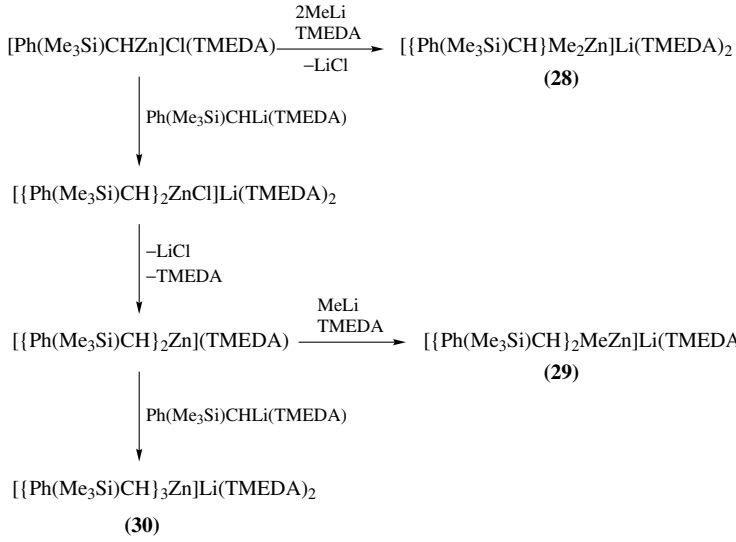

SCHEME 4

highly simplified view, the bonding of the benzylic group to zinc can be regarded as the coordination of a benzyl anion to a molecule of dimethylzinc. Also in **29** the bond distances between the benzylic carbon atoms and zinc compared to that of the methyl carbon atom are elongated [Zn−C(1) 2.089(6), Zn−C(3) 2.084(5) vs. Zn−C(2) 1.989(8) Å]. It is remarkable that the bond angle between the two bulky benzylic groups in **29** is the smallest one [C(1)−Zn−C(3) 115.2°] of the bond angles around zinc [C(1)−Zn−C(2) 125.1(3) and C(2)−Zn−C(3) 119.7(3)°]. However, these bulky groups are oriented in such a way that the steric repulsion between them is minimal (Figure 14).

Due to the presence of two chiral benzylic centres in **29** the possible formation of two diastereoisomers must be expected. The ^{1}H and ^{13}C NMR spectra of **29** indeed

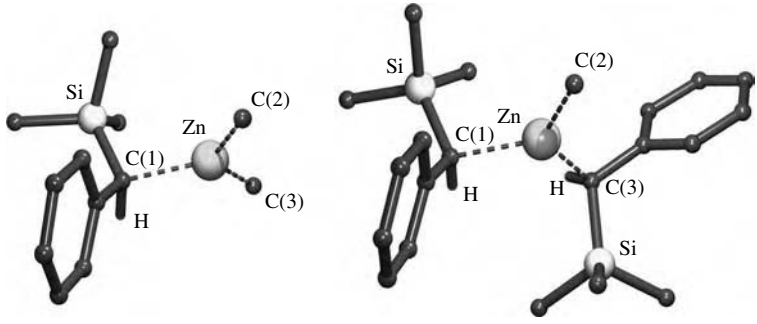

(28) **(29)**

FIGURE 14. Molecular geometries of the heteroleptic triorganozincate anions present in **28** and **29**

show two resonance patterns indicating the presence of two diastereoisomers in solution. One diastereoisomer crystallizes preferentially, i.e. the one in which the two chiral benzylic centres have an identical configuration. In Figure 14, the diastereoisomer in which both chiral centres have (*S*)-configuration is shown, but as a requirement of space-group symmetry (Pbca) both enantiomers are present in the crystal lattice.

The heteroleptic triorganozincate (**31**) in which the zincate anion contains one methyl group and two bulky 2,2,4,4,6,6-hexamethyl-2,4,6-trisilacyclohexyl groups (Figure 15) involves solvent-separated ion pairs of which the lithium cation is coordinated by two 1,3,5-trimethyl-1,3,5-triazine molecules[67]. All three nitrogen atoms of each triazine molecule are coordinated to lithium to give a six-coordinated lithium cation. Like in **28** and **29**, the Zn−C bond distances to the silicon-containing substituent are somewhat elongated [Zn−C(1) 2.083(6) and Zn−C(3) 2.063(6) Å] as compared to the Zn−C methyl distance of 2.017(6) Å. In this anion the bond angle between the bulky substituents is again relatively small [C(1)−Zn−C(3) 114.7(2)°] as was also observed in **29** and was attributed to enhanced delocalization of electron density in silicon-containing anion. The coordination geometry of zinc in **31** is close to trigonal planar as indicated by the sum of the bond angles at zinc (360°).

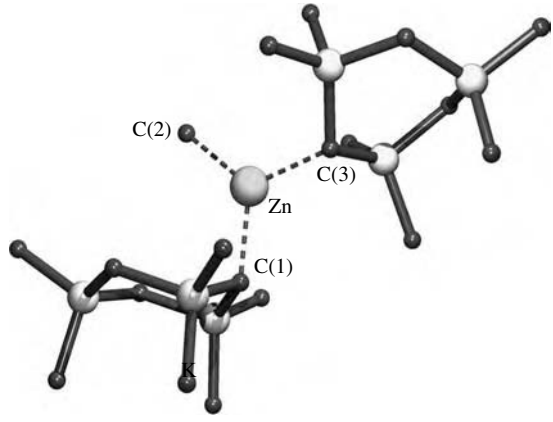

FIGURE 15. Molecular geometry of the heteroleptic triorganozincate anion **31**

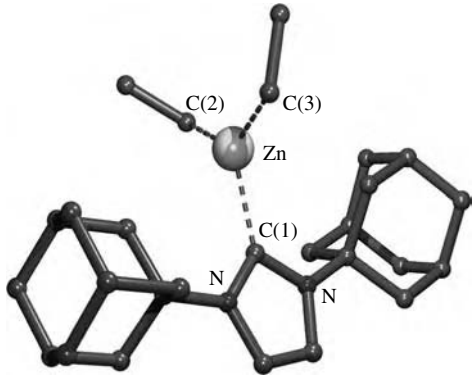

FIGURE 16. Molecular geometry of the neutral compound **32**

The product (**32**) obtained from the reaction of the carbene 1,3-di(1-adamantyl)imidazol-2-ylidene with diethylzinc has been structurally characterized (Figure 16)[68]. This neutral compound should be regarded as containing a (neutral) carbene complexed to diethylzinc. Although the individual bond angles around zinc vary considerably [C(1)−Zn−C(2) 109.8(1), C(1)−Zn−C(3) 118.1(1) and C(2)−Zn−C(3) 132.1°] the sum of these bond angles is 360°, indicating a trigonal planar coordination geometry at zinc. The Zn−C(1) bond distance of 2.096(3) Å is somewhat longer than the Zn−C(ethyl) bonds [Zn−C(2) 1.994(4) and Zn−C(3) 2.009(4) Å].

It has been shown that dialkyl- and diarylmagnesium compounds interact with strongly coordinating agents like cryptands, crown ethers or aza-crown ethers in a disproportionation reaction yielding an ionic structure comprising an alkyl- or arylmagnesium cation and a triorgano-magnesiate anion[69–71]. A similar reaction with dialkylzinc compounds failed[72]. However, according to NMR studies the reaction of a mixture of Et_2Zn and Ph_2Zn with aza-crown ether 14N4 afforded a mixture consisting of the heteroleptic $[Ph_2EtZn]^-$ anion and the homoleptic $[Ph_3Zn]^-$ anion[72] (equation 15).

$$Et_2Zn + Ph_2Zn \xrightarrow[C_6H_6]{14N4} [EtZn(14N4)]^+ + [Ph_2EtZn]^- + [Ph_3Zn]^- \qquad (15)$$

So far, only zincates have been considered in which the organic groups are bonded to zinc via a carbon atom. However, also organozincates are known in which one of the groups is bound to zinc via an electronegative heteroatom. The heteroleptic organozinc compounds [EtZnX] containing an electronegative X group (X = Cl, Br, I or OR) undergo a similar disproportionation reaction as described above, resulting in the formation of $[Et_2ZnX]^-$ anions[73].

Furthermore, reaction of $(Me_3SiCH_2)_2Zn$ with $(Me_3Si)_2NLi$ in the presence of 1,3,5-trimethyl-1,3,5-triazine (TMTA) afforded compound (**33**) (equation 16)[67].

$$(Me_3SiCH_2)_2Zn + (Me_3Si)_2NLi \xrightarrow[THF]{TMTA} \underset{(\mathbf{33})}{[(Me_3SiCH_2)_2(Me_3Si)_2NZn]Li(TMTA)} \qquad (16)$$

An X-ray crystallographic study of **33** shows this compound to be neutral with two Me_3SiCH_2 groups η^1-bonded to zinc while the amide group is μ^2-bonded via its nitrogen

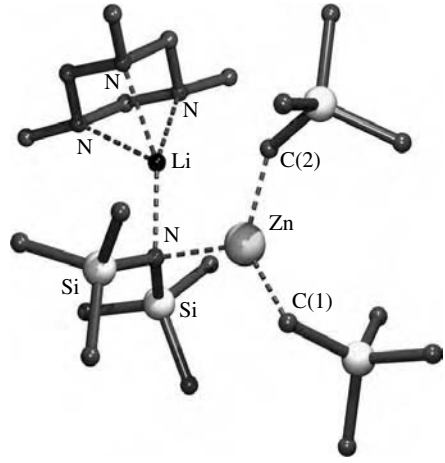

FIGURE 17. Molecular geometry of **33**

atom between zinc and lithium (Figure 17). The TMTA molecule is tridentate coordinated to lithium. The Zn−C bond distances [Zn−C(1) 2.025(14) and Zn−C(2) 2.030(13) Å] are in the expected range for organozincates. The $(Me_3Si)_2N$ group is symmetrically bonded between lithium and zinc [Zn−N 2.131(9) and Li−N 2.083(23) Å]. The Zn−N bond distance in **33** is rather elongated compared to that in linear $[(Ph_2MeSi)_2N]_2Zn$[74], which is 1.850(3) Å, most likely as a consequence of the bridging nature of the $(Me_3Si)_2N$ anion. In this respect it should be noted that the N−Li distances found in trimeric $[(Me_3Si)_2NLi]_3$ range from 1.994(13) to 2.022(13) Å[75]. The Zn−N−Li bond angle of 89.5(7)° is rather acute, probably as a result of a secondary interaction of the α-carbon atom of one of the Me_3SiCH_2 groups with lithium [Li···C(2) 2.74 Å]. The sum of the bond angles around zinc is 259.9°, indicating a trigonal planar coordination geometry, while the lithium atom has a slightly distorted tetrahedral geometry as a result of the additional tridentate coordination of the TMTA molecule.

Also, alkali metal alkoxides interact with diorganozinc compounds to give heteroleptic zincates containing alkoxide moieties, as indicated by NMR spectroscopic studies[76,77]. The structure in the solid state of the product $[Et_2ZnOBu\text{-}t]K$, **34**, obtained from the reaction of Et_2Zn with *t*-BuOK, was established by X-ray crystallography[76]. In the solid state, compound **34** consists of dimers of which the two dimeric halves are symmetry related via an inversion centre. Two *t*-butoxy groups bridge in a symmetric way [Zn−O bond distances 2.091(4) and 2.097(4) Å] between two Et_2Zn units, forming a flat O−Zn−O−Zn arrangement (Figure 18). One of the potassium atoms is located below, and the other one above this plane. Each potassium atom has interactions with both oxygen atoms, one relatively short [2.626(5) Å] and one relatively long [3.734(5) Å]. The acute O−Zn−O bond angle of 79.56(2)° is compensated by a Zn−O−Zn angle of 100.4(3)°. Moreover, this acute angle causes the C−Zn−C angle to open up to 116.2(3)°. Each potassium atom has interactions with the α-C atoms of one of the ethyl groups of both halves of the dimer (both 3.065 Å). Each potassium atom also has an interaction, although much longer (3.331 Å), with an α-C atom of an ethyl group in a neighbouring dimeric unit.

The interesting compound **35** was prepared according to the sequence shown in Scheme 5[78]. It is notable that the last step involves *ortho*-metallation of one of

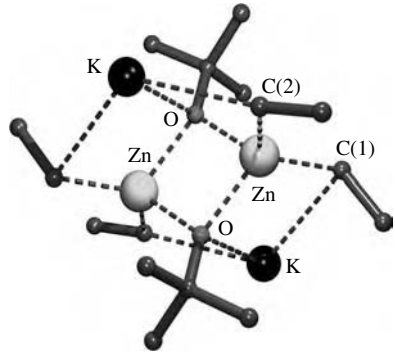

FIGURE 18. The dimeric heteroleptic zincate unit as present in the solid state of **34**

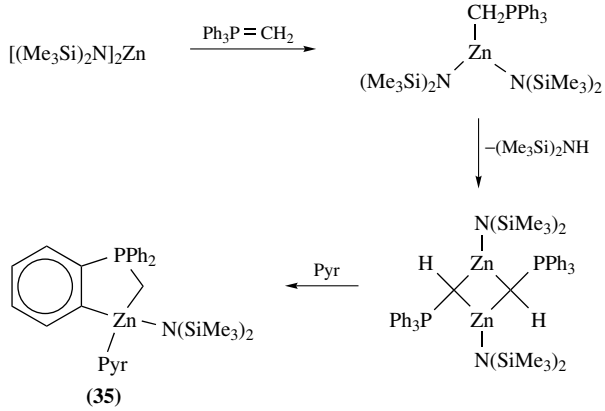

SCHEME 5

the phenyl phosphorus groups. This compound can be regarded as a *C*,*C′-ortho*-chelated heterozincate with two Zn−C bonds, one Zn−N amido bond and an additional coordinating pyridine molecule. Formally, the negative charge is located at zinc and the positive charge at the phosphorus atom.

The molecular geometry of **35** was established by an X-ray crystallographic study (Figure 19). The zinc centre has a distorted tetrahedral coordination geometry with unlike C−Zn distances of which the Zn−C(2) distance [2.137(4) Å] is quite long. The acute C(1)−Zn−C(2) bond angle of 92.9(1)° is a consequence of the bite angle of the five-membered C−P−C−C chelate ring.

According to ^{13}C NMR data, reaction of lithium tetramethylpiperidine (TMP) and *t*-Bu_2Zn, in a 1:1 molar ratio (Scheme 6) affords the heteroleptic zincate [*t*-Bu_2Zn(TMP)]Li (**36**)[79]. An interesting feature of this compound is that it is capable of metalate arenes that contain a directing metalating group (DMG) in *ortho*-position and thus allow further derivatization by reaction of the zincate intermediate with electrophiles (E^+).

The *in situ* formation of dialkylhydrido zincates [R_2HZn]M (M = Li or Na), which have been used as highly selective and mild reducing agents, is notable[80]. Unfortunately, no structural data for this type of zincates are available yet.

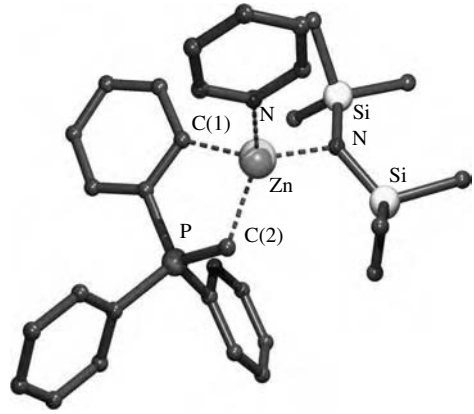

FIGURE 19. Molecular geometry of **35** in the solid state

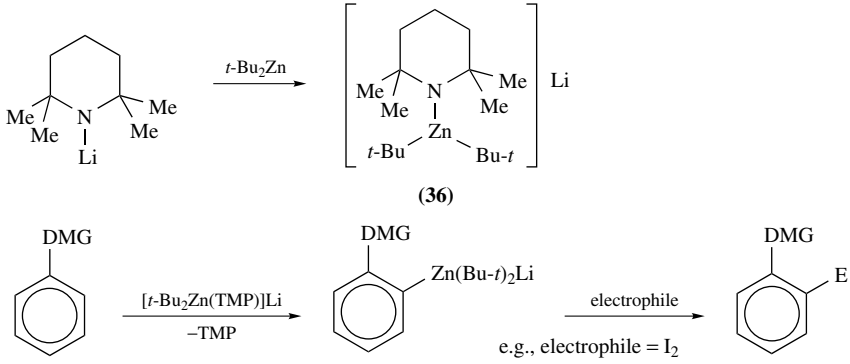

SCHEME 6

III. DIALKYL- AND DIARYLZINC COMPOUNDS

A. Donor-base-free, σ,σ-Bonded Homoleptic R_2Zn and Heteroleptic $RR'Zn$ Compounds

Although dialkylzinc compounds have been known for more than 150 years, the actual structural characterization of these compounds in the solid state by X-ray diffraction studies started only 15 years ago. Such investigations were hampered particularly by the physical properties of these compounds; many of them are low-boiling liquids which, moreover, are extremely sensitive towards oxygen and moisture. It was suggested, based on molar heats of evaporation and molecular weight determinations in solvents like benzene, heptane and dioxane, that dialkylzinc compounds exist as monomers[81,82]. The electronic configuration of zinc in the ground state, observed IR frequencies for Me_2Zn[83] and the observed polarization of Raman frequencies[84] indicated that dialkylzinc compounds adopt a linear C−Zn−C arrangement in which the zinc atom is sp-hybridized.

The first quantitative structural parameters (C−Zn bond distances) in Me_2Zn [1.930(2) Å], Et_2Zn [1.950(2) Å] and *n*-Pr_2Zn [1.952(2) Å] became available from gas-phase electron diffraction studies[42]. Later, the same authors extended these studies, in

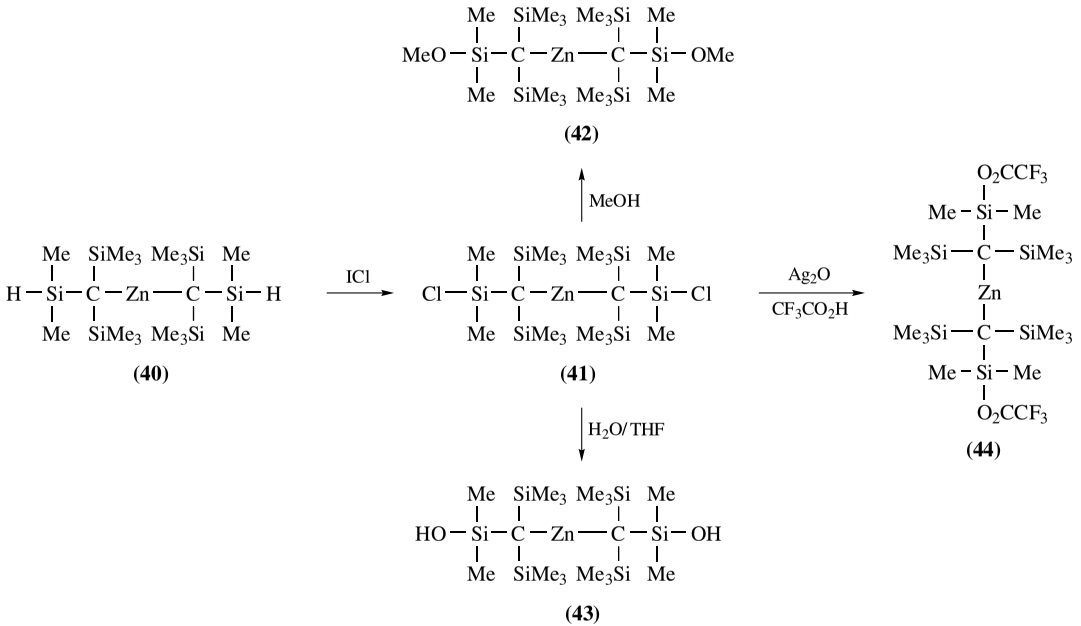
Me SiMe3 Me3Si Me
MeO Si C Zn C Si OMe
Me SiMe3 Me3Si Me
(42)
MeOH
Me SiMe3 Me3Si Me
H Si C Zn C Si H
Me SiMe3 Me3Si Me
(40)
ICl
Me SiMe3 Me3Si Me
Cl Si C Zn C Si Cl
Me SiMe3 Me3Si Me
(41)
Ag2O
CF3CO2H
H2O/THF
Me SiMe3 Me3Si Me
HO Si C Zn C Si OH
Me SiMe3 Me3Si Me
(43)
O2CCF3
Me Si Me
Me3Si C SiMe3
Zn
Me3Si C SiMe3
Me Si Me
O2CCF3
(44)

SCHEME 7

combination with DFT computational studies, to *i*-Pr_2Zn, *t*-Bu_2Zn, *neo*-$Pent_2Zn$ and $(Me_3SiCH_2)_2Zn$[85].

The trimethylsilylmethyl-substituted diorganozinc compounds $(Me_3SiCH_2)_2Zn$ (**37**)[86], $[(Me_3Si)_2CH)]_2Zn$ (**38**)[87] and $[(Me_3Si)_3C]_2Zn$ (**39**)[88] were prepared from the corresponding Grignard or organolithium reagents. Whereas **37** and **38** are pyrophoric liquids and extremely sensitive towards hydrolysis, compound **39** is a crystalline material having a melting point of about 300 °C. Moreover, this compound is air-stable and its resistance towards hydrolysis was demonstrated by the fact that it could be purified by steam distillation techniques[88]. The inertness of the Zn−C carbon bonds in tris(silyl-substituted) methylzinc derivatives was further demonstrated by reaction of $[(HMe_2Si)(Me_3Si)_2C]_2Zn$ (**40**) with various electrophiles like ICl, Br_2 and I_2 and subsequent substitution reactions resulting in compounds of general type $[(XMe_2Si)(Me_3Si)_2C]_2Zn$ with X = Cl, Br, I, F, OH, OMe, O_2CCF_3, O_2CH or NCS[89]. As representative examples, the synthetic pathways towards $[(ClMe_2Si)(Me_3Si)_2C]_2Zn$ (**41**), $[(MeOMe_2Si)(Me_3Si)_2C]_2Zn$ (**42**), $[(HOMe_2Si)(Me_3Si)_2C]_2Zn$ (**43**) and $[F_3CCO_2Me_2Si)(Me_3Si)_2C]_2Zn$ (**44**) are shown in Scheme 7.

The structures of **39**[87], **42**[90], **43**[90] and **44**[89] in the solid state were determined by X-ray crystal structure determinations. The Zn−C bond distances and angles in these compounds are comparable (Table 3). As a representative example the structure of **39** is shown in Figure 20.

Compounds **39**, **42** and **44** exist as discrete monomeric molecules. The Zn−C bond distances are close to the values of simple dialkylzinc compounds obtained from gas-phase electron diffraction studies and are also close to the values predicted by DFT computational studies[85]. Because the zinc atoms in **39**, **42** and **44** are located at special positions in the crystallographic unit cell (at 0.25, 0.25, 0.5 in **39**, and at 0, 0, 0 in both **42** and **44**) the C−Zn−C bond angles are by definition 180° as a consequence of space-group symmetry. Compound **43** forms dimers in the solid state via hydrogen bridges between

TABLE 3. Structural features of the $[XSiMe_2(Me_3Si)_2C]_2Zn$ compounds **39**, **42–44**

Bond distances (Å)	**39**	**42**	**43**	**44**
Zn−C(1)	1.982(2)	1.980(4)	1.965(2)	1.974(3)
Zn−C(2)	1.982(2)	1.980(4)	1.970(2)	1.974(3)
Bond angles (°)				
C(1)−Zn−C(2)	180	180	175.9(1)	180

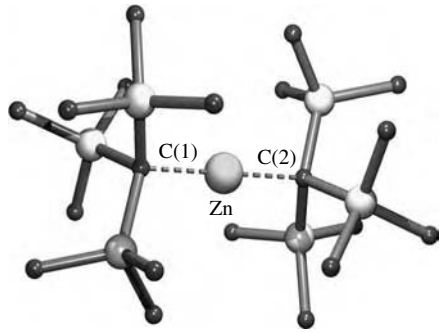

FIGURE 20. Molecular geometry of **39** in the solid state

the two terminal SiOH groups and the two oxygen atoms of an adjacent molecule. The two halves of the dimer are symmetry related via an inversion centre. The two OH groups in each molecule are inequivalent, one oxygen atom, O(1), donating its hydrogen atom intramolecularly and accepting a hydrogen atom intermolecularly, while the other oxygen atom, O(2), shows the complementary behaviour (Figure 21).

The X-ray crystal structure determination of bis[2,2,4,4,6,6-hexamethyl-2,4,6-trisilacyclohexyl]zinc (**45**) shows that this compound exists as a monomer in the solid state[91] (Figure 22). The observed Zn−C bond distance of 1.937(2) Å is remarkably short. The zinc atom is located at a crystallographic inversion centre and consequently enforces a perfectly linear C−Zn−C arrangement. The Zn−C(1)−Si and Si−C−Si bond angles of 110 and 117°, respectively, indicate that a considerable planarization of C(1) has occurred. That such a planarization of the carbon atoms bound to zinc is most likely also present in the structure of **45** in solution was concluded from their exceptional low field shift of 13 ppm and the small $^{1}J(^{13}C-^{1}H)$ and $^{1}J(^{13}C-^{29}Si)$ coupling constants observed in its ^{13}C NMR spectrum.

Dialkylzinc compound **46** contains two 2,4-di-*tert*-butyl-2,4-dienyl anions (Figure 23). In the solid state the two organic groups are η^1-bonded to zinc via C(1) with a Zn−C

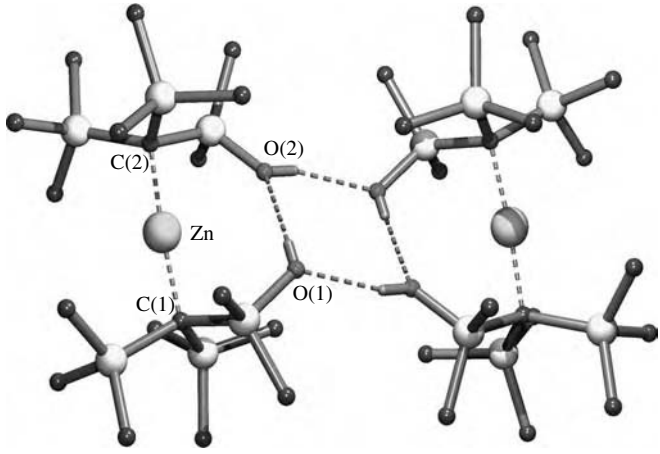

FIGURE 21. Molecular geometry of dimeric **43**

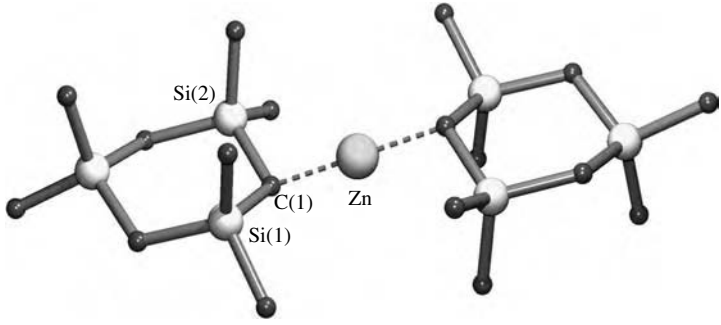

FIGURE 22. Structure in the solid state of **45**

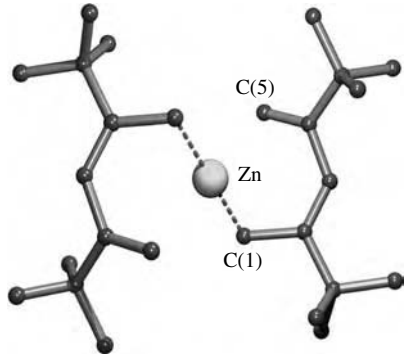

FIGURE 23. Molecular geometry of **46** in the solid state

distance of 1.969(8) Å[92]. Also in this case the molecule is located on a crystallographic inversion centre and consequently the C−Zn−C bond angle is by definition 180°. The alternating long–short–long–short bond distances in the carbon backbone are indicative for a localized diene system. Both dienyl ligands are present in the U conformation and orientated in such a way that they bring C(5) in relatively close proximity (2.850 Å) to the zinc atom (Figure 23). In solution, a ^{1}H NMR spectroscopic study of **46** shows a perfectly symmetric resonance pattern for the dienyl ligand, indicating equivalence of the two sides of the ligand. This pattern remains unchanged down to temperatures below −100 °C, pointing to a process involving a 1,5-metal shift with a low activation barrier.

Reaction of cyclic lithiate (**47**) with $ZnCl_2$ affords a unique 1-zinca-3,6-disilacycloheptane (**48**) (equation 17)[93]. Like its acyclic analogs **39–44** (*vide supra*), compound **48** is air-stable and no hydrolysis was observed after treatment with aqueous THF during a period of 5 h at 80 °C.

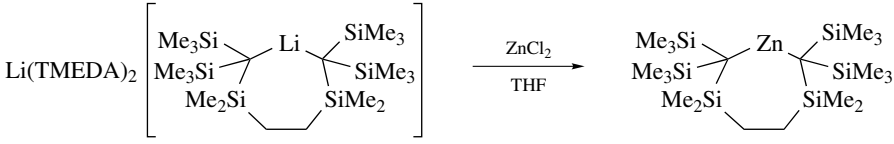

(47) **(48)** (17)

The cyclic nature of **48** was confirmed by an X-ray crystal structure determination (Figure 24). The observed Zn−C bond distances of 1.963(7) and 1.962(7) Å are in the range expected for dialkylzinc compounds. The C(1)−Zn−C(2) bond angle of 169.7(3)° slightly deviates from linear, but the other bond angles in the seven-membered ring are close to the ideal tetrahedral value, indicating minimal ring strain.

$(Me_3Si)_3CZnCH(SiMe_3)_2$ (**49**) and $(Me_3Si)_3CZnPh$ (**50**) are the only examples of heteroleptic diorganozinc compounds the structures of which were determined by X-ray crystal structure determinations (Figure 25)[59]. These compounds have been prepared from the reaction of $(Me_3Si)_3CZnCl$ with one equivalent of $(Me_3Si)_2CHLi$ or PhLi, respectively. It should be noted that **49** and **50** are not accessible via a redistribution reaction of the corresponding symmetric diorganozinc compounds, i.e. **49** from $[(Me_3Si)_3C]_2Zn$ and $[(Me_3Si)_2CH]_2Zn$, and **50** from $[(Me_3Si)_3C]_2Zn$ and Ph_2Zn, respectively, due to the inertness of $[(Me_3Si)_3C]_2Zn$ towards any reaction[87]. The Zn−C bond distances in **49** differ only slightly, Zn−C(1) 1.971(3) and Zn−C(2) 1.946(4) Å, while the C(1)−Zn−C(2)

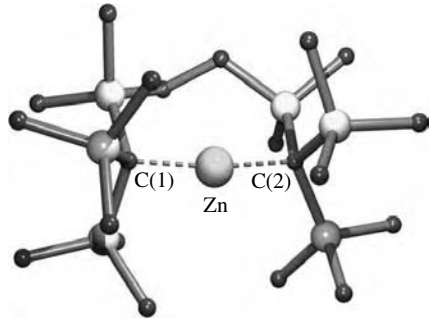

FIGURE 24. Solid state structure of **48**

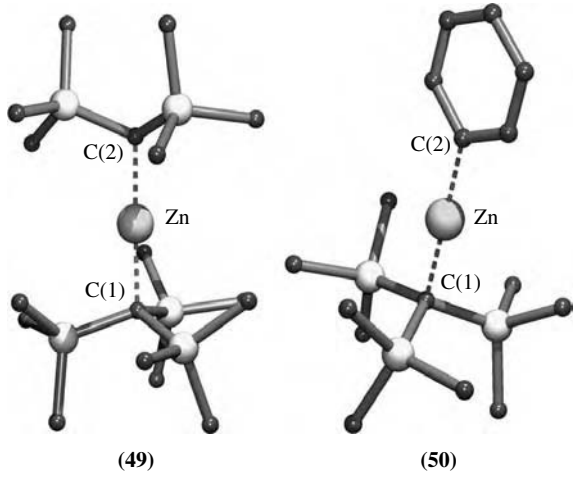

(49) **(50)**

FIGURE 25. Molecular geometry of the heteroleptic diorganozinc compounds **49** and **50** in the solid state

bond angle is close to linear. In **50** the bond distance between the aryl carbon atom and zinc [1.1917(10) Å] is slightly shorter than the Zn−C(1) (alkyl) distance [1.956(10) Å], but this is to be expected because the two carbon atoms involved have different hybridization states. The C(1)−Zn−C(2) bond angle of 177.6(4)° in **50** is very close to the ideal value of 180° for a linear arrangement.

A rather exotic diorganozinc compound **52** is obtained from the reaction of geminal dilithium compound **51** with 3 equivalents of $ZnCl_2$. The structure is shown schematically in equation 18[94]. The short Zn−C bond distances of 1.908(3) and 1.911(3) Å are as expected for sp^2-hybridized carbon atoms bound to zinc. Also, the almost linear C−Zn−C bond angle of 178.6° is in agreement with this type of compounds. At each of the terminal parts of the ligands a Zn−Cl cation is bonded to two nitrogen atoms of each of the PN functionalities. The N−Zn−Cl and N−Zn−N bond angles around these zinc atoms are 120° within experimental error, indicating a perfectly trigonal planar coordination geometry for these zinc atoms. The fact that in the six-membered Zn−N−P−C−P−N

ring the Zn−N bond distances as well as the C−P distances and the P−N distances are almost equal, indicates a considerable conjugation in this ring.

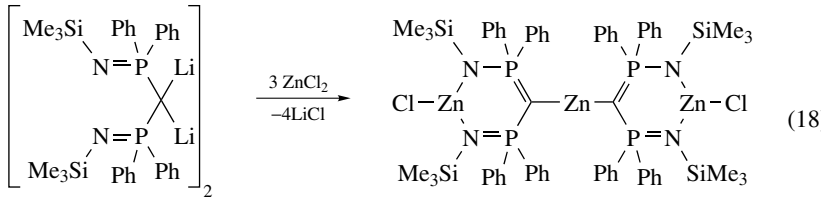

(51) (52) (18)

The X-ray crystal structure determination of diphenylzinc (**53**) reveals a unique structure[9]. It was known already that in apolar solvents like benzene and hexane Ph_2Zn exists as discrete monomeric species[9,95]. Therefore, it was to be expected that also in the solid Ph_2Zn would have a linear monomeric structure like dialkylzincs and other diarylzinc compounds. It appeared, however, that in the solid state Ph_2Zn exists as a dimer comprising two PhZn units linked by two μ-bridging phenyl groups (Figure 26). Such a structural motif, i.e. electron-deficient multi-centre bonding of alkyl or aryl groups is quite common for other metals like Li, Mg, Cu, Ag, Au, Al, etc. but unprecedented, at the time of its discovery, for dialkyl or diarylzinc compounds. The zinc atoms in **53** are three-coordinate as a result of bonding to one terminal and two bridging phenyl groups. Although the individual bond angles around zinc [C(1)−Zn(1)−C(2) 141.5(2), C(1)−Zn(1)−C(4) 115.1(2), C(2)−Zn(1)−C(4) 102.6(2)°] deviate considerably from the ideal value of 120°, the sum of these bond angles (359.4°) is close to 360°, pointing to a trigonal-planar coordination geometry. The Zn(1)−C(1) bond distance of 1.951(5) Å between zinc and the terminal phenyl group is in the expected range. The asymmetric bonding of the bridging aryl groups to the two zinc atoms, with one relatively short [Zn(1)−C(2) 2.016(3) Å] and one relatively long [Zn(1)−C(4) 2.364(5) Å] bond, is remarkable. This dimeric structure may be regarded as consisting of two associated monomeric molecules, i.e. [C(1)Zn(1)(C2)] and [C(3)Zn(2)C(4)]. The two monomers are linked by interactions of the aryl π-system in one of the monomeric units via its *ipso*-carbon atom with the zinc atom of the other monomeric unit, i.e. C(2) with Zn(2) and C(4) with Zn(1).

The structures of dimesitylzinc (**54**)[96], bis[2,4,6-tris(trifluoromethyl)phenyl]zinc (**55**)[97] and bis(pentafluorophenyl)zinc (**56**)[98] have comparable structural features. They are discrete monomeric molecules with a linear C−Zn−C arrangement at zinc (Figure 27). The

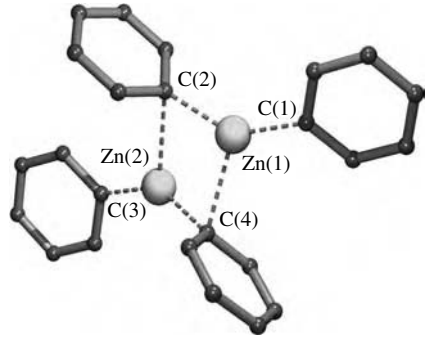

FIGURE 26. Dimeric structure of Ph_2Zn (**53**) in the solid state

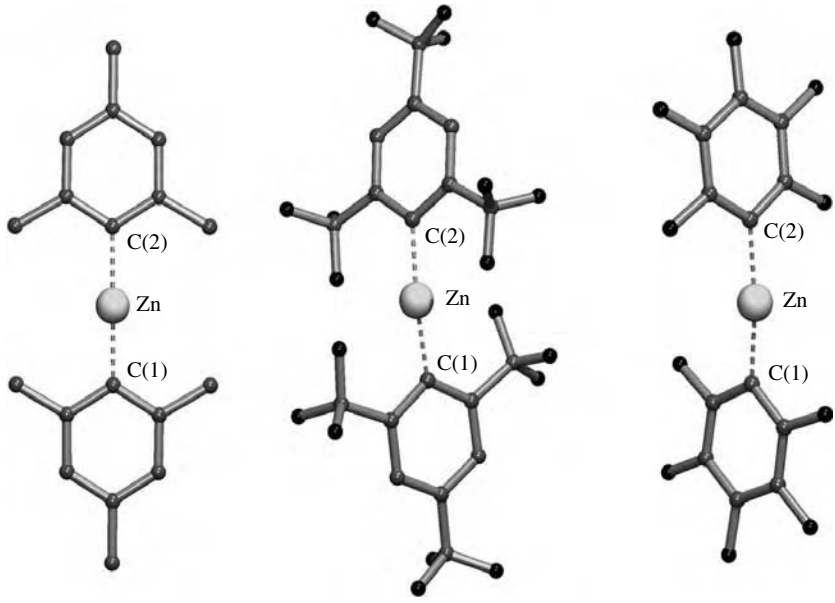

(54) **(55)** **(56)**

FIGURE 27. Structures of the arylzinc compounds **54**, **55** and **56** in the solid state

observed Zn−C bond distances [1.9422(19) Å in **54**, 1.949(3) and 1.950(3) Å in **55** and 1.930(4) and 1.926(4) Å in **56**] are as expected for sp^2-carbon atoms bound to zinc. In **54**, the zinc atom is located on a crystallographic inversion centre and therefore the C−Zn−C bond angle is strictly 180° while the two aryl groups are coplanar with respect to each other. In **55** and **56** such a symmetry is not present, but the observed C−Zn−C bond angles [170.0(1)° in **55** and 172.6(2)° in **56**] are close to linear. In **55** the aryl rings are twisted by 67.1 and in **56** by 76.7°. In the former compound this twist has been explained by minimization of the steric congestion and electrostatic repulsion of the *ortho*-CF_3 groups[97]. In the latter compound the twist seems to be dictated by intermolecular stacking interactions between adjacent molecules[98]. In **55**, the zinc atom has additional interactions with one fluorine atom of each of the *ortho*-CF_3 groups (average Zn−F distance 2.60 Å) which are shorter than the sum of the Van der Waals radii of the constituent atoms.

B. Diorganozinc Compounds Containing Multi-hapto Bonded Groups

With the discovery of ferrocene by two independent groups at the end of 1951[99–101] and its structural elucidation and the subsequent development of metal-cyclopentadienyl chemistry, a new era started in organometallic chemistry. It has been well-established that dicyclopentadienyl compounds of the transition metals have a ferrocene-like structure. On the other hand, cyclopentadienides of the main-group metals tend to form polymers with bridging cyclopentadienyl groups, although exceptions are known[102, 103]. Zinc occupies a borderline position between the transition metals and the main-group metals and the question arises whether the structure of dicyclopentadienylzinc is intermediate between both categories of cyclopentadienyl metal compounds.

Dicyclopentadienylzinc, Cp_2Zn, was first prepared by Fischer and coworkers in 1969 and, based on the similarities of the IR spectra between Cp_2Zn and Cp_2Mg, a ferrocene-like sandwich structure with predominantly ionic cyclopentadienyl–metal interactions was proposed[104]. A similar structure, but with centrally σ-bonded cyclopentadienyl rings, was also suggested because in the ^{1}H NMR spectrum of Cp_2Zn all protons are equivalent[105]. Other authors formulated dicyclopentadienylzinc as $(\eta^1\text{-Cp})_2Zn$, probably by analogy with the monohapto structure, suggested[105] and later established by X-ray crystallography for Cp_2Hg[106].

The first cyclopentadienylzinc compound that was structurally characterized by an X-ray crystallographic study is cyclopentadienyl(methyl)zinc, Cp(Me)Zn (**57**)[107]. The structure of **57** in the solid state consists of puckered chains of methylzinc fragments, linked by bridging cyclopentadienyl groups (Figure 28).

Due to disorder in the cyclopentadienyl groups the exact bonding of the cyclopentadienyl group to zinc remained uncertain, but it has been suggested that the cyclopentadienyl group is η^3-bonded to one zinc atom and η^2-bonded to the other one. In solution, however, cryoscopic measurements in benzene pointed to the existence of discrete monomeric species. IR and ^{1}H NMR studies of solutions of **57** are consistent with η^5-binding of the cyclopentadienyl group to zinc in a symmetric C_{5v} structure.

Sixteen years after its first synthesis had been reported[104], dicyclopentadienylzinc, Cp_2Zn (**58**), was structurally characterized in the solid state by an X-ray crystal structure determination[108]. Like in **56**, the structure of **57** in the solid state consists of infinite chains of zinc atoms with bridging cyclopentadienyl groups, while a terminal Cp group is bonded to each zinc atom. The chain contains two crystallographically independent zinc atoms, Zn(1) and Zn(2). The Cp groups bridging zinc atoms of the same type are located at inversion centres, and these Cp groups therefore are disordered (Figure 29). That the terminal Cp groups are not purely η^1-bonded is clearly indicated by the fact that

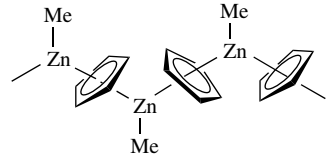

FIGURE 28. Schematic structure of **57** in the solid state

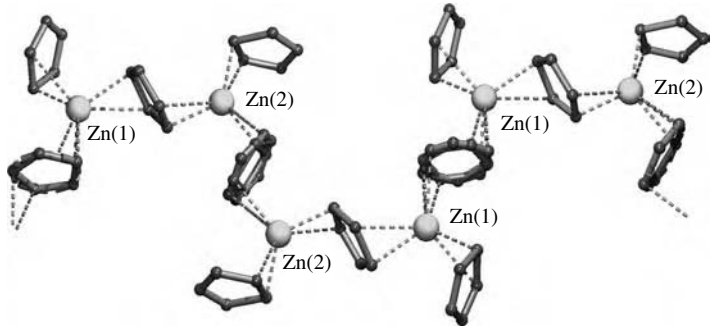

FIGURE 29. Part of the polymeric chain of **58** in the solid state. Note the disordered cyclopentadienyl groups bridging between zinc atoms of the same type

in addition to one short Zn−C interaction [Zn−C 2.04(6) Å, suggesting σ-bonding] a second, relatively short interaction [Zn−C 2.48(6) Å] is present. The Cp group bridging two different types of zinc atoms is asymmetrically bonded with two carbon atoms to one zinc atom [Zn−C 2.04(3) and 2.41(3) Å] and two other carbon atoms to the other zinc atom [Zn−C 2.19(3) and 2.46(2) Å]. Due to disorder in the Cp groups bridging the same type of zinc atoms, their Zn−C bond distances are less certain, but the bonding mode, i.e. two carbon-to-zinc interactions to each zinc atom, is similar.

Structural investigations of monomeric Cp_2Zn in the gas phase by gas-phase electron diffraction studies indicate a structure in which one of the Cp groups is η^5-bonded to zinc while the other Cp group is mainly η^1-bonded[109]. These data were corroborated by DFT calculations. The Zn−C bond distance (2.10 Å) to the η^1-bonded Cp group is considerably longer than expected for a pure σ-Zn−C bond and the angle (95°) between the centre of η^5-bonded Cp group, Zn and C(1), is significantly smaller than expected for a sp^3 carbon atom. This structure is best described as a slip sandwich.

Bis(pentamethylcyclopentadienyl)zinc Cp^*_2Zn (**59**)[110] is a crystalline solid, readily soluble in apolar solvents. Its ^1H and ^{13}C NMR spectra (only one resonance is observed in the ^1H NMR spectrum and two resonances in the ^{13}C NMR spectrum at temperatures down to −100 °C) suggest a highly symmetric structure, most likely similar to that of ferrocene. Although single crystals of **59** suitable for an X-ray structure determination were easily obtained, the structural refinement[111] resulted in a crystallographic 'disaster' (Figure 30). In the solid state **59** exists as discrete monomeric molecules; however, due to the fact that the molecule is located at a crystallographic inversion centre, the zinc atom is disordered over two positions between the cyclopentadienyl rings. Moreover, it appeared that rotational disorder is present in the cyclopentadienyl rings. The data are consistent with a model in which one of the Cp* groups is η^5-bonded and the other one η^1-bonded to zinc, a similar slip sandwich structure as was found in the gas phase for Cp_2Zn. It is obvious that no reliable data with respect to individual bond distances and angles could be obtained. Gas-phase electron diffraction studies of **59** pointed to a slip sandwich structure also in the gas phase[110].

To overcome the problem of crystallographic disorder during the structural characterization by X-ray crystallography, various substituted cyclopentadienyl compounds, i.e. $[t\text{-Bu(Me)}_4C_5]_2Zn$ (**60**)[112], $[Ph(Me)_4C_5]_2Zn$ (**61**)[111], $[(i\text{-Pr})_4C_5H]_2Zn$ (**62**)[113] and $[(Me_3Si)$

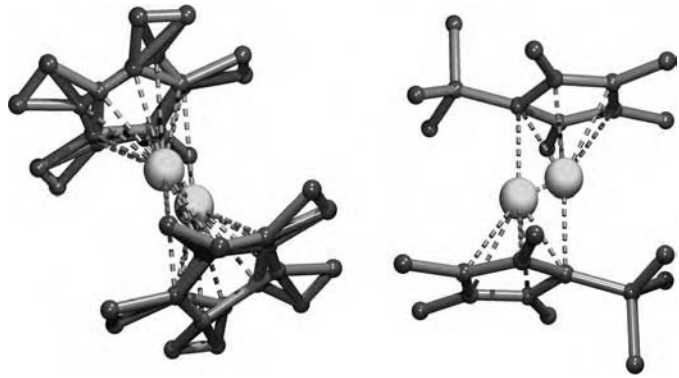

(59) **(60)**

FIGURE 30. Left, the crystallographic 'disaster' of **59**. Right, disordered structure of **60** in the solid state

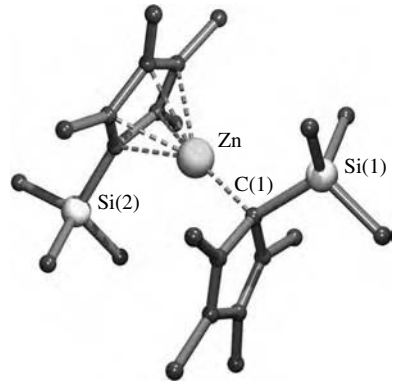

FIGURE 31. Molecular geometry of **63** in the solid state

$Me_4C_5]_2Zn$ (**63**)[112], were prepared and structurally characterized. Unfortunately, in the solid state structures of compounds **60–62**, which are all discrete monomers, the molecules are, as in **59**, located at a crystallographic inversion centre. As a representative example the disordered structure of **60** is shown (Figure 30). The structural features of **60–62** are closely related, i.e. they have a slip sandwich structure in which one of the substituted cyclopentadienyl groups is η^5-bonded to zinc and the other one η^1-bonded to zinc. In the solid state structure of **63**, the disorder as found for **59–62** is not present and therefore this structure could be analysed more in detail (Figure 31)[112]. Although there is a slight difference in Zn–C bond distances [2.154(3) to 2.323(3) Å], indicating a ring slippage of 0.18 Å, such a situation can be regarded as quite normal. Most notable is the way in which the η^1-bonded cyclopentadienyl group (the same carbon atom to which Si is bonded) in **63** is bonded to zinc. The bond angles around C(1) are close to the ideal values of 109.5° and the Zn–C(1) bond distance of 1.953(3) Å is as expected for a Zn σ-bonded to a sp^3 carbon atom. The structure of **63** is not a slip sandwich, as is indicated by the angle of 18° between the two cyclopentadienyl rings, which are perfectly co-planar in **59–62**.

Reaction of Cp^*_2Zn with Et_2Zn afforded, instead of the anticipated Cp*ZnEt, a mixture of Cp*ZnEt and a product, formulated as $Cp^*_2Zn_2$ (**64**)[114]. An X-ray crystallographic structure determination of **64** revealed the unique structural features of this compound (Figure 32). The solid state structure of **64** comprises two metal–metal bonded Cp*Zn moieties in each of which the pentamethylcyclopentadienyl group is η^5-bonded to zinc with almost equal Zn–C distances (2.27–2.30 Å). The linearity of the molecule is shown in the bond angle of 177.4° between Zn(1), the centre of the cyclopentadienyl group, and Zn(2). The most striking feature of **64** is the short [2.305(3) Å] Zn(1)–Zn(2) distance, which is substantially shorter than twice the Pauling single-bond metallic radius (2.50 Å) and therefore indicative for a bonding Zn–Zn interaction. Compound **64** may be regarded as containing a hypothetical Zn_2^{2+} dication, in which formally the oxidation state of zinc is +1. Such a structural motif, i.e. M_2^{2+}, is common for mercury, rare for cadmium but unprecedented for zinc.

^1H and ^{13}C NMR spectroscopic studies of **64** showed that the structure present in the solid state is retained in solution. That the reactivity of **64** is different compared to that of 'normal' organozinc compounds became evident from a hydrolysis reaction of **64** with a carboxylic acid affording the corresponding zinc salt of the carboxylic acid and metallic zinc in a 1:1 ratio and pentamethylcyclopentadiene. This product formation suggests the

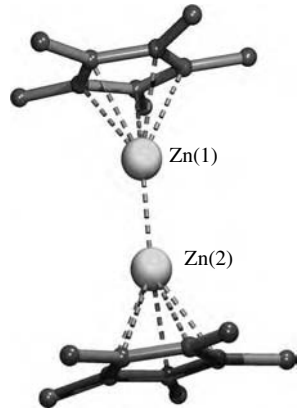

FIGURE 32. Molecular geometry of **64** in the solid state

occurrence of a valence disproportionation of the initially present Zn^{1+} into Zn^{2+} and metallic zinc during or after the hydrolysis of the cyclopentadienyl monoanionic groups.

C. Diorganozinc Compounds Containing Intramolecularly Coordinating Substituents

In the early days of organometallic chemistry it was thought that in many cases the metal–carbon bond would be intrinsically unstable, especially in transition-metal-organic compounds. The two most important pathways by which decomposition of such organometallic compounds may occur are β-hydrogen elimination and thermally induced homolytic cleavage of the metal–carbon bond. To suppress such decomposition pathways several approaches have been put forward, e.g. the use of organic groups lacking β-hydrogen atoms, the introduction of bulky (often trimethylsilyl containing) substituents and the use of organic groups containing a functionalized substituent capable of coordinating to the metal. The isolation and structural characterization of $(Me_3SiCH_2)_4Cu_4$[115] and $(2\text{-}Me_2NCH_2C_6H_4)_4Cu_4$[116] are clear examples of these two approaches and represent the first examples of organocopper compounds sufficiently stable to allow their structural characterization by X-ray crystallography. In $(2\text{-}Me_2NCH_2C_6H_4)_4Cu_4$ the monoanionic, potentially bidentate $2\text{-}Me_2NCH_2C_6H_4$ ligand stabilizes the organocopper compound via intramolecular coordination of the nitrogen to copper. In particular, this ligand was used in the early days to stabilize certain organometallic compounds. Nowadays, about 275 organometallic compounds containing this particular ligand, covering almost the whole periodic system of the elements, have been structurally characterized by X-ray crystallography[5]. When other ligand skeletons and also other heteroatom-functionalized substituents capable of intramolecular coordination are included, several thousands of organometallic derivatives are known[5].

In this respect it is rather surprising that only a few diorganozinc compounds have been reported in which intramolecular coordination of a heteroatom-containing substituent is present. Although the synthesis of $(2\text{-}Me_2NCH_2C_6H_4)_2Zn$ (**65**) was reported already in 1984[117] and it was suggested that, based on the observed ^1H NMR spectra, both nitrogen substituents are involved in nitrogen–zinc coordination, its structure in the solid state has not been established by X-ray crystallography.

A series of dialkylzinc compounds, functionalized with a heteroatom-containing substituent (Scheme 8), has been prepared and was structurally characterized by X-ray crystallographic studies (**66**[118] and **69**[119]) or gas-phase electron diffraction (**66**, **67**[118], **68**[120] and **70**[120]). The relevant structural data are summarized in Table 4 and, as a representative example, the molecular geometry of **66** is shown in Figure 33.

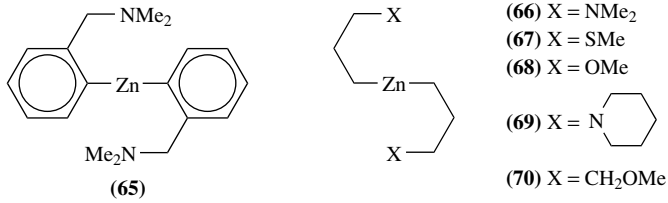

SCHEME 8

All compounds have comparable structural features, the hydrocarbon chains being coiled back to allow the donor atom to coordinate to zinc. The Zn−C bond distances

TABLE 4. Structural data of compounds **66–70**

	X = N(CH$_2$)$_5$ X-ray [a]	X = NMe$_2$ X-ray [a]	X = NMe$_2$ GED [b]	X = SMe GED [b]	X = OMe GED [b]	X = CH$_2$OMe GED [b]
			Bond distances (Å)			
Zn−C(1)	1.992(3)	1.984(5)	1.991(6)	1.966(6)	1.974(4)	1.984(6)
Zn−C(2)	1.992(3)	1.984(5)	1.991(6)	1.966(6)	1.974(4)	1.984(6)
Zn−X(1)	2.404(2)	2.307(4)	2.392(15)	2.732(12)	2.37(3)	2.38(5)
Zn−X(2)	2.404(2)	2.307(4)	2.392(15)	2.732(12)	2.37(3)	2.38(5)
			Bond angles (deg)			
C(1)−Zn−C(2)	155.5(2)	156.4(2)	152(8)	163(15)	175(20)	158(13)
C(1)−Zn−X(1)	84.75(11)	85.6(1)	82(2)	85(2)	77(3)	102(3)
C(1)−Zn−X(2)	110.4(11)	108.2(1)	113(4)	96(2)	106(3)	93(7)
C(2)−Zn−X(1)	110.4(11)	108.2(1)	113(4)	96(2)	106(3)	93(7)
C(2)−Zn−X(2)	84.75(11)	85.6(1)	82(2)	85(2)	77(3)	102(3)
X(1)−Zn−X(2)	107.47(12)	109.7(1)	117(4)	173(12)	111(20)	92(10)

[a] Data obtained from single-crystal X-ray diffraction.
[b] Data obtained from gas-phase electron diffraction.

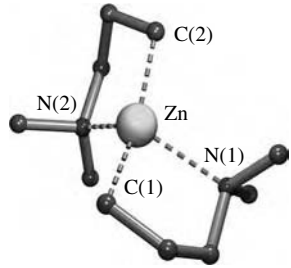

FIGURE 33. Molecular geometry of **66** in the solid state

are as expected, but the coordination bonds of the heteroatoms to zinc are extremely long. A considerable distortion of the tetrahedral coordination geometry at zinc appears from the various bond angles around zinc. The C(1)−Zn−C(2) bond angles are all considerably larger (147.1° in **69** to almost 180° in **67**) than the ideal tetrahedral value of 107°. The C−Zn−X bond angles in the chelate rings of **67–69** are exceptionally small (Table 4), but this is most likely a consequence of the bite angle of the bidentate ligand in combination with the long Zn−X bond length. It should be noted that in **70** this bond angle has a more normal value of 102°, but in this compound more flexible six-membered chelate rings are present. Especially in **68** all bond angles are rather extreme, and point rather to a distorted square planar (with the carbon atoms in *trans*-position) than a tetrahedral coordination geometry at zinc. Also, the diphenylphosphino analog $[Ph_2P(CH_2)_3]_2Zn$ (**71**) has been prepared and structurally characterized by X-ray crystallography[121]. Its structural features are closely related to those of **66–70**.

Reaction of $MeN(CH_2CH_2CH_2Li)_2$ with $ZnCl_2$ afforded a macrocyclic product (**67**) containing two zinc atoms, which was structurally characterized by X-ray crystallography (Figure 34)[119]. Each of the propyl groups of one ligand are bonded to a different zinc atom, while the nitrogen atoms are intramolecularly coordinated to the zinc atoms rendering them three-coordinate. The two halves of the macrocycle are symmetry related via an inversion centre. The Zn−C bond distances [Zn−C(1) 1.979(3), Zn−C(2) 1.983(3) Å] are in the range as expected for dialkylzinc compounds but the Zn−N coordination bond [2.216(2) Å] is rather long. Consequently, the N−Zn−C(1) bond angle in the chelate ring is acute (87.38°). The fact that the sum of the bond angles around zinc is close to 360° implies that the C(1), C(2), Zn and N atoms essentially lie in the same plane. This together with the large C(1)−Zn−C(2) bond angle [156.38(13)°] suggest that the coordination geometry at zinc is T-shaped rather than trigonal planar.

Reaction of two equivalents of 2-[(dimethylamino)methyl]ferrocenyllithium with $ZnCl_2$ affords the corresponding diorganozinc compound (**68**) in which two 2-[(dimethylamino) methyl]ferrocenyl ligands are *C*,*N*-chelate bonded to zinc[122]. Due to the chirality of the bidentate ligands **68** exists in two diastereoisomeric forms. Indeed, in solution a *meso* one and an (*S*,*S*)/(*R*,*R*) enantiomeric pair in a 1:4 ratio were observed by ^1H and ^{13}C NMR spectroscopy. However, it is only the (*S*,*S*)/(*R*,*R*) enantiomeric pair that preferentially crystallizes from solution. An X-ray crystallographic study of such crystals afforded the structure of (*R*,*R*)/(*S*,*S*)-**68** in the solid state (Figure 35).

The Zn−C bond lengths [Zn−C(1) 1.948(2), Zn−C(2) 1.945(2) Å] are in the range expected for sp^2-hybridized carbon atoms bound to zinc. Also in this case the Zn−N coordinate bonds [Zn−N(1) 2.3091(16), Zn−N(2) 2.3622(16) Å] are rather long. The zinc atom has an extremely distorted tetrahedral coordination geometry, which is expressed by the large C(1)−Zn−C(2) and N(1)−Zn−N(2) bond angles of 155.54(8)° and 115.25(6)°, respectively. The bite angles [C(1)−Zn−N(1) 82.02(7)° and C(2)−Zn−C(2) 83.06(8)°]

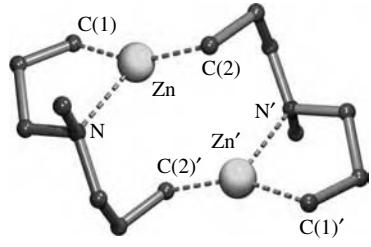

FIGURE 34. Structure of macrocycle **67** in the solid state

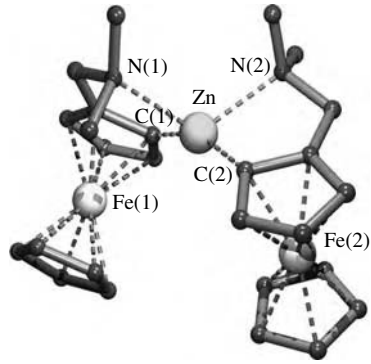

FIGURE 35. Molecular geometry of the (*R*,*R*)-diastereoisomer of **68** in the solid state

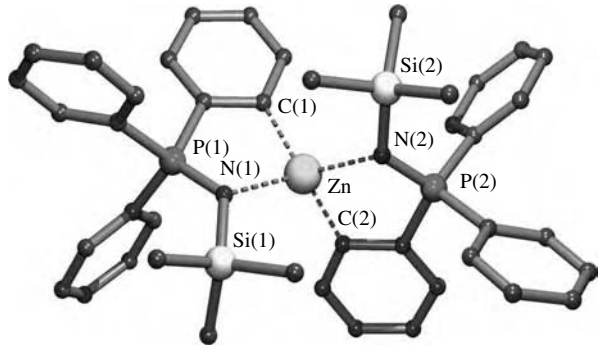

FIGURE 36. Molecular geometry of the bis-iminophosphorane zinc compound **69**

of the *C*,*N*-chelating ligands are small, but typical for this ligand system, and are mainly determined by the radius of the bonded metal.

Compound **69**[123] contains two *C*,*N*-chelate-bonded iminophosphorane ligands and was obtained from the reaction of $ZnCl_2$ with two equivalents of the corresponding *ortho*-lithiated derivative[124]. An X-ray structure determination of **69** revealed a molecular geometry as shown in Figure 36. Because the zinc atom is located on a crystallographic inversion centre, the two *C*,*N*-chelate-bonded ligands are symmetry-related.

The Zn−C bond lengths [2.008(5) Å] are as expected for diarylzinc compounds, but the Zn−N coordinate bonds [2.158(4) Å] are considerably shorter than those in the diorganozinc compounds described above containing an intramolecular coordinating nitrogen atom (e.g. **68**). The zinc atom in **69** has a distorted tetrahedral coordination geometry. The C−Zn−C and N−Zn−N bond angles, 129.28(21)° and 116.07(13)° respectively, are larger than the ideal tetrahedral value. The C−Zn−N bond angles [89.33(18)°] in the five-membered chelate rings are acute, but not as acute as in **68**. This is a consequence of the shorter Zn−N bond lengths in **69** compared to those in **68**.

The structural features of a series of organometallic compounds $[NC_5H_4C(SiMe_3)_2\text{-}2]_2M$ (M = Mg, Zn, Cd, Hg) containing the monoanionic, potentially *C*,*N*-bidentate coordinating $[NC_5H_4C(SiMe_3)_2\text{-}2]$ anion have been studied[125]. It appeared that the Mg,

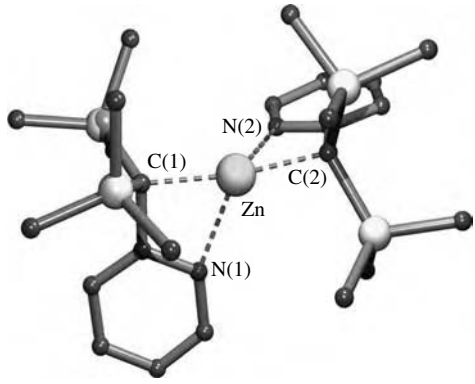

FIGURE 37. Structure of $[NC_5H_4C(SiMe_3)_2\text{-}2]_2Zn$ (**70**)

Zn and Cd compounds are isostructural, having two ligands that are *C*,*N*-chelate bonded to the metal. This is in contrast with the mercury compound in which only the carbon atoms are bonded to the metal in an almost ideal linear C−Hg−C [179.5(3)°] arrangement. In the zinc compound (**70**) both the Zn−C bonds (2.07 Å) and the Zn−N bonds (2.29 Å) are rather long. The coordination geometry around zinc is extremely distorted from tetrahedral (Figure 37). In fact, the C−Zn−C bond angle of 164° suggests a linear rather than a tetrahedral arrangement. On the other hand, the C−Zn−N bond angles in the four-membered chelate ring are extremely acute (67.0°), a consequence of the combination of a four-membered chelate ring with a rather long Zn−N bond.

The bis(benzoyloxymethyl)zinc (**71**) was prepared either from zinc benzoate and diazomethane or from benzoyloxymethyl iodide and Et_2Zn under photolysis conditions (Scheme 9)[126]. Such an acyloxymethylzinc compound appeared to be a reactive carbenoid capable of reacting with a variety of non-functionalized alkenes to afford cyclopropanes in excellent yields (Scheme 9).

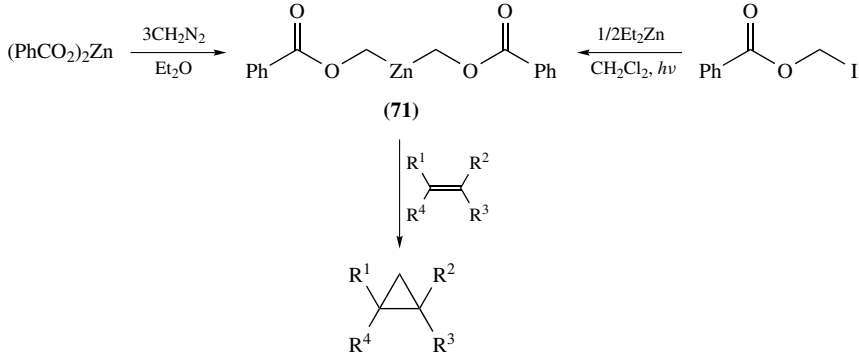

SCHEME 9

During these studies, **71** was obtained as a crystalline material and its structure in the solid state was established by an X-ray crystal structure determination[126]. In **71** the two benzoyloxymethyl groups are symmetry-related via an inversion centre at the zinc position

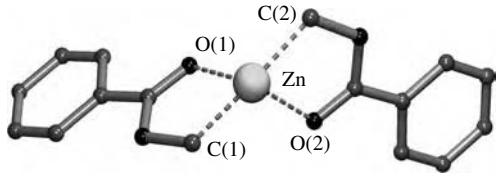

FIGURE 38. Molecular geometry of bis(benzoyloxymethyl)zinc (**71**) in the solid state

and *C*,*O*-chelate-bonded to zinc, rendering the zinc atom four-coordinate (Figure 38). The Zn−C bond length [1.978(2) Å] is in the range expected for an alkylzinc compound. The bond angles around zinc [C(1)−Zn−C(2) 159.35(13)°, O(1)−Zn−O(2) 124.01(18)°, C(1)−Zn−O(1) 80.66(7)° and C(1)−Zn−O(2) 113.53(8)°] point to a distorted square-bipyramidal environment at zinc.

Reaction of α,α'-bis(2-pyridyl)methyllithium with Me_2Zn afforded the unexpected transmetalation product $[MeZnCH(Py)_2]_2$ (**72**) instead of the anticipated triorganozincate[127]. An X-ray crystal structure determination of **72** revealed a dimeric molecule (Figure 39) in which the monomeric parts are arranged in a head-to-tail fashion. In each monomeric part a methylzinc unit is chelate-bonded between the two nitrogen atoms [Zn−N(1) 2.044(2), Zn−N(2) 2.035(2) Å] of one dipyridylmethane unit and bonded to the C_α atom of the other dipyridylmethane unit. The (methyl)−C−Zn bond distance [1.974(3) Å] is quite normal, but the C_α−Zn bond distance [2.269(3) Å] is considerably elongated. This is most likely a consequence of considerable steric strain as the result of two almost eclipsed pyridyl rings (Figure 39).

A rather exotic organozinc compound was obtained starting from 2-pyridylbis(trimethylsilyl)methane, which essentially is the same ligand as is present in deprotonated form in **70** (*vide supra*). Its monolithio derivative was treated with $SbCl_3$ and subsequently with Et_2Zn affording, along with other products, tetrameric $\{[(2\text{-pyridyl})(Me_3Si)C]Zn\}_4$ (**73**) as a crystalline material[128]. An X-ray crystal structure determination revealed a cage-like structure in which four bis-anionic $[(2\text{-pyridyl})(Me_3Si)C]^{2-}$ ligands are bonded to four zinc atoms (Figure 40). As a requirement of the space-group symmetry the tetrameric aggregate has S_4 crystallographic symmetry. The structure consists of a tetrahedron of zinc atoms, while each $[(2\text{-pyridyl})(Me_3Si)C]^{2-}$ ligand spans the face of the tetrahedron with the C_α atom bridge-bonded between two zinc atoms and the pyridyl nitrogen

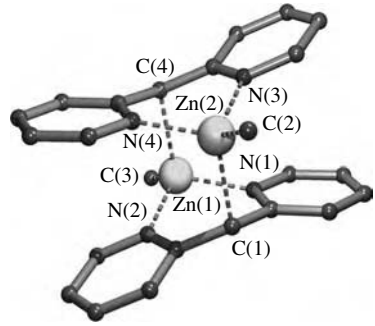

FIGURE 39. Solid state structure of dimeric **72**

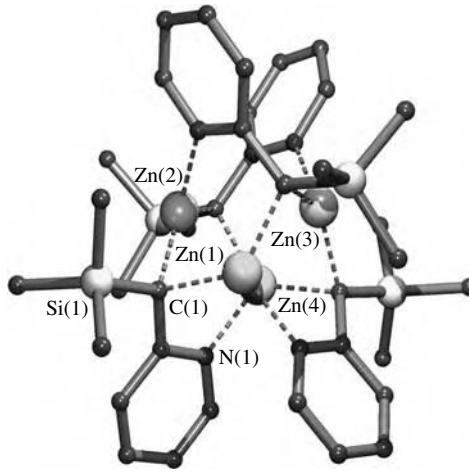

FIGURE 40. Cage-like structure of tetrameric **73** in the solid state

atom coordinating to the third zinc atom. Consequently, the zinc atoms in **73** are three-coordinate. The bridging carbon atom is bonded slightly asymmetric between the two zinc atoms, as is reflected in a small difference in bonding distances [Zn(1)−C(1) 2.040(7), Zn(1)−C(2) 2.024(7) Å]. The Zn−N coordinate bond [2.031(5) Å] is rather short, and most likely is a consequence of its sp^2 character and of the fact that this nitrogen atom is bonding to a three-coordinate zinc centre.

D. Donor–Acceptor Complexes of Diorganozinc Compounds

That diorganozinc compounds are capable of forming donor–acceptor complexes was discovered around 1960. The discovery that ethers like dioxane and DME form well-defined complexes with Me_2Zn[129] and that nitrogen-, phosphorus- and arsenic-containing donor molecules interact with a variety of dialkyl and diaryl zinc compounds to form isolable adducts[130] started a renaissance in the chemistry of organozinc coordination compounds. Before that time it was generally accepted that diorganozinc compounds are unable to form such adducts. Nowadays, it is well-established that diorganozinc compounds readily form complexes with donor molecules[81,82]. Generally, in such complexes two donor atoms interact with the diorganozinc moiety leading to a (distorted) tetrahedral coordination geometry at zinc. More rare are complexes in which only one donor atom is coordinated to zinc, to give trigonal planar coordination at zinc. With one exception, all diorganozinc coordination complexes of which the structure has been determined by X-ray crystallography contain either Zn−N or Zn−O coordination bonds.

Although compounds like $Me_2Zn(OMe_2)$[131] and $Me_2Zn(NMe_3)$[132], which were presumed to contain three-coordinate zinc, have been known for a long time, only very few structures of compounds containing such a structural motif have been established by X-ray crystallography, and these are relatively recent.

Bis[(dimethylisopropoxysilyl)methyl]zinc (**74**) has proven to be a valuable reagent in the nickel-catalysed cross-coupling reactions with alkenylsulfoximines, giving allylic silanes with complete retention of configuration[133]. An X-ray crystal structure determination of **74** showed this compound to exist in the solid state as a coordination polymer (Figure 41)[134]. In **74**, in addition to the two covalent Zn−C bonds [Zn−C(1) 1.953(7)

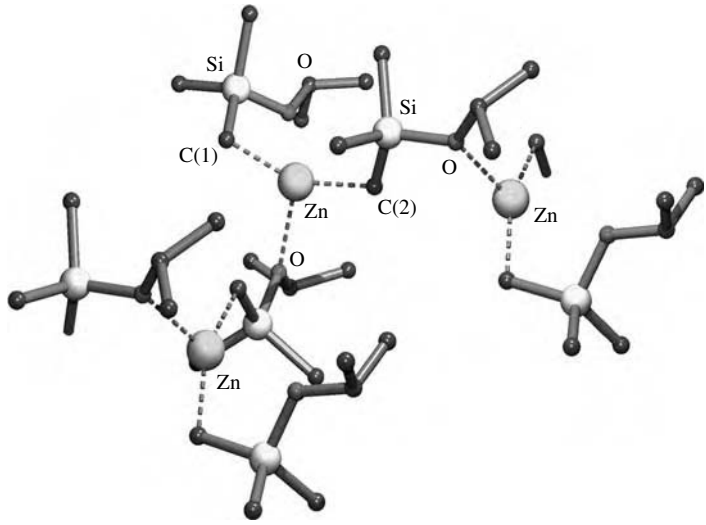

FIGURE 41. Part of the polymeric structure of **74** in the solid state

and Zn−C(2) 1.988(6) Å], the oxygen atom of an isopropoxy group of a neighbouring molecule is coordinated to the zinc atom [Zn−O 2.252(4) Å]. The bond angles around zinc [O−Zn−C(1) 104.2(2)°, O−Zn−C(2) 103.5(2)° and C(1)−Zn−C(2) 152.3(3)°] point to a trigonal planar coordination geometry at zinc. As a result of intermolecular coordination, the molecules are arranged in helices which are perpendicular to the *bc* plane of the unit cell.

A surprising compound (**75**) was obtained as a by-product in low yield from the synthesis of a barium zincate starting from $(Me_3SiCH_2)_2Zn$ and metallic barium in heptane/THF[57]. The X-ray crystal structure determination of this compound revealed a central Ba_2O_2 core arranged in a four-membered ring with three THF molecules coordinated to each barium atom. Each of the oxygen atoms of the central ring is coordinated to the two zinc atoms of a $Me_3SiCH_2ZnCH_2SiMe_2CH_2ZnCH_2SiMe_3$ molecule with bond distances of Zn(1)−O(1) 1.964(3) and Zn(2)−O(1) 1.972(3) Å, respectively (Figure 42). The Zn−C bond distances [Zn(1)−C(1) 2.025(4), Zn(1)−C(2) 1.995(4), Zn(2)−C(3) 2.006(4) and Zn(2)−C(4) 2.043(4) Å] are in the range as expected for sp^3-hybridized carbon atoms bound to zinc. Each of the terminal Me_3SiCH_2 to Zn bonds is slightly elongated due to additional interactions with the respective barium atoms (C−Ba 3.22 Å, average). The zinc atoms have a trigonal planar coordination geometry, as is indicated by the respective bond angles around zinc [O(1)−Zn(1)−C(1) 110.0(2)°, O(1)−Zn(1)−C(2) 116.5(2)°, C(1)−Zn(1)−C(2) 132.6(2)° and O(1)−Zn(2)−C(3) 120.1(2)°, O(1)−Zn(2)−C(4) 110.9(1)°, C(3)−Zn(2)−C(4) 129.0(2)°].

From the reaction of bis[bis(trimethylsilyl)methyl]zinc with 1,3,5-trimethyl-1,3,5-triazine (TMTA) the mono-adduct $[(Me_3Si)_2CH]_2Zn(TMTA)$ (**76**) was isolated as a crystalline material[60]. The X-ray crystal structure determination of **76** revealed a structure in which the zinc atom is three-coordinate as a result of two binding two η^1-$(Me_3Si)_2CH$ groups [Zn−C(1) 1.985(3) and Zn−C(2) 2.002(3) Å] and one of the nitrogen atoms of the TMTA molecule (Figure 43). The latter Zn−N coordinate bond is relatively long [2.387(2) Å]. Whereas the C(1)−Zn−C(2) bond angle [157.4(1)°] deviates considerably

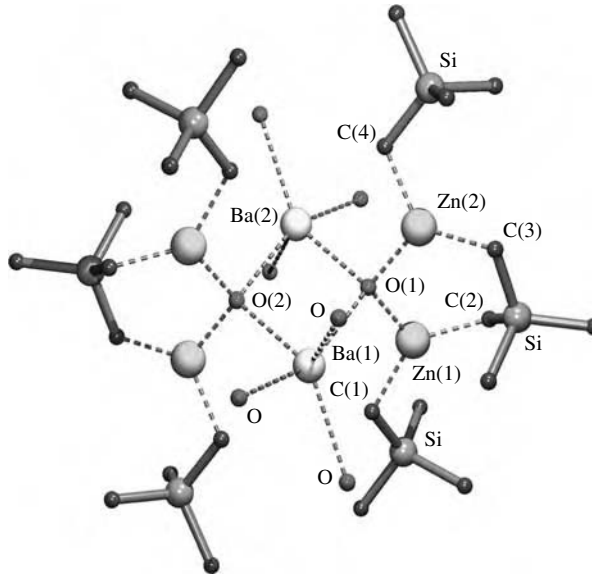

FIGURE 42. Molecular geometry of **75** in the solid state. Note that the CH_2 groups of the coordinated THF molecules are omitted for clarity

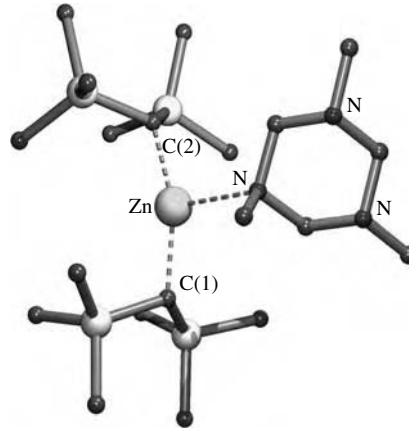

FIGURE 43. Solid state structure of coordination complex **76**

from the ideal value of 120°, the sum of the bond angles around zinc of 360° indicates a perfectly planar arrangement at zinc. That the Zn−N coordination bond is relatively weak indeed is indicated by the fact that **76** is dissociated to a large extent into $[(Me_3Si)_2CH]_2Zn$ and free TMTA when dissolved in apolar solvents like benzene.

Reaction of tri(*tert*-butyl)sulfurtriimide with one equivalent of MeLi followed by an *in situ* reaction with one equivalent of Me_2Zn afforded the bimetallic compound **77** (equation 19)[135]. The molecular geometry of **77** was unambiguously established by an

X-ray crystal structure determination. The lithium atom is *N*,*N*-chelate bonded to the monoanionic ligand while a tetrahedral coordination geometry at lithium is reached by the coordination of two additional THF molecules. The presence of considerable conjugation in this part of the molecule is reflected by the almost equal N−Li distances [2.014(4) and 2.000(4) Å] and almost equal S−N distances [1.5607(17) and 1.5622(17) Å]. The third nitrogen atom acts as a neutral donor to the dimethylzinc molecule [Zn−N 2.1374(17) Å] rendering the zinc atom trigonal planar.

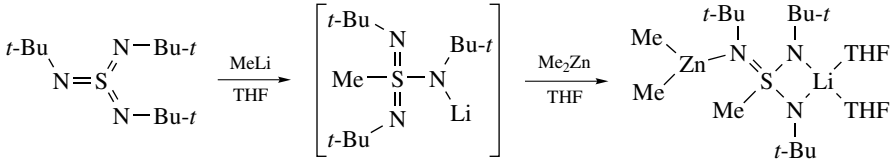

(77) (19)

For a long time it has been known that dialkylzinc compounds can deprotonate secondary carboxylic amides affording heteroleptic alkylzinc carboxylic amides which, according to molecular weight determinations in solution, are highly aggregated species[136]. The actual structural elucidation of these compounds by X-ray crystallography is from a more recent date and will be discussed elsewhere in this chapter. These alkylzinc carboxylic amides react with *t*-BuLi to afford the novel species **78** and **79** (Scheme 10). The author describes **78** and **79** as organozincates, but in fact they are lithium enolates in which the terminal imino-nitrogen atoms are coordinated to a *t*-Bu_2Zn moiety[137].

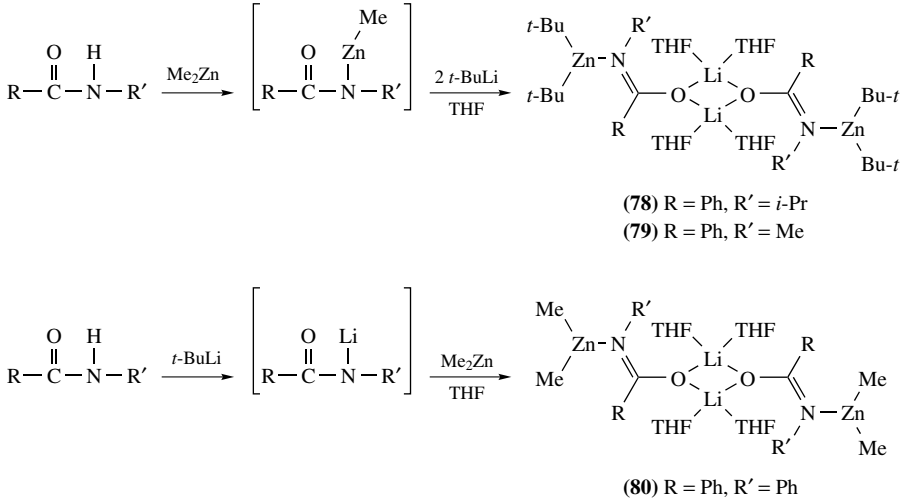

(78) R = Ph, R′ = *i*-Pr
(79) R = Ph, R′ = Me

(80) R = Ph, R′ = Ph

SCHEME 10

Another synthetic approach towards the synthesis of compound **80** involves prior deprotonation of the carboxylic amide with *t*-BuLi, which is then followed by reaction with dimethylzinc (Scheme 10). All three compounds have similar structural features, i.e. they are dimers as a result of two *O*-bridging enolate anions between two lithium atoms. The

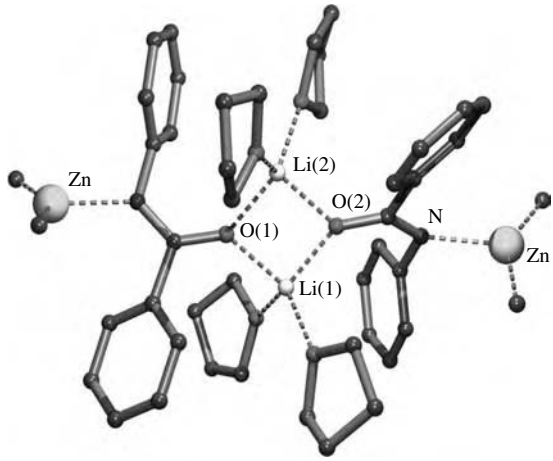

FIGURE 44. Molecular geometry of **80** in the solid state

terminal imino-nitrogen atoms are coordinated to the dialkylzinc units. The solid state structure of **80** is shown in Figure 44 as a representative example.

That a particular combination of substituents, i.e. R and R′ and the diorganozinc compound, may influence the overall structure of this type of compounds was shown by the X-ray crystal structure determination of the *t*-Bu_2Zn derivative of **80**. The latter structure consists of a tetrameric aggregate in which the four enolate oxygen atoms and the four lithium atoms are arranged in a 'ladder'-type arrangement while two of the imino-nitrogen atoms are involved in nitrogen–lithium coordination and the other two imino-nitrogens are coordinated to *t*-Bu_2Zn units.

The structural features of the dialkylzinc units in these compounds are closely related, i.e. the zinc atoms are trigonal-planar coordinated, with C−Zn distances as expected. The Zn−N coordination bonds range from 2.078 to 2.184 Å and the C−Zn−C bond angles range from 132° to 145°.

So far, only coordination complexes of diorganozinc compounds were considered in which one additional ligand is coordinated via its heteroatom to zinc, thus affording a trigonal planar coordination geometry at zinc. This is a rather rare situation for zinc, and complexes containing either two monodentate or one bidentate chelating ligand, thus affording a (distorted) tetrahedral coordination geometry, are far more common for zinc. With one exception the heteroatoms involved in coordination to zinc are always either oxygen or nitrogen atoms (at least for compounds of which the structure was established by an X-ray crystal structure determination). Due to the rather soft character of zinc in diorganozinc compounds, the Zn−N coordination bonds in these complexes are generally stronger than corresponding Zn−O coordination bonds.

It should be noted that most diorganozinc coordination complexes having a tetrahedral coordination geometry are discrete monomers in which the Zn−C bond distances in the diorganozinc moieties are as expected for sp^3 (in alkylzinc) or sp^2 (in arylzinc) carbon atoms. However, C−Zn−C bond angles may vary and seem to be dependent on the nature of the particular heteroatom that is involved in coordination to zinc. Also, the Y−Zn−Y (Y = coordinating heteroatom) bond angle may vary, depending on the particular ligand.

In Table 5, relevant structural features of diorganozinc complexes containing two coordinating oxygen atoms are compiled; only those compounds that have special structural features will be discussed in more detail.

TABLE 5. Relevant structural features of R_2ZnL_2 complexes (L = O-coordinating ligand)

Compound	R	L	Zn−O	C−Zn−C	O−Zn−O	Reference
81	C_6F_5	THF	2.093(2), 2.113(3)	132.1(2)	92.4(1)	138
82	1-fluorenyl	THF	2.095(4), 2.114(5)	117.6(2)	89.3(2)	139
83	[a]	THF	2.209(1), 2.272(1)	130.3(6)	85.7(5)	140
84	C_6H_5	DME	2.287(4), 2.259(4)	146.6(2)	72.16(14)	141
85	CH_2I	[b]	2.10(1), 2.20(1)	138.4(7)	72.7(4)	142
86	C_2H_5	Ni[Salen]	2.321(6), 2.321(6)	147.9(4)	63.1(2)	143
87	C_6H_5	[c]	2.274(6), 2.264(6)	139.6(3)	71.6(2)	144
88	C_6H_5	[d]	2.239(3), 2.328(3)	146.7(2)	72.4(1)	144
89	C_6H_5	[e]	2.300(3), 2.310(3)	145.5(2)	72.68(9)	144

[a] 1,2-C_6H_4.
[b] (*R*)-2,3-Dimethoxy-4,7,7-trimethylbicyclo[2.2.1]heptane.
[c] 2-Bromo-1,3-xylyl 15-crown-4.
[d] 2-Bromo-1,3-xylyl 18-crown-5.
[e] 1,3-Xylyl 18-crown-5.

A common structural feature of compounds **81–89** is their distorted tetrahedral coordination geometry at zinc. A trend that can be observed in Table 5 is that with increasing Zn−O distances, the C−Zn−C angle also increases and consequently the O−Zn−O angle decreases. From a structural point of view **83** has interesting structural features. In this complex two 1,2-phenylene dianionic units are *C*, *C*-bridge bonded between two zinc atoms (Figure 45) and it represents one of the few examples of polymetallated compounds for which the structure has been established by an X-ray crystal structure determination[140].

It is interesting to compare the structure of **84** and of the diglyme complex of Ph_2Zn (**90**) (Figure 46)[141]. In the latter compound all three oxygen atoms of the diglyme ligand are involved in coordination to zinc, resulting in the formation of an unprecedented and still unique example of pentacoordination in diarylzinc chemistry. It is remarkable that the Ph_2Zn units in both complexes are almost identical, which is obvious from the comparable C(1)−Zn−C(2) bond angles [146.6(2)° in **84** and 149.7(3)° in **90**]. However, in **90** all O−Zn bond distances are longer than those in **84**, i.e. 2.483(5), 2.330(5) and 2.509(6) Å in **90** vs. 2.287(4) and 2.259(4) Å in **84**. The coordination geometry at zinc in **90** is neither a trigonal bipyramid nor a square planar pyramid and its configuration does not lie on the Berry pseudo-rotation path between the two.

It is remarkable that in the diphenylzinc crown-ether complexes **87–89** the Ph_2Zn unit is placed outside the crown, in contrast to the Ph_2Mg analog of **89** which exists in the

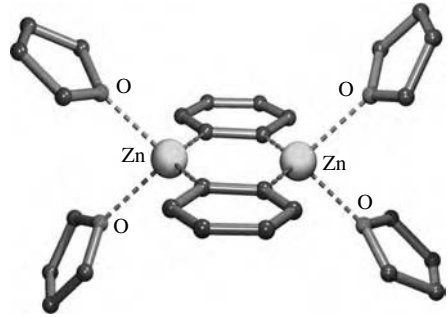

FIGURE 45. Structure of **83** in the solid state

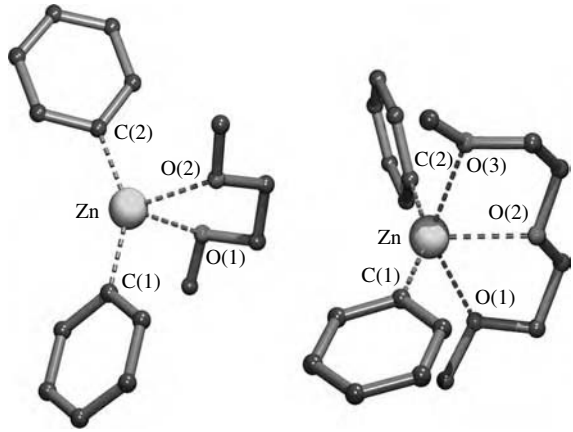

(84) **(90)**

FIGURE 46. Solid state structures of **84** and **90**

solid state as an organometallic rotaxane[145]. In **87–89** the crown ether acts as a bidentate chelating ligand. In fact, in these compounds the structure around zinc is identical to that in the DME complex of Ph_2Zn (Table 5).

Both Et_2Zn and Ph_2Zn form rotaxane structures with 18-crown-6, **91** and **92**, respectively (Figure 47)[146, 147]. In **91**, the zinc atom is located on a crystallographic inversion centre and consequently the C(1)−Zn−C(2) bond angle is 180°. The Zn−O bond distances are extremely long [2.837(3), 2.890(3) and 2.873(3) Å]. Compound **92** has a less symmetric structure but the C−Zn−C bond angle of 174.5(1)° is close to linear. Also, in this compound the Zn−O distances are extremely long [2.634(3) to 3.024(3) Å]. In fact, these compounds may be regarded as clathrates containing a diorganozinc encapsulated within

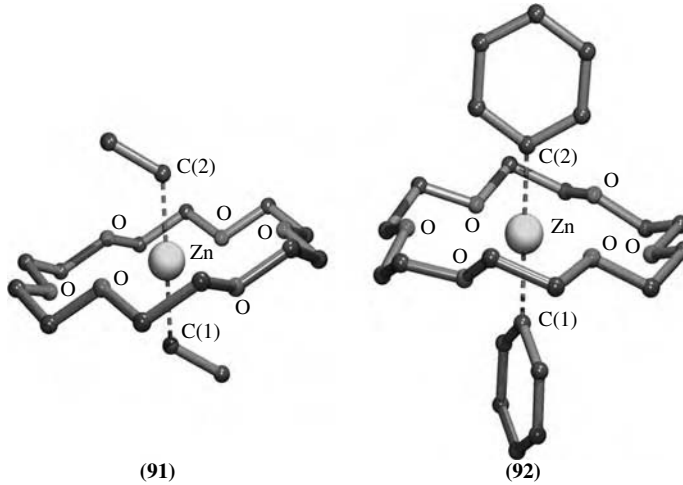

(91) **(92)**

FIGURE 47. Solid state structures of the organometallic rotaxanes **91** and **92**

a crown ether but with very weak Zn−O bonds. The formation of these organometallic rotaxanes has been explained by a mechanism involving a 'peripherally'-crown-ether-coordinated diorganozinc that subsequently disproportionates to triorganozincates and monoorganozinc cations encapsulated in the crown ether[148].

The structure of the diphenylzinc tetrahydrothiophene complex (**93**) is the only example of a diorganozinc compound in which Zn−S coordination bonds are present[149]. Like in diphenylzinc itself[9] the solid state structure of **93** consists of dimeric molecules in which two of the phenyl groups are bridging between two zinc atoms and each of the zinc atoms contains a terminal phenyl group. In addition, one tetrahydrothiophene molecule is coordinated to each zinc atom via its sulfur atom (Figure 48). The bridging aryl group in **93** is less asymmetrically bonded [Zn(1)−C(1) 2.114(2) and Zn(2)−C(1) 2.261(2) Å] compared with these bridges in the diphenylzinc dimer. The Zn−S bond distance is 2.5025(5) Å, which is slightly longer than the sum of the covalent radii (2.35 Å), indicating a relatively weak coordination of the ligand. The bond angles around zinc are close to the ideal tetrahedral value, indicating a slightly distorted tetrahedral geometry at zinc.

The complex of dimethylzinc with 2-(1-methoxypropyl)ferrocenylaldimine, in which the 2-(1-methoxypropyl)ferrocenylaldimine ligand is *N*,*O*-chelate-bonded to zinc [Zn−N 2.213(2), Zn−O 2.381(2) Å], is the only example of a diorganozinc coordination complex in which in one complex both Zn−N and Zn−O coordination occurs[149]. The coordination geometry at zinc is distorted tetrahedral with a larger C−Zn−C (141.6°) and a smaller N−Zn−O (74.9°) bond angle.

The only two structurally characterized complexes of diorganozinc compounds, in which two monodentate N-coordinating ligands are present, are $Me_2Zn[(CH_2NMe)_3]_2$ [$(CH_2NMe)_3$ = hexahydro-1,3,5-trimethyl-1,3,5-triazine] and $(CF_3)_2Zn(Pyr)_2$. In both complexes the zinc atoms have a distorted tetrahedral coordination geometry. In $Me_2Zn[(CH_2NMe)_3]_2$, the Zn−N bond distance is relatively long [2.410(4) Å] combined with a N−Zn−N bond angle of 105.6 (2)° and a C−Zn−C bond angle of 145.1 (2)°[150]. The structural features of $(CF_3)_2Zn(Pyr)_2$ are similar[151], although the Zn−N coordination bonds are relatively short [2.075(2) and 2.082(2) Å]. However, the Zn−C bond lengths [2.056(3) and 2.069(4) Å] are slightly elongated compared to those found in other sp^3 C−N bonding motifs.

Diethylzinc forms a 1:1 complex with DABCO, Et_2Zn(DABCO) (**94**). An X-ray crystal structure determination revealed that Et_2Zn(DABCO) exists in the solid state as a coordination polymer in which Et_2Zn units are linked by the two coordinating nitrogen atoms

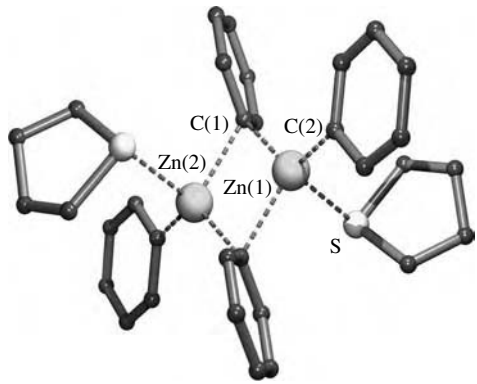

FIGURE 48. Solid state structure of dimeric **93**

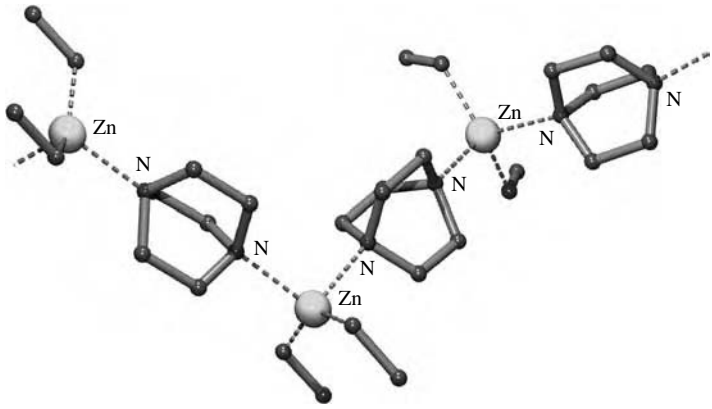

FIGURE 49. Polymeric structure of **94** in the solid state

of DABCO molecules (Figure 49)[152]. Also in this case, the zinc atoms have a distorted tetrahedral coordination geometry.

Ethylzinc-enamine (**95**) undergoes a condensation reaction with aldehydes, affording ethylzinc-aldolates (equation 20)[153]. Such ethylzinc-aldolates are dimers, due to bridging of the aldolate-oxygen atoms between two zinc atoms. The structural features of this type of compounds will be discussed elsewhere in this chapter.

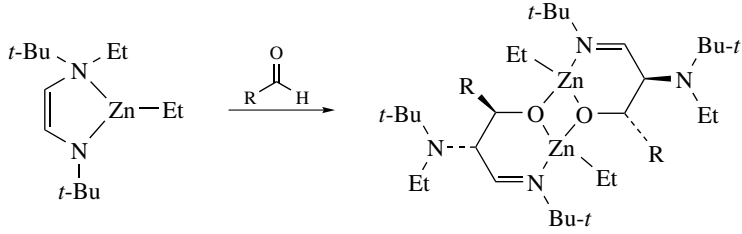

(20)

(95) **(96)** R = 4-Pyr

When **95** is reacted with 4-pyridinecarboxaldehyde, ethylzinc aldolate (**96**) is obtained (equation 20). When a solution of **96** is treated with excess diethylzinc, a crystalline material (**97**) is obtained which appears to be a coordination polymer. This polymer consists of dimeric ethylzinc-aldolate units, linked to a polymeric chain via coordination of the peripheral pyridyl groups to diethylzinc units (Figure 50)[154]. The diethylzinc units in **97** are distorted tetrahedral with C−Zn−C and N−Zn−N angles of 145.7(6)° and 89.4(4)°, respectively.

The large majority of diorganozinc complexes of which the structure in the solid state has been elucidated are those in which a *N*,*N*-chelating ligand is coordinated to the zinc atom. The relevant structural features of all these compounds are summarized in Table 6.

The geometry at zinc in all compounds is comparable, i.e. the zinc atoms have a distorted tetrahedral coordination geometry. The Zn−C bond lengths are as expected for sp^3-bonded carbon atoms to zinc. A larger variation is seen in the C−Zn−C bond angles and the Zn−N coordinate bond lengths. The N−Zn−N angles seem to be governed by the bite angle of the particular chelate ligand involved. When TMEDA complexes **98–103**

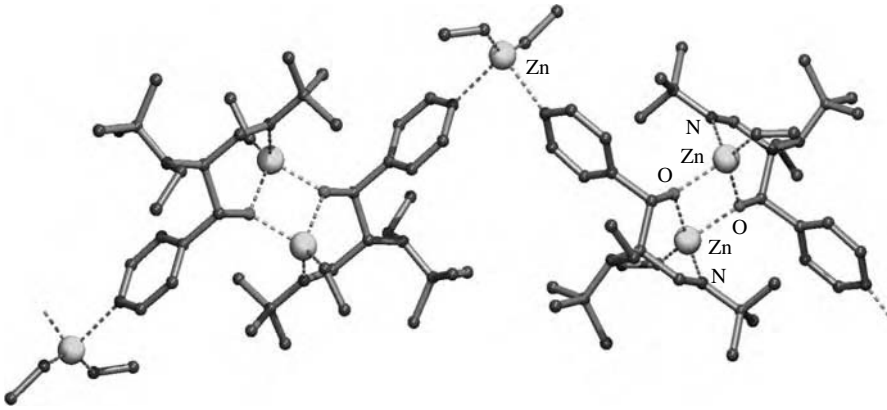

FIGURE 50. Part of the polymeric chain of coordination polymer **97**

TABLE 6. Relevant structural features of R_2ZnN_2 complexes ($N_2 = N,N$-chelating ligand)

Compound	R	N_2	Zn−N (Å)	C−Zn−C (°)	N−Zn−N (°)	Reference
98	Me	TMEDA	2.260(8), 2.278(8)	135.8(3)	79.8(3)	155
99	Me_3CCH_2	TMEDA	2.411(4), 2.411(4)	148.3(1)	77.3(2)	155
100	Et	TMEDA	2.293(5), 2.293(5)	118	80.7(2)	128
101	Bn	TMEDA	2.202(3), 2.209(3)	122.2(2)	82.7(1)	156
102	$Ph(Me_3Si)CH$	TMEDA	2.329(4), 2.314(4)	141.6(2)	79.6(1)	156
103	$Ph(Me_3Si)CH$, Me [a]	TMEDA	2.207(2), 2.260(2)	131.1(1)	81.57(7)	157
104	Me	Sparteine	2.222(5), 2.256(6)	128.2(4)	80.4(2)	158
105	Me	N_4-aza crown [b]	2.282(3), 2.282(3)	125.5(2)	87.21(9)	159
106	Me	N_6-aza crown [c]	2.331(2), 2.257(2)	138.1(1)	80.35(7)	159
107	Me	(*S*,*S*)-ebpe [d]	2.230(3), 2.230(3)	134.8(2)	80.3(2)	160
108	Me	2,2′-bipy [e]	2.116(9), 2.116(9)	127.9(1)	74.3(6)	161
109	$(Me_3Si)_2CH$	2,2′-bipy [e]	2.179(4), 2.196(5)	126.4(2)	74.1(3)	162
110	ICH_2	2,2′-biqui [f]	2.135(7), 2.141(6)	125.5(3)	76.8(2)	163
111	$ClCH_2$	2,2′-biqui [f]	2.117(4), 2.137(4)	127.7(3)	77.0(2)	163
112	Me	*t*-BuDAB [g]	2.207(7), 2.225(7)	137.3(3)	75.0(2)	164

[a] The R_2Zn moiety contains two different R groups.
[b] 1,4,8,11-Tetramethyl-1,4,8,11-tetraazacyclotetradecane.
[c] 1,4,7,10,13,16-Hexamethyl-1,4,7,10,13,16-hexaazacyclooctadecane.
[d] (*S*,*S*)-*N*,*N*′-Ethylenebis(1-phenylethylamine).
[e] 2,2′-Bipyridine.
[f] 2,2′-Biquinoline.
[g] 1,4-Di-*tert*-butyl-1,4-diaza-1,3-butadiene.

are compared, the general trend is that the C−Zn−C bond angle increases with increasing steric bulk of the organic groups bound to zinc. Me_2Zn(TMEDA) (**98**) is an exception in that it has a relatively large C−Zn−C bond angle [135.8(3)°] while this compound has the least sterically demanding groups bound to zinc.

It is interesting to note that the Me_2Zn complexes of the macrocyclic amines N_4-aza crown and N_6-aza crown (Table 6)[159], **105** and **106**, respectively, display a different coordination behaviour. Both macrocyclic amines coordinate to two Me_2Zn units each, using two nitrogen atoms. In **105**, the two Me_2Zn units are coordinated in such a way that two six-membered chelate rings are formed. In **106**, the only possibility is the formation of five-membered chelate rings.

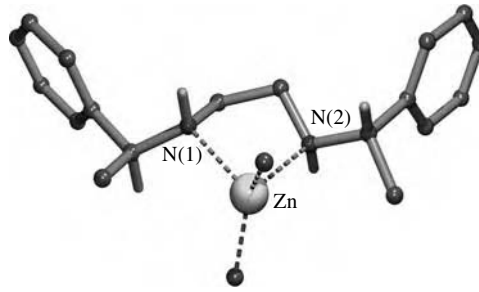

FIGURE 51. Solid state structure of $Me_2Zn[(S,S)$-ebpe] (**107**)

The complex of Me_2Zn with (*S*,*S*)-ebpe, **107**, has been applied successfully as catalyst in the enantioselective reduction of ketones by polymethylhydrosiloxane and combines excellent product yields with high ee values[160]. Its structure comprises the *N*,*N*-chelate coordination of the ebpe ligand to the Me_2Zn unit (Figure 51). It is remarkable that in this case the two secondary amine functionalities are coordinated to zinc and leave the Zn−C bonds unaffected. Indeed, usually secondary amines undergo a fast deprotonation reaction with dialkylzinc compounds.

It has already been known for a long time that haloalkylzinc compounds are excellent reagents in cyclopropanation reactions[165]. Such compounds, however, are rather unstable and are usually prepared *in situ*. It appears that 2,2′-bipyridine and 2,2′-biquinoline stabilize these haloalkylzinc compounds to a large extent[163]. Compounds **110** and **111** (Table 6) are examples of stabilized cyclopropanating reagents that can be stored as solid materials over a longer period of time.

The diorganozinc coordination complexes considered so far are all colourless materials. However, the bipyridine complexes **108** and **109**, the biquinoline complexes **110** and **111** and the *t*-BuDAB complex **112** (Table 6) are intensely coloured. This feature has been studied for a series of R_2Zn(*t*-BuDAB) complexes (R = Me, Et, *i*-Pr, *t*-Bu)[166, 167]. It appeared that the absorption maximum is dependent on the nature of the R group bound to zinc and shifts to longer wavelengths in the order R = Me, primary-alkyl, secondary-alkyl, tertiary-alkyl (Table 7). It has been suggested that the intense colour of these complexes is caused by a $S_0 \rightarrow S_1$ LLCT transition $\sigma(\text{Zn}-\text{C}) \rightarrow \pi^*$ (*t*-BuDAB)[164, 167]. Furthermore, it appeared that in contrast to, e.g., R_2Zn(bipy) complexes, which are stable compounds, the R_2Zn(*t*-BuDAB) complexes are intrinsically unstable and undergo an intramolecular reaction. This was a serendipitous observation when Et_2Zn was reacted with *t*-BuDAB. An *N*-alkylated product was obtained instead of the anticipated Et_2Zn(*t*-BuDAB) complex[167]. The temperature at which the intramolecular reaction starts in the initially formed R_2Zn(*t*-BuDAB) complexes depends on the nature of the R group bound to zinc (Table 7). Computational studies on R_2Zn(*t*-BuDAB) complexes, R = Me, Et, *i*-Pr, *t*-Bu, showed that the LUMOs of these complexes, which are localized within the chelated ligand, have comparable energy levels. However, the HOMO energies increase in the series R = Me < Et < *i*-Pr < *t*-Bu. This is also reflected in the stabilities of the corresponding complexes with R_2Zn of which *t*-Bu_2Zn(*t*-BuDAB) is only stable below −90 °C and Me_2Zn(*t*-BuDAB) is stable at room temperature (Table 7).

The initial reaction step when the temperature of the R_2Zn(*t*-BuDAB) complex reaches its conversion temperature (Table 7) is an intramolecular SET leading to the [RZn(*t*-BuDAB)]$^{\bullet}$/R$^{\bullet}$ radical pair (Scheme 11)[164, 168]. The further reaction path depends on the nature of the R group. When R = Me, a mixture of products **B**, **C** and **D** (Scheme 11)

TABLE 7. Characteristic features of $R_2Zn(t\text{-BuDAB})$ complexes

R	Colour	λ_{max} (nm)	Conversion temp (°C)
Me	orange	390	25
Et	red	490	−50
i-Pr	blue	590	−70
t-Bu	purple	650	−90

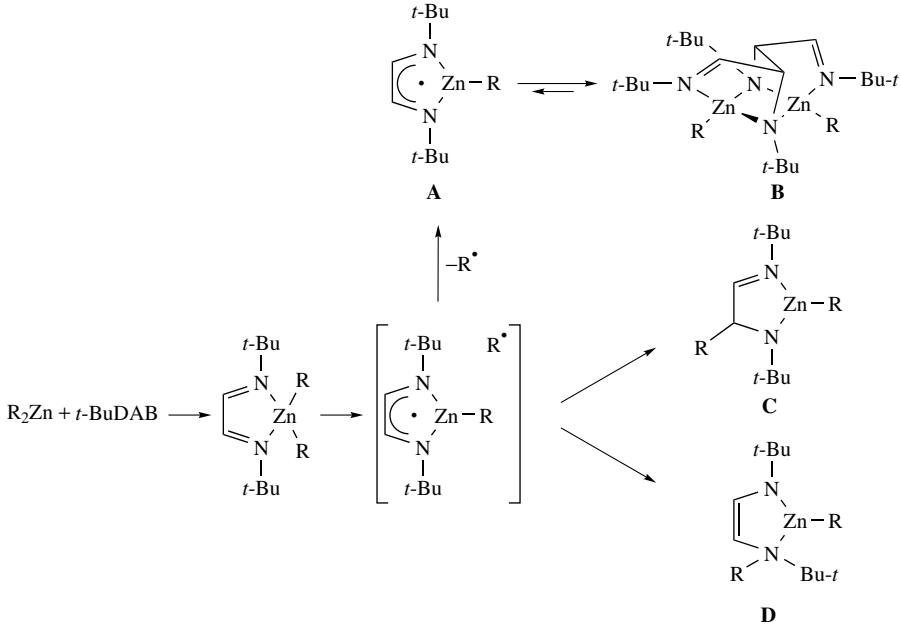

SCHEME 11

in 2:1:1 ratio is obtained. The formation of **B** involves a pathway in which the R radical escapes from the solvent cage followed by dimerization of the organometallic $RZn(t\text{-BuDAB})$ radical **A**. The formation of products **C** and **D** is the result of transfer of the R radical to the imine carbon atom and the imine nitrogen atom, respectively. When R is any primary alkyl group, the predominant product is **D** and traces of **B** are observed. When R is a secondary alkyl group, a mixture of **C** and **D** (2:1 ratio) and traces of **B** are obtained. When R = *t*-Bu, almost exclusively **C** in addition to traces of **B** are obtained.

The formation of the $RZn(t\text{-BuDAB})$ radicals is notable and it appeared that these radicals are examples of persistent organometallic radicals in equilibrium with their C−C coupled dimer. These dimers could be independently synthesized in high yield from the reaction of (*t*-BuDAB)K and the corresponding RZnCl compound. The rate constant of the equilibrium between the persistent radical and its C−C coupled dimer is sufficiently small to study the dimers by NMR spectroscopy and the radicals by ESR spectroscopy[164, 169]. The obtained ESR data are in agreement with a structure for the radical in which the zinc atom adopts a trigonal planar geometry. In this respect it should be noted that the *in situ*

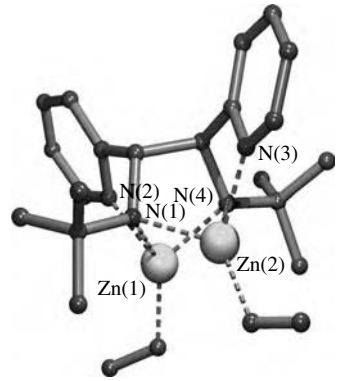

FIGURE 52. Solid state structure of **113**

formation of EtZn(bipy) radicals from the reaction of (bipy)K and EtZnCl has also been reported[170].

For one of the C−C coupled dimers, i.e. the one with $R = Me_3SiCH_2$ (**113),** the structure in the solid state was unambiguously established by an X-ray crystal structure determination[169]. The structure comprises a C−C coupled dimer of the *t*-BuDAB ligand in which the length of the formed C−C bond (1.62 Å) is notable and it is considerably longer than expected for a normal sp^3-C−sp^3-C bond. Each of the two imido nitrogen atoms bridges between two EtZn units while each of the terminal imino nitrogen atoms coordinates to a zinc atom, thus rendering each zinc atom a distorted tetrahedral coordination geometry. A similar structure was observed for the C−C coupled dimer (**113**) (Figure 52), obtained from dimerization of the corresponding radical EtZn(pyca) from the thermolysis reaction of Et_2Zn(pyca) (pyca = *N*-*tert*-butyl-2-pyridinecarbaldimine)[168, 171]. These R_2Zn(pyca) complexes show a similar intramolecular reactivity to that observed for the R_2Zn(*t*-BuDAB) complexes, but more forcing conditions are required (boiling toluene). Moreover, the pathway resulting in *N*-alkylated products (Scheme 11) is blocked, because this would require de-aromatization of the pyridyl group, which is an energetically highly unfavourable process.

IV. HETEROLEPTIC RZnY COMPOUNDS

A. Introduction

In heteroleptic monoorganozinc compounds one organic group is σ-bonded via a carbon atom to the zinc atom. The other group, Y, is bound to zinc via an electronegative heteroatom. Examples of such groups are halogen atoms, oxygen-containing groups like alkoxides, enolates and carboxylates, nitrogen-containing groups like primary and secondary amides, and other groups functionalized with heteroatoms like sulfur, phosphorus, arsenic and selenium. These monoorganozinc–hetero compounds are among the first organozinc compounds discovered; cf. EtZnI by Frankland in 1849[1].

Three major synthetic pathways towards heteroleptic monoorganozinc compounds are available (Scheme 12). The first one involves the reaction of an organic halide with activated metallic zinc as applied in the original synthesis of EtZnI from EtI and Zn[1]. Other examples are the formation of the Reformatsky reagent from α-bromoesters and metallic zinc[172, 173], the formation of the Simmons–Smith reagent, ICH_2ZnI, from CH_2I_2 and metallic zinc[174] and the formation of polyfunctional organozinc reagents[175].

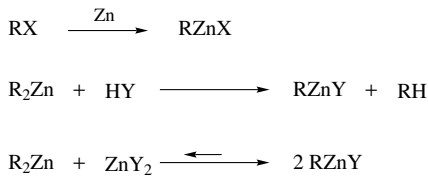

X = Br, I
Y = heteroatom-functionalized organic group

SCHEME 12

The second important route involves the protonolysis of one of the alkyl or aryl groups of dialkyl- or diarylzinc compounds by an organic molecule containing an acidic proton bound to a heteroatom, e.g. alcohols[176, 177] and primary[178] and secondary amines[176, 179]. It is remarkable that one of the alkyl or aryl groups can be removed selectively. When one of the organic groups is protolysed, the reactivity of the remaining zinc–carbon bond is much diminished[82]. It is possible to remove this second organic group, but that in general requires forcing conditions.

The third reaction pathway involves the redistribution reaction of a dialkyl- or diarylzinc compound with a zinc salt. An example of this route is the formation of the unsolvated organozinc halides EtZnCl, EtZnBr and EtZnI from the reaction of pure Et_2Zn with the corresponding zinc halide in a 1:1 ratio[180].

Due to the presence of an electronegative group directly bound to zinc, the Lewis acidity of the zinc atom in the heteroleptic monoorganozinc compounds is enhanced and they readily form complexes with donor molecules, in which the zinc atom has a tetrahedral coordination geometry. A typical feature of such heteroleptic monoorganozinc compounds is their tendency to form aggregates[181]. With only a very few exceptions often very complicated, aggregated structures occur as a result of the presence of heteroatoms, that are bridging and act as multi-electron donors, between zinc atoms.

A factor that always should be taken into account in case of heteroleptic monoorganozinc compounds, especially in solution, is the existence of Schlenk equilibria (equation 21).

$$2\ RZnY \rightleftharpoons R_2Zn + ZnY_2 \tag{21}$$

The equilibrium position is dependent on several factors: (i) the nature of the groups bound to zinc, (ii) the nature and polarity of the solvent and (iii) the presence of additional donor molecules. It is therefore dangerous to draw conclusions from structural information about materials that crystallize from these equilibrium mixtures. Such solid materials are not necessarily representative for the 'bulk' material.

Based on the heteroatom directly bound to zinc, the structures of heteroleptic monoorganozinc compounds can be divided into several subclasses that will be discussed separately below. These subclasses are (i) monoorganozinc cations (i.e. compounds consisting of ion pairs), (ii) monoorganozinc halides, (iii) monoorganozinc compounds with one oxygen atom σ-bonded to zinc, (iv) monoorganozinc compounds with one nitrogen atom σ-bonded to zinc and (v) monoorganozinc compounds containing anions σ-bonded to zinc via other heteroatoms.

B. Monoorganozinc Cations

In the presence of crown ethers, aza-crowns or cryptands, the formation of monoorganozinc cations has been observed in solution when diorganozinc compounds

are treated with Lewis acids that are capable of accepting an alkyl anion, e.g. Et_3Al[73]. Similarly, a 1:1 mixture of Et_2Zn and Ph_2Zn in the presence of 14N4 (1,4,8,11-tetramethyl-1,4,8,11-tetraazacyclotetradecane) undergoes a disproportionation reaction leading to a $[EtZn(14N)]^+$ cation and a $[MePh_2Zn]^-$ anion[72]. Furthermore, it has been suggested that crown ether-complexed monoorganozinc cations play an important role in the formation of diorganozinc-crown ether rotaxanes[148].

The reaction of Et_2Zn with Jutzi's acid $[(Et_2O)H][B(C_6F_5)_4]$ in a 1:1 molar ratio in diethyl ether as a solvent proceeds quantitatively under the formation of $[EtZn(OEt_2)_3][B(C_6F_5)_4]$ (**114**) and one equivalent of ethane[182]. The structure of **114** in the solid was established by an X-ray crystal structure determination. The monoclinic unit cell contains four $[EtZn(OEt_2)_3]^+$ cations (Figure 53) and four $[B(C_6F_5)_4]^-$ anions that have no further interactions. The $[EtZn(OEt_2)_3]^+$ cation has a slightly distorted tetrahedral geometry as a result of the coordination of three additional diethyl ether molecules. The C−Zn−O bond angles range from 115.37(10)° to 123.60(9)°. The Zn−C(1) bond distance of 1.964(3) Å is of the same order as in neutral dialkylzinc compounds. The Zn−O distances of 2.1096(17), 2.0313(18) and 2.073(18) Å are considerably shorter than the Zn−O coordination bonds in neutral diorganozinc-*O*-coordination complexes, most likely as a consequence of the enhanced Lewis acidity of monoorganozinc cations.

A series of EtZn cationic complexes, stabilized by coordination of *N*-alkylated 1,3,5-triazacyclohexanes with weakly coordinating counter anions like ClO_4^-, BF_4^- or $B(C_6F_5)_4^-$, has been reported. These complexes are readily available via protonolysis of Et_2Zn with an acidic tertiary ammonium salt in the presence of the corresponding triazacyclohexane[183]. The structure in the solid state of one of these complexes, i.e. the one containing a 1,3,5-tribenzyl-1,3,5-triazacyclohexane ligand complexed to a EtZn cation and a PF_6 counter-anion (**115**), has been determined by X-ray crystallography[184]. As a result of the coordination of all three nitrogen atoms of the ligand to the EtZn cation the zinc atom has a distorted tetrahedral geometry (Figure 54). As a consequence of the rather rigid configuration of the ligand the N−Zn−N angles are acute [62.37(6)°, 63.20(7)° and 62.37(6)°], but the C−Zn−N angles [137.31(9)°, 153.33(13)° and 137.31(9)°] are larger than expected for a tetrahedral geometry. In the crystal lattice two *trans*-orientated fluorine atoms of the PF_6 anion have interactions (2.85 Å) with the zinc atoms of two neighbouring EtZn cations, leading to a one-dimensional chain structure.

The synthesis and structural characterization of a compound containing *p*-tolylzinc cations complexed to a *N*,*N*,*N*,*N*-tetradentate ligand with a tetraphenylcyclopentadienyl anion as the counterpart has been reported[185]. It seems that all four nitrogen atoms are involved in coordination to zinc, thus giving a penta-coordinate EtZn cation. However,

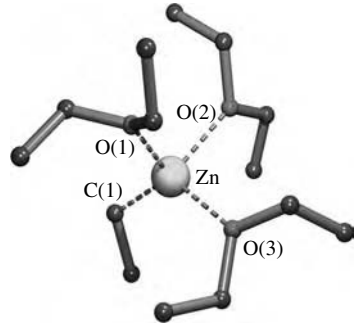

FIGURE 53. The $[EtZn(OEt_2)_3]^+$ cationic part of the structure in the solid state of **114**

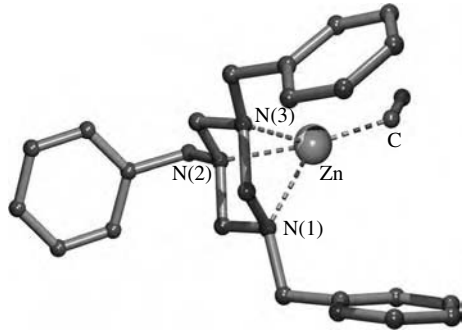

FIGURE 54. Cationic part of the solid state structure of **115**

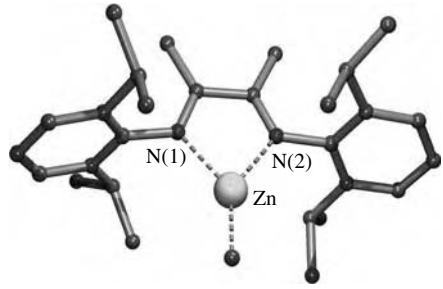

FIGURE 55. Solid state structure of the cationic part of **116**

due to the poor quality of the X-ray data and crystallographic disorder in the ligand part, no reliable data with respect to bond distances and angles can be given.

When $Me_2Zn(DAD)$ [DAD = $(C(Me)NC_6H_3Pr_2\text{-}i\text{-}2,6)_2$] is treated with the strong Lewis acid $(C_6F_5)_3B$, one of the methyl groups is transferred from zinc to boron, giving the ionic complex $[MeZn(DAD)][MeB(C_6F_5)_3]$[186]. Likewise, the selective protonolysis of one of the methyl groups of Me_2Zn with $[DADH][B(C_6F_5)_4]$, which contains an acidic proton, gives $[MeZn(DAD)][B(C_6F_5)_4]$ (**116**) and methane in quantitative yield. The solid state structure of **116** comprises the packing of isolated $[MeZn(DAD)]^+$ cations (Figure 55) and $[B(C_6F_5)_4]^-$ anions in the crystal lattice. In the methylzinc cation both nitrogen atoms of the DAD ligand are bound to zinc [Zn−N 2.035(2) and 2.045(2) Å]. Within experimental error the sum of the bond angles around zinc is 360°, indicating a perfectly planar trigonal coordination geometry around zinc. It has been demonstrated that compound **116** is active as an initiator in the ring-opening polymerization of epoxides.

C. Monoorganozinc Compounds RZnY with Y = Halogen

Although the simple alkylzinc halides RZnX (R = Me or Et, X = Cl, Br, I) were among the first known organozinc compounds[1], for a long time nothing was known about the actual structures of such compounds in solution or in the solid state. The constitution of these compounds in solution seemed to depend on the particular solvent employed[187–190]. It should be noted that in ethereal solutions, the possibility of the presence of a Schlenk equilibrium should always be considered. In these solvents the organozinc halides most

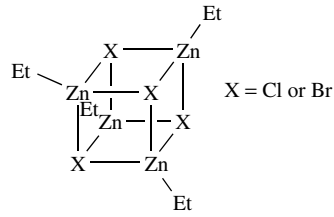

FIGURE 56. Proposed hetero-cubane structures for EtZnCl and EtZnBr

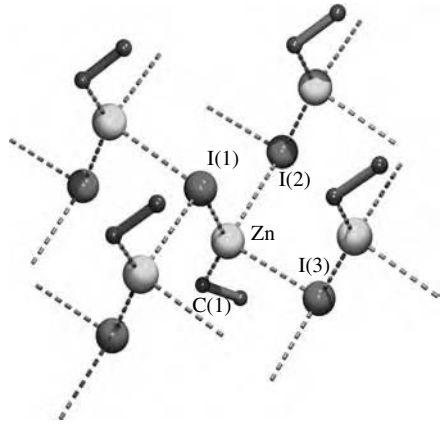

FIGURE 57. Part of the polymeric structure of **117** in the solid state

likely exist as equilibrium mixtures of the parent diorganozinc compound, a solvated zinc dihalide and the organozinc halide itself. However, in apolar solvents like benzene, molecular weight determinations by cryoscopy indicated that EtZnCl and EtZnBr exist as discrete tetrameric aggregates[189]. Based on these observations a hetero-cubane-like structure was proposed for these compounds (Figure 56).

EtZnI (**117**) behaves differently because no clear solutions of this compound could be obtained in apolar solvents. Crystals of **117** suitable for an X-ray crystal determination could be obtained by crystallization of crude **117** from EtI as a solvent[189]. The solid state structure of **117** involves the packing of four EtZnI units in an orthorhombic unit cell in such a way that each of the zinc atoms has additional bonding interactions with two iodine atoms of neighbouring EtZnI units, thus forming a coordination polymer (Figure 57)[191].

In the structure of **117** the Zn−C bond distance of 1.95 Å is as expected for a sp^3-hybridized carbon atom bound to zinc. Each of the zinc atoms has one relatively short (2.64 Å) and two longer (2.91 Å) Zn−I bonds. The zinc atom has a distorted tetrahedral coordination geometry [C(1)−Zn−I(1) 106°, C(1)−Zn−I(2) 144°, C(1)−Zn−I(3) 106° and I(1)−Zn−I(3) 144°] and the geometry of the iodine atoms is close to pyramidal.

It has been well-established that monoorganozinc halides readily form coordination complexes with bidentate ligands like 2.2′-bipyridine and TMEDA[82]. Invariably, such complexes are monomolecular species. The structures of four TMEDA complexes of RZnCl compounds have been established by X-ray crystal structure determinations. These

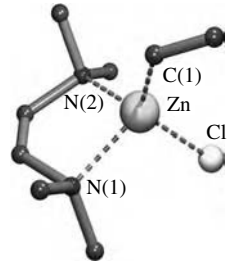

FIGURE 58. Solid state structure of EtZnCl(TMEDA) (**118**)

complexes are EtZnCl(TMEDA)[128], Ph(Me$_3$Si)CHZnCl(TMEDA)[157], the TMEDA complex of 2,2,4,4-tetramethyl-2,4-disilacyclobutylzinc chloride[192] and the TMEDA complex of 2,4-pentadienylzinc chloride[193]. The structures of these compounds are very closely related with respect to bond distances and bond angles at the zinc centre. As a representative example the details of the structure of EtZnCl(TMEDA) (**118**) are given in Figure 58.

In compound **118** the TMEDA ligand is *N*,*N*-chelate-bonded to zinc [Zn−N 2.138(7) Å], resulting in a distorted tetrahedral coordination geometry at zinc. This is reflected in the bond angles around zinc [C(1)−Zn−Cl 124.9(4)°, C(1)−Zn−N both 116.1(3)°, Cl−Zn−N both 103.8(2)° and N(1)−Zn−N(2) 84.4(3)°]. The Zn−C(1) distance of 1.94(1) Å is as expected for a Zn−C bond. The Zn−Cl bond is 2.269(3) Å, which is shorter than the sum of the van der Waals radii.

$CF_3CCl_2ZnCl(DMF)_2$, which is a key intermediate in the one-pot synthesis of CF_3CCl_2-substituted alcohols[194], can be prepared directly from CF_3CCl_3 and metallic zinc in the presence of DMF. An X-ray crystal structure determination of this compound revealed a monomolecular molecule, with the CF_3CCl_2 group and the chloride atom σ-bonded to zinc and two DMF molecules coordinated to zinc via their oxygen atoms[195]. The Zn−C bond length of 2.021(7) is slightly elongated compared to the value observed in other alkylzinc compounds. With the exception of the C−Zn−Cl bond angle of 122.2(3)°, all other bond angles around zinc are close to the ideal tetrahedral value.

When 2-cyanoethylzinc iodide is recrystallized from THF, a crystalline material is obtained. This material appeared to be the mono-THF adduct of 2-cyanoethylzinc iodide which exists in the solid state as a coordination polymer via coordination of the cyanide functionality to an adjacent zinc atom. Coordination saturation at zinc is reached by the coordination of an additional THF molecule. No further structural data have been given for this compound[196].

The reaction of (2-iodo-1,3-xylene)-15-crown-4 with Ph_2Zn for several weeks afforded a remarkable zinc−iodide exchange reaction, resulting in the formation of arylzinc iodide (**119**) (Figure 59)[197]. In **119** the zinc atom is σ-bonded to the C(1)−aryl carbon atom, while two of the oxygen atoms, O(2) and O(3), of the crown ether moiety are intramolecularly coordinated to zinc, resulting in a slightly distorted tetrahedral coordination geometry. This compound is the only example of an arylzinc halide of which the structure was established by an X-ray crystal structure determination.

The solid state structure of the Simmons−Smith reagent, ICH_2ZnI, encapsulated in 18-crown-6 has been established by X-ray crystallography[198]. This complex (**120**) has a rotaxane structure in which, in addition to the Zn−C(1) bond [1.995(9) Å] and the Zn−I(2) bond [2.513(2) Å], three oxygen atoms of the 18-crown-6 moiety are involved in coordination to zinc [Zn−O(1) 2.34(1), Zn−O(2) 2.56(1) and Zn−O(3) 2.60(1) Å].

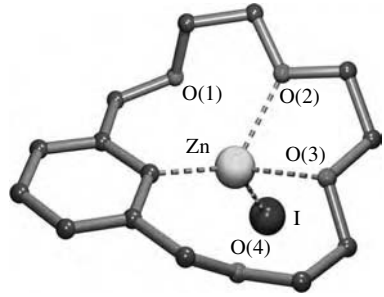

FIGURE 59. Structure of arylzinc iodide **119** in the solid state

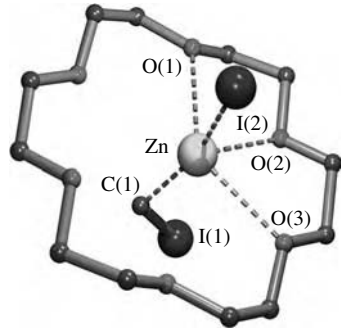

FIGURE 60. The rotaxane structure of **120** in the solid state

This results in a highly distorted trigonal bipyramidal coordination geometry at zinc (Figure 60). The solid state structure of the dibenzo-18-crown-6 analog of **120** has also been established by an X-ray crystal structure determination. Its structural features are closely related to those of **120**.

Reaction of the intramolecular chelating copper alkoxides **121** or **122** with $(Me_3Si)_3CZnCl$ afforded complexes **123** and **124** (equation 22)[199]. In these complexes the copper bis(alkoxide) moiety acts as an *O*,*O*-chelating ligand coordinated to zinc.

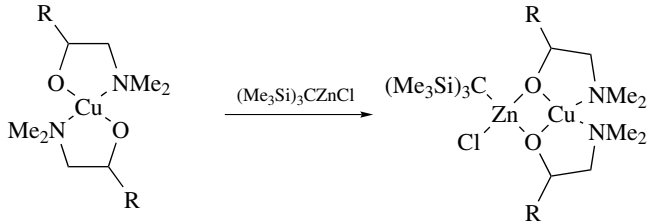

(22)

(121) R = Me
(122) R = Me_2NCH_2

(123) R = Me
(124) R = Me_2NCH_2

The structures of both **123** and **124** were established by X-ray crystal structure determinations. With respect to the zinc environment the structural features of these complexes are

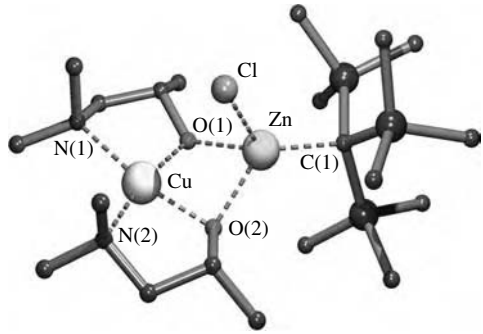

FIGURE 61. Solid state structure of **123**

closely related and, as a representative example, the structure of **123** is shown (Figure 61). The geometry at zinc is distorted tetrahedral; the C(1)−Zn−Cl angle of 120.5(3)° is comparable to the values observed in RZnCl(TMEDA) complexes[128, 157, 192]. The C(1)−Zn−O angles [130.7(3)° and 129.8(3)°] are larger and the O−Zn−Cl angles [93.2(2)° and 93.7(2)°] are smaller than the ideal tetrahedral value. The O−Zn−O angle [76.0(3)°] is extremely small and is a consequence of the bite angle of the *O*,*O*-chelating ligand. Furthermore, it is interesting to note that in both **123** and **124** two chiral carbon centres are present in the alkoxide ligand, but only the achiral *meso*-isomers, with approximately C_S symmetry, crystallize from solutions.

With the exception of EtZnI, which in the solid state forms an aggregated structure (*vide supra*), the structures of the organozinc halide complexes discussed so far are of discrete mononuclear molecules. The presence of the halogen atom bonded to zinc in monoorganozinc halogenides opens the possibility to form dimers via halogen bridges. The formation of such dimers in solid state structures was first reported for $[CF_3CCl_2ZnCl(OEt_2)]_2$. Here, a central Zn−Cl−Zn−Cl square is present and to each of the zinc atoms a CF_3CCl_2 group is bonded and a coordinating diethyl ether molecule[151]. The central four-membered Zn−Cl−Zn−Cl ring is flat and, as a consequence, the zinc atoms have a highly distorted tetrahedral coordination geometry. Although dimerization via halogen bridges was unambiguously established by an X-ray crystal structure determination, further structural details could not be obtained due to crystallographic disorder of the coordinating diethyl ether molecules.

In the solid state $[(PhMe_2Si)_3C]ZnCl$ (**125**) forms chloride-bridged dimers, as was established by an X-ray crystal structure determination[200]. In **125** the two chlorine atoms bridge the two zinc atoms (Figure 62) in a symmetrical manner [Zn(1)−Cl(1) 2.303(3) and Zn(2)−Cl(1) 2.365(3) Å]. The two zinc atoms have a trigonal planar coordination geometry [C(1)−Zn(1)−Cl(1) 137.9(2)°, C(1)−Zn(1)−Cl(2) 133.9(2)° and Cl(1)−Zn(1)−Cl(2) 88.2(1)°]. In the presence of THF, **125** forms an adduct in which, according to its ^1H NMR spectrum, one THF molecule per zinc atom is present, most likely having a structure comparable to that of the $[CF_3CCl_2ZnCl(OEt_2)]_2$ dimer described above.

The organozinc bromide RZnBr (**126**), in which R is the monoanionic, potentially bidentate coordinating $[NC_5H_4C(SiMe_3)_2\text{-}2]^-$ ligand, also forms bromine-bridged dimers in the solid state (Figure 63)[201]. In the centrosymmetric dimer, the $[NC_5H_4C(SiMe_3)_2\text{-}2]^-$ ligand is σ-bonded via its α-carbon atom [Zn−C 2.037(4) Å] and an additional coordinate bond is formed with the pyridyl nitrogen atom [Zn−N 2.077(4) Å]. The bromine atoms bridge rather symmetrically between the two zinc atoms in the dimer [Zn−Br(1) 2.5398(7) and Zn−Br(2) 2.4601(6) Å].

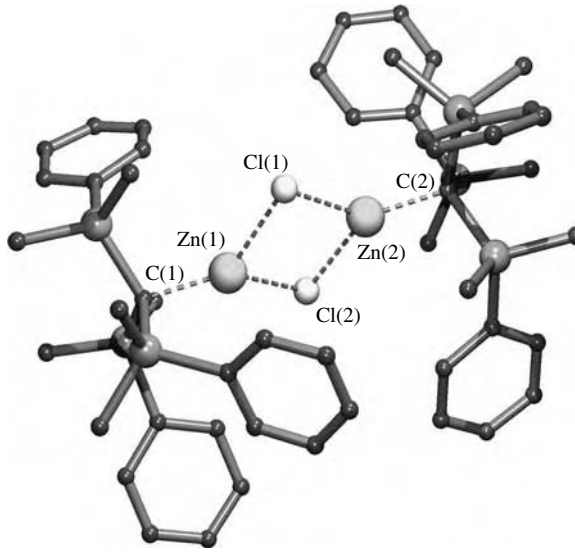

FIGURE 62. Solid state structure of dimeric **125**

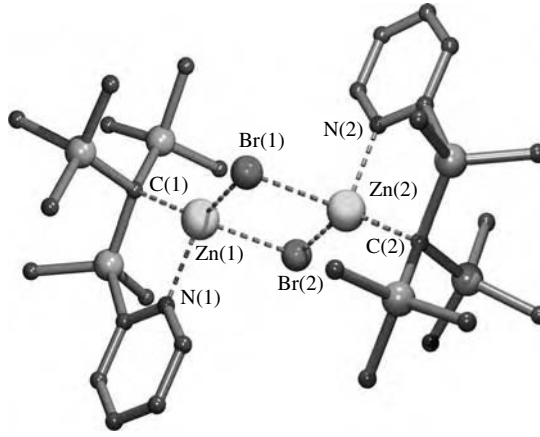

FIGURE 63. Solid state structure of dimeric **126**

A similar structure, in which a heteroatom-containing substituent is intramolecularly coordinated to zinc, was observed for $[\{(Me_3Si)_2(Me_2NSiMe_2)C\}ZnBr]_2$ (**127**) (Figure 64)[202]. Also in this dimer the bromine atoms bridge symmetrically between the two zinc atoms [Zn(1)−Br(1) 2.4614(4) and Zn(2)−Br(1) 2.4963(4) Å], while two $[(Me_3Si)_2(Me_2NSiMe_2)C]^-$ ligands are *C*,*N*-chelate-bonded [Zn(1)−C(1) 2.045(3) and Zn(1)−N(1) 2.152(2) Å] to the zinc atoms.

Also, other metal halides can aggregate with monoorganozinc halogenides, as was shown by the X-ray crystal structure determination of $[(Me_3Si)_2(MePhNSiMe_2)C]ZnBr_2Li$

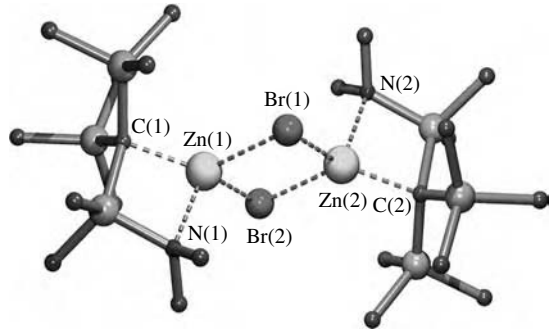

FIGURE 64. Structure of dimeric **127** in the solid state

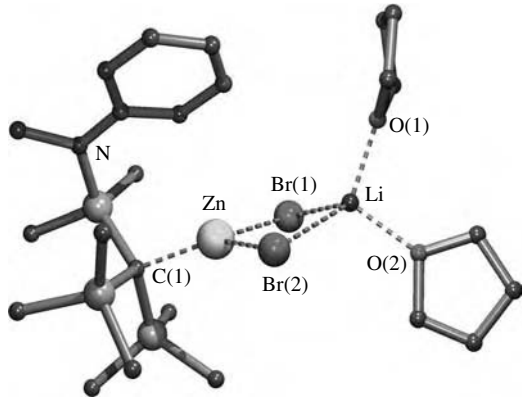

FIGURE 65. Solid state structure of the $RZnBr_2Li(THF)_2$ aggregate **128**

$(THF)_2$ (**128**) (Figure 65)[202]. In this compound two bromine atoms are bridging between zinc and lithium. The Zn−Br(1)−Li−Br(2) ring is folded with an angle of 17° along the Br···Br vector. Surprisingly, the nitrogen atom of the organosilicon fragment is not coordinated to the zinc atom, thus leaving this zinc atom three-coordinate. Most probably, the *N*-methylaniline group is too weakly basic to coordinate to the zinc centre. A tetrahedral coordination geometry at the lithium atom is reached by the coordination of two additional THF molecules.

Dimeric $[2\text{-}(Me_2NCH_2CH_2)\text{-}1,3,4\text{-}(i\text{-}Pr)_3C_5HZnCl]_2$ (**129**) is the only example of a cyclopentadienylzinc halogenide of which the structure has been established by an X-ray crystal structure determination[203]. The centrosymmetric dimer is formed via two bridging chlorine atoms [Zn(1)−Cl(1) 2.3332(10) and Zn(2)−Cl(1) 2.3850(10) Å] between the two zinc atoms (Figure 66). The substituted cyclopentadienyl group is η^1-bonded via C(1) to zinc [Zn(1)−C(1) 2.063(3) Å], while the NMe_2 functionality is coordinated intramolecularly to zinc, affording a six-membered chelate ring [Zn(1)−N(1) 2.124(3) Å]. Each of the zinc atoms has a slightly distorted tetrahedral coordination geometry.

The synthesis of β-hydroxy acids via their esters from ketones and the Reformatsky reagent[172] is still one of the best approaches for this class of compounds. This reagent,

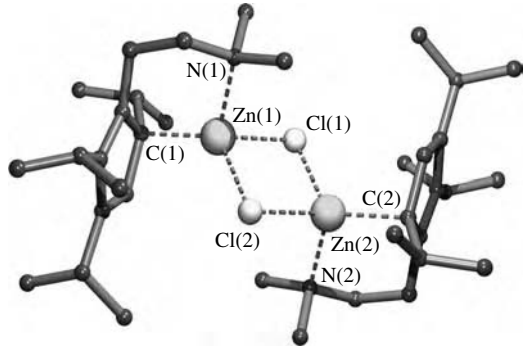

FIGURE 66. Solid state structure of the dimeric cyclopentadienylzinc chloride (**129**)

simply formulated as $(RO)OCCH_2ZnBr$, is generated *in situ* from the corresponding bromo ester and zinc powder in the presence of a ketone. It was thought that this reagent would act as a monoorganozinc halide, i.e. a *C*-metallated species, that adds to a carbonyl group like a Grignard reagent. However, there is ample evidence that the Reformatsky reagent also has properties in accordance with an enolate type structure, i.e. an *O*-metallated species[204, 205]. A complicating factor in the study of the nature of the Reformatsky reagent in solution is the dependence of its spectroscopic properties on the polarity of the solvent. The changes in both the IR and NMR spectra with solvent polarity have been explained in terms of an equilibrium between a *C*-metallated and an *O*-metallated species. Aggregation-state studies by ebulliometry and cryoscopy have shown that in polar solvents like THF, pyridine and dioxane the Reformatsky reagent exists as a dimer, and that only in extremely polar solvents like DMSO is a monomeric species present[206].

The debate about its structural constitution (at least in the solid state) came to an end by the structural elucidation in the solid state of the THF adduct of $(t\text{-BuO})OCCH_2ZnBr$ by X-ray crystallography[206]. It appeared that this compound $[(t\text{-BuO})OCCH_2ZnBr(THF)]_2$ (**130**) exists as a centrosymmetric dimer (Figure 67). This dimer itself consists of a nonplanar eight-membered $(ZnCCO)_2$ ring, each zinc atom being surrounded by a σ-bonded carbon atom [Zn−C 1.98(2) Å], a bromine atom [Zn−Br 2.346(3) Å], a coordinating carbonyl oxygen atom [Zn−O 2.02(1) Å] and a coordinating THF molecule [Zn−O 2.05(1) Å]. The bond angles around zinc point to a slightly distorted tetrahedral geometry. The Zn−C bond distance of 1.98(2) Å has the value expected for a normal Zn−C single bond. The C−O carbonyl bond of 1.31(2) Å is elongated compared to an isolated carbonyl C−O bond, but that is not unexpected, since the oxygen atom is coordinated to zinc. This also explains the shift of C−O carbonyl IR frequency to a lower wave number.

Compound **131** is a rather exotic one and may be described as consisting of one molecule of $[(Me_3Si)_3C]ZnCl$ and one molecule of $[(Me_3Si)_3C]Zn$(2,5-(di-*tert*-butyl)pyrrolidinyl) aggregated in one structure (Figure 68)[207]. In **131**, two $[(Me_3Si)_3C]Zn$ units are linked together via a bridging chlorine atom between the two zinc atoms with equal Zn−Cl distances of 2.410(1) Å. Also, the 2,5-di(*tert*-butyl)pyrrolidinyl ligand bridges between the two zinc atoms, and is σ-bonded with its nitrogen atom [Zn(1)−N 2.151(6) Å] to one of the zinc atoms and η^2-bonded with C(3) [2.190(7) Å] and C(4) [2.194(7) Å] to the other zinc atom. As a consequence of the bonding mode of the 2,5-di(*tert*-butyl)pyrrolidinyl ligand, Zn(1) is three-coordinate and Zn(2) is four-coordinate.

The structural elucidation of the THF adduct of thiazolylzinc bromide (**132**) showed it to be a centrosymmetric dimer (Figure 69)[208]. The two thiazolyl anions are each

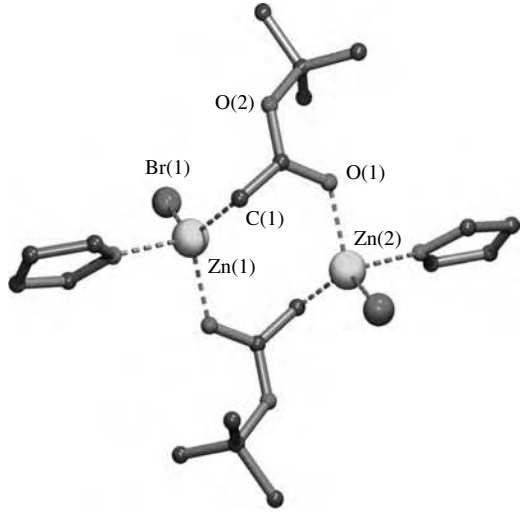

FIGURE 67. Solid state structure of the Reformatsky reagent $[(t\text{-BuO})OCCH_2ZnBr(THF)]_2$ (**130**)

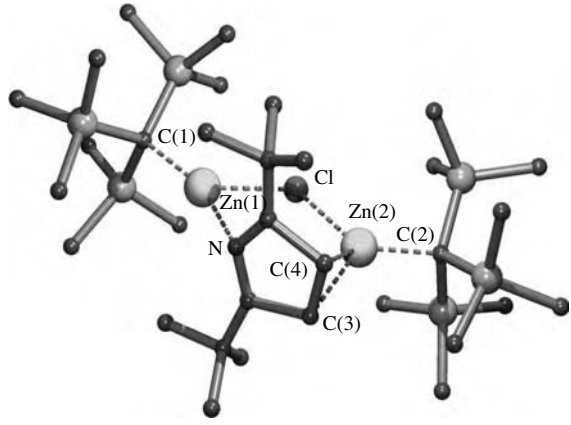

FIGURE 68. Solid state structure of **131**

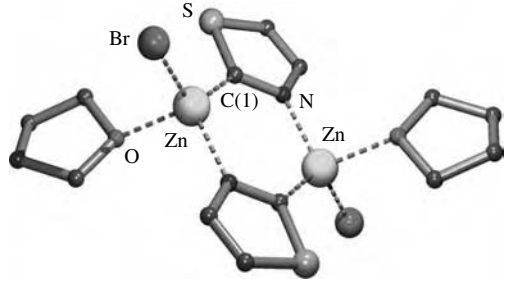

FIGURE 69. Solid state structure of carbenoid compound **132**

bridge-bonded between the two zinc atoms, with C(1) to one of the zinc atoms [Zn−C(1) 2.000 Å] and with the nitrogen atom [Zn−N 2.021 Å] to the other zinc atom. The bromine atom and a coordinating THF molecule complete the four-coordination at zinc. That the carbon atom bound to zinc has carbene character was concluded from the various bonding distances in the thiazolyl anion, and was corroborated by computational studies.

The compound containing a benzoxazole anion and a ZnCl cation forms an adduct with THF, the structural features of which are very closely related to those of **132**[209].

The only example of an organozinc fluoride of which the structure in the solid state has been established by an X-ray crystal structure determination is MeZnF aggregated with Cp^*TiF_3[210]. In this aggregate two $(Cp^*TiF)_2(\mu\text{-}F)_4(\mu_3\text{-}F)(ZnMe)$ units are connected by two $Ti(\mu\text{-}F)-Zn$ bridges.

D. Monoorganozinc Compounds RZnY with Y = OR

A large number of monoorganozinc compounds, in which in addition to the covalently bonded carbon atom an oxygen atom is covalently bound, have been structurally elucidated. These compounds include alkoxides, aryloxides, enolates, β-diketonates, carboxylates, phosphates and siloxanes. As a consequence of the tendency of zinc to attain tetrahedral coordination geometry, in combination with the presence of a potentially multi-electron-donating anionic RO^- group, these compounds usually are aggregated via oxygen bridges between zinc atoms. Only a very few compounds are known that exist (in the solid state) as discrete monomers. These compounds contain either very bulky substituents in close proximity to the zinc atom which prevent aggregation, or contain suitably orientated heteroatom-functionalized substituents capable of coordinating to the zinc atom.

Methylzinc 2,6-di-*tert*-butyl(phenoxide) forms a neutral complex (**133**) with the guanidine ligand *i*-PrN = $C(NMe_2)(NHPr\text{-}i)$, of which the structure in the solid state was established by an X-ray crystal structure determination (Figure 70)[211]. In **133**, the methyl group and the 2,6-di-*tert*-butylphenoxide group are both η^1-bonded to zinc [Zn−O 1.9511(15) Å] while the guanidine ligand forms one coordinate bond [Zn−N(1) 1.9952(18) Å] with its imine nitrogen atom to zinc. As a result the zinc atom has planar trigonal coordination geometry (sum of the bond angles around zinc 359.6°). It is notable that the guanidine amine-hydrogen atom forms an intramolecular hydrogen bridge with the phenolate oxygen atom. This might be an additional stabilizing factor for this structure.

Compounds **134**[212], **135**[213] and **136**[214] (Figure 71) are alkylzinc alkoxides and aryloxides that exist as discrete monomeric molecules in the solid state. These compounds have in common that in addition to the covalently bonded alkoxy or aryloxy group, two

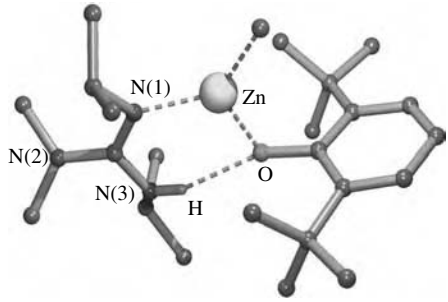

FIGURE 70. Solid state structure of monomeric guanidine complex **133**

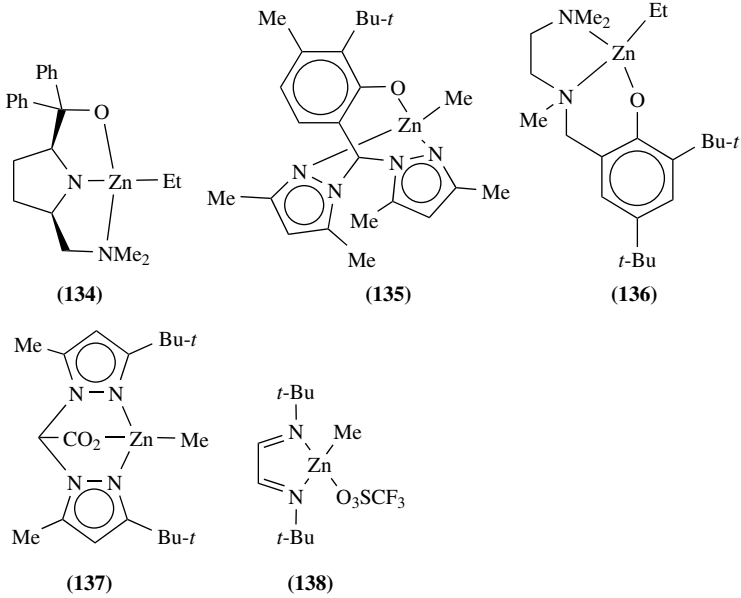

FIGURE 71. Monomeric alkylzinc-oxygen compounds

nitrogen atoms are intramolecularly coordinated to the zinc atom. As a result the zinc atoms in these compounds have a distorted tetrahedral coordination geometry.

Compound **137**[215] is an example of a monomeric methylzinc carboxylate (Figure 71). In this compound the carboxylate group is η^1-bonded to zinc via one of its oxygen atoms, while tetrahedral coordination geometry at zinc is reached via intramolecular coordination of the nitrogen atoms of the two pyrazolyl moieties. The solid state structure of an analog of **137** containing one 3,5-di-*tert*-butylpyrazolyl group and one 3,5-dimethylpyrazolyl group has also been established[216]. This compound is isostructural with **137**.

An X-ray crystal structure determination of methylzinc triflate DAB complex **138** (Figure 71) (DAB = 1,4-di-*tert*-butyl-1,4-diaza-1,3-butadiene) showed it to be a monomeric compound in which the triflate group is η^1-bonded to zinc with one of its oxygen atoms while the DAB ligand is *N*,*N*-chelate-bonded to zinc[161]. Thus compound **138** is a neutral compound in which the zinc atom has a distorted tetrahedral coordination geometry instead of the anticipated ionic structure comprising a trigonal monoorganozinc cation and a triflate anion.

Of the RZnY compounds in which the Y group is an organic group bound via oxygen, the organozinc alkoxy or aryloxy compounds are the largest group of which the solid state structures have been determined. For this type of compounds three basic structural motifs have been observed. The first one involves the formation of dimers **A** (Figure 72) in which two alkoxy or aryloxy groups bridge between two zinc atoms. The zinc atoms are trigonal planar coordinate. Either the organic group bound to zinc (R^1) or the organic group bound to oxygen (R^2) contains bulky substituents that prevent the formation of higher aggregates. The second motif **B** (Figure 72) is an extension of the first one. The organic group bound to zinc contains a heteroatom-functionalized substituent capable of forming a coordination bond to zinc, affording oxygen-bridged dimers in which the zinc atoms have a tetrahedral coordination geometry. The third motif **C** (Figure 72) involves

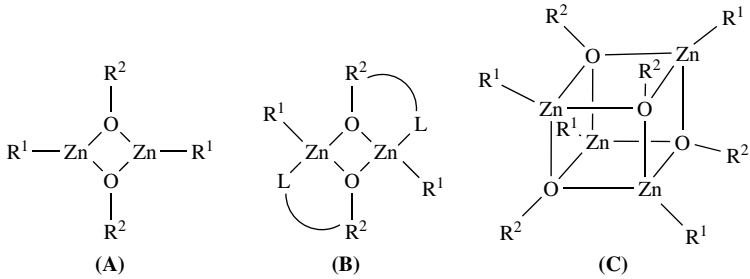

FIGURE 72. The three basic structural motifs observed for R^1ZnOR^2 compounds

the formation of a hetero-cubane structure in which each of the alkoxy or aryloxy groups is μ^3-bonded to three zinc atoms. A similar structure has been proposed for $[EtZnCl]_4$ and $[EtZnBr]_4$[189].

The solid state structure of tris(dimethylphenylsilyl)methylzinc hydroxide (**139**)[217] (Figure 73) is an example of structural motif **A**. Two hydroxy groups are symmetrically bridge-bonded [Zn(1)−O(1) 1.908(7) and Zn(2)−O(1) 1.891(6) Å] between the two zinc atoms affording a flat central Zn−O−Zn−O square. The two halves of the dimer are symmetry-related via a crystallographic centre of symmetry. Each of the zinc atoms has planar trigonal geometry (the sum of the bond angles around zinc is 360° within experimental error). The substituent at the oxygen atom (in this case hydrogen) is the smallest one possible, but the bulky tris(dimethylphenylsilyl)methyl groups, one at each zinc atom, prevent the formation of higher aggregates.

In dimeric ethylzinc 2,6-di-*tert*-butylphenoxide (**140**)[218] the bulk of the groups at zinc and oxygen is reversed. Also here, the centrosymmetric dimer consists of a central flat Zn−O−Zn−O square [Zn(1)−O(1) 1.970(1) and Zn(2)−O(1) 1.990(1) Å], but now to each zinc atom a relatively small ethyl group is bonded while the bulky 2,6-di-*tert*-butylphenoxy groups prevent the formation of higher aggregates (Figure 73).

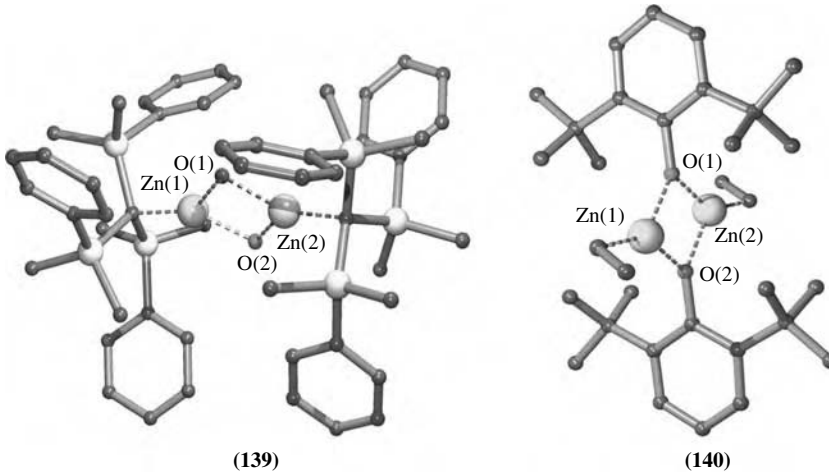

FIGURE 73. Solid state structures of dimeric **139** and **140**

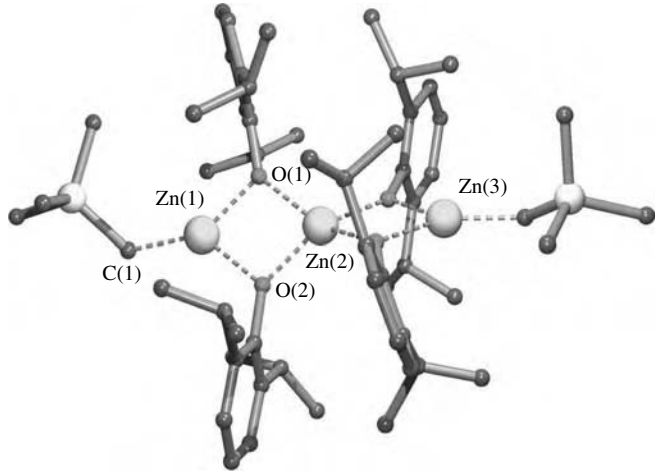

FIGURE 74. Solid state structure of metalla-spirocyclic compound **141**

X-ray crystal structure determinations of $[EtZnOB(Mes)_2]_2$[219], $[Me_3SiCH_2ZnOC_6H_3(Pr\text{-}i)_2\text{-}2,6]_2$[220] and $[Me_3SiCH_2ZnOC_6H_3(Bu\text{-}t)_3\text{-}2,4,6]_2$[220] revealed structures for these compounds which are identical to those observed for **139** and **140**.

That the stoichiometry of the reactants during the synthesis of such compounds, which are usually prepared by selective alcoholysis of one of the alkyl groups of the corresponding dialkylzinc compound, has to be exactly 1:1 became evident from the isolation and structural characterization of **141**[220] (Figure 74). Formally, this compound may be regarded as consisting of two molecules of $Me_3SiCH_2ZnOC_6H_3(Pr\text{-}i)_2$-2,6 and one molecule of $[2,6\text{-}(i\text{-}Pr)_2C_6H_3O]_2Zn$ which are aggregated to one structure. The structure of this compound comprises an almost linear array of three zinc atoms that are bridged by the oxygen atoms of four diisopropylphenoxy groups [Zn(1)−O(1) 1.950(2) and Zn(2)−O(1) 1.985(2) Å]. To each of the terminal zinc atoms one Me_3SiCH_2 group is bonded. Consequently, the terminal zinc atoms each have a planar trigonal geometry and the central zinc atom is distorted tetrahedral. This compound is an example of a metalla-spirocyclic compound. Identical structural motifs have been observed in the solid state structures of the compounds obtained from the reaction of dimethylzinc with either triphenylsilanol or tris(isopropyl)silanol, i.e. $Me_2Zn_3(OSiPh_3)_4$[221] and $Me_2Zn_3[OSi(Pr\text{-}i)_3]_4$[222], respectively. It should be noted that a similar reaction of Me_2Zn or Et_2Zn with diorganosilane diols[221] or monoorganosilane triols[223] affords structurally much more complicated polyhedral organozinc siloxanes.

The second structural motif, **B** (Figure 72), involves also a dimeric structure in which two alkoxy oxygen atoms bridge between two zinc atoms, but now an additional intramolecular coordinating substituent is present, resulting in the formation of four-coordinate zinc atoms. Most of these structural investigations are aimed at the elucidation of the mechanism of the enantioselective addition of organozinc compounds to aldehydes[224], a topic that will be discussed in Chapter 13.

It has been shown that the β-amino alcohol (−)-3-*exo*-(dimethylamino)isoborneol (DAIB) serves as an excellent chiral auxiliary in the enantioselective addition of Et_2Zn to aldehydes[225]. As a model compound for the anticipated intermediate, the structure of MeZn(DAIB) (**142**) in the solid state was determined by X-ray crystallography[226]. In the

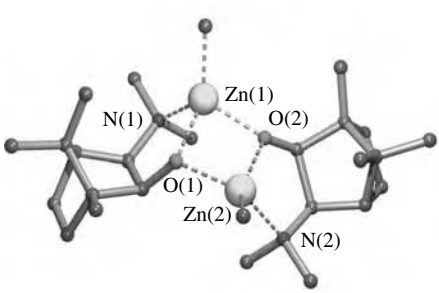

(142)

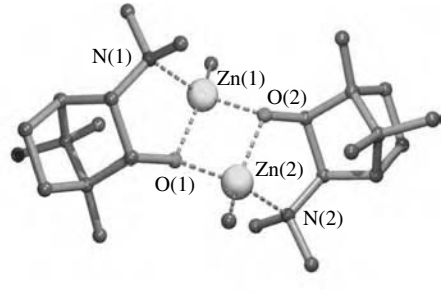

(143)

FIGURE 75. Enantiopure $[MeZn(DAIB)]_2$ (**142**) and *meso*-$[MeZn(DAIB)]_2$ (**143**)

solid state **142** exists as a dimer (Figure 75) via bridging of two alcoholate oxygen atoms between two zinc atoms [Zn(1)−O(1) 1.98(1) and Zn(2)−O(1) 2.05(1) Å]. To each of the zinc atoms one dimethylamino substituent is intramolecularly coordinated [Zn(1)−N(1) 2.25(2) Å] and as a consequence the zinc centra are tetrahedrally coordinated. It is notable that both nitrogen atoms approach the zinc atoms from the same side of the central Zn−O−Zn−O plane affording an overall *syn*-geometry. The crystallized material, obtained from the reaction of racemic DAIB and Me_2Zn, appeared to consist of a *meso*-dimer (**143**) of MeZn(DAIB). In this dimer the coordinating nitrogen atoms approach the Zn−O−Zn−O plane from opposite sides, thus giving an overall *anti*-geometry.

During these studies also the solid state structures of an oxygen-bridged dimeric compound containing two different alcoholate moieties, i.e. a chiral DAIB anion and achiral $Me_2NCH_2CMe_2O$, have been established as well as the symmetric dimer containing two $Me_2NCH_2CMe_2O$ moieties[227]. Both structures have structural properties that are closely related to that of **143**; in both structures the intramolecular-coordinating nitrogen atoms approach the Zn−O−Zn−O plane from opposite sides.

During studies of its application as a catalyst in the enantioselective addition of dialkylzinc compounds to aldehydes and its stereochemical tuning, a series of methylzinc derivatives of *exo*-(2-aryl-substituted) fenchyl alcohols (Figure 76) have been prepared and structurally characterized in the solid state[228–230].

Like the isoborneol derivatives the methylzinc fenchyl alcoholates are dimers via alcoholate-oxygen bridges in a central Zn−O−Zn−O plane, while the two methoxy substituents each coordinate intramolecularly to a zinc atom. In the homo-chiral dimers with R = H or Me the methyl groups bound to the zinc atoms and the two coordinating oxygen atoms are in *syn*-position with respect to the Zn−O−Zn−O plane[228]. As expected, in the heterochiral derivatives with R = *t*-Bu or Me_3Si (**144**) (Figure 77), obtained from the corresponding racemic fenchyl alcohols, both the methyl groups and the coordinating

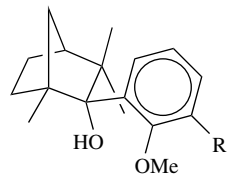

R = H, Me, *t*-Bu, Me_3Si

FIGURE 76. *Exo*-(2-aryl-substituted) fenchyl alcohols

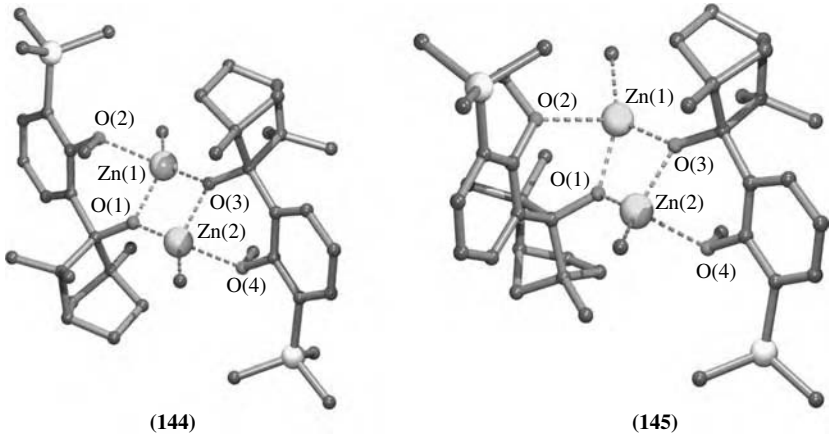

(144) **(145)**

FIGURE 77. Dimeric heterochiral (**144**) and homochiral (**145**) MeZn fenchyl acoholates

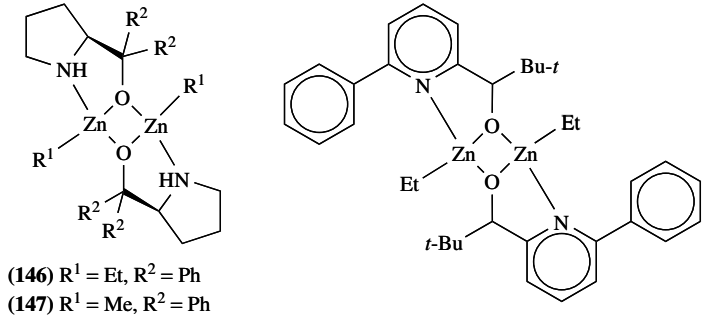

(146) R^1 = Et, R^2 = Ph
(147) R^1 = Me, R^2 = Ph
(148) R^1 = Et, R^2 = 4-$CF_3C_6H_4$

(149)

FIGURE 78. Alkylzinc alkoxides derived from functionalized pyrrolidinyl-2-methanol **146–148** and 2-pyridylmethanol **149**

oxygen atoms are in *anti*-position[229,230]. In contrast, in the homochiral derivatives with R = *t*-Bu or Me_3Si (**145**) (Figure 77) the methyl groups bonded to zinc are *syn*-orientated but the coordinating methoxy groups are in *anti*-position.

Chiral (*S*)-α,α-diphenylpyrrolidinyl-2-methanol reacts with Et_2Zn or Me_2Zn to give the corresponding homochiral dimeric EtZn-alcoholate (**146**)[231] and MeZn-alcoholate (**147**)[232] (Figure 78). The dimeric nature of these compounds was established by X-ray crystal structure determinations. Also in these structures the basic structural motif is a central Zn−O−Zn−O square (bridging oxygen atoms of the alcoholate moieties). In both structures the two pyrrolidinyl nitrogen atoms coordinate each to a zinc atom in such a way that these nitrogen atoms are in *anti*-position with respect to the Zn−O−Zn−O plane. Accordingly, the organic groups bound to zinc (Et in **146** and Me in **147**) are also in *anti*-position. Introduction of a CF_3 group in the *para*-position of the phenyl groups does not only influence the reactivity and selectivity of these compounds, when used as catalysts for the asymmetric copolymerization of cyclohexene oxide and CO_2[231], but also has a large influence on their actual structures in the solid state. The tetra 4-CF_3

derivative of **146**, namely **148** (Figure 78), is also a dimer, but now both the ethyl groups bound to zinc and the coordinated nitrogen atoms are *anti*-orientated with respect to the Zn−O−Zn−O plane.

The ethylzinc alcoholate (**149**) prepared from racemic *α-tert*-butyl-6-phenyl-2-pyridylmethanol and Et_2Zn exists in the solid state as a hetero chiral dimer (Figure 78)[233]. Also in this case the alcoholate oxygen atoms bridge between two zinc atoms, affording a central Zn−O−Zn−O plane. The pyridyl nitrogen atoms are coordinated in such a way to the zinc atoms [Zn−N 2.185(2) Å] that they are in *anti*-position with respect to this plane.

The reaction of Me_2Zn with *rac*-1-phenyl-2-(*N*-methylamino)ethanol or (*S*)-*N*-methyl-2-pyrrolidinemethanol affords the corresponding methylzinc alcoholates[232]. In the solid state, these compounds, **150** and **151** respectively, are trimeric aggregates (Figure 79). In both **150** and **151** three zinc atoms and three bridging oxygen atoms are arranged in a six-membered ring. In **150** this ring adopts a half-boat conformation and in **151** a half-chair conformation. The nitrogen atom of each ligand coordinates to a zinc atom, resulting in five-membered chelate rings and four-coordinate zinc atoms.

The formation of tetrameric aggregates with a hetero-cubane structure is a structural motif that is observed for several alkylzinc alkoxides in the solid state (Figure 80). In these structures the alkoxy group is μ^3-bonded with its oxygen atom to three zinc atoms. The structural elucidation of $[MeZnOMe]_4$ (**152**) represented the first example of such a structural motif in organozinc alkoxide chemistry[234, 235]. Later, similar structures were observed for alkylzinc alkoxides containing other alkoxy groups (**153**, $R^2 = t$-BuO)[236, 237] and/or other organic groups (**154**, $R^1 = Me_3SiCH_2$, R^2 = 1-Ad[220], **155** and **156**, R^1 = halomethyl, R^2 = benzyloxy[238]) bound to zinc. Also, compounds containing a diorganoboryl oxide (**157**)[239] or a triorganosiloxy group (**158**)[222] form tetrameric aggregates with a hetero-cubane structure.

More complicated structures of alkylzinc alkoxides have been observed in the solid state with the stoichiometry $R^1{}_6Zn_7(OR^2)_8$. These compounds have a hetero-di-cubane structure (two hetero-cubanes sharing a corner), and have been observed for $Me_6Zn_7(OMe)_8$ (**159**)[240, 241], $Et_6Zn_7(OMe)_8$ (**160**)[242] and $(ICH_2)_6Zn_7(OMe)_8$ (**161**)[243] (Figure 80).

As a representative example the solid state structure of $[MeZnOMe]_4$ (**152**) is shown (Figure 81). The four zinc atoms and the four oxygen atoms of the four μ^3-bridging methoxy groups are arranged in such a way that a slightly distorted cube is formed.

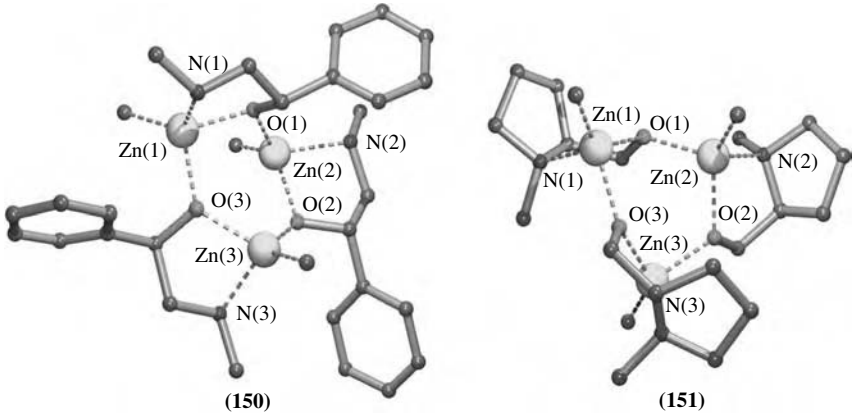

FIGURE 79. Solid state structures of trimeric aggregates **150** and **151**

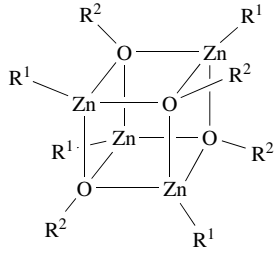

(152) $R^1 = R^2 = Me$
(153) $R^1 = Me$, $R^2 = t\text{-Bu}$
(154) $R^1 = Me_3SiCH_2$, $R^2 = 1\text{-Ad}$
(155) $R^1 = ICH_2$, $R^2 = 4\text{-}MeOC_6H_4CH_2$
(156) $R^1 = ClCH_2$, $R^2 = 4\text{-}MeOC_6H_4CH_2$
(157) $R^1 = Et$, $R^2 = 9\text{-BBN}$
(158) $R^1 = Me$, $R^2 = Et_3Si$

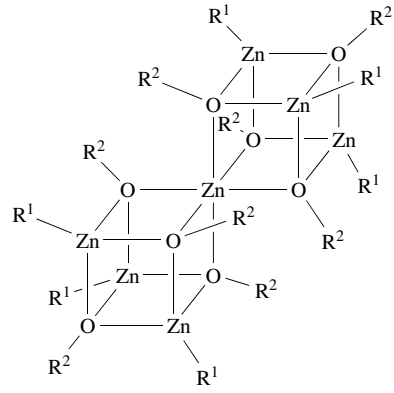

(159) $R^1 = R^2 = Me$
(160) $R^1 = Et$, $R^2 = Me$
(161) $R^1 = ICH_2$, $R^2 = Me$

FIGURE 80. Alkylzinc alkoxides having a hetero-cubane structure

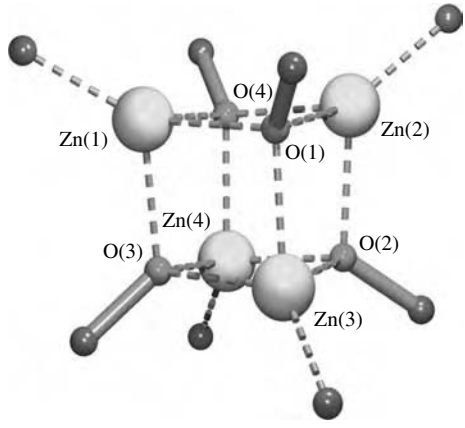

FIGURE 81. Solid state structure of tetrameric methylzinc methoxide

The Zn−O distances in one μ^3-bridging unit are almost equal [O(1)−Zn(1) 2.114(15), O(1)−Zn(2) 2.052(17) and O(1)−Zn(3) 2.069(13) Å]. The slight distortion of the cube is indicated by the observation that all Zn−O−Zn angles are slightly larger (average 96°) than 90° and the O−Zn−O angles are slightly smaller (average 84°) than 90°.

Also, mixed methylzinc alkoxide–alkali metal alkoxide compounds exhibit a hetero-cubane structure in the solid state. In $Me_2Zn_2Li_2(OBu\text{-}t)_4(THF)_2$ (**162**)[244] and $Me_2Zn_2K_2(OSiMe_3)_4(THF)_4$ (**163**)[245], two of the alkoxy groups are μ^3-bridge-bonded between two zinc atoms and one alkali metal atom and consequently the other two alkoxy groups are μ^3-bridge bonded between one zinc atom and two alkali metal atoms (Figure 82). In **162**, tetrahedral coordination geometry at the lithium atoms is reached by the coordination of

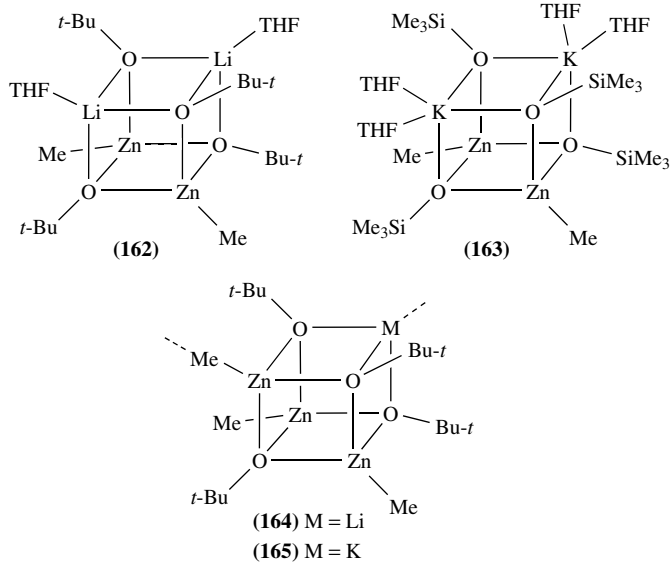

FIGURE 82. Structures of the hetero-cubanes **162–165**

a THF molecule, while in **163** the potassium atoms are penta-coordinate via coordination of two THF molecules.

The mixed methylzinc alkoxide–alkali metal alkoxide compounds $Me_3ZnM(OBu\text{-}t)_4$ [M = Li (**164**)[246] and M = K (**165**)[245]] form infinite polymeric chains of hetero-cubane units by bridging of one of the methyl groups between zinc and the lithium atom in an adjacent hetero-cubane unit (Figure 82). Unfortunately, in **164** crystallographic site disorder is present for the top two metals in the cube (Figure 82); both positions refine for a site occupancy of 50% Zn and 50% Li. Moreover, the bridging methyl group is located at a crystallographic inversion centre in between Zn/Li and its symmetry equivalent. It is therefore impossible to distinguish unambiguously between Zn–Me···Li and Li–Me···Zn bonding modes. In **165**, this disorder is not present and the bonding of the bridging methyl group is rather asymmetric [Zn–C 2.00(1) and K–C 3.20(1) Å].

A series of alkylzinc alkoxides in which the alkoxide is an α-substituted 2-pyridinemethanol group has been prepared[247]. Based on aggregation-state studies by cryoscopy in benzene, it appeared that depending on the particular α-substituent these compounds exist in solution either as dimers or as trimers. An X-ray crystal structure determination of one of these compounds, i.e. $Me_3SiCH_2ZnOCH_2$-2-Pyr, showed that this compound exists in the solid state as a cyclic tetramer[247]. The four alkylzinc alkoxide units are linked via μ^2-bridging alcoholate groups to give a central puckered eight-membered Zn_4O_4 ring, in which the Zn–O distances are almost equal [average value 1.985(1) Å]. The pyridyl nitrogen atoms each coordinate to a zinc atom, resulting in slightly distorted tetrahedrally coordinated zinc atoms.

A rather unexpected product was obtained from the reaction of 2-(methylthio)ethanol and Me_2Zn in dichloromethane as a solvent. Instead of the anticipated methylzinc alkoxy compound, a product was obtained with the constitution $Me_4Zn_4(OCH_2CH_2SMe)_2Cl_2$ (**166**)[248]. The only possible explanation for the formation of this product is that the chloride present originates from the solvent dichloromethane. An X-ray crystal structure

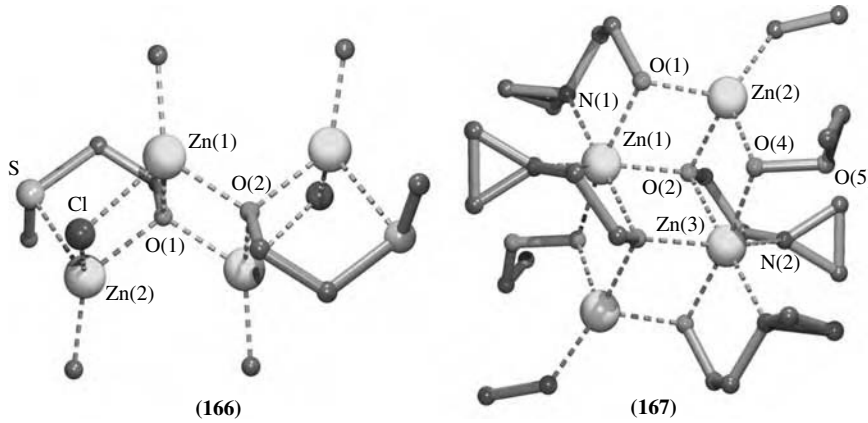

FIGURE 83. Solid state structures of compounds **166** and **167**

determination revealed that **166** can be regarded as consisting of two molecules of $MeZnOCH_2CH_2SMe$ and two molecules of MeZnCl, aggregated in one structure via two μ^3-bridging alkoxides and two μ^2-bridging chlorides (Figure 83). The four zinc atoms, the two oxygen atoms and the two chlorine atoms are aggregated in a ladder-type arrangement. The two central zinc atoms are four-coordinate as a result of the σ-bonded methyl group, two Zn−O bonds [Zn(1)−O(1) 2.101(2) and Zn(1)−O(2) 2.043(2) Å] and one Zn−Cl bond [2.370(1) Å]. To the peripheral MeZn unit one oxygen [Zn(2)−O(1) (2.072(2) Å] and one chlorine atom are bonded [2.365(1) Å], while tetrahedral coordination is reached by intramolecular coordination of the sulfur atom [Zn−S 2.475(2) Å].

Reaction of Et_2Zn with 1-aziridine-ethanol affords the corresponding ethylzinc alcoholate in quantitative yield, which, according to molecular weight determinations, exists in benzene solution as a trimeric aggregate. Treatment of this solution with dry oxygen affords a crystalline material (**167**), which according to its X-ray crystal structure determination consists of four zinc atoms, two ethyl groups, four ethoxyaziridine groups and two ethylperoxo groups. The basic skeletal arrangement of **167** can be best described as an inversion-related, corner-removed face-shared cube (the four zinc atoms are located at the four corners of a defective double hetero-cubane) (Figure 83)[241]. The central zinc atoms [Zn(1) and Zn(3)] are octahedrally coordinated as a result of four Zn−O bonds and two intramolecular Zn−N coordinate bonds. The two other zinc atoms are four-coordinated via one σ-C−Zn bond and three Zn−O bonds. The most interesting feature of **167** is the presence of μ^2-bridging ethylperoxo groups, which is unprecedented for organozinc compounds.

Treatment of the linked phenol tris(3,5-di-*tert*-butyl-2-hydroxyphenyl)methane, abbreviated as $[HOC_6H_2(Bu\text{-}t)_2]_3CH$, with Et_2Zn affords a variety of complex aggregated compounds of which the structures have been determined by X-ray crystallography[249]. The stoichiometries of these compounds are $Et_6Zn_6\{[OC_6H_2(Bu\text{-}t)_2]_3CH\}_2$, $Et_4Zn_5\{[OC_6H_2(Bu\text{-}t)_2]_3CH\}_2$, $Et_2Zn_4\{[OC_6H_2(Bu\text{-}t)_2]_3CH\}_2$ and $Et_3Zn_3\{[OC_6H_2(Bu\text{-}t)_2]_3CH\}_2(THF)_3$.

A special class of linked phenols are the so-called calixarenes. Reaction of *p-t*-Bu-calix[4]arene, abbreviated (H_4L), with excess Et_2Zn in the presence of TMEDA affords the fully deprotonated calixarene complex $Et_2Zn_5(L)_2(TMEDA)_2$ (**168**), the structure of which was determined in the solid state (Figure 84)[250]. The two calixarenes are fused by three zinc atoms. One of these is coordinated by two oxygen atoms from each calixarene unit. The other two zinc atoms, connecting the calixarenes, are five-coordinate, bound by

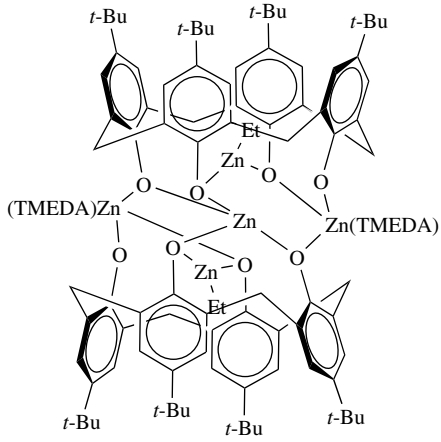

(168)

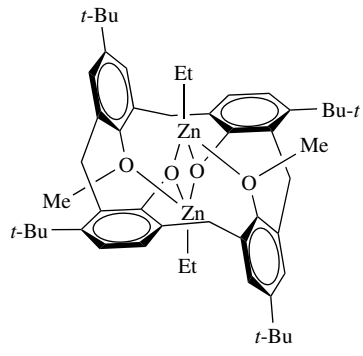

(169)

FIGURE 84. Schematic structures of **168** and **169**

one oxygen on one calixarene, two adjacent oxygen atoms on the other calixarene unit and two nitrogen atoms of one TMEDA molecule. The ethyl groups are located *endo* relative to the cone of the calixarenes with an associated trigonal-planar zinc atom also bound by two oxygen atoms from opposite aromatic rings in the same calixarene.

A similar reaction of 1,3-dimethyl ether *p-t*-Bu-calix[4]arene, abbreviated as (H_2L), with Et_2Zn affords a monomeric compound $(EtZn)_2$(L) (**169**) with a less complex structure (Figure 84)[250]. The zinc atoms in this compound form a flat Zn−O−Zn−O arrangement together with the phenolate oxygen atoms. To each zinc atom one ethyl group is bonded, and tetrahedral coordination is reached by the additional coordination of one methoxy group.

The corresponding, sterically more demanding, 1,3-dibenzyl ether analog also forms a monomeric $(EtZn)_2$−calixarene complex, but with a somewhat different structure[251]. Here, the calixarene unit is in the pinched-cone conformation with one EtZn group capped by all four oxygen atoms rendering this zinc atom five-coordinate, while the other EtZn group is fully immersed in the calixarene cavity and is three-coordinate via bonding to two oxygen atoms.

Because zinc enolates are intrinsically reactive species, especially towards carbonyl compounds, the attempted synthesis of such species often results in the formation of self-condensation products which are often polymeric materials[252]. Only in a few cases could pure organozinc enolates be isolated and structurally characterized.

Three ethylzinc enolates containing a tertiary nitrogen atom in β-position to the enolate oxygen atom have been prepared and were structurally characterized by X-ray crystallography. The structures of these compounds are shown schematically in Figure 85.

In the solid state, compound **170**[253] exists as a dimer (Figure 85). Two enolate moieties bridge with their oxygen atoms between two zinc atoms [Zn−O 2.02(1) and 2.12(1) Å] affording a central flat Zn−O−Zn−O ring. The nitrogen substituents each coordinate to a zinc atom [Zn−N 2.21(2) Å]. Both the ethyl groups bound to zinc and the two coordinating nitrogen atoms are in *syn*-position with respect to the central Zn−O−Zn−O plane. Ethylzinc enolate (**171**) (Figure 85) has an overall structural motif identical to that of **170**. This compound was obtained as an unexpected product from the reaction of CpZnEt and ethyl *N*,*N*-diethylglycinate[254].

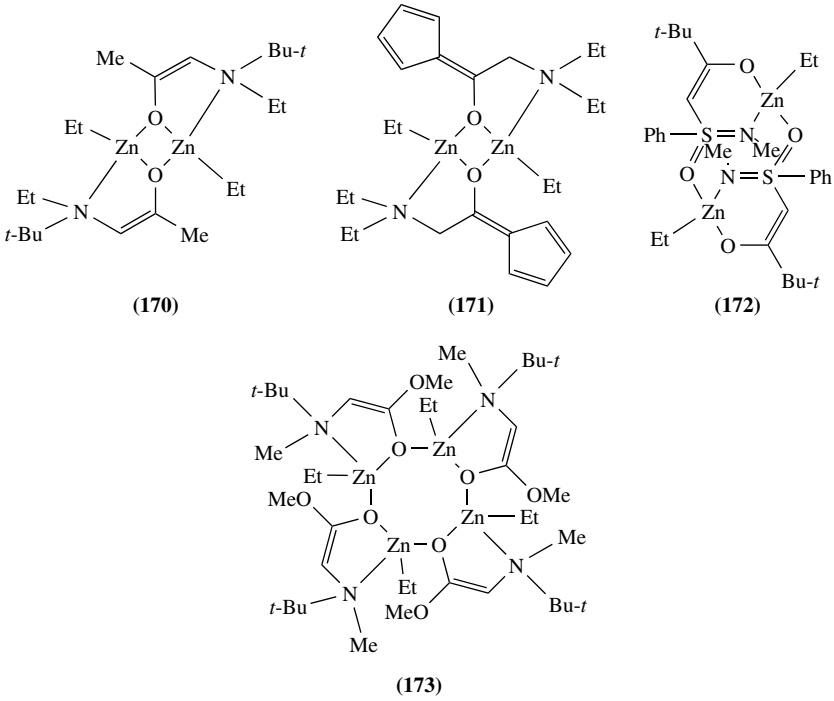

FIGURE 85. Schematic structures of zinc enolates stabilized by intramolecular nitrogen coordination

Compound **172** (Figure 85) is an ethylzinc enolate derived from a β-ketosulfoximine[255]. Also, this compound exists in the solid state as a dimer, but surprisingly dimer formation does not occur via μ^2-bridging of the enolate–oxygen atoms, but by coordination of the oxygen atom bound to sulfur to the zinc atom in the other half of the dimer.

Ethylzinc enolate (**173**) is an alkylzinc enolate derived from an α-amino acid ester. Such derivatives have proven to be valuable intermediates in their zinc-mediated condensation with imines to β-lactams[256]. In the solid state **173** is a tetrameric aggregate (Figure 85)[257] via four μ^2-bridging enolate–oxygen atoms [Zn–O distances range from 2.028(5) to 2.076(6) Å] in a central puckered $(ZnO)_4$ eight-membered ring. Each of the zinc atoms in the ethylzinc moieties is tetrahedrally coordinated via intramolecular coordination, in a five-membered chelate ring, to the nitrogen atom of the amino substituent.

Organozinc β-diketonato compounds also belong formally to the class of organozinc enolates. EtZn(acac) exists in the solid state as a dimer, but due to the poor quality of the crystal data only the basic structural motif, i.e. dimer formation via μ^2-oxygen bridges of two acac anions between two zinc atoms, could be established[258]. It appeared that PhZn(acac) is an unstable compound in solution and spontaneously disproportionates into Ph_2Zn and a compound having the stoichiometry $Ph_2Zn_3(acac)_4$ (**174**)[259]. An X-ray crystal structure determination[260] of **174** (Figure 86) revealed an arrangement of the three zinc atoms that considerably deviates from linear [<Zn(1)–Zn(2)–Zn(3) 142.5°]. Two of the acac anions are μ^2-bridge-bonded between the central zinc atom and each one to a different peripheral zinc atom. The other oxygen atom is also bound to the central zinc atom. Only a slight variation in Zn–O distances (2.006 to 2.051 Å) is observed. The

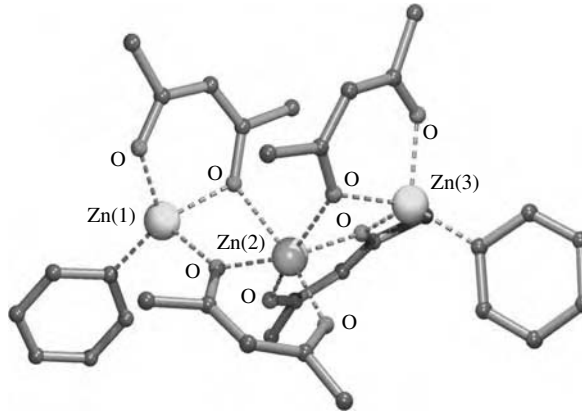

FIGURE 86. Solid state structure of **174**

other two acac anions are also μ^2-bridge-bonded between the central zinc atom and the two peripheral zinc atoms, but in a less symmetric way. The Zn−O bond lengths to the central zinc atom are considerably longer (average 2.278 Å) than those to the peripheral zinc atoms (average 2.017 Å). The other oxygen atoms of those two acac ligands are each bonded to a peripheral zinc atom. These bonding modes render the central zinc atom octahedrally coordinated and the peripheral zinc atoms four-coordinated.

Also, the structures of two organozinc pivaloylacetone derivatives associated with methylzinc methoxide or phenylzinc phenoxide were determined by X-ray crystallography. The complex structures of these compounds, $Et_2Zn_4(Pac)_4(OMe)_2$ (**175**)[252] and $Ph_2Zn_4(Pac)_4(OPh)_2$ (**176**)[261] (Pac = pivaloylacetone anion), are shown schematically in Figure 87.

The structures of only very few organozinc carboxylates (or containing related anionic ligands like carbamates) are known. The structure of $Me_4Zn_4(O_2CNEt_2)_4$[262] has been determined. It is a cage-like structure of two puckered Zn_2O_3C rings, which are linked by bridging oxygen atoms.

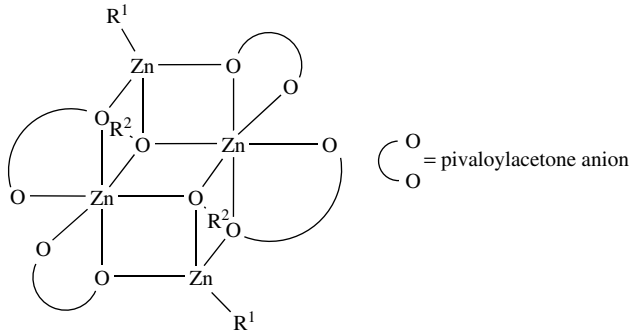

(175) R^1 = Et, R^2 = Me
(176) $R^1 = R^2$ = Ph

FIGURE 87. Schematic structures of **175** and **176**

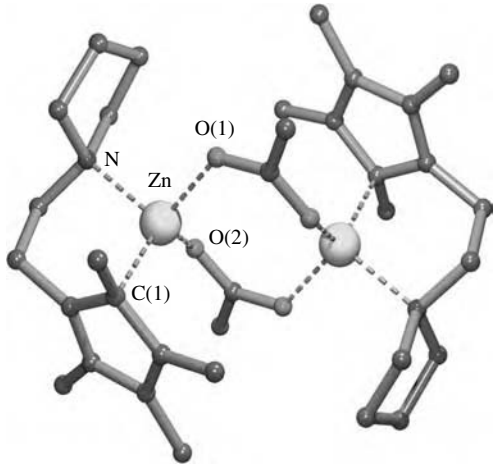

FIGURE 88. Solid state structure of acetate bridged organozinc dimer **177**

The penta-substituted-cyclopentadienylzinc acetate derivative $[(CH_2)_4N(CH_2)_2C_5Me_4ZnO_2CMe]_2$ (**177**) (Figure 88) exists in the solid state as a centro-symmetric dimer via acetate bridges [Zn−O(1) 1.9635(16) and Zn−O(2) 1.9779(15) Å][203]. The cyclopentadienyl group is η^1-bonded to zinc [Zn−C(1) 2.110(2) Å]. Intramolecular coordination of the nitrogen atom of the substituent to zinc [Zn−N 2.124(3) Å] makes this zinc atom tetrahedrally coordinated. A similar compound, in which one of the bridging acetate groups is replaced by a μ^2-bridging OEt group, which has closely related structural features, has been reported by the same authors[263].

A few organozinc compounds containing the t-$BuPO_3$ bis-anion have been reported[263, 264]. They form complex aggregated structures containing up to ten zinc atoms, but are of less interest for organozinc chemists.

E. Monoorganozinc Compounds RZnY with Y = NR_2

Monoorganozinc compounds in which the second group is oxygen-bonded to zinc usually exist as aggregated species and discrete monomolecular structures are exceptions. However, for the monoorganozinc compounds in which the second group is bound via nitrogen to zinc, many more structures of discrete mononuclear species are known.

Tris(trimethylsilyl)methylzinc bis(trimethylsilyl)amide (**178**) is the only example of an organozinc amide in which the zinc atom is two-coordinate, of which the structure has been determined in the solid state (Figure 89)[157]. The Zn−C bond distance [1.944(2) Å] is as expected for a σ-bonded zinc atom. The C−Zn−N bond angle [177.8(1)°] is close to linear. The Zn−N distance is extremely short [1.846(2) Å], but this is a logical consequence of the sp-hybridization of the zinc atom and the sp^2-hybridization of the amide–nitrogen atom. The latter is indicated by the fact that the sum of the bond angles around this nitrogen atom is 359.7°.

In the ethylzinc diphenylamide derivative (**179**)[265] (Figure 89), the zinc atom has a trigonal planar coordination geometry (sum of the bond angles around zinc is 359.8°). Three-coordination at zinc is reached by intramolecular coordination of the phosphorus atom [Zn−P 2.4450(14) Å]. In this compound the amide–nitrogen atom is also sp^2-hybridized. This bonding mode (both the zinc atom and the nitrogen atoms are

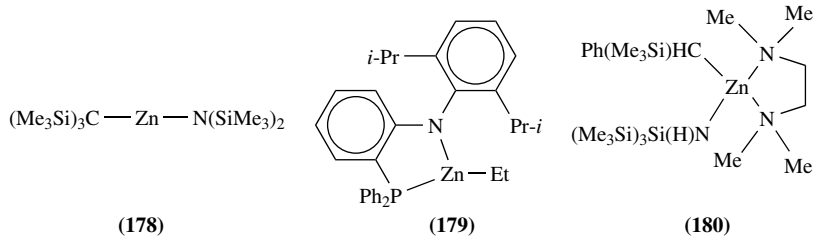

(178) **(179)** **(180)**

FIGURE 89. Schematic structures of **178**, **179** and **180**

sp^2-hybridized) results in a somewhat longer Zn−N bond distance in **179** [1.911(4) Å] compared to the value observed in **178**.

In the organozinc amide complex (**180**)[156] (Figure 89), the zinc atom has a distorted tetrahedral coordination geometry as the result of the coordination by the nitrogen atoms of a TMEDA molecule. The Zn−N bond distances [2.182(3) and 2.252(3) Å] of the coordinating TMEDA molecule are considerably longer than the Zn−N amide σ-bond [1.904(3) Å].

Organozinc β-diketoiminates form a class of compounds of which the structures have been extensively studied, especially those with sterically demanding 2,6-diisopropylphenyl groups present on the nitrogen atoms. A series of compounds with various organic groups bound to zinc, i.e. **181**[266], **182**[267], **183**[266], **184**[266] and **185**[268] (Figure 90), have been prepared and were structurally characterized in the solid state. All compounds have comparable structural features. The bidentate monoanionic diketoiminate ligand is chelate-bonded to the zinc atom with almost equal Zn−N bond distances (average 1.96 Å), resulting in a central six-membered Zn−N−C−C−C−N ring. In **181**, **182** and **185** this ring is flat, but in **183** and **184** this ring is puckered in a boat conformation with the zinc atom at the bow and the opposite C atom at the stern. In all compounds the zinc atom has a trigonal planar coordination geometry. In compound **186**[269] (Figure 90), a potentially intramolecularly coordinating substituent was introduced by replacing one of the 2,6-diisopropylphenyl groups by a 2-methoxyphenyl group, to enforce four-coordination at zinc. However, an X-ray crystal structure determination revealed a structure identical to that of **181–185**.

The solid state structure of **187**[270] (Figure 90), in which a cyanide group is present on the central carbon atom of the diketoiminate fragment, is different. This compound forms

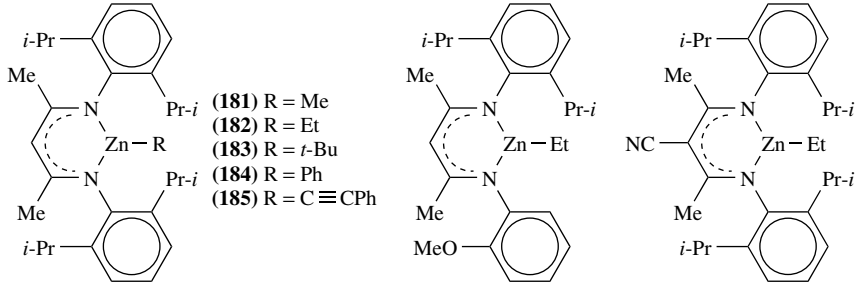

(186) **(187)**

FIGURE 90. Schematic structures of the organozinc diketoiminates **181–187**

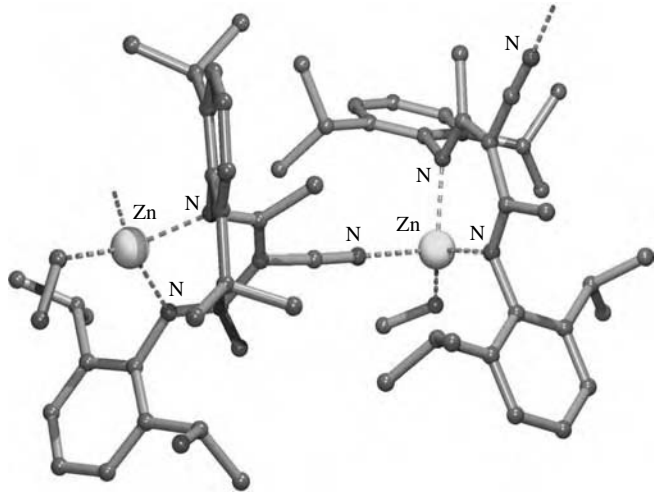

FIGURE 91. Part of the polymeric structure of **187**

linear polymeric chains in the solid state (Figure 91) via coordination of the nitrogen atom of the cyanide group to the zinc atom in a neighbouring molecule [Zn−N 2.136(5) Å], resulting in distorted tetrahedral zinc centres. The pentafluorophenyl analogon of **184**, when recrystallized from THF, forms an adduct in which the THF molecule is coordinated to the zinc atom in a distorted tetrahedral geometry[271].

The solid state structures of the methylzinc iminophosphorane compounds **188**[272] and **189**[273] (Figure 92) show large similarities with those of the organozinc diketoiminates described above. The monoanionic bis(iminophosphorane) ligand is *N*,*N*-chelate-bonded to zinc, resulting in a central Zn−N−P−C−P−N six-membered ring. In both structures the six-membered ring adopts a distorted boat conformation. Trigonal planar coordination

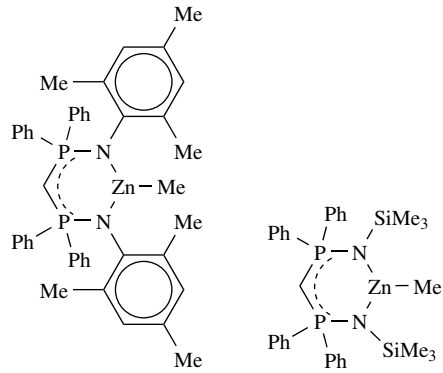

(188) **(189)**

FIGURE 92. Schematic structures of the methylzinc bis(iminophosphorane) compounds **188** and **189**

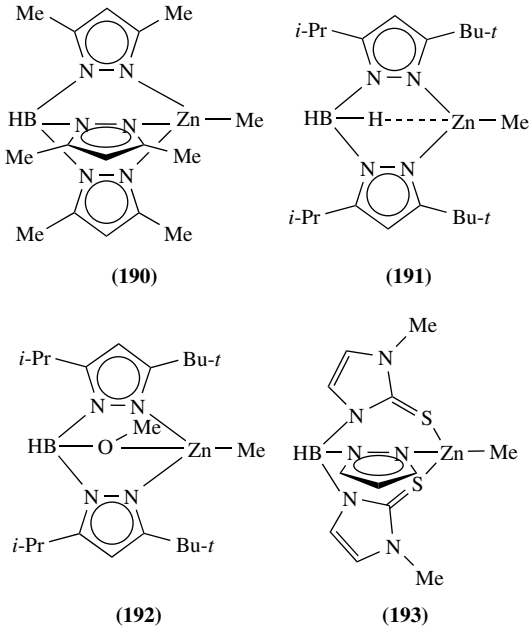

FIGURE 93. Schematic structures of organozinc pyrazolylhydroborato compounds

of the zinc atoms is indicated by the sum of the bond angles around zinc of 360° in both compounds.

Another class of organozinc–nitrogen compounds that have been studied intensively by X-ray crystallography are the tris(pyrazolyl)hydroborato-based systems. The structural details of the 2,4-dimethyl derivative **190**[274] (Figure 93) are given below. It should be noted that the structures of a number of compounds that only differ from **190** in the nature of the substituents present on the pyrazolyl fragment have been determined[275–278]. The structural features of all these compounds are identical. They are monomeric compounds in which the tripodal tris(pyrazolyl)hydroborato fragment caps the zinc atom with its three nitrogen atoms to give a distorted tetrahedral coordination at zinc. In **190** (Figure 94), the three Zn–N distances are almost equal [2.048(6), 2.056(4) and 2.056(4) Å]. Due to the particular architecture of the ligand system all N–Zn–C angles (average 125.0°) are larger than the ideal tetrahedral value and consequently the N–Zn–N angles (average 90.1°) are smaller. Another way to describe these complexes is in terms of an organozinc cation which is capped by the three nitrogen atoms of the tris(pyrazolyl)hydroborato anion.

In compound **191**[279] one of the pyrazolyl groups is lacking and thus only two nitrogen atoms can coordinate to zinc [Zn–N 2.018(5) and 2.021(5) Å]. This leads to a trigonal planar geometry at zinc (the sum of the bond angles around zinc is 360° within experimental error). It has been suggested that an additional weak interaction exists between one of the hydrides and zinc.

Compound **192** (Figure 93) was designed to mimic the binding of zinc to the peptide backbone in thermolysin[280]. The overall structure of **192** shows large similarities with that of **190**, but now two nitrogen atoms [Zn–N 2.101(6) and 2.036(6) Å] and the oxygen atom of the methoxy group [Zn–O 2.182(5) Å] are involved in bonding to zinc.

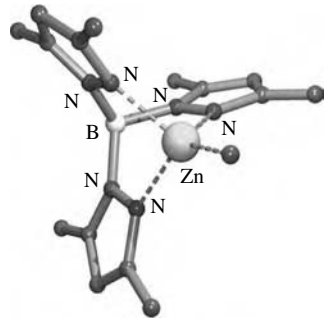

FIGURE 94. Solid state structure of methylzinc tris(pyrazolyl)borato compound **190**

The bis(mercaptoimidazolyl)(pyrazolyl)hydroborato unit present in **193**[281] (Figure 93) coordinates via both sulfur atoms [Zn−S 2.404(1) and 2.410(1) Å] of the two mercaptoimidazolyl moieties and the nitrogen atom [Zn−N 2.043(4) Å] of the pyrazolyl group to zinc. Because this ligand system is more flexible than the tris(pyrazolyl)hydroborate, the bond angles around zinc are closer to the tetrahedral value than in **190**.

X-ray crystal structure determinations of compounds **194**, **195** and **196** (Figure 95) revealed that these compounds exist in the solid state as discrete monomers[282]. In **194**, the zinc atom is trigonal planar coordinated as a result of the *N*,*N*-chelate-bonding [Zn−N 2.007(1) and 1.995(1) Å]. The N−Zn−N bond angle is rather acute [73.83(6)°], but that is a logical consequence of the small bite angle of the ligand.

In **195**, the zinc atom is four-coordinate as a result of the *N*,*S*-chelating ligand [Zn−N 2.009(3) and Zn−S 2.449(1) Å] and the additional coordination of a THF molecule [Zn−O 2.241(3) Å]. The selenium analog **196** is isostructural with **195**.

It has been known for a long time that organozinc amides derived from secondary or primary amines usually exist as dimers in solution[176]. However, depending on the particular groups bound to zinc and/or nitrogen, examples of higher aggregates are also known.

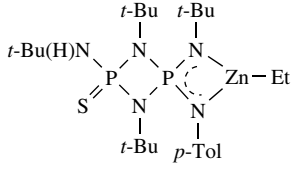

(194)

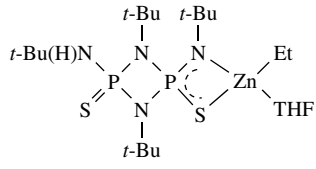

(195)

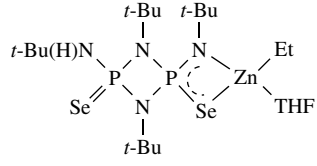

(196)

FIGURE 95. Schematic structures of **194, 195** and **196** in the solid state

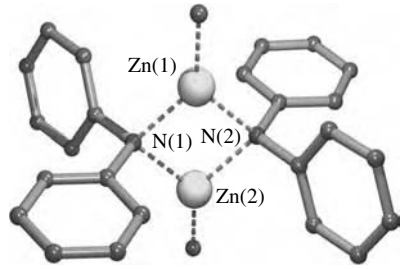

FIGURE 96. Solid state structure of **197**

The first organozinc amide of which the dimeric structure in the solid state was unambiguously established is $[MeZnNPh_2]_2$ (**197**) (Figure 96)[283]. In **197**, two diphenylamide groups are μ^2-bridge bonded via their nitrogen atoms between two methylzinc units, resulting in a central flat Zn−N−Zn−N square. All Zn−N distances are equal within experimental error [average value 2.072(8) Å]. The zinc atoms have a planar trigonal geometry. Because the N−Zn−N bond angle is 90°, consequently the N−Zn−C bond angles (134.4 and 134.6°) deviate considerably from the ideal trigonal value of 120°.

The solid state structures of the organozinc amides **198**[284], **199**[284] and **200**[285] (Figure 97), derived from the corresponding primary amines, are isostructural with that of **197**. In principle, two isomers exist of each of these structures, i.e. one with the groups at the nitrogen atoms located at the same side of the plane defined by the two nitrogen atoms and the two zinc atoms, and one with these groups at opposite sides. It appeared that all these compounds exist as the centrosymmetric dimer, i.e. the one with the two groups at opposite sides.

The ethylzinc amide of mesitylamine crystallizes as a dimeric THF adduct (**201**) (Figure 97)[285]. Also, in this compound the amide nitrogen atom is μ^2-bonded [Zn−N 2.070(5) and 2.076(5) Å] between two zinc atoms. The zinc atoms are distorted tetrahedrally coordinated by additional coordination of a THF molecule [Zn−O 2.240(5) Å].

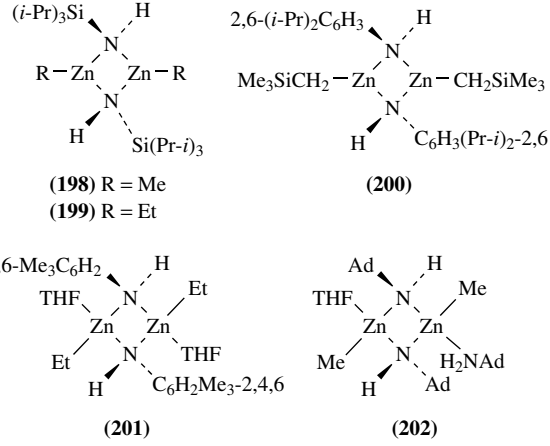

(198) R = Me
(199) R = Et

(200)

(201)

(202)

FIGURE 97. Schematic representation of the structures of **198–202**

The central Zn−N−Zn−N ring is not flat, but folded 30° along the Zn−Zn axis. The two ethyl groups and the two THF molecules are in a *syn* configuration, as are the mesitylamine groups.

The dimeric zinc amide derived from adamantylamine was isolated and structurally characterized as an adduct containing one molecule of coordinated THF and one molecule of coordinated adamantylamine (**202**) (Figure 97)[284]. Its structure shows large similarities with the structure of **201**, but the central Zn−N−Zn−N ring is flat. The two adamantyl groups and the two methyl groups are in *syn*-position and located at the same side of the Zn−N−Zn−N plane. The coordinated THF and adamantylamine are also in *syn*-position but located at the other side of that plane.

The structures of the organozinc amides derived from various diamines, i.e. *N*,*N*,*N*′-trimethylethylenediamine[286], *N*,*N*,*N*′-trimethylpropylenediamine[286], *N*,*N*′-dibenzylethylenediamine[287] and *trans*-1,2-bis(trimethylsilylamino)cyclohexane[288], have also been established. All structures have in common that they are dimers via μ^2-bridging amido nitrogens between the two zinc atoms, forming a central four-membered Zn−N−Zn−N ring, while the second nitrogen atom of each diamine ligand is intramolecularly coordinated to a zinc atom (Figure 98). They only differ in orientation of the various groups present at the central four-membered ring. The two halves of each of the dimers **203**, **204**, **207** and **208** are symmetry-related via an inversion centre. Consequently, the coordinating nitrogen atoms and the Zn-bonded alkyl groups are pairwise located in *anti*-position with respect to the Zn−N−Zn−N plane. In contrast, in **205** and **206** such an inversion centre is not present, but the two halves of the dimer are symmetry-related via a two-fold crystallographic axis. As a result, the two Zn-bonded alkyl groups and the methyl groups at the amide nitrogen are in *syn*-position at one side of the Zn−N−Zn−N ring while the coordinating nitrogen atoms are in *syn*-position at the opposite side.

It appeared to be possible to deprotonate the remaining acidic hydrogen atoms at the coordinating nitrogens in **208** with two additional equivalents of Et_2Zn. The basic structure of the compound obtained $[(EtZn)_2(NSiMe_3)_2$-*c*-C_6H_{10}-1,2$]_2$ (**209**) consists of two *trans*-1,2-bis(trimethylsilylamido)cyclohexane units containing an ethylzinc fragment bonded

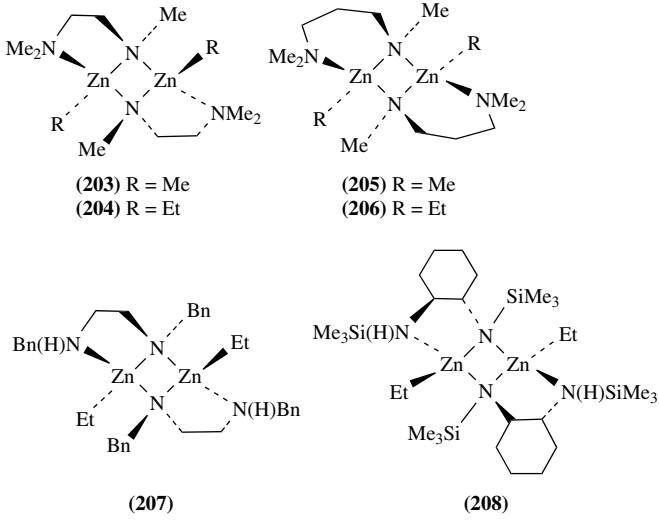

FIGURE 98. Schematic structures of organozinc amides **203–208**

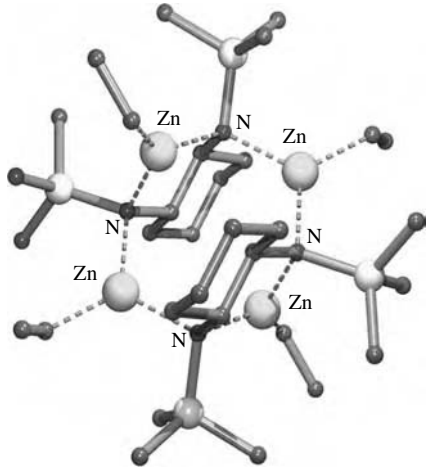

FIGURE 99. Solid state structure of **209**

between the two amido nitrogen atoms, which are linked together by two more ethylzinc moieties, via Zn−N bonds, into a puckered eight-membered ring of alternating nitrogen and zinc atoms (Figure 99)[288]. One of the cyclohexyl fragments is located below that ring and the other one above it.

The alkylzinc amide compounds **210**[289], **211**[290] and **212**[291], derived from the corresponding 2-(aminomethyl)pyridines, have structural features identical to those of **203–208** (Figure 100). They form dimers in which the amide nitrogen atom is μ^2-bridged between

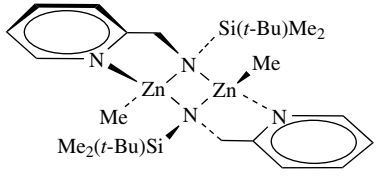

(210)

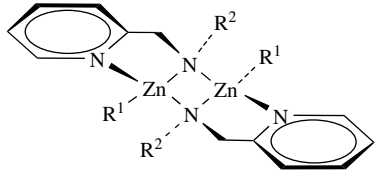

(211) R^1 = Me, R^2 = $(i\text{-Pr})_3$Si
(212) R^1 = $(Me_3Si)_3C$, R^2 = H

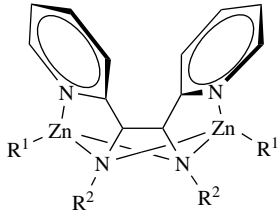

(213) R^1 = Me, R^2 = $(i\text{-Pr})_3$Si
(214) R^1 = Me, R^2 = $Me_2(t\text{-Bu})$Si
(113) R^1 = Et, R^2 = t-Bu

FIGURE 100. Schematic structures of compounds **210–214**

two zinc atoms to give the central Zn−N−Zn−N ring, while the pyridyl nitrogen atoms each coordinate to a zinc atom. These compounds can also exist as two different geometrical isomers. Dimer **210** is centrosymmetric and consequently the central Zn−N−Zn−N ring is flat and the various groups at this ring are pairwise in *anti*-position with respect to this plane. In both **211** and **212** such an inversion centre is not present. The four-membered Zn−N−Zn−N ring in **211** is slightly folded, but essentially flat in **212**. In both **211** and **212** the coordinating pyridyl nitrogen atoms approach the zinc atoms from the same side of the plane (*syn*-position), while the two methyl groups bound to zinc and the amide−nitrogen substituents are in *syn*-position at the other side of the plane. One of the factors that determines the aggregation state of this type of compounds is the bulk of the respective groups present at zinc and nitrogen. This became evident by the structure determination of the methylzinc analog of **212**, which appeared to be a trimeric aggregate in the solid state (*vide infra*).

Thermolysis of the alkylzinc 2-(amidomethyl)pyridines induces an oxidative C−C coupling reaction at the methanide carbon atom. The products **213**[290] and **214**[289] (Figure 100) were structurally characterized by X-ray crystallography. These dimers are isostructural with **113**, which was obtained from the thermal conversion of the diethylzinc complex of *N*-*tert*-butyl-2-pyridylcarbaldimine. Details (Figure 52) are given above (Section III.D).

The structure of the ethylzinc amide derived from 2-(trimethylsilylamino)pyridine (**215**) also consists of a central Zn−N−Zn−N ring via μ^2-N bridging amido groups while the pyridine nitrogen atoms coordinate to the zinc atoms [Zn−N 2.125(5) Å] (Figure 101)[292]. The μ^2-bridging of the amido nitrogen atoms is rather asymmetric [Zn−N 2.061(5) Å within the four-membered chelate ring and 2.245(5) Å to the other zinc atom]. The pyridyl groups are *syn*-orientated with respect to the central Zn−N−Zn−N ring, as are the ethyl groups bound to zinc and the trimethylsilyl groups at the other side of this ring.

The methylzinc guanidinate complex **216** has a similar structure (Figure 101)[211]. In this compound the μ^2-bridging between the zinc atoms is also asymmetric [Zn−N 2.101(3) and 2.201(3) Å]. The orientation of the various groups with respect to the central Zn−N−Zn−N ring is identical to that in **215**. The two guanidinate ligands lie in *syn*-position at one side

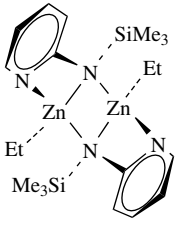

(215)

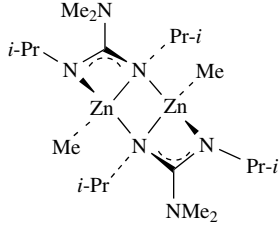

(216)

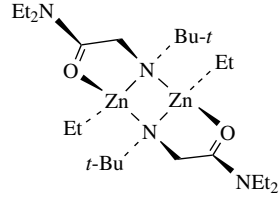

(217)

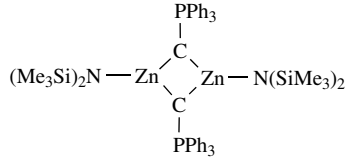

(218)

FIGURE 101. Schematic structures of organozinc amides **215–218**

of the ring and the methyl groups and the isopropyl substituents at the bridging nitrogen atom lie pairwise in *syn*-position at the other side of the ring.

Compound **217** is formed, among other products, from the reaction of the 1-aza-4-oxa-1,3-butadiene, *t*-BuN=C(H)C(=O)NEt$_2$, with Et$_2$Zn[293]. The overall structural features are closely related to the organozinc amides discussed before (Figure 101). The central Zn−N−Zn−N ring formed via μ^2-bridging amido nitrogen atoms [Zn−N 2.069(5) and 2.093(5) Å] is flat. The oxygen atoms of the diethylamido group coordinate each to a zinc atom [Zn−O 2.123(4) Å] and are in *syn*-position with respect to the central plane. Likewise, the two zinc-bonded ethyl groups and the two *t*-butyl groups are in *syn*-position at the other side of that plane.

The structure of dimer **218** is remarkable (Figure 101)[78]. In this compound two carbon atoms are μ^2-bridge-bonded between two zinc atoms [Zn−C 2.066(4) and 2.070(5) Å] and not the amide nitrogen atoms, which are each σ-bonded to a zinc atom [Zn−N 1.930(4) Å]. This 'reversed' bonding mode is most likely a consequence of the ylide character of the bridging carbon atoms. The zinc atoms have trigonal planar coordination geometry. The amide nitrogen atoms are sp^2-hybridized, which is indicated by the sum of the bond angles (360°).

When Cp$_2$Zn and [(Me$_3$Si)$_2$N]$_2$Zn are mixed in a 2:1 molar ratio, a new compound with stoichiometry Cp$_3$Zn$_2$N(SiMe$_3$)$_2$ (**219**) is obtained[294]. The solid state structure of this compound comprises two CpZn units linked to a dimer via one μ^2-N-bridging [Me$_3$Si]$_2$N group [Zn−N 2.005(3) and 2.024(3) Å] and one bridging Cp group (Figure 102). The bonding of the peripheral Cp group to zinc is not pure η^1, as is indicated by one relatively short [2.059(6) Å] and one relatively long [2.473(7) Å] Zn−C bond. This points to a bonding mode which is intermediate between η^1 and η^2. A similar type of bonding is observed for the bridging Cp group. Each of the zinc atoms has one relatively short [average 2.143 Å] and one relatively long [average 2.553 Å] interaction with this Cp group.

The alkylzinc amides derived from the primary amines, 2-(aminomethyl)pyridine (**220**)[291], aniline (**221**)[285], 1-naphthylamine (**222**)[295] and *tert*-butylamine (**223**)[285], have in common that they form trimeric aggregates in the solid state (Figure 103). The three zinc atoms are linked via three μ^2-bridging amide nitrogen atoms, with Zn−N distances in the expected range, to a cyclohexane-like six-membered ring. In **220**, a tetrahedral coordination geometry at zinc is reached by the coordination of a pyridyl nitrogen atom to each zinc atom [average Zn−N 2.160 Å]. In **221** and **222**, the zinc atoms are four-coordinate as the result of coordination of a THF molecule to each zinc atom with Zn−O bond distances ranging from 2.17 to 2.27 Å. In **223**, no additional coordinating ligands

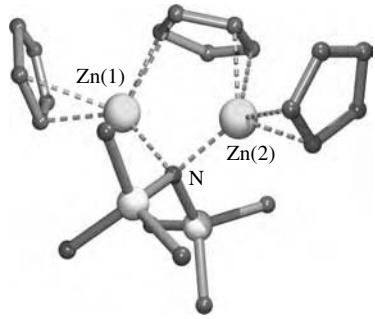

FIGURE 102. Solid state structure of **219**

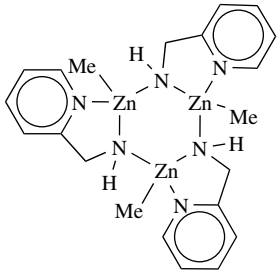

(220)

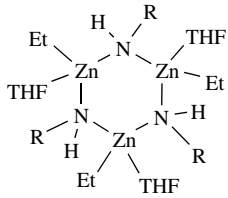

(221) R = Ph
(222) R = 1-naphthyl

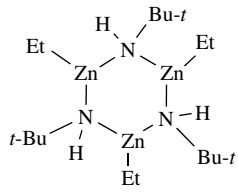

(223)

FIGURE 103. Schematic structures of the trimeric organozinc amides **220–223**

are present and the zinc atoms have trigonal planar coordination geometry. The central six-membered metallacycle in **220** adopts a boat conformation while in **221–223** a chair conformation is present.

The hetero-cubane structural motif, which is often found in organozinc alkoxides (Section IV.D), has also been observed in the solid state structures of a few organozinc phosphaneiminato compounds (Figure 104)[296, 297]. The central core of compounds (**224–226**) consists of a cube of alternating zinc and nitrogen atoms, in which each nitrogen atom is μ^3-bonded to three zinc atoms. These compounds are isostructural and only differ in the nature of the group bound to zinc. Within experimental error the Zn−N distances are equal in each compound [2.088 Å for **224** and 2.088 Å for **225** and 2.069 Å for **226**]. Also, the Zn−N−Zn and N−Zn−N bond angles differ only marginally (<0.5°) from 90°. These values indicate that the central core in these compounds has an almost perfect cubic geometry. Compound **227** is an analog of **225** in which one of the trimethylphospaneiminato groups is replaced by an iodide. As a consequence of the longer Zn−I distances [2.986(3), 2.971(3) and 2.939(3) Å] compared to the Zn−N distances [average 2.055 Å], the geometry of the central cube is less perfect.

Reaction of secondary benzamides with Me_2Zn affords the corresponding methylzinc benzamides (equation 23)[137]. X-ray crystal structure determinations of these compounds revealed complex irregular aggregates in which all nitrogen and oxygen atoms are involved in bonding to zinc.

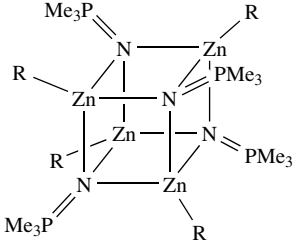

(224) R = Me
(225) R = *n*-Bu
(226) R = C≡CSiMe$_3$

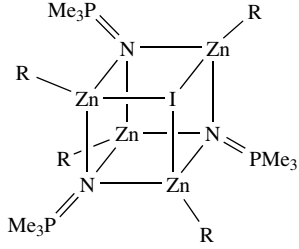

(227) R = *n*-Bu

FIGURE 104. Schematic structures of tetrameric organozinc phosphaneiminates **224–227**

An X-ray crystal structure determination of the product obtained from the reaction of methyl *N*-phenylcarbamate with Et_2Zn (equation 24) shows the formation of a complex aggregate containing two zinc-bonded ethyl groups, four zinc atoms and six deprotonated carbamate molecules, instead of the anticipated ethylzinc carbamate[298].

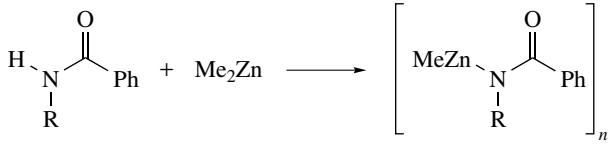

(23)

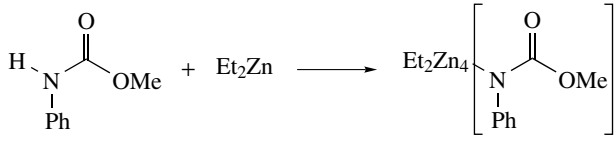

(24)

F. Monoorganozinc Compounds RZnY with Y = Other Heteroatom Bonded Group

Only for a few organozinc compounds, in which in addition to the zinc–carbon bond a zinc–heteroatom bond other than oxygen or nitrogen is present, have structures in the solid state been determined. These structures include those of organozinc compounds in which, in addition to the zinc–carbon bond, a zinc–sulfur, zinc–selenium, zinc–phosphorus or zinc–arsenic bond is present.

Methylzinc thiolate $MeZnSCMe_2CH_2NMe(CH_2)_2Pyr$-2 (**228**) is the only example of a monomeric organozinc thiolate that has been structurally characterized in the solid state (Figure 105)[299]. This compound was used as a precursor for the synthesis of the corresponding formate complex to mimic peptide deformylase. In addition to the zinc–carbon bond [Zn–C 1.986(3) Å] and the Zn–S bond [Zn–S 2.2971(7) Å], the two nitrogen atoms of the ligand system are intramolecularly coordinated to zinc [Zn–N(1) 2.120(2) and Zn–N(2) 2.161(2) Å], rendering the zinc atom distorted tetrahedrally coordinated.

The dimeric structure as present in organozinc–oxygen and –nitrogen aggregates is also observed in the solid state structures of various organozinc thio compounds (Figure 106). The centrosymmetric (trimethylsilyl)methylzinc triphenyl sulfide dimer (**229**)[220] comprises a flat central four-membered ring of alternating zinc and sulfur atoms. The Zn–S–Zn bridge is slightly asymmetric [Zn–S 2.381(1) and 2.416(1) Å]. The zinc atoms are trigonal

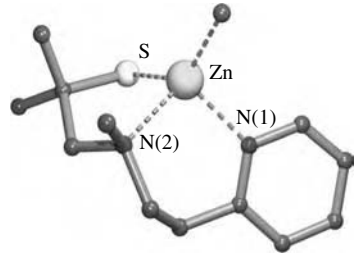

FIGURE 105. Solid state structure of the monomeric organozinc thiolate **228**

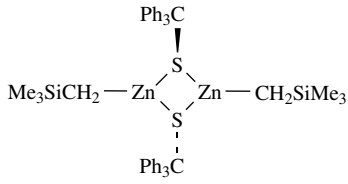

(229)

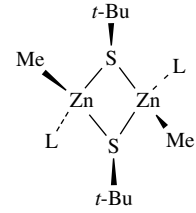

(230a) L = Pyr
(230b) L = TMTA

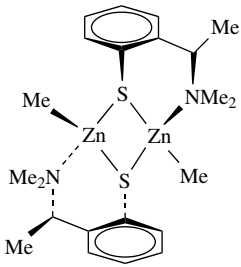

(231)

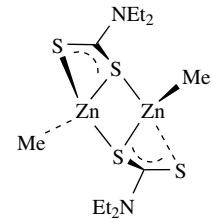

(232)

FIGURE 106. Schematic structures of dimeric organozinc thiolates **229–232**

planar coordinated and the two Ph_3C substituents are in *anti*-position with respect to the central plane.

Methylzinc *tert*-butyl sulfide forms with pyridine or 1,3,5-trimethyl-1,3,5-triazine (TMTA) the dimeric complexes **230a** and **230b**[300]. In both compounds the central four-membered Zn−S−Zn−S ring is folded, to 13° in **230a** and 40° in **230b**. The two coordinating pyridine ligands in **230a** approach the zinc atoms from the same side of the ring (*syn*-position) [Zn−N 2.141(5) and 2.156(5) Å] as the two coordinating TMTA ligands do in **230b** [Zn−N 2.205(5) and 2.216(5) Å]. Both in **230a** and in **230b** the two methyl groups at zinc and the two coordinating ligands are in *syn*-position at the other side of ring.

The enantiopure methylzinc thiolate containing the 2-[(*R*)-1-(dimethylamino)ethyl] thiophenolate ligand (**231**) has proven to be an excellent catalyst for the enantioselective addition of diorganozinc compounds to aldehydes[301]. An X-ray crystal structure determination (Figure 107) showed that this compound in the solid state also exists as a dimer[302]. Its structure comprises a central, almost flat, Zn−S−Zn−S four-membered ring as the result of two μ^2-bridging arylthiolate groups with almost equal Zn−S bond lengths [average 2.414 Å]. Both nitrogen atoms of the substituent are intramolecularly coordinated to a zinc atom [Zn−N 2.101(4) and 2.107(4) Å], forming a six-membered chelate ring. Remarkably, in one of the chelate rings the methyl substituent is orientated perpendicular to the plane of the aryl ring, while in the other chelate ring this substituent is in the energetically less favourable in-plane position.

Methylzinc *N*,*N*-diethyldithiocarbamate (**232**) (Figure 106) exists as a centrosymmetric dimer in the solid state[303]. One sulfur atom of each of the dithiocarbamate groups bridges symmetrically [Zn−S 2.512(4) and 2.501(4) Å] between the two zinc atoms to form a flat four-membered ring. The other two sulfur atoms each coordinate to a zinc atom with a considerably shorter bond distance [Zn−S 2.370(3) Å]. As a consequence of

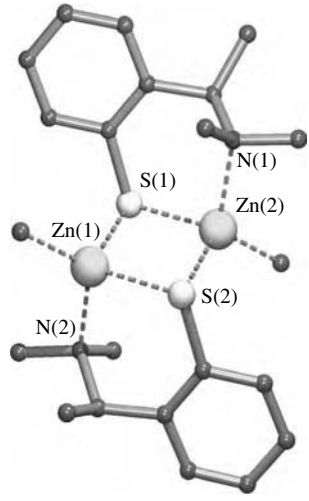

FIGURE 107. Solid state structure of **231**

the small bite angle of the dithiocarbamate chelate, the geometry at the zinc atoms is rather distorted tetrahedral. The solid state structures of the corresponding ethylzinc *N*,*N*-diethyldithiocarbamate[304] and the selenium analogs methylzinc, ethylzinc and (trimethylsilyl)methylzinc *N*,*N*-diethyldiselenocarbamate[305, 306] have been determined, and all are isostructural with **232**.

The solid state structures of methylzinc *tert*-butyl sulfide[307], methylzinc isopropyl sulfide[308] and ethylzinc ethyl sulfide[309] have been determined. All are aggregated clusters. Methylzinc *tert*-butyl sulfide is a pentamer $(MeZnSBu\text{-}t)_5$ in which four of the sulfide groups are μ^3-bonded to four zinc atoms and one sulfide is μ^2-bonded between two zinc atoms (Figure 108). Consequently, four of the zinc atoms have a distorted tetrahedral geometry while the remaining zinc atom is trigonal planar.

Methylzinc isopropyl sulfide is an octamer $(MeZnSPr\text{-}i)_8$ in which all the sulfide groups are μ^3-bridge-bonded to three zinc atoms, rendering them all distorted tetrahedral. No further details are given for this structure.

Ethylzinc ethyl sulfide is a decamer $(EtZnSEt)_{10}$. In this cluster all sulfide groups are μ^3-bonded to three zinc atoms (Figure 108). It is striking that the overall structure of this cluster shows a close resemblance to that of wurtzite.

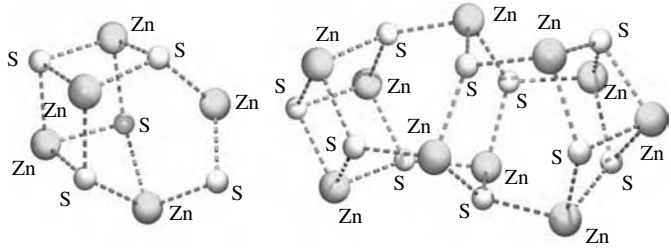

FIGURE 108. Basic arrangement of zinc and sulfur atoms in $(MeZnSBu\text{-}t)_5$ (left) and $(EtZnSEt)_{10}$ (right)

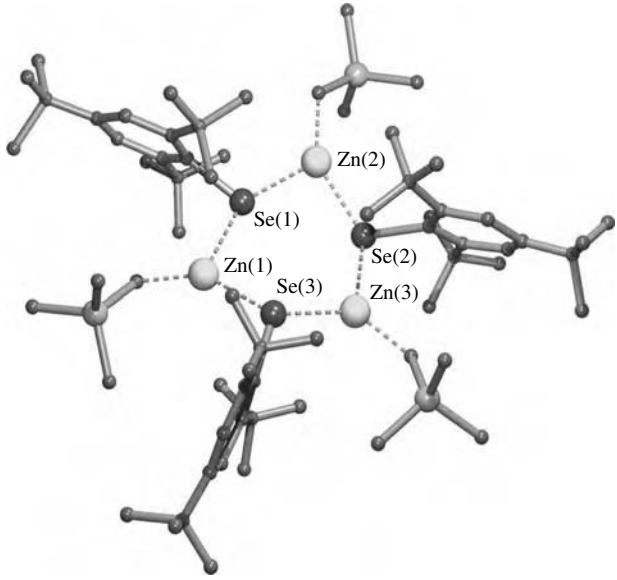

FIGURE 109. Solid state structure of organozinc selenide **233**

Apart from the few organozinc diselenocarbamates (*vide supra*), (trimethylsilyl)methylzinc 2,4,6-tris(*tert*-butyl)phenyl selenide (**233**) is the only compound with direct zinc to selenium bonds of which the structure in the solid state has been established[310]. It is a trimeric aggregate (Figure 109) of which the central core comprises a slightly puckered six-membered ring of alternating zinc and selenium atoms as the result of μ^2-bridging selenide groups with almost equal Zn−Se distances [average 2.445 Å].

In compound **234** (Figure 110), two organozinc moieties directly bound to phosphorus are present[311]. The Zn−P bond lengths are 2.2273(9) and 2.2365(10) Å, while the Zn−C bond lengths [both 1.965(3)Å] are slightly shorter than in homoleptic $[(Me_3Si)_3C]_2Zn$[87]. Due to the steric congestion of the bulky $(Me_3Si)_3C$ groups at the zinc atoms and the i-Pr_3Si groups at phosphorus, the C−Zn−P bond angles [166.5(1)° and 167.0(1)°] deviate from the ideal value of 180° for an sp-hybridized zinc atom. The sum of the bond angles around phosphorus is 319°, indicating a pyramidal geometry. Also, the structure of the corresponding arsenic analog **235** has been reported[312]. Apart from the slightly longer Zn−As bonds [2.3256(7) and 2.3207(7) Å], this compound is isostructural with **234**.

The alkylzinc bis(trimethylsilyl)phosphides (**236**–**238**)[313] and the arsenic analog of **236** (**239**)[314] crystallize as trimeric aggregates (Figure 110). The central part in the organozinc phosphides is a six-membered ring of alternating zinc and phosphorus atoms as a result of μ^2-bridging phosphides between zinc atoms. All zinc−phosphorus distances are in the range of 2.38 to 2.41 Å. In all compounds, the zinc atoms have a trigonal planar geometry. In **238**, the six-membered ring is twisted, but in **236** and **237** this ring has a twist-boat conformation. The arsenic analog **239** is isostructural with **236**. It should be noted that the crystallographic asymmetric unit of isopropylzinc bis(trimethylsilyl)phosphide contains both the trimeric aggregate **238** and a dimer (**240**). This dimer comprises a flat four-membered Zn−P−Zn−P ring as a result of μ^2-bridging phosphido groups with Zn−P distances in the same range as those in the trimeric aggregate. As in the trimer, the

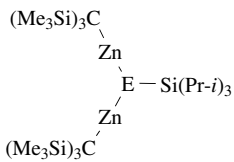

(234) E = P
(235) E = As

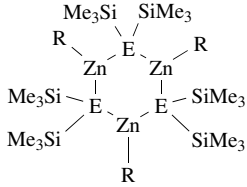

(236) E = P, R = Me
(237) E = P, R = *n*-Bu
(238) E = P, R = *i*-Pr
(239) E = As, R = Me

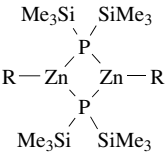

(240) R = *i*-Pr
(241) R = Me_3SiCH_2

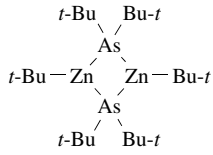

(242)

FIGURE 110. Schematic structures of organozinc-phosphides and -arsenides **234–242**

zinc atoms have a trigonal planar geometry. The solid state structure of the (trimethylsilyl)methyl analog (**241**) of **240** shows a large resemblance to that of **241**[313].

The X-ray crystal structure determination of *tert*-butylzinc bis(*tert*-butyl) arsenide (**242**) revealed a similar structural feature as observed in **240** and **241**, i.e. a flat Zn−As−Zn−As central four-membered ring as a result of μ^2-bridging arsenide groups and trigonal planar zinc atoms[315].

Reaction of dicyclohexylphosphine with Et_2Zn in a 1:1 molar ratio in THF as a solvent affords, after cooling to −30 °C, a crystalline material. An X-ray crystal structure determination showed that this product is the trimeric ethylzinc dicyclohexylphosphide (**243**) (Figure 111)[316]. The structure consists of a central six-membered ring like in the trimeric organozinc phosphides described above. To one of the zinc atoms a molecule of THF is coordinated [Zn−O 2.275(4) Å], rendering this zinc centre tetrahedrally coordinated. The other two zinc atoms have a trigonal planar geometry. The six-membered metallacycle is in the chair conformation.

Similarly, ethylzinc diphenylphosphide (**244**) was prepared from diphenylphosphine and Et_2Zn (Figure 111). An X-ray crystal structure determination revealed a central six-membered metallacycle[317]. To two of the zinc atoms additional diphenylphosphine

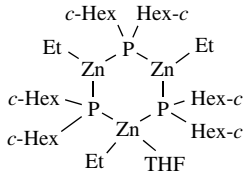

(243)

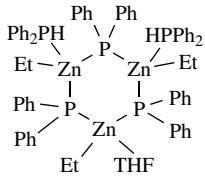

(244)

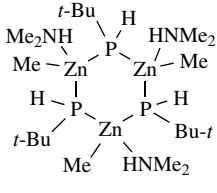

(245)

FIGURE 111. Schematic structures of the organozinc phosphides **243–245**

molecules are coordinated, and the remaining zinc atom is coordinated by a THF molecule, leading to a tetrahedral geometry for all zinc atoms. The Zn−P distances of the coordinated phosphines are slightly longer (average 2.55 Å) than the μ^2-bridge-bonding Zn−P distances (average 2.44 Å). Because the zinc atom and its bonded groups (the ethyl group and the coordinating THF molecule) are crystallographically disordered over two positions, no conclusions can be drawn concerning the actual conformation of the six-membered ring.

The primary phosphine *t*-$BuPH_2$ reacts with Me_2Zn to give a complex [MeZn(P(H)Bu-*t*(*t*-$BuPH_2$)]. After an exchange reaction with $(Me_2N)_3Sb$, compound **245** was obtained as a crystalline material[318]. The structure of **245** comprises again a six-membered metallacycle in a 'half-boat' conformation with μ^2-bonded primary phosphide groups between two zinc atoms. Each of the zinc atoms has a tetrahedral geometry as a result of a coordinating dimethylamine molecule.

V. ORGANOZINC COMPOUNDS CONTAINING A ZINC–TRANSITION METAL BOND

Zinc–transition metal compounds in which a direct zinc to transition metal bond is present ($Zn[Co(CO)_4]_2$ was the first one)[319] have already been known for a long time. However, it was not until 1982 that a compound was isolated and structurally characterized that contained both a zinc-to-carbon and a zinc-to-transition metal bond.

Reaction of $HCo(N_2)(PPh_3)_3$ with Cp_2Zn affords $(CpZn)_2Co(Cp)(PPh_3)$ (**246**), which was structurally characterized in the solid state by X-ray crystallography (Figure 112)[320]. The structure of **246** consists of a central cobalt atom, which is surrounded in roughly tetrahedral fashion by two zinc atoms, a phosphorus atom and an η^5-bonded cyclopentadienyl group. In the two CpZn units the cyclopentadienyl groups are η^5-bonded to zinc with an average Zn−C distance of 2.34 Å. The angles Co−Zn to the centre of the Cp groups are not linear, but slightly bent, 160.6° and 162.9°, respectively. The Zn−Co distances are slightly shorter [2.2893(5) and 2.2882(5) Å] than these distances in $Zn[Co(CO)_4]_2$ [2.305(2) Å].

Likewise, $CpZnNbH_2Cp_2$ (**247**) was obtained from the reaction of Cp_2Zn with Cp_2NbH_3 and was structurally characterized (Figure 112)[321]. The structural geometry of **247** resembles that of Cp_2NbH_3[322], with the central hydrogen atom replaced by a CpZn group. The Cp ring is bound in a nearly symmetrical η^5-fashion to zinc, with its centre displaced slightly off the Nb−Zn axis (0.15 Å).The Zn−Nb distance of 2.5407(7) Å indicates the presence of a normal Zn−Nb single bond. The Nb−H distance [1.69(4) Å] is typical for a terminal Nb−H bond, but the slight bridging character of these hydrides to zinc is indicated by Zn−H distances of 1.97(4) Å and relatively small H−Zn−Nb angles of 51.1°.

$(Cp_2Zn)_2Ta(H)(MeCp)_2$ (**248**) was prepared in a similar way to the niobium compound **247**. Its structural characterization[323] in the solid state revealed a structure (Figure 112)

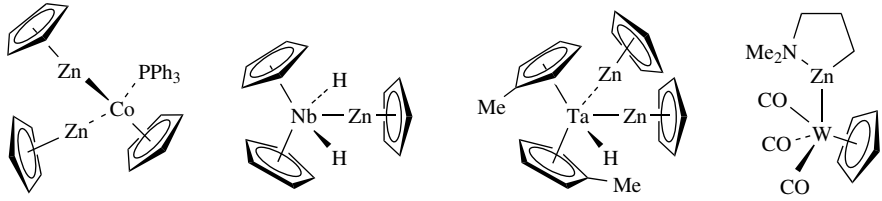

(246) **(247)** **(248)** **(249)**

FIGURE 112. Schematic structures of organozinc–transition metal compounds **246–249**

close to that of Cp_2TaH_3 in which two of the hydrogen atoms are replaced by zinc atoms. In the CpZn units the Cp groups are η^5-bonded to zinc with an average C−Zn distance of 2.37 Å. The two Zn−Ta bonds (2.59 Å) are equal within experimental error and are typical for normal Zn−Ta single bonds. The acute Zn−Ta−Zn bond angle [62.8(1)°] results in a very close approach of the two non-bonded zinc atoms (2.699 Å).

The organozinc tungsten compound **249** (Figure 112) was prepared by a redistribution reaction of the symmetric diorganozinc compound $[Me_2N(CH_2)_3]_2Zn$ with $[CpW(CO)_3]_2$. Its structural characterization in the solid state revealed an organozinc part in which the dimethylaminopropyl group is σ-bonded to zinc and the nitrogen atom is intramolecularly coordinated to zinc [2.19(3) Å][324]. This organozinc part is connected to a $CpW(CO)_3$ unit via a direct Zn−W bond [2.685(3) Å]. The overall structural geometry of **249** can be described as consisting of a central tungsten atom, surrounded in a tetragonal pyramidal fashion by a cyclopentadienyl group in the apical position and three CO molecules and a zinc atom in the basal positions.

Rather unexpected products have been obtained from the reaction of Cp_2Zn with zero-valent nickel compounds. The reaction of Cp_2Zn with $Ni(COD)_2$ (COD = 1,5-cyclooctadiene) in the presence of PPh_3 afforded a product (**250**) of which the X-ray crystal structure determination revealed a structure consisting of a CpNi unit in which the Cp group is η^5-bonded to nickel and a PPh_3 molecule which is coordinated to nickel (Figure 113)[325]. Two zinc atoms are bonded via direct Zn−Ni bonds [Zn−Ni 2.379(5) and 2.383(5) Å] to nickel. To each of the zinc atoms, one Cp group is bonded via an η^1-interaction [Zn−C 2.01(4) and 2.09(4) Å]. Finally, one Cp group bridges via two η^2-interactions between the two zinc atoms. It is notable that these η^2-interactions have one short (average 2.20 Å) and one longer (average 2.44 Å) Zn−C contact.

When the same reaction of Cp_2Zn with $Ni(COD)_2$ was carried out in the absence of PPh_3, an entirely different product having the stoichiometry $Cp_6Zn_4Ni_2$ (**251**) was obtained[326]. An X-ray crystal structure determination revealed the formation of a cluster compound, consisting of an octahedral arrangement of two apical nickel atoms and four equatorial zinc atoms. The octahedron is compressed along the Ni−Ni axis giving eight Ni−Zn bonds of 2.398(2) Å and one long Ni−Ni bond of 2.571(1) Å. To each of the nickel and zinc atoms one Cp group is η^5-bonded. Overall, the structure has a spherical shape (Figure 113). Due to the crystallographic symmetry in the tetragonal space-group $P4_2/mnm$, the Cp groups bound to nickel are two- and those to zinc four-fold disordered.

To overcome this disorder, the same synthetic procedure was used with the substituted cyclopentadienyl compounds bis(*tert*-butylcyclopentadienyl)zinc and bis[(trimethylsilyl) cyclopentadienyl]zinc[327]. Indeed, the corresponding Zn_4Ni_2 clusters were formed, in which the geometry of the central cluster core and the bonding of the cyclopentadienyl groups

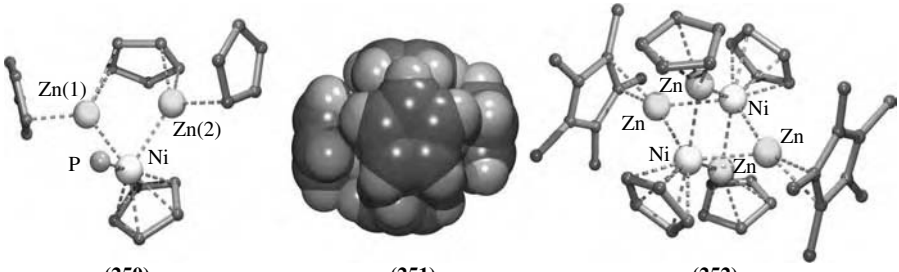

(250) **(251)** **(252)**

FIGURE 113. Solid state structure of **250**. Space filling model of **251**. Solid state structure of **252**

to nickel is identical to that in **251**. The only difference is the hapticity of the bonding of the cyclopentadienyl groups to zinc. In the *tert*-butyl-substituted analog, two of the cyclopentadienyl groups are η^5-bonded to two zinc atoms that are in *trans*-position and the other two cyclopentadienyl groups are η^1-bonded to the other two zinc atoms. Likewise, in the trimethylsilyl derivative two of the cyclopentadienyl groups are η^3-bonded and the other two η^1-bonded.

Reaction of Cp_2Zn, Cp^*_2Zn and $Ni(COD)_2$ in 1:1:1 ratio afforded a similar Zn_4Ni_2 cluster compound **252**[328]. In **252** (Figure 113), two Cp groups are η^5-bonded to the nickel atoms, while a Cp* group is bonded to each of two *trans*-positioned zinc atoms in a η^2-fashion [Zn−C 2.18(1) and 2.24(1) Å]. To the other two zinc atoms Cp groups are bonded. Due to relatively large thermal motions of these Cp groups, their exact bonding mode to zinc could not be determined, but most likely they are intermediate between the η^2- and η^3-bonding modes.

It has been shown that one of the μ^3-bridging hydrogen atoms in the $Cp^*_3Ru_3H_5$ cluster can be easily replaced by a main group organometallic fragment like MeGa, EtAl, *i*-PrMg or EtZn[329]. The X-ray crystal structure determination of the product $Cp^*_3RuZnEtH_4$ (**253**) obtained from the reaction of $Cp^*_3Ru_3H_5$ with Et_2Zn shows that the main structural features of the originating $Cp^*_3Ru_3H_5$ cluster are retained, but one of the μ^3-bridging hydrogen atoms is replaced by a μ^3-bridging EtZn group (Figure 114), with almost equal Zn−Ru distances of 2.6747(10), 2.6561(8) and 2.6561(8) Å.

The organozinc rhodium compounds $[(i\text{-Pr})_2P(CH_2)_3P(Pr\text{-}i)_2RhZnCH_2C_6H_5]_2(\mu\text{-H})_2$ (**254**) and $[(i\text{-Pr})_2P(CH_2)_3P(Pr\text{-}i)_2RhZnCp]_2(\mu\text{-H})_2$ (**255**) (Figure 114) were obtained from the reaction of $[(i\text{-Pr})_2P(CH_2)_3P(Pr\text{-}i)_2Rh]_2(\mu\text{-H})_2$ with $(PhCH_2)_2Zn$ and with Cp_2Zn, respectively[330, 331]. The solid state structure of **254** consists of two $(i\text{-Pr})_2P(CH_2)_3P(Pr\text{-}i)_2Rh$ fragments that are linked into a dimer via two μ^2-bridging hydrogen atoms and two symmetrically μ^2-bridging benzylzinc fragments [Zn−Rh 2.513(1) and 2.558(1) Å] between the rhodium atoms.

Compound **255** also contains two μ^2-bridging zinc atoms between the rhodium atoms, but in a less symmetrical manner than in **254**. This asymmetry is reflected by the difference in bonding distances between rhodium and zinc in one of the bridges [Zn−Rh 2.6115 and 2.4812 Å]. Only one μ^2-bridging hydrogen is present between the rhodium atoms. It is remarkable that the other hydrogen atom occupies a μ^2-bridging position between one of the rhodium atoms and one of the zinc atoms [Rh−H 1.57 and Zn−H 1.66 Å]. It is notable that the Cp groups in the organozinc moieties are η^3-bonded to zinc.

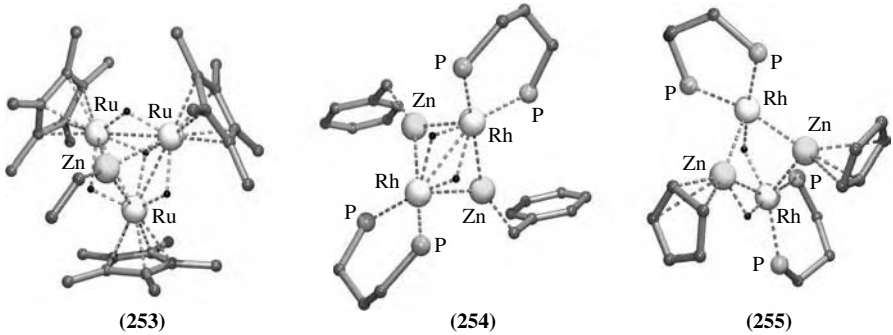

(253) **(254)** **(255)**

FIGURE 114. Solid state structures of the organozinc–transition metal compounds **253–255**. Note that in **254** and **255** the *i*-Pr groups at phosphorus are omitted for clarity

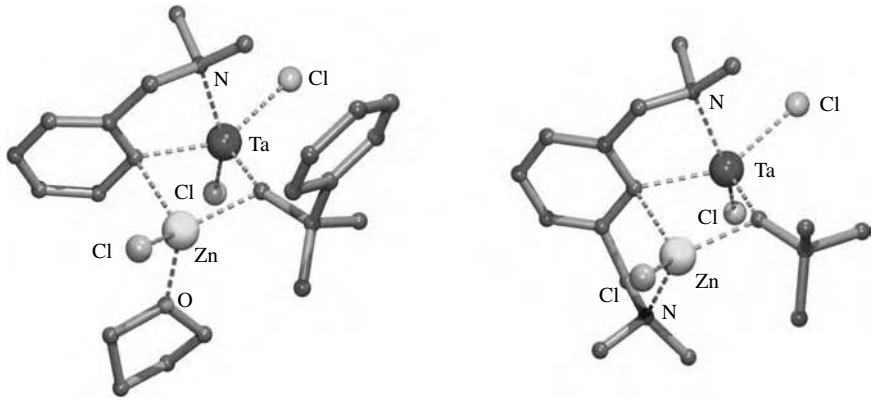

(256) **(257)**

FIGURE 115. Solid state structures of the organozinc–tantalum compounds **256** and **257**

Formally, compounds 2-$Me_2NCH_2C_6H_4TaZn(CH_2CMe_2Ph)Cl_3(THF)$ (**256**) and 2,6-$(Me_2NCH_2)_2C_6H_3TaZn(CH_2CMe_3)Cl_3$ (**257**) (Figure 115) do not belong to the class of organozinc compounds containing a zinc–transition metal bond. However, they are interesting compounds in that they contain both a bridging aryl group and a bridging alkylidyne fragment between a zinc atom and a tantalum atom. X-ray crystal structure determinations confirmed the molecular geometries of both compounds[332, 333].

The overall structures of **256** and **257** show large similarities. The aryl groups bridge in a rather symmetrical manner between zinc and tantalum [in **256**, Zn–C 2.27(2) and Ta–C 2.23(2) Å; in **257**, Zn–C 2.25(1) and Ta–C 2.32(1) Å]. The bridge bonding of the alkylidyne carbon between zinc and tantalum is less symmetric [in **256**, Zn–C 2.14(2) and Ta–C 1.84(2) Å; in **257**, Zn–C 2.114(6) and Ta–C 1.862(6) Å]. In **256**, the tantalum atom has a geometry intermediate between a trigonal bipyramidal and a square pyramidal one. Also, an additional THF molecule is coordinated to the zinc centre [Zn–O 1.99(2) Å], resulting in a distorted tetrahedral geometry. In **257**, the tantalum atom likewise has a geometry intermediate between that of a trigonal bipyramid and a square pyramid. However, here the second (dimethylamino)methyl substituent is coordinated intramolecularly to the zinc centre [Zn–N 2.101(5) Å] rendering this zinc atom distorted tetrahedrally surrounded. The Ta–Zn non-bonding distances in **256** and **257** are almost equal, 2.740(5) Å and 2.729(1) Å, respectively.

VI. CONCLUSIONS

In this chapter it has become clear that knowledge about the actual solution structures of organozinc reagents is often a pre-requisite to better understand the reaction pathways which operate during reactions in which these organozincs are involved. This is of particular importance for the design of novel synthetic strategies towards (new) organic products which are formed when organozinc reagents are used.

In general, simple dialkylzinc and diarylzinc compounds are monomers in which the zinc atom, as a consequence of its ground-state electronic configuration, is sp hybridized. Thus, such molecules contain a linear C–Zn–C arrangement. The only known exception to this rule is diphenylzinc, which in the solid state is a dimer formed via electron-deficient μ^2-bridging phenyl groups.

In the presence of Lewis bases, diorganozinc compounds form complexes with one or two donor molecules. In the 1:2 complexes, the zinc atom typically has a (distorted) tetrahedral coordination geometry. In contrast, 1:1 complexes contain a zinc atom with a rare trigonal planar geometry. This is only observed when either the coordinating ligand and/or the diorganozinc molecule contain sterically demanding groups.

A variety of structural motifs are observed in the solid state for the heteroleptic monoorganozinc compounds RZnY. In this case, Y is either a halide or a heteroatom bonded group. Such a group Y might be σ-bonded to zinc (affording monomers) or μ^2- or μ^3-bridge-bonded between two and three zinc atoms, respectively. In the latter two cases, aggregated structures (dimers, trimers, tetramers or higher aggregates) are invariably formed. For solutions containing RZnY species, the existence of a Schlenk equilibrium between RZnY and both R_2Zn and ZnY_2 should always be considered. Moreover, equilibria between two or more higher aggregates cannot be excluded. Such equilibria are naturally driven by thermodynamics. It should be noted that the formation of solid (crystalline) material from such solutions may be influenced by additional factors such as differences in the solubilities of the respective aggregates and packing effects in the crystal lattice. Consequently, caution should be taken when one is drawing conclusions about the structure of aggregates present in solution based on data obtained from solid state (X-ray) crystal structures. It is perhaps more prudent to regard these solid state structures as resting states, and hence they may represent only one of the many structural forms that can be present in solution.

VII. REFERENCES

1. E. Frankland, *Liebigs Ann. Chem.*, **71**, 171 (1849).
2. J. A. Wanklyn, *Liebigs Ann. Chem.*, **107**, 125 (1858).
3. K. H. Thiele, *Z. Anorg. Allg. Chem.*, **319**, 183 (1962).
4. R. Garth Kidd and R. J. Goodfellow, in *NMR and the Periodic Table* (Eds. R. K. Harris and B. E. Mann), Chap. 8, Academic Press, London, 1978, pp. 260–261.
5. Cambridge Structural Database, release 5.26, February 2005.
6. W. Strohmeier and K. Nützel, *Z. Elektrochem.*, **59**, 538 (1959).
7. J. T. B. H. Jastrzebski and G. van Koten, in *Modern Organocopper Chemistry* (Ed. N. Krause), Chap. 1, Wiley-VCH, Weinheim, 2002, pp. 1–44.
8. T. Stey and D. Stalke, in *The Chemistry of Organolithium Compounds*, Part 1 (Eds. Z. Rappoport and I. Marek), Chap. 2, Wiley, Chichester, 2004, pp. 47–120.
9. P. R. Markies, G. Schat, O. S. Akkerman, F. Bickelhaupt, W. J. J. Smeets and A. L. Spek, *Organometallics*, **9**, 2243 (1990).
10. E. Rijnberg, J. T. B. H. Jastrzebski, J. Boersma, H. Kooijman, N. Veldman, A. L. Spek and G. van Koten, *Organometallics*, **16**, 2239 (1997).
11. P. W. J. de Graaf, J. Boersma and G. J. M. van der Kerk, *J. Organometal. Chem.*, **78**, C19 (1974).
12. J. Soulati, K. L. Henold and J. P. Oliver, *J. Am. Chem. Soc.*, **93**, 5694 (1971).
13. K. L. Henold, J. Soulati and J. P. Oliver, *J. Am. Chem. Soc.*, **91**, 3171 (1969).
14. E. Wissing, J. T. B. H. Jastrzebski, J. Boersma and G. van Koten, *J. Organometal. Chem.*, **459**, 11 (1993).
15. J. A. Wanklyn, *Liebigs Ann. Chem.*, **108**, 67 (1858).
16. J. A. Wanklyn, *Liebigs Ann. Chem.*, **140**, 211 (1866).
17. G. Wittig, F. J. Meyer and G. Lange, *Liebigs Ann. Chem.*, **571**, 167 (1951).
18. G. Wittig and G. Hornberger, *Liebigs Ann. Chem.*, **577**, 11 (1952).
19. H. Gilman and L. A. Woods, *J. Am. Chem. Soc.*, **67**, 520 (1945).
20. D. T. Hurd, *J. Org. Chem.*, **13**, 711 (1948).
21. R. Nast and R. Müller, *Chem. Ber.*, **91**, 2861 (1958).
22. K. Issleib and H. O. Fröhlich, *Chem. Ber.*, **95**, 375 (1962).
23. Fr. Hein and H. Schramm, *Z. Anorg. Allg. Chem.*, **158**, 153 (1926).
24. Fr. Hein and Fr. A. Segitz, *Z. Phys. Chem.*, **151**, 234 (1930).

25. D. Seyferth, *Organometallics*, **20**, 2940 (2001).
26. W. Tochtermann, *Angew. Chem., Int. Ed. Engl.*, **5**, 351 (1966).
27. G. Wittig, *Quart. Rev.*, 191 (1966).
28. N. Krause (Ed.), *Modern Organocopper Chemistry*, Wiley-VCH, Weinheim, 2002.
29. A. E. H. Wheatley, *New J. Chem.*, **28**, 435 (2004).
30. D. J. Linton, P. Schooler and A. E. H. Wheatley, *Coord. Chem. Rev.*, **223**, 53 (2001).
31. E. C. Ashby, L-C. Chao and J. Laemmle, *J. Org. Chem.*, **39**, 3258 (1974).
32. Y. Okuda, K. Wakamatsu, W. Tückmantel, K. Oshima and H. Nozaki, *Tetrahedron Lett.*, **26**, 4629 (1985).
33. M. Uchiyama, M. Koike, M. Kameda, Y. Kondo and T. Sakamoto, *J. Am. Chem. Soc.*, **118**, 8733 (1996).
34. T. Takada, H. Sakurai and T. Hirao, *J. Org. Chem*, **66**, 300 (2001).
35. M. Uchiyama, M. Kameda, O. Mishima, N. Yokoyama, M. Koike, Y. Kondo and T. Sakamoto, *J. Am. Chem. Soc.*, **120**, 4934 (1998).
36. S. Mori, A. Hirai, M. Nakamura and E. Nakamura, *Tetrahedron*, **56**, 2805 (2000).
37. M. Uchiyama, S. Nakamura, T. Ohwada, M. Nakamura and E. Nakamura, *J. Am. Chem. Soc.*, **126**, 10897 (2004).
38. F. Kaufmann, A. Geraudelle, B. Kaempf, F. Schué, A. Deluzarche and A. Maillard, *J. Organomet. Chem.*, **24**, 13 (1970).
39. M. Uchiyama, Y. Kondo and T. Sakamoto, *J. Synth. Org. Chem. Jpn.*, **57**, 1051 (1999).
40. M. Uchiyama, Y. Kondo, T. Miura and T. Sakamoto, *J. Am. Chem. Soc.*, **119**, 12372 (1997).
41. E. Weiss and R. Wolfrum, *Chem. Ber.*, **101**, 35 (1968).
42. A. Almenningen, T. U. Helgaker, A. Haaland and S. Samdal, *Acta Chem. Scand., Ser. A*, **36**, 159 (1982).
43. E. Weiss and E. A. C. Lucker, *J. Organomet. Chem.*, **2**, 197 (1964).
44. H. Dietrich, *Acta Crystallogr.*, **16**, 681 (1963).
45. E. Weiss and H. Plass, *J. Organomet. Chem.*, **14**, 21 (1968).
46. D. Stalke, *Chem. Soc. Rev.*, **27**, 171 (1998).
47. U. Cremer, I. Pantenburg and U. Ruschewitz, *Inorg. Chem.*, **42**, 7716 (2003).
48. A. J. Edwards, A. Fallaize, P. R. Raithby, M.-A. Rennie, A. Steiner, K. L. Verhorevoort and D. S. Wright, *J. Chem. Soc., Dalton Trans.*, 133 (1996).
49. H.-O. Fröhlich, B. Kosan, B. Müller and W. Hiller, *J. Organomet. Chem.*, **441**, 177 (1992).
50. H.-O. Fröhlich, B. Kosan, B. Undeutsch and H. Görls, *J. Organomet. Chem.*, **472**, 1 (1994).
51. R. Wyrwa, H.-O. Fröhlich and H. Görls, *Organometallics*, **15**, 2833 (1996).
52. J. T. B. H. Jastrzebski, G. van Koten, M. Konijn and C. H. Stam, *J. Am. Chem. Soc.*, **104**, 5490 (1982).
53. A. Osman, R. G. Steevensz, D. G. Tuck, H. A. Meinema and J. G. Noltes, *Can. J. Chem.*, **62**, 1698 (1984).
54. G. van Koten, J. T. B. H. Jastrzebski, F. Muller and C. H. Stam, *J. Am. Chem. Soc.*, **107**, 697 (1985).
55. G. van Koten, J. T. B. H. Jastrzebski, C. H. Stam and N. C. Niemann, *J. Am. Chem. Soc.*, **106**, 1880 (1984).
56. A. P. Purdy and C. F. George, *Organometallics*, **11**, 1955 (1992).
57. M. Westerhausen, C. Gückel, T. Habereder, M. Vogt, M. Warchhold and H. Nöth, *Organometallics*, **20**, 893 (2001).
58. M. Westerhausen, C. Gückel, H. Piotrowski and M. Vogt, *Z. Anorg. Allg. Chem.*, **628**, 735 (2002).
59. M. Westerhausen, B. Rademacher, W. Schwarz, J. Weidlein and S. Henkel, *J. Organomet. Chem.*, **469**, 135 (1994).
60. M. Westerhausen, B. Rademacher and W. Schwarz, *Z. Anorg. Allg. Chem.*, **619**, 675 (1993).
61. E. Rijnberg, J. T. B. H. Jastrzebski, J. Boersma, H. Kooijman, A. L. Spek and G. van Koten, *J. Organomet. Chem.*, **541**, 181 (1997).
62. S. R. Boss, M. P. Coles, R. Haigh, P. B. Hitchcock, R. Snaith and A. E. H. Wheatley, *Angew. Chem., Int. Ed.*, **42**, 5593 (2003).
63. M. A. Putzner, B. Neumüller and K. Dehnicke, *Z. Anorg. Allg. Chem.*, **623**, 539 (1997).
64. M. Krieger, G. Geiseler, K. Harms, J. Merle, W. Massa and K. Dehnicke, *Z. Anorg. Allg. Chem.*, **624**, 1387 (1998).
65. K. H. Thiele, H. Görls and W. Seidel, *Z. Anorg. Allg. Chem.*, **624**, 555 (1998).

66. M. Westerhausen, M. Wieneke, W. Ponikwar, H. Nöth and W. Schwarz, *Organometallics*, **17**, 1438 (1998).
67. M. Westerhausen, B. Rademacher, W. Schwarz and S. Henkel, *Z. Naturforsch., B: Chem. Sci.*, **49**, 199 (1994).
68. A. L. Arduengo III, H. V. R. Dias, F. Davidson and R. L. Harlow, *J. Organomet. Chem.*, **462**, 13 (1993).
69. E. P. Squiller, R. R. Whittle and H. G. Richey Jr., *J. Am. Chem. Soc.*, **107**, 432 (1985).
70. D. M. Kushlan, *J. Am. Chem. Soc.*, **109**, 2510 (1987).
71. A. D. Pajerski, M. Parvez and H. G. Richey Jr., *J. Am. Chem. Soc.*, **110**, 2660 (1988).
72. R. M. Fabicon, A. D. Pajerski and H. G. Richey Jr., *J. Am. Chem. Soc.*, **113**, 6680 (1991).
73. R. M. Fabicon and H. G. Richey Jr., *Organometallics*, **20**, 4018 (2001).
74. P. P. Power, K. Ruhlandt-Senge and S. C. Shoner, *Inorg. Chem.*, **30**, 5013 (1991).
75. R. D. Rogers, J. L. Atwood and R. Grüning, *J. Organomet. Chem.*, **157**, 229 (1978).
76. R. M. Fabicon, M. Parvez and H. G. Richey Jr., *J. Am. Chem. Soc.*, **113**, 1412 (1991).
77. R. M. Fabicon and H. G. Richey Jr., *J. Chem. Soc., Dalton Trans.*, 783 (2001).
78. M. Steiner, H. Grützmacher, H. Prtizkow and L. Zsolnai, *Chem. Commun.*, 285 (1998).
79. Y. Kondo, M. Shilai, M. Uchiyama and T. Sakamoto, *J. Am. Chem. Soc.*, **121**, 3539 (1999).
80. M. Uchiyama, S. Furumoto, M. Saito, Y. Kondo and T. Sakamoto, *J. Am. Chem. Soc.*, **119**, 11425 (1997).
81. K. Nützel, in *Houben-Weyl: Methoden der Organischen Chemie* (Ed. E. Müller), Vol. 13/2a, Thieme, Stuttgart, 1973, p. 554.
82. J. Boersma, in *Comprehensive Organometallic Chemistry* (Eds. G. Wilkinson, F. G. A. Stone and E. W. Abel), Vol. 2, Pergamon, Oxford, 1982, p. 823.
83. H. S. Gutowsky, *J. Chem. Phys.*, **17**, 128 (1949).
84. S. Venkateswaran, *Indian J. Phys.*, **5**, 145 (1930).
85. A. Haaland, J. C. Green, G. C. McGready, A. J. Downs, E. Gullo, M. J. Lyall, J. Timberlake, A. V. Tutukin, H. V. Volden and K.-A. Østby, *Dalton Trans.*, 4356 (2003).
86. S. Moorehouse and G. Wilkinson, *J. Chem. Soc., Dalton Trans.*, 2187 (1974).
87. M. Westerhausen, B. Rademacher and W. Poll, *J. Organomet. Chem.*, **421**, 175 (1991).
88. C. Eaborn, N. Retta and J. D. Smith, *J. Organomet. Chem.*, **190**, 101 (1980).
89. S. S. Al-Juaid, C. Eaborn, A. Hebtemariam, P. B. Hitchcock and J. D. Smith, *J. Organomet. Chem.*, **437**, 41 (1992).
90. F. I. Aigbirhio, S. S. Al-Juaid, C. Eaborn, A. Habtemariam, P. B. Hitchcock and J. D. Smith, *J. Organomet. Chem.*, **405**, 149 (1991).
91. M. Westerhausen and B. Rademacher, *J. Organomet. Chem.*, **443**, 25 (1993).
92. R. D. Ernst, J. W. Freeman, P. N. Swepston and D. R. Wilson, *J. Organomet. Chem.*, **402**, 17 (1991).
93. C. Eaborn, M. S. Hill, P. B. Hitchcock, J. D. Smith, S. Zhang and T. Ganicz, *Organometallics*, **18**, 2342 (1999).
94. T. Bollwein, M. Westerhausen and A. Pfitzner, *Z. Naturforsch., B: Chem. Sci.*, **58**, 493 (2003).
95. W. Strohmeier, K. Hümpfner, K. Miltenberger and F. Seifert, *Z. Elektrochem.*, **63**, 537 (1959).
96. S. C. Cole, M. P. Coles and P. B. Hitchcock, *Dalton Trans.*, 3663 (2003).
97. S. Brooker, N. Bertel, D. Stalke, M. Noltemeyer, H. W. Roesky, G. M. Sheldrick and F. T. Edelmann, *Organometallics*, **11**, 192 (1992).
98. Y. Sun, W. E. Piers and M. Parvez, *Can. J. Chem.*, **76**, 513 (1998).
99. T. J. Kealy and P. L. Pauson, *Nature*, **168**, 1039 (1951).
100. S. A. Miller, J. A. Tebboth and J. F. Tremaine, *J. Chem. Soc.*, 632 (1952).
101. P. Laszlo and R. Hoffman, *Angew. Chem., Int. Ed.*, **39**, 123 (2000).
102. W. Bünder and E. Weiss, *J. Organomet. Chem.*, **92**, 1 (1975).
103. W. Bünder and E. Weiss, *Z. Naturforsch., B: Chem. Sci.*, **33**, 1235 (1978).
104. E. O. Fischer, H. P. Hoffmann and A. Treiber, *Z. Naturforsch., B: Chem. Sci.*, **14**, 599 (1969).
105. J. Lorberth, *J. Organomet. Chem.*, **19**, 189 (1969).
106. B. Fischer, G. P. M. van Mier, J. Boersma, G. van Koten, W. J. J. Smeets and A. L. Spek, *Recl. Trav. Chim. Pays-Bas*, **107**, 259 (1988).
107. T. Aoyagi, H. M. M. Shearer, K. Wade and G. Whitehead, *J. Organomet. Chem.*, **146**, C29 (1978).
108. P. H. M. Budzelaar, J. Boersma, G. J. M. van der Kerk, A. L. Spek and A. J. M. Duisenberg, *J. Organomet. Chem.*, **281**, 123 (1985).

109. A. Haaland, S. Samdal, N. V. Tverdova, G. V. Girichev, N. I. Giricheva, S. A. Shlykov, O. G. Garkusha and B. V. Lokshin, *J. Organomet. Chem.*, **684**, 351 (2003).
110. R. Blom, J. Boersma, P. H. M. Budzelaar, B. Fischer, A. Haaland, H. V. Volden and J. Weidlein, *Acta Chem. Scand., Ser. A*, **40**, 113 (1986).
111. B. Fischer, P. Wijkens, J. Boersma, G. van Koten, W. J. J. Smeets, A. L. Spek and P. H. M. Budzelaar, *J. Organomet. Chem.*, **376**, 223 (1989).
112. R. Rernández, I. Resa, D. del Río, E. Carmona, E. Gutiérrez-Puebla and Á. Monge, *Organometallics*, **22**, 381 (2003).
113. D. J. Burkey and T. P. Hanusa, *J. Organomet. Chem.*, **512**, 165 (1996).
114. I. Resa, E. Carmona, E. Gutiérrez-Puebla and A. Monge, *Science*, **305**, 1136 (2004).
115. J. A. J. Jarvis, B. T. Kilbourn, R. Pearce and M. F. Lappert, *J. Chem. Soc., Chem. Commun.*, 475 (1973).
116. J. M. Guss, R. Mason, I. Søtofte, G. van Koten and J. G. Noltes, *J. Chem. Soc., Chem. Commun.*, 446 (1972).
117. A. Osman, R. G. Steevensz, D. G. Tuck, H. A. Meinema and J. G. Noltes, *Can. J. Chem.*, **62**, 1698 (1984).
118. J. Dekker, J. Boersma, L. Fernholt, A. Haaland and A. L. Spek, *Organometallics*, **6**, 1202 (1987).
119. H. Schumann, S. Freitag, F. Girsdies, H. Hemling and G. Kociok-Köhn, *Eur. J. Inorg. Chem.*, 245 (1998).
120. J. Boersma, L. Fernholt and A. Haaland, *Acta Chem. Scand., Ser. A*, **38**, 523 (1984).
121. J. Dekker, J. W. Münninghoff, J. Boersma and A. L. Spek, *Organometallics*, **6**, 1236 (1987).
122. N. Seidl, K. Jacob, P. Zanello and M. Fontani, *J. Organomet. Chem.*, **620**, 243 (2001).
123. S. Wingerter, H. Gornitzka, G. Bertrand and D. Stalke, *Eur. J. Inorg. Chem.*, 173 (1999).
124. A. Steiner and D. Stalke, *Angew. Chem., Int. Ed. Engl.*, **34**, 1752 (1995).
125. M. J. Henderson, R. I. Papasergio, C. L. Raston, A. H. White and M. F. Lappert, *J. Chem. Soc., Chem. Commun.*, 672 (1986).
126. A. B. Charette, A. Beauchemin and S. Francoeur, *J. Am. Chem. Soc.*, **123**, 8139 (2001).
127. H. Gornitzka, C. Hemmert, G. Bertrand, M. Pfeiffer and D. Stalke, *Organometallics*, **19**, 112 (2000).
128. P. C. Andrews, C. L. Raston, B. W. Skelton and A. H. White, *Organometallics*, **17**, 779 (1998).
129. K. H. Thiele, *Z. Anorg. Allg. Chem.*, **322**, 71 (1963).
130. J. G. Noltes and J. W. G. van den Hurk, *J. Organomet. Chem.*, **1**, 377 (1963).
131. K. H. Thiele, *Z. Anorg. Allg. Chem.*, **319**, 183 (1962).
132. K. H. Thiele, *Z. Anorg. Allg. Chem.*, **325**, 156 (1963).
133. H.-J. Gais and G. Bülow, *Tetrahedron Lett.*, **33**, 461 (1992).
134. H.-J. Gais, G. Bülow and G. Raabe, *J. Am. Chem. Soc.*, **115**, 7215 (1993).
135. B. Walfort, A. P. Leedham, C. A. Russell and D. Stalke, *Inorg. Chem.*, **40**, 5668 (2001).
136. J. G. Noltes and J. Boersma, *J. Organomet. Chem.*, **16**, 345 (1969).
137. S. R. Boss, R. Haigh, D. J. Linton, P. Schooler, G. P. Shields and A. E. H. Wheatley, *Dalton Trans.*, 1001 (2003).
138. M. Weidenbruch, M. Herrndorf, A. Schäfer, S. Pohl and W. Saak, *J. Organomet. Chem.*, **361**, 139 (1989).
139. B. Fischer, J. Boersma, G. van Koten, W. J. J. Smeets and A. L. Spek, *Organometallics*, **8**, 667 (1989).
140. M. Schreuder Goedheijt, T. Nijbacker, O. S. Akkerman, F. Bickelhaupt, N. Veldman and A. L. Spek, *Angew. Chem., Int. Ed. Engl.*, **35**, 1550 (1996).
141. P. R. Markies, G. Schat, O. S. Akkerman, F. Bickelhaupt and A. L. Spek, *J. Organomet. Chem.*, **430**, 1 (1992).
142. S. E. Denmark, J. P. Edwards and S. L. Wilson, *J. Am. Chem. Soc.*, **114**, 2592 (1992).
143. S. J. Dzugan and V. L. Goedken, *J. Organomet. Chem.*, **356**, 249 (1988).
144. P. R. Markies, G. Schat, O. S. Akkerman, F. Bickelhaupt, W. J. J. Smeets and A. L. Spek, *Organometallics*, **10**, 3538 (1991).
145. P. R. Markies, T. Nomoto, O. S. Akkerman, F. Bickelhaupt, W. J. J. Smeets and A. L. Spek, *J. Am. Chem. Soc.*, **110**, 4845 (1988).
146. A. D. Pajerski, G. L. BergStresser, M. Parvez and H. G. Richey, Jr., *J. Am. Chem. Soc.*, **110**, 4844 (1988).

147. R. M. Fabicon, M. Parvez and H. G. Richey, Jr., *Organometallics*, **18**, 5163 (1999).
148. J. E. Chubb and H. G. Richey, Jr., *Organometallics*, **17**, 3204 (1998).
149. E. Hecht, *Z. Anorg. Allg. Chem.*, **627**, 2351 (2001).
150. M. B. Hursthouse, M. Motevalli, P. O'Brien, J. R. Walsh and A. C. Jones, *Organometallics*, **10**, 3196 (1991).
151. J. Behm, S. Lotz and W. A. Herrmann, *Z. Anorg. Allg. Chem.*, **619**, 849 (1993).
152. X. Huang, H. Sun, X. Wang, Y. J. Liu, X. You and X. Sun, *Main Group Met. Chem.*, **19**, 161 (1996).
153. E. Wissing, R. W. A. Havenith, J. Boersma and G. van Koten, *Tetrahedron Lett.*, **33**, 7933 (1992).
154. E. Wissing, R. W. A. Havenith, J. Boersma, W. J. J. Smeets, A. L. Spek and G. van Koten, *J. Org. Chem.*, **58**, 4228 (1993).
155. P. O'Brien, M. B. Hursthouse, M. Motevalli, J. R. Walsh and A. C. Jones, *J. Organomet. Chem.*, **449**, 1 (1993).
156. M. Westerhausen, M. Wieneke, B. Rademacher and W. Schwarz, *Chem. Ber./Recueil*, **130**, 1499 (1997).
157. M. Westerhausen, M. Wieneke and W. Schwarz, *J. Organomet. Chem.*, **522**, 137 (1996).
158. M. Motevalli, P. O'Brien, A. J. Robinson, J. R. Walsh and P. B. Wyatt, *J. Organomet. Chem.*, **461**, 5 (1993).
159. C. M. Coward, A. C. Jones, A. Steiner, J. F. Bickley, L. M. Smith and M. E. Pemble, *J. Chem. Soc., Dalton Trans.*, 3480 (2000).
160. H. Mimoun, J. Y. de Saint Laumer, L. Giannini, R. Scopelliti and C. Floriani, *J. Am. Chem. Soc.*, **121**, 6158 (1999).
161. E. Wissing, M. Kaupp, J. Boersma, A. L. Spek and G. van Koten, *Organometallics*, **13**, 2349 (1994).
162. M. Westerhausen, B. Rademacher and W. Schwarz, *J. Organomet. Chem.*, **427**, 275 (1992).
163. A. B. Charette, J.-F. Marcoux, C. Molinaro, A. Beauchemin, C. Brochu and É. Isabel, *J. Am. Chem. Soc.*, **122**, 4508 (2000).
164. M. Kaupp, H. Stoll, H. Preuss, W. Kaim, T. Stahl, G. van Koten, E. Wissing, W. J. J. Smeets and A. L. Spek, *J. Am. Chem. Soc.*, **113**, 5606 (1991).
165. H. E. Simmons, T. L. Cairns, S. A. Vladuchick and C. M. Hoiness, *Org. React.*, **20**, 1 (1973).
166. E. Wissing, E. Rijnberg, P. A. van der Schaaf, K. van Gorp, J. Boersma and G. van Koten, *Organometallics*, **13**, 2609 (1994).
167. J. M. Klerks, J. T. B. H. Jastrzebski, G. van Koten and K. Vrieze, *J. Organomet. Chem.*, **224**, 107 (1982).
168. G. van Koten, J. T. B. H. Jastrzebski and K. Vrieze, *J. Organomet. Chem.*, **250**, 49 (1983).
169. E. Wissing, S. van der Linden, E. Rijnberg, J. Boersma, W. J. J. Smeets, A. L. Spek and G. van Koten, *Organometallics*, **13**, 2602 (1994).
170. J. Boersma, A. Mackor and J. G. Noltes, *J. Organomet. Chem.*, **99**, 337 (1975).
171. A. L. Spek, J. T. B. H. Jastrzebski and G. van Koten, *Acta Crystallogr.*, **C43**, 2006 (1987).
172. S. N. Reformatsky, *Ber. Dtsch. Chem. Ges.*, **20**, 1210 (1887).
173. M. Gaudemar, *Organomet. Rev. A.*, **8**, 183 (1972).
174. H. E. Simmons and R. D. Smith, *J. Am. Chem. Soc.*, **81**, 4256 (1959).
175. P. Knochel and R. D. Singer, *Chem. Rev.*, **93**, 2117 (1993).
176. G. E. Coates and D. Ridley, *J. Chem. Soc.*, 1870 (1965).
177. J. M. Bruce, B. C. Cutsforth, D. W. Farren, F. G. Hutchinson, F. M. Rabagliati and D. R. Reed, *J. Chem. Soc. (B)*, 1020 (1966).
178. M. H. Abraham and J. A. Hill, *J. Organomet. Chem.*, **7**, 23 (1967).
179. J. G. Noltes, *Recl. Trav. Chim. Pays-Bas*, **84**, 126 (1965).
180. J. Boersma and J. G. Noltes, *Tetrahedron Lett.*, 1521 (1966).
181. P. O'Brien, in *Comprehensive Organometallic Chemistry II* (Eds. E. W. Abel, F. G. A. Stone and G. Wilkinson), Vol. 3, Pergamon, Oxford, 1995, p. 175.
182. D. A. Walker, T. J. Woodman, D. L. Hughes and M. Bochmann, *Organometallics*, **20**, 3772 (2001).
183. M. Haufe, R. D. Köhn, R. Weimann, G. Seifert and D. Zeigan, *J. Organomet. Chem.*, **520**, 121 (1996).
184. M. Haufe, R. D. Köhn, G. Kociok-Köhn and A. C. Filippou, *Inorg. Chem. Commun.*, **1**, 263 (1998).

185. H. Tang, M. Parvez and H. G. Richey Jr., *Organometallics*, **19**, 4810 (2000).
186. M. D. Hannant, M. Schormann and M. Bochmann, *J. Chem. Soc., Dalton Trans.*, 4071 (2002).
187. A. Job and R. Reich, *Bull. Soc. Chim. Fr.*, **33**, 1414 (1923).
188. M. H. Abraham and P. H. Rolfe, *J. Organomet. Chem.*, **7**, 35 (1967).
189. J. Boersma and J. G. Noltes, *Tetrahedron Lett.*, 1521 (1966).
190. J. Boersma and J. G. Noltes, *J. Organomet. Chem.*, **8**, 551 (1967).
191. P. T. Moseley and H. M. M. Shearer, *J. Chem. Soc., Dalton Trans.*, 65 (1973).
192. B. Rademacher, W. Schwarz and M. Westerhausen, *Z. Anorg. Allg. Chem.*, **621**, 1395 (1995).
193. H. Yasuda, Y. Ohnuma, A. Nakamura, Y. Kai, N. Yasuoka and N. Kasai, *Bull. Chem. Soc. Jpn.*, **53**, 1101 (1980).
194. R. W. Lang, *Helv. Chim. Acta*, **69**, 881 (1986).
195. D. Belluš, B. Klingert, R. W. Lang and G. Rihs, *J. Organomet. Chem.*, **339**, 17 (1988).
196. T. N. Majid, M. Chang, P. Yeh and P. Knochel, *Tetrahedron Lett.*, **30**, 5069 (1989).
197. G.-J. Gruter, O. S. Akkerman, F. Bickelhaupt, W. J. J. Smeets and A. L. Spek, *Recl. Trav. Chim. Pays-Bas*, **112**, 425 (1993).
198. A. B. Charette, J.-F. Marcoux and F. Bélanger-Gariépy, *J. Am. Chem. Soc.*, **118**, 6792 (1996).
199. R. Becker, J. Weiss, M. Winter, K. Merz and R. Fischer, *J. Organomet. Chem.*, **630**, 253 (2001).
200. S. S. Al-Juaid, C. Eaborn, A. Habtemariam, P. B. Hitchcock, J. D. Smith, K. Tavakkoli and A. D. Webb, *J. Organomet. Chem.*, **462**, 45 (1993).
201. C. Eaborn, M. S. Hill, P. B. Hitchcock and J. D. Smith, *J. Chem. Soc., Dalton Trans.*, 2467 (2002).
202. D. Azarifar, M. P. Coles, S. M. El-Hamruni, C. Eaborn, P. B. Hitchcock and J. D. Smith, *J. Organomet. Chem.*, **689**, 1718 (2004).
203. D. J. Darensbourg, J. R. Wildeson and J. C. Yarbrough, *Organometallics*, **20**, 4413 (2001).
204. W. R. Vaughan, S. C. Bernstein and M. E. Lorber, *J. Org. Chem.*, **30**, 1790 (1965).
205. W. R. Vaughan and H. P. Knoes, *J. Org. Chem.*, **35**, 2394 (1970).
206. J. Dekker, P. H. M. Budzelaar, J. Boersma, G. J. M. van der Kerk and A. L. Spek, *Organometallics*, **3**, 1403 (1984).
207. M. Westerhausen, M. Wieneke, H. Nöth, T. Seifert, A. Pfitzner, W. Schwarz, O. Schwarz and J. Weidlein, *Eur. J. Inorg. Chem.*, 1175 (1998).
208. C. Hilf, F. Bosold, K. Harms, J. C. W. Lorenz, M. Marsch, M. Schmeczek and G. Boche, *Chem. Ber.*, **130**, 1201 (1997).
209. G. Boche, F. Bosold, H. Hermann, M. Marsch, K. Harms and J. C. W. Lorenz, *Chem. Eur. J.*, **4**, 814 (1998).
210. P. Yu, P. Müller, H. W. Roesky, M. Noltemeyer, A. Demsar and I. Usón, *Angew. Chem., Int. Ed. Engl.*, **38**, 3319 (1999).
211. M. P. Coles and P. B. Hitchcock, *Eur. J. Inorg. Chem.*, 2662 (2004).
212. E. J. Corey, P.-W. Yuen, F. J. Hannon and D. A. Wierda, *J. Org. Chem.*, **55**, 784 (1990).
213. B. S. Hammes and C. J. Carano, *Inorg. Chem.*, **38**, 4593 (1999).
214. C. K. Williams, L. E. Breyfogle, S. K. Choi, W. Nam, V. G. Young Jr., M. A. Hillmyer and W. B. Tolman, *J. Am. Chem. Soc.*, **125**, 11350 (2003).
215. B. S. Hammes, M. T. Kieber-Emmons, J. A. Letizia, Z. Shirin, C. J. Carrano, L. N. Zakharov and A. L. Rheingold, *Inorg. Chim. Acta*, **346**, 227 (2003).
216. I. Hegelmann, A. Beck, C. Eichhorn, B. Weibert and N. Burzlaff, *Eur. J. Inorg. Chem.*, 339 (2003).
217. S. S. Al-Juaid, N. H. Buttrus, C. Eaborn, P. B. Hitchcock, A. T. L. Roberts, J. D. Smith and A. C. Sullivan, *J. Chem. Soc., Chem. Commun.*, 908 (1986).
218. M. Parvez, G. L. Bergstresser and H. G. Richey Jr., *Acta Crystallogr.*, **C48**, 641 (1992).
219. R. Anulewicz-Ostrowska, S. Lulinski, E. Pindelska and J. Serwatowski, *Inorg. Chem.*, **41**, 2525 (2002).
220. M. M. Olmstead, P. P. Power and S. C. Shoner, *J. Am. Chem. Soc.*, **113**, 3379 (1991).
221. K. Merz, H.-M. Hu, S. Rell and M. Driess, *Eur. J. Inorg. Chem.*, 51 (2003).
222. M. Driess, K. Merz and S. Rell, *Eur. J. Inorg. Chem.*, 2517 (2000).
223. G. Anantharaman, V. Chandrasekhar, U. N. Nehete, H. W. Roesky, D. Vidovic and J. Magull, *Organometallics*, **23**, 2251 (2004).
224. K. Soai and S. Niwa, *Chem. Rev.*, **92**, 833 (1992).
225. M. Kitamura, S. Suga, K. Kawai and R. Noyori, *J. Am. Chem. Soc.*, **108**, 6071 (1986).

226. M. Kitamura, S. Okada, S. Suga and R. Noyori, *J. Am. Chem. Soc.*, **111**, 4028 (1989).
227. M. Kitamura, S. Suga, M. Niwa and R. Noyori, *J. Am. Chem. Soc.*, **117**, 4832 (1995).
228. B. Goldfuss, S. I. Khan and K. N. Houk, *Organometallics*, **18**, 2927 (1999).
229. B. Goldfuss, M. Steigelmann and F. Rominger, *Eur. J. Org. Chem.*, 1785 (2000).
230. M. Steigelmann, Y. Nisar, F. Rominger and B. Goldfuss, *Chem. Eur. J.*, **8**, 5211 (2002).
231. K. Nakano, K. Nozaki and T. Hiyama, *J. Am. Chem. Soc.*, **125**, 5501 (2003).
232. E. Hecht, *Z. Anorg. Allg. Chem.*, **626**, 2223 (2000).
233. C. Bolm, G. Schlingloff and K. Harms, *Chem. Ber.*, **125**, 1191 (1992).
234. H. M. M. Shearer and C. B. Spencer, *J. Chem. Soc., Chem. Commun.*, 194 (1966).
235. H. M. M. Shearer and C. B. Spencer, *Acta Crystallogr.*, **B36**, 2046 (1980).
236. W. A. Herrmann, S. Bogdanović, J. Behm and M. Denk, *J. Organomet. Chem.*, **430**, C33 (1992).
237. A. D. Bond, D. J. Linton and A. E. H. Wheatley, *Acta Crystallogr.*, **E57**, m298 (2001).
238. A. B. Charette, C. Molinaro and C. Brochu, *J. Am. Chem. Soc.*, **123**, 12160 (2001).
239. S. Luliński, I. Madura, J. Serwatowski and J. Zachara, *Inorg. Chem.*, **38**, 4937 (1999).
240. M. L. Ziegler and J. Weiss, *Angew. Chem.*, **82**, 931 (1970).
241. J. Lewiński, W. Marciniak, J. Lipkowski and I. Justyniak, *J. Am. Chem. Soc.*, **125**, 12698 (2003).
242. M. Ishimori, T. Hagiwara, T. Tsuruta, Y. Kai, N. Yasuoka and N. Kasai, *Bull. Chem. Soc. Jpn.*, **49**, 1165 (1976).
243. A. Charette, A. Beauchemin, S. Francoeur, F. Bélanger-Gariépy and G. D. Enright, *Chem. Commun.*, 466 (2002).
244. R. P. Davies, D. J. Linton, P. Schooler, R. Snaith and A. E. H. Wheatley, *Chem. Eur. J.*, **7**, 3696 (2001).
245. K. Merz, S. Block, R. Schoenen and M. Driess, *Dalton Trans.*, 3365 (2003).
246. A. D. Bond, D. J. Linton, P. Schooler and A. E. H. Wheatley, *J. Chem. Soc., Dalton Trans.*, 3173 (2001).
247. P. A. van der Schaaf, E. Wissing, J. Boersma, W. J. J. Smeets, A. L. Spek and G. van Koten, *Organometallics*, **12**, 3624 (1993).
248. J. Lewiński, W. Marciniak, Z. Ochal, J. Lipkowski and I. Justyniak, *Eur. J. Inorg. Chem.*, 2753 (2003).
249. M. B. Dinger and M. J. Scott, *Inorg. Chem.*, **40**, 1029 (2001).
250. M. G. Gardiner, S. M. Lawrence, C. L. Raston, B. W. Skelton and A. H. White, *Chem. Commun.*, 2491 (1996).
251. E. Bukhaltsev, I. Goldberg and A. Vigalok, *Organometallics*, **23**, 4540 (2004).
252. J. Dekker, A. Schouten, P. H. M. Budzelaar, J. Boersma, A. L. Spek and A. J. M. Duisenberg, *J. Organomet. Chem.*, **320**, 1 (1987).
253. M. R. P. van Vliet, G. van Koten, P. Buysingh, J. T. B. H. Jastrzebski and A. L. Spek, *Organometallics*, **6**, 537 (1987).
254. J. T. B. H. Jastrzebski, J. Boersma, G. van Koten, W. J. J. Smeets and A. L. Spek, *Recl. Trav. Chim. Pays-Bas*, **107**, 263 (1988).
255. C. Bolm, J. Müller, M. Zehnder and M. Neuburger, *Chem. Eur. J.*, **1**, 312 (1995).
256. J. T. B. H. Jastrzebski and G. van Koten, *Bioorg. Med. Chem. Lett.*, **3**, 2351 (1993).
257. F. H. van der Steen, J. Boersma, A. L. Spek and G. van Koten, *Organometallics*, **10**, 2467 (1991).
258. D. Walther, T. Döhler, N. Theyssen and H. Görls, *Eur. J. Inorg. Chem.*, 2049 (2001).
259. J. Boersma, F. Verbeek and J. G. Noltes, *J. Organomet. Chem.*, **33**, C53 (1971).
260. A. L. Spek, *Cryst. Struct. Commun.*, **2**, 535 (1973).
261. J. Boersma, A. L. Spek and J. G. Noltes, *J. Organomet. Chem.*, **81**, 7 (1974).
262. I. Abrahams, M. A. Malik, M. Motevalli and P. O'Brien, *J. Chem. Soc., Dalton Trans.*, 1043 (1995).
263. Y. Yang, J. Pinkas, M. Noltemeyer, H.-G. Schmidt and H. W. Roesky, *Angew. Chem., Int. Ed.*, **38**, 664 (1999).
264. G. Anantharaman, V. Chandrasekhar, M. G. Walawalkar, H. W. Roesky, D. Vidovic, J. Magull and M. Noltemeyer, *Dalton Trans.*, 1271 (2004).
265. L.-C. Liang, W.-Y. Lee and C.-H. Hung, *Inorg. Chem.*, **42**, 5471 (2003).
266. J. Prust, A. Stasch, W. Zheng, H. W. Roesky, E. Alexopoulos, I. Usón, D. Böhler and T. Schuchardt, *Organometallics*, **20**, 3825 (2001).

267. M. Cheng, D. R. Moore, J. J. Reczek, B. M. Chamberlain, E. B. Lobkovsky and G. W. Coates, *J. Am. Chem. Soc.*, **123**, 8738 (2001).
268. J. Prust, H. Hohmeister, A. Stasch, H. W. Roesky, J. Magull, E. Alexopoulos, I. Usón, H.-G. Schmidt and M. Noltemeyer, *Eur. J. Inorg. Chem.*, 2156 (2002).
269. A. P. Dove, V. C. Gibson, E. L. Marshall, A. J. P. White and D. J. Williams, *Dalton Trans.*, 570 (2004).
270. S. D. Allen, D. R. Moore, E. B. Lobkovsky and G. W. Coates, *J. Organomet. Chem.*, **683**, 137 (2003).
271. S. Aboulkacem, W. Tyrra and I. Pantenburg, *Z. Anorg. Allg. Chem.*, **629**, 1569 (2003).
272. M. S. Hill and P. B. Hitchcock, *J. Chem. Soc., Dalton Trans.*, 4694 (2002).
273. A. Kasani, R. McDonald and R. G. Cavell, *Organometallics*, **18**, 3775 (1999).
274. A. Looney, R. Han, I. B. Gorrell, M. Cornebise, K. Yoon, G. Parkin and A. L. Rheingold, *Organometallics*, **14**, 274 (1995).
275. R. Alsfasser, A. K. Powell, S. Trofimenko and H. Vahrenkamp, *Chem. Ber.*, **126**, 685 (1993).
276. J. L. Kisko, T. Fillebeen, T. Hascall and G. Parkin, *J. Organomet. Chem.*, **596**, 22 (2000).
277. M. H. Chisholm, N. W. Eilerts, J. C. Huffman, S. S. Iyer, M. Pacold and K. Phomphrai, *J. Am. Chem. Soc.*, **122**, 11845 (2000).
278. H. V. R. Dias and W. Jin, *Inorg. Chem.*, **42**, 5034 (2003).
279. C. M. Dowling and G. Parkin, *Polyhedron*, **20**, 285 (2001).
280. C. M. Dowling and G. Parkin, *Polyhedron*, **15**, 2463 (1996).
281. C. Kimblin, B. M. Bridgewater, T. Hascall and G. Parkin, *J. Chem. Soc., Dalton Trans.*, 1267 (2000).
282. G. R. Lief, D. F. Moser, L. Stahl and R. J. Staples, *J. Organomet. Chem.*, **689**, 1110 (2004).
283. N. A. Bell, H. M. M. Shearer and C. B. Spencer, *Acta Crystallogr.*, **C39**, 1182 (1983).
284. M. Westerhausen, T. Bollwein, A. Pfitzner, T. Nilges and H.-J. Deiseroth, *Inorg. Chim. Acta*, **312**, 239 (2001).
285. M. M. Olmstead, W. J. Grigsby, D. R. Chacon, T. Hascall and P. P. Power, *Inorg. Chim. Acta*, **251**, 273 (1996).
286. M. A. Malik, P. O'Brien, M. Motevalli and A. C. Jones, *Inorg. Chem.*, **36**, 5076 (1997).
287. V. Bette, A. Mortreux, C. W. Lehmann and J.-F. Carpentier, *Chem. Commun.*, 332 (2003).
288. D. Chakraborty and E. Y.-X. Chen, *Organometallics*, **22**, 769 (2003).
289. M. Westerhausen, T. Bollwein, N. Makropoulos, T. M. Rotter, T. Habereder, M. Suter and H. Nöth, *Eur. J. Inorg. Chem.*, 851 (2001).
290. M. Westerhausen, T. Bollwein, N. Makropoulos, S. Schneiderbauer, M. Suter, H. Nöth, P. Mayer, H. Poitrowski, K. Polborn and A. Pfitzner, *Eur. J. Inorg. Chem.*, 389 (2002).
291. M. Westerhausen, T. Bollwein, P. Mayer and H. Poitrowski, *Z. Anorg. Allg. Chem.*, **628**, 1425 (2002).
292. L. M. Engelhardt, G. E. Jacobsen, W. C. Patalinghug, B. W. Skelton, C. L. Raston and A. H. White, *J. Chem. Soc., Dalton Trans.*, 2859 (1991).
293. M. R. P. van Vliet, G. van Koten, J. F. Modder, J. A. M. van Beek, W. J. Klaver, K. Goubitz and C. H. Stam, *J. Organomet. Chem.*, **319**, 285 (1987).
294. P. H. M. Budzelaar, J. Boersma, G. J. M. van der Kerk and A. L. Spek, *Organometallics*, **3**, 1187 (1984).
295. M. G. Davidson, D. Elilio, S. L. Less, A. Martín, P. R. Raithby, R. D. Snaith and D. S. Wright, *Organometallics*, **12**, 1 (1993).
296. M. Krieger, R. O. Gould, K. Harms, S. Parsons and K. Dehnicke, *Chem. Ber.*, **129**, 1621 (1996).
297. M. Krieger, R. O. Gould, B. Neumüller, K. Harms and K. Dehnicke, *Z. Anorg. Allg. Chem.*, **624**, 1434 (1998).
298. F. A. J. J. van Santvoort, H. Krabbendam, A. L. Spek and J. Boersma, *Inorg. Chem.*, **17**, 388 (1978).
299. S. Chang, R. D. Sommer, A. L. Rheingold and D. P. Goldberg, *Chem. Commun.*, 2396 (2001).
300. M. A. Malik, M. Motevalli, J. R. Walsh, P. O'Brien and A. C. Jones, *J. Mater. Chem.*, **5**, 731 (1995).
301. E. Rijnberg, N. J. Hovestad, A. W. Kleij, J. T. B. H. Jastrzebski, J. Boersma, M. D. Janssen, A. L. Spek and G. van Koten, *Organometallics*, **16**, 2847 (1997).
302. D. M. Knotter, M. D. Janssen, D. M. Grove, W. J. J. Smeets, E. Horn, A. L. Spek and G. van Koten, *Inorg. Chem.*, **30**, 4361 (1991).

303. M. B. Hursthouse, M. A. Malik, M. Motevalli and P. O'Brien, *Organometallics*, **10**, 730 (1991).
304. M. A. Malik, P. O'Brien and M. Motevalli, *Acta Crystallogr.*, **C52**, 1931 (1996).
305. J. B. Hursthouse, M. A. Malik, M. Motevalli and P. O'Brien, *J. Mater. Chem.*, **2**, 949 (1992).
306. M. A. Malik, M. Motevalli, J. R. Walsh and P. O'Brien, *Organometallics*, **11**, 3136 (1992).
307. G. W. Adamson, N. A. Bell and H. M. M. Shearer, *Acta Crystallogr.*, **B38**, 462 (1982).
308. G. W. Adamson and H. M. M. Shearer, *J. Chem. Soc., (D)*, 897 (1969).
309. D. Zeng, M. J. Hampden-Smith and E. N. Duesler, *Inorg. Chem.*, **33**, 5376 (1994).
310. K. Ruhlandt-Senge and P. P. Power, *Inorg. Chem.*, **32**, 4505 (1993).
311. M. Westerhausen, M. Wieneke, K. Doderer and W. Schwarz, *Z. Naturforsch.*, **51b**, 1439 (1966).
312. M. Westerhausen, M. Wieneke and W. Schwarz, *J. Organomet. Chem.*, **572**, 249 (1999).
313. B. Rademacher, W. Schwarz and M. Westerhausen, *Z. Anorg. Allg. Chem.*, **621**, 287 (1995).
314. B. Rademacher, W. Schwarz and M. Westerhausen, *Z. Anorg. Allg. Chem.*, **621**, 1439 (1995).
315. T. J. Groshens, K. T. Higa and R. J. Butcher, *J. Organomet. Chem.*, **463**, 97 (1993).
316. A. J. Edwards, M. A. Paver, P. R. Raithby, C. A. Russell and D. S. Wright, *Organometallics*, **12**, 4687 (1993).
317. M. G. Davidson, A. J. Edwards, M. A. Paver, P. R. Raithby, C. A. Russell, A. Steiner, K. L. Verhorevoort and D. S. Wright, *J. Chem. Soc., Chem. Commun.*, 1989 (1995).
318. A. Bashall, J. M. Cole, F. García, A. Primo, A. Rothenberger, M. McPartlin and D. S. Wright, *Inorg. Chim. Acta.*, **354**, 41 (2003).
319. W. Hieber and U. Teller, *Z. Anorg. Allg. Chem.*, **249**, 43 (1942).
320. P. H. M. Budzelaar, J. Boersma, G. J. M. van der Kerk and A. J. M. Duisenberg, *Inorg. Chem.*, **21**, 3777 (1982).
321. P. H. M. Budzelaar, K. H. den Haan, J. Boersma, G. J. M. van der Kerk and A. L. Spek, *Organometallics*, **3**, 156 (1984).
322. R. D. Wilson, T. F. Koetzle, D. W. Hart, A. Kvick, T. L. Tripton and R. Bau, *J. Am. Chem. Soc.*, **99**, 1775 (1977).
323. P. H. M. Budzelaar, A. A. H. van der Zeijden, J. Boersma, G. J. M. van der Kerk, A. L. Spek and A. J. M. Duisenberg, *Organometallics*, **3**, 159 (1984).
324. P. H. M. Budzelaar, H. J. Alberts-Jansen, K. Mollema, J. Boersma, G. J. M. van der Kerk, A. L. Spek and A. J. M. Duisenberg, *J. Organomet. Chem.*, **243**, 137 (1983).
325. P. H. M. Budzelaar, J. Boersma, G. J. M. van der Kerk, A. L. Spek and A. J. M. Duisenberg, *J. Organomet. Chem.*, **287**, C13 (1985).
326. P. H. M. Budzelaar, J. Boersma, G. J. M. van der Kerk, A. L. Spek and A. J. M. Duisenberg, *Organometallics*, **4**, 680 (1985).
327. B. Fischer, J. Boersma, G. van Koten and A. L. Spek, *New J. Chem.*, **12**, 613 (1988).
328. B. Fischer, H. Kleijn, J. Boersma, G. van Koten and A. L. Spek, *Organometallics*, **8**, 920 (1989).
329. M. Ohashi, K. Matsubara, T. Iizuka and H. Suzuki, *Angew. Chem., Int. Ed.*, **42**, 937 (2003).
330. M. D. Fryzuk, D. H. McConville and S. J. Rettig, *Organometallics*, **9**, 1359 (1990).
331. M. D. Fryzuk, D. H. McConville and S. J. Rettig, *Organometallics*, **12**, 2152 (1993).
332. M. H. P. Rietveld, P. Lohner, M. G. Nijkamp, D. M. Grove, N. Veldman, A. L. Spek, M. Pfeffer and G. van Koten, *Chem. Eur. J.*, **3**, 817 (1997).
333. H. C. L. Abbenhuis, N. Feiken, H. F. Haarman, D. M. Grove, E. Horn, A. L. Spek, M. Pfeffer and G. van Koten, *Organometallics*, **12**, 2227 (1993).

CHAPTER 3

Thermochemistry of organozinc compounds

JOEL F. LIEBMAN

Department of Chemistry and Biochemistry, University of Maryland, Baltimore County, 1000 Hilltop Circle, Baltimore, MD 21250, USA
Fax: +1 410 455 2608; e-mail: jliebman@umbc.edu

and

SUZANNE W. SLAYDEN

Department of Chemistry, George Mason University, 4400 University Drive, Fairfax, VA 22030-4444, USA
Fax: +1 703 993 1055; e-mail: sslayden@gmu.edu

I. INTRODUCTION: SCOPE AND DEFINITIONS

Thermochemical attention in this chapter is directed towards compounds with carbon−zinc bonds, i.e. species that are usually labeled organometallic. The thermodynamic properties that we discuss are restricted to the enthalpy of formation (often called the 'heat of formation'), enthalpy of vaporization and carbon−zinc bond energies. We forego discussion of other thermochemical properties such as entropy, heat capacity or excess enthalpy. The energy units are kJ mol^{-1} where 4.184 kJ is defined to equal 1 kcal.

The chemistry of organozinc compounds
Edited by Z. Rappoport and I. Marek

There are few data for any organozinc compounds. The most numerous are for the dialkylzincs, R_2Zn. Earlier compilations of organozinc thermochemical data can be found in the classic text by Cox and Pilcher[1], a chapter by Pilcher and Skinner in an earlier volume in this series from 1982[2] and in Martinho Simões's evaluated compilation of data as found in the NIST Chemistry WebBook[3].

II. DIALKYLZINC COMPOUNDS

A. Enthalpies of Vaporization

It is rare that the thermochemical database for compounds with a common functional group includes many more enthalpies of vaporization (ΔH_{vap}) than enthalpies of formation. However, that seems to be the situation for the dialkylzinc compounds. In addition to the archival sources for enthalpy data already mentioned in the Introduction, there is a recently published compendium of vaporization enthalpies that includes data reported between 1910–2002[4]. As we have examined the published sources of vaporization enthalpy data, it is apparent that there exists some confusion about the primary origin of some of the data. With only a couple of exceptions, we have obtained the original publications and verified the sources and vaporization enthalpies that appear in Table 1. Unfortunately, the vapor pressures of the dibutylzinc through diheptylzinc compounds were not determined near 298 K and we do not have the auxillary data necessary for correction. The dimethylzinc and diethylzinc species were determined close to 298 K and so temperature adjustments to their enthalpies of vaporization are expected to be negligible. The individually determined values are quite consistent for each of them and the average enthalpies of vaporization for these compounds are 29.9 ± 0.5 and 39.6 ± 1.1 kJ mol^{-1}, respectively. The temperature corrections to the enthalpies of vaporization of the di-*n*-propylzinc and diisopropylzinc species are likewise expected to be inconsequential, although an apparent correction appears in the data from Reference 1.

Acknowledging these problems, we make the following observations about the vaporization enthalpy data. It has long been known[1] that enthalpies of vaporization of several homologous series are linearly correlated with the number of carbon atoms, n, in the molecule for $n \geqslant 2$. Sometimes, but not always, the enthalpy of vaporization of the methyl derivative is anomalous. When all the original data for diethylzinc through diheptylzinc are subjected to a linear regression analysis of enthalpy of vaporization vs. number of carbon atoms in the alkyl group, the slope of the regression equation is 4.4 kJ mol^{-1}, which is similar to those for other homologous functional group series. For example, the slopes for the *n*-alkanes, the di-*n*-alkyl sulfides and the di-*n*-alkyl ethers are 5.0, 4.9 and 4.3 kJ mol^{-1}, respectively. The correlation coefficient for the di-*n*-alkylzinc data is rather low, 0.88, reflecting the variation in the values used in the analysis. The experimental average enthalpy of vaporization of dimethylzinc is *ca* 3 kJ mol^{-1} less than the value calculated from the regression equation.

A simple method for estimating enthalpies of vaporization is the 'CHLP protocol'[19]. The quantities $\tilde{n}_c$ and n_Q in equation 1 refer respectively to the number of quaternary carbon atoms and non-quaternary carbon atoms in the compound, and b is a value that is characteristic of the functional group bonded to the hydrocarbon parent.

$$\Delta H_{vap}(\text{kJ mol}^{-1}) = 4.69\tilde{n}_c + 1.3n_Q + 2.97 + b \quad (1)$$

Recognizing that the enthalpies of vaporization of the higher di-*n*-alkylzincs are not temperature-corrected for 298 K, and the dimethylzinc and perhaps even the diethylzinc enthalpies are anomalous, we calculate the b substituent constant from the data for

TABLE 1. Enthalpies of vaporization of dialkylzinc compounds ($kJ\,mol^{-1}$)

Compound	ΔH_{vap}	Reference
Dimethylzinc	29.9	5
	29.5 [a]	6
	30.4 ± 0.2	7, 8
Diethylzinc	37	9
	40.2 [b]	5
	38.3	10
	37.9	11
	38.8 ± 0.40	7
Di-*n*-propylzinc	40.3	5
	40.6	12
	39.5	13
	42.1 ± 0.4	14
	43 ± 2	15
	45.6 ± 2.5 [c]	1
Diisopropylzinc	41.8 ± 0.5	14
	47.3	16
Di-*n*-butylzinc	42.9	5
	45.3	13
	50.7 ± 0.3	17
	54.4 ± 3.3 [c]	1
Di-*sec*-butylzinc	40.9 ± 0.2	17
Diisobutylzinc	44.6 ± 0.2	17
Di-*t*-butylzinc	49.3 ± 0.8	17
Dipentylzinc	48.6	13
Dihexylzinc	56.2	13
Diheptylzinc	62.3	13

[a] This value is recorded as 29.5 ± 0.4 $kJ\,mol^{-1}$ in Reference 2, but not credited. The citation in Reference 2 is for the enthalpy of formation only, from Reference 18. In the latter study, the authors credit Reference 5 for the enthalpy of vaporization.
[b] This value is recorded as 40.2 ± 2.1 in Reference 2, but not credited. The citation in Reference 2 is for the enthalpy of formation only, from Reference 18. In the latter study, the authors credit Reference 9 for the enthalpy of vaporization. Both 40.2 and 40.2 ± 2.1 with different cited sources have appeared together in compilations, suggesting they are independent measurements.
[c] The enthalpy of vaporization is originally from Reference 13 and corrected by Reference 1. In some compilations, both values have been listed, with different cited sources, suggesting they are independent measurements.

the dipropylzincs. According to equation 1, the enthalpies of vaporization of the two isomers should be the same. The average calculated b value is thus 11 ± 3 $kJ\,mol^{-1}$. Regardless of the accuracy of this number, the b values calculated for other dialkylzincs should be compatible if they had been temperature-corrected. For comparison, the b values for dimethylzinc and diethylzinc are *ca* 17 and 18 $kJ\,mol^{-1}$, respectively. The presumably temperature-corrected enthalpies of vaporization for di-*n*-propylzinc and di-*n*-butylzinc from Reference 1 yield b values of 14.5 and 13.9 $kJ\,mol^{-1}$, respectively. As these are consistent with those calculated from uncorrected original data, we will accept our calculated b value for the dialkylzincs when it is necessary to estimate an enthalpy of vaporization.

B. Enthalpies of Formation

Depending on the R group, enthalpies of formation ($\Delta_f H_m$) shown in Table 2 have been obtained using either reaction and/or combustion calorimetry. Although there are fewer values for enthalpies of formation than for enthalpies of vaporization, there is still some confusion about the source, as well as the numerical value, of some of the data. To the extent possible, the sources have been obtained and the enthalpies of formation recorded in Table 2. Only the liquid phase enthalpies of formation are listed for those compounds that have multiple determinations of enthalpies of formation and of vaporization.

With the exception of the methyl derivative, the quality of the data in a homologous series, RZ, is revealed by the extent of the linear correlation of the enthalpies of formation with the number of carbon atoms in the hydrocarbon group, R. The methyl-substituted species frequently deviates from the correlation. For a Z atom or group that is more electronegative than carbon, the enthalpy of formation of MeZ is more positive than the value extrapolated from the straight line, while for more electropositive Z, the deviation is in the opposite direction[21]. Figure 1 is a plot of the liquid enthalpies of formation[1] of dimethyl-, diethyl-, di-*n*-propyl- and di-*n*-butylzinc vs. the number of carbon atoms in an alkyl ligand. Regarding dimethylzinc, its enthalpy of formation deviates in the expected direction for a methyl group bonded to a more electropositive element, that is, the enthalpy of formation of dimethylzinc is more negative than that for diethylzinc.

TABLE 2. Enthalpies of formation of organozinc compounds (kJ mol^{-1})

Compound	$\Delta_f H_m$ (lq)	$\Delta_f H_m$ (g)	Reference
Dimethylzinc	26.4 ± 4.2		18
	27.2		12
	25.1 ± 8.4 [a]		1
	20.8 ± 1.2 [b]		2
Diethylzinc	18.0 ± 4.2		18
	17.2		12
	16.7 ± 6.3 [c]		1
Dipropylzinc	−56.9		12
	-57.7 ± 23.4		1
	-59.3 ± 23 [d]		2
Di-*n*-butylzinc	−104.2		12
	-104.2 ± 23.8 [e]		1
	-105.9 ± 23.5 [d]		2
Dineopentylzinc	$-174. \pm 14.$	$-121. \pm 17.$	20
Bis(trimethylsilylmethyl)zinc	-409.7 ± 19	-355.3 ± 21	20

[a] This is the selected value given in this archival source, which is a composite of the enthalpies of formation from References 12 and 18. The enthalpy of formation given in Reference 18, itself a composite of three different reaction enthalpies, is 6.3 kcal mol^{-1}. Only one of these reaction enthalpies was chosen for inclusion in Reference 1, 5.4 kcal mol^{-1}.

[b] The enthalpy of formation found from this source is credited to Reference 18. No information was given concerning the correction made to the original data. These data are not independent measurements.

[c] This is the selected value given in this archival source, which is a composite of the enthalpies of formation from References 12 and 18 and a value of 4.9 ± 0.7 kcal mol^{-1} from W. F. Lautsch, A. Tröber, W. Zimmer, L. Mehner, W. Linck, H.-M. Lehman, H. Brandenberger, H. Korner, H.-J. Metschker, K. Wagner and R. Kaden, *Z. Chem.*, **3**, 415 (1963). This value also appears in Reference 2, where it is mistakenly credited to Reference 18.

[d] The enthalpy of formation found from this source is credited to Reference 12. No information was given concerning the correction made to the original data. These data are not independent measurements.

[e] This corrected value was credited to Reference 12.

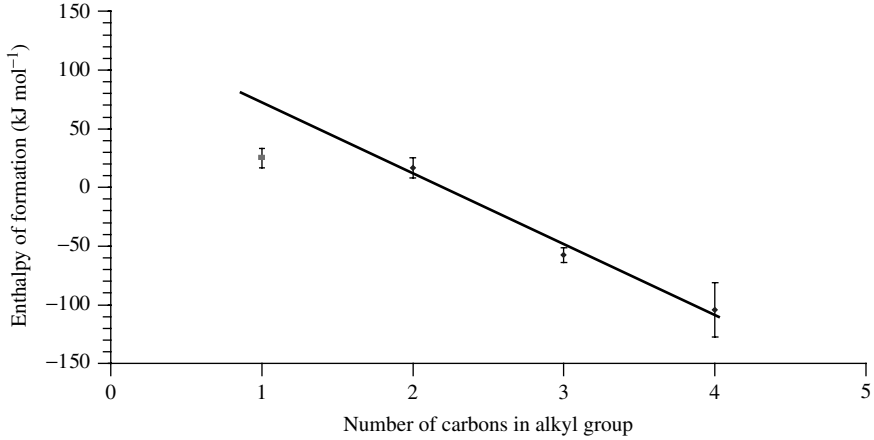

FIGURE 1. Enthalpies of formation of di-*n*-alkylzincs (liquid, kJ mol^{-1})

Assessing the quality of the data for the remaining di-*n*-alkylzinc species is a problem. The three data points are clearly not linearly related. An unweighted least squares regression analysis gives a slope, or 'methylene increment', of -30.2 kJ mol^{-1}. The slope value, which represents the difference between successive members of the homologous series, is much more negative than is typical for other homologous series, even acknowledging that somewhat more reliable values are obtained when the number of carbon atoms in R is greater than 4. For example, the slopes of the regression line for the liquid and gaseous *n*-alkanes (*n*-R-$(CH_2)_x$-H) are -25.6 and -20.6 kJ mol^{-1}, respectively. However, for the only two *n*-alkyl lithiums for which there are enthalpy of formation data, ethyl and butyl lithium, the gas phase methylene increment is *ca* -32 kJ mol^{-1} [22].

No enthalpy of formation data are available from the literature for any of the branched isomers of either dipropylzinc or dibutylzinc. The enthalpy of formation of dineopentylzinc[20] is the only value available for any of the dipentylzinc isomers.

A recent study[23] combined quantum chemical calculations and electron diffraction/photoelectron spectroscopy to derive the following dialkylzinc gas phase enthalpies of formation: ethyl, 57 ± 8; *n*-propyl, 10 ± 8; isopropyl, 32 ± 8; *t*-butyl, -17 ± 8; neopentyl, -117 ± 8 kJ mol^{-1}. The benchmark value of 53 ± 1 kJ mol^{-1} was chosen for the gas phase enthalpy of formation of dimethylzinc. Compared to the experimental values, the diethyl and dineopentyl values are very close, but the *n*-propyl enthalpy of formation is just barely within the combined large error bars. The methylene increment from the theoretically derived values of diethylzinc and di-*n*-propylzinc is -23.5 kJ mol^{-1}, a value that is consistent with other gas phase homologous series. Using this increment, the enthalpies of formation of gaseous di-*n*-butylzinc and di-*n*-pentylzinc are calculated to be -37 and -84 kJ mol^{-1}, respectively.

For isomeric alkanes substituted with an electronegative atom, such as *n*-, *sec*- and *t*-butyl bromide, alkyl group branching at the carbon bonded to the substituent atom increases the thermodynamic stability in both the liquid and gaseous phases. The increasing stability parallels the alkyl group carbocation stability. In contrast, branching at a carbon bonded to a more electropositive group thermodynamically destabilizes the isomer. The calculated isomerization enthalpy of the theoretically-derived enthalpies of formation for the dipropylzincs is 22 kJ mol^{-1}, or 11 kJ mol^{-1} for each propyl group.

The isomerization enthalpy of the *n*-propyl and isopropyl lithiums is *ca* 15 kJ mol^{-1} [22]. These isomerization enthalpy absolute values are nearly the same as that for diisopropyl or di-*sec*-butyl ether, *ca* 11 kJ mol^{-1} per alkyl group[24]. From the above-estimated enthalpy of formation of di-*n*-butylzinc and the calculated enthalpy of formation of di-*t*-butylzinc from Reference 23, the isomerization enthalpy is 10 kJ mol^{-1} per butyl group. We might have expected the primary/tertiary isomerization enthalpy to be larger than the primary/secondary isomerization. The isomerization enthalpy of *t*-butyl methyl ether to *n*-butyl methyl ether or of *t*-butyl *n*-butyl ether to di-*n*-butyl ether is *ca* 23–25 kJ mol^{-1}. Because of destabilizing steric effects in the di-*t*-butyl ether, its isomerization enthalpy to the di-*n*-butyl ether is *ca* 11 kJ mol^{-1} per butyl group[24]. However, the carbon–zinc bond is longer than the carbon–oxygen bond, and the C–Zn–C bond angle is 180°, and so steric effects would not seem a satisfactory rationalization. Dineopentylzinc, with branching at the β-carbon instead of the α-carbon, is calculated to be *ca* 33 kJ mol^{-1} per pentyl group more stable than its non-branched isomer, di-*n*-pentylzinc, both of them primary alkyl groups. Unfortunately, there are no enthalpies of formation known to the authors for any neopentyl-Z species with which to make a comparison. The isomerization enthalpy[25] of *n*-pentane to neopentane, examples of pentyl-H species, is −21 kJ mol^{-1}, compared to the *ca* 17 kJ mol^{-1} for each of the pentyl groups bonded to Zn. For the related example of pentyl–CH_3 species, the isomerization enthalpy is −19 kJ mol^{-1}.

C. Bond Energies

Much of the enthalpy of formation data for the dialkylzincs was reported from two separate sources in 1949[12, 18]. From these measurements each group derived the mean bond dissociation energies of the dialkylzinc compounds. From Reference 12, the mean C–Zn bond energies were 172 kJ mol^{-1} for Me_2Zn and 150 kJ mol^{-1} for Et_2Zn (and by assumption for the *n*-Pr_2Zn and *n*-Bu_2Zn species also). From Reference 18, the mean bond energies for the Me_2Zn and Et_2Zn compounds were reported as 171 and 144 kJ mol^{-1}, respectively.

A contemporary source for the mean bond energies combined quantum chemical calculations and electron diffraction/photoelectron spectroscopy[23] and used a combination of the experimentally-determined enthalpies of formation and vaporization for dimethylzinc as a benchmark. The average C–Zn bond energy for Me_2Zn was reported as 186 ± 2 kJ mol^{-1}. Compatible mean bond energies were found when either literature enthalpy of formation data or DFT calculations were employed. The DFT calculated energies are (kJ mol^{-1}): Et_2Zn, 156 ± 8; *n*-Pr_2Zn, 159 ± 8; *i*-Pr_2Zn, 132 ± 8; *t*-Bu_2Zn, 116 ± 8; neoPen_2Zn, 162 ± 8; and $(Me_3SiCH_2)_2Zn$, 179 ± 8.

We are told in Reference 23 that there is a good correlation between the organozinc species homolytic bond energies and both the corresponding R–H and the R–Zn bond lengths. The correlations include the Si-containing bis(trimethylsilylmethyl)zinc compound that has a comparatively shorter and stronger C–Zn bond, just as trimethylsilylmethane has a shorter and stronger C–H bond compared to other saturated alkanes.

From the data and accompanying analysis in a study of catalyzed chain growth polymerization of diethylzinc and *n*-alkene synthesis[26], we deduce that the reaction 2

$$\begin{aligned} &CH_3CH_2(CH_2CH_2)_aZn(CH_2CH_2)_bCH_2CH_3 + CH_3CH_2(CH_2CH_2)_cZn(CH_2CH_2)_dCH_2CH_3 \\ &\quad\longrightarrow CH_3CH_2(CH_2CH_2)_wZn(CH_2CH_2)_xCH_2CH_3 \\ &\quad + CH_3CH_2(CH_2CH_2)_yZn(CH_2CH_2)_zCH_2CH_3 \end{aligned} \tag{2}$$

is essentially thermoneutral for all balanced equations where a, b, c, d, w, x, y, $z \geqslant 0$. This is another way of saying that D(Zn–C) is a constant for all alkyl groups, except

for the dimethylzinc, in both symmetrical and unsymmetrical di-*n*-alkylzinc homologous series. These authors also inferred that D(Zn−Me) is larger than D(Zn−R) for longer alkyls.

In a recent synthesis of a mixed zinc/cadmium telluride alloy, a mixture of dimethylcadmium and diethylzinc was employed[27]. The original authors interpreted the results by assuming that the redistribution reaction 3 is essentially thermoneutral since the difference between the enthalpies of formation for the symmetrical dialkylzincs is small.

$$Me_2Zn + Et_2Zn \longrightarrow 2MeEtZn \tag{3}$$

While none of these results is particularly surprising, it is encouraging to have confirmation.

A corollary of the aforementioned two results is that reaction 4 is also thermoneutral for all balanced equations where a, b, c, d, w, x, y, $z \geqslant 0$.

$$CH_3(CH_2)_aZn(CH_2)_bCH_3 + CH_3(CH_2)_cZn(CH_2)_dCH_3 \longrightarrow CH_3(CH_2)_wZn(CH_2)_xCH_3 + CH_3(CH_2)_yZn(CH_2)_zCH_3 \tag{4}$$

Likewise, reaction 5 is expected to be thermoneutral for all hydrocarbon groups R.

$$Me_2Zn + R_2Zn \longrightarrow 2MeZnR \tag{5}$$

III. MONOALKYLZINC SPECIES

Not surprisingly, the data for the univalent monoalkylzinc species are both sparse and problematic. After all, these species are most logically and synthetically derived from their divalent counterparts and we have already enunciated difficulties with their thermochemical study. Martinho Simões[3] has compiled three values for the enthalpy of formation of the monomethyl species, 190 ± 17, 193 ± 11 and 172.4 ± 6.5 kJ mol^{-1} that rely on an enthalpy of formation of gas phase dimethylzinc of 52.9 ± 1.3 kJ mol^{-1}. From the same source and with a benchmark value for gaseous diethylzinc of 55.5 ± 3.9, the enthalpies of formation of the monoethyl species are 175 ± 17, 167 and 155.7 ± 9.5 kJ mol^{-1}. The average values for the enthalpies of formation of MeZn and EtZn are thus 186 and 166 kJ mol^{-1}, respectively, both with large uncertainties. The enthalpy of formation of gaseous zinc (from Reference 28) is 130.7 kJ mol^{-1} with an uncertainty safely under 1 kJ mol^{-1}. Accordingly, reaction 6 is endothermic by *ca* 186 and 146 kJ mol^{-1} for R = Me and Et, respectively.

$$R_2Zn(g) + Zn(g) \longrightarrow 2RZn(g) \tag{6}$$

We thus conclude that the R−Zn bond in the univalent monoalkylzinc species is considerably weaker than the 'average' bonds in the divalent dialkylzincs, and *a fortiori*, the first C−Zn bond strength.

We can be more quantitative by using equation 7 where $n = 1$ and 2. From the recommended enthalpies of formation of methyl and ethyl radical of 147 ± 1 and 119 ± 2 kJ mol^{-1} from Reference 29, we deduce the first bond strength of Me_2Zn to be 280 kJ mol^{-1} and that of Et_2Zn to be 230 kJ mol^{-1}. By contrast, the Me−Zn bond strength in MeZn is 92 kJ mol^{-1} and the Et−Zn bond strength in EtZn is 84 kJ mol^{-1}. It would appear that compounds containing univalent zinc are unequivocally unstable compared to corresponding species with zinc in its divalent oxidation state.

$$R_nZn \longrightarrow R_{n-1}Zn + R \tag{7}$$

IV. DIMETHYLZINC RADICAL CATION AND METHYLZINC CATION

The formation (and accompanying fragmentation) of dimethylzinc to produce the dimethylzinc radical cation, $Me_2Zn^{\bullet+}$, has been studied by photoelectron spectroscopy[30]. The energies of reaction 8 are $n = 0$, 9.00 ± 0.02; $n = 1$, 10.22 ± 0.02; and $n = 2$, 13.13 ± 0.13 eV.

$$Me_2Zn^{\bullet+} \longrightarrow (Me)_{2-n}Zn^{+} + nMe^{\bullet} \tag{8}$$

From these data, we derive the $MeZn^{\bullet+}-Me$ bond energy as the difference between the fragmentation energies for $n = 1$ and $n = 0$: 1.22 ± 0.03 eV or 118 ± 3 kJ mol^{-1}. The $Me-Zn^{+}$ bond energy is the difference between the fragmentation energies for $n = 1$ and $n = 2$: 2.89 ± 0.13 eV or 278 ± 13 kJ mol^{-1}. It is noteworthy that the $MeZn^{\bullet+}-Me$ bond is so much weaker than MeZn−Me, the aforementioned first bond energy of the corresponding neutral, dimethylzinc. Likewise, the $Me-Zn^{\bullet+}$ bond is so much stronger than that of the corresponding neutral, monomethylzinc.

V. ZINC–CYANIDE COMPLEXES

The zinc−cyanide complexes are on the interface of organic and inorganic chemistry. We include them here because of their Zn−C bond. (Perhaps this will encourage thermochemical investigations on the isoelectronic alkynylzinc species, much as there has been interest in both cyano and alkynyl silver-containing species[31].) The species $Zn(CN)_2$, $Zn(CN)_3^{-}$ and $Zn(CN)_4^{2-}$ have all been thermochemically characterized in aqueous solution by thermometric titration[32]. The enthalpy of reaction values kJ mol^{-1} are shown for reactions 9–11.

$$Zn^{2+} + 2CN^{-} \longrightarrow Zn(CN)_2 \qquad H^{\circ} = -45.2 \pm 2.1 \tag{9}$$

$$Zn^{2+} + 3CN^{-} \longrightarrow Zn(CN)_3^{-} \qquad H^{\circ} = -80.3 \pm 2.1 \tag{10}$$

$$Zn^{2+} + 4CN^{-} \longrightarrow Zn(CN)_4^{2-} \qquad H^{\circ} = -116.3 \pm 2.1 \tag{11}$$

As also reported in Reference 32, the enthalpy of reaction 11 was also determined calorimetrically to have the indistinguishable value of -116.7 ± 0.4 kJ mol^{-1}.

From a standard archive for inorganic species[28], the enthalpies of formation of aqueous Zn^{2+} and CN^{-} are −153.9 and 150.6 kJ mol^{-1} respectively, from which we derive the enthalpies of formation of aqueous $Zn(CN)_2$, $Zn(CN)_3^{-}$ and $Zn(CN)_4^{2-}$ as 102.1, 217.6 and 332.2 kJ mol^{-1}. By contrast, the enthalpy of formation[32] of solid $Zn(CN)_2$ is 95.8 kJ mol^{-1} [33].

While there are no thermochemical data available for the $(ZnCN)^{+}$ ion or related neutral, the latter species, in its gas phase, was found to have a $2\sum$ ground state with an atypically short CN bond length[34]. Valence isoelectronic to the latter species is the $(ZnCS)^{+}$ ion for which a 0 K gas phase bond energy of 149 ± 23 kJ mol^{-1} was recently determined[35].

VI. REFERENCES AND NOTES

1. J. D. Cox and G. Pilcher, *Thermochemistry of Organic and Organometallic Compounds*, Academic Press, London, 1970.
2. G. Pilcher and H. A. Skinner, 'Thermochemistry of organometallic compounds', in *The Chemistry of the Metal−Carbon Bond*, Vol. 1 (Eds. F. R. Hartley and S. Patai), Wiley, Chichester, 1982.
3. J. A. Martinho Simões, 'Organometallic Thermochemistry Database', in *NIST Chemistry WebBook*, *NIST Standard Reference Database Number* 69 (Eds. P. J. Linstrom and W. G. Mallard), March 2003, National Institute of Standards and Technology, Gaithersburg, MD 20899 (http://webbook.nist.gov).

4. J. S. Chickos and W. E. Acree, Jr., *J. Phys. Chem. Ref. Data*, **32**, 519 (2003).
5. C. H. Bamford, D. L. Levi and D. M. Newitt, *J. Chem. Soc.*, 468 (1946).
6. L. H. Long and J. Cattanach, *J. Inorg. Nucl. Chem.*, **20**, 340 (1961).
7. A. E. Sokolovskii and A. K. Baev, *J. Gen. Chem. USSR*, **54**, 89 (1984).
8. A. K. Baev, *Russ. J. Inorg. Chem.*, **42**, 587 (1997).
9. F. Hein and H. Schramm, *Z. Physik. Chem. A*, **149**, 408 (1930).
10. The enthalpy of vaporization was calculated by the method of Reference 4 from the vapor pressure–temperature data found in D. R. Stull, *Ind. Eng. Chem.*, **39**, 517 (1947) cited from Hein and Schramm, *Z. Physik. Chem.*, **86**, 385 (1914).
11. J. E. House, Jr., *Thermochim. Acta*, **71**, 215 (1983).
12. L. H. Long and R. G. W. Norrish, *Phil. Trans. Roy. Soc. (London)*, **A241**, 587 (1949).
13. L. F. Hatch, G. Sutherland and W. J. Ross, *J. Org. Chem.*, **14**, 1130 (1949).
14. A. E. Sokolovskii and A. K. Baev, *Vestsi Akad. Navuk BSSR, Ser. Khim. Navuk*, 115 (1984) as cited in References 3 and 4.
15. A. K. Baev and M. A. Shishko, *Russ. J. Appl. Chem.*, **75**, 25 (2002) as found in Reference 4; *Chem. Abstr.*, **100**, 127683p (1984).
16. G. W. Thompson, *Chem. Rev.*, **38**, 1 (1946). The author does not provide any experimental detail, but says of the experimental data 'many of these equations were obtained from data of lower quality…'. The enthalpy of vaporization is calculated from the data by the method of Reference 4.
17. A. E. Sokolovskii and A. K. Baev, *Russ. J. Phys. Chem.*, **58**, 1635 (1984).
18. A. S. Carson, K. Hartley and H. A. Skinner, *Trans. Faraday Soc.*, 1159 (1949).
19. J. S. Chickos, D. G. Hesse, J. F. Liebman and S. Y. Panshin, *J. Org. Chem.*, **53**, 3424 (1988); J. S. Chickos, D. G. Hesse and J. F. Liebman, *J. Org. Chem.*, **54**, 5250 (1989).
20. I. E. Gümrükçüoglü, J. Jeffery, M. F. Lappert, J. B. Pedley and A. K. Rai, *J. Organometal. Chem.*, **341**, 53 (1988).
21. J. F. Liebman, J. A. Martinho Simões and S. W. Slayden, *Structural Chemistry*, **6**, 65 (1995).
22. S. W. Slayden and J. F. Liebman, 'Thermochemistry of organolithium compounds', in *The Chemistry of Organolithium Compounds* (Eds. Z. Rappoport and I. Marek), Wiley, Chichester, 2004.
23. A. Haaland, J. C. Green, G. S. McGrady, A. J. Downs, E. Gullo, M. J. Lyall, J. Timberlake, A. V. Tutukin, H. V. Volden and K.-A. Østby, *Dalton Trans.*, 4356 (2003).
24. S. W. Slayden and J. F. Liebman, 'Thermochemistry of ethers, alcohols, arenols, enols and peroxides', in *The Chemistry of Functional Groups, Supplement E: The Chemistry of Hydroxyl, Ether and Peroxide Groups*, Vol. 2 (Ed. S. Patai), Wiley, Chichester, 1993.
25. The enthalpies of formation are taken from J. B. Pedley, R. D. Naylor and S. P. Kirby, *Thermochemical Data of Organic Compounds* (2nd Ed.), Chapman & Hall, New York, 1986.
26. G. J. P. Britovsek, S. A. Cohen, V. C. Gibson and M. van Meurs, *J. Am. Chem. Soc.*, **126**, 10701 (2004).
27. M. J. Kappers, K. J. Wilkerson and R. F. Hicks, *J. Phys. Chem. B*, **101**, 4882 (1997).
28. D. D. Wagman, W. H. Evans, V. B. Parker, R. H. Schumm, I. Halow, S. M. Bailey, K. L. Churney and R. L. Nuttall, 'The NBS Tables of Chemical Thermodynamic Properties: Selected Values for Inorganic and C_1 and C_2 Organic Substances in SI Units', *J. Phys. Chem. Ref. Data*, **11**, Supplement 2 (1982).
29. W. Tsang, 'Heats of formation of organic free radicals by kinetic methods', in *Energetics of Organic Free Radicals* (Eds. J. A. Martinho Simões, A. Greenberg and J. F. Liebman), Blackie Academic and Professional, London, 1996.
30. G. Distefano and V. H. Dibeler, *Intern. J. Mass Spectrom. Ion Phys.*, **59**, 4 (1970).
31. J. F. Liebman, J. A. Martinho Simões and S. W. Slayden, in *The Chemistry of Organic Silver and Gold Compounds* (Eds. S. Patai and Z. Rappoport), Wiley, Chichester, 1999.
32. R. M. Izatt, J. J. Christensen, J. W. Hansen and G. D. Watt, *Inorg. Chem.*, **4**, 718 (1965).
33. Reference 28 also gives the enthalpy of formation of the aqueous $Zn(CN)_4^{-2}$ as 342.3 kJ mol^{-1}, as well as of the solid salt $K_2Zn(CN)_4$ as -100.0 kJ mol^{-1}.
34. M. A. Brewster and L. M. Ziurys, *J. Chem. Phys.*, **117**, 485 (2002).
35. C. Rue, P. D. Armentrout, I. Kretzschmar and H. Schwarz, *J. Phys. Chem. A*, **106**, 9788 (2002).

CHAPTER 4

^{67}Zn NMR, a tool for coordination chemistry problems

ATHANASSIOS G. COUTSOLELOS

Chemistry Department, Laboratory of Bioinorganic Chemistry, University of Crete, PO Box 2208, GR-71003 Heraklion, Crete, Greece
Fax: +30 281 054 5054; e-mail: coutsole@chemistry.uoc.gr

and

GEORGIOS A. SPYROULIAS

Department of Pharmacy, University of Patras, Panepistimioupoli — Rion, GR-26504 Patras, Greece
Fax: +30 261 096 9950; e-mail: gspyroul@upatras.gr

I. INTRODUCTION

Nuclear magnetic resonance (NMR) spectroscopy is a powerful and versatile analytical technique that can provide site-specific information about chemical bonding, structure and dynamics in molecular systems. NMR applications have made a major impact in a variety of disciplines ranging from materials science to molecular biology and bioinorganic

The chemistry of organozinc compounds
Edited by Z. Rappoport and I. Marek

chemistry. Heteronuclear NMR has found an important role when metal ions are involved in the chemical structures and for several cases has assisted in approaching solutions or solid state problems.

^{1}H and ^{13}C NMR spectroscopies are being widely used to characterize Zn(II) organometallic compounds with organic moieties, amino acids or amino acid synthetic analogues based on minor chemical shift differences of the nuclei of the free ligands and the Zn(II) complexes. On the other hand, ^{67}Zn nucleus could be also used to probe the metal binding of organometallic compounds or biopolymers like proteins and enzymes.

II. ^{1}H AND ^{13}C NMR SPECTROSCOPY OF ORGANOMETALLIC COMPOUNDS

Zn^{2+} ion is diamagnetic ($[Ar]d^{10}$), lacking any unpaired electron density, and therefore no influence on the relaxation properties and chemical shifts of the ^{1}H and/or ^{13}C resonances is expected. However, in an attempt to illustrate the differentiation of various Zn ligands bearing oxygen, nitrogen or sulfur donor atoms, experimental NMR data reported in the literature are collected[1–4]. Ligands discussed in this section are either peptides bearing natural amino acids or synthetic organic moieties. These groups bear mainly N and S donor atoms, since the coordination of ligands through oxygen donor atoms, mainly carboxylic acids, sets the Zn metal ion in a three-bond distance from a C atom bearing protons [i.e. Zn−O−C(O)−C**H**R−, where R = H or other group], thus minimizing even further the chemical shift differentiation effect arising from metal binding.

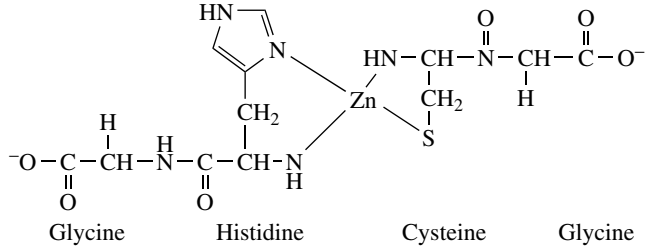

CHART 1. Zn(II) coordination to $^{+}H_3N-His-Gly-COO^{-}$ and $^{+}H_3N-Cys-Gly-COO^{-}$ dipeptides

In the former case, two dipeptides, $^{+}H_3N-His-Gly-COO^{-}$ and $^{+}H_3N-Cys-Gly-COO^{-}$, are bound to a Zn(II) ion, through the two NH terminal dipeptide groups and the imidazole ring of the histidine and the SH group of cysteine residue (see Chart 1)[1]. The authors monitored the chemical shift differences of ^{1}H and ^{13}C nuclei between the free and metal-bound peptides by taking into account (i) the H nuclei of the Cα and Cβ carbon atoms of the cysteine residue, the Cα, Cδ2 and Cε1 (see Chart 2) protons of the histidine residues and those sited at the Cα carbon atoms of the glycyl residues, as well as (ii) the C nuclei of the two COO^{-} terminal groups and the CO carbonyl atoms of the peptide bonds, in concert with the histidine Cα, Cβ, Cγ, Cδ2 and Cε1 carbon atoms, the cysteine Cα and Cβ carbons and the two Cα carbon atoms of glycines (see Chart 2). The largest ^{1}H chemical shift differences were observed for protons that were close to the zinc coordination sites (histidine Nε2 or Nδ2 and cysteine S) and were measured to be only 1.12 and 1.0 ppm for cysteine βCH_2 and histidine Hε1 protons (see Chart 2),

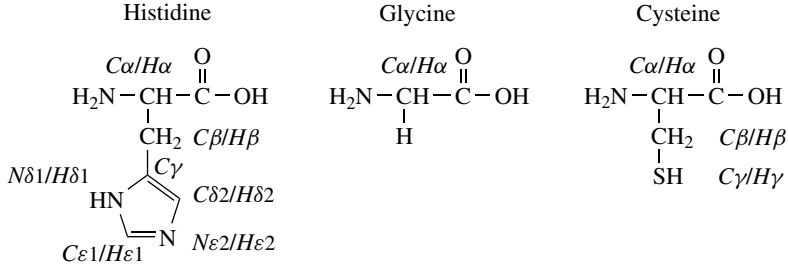

CHART 2. Proton and carbon annotations for histidine, glycine and cysteine amino acids

respectively. The ^{1}H chemical shift difference for the remaining non-labile protons is even smaller and varies from 0.10 to 0.75 ppm.

As far as the ^{13}C chemical shift changes are concerned, the histidine and cysteine carbons bear the most shifted protons. Thus the Cε1 (4.28 ppm) and Cβ (4.90 ppm) carbons together with the histidine Cγ atom (which does not bear a proton) exhibit the largest variation, reaching up to *ca* 12.0 ppm. In contrast to the carbon atoms of COO^{-}, CONH and glycine αCH_2 groups which do not experience any chemical shift variation upon Zn(II) binding, the remaining ^{13}C resonance differences measured varied from 1.60 to 3.40 ppm. These data suggest that ^{1}H resonances are not considerably influenced by Zn(II) metal coordination and that ^{13}C signals are stronger indicators for monitoring the metal binding process of Zn(II) bioinorganic compounds through NMR spectroscopy.

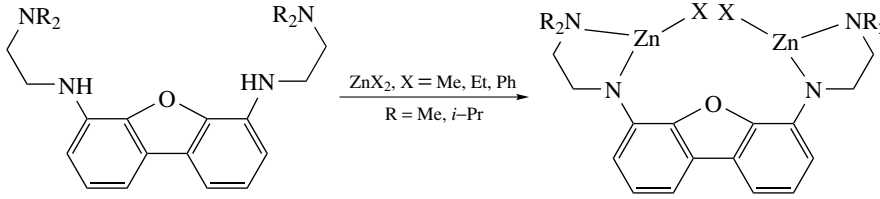

CHART 3. Zn chelating agents studied in their free and Zn(II)-bound form through ^{1}H/^{13}C NMR spectroscopy[4]

The minimal effect on proton chemical shifts in Zn organometallic compounds has been also observed through NMR studies of Zn(II) complexes with synthetic organic chelating compounds by Hlavinka and Hagadorn in a recent article[4]. In this study various tetraamino chelating agents were synthesized and used for the binding of two Zn(II) atoms per molecule. Each metal coordinates through the two nitrogen atoms of the ligand, while the other two positions of its coordination spheres are occupied by the ligands of the Zn metalation agent. Despite the nature of the ligand (different alkyl group at the terminal nitrogen atom) the chemical shift differences of the non-labile protons, sited either at the aromatic rings of the ligand or at the *N*-alkyl group (R = Me, *i*-Pr; see Chart 3), which are observed upon Zn(II) binding, vary between 0.10 and 0.55 ppm.

Other reports concerning chemically modified amino acid as metal chelating agents[5] used for the carbonic anhydrase active site model reconstruction are in close agreement with the small contribution of Zn(II) binding to the proton chemical shift variation discussed above. NMR experiments carried out in DMSO-d_6, at 300 K, and the observed

chemical shift difference for histidine imidazole Hε1 proton between its free and Zn(II)-bound form is measured to be only *ca* 0.50 ppm, while minimal changes for Hδ2 of *ca* 0.15 ppm have been observed as well. However, it is noteworthy that the striking difference between the ^{1}H NMR spectra of free and bound ligands in this study is the signal broadening. All histidine imidazole ring proton resonances in Zn(II) complexes are considerably broadened when compared with the proton signals of the free histidyl residue. Except for the two shifted signals which are also remarkably broadened, the remaining his imidazole ring signals have lost the hyperfine structure. ^{1}H resonance broadening usually reflects the difference in nuclei relaxation properties, providing indirect evidence for differences in the magnetic environment of the affected nuclei due to metal coordination, but it is also observed in the case of metal chelating agents with medium Zn(II) binding affinity. When Zn(II) metal is in an exchange equilibrium between its complexed (bound) and free form in solution, this effect is illustrated through signal broadening of the vicinal proton resonances.

Overall, what is reported above are some recent data from the field of the organometallic chemistry of Zn(II) compounds using a variety of metal chelating agents. All reflect the small effect of zinc binding on the NMR spectral parameters of the complexes with respect to the free organic ligands. However, a comparison between ^{1}H and ^{13}C data suggests that ^{13}C NMR spectroscopy provides safer evidence for the coordination of organic moieties to the Zn(II) metal than the ^{1}H NMR spectroscopy.

III. ^{67}Zn NMR SPECTROSCOPY OF ORGANOMETALLIC COMPOUNDS AND BIOMACROMOLECULES

From an NMR perspective, ^{67}Zn (the only NMR-active zinc isotope) is among a number of potentially important but insensitive metal nuclei such as ^{43}Ca and ^{25} Mg. However, ^{67}Zn NMR spectra of aqueous Zn^{+2} are different from ^{43}Ca and ^{25}Mg NMR spectra of aqueous Ca^{2+} and Mg^{2+} in some respects. For example, ^{67}Zn NMR spectra of aqueous Zn^{2+} have marked concentration dependences in terms of the half-band widths ($\Delta\nu_{1/2}$) compared with those of ^{43}Ca and ^{25}Mg NMR spectra of aqueous Ca^{2+} and Mg^{2+}[6–8].

It has been found that the temperature effects of the ^{67}Zn NMR signals are markedly different from each other, depending upon the molecular weights of ligand molecules[4]. The intensity of ^{67}Zn NMR signals (or resonances) arises from the fact that ^{67}Zn is a quadrupolar nucleus (spin 5/2, $Q = 0.15 \times 10^{-28}$ m^{-2}) with low natural abundance (4.11%) and a small magnetogyric ratio ($\gamma = 1.6768 \times 10^{7}$ rad T^{-1} s^{-1}). Consequently, ^{67}Zn NMR experiments are remarkably difficult. In addition to the low intrinsic sensitivity, solution state ^{67}Zn NMR is further hampered by the fact that molecular tumbling motion always induces efficient ^{67}Zn quadrupole relaxation, resulting in short lifetimes of Zeeman energy levels, which lead to broad NMR lines.

Until 1999, ^{67}Zn NMR of liquid samples was limited to studies of either highly symmetric species or unsymmetrical complexes undergoing rapid exchange with large excessive $[Zn(H_2O)_6]^{2+}$ concentrations[8–11]. Despite the biological relevance of zinc ions, the aforementioned practical difficulties have made ^{67}Zn NMR a nearly forgotten area. In the past, NMR studies of the metal binding sites of zinc-containing proteins have essentially relied on the utility of a surrogate probe, by which they replaced the native ^{67}Zn with another metal ion, e.g. $Co^{2+/3+}$, with more favorable spectroscopic properties[12]. Recently, NMR-active ^{113}Cd ions were employed as a surrogate probe for ^{67}Zn[13,14]. Indeed, ^{113}Cd NMR has been widely employed in the spectroscopic study of metalloproteins which bear Zn(II) in their native state[15]. The adaptable ligand coordination, number and geometry of Cd(II) are rather similar to Zn(II) and in many cases where Cd(II) has replaced Zn(II), the catalytic activity of the metalloenzymes has been retained even to a low extent[16].

In particular, in Cd(II)-Thermolysin derivative (a zinc metalloprotease with proteolytic activity similar to carboxypeptidase A), the X-ray structure has provided evidence for isostructural replacement of Zn(II) by Cd(II)[17,18]. In general, the ^{113}Cd chemical shift is very sensitive to the nature, number and coordination type of the amino acid ligands and ^{113}Cd resonances are commonly detected by direct observation ($I = 1/2$, and 63% sensitivity compared with ^{13}C) or by inverse detection of ^{113}Cd scalar-coupled to ^{1}H.

A variety of inverse experiments which require a time delay for transfer of magnetization between ^{1}H and ^{113}Cd spins, such as ^{1}H–^{113}Cd HMQC, ^{113}Cd-edited ^{1}H–^{1}H COSY or ^{1}H–^{113}Cd hetero-TOCSY experiments[13] and 2D ^{1}H–^{15}N HMQC without Cd excitation pulses, are applied for successful identification of histidines coordinated to Cd(II) metal[19]. The latter technique provides geometrical information for the metal coordination sphere through the determination of $^{3}J_{\mathrm{H-Cd}}$ and $^{1}J_{\mathrm{N-Cd}}$ for ^{113}Cd-bound imidazole rings[17–19].

The reported data as far as ^{67}Zn NMR is concerned are sporadic, and very limited due to difficulties from a technical point of view, the nature of the ^{67}Zn nucleus, as well as all factors responsible for the latter such as concentration, the nature of the proximity ligands etc. A descriptive analysis of the last reported data concerning ^{67}Zn NMR studies will be developed with respect to the role of Zn ion or element in materials science or bioinorganic chemistry in both solution and solid state.

IV. THEORETICAL INTRODUCTION AND TECHNICAL DIFFICULTIES

Zinc is required as an integral constituent in a large number of enzymes[20,21]. To study the catalytic or structural role of zinc ions in these biological systems, it is desirable to have a technique that can probe the chemical environment at the zinc site. In the absence of X-ray crystallographic data, direct detection of the Zn(II) ions bound to a biological macromolecule is a difficult task, because routine analytical techniques such as UV/vis, electron spin resonance (ESR) and solution NMR spectroscopy are not suitable for studying diamagnetic d^{10} Zn(II) ions. As a result, spectroscopic studies of metal-binding sites in zinc-containing proteins have reported on the utility of surrogate metal probes (e.g. Mn, Co and Cd)[22,23].

Recently, solid-state ^{67}Zn NMR spectroscopy has emerged as a viable method for detecting Zn(II) ions even in large molecular systems[23–29]. During these ^{67}Zn NMR studies, it has become increasingly apparent that a better understanding of the ^{67}Zn NMR properties is needed. One fundamental question is how the ^{67}Zn NMR tensors, both the chemical shift tensor and the electric field gradient (EFG) tensor, are related to the chemical environment and molecular structure. One way to decipher this NMR property/structure relationship is to use quantum-mechanical calculations. To the best of our knowledge, quantum-mechanical ^{67}Zn EFG calculations have been attempted only for simple ionic solids such as ZnO[30], $ZnAl_2O_4$ and $ZnFe_2O_4$[31]; no theoretical study has been reported for the ^{67}Zn EFG tensors in Zn(II) coordination complexes. The fact that a reasonable amount of reliable ^{67}Zn EFG data has been accumulated in the past several years from experimental solid-state NMR studies makes the theoretical examination of ^{67}Zn EFG tensors timely and possible. Recently, Ida and Wu[32], have reported a systematic quantum-mechanical investigation for the ^{67}Zn EFG tensors in six Zn(II) coordination complexes: zinc acetate dihydrate (**1**), bis(acetato)bis(imidazole)zinc (**2**), tetrakis(imidazolo)zinc perchlorate (**3**), tetrakis(thiourea)zinc nitrate (**4**), zinc formate dihydrate (**5**) and bis(acetato)bis(urea)zinc (**6**) (Figure 1).

These Zn(II) coordination complexes were chosen because both reliable X-ray crystallographic and solid-state ^{67}Zn NMR data are available in the literature. Furthermore, single-crystal ^{67}Zn NMR studies have been reported for compounds **1** and **5**, so that not only the magnitude but also the orientation of the ^{67}Zn EFG tensor is known in

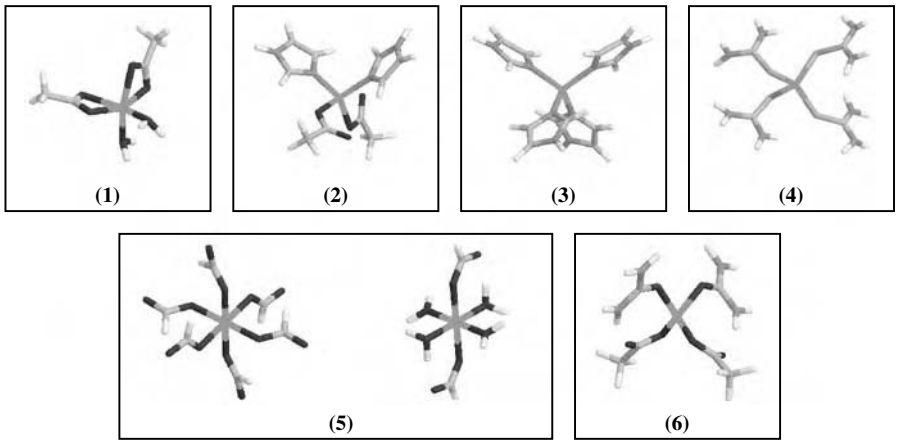

FIGURE 1. Molecular clusters models for compounds 1–6[32]. Reproduced with permission from Reference 32

the molecular frame of reference. This precise information is useful in determining the accuracy of the computed EFG results. The primary objective of the mentioned study is to evaluate the applicability of current computational methods for calculating ^{67}Zn EFG tensors in molecular complexes.

The authors have used a general molecular cluster approach to model the Zn(II) site in the crystal lattice. For Zn(II) coordination complexes examined in this study, the Zn(II) center is generally surrounded by ligand molecules such as imidazole and acetate groups. This is somewhat different from the ionic network solids such as ZnO and $ZnAl_2O_4$, for which it is important to take into consideration the lattice periodicity. For this reason, they usually include ligand molecules only from the first coordination sphere. The only exception to this general statement is that, if the Zn center of interest is bound to water molecules and the water molecules are involved in extensive hydrogen bonding, ligands from the second coordination sphere must be included in the cluster model. This finding is important because water molecules often participate in Zn(II) ion binding in zinc-containing proteins. The implication of this study is that it is possible to predict ^{67}Zn EFG tensors for the Zn(II) sites in proteins. Although the above study is focused on EFG tensors, it should also be possible to examine the ^{67}Zn magnetic (or chemical) shielding tensors using quantum-mechanical computations. Very little is known in this latter area; however, it is hoped that the work of Ida and Wu will encourage further quantum-mechanical studies of these fundamental ^{67}Zn NMR tensors and that new reports on this issue will appear in the near future[32].

V. SOLID-STATE NMR

Solid-state NMR is a branch of NMR spectroscopy that deals with solid or solid-like systems and is presently undergoing rapid expansion as a result of the significant advances in both NMR methodology and instrumentation that have occurred recently. To date, most successful solid-state NMR applications to biological systems have utilized spin-1/2 nuclei such as ^{13}C, ^{15}N and ^{31}P. For a large number of biologically important elements, however, the only NMR active isotopes are those with nuclear spins greater than one half. Such nuclei have a non-spherical charge distribution and are known as quadrupolar nuclei, for example ^{17}O ($S = 5/2$), ^{23}Na ($S = 3/2$), ^{25}Mg ($S = 5/2$), ^{39}K ($S = 3/2$), ^{43}Ca ($S = 7/2$),

^{67}Zn ($S = 5/2$) and ^{59}Co ($S = 9/2$), to mention just a few. It should be noted that all of these examples are half-integer spins. In fact, there is another type of quadrupolar nuclei for which the spin number is an integer, such as ^{2}H ($S = 1$), ^{6}Li ($S = 1$), ^{14}N ($S = 1$) and ^{10}B ($S = 3$). The integer spins have quite different NMR properties compared with those of half-integer nuclei; consequently, the techniques used to record solid-state NMR spectra of integer nuclei are unique.

In a recent study, Lipton and coworkers[33] described a new probe which has been completely redesigned in order to perform solid-state NMR spectroscopy of half-integer quadrupolar nuclides, such as Zn and Mg. This new probe includes a cross coil and variable capacitors that are operational at cryogenic temperatures. However, even with this new probe the most important issue, which had to be resolved, was the optimal sensitivity. In order to apply this technique in large molecules, such as proteins, enzymes etc., one should considerably enhance sensitivity considering that spins of interest (^{67}Zn) are found in a dilute environment. While the metal ion under investigation has an atomic mass below 100, the biopolymer has a molecular weight which ranges from 10 to 50 kDa. As the authors stated[33] after performing a number of technical modifications, the new probe reached an improvement in signal-to-noise ratio of approximately 15%. The application of this technology to a biologically interesting molecule, the carbonic anhydrase, is presented below (see Section VI).

VI. INTEREST FOR BIOINORGANIC CHEMISTRY

Zinc plays a key role in the active binding site for a range of important metalloproteins[34]. For example, Zn^{2+} is important for the function of pencillamine[6], insulin[35], carboxypeptidase A[34], thermolysin[37], phospholipase C[38], Angiotensin Converting Enzyme[39] and Anthrax Lethal Factor[40]. To understand the enzymatic function of these metalloproteins, it is of interest to study the Zn^{2+} coordination environment with a variety of ligands, i.e. N, O and S donor atoms. Information on Zn^{2+} complexation may potentially be obtained from liquid-state ^{67}Zn NMR (isotropic chemical shifts, δiso; T_1 and T_2 relaxation)[41,42]. However, the large ^{67}Zn linewidth and poor receptivity will prevent useful data from being obtained on biological compounds via liquid-state NMR. Furthermore, the Zn^{2+} coordination is particularly reflected in the ^{67}Zn ($I = 5/2$) quadrupole coupling, an interaction which may be obtained only indirectly from liquid-state relaxation studies. Solid-state ^{67}Zn NMR is a more direct and informative probe for the local structure but is unfortunately associated with broad line shapes due to a large quadrupole moment.

To circumvent these problems it has been popular to replace Zn^{2+} with $^{113}Cd^{2+}$ ($I = 1/2$) and use empirical relations between ^{113}Cd chemical shielding anisotropy (CSA) and structure[15–18,43,44] to obtain information about metal coordination in metalloenzymes[45,46]. Nevertheless, ^{67}Zn NMR should be the method of choice for Zn metalloproteins. This approach removes the potential ambiguities regarding changes in local structure induced by Cd^{2+} replacement and may be used to investigate the utility of the ^{113}Cd surrogate probe strategy. Among the few ^{67}Zn solid-state NMR studies reported so far[47,48], one has involved the detection of a 40-kHz-wide powder pattern at 11.7 T for $Zn(CH_3COO)_2{\bullet}2H_2O$[42] using the quadrupolar echo (QE) experiment[49].

For large-weight Zn^{2+} complexes with broad (50–150 kHz) second-order quadrupolar powder patterns ^{67}Zn QE NMR may be an experimental challenge. In such cases the sensitivity must be enhanced by isotope enrichment combined with, e.g., cross polarization (CP) from ^{1}H[50], low-temperature acquisition[51] or sampling of the free-induction decay (FID) in the presence of a train of refocusing pulses[52–54].

Low-temperature experiments are technically difficult and may cause the sample to be in a phase different from that at ambient temperature. Similarly, CP is demanding since it

requires the matching of an rf field amplitude on the ^{67}Zn channel of about 50 kHz with a threefold larger amplitude on the ^{1}H channel to obtain an efficient spin-lock. Ellis and coworkers[54] have demonstrated that ^{67}Zn QCPMG NMR represents a feasible approach to study Zn^{2+} coordination in model complexes for metalloenzyme derivatives. The QCPMG experiment[54] (equation 1)

$$(\pi/2)_x - \tau_1 - (\pi)_y - \tau_2 - \text{Acq.}(1/2\tau_a) - [\tau_3 - (\pi)_y - \tau_4 - \text{Acq.}(\tau_a)]^{\text{M}} - \text{Acq.}(\tau_d) \quad (1)$$

splits the QE line shape for the central transition into a manifold of spin-echo sidebands separated by $1/\tau_a$, where τ_a is the interpulse acquisition period with ^{1}H decoupling (M is the number of echo repetitions and τ_d an additional acquisition time to ensure full decay of the signal). Depending on the sideband separation, QCPMG may enhance the sensitivity by an order of magnitude compared to QE while maintaining information on the anisotropic interactions[54].

The applicability of the method is demonstrated using ^{67}Zn-enriched zinc formate dihydrate $Zn(OOCH)_2 \cdot 2H_2O$[55] and zinc diimidazole diacetate $Zn(OOCCH_3)_2(C_3H_4N_2)_2$[56]. These complexes are representatives of Zn^{2+} in an all-oxygen six-coordination sphere and in a 2-O, 2-N four-coordination sphere, respectively.

As a conclusion, they have demonstrated that ^{67}Zn QCPMG NMR, through its significant sensitivity enhancement compared to QE NMR, represents a powerful method in studies of zinc complexes. By the determination of relationships between the coordination geometry and the parameters for chemical shielding and quadrupole coupling tensors, they anticipate that ^{67}Zn QCPMG NMR will play a critical role in solid-state investigations of ^{67}Zn-enriched metalloproteins. Employing improved instrumentation, the sensitivity of the ^{67}Zn QCPMG experiment will be further improved by combination with CP and acquiring the spectra at cryogenic temperatures.

As mentioned above, the ligating units for zinc complexation in biological enzymes such as zinc fingers[57], zinc twists, zinc clusters[58], alcohol dehydrogenase[59], metallothioneins[60] and carbonic anhydrase[61] are bis(cysteinyl) or bis(histidinyl) derivatives. These protein sequences His−X−His or Cys−Y−Cys (X, Y are 1–4 amino acids) offer N or S atoms for coordination, while in some cases residues with oxygen atom donors or H_2O were found in a coordination sphere of Zn(II) metal. The zinc ion is responsible for protein folding and catalytic binding of H_2O or CO_2. Tripeptides with bis(histidinyl) sequences have been investigated by Gockel and coworkers[62]. Other authors have described tripodal histidine ligands[63], pyrazolylborate ligands[64] and macrocyclic polyamines[65]. For all these cases, NMR spectroscopy was a powerful tool in order to clarify not only the three-dimentional structure of metalloenzymes, but also the electronic and coordination properties of their metal centers.

Toward this direction, a His−X−His pseudotripeptide zinc complex (X is an *N*-alkyl glycine derivative) similar to the catalytic center of the carbonic anhydrase was computer-designed and experimentally synthesized[66]. The authors applied 2D-NMR techniques in order to achieve the complete resonance assignment of all protons, carbon nuclei as well as of all nuclear overhauser effect signals. The three-dimensional structure of the complex was determined with the COSMOS (computer simulation of molecular structures) force field by applying ^{13}C bond polarization theory, chemical shift pseudoforces and restrictions for NOE distances. From molecular dynamics simulations, simulated annealing protocols and geometry optimizations, the three best structures (in terms of energy and optimized force-field parameters) were used for a final investigation by density functional theory. This detailed structural analysis of a zinc complex in combination with the profound analysis of the NMR parameters provides an excellent probe for Zn–ligand interaction through NMR. Despite the fact that no ^{67}Zn NMR experiments were performed for this

Zn-organometallic compound and the complex was synthesized with the aim of modeling the active site of carbonic anhydrase during its first catalytic step, the acquisition of the NMR properties of ^{13}C nucleus at this Zn complex could be further exploited in studies where the zinc ion would be replaced by a ^{67}Zn nucleus.

VII. INTEREST FOR MATERIAL–SOLID-STATE CHEMISTRY

A wide array of ferroelectric, piezoelectric and pyroelectric materials have titanium, zirconium and zinc metal cations as part of their elemental composition[67–69]. Many electrical materials based on titanium oxide (titanates) and zirconium oxide (zirconates) are known to have structures based on perovskite-type oxide lattices[67–69]. Barium titanate, $BaTiO_3$ and a diverse compositional range of PZT materials (lead zirconate titanates, $Pb_xZr_yTi_{1-y}O_3$) and PLZT materials (lead lanthanum zirconate titanates, $Pb_xLa_{1-x}Zr_yTi_{1-y}O_3$) are among these perovskite-type electrical materials.

Some materials containing the zinc cation, such as ZnO and ZnS, are also piezoelectric[67–70]. The structural characterization of the barium, titanium, zirconium and zinc cation sites in these types of materials would aid our understanding of their chemical and physical properties, and multinuclear NMR should be helpful in this regard. The synthesis of various metal oxide ceramics often employs solid-state reactions that involve the thermal decomposition of metal hydroxide and metal chelate precursors or the use of metal alkoxide sol-gel precursor[71–76]. In particular, PZT and PLZT ceramics have been synthesized from solid-state reactions of oxides or carbonates of the metal cations and from solutions containing $ZrOCl_2{\bullet}8H_2O$ and $TiOSO_4$[74,75]. In addition to a knowledge of the metal cation chemistry, the structural characterization of the hydrogen atom chemistry of metal oxide precursor materials would be of use in helping to develop and understand synthetic pathways for the production of electrical materials, and ^{1}H NMR should also be the method of choice in order to address this issue.

There are a large number of scientifically and industrially important zinc products and compounds for which it would be valuable to have a characterization method, such as NMR, complementary to powder X-ray diffraction. The observation of ^{67}Zn NMR in cubic compounds, e.g. ZnS (sphaelerite), ZnSe and ZnTe[77–80] was reported from Mössbauer[78,79] and NQR[80] measurements, which yield a variety of coupling constants at 4.2 K, viz. 13:8.4/MHz[77], 12:45.2/MHz[76] and 13:620.8/MHz[77–80].

The first observation of ^{67}Zn NMR in zinc metal was by Abart and coworkers[49a] in a measurement at 4.2 K, using a field sweeping technique, which yielded a value of $C_q = 12 : 73(4)$ MHz. No subsequent NMR observation has been reported. A measure of the temperature dependence of the ^{67}Zn nuclear quadrupole coupling in zinc metal has been obtained from time differential perturbed angular correlation (TDPAC) measurements[81] using an excited state of ^{67}Zn ($I = 9/2$; 605 keV). However, the use of liquid helium temperatures and exotic short-lived isotopes precludes the adoption of these techniques for general material characterization.

The observation of ^{67}Zn NMR in zinc metal by Fourier transform NMR at a fixed frequency and around 295 K is reported by Bastow[82]. The precision in determination of edge singularities of the central $(-1/2, 1/2)$ powder lineshape, together with the sharp definition of the inner satellite transitions at 295 K, permitted an accurate determination of the isotropic Knight shift, together with the first determination of the axial component of the Knight shift. Temperature dependence for the Knight shift was also measured, for the first time, up to nearly two thirds of the melting point.

Wu[24] has also reported solid-state ^{67}Zn NMR spectra for ZnO, ZnS, $ZnSO_4{\bullet}7H_2O$ and $Zn(CH_3COO)_2$. From the ^{67}Zn NMR spectra obtained for stationary and magic-angle spinning (MAS) powder samples, useful parameters of chemical shift anisotropy (CSA)

and nuclear coupling constant (NQCC) are determined. These results demonstrate the feasibility of natural abundance ^{67}Zn NMR studies on solids.

Recently, Ellis and coworkers[29] determined the crystal structure, quadrupole coupling parameters and the orientation of the electric field gradient tensors for each site of zinc formate dihydrate. According to this work there are two distinct sites in the asymmetric unit: one containing four in-plane waters with two bridging formates, the other containing six bridging formates. The solid-state NMR lineshapes have been assigned to their respective sites by using isotopic labeling and cross-polarization methods. The hydrated site corresponds to the lineshape having a quadrupole coupling constant (Cq) of 9.6 MHz and the anhydrous site has a Cq of 6.2 MHz. The absence of chemical shielding contributions to the observed lineshapes has been verified with a high-field solid-state NMR experiment performed at 18.8 T.

Finally, Bastow[83] used ^{67}Zn NMR as a probe to measure the electric field gradients at the metal site in the zinc halides ZnF_2, γ-$ZnCl_2$, $ZnBr_2$, ZnI_2 and Rb_2ZnCl_4 at room temperature. In addition, two hydration states have been detected for $ZnSO_4$. For ZnF_2 and γ-$ZnCl_2$, an *ab initio* calculation of the electric field gradient at the Zn site using the WIEN code agrees with the experimentally observed values.

VIII. APPLICATIONS

A representative collection of various applications of ^{67}Zn NMR will be described in this section. As already mentioned in a previous section, the zinc ion is responsible for protein folding and catalytic binding of H_2O or CO_2. For all these cases, NMR spectroscopy was a powerful tool in order to clarify the three-dimentional structure of metalloenzymes.

The basic thrust of Ellis group's developmental efforts over the past several years has been to characterize Zn^{2+} and Mg^{2+} sites in proteins using NMR spectroscopy. The simplicity of this sentence belies the fact that as little as a few years ago most of the NMR community would have described such an experiment as prohibitively difficult. The mentioned group developed a means to directly observe these metals in proteins via a low-temperature solid-state NMR experiment[28,29]. Therefore, their interest is to exploit this new technology to define the mechanistic details of how divalent metal cations (Zn^{2+}, Mg^{2+} and Ca^{2+}) augment the chemistry of the proteins to which they bind. Moreover, they want to establish a relationship between magnetic resonance parameters for the metal and the structure of these metals in metalloproteins. The magnetic resonance parameters are sensitive measures of charge, ligand type and number, and the symmetry of the metal site. All these parameters are a reflection of the potential chemistry that occurs at the metal site. Therefore, such relationships should aid in the development and delineation of the correlation between structure and function for this important class of proteins.

Indeed, Ellis's group provided some very nice examples of the application of ^{67}Zn NMR spectroscopy when applied to proteins, such as the Minimal DNA Binding Domain of Human Nucleotide Excision Repair Protein XPA[84] and the Human Carbonic Anhydrase[85].

The former is a protein of 14.7 kDa involved in the multienzyme nucleotide excision repair (NER) pathway with a determined NMR solution structure[86]. In this protein, the Zn^{2+} possesses rather a structural than a catalytic role. ^{67}Zn NMR spectra were acquired using a rather sophisticated probe (for details, see Reference 87) and operating at temperatures 5–250 K. Data acquisition was performed with the application of spin-echo methods for enhanced sensitivity[33,84,86]. Specifically, experiments were carried out at 25 K using a combination of CP (cross-polarization)[50] and spikelet echo pulse sequences[54,87] which provide a considerable increase in signal-to-noise ratio (of the order of 30) relative to a classical quadrupole echo pulse sequence. The proton field strength applied to the above measurements was 60 kHz with a matching field of 20 kHz for zinc and a contact time

of 30 ms. Data collection has been performed with the accumulation of 1090 transients and a selective π pulse to be set at 4 μs. Experimental data and simulations, such as line-shape parameters and isotropic chemical shifts, available for tetrakis(thiourea)zinc nitrate complex suggest that a model of a zinc metal ion coordinated to 4 sulfur atoms could account for the ^{67}Zn spectrum of XPA protein. This work of Ellis and coworkers represents the first NMR-based direct observation of the Zn^{2+} site of a metalloprotein.

The latter Human Carbonic Anhydrase Isozyme II (CAII) is a well-studied protein with a large number of crystal structures available so far[88]. CAII catalyzes the reaction of CO_2 with water and the mechanism of this reaction, as any reaction catalyzed by a Zn^{2+} enzyme, is based on the water activation through ionization, where polarization accompanied by slight structural rearrangement in catalytic sites frequently involving zinc ligands' displacement. In CAII, Zn^{2+} is bound to three histidines while a hydroxide plays the role of the fourth metal ligand. His94 and His96 are coordinated to Zn^{2+} through the Nε2 nitrogen atom of the imidazole ring while the third histidine, His 119, is coordinated with the other nitrogen atom of imidazole, namely Nδ1. The protonated nitrogens of these three histidines are hydrogen-bonded to the backbone or side-chain atoms of some residues found in close spatial proximity, such as Gln92, Glu117 and Asn244. The residues involved in this H-bond network seem to control the apparent pK_a of the presumed zinc–water[89] and enhance the zinc affinity in CAII[90]. Ellis and coworkers[85] applied ^{67}Zn solid-state NMR spectroscopy in order to study the pH dependence of the metal site by monitoring the ^{67}Zn NMR parameters and probing the nature of the fourth ligand. Measurements were carried out for protein samples at different pH, at 9.4 T (400 MHz for ^{1}H) and 18.8 T (800 MHz for ^{1}H) with a modified probe, different than that used for the ^{67}Zn NMR investigation of the XPA protein described above, and at a temperature of 10–20 K depending on protein concentration and paramagnetic doping. Basic NMR parameters were set for proton pulse width at 5.5 μs using a ^{67}Zn Hartman–Hahn matching field 3 times less and a ^{67}Zn-selective π pulse width of 5.5 μs, and recycle time form 10 s (at 9.4 T) to 20 and 60 s (at 18.8 T). The extracted values of *Cq* are found to be similar (*ca* 10 MHz) despite the different pH values of protein samples, indicating that ^{67}Zn NMR parameters are not affected by the type of the zinc ligand (water or hydroxide).

The authors attempted to fit the experimental NMR data to potential conformations of CAII's active site. Therefore, they developed three possible models (representing potential coordination states of the CAII zinc site) through the application of *ab initio* electronic structure calculation to the protein's active site determined by X-ray crystallography by Liljas and coworkers[91]. The first minimal model considers the three zinc-bound histidines and a water molecule or a hydroxide ion and the second consists of the first models with five additional water molecules. The third, the most complicated, takes into consideration the second one adding new structural elements, which represent the side-chains of the residues (Gln92, Glu117 and Asn244, the former two represented as formic acids and the latter as formamide) proposed to be hydrogen bonded to the protonated nitrogen atoms of histidine zinc-ligands. The *ab initio* calculations fit rather well with NMR-derived *Cq* values, that is around 10 MHz for the second and third model but not for the first one, suggesting that the hydroxide occupies the fourth position in the Zn^{2+} coordination sphere in CAII when the enzyme exists in a pH range of 5.0–8.5. These data are found rather consistent with previous EXAFS data, which had also suggested the hydroxide as the fourth zinc ligand[92].

The biological implication of this study is highly relevant to the fact that the enzyme's mechanism is pH-dependent and, in the case that a hydroxide is the fourth zinc ligand at pH 5, the deprotonation of the $Zn-OH_2$ could not be simply described by the acid/base equilibrium with a pK_a value close to 7.0. The combination of the ^{67}Zn NMR spectroscopy data and *ab initio* structure calculations supports the existence of a hydroxide instead of

a water throughout the pH range examined. This study on the 30 kDa CAII provides convincing evidence for the potential role and application of the ^{67}Zn NMR spectroscopy to the study of ^{67}Zn-loaded metalloproteins of rather high molecular mass, providing new insights not only for the structural determination of the enzyme's active site but also valuable information for its function mechanism.

Another interesting example is the applicability of the zinc complex of L-carnosine (L-CAZ; generic name Polaprezinc) for medical use. This is the first drug for oral administration in which zinc plays an essential role. L-CAZ was approved as an anti-ulcer drug of membrane protection type[80]. Characterization of L-CAZ was achieved by various spectroscopic methods along with elemental analysis. Zinc ion coordinates with L-carnosine to form a quadridentate 1:1 complex of polymeric nature in order to maintain low strain of chelate rings. L-CAZ can remain in the stomach juice without rapid dissociation and adhere specifically to ulcerous lesion, after which L-carnosine and zinc are released to heal the ulcer. L-CAZ exhibited high efficacy in clinical use without any serious side effect. L-CAZ exhibited an inhibitory effect on helicobacter pylori. Physicochemical aspects of carnosine, zinc and the zinc complex can explain favorable features of L-CAZ as a drug.

Recent advantages in the technology of NMR instrumentation (magnets, probes, amplifiers etc.) and NMR spectroscopy methodology could probably lead to more effective studies on exotic nuclei such as ^{67}Zn and Zn-organometallic compounds or Zn-metalloproteins and enzymes, with apparent interest either for materials science or for bioinorganic chemistry. Until then, NMR studies of ^{67}Zn-enriched compounds would possibly need the cooperative use of theoretical calculations and X-ray-derived structural information in order to characterize the magnetic and electronic properties of ^{67}Zn nucleus. To this aim, the new technological and methodological achievements of the group of Ellis could be applied in new Zn-organometallic or Zn-containing polypeptides in order to accumulate additional NMR data and to expand our knowledge base about the properties and features of ^{67}Zn nuclei in a variety of coordination environments.

IX. REFERENCES

1. P. R. Reddy, M. Radhika and K. S. Rao, *J. Chem. Sci.*, **116**, 221 (2004).
2. N. Niklas, A. Zahl and R. Alsfasser, *Dalton Trans.*, 778 (2003).
3. B.-H. Ye, X.-Y. Li, I. D. Williams and X.-M. Chen, *Inorg. Chem.*, **41**, 6426 (2002).
4. M. L. Hlavinka and J. R. Hagadorn, *Organometallics*, **24**, 5335 (2005).
5. U. Herr, W. Spahl, G. Trojandt, W. Steglich, F. Thaler and R. van Eldik, *Bioorg. Med. Chem.*, **7**, 699 (1999).
6. T. Shimizu and M. Hatano, *Biochem. Biophys. Res. Commun.*, **104**, 1356 (1982).
7. T. Shimizu, M. Kodaka and M. Hatano, *Biochem. Biophys. Res. Commun.*, **106**, 988 (1982).
8. T. Shimizu and M. Hatano, *Inorg. Chim. Acta*, **76**, L177 (1983).
9. M. Kodaka, T. Shimizu and M. Hatano, *Inorg. Chim. Acta*, **78**, L55 (1983).
10. P. Granger, in *Transition Metal Nuclear Magnetic Resonance* (Ed. P. S. Prigosin), Elsevier Science Publishers B. V., Amsterdam, 1991, pp. 285–346.
11. A. Delville and C. Detellier, *Can. J. Chem.*, **64**, 1845 (1986).
12. (a) R. A. Santos, E. S. Gruff, S. A. Koch and G. S. Harbison, *J. Am. Chem. Soc.*, **112**, 9257 (1990).
    (b) R. A. Santos, E. S. Gruff, S. A. Koch and G. S. Harbison, *J. Am. Chem. Soc.*, **113**, 469 (1991).
13. K. McAteer, A. S. Lipton and P. D. Ellis, in *Encyclopedia of Nuclear Magnetic Resonance* (Eds. D. M. Grant and R. K. Harris), Wiley, Chichester, 1996, pp. 1085–1091.
14. (a) J. E. Coleman and B. L. Vallee, *J. Biol. Chem.*, **235**, 390 (1960).
    (b) J. E. Coleman and B. L. Vallee, *J. Biol. Chem.*, **236**, 2244 (1961).
    (c) S. Lindskog, *J. Biol. Chem.*, **238**, 945 (1963).
    (d) B. L. Vallee and R. J. P. Williams, *Proc. Natl. Acad. Sci. U.S.A.*, **59**, 498 (1968).
    (e) S. A. Latt, D. S. Auld and B. L. Vallee, *Proc. Natl. Acad. Sci. U.S.A.*, **67**, 1383 (1970).

15. G. Öz, D. L. Pountney and I. M. Armitage, *Biochem. Cell Biol.*, **76**, 223 (1998).
16. I. M. Armitage, A. J. M. Schoot Uiterkamp, J. F. Chlebowski and J. E. Coleman, *J. Magn. Reson.*, **29**, 375 (1978).
17. D. R. Holland, A. C. Hausrath, D. Juers and B. W. Matthews, *Protein Sci.*, **4**, 1955 (1995).
18. (a) K. H. Gardner and J. E. Coleman *J. Biomol. NMR*, **4**, 761 (1994).
(b) D. H. Live, C. L. Kojiro, D. Cowburn and J. L. Markley, *J. Am. Chem. Soc.*, **107**, 3043 (1985).
19. C. Damblon, C. Prosperi, L.-Y. Lian, I. Barsukov, R. P. Soto, M. Galleni, J.-M. Frère and G. C. K. Roberts, *J. Am. Chem. Soc.*, **121**, 11575 (1999).
20. J. J. R. Frausto da Silva and R. J. P. Williams, *The Biological Chemistry of the Elements*, Oxford University Press, Oxford, 1991.
21. S. J. Lippard and J. M. Berg, *Principles of Bioinorganic Chemistry*, University Science Books, Mill Valley, CA, 1994.
22. M. F. Summers, *Coord. Chem. Rev.*, **86**, 43 (1988).
23. G. Wu, *Biochem. Cell Biol.*, **76**, 429 (1998).
24. G. Wu, *Chem. Phys. Lett.*, **298**, 375 (1998).
25. S. Sham and G. Wu, *Can. J. Chem.*, **77**, 1782 (1999).
26. T. Vosegaard, U. Andersen and H. J. Jakobsen, *J. Am. Chem. Soc.*, **121**, 1970 (1999).
27. A. S. Lipton, G. W. Buchko, J. A. Sears, M. A. Kennedy and P. D. Ellis, *J. Am. Chem. Soc.*, **123**, 992 (2001).
28. A. S. Lipton, J. A. Sears and P. D. Ellis, *J. Magn. Reson.*, **151**, 48 (2001).
29. A. S. Lipton, M. D. Smith, R. D. Adams and P. D. Ellis, *J. Am. Chem. Soc.*, **124**, 410 (2002).
30. D. W. Mitchell, S. B. Sulaiman, N. Sahoo, T. P. Das, W. Potzel and G. M. Kalvius, *Phys. Rev. B*, **44**, 6728 (1991).
31. D. W. Mitchell, T. P. Das, W. Potzel, W. Schiess, H. Karzel, M. Steiner, M. Köfferlein, U. Hiller, G. M. Kalvius, A. Martin, W. Schäfer, G. Will, I. Halevy and J. Gal, *J. Phys. Rev.*, **B 53**, 7684 (1996).
32. R. Ida and G. Wu, *J. Phys. Chem. A*, **106**, 11234 (2002).
33. A. S. Lipton, R. W. Heck, J. A. Sears and P. D. Ellis, *J. Magn. Reson.*, **168**, 66 (2004).
34. L. Stryer, *Biochemistry*, 4th edn., W. H. Freeman and Company, New York, 1995.
35. M. L. Brader, *J. Am. Chem. Soc.*, **119**, 7603 (1997).
36. (a) W. N. Lipscomb, J. A. Harstuck, F. A. Quiocho and G. N. Reeke Jr., *Proc. Natl. Acad. Sci. U.S.A.*, **64**, 28 (1969).
(b) D. W. Christianson and W. N. Lipscomb, *Acc. Chem. Res.*, **22**, 62 (1989).
37. B. W. Matthews, L. H. Weaver and W. R. Kester, *J. Biol. Chem.*, **249**, 8030 (1974).
38. E. Hough, L. K. Hansen, B. Birknes, K. Lynge, S. Hansen, A. Hordvik, C. Little, E. Dodson and Z. Derewenda, *Nature*, **338**, 357 (1989).
39. R. Natesh, S. L. U. Schwager, E. D. Sturrock and K. R. Acharya, *Nature*, **421**, 551 (2003).
40. A. D. Pannifer, T. Y. Wong, R. Schwarzenbacher, M. Renatus, C. Petosa, J. Bienkowska, D. B. Lacy, R. J. Collier, S. Park, S. H. Leppla, P. Hanna and R. C. Liddington, *Nature*, **414**, 229 (2001).
41. G. E. Maciel, L. Simeral and J. J. H. Ackerman, *J. Phys. Chem.*, **81**, 263 (1977).
42. T. Shimizu and M. Hatano, *Inorg. Chem.*, **24**, 2003 (1985).
43. R. S. Honkonen and P. D. Ellis, *J. Am. Chem. Soc.*, **106**, 5488 (1984).
44. A. S. Lipton, S. S. Mason, S. M. Myers, D. L. Reger and P. D Ellis, *Inorg. Chem.*, **35**, 7111 (1996) and references cited therein.
45. M. A. Kennedy and P. D. Ellis, *J. Am. Chem. Soc.*, **111**, 3195 (1989).
46. K. McAteer, A. S. Lipton, M. A. Kennedy and P. D. Ellis, *Solid State Nucl. Magn. Reson.*, **7**, 229 (1996).
47. A. C. Kunwar, G. L. Turner and E. Oldfield, *J. Magn. Reson.*, **69**, 124 (1986).
48. (a) T. J. Bastow and S. N. Stuart, *Phys. Status Solidi B*, **145**, 719 (1988).
(b) S. F. Dec, M. F. Davis, G. E. Maciel, C. E. Bronnimann, J. F. Fitzgerald and S. Han, *Inorg. Chem.*, **32**, 955 (1993).
(c) G. Wu, S. Kroeker and R. E. Wasylishen, *Inorg. Chem.*, **34**, 1595 (1995).
(d) T. J. Bastow, *J. Phys.: Condens. Matter*, **8**, 11309 (1996).
49. (a) I. Solomon, *Phys. Rev.*, **110**, 61 (1958).
(b) J. H. Davis, K. R. Jeffrey, M. Bloom, M. I. Valic and T. P. Higgs, *Chem. Phys. Lett.*, **42**, 390 (1976).

50. A. Pines, M. G. Gibby and J. S. Waugh, *J. Chem. Phys.*, **56**, 1776 (1972).
51. P. L. Kuhns and J. S. Waugh, *J. Chem. Phys.*, **97**, 2166 (1992).
52. M. Bloom and E. Sternin, *Biochemistry*, **26**, 2101 (1987).
53. J. T. Cheng and P. D. Ellis, *J. Phys. Chem.*, **93**, 2549 (1989).
54. F. H. Larsen, H. J. Jakobsen, P. D. Ellis and N. C. Nielsen, *J. Phys. Chem. A*, **101**, 8597 (1997).
55. F. H. Larsen, A. S. Lipton, H. J. Jakobsen, N. C. Nielsen and P. D. Ellis, *J. Am. Chem. Soc.*, **121**, 3783 (1999).
56. W. DeW. Horrocks Jr., J. N. Ishley, B. Holmquist and J. S. Thompson, *J. Inorg. Biochem.*, **12**, 131 (1980).
57. (a) A. Klug and D. Rhodes, *Trends Biochem. Sci.*, **12**, 464 (1987).
    (b) B. A. Krizek, B. T. Amann, V. J. Kilfoil, D. L. Merkle and J. M. Berg, *J. Am. Chem. Soc.*, **113**, 4518 (1991).
58. R. Marmorstein, M. Carey, M. Ptashne and S. C. Harrison, *Nature*, **356**, 408 (1992).
59. E. Magonet, D. Hayen, D. Delforge, F. Delaire and J. Remacle, *Biochem. J.*, **287**, 361 (1992) and references cited therein.
60. M. J. Stillman, C. F. Shaw and K. T. Suzuki, *Methallothioneins*, VCH, Weinheim (1992).
61. X. Zhang, C. D. Hubbard and R. van Eldrik, *J. Phys. Chem.*, **100**, 9161 (1996).
62. P. Gockel, M. Gelinsky, R. Vogler and H. Vahrenkamp, *Inorg. Chim. Acta*, **272**, 115 (1998).
63. U. Herr, W. Spahl, G. Trojandt, W. Steglich, F. Thaler and R. van Eldrik, *Bioorg. Med. Chem.*, **7**, 699 (1999).
64. R. Alsfasser, M. Ruf, S. Trofimenko and H. Vahrenkamp, *Chem. Ber.*, **126**, 703 (1993).
65. E. Kimura, *Prog. Inorg. Chem.*, **41**, 443 (1994); R. van Eldrik, *Coord. Chem. Rev.*, **182**, 373 (1999).
66. R. Witter, L. Seyfart, G. Greiner, S. Reissmann, J. Weston, E. Anders and U. Sternberg, *J. Biomol. NMR*, **24**, 277 (2002).
67. B. Jaffe, W. R. Cook and H. Jaffe, *Piezoelectric Ceramics*, Academic Press, London, 1979.
68. R. Buchanan (Ed.), *Ceramic Materials for Electronics*, Marcel Dekker, New York, 1986.
69. K. Wakino, in *Fine Ceramics* (Ed. S. Saito), Elsevier, New York, 1985, pp. 251–261.
70. A. R. West, *Basic Solid State Chemistry*, Wiley, New York, 1998, pp. 331–341.
71. A. Amin, M. A. Spears and B. M. Kulwicki, *J. Am. Ceram. Soc.*, **66**, 733 (1983).
72. T. T. Fang and H. B. Lin, *J. Am. Ceram. Soc.*, **72**, 1899 (1989).
73. W. Hertl, *J. Am. Ceram. Soc.*, **71**, 879 (1988).
74. J. J. Ritter, R. S. Roth and J. E. Blendell, *J. Am. Ceram. Soc.*, **69**, 155 (1986).
75. K. Kezuka, Y. Hayashi and T. Yamaguchi, *J. Am. Ceram. Soc.*, **72**, 1660 (1989).
76. G. H., Hacrtling and C. E. Land, *J. Am. Ceram. Soc.*, **54**, 1 (1971).
77. J. Abart, E. Pelangie, W. Socher and J. Voitlander, *J. Chem. Phys.*, **78**, 5468 (1983).
78. W. T. Vetterling and R. V. Pound, in *Workshop on New Directions in Mössbauer Spectroscopy* (Argonne, 1977) (Ed. G. J. Perlow), *AIP Conf. Proc.*, **38**, 27 (1977).
79. M. Steiner, W. Potzel, H. Karzel, W. Schiessl, M. Kofferlein, G. M. Kalvius and P. Blaha, *J. Phys.: Condens. Matter*, **8**, 3581 (1996). See also W. Potzel, A. Forster and G. M. Kalvius, *Phys. Lett.*, **67A**, 421 (1978).
80. E. N. Kaufman, J. R. Brookeman, P. C. Canepa, T. A. Scott, D. H. Rasmussen and J. H. Perepezko, *Solid State Commun.*, **29**, 375 (1979).
81. J. Christiansen, P. Heubes, R. Keitel, W. Klinger, W. Loeffler, W. Sandner and W. Witthuhn, *Z. Phys. B*, **24**, 117 (1976).
82. T. J. Bastow, *J. Phys.: Condens. Matter*, **8**, 11309 (1996).
83. T. J. Bastow, *Chem. Phys. Lett.*, **380**, 516 (2003).
84. S. A. Lipton, G. W. Buchko, J. A. Sears, M. A. Kennedy and P. D. Ellis, *J. Am. Chem. Soc.*, **123**, 992 (2001).
85. S. A. Lipton, R. W. Heck and P. D. Ellis, *J. Am. Chem. Soc.*, **126**, 4735 (2004).
86. T. Ikegami, I. Kuraoka, M. Saijo, N. Kodo, Y. Kyogoku, K. Morikawa, K. Tanaka and M. Shirakawa, *Nat. Struct. Biol.*, **5**, 701 (1998).
87. A. S. Lipton, R. W. Heck, J. A. Sears and P. D. Ellis, *J. Magn. Reson.*, **168**, 66 (2004).
88. D. W. Cristianson and C. A. Fierke, *Acc. Chem. Res.*, **29**, 331 (1996).

89. C. A. Lesburg and D. W. Christianson, *J. Am. Chem. Soc.*, **117**, 6838 (1995).
90. L. L. Kiefer, S. A. Paterno and C. A. Fierke, *J. Am. Chem. Soc.*, **117**, 6831 (1995).
91. H. Hakansson, M. Carlsson, L. A. Svensson and L. A. Liljas, *J. Mol. Biol.*, **227**, 1192 (1992).
92. (a) V. Yachandra, L. Powers and T. G. Spiro, *J. Am. Chem. Soc.*, **105**, 6596 (1983).
(b) J. C. Amiss and S. J. Gurman, *J. Synchrotron Rad.*, **6**, 387 (1999).

CHAPTER 5

Mass spectrometry of organozinc compounds

SERGIU P. PALII

Department of Chemistry, University of Florida, P.O. Box 117200, Gainesville, FL 32611-7200, USA
Fax: +1 352 392 0872; e-mail: palii@ufl.edu

and

DMITRI V. ZAGOREVSKII

Department of Chemistry and Chemical Biology, Rensselaer Polytechnic Institute, 209C Cogswell Laboratories, 110 8th Str., Troy, NY 12180, USA
Fax: +1 518 276 4887; e-mail: zagord@rpi.edu

The chemistry of organozinc compounds
Edited by Z. Rappoport and I. Marek

I. ABBREVIATIONS

acacH	acetylacetone
CI	chemical ionization
CID	collision-induced dissociation
CIDI	collision-induced dissociative ionization
Cp	cyclopentadienyl
Cp*	pentamethylcyclopentadienyl
DC/FT	dc discharge/flow tube (ion source)
DMAP	4-(*N*,*N*-dimethylamino)pyridine
DMSO	dimethyl sulfoxide
EI	electron ionization
ESI	electrospray ionization
FAB	fast atom bombardment
FT-ICR	Fourier transform-ion cyclotron resonance
GIB	guided ion beam (mass spectrometer)
HPMS	high-pressure mass spectrometry
ICP	inductively coupled plasma
IE	ionization energy
IP	ionization potential
LA	laser ablation
LD	laser desorption
LV	laser vaporization
M	neutral molecule
M^+	molecular ion
Me	methyl
Met	metal atom
MI	metastable ion
MOCVD	metalorganic chemical vapor deposition
MOVPE	metalorganic vapor phase epitaxy
MS	mass spectrometry
OMCVD	organometallic chemical vapor deposition
OMVPE	organometallic vapor phase epitaxy
PES	photoelectron spectroscopy
SIFT	selected-ion flow tube (mass spectrometer)
SIMS	secondary ion mass spectrometry
Solv	solvent molecule
SWIFT	stored waveform inverse Fourier transform
THF	tetrahydrofuran
TOF	time-of-flight (mass spectrometer)
X	halogen atom

II. INTRODUCTION

Zinc compounds have found practical uses since prehistoric times. As a metal, zinc was recognized in the 14th century. The publication of the pioneering works of Edward Frankland[1–3] in the mid-19th century marked the beginnings of organozinc chemistry, as well as the birth of a larger research field—organometallic chemistry[4].

TABLE 1. Isotopic composition of natural zinc [a]

Isotope	Atomic mass (u)	Mole fraction
^{64}Zn	63.929 1461(18)	0.482 68(321)
^{66}Zn	65.926 0364(17)	0.279 75(77)
^{67}Zn	66.927 1305(17)	0.041 02(21)
^{68}Zn	67.924 8473(17)	0.190 24(123)
^{70}Zn	69.925 325(4)	0.006 31(9)

[a] For details see *IUPAC Technical Report*[8].

Dimethylzinc was the first organozinc compound to be studied by mass spectrometry (MS), as part of early MS studies performed by Aston aiming to examine natural abundances of Zn isotopes[5]. Soon thereafter, Bainbridge[6] showed that Aston's data were imprecise because the formation of hydride ions $[ZnH]^+$ was overlooked, and therefore their contribution to the measured abundances of Zn isotopes was not taken into consideration. In the years that followed, numerous studies addressed the subject of Zn isotopic abundances[7,8]. In 2001, the data presented in Table 1 were accepted as the most accurate[8]. It was by mass spectrometry that this best measurement from a single terrestrial source was obtained.

Given that Zn is a polyisotopic element, the mass spectra of its compounds are difficult to interpret if there is an overlapping of isotope clusters of the fragment ions. On the other hand, if such overlapping does not occur, the presence of polyisotopic elements (e.g. Zn, Cl, Br etc.) with their distinctive signature greatly facilitates the assignment of the isotope clusters in a mass spectrum. Figure 1 shows the isotopic distributions of the Zn^+, $[Zn_2]^+$, $[ZnCl]^+$ and $[ZnBr]^+$ ions as calculated by the AELITA software[9]. It should be noted that the MS detection of $[(Zn)_a]^+$, $[(Zn)_aL_b]^+$ and $[ZnX_c]^+$ ions (where L = ligand, X = polyisotopic halide, a and $b \geqslant 2$, $c = 1$ or 2) derived from different precursors was reported by many authors[10–24]. These experimental data are in good agreement with the computer-simulated isotopic distribution.

The progress of the mass spectrometry of organozinc compounds has paralleled the development of new MS techniques. The first complexes studied by MS should have been volatile. However, the development of ionization methods such as fast atom bombardment, electrospray ionization and laser ionization has allowed the analysis of non-volatile, high molecular weight and ionic complexes. The evolution of methods of studying unimolecular

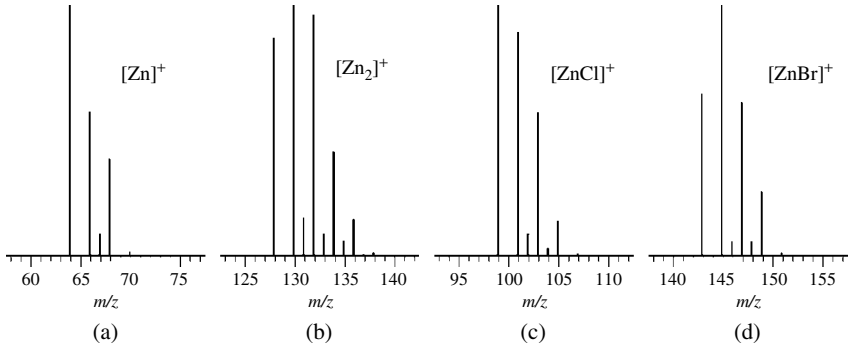

FIGURE 1. Graphical representation of the relative isotope peak intensities for (a) Zn^+, (b) $[Zn_2]^+$, (c) $[ZnCl]^+$ and (d) $[ZnBr]^+$ ions as calculated by the AELITA software[9]

and ion/molecule reactions of mass-selected ions has made further progress possible. For example, Marshall and coauthors[25] exploited the performance of Fourier transform-ion cyclotron resonance mass spectrometry (FT-ICR MS) in the study of the self-chemical ionization (self-CI) of diethylzinc. In their work, the stored waveform inverse Fourier transform (SWIFT) dipolar excitation was used to isolate isotopic species containing ^{64}Zn and ^{12}C and to study their reaction with neutral diethylzinc.

This review intends to summarize the data available on the mass spectrometry of organozinc compounds. Analytical applications of MS to the characterization of compounds having a Zn−C bond will be the major focus of the present work. Physico-chemical parameters of organozinc derivatives will also be reported, along with gas phase reactions resulting in the dissociation or formation of zinc−carbon bond(s).

III. MASS SPECTROMETRY OF ORGANOZINC COMPOUNDS

A. Dialkylzinc and Dihaloalkylzinc Compounds

The first dialkylzinc compound to be studied in detail by electron ionization (EI) mass spectrometry was $Zn(CH_3)_2$ (**1**)[26]. The mass spectrum registered with a time-of-flight (TOF) instrument at the electron energy 70 eV is shown in Table 2. Under the conditions of this experiment, the peak corresponding to the fragment ion $[ZnCH_3]^+$ was the most abundant. This observation demonstrated that the cleavage of the Zn−C bond in the molecular ion (M^+) with the release of the CH_3 group dominates the fragmentation process. The ions with *m/z* 78, *m/z* 77 and *m/z* 76 (Table 2) corresponded to the loss of hydrogen atoms from the $[ZnCH_3]^+$ ion. Rearrangement reactions resulted in the formation of $[ZnH]^+$ and $[HZnCH_3]^+$ ions having a metal−hydrogen bond which was absent in the parent molecule. It was established that the abundance ratio of ions in the mass spectrum of dimethylzinc depends on the energy of the ionizing electrons, as illustrated in Figure 2. This experiment showed that at ionization energies lower than *ca* 25 eV, the decrease in the abundance of the molecular ion $[Zn(CH_3)_2]^+$ correlated with an increase in the abundance of the fragment ion $[ZnCH_3]^+$. At ionization energies exceeding *ca* 25 eV, the latter ion dominated the mass spectrum. In the interval between 35 and 70 eV, the fractional abundance of the ions underwent only a slight change. It was concluded[26] that the curve describing the fragment ions $[ZnCH_3]^+$, represented on the clastogram in Figure 2, indicated their participation as intermediates in the consecutive unimolecular decompositions of **1** in the gas phase under EI (equations 1 and 2):

$$[Zn(CH_3)_2]^+ \longrightarrow [ZnCH_3]^+ + CH_3^\bullet \quad (1)$$

$$[ZnCH_3]^+ \longrightarrow Zn^+ + CH_3^\bullet \quad (2)$$

TABLE 2. Relative intensities of the principal ions observed in the EI mass spectrum (70 eV) of dimethylzinc[26]

Ion	*m/z* [a]	Relative intensity (%)
$[Zn(CH_3)_2]^+$	94	36.6
$[HZnCH_3]^+$	80	7.6
$[ZnCH_3]^+$	79	100
$[ZnCH_2]^+$	78	9.0
$[ZnCH]^+$	77	2.8
$[ZnC]^+$	76	1.3
$[ZnH]^+$	65	2.3
$[Zn]^+$	64	16.6
$[CH_3]^+$	15	21.4

[a] *m/z* values are given for ions containing ^{64}Zn, ^{12}C and ^{1}H isotopes.

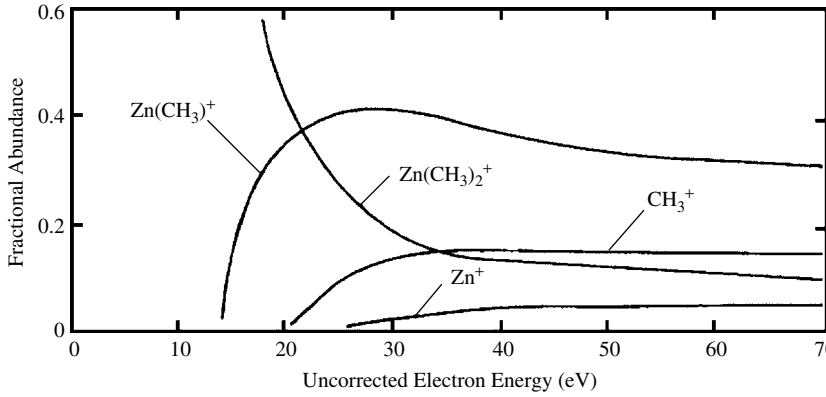

FIGURE 2. The fractional intensities of the ions produced from dimethylzinc by EI as a function of the ionizing energy of the electrons. Adapted from Reference 26

The comparative mass spectrometric behavior of compound **1** and other compounds of the general formula $Met(CH_3)_n$ (where Met = metal atom) has also been reported[18,26].

Diethylzinc $Zn(C_2H_5)_2$ **(2)** was investigated by the FT-ICR MS technique under the conditions of EI[27] and self-CI[25]. The EI mass spectrum of compound **2** consisted of numerous ions, the most abundant being $[Zn(C_2H_5)_2]^+$, $[ZnC_2H_5]^+$, Zn^+ and $[C_2H_5]^+$. Other Zn-containing ions detected were $[ZnC_2H_4]^+$, $[ZnC_2H_3]^+$ and $[ZnH]^+$. In addition, the organic ions $[C_2H_a]^+$ ($a = 1–6$), $[C_3H_b]^+$ ($b = 2–7$) and $[C_4H_c]^+$ ($c = 2, 3, 5–9$) were registered[27]. The formation of organic ions containing a single carbon atom has not been observed over the ionization energy range of up to 200 eV. Figure 3 shows the total ionization cross section of diethylzinc and the partial ionization cross sections for the production of Zn-containing ions[27]. Zn-containing ions dominated the ion production, occupying about two-thirds of the total cross section over most of the 10–200 eV electron energies studied. The total ionization cross section reached a maximum at *ca* 80 eV.

Marshall and coworkers[25] observed that the ions formed from compound **2** under EI reacted with the neutral diethylzinc background, giving rise to new products (Figure 4). This process progressed as a function of the time allocated for the reactions taking place in the ICR cell (Figure 5). Theoretical calculations by the ZINDO/1 semi-empirical method were performed to assist the interpretation of the experimental observations. The geometries of various Zn-containing species were optimized, and their energies were calculated[25]. Scheme 1 summarizes the proposed pathway for diethylzinc self-CI. The examination of the reaction between $^{64}Zn^+$ and neutral diethylzinc revealed that bare metal ions react primarily by charge transfer to produce $[Zn(C_2H_5)_2]^+$ with m/z 122. The latter molecular ion of compound **2** produced by charge transfer should possess much less internal energy than if produced by EI. The product ion spectra from the charge transfer reaction closely resembled those from the EI-generated M^+, suggesting that the sampled reaction pathways are not highly endothermic[25].

The detailed examination of ion/molecule reactions between organic or Zn-containing ions produced from **2** under EI and neutral diethylzinc was also reported recently[27]. Several ions containing two metal atoms ($[Zn_2C_2H_5]^+$, $[Zn_2C_4H_{11}]^+$ and $[Zn_2C_6H_{15}]^+$) were detected as the intermediate products, but no larger Zn cluster ions were observed. Ionic species (including intermediates) reacted further with the neutral $Zn(C_2H_5)_2$ to form the $[ZnC_8H_{17}]^+$ ion as final product[27].

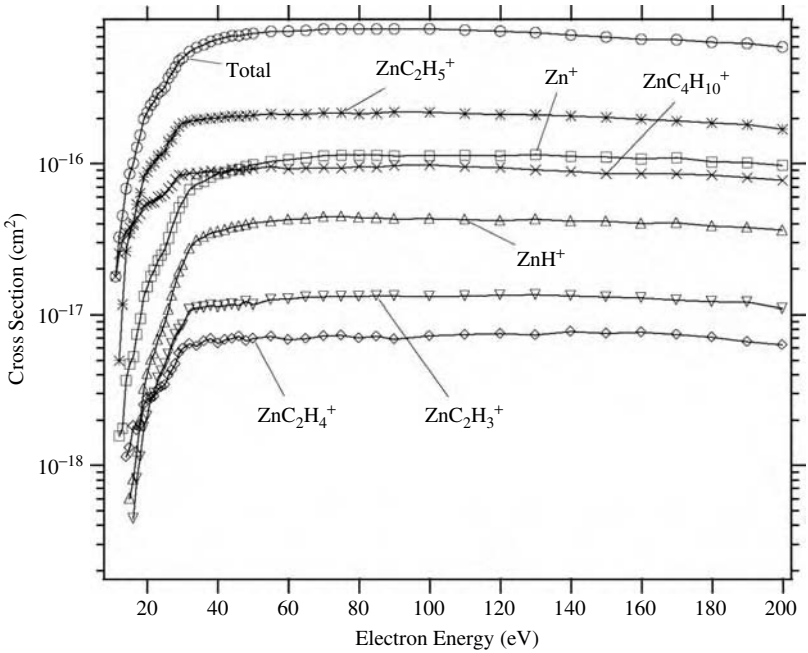

FIGURE 3. Total ionization cross section of diethylzinc and partial ionization cross sections for the production of the Zn-containing ions. Reproduced by permission of Elsevier from Reference 27

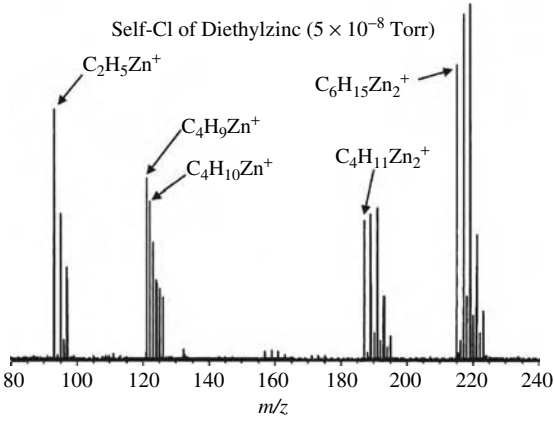

FIGURE 4. Self-chemical ionization FT-ICR mass spectrum of diethylzinc. Electron energy: 70 eV; diethylzinc neutral reagent pressure: 5×10^{-8} Torr. Reproduced by permission of John Wiley & Sons Ltd. from Reference 25

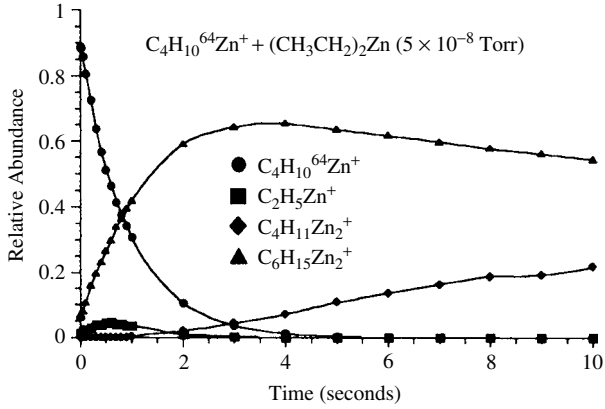

FIGURE 5. Progress curve for the reaction of $[^{64}Zn(^{12}C_2H_5)_2]^+$ with natural-abundance diethylzinc neutral (5×10^{-8} Torr). Reproduced by permission of John Wiley & Sons Ltd. from Reference 25

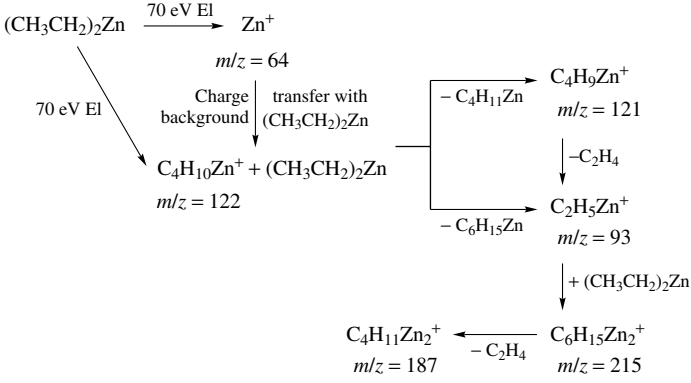

SCHEME 1. Proposed pathway for the reaction of $[^{64}Zn(^{12}C_2H_5)_2]^+$ with neutral diethylzinc (5×10^{-8} Torr). Reproduced by permission of John Wiley & Sons Ltd. from Reference 25

A series of bis(perfluoroalkyl)zinc [$Zn(C_2F_5)_2$•$2CH_3CN$ **(3)**, $Zn(C_2F_5)_2$•2THF **(4)**, $Zn(C_2F_5)_2$•2DMSO **(5)**, $Zn(C_3F_7\text{-}n)_2$•$2CH_3CN$ **(6)**, $Zn(C_3F_7\text{-}n)_2$•2THF **(7)**, $Zn(C_3F_7\text{-}i)_2$•$2CH_3CN$ **(8)**, $Zn(C_3F_7\text{-}i)_2$•2THF **(9)**, $Zn(C_4F_9\text{-}n)_2$•$2CH_3CN$ **(10)**, $Zn(C_4F_9\text{-}n)_2$•2THF **(11)**, $Zn(C_6F_{13}\text{-}n)_2$•$2CH_3CN$ **(12)**, $Zn(C_6F_{13}\text{-}n)_2$•2THF **(13)**, $Zn(C_7F_{15}\text{-}n)_2$•$2CH_3CN$ **(14)**, $Zn(C_8F_{17}\text{-}n)_2$•$2CH_3CN$ **(15)** and $Zn(C_8F_{17}\text{-}n)_2$•2THF **(16)**] have been studied by EI mass spectrometry[28]. Mass spectra of perfluoropropyl derivatives are listed in Table 3 as examples. Generally, halocarbon derivatives are notorious for generating rearranged ions and neutrals with Met−X bonds under EI. Compounds **3–16** are not exceptions. The mass spectra of **3–8** and **10–16** contained at least one of the ions $[ZnF]^+$ and $[ZnF•Solv]^+$ [where Solv = solvent molecule (CH_3CN, DMSO or THF)]. Many of these compounds also generated rearranged ions such as $[ZnCF_3]^+$. The dissociation of the Zn−C bond is another abundant reaction. No ions having two perfluoroalkyl groups at the metal atom were detected. A remarkable characteristic of the EI mass spectra of these compounds was that the Zn−Solv bonds were more stable than

TABLE 3. Relative intensities of ions (m/z (rel. int.) [ion]) observed in the EI mass spectra of some bis(perfluoroalkyl)zinc compounds[28]

$Zn(C_3F_7\text{-}n)_2\bullet 2CH_3CN$ (20 eV, 70 °C)	$Zn(C_3F_7\text{-}n)_2\bullet 2THF$ (20 eV, 65 °C)	$Zn(C_3F_7\text{-}i)_2\bullet 2CH_3CN$ (20 eV, 65 °C)	$Zn(C_3F_7\text{-}i)_2\bullet 2THF$[a] (20 eV, 140 °C)
333[b] (0.2%) $[Zn(C_3F_7)C_2F_4]^+$	339 (0.4%) $[ZnC_3F_5\bullet 2THF]^+$	274 (1.5%) $[ZnC_3F_7\bullet CH_3CN]^+$	402 (0.7%) $[Zn(C_3F_7)_2]^+$
283 (9.5%) $[ZnC_4F_9]^+$	305 (0.9%) $[ZnC_3F_7\bullet THF]^+$	173 (0.5%) $[ZnCF_3CH_2CN]^+$	305 (3.9%) $[ZnC_3F_7\bullet THF]^+$
274 (2.4%) $[ZnC_3F_7\bullet CH_3CN]^+$	283 (4.7%) $[ZnC_4F_9]^+$	131 (100%) $[C_3F_5]^+$	42 (100%) $[CH_2CO]^+$
233 (7.3%) $[ZnC_3F_7]^+$	233 (3.2%) $[ZnC_3F_7]^+$	124 (10.0%) $[ZnF\bullet CH_3CN]^+$	
210 (1.9%) $[ZnC_2F_5\bullet HCN]^+$	155 (3.2%) $[ZnF\bullet THF]^+$	83 (0.7%) $[ZnF]^+$	
193 (1.2%) $[Zn(CF_3)F\bullet CH_3CN]^+$	133 (5.0%) $[ZnCF_3]^+$	64 (2.9%) $[Zn]^+$	
133 (10.0%) $[ZnCF_3]^+$	64 (4.3%) $[Zn]^+$		
124 (12.0%) $[ZnF\bullet CH_3CN]^+$	42 (100%) $[CH_2CO]^+$		
83 (2.0%) $[ZnF]^+$			
64 (6.2%) $[Zn]^+$			
41 (100%) $[CH_3CN]^+$			

[a]The ions $[ZnC_3F_7I]^+$ (m/z 360; rel. int.: 3.9%), $[unknown]^+$ (m/z 307; rel. int.: 10.4%) and $[ZnFI]^+$ (m/z 210; rel. int.: 2.9%) are also present in the mass spectrum and derive from the starting reagents used in the synthesis of compound $Zn(C_3F_7\text{-}i)_2\bullet 2THF$.
[b]In all cases, m/z values are given for ions containing ^{64}Zn, ^{19}F, ^{16}O, ^{14}N, ^{12}C and ^{1}H isotopes.

the Zn–perfluroalkyl bond. The isomers Zn(*n*-C_3F_7)$_2$•Solv and Zn(*i*-C_3F_7)$_2$•Solv (the pair **6** and **8** and the pair **7** and **9**, respectively) displayed some differences in the mass spectra (Table 3); unfortunately, the experimental conditions (the temperature) under which the samples have been measured were not the same for the isomeric samples. For that reason, it is not possible to discuss isomer differentiation by means of MS in this particular case.

B. Other Organozinc Compounds with the General Formula ZnR_2

Dicyclopentadienylzinc $ZnCp_2$ **(17)** [where Cp = cyclopentadienyl (C_5H_5)] generated a simple mass spectrum consisting of the $[ZnCp_2]^+$, $[ZnCp]^+$ and $[Zn]^+$ ions[29]. The character of the interactions between Zn^{2+} and $(Cp^-)_2$ is electrostatic rather than covalent[30]. This might be the key explanation of the easy dissociation of Zn–Cp bond(s) during the MS experiment. The structure and the energetics of the $[ZnCp]^+$ ion have also been investigated by computational methods[31, 32]. It was predicted that the $[ZnCp]^+$ ion would preferably exist as a η^2- or η^1-bound structure[32].

Three isomeric R_2Zn complexes [R = 1-norbornyl **(18)**, R = 2-norbornyl **(19)**, R = 7-norbornyl **(20)** (norbornyl (C_7H_{11}) = bicyclo[2.2.1]heptyl)] generated organic and Zn-containing ions under EI[33]. Only compound **19** produced stable molecular ions. Compound **18** generated $[ZnR]^+$ and $[R]^+$, compound **19** gave rise to $[ZnR_2]^+$, $[ZnR]^+$ and $[R]^+$, whereas compound **20** produced $[ZnR]^+$, $[R_2]^+$ and $[R]^+$. The formation of the dimeric organic ion $[R_2]^+$ from the M^+ of compound **20** is presumably promoted by the metal center.

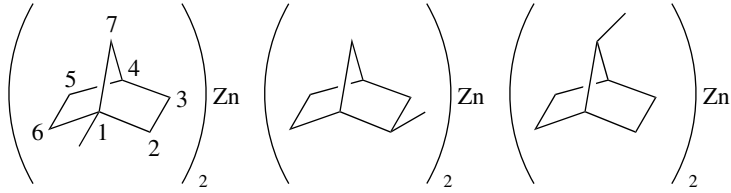

(18) **(19)** **(20)**

The EI mass spectrum of the bis[2,4,6-tris(trifluoromethyl)phenyl]zinc **(21)** showed a weak signal due to molecular ion. The spectrum was dominated by the $[C_6H_2(CF_3)_2CF_2]^+$ ion formed as a result of the rearrangement process in which a halogen atom from the ligand migrated to the remaining organozinc fragment[34].

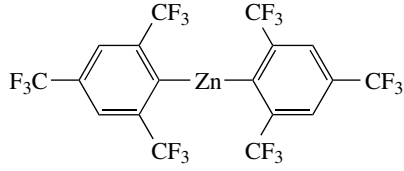

(21)

The investigation of the exchange of organyl groups between various dialkylzinc complexes, ZnR'_2 and ZnR''_2, has been performed by EI MS. The observation of M^+ of the mixed compounds $ZnR'R''$ confirmed that the alkyl exchange took place in the gas phase[35].

C. Miscellaneous Complexes Containing a Zn–C Bond

1. Cubane-like zinc-containing clusters

Mass spectrometry was used to confirm the existence of $[Me_4Zn_4(OR')_4]$ tetramers (R′ = Me, Et, *i*-Pr, *t*-Bu) in the vapor phase[17,18,36–38]. All compounds showed $[Me_3Zn_4(OR')_4]^+$ ions in the EI mass spectra. The MS detection of ionic aggregates having more than four monomeric RZnOR′ units has also been reported[17].

Schröder and coworkers[39] performed a detailed study of the sequential dissociations of the tetranuclear zinc cluster-ion $[Me_3Zn_4(OC_3H_7\text{-}i)_4]^+$ formed by the dissociative electron ionization of neutral tetrameric methylzinc isopropoxide $[MeZn(OC_3H_7\text{-}i)]_4$ **(22)**. This compound has an unusual structure, which consists of a cubic Zn_4O_4 core. A variety of tandem mass spectrometry experiments was performed using a four-sector instrument with a BEBE configuration (B: magnetic sector, E: electric sector). This instrument allowed metastable ion (MI), collision-induced dissociation (CID) and collision-induced dissociative ionization (CIDI) studies of metal-containing mass-selected ions. A selectively deuteriated complex $[(CH_3)Zn(OC_3D_7\text{-}i)]_4$ (**23**) was synthesized and studied to assist the interpretation of experimental results. Also, a mass spectrometer with a QHQ configuration (Q: quadrupole, H: hexapole) equipped with an electrospray ionization (ESI) source was used to produce and investigate under CID conditions the $[Zn(OC_3H_7\text{-}i)]^+$ ion solvated with two *i*-PrOH molecules generated from the $[Zn(NO_3)(i\text{-}C_3H_7OH)_3]^+$ precursor ion[39].

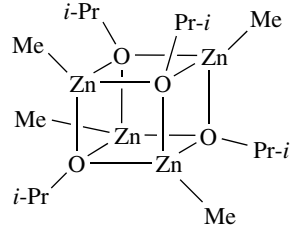

(22)

This study revealed that after the loss of the neutral $MeZn(OC_3H_7\text{-}i)$ fragment from the tetranuclear ion $[Me_3Zn_4(OC_3H_7\text{-}i)_4]^+$, the $[Me_2Zn_3(OC_3H_7\text{-}i)_3]^+$ ion was produced. In the latter trinuclear cluster-ion, a hydrogen migration led to the expulsion of a neutral acetone molecule and the formation of $[Me_2Zn_3(OC_3H_7\text{-}i)_2(H)]^+$. Further dissociation generated the neutral entity $HZn(OC_3H_7\text{-}i)$ and the cluster-ion $[Me_2Zn_2(OC_3H_7\text{-}i)]^+$. The resulting binuclear ion $[Me_2Zn_2(OC_3H_7\text{-}i)]^+$ lost neutral species (Zn, C, H_4) with 80 u (for the ^{64}Zn and ^{12}C isotopes). CIDI experiments showed that the neutral entity (Zn, C, H_4) represents insertion species $HZnCH_3$, rather than $(Zn + CH_4)$, contrary to the expectations that $(Zn + CH_4)$ would be more stable. Finally, the $[CH_3Zn(OC(CH_3)_2)]^+$ ion released a neutral acetone molecule and generated the $[CH_3Zn]^+$ species[39].

Negative-ion ESI mass spectrometry has been employed to investigate the mechanisms of the synthesis of the heterobimetallic clusters $[((THF)Li)_2(MeZn)_2(OBu\text{-}t)_4]$ **(24)**, $[((THF)_2K)_2(MeZn)_2(OSiMe_3)_4]$ **(25)** and $[K(MeZn)_3(OBu\text{-}t)_4]$ **(26)** in solution[11]. Compounds **24–26** possess distorted heterocubane skeletons: $Li_2Zn_2O_4$, $K_2Zn_2O_4$ and KZn_3O_4, respectively.

In this way, the reaction mixtures for the synthesis of the **24–26** clusters have been subjected to negative-ion ESI MS analysis and several negatively charged intermediates have been detected. Some identified species were cluster anions: $[C_{36}H_{80}Li_3O_8Zn_2]^- \equiv [(Me_2ZnOBu\text{-}t)_2 + Li^+ + (LiOBu\text{-}t)_2 + 4THF]^-$ (for compound

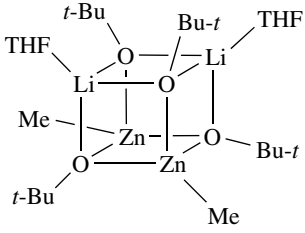

(24)

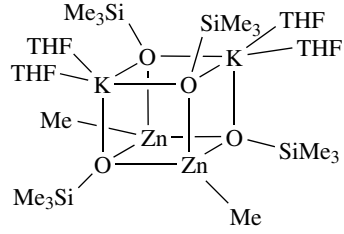

(25)

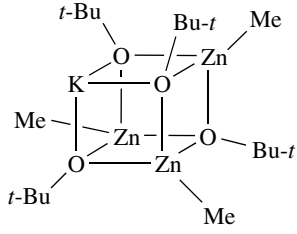

(26)

24), $[C_{10}H_{30}KO_2Si_2Zn_2]^- \equiv [K(Me_2ZnOSiMe_3)_2]^-$ and $[C_{14}H_{42}KO_4Si_4Zn_2]^- \equiv [K\{MeZn(OSiMe_3)_2\}_2]^-$ (for compound **25**) and $[C_{19}H_{45}O_4Zn_3]^- \equiv [(MeZn)_3(OBu\text{-}t)_4]^-$ (for compound **26**)[11].

Compounds **22–26** possess heterocubane structures in which four metal atoms are linked via μ_3-O bridges of the OR′ or $OSiMe_3$ groups, forming the Met_4O_4 skeleton. Heterocubane clusters with a Zn_4N_4 skeleton have also been encountered. Such clusters include the tetrameric complexes $[MeZn(NPMe_3)]_4$ **(27)** and $[(n\text{-}C_4H_9)Zn(NPMe_3)]_4$ **(28)**, which gave rise to the $[Me_3Zn_4(NPMe_3)_4]^+$ (*m/z* 667) and $[(n\text{-}C_4H_9)_3Zn_4(NPMe_3)_4]^+$ (*m/z* 793) ions, respectively at the electron energy 70 eV[40].

Generally, the cubane-like zinc-containing clusters with Zn_4A_4 cores (where A = O or N) (e.g. **22**, **23**, **27** and **28**) generate primarily $[R_3Zn_4(OR')_4]^+$ or $[R_3Zn_4(NR'')_4]^+$ ions under EI conditions. Both types of ions are the result of the dissociation of the Zn−C bond while the cubane skeleton remains intact. Another cluster, $[(n\text{-}C_4H_9)_4Zn_4I(NPMe_3)_3]$ (**29**), in which four zinc atoms are linked via three μ_3-N bridges of the phosphaneiminato groups and one iodine atom, released $n\text{-}C_4H_9^{\bullet}$ and $n\text{-}C_4H_9I$ species and gave rise to the $[(n\text{-}C_4H_9)_2Zn_4(NPMe_3)_3]^+$ (*m/z* 646) ion under dissociative electron ionization (70 eV)[40]. In this case, the skeleton Zn_4N_3I did not survive the dissociative EI conditions. In point of

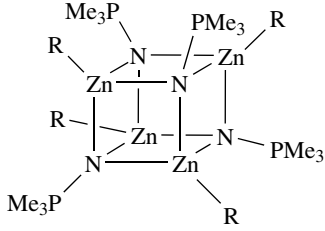

(27) R = Me

(28) R = *n*-Bu

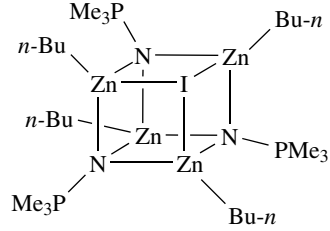

(29)

fact, the Zn_4N_3I core has been expected to be weaker than the Zn_4N_4 one. These expectations have been based on crystal-structure determinations[40] showing that the Zn_4N_3I core in compound **29** is distorted, whereas in the Zn_4N_4 core, all bond angles are close to 90°, making it more stable.

2. Binuclear and dimeric zinc complexes

Additionally, mass spectrometry methods have been successfully applied for the identification of other Zn-containing complexes. Among them are compounds containing two Zn atoms[10,41,42] **(30–32)**, as well as some complexes that exist as dimers in the condensed phase according to different physical methods[42–47] **(33–42)**. For all these compounds, isotope clusters with isotopic distributions similar to the graphical representations in Figure 1b (for $[Zn_2]^+$) were expected, provided that the binuclear species or dimer entities are able to survive the ionization process.

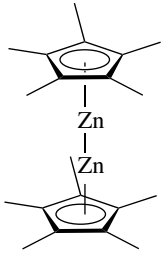

(30)

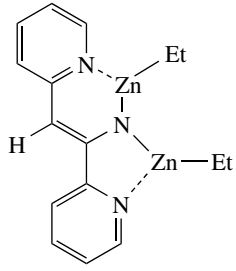

(31)

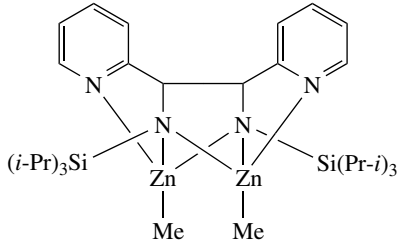

(32)

Decamethyldizincocene $Zn_2(\eta^5\text{-}C_5Me_5)_2$ **(30)** represents a stable compound of $Zn^{(I)}$ with a Zn—Zn bond. The high-resolution mass spectrum of **30** contained the expected isotope cluster for the molecular ion $[Zn_2(Cp^*)_2]^+$ (where Cp* stands for pentamethylcyclopentadienyl)[10]. For the binuclear compound **31**, M^+ and $[M - Et]^+$ ions of low intensities were detected under EI[41]. Complex **32** did not produce Zn-containing ions under similar experimental conditions. The detected ion with the highest mass was $[C_{15}H_{28}N_2Si]^+$, representing half of the nitrogen-containing ligand[42].

The structures of the dimeric molecules **33** and **34** with a Zn_2N_2 central ring display a close similarity, but their EI mass spectra were very different[42,43]. Complex **33** produced only one metal-containing ion $[M/2]^+$ of low abundance, which stands for the ionized monomer, whereas **34** generated M^+ and $[M - Me]^+$, along with a few abundant organic fragment ions. The dimer compounds **35–38** having a Zn_2N_2 ring were also subjected to electron ionization. Complexes **35** and **36** produced only organic fragment ions[44]; complex **37**[44] generated a very abundant fragment ion [(adamantylamine)Zn]$^+$, whereas complex **38** gave rise to the $[\{Me_2NC(NPr\text{-}i)_2\}_2Zn]^+$, $[\{Me_2NC(NPr\text{-}i)_2\}_2Zn - NMe_2]^+$ and $[\{Me_2NC(NPr\text{-}i)_2\}Zn]^+$ ions[45].

The reaction of diethylzinc with acetylacetone (acacH) in toluene resulted in the dimeric compound $[EtZn(acac)]_2$ **(39)**, which consists of a four-membered Zn_2O_2 ring[46]. The EI mass spectrum of **39** displayed three groups of peaks, attributed to the $[Zn(acac)_2]^+$ (m/z 262), $[EtZn(acac)]^+$ (m/z 192) and $[Zn(acac)]^+$ (m/z 163) ions. The ion with m/z 192 simply represents a monomer fragment, whereas the ion with m/z 262 can be written as $[M - Et_2Zn]^+$.

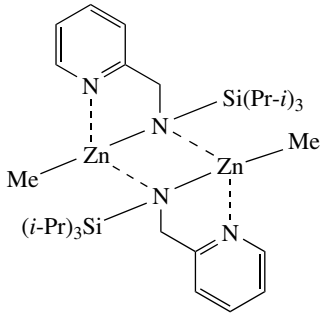

(33)

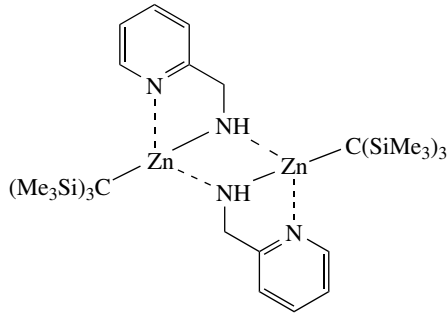

(34)

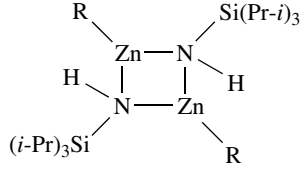

(35) R = Me

(36) R = Et

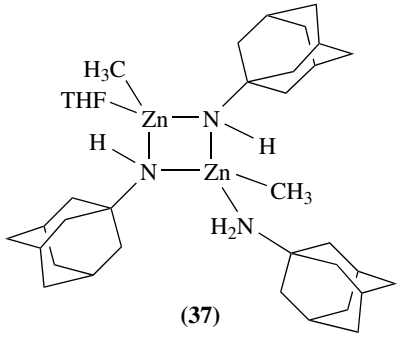

(37)

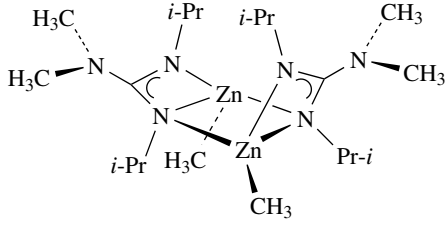

(38)

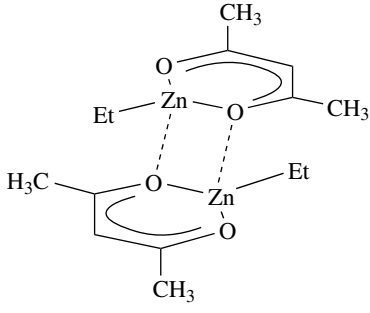

(39)

A crystallographic study of $MeZnS_2CNEt_2$ **(40)** revealed that in the crystal phase, this complex exists in the dimeric $[MeZnS_2CNEt_2]_2$ form. Unfortunately, no clear conclusion could be drawn about the structure of this compound in either the solution or the gas phase[47]. Mass spectra of **40** and related compounds $MeZnS_2CNMe_2$ **(41)** and $EtZnS_2CNMe_2$ **(42)** contained peaks attributed to the M^+ of the monomers and to the $[Zn(dialkyldithiocarbamate)_2]^+$ ions[47].

3. Monomeric RZnL complexes (L = polydentate ligand)

Compounds **43–59** represent monomeric RZnL complexes (where L = bidentate or tridentate ligand)[48–54]. The mass spectra of these species have been measured by either EI MS, CI MS or fast atom bombardment (FAB) MS. Compounds **43** and **44** generated M^+ of low abundances in the EI MS conditions[48]. Under the same conditions, $[N\{P(NMe_2)_2NSiMe_3\}_2ZnMe]$ **(45)** produced abundant $[M - Me]^+$ ions, whereas $[N\{P(NMe_2)_2NSiMe_3\}_2ZnEt]$ **(46)** generated M^+ and $[M - ZnEt]^+$ ions[49]. Complex **47** was subjected to FAB MS, and $[M - Et]^+$ and $[M - ZnEt]^+$ ions were detected[50]. Under CI MS conditions[51] (reagent gas: NH_3 or CH_4), complexes **48–50** produced protonated molecules $[M + H]^+$.

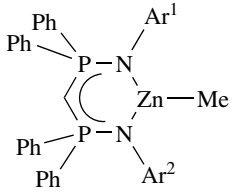

(43) $Ar^1 = Ar^2 = 2,4,6\text{-}Me_3C_6H_2$

(44) $Ar^1 = 2,4,6\text{-}Me_3C_6H_2$, $Ar^2 = Ph$

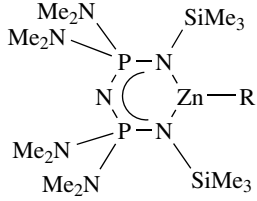

(45) R = Me

(46) R = Et

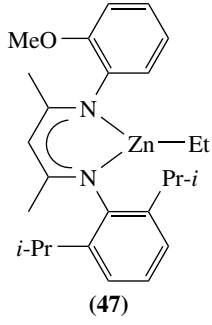

(47)

In compounds **43–50**, the metal center interacts with a bidentate ligand through two N donor atoms, forming a six-membered ring. In complexes **51–53**, $Zn^{(II)}$ coordinates with the bidentate ligands, forming five-membered rings. The EI mass spectrum of **51** displayed M^+, $[M - Me]^+$ and $[M - ZnMe]^+$ ions[52]. At 70 eV, **52** and **53** released bidentate ligands and produced the fragment ions $[\{Ph(Me_3Si)CH\}ZnMe]^+$ and $[\{Ph(Me_3Si)CH\}ZnCl]^+$, respectively, as the most abundant Zn-containing species[53].

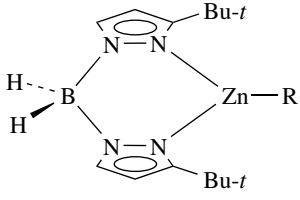

(48) R = Me

(49) R = Et

(50) R = *t*-Bu

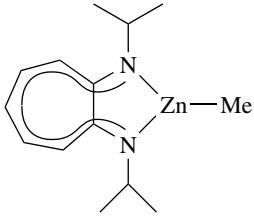

(51)

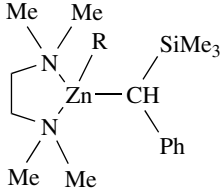

(52) R = Me

(53) R = Cl

Compounds **54–56**[54] and **57–59**[51] contain a ZnR group coordinated to tridentate ligands. At the electron ionization energy 70 eV, **54** and **55** gave rise to abundant fragmentation and generated some Zn-containing ions. In the case of **54**, the ions $[M - Me]^+$, $[M - CO_2]^+$, $[M - C_4H_9]^+$ and $[M - CO_2 - C_4H_9]^+$ were detected. Complex **55** produced $[M - Et]^+$, $[M - Et - CO_2]^+$ and $[M - CO_2 - C_4H_9]^+$ ions. Compound **56** was analyzed by FAB mass spectrometry using 3-nitrobenzyl alcohol as matrix[54]. Interestingly, under these experimental conditions, some protonated dimer-like species as well as some Zn-containing fragment ions were registered: $[M_2H - Me]^+$, $[M_2H - Me - CO_2]^+$, $[M + H]^+$, $[M - Me]^+$, $[M - CO_2]^+$ etc. The CI (reagent gas: NH_3 or CH_4) mass spectra of **57–59** consisted only of the $[M + H]^+$ species[51].

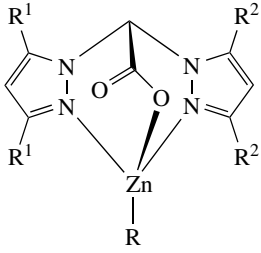

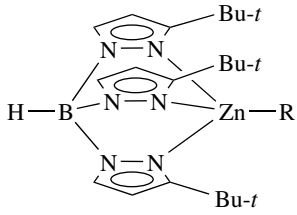

(**54**) R = Me, $R^1 = R^2 = t$-Bu

(**55**) R = Et, $R^1 = R^2 = t$-Bu

(**56**) $R = R^1$ = Me, $R^2 = t$-Bu

(**57**) R = Me

(**58**) R = Et

(**59**) R = C≡C—Ph

4. Other species containing organozinc fragments

Two isomeric complexes, **60** and **61**, have been analyzed by CI MS (reagent gas: CH_4), producing $[M + 1]^+$ and $[M + 29]^+$ ions[55]. Electron ionization mass spectrometry was applied in the analysis of the product of the reaction between $Zn(CF_3)Br{\bullet}2CH_3CN$ **(62)** and 4-(*N*,*N*-dimethylamino)pyridine (DMAP). The EI (20 eV) mass spectrum of the product, $Zn(CF_3)Br{\bullet}$DMAP **(63)**, was recorded at 280 °C and consisted mainly of $[C_6H_3BrF_2NZn]^+$, $[ZnBr_2]^+$ and $[ZnBr]^+$ ions. At lower temperatures, this compound did not yield any Zn-containing ions, and the spectra were dominated by the peaks of the $[DMAP]^+$ and $[C_2H_6N]^+$ ions[56].

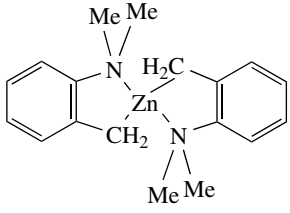

(60)

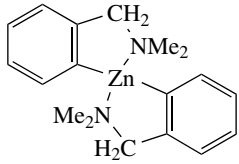

(61)

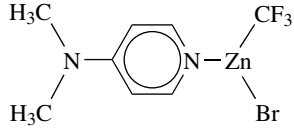

(63)

Ferrocenyl-containing zinc complexes **64** and **65** were analyzed by EI mass spectrometry[57,58]. For **64**, the intact M^+ has been recorded at 70 eV[57]. EI mass spectra for the other heterometallic compounds, such as $Zn^{(II)}$-containing mixed-valence $Mn^{(VI)}Mn^{(V)}$

complexes $Mn_2(NBu\text{-}t)_2(\mu\text{-}NBu\text{-}t)_4ZnMe$ **(66)** and $Mn_2(NBu\text{-}t)_2(\mu\text{-}NBu\text{-}t)_4ZnCH_2Bu\text{-}t$ **(67)**, were also reported[59]. Cluster **66** generated M^+, $[M - ZnMe]^+$, $[M - ZnMe - Me]^+$ and $[M - ZnMe - NBu\text{-}t - Me]^+$ ions, and complex **67** gave rise to M^+, $[M - Me]^+$ and $[M - ZnCH_2Bu\text{-}t]^+$ ions.

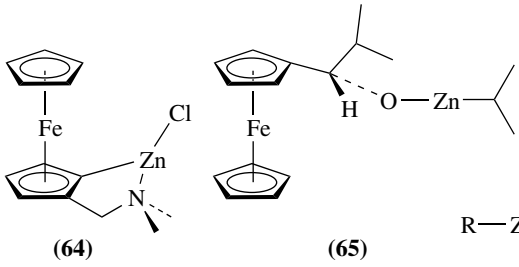

(64) **(65)**

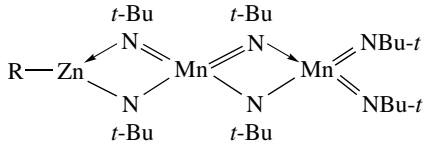

(66) R = Me

(67) $R = CH_2Bu\text{-}t$

Three zincate species with the general formula $[Li(tmeda)_2]^+[Me_{3-n}Zn\{CH(SiMe_3)Ph\}_n]^-$ [where tmeda = 1,2-bis(dimethylamino)ethane, $n = 1$ for **68**, $n = 2$ for **69** and $n = 3$ for **70**] have been subjected to EI MS analysis[60]. At the electron energy 70 eV, the mass spectra displayed peaks of the organic ions $[tmeda]^+$ and/or $[SiMe_3]^+$ and $[CH(SiMe_3)Ph]^+$, as well as peaks attributed to the $[ZnR_2]^+$, $[MeZnR]^+$, $[ZnR]^+$ and $[ZnMe_2]^+$ ions for **68**; $[ZnR_2]^+$, $[ZnR_2 - Me]^+$, $[MeZnR]^+$ and $[ZnR]^+$ ions for **69**; $[ZnR_2]^+$ and $[ZnR]^+$ ions for **70** [when $R = CH(SiMe_3)Ph$].

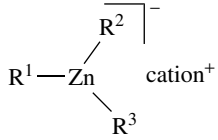

(68) $R^1 = CH(SiMe_3)Ph$, $R^2 = R^3 = Me$, $cation^+ = [Li(1,2\text{-bis(dimethylamino)ethane}_2)]^+$

(69) $R^1 = R^2 = CH(SiMe_3)Ph$, $R^3 = Me$, $cation^+ = [Li(1,2\text{-bis(dimethylamino)ethane}_2)]^+$

(70) $R^1 = R^2 = R^3 = CH(SiMe_3)Ph$, $cation^+ = [Li(1,2\text{-bis(dimethylamino)ethane}_2)]^+$

To summarize, mass spectrometry has successfully been used for the identification of compounds containing a Zn–C bond, which have a large diversity of structures and complexity. These complexes have been subjected to different ionization methods (such as EI, CI, FAB and ESI) and in many cases they generated numerous Zn-containing fragment ions. Under soft (CI or FAB) experimental conditions, some of these compounds produced protonated molecules $[M + H]^+$ or even protonated dimer-like species $[M_2H - R]^+$. Electron ionization was successful for the characterization of many volatile Zn-containing compounds. Peaks of molecular ions M^+ were frequently observed, but the majority of the mass spectra were dominated by Zn–C bond dissociation products.

The formation of Zn−C bonds was observed as a result of the dissociative ionization of various compounds or ion/molecule reactions. Rearrangements of organozinc ions are a source for new Zn−C bonds. An example is the formation of the $[ZnC_6H_5]^+$ ion from the $Zn^{(II)}$ chelate complex of bis(monothiodibenzoylmethane) **(71)** under EI[61]. A similar rearrangement process was reported to occur under EI for the $Zn^{(II)}$ chelate of bis(benzoylmethane) **(72)**[62]. The generation of the new $Zn-CF_3$ bond was observed as a consequence of rearrangements taking place in bis(perfluoroalkyl)zinc (compounds **3–16**) subjected to EI MS at 20 eV and $T < 95\,^{\circ}C$[28].

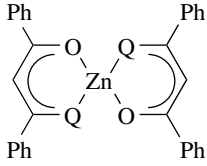

(71) Q = S

(72) Q = O

Dance and coworkers[12, 63] reported a study involving the laser ablation (LA) of $Zn^{(II)}$ cyanide, $Zn(CN)_2$ **(73)** and the FT-ICR MS characterization of the resulting long series of ions with the general formula $[Zn_n(CN)_{2n+1}]^-$, comprising 27 members, from $[Zn(CN)_3]^-$ to $[Zn_{27}(CN)_{55}]^-$ ($n = 1-27$). The $[Zn_n(CN)_{2n+1}]^-$ anions were obtained by ablation at 1064 nm (power density *ca* 1.8×10^4 MW cm^{-2}). In the positive-ion mode measurements at the same radiation, only Zn^+ and minor contributions from the $[Zn_2]^+$ and $[Zn(CN)]^+$ species were observed. The only Zn-containing ions registered at a radiation of 532 nm were $[Zn(CN)_3]^-$ in the negative-ion mode and Zn^+ in the positive-ion mode. The $[CN]^-$ and polyatomic $[C_xN_y]^-$ ions were also produced during LA. In addition, *in silico* simulation of the possible structures of many of the detected ionic species has been reported, and helical structures were proposed for ions in the series $[Zn_n(CN)_{2n+1}]^-$.

IV. ORGANOZINC ION STRUCTURE AND ENERGETICS

A. Energetics and Photodissociation Studies

The quantity of energy that a gaseous molecule must absorb in order for an electron to be removed from the molecule is called the ionization energy (IE). The lowest IE, or the first ionization potential (IP), corresponds to the ground electronic state of the positive ion. In general, the IEs are deduced from photoionization experiments on neutral species, in which the resulting positive ions are recorded mass spectrometrically. These apparatuses are usually equipped with a monochromatic source of radiation. EI MS with a monoenergetic electron beam is an alternative method of IE measurements. Photoelectron spectroscopy (PES) represents yet another tool in the arsenal of physical methods used for determining IE values.

The He I photoelectron spectra of ZnR_2 [where R = Me **(1)**, Et **(2)**, *t*-Bu **(74)** and neopentyl **(75)**] (Figure 6) have been measured and the ionization energies were calculated[64]. For all four compounds, the corresponding first energy bands were distinctive and their values decrease in the order $Me_2Zn > Et_2Zn >$ (neopentyl)$_2Zn > t\text{-}Bu_2Zn$. The vertical IEs are presented in Table 4. The PES data of dimethylzinc were in good agreement with those described in an earlier report[65]. The appearance energies and heats

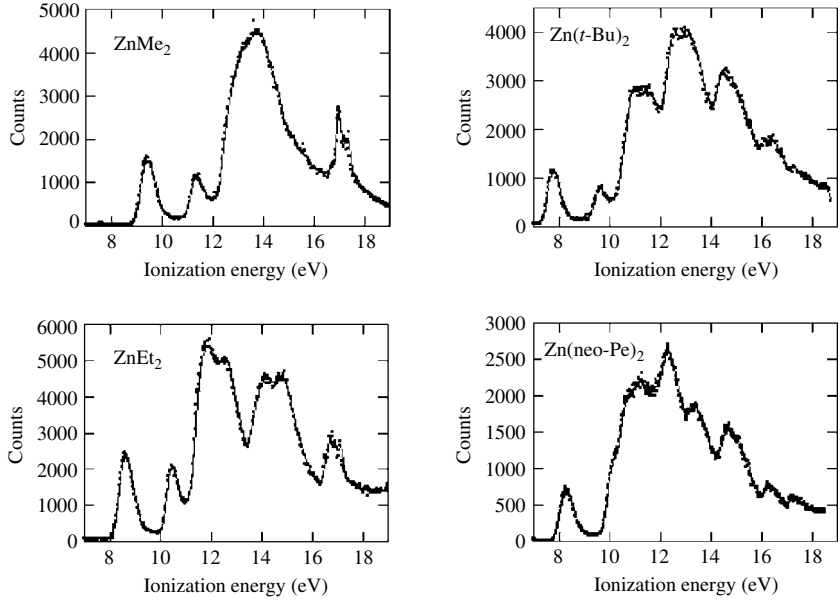

FIGURE 6. He I photoelectron spectra of ZnR_2, R=Me, Et, *t*-Bu and neopentyl. Reproduced by permission of The Royal Society of Chemistry from Reference 64

TABLE 4. Orbital energies, calculated and experimental ionization energies (eV) for Me_2Zn, Et_2Zn, *t*-Bu_2Zn and neopentyl$_2$Zn. For the 3*d* electrons the orbital energy and calculated IE are those of the δ symmetry orbital while the experimental IE is that of the band maximum[64]

R_2Zn	Orbital energy		IE calc	IE exp
Me_2Zn	σ_u	−5.937	9.25	9.40
	σ_g	−7.775	11.16	11.36
	Zn *d*	−10.92	18.11	16.95
Et_2Zn	σ_u	−5.414	8.29	8.63
	σ_g	−7.075	9.89	10.46
	Zn *d*	−10.87	17.46	16.70
t-Bu_2Zn	σ_u	−4.752	7.34	7.80
	σ_g	−6.531	9.09	9.63
	Zn *d*	−10.76	17.38	16.13
neopentyl$_2$Zn	σ_u	−5.323	8.00	8.33
	σ_g	−6.805	9.41	10.20
	Zn *d*	−10.72	17.43	16.30

of formation of the principal positive ions generated by dimethylzinc determined from mass spectrometric[26] and from photoionization studies[66] have also been reported.

The Met^+-L bond dissociation energies were measured for some Zn-containing gas phase cations using different methods[66–77]. Armentrout[78] reviewed guided ion beam studies of transition metal–ligand thermochemistry and reported the following

values: $D^o(Zn^+-H) = 2.36$ eV, $D^o(Zn^+-CH_3) = 2.90$ eV, $D^o(Zn^+-O) = 1.67$ eV and $D^o(Zn^+-S) = 2.05$ eV. It has also been determined that $D^o(Zn^+-CS) = 1.54 \pm 0.24$ eV[77]. Buckner and coworkers[15] generated $[Zn_2]^+$ from ZnO by laser desorption. The charge transfer reactions of $[Zn_2]^+$ indicated that $IE(Zn_2) = 9.0 \pm 0.2$ eV, from which the bond dissociation energy $D^o(Zn^+-Zn) = 0.56 \pm 0.2$ eV has been deduced[15].

The photochemistry of $Zn^+-(CH_4)$ and $Zn^+-(CH_3OH)$ complexes has been studied in detail[79,80]. In that context, the possibility of the formation of a metal-hydroxo insertion complex $[HO-Zn-CH_3]^+$ (the isomer of $[Zn-(CH_3OH)]^+$) has also been discussed[80]. In other series of studies, the mechanism of dimethylzinc[66,81–86], zinc monoethyl cation[87], diethylzinc[13,82–85,88], diethylzinc dimer[13] and dipropylzinc[85] photolysis has been investigated by photoionization techniques. It was the study of Borsella and Larciprete[84] that first observed different gas phase photodissociation mechanisms for Me_2Zn and Et_2Zn by using one- and two-color multiphoton ionization combined with TOF MS.

B. Gas Phase Ion/Molecule Reactions

Generally, gas phase ion/molecule reactions have been carried out with various MS techniques. In the last few decades, FT-ICR MS made a significant contribution to these studies[89–95]. The majority of gas phase reactions between organometallic or bare metal ions and neutral organic molecules correspond to one or several of the following processes: ligand substitution, dehydration of alcohols, dehydrohalogenation of alkyl halides, H_2 elimination from organic species, cleavage of C–C bonds and generation of small organic species from larger entities. A significant part of the gaseous ion/molecule reactions have been explained by assuming that the first step of the interaction is a Met^+ insertion into a bond of the organic molecule, generating insertion intermediates[92].

Reports about gas phase reactions involving Zn-containing ions, bare Zn^+ or gaseous Zn atoms are scarce. Danchevskaya and coworkers[96] studied the mechanism of methanol dehydrogenation in Zn vapors in the EI mass spectrometer, and the main intermediate product was determined to be ZnOMe. Schildcrout[97,98] reported the formation of the $[Zn_2L_3]^+$, $[Zn_2L_4]^+$ and $[Zn_3L_5]^+$ ions from the monomeric compound ZnL_2 (where L stands for β-diketonate) at high-pressure MS conditions. Po and coworkers[67] investigated the reactions of gaseous Zn atoms with H_3^+ (D_3^+) and CH_5^+ (CH_4D^+). However, the gas phase ion chemistry of Zn^+ with predilection to the ion/molecule reactions began only in 1980s[68,71–73,99], although to that date, studies involving many other metal ions in ion/molecule reactions had already been reported[95].

Given the relatively high ionization energy of atomic Zn (9.394 eV)[100], Zn^+ reacts with many neutral molecules (M) through charge transfer to produce M^+. Also, for some molecules reacting with Zn^+ ions, both charge transfer and M addition in different ratios were observed. The reports of such interactions, along with other gas phase ion/molecule reactions involving Zn-containing and C-containing species, are summarized in Table 5. Finally, examples when Zn^+ are unreactive toward the substrate have also been reported[103]. For instance, the ionization energy of H_2S (10.47 eV) is higher than that of Zn^+, and consequently the charge transfer or formation of any other products was not found[103]. The reactivity of diethylzinc under EI in FT-ICR MS conditions has been described as self-CI (Figure 4 and Scheme 1)[25]. The final product in the cascade of ion/molecule reactions between Zn-containing ions and neutral diethylzinc background has been determined to be a $[ZnC_8H_{17}]^+$ ion[27] (Table 5).

Schwarz and coworkers[92,110] studied the reactions of first-row transition-metal ions with different organic molecules and revealed a distinct influence of the individual Met^+ on the processes occurring in investigated systems. For example, by comparison with other metal ions, the studied closed *d*-shell ions Cu^+ and Zn^+ reacted with 2-methylbutanenitrile

TABLE 5. Gas phase ion/molecule reactions involving Zn-containing and C-containing species[a]

Ionization (MS)[b]	Cation	Reagent	Major product ion(s)	Other ions[c]	Reference
EI (GIB)	Zn^+	CH_3R[d]	$[ZnCH_3]^+$, $[R]^+$	$[ZnH]^+$, $[RCH_2]^+$, $[RCH_3]^+$	72
LV (HPMS)	Zn^+	*i*-C_4H_8	$[C_4H_8]^+$	—	118
ICP (SIFT)	Zn^+	C_6H_6	$[C_6H_6]^+$	$[Zn(C_6H_6)]^+$, $[Zn(C_6H_6)_2]^+$, $[Zn(C_6H_6)_3]^+$	121
LA (FT-ICR)	Zn^+	C_6H_6	$[C_6H_6]^+$	—	103
LA (FT-ICR)	Zn^+	$C_6H_5CH_3$	$[C_7H_8]^+$	—	103
LA (FT-ICR)	Zn^+	*p*-$(CH_3)_2C_6H_4$	$[C_8H_{10}]^+$	$[C_7H_7]^+$	103
LA (FT-ICR)	Zn^+	1,3,5-$(CH_3)_3C_6H_3$	$[C_9H_{12}]^+$	$[C_8H_{10}]^+$	103
SIMS	Zn^+	L[e]	$[L]^+$	—	120
LV (FT-ICR)	Zn^+	C_6H_5F	$[C_6H_5F]^+$	—	113
LV (FT-ICR)	Zn^+	C_6H_5Cl	$[C_6H_5Cl]^+$	$[C_6H_5]^+$	113
LV (FT-ICR)	Zn^+	C_6H_5Br	$[C_6H_5Br]^+$	$[C_6H_5]^+$	113
LV (FT-ICR)	Zn^+	C_6H_5I	$[C_6H_5I]^+$	$[C_6H_5]^+$	113
ICP (SIFT)	Zn^+	C_6F_6	$[Zn(C_6F_6)]^+$	$[ZnF]^+$	122
LA (FT-ICR)	Zn^+	Me_2O_2	$[C_2H_6O_2]^+$	—	119
LD (FT-ICR)	Zn^+	$NCCH(CH_3)C_2H_5$	$[Zn(NCCH(CH_3)C_2H_5)]^+$	$[Zn,H,C,N]^+$, $[NCCH(CH_3)C_2H_5]^+$	110
LD (FT-ICR)	Zn^+	$NCCH(C_2H_5)_2$	$[NCCH(C_2H_5)_2]^+$	$[Zn(NCCH(C_2H_5)_2]^+$	116
LD (FT-ICR)	Zn^+	*i*-PrNCO	$[Zn(HNCO)]^+$	$[Zn(C_3H_6)]^+$	111, 114, 117
LD (FT-ICR)	Zn^+	*s*-BuNCO	$[Zn(HNCO)]^+$	$[C_4H_9]^+$, $[Zn(C_4H_8)]^+$	117
LD (FT-ICR)	Zn^+	*t*-BuNCO	$[Zn(HNCO)]^+$	$[C_4H_9]^+$, $[Zn(C_4H_8)]^+$, $[C_4H_8]^+$	117
LD (FT-ICR)	Zn^+	*t*-PenNCO	$[Zn(HNCO)]^+$	$[C_5H_{11}]^+$, $[Zn(C_5H_{10})]^+$, $[C_5H_{10}]^+$	117
LD (FT-ICR)	Zn^+	*n*-C_4H_9NCS	$[C_4H_9NCS]^+$	$[Zn(HNCS)]^+$	115
LA (FT-ICR)	Zn^+	C_6H_5SH	$[C_6H_5SH]^+$	$[C_6H_6]^+$	103
LA (FT-ICR)	Zn^+	*p*-FC_6H_4SH	$[FC_6H_4SH]^+$	$[C_6H_4SH]^+$	103
LA (FT-ICR)	Zn^+	*n*-C_3H_7SH	$[C_3H_7SH]^+$ $[C_3H_7SH_2]^+$ $[Zn(C_3H_7SH)]^+$	$[Zn(C_3H_7SH)(C_3H_7S)]^+$ $[Zn(C_3H_7SH)_2(C_3H_7S)]^+$ $[C_2H_4SH]^+$, $[ZnS]^+$	103
LA (FT-ICR)	Zn^+	*n*-C_4H_9SH	$[C_4H_9SH_2]^+$ $[Zn(C_4H_9SH)]^+$	$[Zn(C_4H_9SH)_2]^+$ $[Zn(C_4H_9S)(C_4H_9SH)]^+$ $[Zn(C_4H_9S)(C_4H_9SH)_2]^+$ $[ZnS(C_4H_9S)(C_4H_9SH)]^+$	103
LA (FT-ICR)	Zn^+	*i*-C_4H_9SH	$[C_4H_9SH]^+$	$[Zn(C_4H_9SH)]^+$ $[C_4H_9SH_2]^+$, $[C_4H_8]^+$	103

LA (FT-ICR)	Zn^+	*s*-C_4H_9SH	$[ZnC_4H_8]^+$ $[Zn(C_4H_9SH)]^+$	$[C_4H_9SH]^+$, $[C_4H_9SH_2]^+$ $[Zn(SH)(C_4H_9SH)]^+$ $[Zn(C_4H_9S)(C_4H_9SH)]^+$ $[Zn(C_4H_9S)(C_4H_9SH)_2]^+$	103
LA (FT-ICR)	Zn^+	*t*-C_4H_9SH	$[C_4H_9SH_2]^+$	$[C_4H_9SH]^+$, $[C_4H_9]^+$ $[Zn(C_4H_9SH)]^+$	103
DC/FT (GIB)	Zn^+	COS	$[ZnS]^+$	—	77
DC/FT (GIB)	Zn^+	CS_2	$[CS_2]^+$	$[ZnS]^+$, $[ZnCS]^+$	77
LD (FT-ICR)	$[Zn_2]^+$	*c*-C_6H_{10}	$[C_6H_{10}]^+$	—	15
LD (FT-ICR)	$[Zn_2]^+$	alkenes[f]	[Zn(alkene)]$^+$	—	15
LD (FT-ICR)	$[Zn_2]^+$	alcohols[g]	[Zn(alcohol)]$^+$	—	15
EI (HPMS)	$[CH_4D]^+$	Zn(g)[h]	$[ZnH]^+$	—	67
EI (HPMS)	$[C_2H_6D]^+$	Zn(g)	$[ZnH]^+$	—	67
EI (FT-ICR)	$[C_2H_3]^+$	$Zn(C_2H_5)_2$	$[ZnC_2H_5]^+$	$[ZnC_4H_9]^+$, $[ZnC_4H_{10}]^+$	27
EI (FT-ICR)	$[C_2H_5]^+$	$Zn(C_2H_5)_2$	$[ZnC_2H_5]^+$	$[ZnC_4H_9]^+$, $[ZnC_4H_{10}]^+$	27
EI (FT-ICR)	$[C_3H_5]^+$	$Zn(C_2H_5)_2$	$[ZnC_2H_5]^+$	$[ZnC_4H_9]^+$, $[ZnC_4H_{10}]^+$	27
EI (FT-ICR)	Ar^+	$Zn(C_2H_5)_2$	$[ZnC_2H_5]^+$, $[C_2H_5]^+$	$[C_2H_3]^+$, Zn^+, $[ZnH]^+$, $[Zn(C_2H_5)_2]^+$, $[ZnC_4H_9]^+$, $[C_4H_7]^+$	27
EI (FT-ICR)	Zn^+	$Zn(C_2H_5)_2$	$[Zn(C_2H_5)_2]^+$	$[ZnC_2H_5]^+$, $[Zn_2C_2H_5]^+$	27
EI (FT-ICR)	$[ZnC_2H_5]^+$	$Zn(C_2H_5)_2$	$[ZnC_4H_9]^+$	$[Zn_2C_6H_{15}]^+$, $[Zn_2C_4H_{11}]^+$	27
EI (FT-ICR)	$[Zn(C_2H_5)_2]^+$	$Zn(C_2H_5)_2$	$[Zn_2C_6H_{15}]^+$	$[ZnC_8H_{17}]^+$, $[Zn_2C_4H_{11}]^+$	27
EI (FT-ICR)	$[ZnC_4H_9]^+$	$Zn(C_2H_5)_2$	$[Zn_2C_6H_{15}]^+$	$[ZnC_8H_{17}]^+$, $[Zn_2C_4H_{11}]^+$	27
EI (FT-ICR)	$[Zn_2C_4H_{11}]^+$	$Zn(C_2H_5)_2$	$[ZnC_8H_{17}]^+$	$[Zn_2C_6H_{15}]^+$	27
EI (FT-ICR)	$[Zn_2C_6H_{15}]^+$	$Zn(C_2H_5)_2$	$[ZnC_8H_{17}]^+$	—	27
Self-CI (FT-ICR)	Zn^+	$Zn(C_2H_5)_2$	$[Zn(C_2H_5)_2]^+$	—	25
Self-CI (FT-ICR)	$[ZnC_2H_5]^+$	$Zn(C_2H_5)_2$	$[Zn_2C_6H_{15}]^+$	$[Zn_2C_4H_{11}]^+$	25
Self-CI (FT-ICR)	$[Zn(C_2H_5)_2]^+$	$Zn(C_2H_5)_2$	$[ZnC_2H_5]^+$	$[ZnC_4H_9]^+$	25
EI (FT-ICR)	$[Cp_2ZrCH_3]^+$	$Zn(CH_3)_2$	$[Cp_2Zr(\mu\text{-}CH_2)(\mu\text{-}CH_3)Zn]^+$	[i]	112

[a] For other reports describing gas phase ion/molecule reactions involving Zn-containing species which are not included in this table, refer to References 67, 71, 75, 76, 96–99, 101–109.
[b] See Abbreviation section for meaning of acronyms.
[c] Dash = no observed ions.
[d] R = CH_3, C_2H_5, *i*-C_3H_7, *t*-C_4H_9.
[e] L = dimethyl[2.*n*]paracyclophane-enes (n = 3, 4, 5, 6).
[f] alkenes = C_2–C_7 alkenes.
[g] alcohols = C_1–C_3 alcohols.
[h] Zn(g) = zinc vapor.
[i] CID spectrum of $[Cp_2Zr(\mu\text{-}CH_2)(\mu\text{-}CH_3)Zn]^+$ revealed peaks due to $[Cp_2ZrCH_3]^+$, $[ZrCp]^+$ and $[ZnCH_3]^+$

differently, in particular by forming intermediates of ion/dipole complexes[110]. The detection of the $[Zn(HNCS)]^+$ product ion in the reaction between Zn^+ and butyl isothiocyanate has also been rationalized in terms of the ion/dipole mechanism[115]. In another study, there were no indications of any C−C or C−H bond activation of cyclohexane by Zn^+ ion, although some other metal ions generated $[Met(C_3H_6)]^+$ or mediated single or multiple dehydrogenation of *c*-C_6H_{12} yielding $[Met(benzene)]^+$ as the main product ion[104].

For $[Zn_2]^+$, a rapid displacement of a Zn atom in reactions with alcohols and alkenes was observed[15]. This process is consistent with the weak bonding in the $[Zn_2]^+$ ion.

Literature analysis shows that various ionization methods have been applied in the studies concerning the gas phase ion chemistry of Zn^+. Presumably, in many of the described experiments (Table 5), Zn^+ ions are in the ground electronic state. This is assumed because of the large energy difference (6.01 eV)[72] between the ground state ($3d^{10}4s^1$) and the first excited state ($3d^{10}4p^1$) of Zn^+. Georgiadis and Armentrout[72] used EI with an electron energy of 15 eV ensuring only the generation of ground state Zn^+ ions.

C. *In silico* Studies of Organozinc Ion Structures

Computational chemistry procedures describing the geometry and thermochemistry of gaseous ions are often used to predict and support experimental data. This approach has also been employed to investigate the structure and energetics of some organozinc ions at different levels of theory. Cations and anions having a Zn−C bond which were studied *in silico* are listed in Tables 6 and 7, respectively.

TABLE 6. Zn−C bond-containing cations studied *in silico*

No.	Cation	Zn bonding environment	Reference
1	$[ZnC]^+$	$[Zn-C]^+$	125
2	$[ZnCH]^+$	$[Zn-CH]^+$	126
3	$[Zn(C, H, N)]^+$	$[Zn-CNH]^+$	123, 124
4	$[Zn(C, H, N)]^+$	$[H-Zn-CN]^+$	123, 124
5	$[ZnCH_2]^+$	$[Zn-CH_2]^+$	126, 127
6	$[ZnCH_2]^{2+}$	$[Zn-CH_2]^{2+}$	127
7	$[ZnCH_3]^+$	$[Zn-CH_3]^+$	126, 128–135
8	$[ZnCH_4]^+$	$[Zn-CH_4]^+$	79
9	$[Zn(CH_3OH)]^+$	$[HO-Zn-CH_3]^+$	80
10	$[Zn(C_2, H_3, N)]^+$	$[Zn-CNCH_3]^+$	123, 124
11	$[Zn(C_2, H_3, N)]^+$	$[Zn-CH_2CNH]^+$	123, 124
12	$[Zn(C_2, H_3, N)]^+$	$[H-Zn-CNCH_2]^+$	123, 124
13	$[Zn(C_2, H_3, N)]^+$	$[H-Zn-CH_2CN]^+$	123, 124
14	$[Zn(C_2, H_3, N)]^+$	$[H-Zn-CH_2NC]^+$	123, 124
15	$[Zn(C_2, H_3, N)]^+$	$[NC-Zn-CH_3]^+$	123, 124
16	$[Zn(C_2, H_3, N)]^+$	$[CN-Zn-CH_3]^+$	123, 124
17	$[ZnC_2H_5]^+$	$[Zn-CH_2CH_3]^+$	25, 87
18	$[Zn(CH_3)_2]^+$	$[H_3C-Zn-CH_3]^+$	130–132, 136
19	$[ZnC_4H_9]^+$	$[(C_2H_4)-Zn-(C_2H_5)]^+$	25
20	$[ZnC_4H_{10}]^+$	$[(C_2H_5)-Zn-(C_2H_5)]^+$	25
21	$[Zn(C_5H_5)]^+$	$[Zn(\eta^1\text{-}C_5H_5)]^+$	32
22	$[Zn(C_5H_5)]^+$	$[Zn(\eta^2\text{-}C_5H_5)]^+$	32
23	$[Zn(C_5H_5)]^+$	$[Zn(\eta^5\text{-}C_5H_5)]^+$	31, 32
24	$[Zn(C_6H_6)]^+$	$[Zn-(C_6H_6)]^+$	121
25	$[Zn(C_6H_6)_2]^+$	$[(C_6H_6)-Zn-(C_6H_6)]^+$	121
26	$[Zn_2CH_2]^+$	$[Zn-CH_2-Zn]^+$	137
27	$[Zn_2C_2]^+$	$[Zn-C\equiv C-Zn]^+$	137

TABLE 7. Zn−C bond-containing anions studied *in silico*

No.	Anion	Zn bonding environment	Reference
1	$[ZnC]^-$	$[Zn-C]^-$	125
2	$[ZnCH_3]^-$	$[Zn-CH_3]^-$	133
3	$[Zn(CH_3)_3]^-$	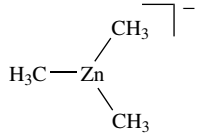	138
4	$[Zn(CH_3)_4]^{2-}$	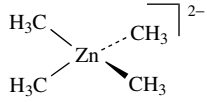	138
5	$[Zn(C_5H_5)]^-$	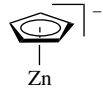	31
6	$[H_2Zn(C_5H_5)]^-$	$[H_2-Zn-(C_5H_5)]^-$	32
7	$[Zn_n(CN)_{2n+1}]^-$	$[(NC)_2Zn\{(\mu\text{-}CN)Zn(CN)\}_{n-1}(CN)]^-$	12

Calculations by the MNDO (modified neglect of diatomic overlap) method with full optimization of geometry were carried out for [Zn, N, C, H]$^+$ ions indicating the possible existence of four stable isomers (Figure 7). According to the same semi-empirical method, [Zn, N, C_2, H_3]$^+$ ions can form nine stable isomeric structures (Figure 7)[123, 124]. In a separate study by density functional theory, self-assembled helicate architectures have been proposed for ions of the $[Zn_n(CN)_{2n+1}]^-$ series[12].

Three isomeric structures were predicted for $[ZnCp]^+$ ions[32]. The most stable was determined to be the η^2-bound isomer. The η^1- and η^5-bound structures were *ca* 0.14 and 0.35 eV higher in energy than the η^2-bound isomer. All structures were optimized using a package of *ab initio* programs[32]. For the $[ZnCp]^-$ ion, only the η^5-bound structure has been examined[31].

V. OTHER STUDIES INVOLVING MASS SPECTROMETRY

Zinc-containing complexes have applications in many areas. The monitoring of compound purity, degradation or modification during different processes is sometimes crucial for the success of the endeavor. Mass spectrometry has become a common tool for prompt analysis and has been applied to investigations involving a variety of Zn-containing species[139–177].

A. Mass Spectrometric Investigation of Pyrolysis of Zinc-containing Species

Thermal decomposition of $Zn(CH_3)_2$ or its co-pyrolysis with other organoelement compounds has been studied mass spectrometrically[139–142]. Only two Zn-containing ions ($[ZnCH_3]^+$ and $[Zn]^+$) were detected at 100 °C from the co-pyrolysis of an equimolar mixture of *t*-butyl(allyl)selenium and dimethylzinc[140]. The relative intensities of the peaks corresponding to the $[ZnCH_3]^+$ and $[Zn]^+$ ions diminish as the temperature increases, becoming negligible at $T > 320$ °C.

The pyrolysis of $Zn(C_2H_5)_2$ and that of organotellurium compounds have been studied both separately and in combination by using an isothermal reactor coupled with a MS

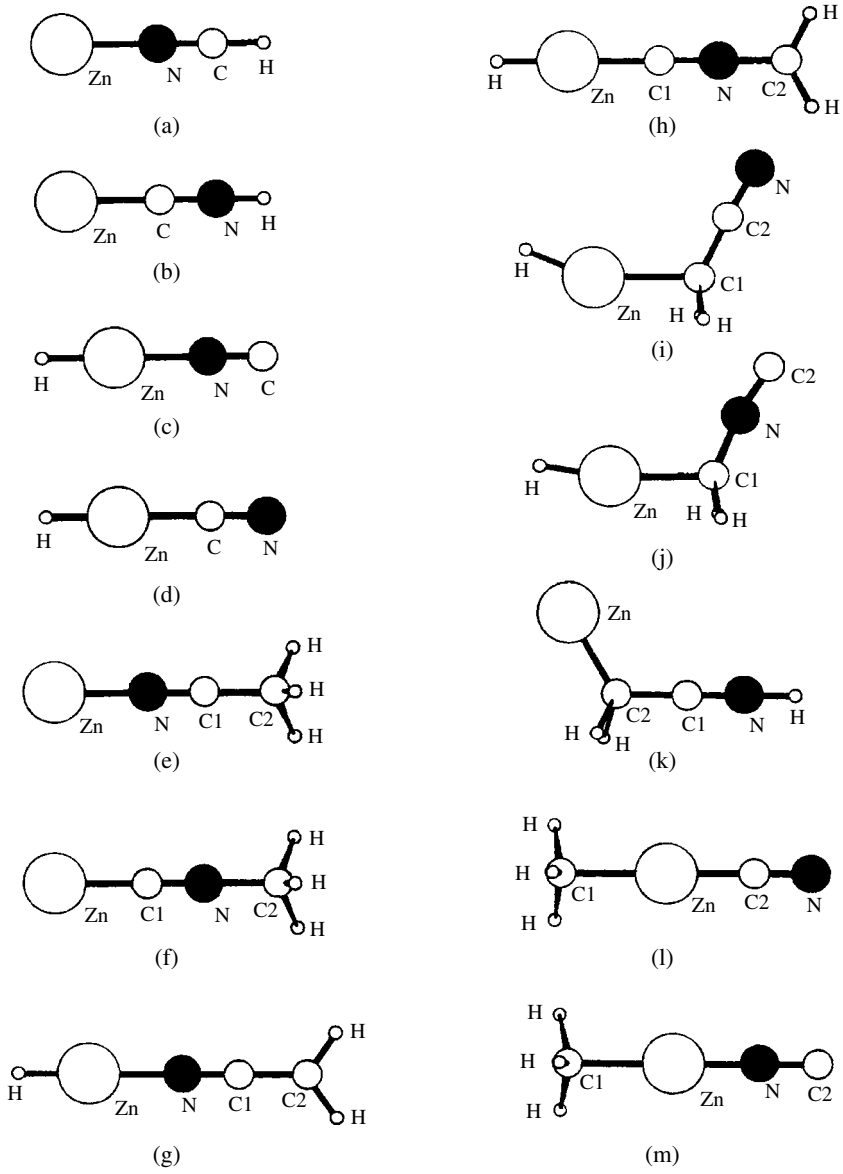

FIGURE 7. The calculated structures of (a)–(d) four isomers of [Zn, N, C, H]$^+$ ions and (e)–(m) nine isomers of [Zn, N, C_2, H_3]$^+$ ions using the MNDO method with full optimization of geometry. Reproduced by permission of John Wiley & Sons Ltd. from Reference 123

instrument[142–146]. At room temperature, $[Zn(C_2H_5)_2]^+$, $[ZnC_2H_5]^+$, $[Zn]^+$ and $[C_2H_5]^+$ ions were detected. These ions were clearly produced from $Zn(C_2H_5)_2$ under EI. When the temperature was increased to 400 °C, the abundances of all these ions decreased, and several new peaks appeared in the mass spectra. These new peaks corresponded to the $[C_2H_4]^+$, $[C_3H_7]^+$ and $[C_4H_{10}]^+$ ions, which were derived from the *n*-butane newly formed during pyrolysis[143–145].

Unexpectedly, thermal decomposition of bis(pyridine)bis(trifluoromethyl)zinc, $Zn(CF_3)_2 \cdot 2C_5H_5N$ **(76)**, gave rise to CF_3H, which is believed to be a result of proton abstraction from pyridine by the trifluoromethyl group. Pyridine has been identified as the major product of the decomposition. No Zn-containing ions were detected for **76**[147].

Recently, the *in situ* thermal decomposition monitoring capability of TOF-SIMS has been reported, in which zinc acetate dihydrate, $Zn(CH_3COO)_2 \cdot 2H_2O$ **(77)**, decomposed to form ZnO nanoparticles[148]. The only organozinc ions detected at room temperature were $[ZnCH_3]^+$ (in the positive-ion mode) and $[OZnCH_3]^-$ (in the negative-ion mode), both of relatively low abundances.

B. Monitoring of Organometallic Vapor Phase Epitaxy by Mass Spectrometry

Organozinc compounds have an extensive use in the electronics industry for the manufacture of various Zn-containing semiconductor materials through the vapor phase growth technique of organometallic chemical vapor deposition (OMCVD). This technique is also known as MOCVD (metalorganic chemical vapor deposition), MOVPE (metalorganic vapor phase epitaxy) and OMVPE (organometallic vapor phase epitaxy). Mass spectrometry is used extensively in this field to monitor the purity of organometallic precursors, the incorporation of alkyl fragments (e.g. carbon) in the epitaxial layers or the incorporation of the desired dopants in the final semiconductor materials[158–177].

VI. CONCLUSIONS

Mass spectrometry has found various applications in the chemistry of zinc–carbon bonds. The availability of a variety of ionization techniques has made possible the identification of different types of organozinc compounds—volatile, neutral, ionic, dimeric, polymetallic, solvent-containing etc. In the majority of the reported cases, molecular species have been observed. The experimental results demonstrated that Zn–C bonds are rather weak and easily cleaved upon or after ionization. It is obvious, however, that expanding mass spectrometry-based methods of analysis of zinc complexes will greatly benefit this field of chemistry, as well as facilitate applications of organozinc compounds to material sciences.

It should also be noted that significant progress has been made in the measuring of thermochemical parameters of organozinc complexes. Ionization energies were measured and the dissociation characteristics of ions were determined. The experimental results for gaseous Zn-containing ions were supported by quantum-chemical calculations.

The study of gas phase reactions between ions and neutral species is an application of mass spectrometry to organozinc chemistry with only partially explored potential. These experiments could be useful for the understanding of mechanisms of selected reactions as well as for the structural characterization of unstable intermediates.

VII. REFERENCES

1. E. Frankland, *Liebigs Ann. Chem.*, **71**, 171 (1849); *J. Chem. Soc.*, **2**, 263 (1850).
2. E. Frankland, *Liebigs Ann. Chem.*, **71**, 213 (1849); *J. Chem. Soc.*, **2**, 297 (1850).
3. E. Frankland, *Experimental Researches in Pure, Applied and Physical Chemistry*, John van Voorst, London, 1877.

4. D. Seyferth, *Organometallics*, **20**, 2940 (2001).
5. F. W. Aston, *Phil. Mag.*, **45**, 934 (1923); *Proc. R. Soc. London*, **A130**, 302 (1931); **A149**, 396 (1935); *Nature*, **122**, 345 (1928); **130**, 847 (1932).
6. K. T. Bainbridge, *Phys. Rev.*, **39**, 847 (1932).
7. J. R. de Laeter, *Applications of Inorganic Mass Spectrometry*, Wiley, New York, 2001.
8. J. R. de Laeter, J. K. Böhlke, P. de Bièvre, H. Hidaka, H. S. Peiser, K. J. R. Rosman and P. D. P. Taylor, *Pure Appl. Chem.*, **75**, 683 (2003).
9. Yu. N. Sukharev, Yu. S. Nekrasov, N. S. Molgachova and E. E. Tepfer, *Org. Mass Spectrom.*, **26**, 770 (1991).
10. I. Resa, E. Carmona, E. Gutierrez-Puebla and A. Monge, *Science*, **305**, 1136 (2004).
11. K. Merz, S. Block, R. Schoenen and M. Driess, *J. Chem. Soc., Dalton Trans.*, 3365 (2003).
12. I. G. Dance, P. A. W. Dean, K. J. Fisher and H. H. Harris, *Inorg. Chem.*, **41**, 3560 (2002).
13. H.-Q. Hou, Z. Zhang, U. Ray and M. Vernon, *J. Chem. Phys.*, **92**, 1728 (1990).
14. I. Katakuse, T. Ichihara, M. Morris, T. Matsuo, T. Sakurai and H. Matsuda, *Int. J. Mass Spectrom. Ion Proc.*, **91**, 85 (1989).
15. S. W. Buckner, J. R. Gord and B. S. Freiser, *J. Chem. Phys.*, **88**, 3678 (1988).
16. K. Skudlarski, J. Dudek and J. Kapał, *J. Chem. Thermodynamics*, **19**, 151 (1987).
17. B. Adler, A. Lachowicz and K.-H. Thiele, *Z. Anorg. Allg. Chem.*, **423**, 27 (1976).
18. M. R. Litzow and T. R. Spalding, *Mass Spectrometry of Inorganic and Organometallic Compounds*, Chap. 5, Elsevier, Amsterdam, 1973, pp. 97–113.
19. K. Matsumoto, N. Kiba and T. Takeuchi, *Anal. Chem.*, **43**, 1691 (1971).
20. H. Bloom, B. V. O'Grady, R. G. Anthony and V. C. Reinsborough, *Aust. J. Chem.*, **23**, 843 (1970).
21. R. W. Kiser, J. G. Dillard and D. L. Dugger, '*Mass Spectrometry of Inorganic Halides*' in *Mass Spectrometry in Inorganic Chemistry, Adv. Chem. Ser.*, **72**, 153 (1968).
22. F. J. Keneshea and D. Cubicciotti, *J. Chem. Phys.*, **40**, 191 (1964).
23. A. Büchler, J. L. Stauffer and W. Klemperer, *J. Chem. Phys.*, **40**, 3471 (1964).
24. A. Büchler, J. L. Stauffer and W. Klemperer, *J. Am. Chem. Soc.*, **86**, 4544 (1964).
25. M. A. Freitas, S. R. Dillon, R. C. Dougherty and A. G. Marshall, *Rapid Commun. Mass Spectrom.*, **13**, 1622 (1999).
26. R. E. Winters and R. W. Kiser, *J. Organomet. Chem.*, **10**, 7 (1967).
27. C. Q. Jiao, C. A. DeJoseph, Jr. and A. Garscadden, *Int. J. Mass Spectrom.*, **235**, 83 (2004).
28. D. Naumann, C. Schorn and W. Tyrra, *Z. Anorg. Allg. Chem.*, **625**, 827 (1999).
29. A. Haaland, S. Samdal, N. V. Tverdova, G. V. Girichev, N. I. Giricheva, S. A. Shlykov, O. G. Garkusha and B. V. Lokshin, *J. Organomet. Chem.*, **684**, 351 (2003).
30. V. M. Rayón and G. Frenking, *Chem. Eur. J.*, **8**, 4693 (2002).
31. V. G. Zakrzewski and J. V. Ortiz, *J. Phys. Chem.*, **98**, 13198 (1994).
32. P. H. M. Budzelaar, J. J. Engelberts and J. H. van Lenthe, *Organometallics*, **22**, 1562 (2003).
33. K.-H. Thiele, V. Dimitrov and J. Thielemann, *Z. Anorg. Allg. Chem.*, **483**, 145 (1981).
34. S. Brooker, N. Bertel, D. Stalke, M. Noltemeyer, H. W. Roesky, G. M. Sheldrick and F. T. Edelmann, *Organometallics*, **11**, 192 (1992).
35. H. Nehl and W. R. Scheidt, *J. Organomet. Chem.*, **289**, 1 (1985).
36. G. Allen, J. M. Bruce, D. W. Farren and F. G. Hutchinson, *J. Chem. Soc., B*, 799 (1966).
37. J. M. Bruce, B. C. Cutsforth, D. W. Farren, F. G. Hutchinson, F. M. Rabagliati and D. R. Reed, *J. Chem. Soc., B*, 1020 (1966).
38. K.-H. Thiele, B. Adler, H. Grahlert and A. Lachowicz, *Z. Anorg. Allg. Chem.*, **403**, 279 (1974).
39. D. Schröder, H. Schwarz, S. Polarz and M. Driess, *Phys. Chem. Chem. Phys.*, **7**, 1049 (2005).
40. M. Krieger, R. O. Gould, K. Harms, S. Parsons and K. Dehnicke, *Chem. Ber.*, **129**, 1621 (1996).
41. M. Westerhausen, A. N. Kneifel and A. Kalisch, *Angew. Chem., Int. Ed.*, **44**, 96 (2005).
42. M. Westerhausen, T. Bollwein, N. Makropoulos, S. Schneiderbauer, M. Suter, H. Nöth, P. Mayer, H. Piotrowski, K. Polborn and A. Pfitzner, *Eur. J. Inorg. Chem.*, 389 (2002).
43. M. Westerhausen, T. Bollwein, P. Mayer and H. Piotrowski, *Z. Anorg. Allg. Chem.*, **628**, 1425 (2002).
44. M. Westerhausen, T. Bollwein, A. Pfitzner, T. Nilges and H.-J. Deiseroth, *Inorg. Chim. Acta*, **312**, 239 (2001).

45. M. P. Coles and P. B. Hitchcock, *Eur. J. Inorg. Chem.*, 2662 (2004).
46. D. Walther, T. Döhler, N. Theyssen and H. Görls, *Eur. J. Inorg. Chem.*, 2049 (2001).
47. M. B. Hursthouse, M. A. Malik, M. Motevalli and P. O'Brien, *Organometallics*, **10**, 730 (1991).
48. M. S. Hill and P. B. Hitchcock, *J. Chem. Soc., Dalton Trans.*, 4694 (2002).
49. S. K. Pandey, A. Steiner, H. W. Roesky and D. Stalke, *Inorg. Chem.*, **32**, 5444 (1993).
50. A. P. Dove, V. C. Gibson, E. L. Marshall, A. J. P. White and D. J. Williams, *J. Chem. Soc., Dalton Trans.*, 570 (2004).
51. A. Looney, R. Han, I. B. Gorrell, M. Cornebise, K. Yoon, G. Parkin and A. L. Rheingold, *Organometallics*, **14**, 274 (1995).
52. J.-S. Herrmann, G. A. Luinstra and P. W. Roesky, *J. Organomet. Chem.*, **689**, 2720 (2004).
53. M. Westerhausen, M. Wieneke and W. Schwarz, *J. Organomet. Chem.*, **522**, 137 (1996).
54. I. Hegelmann, A. Beck, C. Eichhorn, B. Weibert and N. Burzlaff, *Eur. J. Inorg. Chem.*, 339 (2003).
55. J. L. Atwood, D. E. Berry, S. R. Stobart and M. J. Zaworotko, *Inorg. Chem.*, **22**, 3480 (1983).
56. S. V. Pasenok, N. V. Kirij, Yu. L. Yagupolskii, D. Naumann, W. Tyrra and A. Fitzner, *Z. Anorg. Allg. Chem.*, **625**, 834 (1999).
57. N. Seidel, K. Jacob, P. Zanello and M. Fontani, *J. Organomet. Chem.*, **620**, 243 (2001).
58. K. Soai, T. Hayase and K. Takai, *Tetrahedron: Asymmetry*, **6**, 637 (1995).
59. A. A. Danopoulos, G. Wilkinson, T. K. N. Sweet and M. B. Hursthouse, *J. Chem. Soc., Dalton Trans.*, 205 (1995).
60. M. Westerhausen, M. Wieneke, W. Ponikwar, H. Nöth and W. Schwarz, *Organometallics*, **17**, 1438 (1998).
61. M. Das and S. E. Livingstone, *Aust. J. Chem.*, **28**, 513 (1975).
62. M. J. Lacey, C. G. MacDonald and J. S. Shannon, *Org. Mass Spectrom.*, **1**, 115 (1968).
63. I. G. Dance, P. A. W. Dean and K. J. Fisher, *Angew. Chem., Int. Ed. Engl.*, **34**, 314 (1995).
64. A. Haaland, J. C. Green, G. S. McGrady, A. J. Downs, E. Gullo, M. J. Lyall, J. Timberlake, A. V. Tutukin, H. V. Volden and K.-A. Østby, *J. Chem. Soc., Dalton Trans.*, 4356 (2003).
65. G. M. Bancroft, D. K. Creber, M. A. Ratner, J. W. Moskowitz and S. Topiol, *Chem. Phys. Lett.*, **50**, 233 (1977).
66. G. DiStefano and V. H. Dibeler, *Int. J. Mass Spectrom. Ion Phys.*, **4**, 59 (1970).
67. P. L. Po, T. P. Radus and R. F. Porter, *J. Phys. Chem.*, **82**, 520 (1978).
68. M. M. Kappes and R. H. Staley, *J. Phys. Chem.*, **85**, 942 (1981).
69. P. B. Armentrout, L. F. Halle and J. L. Beauchamp, *J. Am. Chem. Soc.*, **103**, 6501 (1981).
70. M. L. Mandich, L. F. Halle and J. L. Beauchamp, *J. Am. Chem. Soc.*, **106**, 4403 (1984).
71. J. E. Bartmess and J. G. Kester, *Inorg. Chem.*, **23**, 1877 (1984).
72. R. Georgiadis and P. B. Armentrout, *J. Am. Chem. Soc.*, **108**, 2119 (1986).
73. R. Georgiadis and P. B. Armentrout, *J. Phys. Chem.*, **92**, 7060 (1988).
74. R. Georgiadis, E. R. Fisher and P. B. Armentrout, *J. Am. Chem. Soc.*, **111**, 4251 (1989).
75. D. E. Clemmer, N. F. Dalleska and P. B. Armentrout, *J. Chem. Phys.*, **95**, 7263 (1991).
76. B. L. Kickel and P. B. Armentrout, *J. Phys. Chem.*, **99**, 2024 (1995).
77. C. Rue, P. B. Armentrout, I. Kretzschmar, D. Schröder and H. Schwarz, *J. Phys. Chem. A*, **106**, 9788 (2002).
78. P. B. Armentrout, *Int. J. Mass Spectrom.*, **227**, 289 (2003).
79. W.-Y. Lu, T.-H. Wong and P. D. Kleiber, *Chem. Phys. Lett.*, **347**, 183 (2001).
80. W.-Y. Lu, T.-H. Wong, Y. Sheng, A. T. Lytle and P. D. Kleiber, *J. Phys. Chem. A*, **107**, 984 (2003).
81. C. F. Yu, F. Youngs, K. Tsukiyama, R. Bersohn and J. Preses, *J. Chem. Phys.*, **85**, 1382 (1986).
82. R. Larciprete and E. Borsella, *Chem. Phys. Lett.*, **147**, 161 (1988).
83. R. Larciprete and E. Borsella, *Il Nuovo Cimento della Società Italiana di Fisica, D: Condensed Matter, Atomic, Molecular and Chemical Physics, Fluids, Plasmas, Biophysics*, **11D**, 1603 (1989); *Chem. Abstr.*, **112**, 217120e (1990).
84. E. Borsella and R. Larciprete, *Appl. Surf. Sci.*, **36**, 221 (1989).
85. R. L. Jackson, *J. Chem. Phys.*, **96**, 5938 (1992).
86. J. A. Elias, P. J. Wisoff and W. L. Wilson, Jr., *J. Appl. Phys.*, **74**, 6962 (1993).
87. M. B. Pushkarsky, V. L. Stakhursky and T. A. Miller, *J. Phys. Chem. A*, **104**, 9184 (2000).

88. P. F. Seidler, *J. Phys. Chem.*, **98**, 2095 (1994).
89. K. J. Fisher, *Prog. Inorg. Chem.*, **50**, 343 (2001).
90. B. S. Freiser, *Acc. Chem. Res.*, **27**, 353 (1994).
91. K. Eller, *Coord. Chem. Rev.*, **126**, 93 (1993).
92. K. Eller and H. Schwarz, *Chem. Rev.*, **91**, 1121 (1991).
93. D. H. Russell (Ed.), *Gas Phase Inorganic Chemistry*, Plenum Press, New York, 1989.
94. J. Allison, *Prog. Inorg. Chem.*, **34**, 627 (1986).
95. T. R. Spalding, '*Mass Spectrometry of Organometallic Compounds*', Chap. 22 in *The Chemistry of the Metal–Carbon Bond* (Eds. F. R. Hartley and S. Patai), Vol. 1, Wiley, New York, 1982, pp. 919–969.
96. M. N. Danchevskaya, G. P. Panasyuk and N. I. Kobozev, *Zh. Fiz. Khim.*, **35**, 2125 (1961); *Chem. Abstr.*, **56**, 9457e (1962).
97. S. M. Schildcrout, *J. Phys. Chem.*, **80**, 2834 (1976).
98. S. M. Schildcrout, *Inorg. Chem.*, **19**, 224 (1980).
99. S. J. Babinec and J. Allison, *J. Am. Chem. Soc.*, **106**, 7718 (1984).
100. C. M. Brown, S. G. Tilford and M. L. Ginter, *J. Opt. Soc. Am.*, **65**, 1404 (1975).
101. D. E. Clemmer and P. B. Armentrout, *J. Chem. Phys.*, **97**, 2451 (1992).
102. D. Schröder and H. Schwarz, *Angew. Chem., Int. Ed. Engl.*, **32**, 1420 (1993).
103. J. H. El-Nakat, I. G. Dance, K. J. Fisher and G. D. Willett, *Polyhedron*, **13**, 409 (1994).
104. K. Seemeyer, D. Schröder, M. Kempf, O. Lettau, J. Müller and H. Schwarz, *Organometallics*, **14**, 4465 (1995).
105. I. G. Dance, K. J. Fisher and G. D. Willett, *Inorg. Chem.*, **35**, 4177 (1996).
106. G. K. Koyanagi, D. Caraiman, V. Blagojevic and D. K. Bohme, *J. Phys. Chem. A*, **106**, 4581 (2002).
107. M. Y. Combariza and R. W. Vachet, *J. Phys. Chem. A*, **108**, 1757 (2004).
108. M. Y. Combariza, J. T. Fermann and R. W. Vachet, *Inorg. Chem.*, **43**, 2745 (2004).
109. B. S. Fox-Beyer, Z. Sun, I. Bălteanu, O. P. Balaj and M. K. Beyer, *Phys. Chem. Chem. Phys.*, **7**, 981 (2005).
110. K. Eller, W. Zummack and H. Schwarz, *J. Am. Chem. Soc.*, **112**, 621 (1990).
111. K. Eller and H. Schwarz, *Ber. Bunsenges. Phys. Chem.*, **94**, 1339 (1990).
112. A. R. Siedle, R. A. Newmark, J. N. Schroepfer and P. A. Lyon, *Organometallics*, **10**, 400 (1991).
113. A. Bjarnason, *Organometallics*, **10**, 1244 (1991).
114. K. Eller and H. Schwarz, *Int. J. Mass Spectrom. Ion Proc.*, **108**, 87 (1991).
115. K. Eller, S. Akkök and H. Schwarz, *Helv. Chim. Acta*, **74**, 1609 (1991).
116. K. Eller, S. Karrass and H. Schwarz, *Organometallics*, **11**, 1637 (1992).
117. K. Eller, D. Schröder and H. Schwarz, *J. Am. Chem. Soc.*, **114**, 6173 (1992).
118. G. M. Daly, Y. B. Pithawalla, Z. Yu and M. S. El-Shall, *Chem. Phys. Lett.*, **237**, 97 (1995).
119. R. Wesendrup, C. A. Schalley, D. Schröder and H. Schwarz, *Chem. Eur. J.*, **1**, 608 (1995).
120. H.-F. Grützmacher, S. Zorić and C. Wellbrock, *Int. J. Mass Spectrom.*, **210/211**, 311 (2001).
121. G. K. Koyanagi and D. K. Bohme, *Int. J. Mass Spectrom.*, **227**, 563 (2003).
122. D. Caraiman, G. K. Koyanagi and D. K. Bohme, *J. Phys. Chem. A*, **108**, 978 (2004).
123. S. P. Palii, N. I. Raevskii, D. V. Zagorevskii, K. M. Indrichan, Yu. A. Borisov, N. V. Gerbeleu and Yu. S. Nekrasov, *Org. Mass Spectrom.*, **26**, 742 (1991).
124. S. P. Palii, *Ph.D. Thesis*, Institute of Chemistry of the Academy of Sciences of the Republic of Moldova (Chişinău, Moldova) and Physico-Chemistry Institute of the Ukrainian Academy of Sciences (Odessa, Ukraine, USSR), 1991.
125. G. L. Gutsev, L. Andrews and C. W. Bauschlicher, Jr., *Theor. Chem. Acc.*, **109**, 298 (2003).
126. J. Li, D. Feng and S. Feng, *Science in China, Series B: Chem.*, **42**, 283 (1999).
127. M. A. San Miguel, A. Márquez and J. Fernández Sanz, *J. Am. Chem. Soc.*, **118**, 429 (1996).
128. T. Ziegler, V. Tschinke and A. Becke, *J. Am. Chem. Soc.*, **109**, 1351 (1987).
129. J. B. Schilling, W. A. Goddard III and J. L. Beauchamp, *J. Am. Chem. Soc.*, **109**, 5573 (1987).
130. M. J. S. Dewar and K. M. Merz, Jr., *Organometallics*, **5**, 1494 (1986).
131. M. J. S. Dewar and K. M. Merz, Jr., *Organometallics*, **7**, 522 (1988).
132. J. J. P. Stewart, *J. Comput. Chem.*, **12**, 320 (1991).
133. V. G. Zakrzewski and J. V. Ortiz, *J. Chem. Phys.*, **100**, 6508 (1994).
134. V. A. Shagun, S. G. Shevchenko and Yu. L. Frolov, *J. Struct. Chem. (Transl. of Zh. Strukt. Khim.)*, **44**, 736 (2003).

135. E. N. Brothers, D. Suarez, D. W. Deerfield II and K. M. Merz, Jr., *J. Comput. Chem.*, **25**, 1677 (2004).
136. E. Fang and F. J. Grieman, *Main Group Met. Chem.*, **17**, 447 (1994).
137. C. Jiménez Calzado and J. Fernández Sanz, *J. Mol. Struct. (Theochem)*, **390**, 61 (1997).
138. S. Mori, A. Hirai, M. Nakamura and E. Nakamura, *Tetrahedron*, **56**, 2805 (2000).
139. D. C. Topor, *J. Chim. Phys. Phys.-Chim. Biol.*, **63**, 347 (1966).
140. M. Danek, J.-S. Huh, K. F. Jensen, D. C. Gordon and W. P. Kosar, *Chem. Mater.*, **7**, 731 (1995).
141. J. C. Wenger, D. J. Oakes, M. R. S. McCoustra and M. A. Chesters, *Surf. Sci.*, **360**, 81 (1996).
142. W. S. Kuhn, B. Qu'Hen and O. Gorochov, *Prog. Cryst. Growth Charact. Mater.*, **31**, 1 (1995).
143. H. Dumont, A. Marbeuf, J.-E. Bourée and O. Gorochov, *J. Mater. Chem.*, **2**, 923 (1992).
144. H. Dumont, A. Marbeuf, J.-E. Bourée and O. Gorochov, *J. Mater. Chem.*, **3**, 1075 (1993).
145. H. Dumont, A. Marbeuf, J.-E. Bourée and O. Gorochov, *Mater. Sci. Eng.*, **B17**, 41 (1993).
146. B. Qu'Hen, W. S. Kuhn, A. Lusson and O. Gorochov, *J. Cryst. Growth*, **159**, 138 (1996).
147. E. K. S. Liu, *Inorg. Chem.*, **19**, 266 (1980).
148. A. V. Ghule, K. Ghule, C.-Y. Chen, W.-Y. Chen, S.-H. Tzing, H. Chang and Y.-C. Ling, *J. Mass Spectrom.*, **39**, 1202 (2004).
149. G. A. Razuvaev, G. G. Petukhov, R. F. Galiulina and N. N. Shabanova, *Zh. Obshch. Khim.*, **34**, 3812 (1964); *Chem. Abstr.*, **62**, 9163f (1965).
150. L. M. Dyagileva, E. I. Tsyganova, V. I. Faerman and Yu. A. Aleksandrov, *Zh. Fiz. Khim.*, **61**, 2260 (1987); *Chem. Abstr.*, **107**, 205777h (1987).
151. N. D. Grishnova, P. E. Gaivoronskii, I. V. Donnikov, A. N. Moiseev, Yu. M. Salganskii and N. V. Shushunov, *Vysokochistye Veshchestva*, 172 (1987); *Chem. Abstr.*, **107**, 108562b (1987).
152. N. D. Grishnova, Yu. A. Kurskii, M. A. Lopatin, A. N. Moiseev, Yu. M. Salganskii, P. G. Sennikov, V. G. Tsvetkov and N. V. Shushunov, *Vysokochistye Veshchestva*, 48 (1987); *Chem. Abstr.*, **107**, 29019b (1987).
153. V. N. Votintsev, A. N. Moiseev and A. S. Nikishin, *Vysokochistye Veshchestva*, 100 (1989); *Chem. Abstr.*, **111**, 137016q (1989).
154. A. M. Gordeev, N. D. Grishnova, P. E. Gaivoronskii, A. N. Moiseev, V. M. Polyakov, Yu. M. Salganskii, V. N. Shishov and N. V. Shushunov, *Vysokochistye Veshchestva*, 124 (1990); *Chem. Abstr.*, **113**, 115462w (1990).
155. G. G. Devyatykh, V. A. Sidorov, E. M. Gavrishchuk and A. N. Moiseev, *Vysokochistye Veshchestva*, 95 (1993); *Chem. Abstr.*, **119**, 163418g (1993).
156. A. A. Oleinik, V. A. Dodonov, G. N. Lysenko and O. N. Druzhkov, *Russ. Chem. Bull.*, **43**, 1577 (1994); *Chem. Abstr.*, **123**, 67022k (1995).
157. A. A. Skatova, S. K. Ignatov, V. A. Dodonov, A. G. Razuvaev and O. N. Druzhkov, *Russ. Chem. Bull.*, **44**, 1832 (1995); *Chem. Abstr.*, **124**, 261217p (1996).
158. J. I. Davies, M. J. Parrott and J. O. Williams, *J. Cryst. Growth*, **79**, 363 (1986).
159. J. I. Davies, G. Fan, M. J. Parrott and J. O. Williams, *J. Chem. Soc., Chem. Commun.*, 68 (1986).
160. H. Ogawa and M. Nishio, *J. Appl. Phys.*, **64**, 6750 (1988).
161. K. P. Giapis, K. F. Jensen, J. E. Potts and S. J. Pachuta, *Appl. Phys. Lett.*, **55**, 463 (1989).
162. S. Patnaik and K. F. Jensen, *J. Cryst. Growth*, **107**, 390 (1991).
163. A. I. Romanychev, *Zh. Prikl. Khim.*, **65**, 2672 (1992); *Chem. Abstr.*, **120**, 257740d (1994).
164. S. Patnaik, K.-L. Ho, K. F. Jensen, D. C. Gordon, R. U. Kirss and D. W. Brown, *Chem. Mater.*, **5**, 305 (1993).
165. M. Danek, S. Patnaik, K. F. Jensen, D. C. Gordon, D. W. Brown and R. U. Kirss, *Chem. Mater.*, **5**, 1321 (1993).
166. D. Rajavel and J. J. Zinck, *J. Electron. Mater.*, **22**, 803 (1993).
167. J. Cheon, L. H. Dubois and G. S. Girolami, *Chem. Mater.*, **6**, 2279 (1994).
168. G. H. Fan, N. Maung, T. L. Ng, P. F. Heelis, J. O. Williams, A. C. Wright, D. F. Foster and D. J. Cole-Hamilton, *J. Cryst. Growth*, **170**, 485 (1997).
169. S. Stolyarova, N. Amir and Y. Nemirovsky, *J. Cryst. Growth*, **186**, 55 (1998).
170. S. Sinharoy, M. A. Stan, A. M. Pal, V. G. Weizer, M. A. Smith, D. M. Wilt and K. Reinhardt, *J. Cryst. Growth*, **221**, 683 (2000).
171. M.-K. Lee, S.-S. Pan and B.-T. Tsay, *Jpn. J. Appl. Phys.*, **39**, L374 (2000).
172. C. R. Eddy, Jr., D. Leonhardt, V. A. Shamamian and J. E. Butler, *J. Electron. Mater.*, **30**, 538 (2001).

173. H. Kleinwechter, C. Janzen, J. Knipping, H. Wiggers and P. Roth, *J. Mater. Sci.*, **37**, 4349 (2002).
174. W. Xu, Z. Ye, T. Zhou, B. Zhao, L. Zhu and J. Huang, *J. Cryst. Growth*, **265**, 133 (2004).
175. Y. Fujita and R. Nakai, *J. Cryst. Growth*, **272**, 795 (2004).
176. C. A. Hampel, C. Blaauw, I. D. Calder, R. Glew, D. Macquistan, T. Bryskiewicz and S. Guillon, *J. Vac. Sci. Technol. A*, **22**, 912 (2004).
177. T. M. Barnes, S. Hand, J. Leaf and C. A. Wolden, *J. Vac. Sci. Technol. A*, **22**, 2118 (2004).

CHAPTER 6

Dynamic behavior of organozinc compounds

ALBERT GUIJARRO

Departamento de Química Orgánica, and Instituto de Síntesis Orgánica (ISO), Universidad de Alicante, Ap. 99, E-03080, Alicante, Spain
Fax: +34 96 590 3549; e-mail: aguijarro@ua.es

The chemistry of organozinc compounds
Edited by Z. Rappoport and I. Marek

I. INTRODUCTION

The dynamic behavior of organozinc compounds in solution involves, in a first approach, four independent processes: (a) exchange, (b) inversion, (c) aggregation and (d) coordinating-ligand exchange (Scheme 1). In principle, all these processes involve to a certain extent more or less profound changes of the C−Zn bonds, sometimes being major changes (exchange and inversion), but sometimes only marginal changes (e.g. in the populations of this bond when coordinating-ligand exchange occurs). Only (a) exchange and (b) inversion, i.e. the processes that affect entirely the integrity of the C−Zn bond, have been studied in sufficient detail from the point of view of their dynamics.

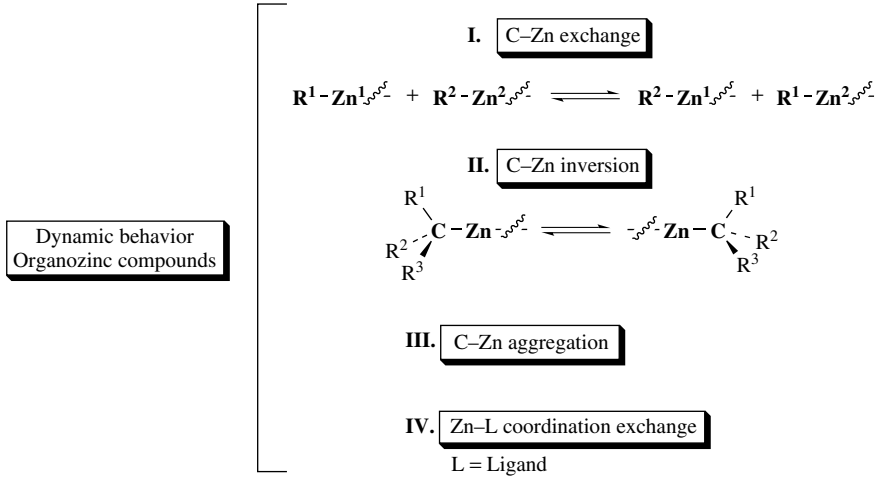

SCHEME 1. The dynamic behavior of organozinc compounds involves C−Zn exchange and C−Zn bond inversion as main processes. Aggregation and ligand exchange dynamics complete the overall picture describing the dynamics of these compounds

The description of their kinetics and mechanisms will be the main subject of discussion in this chapter. Although this is the best explored area of organozinc dynamics, it is far from being complete and further research waits to be done in this field. On the other hand, aggregation dynamics either affects—but only partially—the integrity of the C−Zn bond, or does not affect it at all, depending on whether the C−Zn bond takes part or not in the aggregation process. Much less work has been reported describing the dynamics of aggregation processes for organozinc reagents, in spite of the large volume of structural data available. When so, it will be discussed throughout the text.

Similar arguments apply to the coordinating-ligand exchange processes. Kinetics describing these processes for organozinc compounds are seldom found in the literature,

in spite of the enormous amount of descriptive structural work published on the detailed crystalline structures of organozinc complexes. Sometimes, the distinction between one or another process is not so clear. Dimeric diphenylzinc, $(Ph_2Zn)_2$, which is the stable form of Ph_2Zn in the solid state (see Section II.A.2), has an aryl-bridging structure analogous to the transition state that currently explains the dynamics of the alkyl exchange in dialkylzinc reagents (Section II.A.1), and will be treated in that section.

Another example is tetrameric methoxy(methyl)zinc, $(MeZnOMe)_4$. The mechanism can be treated both as an aggregative process as well as a ligand coordination exchange process. It reveals aggregation due solely to oxygen bridging, with no direct participation of the C−Zn bond, and will be mentioned only briefly.

Each of these dynamic processes can be considered to apply to different kinds of organozinc compounds. In general, most compounds that bear at least one C−Zn bond can be classified into three main groups depending on the number of net C−Zn bonds present in the compound, taken as a monomeric molecular structure regardless of any associative behavior. Consequently, in the first group there are the compounds with only one net C−Zn bond with general formula RZnX, including organozinc halides, but also alkoxides, amides etc. with X = Hal, OR, NR_2 etc. respectively. In a second group having two net carbons bound to zinc we find the diorganozinc compounds, R_2Zn, while anionic organozinc or zincates, R_3Zn^-, R_4Zn^{-2}, have three or more R groups directly bound to the metal and belong to the third group. The dynamics of these families of compounds may differ substantially among them, and often also within the same group. When possible they will be treated separately.

II. DYNAMICS OF CARBON−ZINC BOND EXCHANGE: C−Zn EXCHANGE

Equilibria exchanging alkyl or other organic groups between organozinc compounds have been classified as (A) intermolecular exchange, (B) metallotropic exchange (or shift) and (C) exchange with other metals.

A. Intermolecular C−Zn Exchange

1. Alkyl−Zn exchange in dialkylzinc compounds

a. Alkyl−Zn exchange in dimethylzinc and related compounds. The exchange of methyl groups in dimethylzinc (Me_2Zn) is a representative example of the general dynamics of exchange of alkyl groups. Early reports showed that no carbon−proton coupling was observed by 15 MHz ^{13}C-NMR (60 MHz for proton) in Me_2Zn at room temperature[1]. The system exchanges rapidly its methyl groups in an intermolecular fashion and no $^3J_{CH}$ corresponding to the potential $^1H_3C-Zn-^{13}CH_3$ coupling was recorded under these conditions. More recently, this coupling has been recorded at higher frequencies and much lower temperatures. Using fully ^{13}C-labeled samples, in the absence of ^{1}H-decoupling, the spectrum of Me_2Zn-$^{13}C_2$ results in magnetic inequivalence of chemically equivalent carbon and proton nuclei, as a consequence of the difference in the C,H couplings between a given carbon atom and its protons and those protons attached to the other ^{13}C in the same molecule. Under slow exchange rate conditions, the spin system turns into a higher order coupling pattern type $A_3A'_3XX'$, the set of absorptions being given in Figures 1a and 1b. The ^{1}H-coupled ^{13}C-NMR spectrum was recorded at 150 MHz (600 MHz for ^{1}H) at −80 °C. This approach permits the calculation of all coupling constants of the spin system including the $^3J_{CH}$ (−1.0 Hz) and $^2J_{CC}$ (18.4 Hz) as the most relevant ones (Figure 1)[2]. The spectrum proved to be nearly equivalent to the lithium dimethylcuprate Me_2CuLi (Figure 1c), which is isoelectronic and isospin with Me_2Zn, with only slight

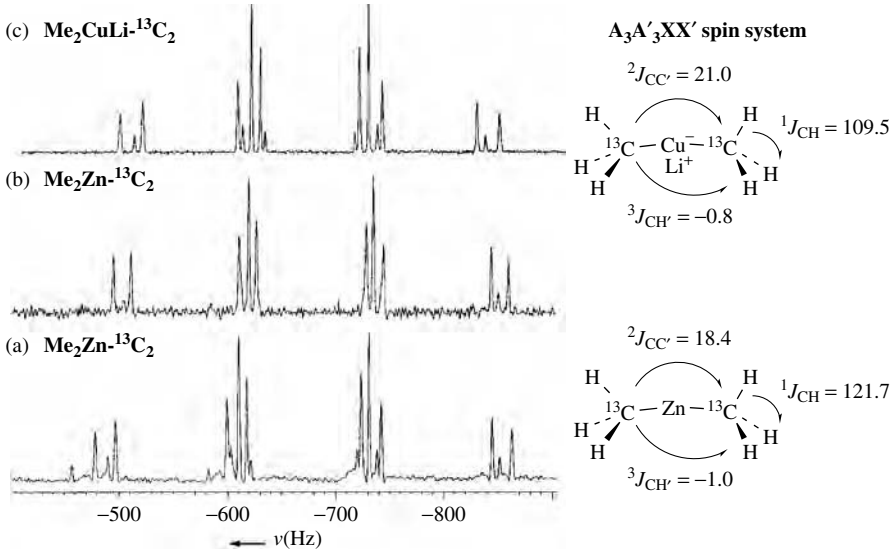

FIGURE 1. ^{1}H coupled ^{13}C-NMR spectra at $-80\,^{\circ}C$ of (a) Me_2Zn-$^{13}C_2$ in hexane, (b) Me_2Zn-$^{13}C_2$ in THF-d_8, (c) isoelectronic Me_2CuLi-$^{13}C_2$ in THF-d_8. (Reproduced by permission of Wiley-VCH from Reference 2)

differences in the coupling constants. Although no dynamic NMR study was carried out to obtain activation barriers, a rough estimate of a lower limit for the exchange at $-80\,^{\circ}C$ is $\Delta G^{\neq} > 10$ kcal mol^{-1} (see Appendix).

For a long time, mechanisms for the exchange have been suggested, including the most likely one involving alkyl-bridged transition state **1** (equation 1)[3].

$$R^1{}_2Zn + R^2{}_2Zn \rightleftharpoons \left[R^1Zn(R^1)(R^2)ZnR^2 \right]^{\neq} \rightleftharpoons 2\,R^1R^2Zn \qquad (1)$$

(1)

However, until very recently, the structure of the transition state for the exchange process was not studied in detail by means of calculations[4]. Dimethylzinc, like other dialkylzinc compounds, is a monomer in the solid state (mp $= -29\,^{\circ}C$) as well as in solution in both polar or nonpolar solvents. The basic structural features are maintained either in the pure state or in hydrocarbon solvents, while in polar coordinating solvents such as ethers soluble coordination complexes are formed. The structure of dimethylzinc in the gas phase is consistent with a linear geometry[5], the two highest occupied molecular orbitals were found to be symmetrical and antisymmetrical C−Zn−C three-center orbitals, while the low-lying $3d^{10}$ electrons remain essentially nonbonding[6]. The experimental C−Zn bond distance is 1.93 Å[7], as observed by Raman rotational spectroscopy. With this configuration, the coordination behavior of dimethylzinc is determined largely by electrostatic interactions, and ligand field effects are absent. In this sense, the organometallic chemistry of Zn has certain analogies to that of Mg; their differences can be often explained in terms

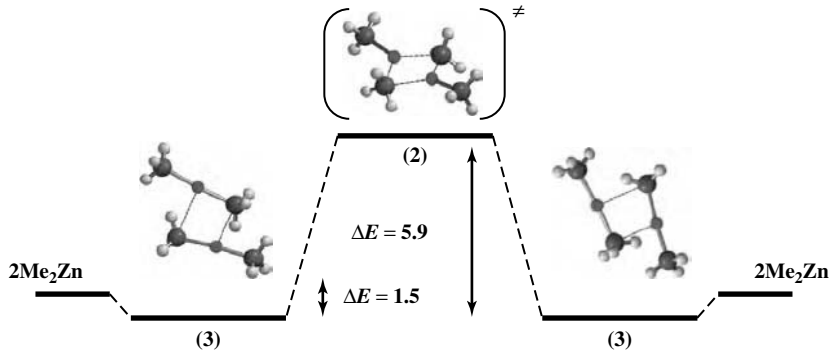

FIGURE 2. Calculated mechanism for the degenerate exchange of methyls between two Me_2Zn molecules. Relative electronic energies ΔE (kcal mol^{-1}) are given

of electronegativity. With covalent, but rather polar C−Zn bonds (Zn Pauling electronegativity is 1.65)[8], dimethylzinc and related compounds appear as electron-deficient species unable to attain coordination saturation with this configuration. Although ΔG° is unfavorable for the association of simple dialkylzinc reagents, the bridging of alkyl groups between two zinc centers can provide low-energy pathways to facilitate the intermolecular exchange of alkyl groups. The mechanism for the most simple exchange of this kind, i.e. the degenerate exchange of Me between two molecules of Me_2Zn, has been carried out using density functional theory (DFT) with the B3LYP functional, and LACVP* basis set including Hay and Wadt's effective core potentials (ECP) for zinc, and 6–31G* basis set for the geometry and energy optimizations of the other atoms[4]. A four-center transition state (**2** in Figure 2) was located, in which bridging methyl groups are 2.27 Å equidistant from each Zn atom in an approximately C_{2v} overall symmetry. The calculated C−Zn distances are given in Scheme 2.

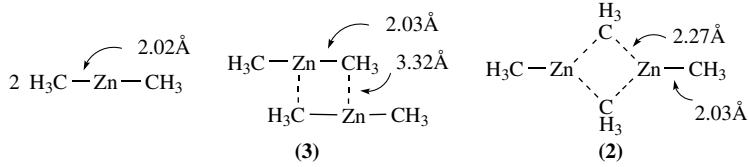

SCHEME 2. Calculated C−Zn distances, d_{C-Zn} (Å), for the reagents (Me_2Zn), transition state (**2**) and dimeric intermediates (**3**) in Figure 2

According to these *ab initio* calculations, the transition state **2** is reached from a previous loosely bound dimer **3** which is only $\Delta E = 1.53$ kcal mol^{-1} more stable than two monomer molecules. From the geometry of the dimer **3**, the d_{C-Zn} is only barely affected in respect to the isolated Me_2Zn (Scheme 2). It is likely that this dimer is undetected in the actual equilibrium due to the very unfavorable entropic factor $-T\Delta S$ of dimerization that easily surpasses the small stabilizing enthalpy. The transition state **2** is located at $\Delta E = 5.93$ kcal mol^{-1} above this dimer. The actual experimental barrier, $\Delta G^{\neq} = \Delta H^{\neq} - T\Delta S^{\neq}$, is expected to be somewhat higher than this value, due to an anticipated more negative entropy of formation of transition state **2** with respect to dimer **3**, the former being held together tighter by hypervalent C and Zn atoms, therefore

reducing the degrees of freedom (for actual experimental barriers involving Me_2Zn in related exchanges, see Section II.C.1). In this transition state the carbons undergoing exchange have a front-side interaction with both Zn atoms, preserving the configuration of the exchanging carbon. According to this mechanism, the stereochemical integrity of the migrating groups is retained throughout the exchange. From these studies, the enthalpy barriers found for the methyl exchange predict that the exchange is a kinetically feasible process and occurs with *retention* of the configuration of the exchanging methyl. It can also be inferred that aggregation between dialkylzinc species is not thermodynamically favored since entropic factors should prevail over those for a weakly bound dimer, which is the only energy minimum on the energy surface.

In contrast, aggregation through bridging alkyl groups between two metal centers is one of the ways that other electron-deficient alkylmetals relieve, at least partially, their electronic demand. Me_2Mg exists as a long-chain polymer where the metal atoms are connected by pairs of methyl bridges (Mg–C distance 2.24 Å) with an almost tetrahedral arrangement of four methyl groups around each metal atom (Scheme 3, a)[9]. A rather more complicated dynamic scenario is found in solution, although the main structural features of the system remain intact if the solvent is not highly coordinating. In diethyl ether solutions, Me_2Mg is associated to a certain degree which is strongly concentration and temperature dependent[10]. The insertion of ether solvent molecules breaks down the chains (Scheme 3, b), but exchange is fast and a single sharp signal for all CH_3 groups is observed at 30 °C by 100 MHz ^{1}H-NMR. Below −30 °C a small downfield absorption was attributed to bridging CH_3 groups by ^{1}H-NMR, while the bulk of the solvated monomers (Scheme 3, c) along with the terminal nonbridging methyl groups of the associated species remained upfield. For more coordinating solvents, the amount of solvated monomers prevails and Me_2Mg remains monomeric in THF over a wide concentration range. In the light of these facts and other observations both for Me_2Mg and other dialkylmagnesium reagents[11], which assign a bimolecular order to the mechanism of alkyl exchange in dialkylmagnesium reagents[12], the intermediate in the exchange reactions is envisaged as a dimeric alkyl bridging structure such as (d) in Scheme 3, or another species with a similar binding pattern. Depending on the solvent, conditions etc. the structure (d) could be either a true intermediate or a transition state.

The transition state proposed for the alkyl exchange in dialkylzinc reagents shows also many analogies with that for other alkylmetals which are dimeric in the ground state

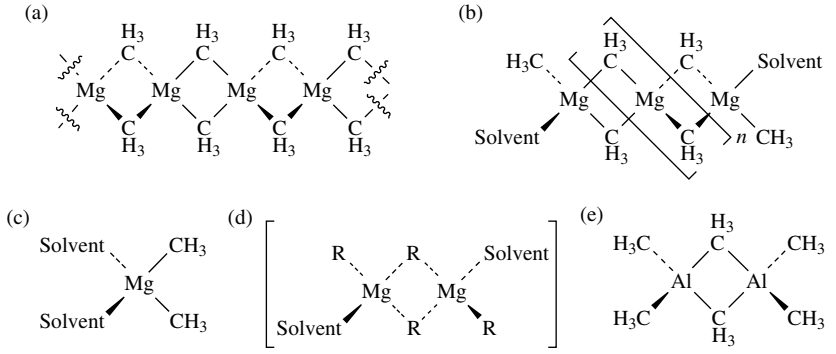

SCHEME 3. Aggregative behavior of Me_2Mg and Me_3Al: (a) Polymeric Me_2Mg (solid state), (b) suggested structure for the aggregates in weakly coordinating solvents, (c) coordinated monomeric Me_2Mg, (d) suggested intermediate/transition state in the mechanism of the alkyl exchange in R_2Mg reagents, (e) structure of $(Me_3Al)_2$ in solid and hydrocarbon solution

and also with rapidly exchanging systems at room temperature like trialkylaluminums Al_2R_6. Trimethyl aluminum is dimeric in the solid state[13] and maintains its associated structure with methyl bridging groups in hydrocarbon solution (Scheme 3, e)[14]. The system dynamically exchanges all methyls in hydrocarbon solution at room temperature, giving separated absorptions for the bridging and terminal methyls only at $-75\,^{\circ}C$ by 56.5 MHz ^{1}H-NMR. The activation parameters for the methyl exchange were obtained by both ^{13}C-NMR[15] and ^{67}Al-NMR experiments[16].

b. Alkyl–Zn exchange in primary, secondary and other dialkylzinc compounds. Alkyl group exchange between mixtures of different dialkylzinc compounds has been difficult to detect by ^{1}H-NMR, e.g. using mixtures of $Et_2Zn + Me_2Zn$ or t-Bu_2Zn[17]. That could be explained in terms of a relatively stable mixed dialkylzinc compound present as a major component that precludes the observation of minor components of the equilibrium. Apparently, a relatively large thermodynamic constant K favors the formation of mixed species (equation 2).

$$Et_2Zn \quad + \quad Me_2Zn \quad \underset{}{\overset{K}{\rightleftharpoons}} \quad 2\ EtZnMe \tag{2}$$

An approximate determination of K has been carried out by means of calorimetric experiments for a number of diorganozinc pairs, including dialkyl, diallyl and diarylzinc compounds in toluene, assuming that $\Delta G_r^{\circ} \approx \Delta H_r^{\circ}$ (equation 3)[3]. In general, the equilibrium is shifted to the side of the mixed species, especially when the organic groups bound to zinc are much different. The actual existence of these mixed diorganozinc reagents was evidenced by MS analyses of the reaction mixtures, by observation of the molecular ions corresponding to the R^1R^2Zn mixed species. Also, the formation of mixed R^1R^2Zn compounds could be observed by ^{13}C-NMR, using secondary dialkylzinc reagents[18]. The spectrum for s-Bu_2Zn (**4**) shows splitting of the ^{13}C signals (25.5 MHz, THF-d_8) due to the presence of *meso* and *racemic* s-Bu_2Zn diastereomers, in approximately the same amount (equation 4 and Figure 3a). The s-Bu exchange at $-30\,^{\circ}C$ (temperature at which the spectra was recorded) is slower than the experimental NMR time and splitting was also discernible at up to $35\,^{\circ}C$. The addition of one equivalent of i-Pr_2Zn (**5**) (Figure 3b) displays a spectrum of the equilibrium mixture in equation 5 (Figure 3c). In it, a new set of signals corresponding to the mixed species **6** appears, displaying the distinctive feature of the nonequivalence of the C6′ and C6″ methyls, as expected from an asymmetric environment. Unfortunately, no line-shape analysis of the temperature-dependent resonances was carried out to determine the actual activation parameters. Still, for the exchange in equation 4, it was possible to give roughly a lower limit for the activation barrier[18]. Statistically, only half of the encounters will cause changes in the chemical shifts of the molecules involved. Making an approximate use of the equations in the Appendix (Section IV) on the observed splitting for C3 ($\Delta\nu = 0.8$ Hz), a lower limit for the exchange barrier is placed at $\Delta G^{\neq} > 17$ kcal mol^{-1} at $35\,^{\circ}C$ in THF-d_8[18].

$$R^1{}_2Zn \quad + \quad R^2{}_2Zn \quad \underset{}{\overset{K}{\rightleftharpoons}} \quad 2\ R^1R^2Zn \tag{3}$$

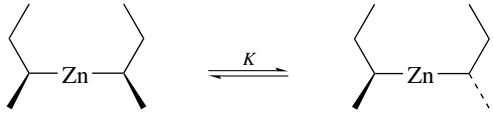

$K = ca\ 1$ (4)

(*RS*,*SR*)-(**4**) (*RS*,*RS*)-(**4**)

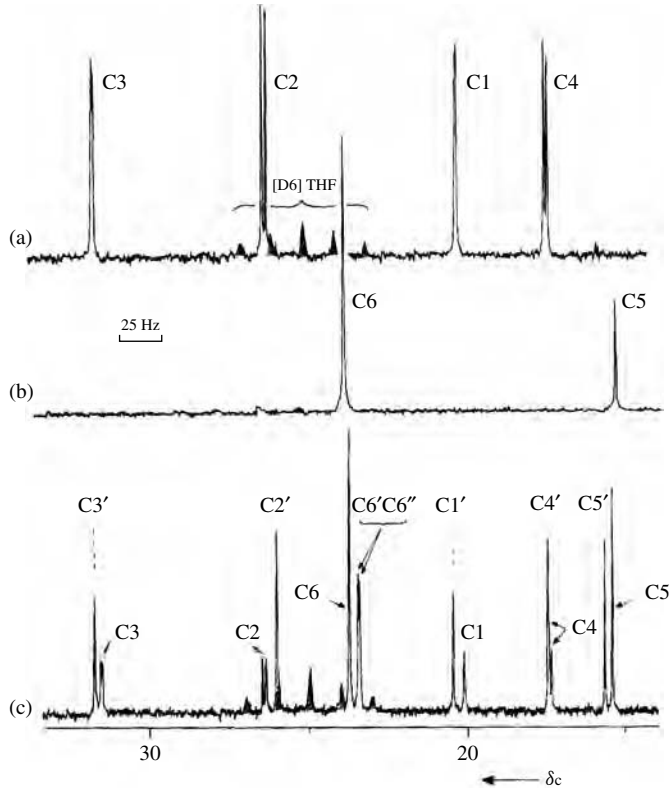

FIGURE 3. 25.5 MHz ^{13}C-NMR of compounds **4–6** (δ_C in ppm, −30 °C, THF-d_8). (a) Spectrum of the mixture of diastereomers of *s*-Bu_2Zn (**4**). (b) Spectrum of *i*-Pr_2Zn (**5**). (c) Spectrum of a 1:1 mixture of **4** + **5** according to equation 5. Reproduced by permission of Wiley-VCH from Reference 18

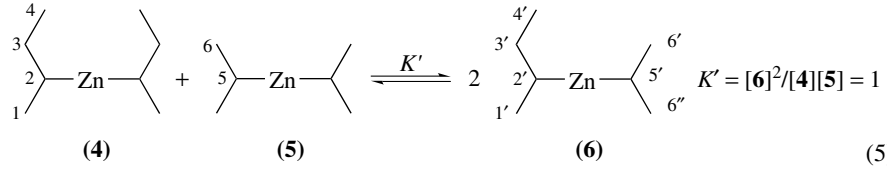

(5)

2. Exchange with aryl, alkenyl and alkynylzinc compounds

The bridged structures proposed for the alkyl exchange, such as those in equation 1 or in Figure 2, are assumed to be transition states. As the alkyl groups are replaced by more electronegative sp^2 or *sp* carbon groups, a higher tendency to aggregate occurs. This is caused by an increased electron impoverishment of the metal center, among other factors. As a result, bridged structures can become either relative energy minima (or intermediates), as well as absolute minima (e.g. if dimers are the most stable form of the compound). This is the case of aryl, alkenyl and alkynylzinc compounds.

Diphenylzinc (Ph_2Zn, **7**) was determined earlier to be monomeric in benzene or cyclohexane[19], and more recently in hexane[20], but exists as a bridged dimer in the solid state, in clear contrast to normal dialkylzinc derivatives which are monomeric also in the solid state. The dimerization of Ph_2Zn has been studied theoretically[4]. Calculations, identical to those described in Section II.A.1.a for Me_2Zn, were carried out on dimeric diphenylzinc, affording the Ph-bridging structure **8**, whose main structural features fully coincide with the reported structure of solid state Ph_2Zn. Interestingly, gas phase calculations locate dimer **8** in a deep energy well below the energy of two isolated Ph_2Zn molecules (equation 6). Although no experimental data have been found for the kinetics of this exchange and presumably small entropic contributions have not been estimated, activation barriers should be very low. The case of the mixed exchange $Ph_2Zn + Et_2Zn$, which is of certain synthetic importance, has been computer simulated (equation 7). Both reagents (**9**) and products (**11**) occur as weakly associated electrostatic dimers in the gas phase, as seen previously for Me_2Zn. The heat of reaction (zero point energy corrections neglected) favors the formation of mixed product PhZnEt. The activation enthalpy barrier in the forward direction is very small too, $\Delta H^{\neq} = 1.3$ kcal mol^{-1}. **10** was identified as a true transition state, and it is substantially stabilized compared to the analogous $MeZn(\mu\text{-}Me)_2ZnMe$ transition state (**2** in Figure 1).

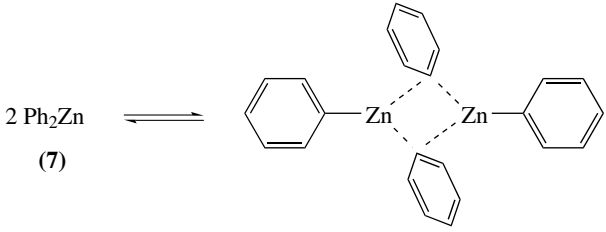

(6)

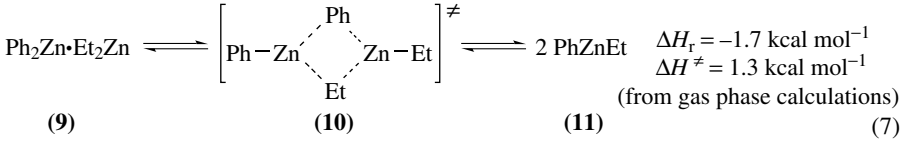

(7)

The extent of participation of bridged structures required for stabilization has not been studied for vinylzinc derivatives. Divinylzinc, $(CH_2{=}CH)_2Zn$, is monomeric in benzene solution, but has a higher melting and boiling point than its saturated analogue[21], indicating larger intermolecular interactions in condensed phases. A similar behavior to that found for Ph_2Zn seems reasonable. In the case of alkynylzinc reagents, dipropynylzinc $(MeC{\equiv}C)_2Zn$ or di(phenylethynyl)zinc $(PhC{\equiv}C)_2Zn$ are solids displaying low solubility in nonpolar organic solvents, indicating a highly associated nature[22]. For instance, di-1-octynylzinc $[CH_3(CH_2)_5C{\equiv}C]_2Zn$ is polymeric in the solid state and only moderately soluble in benzene, forming lower aggregates[23]. Permanent aggregation by alkynyl bridges (such as **12**, polymeric chain) is thought to be the reason for their unexpected physical properties. $EtZnC{\equiv}C(CH_2)_nNMe_2$ or $Zn[C{\equiv}C(CH_2)_nNMe_2]_2$ ($n = 1$–4) show oligomeric or polymeric association in benzene[24]. Thus, $EtZnC{\equiv}C(CH_2)_2NMe_2$ was found to be trimeric in benzene, **13**, with bridging alkynyl groups holding together the structure, in spite of the coordinating NMe_2 groups. However, $EtZnC{\equiv}C(CH_2)_2NMe_2$ is monomeric in pyridine. No experimental data for alkynyl exchange are available. However, the existence of readily accessible aggregates such as **12** or **13** suggest again very low activation barriers.

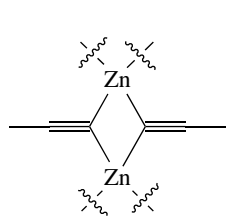

(12)

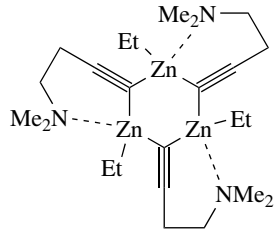

(13)

3. Alkyl–Zn exchange in organozinc salts

a. Alkyl–Zn exchange in organozinc salts–diorganozinc compounds. Organozinc halides are the most representative class of organozinc salts used in organic chemistry. They can be obtained and crystallized either in solvated or unsolvated form. Ethylzinc chloride or bromide readily dissolve in hydrocarbon solvents, being associated as tetramers in benzene[25]. These structures are easily disaggregated by coordinating ligands such as TMEDA [$Me_2N(CH_2)_2NMe_2$] or 2,2′-bipyridyl. In more coordinating solvents such as Et_2O they are monomeric (equation 8)[26]. Although the coordination chemistry (including aggregation) of organozinc salts is very diverse[27] and a large amount of structural data are available[28], little has been studied about its kinetics, being generally implicit that ligand exchange and its aggregative role is a fast process compared with C−Zn exchange.

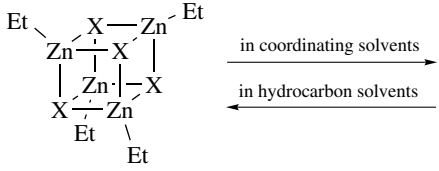

X = Cl, Br, OMe (8)

Alkyl group exchange between alkylzinc salts and dialkylzinc compounds is a fast equilibrium (equation 9). Only one set of ethyl group absorptions—one triplet and one quartet—is present in the 100 MHz ^{1}H-NMR spectra of a mixture of EtZnX (X = Cl, Br, I) and Et_2Zn in toluene, although in the absence of exchange these compounds should display chemical shift differences for the α-protons of more than 20 Hz, with the higher field signal corresponding to Et_2Zn. The situation is similar for other organozinc salts RZnX, with X = OR, NR_2 or SR[29]. The chemical shifts of the methylene group $\delta(CH_2)$ from mixtures obtained by varying the molar fraction (x) of EtZnX showed an excellent linear relationship with x, as long as no interferences due to deficient solubility occurred. This indicates that a fast exchange is operating and only averaged $\delta(CH_2)$ values are observed. The exchange is very fast indeed and these equilibria could not be frozen even at −60 °C, displaying pre-exchange lifetimes of $\tau_{EtZn} < 0.004$ s[29], corresponding to activation barriers of $\Delta G^{\neq} < 10$ kcal mol^{-1} at −60 °C.

$$R^1{}_2Zn + R^2ZnX \rightleftharpoons R^1R^2Zn + R^1ZnX \rightleftharpoons \text{etc.} \tag{9}$$

In THF, however, the exchange equilibrium of a mixture of EtZnI and Et_2Zn displayed coalescence by 100 MHz ^{1}H-NMR around −55 °C and fully separated signals down to −70 °C[30], approximately corresponding to $\Delta G^{\neq}$ of *ca* 11 kcal mol^{-1} at −55 °C. The

mechanism of the alkyl exchange in Grignard reagents (RMgX) has a number of points in common with the exchange involving organozinc halides. It has been investigated at low temperature, where exchange is slow on the NMR time-scale (100 MHz ^{1}H-NMR)[31]. The presence of a good bridging group with lone pairs facilitates the exchange. Consequently, bridged complexes such as **14** have been proposed as intermediates for this exchange[10]. For analogy, and based on the observation that RZnX has apparently lower activation barriers for the R exchange than R_2Zn, the heteroatom-bridged transition state **15** appears a likely candidate to explain this fast exchange process (equation 10).

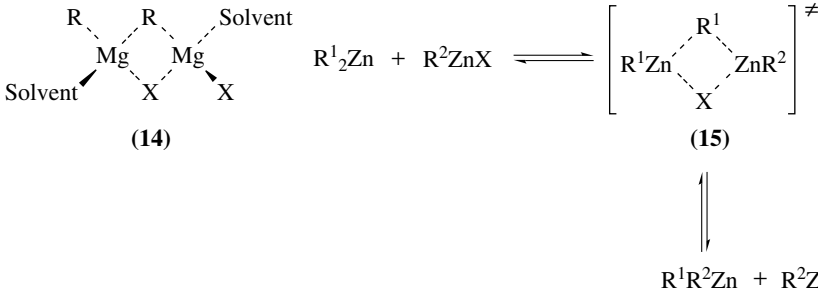

(10)

b. The Schlenk equilibrium. A Schlenk-type equilibrium is, in principle, always present in organozinc halides (equation 11), although it generally lies well to the right in both hydrocarbon or ether solvents[22]. Radioactive labeling showed in early studies that the scrambling of the zinc in $^{65}ZnCl_2 + Et_2Zn \leftrightarrows ZnCl_2 + Et_2{}^{65}Zn$ takes place easily at room temperature in Et_2O and leads to statistical distribution of ^{65}Zn[32]. In fact, ethylzinc halides (X = Cl, Br) can be prepared as a crystalline solid from neat diethylzinc and a zinc halide, $ZnX_2 + Et_2Zn \rightarrow 2$ EtZnX, and can be recrystallized from pentane[25]. Extrapolation of the chemical shift of the methylene group $\delta(CH_2)$ obtained from different EtZnCl/Et_2Zn mixtures of increasing molar fraction in toluene to $x_{EtZnCl} = 1$ afforded the identical value of $\delta(CH_2)$ to that obtained for the actual pure EtZnCl in the same solvent. This is clear evidence that equilibrium 11 is completely shifted to the right in toluene[29]. Estimates of K for EtZnI by 100 MHz ^{1}H-NMR gave $K \geqslant 500$ at $-70\,^\circ$C in THF[30]. At room temperature, IR and Raman spectroscopy also indicate Schlenk equilibria that are largely shifted to the right ($K \geqslant 100$, equation 11) for mixtures of Me_2Zn or Et_2Zn with ZnX_2, X = Cl, Br, I in THF[33]. Indeed, dissolving ZnX_2 in R_2Zn, when possible, constitutes a direct way to prepare RZnX if coordinating solvents are to be avoided. Sometimes it is possible to shift this equilibrium to the right, e.g. by removing/precipitating the zinc halide from solution with complexating agents (2,2′-bipyridyl, chelating agents), by distillation of the volatile R_2Zn if it is volatile, or simply by changing the solvent if the organozinc halide is not fully stable in it (e.g. MeZnI precipitates ZnI_2 in benzene or toluene)[29].

$$\text{Schlenk equilibrium:}\quad R_2Zn + ZnX_2 \overset{k}{\rightleftharpoons} 2\ RZnX \qquad K = \frac{[RZnX]^2}{[R_2Zn][ZnX_2]} \tag{11}$$

The Schlenk equilibria for pentafluorophenylzinc halides (C_6F_5ZnX) has been followed by ^{19}F-NMR in coordinating solvents, where all the species are monomeric. In THF at 35 °C, the equilibrium constants for $(C_6F_5)_2Zn + ZnX_2 \leftrightarrows 2\ C_6F_5ZnX$ were $K = 18.1$ (X = Cl), 16.3 (X = Br) and 7.5 (X = I), and the rate of exchange of C_6F_5 groups were in the order X = Cl > Br > I[34]. Grignard reagents (RMgX) instead display larger differences between X = Cl and X = Br when the Schlenk equilibrium is considered (Table 1, entries

TABLE 1. Experimental values for the Schlenk equilibrium $MX_2 + Me_2M \leftrightarrows 2\ MeMX$, M = Mg, Zn (equation 11)

	RMX	Solvent	T (K)	K (technique)	Reference
1	MeMgBr	Et_2O	298	450 (UV)	35
2	MeMgCl	THF	298	1.0 (NMR)	10
3	MeMgBr	PhH	298	very small (mol. weight det.)	36
4	MeZnBr	Et_2O	298	very large (IR, Raman)	33
5	MeZnI	THF	183	>500 (NMR)	30
6	MeZnCl	PhMe	298	very large (NMR)	29

1–3). While the equilibrium favors the formation of RMgX (X = Br, Cl) in Et_2O[35], it is not so in THF[10], and it is totally reversed in hydrocarbon solvents[36]. Similar behavior in varying solvents is found for different organomagnesium halides such as $EtMgX$[37,38], and $PhMgX$[38,39]. The nature of the solvent has been found to be among the most important factors determining the position of the Schlenk equilibrium, and its influence has also been the subject of a theoretical study[40]. On the contrary, as seen above, organozinc halides RZnX (X = Cl, Br) are generally the dominant species in the Schlenk equilibrium regardless of the solvent (Table 1, entries 4–6).

4. Alkyl exchange in zincates

Organozincates are anionic complexes with a central zinc atom surrounded by 3 or 4 organic anionic ligands and stabilized by their corresponding counterions, with a general formula $R_3Zn^-M^+$ or $R_4Zn^{-2}\ 2M^+$. They can be stoichiometrically formulated in principle by addition of the corresponding amount of RLi or RMgX to ZnX_2, RZnX or R_2Zn to fulfill the empirical formula. The ^{1}H-NMR spectrum of MeLi/Me_2Zn mixtures, for instance, consists of a single sharp resonance at room temperature whose chemical shift depends on the Li/Zn amount, having a continuous shift upfield as the amount of MeLi increases, with an upper limit located in the chemical shift of pure MeLi. This is indicative that fast exchange of Me groups between the different organozincate species and between organozincate and organolithium species occurs in solution[41]. Lowering the temperature down to −78 °C, the ^{1}H-NMR spectra affords only one methyl resonance for the organozincate species in THF[42,43a], along with the excess of MeLi that gives now a separate signal. Splitting in Et_2O is more complex, from which it is implied that both aggregation and exchange processes between different species take place[41]. The activation barriers for the exchange between the signal corresponding to the zincate species and the excess MeLi has been studied by both ^{1}H- and ^{7}Li-NMR. The observed Arrhenius activation energy for the methyl group exchange and ^{7}Li exchange was $E_a = 10.7$ and 9.0 kcal mol^{-1}, respectively, with comparable although slightly higher barriers for the MeLi–Me_2Mg system and slightly lower barriers for the MeLi–Me_2Cd *ate* systems. For comparative purposes, raw experimental data have been reprocessed and activation parameters have been recalculated, being expressed here in terms of activation enthalpy and entropy: $\Delta H^{\neq} = 10.3$ kcal mol^{-1} and $\Delta S^{\neq} = -8.8$ cal mol^{-1} K^{-1} for the CH_3 group exchange and $\Delta H^{\neq} = 8.5$ kcal mol^{-1} and $\Delta S^{\neq} = -13.3$ cal mol^{-1} K^{-1} for the Li exchange (solution of MeLi–Me_2Zn of 3.66:1 ratio in THF in the range of temperatures −40 °C to 0 °C). At 25 °C it corresponds to a free energy of activation of $\Delta G^{\neq} = 12.9$ kcal mol^{-1} and $\Delta G^{\neq} = 12.5$ kcal mol^{-1} for the CH_3 group exchange and the Li exchange, respectively. These values are always referred to the actual dynamic process observed experimentally, with no inferences on possible mechanisms of the exchange process. The structure of triorganozincates is known

in the solid phase. Potassium trimethylzincate Me_3ZnK has a trigonal-planar coordination at the zinc atom[44], while lithium tetramethylzincate anion is tetrahedral[45]. However, in solution the existence of Me_4ZnLi_2 as a single entity[43], in contrast to the hypothesis that this is an artifact originated by rapid signal averaging, remained unsettled for some time. The question was settled by the low-temperature ^{1}H-coupled ^{13}C-NMR spectrum of fully ^{13}C labeled reagents, which result, as shown for Me_2Zn (Section II.A.1.a), in magnetic inequivalence of the chemically equivalent carbon atoms in Me_3ZnLi-$^{13}C_3$ and Me_4ZnLi_2-$^{13}C_4$[2]. This magnetic inequivalence which allows the observation of the carbon–carbon coupling constants over two bonds, $^{13}C-Zn-^{13}C$, provides a direct way to reveal the actual coordination of the zinc atom in solution. The ^{1}H-coupled ^{13}C-NMR spectrum (150 MHz) of Me_3ZnLi-$^{13}C_3$ (0.08 M) was recorded at $-80\,^\circ$C in THF-d_8. The Me exchange is slow at this temperature, the spectra displaying an $A_3A'_3A''_3XX'X''$ spin system consistent with a $Me_3Zn^-C_3$ or D_3 symmetric anion, and permitting the calculation of all coupling constants including the relevant one $^2J_{CC}$ (14.0 Hz). The situation for Me_4ZnLi_2-$^{13}C_4$ was similar ($A_3A'_3A''_3A'''_3XX'X''X'''$ spin system, $^2J_{CC} = 12.2$ Hz) confirming the actual existence of such tetrahedral species in solution, with the exception that the equilibrium $Me_3ZnLi + MeLi \leftrightarrows Me_4ZnLi_2$ is shifted to the left, giving a very weak set of resonances for Me_4Zn^-. The exchange rate as well as the former equilibrium depend on the concentration, indicating molecular orders higher than 1.

B. Metallotropic Exchange in Organozinc Reagents

The metallotropic exchange or shift in allylzinc, 2,4-dienylzinc and other related organozinc compounds involves the migration of the Zn atom through an unsaturated hydrocarbon system with the corresponding bond reorganizations. In principle, it can have a concerted character, being then subjected to the conservation of the orbital symmetry rules, or it may have an actual dissociation step involving ionic (or other) intermediates.

1. Allylzinc reagent dynamics

In general, allylzinc compounds are fluxional systems that have low energy barriers for an apparent 1,3-migration of the Zn atom. They are conveniently described as σ-bonded allylic organozinc species rapidly equilibrating between all possible isomeric forms at room temperature, the final equilibrium composition being given by the relative stability of each component (**16–18**, equation 12)[22]. Other conceivable limiting structures, such as a fully delocalized π-allylzinc system, or even allyl anions [$CH_2{=}CHCH_2^- \leftrightarrow {}^-CH_2CH{=}CH_2$] can, in principle, be ruled out in the liquid phase on the basis of their IR or Raman spectra, especially in the range of the C=C bond vibrations[46].

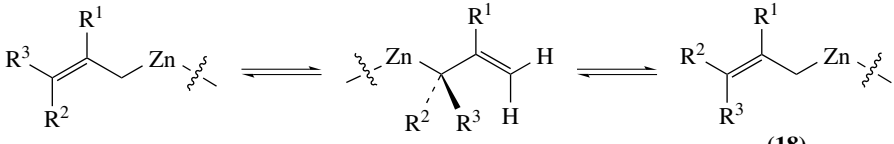

(16) **(17)** **(18)** (12)

Some representative examples follow. The ^{1}H-NMR spectra of diallylzinc (**19**), bis(2-methylallyl)zinc (**20**), bis(3-methylallyl)zinc (**21**) and bis(3,3-dimethylallyl)zinc (**22**) are typical fluxional systems whose dynamics have been studied over the range of temperatures $-125\,^\circ$C to $100\,^\circ$C[47]. Diallylzinc (**19**) shows the four α- and γ-protons as chemically

and magnetically equivalent, displaying together with the β-proton an AX_4 spin pattern between $-40\,^{\circ}C$ to $100\,^{\circ}C$, with a $^3J_{AX} = 10.8$ Hz. This is approximately an intermediate value between the *cis*- and *trans*-vinyl coupling averaged with the ^3J coupling of the β-proton and the free-rotating CH_2Zn group. Below $-120\,^{\circ}C$ a different spin system is observed, consistent with an $AMNX_2$ which can be assigned to the static σ-allyl form of **19**. Coalescence is observed at $T_C = -75\,^{\circ}C$ at 80 MHz. From the IR spectrum in THF, the C=C stretching frequencies appear at $\nu_{C=C} = 1602\ cm^{-1}$, indicating that the σ-allyl form is present in solution at rt. **20** behaves similarly, displaying a A_4X_3 spin system at higher temperature than T_C and a ABM_3X_2 spin system at lower temperature. The IR stretching of **20** in THF is $\nu_{C=C} = 1604\ cm^{-1}$. The spectra of **21** and **22** at $30\,^{\circ}C$ are just what would be expected from the structures represented, with rapidly equilibrating mixtures of the (*Z*)- and (*E*)- isomers (**16** and **18** in equation 12) and undetectable amounts of the thermodynamically less stable, most substituted R^2R^3CZn isomer **17**. The interconversion of allylic isomers is rapid at rt, and the chemical shifts and coupling constants of the protons in **21** and **22** are an average of those in the isomeric forms **16** $\rightleftarrows$ **17** $\leftrightarrows$ **18**, weighted according to their relative concentrations. Thus, for instance, the olefinic vicinal coupling in **21**, $H^2C{=}CH^3$, is $^3J_{H2H3} = 12.4$ Hz. This value is considered an average of the expected *cis*- and *trans*-olefin coupling, both isomers being the two major components of the equilibrium mixture. The corresponding equilibria involving the diallylmagnesium species as well as allylmagnesium halides have lower activation barriers[48,49]. Diallylmagnesium $(CH_2{=}CHCH_2)_2Mg$ (**23**) displays a symmetric A_4X pattern down to $-120\,^{\circ}C$ by ^{1}H-NMR in THF[50], and so does allylmagnesium bromide in Et_2O down to $-80\,^{\circ}C$ (60 MHz)[51].

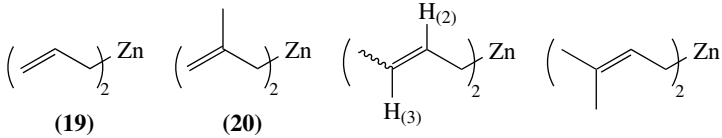

(19) **(20)** **(21)** **(22)**

Spin system (80 MHz ^{1}H-NMR)	A_4X (25 °C)	A_4X_3 (25 °C)	Major isomers detected
	$AMNX_2$ (−120 °C)	ABM_3X_2 (−110 °C)	

The mechanism of the exchange has been studied for **19** and **20**[52]. Plotting $\ln k_{exp}$ against ln [**20**] affords a slope of 1.2 ± 0.3. From $1/\tau = k_{exp} = k_2/4\ [\mathbf{20}]^{n-1}$, the kinetic data indicate that the reaction order for this exchange is approximately 2 in THF. The proposed mechanism resembles the vinylogous form of the bimolecular alkylzinc exchange (equation 13, **19a** = rearranged **19**), rather than unimolecular pathways in the sense of a true [1,3]-metallotropic rearrangement (equation 14, left, **19a** = rearranged **19**). Concerted all-suprafacial via transition state **24** is an allowed process by orbital symmetry in contrast with the conceivable bimolecular process via transition state **25**, in which both allylzinc reagents would scramble at once. Additionally, inversion involving perhaps an ionic step as in equation 14 involving the ion pair **26**, which might occur in highly solvating environments, should not be ruled out in other scenarios[52].

The activation parameters reported for the exchange process in **19** and **20** are definitively lower than the expected values for saturated systems (Table 2, compare to Me_2Zn exchange barriers shown in Section II.C.1). Values in Table 2 are referred to the experimental rate of exchange k_{exp} at the given concentration, i.e. which is neither concentration nor statistically corrected according to the molecularity of the reaction. The actual rate

of exchange is still faster, $k_2 = 4k_{exp}/[\mathbf{19}]$, assuming that the mechanism of equation 13 applies, and therefore only one of the four allyl groups in the transition state **24** do actually scramble per encounter. If we wish to refer the activation parameters to the actual bimolecular rate constant k_2, the implementation of the concentration and the statistical correction factor would result in a slightly modified entropy of activation: $\Delta S^{\neq}_{(k_2)} = \Delta S^{\neq} + R \ln (4/[\mathbf{19}])$, $R = 1.987$ cal mol^{-1} K^{-1}, while $\Delta H^{\neq}$ would remain unchanged.

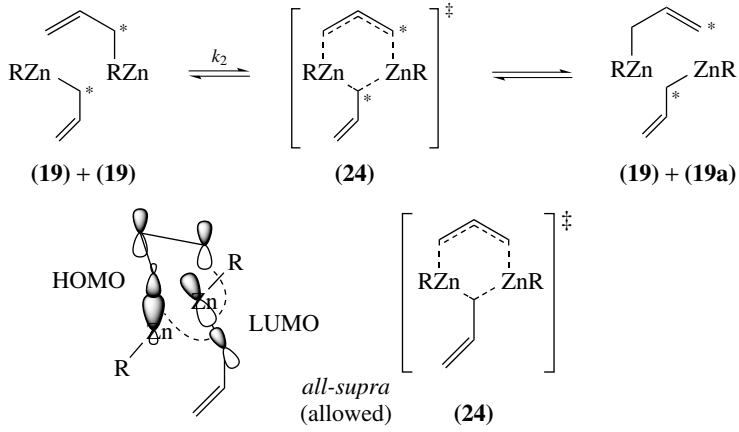

(13)

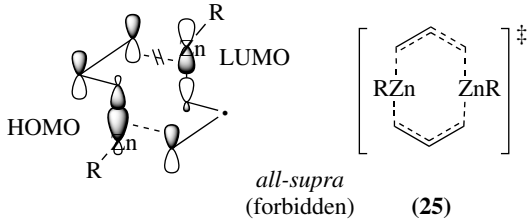

(14)

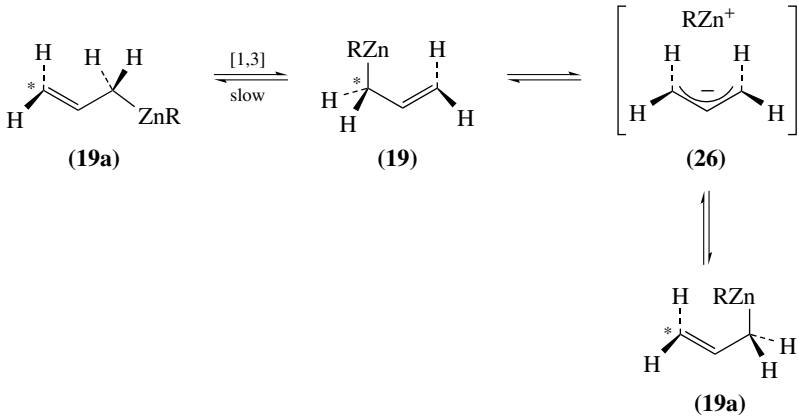

The structural features in the solid phase can be strikingly different. Solid-phase ^{13}C-NMR spectroscopy indicates that the basic energy difference for allylzinc derivatives

TABLE 2. Experimental activation parameters for allylic organozinc exchange [a]

Compound	Conc. (m) [b]	Solvent	$\Delta H^{\neq}$	$\Delta S^{\neq}$	$\Delta G^{\neq}_{298}$ [c]	Range of T (°C)
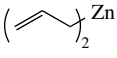	1.7	THF	8.8 ± 0.2	-3.8	9.9	$-30°$ to $-90°$
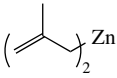	1.5	THF	8.3 ± 0.3	-8.0	10.7	$0°$ to $-90°$

[a] By 80 MHz ^{1}H-NMR, in THF (also THF/Et_2O mixtures in original reference 47). $\Delta H^{\neq}$ and $\Delta G^{\neq}$ are in kcal mol^{-1} and $\Delta S^{\neq}$ in cal mol^{-1} K^{-1}.
[b] In mol per kg of solvent (molality).
[c] Extrapolated to 25 °C.

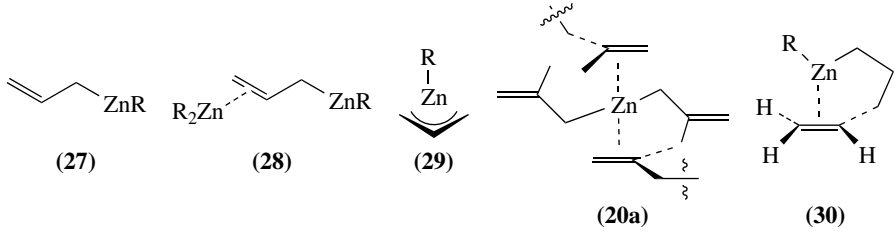

(27) **(28)** **(29)** **(20a)** **(30)**

in the σ-allylic form (**27**), π-complexing σ-allylic form (**28**) and π-allylic form (**29**) might be rather small in the crystalline phase. Indeed, CPMAS-^{13}C-NMR spectroscopy (cross-polarization–magic angle spinning) of diallylzinc, $(CH_2 = CHCH_2)_2Zn$ and of 2-methylallylzinc chloride, $CH_2 = C(CH_3)CH_2ZnCl$, show identical absorptions for the C_α and C_γ nuclei, indicating a η^3-coordination with the Zn atom in the crystal phase[53]. Both compounds restore the σ-allylic form in THF solution, as seen by the ^{13}C-NMR spectrum at -100 °C. In solution of coordinating solvents the preferred structure is the solvated form of **27**, which displays a complete set of absorptions for every carbon atom below T_C. π-Complexing interactions as in **28** have been detected in the crystal structure of unsolvated **20**, a fragment of which has been represented as **20a**. In this crystal structure, the π-interactions complete along with the σ-allylic bonds the binding interactions surrounding the Zn atom in the solid phase. Also, ^{1}H-NMR studies of dipent-4-enylzinc (**30**) strongly support some intramolecular π-complexation between the zinc atom and the double bond, forcing **30** to adopt the shown conformation[54]. Vibrational spectroscopy may reflect this interaction as a shift to lower frequencies in the $\nu_{C=C}$ stretching frequency, so structural assumptions regarding alkenylzinc compounds based on IR spectroscopy should be carefully contrasted.

2. 2,4-Dienylzinc reagent dynamics

The dynamics of the penta-2,4-dienylzinc systems have also been studied in detail[55]. Bis(2,4-pentadienyl)zinc•TMEDA (**31**) (TMEDA complexation impairs thermal stability) exists as a 4:1 mixture of interconverting (*E*)- and (*Z*)-isomers in the σ-allylic form ($^1\eta$) which can be seen separately by 100 MHz ^{1}H-NMR at 38 °C in C_6D_6. The corresponding penta-2,4-dienylzinc chloride•TMEDA (**32**) exists solely as the (*E*)-structure both in solution and in the solid state. In the crystal structure of (***E***)**-32** the $^1\eta$-coordination

of the pentadienyl group is present, as well as the W-shaped conformation of the (*E*)-alkenedienyl chain (equation 15).

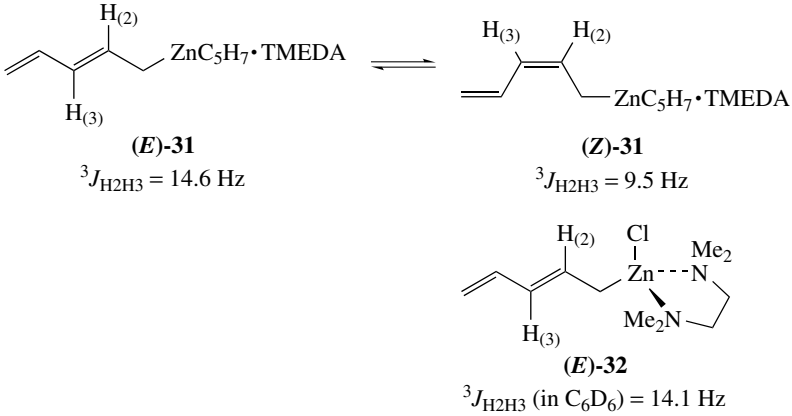

(*E*)-31
$^3J_{H2H3} = 14.6$ Hz

(*Z*)-31
$^3J_{H2H3} = 9.5$ Hz

(*E*)-32
$^3J_{H2H3}$ (in C_6D_6) = 14.1 Hz

(15)

Under the reported experimental conditions, **(*Z*)-31**, having the proper geometry, may very likely undergo a potential [1,5]-metallotropic rearrangement. If so, such a process is slow on the NMR time scale. As a result, **(*Z*)-31** displays 6 different absorptions by ^{1}H-NMR [2H1 to H4 + (*Z*)-H5 + (*E*)-H5]. Unfortunately, the limited thermal stability of **31** prevents NMR experiments at higher temperature in order to test this hypothesis. When faster than the NMR time scale, the [1,5]-metallotropic rearrangement imparts a higher symmetry to the penta-2,4-dienyl structure as seen by NMR and this is clearly reflected in the spectra. This is the case of bis(2,4-dimethylpenta-2,4-dienylzinc)•TMEDA complex (**33a**). In **33a**, the steric effects of the two methyl substituents at C2 and C4 positions facilitate the formation of the U-shaped conformation required for the [1,5]-shift. In the spectrum of **33a** two sets of signals in 10:9 ratio were observed. From the 100 MHz ^{1}H-NMR at 10 °C in C_6D_6, **33a** is present in two forms displaying different rates in their fluxional dynamics. The **(*Z*)-33a** gives a spectrum consistent with an NMR time-averaging structure of high symmetry (three signals, corresponding to 2H1 = 2H5, H3 and Me2 = Me4), as a result of a fast [1,5]-metallotropic rearrangement (equation 16), whereas **(*E*)-33a**, incapable of achieving a suitable conformation with close C1 and C5 positions, displays lower symmetry by ^{1}H-NMR under the same conditions (i.e. absorptions, corresponding to 2H1, H3, 2H5, Me2 and Me4). In cyclic systems, such as bis(cyclohepta-2,4-dienyl)zinc (**34a**), the occurrence of this [1,5]-metallotropic rearrangement is especially facile and **34a** displays also an NMR time-averaging symmetric structure of only 5 signals (H1 = H5, H2 = H4, H3, α-H6 = α-H7 and β-H6 = β-H7) according to the equilibrium in equation 17, which is fast under the given experimental conditions (100 MHz ^{1}H-NMR at −20 °C, toluene-d_8). Interestingly, the appearance of two sets of signals for (*Z*)- and **(*E*)-33a** also indicates that the potential [1,3]-metallotropic rearrangement (or Zn-allylic rearrangement), which on the ground of orbital symmetry rules requires an intricate *antarafacial* migration of the Zn atom, does not take place at comparable rates (equation 18). This [1,3]-metallotropic rearrangement would interconvert **(*Z*)-33a** ⇆ **(*E*)-33a**, which would afford for **33a** a spectrum with only one averaged set of signals (as for **21**, see Section II.B.1). The analogous magnesium substrate, **33b**, along with a range of other different bis(2,4-dienyl)magnesium compounds has also been studied by NMR and showed a fluxional behavior[56]. Instead of the spectrum of a (*E*), (*Z*)

mixture, only one set of signals [a time-averaged highly symmetric structure like (***Z***)-**33a**] is observed for **33b**, under identical experimental conditions (100 MHz ^{1}H-NMR at 10 °C in C_6D_6) (equation 18). The dienyl cyclic magnesium derivative **34b** displays inevitably also a time-averaged highly symmetric structure. In summary, the activation barriers are lower for penta-2,4-dienylmagnesium derivatives in these processes, in analogy with the dynamics displayed by the allyl-Zn vs. allyl-Mg systems. The higher ionic character of the C−Mg bond can explain these facts. Higher covalency of the C−Zn bond does not favor [1,3]-suprafacial shifts, which are thermally forbidden by the orbital symmetry rules.

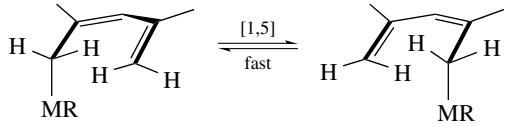

(16)

(***Z***)-(**33a**) MR = ZnC_7H_{11}•TMEDA
(***Z***)-(**33b**) MR = MgC_7H_{11}•TMEDA

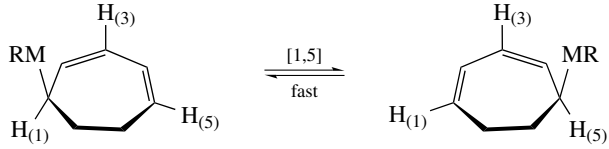

(17)

(34a) MR = ZnC_7H_9•TMEDA
(34b) MR = MgC_7H_9•nTHF

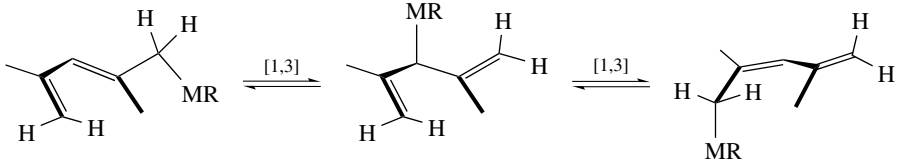

(***E***)-(**33a**) MR = ZnC_7H_{11}•TMEDA (slow [1,3] shift) (***Z***)-(**33a**)
(***E***)-(**33b**) MR = MgC_7H_{11}•TMEDA (fast [1,3] shift) (***Z***)-(**33b**) (18)

3. Zincocene dynamics

Dicyclopentadienylzinc or zincocene, $(C_5H_5)_2Zn$ (or Cp_2Zn), is a polymeric solid formed of infinite chains with both σ- and π-type interactions between Zn and Cp groups[57]. Nearly insoluble in nonpolar organic solvents, it can be dissolved in polar solvents showing a sharp single ^{1}H-NMR absorption, indicative of equivalence of the ring protons in the NMR time scale, a consequence of a fluxional behavior having a low energy barrier[58]. Recent structure refinements of gas electron diffraction data and density functional theory (DFT) calculations at the B3LYP/LanL2DZ level, and other theoretical studies, show that $(C_5H_5)_2Zn$ has an η^5,η^1 slip sandwich molecular structure in the gas phase (Scheme 4, a)[59]. Dynamic study of these systems are better carried out with bis(pentamethylcyclopentadienyl)zinc, $(C_5Me_5)_2Zn$, which is monomeric in the solid state as well as in other phases, in contrast to the parent compound. The structure in the solid[60] and vapor phase[61] is also described with both η^1- and η^5-donation to the metal. The $(C_5Me_5)_2Zn$ dissolves very well in apolar solvents. Low-temperature ^{1}H-NMR spectra (200 MHz, −100 °C, toluene-d_8) showed only a single 30H singlet at 1.98 ppm for all

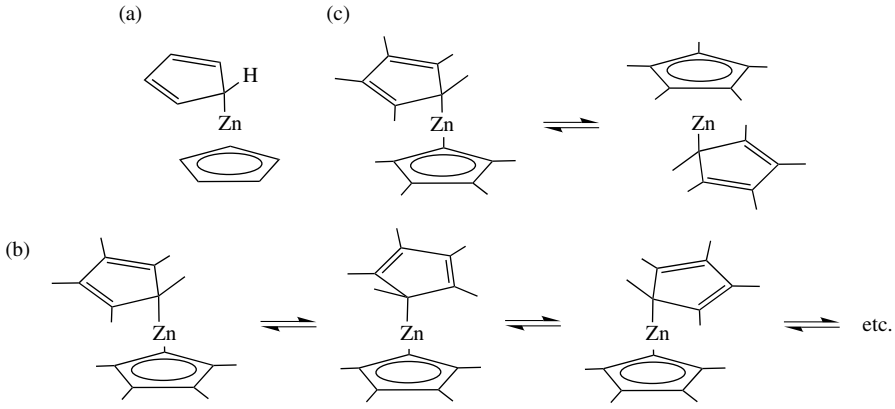

SCHEME 4. (a) Structure of gas phase Cp_2Zn; (b) and (c) are fast equilibria describing [1,5]-metallotropic rearrangement and fluxional behavior of $[C_5(CH_3)_5]_2Zn$, with a fast exchange between η^1- and η^5-hapticity of both rings, respectively, resulting in an average signal by NMR

averaged methyl signals $[C_5(CH_3)_5]_2Zn$, and ^{13}C-NMR (125 MHz, $-100\,^{\circ}C$, toluene-d_8) showed only two signals at 11.05 and 111.62 ppm corresponding to the averaged 10C methyl and averaged 10C cyclopentadienyl signals. Assuming a η^5,η^1-structure similar to that found in the solid or gas state, two different fluxional processes that are fast on the NMR time scale would render all ring atoms equal. The first dynamic exchange corresponds to a fast [1,5]-metallotropic (or sigmatropic) shift of the monohapto bonded ring (Scheme 4, b). The second probably involves a fast exchange between η^1- and η^5-hapticity of both rings (Scheme 4, c). These equilibria could not be slowed down by varying temperature (VT) NMR. Attempts to freeze this fluxional behavior using lower symmetry derivatives, such as $[C_5(CH_3)_4Ph]_2Zn$, failed, affording spectra with a similar dynamic pattern. Interestingly, in the solid state the structure is disordered, with the Zn atom scrambled between two equivalent sites, each of which is η^1-bonded to one ring and η^5-bonded to the other. This indicates that the barriers are very low indeed. For several other substituted metallocenes, these kinds of barriers are in the range of 0.2–1 kcal mol^{-1} [60].

C. Alkyl–Zn Exchange with Other Organometallic Compounds

1. Methyl–Zn exchange between Me_2Zn and Me_nM, M = Zn, Cd, Hg, Mg, In

Soon after the alkyl-bridging structure for dimeric trimethylaluminum $(Me_3Al)_2$ (Scheme 3e, in Section II.A.1.a) was determined in the solid state, as well as observed in the gas phase and in solution[14], similar structures were proposed to explain the mechanism of the alkyl exchange in alkylmetals of the group IIa or IIb[62]. Rough measurement of the Me_2Zn–Me_2Cd system in solvents of different polarity at 25 °C showed pre-exchange mean lifetimes of $\tau_A = 0.09$–0.19 s for $[Me_2Zn] = [Me_2Cd] = 1M$ (apparent exchange rate $= 1/\tau_A$; for a definition of τ_A and other kinetic parameters see Appendix, Section IV.A)[63]. The effect of the solvent is small (small rate increase on increasing the solvent donor ability) and there is no correlation of the exchange rate with the dielectric constant of the solvent, which was varied from $\varepsilon_e = 2.0$ for cyclohexane to 36.1 for nitrobenzene. Accordingly, the rate-determining step for the exchange does not form ionic charges. Interpretation of these one-point data in terms of activation

barriers, e.g. in cyclohexane or pyridine, and assuming bimolecular exchange, affords $\Delta G^{\neq}(\text{Cy}) = 16.4$ kcal mol^{-1} and $\Delta G^{\neq}(\text{Py}) = 15.6$ kcal mol^{-1} at 25 °C (from averaged $k_{\text{apparent}} = 1/\tau_{\text{MeCd}}/[\text{Me}_2\text{Zn}] = 3.0$ and 11.7 M^{-1} s^{-1}, respectively, $k_2 = 2k_{\text{apparent}}$). A much faster exchange rate was found for the Me_2Zn–Me_2Mg system ($\tau_A < 0.009$ s) compared to the Me_2Zn–Me_2Cd system at 32 °C in THF, while the $(CH_3)_2Zn$–$(CD_3)_2Hg$ system exchanges much slower, showing no signs of scrambling after 8 days[64]. A complete line-shape analysis by 100 MHz variable-temperature NMR of the exchanging system Me_2Zn–Me_2Cd in hydrocarbon media provided a more precise estimate of the actual activation parameters and order of this reaction[65]. At 70 °C the system allowed the observation of the bimolecular rate constant $k_2 = 36$ l mol^{-1} s^{-1} (averaged corrected) and an activation energy of $E_a = 17.0$ kcal mol^{-1} [66]. The graphical and/or numerical raw experimental data found in References 62–66 have been mapped and/or recalculated and plotted again according to the transition state theory—a more actual treatment of kinetic data—as well as in the original Arrhenius format for verification (see Appendix, Section IV.B). This has been done in order to compare activation parameters for different exchanging processes, normally obtained under different experimental conditions, using current terminology ($\Delta H^{\neq}$ and $\Delta S^{\neq}$). It likely provides somewhat more reliable activation parameters than the original work, based on Arrhenius plots, which is less accurate for extrapolation to other temperatures as used by the original authors (see Section IV.B). In addition, some of the original work contained some inconsistencies and errors in the treatment of data, mentioned in part by the authors[66], that has been corrected here. The general protocol followed is described in Scheme 5 for the Me_2Zn–Me_2Cd exchanging system. According to the chemical equilibrium represented and the transition state theory, the rate of exchange is given by the product of the concentration of the activated complex times k_{-2} (equation 19). The equilibrium is degenerate. Applying steady-state conditions, equation 20 results, and the exchange rate can be expressed in terms of the concentration of reagents [Me_2Zn] and [Me_2Cd], which are constant values (equation 21). The pre-exchange lifetimes for methyl bound to zinc, Me–Zn (τ_{MeZn}), and to cadmium, Me–Cd (τ_{MeCd}), are given by equations 22 and 23 and are measured experimentally. A statistical factor of 2 is introduced, since the chemical equilibrium via **35a** exchanges only one of the two methyl groups in each molecule of reagents, so fast exchange on the NMR time scale of all Me–Zn (or Me–Cd) implies a twofold faster chemical exchange. From that, the apparent rate constant of the experiment is $k_{\text{apparent}} = k_2/2$, and experimental validation of the equivalence in equation 24 at different concentration of Me_2Zn and Me_2Cd ensures the bimolecular order of the exchange reaction. Finally, by transferring the data obtained from variable-temperature (VT) NMR experiments to the Eyring equation (see Appendix, Section IV.B.1), the activation parameters $\Delta H^{\neq}$ and $\Delta S^{\neq}$ are obtained.

The methyl-bridged activated complex **35a** may play indistinctly the role of true transition state or intermediate under the mechanistic treatment given in Scheme 5. The corresponding activation parameters, $\Delta H^{\neq} = 16.3 \pm 1$ kcal mol^{-1} and $\Delta S^{\neq} = -4.2$ cal mol^{-1} K^{-1}, were obtained from kinetic data at 60–80 °C in methylcyclohexane, and a free energy of activation $\Delta G^{\neq} = 17.5$ kcal mol^{-1} at 25 °C was obtained by extrapolation. The original work dealt with the Arrhenius activation energy, $E_a = 17.0$ kcal mol^{-1} and $\Delta S^{\neq} = -3$ cal mol^{-1} K^{-1} at 25 °C[66]. It should be noted that the precision of the apparently small $\Delta S^{\neq}$ values based—in this case—on a rather small number of data points and a narrow temperature range is rather low. The situation is different for the Me_2Zn–Me_3In system (Scheme 6). More precise data ($\Delta H^{\neq} = 8.6 \pm 0.2$ kcal mol^{-1}, $\Delta S^{\neq} = -16$ cal mol^{-1} K^{-1}) were obtained for this exchange in Et_2O. The exchange is faster ($\Delta G^{\neq} = 13.2$ kcal mol^{-1} at 25 °C) than the Me_2Zn–Me_2Cd exchange, in agreement with other observations involving Group III metals[15, 62, 63, 67]. A similar bridged activation complex **35b** is proposed. To explore whether the electronegativity differences between the metals play

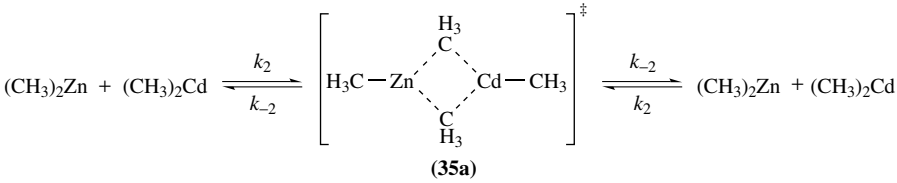

(35a)

$Me_2Zn + Me_2Cd$ (80–60 °C in MeCy)

$k_2 = 36\ l\ mol^{-1}s^{-1}$ (70 °C) $\Delta H^{\neq} = 16.3$ kcal mol^{-1}

$E_a = 17.0$ kcal mol^{-1} $\Delta S^{\neq} = -4.2$ cal mol^{-1} K^{-1} $\Big\}$ $\Delta G^{\neq} = 17.5$ kcal mol^{-1} (25 °C)

$$\text{rate}_{\text{exchg.}} = k_{-2}[\mathbf{35a}] \tag{19}$$

$$d[\mathbf{35a}]/dt = 0; \quad k_{-2}[\mathbf{35a}] = k_2[Me_2Zn][Me_2Cd] \tag{20}$$

$$\text{rate}_{\text{exchg.}} = k_2[Me_2Zn][Me_2Cd] \tag{21}$$

$$\frac{1}{\tau_{CdMe}} = \frac{k_2[Me_2Zn][Me_2Cd]}{2[Me_2Cd]} = \frac{k_2}{2}[Me_2Zn] \tag{22}$$

$$\frac{1}{\tau_{ZnMe}} = \frac{k_2[Me_2Zn][Me_2Cd]}{2[Me_2Zn]} = \frac{k_2}{2}\ [Me_2Cd] \tag{23}$$

$$k_2 = \frac{2}{\tau_{CdMe}[Me_2Zn]} = \frac{2}{\tau_{ZnMe}[Me_2Cd]} \tag{24}$$

SCHEME 5. Rate equations and activation parameters for the methyl exchange in the Me_2Zn–Me_2Cd system

a role in affecting the energy of the activation complex, and since, to the best of our knowledge, the self-exchange in Me_2Zn has not been measured, the self-exchange of Me_2Cd was studied. Detection of intermolecular exchange of methyl groups in Me_2Cd is relatively easy, by using the spectral changes which accompany such exchange on the ^{111}Cd–Me (12.9%, spin 1/2) and ^{113}Cd–Me (12.3%, spin 1/2) spin–spin couplings. Both isotopes give similar splitting patterns and are taken as one (of 25.2% abundance)[68]. A statistical factor of 4 instead of 2 (see equation 22 and below) is introduced, since only half of the exchanges actually change the spin system, and effective concentrations of magnetically active $[Me_2Cd^*] = 0.252[Me_2Cd]$ are employed. The activation parameters for the exchange in Et_2O are $\Delta H^{\neq} = 5.0 \pm 0.2$ kcal mol^{-1}, $\Delta S^{\neq} = -34$ cal mol^{-1} K^{-1} (Scheme 6). Not only is the activation barrier ($\Delta G^{\neq} = 15.3$ kcal mol^{-1} at 25 °C) smaller than in the Me_2Zn–Me_2Cd system, but the contribution of its components $\Delta H^{\neq}$ and $\Delta S^{\neq}$ differs notably. Here, the activation entropy is large and negative, whereas enthalpy contributes less to the overall barrier. This is expected for bridged structures such as **35c**, which in some cases might be even the lowest minima on the potential energy surface for highly electron-deficient species as seen e.g. for $[Me_2Mg]_2$ in Section II.A.1.a. A better correlation with the activation parameters of the Me_2Zn–Me_2Cd exchange is found for the exchange of *neat* Me_2Cd, $\Delta H^{\neq} = 15.2 \pm 0.1$ kcal mol^{-1}, $\Delta S^{\neq} = -8.8$ cal mol^{-1} K^{-1}, corresponding to a free energy of activation at 25 °C of $\Delta G^{\neq} = 17.8$ kcal mol^{-1} (Scheme 6), remarkably similar to the values for Me_2Zn–Me_2Cd exchange in hydrocarbon solvent. To our surprise, the results in Et_2O seem to fit better the theoretical studies

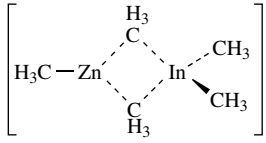

(35b)

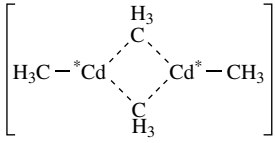

(35c)

$Me_2Zn + Me_3In$ (10 to −20 °C in Et_2O)

$k_2 = 175\ mol^{-1}s^{-1}$ (−8.8 °C) $\Delta H^{\neq} = 8.6$ kcal mol^{-1}
$E_a = 9.1$ kcal mol^{-1} $\Delta S^{\neq} = -16$ cal mol^{-1} K^{-1} } $\Delta G^{\neq} = 13.2$ kcal mol^{-1} (25 °C)

Me_2Cd (35 to −1.5 °C in Et_2O)

$k_2 = 51\ l\ mol^{-1}s^{-1}$ (33.3 °C) $\Delta H^{\neq} = 5.0$ kcal mol^{-1}
$E_a = 5.6$ kcal mol^{-1} $\Delta S^{\neq} = -34$ cal mol^{-1} K^{-1} } $\Delta G^{\neq} = 15.3$ kcal mol^{-1} (25 °C)

Me_2Cd (94–38 °C neat)

k_2 = not determined experimentally $\Delta H^{\neq} = 15.2$ kcal mol^{-1}
$E_a = 15.7$ kcal mol^{-1} $\Delta S^{\neq} = -8.8$ cal mol^{-1} K^{-1} } $\Delta G^{\neq} = 17.8$ kcal mol^{-1} (25 °C)

SCHEME 6. Activation parameters for the methyl exchange in the Me_2Zn–Me_3In and Me_2Cd systems

for Me_2Zn exchange in the gas phase (Section II.A.1.a) than the experimental values in apolar media. The reason for this apparently abnormal behavior may lie in the reported very weakly bound electrostatic dimer **3** in Figure 2 and Scheme 2, with almost intact H_3C−Zn bond. This dimer might exist only in low dielectric constant media, providing a low $\Delta S^{\neq}$ reaction pathway (since it is already a dimer) and high $\Delta H^{\neq}$, since reorganization of bonds to form bridges probably requires virtually no solvation. In contrast, in more polar solvents, dimer **3** is dissociated. The absence of dimer **3** results in higher $\Delta S^{\neq}$ pathways (due to the monomeric reagents) and lower $\Delta H^{\neq}$ due to solvent stabilization in the bridge-formation step. Interestingly, the self-exchange of Me_2Cd is strongly catalyzed by Cd alkoxides and peroxides that could originate from water or oxygen impurities[69], as well as by halides ($CdBr_2$)[68]. The oxygen or halide atoms are probably bridge-forming groups, facilitating the dimerization and subsequent exchange of alkyl groups, as will be seen in the next section.

2. Influence of the alkyl group on the exchange rate

The influence of the nature of the alkyl group on the rate of exchange of R_2Zn has been investigated for the reaction of R_2Zn and PhHgCl using a variety of alkyl groups[70]. The reaction is bimolecular ($k_2 = 0.64\ l\,mol^{-1}\,s^{-1}$ in THF at 0 °C, $\Delta G^{\neq}$ is *ca* 16.2 kcal mol^{-1}) and the relative rate constants for exchange of R_2Zn with PhHgCl (in Et_2O at 35 °C) are Me_2Zn (rate = 1), Et_2Zn (4.5), Pr_2Zn (17) and *i*-Pr_2Zn (*ca* 22). These results indicates that electronically rich C−Zn bonds undergo faster electrophilic substitution of ZnR by HgPh, probably through an $S_Ei(S_ECi)$ mechanism (chlorine assisted internal electrophilic substitution) (Scheme 7). Electron-donating substituents stabilize the electron-deficient

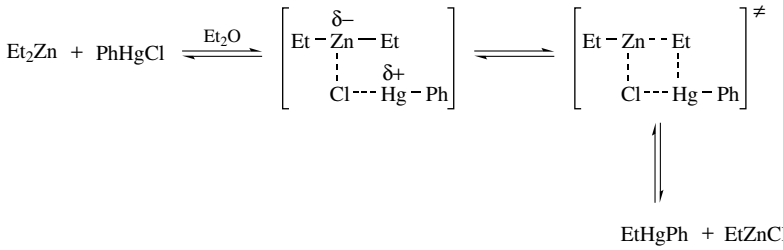

SCHEME 7. The electrophilic substitution of Et_2Zn by PhHgCl follows a second order rate law with an activation barrier of $\Delta G^{\neq} = 16.2$ kcal mol^{-1} (0 °C). This barrier can be lowered by replacing the ethyl groups at the zinc by more electron-donating alkyl groups, indicating an electronically deficient transition state

transition state. Differently, the reactivity profile is, however, flat in THF at 25 °C for the same group of reagents. The term 'flat profile' is used in competitive kinetics denoting identical rates regardless of the substituents (i.e. relative rates = 1 for all substituents). This negligible electronic effect of the R group on the reaction rate indicates that the rate-determining step of the reaction may be the de-coordination of solvent molecules from a hypothetical robust coordination complex around the Zn atom. The reactivity profile in Et_2O for this reaction is similar to those of other S_E processes involving other group IIb organometallic compounds such as $RHgR' + AcOH \rightarrow RH$[71] or $RHgBr + Br_2 \rightarrow RBr$[72], governed by both electronic and steric effects, for which the relative reaction rates are also R = Me < Et < *i*-Pr < *t*-Bu.

3. Alkyl–Zn exchange with organoboranes

The alkylboron–alkylzinc exchange process, $3R^1{}_2Zn + 2R^2{}_3B \leftrightarrows 3R^2{}_2Zn + 2R^1{}_3B$, is an equilibrium discovered in 1960[73]. The exchange $Et_3B + Me_2Zn \rightarrow Me_3B + Et_2Zn$ afforded 79% of products as isolated yield, the equilibrium being shifted to the right by distillation of Me_3B (bp = −20 °C). The exchange was found to be a convenient way to obtain different organozinc compounds starting from readily available Me_2Zn or Et_2Zn and more elaborated alkylboranes. Exchange reactions are rapid and can be shifted to completion by removal of the readily volatile Me_3B or Et_3B component[74]. Dialkyl[73], diaryl[75], diallyl[74] and dibenzylzinc compounds[75] are all suitable reagents in this strategy. More recently[76], this exchange has found direct synthetic application of organozinc compounds taking advantage of the extensive developments in organoboron chemistry[77], that supplies readily available, stereochemically well-defined organoboranes by hydroboration[78].

The mechanism of exchange between Me_2Zn and Me_3B has been studied using computational methods by the density functional theory (DFT) at the B3PW91 level, with a 6-31G* basis set for geometry optimizations[79]. A nonstraightforward reaction pathway was found for this exchange, which involves the participation of at least two intermediates (Figure 4). Reagents and products of the exchange are identical, therefore the energy profile is symmetrical and only half of it is shown in Figure 4. Zero point energy corrections aside, at the bottom energy level (relative electronic energy $\Delta E = 0$ kcal mol^{-1}) the two substrates form a weakly bonded dimer of electrostatic nature, **36**, with little geometry distortion with respect to the isolated molecules. As the two monomers approach, a symmetrical (C_s) four-membered ring intermediate of high energy, **37**, is formed, located at $\Delta E = 6$ kcal mol^{-1}. As expected, in **37**, the B, Zn and ring C atoms are all hypervalent. The barrier for this conversion is $\Delta E = 6.6$ kcal mol^{-1} and the transition state is identified

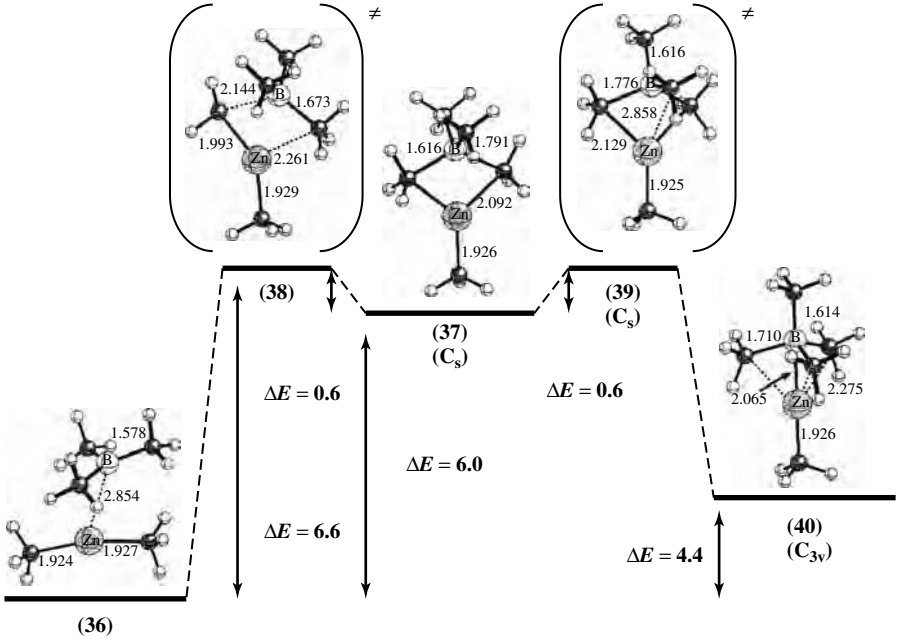

FIGURE 4. Calculated mechanism for the degenerate exchange of Me between Me_2Zn and Me_3B molecules. Relative ΔE in kcal mol^{-1} and bond distances in Å. Only half of the symmetric energy profile is shown; the complete surface follows the reverse sequence from **40** to **36**

as **38**. A second high-energy intermediate is found along the way in the forward direction. Through a small barrier (identified as **39**), the intermediate **37** reorganizes to another intermediate, **40**, of lower energy and higher symmetry (C_{3v}, $\Delta E = 4.4$ kcal mol^{-1}). The structure of this second intermediate is interesting and resembles, in principle, that of tetramethylborates (i.e. the hypothetical $[Me_4B]^-$ $[ZnMe]^+$). Analysis of the MOs indicates, however, a covalent character of the B−Zn single bond, with a significant admixture of 3*d* orbitals of Zn along with a major contribution of *s*-*p* orbitals of B and Zn. In both intermediates, the carbons undergoing exchange have a front-side interaction with the B and Zn atoms, preserving the configuration of the exchanging carbon, i.e. the migration occurs with *retention* of the configuration, and so is observed experimentally[80]. From **40**, the route to separate monomers follows the reverse sequence **40** → **39** → **37** → **38** → **36** (Figure 4).

The actual experimental barrier, $\Delta G^{\neq} = \Delta H^{\neq} - T\Delta S^{\neq}$, is expected to be, to some extent, higher than the calculated barrier ($\Delta H_r = 6.6$ kcal mol^{-1}), due to an anticipated negative entropy contribution for the rearrangement **36** → **38**, consequent with an increase in the number of binding sites and loss of degrees of freedom. Also, the steric demand is brought to minima in the given example. The hypercoordinated nature of the intermediate **37** will impose increased barriers of exchange to systems substituted by bulkier groups. Still, provided that these barriers are not prohibitive, the longer C−Zn bond compared to the C−B bond and the decrease in coordination number from B to Zn release steric tensions of a hypothetic bulky group R in the $R_3B \rightarrow R_2Zn$ exchange process, shifting the equilibrium toward the products.

III. DYNAMICS OF INVERSION AT CARBON BONDED TO ZINC: C−Zn INVERSION

The inversion of the configuration of the carbon in C−Zn bonds involves cleavage and reconstruction of this bond from the back side of the carbon, the integrity of this bond being entirely affected. The rates of this process are much slower than the C−Zn exchange, which occurs with retention of the configuration as seen in the previous section, and it is strongly dependent on the substitution and/or hybridization of the carbon bonded to zinc. In practice, only primary, allylic and benzylic organozinc systems, and to a lesser extent secondary organozinc compounds, are those systems in which inversion of configuration has actually been established. In general, mechanisms for these processes have not been devised beyond doubt, although the current proposals, based mainly on observation of analogous systems with other metals, will be briefly outlined in each case.

A. Inversion at a Primary Alkyl Carbon Bonded to Zinc

Among the different organometallic reagents utilized in organic chemistry, organozinc compounds occupy an intermediate position in terms of electronegativity of the metal. As a general trend, it is accepted that for organometallic reagents devoid of functionality, the more covalently bonded species are those which display the higher inversion barriers at the carbon center (or *topoisomerization* barriers)[81], and vice versa. A comparative study (Table 3) has been carried out comparing the dynamic behavior of different neohexylorganometallic reagents (neohexyl = 3,3-dimethylbutyl), including neohexylLi, $(neohexyl)_2Mg$, $(neohexyl)_2Zn$, $(neohexyl)_3Al$ and $(neohexyl)_2Hg$[82]. By ^{1}H-NMR, the chemical shift of both methylenic groups move essentially linearly upfield with decreasing electronegativity of the metal, indicating that shielding effects are mainly due to higher polarization of the C−M bond, while anisotropic effects from the metal orbitals are unimportant. If the inversion is slow compared to the NMR time scale, the CH_2CH_2 group of the neohexyl displays, in all cases, an AA′BB′ spin system. This is achieved at room temperature for all organometallic reagents but for neohexylLi, which required lower temperatures at 60 MHz ^{1}H-NMR. The values of the vicinal coupling constants [e.g. $J_{AB} = 4.7$ Hz, $J_{AB'} = 13.3$ Hz for $(neohexyl)_2Zn$] indicate in all cases that the preferred conformations are *anti*, as shown in equation 25. Increasing the temperature of the Et_2O solutions of neohexylLi, $(neohexyl)_2Mg$ and $(neohexyl)_2Zn$ results in a gradual change from the AA′BB′ type of spectrum to the A_2B_2 one for the CH_2CH_2 group, with the consequent simplification of the spectrum. These changes result from the averaging of the vicinal coupling constants which, in the way it occurs, is consistent only with

TABLE 3. ^{1}H-NMR spectra of neohexylmetallic compounds in Et_2O under slow inversion conditions[82]

RM[a]	RLi	R_2Mg	R_2Zn	R_3Al	R_2Hg
Temp. (°C)	−18	30	30	30	30
M electronegativity (Pauling)	1.0	1.2	1.6	1.5	1.9
δ (CH_2CH_2M) (ppm)	−1.08	−0.68	+0.15	−0.20	+1.01
δ (CH_2CH_2M) (ppm)	1.35	1.39	1.47	1.25	1.58
J_{AB} (Hz)	3.5	4.0	4.7	3.9	5.1
$J_{AB'}$ (Hz)	15.5	14.2	13.3	14.2	11.8
$J_{AA'}$ (Hz)	−12.1	−12.5	−12.4	−13.4	−12.5
$J_{BB'}$ (Hz)	−13.05	−13.4	−13.6	−13.4	−13.6
Conc. In Et_2O (mol%)	10-5	6-1	1	1	15-5

[a] R = $(CH_3)_3CCH_2CH_2$.

inversion of the configuration in the α-carbon. The AA′BB′ spectra of $(neohexyl)_3Al$ and $(neohexyl)_2Hg$ is retained up to 150–163 °C, indicating that these substances are configurationally stable in Et_2O under the given experimental conditions.

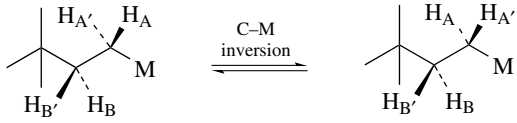

Spin system by NMR

slow inversion: AA′BB′
fast inversion: A_2B_2 (25)

M = Li, MgR, ZnR, AlR_2, HgR

The inversion rates for the lithium, magnesium and zinc compounds gave reasonably linear Arrhenius plots, from which the values of activation energy E_a could be obtained. Similarly to the previous sections devoted to the C−Zn bond exchange (Section II.C.1), the graphical and/or numerical raw experimental data have been replotted according to the transition state theory, as well as to the original Arrhenius format, for comparative purposes (see Appendix). However, unlike Section II.C.1, since a unique mechanism of inversion has not been unequivocally established, the activation parameters are referred to the observed rates of inversion, $k_{obsd.} = 1/\tau_A$, without inferences to the mechanism/order of the reaction. This is equivalent to assuming that reactions are first order in the organometallic reagent, and that no statistical factors were applied when pertinent. Table 4 contains the activation parameters for the inversion of the C−metal bond of several primary organometallic species, as measured by ^{1}H-NMR spectroscopy in Et_2O at the concentrations given in Table 3. For the primary diorganozinc compound, the activation parameters measured in the range 80–145 °C were $\Delta H^{\neq} = 24.9 \pm 2$ kcal mol^{-1} and $\Delta S^{\neq} = +12.8$ cal mol^{-1} K^{-1}. Extrapolation affords $\Delta G^{\neq} = 21.1$ kcal mol^{-1} for the inversion process at 25 °C. Compared to the analogous organolithium and organomagnesium reagents, the rates of inversion are slower as would be expected from the metal electronegativity (Table 3). However, the differences between these processes may be more profound, as could be inferred from the poor $\Delta H^{\neq}/\Delta S^{\neq}$ correlation for the Li, Mg and Zn inversion processes[83]. Although the available data are statistically too limited to make many assumptions, the departure of organolithium from a common inversion mechanism[84] might be the reason for this far from linear correlation. On the other hand, the neohexylaluminum is trivalent on the Al atom, which could confer extra congestion on the transition state with consequent higher barrier, despite a favorable electronegativity compared to Zn. Unfortunately, inversion barriers in organozinc reagents have been seldom studied and data available for their interpretation are scarce. In contrast, inversion barriers in organomagnesium (and organolithium) reagents have been studied much more in detail. The situation for these metals is further complicated by their different aggregative behavior. Although no study on the concentration dependence of inversion rates was conducted for dineohexylzinc, no change in inversion rate was detected for dineohexylmagnesium and neohexyllithium over the range of concentration displayed in Table 3. Hence, a general mechanism is proposed in which inversion appeared to be a first-order process and the general dependence of the inversion rate on the nature of the metal suggests a dissociation–recombination (or S_E1) mechanism[82]. Significantly, these experimental data do not exclude the participation of aggregates. Alternatively, associated species—dimers, trimers etc.—could have displayed *apparent* first-order inversion rates provided that their stoichiometric changes remain practically constant over the range of concentrations studied[82]. Indeed, other studies on primary organomagnesium reagents [R_2Mg, RMgX: X = Cl, Br, I; R = $CH_3CH_2CH(CH_3)CH_2$] conclude that there is an actual dependence on the concentration, indicating higher reaction orders, and that inversion takes place in a dimeric species. An intra-aggregate electrophilic transfer of the

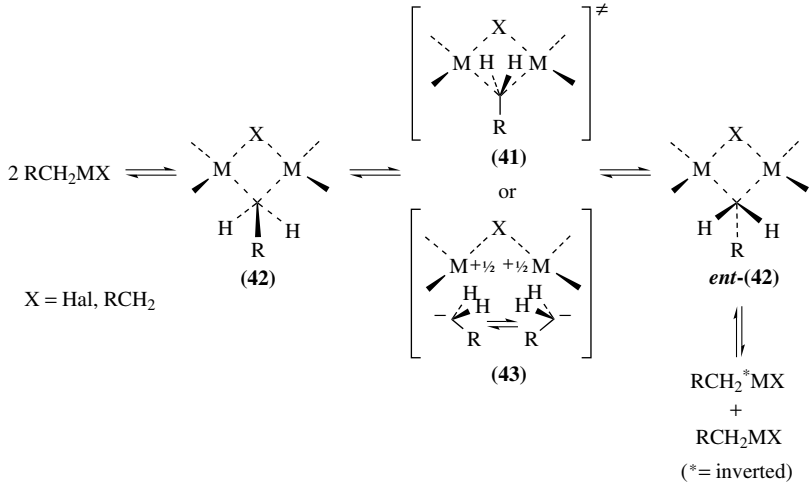

SCHEME 8. Proposed mechanisms of inversion of the carbon–metal bonds in RCH_2MX involving aggregates. (a) Though an S_Ei mechanism, with a possible transition state like **41**, and (b) involving the formation of ion pairs (**43**) as intermediates. M = Zn, Mg, groups and solvating solvents in the periphery of **41**–**43** are not specified

bridged group between the two magnesium atoms in the dimeric transition state for symmetrical exchange was proposed (Scheme 8, transition state **41**)[85]. This S_Ei process is first order in the reagent when it is dimeric (e.g. RMgCl in Et_2O, $ca < 0.1$ M) but becomes second order when the RMgX (X = Br, I) is monomeric ($ca < 0.1$ M), according to the experimental observations. It should be pointed out also that complex reaction orders seem to operate at higher concentrations, due in part to insufficient solvation.

Organozinc reagents could participate in lower energy pathways for the inversion via aggregate formation, in the same way the concentration dependence of primary Grignard reagent inversion has been rationalized. Organozinc reagents easily form dimeric structures involved in the exchange process and dimers can even become the more stable species depending on the nature of the substituents (Sections II.A.1 and II.A.2). The case of organoaluminum reagents is of significance in this respect. While inversion rates for the primary reagents trineohexyl aluminum[82] or triisohexyl aluminum[86] were too slow to be measured in Et_2O, they could be measured in hydrocarbon solvents such as *n*-pentane or toluene[86], where stabilization through dimers is well established (see Section II.A.1.a). The geometry of **42** evokes that of Me_6Al_2. From neutron diffraction at low temperature of Me_6Al_2, the two bridging CH_3 groups adopt a staggered conformation with respect to each other in a molecule with C_{2h} symmetry[87], as would be the case in **42** for X = RCH_2. An aggregate may provide mechanistic opportunities for a carbanion to interact with a metal cation from one face, or with another cation from the other face, providing easier inversion pathways than a simple S_E1. In Scheme 8, an ionic mechanism for inversion involving dimeric organozinc reagents is proposed. By C–Zn heterolytic bond cleavage a fast inverting carbanion is formed, which is stabilized by ion-pair formation with a delocalized bis-organometallic countercation (**43**). Collapse of the inverted carbanion with the rear metal cation involves relatively little internal atomic rearrangement, in conformity with the least motion principle. The process results in inversion of one of the two organozinc molecules after dimer dissociation. The advantage of this ionic mechanism via **43** over

the concerted S_Ei route via **41** is that (a) it displays the correct $\Delta H^{\neq}$/MX electronegativity profiles corresponding to a heterolytic cleavage yielding ion-paired intermediates (see below), and (b) it can account for the positive activation entropy $\Delta S^{\neq}$ values displayed by the inversion process, based on the dissociation step (particularly with less polar, unassociated substrates such as R_2Zn). Large positive $\Delta S^{\neq}$ values are particularly difficult to accommodate in the context of a concerted mechanism via transition state **41**, for which activation profiles with negative $\Delta S^{\neq}$ values are expected, in analogy with the bimolecular exchange processes reported in Section II.C.1.

The reason for including the kinetic parameters of RMgX inversion in Table 4 is to get some insights of the corresponding activation parameters for RZnX (R = primary alkyl) from the available data for Grignard and diorganomagnesium reagents. Reactions passing through the same type of rate-determining transition state are likely to display isokinetic relationships or, in terms of the activation parameters, a good $\Delta H^{\neq}/\Delta S^{\neq}$ linear compensation effect[83,88]. An analysis of the activation parameters for R_2Mg and RMgX indicates that they actually do follow good isokinetic relationships[89], in spite of the large variation in magnitude of $\Delta H^{\neq}$ and $\Delta S^{\neq}$ (Table 4). An isokinetic finite temperature $T_{iso} = 336$ K is obtained for the RMgX and R_2Mg inversion process in Et_2O. An attempt to assign this isokinetic temperature to a vibrational resonant condition of the solvent–reactants system following isokinetic theories[89], affords a far-IR frequency of $\nu = 254\ cm^{-1}$, which may actually correspond to a skeletal vibration of the solvent according to the vibrational analysis of Et_2O (B3LYP/6-31+G**, $\nu = 252\ cm^{-1}$, B_1 symmetry). Also, the effect of the halide on the $\Delta H^{\neq}$ of RMgX is linear {[$R^2 = 0.9999$] vs. Pauling's electronegativity of the halide, [X = Cl (3.0), Br (2.8) and I (2.5)]}. This can be interpreted in terms of the effective electronegativity displayed by the Mg atom attached to it, which polarizes the C–Mg bond, showing the lower enthalpy barriers for the more polarized bonds. These apparently smooth behaviors displayed by the organomagnesium series, and the lack of experimental data on organozinc activation parameters, prompted us to propose an analogous isokinetic relationship for the organozinc series. If, as suspected, the halide effect acts in a similar manner in the actual organozinc reagents, the actual activation barriers for inversion presumably will resemble those in Table 5, obtained from Figure 5, taking as starting point the experimental activation parameters obtained for dineohexylzinc (Table 4).

The 500 MHz ^{1}H-NMR of the primary organozinc iodides **44a** and **44b** have been reported[93]. The methylenic protons α to the zinc atom occur as the AB part of an ABC spin system, indicating slow inversion rates. Applying equation 34 (see Appendix, Section IV.A) to the given chemical shifts and coupling constants, a lower limit for the free activation energy can be established as $\Delta G^{\neq} > 15$ kcal mol^{-1} in DMF-d_7 or THF-d_8 at 25 °C. No further attempts to approach closer to the coalescence temperature were undertaken (equation 26).

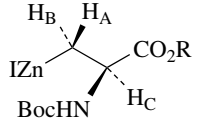

(44a) R = Bn
(44b) R = Me

500 MHz ^{1}H-NMR, DMF-d_7, 25 °C
44a: ABC system, $\nu_A - \nu_B = 0.06$ ppm, $J_{AB} = 12.5$ Hz
44b: ABC system, $\nu_A - \nu_B = 0.04$ ppm, $J_{AB} = 12.8$ Hz

$\rightarrow \Delta G^{\neq} > 15$ kcal mol^{-1} (26)

TABLE 4. Experimental activation parameters for the primary carbon–metal bond inversion as measured in Et_2O by VT-NMR [a]

Structure		M	$\Delta H^{\neq}$	$\Delta S^{\neq}$	$\Delta G^{\neq}_{298}$	Reference
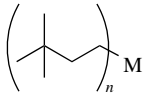	$n = 1$	Li	13.8	−3.5	14.9	82 [b]
	$n = 2$	Mg	18.7	−0.4	18.8 [c]	90 [b]
	$n = 2$	Zn	24.9	+12.8	21.1 [c]	82 [b]
	$n = 3$	Al	—	—	slow	82
	$n = 2$	Hg	—	—	slow	82
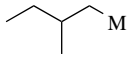		Li [d]	14.8	−3	15.7	91
		MgR [e]	18.2	+5	16.7	92
		MgI	20.4	+11	17.1	85
		MgBr	12.0	−11	15.3	92
		MgCl	6.2	−28	14.5	85

[a] Solvent is diethyl ether, unless otherwise stated. Different experimental conditions, such as concentration or the method of preparation of the organometallic compound, can be found in the different references. $\Delta H^{\neq}$, $\Delta G^{\neq}$ (kcal mol^{-1}); $\Delta S^{\neq}$ (cal mol^{-1} K^{-1}).
[b] Originally given as Arrhenius plots, these parameters were recalculated from raw data found in the reference. Reactions are considered first order in the organometallic species.
[c] Extrapolated to 298 K.
[d] In pentane.
[e] R = 2-methylbutyl.

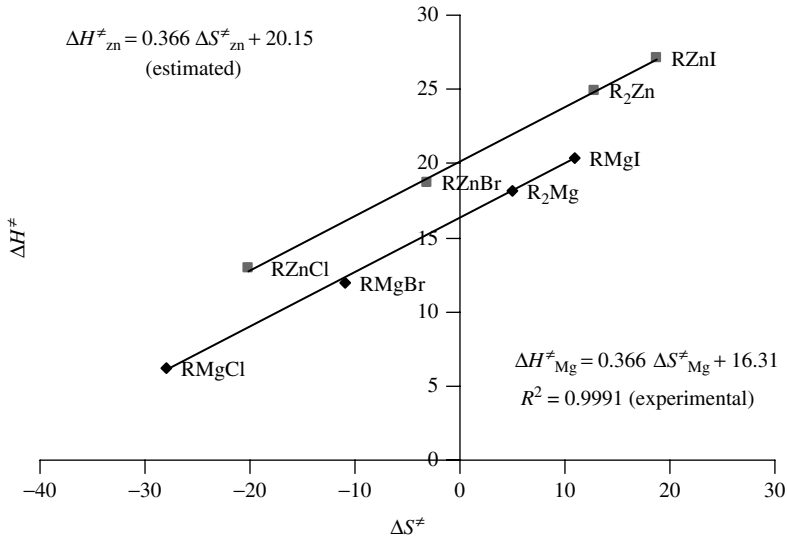

FIGURE 5. Plot of experimental $\Delta H^{\neq}$ vs. $\Delta S^{\neq}$ displaying a compensation effect for the RMgX series (R = 2-methylbutyl) with a fair slope, $T_{iso} = 366$ K in Et_2O. $\Delta H^{\neq}$ and $\Delta G^{\neq}$ are in kcal mol^{-1} and $\Delta S^{\neq}$ in cal mol^{-1} K^{-1}. Assuming a similar isokinetic behavior for the RZnX series, an estimate of the activation parameters can be obtained, which is plotted in the top line and detailed in Table 5

TABLE 5. Estimated activation parameters for primary organozinc inversion in Et_2O [a]

RZnX	$\Delta H^{\neq}$	$\Delta S^{\neq}$	$\Delta G^{\neq}_{298}$
$(RCH_2)_2Zn$ [b]	24.9	12.8	21.1
RCH_2ZnI	27.1	18.8	21.5
RCH_2ZnBr	18.7	−3.2	20.0
RCH_2ZnCl	12.9	−20.2	19.0

[a] Data inferred from Figure 5 assuming isokinetic behavior as for RMgX. $\Delta H^{\neq}$ and $\Delta G^{\neq}$ are in kcal mol^{-1} and $\Delta S^{\neq}$ in cal mol^{-1}K^{-1}.
[b] Experimental $\Delta H^{\neq}$ value for dineohexylzinc (Table 4).

B. Inversion at a Secondary Alkyl Carbon Bonded to Zinc

Ordinarily, NMR spectrometers are designed for operation between 200 °C and −100 °C or less, allowing the study of a wide range of systems with activation energies ranging between *ca* 5 to 25 kcal mol^{-1} [94]. The information obtained is very valuable when the experimental conditions allow the observation of coalescence or dynamic line broadening, from which activation parameters are obtained. However, in those cases in which the inversion is slow on the NMR time scale, the question about the preservation of the configurational integrity of the organometallic species in a macroscopic time scale remains unanswered. This is the case of most main-group secondary organometallic compounds, which are far more interesting for possible synthetic applications than primary ones (Table 6). Assuming the same electronegativity criteria given for primary organozinc reagents, it is not surprising that secondary organozinc bromides invert slowly under the reported experimental conditions (200 or 100 MHz ^{1}H-NMR, 1.5 M in THF, 150 °C), since neither alkyl secondary organolithium[95] nor organomagnesium[96] reagent inversion rates could be obtained in this way (Table 6).

The stereocontrolled (at the C−Zn center) preparation and reactions of organozinc compounds are, however, an active field of research. Diastereomeric cyclic secondary organozinc halides were prepared as mixtures of isomers that appear to be configurationally stable under the experimental reaction conditions used, although the distribution of products can be electrophile-dependent[100]. Other cyclic and acyclic diastereomerically

TABLE 6. Attempts to measure secondary alkyl carbon–metal bond inversion by NMR [a]

Structure		M	T (°C)	Solvent	MHz	Rate of inversion	Reference
	n = 1, 2, 3 [b]	MgBr	175	diglyme	60	slow	97
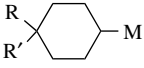	R = *t*-Bu, R′ = H	Li	40	pentane/tol	100/60	slow	98
	R = R′ = Me	MgBr	175	diglyme	60	slow	97
	R = Ph	ZnBr	150	THF [c]	200/100	slow	99
	R = Me	ZnBr	150	THF [c]	200/100	slow	99

[a] The detailed experimental conditions can be found in different references.
[b] For this and other isomeric *gem*-dimethyl cycloalkylmagnesium reagents.
[c] In the presence of one equivalent of a coordinating ligand (see text) using a pressure-NMR tube.

enriched mixed diorganozinc species have also been prepared and their stereochemistry studied after reaction with electrophiles[101]. Hydroboration plus organoboron–organozinc exchange (Section II.C.3) results in access to a variety of configurationally stable secondary organozinc reagents that were trapped with electrophiles after transmetallation, all the steps involving retention of the configuration[102]. Direct observation by NMR of the configuration of organozinc halides by employing chiral solvating agents[103, 104] was attained using C_2 symmetrically substituted ligands, the (+)-2,2′-isopropylidene-bis[(*R*)-4-phenyloxazoline] [(+)-(*R*)-**45**] giving the best results[99]. This chiral ligand displayed two sets of signals in the ^{1}H-NMR spectrum of 2-butylzinc bromide. The dynamic behavior of organometallic compounds in solution involves inversion at carbon bound to metal, carbon–metal exchange and ligand–metal coordination exchange. A fast dynamic equilibrium in solution, the product of these last two processes, generates surprisingly simple NMR spectra at room temperature (Scheme 9a, Figure 6a–c).

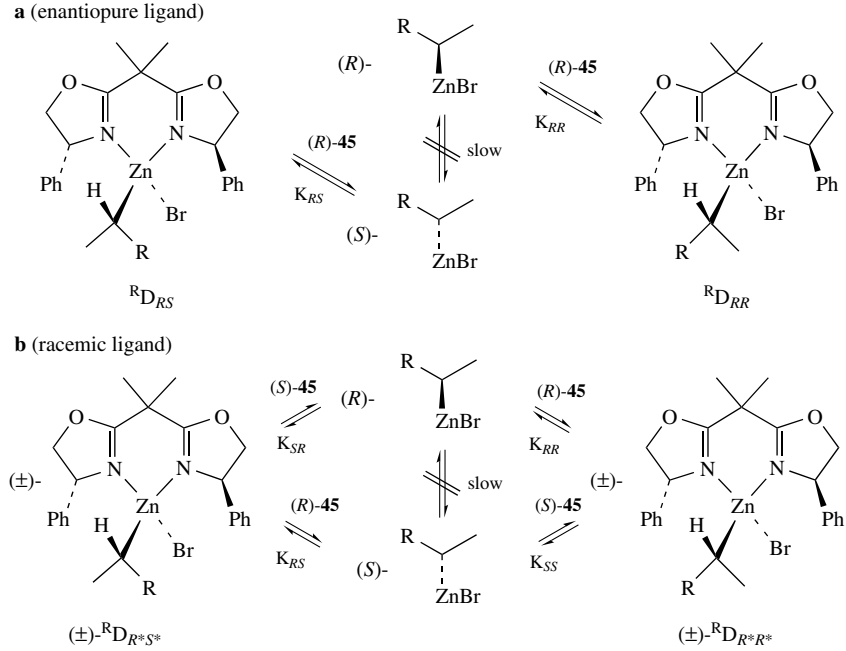

SCHEME 9. Complexation equilibria of 2-butylzinc bromide (R = Et) or 1-phenyl-2-propylzinc bromide (R = Bn) with: (a) (+)-(*R*)-**45**; (b) (±) -(*RS*)-**45**. $K_{RS} = K_{SR} = K_{R*S*}$; $K_{RR} = K_{SS} = K_{R*R*}$. The ratio of the concentration of both diastereomers, measured in the racemic system, is the equilibrium constant between these diastereomers $^{R}D_{RS} \leftrightarrows {}^{R}D_{RR}$; $^{R}K = K_{RR}/K_{RS} = [{}^{R}D_{R*R*}]/[{}^{R}D_{R*S*}]$

The fact that two sets of signals occur, corresponding to both enantiomers of the organozinc reagent (1.0:1 ratio), indicates by itself that inversion of configuration is slow on the NMR time scale, as could be inferred from data in Table 6. A different NMR test to determine the limits of the configurational robustness of the C–Zn bond in organozinc bromides comes from a different line of reasoning, which is described ahead following closely Reference 99. It is a fact that under fast equilibrium conditions, two racemic reagents will generate only *one* set of signals, even though two pairs of diastereomers are formed. Indeed, the use of a racemic ligand afforded a single set of signals, as

expected from a fast complexation equilibrium (Figure 6d, e). Procurement of the spectrum at $-50\,^{\circ}C$ freezes the equilibrium as seen by NMR, and two sets of signals are again observed. These two sets of signals are analogous to those observed using an enantiopure ligand, but appear with different relative proportions (Figure 6f). The ratio now corresponds to the *thermodynamic* equilibrium constant, which depends on the relative stabilities of both diastereomeric complexes and is in general different from 1:1. This ratio is ${}^{Et}K = K_{RR}/K_{RS} = 1.01{:}1$ for 2-butylzinc bromide at $-50\,^{\circ}C$ (R = ethyl, Scheme 9b, Figure 6f), right at the limit of sensitivity of the integration. The reason for

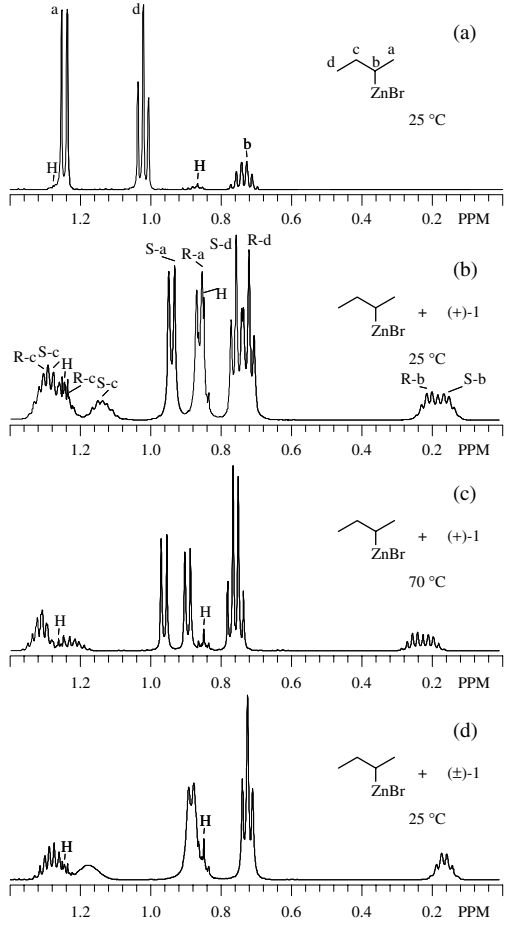

FIGURE 6. 500 MHz ^{1}H-NMR partial spectra of 2-butylzinc bromide in the presence of 1 equivalent of (+)-**45**, or its racemic counterpart (±)-**45**, at different temperatures. The side-product butane is represented by H. Methylene protons (c) are not shown in spectrum (a) due to solvent peak overlap. Assignments of the absolute configurations were made based on predicted anisotropic effects and are represented in spectrum (b). Reproduced by permission of Wiley-VCH from Reference 99

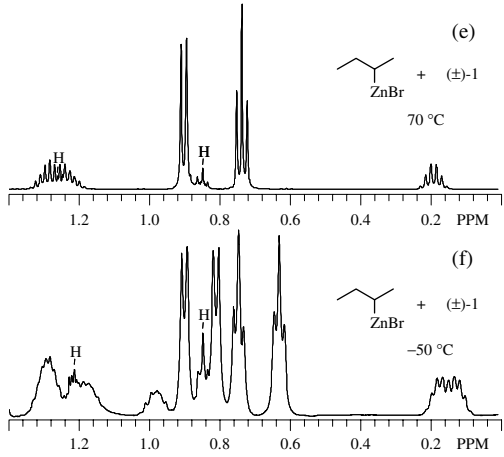

FIGURE 6. (*continued*)

this thermodynamic constant (^{Et}K) for the hypothetical equilibrium $^{Et}D_{RR} \leftrightarrows {}^{Et}D_{RS}$ being so close to 1 is the only limited difference in steric hindrance between Me and Et. Substitution of the Et by the more hindered group Bn modifies the final equilibrium composition, with $^{Bn}K = 2.70$ (R = benzyl, Scheme 9, Figure 7a–7f) at $-30\,^{\circ}C$. By using this last organozinc bromide, the rate of inversion of a secondary C–Zn bond could be measured. The spectrum of 1-phenyl-2-propylzinc bromide in the presence of 1 equivalent of (*R*)-**45** displayed, as expected, two sets of signals in a 1.0:1 ratio, indicating the racemic nature of

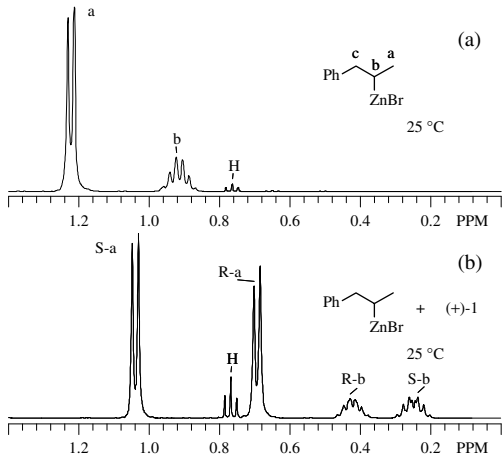

FIGURE 7. 500 MHz ^{1}H-NMR partial spectra of 1-phenyl-2-propylzinc bromide in the presence of 1 equivalent of (+)-**45**, or its racemic counterpart (±) -**45**, at different temperatures. The side-product 1-phenylpropane is represented by H. Methylene protons [c: 2.75–2.95 (2H, m, CH_2) in spectrum (a)] are not shown. Assignments of the absolute configurations were made based both on free energy criteria and predicted anisotropic effects and are represented in spectrum (b). Reproduced by permission of Wiley-VCH from Reference 99

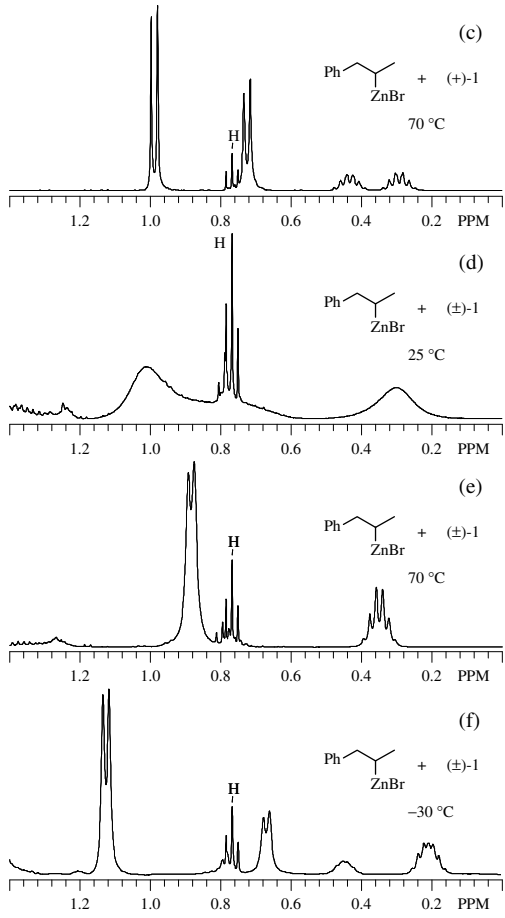

FIGURE 7. (*continued*)

the organozinc reagent (Figure 7b). However, this is not a steady state. It will depend on the inversion rate of the C−Zn bond as to how fast the composition of the enantiomeric mixture will spontaneously evolve from an initial 1:1 ratio to *ca* 2.70:1 ratio, reaching in doing so the thermodynamic equilibrium. This is analogous to saying that the presence of a chiral ligand shifts the composition of the racemic mixture of the organozinc bromide from 1:1 initially to another final value, which corresponds to the new thermodynamic equilibrium in that chiral medium. The racemic ligand approach can be used to obtain a good estimate of the thermodynamic constant corresponding to this new equilibrium. From the rate laws of interconversion of both enantiomers, represented by equation 27, the equations that describe the exponential approach to the final equilibrium can be easily deduced (equation 28). In the simplest approximation to the mechanism of inversion, a monomolecular transition state is assumed. D corresponds to the averaged signal of

the actual diastereomer and the free organozinc reagent, if any, in fast equilibrium, as observed by NMR.

$$D_{RR} \underset{k_{-1}}{\overset{k_1}{\rightleftharpoons}} D_{RS} \qquad K = \frac{k_1}{k_{-1}} \tag{27}$$

$$(1 + K)[D_{RR}] - 1 = \frac{K - 1}{2} e^{-(k_1 + k_{-1})t} \quad \text{or} \quad K - (1 + K)[D_{RS}] = \frac{K - 1}{2} e^{-(k_1 + k_{-1})t} \tag{28}$$

Monitoring a sample of BnCH(ZnBr)Me + (*R*)-**45** by ^{1}H-NMR for 9 days, a slow but perceptible evolution of both diastereomers was observed as they grew toward the predicted ratio ^{Bn}K. By using a logarithmic plot, equation 28 yielded a slope, $k_1 + k_{-1} = 0.00024\ h^{-1}$, from which the half life of the secondary carbon inversion was obtained, $t_{1/2} = 4.0$ months, corresponding to a free energy of activation $\Delta G^{\neq} = 27.2$ kcal mol^{-1} at 25 °C. The data collected represent only the early stages of the evolving system in its approach to the equilibrium. It is therefore only approximate, since the appearance of solids prevented a follow-up of the reaction to completion. As an example of application of this protocol, 2-octylzinc bromide prepared from enantiopure (*R*)-2-bromooctane and activated zinc was unambiguously identified as racemic. This avoids potential interference such as the use of electrophiles in the determination of enantiomeric excesses of organometallic compounds[105].

C. Vinylic Carbon Bonded to Zinc

Divinylzinc, vinyl organozinc halides and, in general, 1-alkenylzinc reagents are configurationally stable by NMR, displaying typical ^{1}H-NMR patterns consistent with fixed *Z*- or *E*-configurations at normal NMR frequencies. Divinylzinc, $(CH_2 = CH)_2Zn$, for instance, shows an ABC spin system by ^{1}H-NMR at 100 MHz with well-defined coupling constants: $^3J_{trans} = 21.9$ Hz, $^3J_{cis} = 15.74$ Hz, $^2J_{gem} = 5.44$ Hz in Et_2O[106]. Inversion barriers are unknown. Alkenylzinc halides and, in general, alkenylzinc compounds maintain their stereochemical integrity in their reaction with electrophiles[107]. Excellent configuration stability has been observed also for electron-poor polyfluorinated substituted vinylzinc halides[108] and *E*- and *Z*-1,2-difluorovinylzinc halides[109, 110] under a macroscopic (or laboratory) time scale.

D. Inversion at Benzylic Carbon Bonded to Zinc

Secondary benzylic organozinc halides have been studied from the point of view of their configuration stability[111]. Configurationally well-defined organozinc compounds can be conveniently prepared from benzyllithium reagents which, due to their fluxional behavior (low inversion barriers), populate the thermodynamically most stable benzyllithium epimer. Within the appropriate organic substitution pattern, this equilibrium can be shifted almost completely so only one diastereomer is virtually detectable. This is the case for certain intramolecularly-chelated benzyllithium reagents, such as **46**. Interestingly, these reagents undergo Li–Zn transmetallation with *inversion* of the configuration at the benzylic carbon, in analogy with other S_E2 reactions displayed by this system. The resulting

benzylic organozinc halides *syn*-**47** display manifestly higher inversion barriers than the original benzyllithium reagents, due to the higher covalent nature of the C–Zn bond[112]. Since *syn*-**47** is counter-thermodynamically configured, the equilibrium *syn*-**47** ⇆ *anti*-**47** tends to be re-established and its dynamics are observable within a macroscopic time scale. This spontaneous process can be studied using the temperature and time-before-quenching variable (Scheme 10). At −30 °C, an inversion process for *syn*-**47** is unnoticeable (*syn*:*anti* = ⩾98 : ⩽2), whereas 2 h at 50 °C is sufficient for the equilibrium to be re-established, by extensive epimerization in the direction of the thermodynamically more stable isomer *anti*-**47** (*anti*:*syn* = ⩾98 : ⩽2).

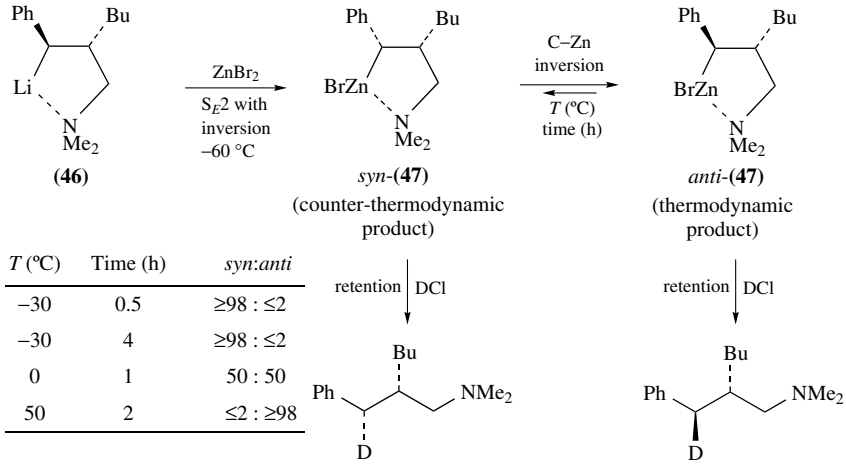

T (°C)	Time (h)	*syn*:*anti*
−30	0.5	≥98 : ≤2
−30	4	≥98 : ≤2
0	1	50 : 50
50	2	≤2 : ≥98

SCHEME 10. The benzylic organozinc reagent *syn*-**47** can be prepared in a near diastereomerically pure form (*syn:anti* **47**⩾98 : ⩽2) by Li–Zn transmetallation occurring with net inversion of the configuration. *Syn*-**47** inverts spontaneously and mostly completely to the thermodynamically more stable *anti*-**47**

For the sake of comparison with other organozinc reagents, an estimate of the activation barrier has been obtained. From the observation that 1 hour was required to reach equal proportions of the *syn* and *anti* diastereomers at 0 °C (i.e. *syn*:*anti* = 50:50), an adaptation of equation 28 (Section III.B) to the initial boundary conditions for the *syn*-**47** ⇆ *anti*-**47** equilibrium results in the expression: $-(k_1 + k_{-1})t_{(50:50)} = \ln[(K-1)/2K]$. From this, the experimental kinetic constant for this reversible process is obtained, $k_{exp} = k_1 + k_{-1} = 0.71\ h^{-1}$, corresponding to a free activation energy of $\Delta G^{\neq} = 20.6$ kcal mol^{-1} at 0 °C in 5:1 hexane–Et_2O. $K = [anti\text{-}\mathbf{47}]/[syn\text{-}\mathbf{47}] = 98/2$ is taken as an estimate of the thermodynamic equilibrium constant. Higher K values affect k_{exp} only marginally (e.g. for $K = \infty$ the error in k_{exp} is less than 3%). In other studies, configurationally labile secondary benzylic organozinc halides were proposed[113]. A fluxional behavior was required to explain the stereochemical outcome of some chirally-induced Pd-catalyzed cross-coupling reactions at room temperature, which afforded up to 86% ee (95% yield) starting with racemic benzylzinc halides. The mechanism of the inversion is not known although a mechanism involving dimers, as proposed for primary organozinc halides, is, in principle, feasible (Scheme 8, Section III.A). Dibenzylzinc is a low melting solid (mp 39.5–41.5 °C) sparingly soluble in hexane, indicating a certain tendency to association. Alternatively, due to the stability of the benzyl carbanion, dissociation and reorganization of ions in a more or less associated form (such as close contact pairs, solvent-separated pairs) could

account for the inversion rates in polar solvents, as proposed for different benzyl alkali derivatives[114].

E. Inversion at Allylic and Propargylic Carbon Bonded to Zinc

The propargylzinc–allenylzinc equilibrium, $RZnCH_2C{\equiv}CH \leftrightarrows H_2C{=}C{=}CHZnR$, is shifted well to the right, as can be inferred from the original ^{1}H-NMR and IR spectral data on diallenylzinc and allenylzinc halides[115], which share certain analogies with allenyllithium ($H_2C{=}C{=}CHLi$)[116]. Calculations on allenylmagnesium reagents[117], an *ab initio* and density functional theory (DFT) study of allenylzinc halides[118] also indicate an allenic nature for the organometallic reagent. If ionic routes are neglected, the inversion of configuration in the propargyl–allenyl organozinc system is markedly different from the inversion of configuration in the sp^3 carbon of allylic organozinc compounds. The latter is inevitably linked to two fast processes: (1) metallotropic shift and (2) free rotation around σ sp^2–sp^3 bond, resulting therefore in easy racemizations, with rates comparable to the slowest of these two steps, i.e. the Zn shift (Sections II.B.1 and II.B.2). For comparison, even at $-60\,^\circ$C in THF, diallylzinc exchange has $\Delta G^{\neq}$ *ca* 9.6 kcal mol^{-1} (Table 2), corresponding to a half-life time of only $t_{1/2} = 0.001$ s. Instead, for the propargyl–allenyl organozinc system, the free rotation step (2) is disabled in the allenyl form, impairing high inversion barriers of racemization in chiral allenylzinc reagents. Indeed, the allenyl zinc reagent **48** has been found to be configurationally stable at a not so low temperature as would be expected for an allylic organozinc derivative, by means of the Hoffmann test[119]. The stability was proven at $-60\,^\circ$C to $-10\,^\circ$C by comparing the stereochemical outcome of the reactions of **48** with both the enantiopure and the racemic form of an electrophilic imine[120]. Additionally, racemic **48** was resolved kinetically by using 0.5 equivalent of the enantiopure (*R*)-imine, which reacted selectively with the enantiomer (S_a)-**48** (matching pair). The remaining (R_a)-**48** (ee up to 88%) (mismatched reacting pair) was found to be configurationally stable at $-60\,^\circ$C on a macroscopic time scale (1–2 hours) (equation 29)[121].

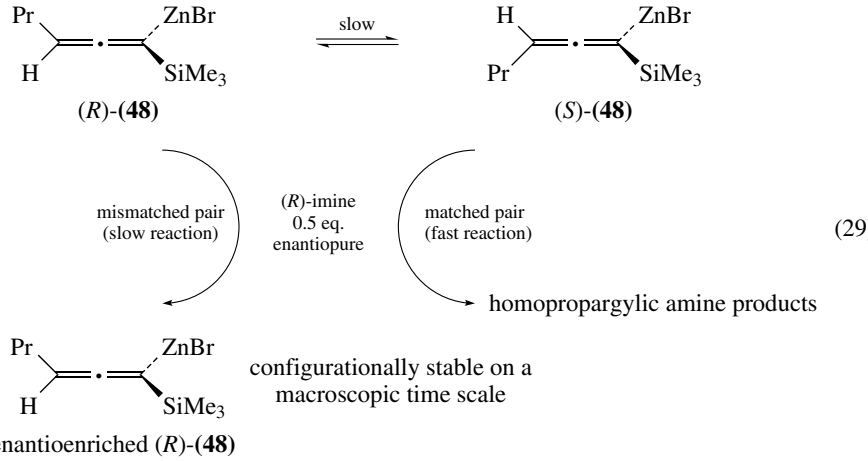

(29)

Regarding the potential mechanism of the propargyl–allenyl organozinc rearrangement (equation 30), neither rates or kinetic reaction orders are available, to the best of our knowledge. The process is conceptually attractive though. In the cases in which the

configuration of the propargyl–allenyl system is preserved—as in equation 29—a dissociative ionic route can be excluded. The metallotropic rearrangement is then either *antarafacial* or *suprafacial* in the propargyl–allenic subunit, but not both, since an alternative mechanism (i.e. one time *supra*-, next time *antara*- occurring indistinctly) would inevitably lead to racemic products [the stereodescriptors *supra*- and *antara*- are referred to the participating orbitals (see **49**) since the perpendicular double bond is irrelevant for orbital admixing with the σ C–Zn orbital, due to orthogonality and torsional constraints]. For potential unimolecular reactions, molecular orbital representation (cf. **49**a) represents the theoretically allowed (although unlikely) migrating pathway leading to an *antarafacial* stereochemistry, while transition state **50** is a tentative *suprafacial* pathway with (unnoticeable) inversion in the Zn atom. The geometry of the system might severely limit these approaches. For the *a priori* more likely bimolecular reactions, adaptations of the models described earlier for allylzinc rearrangement to the geometrical constraints present in propargyl–allenyl structures are in principle valid (Section II.B.1).

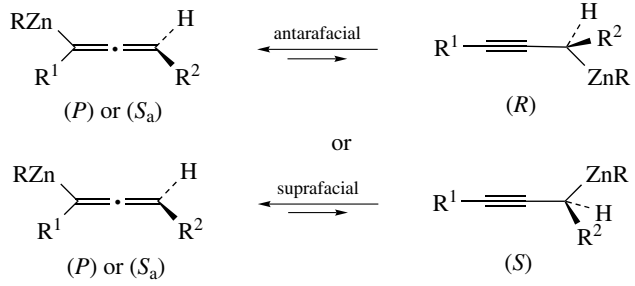

(30)

either *suprafacial* or *antarafacial*, but not both

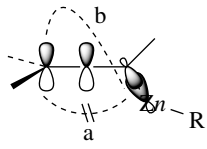

(49) (a) supra–supra (forbidden)
(b) antara–supra (allowed)

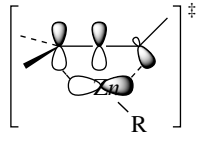

(50) supra–antara (allowed)

IV. APPENDIX

A. Obtention of the Different Activation Parameters by NMR

In general, two methods are used to determine quantitatively the parameters describing the dynamic behavior of molecules by means of NMR. The *complete line-shape analysis* relies upon the theoretical calculation of spectra. Resolving the NMR rate equations (the Bloch equations) for exchanging systems allows one to calculate the spectrum for any given exchange rate, which usually requires computer analysis. Such calculations tell us the number of peaks, their line widths and intensities, i.e. the entire spectral curve or *line shape*. When dynamic processes are present, the *line shape* depends much on the exchange rate k, and thus on the time τ spent by the nuclei in a particular environment, or *lifetime*. For first and second order reactions the expressions defining τ are equations 31 and 32.

$$\text{First order:}\quad \text{A} \xrightarrow{k_1} \text{B},\ \textit{rate} = k_1[\text{A}] \text{ and } \textit{lifetime}, \tau(\text{s}): \quad \frac{1}{\tau_\text{A}} = k_1\ (\text{s}^{-1}) \tag{31}$$

$$\text{Second order: A} + \text{B} \xrightarrow{k_2} \text{C}, \textit{ rate} = k_2[\text{A}][\text{B}], \text{ and}$$

$$\textit{lifetime}, \tau\,(\text{s}) : \frac{1}{\tau_\text{A}} = k_2[\text{B}]; \frac{1}{\tau_\text{B}} = k_2[\text{A}]\ (\text{s}^{-1}) \tag{32}$$

Simulation of the spectra recorded at different temperatures near the region where dynamics produces major changes in the line shape allows us to obtain different values of $1/\tau$. Since each chemical shift difference between exchanging sites, as well as each spin coupling, gives rise to a *coalescence* of its own (when its $\Delta\nu$ or $J \approx k$), the analysis can be extended over a wide range of temperatures covering the different coalescence temperatures of the different signals. From here, k is obtained as a function of T and the activation parameters can be obtained by plotting according to the Arrhenius or Eyring equations.

On the other hand, a simpler treatment comes from the observation of *coalescence*. In an exchanging system, such as A $\leftrightarrows$ B, a nucleus in state A has a chemical shift ν_A (and possibly a coupling constant of J_A), and in state B a chemical shift ν_B (and a coupling constant of J_B). Always referred to the NMR time scale, we talk of *slow exchange* conditions, when we observe the NMR spectra of the two species A and B, from which ν_A, ν_B, J_A and J_B, as well as the constant K of the equilibrium can be obtained. Under *fast exchange* conditions, the observed spectrum is an averaged spectrum in which the chemical shifts and couplings are the weighted averages of the values in A and B. Under *intermediate exchange* conditions, however, we observe broad lines, indicative of a rate process. As the temperature rises, the two sets of signals observed under slow-exchange conditions begin to merge into one broad signal, which becomes sharp at still higher temperatures. When no observable valley between the two merging sets of signals exists, *coalescence* has occurred. The temperature at which this happens is the *coalescence temperature*, T_C. The coalescence temperature itself is not a constant, but is a quantity that depends on the frequency of observation of the spectrometer. The higher the observing frequency, the higher T_C will be observed. From the coalescence, the Bloch equations can be solved analytically for a number of simple cases, which affords directly the rate constant (k_c) of the exchange at the temperature of coalescence. In the simple case of an equilibrium A $\leftrightarrows$ B, and provided that the following restrictions 1–3 are fulfilled,

1. the dynamic process occurring is first order kinetically,
2. the two sites A and B have equal populations (i.e. $K = 1$),
3. the two exchanging nuclei are not coupled to each other,

then the expression that gives k_c as a function of $\Delta\nu$ is given by equation 33,

$$k_\text{c} = \frac{\pi}{\sqrt{2}}\Delta\nu, \quad \text{where } \Delta\nu = \nu_\text{A} - \nu_\text{B}\ (\text{Hz}) \tag{33}$$

Strictly speaking, $\Delta\nu$ must be the chemical shift difference at T_C, obtained by extrapolation from lower temperatures. However, even if these conditions are not fulfilled exactly, equation 33 is often a reasonable approximation for estimating k_c and therefore activation barriers at the temperature T_C. For an exchange process between two nuclei A $\leftrightarrows$ B with a mutual coupling J_AB, equation 34 applies and gives the rate constant at the coalescence temperature,

$$k_\text{c} = \frac{\pi}{\sqrt{2}}\sqrt{\Delta\nu^2 + 6J^2{}_\text{AB}}, \quad \text{where } \Delta\nu = \nu_\text{A} - \nu_\text{B}, \text{ and } J_\text{AB}, \text{ are in Hz} \tag{34}$$

Equations 33 and 34 are valid only for the case given, degenerate states and first-order reactions, but are often used to obtain approximate values of $\Delta G^{\neq}$ [122].

B. Relationships between Activation Parameters

1. The Arrhenius and Eyring equations

In the earlier days of dynamic NMR spectroscopy, most researchers used the Arrhenius equation, founded on the empirical observation that conducting a reaction at a higher temperature increases the reaction rate. By applying the Arrhenius equation (equation 35) it is possible to determine graphically the activation energy E_a of a dynamic process, where T is temperature in K, A is the frequency (or pre-exponential) factor ($\ln A$ relates to the entropy of activation) and R is the universal gas constant ($R = 1.98719\ \mathrm{cal\,mol^{-1}\,K^{-1}}$). Plotting $\ln k$ against $1/T$ yields, for many reactions, a straight line with slope $-E_a/R$.

$$k = A\, e^{\frac{-E_a}{RT}}, \quad \text{from where} \quad \ln k = \ln A - \frac{E_a}{RT} \tag{35}$$

In contrast with the Arrhenius equation, the Eyring equation is a theoretical construct, based on the transition state model. The Eyring equation describes the temperature dependence of the reaction rates. It interrelates the rate constant k with the free energy of activation $\Delta G^{\neq}$, through the pseudo-equilibrium constant of formation of the transition state from reagents, $K^{\neq}$; $K^{\neq}$ can be expressed in different units and is dimension-corrected by c°. Thus the free energy of activation, $\Delta G^{\neq}$ ($\mathrm{kcal\,mol^{-1}}$), is related to $K^{\neq}$ by equation 36 and can be also expressed in terms of $\Delta H^{\neq}$ (enthalpy of activation, in $\mathrm{kcal\,mol^{-1}}$) and $\Delta S^{\neq}$ (entropy of activation, in $\mathrm{cal\,mol^{-1}\,K^{-1}}$ or entropy units, e.u.) using pseudo-thermodynamic relationships, where T is the temperature in K. At present, most investigators prefer to use the Eyring equation (equation 37) to obtain the activation parameters, where k is the rate constant, κ is the transmission coefficient (usually assumed to be exactly 1), k_B is the Boltzmann constant ($k_B = 3{,}29986{\bullet}10^{-24}\ \mathrm{cal\,K^{-1}}$), h is the Plank constant ($h = 1{,}58369{\bullet}10^{-34}$ cal s), c° depends on $K^{\neq}$ (and is the standard concentration $c^{\circ} = 1\ \mathrm{mol\,l^{-1}}$ if $K^{\neq}$ has units $\mathrm{l\,mol^{-1}}$ etc.) and R is the universal gas constant.

$$-RT\ln(K^{\neq}c^{\circ}) = \Delta G^{\neq} = \Delta H^{\neq} - T\Delta S^{\neq} \tag{36}$$

$$k = \kappa\frac{k_B T}{hc^{\circ}}e^{\frac{-\Delta G^{\neq}}{RT}}; \quad \ln\frac{k}{T} = -\frac{\Delta H^{\neq}}{RT} + \ln\frac{k_B}{h} + \frac{\Delta S^{\neq}}{R} \tag{37}$$

The quantities $\Delta H^{\neq}$ and $\Delta S^{\neq}$ are obtained by plotting $\ln k/T$ against $1/T$ (equation 37, right), obtained by combining equation 36 and the Eyring equation (equation 37, left).

The activation parameters of the Arrhenius and Eyring equations can be related using the expression in equation 38, with T the mean temperature within the experimental range. Equation 38 originates from the thermodynamic definition of enthalpy and, assuming ideal gas behavior (a condition not always fulfilled): $\Delta H = \Delta(E + pV) = \Delta E + \Delta nRT$. For a reaction of the type $A + B \leftrightarrows [AB]^{\neq}$, $\Delta n = -1$, and identifying the internal energy ΔE as the activation energy E_a in going from reactants to activated complexes, equation 38 (left) is obtained. By substituting equation 38 (left) in the Eyring equation, the expression for the pre-exponential factor is also obtained (equation 38, right). When extrapolations

of the activation barriers to other temperatures need to be done, equation 36 can be used since $\Delta H^{\neq}$ and $\Delta S^{\neq}$ are usually assumed to vary little with the temperature.

$$\Delta H^{\neq} = \Delta E_a - RT; \quad A = e\frac{k_B T}{h} e^{\frac{\Delta S^{\neq}}{R}} \tag{38}$$

The activation parameters are subjected to errors, especially in the precise determination of temperatures such as T_C, the frequency separation ($\Delta\nu$), line widths, coupling constants, variation of the concentration with the temperature etc. Although the experimental determination of the activation parameters could have been performed accurately, it should not be pretended to possess excessive accuracy. Caution is advised especially with entropies of activation, due to the inherent imprecision of the method (ordinates at the origin from least-squares line fitting)[94, 123].

V. REFERENCES

1. F. J. Weigert, M. Winokur and J. D. Roberts, *J. Am. Chem. Soc.*, **90**, 1566 (1968).
2. T. A. Mobley and S. Berger, *Angew. Chem., Int. Ed.*, **38**, 3070 (1999).
3. H. Nehl and W. R. Scheidt, *J. Organomet. Chem.*, **289**, 1 (1985).
4. M. Fontes, X. Verdaguer, L. Sola, M. A. Pericas and A. Riera, *J. Org. Chem.*, **69**, 2532 (2004).
5. (a) I. S. Butler and M. L. Newbury, *Spectrochim. Acta, Part A*, **33A**, 669 (1977).
   (b) H. W. Thompson, J. W. Linnett and F. J. Wagstaffe, *Trans. Faraday Soc.*, **36**, 797 (1940).
6. A. Haaland, J. C. Green, G. S. McGrady, A. J. Downs, E. Gullo, M. J. Lyall, J. Timberlake, A. V. Tutukin, H. V. Volden and K.-A. Ostby, *Dalton Trans.*, 4356 (2003).
7. K. S. Rao, B. P. Stoicheff and R. Turner, *Can. J. Phys.*, **38**, 1516 (1960).
8. N. N. Greenwood and A. Earnshaw (Eds.), *Chemistry of the Elements*, 2nd edn., Butterworth-Heinemann, Oxford, 1997, p. 1205.
9. E. Weiss, *J. Organomet. Chem.*, **2**, 314 (1964).
10. (a) E. C. Ashby and G. E. Parris, *J. Am. Chem. Soc.*, **93**, 1206 (1971).
    (b) E. C. Ashby, G. E. Parris and F. Walker, *J. Chem. Soc., Chem. Commun.*, 1464 (1969).
11. G. M. Whitesides, F. Kaplan and J. D. Roberts, *J. Am. Chem. Soc.*, **85**, 2167 (1963).
12. H. O. House, R. A. Latham and G. M. Whitesides, *J. Org. Chem.*, **32**, 2481 (1967).
13. (a) G. S. McGrady, J. F. C. Turner, R. M. Ibberson and M. Prager, *Organometallics*, **19**, 4398 (2000).
    (b) P. H. Lewis and R. E. Rundle, *J. Chem. Phys.*, **21**, 986 (1953).
    (c) J. C. Huffman and W. E. Streib, *J. Chem. Soc., Chem. Commun.*, 911 (1971).
14. N. Muller and D. E. Pritchard, *J. Am. Chem. Soc.*, **82**, 248 (1960).
15. O. Yamamoto and M. Yanagisawa, *Bull. Chem. Soc. Jpn.*, **51**, 1231 (1978).
16. Z. Cerny, J. Fusek, O. Kriz, S. Hermanek, M. Solc and B. Casensky, *J. Organomet. Chem.*, **386**, 157 (1990).
17. J. G. Noltes and J. Boersma, *J. Organomet. Chem.*, **9**, 1 (1967).
18. R. Mynott, B. Gabor, H. Lehmkuhl and I. Doering, *Angew. Chem.*, **97**, 332 (1985).
19. W. Strohmeier, K. Humpfner, K. Miltenberger and F. Seifert, *Z. Elektrochem.*, **63**, 537 (1959).
20. P. R. Markies, G. Schat, O. S. Akkerman and F. Bickelhaupt, *Organometallics*, **9**, 2243 (1990).
21. D. K. Breitinger and C. E. Zybill, in *Synthetic Methods of Organometallic and Inorganic Chemistry* (Ed. W. A. Herrmann), Vol. 5, Thieme, Stuttgart, 1999, pp. 109–165.
22. J. Boersma, in *Comprehensive Organometallic Chemistry* (Ed. G. Wilkinson, F. G. A. Stone and E. W. Abel), Vol. 2, Pergamon Press, Oxford, 1982, pp. 823–862.
23. E. A. Jeffery and T. Mole, *J. Organomet. Chem.*, **11**, 393 (1968).

24. J. Boersma, *J. Organomet. Chem.*, **189**, 1 (1980).
25. J. Boersma and J. G. Noltes, *Tetrahedron Lett.*, 1521 (1966).
26. J. Boersma and J. G. Noltes, *J. Organomet. Chem.*, **13**, 291 (1968).
27. P. A. van der Schaaf, E. Wissing, J. Boersma, W. J. J. Smeets, A. L. Spek and G. van Koten, *Organometallics*, **12**, 3624 (1993).
28. P. O'Brien, in *Comprehensive Organometallic Chemistry II* (Eds. E. W. Abel, F. G. A. Stone and G. Wilkinson), Vol. 3, Elsevier Science, Oxford, 1995, pp. 175–196.
29. J. Boersma and J. G. Noltes, *J. Organomet. Chem.*, **8**, 551 (1967).
30. D. F. Evans and G. V. Fazakerley, *J. Chem. Soc., A*, 182 (1971).
31. D. F. Evans and G. V. Fazakerley, *J. Chem. Soc., A*, 184 (1971).
32. R. E. Dessy and G. R. Coe, *J. Org. Chem.*, **28**, 3592 (1963).
33. D. F. Evans and I. Wharf, *J. Chem. Soc., A*, 783 (1968).
34. D. F. Evans and R. F. Phillips, *J. Chem. Soc., Dalton Trans.*, 978 (1973).
35. (a) E. C. Ashby, J. Laemmle and H. M. Neumann, *J. Am. Chem. Soc.*, **93**, 4601 (1971).
    (b) E. C. Ashby, J. Laemmle and H. M. Neumann, *J. Am. Chem. Soc.*, **94**, 5421 (1972).
36. E. C. Ashby and R. Reed, *J. Org. Chem.*, **31**, 971 (1966).
37. M. B. Smith and W. E. Becker, *Tetrahedron Lett.*, 3843 (1965).
38. M. B. Smith and W. E. Becker, *Tetrahedron*, **23**, 4215 (1967).
39. M. B. Smith and W. E. Becker, *Tetrahedron*, **22**, 3027 (1966).
40. J. Tammiku-Taul, P. Burk and A. Tuulmets, *J. Phys. Chem. A*, **108**, 133 (2004).
41. L. M. Seitz and T. L. Brown, *J. Am. Chem. Soc.* **88**, 4140 (1966).
42. L. M. Seitz and B. F. Little, *J. Organomet. Chem.* **18**, 227 (1969).
43. (a) M. Uchiyama, M. Koike, M. Kameda, Y. Kondo and T. Sakamoto, *J. Am. Chem. Soc.* **118**, 8733 (1996).
    (b) M. Uchiyama, Y. Kondo, T. Miura and T. Sakamoto, *J. Am. Chem. Soc.* **119**, 12372 (1997).
    (c) M. Uchiyama, M. Kameda, O. Mishima, N. Yokoyama, M. Koike, Y. Kondo and T. Sakamoto, *J. Am. Chem. Soc.*, **120**, 4934 (1998).
44. E. Weiss, *Angew. Chem., Int. Ed. Engl.*, **32**, 1501 (1993).
45. E. Weiss and R. Wolfrum, *Chem. Ber.*, **101**, 35 (1968).
46. K. H. Thiele, G. Engelhardt, J. Koehler and M. Arnstedt, *J. Organomet. Chem.*, **9**, 385 (1967).
47. R. Benn, E. G. Hoffmann, H. Lehmkuhl and H. Nehl, *J. Organomet. Chem.*, **146**, 103 (1978).
48. D. A. Hutchison, K. R. Beck, R. A. Benkeser and J. B. Grützner, *J. Am. Chem. Soc.*, **95**, 7075 (1973).
49. M. Staehle and M. Schlosser, *J. Organomet. Chem.*, **220**, 277 (1981).
50. H. E. Zieger and J. D. Roberts, *J. Org. Chem.*, **34**, 1976 (1969).
51. (a) G. M. Whitesides, J. E. Nordlander and J. D. Roberts, *J. Am. Chem. Soc.*, **84**, 2010 (1962).
    (b) G. M. Whitesides, J. E. Nordlander and J. D. Roberts, *Discuss. Faraday Soc.*, **34**, 185 (1962).
52. E. G. Hoffmann, H. Nehl, H. Lehmkuhl, K. Seevogel and W. Stempfle, *Chem. Ber.*, **117**, 1364 (1984).
53. R. Benn, H. Grondey, H. Lehmkuhl, H. Nehl, K. Angermund and C. Krueger, *Angew. Chem.*, **99**, 1303 (1987).
54. J. St. Denis, J. P. Oliver and J. B. Smart, *J. Organomet. Chem.*, **44**, C32 (1972).
55. H. Yasuda, Y. Ohnuma, A. Nakamura, Y. Kai, N. Yasuoka and N. Kasai, *Bull. Chem. Soc. Jpn.*, **53**, 1101 (1980).
56. H. Yasuda, M. Yamauchi, A. Nakamura, T. Sei, Y. Kai, N. Yasuoka and N. Kasai, *Bull. Chem. Soc. Jpn.*, **53**, 1089 (1980).
57. P. H. M. Budzelaar, J. Boersma, G. J. M. Van der Kerk, A. L. Spek and A. J. M. Duisenberg, *J. Organomet. Chem.*, **281**, 123 (1985).
58. O. G. Garkusha, B. V. Lokshin and G. K. Borisov, *J. Organomet. Chem.*, **553**, 59 (1998).
59. (a) A. Haaland, S. Samdal, N. V. Tverdova, G. V. Girichev, N. I. Giricheva, S. A. Shlykov, O. G. Garkusha and B. V. Lokshin, *J. Organomet. Chem.*, **684**, 351 (2003).
    (b) B. V. Lokshin, O. G. Garkusha, Y. A. Borisov and N. E. Borisova, *Russ. Chem. Bull.*, **52**, 831 (2003).
60. B. Fischer, P. Wijkens, J. Boersma, G. Van Koten, W. J. J. Smeets, A. L. Spek and P. H. M. Budzelaar, *J. Organomet. Chem.*, **376**, 223 (1989).

61. (a) R. Blom, A. Haaland and J. Weidlein, *J. Chem. Soc., Chem. Commun.*, 266 (1985).
(b) R. Blom, J. Boersma, P. H. M. Budzelaar, B. Fischer, A. Haaland, H. V. Volden and J. Weidlein, *Acta Chem. Scand., Ser. A*, **40**, 113 (1986).
62. A. L. Allred and C. R. McCoy, *Tetrahedron Lett.*, 25 (1960).
63. C. R. McCoy and A. L. Allred, *J. Am. Chem. Soc.*, **84**, 912 (1962).
64. R. E. Dessy, F. Kaplan, G. R. Coe and R. M. Salinger, *J. Am. Chem. Soc.*, **85**, 1191 (1963).
65. K. L. Henold, J. Soulati and J. P. Oliver, *J. Am. Chem. Soc.*, **91**, 3171 (1969).
66. J. Soulati, K. L. Henold and J. P. Oliver, *J. Am. Chem. Soc.*, **93**, 5694 (1971).
67. Z. Cerny, J. Fusek, O. Kriz, S. Hermanek, M. Solc and B. Casensky, *J. Organomet. Chem.*, **386**, 157 (1990).
68. W. Bremser, M. Winokur and J. D. Roberts, *J. Am. Chem. Soc.*, **92**, 1080 (1970).
69. N. S. Ham, E. A. Jeffery, T. Mole, J. K. Saunders and S. N. Stuart, *J. Organomet. Chem.*, **8**, P7 (1967).
70. M. H. Abraham and P. H. Rolfe, *J. Organomet. Chem.*, **8**, 385 (1967).
71. W. A. Nugent and J. K. Kochi, *J. Am. Chem. Soc.*, **98**, 5979 (1976).
72. (a) L. M. Sayre and F. R. Jensen, *J. Am. Chem. Soc.*, **101**, 6001 (1979).
(b) L. M. Sayre and F. R. Jensen, *J. Am. Chem. Soc.*, **101**, 1900 (1979).
73. L. I. Zakharkin and O. Y. Okhlobystin, *Zh. Obshch. Khim.*, **30**, 2134 (1960); *Chem. Abstr.*, **55**, 48478 (1961).
74. K. H. Thiele and P. Zdunneck, *J. Organomet. Chem.*, **4**, 10 (1965).
75. K. H. Thiele and J. Koehler, *J. Prakt. Chem.*, **32**, 54 (1966).
76. (a) F. Langer, J. Waas and P. Knochel, *Tetrahedron Lett.*, **34**, 5261 (1993).
(b) E. Hupe, M. I. Calaza and P. Knochel, *J. Organomet. Chem.*, **680**, 136 (2003).
77. (a) H. C. Brown and B. Singaram, *Pure Appl. Chem.*, **59**, 879 (1987).
(b) I. Beletskaya and A. Pelter, *Tetrahedron*, **53**, 4957 (1997).
(c) H. C. Brown, *Pure Appl. Chem.*, **47**, 49 (1976).
78. (a) K. Burgess and W. A. Van der Donk, in *Advanced Asymmetric Synthesis*, Blackie Academic & Professional, an imprint of Chapman & Hall, London, 1996, p. 181.
(b) H. C. Brown, P. K. Jadhav and B. Singaram, *Mod. Synth. Methods*, **4**, 307 (1986).
(c) H. C. Brown and P. K. Jadhav, *Asymmetric Synth.*, **2**, 1 (1983).
79. E. Hupe, P. Knochel and K. J. Szabo, *Organometallics*, **21**, 2203 (2002).
80. E. Hupe and P. Knochel, *Org. Lett.*, **3**, 127 (2001).
81. G. Binsch, E. L. Eliel and H. Kessler, *Angew. Chem., Int. Ed. Engl.*, **10**, 570 (1971).
82. M. Witanowski and J. D. Roberts, *J. Am. Chem. Soc.*, **88**, 737 (1966).
83. J. E. Leffler, *J. Org. Chem.*, **20**, 1202 (1955).
84. H. J. Reich, M. A. Medina and M. D. Bowe, *J. Am. Chem. Soc.*, **114**, 11003 (1992).
85. G. Fraenkel, C. E. Cottrell and D. T. Dix, *J. Am. Chem. Soc.*, **93**, 1704 (1971).
86. G. Fraenkel, D. T. Dix and M. Carlson, *Tetrahedron Lett.*, 579 (1968).
87. G. S. McGrady, J. F. C. Turner, R. M. Ibberson and M. Prager, *Organometallics*, **19**, 4398 (2000).
88. L. Liu and Q.-X. Guo, *Chem. Rev.*, **101**, 673 (2001).
89. (a) W. Linert, *Chem. Soc. Rev.*, **23**, 429 (1994).
(b) W. Linert and R. F. Jameson, *Chem. Soc. Rev.*, **18**, 477 (1989).
90. G. M. Whitesides, M. Witanowski and J. D. Roberts, *J. Am. Chem. Soc.*, **87**, 2854 (1965).
91. G. Fraenkel, W. E. Beckenbaugh and P. P. Yang, *J. Am. Chem. Soc.*, **98**, 6878 (1976).
92. G. Fraenkel and D. T. Dix, *J. Am. Chem. Soc.*, **88**, 979 (1966).
93. R. F. W. Jackson, R. J. Moore, C. S. Dexter, J. Elliott and C. E. Mowbray, *J. Org. Chem.*, **63**, 7875 (1998).
94. M. Oki, '*Applications of Dynamic NMR Spectroscopy to Organic Chemistry*', in *Methods in Stereochemical Analysis, Vol. 4* (Ed. A. P. Marchand), VCH Publishers, Deerfield Beach, 1985, p. 3.
95. (a) A. Basu and S. Thayumanavan, *Angew. Chem., Int. Ed.*, **41**, 716 (2002).
(b) D. Hoppe and T. Hense, *Angew. Chem., Int. Ed. Engl.*, **36**, 2283 (1997).
(c) P. Beak, A. Basu, D. J. Gallagher and Y. S. Park, *Acc. Chem. Res.*, **29**, 552 (1996).
(d) D. Iula and R. E. Gawley, *J. Org. Chem.*, **65**, 6169 (2000).
(e) H. J. Reich, J. E. Holladay, T. G. Walker and J. L. Thompson, *J. Am. Chem. Soc.*, **121**, 9769 (1999).

(f) H. J. Reich and K. J. Kulicke, *J. Am. Chem. Soc.*, **118**, 273 (1996).
(g) H. J. Reich and K. J. Kulicke, *J. Am. Chem. Soc.*, **117**, 6621 (1995).
96. (a) R. W. Hoffmann, *Chem. Soc. Rev.*, **32**, 225 (2003).
(b) R. W. Hoffmann and B. Hoelzer, *J. Am. Chem. Soc.*, **124**, 4204 (2002).
(c) R. W. Hoffmann and B. Holzer, *Chem. Commun.*, 491 (2001).
(d) R. W. Hoffmann, B. Holzer, O. Knopff and K. Harms, *Angew. Chem., Int. Ed.*, **39**, 3072 (2000).
97. E. Pechhold, D. G. Adams and G. Fraenkel, *J. Org. Chem.*, **36**, 1368 (1971).
98. (a) W. H. Glaze, C. M. Selman, A. L. Ball, Jr. and L. E. Bray, *J. Org. Chem.*, **34**, 641 (1969).
(b) W. H. Glaze and C. M. Selman, *J. Organometal. Chem.*, **11**, P3 (1968).
(c) W. H. Glaze and C. M. Selman, *J. Org. Chem.*, **33**, 1987 (1968).
99. A. Guijarro and R. D. Rieke, *Angew. Chem., Int. Ed.*, **39**, 1475 (2000).
100. R. Duddu, M. Eckhardt, M. Furlong, H. P. Knoess, S. Berger and P. Knochel, *Tetrahedron*, **50**, 2415 (1994).
101. (a) C. Darcel, F. Flachsmann and P. Knochel, *Chem. Commun.*, 205 (1998).
(b) A. Boudier, F. Flachsmann and P. Knochel, *Synlett*, 1438 (1998).
102. (a) A. Boudier, C. Darcel, F. Flachsmann, L. Micouin, M. Oestreich and P. Knochel, *Chem. Eur. J.*, **6**, 2748 (2000).
(b) P. Knochel, A. Boudier, L. O. Bromm, E. Hupe, J. A. Varela, A. Rodriguez, C. Koradin, T. Bunlaksananusorn, H. Laaziri and F. Lhermitte, *Pure Appl. Chem.*, **72**, 1699 (2000).
103. D. Parker, *Chem. Rev.*, **91**, 1441 (1991).
104. R. W. Hoffmann, W. Klute, R. K. Dress and A. Wenzel, *J. Chem. Soc., Perkin Trans. 2*, 1721 (1995).
105. (a) A. Guijarro and R. D. Rieke, *Angew. Chem., Int. Ed. Engl.*, **37**, 1679 (1998).
(b) A. Guijarro, D. M. Rosenberg and R. D. Rieke, *J. Am. Chem. Soc.*, **121**, 4155 (1999).
106. H. D. Visser and J. P. Oliver, *J. Organomet. Chem.*, **40**, 7 (1972).
107. J. A. Marshall and P. Eidam, *Org. Lett.*, **6**, 445 (2004).
108. S. W. Hansen, T. D. Spawn and D. J. Burton, *J. Fluorine Chem.*, **35**, 415 (1987).
109. (a) C. R. Davis and D. J. Burton, *Tetrahedron Lett.*, **37**, 7237 (1996).
(b) Q. Liu and D. J. Burton, *Tetrahedron Lett.*, **41**, 8045 (2000).
110. C. R. Davis and D. J. Burton, *J. Org. Chem.*, **62**, 9217 (1997).
111. S. Klein, I. Marek and J.-F. Normant, *J. Org. Chem.*, **59**, 2925 (1994).
112. S. Norsikian, I. Marek, S. Klein, J. F. Poisson and J. F. Normant, *Chem. Eur. J.*, **5**, 2055 (1999).
113. T. Hayashi, T. Hagihara, Y. Katsuro and M. Kumada, *Bull. Chem. Soc. Jpn.*, **56**, 363 (1983).
114. (a) D. Hoppe, A. Carstens and T. Krämer, *Angew. Chem., Int. Ed. Engl.*, **29**, 1424 (1990).
(b) R. W. Hoffmann, R. K. Dress, T. Ruhland and A. Wenzel, *Chem. Ber.*, **128**, 861 (1995).
115. K. H. Thiele and D. Gaudig, *Z. Anorg. Allg. Chem.*, **365**, 301 (1969).
116. H. J. Reich, J. E. Holladay, T. G. Walker and J. L. Thompson, *J. Am. Chem. Soc.*, **121**, 9769 (1999).
117. C. Lambert, P. v. R. Schleyer and E. U. Wurthwein, *J. Org. Chem.*, **58**, 6377 (1993).
118. B. W. Gung, X. Xue, N. Knatz and J. A. Marshall, *Organometallics*, **22**, 3158 (2003).
119. R. W. Hoffmann, J. Lanz, R. Metternich, G. Tarara and D. Hoppe, *Angew. Chem., Int. Ed., Engl.*, **26**, 1145 (1987).
120. J.-F. Poisson, F. Chemla and J. F. Normant, *Synlett*, 305 (2001).
121. J. F. Poisson and J. F. Normant, *J. Am. Chem. Soc.*, **123**, 4639 (2001).
122. M. Raban, D. Kost and E. H. Carlson, *J. Chem. Soc., Chem. Commun.*, 656 (1971).
123. (a) M. J. Pilling and P. W. Seakins (Eds.), *Reaction Kinetics*, Oxford University Press, New York, 1995.
(b) H. Friebolin (Ed.), *Basic One- and Two-Dimensional NMR Spectroscopy*, VCH Publishers, New York, 1991.
(c) J.-J. Delpuech (Ed.), *Dynamics of Solutions and Fluid Mixtures by NMR*, Wiley, Chichester, 1995.

CHAPTER 7

Cyclopropanation mediated by zinc organometallics

ANDRÉ B. CHARETTE

Department of Chemistry, Université de Montréal, P.O. Box 6128, Station Downtown, Montréal, Québec, Canada H3C 3J7
Fax: +1 514 343 5900; e-mail: andre.charette@umontreal.ca

I. INTRODUCTION

The landmark discovery by Simmons and Smith that iodomethylzinc iodide could convert a wide variety of alkenes into the corresponding cyclopropanes (equation 1)[1,2] constitutes one of the most important methods for the generation of the simplest cycloalkane[3–5].

The chemistry of organozinc compounds
Edited by Z. Rappoport and I. Marek

Since then, not only has the scope of the reaction been widely studied, but also structural variations of the reagents and the reaction conditions in order to further increase its synthetic utility. The following sections will present the latest, state-of-the-art methodologies for the generation of cyclopropane derivatives using zinc carbenoid reagents.

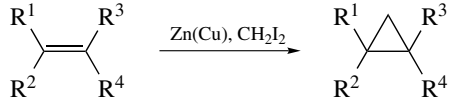

(1)

II. PREPARATION AND STRUCTURE OF ZINC CARBENOIDS

A. Unsubstituted Halomethylzinc Carbenoids

Iodomethylzinc iodide was first prepared in 1929 by Guy Emschwiller[6] when he gently heated a zinc–copper couple with diiodomethane in ether (equation 2).

$$Zn-Cu \xrightarrow[\text{ether}]{CH_2I_2} IZnCH_2I \qquad (2)$$

In this first report, the structure $IZnCH_2I$ was postulated based on three observations: the reagent reacted with iodine to afford diiodomethane and zinc iodide; it reacted with water to form iodomethane, zinc hydroxide and zinc iodide; and finally it reacted with an aqueous solution of oxygen to generate zinc iodide and an aqueous solution of formaldehyde. It was only twenty-nine years later that Simmons and Smith reported the seminal observation that iodomethylzinc iodide reacted with alkenes to generate the corresponding cyclopropane in high yields. This method required ether as solvent and an activated form of zinc. Their original procedure, which required heating a mixture of zinc dust and cupric oxide under a hydrogen atmosphere[7], was soon replaced by a more practical and less tedious treatment of zinc powder with a cupric sulfate solution[8,9]. Many activating procedures are available: the LeGoff modification involves the treatment of zinc dust with a hot solution of cupric acetate in acetic acid[10]. Cuprous chloride under nitrogen has also been used as an activator[11,12]. A zinc–silver couple has been found to be useful giving, in some cases, more efficient cyclopropanation reactions when compared to those obtained with the zinc–copper couple[13]. Commercial zinc dust is only suitable for the reagent preparation if it does not contain lead impurities[14]. If traces of lead are present, then the formation of the *gem*-dizinc species is favored. Other zinc activators include acetyl chloride[15], TMSCl[14,16], $TiCl_4$[17], heating[18] or sonication[19]. However, activation procedures using $CuSO_4$[8], $Cu(OAc)_2$[10] or CuCl[11] are still used in >90% of all the examples in which diiodomethane is used as the reagent precursor. Alternatively, highly reactive zinc powder suitable for reagent formation from dibromomethane can be prepared by *in situ* reduction of zinc(II) salts[20].

One major limitation inherent to the preparative methods of these reagents is that an ethereal solvent must necessarily be used (most commonly ether, THF or DME). In these solvents, the electrophilic character of the reagent is significantly diminished due to the presence of basic ligands[5]. For this reason, several new reagents were developed using alternative procedures that allowed the use of noncomplexing solvents. A major breakthrough in this area was reported by Furukawa and coworkers when they found that

the replacement of zinc metal by diethylzinc led to the formation of a reactive species that was an efficient cyclopropanating reagent (equation 3)[21,22].

$$Et_2Zn \xrightarrow[\text{Compatible Solvents: } CH_2Cl_2, \text{ hexanes, toluene } ClCH_2CH_2Cl, \text{ benzene, ether etc.}]{CH_2I_2} EtZnCH_2I \quad (3)$$

This alkyl exchange reaction proceeds smoothly in a wide range of solvents. It is believed that traces of molecular oxygen are necessary to initiate the alkyl group exchange[23,24]; however, the adventitious oxygen present as an impurity is sufficient to initiate the process. The reactivity profile of $Zn(CH_2X)_2$ (X = I, Cl), prepared from Et_2Zn and a two-fold excess of XCH_2I (X = I, Cl) (equation 4), indicates that these reagents are sometimes more effective than those derived from zinc metal[25]. Bis(chloromethyl)zinc in 1,2-dichloroethane has been used to cyclopropanate less reactive alkenes.

$$Zn(CH_2Cl)_2 \xleftarrow[\text{Compatible Solvents: } CH_2Cl_2, \text{ hexanes, toluene } ClCH_2CH_2Cl, \text{ benzene, ether etc.}]{2\ ClCH_2I} Et_2Zn \xrightarrow[\text{Compatible Solvents: } CH_2Cl_2, \text{ hexanes, toluene } ClCH_2CH_2Cl, \text{ benzene, ether etc.}]{2\ CH_2I_2} Zn(CH_2I)_2 \quad (4)$$

A homogeneous solution of the bis(iodomethyl)zinc•DME complex in dichloromethane can be prepared by adding diethylzinc to 1 equivalent of 1,2-dimethoxyethane in dichloromethane followed by 2 equivalents of diiodomethane[26]. The presence of DME makes the preparation of the reagent safer by ensuring that the mixture is constantly homogeneous. This reagent has been useful in enantioselective cyclopropanation reactions (*vide infra*).

The second major advantage of this method is that a wide range of new cyclopropanating reagents with new properties became available. If a sufficiently acidic compound reacts with diethylzinc, a mixed zinc species is formed (equation 5). The second ethyl group can then be exchanged with an iodomethyl unit to generate a potentially reactive iodomethylzinc species.

$$Et-Zn-Et \xrightarrow[(-EtH)]{R-X-H} RX-Zn-Et \xrightarrow[(-EtI)]{CH_2I_2} RX-Zn-CH_2I \quad (5)$$

Shi and coworkers have reported that several carboxylic acids react with diethylzinc/diiodomethane to generate mixed species, which have the general structure $R'COOZnCH_2I$ and are effective cyclopropanating reagents[27]. Among them, the reagent derived from a 1:1:1 mixture of trifluoroacetic acid (RXH = CF_3COOH), diethylzinc and diiodomethane is quite effective for the cyclopropanation of simple alkenes[28]. Care must be taken since the reaction between diethylzinc and trifluoroacetic acid is quite exothermic. Alternatively, Charette and coworkers have reported that mixed reagents derived from phenols (equation 6)[29] or phosphoric acids (equation 7)[30] are effective reagents as well.

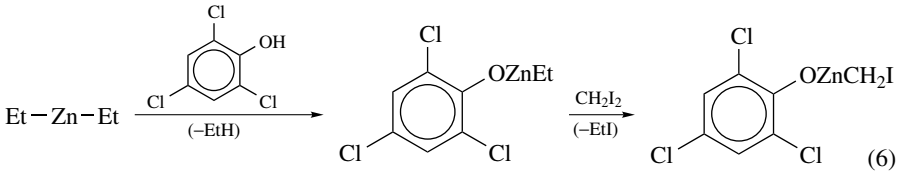

(6)

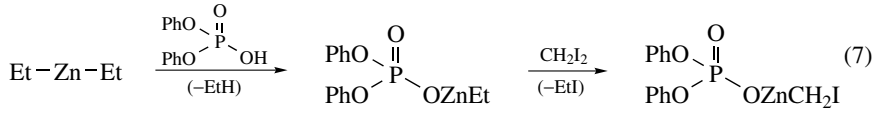

(7)

Another approach for the preparation of $IZnCH_2I$ involves the alkyl exchange reaction between EtZnI (prepared from Zn metal and EtI) and CH_2I_2[31]. This method is especially useful if the reagent has to be prepared on a large scale and if Et_2Zn is not a viable option.

Shortly after Simmons and Smith's seminal publication, Wittig and coworkers[32, 33] reported that the treatment of zinc iodide with either 1 or 2 equiv of diazomethane also produces $IZnCH_2I$ or the analogous bis(iodomethyl)zinc reagent [$Zn(CH_2I)_2$]. However, this method for the preparation of the reagent has been far eclipsed by the others.

B. α-Substituted Halomethylzinc Carbenoids

α-Substituted zinc carbenoids can be prepared by reacting diethylzinc or zinc metal with more substituted dihaloalkanes. These more highly substituted reagents are effective at generating 1,2,3-substituted cyclopropanes as long as the organozinc reagents do not have the possibility to undergo a β-hydride elimination. Table 1 presents substituted precursors that have been used to generate highly substituted cyclopropane derivatives.

In the cases where their potential decomposition via a β-hydride elimination pathway is possible, a large excess of the reagent and careful temperature control is necessary to get a high yield of the cyclopropane. The reagent formation is more effective if a diiodo precursor is used instead of dibromides and activated dichlorides, but these latter two have also been successfully converted into suitable reagents.

TABLE 1. Known α-substituted zinc carbenoids in cyclopropanation reactions

Substituted dihalide	Metal reagent	Carbene unit	Reference
$MeCHI_2$	Zn/Cu	MeCH	34
	EtZnI		35
	Zn/Ag		36
	Et_2Zn		37
$MeCHBr_2$	Zn/Cu	MeCH	38
$TIPSOCH_2CH_2CHI_2$	Et_2Zn	$TIPSOCH_2CH_2CH$	39
Me_2CBr_2	Zn	Me_2C	40
Me_2CI_2	Et_2Zn		41, 42
$PhCHCl_2$	Zn	PhCH	40
$PhCHBr_2$	Zn		40
$PhCHI_2$	Et_2Zn		37
CHI_3	Et_2Zn	CHI	43
$CHBr_3$	Et_2Zn	CHBr	44
$CHCl_3$	Zn	CHCl	40
$CHBrCl_2$	Zn	CHCl	40
$CHBr_2Cl$	Zn	CHCl	40
$CHFI_2$	Et_2Zn	CHF	43
CF_2Br_2	Zn	CF_2	45
CHI_3	Et_2Zn or EtZnI	CHZnX	46

The use of iodoform as the reagent precursor under Furukawa's conditions gives rise to a more complex scenario, since the additional C−I bonds can further react with an ethylzinc species (equation 8)[46]. The reaction of the iodo-substituted zinc carbenoid with an alkene will generate an iodo-substituted cyclopropane, whereas that involving the *gem*-dizinc carbenoid will lead to a cyclopropylzinc product. The evidence for the formation of a *gem*-dizinc carbenoid was obtained not only by the analysis of the cyclopropanation products but also by the formation of d_2-iodomethane upon quenching the reagent with D_2O/DCl.

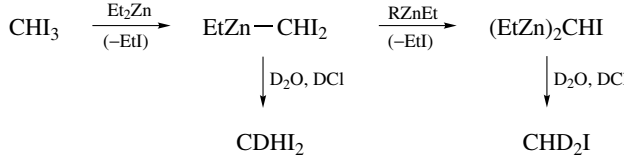

(8)

Improved preparation and reactivity of the *gem*-dizinc reagent was accomplished by using a mixture of ZnI_2, $EtZnI{\bullet}2OEt_2$ and CHI_3[47]. The presence of ZnI_2 allows for shorter reaction times and cleaner reactions, particularly with less reactive substrates.

Functionalized zinc carbenoids have been prepared from diiodoalkanes and diethylzinc and used in stereoselective transformations, but their use is limited by the availability of the diiodoalkane[48–50] and the stability of the resulting zinc carbenoid. Alternatively, the reaction of a diazoalkane with ZnI_2 can be used to access complex zinc carbenoids, but with modest efficiency (equation 9)[51].

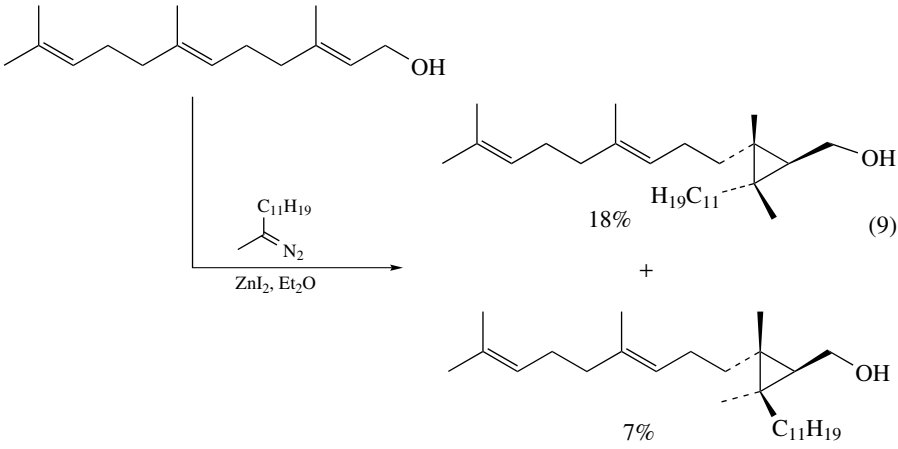

(9)

Functionalized zinc carbenoids have been prepared from carbonyl compounds by an indirect strategy[52]. The deoxygenation of a carbonyl compound to an organozinc carbenoid can be induced by a reaction with zinc and TMSCl. Therefore, the aldehyde or ketone, when treated with TMSCl or 1,2-bis(chlorodimethylsilyl)ethane in the presence of an alkene, generates the cyclopropanation product. This method is quite effective for the production of alkoxy-substituted cyclopropane derivatives. A 55% yield of the

desired trimethylsilylethoxycyclopropane was obtained when an orthoester was used as the carbenoid precursor (equation 10)[53].

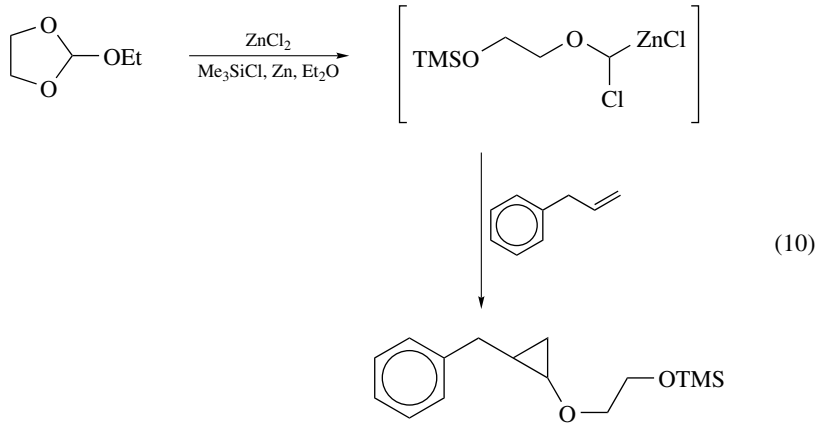

(10)

cis/*trans*: 3/1 (55%)

C. Solid and Solution Structures of Halomethylzinc Reagents

Shortly after its discovery, it was clearly established that the Simmons–Smith cyclopropanation reaction involving halomethylzinc reagents proceeded in a concerted fashion with retention of configuration with regards to the double bond geometry[3]. Conversely, the exact structure of the halomethylzinc derivatives, both in solution and in the solid state, has been speculated for many years. Yet, it is only in the early 1990s that the first X-ray crystal structure of bis(iodomethyl)zinc was reported (Figure 1, **1**)[54,55]. Since then, several crystal structures have been published, including complexes derived from bis(chloromethyl)zinc[56], iodomethylzinc iodide[57] and iodomethylzinc diphenylphosphate[30] (Figure 1, **2**–**6**). The halomethylzinc complexes are all monomeric except in the case of iodomethylzinc diphenylphosphate, which crystallizes as a dimer in the presence of THF. Although the preferred geometry for diorganozinc reagents is linear, the presence of basic solvents and ligands during the crystallization process generally leads to the formation of tetrahedral zinc centers. As anticipated, the dihedral angle X(C)–Zn–C in tetrahedral structures becomes smaller as the basicity of bidentate ligands increases. It is also important to point out that there is no evidence of any inter- or intramolecular iodide–zinc interactions. Such an interaction was postulated as being the starting event in the cyclopropanation process occurring through a butterfly-type transition structure (*vide infra*)[3].

It is also interesting to point out that bipyridine•$RZnCH_2X$ complexes are not reactive in the cyclopropanation reaction due to the high basicity of the bipyridine ligand. However, the addition of zinc iodide promotes the cyclopropanation reaction since uncomplexed $IZnCH_2X$ can be formed via an iodide–halomethyl group exchange. This approach has been used in catalytic asymmetric cyclopropanation reactions (*vide infra*).

In addition, crystal structures of several halomethylzinc alkoxides[58,59] and an acyloxymethylzinc reagent[60] have been reported (Figure 2, **7**–**9**). Iodo- and chloromethylzinc alkoxides exist as tetramers in cubane or bis(cubane)-like structures. However, these

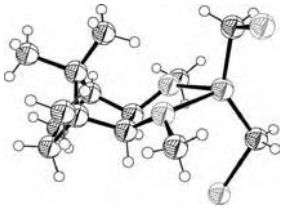

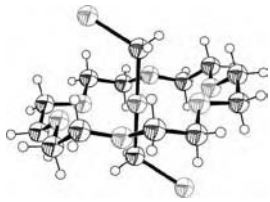

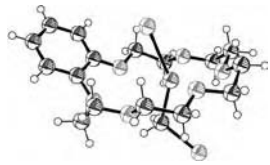

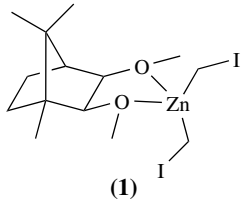

(1)

$Zn(CH_2I)_2$•18-crown-6

(2)

$IZnCH_2I$•benzo-18-crown-6

(3)

$Zn(CH_2I)_2$•bis(quinoline)

(4)

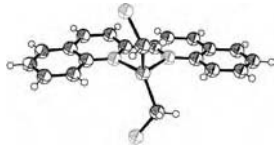

$Zn(CH_2Cl)_2$•bis(quinoline)

(5)

$[(PhO)_2P(O)OZnCH_2I$•$THF]_2$

(6)

FIGURE 1. X-ray crystal structures of common cyclopropanating reagents

species are not sufficiently electrophilic to act as cyclopropanating reagents in the absence of Lewis acids. The structure of (benzoyloxymethyl)zinc (**10**) has also been reported. Although this is not an effective cyclopropanating reagent, the analogous acyloxymethylethylzinc and acyloxymethylzinc iodide bearing a perfluoropentanoyl group are sufficiently reactive to cyclopropanate a wide range of alkenes.

The solution structure of halomethylzinc derivatives has been the subject of several debates. Among those, the possible Schlenk equilibrium between $IZnCH_2I$ and $Zn(CH_2I)_2/ZnI_2$ has been invoked to account for the stereochemical outcome of some cyclopropanation reactions[3], but little has been established unequivocally. Recently, in-depth low temperature spectroscopic studies of iodomethylzinc complexes have clearly established that the equilibrium between these species lies heavily on the side of $IZnCH_2I$ (equation 11)[61,62].

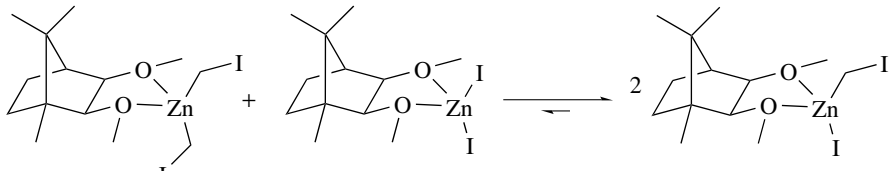

(11)

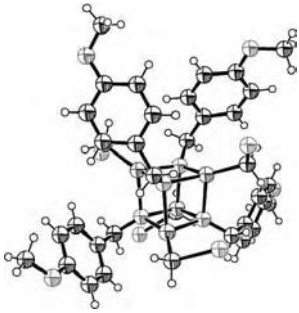

$[p\text{-}MeOC_6H_4CH_2OZnCH_2I]_4$

(7)

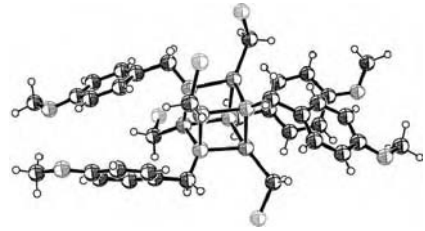

$[p\text{-}MeOC_6H_4CH_2OZnCH_2Cl]_4$

(8)

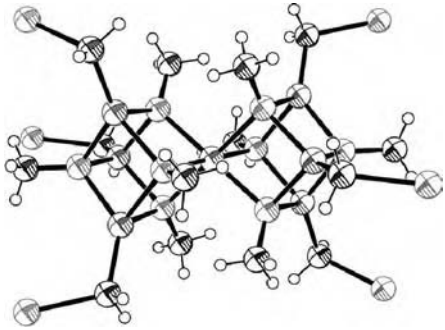

$[(MeO)_8Zn_7(CH_2I)_6]$

(9)

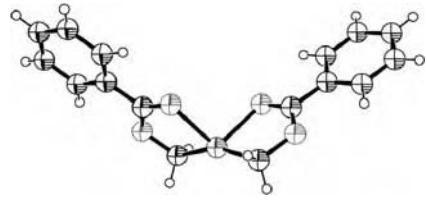

$(PhC(O)OCH_2)_2Zn$

(10)

FIGURE 2. X-ray crystal structures of unreactive zinc carbenoids

This observation is in agreement with the behavior of organozinc iodides (RZnI)[63–65], but is in sharp contrast with what has been reported for $BrZnCH_2Br$[66]. Many soluble halomethylzinc complexes have been fully characterized in solution by ^1H and ^{13}C NMR spectroscopies, and the characteristic chemical shifts are shown in Table 2.

TABLE 2. ^1H and ^{13}C chemical shifts for $ZnCH_2X$ species[30,56,61]

Complex (Solvent)	^1H NMR ($ZnCH_2X$)	^{13}C NMR ($ZnCH_2X$)
$IZnCH_2I$•2THF (CD_2Cl_2)	1.34	−17.4
$Zn(CH_2I)_2$•2THF (CD_2Cl_2)	1.38	−17.3
$EtZnCH_2I$•DME (CD_2Cl_2)	1.42	—
$(PhO)_2P(O)OZnCH_2I$ ($CDCl_3$)	1.34–1.27	−25.4
$Zn(CH_2I)_2$•bipyridine (CD_2Cl_2)	1.49	−12.2
$Zn(CH_2Cl)_2$•bipyridine (CD_2Cl_2)	2.71	32.9
$IZnCH_2I$•bipyridine (CD_2Cl_2)	1.64	−14.6
$CF_3COOZnCH_2I$•bipyridine (CD_2Cl_2)	1.61	−20.5

The solution structure of the Furukawa reagent ($EtZnCH_2I$) has been established by ^1H and ^{13}C NMR as well[61]. This reagent is in equilibrium with Et_2Zn and $Zn(CH_2I)_2$ (equation 12), but it has a limited lifetime: it will either undergo cyclopropanation or it will rearrange to PrZnI.

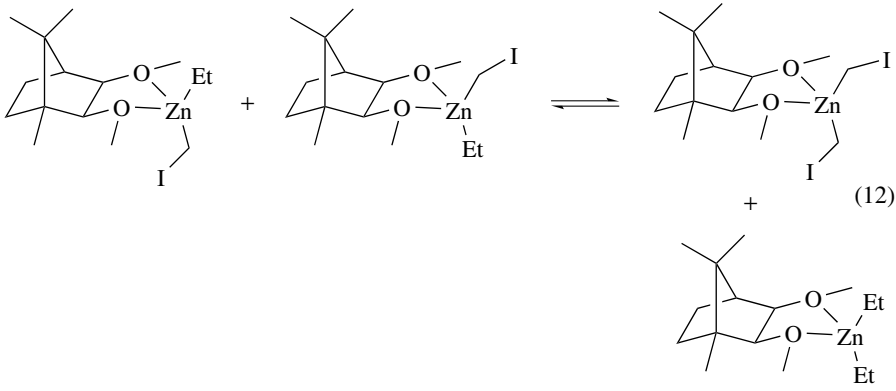

(12)

III. MECHANISM OF THE CYCLOPROPANATION OF ALKENES USING ZINC CARBENOIDS

The first mechanistic picture of the cyclopropanation of alkenes using halomethylzinc reagents was provided early on by Simmons and coworkers (Figure 3, **A**)[3]. A three-centered transition structure was proposed to account for the observed stereospecificity of the reaction relative to the alkene geometry. The methylene delivery occurs in a concerted, asynchronous process leading to the cyclopropane and zinc halide. The reagents are electrophilic in nature, and the reaction is relatively sensitive to both the nucleophilicity of the alkene and the steric crowding around the alkene. DFT studies of the Simmons–Smith reaction between chloromethylzinc chloride and ethylene using various basis sets corroborated this butterfly-type transition structure, and the activation energy was calculated to be 24.7 (B3LYP, transition structure **B** in Figure 3)[67], 21.4[68] and 17.3 kcal mol^{-1} (B3LYP/6-31 A)[69]. Similar calculations for the cyclopropanation of ethylene with iodomethylzinc iodide led to lower activation energies of 11.4–14.6[70], 17.0[68] and 21.2 kcal mol^{-1}[71]. The activation energy of the cyclopropanation reaction is dependent upon the leaving group ability of the halomethylzinc reagent. The order of reactivity goes from I < Br < Cl < F, the cyclopropanation of ethylene with fluoromethylzinc fluoride possessing an activation energy of 31.9 kcal mol^{-1}[68]. It has also been calculated that the cyclopropanation reaction of ethylene with halo-substituted iodomethylzinc aryloxides (such as that in equation 6) proceeds with an activation energy of about 1 kcal mol^{-1} lower relative to that with iodomethylzinc iodide. The butterfly-type model was refined a few years later when it was calculated and concluded that the presence of a Lewis acid (such as $ZnCl_2$) decreased the activation energy by a few kcal mol^{-1} (Figure 3, **C**). A more substantial decrease in the activation energy was calculated for the cyclopropanation of zinc alkoxides derived from allylic alcohols.

The cyclopropanation reaction using *gem*-dizinc carbenoids has also been theoretically studied by Phillips and coworkers[72]. The *gem*-dizinc carbenoids react with ethylene via a synchronous attack with an activation energy of about 15 kcal mol^{-1} (Figure 3, **D**). It was also predicted that the reaction could be accelerated by the addition of zinc iodide.

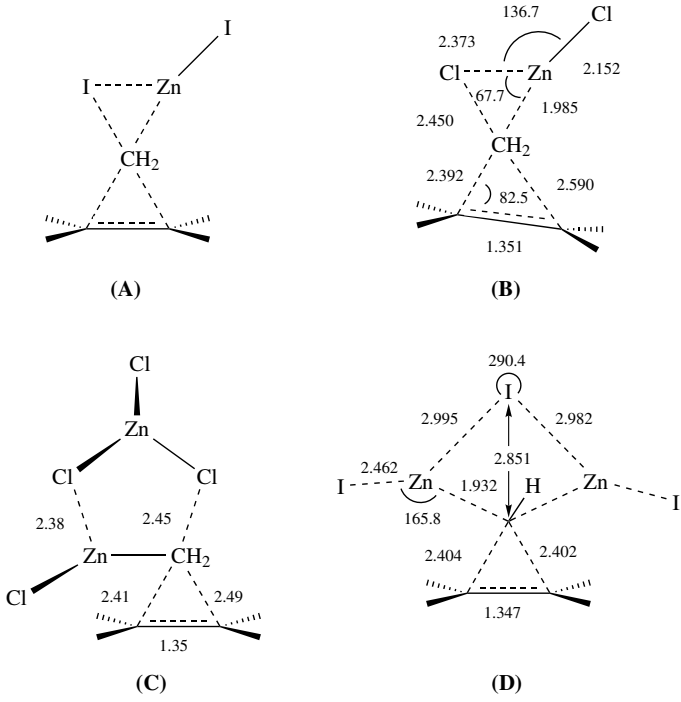

FIGURE 3. Transition state models for the Simmons–Smith cyclopropanation reaction

IV. SYNTHETIC SCOPE OF THE CYCLOPROPANATION USING ZINC CARBENOIDS

A. Nature of the Reaction Solvent, Additives and Reaction Temperature

Traditionally, cyclopropanation reactions using iodomethylzinc carbenoids were performed in ether. This restriction arose from preparation of the reagent that involved the oxidative addition reaction between zinc and diiodomethane. However, it has been recognized that the solvent used in the zinc-mediated cyclopropanation reactions plays an extremely important role due to the electrophilic nature of the zinc carbenoid and the Lewis acidity of the reagent. Chlorinated solvents, such as dichloromethane and 1,2-dichloroethane, have become the solvents of choice since they are nonbasic, unreactive toward the zinc reagents and polar enough to solubilize the substrates. However, these solvents require the use of diethylzinc as a reagent precursor. When basic solvents are used, the rate of cyclopropanation usually decreases as the basicity of the solvent increases. It is sometimes desirable to add Lewis basic additives in the cyclopropanation reaction, namely to avoid premature decomposition of the reagent and to ensure homogeneous reactions. The DME complex of bis(iodomethylzinc) is a useful reagent prepared by mixing 1 equivalent of 1,2-dimethoxyethane and diethylzinc with 2 equivalents of diiodomethane[26]. It should also be pointed out that the majority of the reagents are not thermally stable. Therefore, carrying out the reactions above room temperature may be detrimental to the

yields due to premature reagent decomposition. Finally, it has been speculated that traces of oxygen are necessary to induce the alkyl group exchange between diethylzinc and diiodomethane using the Furukawa procedure. It may be necessary to introduce a small amount of oxygen to facilitate the reagent formation; however, in most instances, residual oxygen is sufficient to promote reagent formation.

B. Achiral Alkenes

The cyclopropanation of simple alkenes using halomethylzinc carbenoids has been part of the synthetic organic chemist toolbox for many years. Alkyl-substituted alkenes are generally good starting materials for the generation of cyclopropanes. For example, cyclooctene has been converted into bicyclo[6.1.0]nonane using several zinc reagents (equation 13)[14,73].

(13)

Zn/Cu, CH_2I_2, Et_2O, 40 °C, 8 h	96%
Et_2Zn, CH_2I_2, PhH, 50 °C	98%
Et_2Zn, CH_2ICl, PhH, 50 °C	99%

The reaction was generally faster with electron-rich alkenes; however, steric hindrance must also be taken into consideration. For example, the relative rate of cyclopropanation of substituted cyclohexenes is shown in equation 14[74].

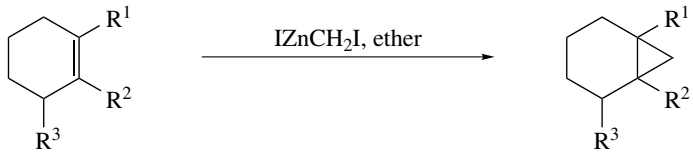

(14)

	$k_{alkene}/k_{cyclohexene}$
$R^1 = H, R^2 = H, R^3 = H$	1.00
$R^1 = H, R^2 = Me, R^3 = H$	2.14
$R^1 = Me, R^2 = Me, R^3 = H$	0.94
$R^1 = H, R^2 = H, R^3 = Me$	0.58

Aryl-substituted alkenes also react with halomethylzinc carbenoids to generate the cyclopropane derivatives (equations 15 and 16). These substrates are excellent tests for new cyclopropanating reagents, since they are usually converted into the cyclopropanes in lower yields than their alkyl-substituted analogues. Classical zinc carbenoids (Simmons–Smith, Furukawa and Wittig) converted styrene into the corresponding cyclopropanes in relatively low yields (32–50%) (equation 15)[3]. Conversely, Denmark's protocol using chloroiodomethane[25] as reagent precursor was quite effective, providing a

>98% conversion for this transformation. Shi's TFA[28] ($CF_3COOZnCH_2I$) and Charette's trichlorophenol[29] (see equation 6) derived reagents were also effective for this reaction.

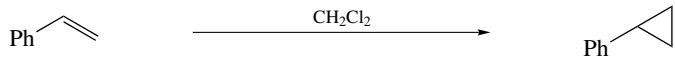

Zn/Cu, CH_2I_2, ether, reflux	32%
$EtZnCH_2I$ (2 equiv), 0 °C	50%
$Zn(CH_2I)_2$ (1 equiv), 0 °C	47%
$Zn(CH_2Cl)_2$ (1 equiv), 0 °C	>98%
$CF_3COOZnCH_2I$ (2 equiv), 20 min, rt	85%
2,4,6-$Cl_3C_6H_2OZnCH_2I$ (2 equiv), 12 h, rt	>98% (91% isolated)

(15)

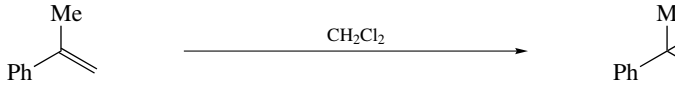

Zn/Cu, CH_2I_2, ether, reflux	61%
$EtZnCH_2I$ (2 equiv), 0 °C	85%
$Zn(CH_2I)_2$ (1 equiv), 0 °C	86%
$Zn(CH_2Cl)_2$ (1 equiv), 0 °C	>98%
$CF_3COOZnCH_2I$ (1.5 equiv), 12 h, rt	>95% (84% isolated)
2,4,6-$Cl_3C_6H_2OZnCH_2I$ (2 equiv), 12 h, rt	>98% (94% isolated)
$(PhO)_2P(O)OZnCH_2I$ (1.5 equiv), 12 h, rt	95%

(16)

The introduction of a methyl substituent increases the nucleophilic character of the alkene; therefore, it is not surprising to observe that α-methylstyrene was converted into the corresponding cyclopropane in slightly higher yields with most reagents (equation 16). The lower yield observed using the Simmons–Smith reagent with both substrates probably derives from the selection of ether as the solvent rather than a lower reactivity of the reagent.

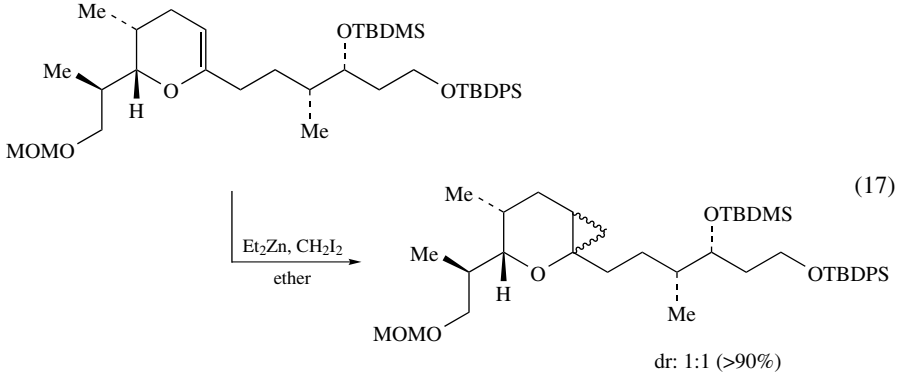

(17)

dr: 1:1 (>90%)

Since the cyclopropanation reaction using zinc carbenoids is usually faster with electron-rich alkenes, it is not surprising to observe that enol ethers are nicely converted into cyclopropyl ethers in high yields (equation 17)[75].

Although *O*-alkyl-substituted enol ethers react smoothly with zinc carbenoids (equation 18)[76], higher yields are usually obtained with the Furukawa reagent using a slight excess of diethylzinc to scavenge zinc iodide (and convert it into the less Lewis acidic ethylzinc iodide as it is formed) (see equation 18 vs 19)[77].

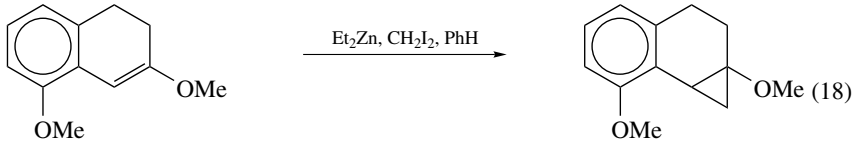

74% (18)

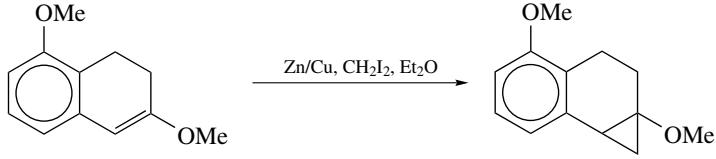

30% (19)

Trimethylsilyloxy-substituted alkenes are by far the most widely used enol ethers because of their straightforward preparation from the corresponding ketones (equation 20)[78–82]. The electron-rich character of silyl enol ethers allows for highly chemoselective cyclopropanations in the presence of additional double bonds (equation 21)[83].

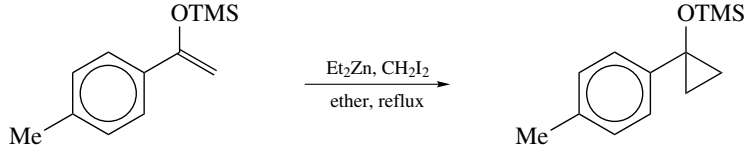

80% (20)

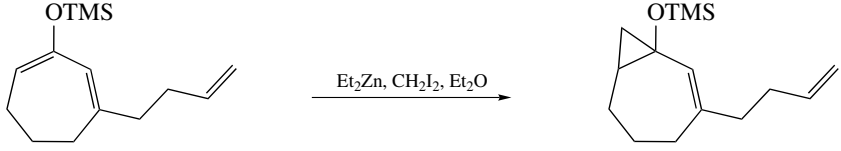

>72% (21)

Enol esters have been used under Simmons–Smith conditions, and the products are valuable precursors for cyclopropanols. Alternatively, the lithium enolate which can be obtained from the corresponding enol ester can be converted into the cyclopropanol derivative[84] (equation 22)[85]. The direct cyclopropanation of zinc or lithium enolates using

zinc reagents[86] is known, but samarium/diiodomethane is usually the reagent of choice for this transformation[87,88].

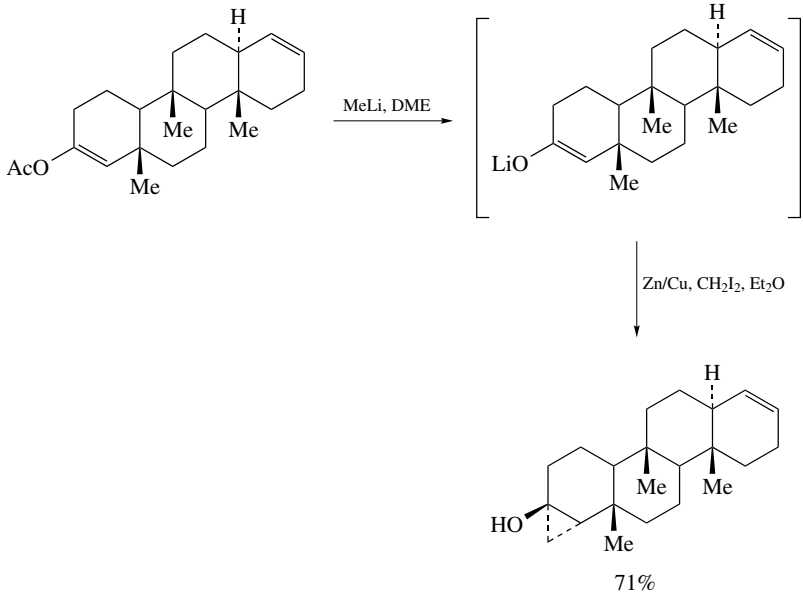

(22)

71%

Treatment of a readily enolizable 1,3-dicarbonyl derivative with a mixture of diethylzinc and diiodomethane generates a 1,4-dicarbonyl by a chain extension process through the corresponding cyclopropanol derivative (equation 23)[89]. Several enolizable starting materials such as β-ketophosphonates[90], β-keto amides[91] and amino acid skeletons[92] have been subjected to these chain extension conditions.

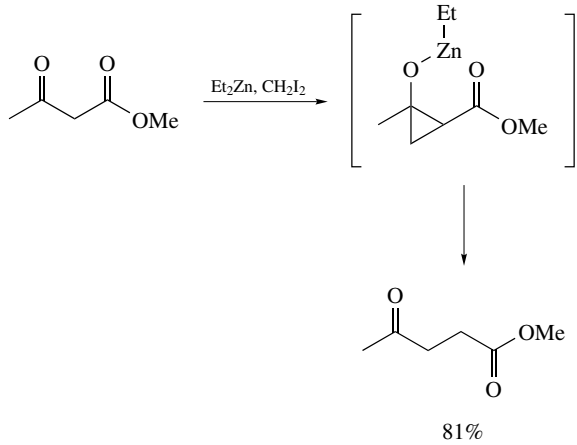

(23)

81%

The cyclopropanation of *N*-substituted alkenes has been reported in a very few cases. Problems arising from *N*-alkylation by the electrophilic zinc reagents were sometimes

observed even if the reagent stoichiometry and the temperature were carefully controlled (equations 24 and 25)[93,94]. The introduction of an electron-withdrawing protecting group on nitrogen to avoid alkylation side reactions decreases the nucleophilicity of the alkene, and lower yields were observed unless highly electrophilic reagents were used (equation 26)[95].

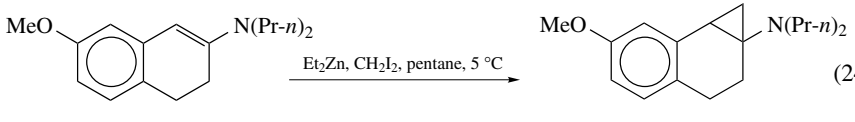

26% (24)

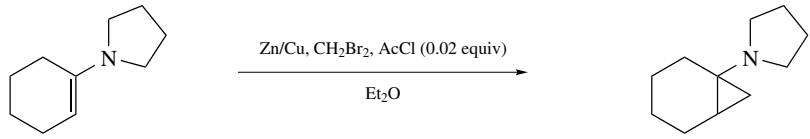

22% (25)

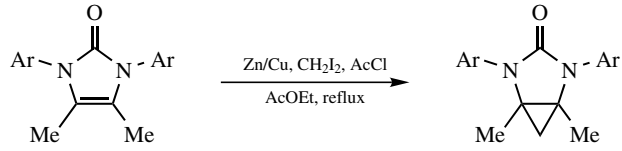

21% (26)

The synthesis of halo-substituted cyclopropanes using zinc carbenoids can be accomplished using three different approaches: by the cyclopropanation of a halo-substituted alkene, by the cyclopropanation using a halo-substituted zinc carbenoid, or by the cyclopropanation using *gem*-dizinc carbenoids followed by trapping the cyclopropylzinc with an electrophilic halide source.

The cyclopropanation of vinyl halides is efficient for fluoro- (equation 27)[96], chloro- (equation 28)[97,98], bromo- (equation 29)[99] and iodo-substituents (equation 30)[100]. However, the selection of the right reagent is sometimes necessary. For example, the efficiency of the cyclopropanation of (*E*)-3-chloro-2-propen-1-ol is highly dependent upon the choice of the reagent (equation 28)[97]. In general, the new generation of reagents are more effective for carrying this transformation than the Simmons–Smith reagent in ether.

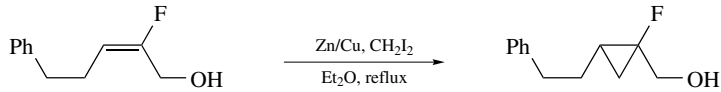

78% (27)

$Zn(CH_2I)_2$•DME (2 equiv), CH_2Cl_2	72%	(28)
$CF_3COOZnCH_2I$ (2.5 equiv), CH_2Cl_2	>95%	
4-Cl-2,6-$Me_2C_6H_2OZnCH_2I$ (2.5 equiv)	>95%	

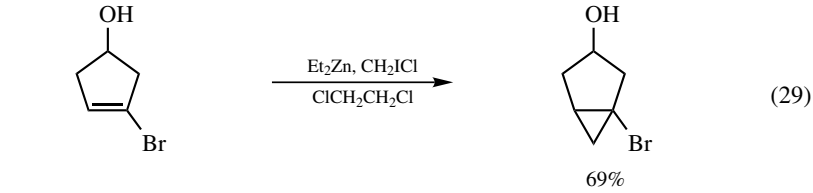

(29)

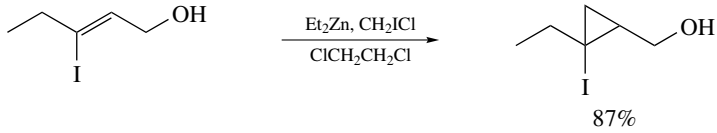

(30)

It has been shown that bis(chloromethyl)zinc in 1,2-dichloroethane (Denmark's modification) is particularly effective for the cyclopropanation of iodo-substituted allylic alcohols (equation 30)[100]. The cyclopropanation of dihalo-substituted alkenes is a lot more difficult due to the significant decrease in the nucleophilicity of the alkene, thus resulting in much lower yields of the desired products (equation 31)[97]. In this case, significant amounts of *O*-methylation were also observed.

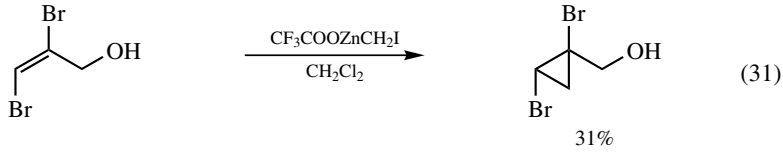

(31)

The second approach for the synthesis of halo-substituted cyclopropane derivatives involves the use of dihalomethylzinc carbenoids. These carbenoids are typically prepared by mixing diethylzinc with the appropriate trihalomethane reagent (Table 1, Section II.B). Although it is generally better if a dihaloiodomethane is used as the reagent precursor, the presence of a carbon–iodine bond is not necessary. The resulting carbenoids, generated from trihalomethane derivatives, are fairly reactive, but the reaction suffers from a general lack of diastereocontrol (equations 32 and 33)[101,44].

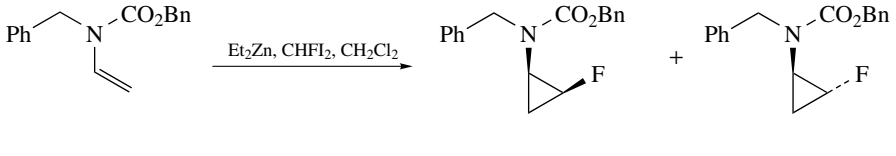

dr: 69:31 (79%) (32)

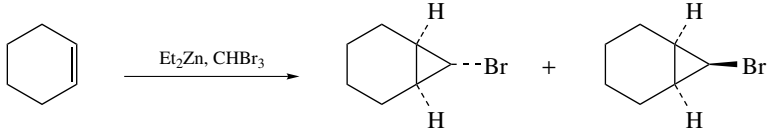

dr: 1:1.3 (52%) (33)

An alternative stereocontrolled approach involves the use of *gem*-dizinc reagents to generate the corresponding cyclopropylzinc species, which was then trapped with iodine

or bromine to generate the halo-substituted cyclopropane (equation 34)[46]. The reaction proceeds with complete diastereocontrol using the dibenzyl ether derived from *cis*-2-butene-1,4-diol. It is important to mention that the cyclopropylzinc intermediate could also be trapped with other electrophiles, such as acid chlorides, upon further transmetalation with CuCN.

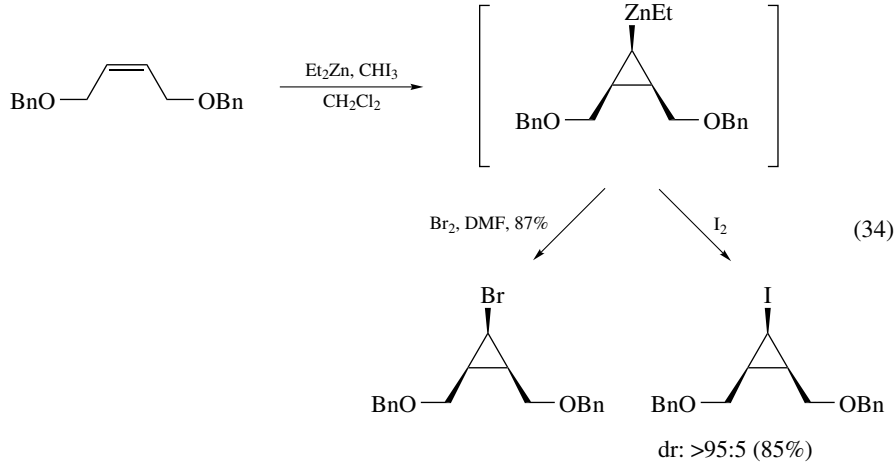

(34)

dr: >95:5 (85%)

A modification to the original *gem*-dizinc protocol to improve the scope of the reaction was also reported[47]. Ethylzinc iodide was used as the carbenoid precursor, and the reaction was run in the presence of zinc iodide. Under these conditions, simple allylic ethers could be converted into iodo-cyclopropanes in high yields and diastereocontrol (equation 35).

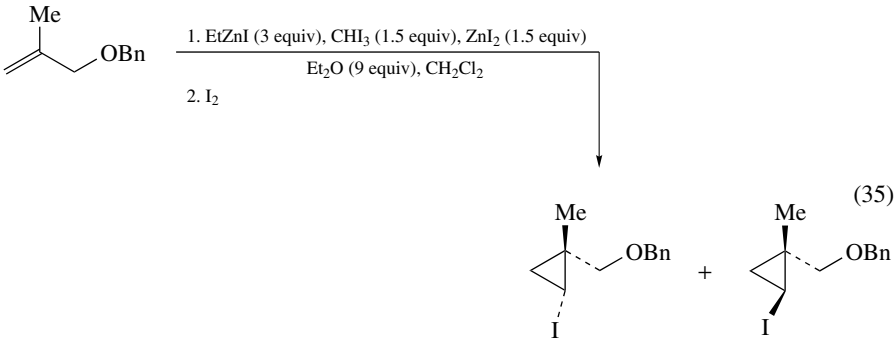

(35)

dr: 96:4 (76%)

It is also possible to perform a zinc–boron exchange if trimethylborate is added to the cyclopropylzinc species (equation 36)[102]. However, the presence of a zinc alkoxide

is mandatory for this transmetalation to take place. If the dibenzyl ether of *cis*-2-butene-1,4-diol was used, no zinc–boron exchange was observed.

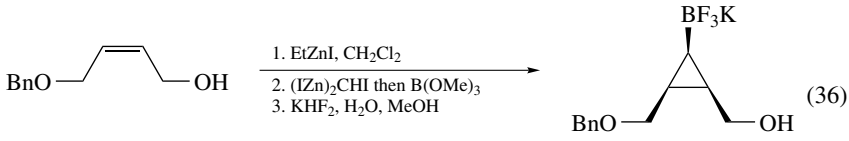

(36)

dr: >95:5 (63%)

The cyclopropanation of vinyl organometallic and heteroatom substituted vinylic compounds has also been reported using zinc carbenoids. Vinylboronates (equation 37)[103], -alanes (equation 38)[104], -zincs (equation 39)[105], -stannanes (equation 40)[106], -phosphonates (equation 41)[107], -germanes (equation 42)[108], and silanes (equation 43)[109,110] could be readily converted into cyclopropane derivatives.

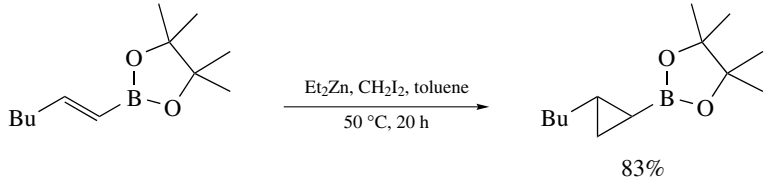

(37)

83%

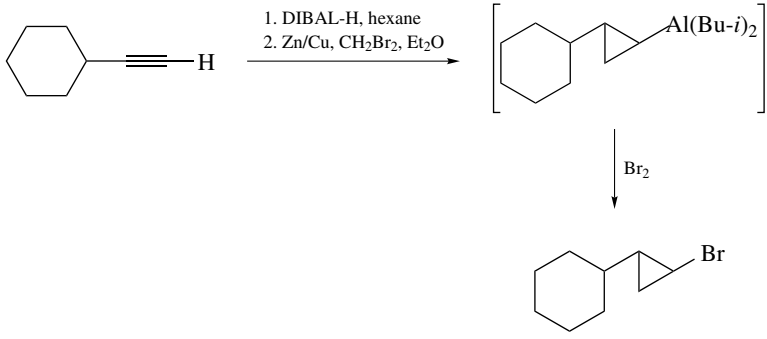

(38)

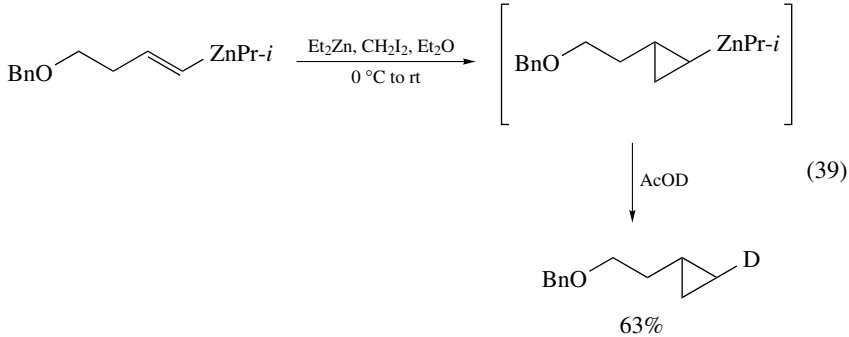

(39)

63%

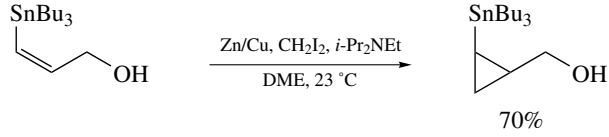

(40)

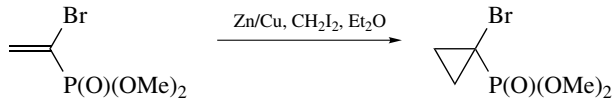

(41)

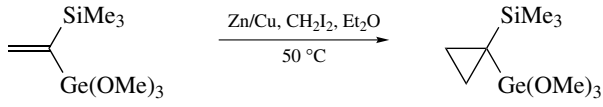

(42)

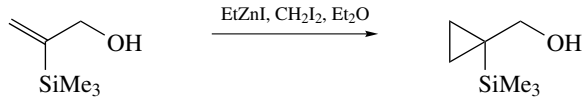

(43)

The intramolecular version of the cyclopropanation of alkenes using zinc carbenoids has not been extensively studied. One major limitation is the need to prepare the precursor, since there are relatively few mild methods to generate 1,1-diiodoalkanes (equation 44)[111].

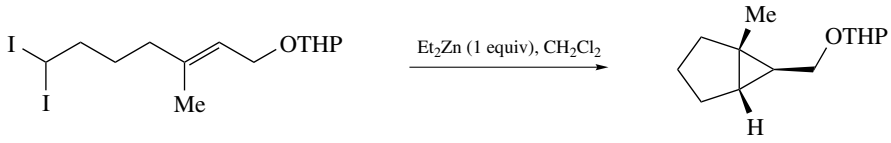

(44)

The most widely found method involves the preparation of the carbenoid from the corresponding carbonyl derivative (equation 45)[112].

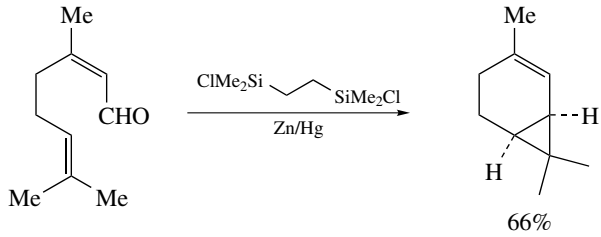

(45)

The cyclopropanation of alkenes using zinc carbenoids displays excellent chemoselectivities. A large number of functional groups are compatible with these reagents, such as alkynes, silanes, stannanes, germanes, alcohols, ethers, sulfonate esters, aldehydes,

ketones, carboxylic acids and derivatives, carbonates, carbamates, imidates, oxime ethers, boronates, phosphonates, sulfones, sulfonates, sulfonylimines and sulfoximines.

In some cases, the experimental conditions had to be modified to minimize the formation of by-products. For example, the proto-destannylation side reaction with tin-containing substrates can be minimized by adding diisopropylethylamine (equation 40)[113]. The compatibility of acid-sensitive functionalities can be increased by scavenging ZnI_2, because it is formed as the reaction proceeds. It is usually better to use the Et_2Zn/CH_2I_2 combination with excess Et_2Zn to scavenge ZnI_2, since these species will equilibrate to form the less Lewis acidic EtZnI. Alternatively, to avoid side reactions with acid-sensitive substrates, it is sometimes important to quench the reaction with pyridine to scavenge ZnI_2 and the excess reagent prior to the addition of water[13].

Highly Lewis basic and nucleophilic functional groups are not compatible with zinc carbenoids. The methylation or ylide formation of heteroatoms is one of the most important side reactions of these reagents. For example, amines, thioethers and phosphines readily react with the zinc reagents to generate ammonium salts[114], sulfonium[115] and phosphonium ylides[116, 117]. Terminal alkynes generally lead to a large number of by-products[118].

C. Stereoselective Cyclopropanation of Chiral Alkenes

The stereoselective cyclopropanation of chiral alkenes can be divided into two classes: cyclic and acyclic alkenes. Furthermore, within each class, a subdivision exists involving those that contain a proximal basic group that can direct the cyclopropanation reaction of zinc carbenoids and the others that do not. The discrimination of reactivity between alkenes that possess a proximal basic group and those that do not was first highlighted early on when Simmons and Smith noticed that the cyclopropanation of 1-(*o*-methoxyphenyl)-1-propene was more efficient than that of the related *meta* and *para* isomers (equation 46)[2].

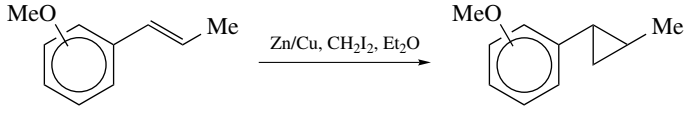

(46)

2-MeO	70%
3-MeO	60%
4-MeO	63%

This observation was corroborated with other simple cyclic and acyclic molecules, such as geraniol or its corresponding benzyl ether, which are cyclopropanated at the allylic alcohol and ether position with high chemoselectivity (equation 47)[119]. This observation is counterintuitive given the reaction components, since one would expect that the most electron-rich alkene will react faster with the electrophilic reagent. It has been suggested that proximal basic groups could 'direct' the delivery of the methylene unit through a rate enhancement due to a complex induced proximity effect.

Mechanistically, the reaction initially proceeds through the formation of the zinc alkoxide, which then complexes a second equivalent of the reagent, and then undergoes a pseudo-intramolecular cyclopropanation (equation 48). It is therefore implicit that 2 equivalents of zinc are needed in these reactions, since the ethylzinc alkoxide does not form the corresponding iodomethylzinc alkoxide in the presence of iodomethane, and the latter does not cyclopropanate alkenes in the absence of a Lewis acid.

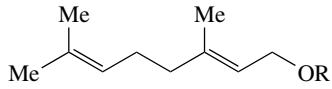

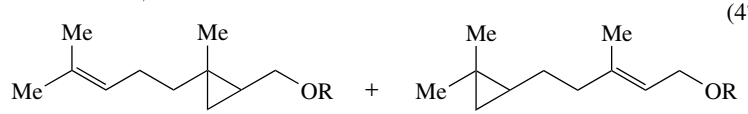

(47)

R = H; $EtZnCH_2I$ 74% 2%

R = Bn; $Zn(CH_2I)_2$ >97% <1%

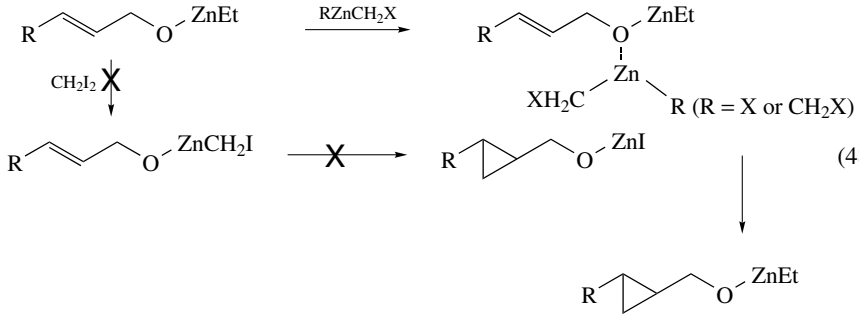

(48)

1. Stereoselective cyclopropanation of cyclic alkenes

It was recognized early on that the directing ability of proximal basic groups could be elegantly used to control the diastereoselectivity in the cyclopropanation of cyclic alkenes (equation 49)[22, 120, 121].

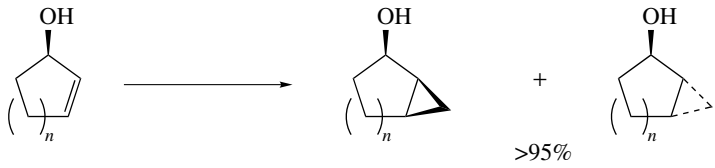

>95%

n = 1, Zn/Cu, CH_2I_2	dr: >99:1
n = 2, Zn/Cu, CH_2I_2	dr: >99:1
n = 2, Et_2Zn, CH_2I_2	dr: >99:1
n = 2, Et_2Zn, $ClCH_2I$	dr: >99:1
n = 3, Zn/Cu, CH_2I_2	dr: 90:10
n = 4, Zn/Cu, CH_2I_2	dr: <1:99
n = 5, Zn/Cu, CH_2I_2	dr: <1:99

(49)

The reaction proceeded with extremely high *syn* diastereocontrol with five- and six-membered cyclic allylic alcohols with a variety of zinc carbenoids. One particularly interesting example of a highly functionalized starting material is in the introduction of the C19 methyl group of taxusin through a highly chemo- and diastereoselective cyclopropanation (equation 50)[122].

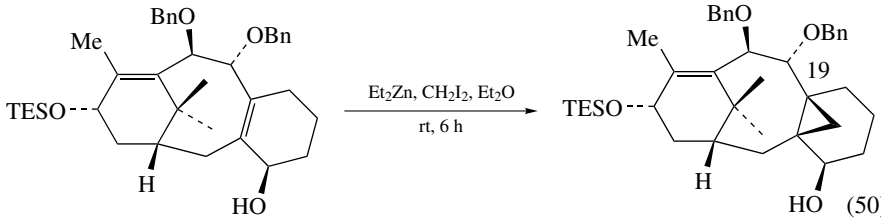

(50)

The conformation of the hydroxy group relative to the alkene and the relative steric hindrance around it must also be taken into consideration when planning a synthesis. For example, the cyclopropanation of a tricyclic precursor in the synthesis of myrocin produced the *anti* cyclopropyl alcohol derivative (equation 51)[123]. This reaction is probably still hydroxy directed by the fixed equatorial OH group, but the attack on the less hindered face of the alkene is favored.

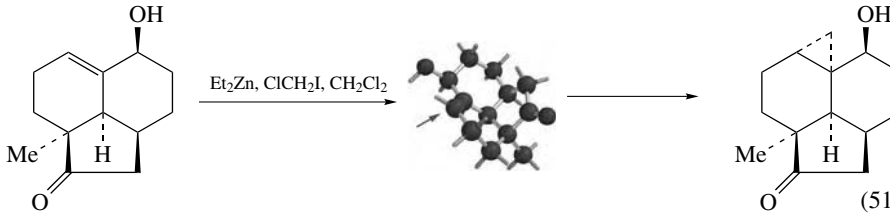

(51)

In the case of the seven-membered ring, the diastereoselection dropped to 9:1 using the Simmons–Smith reagent. A reversal of relative stereocontrol was observed with eight- and nine-membered cyclic allylic alcohol derivatives. This reversal was explained using a simple conformational analysis of the ground state in which attack from the hydroxy side of the most stable conformation led to the *anti* isomer (Figure 4).

This isomer was also formed with larger rings containing both *cis*- and *trans*-alkenes. In these cases with more flexible ring systems, the diastereochemical outcome is explained

FIGURE 4. Ground state conformation of 2-cycloocten-1-ol and 2-cyclononen-1-ol

by minimizing the A-1,3 strain. This reaction, using Denmark's conditions, was a key step in Oppolzer's synthesis of (*R*)-muscone (equation 52)[124].

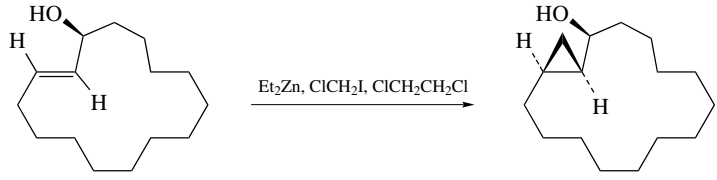

(52)

dr: >99:1 (91%)

It is also important to point out that the directing ability of basic groups is not limited to alcohols (or, more accurately, zinc alkoxides). Esters and ethers (benzyl, THP, MOM, MEM etc.) can also direct the cyclopropanation reaction. The cyclopropanation of tri-*O*-benzyl-D-glucal produced the corresponding *syn* cyclopropane in high yield (equation 53)[125].

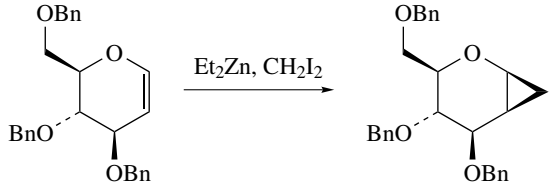

(53)

dr: >95:5 (92%)

Finally, a homoallylic THP ether may be involved in directing the cyclopropanation reaction of a trimethylsilyl enol ether (equation 54)[126]. The lower diastereoselectivity may be a consequence of the remote position of the directing group (homoallylic position).

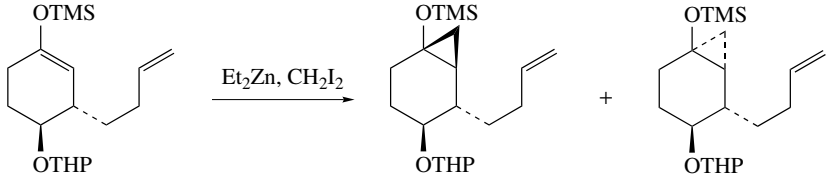

dr: 91:9 (87%) (54)

To calibrate the relative directing ability of various basic groups, Charette and Marcoux examined the diastereoselectivities of the cyclopropanation of monoprotected *trans*-2-cyclohexene-1,4-diols as a function of the protecting group and the number of equivalents of the reagent (equation 55)[127]. One striking feature is that a zinc alkoxide was found to be a better directing group than a benzyl ether when only 1 extra equivalent of the zinc carbenoid was used. However, this diastereoselectivity was completely reversed when 9 equivalents of the reagent was used. A possible explanation for this observation is that when an excess reagent is used, the weaker complex gives rise to the methylene delivery (the zinc reagent is more electrophilic in the weaker complex). When only 1 equivalent was used, the reagent was preferentially complexed to the more basic zinc alkoxide; therefore, the reaction became alkoxy directed. This trend, although not as striking, was

also observed for acetyl and benzyloxymethyl (BOM) protecting groups. In both cases, again the amount of product resulting from a non-alkoxy directed reaction increased as the number of equivalents of reagent increased. However, a triisopropylsilyl ether did not act as a directing group in this reaction.

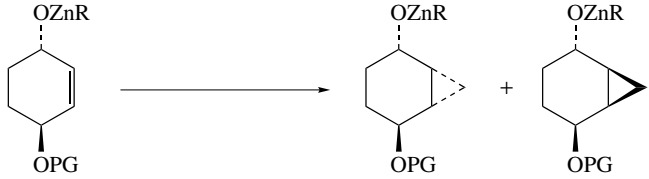

PG = Bn	$Zn(CH_2I)_2$ (1 equiv)	dr: >25:1 (>95%)	(55)
PG = Bn	$EtZnCH_2I$ (9 equiv)	dr: 1:>25 (>95%)	
PG = Ac	$Zn(CH_2I)_2$ (1 equiv)	dr: >10:1 (85%)	
PG = Ac	$Zn(CH_2I)_2$ (9 equiv)	dr: 5:1 (>95%)	
PG = BOM	$Zn(CH_2I)_2$ (1 equiv)	dr: >10:1 (25%)	
PG = BOM	$Zn(CH_2I)_2$ (9 equiv)	dr: 1:3 (95%)	
PG = TIPS	$Zn(CH_2I)_2$ (1 equiv)	dr: >10:1 (25%)	
PG = TIPS	$Zn(CH_2I)_2$ (9 equiv)	dr: >10:1 (>95%)	

Another example of the superiority of the alkoxy group as a directing group was reported by Johnson in his synthesis of enantiomerically pure cyclopropyl ketones after auxiliary cleavage (equation 56)[128]. In that case, the product resulting from a sulfoximine directed cyclopropanation was never observed.

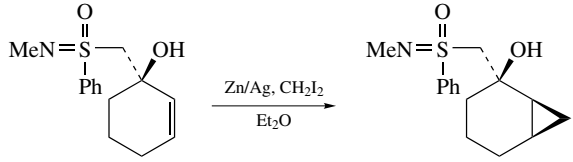

(56)

dr: >95:5 (>90%)

In the absence of directing groups, the sense of induction in the cyclopropanation of cyclic alkenes is predicted on the basis of the minimization of steric interactions. An intermediate in the synthesis of (+)-acetoxycrenulide was prepared by this key reaction in which the carbenoid attack occurred from the side opposite to the methyl group of this highly functionalized alkene (equation 57)[129].

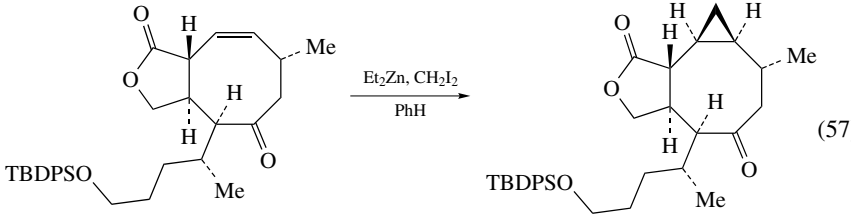

(57)

dr: >95:5 (92%)

2. Stereoselective cyclopropanation of acyclic alkenes

The diastereoselective cyclopropanation of acyclic allylic alcohols is a very useful synthetic transformation. It was recognized early on by Pereyre and coworkers that the cyclopropanation of *Z*-substituted chiral allylic alcohol was highly *syn* selective (equation 58)[130]. It was later shown that most zinc carbenoids react with these substrates with high *syn* stereocontrol.

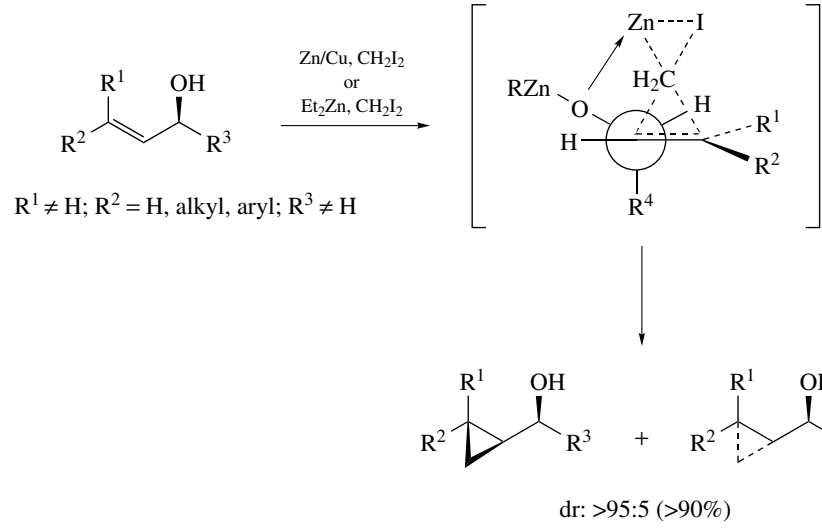

$R^1 \neq H$; $R^2 = H$, alkyl, aryl; $R^3 \neq H$

dr: >95:5 (>90%)

(58)

The level of diastereoselection in the cyclopropanation of chiral acyclic *E*-allylic alcohols is highly dependent upon the choice of the reagent, the stoichiometry and the solvent. Charette has shown that, with simple *E*-substituted chiral allylic alcohols, the use of an excess of the Furukawa reagent in dichloromethane provided the highest *syn* stereocontrol (equation 59)[131].

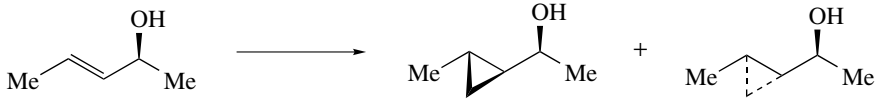

(59)

Zn/Cu, CH_2I_2, Et_2O	dr: 57:43 (no yield given)
Et_2Zn (5 equiv), CH_2I_2 (5 equiv), Et_2O	dr: 82:18 (50%)
Et_2Zn (5 equiv), CH_2I_2 (5 equiv), CH_2Cl_2	dr: 88:12 (>95%)

The level of *syn* induction increases as the size of the *E*-substituent increases as well as the size of the allylic substituent. An interesting application of these reaction conditions was reported in the synthesis of an advanced intermediate in halicholactone synthesis (equation 60)[132]. It is important to note that the reaction proceeded not only with excellent diastereocontrol, but also with complete chemoselectivity in favor of the allylic alcohol double bond. However, the participation of the trimethylsilylethoxymethyl (SEM)

ether cannot be excluded since it would lead to the same diastereomer upon minimizing the allylic strain.

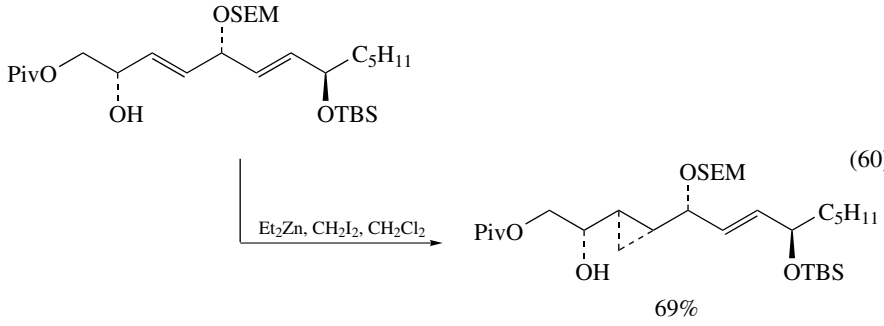

(60)

A clever access to diastereomerically and enantioenriched *syn* cyclopropylmethanol derivatives was reported by Walsh and coworkers (equation 61)[133]. This methodology features an initial asymmetric carbon–carbon bond-forming process by a catalytic asymmetric addition of an organozinc species to an aldehyde in the presence of Nugent's catalyst. The resulting chiral acyclic allylic zinc alkoxide was directly treated with Furukawa reagent to produce the corresponding *syn* cyclopropyl methanol derivative with outstanding enantio- and diastereocontrol.

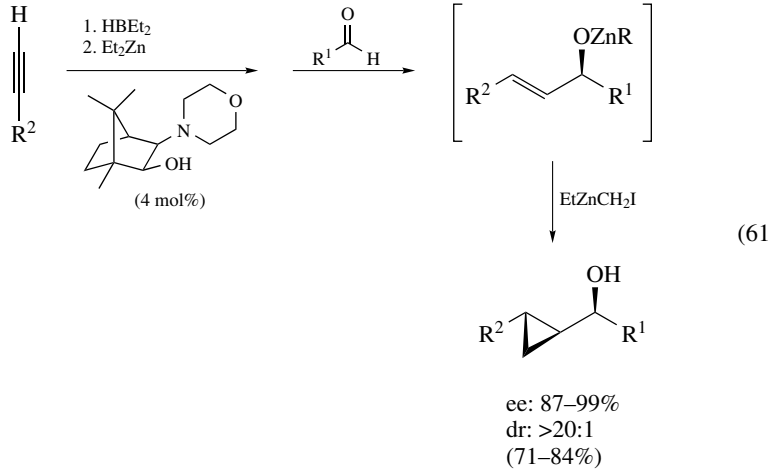

(61)

Alternatively, the use of the reagent prepared by mixing trifluoroethanol, diethylzinc and iodoform led to the formation of the corresponding iodocyclopropane with outstanding diastereocontrol (equation 62).

Charette and coworkers have shown that the diastereoselective cyclopropanation of chiral allylic alcohols with *gem*-dizinc carbenoids proceeds with high diastereocontrol for protected 2-butene-1,4-diol derivatives (equation 63)[134]. The minimization of the A-1,3 strain and the formation of a zinc chelate in the product is believed to be responsible for

the sense of induction. *E*-Substituted chiral allylic alcohols can also be used, but the level of induction is highly dependent upon the nature of the substituents.

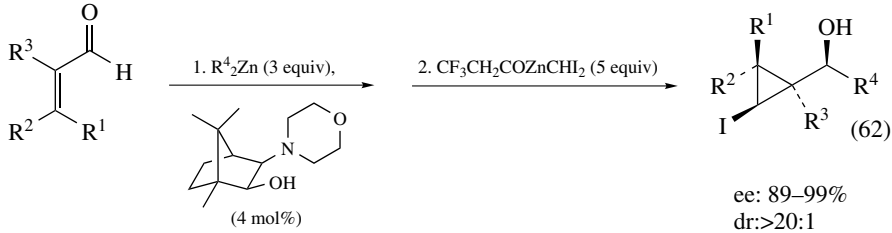

(62)

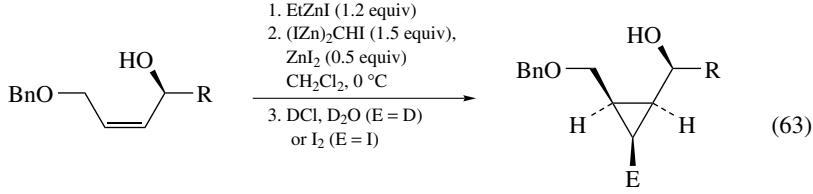

(63)

In addition, if this reaction was run in the presence of trimethylborate, a usual zinc–boron exchange led to the cyclopropylboron derivative that could be used in Suzuki coupling to give rise to trisubstituted cyclopropanes (equation 64)[102].

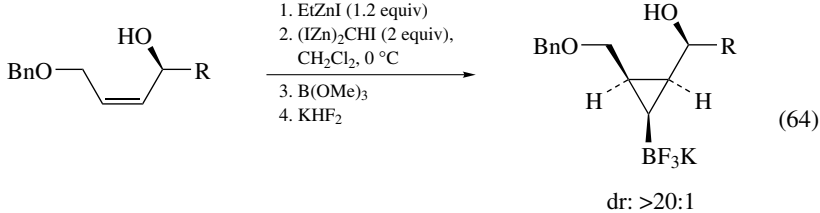

(64)

As one might expect, the diastereoselectivities with homoallylic alcohols are quite substrate-dependent. One successful example involves the cyclopropanation of allyl silanes[135, 136], which could be cyclopropanated with a high level of diastereocontrol (equations 65 and 66).

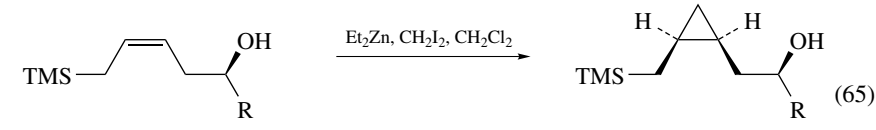

(65)

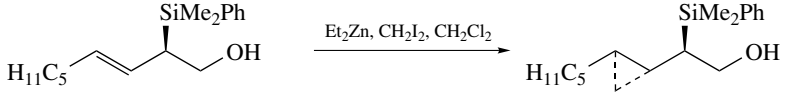

(66)

dr: 98:2 (83%)

The model involving the minimization of the A-1,3 allylic strain followed by an alkoxy-directed cyclopropanation is quite reliable to predict the sense of induction in the cyclopropanation of chiral acyclic allylic alcohols. However, the application of this model is not as straightforward in the case of allylic ethers. Indeed, it was shown that the cyclopropanation of benzyl ethers led to a major *anti* or *syn* isomer depending upon the nature of the substituents (equation 67)[137].

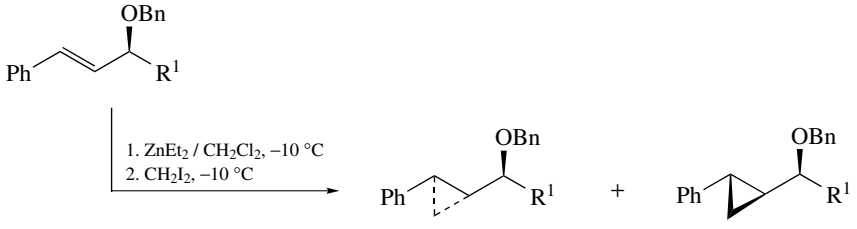

R^1 = Me dr: 90:10 (94%)
R^1 = Et dr: 67:33 (94%)
R^1 = *i*-Pr dr: 5:95 (94%)

(67)

It was later found that the *anti* selectivities could be greatly improved by using silyl ethers and the more reactive Shi's reagent (equation 68)[138]. The transition structure in which the C−O bond eclipses the C=C bond was proposed to account for the sense of induction and is based on the work of Gung and coworkers[139]. It should also be mentioned that *Z*-alkyl-substituted allylic silyl ethers led to the *anti* isomer as well, and their *Z*-aryl-substituted analogues led to the *syn* isomer.

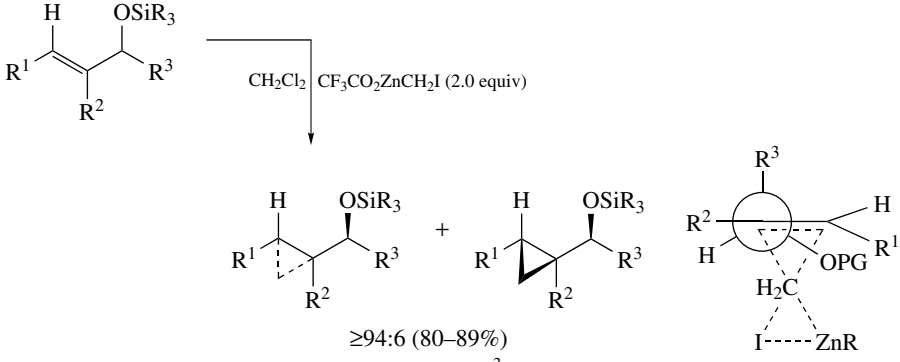

≥94:6 (80–89%)
except when R^3 = *i*-Pr:
dr: 70:30 (78%)

R^1 = aryl, alkyl; R^2 = H, alkyl; R^3 = alkyl

(68)

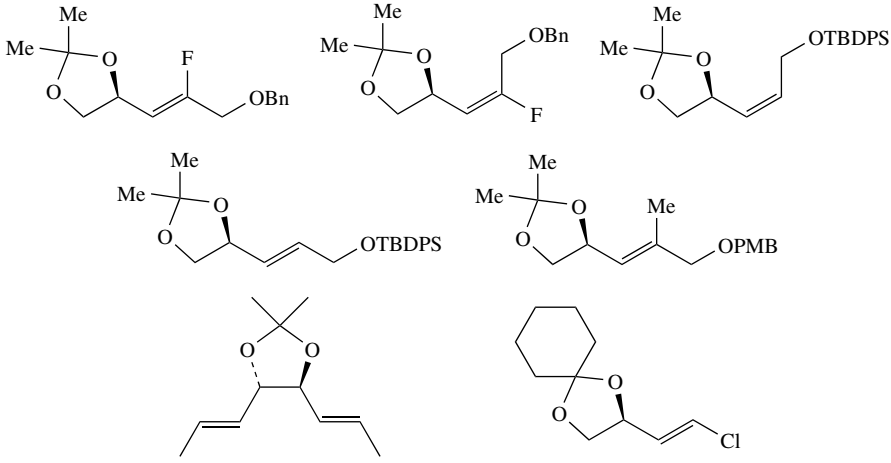

FIGURE 5. Starting materials producing a *syn*-selective cyclopropanation using $RZnCH_2X$ in chlorinated solvents

There are numerous examples of highly *syn* diastereoselective cyclopropanation of allylic ethers in the literature, and most of them are alkenes prepared from protected glyceraldehyde. Some examples are illustrated in Figure 5[96, 140–143]. In almost all cases, the reagent used was prepared from diethylzinc and diiodo- or chloroiodomethane. One exception was for the less reactive *E*-vinyl chloride, for which iodomethylzinc trifluoroacetate was used[144].

The cyclopropanation of allylic alcohols in which a non-Lewis basic stereogenic center is located at the other allylic position does not generally proceed with high enantiocontrol[145]. One interesting exception is the cyclopropanation of *E*-vinylcyclopropanes, which produced the *anti* isomer with high induction (equation 69)[146].

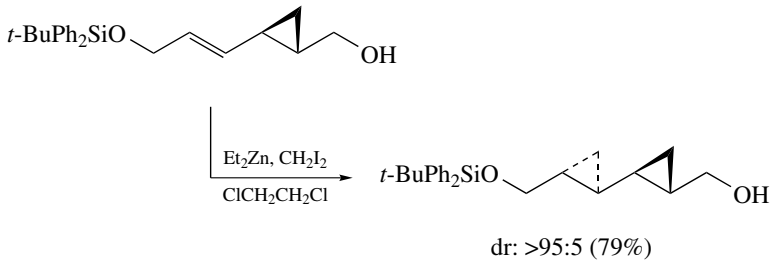

(69)

dr: >95:5 (79%)

The cyclopropanation of fully protected chiral allylic amines afforded poor diastereoselectivities (equation 70)[147]. However, Wipf and coworkers have shown that a chiral allylic amine generated *in situ* by a sequential hydrozirconation/Zr–Zn transmetalation/imine addition reacted upon addition of diiodomethane to generate the corresponding *anti* cyclopropyl isomer with outstanding diastereocontrol (equation 71)[148, 149]. The reaction is quite interesting mechanistically, since it implies that a methylzinc amide can exchange with diiodomethane to produce an iodomethylzinc amide. It is postulated that

the latter undergoes an intramolecular cyclopropanation which could be facilitated by the presence of a zirconocene complex.

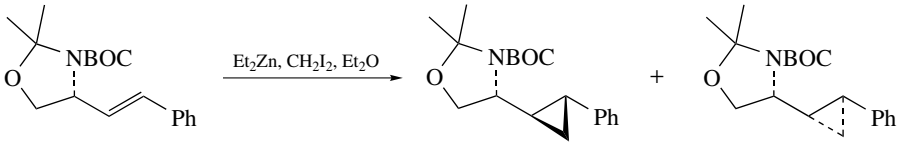

dr: 3:1 (50%) (70)

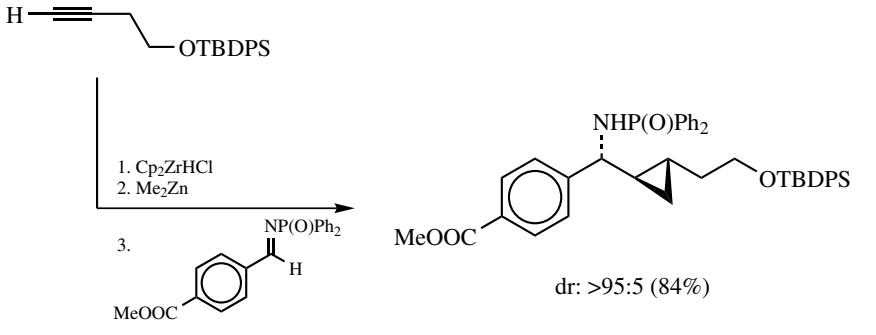

dr: >95:5 (84%) (71)

D. Stereoselective Cyclopropanation of Alkenes using Chiral Auxiliaries

Several covalently attached chiral auxiliaries are available to cyclopropanate various classes of alkenes. In general, the only reagents that have been used are the unsubstituted iodomethylzinc carbenoids. Attempts to generate more highly substituted cyclopropane derivatives with α-substituted iodoalkylzinc carbenoids have failed to give a useful level of diastereoselection. Substituted cyclopropylmethanol derivatives can be prepared using carbohydrate derived chiral auxiliaries (Figure 6)[150]. Although the reactions are highly diastereoselective, a large excess of the zinc reagent is necessary for high yields and stereochemical induction. A first equivalent is necessary to deprotonate the free hydroxy group, and the excess is a consequence of having numerous basic groups. Both the L-rhamnose (**12**) and α-glucoside (**13**) auxiliaries act as pseudo-mirror images of the β-glucoside (**11**)[151].

In all cases, the cleavage of the auxiliary could not be accomplished under acidic conditions due to the sensitivity of the cyclopropylmethanol unit. Cleavage by ring contraction of the corresponding C-2 *O*-triflyl derivative afforded the cyclopropylmethanols in good yield (equation 72)[152].

Since the reaction is highly diastereoselective with most substituted allylic alcohols, application of this methodology to the synthesis of all isomers of coronamic acid is particularly well suited[153]. In an attempt to decrease the number of equivalents of the reagent needed and to establish the minimum stereochemical requirements of the auxiliary for high induction, the cyclohexanediol derivative (**14**) was developed (see Figure 6). The cyclopropanation was highly diastereoselective with only three equivalents of the reagent. Destructive cleavage of the auxiliary to produce the cyclopropylmethanol in high yield could be accomplished by transforming first the alcohol moiety into iodide and then by treating the resulting iodide with BuLi[154].

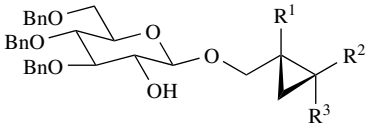

(11)

Et_2Zn (10 equiv), CH_2I_2 (10 equiv)
toluene

dr >95:5
(>95%)

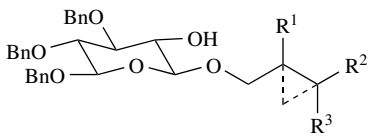

(12)

Et_2Zn (10 equiv), CH_2I_2 (10 equiv)
toluene

dr >95:5
(>95%)

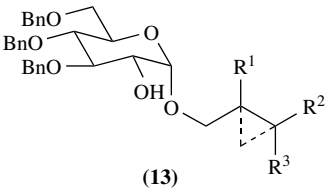

(13)

Et_2Zn (10 equiv), CH_2I_2 (10 equiv)
t-BuOMe

dr >95:5
(83–93%)

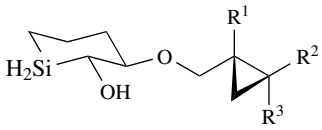

(14)

Et_2Zn (3 equiv)
$ClCH_2I$ (3 equiv)
toluene

dr >93:7
(90–98%)

FIGURE 6. Carbohydrate derived chiral auxiliaries for the cyclopropanation of allylic alcohols

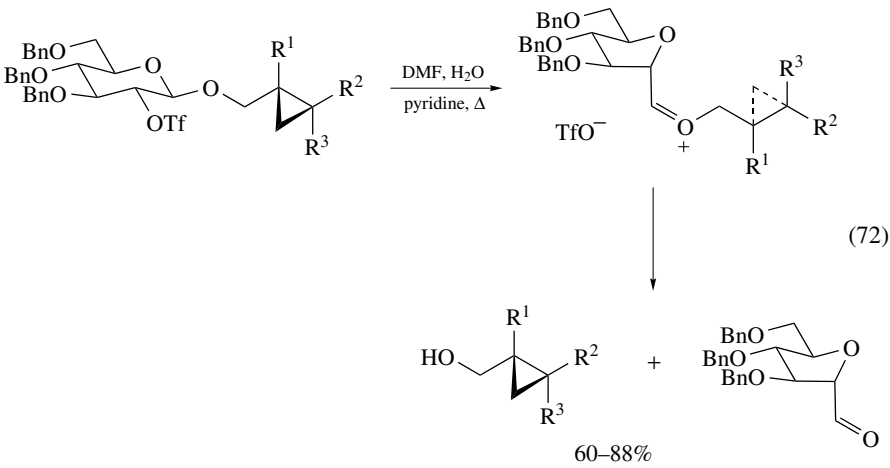

(72)

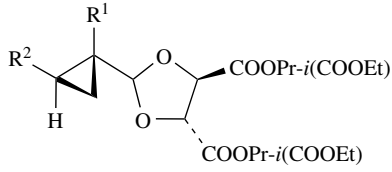

(**15**)

Et_2Zn (5 equiv)
CH_2I_2 (10 equiv)
hexane

dr: 93:7 to 97:3
(50–95%)

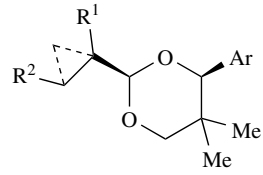

(**16**)

Et_2Zn (3-5 equiv)
CH_2I_2 (6-10 equiv)
toluene

dr: 60:40 to 89:11
(34–67%)

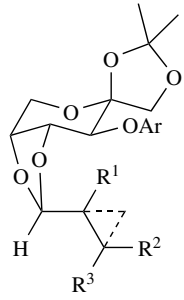

(**17**)

Et_2Zn (5 equiv)
CH_2I_2 (10 equiv)
$(CH_2Cl)_2$

dr: 61:39 to 81:19
(45–90%)

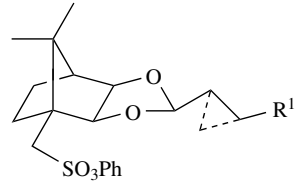

(**18**)

Et_2Zn (5 equiv)
CH_2I_2 (10 equiv)
CH_2Cl_2

dr: >99:1
(76–95%)

FIGURE 7. 1,2- and 1,3-diol derived chiral auxiliaries for the cyclopropanation of acyclic α,β-unsaturated carbonyl

Chiral acetals have also been used as chiral auxiliaries for the enantioselective cyclopropanation of α,β-unsaturated carbonyl derivatives (Figure 7). Yamamoto's tartrate derived auxiliaries (**15**) based on the ether-directed cyclopropanation allowed the efficient preparation of cyclopropylcarboxaldehyde derivatives[155,156]. The reaction proceeded with high diastereocontrol, and the auxiliary could be cleaved under mild acidic conditions (equation 73).

Other chiral auxiliaries for the cyclopropanation of α,β-unsaturated aldehydes have also been developed (Figure 7, **16**–**18**)[157–159]. α,β-Unsaturated chiral amides have also been used in auxiliary-based reactions but the addition of diethyl tartrate as chiral additives was necessary for high diastereoselectivities[160].

Two approaches allow for the preparation of enantiomerically enriched bicyclo[n, 1.0] systems using zinc carbenoids. The first, developed by Johnson, involves the directed

Simmons–Smith cyclopropanation of β-hydroxysulfoximines (equation 74)[161]. However, access to the pure bicyclo[3.1.0] derivative required chromatographic separation of the diastereomeric sulfoximine adducts.

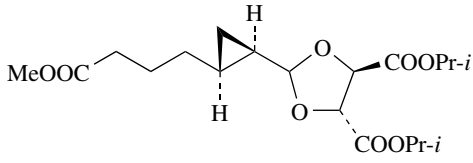

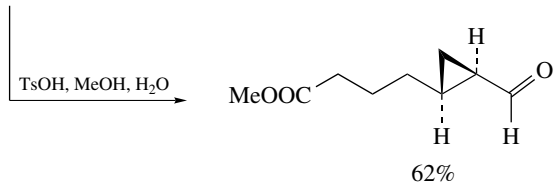

62%

(73)

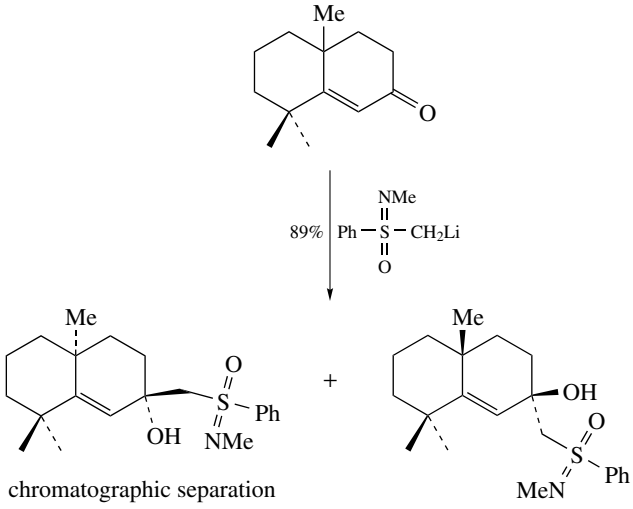

(74)

A second general approach featuring the use of C_2 symmetric diols as chiral auxiliaries was developed by Mash (equation 75)[162, 163]. The reaction proceeded with good to excellent diastereocontrol with 5- to 16-membered cyclic enones, and cleavage of the auxiliary could be smoothly accomplished under mild acidic conditions (equation 75). This reaction was applied to several syntheses of natural products such as modhephene[164], muscone[165], chokol[166] and β-eudesmol[167].

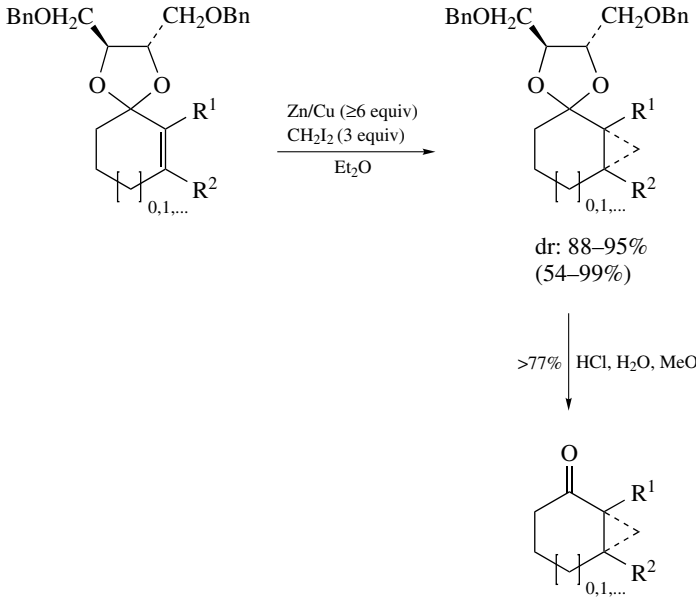

(75)

A detailed mechanistic investigation of the structural requirements of the chiral auxiliary for high induction was reported[168, 169], but it was only a few years later that a more effective second-generation chiral auxiliary was developed using bulkier substituents on the dioxolane ring (equation 76)[170].

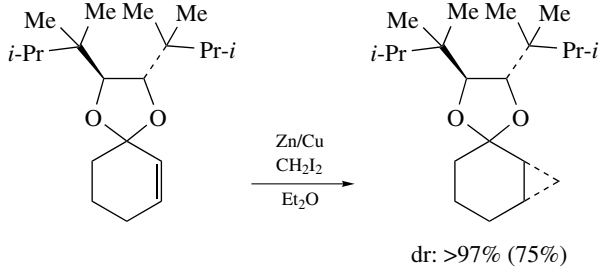

(76)

A chiral auxiliary-based approach has been developed for the preparation of chiral, non-racemic cyclopropylmethylamines that are not protected with electron-withdrawing groups. The cyclopropanation of allylic tertiary amines bearing a β-hydroxide occurred

cleanly and with high diastereoselectivity to generate the cyclopropylmethylamine (equation 77)[171]. Cleavage of the auxiliary could be achieved upon treatment with methyl iodide followed by heating. It should be pointed out that the alcohol (or the intermediate zinc alkoxide) protects the basic nitrogen atom from being alkylated by the electrophilic zinc reagent.

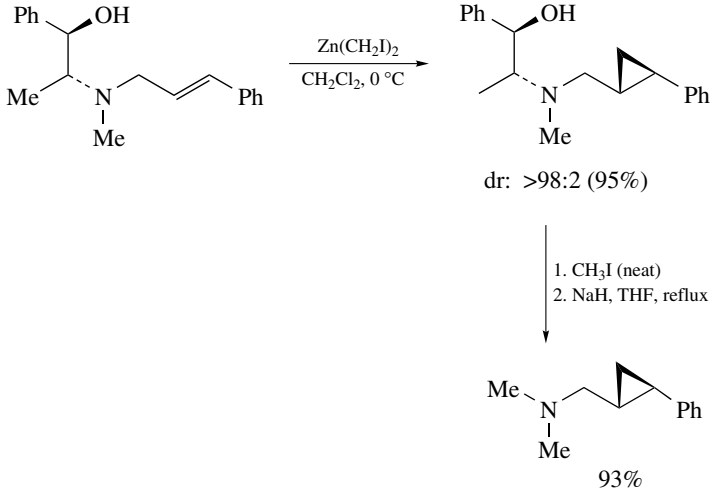

(77)

A very useful class of chiral auxiliaries has been developed for alkenes substituted with a heteroatom. These auxiliaries, attached to the heteroatom, allow for the preparation of enantiomerically enriched cyclopropanols, cyclopropylamines and cyclopropylboronic acids. Tai and coworkers have developed a method to efficiently generate substituted cyclopropanol derivatives using the cyclopropanation of a chiral enol ether (equation 78)[172]. The reaction proceeds with very high diastereocontrol with five- to eight-membered ring sizes as well as with acyclic enol ethers. The potential problem with the latter is the control of the double bond geometry upon enol ether formation. A detailed mechanistic study involving two zinc centers in the transition structure has been reported[173].

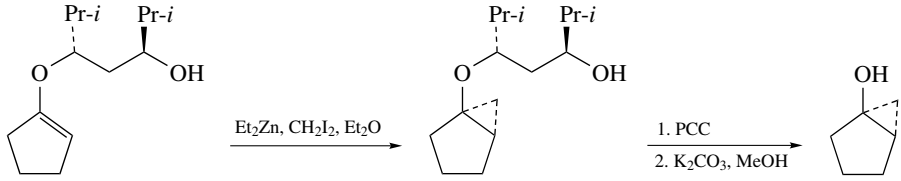

dr: >99% (81%) (78)

An alternate strategy to access cyclopropanol derivatives[174] from an acyclic precursor has been reported by Imai and coworkers (equation 79)[175]. Alkyne hydroboration followed by treatment of the resulting boronic acid with tetramethyltartramide produced the cyclopropanation precursor. A subsequent diastereofacial cyclopropanation afforded the

corresponding cyclopropylboronate ester, which could be oxidized to the cyclopropanol under mild basic conditions.

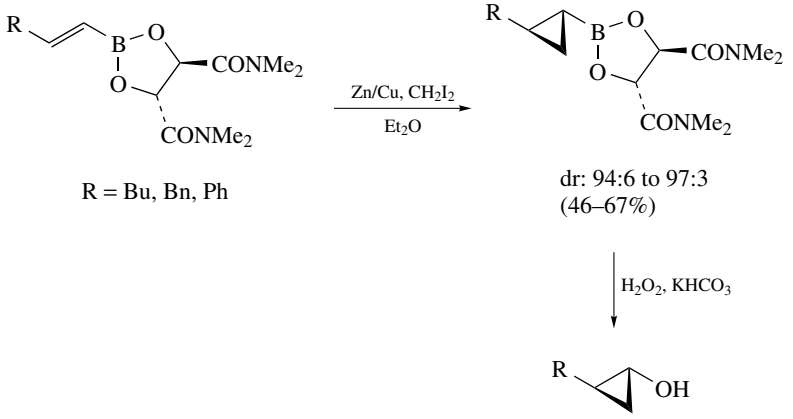

Other chiral auxiliaries have been tested, such as those derived from TADDOL ligands, but, in these cases, better diastereocontrol was achieved using palladium acetate/diazomethane[176] or using double differentiation with a chiral catalyst (*vide infra*).

The cyclopropanation of a chiral enamide has been investigated for the preparation of fluoro-substituted cyclopropylamines. Unfortunately, the reaction produced a mixture of all four possible stereoisomers when the chiral starting material was submitted to the α-fluoro iodomethylzinc carbene (equation 80)[177].

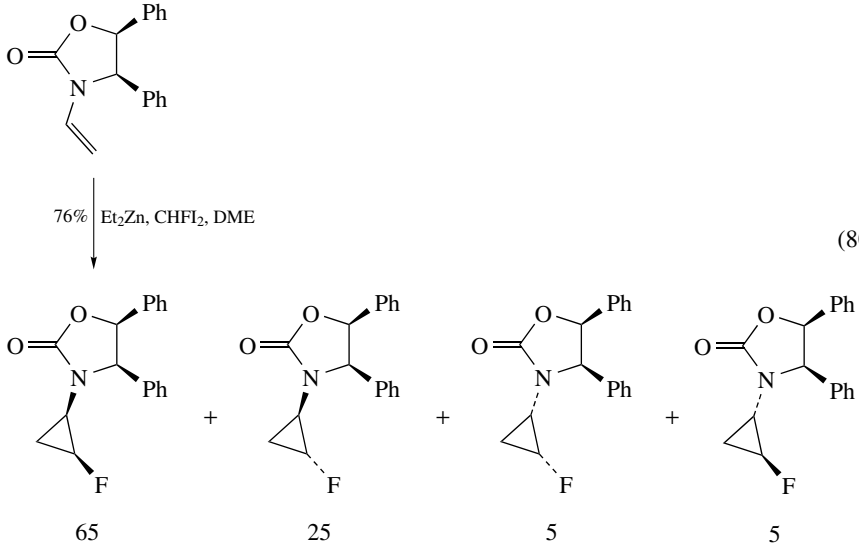

Finally, it is also possible to prepare an enantiomerically pure 1-amino-2-alkoxycyclopropane using a cyclic dihydrooxazole that is readily available from serine or threonine (equation 81)[178].

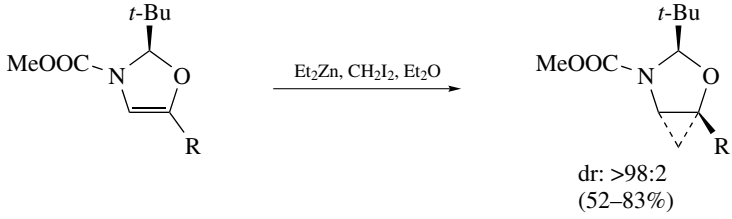

dr: >98:2
(52–83%) (81)

E. Stereoselective Cyclopropanation of Alkenes using Stoichiometric Chiral Reagents

The cyclopropanation of alkenes using external stoichiometric chiral additives can be divided according to their general mechanistic scheme into two classes. The enantioselective cyclopropanation of allylic alcohols, in which a pre-association between the corresponding zinc alkoxide and the zinc reagent probably takes place, constitutes the first class. The second class involves the enantioselective cyclopropanation of unfunctionalized alkenes. The latter implies that there will be no association between the reagent and the alkene through alkoxide formation.

The first stoichiometric chiral additives were tested in 1968[179]; the first relatively successful attempts were published by Fujisawa and coworkers in 1992[180], who reported that moderate levels of enantioselection (79% ee for cinnamyl alcohol and 81% ee for *cis*-6-phenyl-2-hexen-1-ol) were observed if 1 equivalent of diethyl tartrate was added to a mixture of the allylic alcohol, diethylzinc and diiodomethane (equation 82).

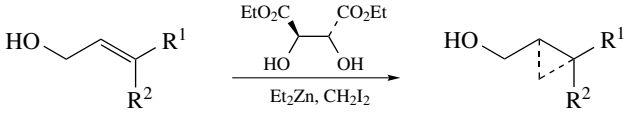

R^1 = Ph, R^2 = H	54% (79% ee)
R^1 = $PhMe_2Si$, R^2 = Me	93% (89% ee)
R^1 = Me, R^2 = $PhMe_2Si$	72% (74% ee)
R^1 = $PhMe_2Si$, R^2 = Bu	84% (87% ee)

(82)

The method was then extended to silyl-substituted allylic alcohols by Ukaji and coworkers[181] and they observed good ee values as well (equation 82).

The tartaric acid scaffold also led to the design of one of the most effective and general methods to generate enantiomerically enriched substituted cyclopropylmethanol derivatives. Indeed, the chiral dioxaborolane ligand **19**, prepared from tetramethyltartramide and butylboronic acid, is a superb chiral additive in allylic alcohol-directed cyclopropanation reactions (equation 83)[182, 183]. The best procedure requires the use of the soluble bis(iodomethyl)zinc•DME complex[26]. The reaction affords high yields and enantiomeric

excesses with a wide range of substituted allylic alcohols, including those containing cis-, trans-, tri- and tetrasubstituted alkenes. The only class of alkenes that consistently produced enantiomeric excesses below 90% are those in which R^1 and $R^2 \neq H$ and $R^3 = H$. The enantioselective cyclopropanation of (*E*)-3-chloro-2-propen-1-ol was used to install the cyclopropane ring of the callipeltoside A side chain[184].

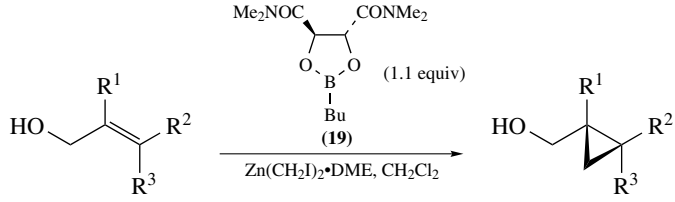

$R^1 = H$, $R^2 = Ph$, $R^3 = H$	95% (94% ee)	
$R^1 = H$, $R^2 = n\text{-}C_3H_7$, $R^3 = H$	80% (93% ee)	
$R^1 = H$, $R^2 = CH_2CH_2Ph$, $R^3 = H$	90% (94% ee)	(83)
$R^1 = H$, $R^2 = SnBu_3$, $R^3 = H$	88% (90% ee)	
$R^1 = H$, $R^2 = I$, $R^3 = H$	83% (90% ee)	
$R^1 = H$, $R^2 = H$, $R^3 = Et$	90% (93% ee)	
$R^1 = H$, $R^2 = H$, $R^3 = I$	90% (93% ee)	
$R^1 = H$, $R^2 = H$, $R^3 = SnBu_3$	73% (90% ee)	
$R^1 = H$, $R^2 = H$, $R^3 = CH_2OBn$	93% (91% ee)	
$R^1 = Me$, $R^2 = Ph$, $R^3 = H$	96% (85% ee)	
$R^1 = H$, $R^2 = Me$, $R^3 = Me$	85% (94% ee)	
$R^1 = CH_2OTIPS$, $R^2 = Me$, $R^3 = Me$	85% (88% ee)	

The reaction has been extended to the chemo- and enantioselective cyclopropanation of polyenes (equations 84 and 85)[185] and allenic alcohols that afforded spiropentane derivatives[186].

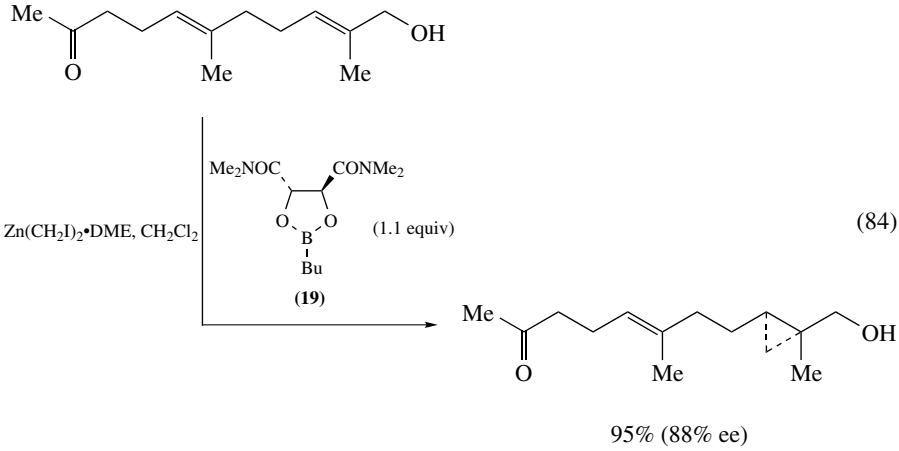

(84)

95% (88% ee)

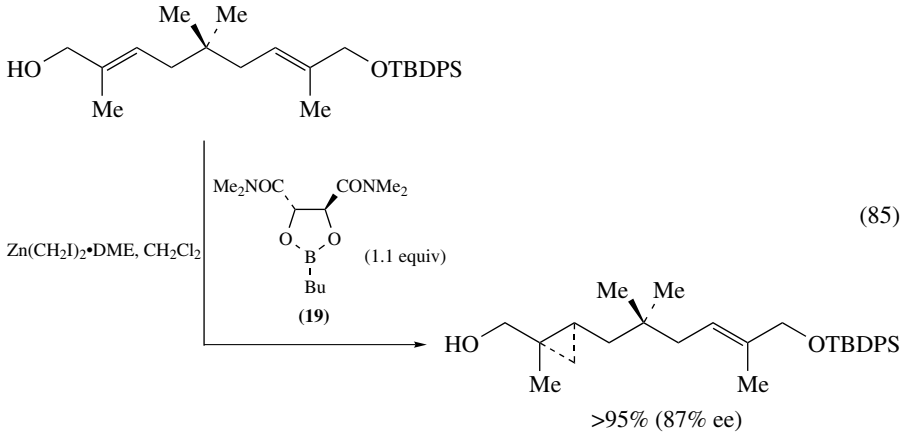

(85)

The enantioselective cyclopropanation leading to 1,2,3-substituted cyclopropane derivatives proceeds with high diastereocontrol (equation 86)[39]. It is quite interesting to observe that the same reaction, when run in the absence of the dioxaborolane ligand, led to lower diastereoselectivity. Other functionalized 1,1-diiodoalkanes can be used as the zinc carbenoid precursor, but it should be noted that up to 2 equivalents of the reagent (4 equivalents of $RCHI_2$) are needed in this process. This reaction has been applied in the synthesis of ambruticin[187].

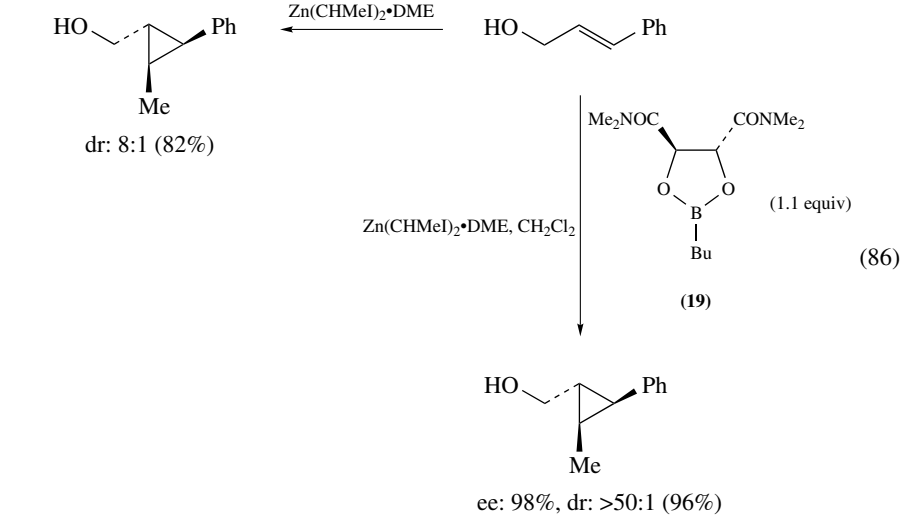

(86)

A case of matched and mismatched pairs was observed in the reagent-controlled cyclopropanation of chiral allylic alcohols. When the chiral, nonracemic allylic alcohol was treated with one enantiomer of the dioxaborolane ligand, the *anti* diastereomer was

formed, whereas treatment with the ligand's antipode led to a much lower diastereomeric ratio (equation 87)[137].

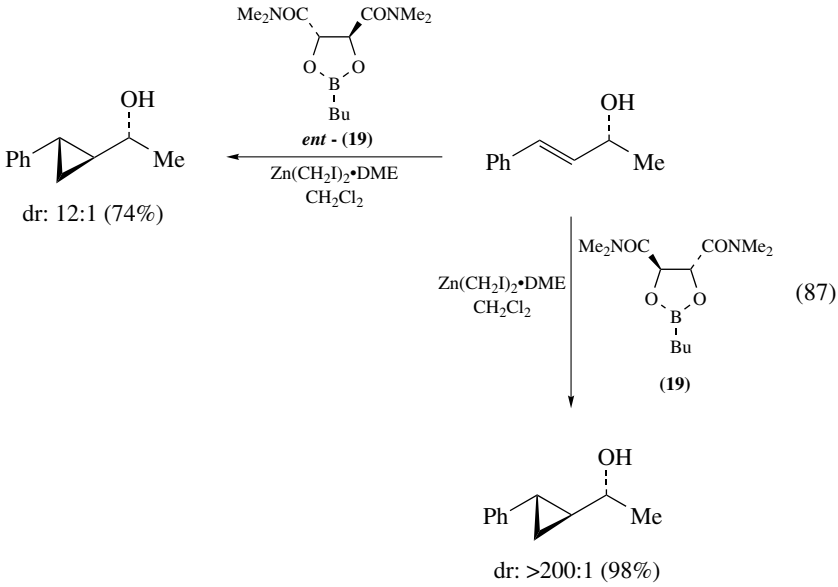

(87)

However, an excellent reagent-controlled cyclopropanation was observed if the stereogenic center was located at the other allylic position (equation 88)[188]. This reaction was used extensively in the bidirectional chain synthesis of the poly(cyclopropane) natural products, FR-900848[189] and U-106305[190].

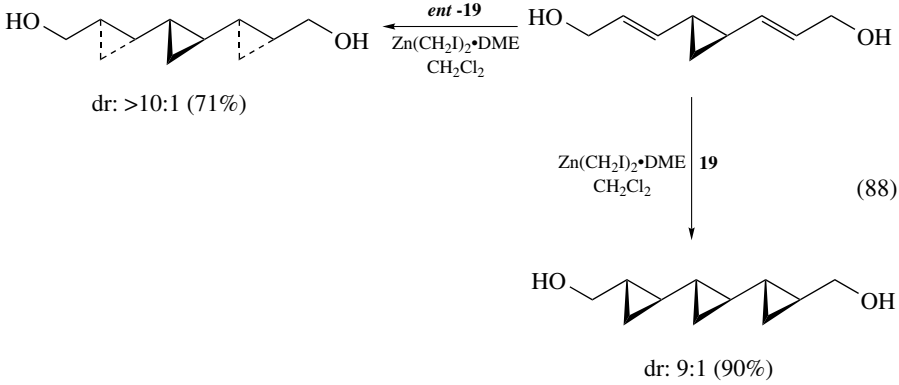

(88)

N,*N*,*N*′,*N*′-Tetraethyl-1,1′-bi-2-naphthol-3,3′-dicarboxamide (**20**) has been shown by Katsuki and coworkers to be quite effective as a stoichiometric additive in the cyclopropanation of allylic alcohols (equation 89)[191]. The best enantioselectivities were obtained with aryl-substituted allylic alcohols; however, 6 equivalents of diethylzinc were needed.

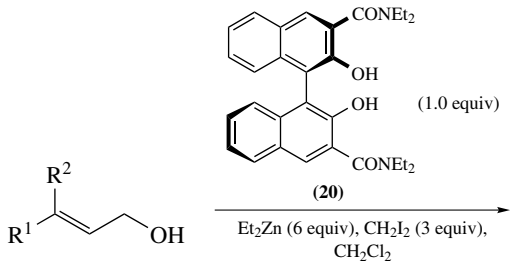

(89)

R^1 = Ph, R^2 = H	55% (94% ee)
R^1 = $PhCH_2CH_2$, R^2 = H	65% (89% ee)
R^1 = $TrOCH_2$, R^2 = H	64% (88% ee)
R^1 = $TBDPSOCH_2$, R^2 = H	59% (87% ee)
R^1 = H, R^2 = $TrOCH_2$	34% (65% ee)

The next classes of reagents developed are those for the cyclopropanation of unfunctionalized alkenes. After early attempts at getting high enantioselectivities for the cyclopropanation of β-methylstyrene using a chiral alcohol (**21**), bis(iodo)methylzinc, diethylzinc, dichloromethane and a Lewis acid (equation 90)[28], Shi and coworkers made a major breakthrough when they found that a simple dipeptide (**22**) derived from valine and proline could be used (equation 91)[192]. However, in either case, the absolute stereochemistry of the cyclopropane has not been determined.

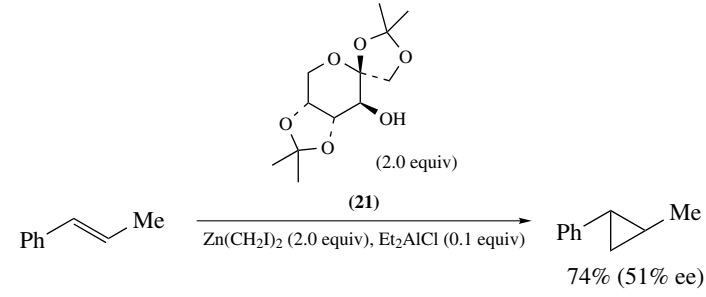

74% (51% ee)

(90)

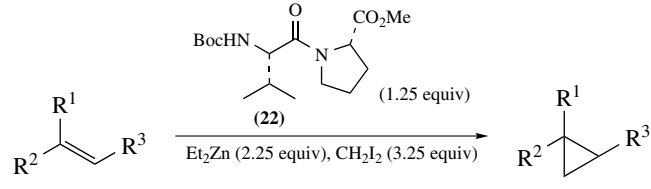

43–84% (72–91% ee)

(91)

The simple peptide, used in stoichiometric amounts, can convert a variety of aryl-substituted alkenes to the corresponding cyclopropane with good to excellent enantioselectivities (Figure 8).

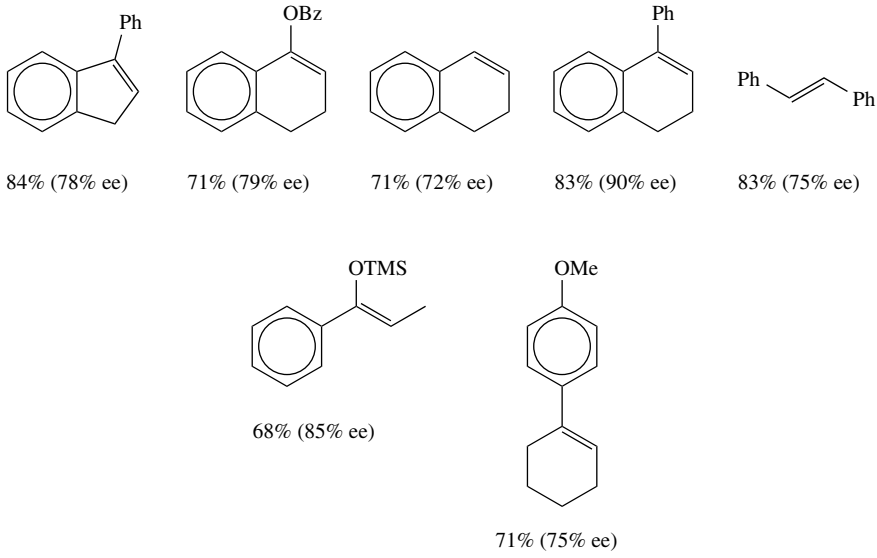

FIGURE 8. Enantioselective cyclopropanation of unfunctionalized alkenes using chiral ligand **22**

An alternate approach has been developed by Charette and coworkers in which chiral iodomethylzinc phosphates were prepared and tested in the cyclopropanation of unfunctionalized alkenes. Although these reagents were not sufficiently reactive to convert aryl-substituted alkenes (such as indene) to the corresponding cyclopropane, they reacted nicely with protected aryl-substituted allylic and homoallylic alcohols (equation 92)[30]. Several 3,3′-disubstituted binols were tested and ligand **23** stood out as being the most effective with this class of compounds. The active reagent in this case is a chiral iodomethylzinc phosphate.

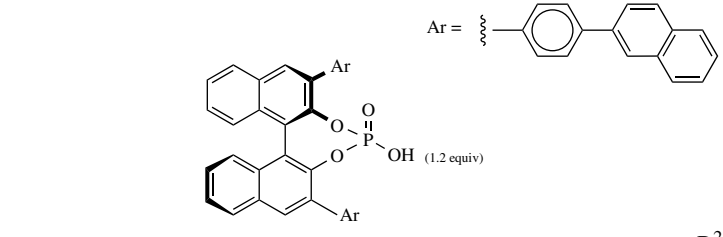

(92)

$R^2 = CH_2OBn$	89% (90% ee)
$R^2 = CH_2OTES$	84% (92% ee)
$R^2 = CH_2CH_2OBn$	85% (93% ee)

F. Stereoselective Cyclopropanation of Alkenes using Chiral Catalysts

The development of a catalytic asymmetric cyclopropanation reaction involving halomethylzinc reagents has been extremely challenging. One issue is that the uncatalyzed, background cyclopropanation reaction between an achiral haloalkylzinc reagent and an alkene is usually a fast process. The notion of using Lewis acids to accelerate the cyclopropanation of alkenes has been contemplated for several decades, but it is only recently that it has produced impressive results. The first ground-breaking work was published by Kobayashi and coworkers, who demonstrated that the addition of only 0.12 equivalent of chiral disulfonamide ligand **24** led to the formation of the cyclopropanated product derived from cinnamyl alcohol in 76% ee (equation 93)[193, 194]. Conversely, stannyl- and silyl-substituted allylic alcohols were also very good substrates[195].

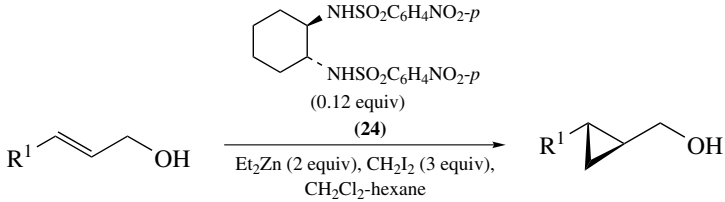

(93)

$R^1 = Ph$ 82% (76% ee)
$R^1 = SnBu_3$ 94% (86% ee)

Denmark and coworkers have reported an in-depth study of this reaction and highlighted the effect of the many variables to optimize the enantioselectivities[62]. They have shown that the rate and selectivity of the catalytic enantioselective cyclopropanation of cinnamyl alcohol utilizing the bis(sulfonamide) **25** was greatly dependent on the order of addition of the reagents[196]. The independent preformation of the ethylzinc alkoxide and bis(iodomethyl)zinc was also found to be very important for high enantiocontrol (equation 94, Figure 9).

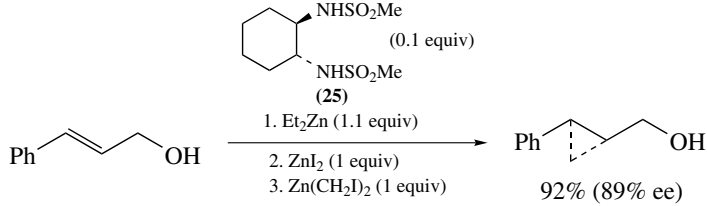

(94)

92% (89% ee)

The reaction also displayed autocatalytic behavior, which was shown to be due to the generation of zinc iodide. This species, in combination with bis(iodomethyl)zinc, undergoes Schlenk equilibration to give iodomethylzinc iodide. This and other observations have led to the proposed transition state model in which three zinc atoms are involved in the cyclopropanation (Figure 10).

Charette and Brochu have reported an alternate protocol for the Lewis acid-catalyzed cyclopropanation reaction of allylic alcohols, in which the uncatalyzed process is suppressed[197]. The addition of $Zn(CH_2I)_2$ (1 equivalent) to an allylic alcohol (1 equivalent)

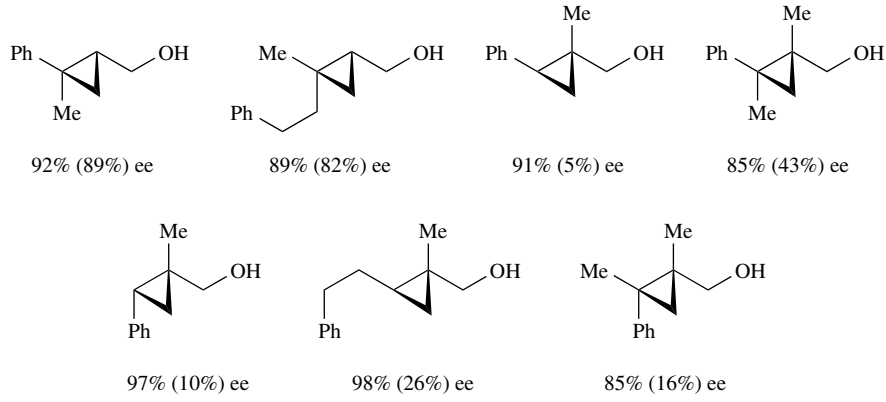

FIGURE 9. Enantioselectivities for the catalytic asymmetric cyclopropanation with ligand **25**

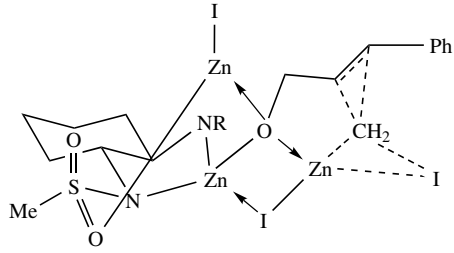

FIGURE 10. Transition state model for the cyclopropanation using chiral ligand **25**

produced the iodomethylzinc alkoxide in quantitative yield along with methyl iodide (equation 95). These species are typically not good methylene transfer agents, but it was found that the addition of a Lewis acid triggers methylene delivery. The use of the titanium–taddolate **26** produced the corresponding cyclopropane derived from aryl-substituted allylic alcohols in up to 92% ee[198]. The enantioselectivities dropped for alkyl-substituted allylic alcohols.

The last two catalytic systems available are intimately based on the stoichiometric ligands **22** and **23**, derived from the dipeptide and the chiral phosphoric acid, respectively. The addition of basic additives to slow down or suppress the background reaction allowed the use of catalytic amounts of the ligand. In his initial report, Shi and coworkers have shown that adding 1 equivalent of ethyl methoxyacetate allowed the catalyst loading to be decreased to 0.25 equiv (equation 96)[199]. Under these conditions, the enantioselectivities are similar to those reported in Figure 7.

Conversely, Charette and coworkers have shown that the chiral phosphate **23** could be used in catalytic amounts for the cyclopropanation of protected allylic alcohols (equation 97)[30]. This was made possible by using DME as the additive to slow down the background cyclopropanation process, leading to racemic cyclopropane (Pathway A). Bis(iodomethyl)zinc was used as the stoichiometric reagent to regenerate the reactive iodomethylzinc phosphate (Pathway B). Excellent enantioselectivities were observed using this protocol; however, the scope of the reaction is still quite limited.

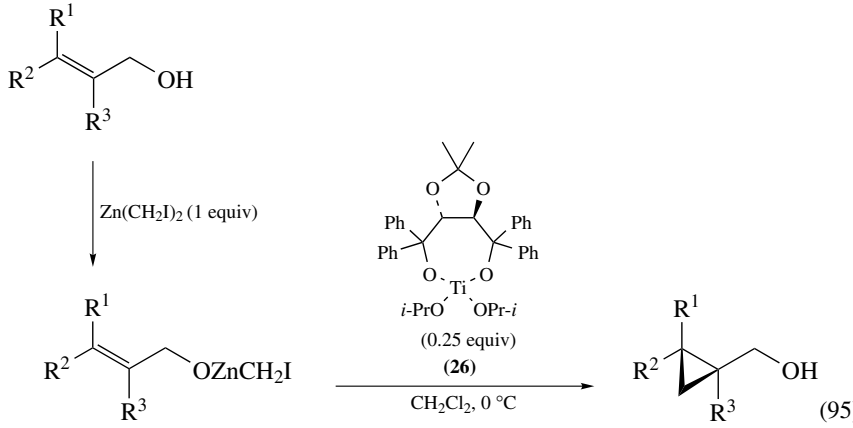

(95)

R^1 = H, R^2 = Ph, R^3 = H	85% (92% ee)
R^1 = Ph, R^2 = H, R^3 = H	62% (72% ee)
R^1 = Ph, R^2 = Me, R^3 = H	80% (88% ee)
R^1 = H, R^2 = Ph, R^3 = Me	80% (50% ee)
R^1 = H, R^2 = 2-Naphthyl, R^3 = H	81% (92% ee)
R^1 = H, R^2 = 1-Naphthyl, R^3 = H	80% (84% ee)
R^1 = H, R^2 = Cinnamyl, R^3 = H	75% (86% ee)
R^1 = H, R^2 = 3,5-$Me_2C_6H_3$, R^3 = H	86% (92% ee)
R^1 = H, R^2 = *n*-Pr, R^3 = H	68% (74% ee)

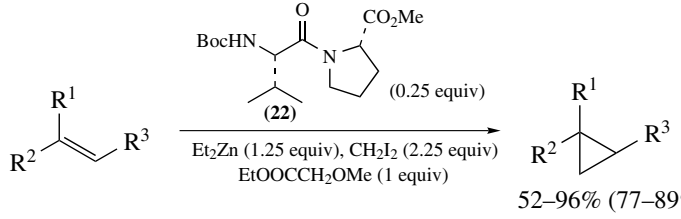

(96)

52–96% (77–89% ee)

V. CONCLUSION

The preceding sections highlighted the substantial progress made in the cyclopropanation of alkenes using haloalkylzinc carbenoids. The Simmons–Smith cyclopropanation and its numerous stereoselective variations have made it one of the most effective reactions to generate three-membered ring derivatives. These reactions have not been used only in natural product synthesis but also in the generation of semisynthetic and synthetic analogues[200, 201]. It is anticipated that further progress will lead to even more versatile and useful reactions that will complement alternative methods to generate cyclopropanes[5].

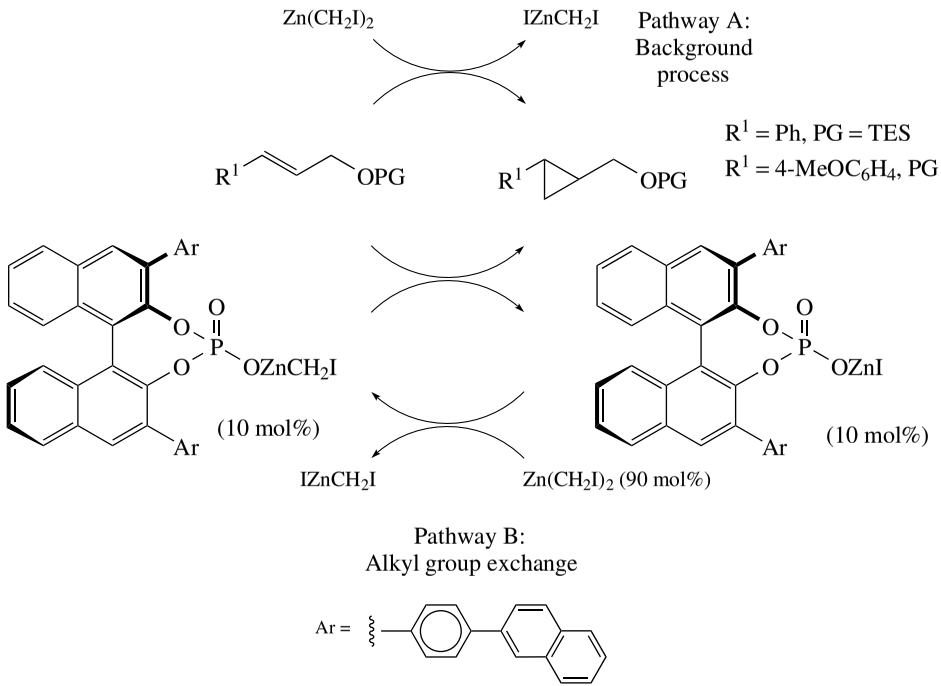
Zn(CH2I)2
IZnCH2I
Pathway A:
Background
process
R1 = Ph, PG = TES 83% (88% ee)
R1 = 4-MeOC6H4, PG = Bn 88% (84% ee)
R1
OPG
R1
OPG
Ar
O
O
P
O
OZnCH2I
Ar
(10 mol%)
Ar
O
O
P
O
OZnI
Ar
(10 mol%)
IZnCH2I
Zn(CH2I)2 (90 mol%)
Pathway B:
Alkyl group exchange
Ar =

(97)

VI. REFERENCES

1. H. E. Simmons and R. D. Smith, *J. Am. Chem. Soc.*, **80**, 5323 (1958).
2. H. E. Simmons and R. D. Smith, *J. Am. Chem. Soc.*, **81**, 4256 (1959).
3. H. E. Simmons, T. L. Cairns, S. A. Vladuchick and C. M. Hoiness, *Org. React.*, **20**, 1 (1973).
4. A. B. Charette and A. Beauchemin, *Org. React.*, **58**, 1 (2001).
5. H. Lebel, J. F. Marcoux, C. Molinaro and A. B. Charette, *Chem. Rev.*, **103**, 977 (2003).
6. G. Emschwiller, *C. R. Hebd. Seance Acad. Sci.*, **188**, 1555 (1929).
7. F. L. Howard, *J. Res. Natl. Bur. Stand., Sect. A*, **24**, 677 (1940).
8. R. S. Shank and H. Shechter, *J. Org. Chem.*, **24**, 1825 (1959).
9. R. D. Smith and H. E. Simmons, *Org. Synth.*, Coll. Vol. 5, 855 (1973).
10. E. LeGoff, *J. Org. Chem.*, **29**, 2048 (1964).
11. R. J. Rawson and I. T. Harrison, *J. Org. Chem.*, **35**, 2057 (1970).
12. U. Schuchardt, J. H. S. Nery and M. A. Zuiani, *J. Braz. Chem. Soc.*, **2**, 61 (1991).
13. J. M. Denis, C. Girard and J. M. Conia, *Synthesis*, 549 (1972).
14. K. Takai, T. Kakiuchi and K. Utimoto, *J. Org. Chem.*, **59**, 2671 (1994).
15. E. C. Friedrich and E. J. Lewis, *J. Org. Chem.*, **55**, 2491 (1990).
16. G. Picotin and P. Miginiac, *J. Org. Chem.*, **52**, 4796 (1987).
17. E. C. Friedrich, S. E. Lunetta and E. J. Lewis, *J. Org. Chem.*, **54**, 2388 (1989).
18. Y. Stenstrom, *Synth. Commun.*, **22**, 2801 (1992).
19. O. Repic and S. Vogt, *Tetrahedron Lett.*, **23**, 2729 (1982).
20. R. D. Rieke, P. T.-J. Li, T. P. Burns and S. T. Uhm, *J. Org. Chem.*, **46**, 4323 (1981).
21. J. Furukawa, N. Kawabata and J. Nishimura, *Tetrahedron Lett.*, 3353 (1966).
22. J. Furukawa, N. Kawabata and J. Nishimura, *Tetrahedron*, **24**, 53 (1968).
23. S. Miyano and H. Hashimoto, *J. Chem. Soc., Chem. Commun.*, 1418 (1971).
24. S. Miyano and H. Hashimoto, *Bull. Chem. Soc. Jpn.*, **46**, 892 (1973).
25. S. E. Denmark and J. P. Edwards, *J. Org. Chem.*, **56**, 6974 (1991).
26. A. B. Charette, S. Prescott and C. Brochu, *J. Org. Chem.*, **60**, 1081 (1995).
27. Z. Q. Yang, J. C. Lorenz and Y. Shi, *Tetrahedron Lett.*, **39**, 8621 (1998).
28. J. C. Lorenz, J. Long, Z. Q. Yang, S. Xue, Y. Xie and Y. Shi, *J. Org. Chem.*, **69**, 327 (2004).
29. A. B. Charette, S. Francoeur, J. Martel and N. Wilb, *Angew. Chem., Int. Ed.*, **39**, 4539 (2000).
30. M. C. Lacasse, C. Poulard and A. B. Charette, *J. Am. Chem. Soc.*, **127**, 12440 (2005).
31. S. Sawada and Y. Inouye, *Bull. Chem. Soc. Jpn.*, **42**, 2669 (1969).
32. G. Wittig and K. Schwarzenbach, *Angew. Chem.*, **71**, 652 (1959).
33. G. Wittig and F. Wingler, *Chem. Ber.*, **97**, 2146 (1964).
34. H. E. Simmons, E. P. Blanchard and R. D. Smith, *J. Am. Chem. Soc.*, **86**, 1347 (1964).
35. E. C. Friedrich, D. B. Taggart and M. A. Saleh, *J. Org. Chem.*, **42**, 1437 (1977).
36. E. C. Friedrich and G. Biresaw, *J. Org. Chem.*, **47**, 1615 (1982).
37. J. Furukawa, N. Kawabata and J. Nishimura, *Tetrahedron Lett.*, 3495 (1968).
38. P. S. Mariano, E. Bay, C. Bracken, T. Rose and D. G. Watson, *J. Org. Chem.*, **45**, 1753 (1980).
39. A. B. Charette and J. Lemay, *Angew. Chem., Int. Ed. Engl.*, **36**, 1090 (1997).
40. S. Durandetti, S. Sibille and J. Perichon, *J. Org. Chem.*, **56**, 3255 (1991).
41. K. J. Stahl, W. Hertzsch and H. Musso, *Liebigs Ann. Chem.*, 1474 (1985).
42. A. B. Charette and N. Wilb, *Synlett*, 176 (2002).
43. J. Nishimura and J. Furukawa, *J. Chem. Soc., Chem. Commun.*, 1375 (1971).
44. S. Miyano, Y. Matsumoto and H. Hashimoto, *J. Chem. Soc., Chem. Commun.*, 364 (1975).
45. W. R. Dolbier, H. Wojtowicz and C. R. Burkholder, *J. Org. Chem.*, **55**, 5420 (1990).
46. A. B. Charette, A. Gagnon and J. F. Fournier, *J. Am. Chem. Soc.*, **124**, 386 (2002).
47. J. F. Fournier and A. B. Charette, *Eur. J. Org. Chem.*, 1401 (2004).
48. P. Charreau, M. Julia and J. N. Verpeaux, *Bull. Soc. Chim. Fr.*, **127**, 275 (1990).
49. L. Aufauvre, I. Marek and P. Knochel, *J. Chem. Soc., Chem. Commun.*, 2207 (1999).
50. J. M. Cloarec and A. B. Charette, *Org. Lett.*, **6**, 4731 (2004).
51. L. J. Altman, R. C. Kowerski and D. R. Laungani, *J. Am. Chem. Soc.*, **100**, 6174 (1978).
52. W. B. Motherwell and L. R. Roberts, *J. Chem. Soc., Chem. Commun.*, 1582 (1992).
53. R. J. Fletcher, W. B. Motherwell and M. E. Popkin, *J. Chem. Soc., Chem. Commun.*, 2191 (1998).
54. S. E. Denmark, J. P. Edwards and S. R. Wilson, *J. Am. Chem. Soc.*, **113**, 723 (1991).

55. S. E. Denmark, J. P. Edwards and S. R. Wilson, *J. Am. Chem. Soc.*, **114**, 2592 (1992).
56. A. B. Charette, J. F. Marcoux, C. Molinaro, A. Beauchemin, C. Brochu and E. Isabel, *J Am. Chem. Soc.*, **122**, 4508 (2000).
57. A. B. Charette, J. F. Marcoux and F. Bélanger-Gariépy, *J. Am. Chem. Soc.*, **118**, 6792 (1996).
58. A. B. Charette, C. Molinaro and C. Brochu, *J. Am. Chem. Soc.*, **123**, 12160 (2001).
59. A. B. Charette, A. Beauchemin, S. Francoeur, F. Bélanger-Gariépy and G. D. Enright, *J. Chem. Soc., Chem. Commun.*, 466 (2002).
60. A. B. Charette, A. Beauchemin and S. Francoeur, *J. Am. Chem. Soc.*, **123**, 8139 (2001).
61. A. B. Charette and J. F. Marcoux, *J. Am. Chem. Soc.*, **118**, 4539 (1996).
62. S. E. Denmark and S. P. O'Connor, *J. Org. Chem.*, **62**, 3390 (1997).
63. R. E. Dessy and G. R. Coe, *J. Org. Chem.*, **28**, 3592 (1963).
64. D. F. Evans and I. Wharf, *J. Chem. Soc., A*, 783 (1968).
65. D. F. Evans and G. V. Fazakerley, *J. Chem. Soc., A*, 182 (1971).
66. B. Fabisch and T. N. Mitchell, *J. Organomet. Chem.*, **269**, 219 (1984).
67. F. Bernardi, A. Bottoni and G. P. Miscione, *J. Am. Chem. Soc.*, **119**, 12300 (1997).
68. H. Hermann, J. C. W. Lohrenz, A. Kuhn and G. Boche, *Tetrahedron*, **56**, 4109 (2000).
69. M. Nakamura, A. Hirai and E. Nakamura, *J. Am. Chem. Soc.*, **125**, 2341 (2003).
70. T. K. Dargel and W. Koch, *J. Chem. Soc., Perkin Trans. 2*, 877 (1996).
71. W. H. Fang, D. L. Phillips, D. Q. Wang and Y. L. Li, *J. Org. Chem.*, **67**, 154 (2002).
72. C. Y. Zhao, D. Q. Wang and D. L. Phillips, *J. Am. Chem. Soc.*, **124**, 12903 (2002).
73. J. J. Eisch, N. E. Burlinson and M. Boleslawski, *J. Organomet. Chem.*, **111**, 137 (1976).
74. B. Rickborn and J. H. H. Chan, *J. Org. Chem.*, **32**, 3576 (1967).
75. R. K. Boeckman Jr, A. B. Charette, T. Asberom and B. H. Johnston, *J. Am. Chem. Soc.*, **113**, 5337 (1991).
76. A. M. Johansson, C. Mellin and U. Hacksell, *J. Org. Chem.*, **51**, 5252 (1986).
77. J. R. M. Lundkvist, L. E. Arvidsson, U. Hacksell and A. M. Johansson, *Acta Chem. Scand., Ser. B*, **40**, 508 (1986).
78. J. M. Conia and C. Girard, *Tetrahedron Lett.*, 2767 (1973).
79. R. Le Goaller and J. L. Pierre, *Bull. Soc. Chim. Fr.*, 1531 (1973).
80. S. Murai, T. Aya and N. Sonoda, *J. Org. Chem.*, **38**, 4354 (1973).
81. G. M. Rubottom and M. I. Lopez, *J. Org. Chem.*, **38**, 2097 (1973).
82. J. R. Van der Vecht, H. Steinberg and T. J. de Boer, *Recl. Trav. Chim. Pays-Bas*, **95**, 149 (1976).
83. K. I. Booker-Milburn and R. F. Dainty, *Tetrahedron Lett.*, **39**, 5097 (1998).
84. H. W. Whitlock Jr. and L. E. Overman, *J. Org. Chem.*, **34**, 1962 (1969).
85. R. E. Ireland, C. J. Kowalski, J. W. Tilley and D. M. Walba, *J. Org. Chem.*, **40**, 990 (1975).
86. S. Ito, H. Shinokubo and K. Oshima, *Tetrahedron Lett.*, **39**, 5253 (1998).
87. T. Imamoto, T. Takeyama and H. Koto, *Tetrahedron Lett.*, **27**, 3243 (1986).
88. T. Imamoto and T. Takeyama, *Tetrahedron Lett.*, **28**, 1307 (1987).
89. J. B. Brogan and C. K. Zercher, *J. Org. Chem.*, **62**, 6444 (1997).
90. C. A. Verbicky and C. K. Zercher, *J. Org. Chem.*, **65**, 5615 (2000).
91. R. Hilgenkamp and C. K. Zercher, *Tetrahedron*, **57**, 8793 (2001).
92. C. R. Theberge and C. K. Zercher, *Tetrahedron*, **59**, 1521 (2003).
93. J. Vallgaarda, L. E. Arvidsson, B. E. Svensson, C. J. Fowler and U. Hacksell, *Eur. J. Med. Chem.*, **28**, 399 (1993).
94. E. C. Friedrich and E. J. Lewis, *J. Org. Chem.*, **55**, 2491 (1990).
95. J. L. Gagnon and W. W. Zajac, *Synth. Commun.*, **26**, 837 (1996).
96. T. Morikawa, H. Sasaki, K. Mori, M. Shiro and T. Taguchi, *Chem. Pharm. Bull.*, **40**, 3189 (1992).
97. A. B. Charette and A. Gagnon, unpublished results.
98. H. B. Huang and J. S. Panek, *Org. Lett.*, **6**, 4383 (2004).
99. W. Yong and M. Vandewalle, *Synlett*, 911 (1996).
100. E. Piers and P. D. Coish, *Synthesis*, 47 (1995).
101. O. Tamura, M. Hashimoto, Y. Kobayashi, T. Katoh, K. Nakatani, M. Kamada, I. Hayakawa, T. Akiba and S. Terashima, *Tetrahedron*, **50**, 3889 (1994).
102. A. B. Charette, S. Mathieu and J. F. Fournier, *Synlett*, 1779 (2005).
103. P. Fontani, B. Carboni, M. Vaultier and G. Mass, *Synthesis*, 605 (1991).
104. G. Zweifel, G. M. Clark and C. C. Whitney, *J. Am. Chem. Soc.*, **93**, 1305 (1971).

105. K. Yachi, H. Shinokubo and K. Oshima, *Angew. Chem., Int. Ed.*, **37**, 2515 (1998).
106. T. N. Mitchell and B. Kowall, *J. Organomet. Chem.*, **490**, 239 (1995).
107. H. Dolhaine and G. Hagele, *Phosphorus Sulfur*, **4**, 123 (1978).
108. V. V. Shcherbinin, K. V. Pavolov, I. P. Shvedov, O. S. Korneva, L. G. Menchikov and O. M. Nefedov, *Russ. Chem. Bull.*, **46**, 1632 (1997).
109. G. J. Wells, T. H. Yan and L. A. Paquette, *J. Org. Chem.*, **49**, 3604 (1984).
110. N. A. Rahman and I. Fleming, *Synth. Commun.*, **23**, 1583 (1993).
111. A. B. Charette and C. Molinaro, unpublished results.
112. W. B. Motherwell and L. R. Roberts, *Tetrahedron Lett.*, **36**, 1121 (1995).
113. E. J. Corey and T. M. Eckrich, *Tetrahedron Lett.*, **25**, 2415 (1984).
114. G. Wittig and K. Schwarzenbach, *Justus Liebigs Ann. Chem.*, **650**, 3127 (1962).
115. Z. Kosarych and T. Cohen, *Tetrahedron Lett.*, **23**, 3019 (1982).
116. D. Seyferth, *Angew. Chem.*, **72**, 36 (1960).
117. G. Wittig and K. Schwarzenbach, *Justus Liebigs Ann. Chem.*, **650**, 1 (1962).
118. C. Dumont, M. Zoukal and M. Vidal, *Tetrahedron Lett.*, **22**, 5267 (1981).
119. A. B. Charette and A. Beauchemin, *J. Organomet. Chem.*, **617**, 702 (2001).
120. C. D. Poulter, E. C. Friedrich and S. Winstein, *J. Am. Chem. Soc.*, **91**, 6892 (1969).
121. A. H. Hoveyda, D. A. Evans and G. C. Fu, *Chem. Rev.*, **93**, 1307 (1993).
122. R. Hara, T. Furukawa, Y. Horiguchi and I. Kuwajima, *J. Am. Chem. Soc.*, **118**, 9186 (1996).
123. S. Yamada, S. Nagashima, Y. Takaoka, S. Torihara, M. Tanaka, H. Suemune and M. Aso, *J. Chem. Soc., Perkin Trans. 1*, 1269 (1998).
124. W. Oppolzer and R. N. Radinov, *J. Am. Chem. Soc.*, **115**, 1593 (1993).
125. R. Murali, C. V. Ramana and M. Nagarajan, *J. Chem. Soc., Chem. Commun.*, 217 (1995).
126. N. Iwasawa, M. Funahashi and K. Narasaka, *Chem. Lett.*, 1697 (1994).
127. A. B. Charette and J. F. Marcoux, *Synlett*, 1197 (1995).
128. C. R. Johnson and M. R. Barbachyn, *J. Am. Chem. Soc.*, **104**, 4290 (1982).
129. T. Z. Wang, E. Pinard and L. A. Paquette, *J. Am. Chem. Soc.*, **118**, 1309 (1996).
130. M. Ratier, M. Castaing, J. Y. Godet and M. Pereyre, *J. Chem. Res. (S)*, 179 (1978).
131. A. B. Charette and H. Lebel, *J. Org. Chem.*, **60**, 2966 (1995).
132. Y. Takemoto, Y. Baba, G. Saha, S. Nakao, C. Iwata, T. Tanaka and T. Ibuka, *Tetrahedron Lett.*, **41**, 3653 (2000).
133. H. Y. Kim, A. E. Lurain, P. Garcia-Garcia, P. J. Carroll and P. J. Walsh, *J. Am. Chem. Soc.*, **127**, 13138 (2005).
134. J. F. Fournier, S. Mathieu and A. B. Charette, *J. Am. Chem. Soc.*, **127**, 13140 (2005).
135. P. Mohr, *Tetrahedron Lett.*, **36**, 7221 (1995).
136. Y. Landais and L. Parra-Rapado, *Tetrahedron Lett.*, **37**, 1205 (1996).
137. A. B. Charette, H. Lebel and A. Gagnon, *Tetrahedron*, **55**, 8845 (1999).
138. A. B. Charette and M. C. Lacasse, *Org. Lett.*, **4**, 3351 (2002).
139. B. W. Gung, J. P. Melnick, M. A. Wolf and A. King, *J. Org. Chem.*, **60**, 1947 (1995).
140. Y. Zhao, T. Yang, M. Lee, D. Lee, M. G. Newton and C. K. Chu, *J. Org. Chem.*, **60**, 5236 (1995).
141. T. Morikawa, H. Sasaki, R. Hanai, A. Shibuya and T. Taguchi, *J. Org. Chem.*, **59**, 97 (1994).
142. Y. Fukuyama, M. Hirono and M. Kodama, *Chem. Lett.*, 167 (1992).
143. A. G. M. Barrett, K. Kasdorf and D. J. Williams, *J. Chem. Soc., Chem. Commun.*, 1781 (1994).
144. D. A. Evans and J. D. Burch, *Org. Lett.*, **3**, 503 (2001).
145. J. Cossy, N. Blanchard and C. Meyer, *J. Org. Chem.*, **63**, 5728 (1998).
146. A. G. M. Barrett and G. J. Tustin, *J. Chem. Soc., Chem. Commun.*, 355 (1995).
147. M. Pilar de Frutos, M. Dolores Fernández, E. Fernández-Alvarez and M. Bernabé, *Tetrahedron Lett.*, **32**, 541 (1991).
148. P. Wipf, C. Kendall and C. R. J. Stephenson, *J. Am. Chem. Soc.*, **123**, 5122 (2001).
149. P. Wipf, C. Kendall and C. R. J. Stephenson, *J. Am. Chem. Soc.*, **125**, 761 (2003).
150. A. B. Charette, B. Côté and J. F. Marcoux, *J. Am. Chem. Soc.*, **113**, 8166 (1991).
151. A. B. Charette, N. Turcotte and J. F. Marcoux, *Tetrahedron Lett.*, **35**, 513 (1994).
152. A. B. Charette and B. Côté, *J. Org. Chem.*, **58**, 933 (1993).
153. A. B. Charette and B. Côté, *J. Am. Chem. Soc.*, **117**, 12721 (1995).
154. A. B. Charette and J. F. Marcoux, *Tetrahedron Lett.*, **34**, 7157 (1993).
155. I. Arai, A. Mori and H. Yamamoto, *J. Am. Chem. Soc.*, **107**, 8254 (1985).

156. A. Mori, I. Arai, H. Yamamoto, H. Nakai and Y. Arai, *Tetrahedron*, **42**, 6447 (1986).
157. R. Ebens and R. M. Kellogg, *Recl. Trav. Chim. Pays-Bas*, **109**, 552 (1990).
158. J. Kang, G. J. Lim, S. K. Yoon and M. Y. Kim, *J. Org. Chem.*, **60**, 564 (1995).
159. P. T. Kaye and W. E. Molema, *J. Chem. Soc., Chem. Commun.*, 2479 (1998).
160. K. Tanaka, H. Uno, H. Osuga and H. Suzuki, *Tetrahedron: Asymmetry*, **5**, 1175 (1994).
161. C. R. Johnson, M. R. Barbachyn, N. A. Meanwell, C. J. Stark, Jr. and J. R. Zeller, *Phosphorus, Sulfur Relat. Elem.*, **24**, 531 (1985).
162. E. A. Mash and K. A. Nelson, *J. Am. Chem. Soc.*, **107**, 8256 (1985).
163. E. A. Mash and K. A. Nelson, *Tetrahedron*, **43**, 679 (1987).
164. E. A. Mash, S. K. Math and C. J. Flann, *Tetrahedron Lett.*, **29**, 2147 (1988).
165. K. A. Nelson and E. A. Mash, *J. Org. Chem.*, **51**, 2721 (1986).
166. E. A. Mash, *J. Org. Chem.*, **52**, 4142 (1987).
167. E. A. Mash and J. A. Fryling, *J. Org. Chem.*, **52**, 3000 (1987).
168. E. A. Mash, S. B. Hemperly, K. A. Nelson, P. C. Heidt and S. Vandeusen, *J. Org. Chem.*, **55**, 2045 (1990).
169. E. A. Mash and S. B. Hemperly, *J. Org. Chem.*, **55**, 2055 (1990).
170. S. M. Yeh, L. H. Huang and T. Y. Luh, *J. Org. Chem.*, **61**, 3906 (1996).
171. V. K. Aggarwal, G. Y. Fang and G. Meek, *Org. Lett.*, **5**, 4417 (2003).
172. T. Sugimura, M. Yoshikawa, T. Futagawa and A. Tai, *Tetrahedron*, **46**, 5955 (1990).
173. T. Sugimura, T. Futagawa, M. Yoshikawa, T. Katagiri, R. Miyashige, M. Mizuguchi, S. Nagano, S. Sugimori, A. Tai, T. Tei and T. Okuyama, *Tetrahedron*, **57**, 7495 (2001).
174. O. G. Kulinkovich, *Chem. Rev.*, **103**, 2597 (2003).
175. T. Imai, H. Mineta and S. Nishida, *J. Org. Chem.*, **55**, 4986 (1990).
176. J. E. A. Luithle and J. Pietruszka, *J. Org. Chem.*, **64**, 8287 (1999).
177. T. Akiba, O. Tamura, M. Hashimoto, Y. Kobayashi, T. Katoh, K. Nakatani, M. Kamada, I. Hayakawa and S. Terashima, *Tetrahedron*, **50**, 3905 (1994).
178. D. Seebach and G. Stucky, *Angew. Chem., Int. Ed. Engl.*, **27**, 1351 (1988).
179. S. Sawada, J. Oda and Y. Inouye, *J. Org. Chem.*, **33**, 2141 (1968).
180. Y. Ukaji, M. Nishimura and T. Fujisawa, *Chem. Lett.*, 61 (1992).
181. Y. Ukaji, K. Sada and K. Inomata, *Chem. Lett.*, 1227 (1993).
182. A. B. Charette and H. Juteau, *J. Am. Chem. Soc.*, **116**, 2651 (1994).
183. A. B. Charette, H. Juteau, H. Lebel and C. Molinaro, *J. Am. Chem. Soc.*, **120**, 11943 (1998).
184. I. Paterson, R. D. M. Davies and R. Marquez, *Angew. Chem., Int. Ed.*, **40**, 603 (2001).
185. A. B. Charette and H. Juteau, *Tetrahedron*, **53**, 16277 (1997).
186. A. B. Charette, E. Jolicoeur and G. A. S. Bydlinski, *Org. Lett.*, **3**, 3293 (2001).
187. P. Liu and E. N. Jacobsen, *J. Am. Chem. Soc.*, **123**, 10772 (2001).
188. A. B. Charette and H. Lebel, *J. Am. Chem. Soc.*, **118**, 10327 (1996).
189. A. G. M. Barrett and K. Kasdorf, *J. Chem. Soc., Chem. Commun.*, 325 (1996).
190. A. G. M. Barrett, D. Hamprecht, A. J. P. White and D. J. Williams, *J. Am. Chem. Soc.*, **119**, 8608 (1997).
191. H. Kitajima, Y. Aoki, K. Ito and T. Katsuki, *Chem. Lett.*, 1113 (1995).
192. J. Long, Y. Yuan and Y. Shi, *J. Am. Chem. Soc.*, **125**, 13632 (2003).
193. H. Takahashi, M. Yoshioka, M. Ohno and S. Kobayashi, *Tetrahedron Lett.*, **33**, 2575 (1992).
194. H. Takahashi, M. Yoshioka, M. Shibasaki, M. Ohno, N. Imai and S. Kobayashi, *Tetrahedron*, **51**, 12013 (1995).
195. N. Imai, K. Sakamoto, H. Takahashi and S. Kobayashi, *Tetrahedron Lett.*, **35**, 7045 (1994).
196. S. E. Denmark and S. P. O'Connor, *J. Org. Chem.*, **62**, 584 (1997).
197. A. B. Charette and C. Brochu, *J. Am. Chem. Soc.*, **117**, 11367 (1995).
198. A. B. Charette, C. Molinaro and C. Brochu, *J. Am. Chem. Soc.*, **123**, 12168 (2001).
199. J. Long, H. F. Du, K. Li and Y. Shi, *Tetrahedron Lett.*, **46**, 2737 (2005).
200. K. C. Nicolaou, P. K. Sasmal, G. Rassias, M. V. Reddy, K. H. Altmann, M. Wartmann, A. O'Brate and P. Giannakakou, *Angew. Chem., Int. Ed.*, **42**, 3515 (2003).
201. P. Wipf, J. T. Reeves, R. Balachandran and B. W. Day, *J. Med. Chem.*, **45**, 1901 (2002).

CHAPTER 8

Functionalized organozinc compounds

PAUL KNOCHEL, HELENA LEUSER, LIU-ZHU GONG, SYLVIE PERRONE and FLORIAN F. KNEISEL

Department of Chemistry, Ludwig-Maximilians-Universität München, Butenandtstr. 5-13, D-81377 München, Germany
Fax: +49 8921 807 7680; e-mail: paul.knochel@cup.uni-muenchen.de

The chemistry of organozinc compounds
Edited by Z. Rappoport and I. Marek

I. INTRODUCTION

Organozincs are known since the preparation of diethylzinc by Frankland in 1849 at Marburg (Germany)[1]. These organometallic reagents were fairly often used to form new carbon–carbon bonds until Grignard[2] discovered in 1900 a convenient preparation of organomagnesium compounds. These reagents were found to be more reactive species toward a broad range of electrophiles and afforded generally higher yields compared to organozincs. However, some reactions were still performed with zinc organometallics such as the Reformatsky reaction[3] or the Simmons–Smith cyclopropanation[4]. The intermediate organometallics (zinc enolate and zinc carbenoid) were more easy to handle and more selective than the corresponding magnesium organometallics. Remarkably, Hunsdiecker and coworkers reported in a German patent of 1943 that organozinc reagents bearing long carbon chains terminated by an ester function can be prepared[5]. This functional group tolerance remained largely ignored by synthetic chemists and it became clear only recently that organozinc compounds are prone to undergo a large range of transmetalations due to the presence of empty low-lying *p*-orbitals which readily interact with the *d*-orbitals of many transition metal salts leading to highly reactive intermediates[6]. One can wonder why unreactive zinc reagents can produce highly reactive organometallic intermediates reacting with many electrophiles which are unreactive toward organozincs. This can be explained by the presence of *d*-orbitals at the transition metal center which makes a number of new reaction pathways available that were not accessible to the zinc precursors since the empty *d*-orbitals of zinc are too high in energy to participate in most organic reactions. It is the combination of the high tolerance of functionalities of organozinc derivatives with a facile transmetalation to many transition metal complexes which makes organozincs such valuable reagents. Especially important are the transmetalation of RZnX reagents to organocopper compounds[6] and to palladium intermediates[7] which allow the performance of cross-coupling reactions with high efficiency (Negishi reaction[7]; Scheme 1).

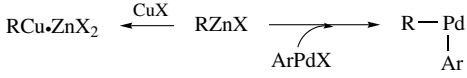

SCHEME 1. Transmetalation of organozinc reagents

Furthermore, the highly covalent character of the carbon–zinc bond[8] affords organozincs configurationally stable at temperatures where the corresponding organo-magnesiums and -lithiums undergo a racemization. This property makes them good candidates for the preparation of chiral organometallics[9]. In this chapter, we will describe the methods of preparation of polyfunctional organozinc compounds followed by a detailed presentation of their reactivity in the absence and in the presence of transition metal catalysts.

II. METHODS OF PREPARATION OF POLYFUNCTIONAL ORGANOZINC REAGENTS

A. Classification

There are three important classes of organozinc reagents: (i) organozinc halides of the general formula RZnX, (ii) diorganozincs of the general formula R^1ZnR^2 in which R^1 and R^2 are two organic groups and (iii) zincates of the general formula $R^1(R^2)(R^3)ZnMet$

in which the metal (Met) is usually Li or MgX. The reactivity of these zinc reagents increases with the excess of negative charge on the zinc center (Scheme 2). The reactivity of organozinc halides strongly depends on the electronegativity of the carbon attached to zinc and on the aggregation of the zinc reagent. A stabilization of the negative carbanionic charge by inductive or mesomeric effects leads to a more ionic carbon–zinc bond and to a higher reactivity.

alkynyl < alkyl < alkenyl ≤ aryl < benzyl < allyl

$RZnX < R_2Zn < R_3ZnMgX < R_3ZnLi$

SCHEME 2. Reactivity order of zinc organometallics

B. Preparation of Polyfunctional Organozinc Halides

1. Preparation by the oxidative addition to zinc metal

The oxidative addition of zinc dust to functionalized organic halides allows the preparation of a broad range of polyfunctional organozinc iodides (Scheme 3) such as **1–5**[10–14]. Several functional groups such as the nitro or azide group inhibit the radical transfer

$$FG-R-I \xrightarrow[THF]{Zn\ dust} FG-R-ZnI$$

FG = CO_2R, enoate, CN, halide, $(RCO)_2N$, $(TMS)_2N$, RNH, NH_2, RCONH, $(RO)_3Si$, $(RO)_2PO$, RS, RSO, RSO_2, PhCOS

R = alkyl, aryl, benzyl, allyl

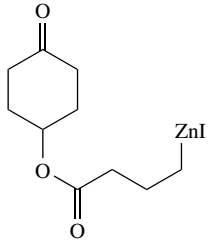

(1)[10]

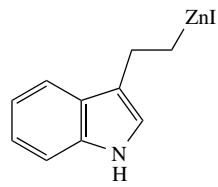

(2)[11]

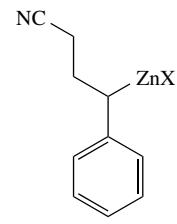

(3)[12]

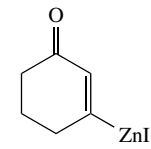

(4)[13]

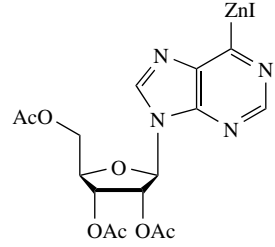

(5)[14]

SCHEME 3. Functionalized organozinc compounds prepared by oxidative addition

reaction leading to the zinc reagent. On the other hand, hydroxyl groups form zinc alkoxides which coat the zinc surface and therefore hamper the reaction; similar behavior was observed for other acidic hydrogen atoms (carboxylic acids, imidazoles). As a general rule, the nature of the zinc dust is less important than its activation. Finely cut zinc foil or zinc dust [commercially available source (*ca* 325 mesh)] can be used. Zinc slowly oxidizes in air and is covered by an oxide layer. Its activation is of great importance; this is done by removing the oxide layer via chemical methods. A very efficient procedure consists of treating zinc with 1,2-dibromoethane (5 mol%) in THF (reflux for 0.5 min) followed by the addition of Me_3SiCl (1–2 mol%; reflux for 0.5 min)[10,15–17].

Under these conditions, a broad range of polyfunctional alkyl iodides are converted to the corresponding organozinc halides in high yields[6]. In the case of primary alkyl iodides, the insertion occurs at 40–50 °C whereas secondary alkyl iodides already react at 25–30 °C. Secondary alkyl bromides also react under these conditions[18], but primary alkyl bromides are usually inert with this type of activation and much better results are obtained by using Rieke zinc[19–21]. Thus, the reduction of zinc chloride with finely cut lithium and naphthalene produces within 1.5 h highly reactive zinc (Rieke zinc).

This activated zinc[22] readily inserts in secondary and tertiary alkyl bromides. Adamantyl bromide (**6**) is converted into the corresponding organozinc reagent (**7**) and its reaction with cyclohexenone in the presence of BF_3•OEt_2 and TMSCl furnishes the 1,4-addition product **8** (Scheme 4). Rieke zinc proves also to be very useful for preparing aryl- and heteroaryl-zinc halides. Thus, the reaction of Rieke zinc with *p*-bromobenzonitrile (**9**) in refluxing THF provides after 3 h the corresponding zinc reagent (**10**) which is benzoylated leading to the ketone **11** in 73% yield (Scheme 5)[18a].

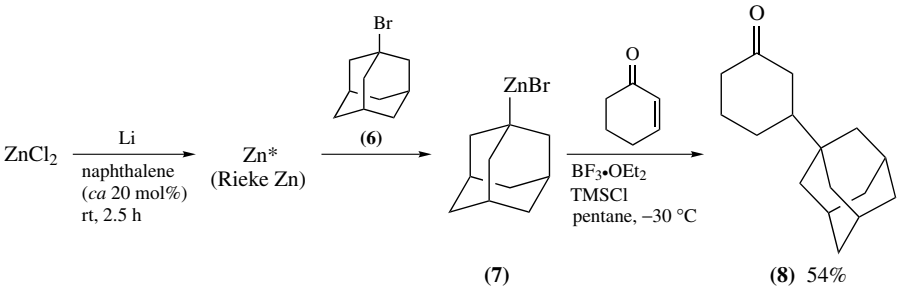

SCHEME 4. Preparation and uses of tertiary alkylzinc reagents using Rieke zinc

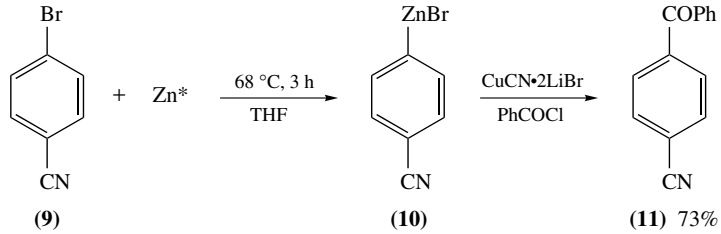

SCHEME 5. Preparation and uses of functionalized arylzinc bromides using Rieke zinc

Interestingly, many electron-deficient heterocyclic and aryl bromides or iodides are sufficiently activated to react with commercially available zinc powder[14]. In the case of

benzylic halides, bromides and even chlorides can be used[12]. Thus, for the functionalized benzylic bromide **12a**, the formation of the corresponding benzylic zinc bromide (**13a**) by the direct insertion of zinc dust is complete within 2 h at 5 °C.

After a Michael addition, the expected conjugated addition product **14a** is formed in 92% yield. The corresponding benzylic chloride (**12b**) requires a reaction time of 48 h leading to the benzylic zinc chloride (**13b**). Allylation of **13b** provides the aromatic benzoate **14b** in 87% yield (Scheme 6). The use of DMSO/THF mixture has a favorable effect, allowing the synthesis of substituted benzylic reagents such as **3**[9]. Similarly, the preparation of alkylzinc iodides is facilitated if the reaction is performed in THF and NMP (*N*-methylpyrrolidinone) mixtures. Such solutions of $MeO_2C(CH_2)_4ZnI$ add to benzaldehyde in the presence of TMSCl (2 equiv) in 70% yield[23]. The use of ultrasound also promotes the formation of organozinc compounds[24]. This procedure proved to be especially useful for the preparation of the Jackson reagent (**15**) derived from serine. The reaction of this zinc derivative with various electrophiles, in the presence of either a copper(I) or palladium(0) catalyst, leads to products of type **16–18**[25] (Scheme 7).

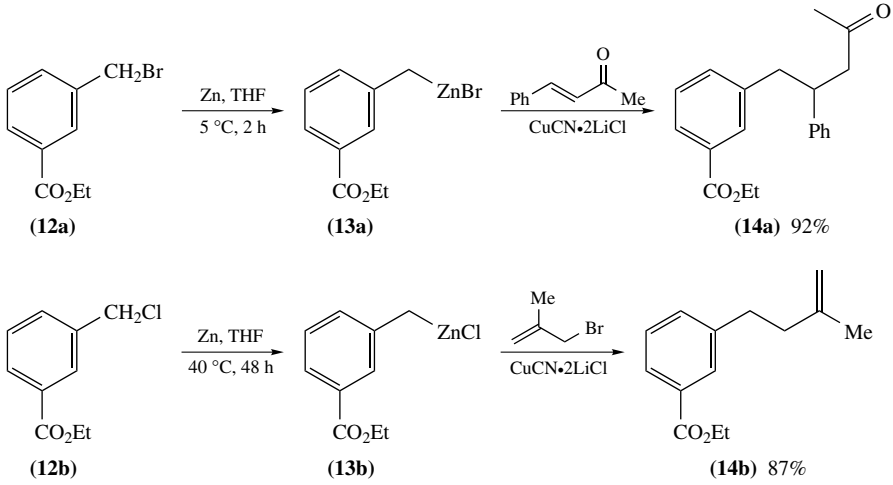

SCHEME 6. Preparation and uses of functionalized benzylic zinc reagents

The decomposition of the zinc reagent **19** leading to methyl but-3-enoate **20** and the zinc amide **21** (Scheme 8) has been extensively studied by Jackson and coworkers[26]. It was found that the zinc species **19a** undergoes the elimination *ca* three times faster than the zinc reagent **19b**. This might be surprising since −NHBoc is not as good a leaving group as $-NHCOCF_3$. It could be explained by the chelation of the Boc group with the zinc metallic center, which enhances the ate character of the metal as well as the electron density of the C−Zn bond and which therefore favors the elimination. This factor seems to be more important than the leaving group ability of −NHR[27]. Interestingly, a free phenolic function is tolerated in cross-coupling reactions.

Organozinc reagents bearing a free NH function in β-position, such as **22**, can be readily prepared by the direct insertion of zinc dust previously activated with TMSCl in DMF leading to the corresponding β-iodoamino derivative **23**. Interestingly, the best reactivity of this chelate stabilized zinc species can be obtained by using catalytic amounts of $CuBr{\bullet}Me_2S$ (5 mol%). In the case of the reaction with propargyl chloride, the corresponding allene **24** is obtained in 60% yield via an S_N2'-mechanism (Scheme 9)[28].

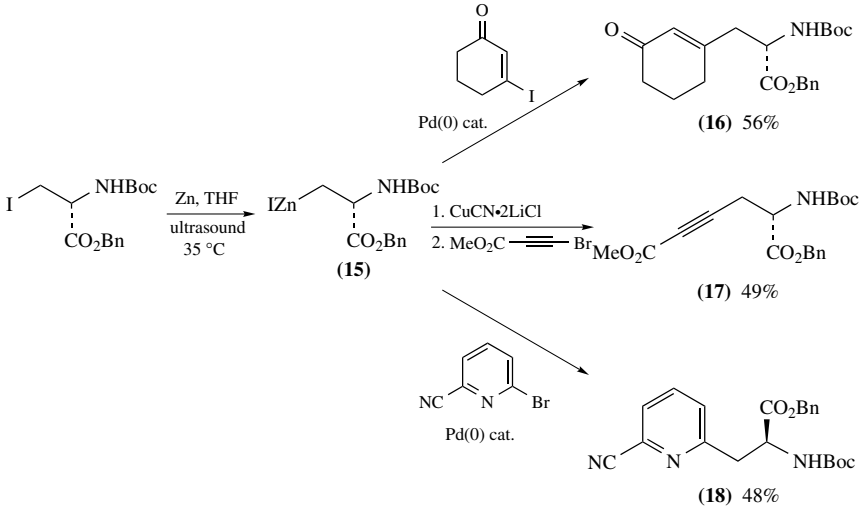

SCHEME 7. Ultrasound-mediated preparation of the Jackson reagent **15** and its uses

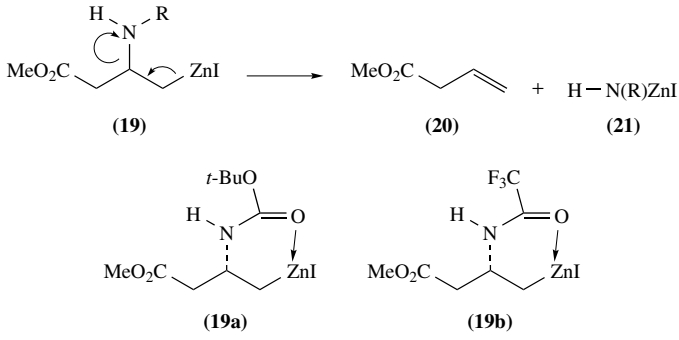

SCHEME 8. Stability of α-amino alkylzinc reagents

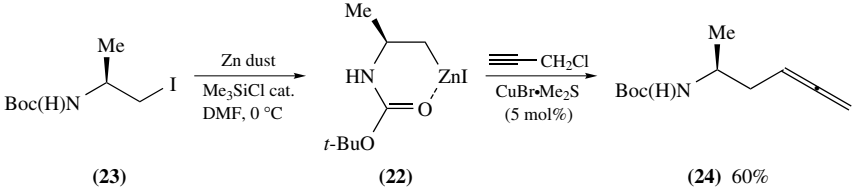

SCHEME 9. Generation of a β-amino alkylzinc reagent in DMF

During the preparation of allylic zinc reagents, the formation of Wurtz-coupling products may be observed, especially if the intermediate allylic radical is well stabilized. However, the direct insertion of zinc foil to allyl bromide in THF at 5 °C is one of the best methods for preparing an allylic anion equivalent. Allylic zinc reagents are more convenient to prepare and to handle than their magnesium and lithium counterparts[15].

Similarly, electron-rich benzylic bromides such as **25a** often lead to homo-coupling products. The use of the corresponding phosphate **25b** and catalytic amounts of LiI in dimethyltetrahydropyrimidinone (DMPU) provides the corresponding zinc reagent in quantitative yield (Scheme 10)[29]. The presence of LiI generates small concentrations of the benzylic iodide, which is converted to the zinc reagent. Little homo-coupling is observed under these conditions.

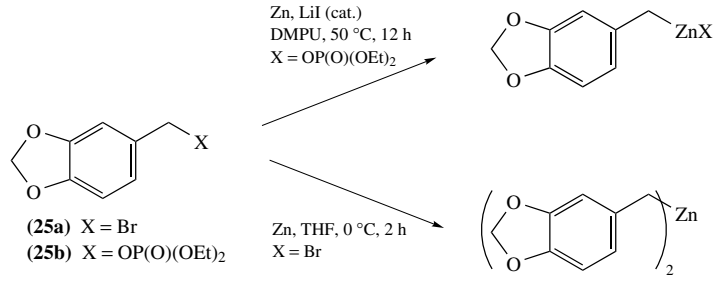

SCHEME 10. Importance of the precursor for the preparation of benzylic zinc reagents

The addition of lithium iodide and bromide mixtures allows also the performance of the zinc insertion with primary alkyl chlorides, tosylates or mesylates as starting material (Scheme 11)[29]. Thus, the alkyl tosylate **26** is converted in *N*,*N*-dimethylacetamide (DMAC) in the presence of lithium iodide (0.2 equiv) and lithium bromide (1.0 equiv) after heating at 50 °C for 12 h to the zinc organometallic **27**. After transmetalation with CuCN•2LiCl, the zinc reagent **27** undergoes an addition-elimination to 3-iodo-2-cyclohexenone leading to the enone **28** in 85% yield. The addition of both lithium iodide and lithium bromide is necessary in order to observe fast reactions. The direct exchange of a sulfonate to the corresponding iodide with LiI is slow and a stepwise reaction first with LiBr leading to the corresponding alkyl bromide, then a reaction with LiI leading to the corresponding iodide is a faster reaction pathway. The chloroalkyl mesylate **29** is converted to the zinc species **30**, which undergoes a substitution reaction with the

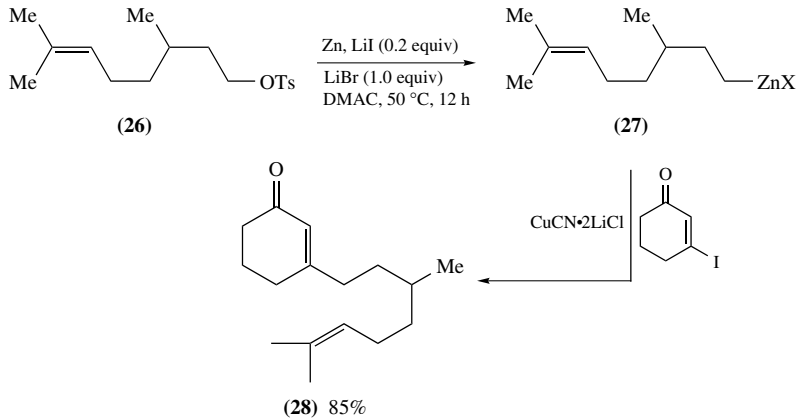

SCHEME 11. Preparation and uses of alkylzinc derivatives starting from alkyl sulfonates

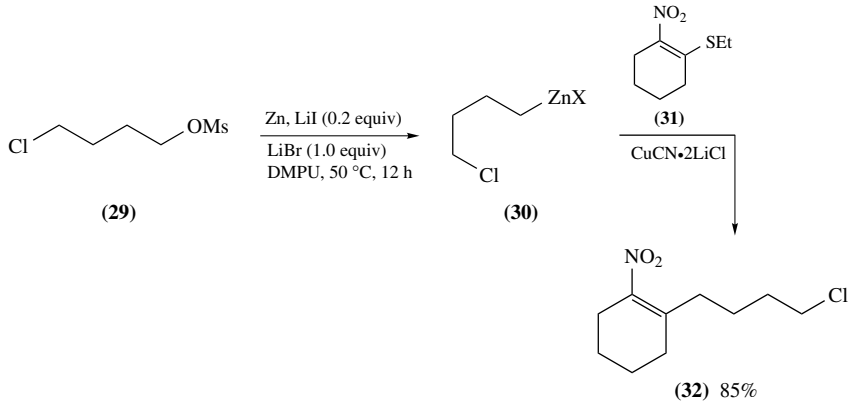

SCHEME 11. (*continued*)

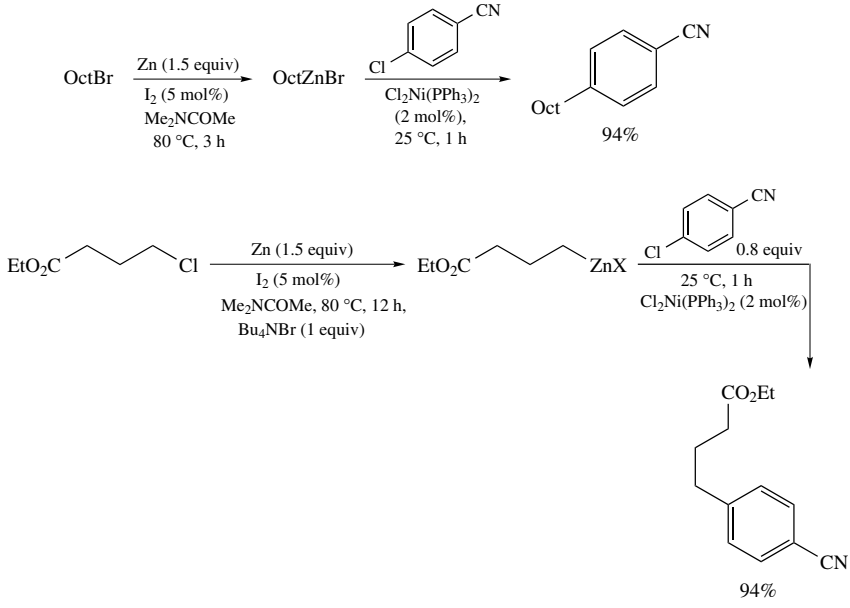

SCHEME 12. Iodine catalyzed formation of organozinc bromides

unsaturated nitro derivative **31** leading to the tetra-substituted nitroolefin **32** in 85% yield (Scheme 11)[29,30].

Alkylzinc bromides bearing various functional groups[31] can be readily prepared by the direct insertion of zinc metal (dust, powder or shot) to alkyl bromides by performing the reaction in the presence of iodine (1–5 mol%) in a polar solvent like DMAC. It is also possible to use alkyl chlorides as starting material. In this case, the reaction is best performed in presence of Bu_4NBr (1 equiv). The resulting zinc reagent undergoes smooth Ni-catalyzed cross-coupling[32] reactions with various aryl chlorides (Scheme 12).

For polyfluorinated organozinc halides, the zinc insertion is conveniently done with a zinc–copper couple (Scheme 13)[33,34]. The preparation of trifluoromethylzinc halides (**33**) is best achieved using the method of Burton[35], which involves the reaction of CF_2Cl_2 or CBr_2F_2 with zinc in DMF. This reaction produces a mixture of CF_3ZnX (**33**) and bis-trifluoromethylzinc (**34**) (Scheme 13)[35].

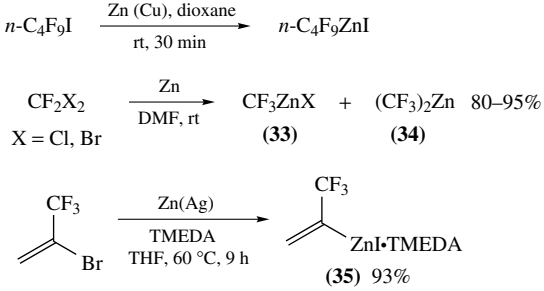

SCHEME 13. Preparation of perfluorinated zinc reagents

Interestingly, the presence of a CF_3 substituent considerably facilitates the zinc insertion. Thus, 2-bromotrifluoropropene reacts with the Zn/Ag couple in the presence of TMEDA leading to the expected zinc reagent **35** in 93% yield[35c–e].

The formation of arylzinc reagents can also be accomplished by using electrochemical methods. With a sacrificial zinc anode and in the presence of nickel 2,2-bipyridyl, polyfunctional zinc reagents of type **36** can be prepared in excellent yields (Scheme 14)[36]. An electrochemical conversion of aryl halides to arylzinc compounds can also be achieved by a cobalt catalysis in DMF/pyridine mixture[37]. The mechanism of this reaction has been carefully studied[38]. This method can also be applied to heterocyclic compounds such as 2- or 3-chloropyridine and 2- or 3-bromothiophenes[39,36d,e]. Zinc can also be electrochemically activated and a mixture of zinc metal and small amounts of zinc formed by electroreduction of zinc halides are very reactive toward α-bromoesters and allylic or benzylic bromides[36f,g].

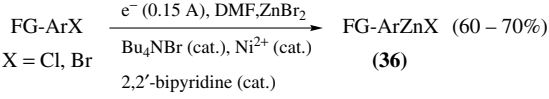

SCHEME 14. Electrochemical preparation of polyfunctional arylzinc halides

The previous results suggest that transition metals may catalyze the zinc insertion reaction. This proves to be the case and the reaction of octyl iodide with Et_2Zn in the presence of $PdCl_2$(dppf) (1.5 mol%) in THF at 25 °C produces OctZnI within 2 h of reaction time in 75–80% yield[40]. A detailed mechanism is given in Scheme 15.

These palladium- or nickel-catalyzed reactions are radical reactions leading to an organometallic product. By using a precursor such as **37** as a 1:1 mixture of diastereoisomers, the palladium-catalyzed cyclization provides in a stereoconvergent way the cyclopentylmethylzinc derivative **38** which, after allylation, produces the unsaturated ester **39** in 71% yield[41]. The intermediate radical cyclizes via a transition state **A** where all the substituents are in an equatorial position. Interestingly, the analogous reaction using $Ni(acac)_2$ as a catalyst allows the preparation of heterocyclic compounds such as **40**. The

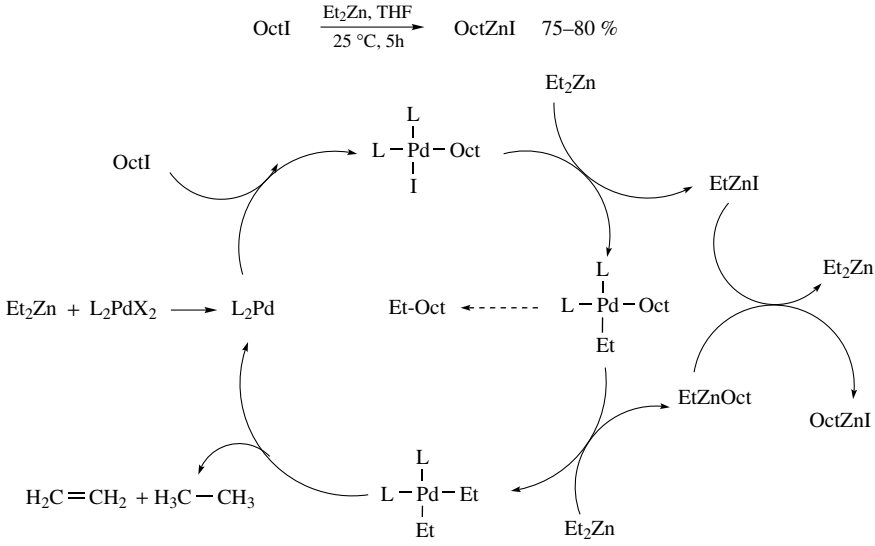

SCHEME 15. Mechanism of the Pd-catalyzed reaction of alkyl iodides with diethylzinc

relative stereochemistry of up to three contiguous centers is set up in this cyclization (Scheme 16)[41].

Application of these methods toward the preparation of natural products, such as (−)-methylenolactocin (**41**) or *cis*-methyl jasmonate (**42**), has been accomplished[42] (Scheme 17).

This reaction can be applied to the preparation of benzylic zinc reagents[40a, 43]. A range of benzylic halides has been reduced with Et_2Zn in the presence of $Pd(PPh_3)_4$ as a catalyst[43]. Other metallic salts catalyze the I/Zn exchange reaction. Thus, mixed metal catalysis using manganese(II) bromide and copper(I) chloride allows the performance of a Br/Zn exchange with various functionalized alkyl bromides of type **43** (Scheme 18)[44]. The reaction proceeds in a polar solvent such as DMPU[45] under very mild conditions.

Interestingly, low-valent cobalt species obtained by the *in situ* reduction of $CoBr_2$ with zinc catalyze the reaction of aryl bromides with zinc dust. The reaction allows the preparation of a range of functionalized arylzinc halides such as **44** (Scheme 19)[45].

In summary, the direct insertion of zinc dust to organic halides is an excellent method for preparing a broad range of polyfunctional organozinc halides bearing various functional groups like an ester[46], an ether, an acetate[47], a ketone, cyano[48], halide[49], *N*,*N*-bis(trimethylsilyl)amino[50], primary and secondary amino, amide, phthalimide[51], sulfide, sulfoxide and sulfone[52], boronic ester[53], enone[54] or a phosphonate[55]. An alternative method is based on transmetalation reactions.

2. Preparation of organozinc halides using transmetalation reactions

A number of transmetalation procedures leading to zinc organometallics can be performed. Many organometallics having a polar C−Met bond are readily transmetalated by the reaction with a zinc salt to the more covalent organozinc compounds. The synthetic

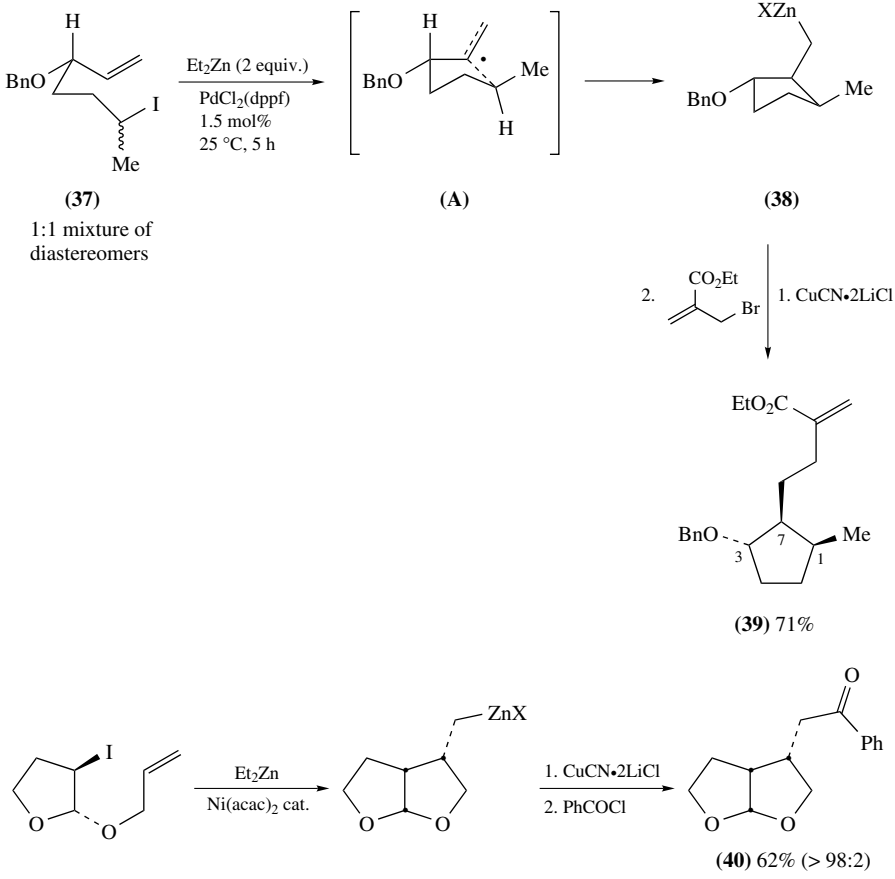

SCHEME 16. Pd- and Ni-catalyzed radical cyclization leading to zinc organometallics

scope of these transmetalations depends on the availability of the starting organometallic species and on its compatibility with functional groups. Although organolithiums are highly reactive organometallic species, it is possible to prepare aryllithium species bearing cyano groups[56] or nitro groups[57] at very low temperature ($-100\,^{\circ}C$ to $-90\,^{\circ}C$). By performing a halogen–lithium exchange reaction, followed by a transmetalation with $ZnBr_2$, functionalized organometallics are prepared which cannot be obtained by the insertion of zinc to the corresponding organic halide. Azides inhibit the direct zinc insertion to an organic halide. However, the reaction of the alkenyl iodide **45** bearing an azide group with *n*-BuLi at $-100\,^{\circ}C$ followed by the transmetalation with ZnI_2 in THF at $-90\,^{\circ}C$ provides the expected zinc reagent **46** in >85% yield (Scheme 20)[58].

The mixed 1,2-bimetallic Zn/Si-reagent **47** is a versatile species which reacts with aldehydes in high diastereoselectivity[59]. It is prepared by a bromine/lithium exchange reaction starting from **48** followed by a transmetalation with $ZnCl_2$ (Scheme 21). The

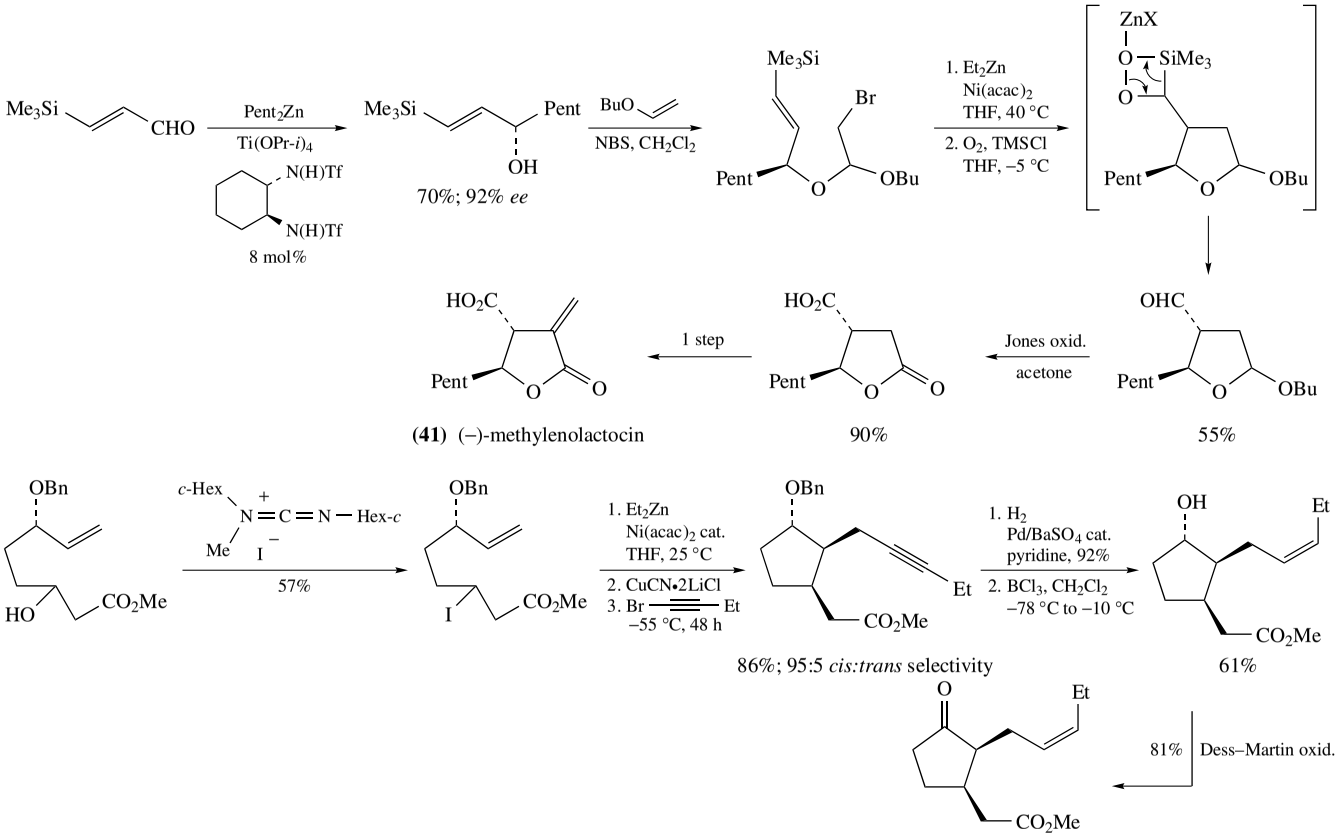

SCHEME 17. Preparation of (−)-methylenolactocin (**41**) and *cis*-methyl jasmonate (**42**)

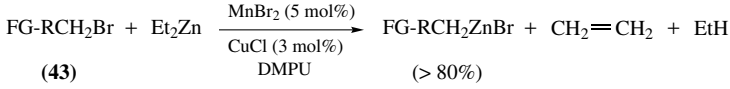

FG = ester, nitrile, chloride

SCHEME 18. Mixed Mn/Cu-catalyzed alkylzinc bromides synthesis

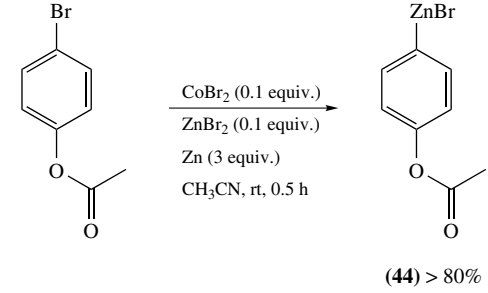

SCHEME 19. Cobalt-mediated insertion of zinc to aryl bromides

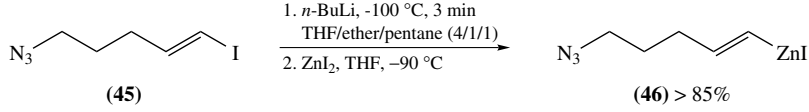

SCHEME 20. Preparation of an alkenylzinc reagent bearing an azide function

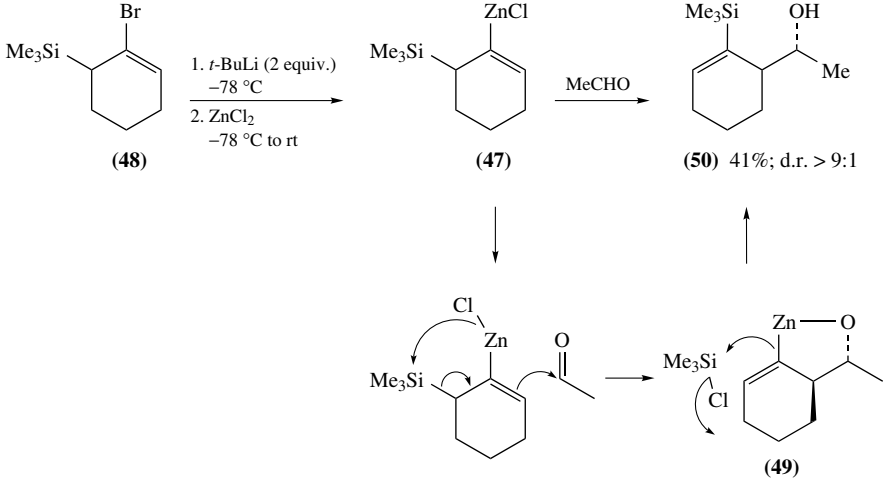

SCHEME 21. Preparation and uses of a zinc/silicon bimetallic of type **47**

reaction with acetaldehyde leads initially to the alkenylzinc species **49** which reacts with Me_3SiCl, providing the alkenylsilane **50** in 41% yield and a diastereoselectivity >9:1. 2-Lithiated oxazoles are unstable and easily undergo a ring-opening to the tautomeric isocyanides. This ring cleavage can be avoided by preparing the corresponding 2-zincated oxazole (**51**), which is much more stable toward a fragmentation reaction (Scheme 22)[60]. The lithiation of the *O*-vinyl carbamate (**52**) with *sec*-BuLi followed by transmetalation with zinc bromide provides the convenient acyl anion derivative **53**, which undergoes smooth Pd(0)-catalyzed cross-coupling reactions (Scheme 22)[61].

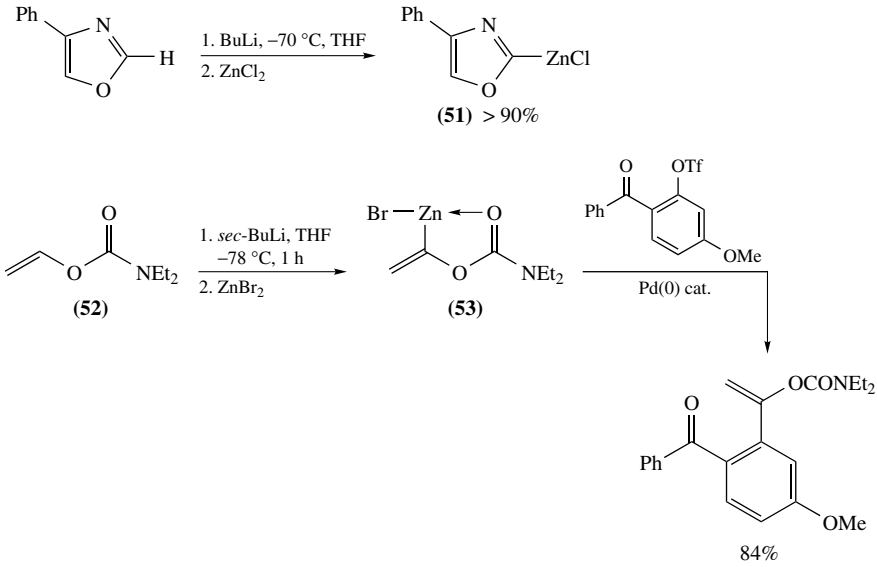

SCHEME 22. Preparation and uses of a zinc reagent via a Li/Zn transmetalation sequence

This reaction sequence has been extended to lithium enolates. The deprotonation of the aminoester **54** with LDA followed by a transmetalation with zinc bromide in ether furnishes a zinc enolate, which readily adds to the double bond providing the proline derivative **55** in high diastereoselectivity (Scheme 23)[62].

Similarly, zincated hydrazone derivatives of type **56** undergo an intermolecular carbozincation of strained cyclopropene rings such as **57**, leading to the adduct **58** with 92% yield[63]. This type of addition can be extended to ethylene[63b]. It proceeds with an excellent stereoselectivity allowing the enantioselective synthesis of α-substituted ketones. Allylic zinc species add as well to cyclopropenone acetals, allowing an enantioselective allylzincation to take place[63d]. This reaction provides an entry to quaternary centers with good stereocontrol. Fluorine-substituted alkenes can be readily lithiated by the reaction with a strong base (Scheme 24).

1-Chloro-2,2-difluorovinylzinc chloride **59** opens the access to a range of fluorine-containing molecules via cross-coupling reactions. Normant and coworkers have prepared this zinc reagent by the deprotonation of 1-chloro-2,2-difluoroethene **60** and transmetalation[64]. These two steps can be combined in one and the lithiation of **60** with *sec*-BuLi in the presence of $ZnCl_2$ provides the corresponding dialkylzinc **61** as a colorless clear solution[65]. Percy and coworkers[66] and Burton and Anilkumar[67] reported that the deprotonation of 1-chloro-2,2,2-trifluoroethane **62** produces, after elimination and

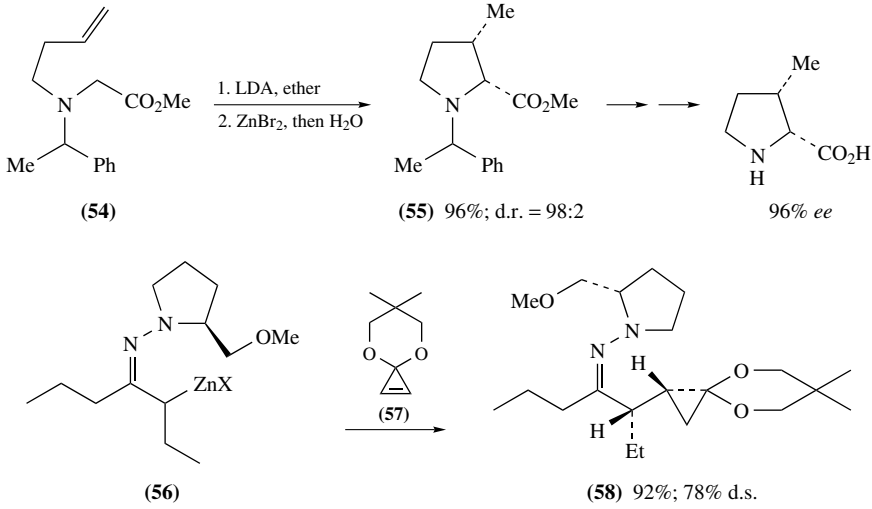

SCHEME 23. Conversion of zinc enolates to organozinc reagents

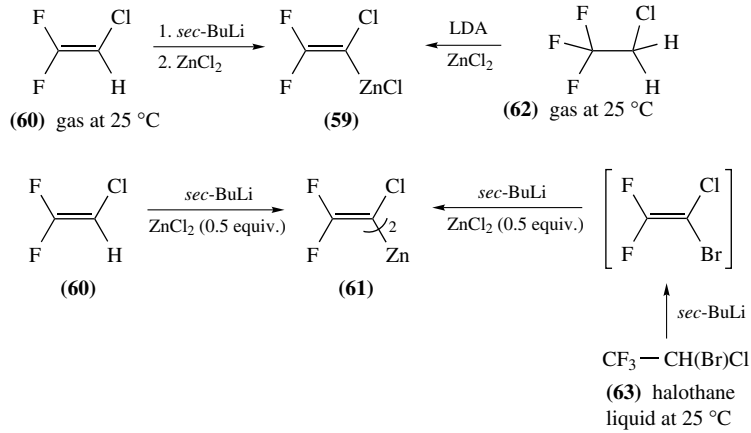

SCHEME 24. Preparation of fluoro-substituted alkenylzincs via lithium intermediates

transmetalation, the zinc reagent **59**. Especially convenient is the deprotonation of liquid halothane (**63**) with *sec*-BuLi in the presence of $ZnCl_2$.

Transmetalations starting from alkenylzirconium species, which are obtained by hydrozirconation using $H(Cl)ZrCp_2$, are readily accomplished[68,69]. Ichikawa, Minami and coworkers have elegantly shown that difluorovinylzinc iodide **64** is obtained by the addition of '$ZrCp_2$' to the alkenyl tosylate **65**[68]. *In situ* transmetalation reactions have also been reported.

A new three-component reaction[70] has been made possible by treating an alkenylzirconium reagent of type **66** with an alkyne **67** and an aldehyde **68** in the presence of catalytic amounts of $Ni(cod)_2$ (10 mol%) and $ZnCl_2$ (20 mol%). The resulting pentadienyl alcohols like **69** are obtained in satisfactory yield. The transmetalation of the

alkenylzirconium species **66** to the corresponding zinc species is essential for the success of the carbometalation reaction[71]. An intramolecular version of the reaction is possible showing the high affinity of the intermediate alkenylzinc derived from **66** for adding to the alkyne **70**. The competitive alternative addition to the aldehyde is not observed. The most general application has been reported by Wipf and Xu[69], who demonstrated that a range of alkenylzirconium species are readily transmetalated to zinc organometallics. Thus, the reaction of the alkenylzirconium **71** with Et_2Zn produces a zinc reagent which adds to an unsaturated aldehyde, furnishing the expected allylic alcohol in excellent yield (Scheme 25)[69]. Organotin compounds have also occasionally been converted to zinc and then copper compounds by generating first an organolithium derivative (Scheme 26)[72]. α-Aminostannanes of type **72** undergo a low-temperature Sn/Li exchange reaction with BuLi in THF and lead after a transmetalation to an organozinc species displaying a

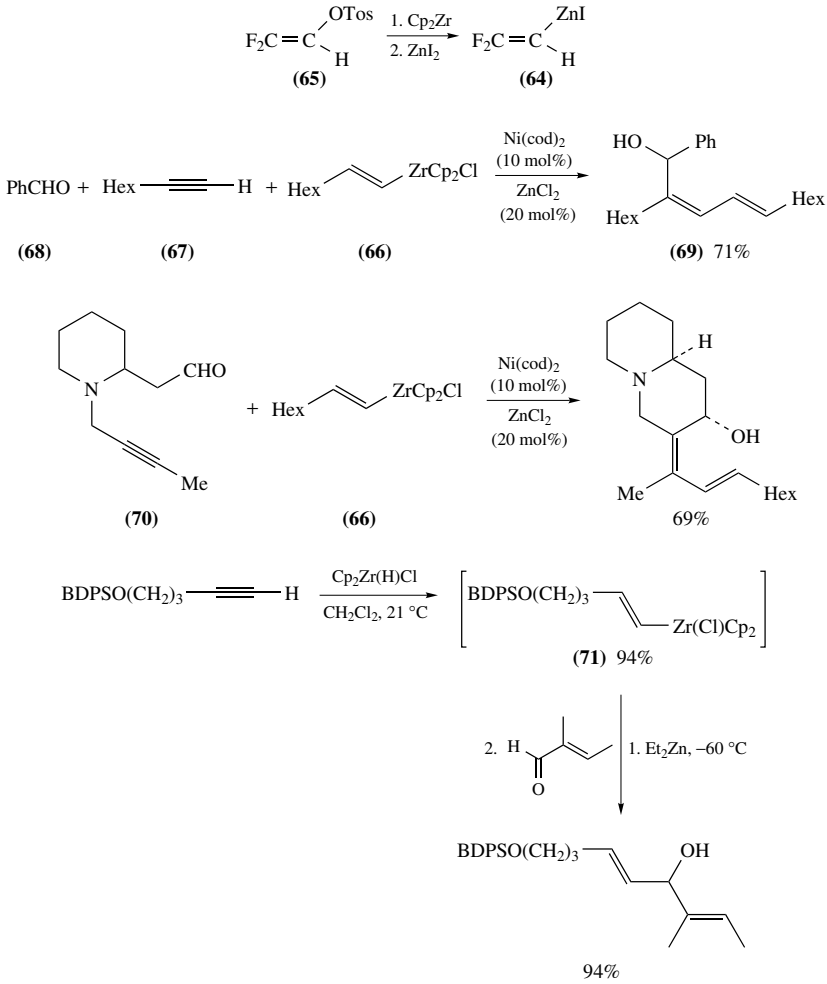

SCHEME 25. Alkenylzinc species obtained from alkenylzirconium derivatives

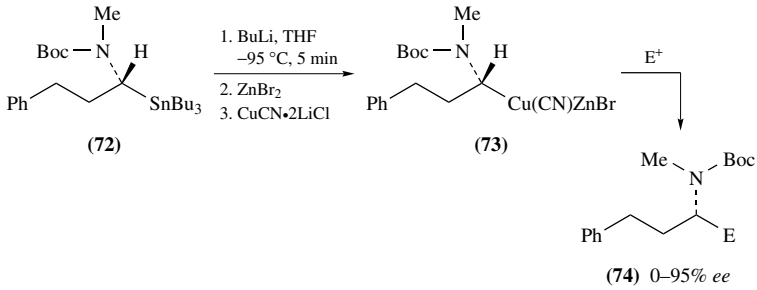

SCHEME 26. Preparation and uses of zinc organometallics starting from tin reagents

moderate reactivity. After a further transmetalation with CuCN•2LiCl, a copper–zinc species such as **73** is obtained. The reaction of **73** with electrophiles (E^+) affords products of type **74** with variable enantioselectivities. Quenching of the copper–zinc reagent **73** with reactive electrophiles proceeds with retention of configuration with up to 95% *ee*.

The weak carbon–mercury bond favors transmetalations of organomercurials[73]. The reaction of functionalized alkenylmercurials, such as **75**, with zinc in the presence of zinc salts like zinc bromide leads to the corresponding zinc reagents **76** in high yield and excellent stereoisomeric purity (Scheme 27)[74]. Interestingly, the required functionalized diorganomercurials can be obtained either by the reaction of functionalized alkylzinc iodides with mercury(I) chloride or by methylene homologation reaction using $(ICH_2)_2Hg$ (Scheme 27)[74].

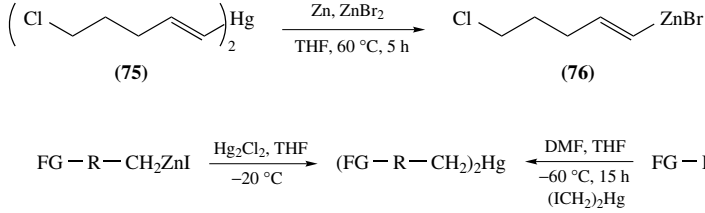

SCHEME 27. Preparation of alkenylzinc bromides from organomercurials

A range of polyfunctional organomagnesium species is available via an iodine–or a bromine–magnesium exchange reaction[75]. Since the carbon–magnesium bond is less polar than a carbon–lithium bond, considerably more functional groups are tolerated in these organometallics and experimentally more convenient reaction conditions can be used. Thus, the reaction of the aryl iodide **77** with *i*-PrMgBr in THF at $-10\,^{\circ}C$ for 3 h provides an intermediate magnesium reagent which, after transmetalation with $ZnBr_2$, furnishes the zinc reagent **78**. Its palladium-catalyzed cross-coupling with the bromofuran **79** provides the cross-coupling product **80** in 52% yield (Scheme 28)[76].

This exchange reaction allows the preparation of various zinc reagents bearing numerous functional groups[75]. Special methods are available for the preparation of organozinc halides, such as insertion reactions using zinc carbenoids like (iodomethyl)zinc iodide[77]. The reaction of an organocopper reagent (**81**) with ICH_2ZnI provides a copper–zinc reagent **82** which reacts with numerous electrophiles (Scheme 29)[78]. This reaction is quite general and allows one, for example, to homologate lithium enolates leading to the zinc homoenolate **83**, which can be readily allylated in the presence of a copper

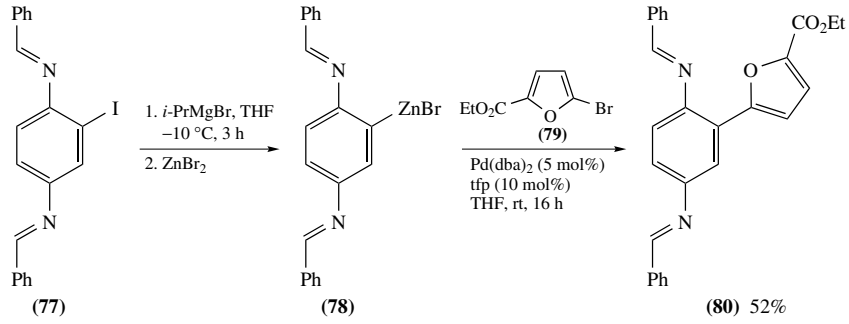

SCHEME 28. Preparation and uses of arylzinc halides via an I/Mg exchange

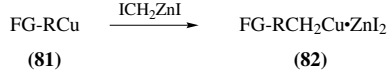

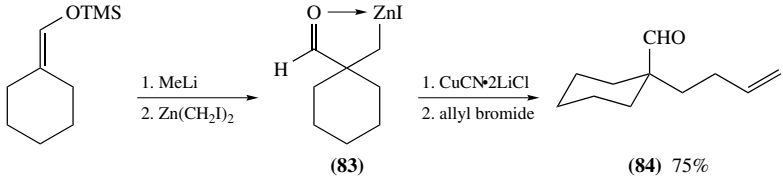

SCHEME 29. Homologation of zinc enolate using a zinc carbenoid

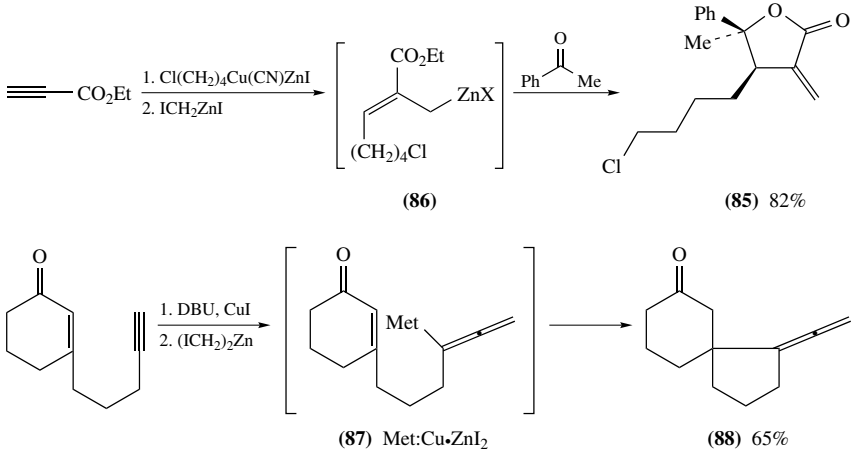

SCHEME 30. Allylic and allenic zinc reagents via methylene homologation

catalyst leading to the aldehyde **84** in 75% yield (Scheme 29)[78, 79]. A one-pot synthesis of γ-butyrolactones such as **85** can be realized via an intermediate allylic zinc species **86** generated by the homologation of an alkenylcopper reagent obtained by the carbocupration of ethyl propiolate (Scheme 30).

Interestingly, an intramolecular trapping of an allenylzinc–copper species **87** generated by the homologation of an alkynylcopper can be achieved leading to the spiro-product **88** in 65% yield (Scheme 30)[79]. This method allows the homologation of silylated lithium carbenoids[80] and can be extended to the performance of polymethylene homologations[78c]. The use of lithium tributylzincates allows the synthesis of alkylated allenylzinc species such as **89**, which react with aldehydes leading to alcohols of type **90** with high diastereoselectivity (Scheme 31)[81, 82].

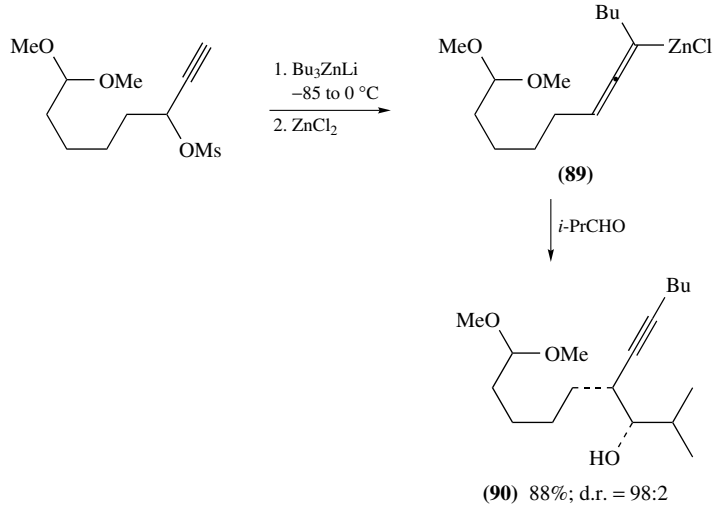

SCHEME 31. Preparation and uses of allenic zinc reagents using lithium trialkylzincates

The reaction of stereomerically well-defined alkenylcopper species **91** obtained by a carbocupration followed by treatment with $(ICH_2)_2Zn$ leads to a selective double methylene insertion providing the chelate-stabilized alkylzinc reagent **92**, which leads after deuteriation with D_2O to the unsaturated sulfoxide **93** in 80% yield. This method has been elegantly extended by Marek, Knochel and coworkers (Scheme 32)[83].

A selective reaction of 1,4-bimetallic alkanes with CuCN•2LiCl allows the preparation of a range of new polyfunctional zinc–copper reagents[84]. Thus, the reaction of 1,4-dizincated butane (**94**) with CuCN•2LiCl, followed by cyclohexenone in the presence of TMSCl (2 equiv), provides the new zinc–copper reagent **95** which reacts with 3-iodo-2-cyclohexenone, furnishing the diketone **96** in 64% yield (Scheme 33)[84].

The preparation of chiral alkylzinc halides by the direct insertion of zinc is complicated due to the radical nature of the zinc insertion. Nevertheless, the strained secondary alkyl iodide **97** is converted to the corresponding chiral secondary organozinc reagent (**98**) with high retention of configuration leading, after stannylation with Me_3SnCl, to the tin derivative **99** in 72% yield[85]. Interestingly, the *trans*-β-iodoester **100** is stereoselectively converted to the *cis*-ester **101** leading, after acylation, to the aminoketone **102**[86]. The chelation with the ester group may be responsible for the *cis*-configuration of the zinc reagent **101** (Scheme 34). ^1H NMR studies[87] confirm that secondary dialkylzincs should display a high configurational stability, although it was noticed that the presence of an excess of zinc(II) salts epimerizes secondary alkylzinc reagents[87].

The importance of chelating for the configurational stability of organozinc reagents has been recently demonstrated by Normant and Marek. The reaction of the bimetallic reagent

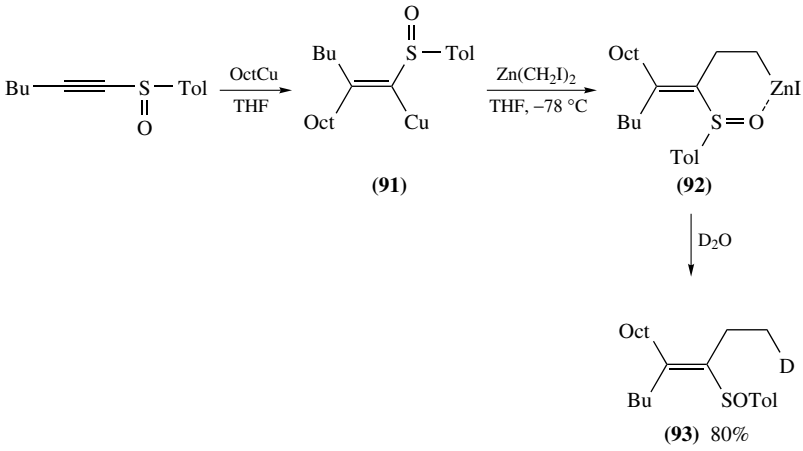

SCHEME 32. Double homologation of alkenyl sulfoxide derivatives

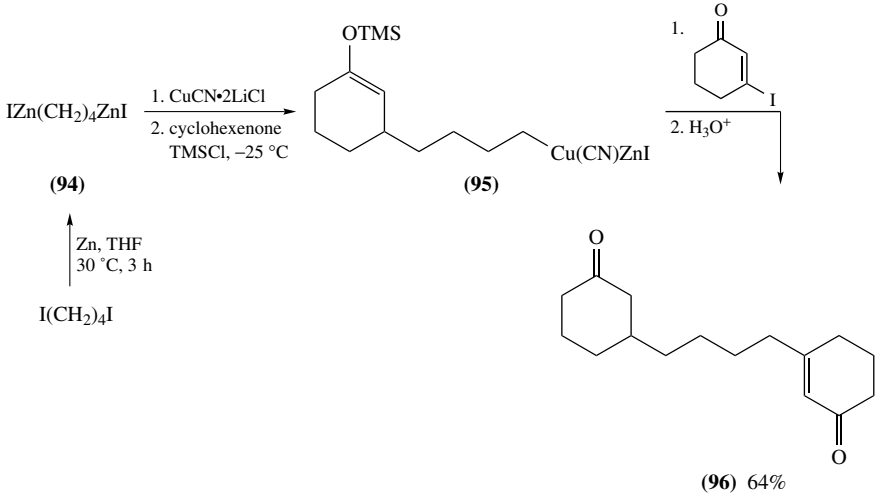

SCHEME 33. Preparation and uses of alkylzinc–copper reagents via the selective reaction of 1,4-dizincated butane

103 prepared by the allylzincation of the alkenyllithium **104** leads, after stereoselective sequential quenching with two electrophiles (MeOD and I_2), to the primary iodide **105** as a 34:66 mixture of diastereomers (Scheme 35)[88]. Also, alkenylzinc reagents such as **106** display a relatively high configurational stability [little racemization is observed at $-65\,^{\circ}C$ (2 h)]. A kinetic resolution with (*R*)-mandelic imine derivate **107** is possible. Thus, treatment of a racemic mixture of the zinc reagent **106** with half of an equivalent of the imine **107** led to a highly preferential reaction with the (S_a)-enantiomer of **106**, leading to the adduct **108**. The remaining unreacted (R_a)-**106** can now be trapped with an

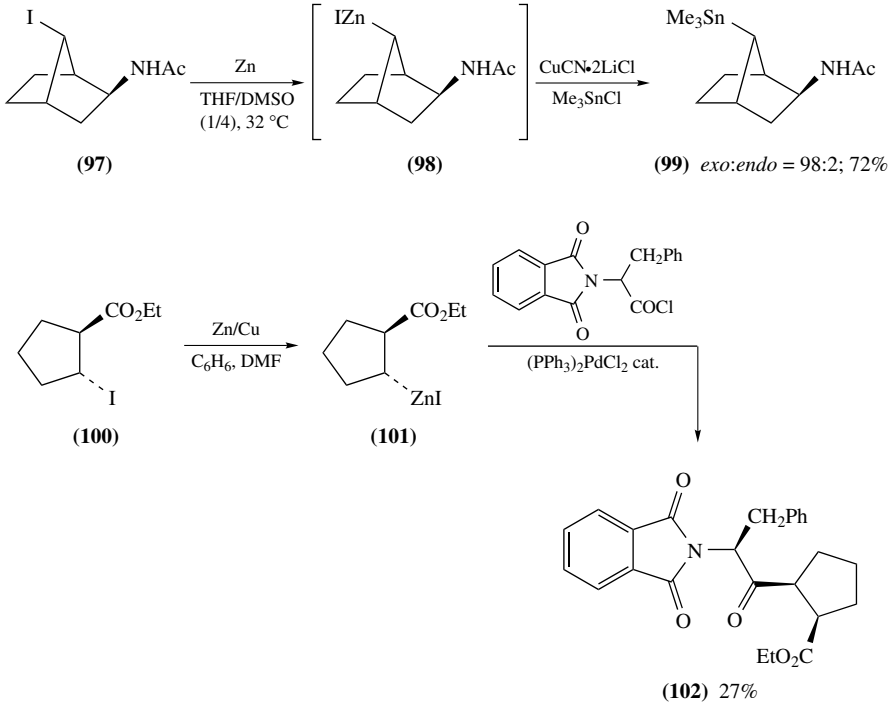

SCHEME 34. Stereoselective preparation of secondary alkylzinc iodides by the direct insertion of zinc

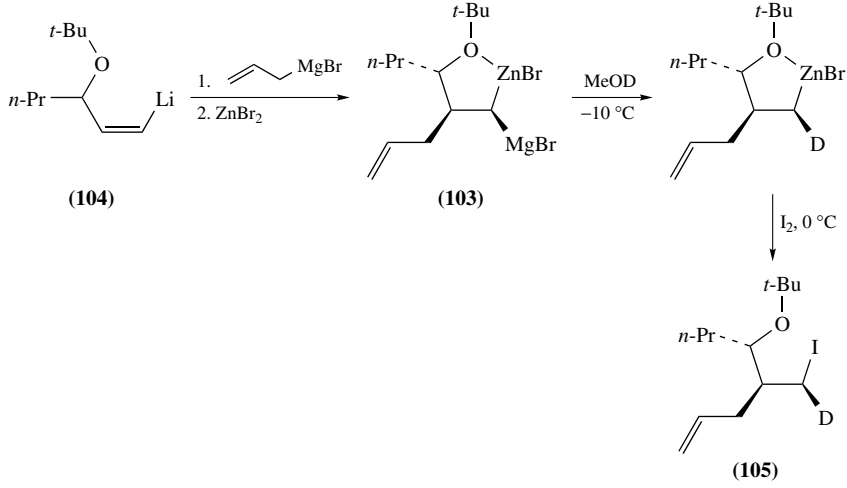

SCHEME 35. Synthesis of chiral organozinc halides

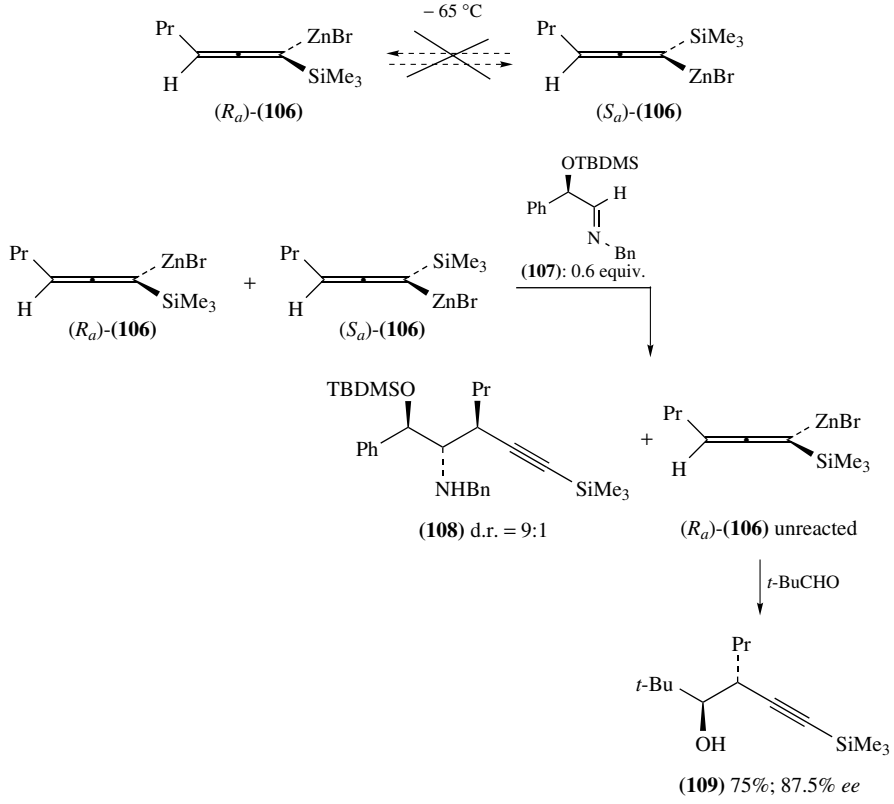

SCHEME 35. (*continued*)

aldehyde such as pivalaldehyde, giving the chiral homopropargylic alcohol **109** in 75% yield and 87.5% *ee*[89]. This kinetic resolution has been used to prepare *anti, anti*-vicinal amino diols in >95% *ee* and d.r. >40:1[90]. In general, diorganozincs are more easily prepared in optically pure form. This will be discussed in detail in the next section. On the other hand, secondary zinc reagents prepared by direct zinc insertion to secondary alkyl iodides are obtained without stereoselectivity[91].

C. Preparation of Diorganozincs

1. Preparation via an I/Zn exchange

Diorganozincs are usually more reactive toward electrophiles than organozinc halides. A wide range of methods is available for their preparation. The oldest is the direct insertion of zinc to an alkyl halide (usually an alkyl iodide) leading to an alkylzinc intermediate which, after distillation, provides the liquid diorganozinc (R_2Zn)[1]. This method is applicable only to non-functionalized diorganozincs bearing lower alkyl chains (up to hexyl) due to the thermal instability of higher homologs. The I/Zn exchange reaction using Et_2Zn allows the

preparation of a broad range of diorganozincs. The ease of the exchange reaction depends on the stability of the newly produced diorganozincs. Thus, diiodomethane smoothly reacts with Et_2Zn in THF at $-40\,^{\circ}C$, providing the corresponding mixed ethyl(iodomethyl)zinc reagent (**110**) with quantitative yield[92]. The I/Zn exchange is catalyzed by the addition of CuI (0.3 mol%). After the evaporation under vacuum of excess Et_2Zn and ethyl iodide formed during the reaction, the resulting diorganozincs **111a–d** are obtained in excellent yields (Scheme 36)[93].

$$ICH_2I + Et_2Zn \xrightarrow[-40\,^{\circ}C]{THF} ICH_2ZnEt \quad \textbf{(110)}\ 90\%$$

$$FG\text{-}RCH_2I + Et_2Zn \xrightarrow[\text{neat, 25–50 }^{\circ}C]{\text{CuI cat.}} (FG\text{-}RCH_2I)_2Zn$$

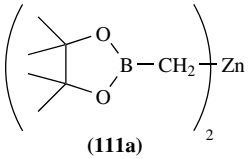

(111a)

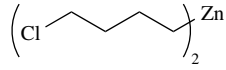

(111b)

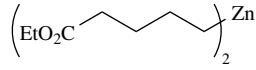

(111c)

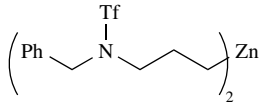

(111d)

SCHEME 36. Diorganozincs obtained by I/Zn exchange

Interestingly, this iodine–zinc exchange can also be initiated by light[94]. Thus, the irradiation (>280 nm) of an alkyl iodide in CH_2Cl_2 in the presence of Et_2Zn (1 equivalent) provides the desired diorganozinc with excellent yields. A more reactive exchange reagent (i-Pr_2Zn) can be used instead of Et_2Zn. This organometallic has to be free of salts if optically active diorganozincs have to be prepared[95]. However, the presence of magnesium salts has a beneficial effect on the rate of exchange and a range of mixed zinc reagents of the type RZn(Pr-i) (**112**) can be prepared under mild conditions (Scheme 37)[96].

Since the isopropyl group is also transferred in the reaction with an electrophile at a comparable rate as the second R group, an excess of electrophile must be added and tedious separations may be required. A more straightforward approach is possible for diarylzincs. In this case, the I/Zn exchange can be performed under very mild conditions[97].

The intermediate formation of a zincate enhances the nucleophilic reactivity of the substituents attached to the central zinc atom and makes it more prone for undergoing an iodine–zinc exchange reaction. Thus, the addition of catalytic amounts of Li(acac) to an aryl iodide and i-Pr_2Zn (Scheme 38) allows the transfer of the two i-Pr groups with the formation of Ar_2Zn and i-PrI (2 equivalents). This method allows the preparation of highly functionalized diarylzinc reagents bearing an aldehyde function like **113** or an isothiocyanate group like **114** (Scheme 39). These diarylzinc reagents undergo typical reactions of diorganozincs. Thus, the acylation of **113** with an acid chloride in the presence

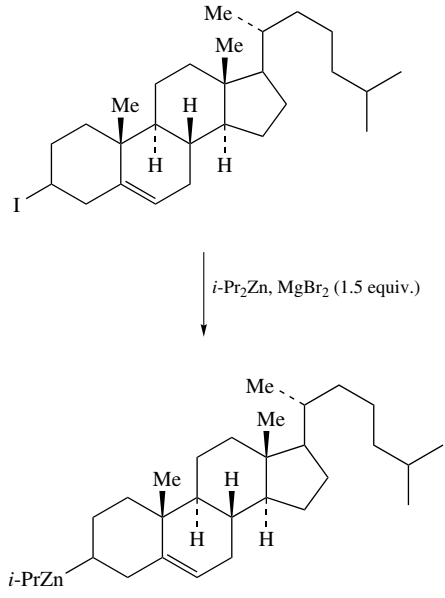

(112) *ca* 60%

SCHEME 37. Preparation of mixed diorganozincs via an I/Zn exchange

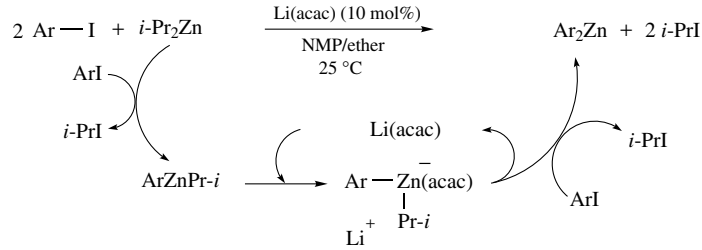

SCHEME 38. Li(acac) catalyzed synthesis of diarylzincs

of Pd(0) provides the polyfunctional ketone **115** in 75% yield, whereas the reaction of the zinc reagent **114** with Me_3SnCl gives the aryltin derivative **116** in 66% yield.

Mixed diorganozincs are synthetically useful intermediates, especially if one of the groups attached to zinc is transferred preferably. The trimethylsilylmethyl group is too unreactive toward most electrophiles and plays the role of a dummy ligand. The preferential transfer of the second R-group attached to zinc is therefore possible in many cases. The reaction of 4-chlorobutylzinc iodide with Me_3SiCH_2Li in THF at $-78\,^{\circ}C$ provides the mixed diorganozinc reagent **117**, which readily undergoes a Michael addition with butyl acrylate in THF:NMP mixtures (Scheme 40)[98]. Barbier-type reactions are also well suited for the synthesis of diarylzincs, although the functional group tolerance of this method has not been investigated in detail[99, 100].

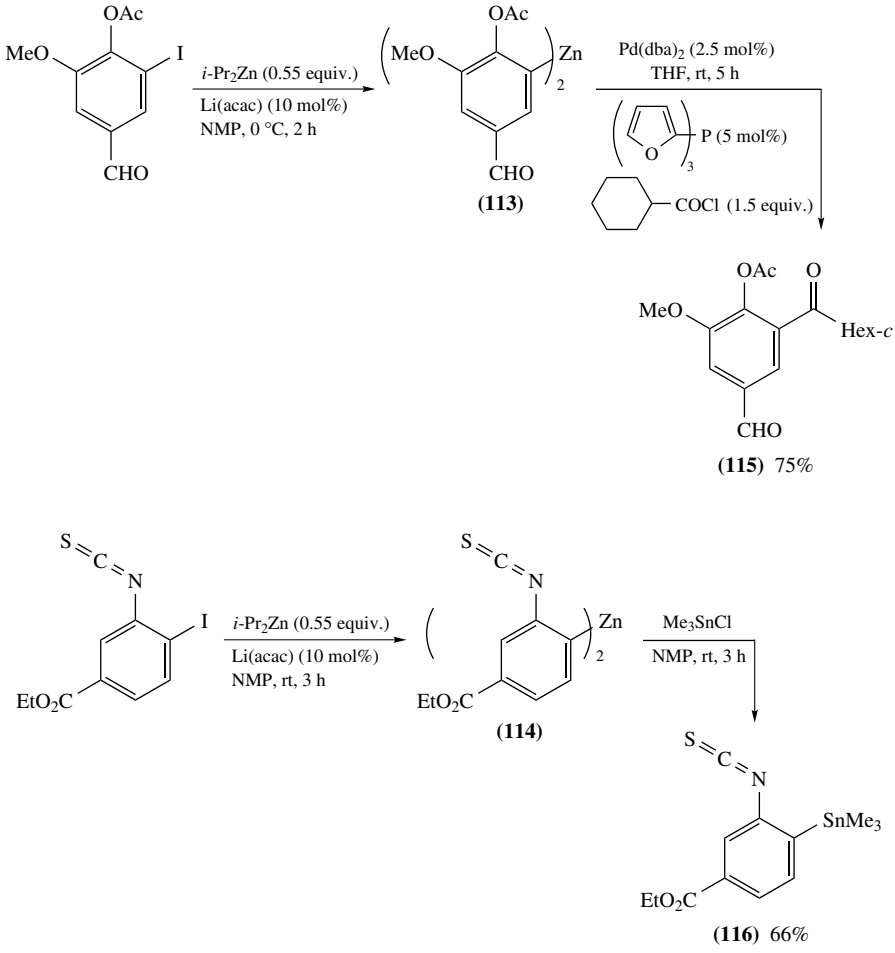

SCHEME 39. Functionalized diarylzincs bearing an aldehyde or an isothiocyanate functional group

The reaction of 4-bromotoluene with lithium in the presence of zinc bromide in ether affords the corresponding zinc reagent **118**, which undergoes a smooth 1,4-addition to sterically hindered enones and leads to the cyclopentanone **119** in 84% yield[99] (Scheme 40).

2. The boron–zinc exchange

Various organoboranes react with Et_2Zn or i-Pr_2Zn providing the corresponding diorganozinc. Pioneered by Zakharin[101], Thiele[102] and coworkers, the method provides a general entry to a broad range of diorganozincs. The exchange reaction proceeds usually under mild conditions and tolerates a wide range of functional groups. It is applicable to the preparation of allylic and benzylic diorganozincs as well as secondary and primary

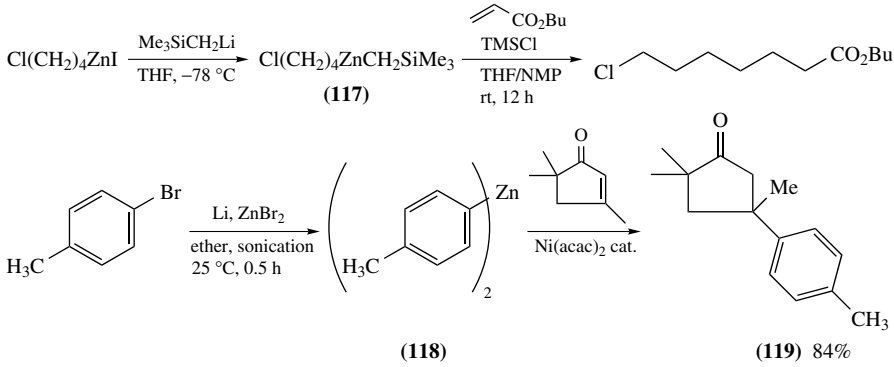

SCHEME 40. Various synthesis and Michael additions of organozincs

dialkylzincs[103] and dialkenylzincs[104]. Remarkably, functionalized alkenes bearing a nitro group or a alkylidenemalonate function are readily hydroborated with Et_2BH[105] prepared *in situ* and converted to diorganozinc reagents such as **120** and **121**. After a copper-catalyzed allylation the expected allylated products **122** and **123** are obtained in high yields (Scheme 41)[103].

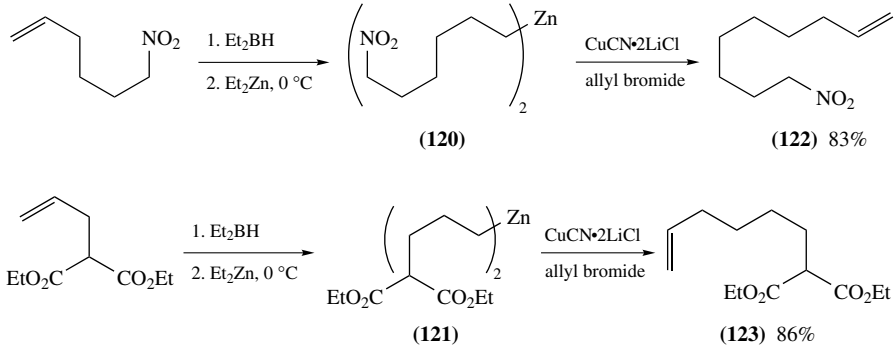

SCHEME 41. Preparation and uses of functionalized diorganozincs using a B/Zn exchange

The hydroboration of dienic silyl enol ethers, such as **124**, with Et_2BH leads to organoboranes which can be converted to new diorganozincs, such as **125** (Scheme 42)[106]. More importantly, this method allows the preparation of chiral secondary alkylzinc reagents.

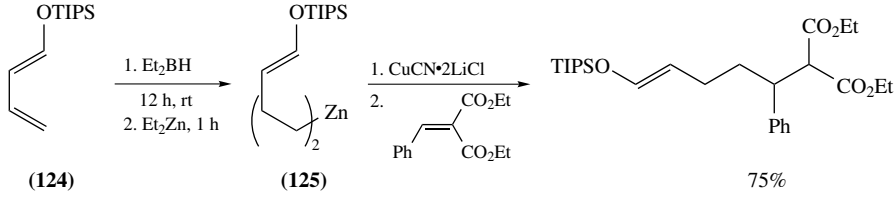

SCHEME 42. Preparation and uses of diorganozincs bearing a silyl ether using a boron–zinc exchange

Thus, the hydroboration of 1-phenylcyclopentene with (−)-IpcBH$_2$ (99% *ee*)[107] produces, after crystallization, the chiral organoborane **126** with 94% *ee*. The reaction of **126** with Et$_2$BH replaces the isopinocamphenyl group with an ethyl substituent (50 °C, 16 h) and provides, after the addition of *i*-Pr$_2$Zn (25 °C, 5 h), the mixed diorganozinc **127**. Its stereoselective allylation leads to the *trans*-disubstituted cyclopentane **128** in 44% yield (94% *ee*; *trans*:*cis* = 98:2); see Scheme 43[108]. This sequence can be extended to open-chain alkenes and *Z*-styrene derivative **129** is converted to the *anti*-zinc reagent **130**, which provides after allylation the alkene **131** in 40% yield and 74% *ee* (dr = 8:92).

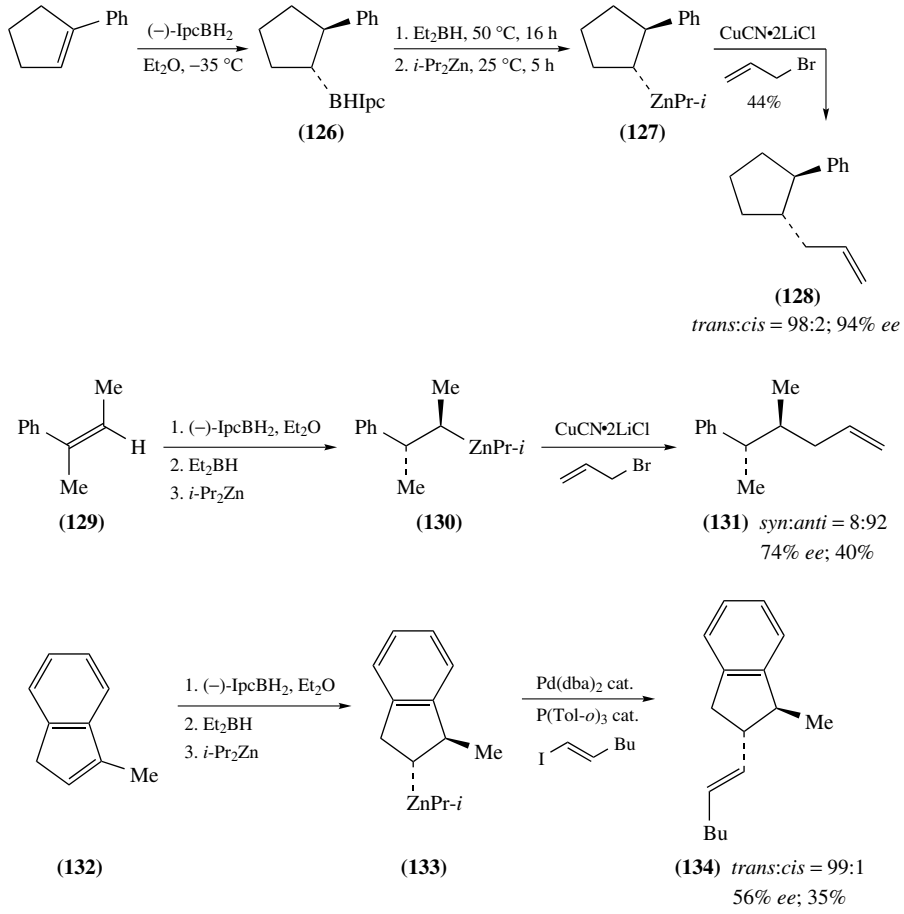

SCHEME 43. Synthesis of chiral secondary alkylzincs via B/Zn exchange

Similarly, the indene derivative **132** is converted by asymmetric hydroboration and B/Zn exchange into the *trans*-indanylzinc reagent **133**, which undergoes a Pd-catalyzed cross-coupling with an *E*-alkenyl iodide leading to the *trans*-*E*-product **134** in 35% yield (Scheme 43)[108b]. Several functionalized alkenes have been converted into chiral secondary alkylzinc reagents[109]. Especially interesting are unsaturated acetals, such as **135**, which

can be hydroborated with (−)-IpcBH$_2$ with high enantioselectivity (91% *ee*) providing, after B/Zn exchange, the mixed zinc reagent **136**.

Its trapping with various electrophiles provides chiral products, such as **137–139**. The deprotection of **139** furnishes the β-alkynylaldehyde **140** in 88% *ee*. The *exo*-alkylidene acetal **141** is converted similarly to the zinc reagent **142**, which can be allylated with an excellent diastereoselectivity (d.r. = 96:4) leading to the ketal **143** (Scheme 44)[109].

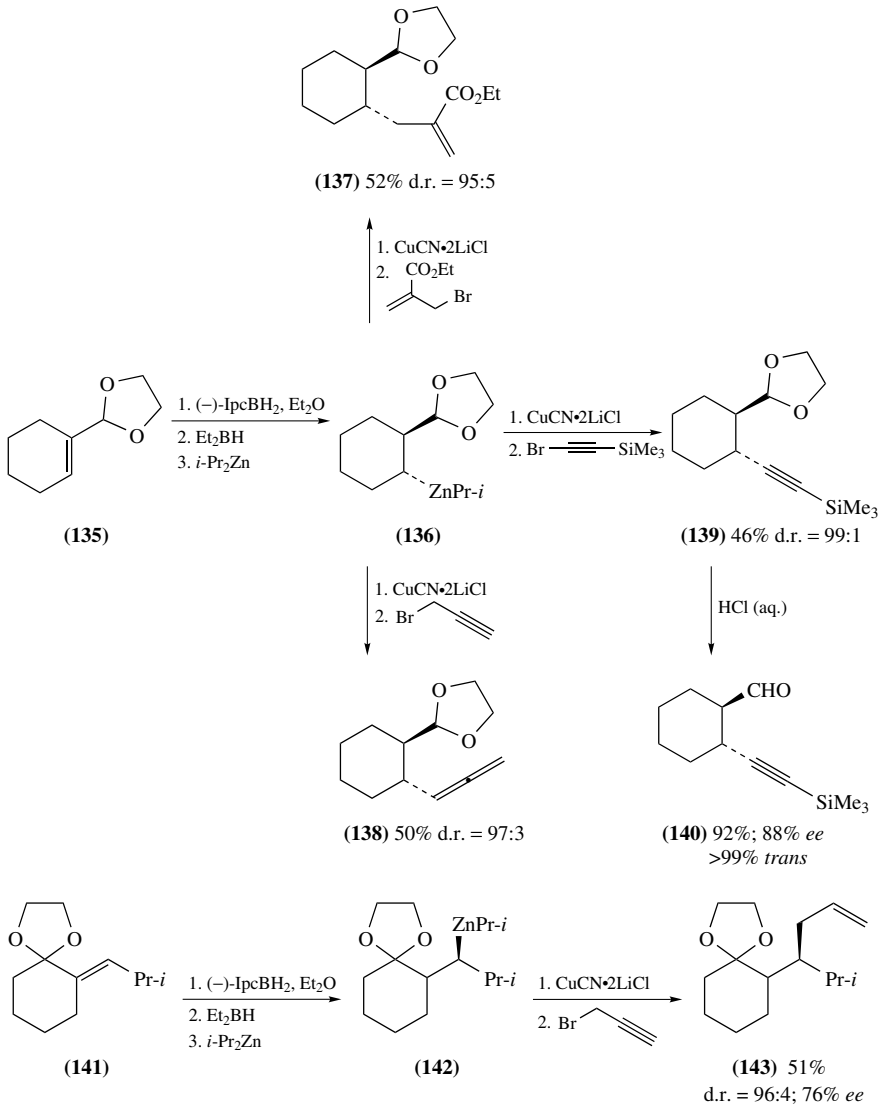

SCHEME 44. Preparation and uses of chiral functionalized zinc organometallics via a boron–zinc exchange

A substrate controlled hydroboration can also be achieved. Thus, the hydroboration of the unsaturated bicyclic olefin **144** occurs with high diastereoselectivity. B/Zn exchange leads to the zinc reagent **145**, which can be acylated with retention of configuration at C(3) leading to the bicyclic ketone with a control of the relative stereochemistry of 4 contiguous chiral centers as shown in product **146** (Scheme 45)[110]. The hydroboration of allylic silanes, such as **147**, proceeds with high diastereoselectivity as demonstrated by Fleming and Lawrence[111]. It is difficult to use the newly formed carbon–boron bond for making new carbon–carbon bonds due to its moderate reactivity. However, the B/Zn exchange converts the unreactive carbon–boron bond to a reactive carbon–zinc bond as in compound **148**. A further transmetalation with the THF soluble salt CuCN•2LiCl provides copper reagents which can be allylated (**149a**), alkynylated (**149b**) or acylated (**149c**); see Scheme 45.

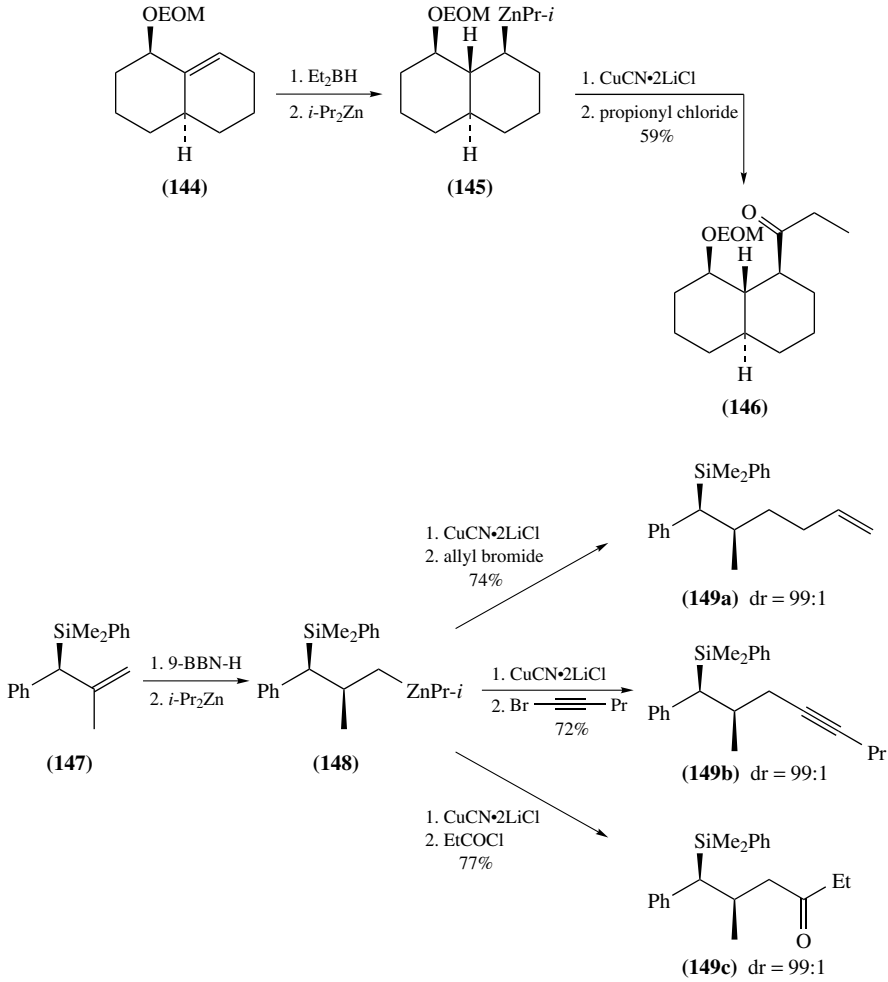

SCHEME 45. Diastereoselective hydroboration and B/Zn exchange

The hydroboration of allylic amine or alcohol derivatives can be used for the preparation of alkylzinc reagents with excellent diastereoselectivity (Scheme 46)[112]. Thus, the diastereoselective hydroboration of the allylic sulfonamide **150**[113] affords, after B/Zn exchange, the zinc reagent **151** which leads, after a copper-catalyzed acylation, to the ketone **152** with 62% yield[112]. Rhodium-catalyzed hydroborations are also compatible with the boron–zinc exchange reaction and the *exo*-methylene silylated alcohol **153** is readily hydroborated with catecholborane[114] in the presence of $ClRh(PPh_3)_3$[115] affording, after boron–zinc exchange, the zinc reagent **154** leading, after allylation, to the *cis*-substituted products **155** and **156**[112]. The boron–zinc exchange can be extended to aromatic systems. The required aromatic boron derivatives can be readily prepared from the corresponding arylsilanes such as **157** by using BCl_3[116].

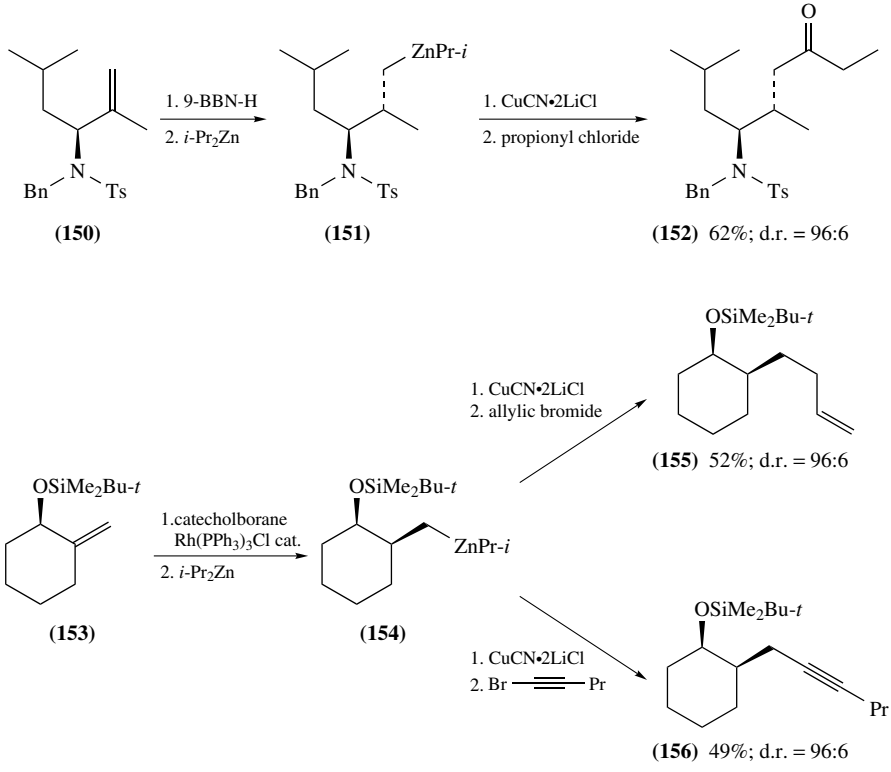

SCHEME 46. Diastereoselective hydroboration of allylic derivatives and B/Zn exchange

The resulting functionalized arylborane **158** readily undergoes a B/Zn exchange leading to the zinc reagent **159**, which can be trapped by various electrophiles, such as propargyl bromide or propionyl chloride, leading respectively to the allene **160** (73%) and to the ketone **161** (72%); see Scheme 47[116].

3. Hydrozincation of alkenes

Diorganozincs can also be prepared by a nickel-catalyzed hydrozincation. The reaction of Et_2Zn with $Ni(acac)_2$ may produce a nickel hydride that adds to an alkene leading,

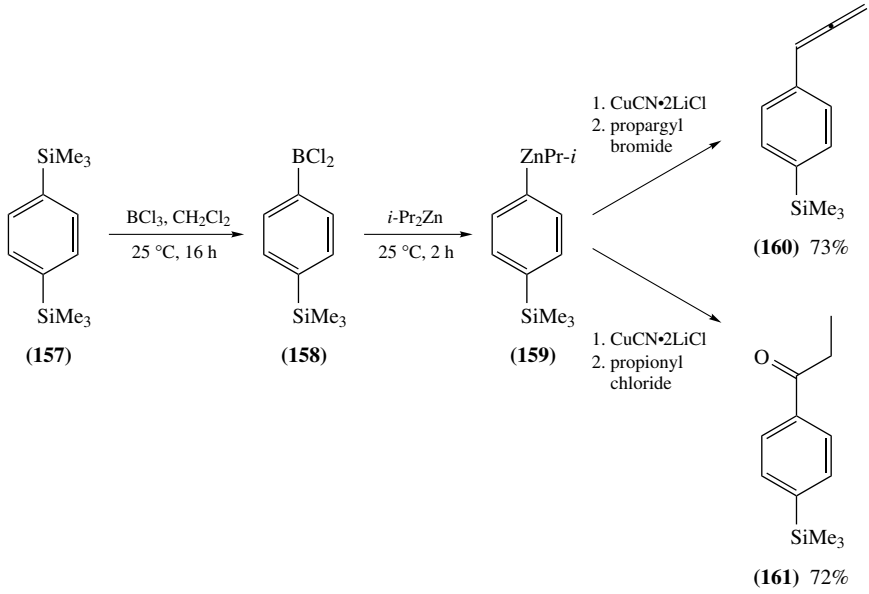

SCHEME 47. Synthesis of arylzinc derivatives via a Si/B/Zn exchange sequence

after transmetalation, with Et_2Zn, to a dialkylzinc. This reaction proceeds in the absence of solvent and at temperatures between 50–60 °C. A number of functionalized olefins, like allylic alcohols or amines, can be used directly. They afford the expected products in 60–75% yield (Scheme 48)[117]. This method is especially well suited for the preparation of functionalized diorganozincs for the asymmetric addition to aldehydes[117].

D. Diverse Methods of Preparation of Allylic Zinc Reagents

Several methods have been described for preparing allylic zinc derivatives. In contrast to alkylzincs, allylic zinc reagents are much more reactive due to the more ionic nature of the carbon–zinc bond in these organometallics. The chemistry displayed by these reagents is not representative of the usually moderate reactivity of organozinc derivatives. Tamaru and coworkers have converted various allylic benzoates to the corresponding organozinc intermediates in the presence of palladium(0) as catalyst.

The resulting allylic zinc reagents of the tentative structure **162** react with aldehydes with high stereoselectivity depending on the substitution pattern (Scheme 49)[118,119]. Substituted allylic zinc reagents can be prepared by the fragmentation of sterically hindered homoallylic alcoholates. This method allows the first access to functionalized allylic reagents. Thus, the treatment of the lithium homoallylic alcoholates **163a** and **163b** with zinc chloride leads to a fragmentation and produces the new allylic reagents **164a** and **164b** (Scheme 50), which have to be immediately trapped with benzaldehyde providing the new homoallylic alcohols **165a** and **165b** in 56–60% yield[120].

The addition of substituted allylic zinc reagents to aldehydes is usually unselective[121]. Furthermore, the direct zinc insertion to substituted allylic halides is complicated by radical homocoupling reactions. Both of these problems are solved by the fragmentation of homoallylic alcohols. Thus, the ketone **166** reacts with BuLi providing a lithium alcoholate which, after the addition of $ZnCl_2$ and an aldehyde, provides the expected addition product

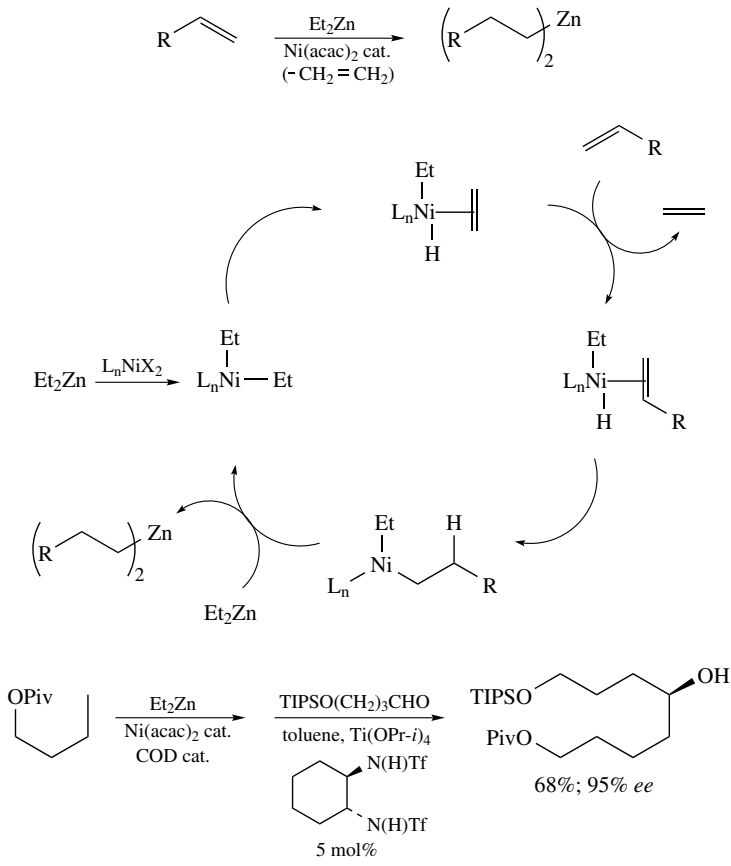

SCHEME 48. Ni-catalyzed hydrozincation of alkenes

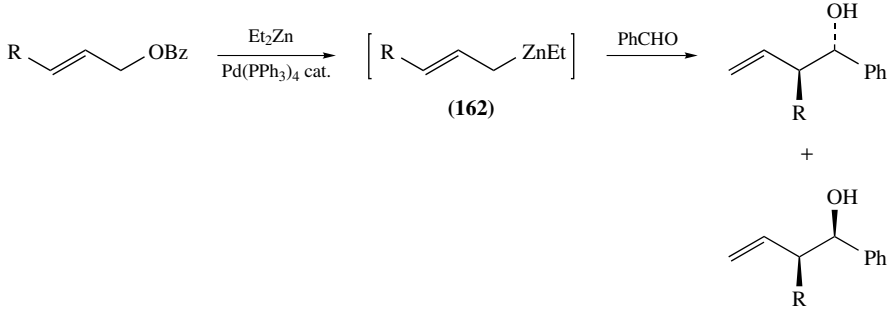

SCHEME 49. Umpolung of the reactivity of allylic systems

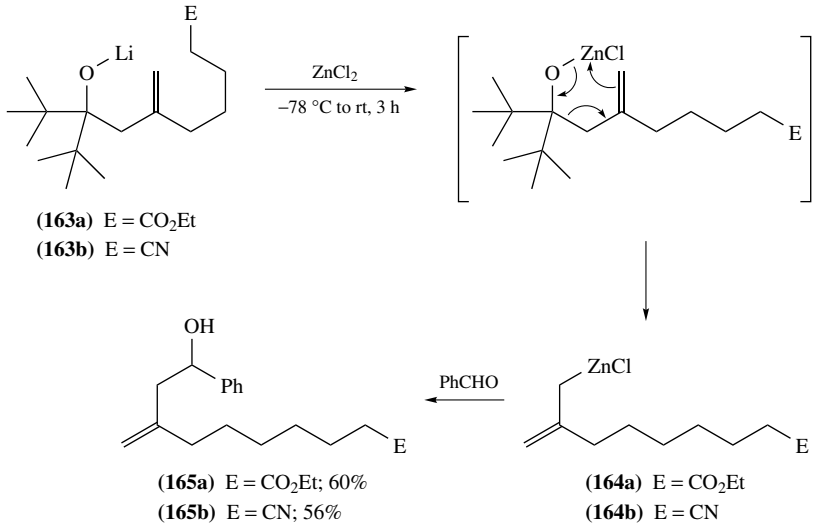

(163a) E = CO_2Et
(163b) E = CN

(165a) E = CO_2Et; 60%
(165b) E = CN; 56%

(164a) E = CO_2Et
(164b) E = CN

SCHEME 50. Preparation and uses of allylic zinc reagents by fragmentation reaction

167 with an excellent diastereoselectivity[120]. Oppolzer and coworkers have shown that the magnesium–ene reaction is a versatile method for adding allylic magnesium reagents to alkenes in an intramolecular fashion[122]. A zinc–ene[123] reaction can be initiated by the addition of BuLi to *tert*-butyl ketone **168** followed by the addition of zinc chloride. The resulting zincated spiro-derivative **169** is quenched with an acid chloride leading to the ketone **170** in 60% and >98% *syn*-diastereoselectivity (Scheme 51)[120d].

E. Preparation of Lithium Triorganozincates

Lithium triorganozincates are best prepared by the reaction of an alkyllithium (3 equivalents) with zinc chloride or by the addition of an alkyllithium to a dialkylzinc in an etheral solvent[124]. Lithium and magnesium trialkylzincates are more reactive compared to dialkylzincs or alkylzinc halides due to the excess of negative charge at the metallic zinc center which confers a higher nucleophilicity to the organic substituents. Thus, lithium trialkylzincates readily undergo 1,4-addition reactions to enones[125]. A methyl group can serve as a dummy ligand allowing a somewhat selective transfer of the alkyl substituent (Scheme 52)[124]. In the presence of chiral nitrogen-chelating ligands, asymmetric 1,4-

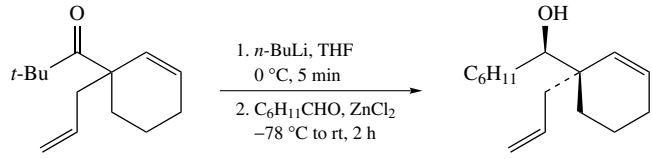

(166)

(167) 76%; *syn*:*anti* < 2:98

SCHEME 51. Diastereoselective reactions of substituted allylic zinc reagents generated by fragmentation

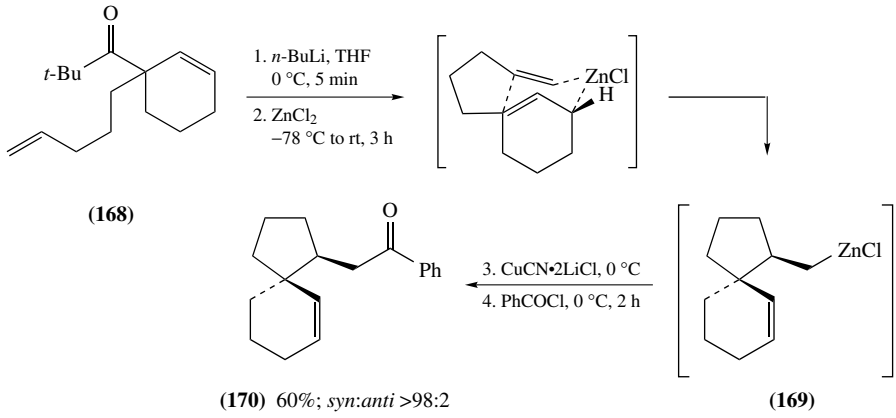

SCHEME 51. (*continued*)

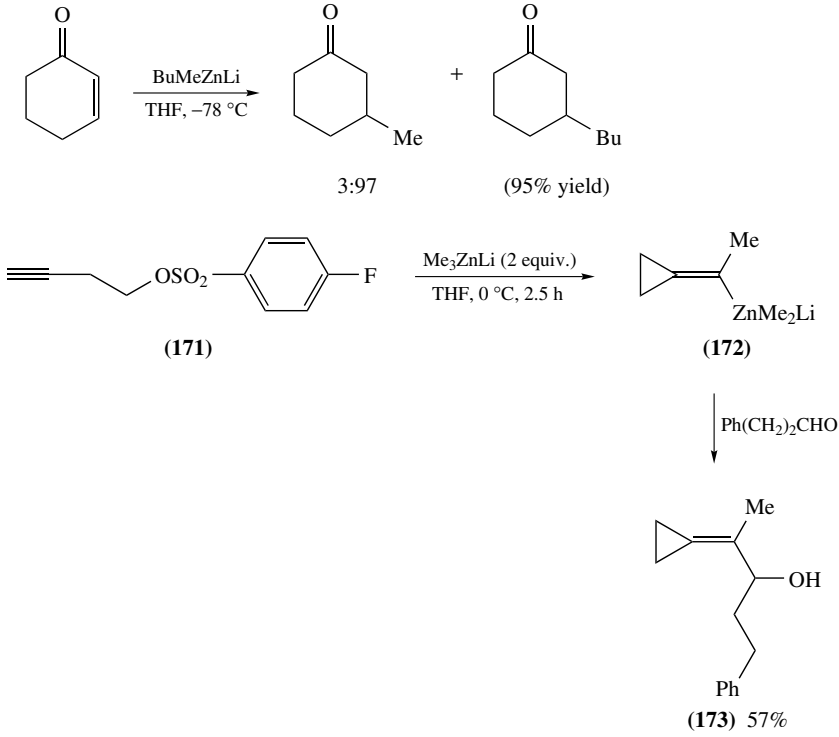

SCHEME 52. Preparation and uses of lithium triorganozincates

addition reactions can be performed with moderate enantioselectivity[126]. Interestingly, the addition of Bu_3ZnLi to nitrostyrene in a chiral solvent mixture of pentane and (*S*,*S*)-1,4-dimethylamino-2,3-dimethoxybutane leads to an optically enriched nitroalkane[127]. Triorganozincates can also be obtained by the reaction of the sulfonate **171** with Me_3ZnLi leading to the cyclopropylidene-alkylzinc reagent **172**. Its reaction with an aldehyde provides the allylic alcohol **173** in 57% yield (Scheme 52)[124d].

Lithium triorganozincates can also be prepared via an I/Zn exchange reaction. The exchange is highly chemoselective and tolerates sensitive functional groups like an epoxide or an ester. The reaction of aryl iodides **174a** and **174b** with Me_3ZnLi provides the functionalized lithium zincates **175a** and **175b**, which undergo respectively a ring closure and an addition to PhCHO leading to the products **176a** and **176b** in satisfactory yields (Scheme 53)[128].

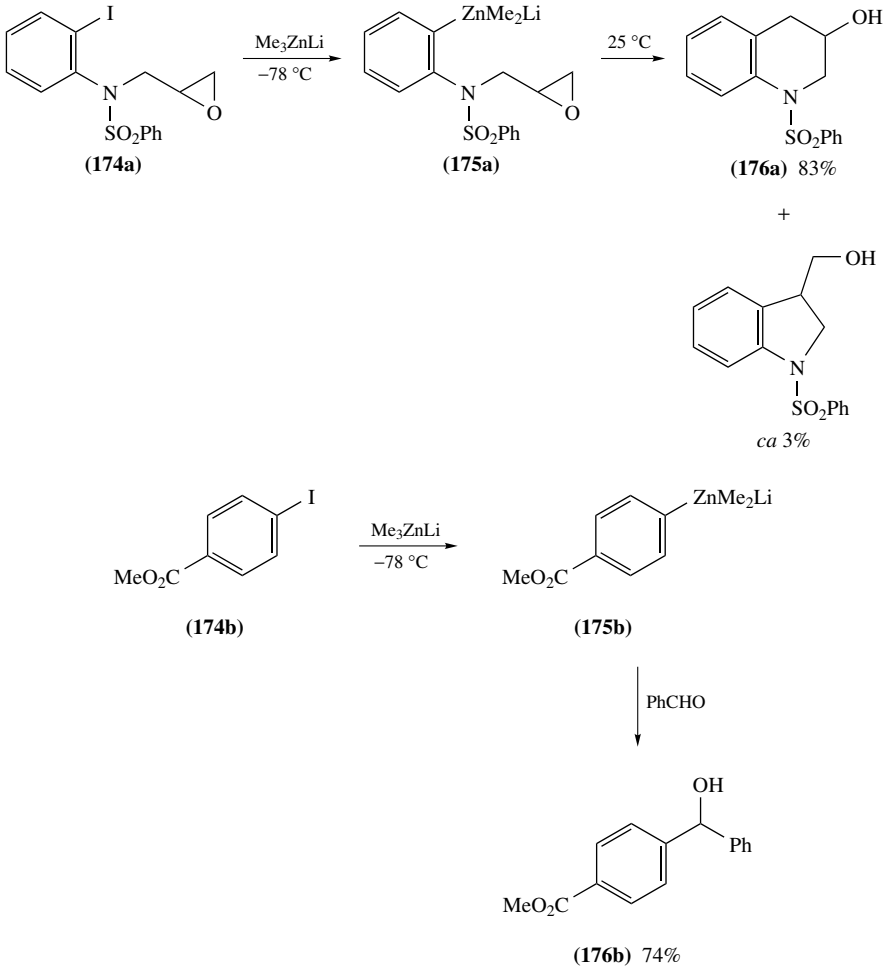

SCHEME 53. Preparation and uses of arylzincates via an I/Zn exchange reaction

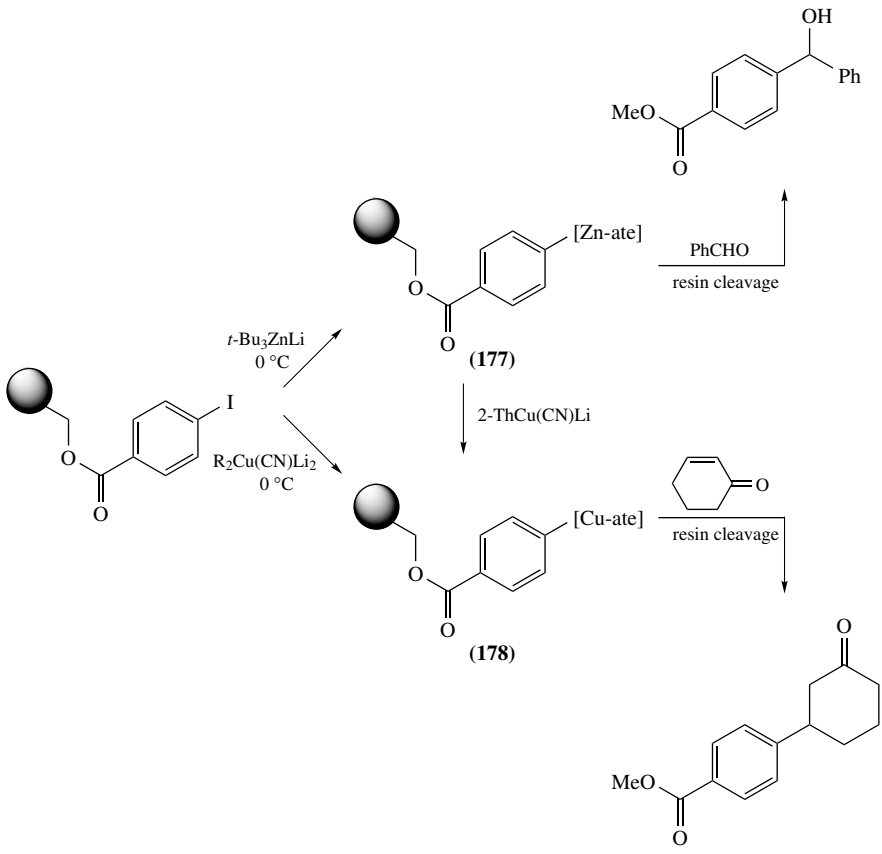

SCHEME 54. Preparation and uses of zincates on the solid phase

Immobilized zincates such as **177** can be prepared by treating serine-bound 4-iodobenzoate with t-Bu_3ZnLi at 0 °C[129]. They react readily with aldehydes. Transmetalation with lithium (2-thienyl)cyanocuprate provides the copper species **178** which undergoes 1,4-additions (Scheme 54). Lithium trialkylzincates can be used for the preparation of benzylic zinc reagents using a very elegant approach of Harada and coworkers. Thus, the treatment of the iodomesylate **179** with Bu_3ZnLi leads to the new zincate **180**, which undergoes a 1,2-migration leading to the benzylic zinc reagent **181**. It is readily quenched with an aldehyde leading to the alcohol **182** in 80% yield (Scheme 55)[130]. Interestingly, lithium and magnesium triarylzincates add to α,β-unsaturated sulfoxides in the presence of catalytic amounts of $Ni(acac)_2$ with good diastereoselectivity (Scheme 55)[131].

III. REACTIONS OF ORGANOZINC REAGENTS

The high covalent degree of the carbon–zinc bond and the small polarity of this bond leads to a moderate reactivity of these organometallics toward many electrophiles. Only powerful electrophiles react in the absence of a catalyst. Thus, bromolysis or iodolysis

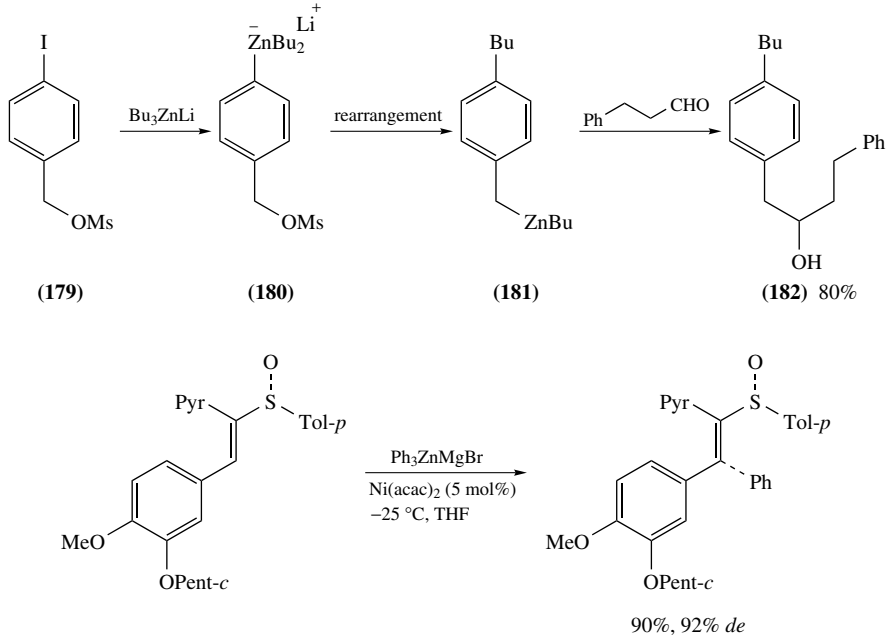

SCHEME 55. Reactivity of lithium trialkylzincates

reactions are high-yield reactions. In general, a direct reaction of organozincs with carbon electrophiles is not efficient and low yields are obtained. The addition of a catalyst is usually needed. The presence of empty *p*-orbitals at the zinc center facilitates transmetalations and a number of transition metal organometallics can be prepared in this way. These reagents are usually highly reactive toward organic electrophiles since the low-lying *d*-orbitals are able to coordinate and activate many electrophilic reagents. Many catalytic or stoichiometric transmetalations using zinc organometallics have been developed in recent years.

A. Uncatalyzed Reactions

Only reactive electrophiles react directly with organozinc derivatives. Allylic zinc reagents and to some extent propargylic zinc reagents are much more reactive. They add readily to carbonyl compounds or imines[132, 133]. Thus, the reaction of the ester substituted allylic zinc derivative **183** with the chiral imine **184** provides the lactam **185** with excellent diastereoselectivity (Scheme 56)[133]. An *in situ* generation of the allylic zinc reagent starting from the corresponding bromide **186** allows the addition to alkynes leading to skipped 1,3-dienes of type **187**[134].

Propargylic zinc derivatives react with aldehydes or ketones with variable selectivity, affording a mixture of allenic and homopropargylic alcohols[135]. However, under appropriate reaction conditions, high enantioselectivities and diastereoselectivities can be achieved. Marshall has shown that chiral propargylic mesylates such as **188** are converted to allenylzinc reagents **189** through treatment with a Pd(0) catalyst. Their addition to an aldehyde such as **190** provides the *anti*-homopropargylic alcohol **191** in 70% yield as a main diastereoisomer (d.r. = 85:15) (Scheme 57)[136].

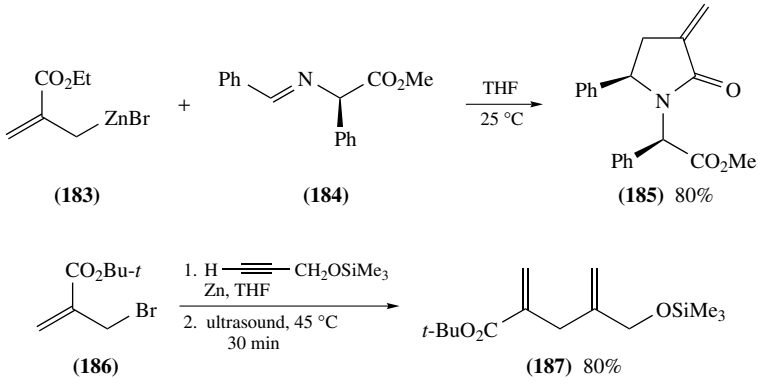

SCHEME 56. Reactions of functionalized allylic zinc reagents

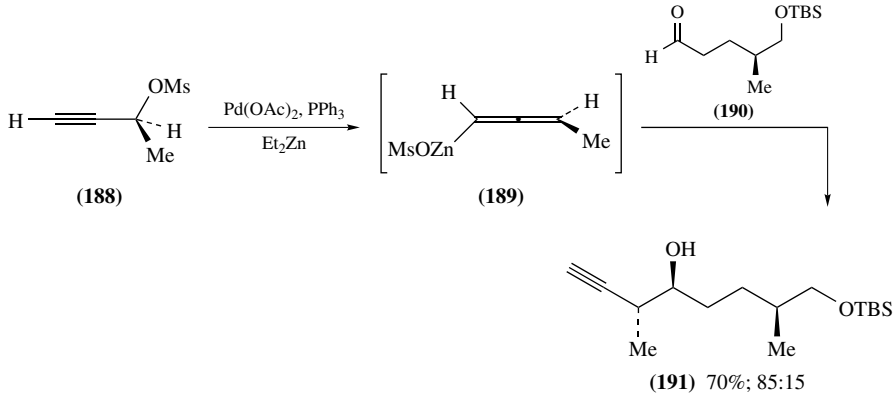

SCHEME 57. Preparation and reactions of chiral allenyl zinc reagents

Interestingly, 1-trimethylsilylpropargyl zinc reagents add to aldehydes with high regio- and diastereoselectivity leading to *anti*-homopropargylic alcohols[137]. The direct oxidation of organozincs with oxygen is an excellent method for preparing hydroperoxides[138]. Recently, a new synthesis of propargylic hydroperoxides has been developed by Harada and coworkers using allenylzinc intermediates[139]. The reaction of the mesylate **192** with the lithium zincate (Bu_3ZnLi; 2 equivalents) produces, after the addition of $ZnCl_2$ (0.5 equivalents), the allenylzinc species **193** which reacts at -40 °C with O_2 in the presence of trimethylsilyl chloride providing the hydroperoxide **194** in 60% yield (Scheme 58)[139].

The moderate reactivity of zinc organometallics is compatible with the preparation of various hydroperoxides with good selectivity. The use of perfluorinated solvents allows one to perform the oxygenation reaction at low temperature owing to the exceptionally high oxygen solubility in these media[140]. Functionalized organozincs prepared by hydrozincation, carbozincation or by boron–zinc exchange can be oxidized to the corresponding alcohols or hydroperoxides depending on the reaction conditions[141]. Tosyl cyanide reacts with a range of zinc organometallics providing the corresponding nitriles in excellent yields[142]. The functionalized alkylzinc species **195** is smoothly converted to the corresponding nitrile **196** in 67% yield. Interestingly, whereas the reaction of tosyl cyanide

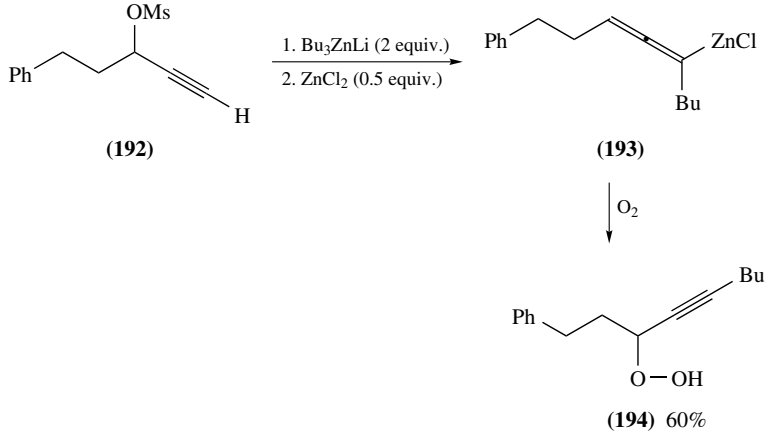

(192) **(193)** **(194)** 60%

SCHEME 58. Preparation of propargylic hydroperoxides

with benzylic bromide produces selectively 1-methylbenzonitrile in 76% yield, the cyanation of the corresponding copper reagent furnishes benzyl cyanide as sole product in 80% yield (Scheme 59)[142]. The reaction of 1,1-mixed bimetallics of magnesium and zinc, such as **197**[143], prepared by the addition of allylzinc bromide to (Z)-octenylmagnesium bromide with tosyl cyanide produces the nitrile **198** in 93% yield (Scheme 59)[142].

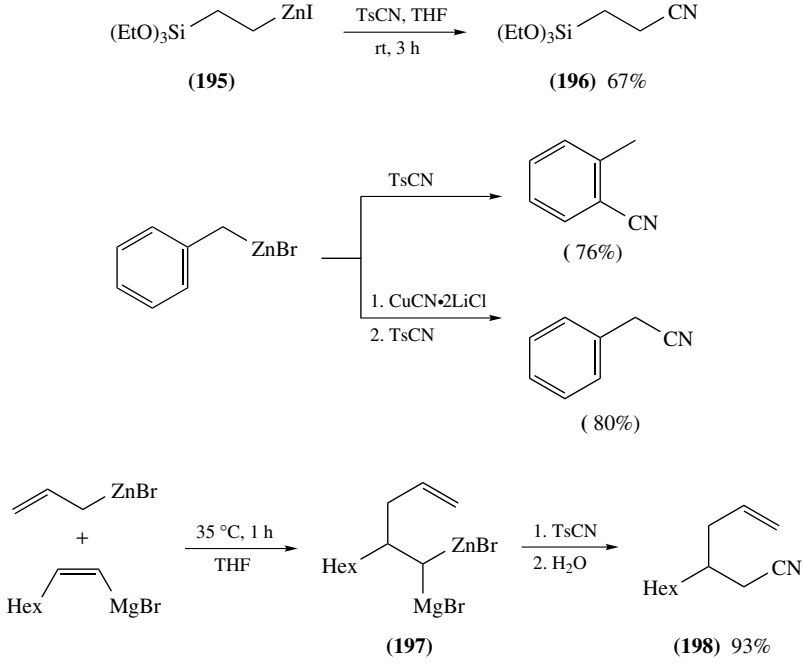

(195) **(196)** 67% **(197)** **(198)** 93%

SCHEME 59. Electrophilic cyanation of organozinc reagents

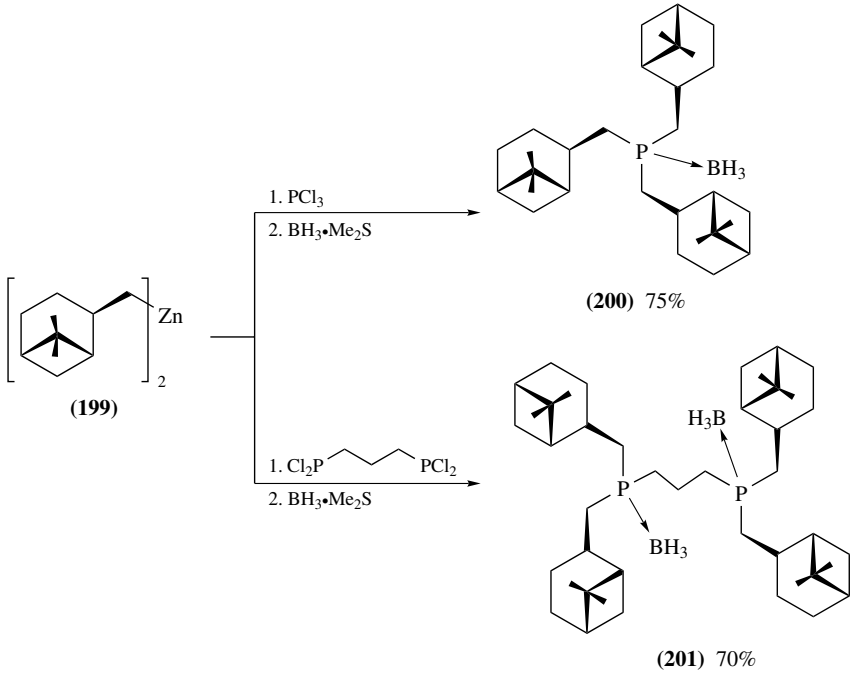

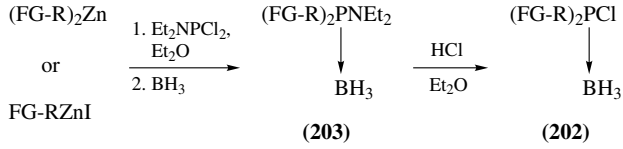

SCHEME 60. Preparation of polyfunctional phosphines

The reaction with various chlorophosphine derivatives leads to polyfunctional phosphines with high yield[144]. The hydroboration of β-pinene with BH_3•Me_2S gives *bis*-myrtanylzinc **199** in quantitative yield (Scheme 60)[144b]. The coupling of **199** with various chlorophosphines or PCl_3 provides new chiral phosphines, such as **200** and **201**. Polyfunctional chlorophosphines protected as their BH_3 complex, such as **202**, can be prepared in two steps by the reaction of Et_2NPCl_2 with polyfunctional organozinc reagents. After protection with BH_3, the borane complexes **203** are obtained in excellent yields. Treatment of **203** with HCl in ether leads to the borane-protected chlorophosphines of type **202** (Scheme 60)[145].

Similarly functionalized organometallics such as the serine-derived zinc–copper derivate **204** react under mild conditions with $ClPPh_2$. The resulting phosphine was protected as a sulfide providing enantiomerically pure **205** in 75% yield. Modification of the protecting groups furnishes the selectively protected diphenylphosphinoserine **206** in 80% yield (Scheme 61)[146a].

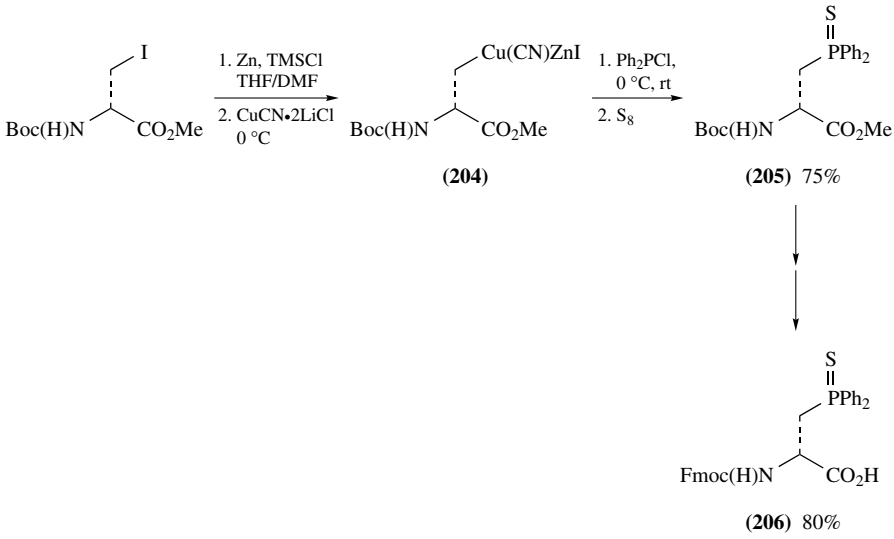

SCHEME 61. Preparation of chiral functionalized phosphines

A combination of a substitution reaction with a chlorophosphine followed by a hydroboration and boron–zinc exchange allows the preparation of the mixed 1,2-diphosphine **207** in good yield (Scheme 62)[145].

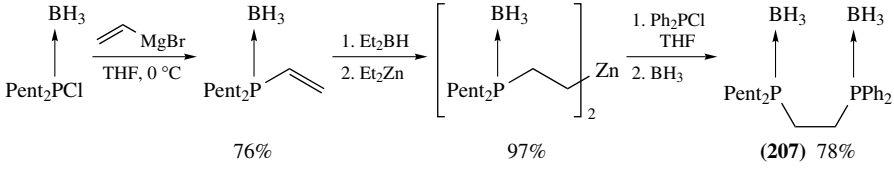

SCHEME 62. Preparation of mixed diphosphines using functionalized zinc organometallics

Reactive organometallic reagents, such as $Cr(CO)_5$•THF, readily add diorganozincs leading, in the presence of CO (1 atm) and $Me_3O^+BF_4^-$ (rt, 2 h), to functionalized Fischer carbene complexes[146b]. Excellent addition reactions are also obtained with iminium trifluoroacetates, such as **208** (Scheme 63). The reaction of the aminal **209** with trifluoroacetic anhydride in CH_2Cl_2 at 0 °C gives the iminium trifluoroacetate **208** with quantitative yield. Its reaction with phenylzinc chloride furnishes the expected amine **210** in 85% yield[147]. Interestingly, this approach can be extended to functionalized organomagnesium reagents[148]. Functionalized diarylzincs such as **211** add to the activated Schiff base **212** leading to amino acid **213** in 62% yield[149].

The formation of activated iminium intermediates derived from nitrogen heterocycles has been reported by Comins[150]. The activation of pyridine derivative such as **214** with phenyl chloroformate provides the pyridinium salt **215**, which smoothly reacts with the zinc homoenolate **216**[151] leading to the addition product **217** in 66% yield[150]. The reaction

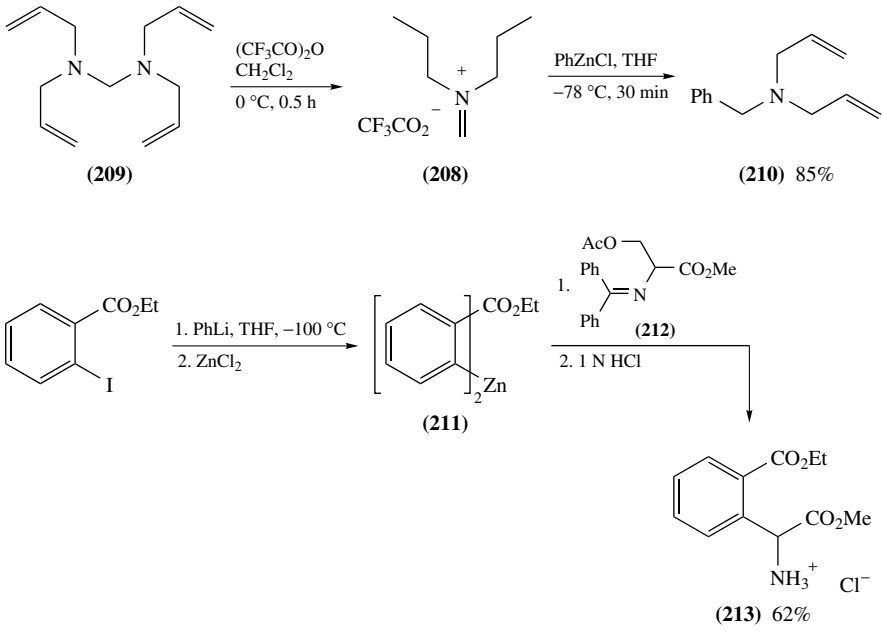

SCHEME 63. Reaction of zinc organometallics with iminium intermediates

of the unsaturated amide **218** with $Ph_3C^+BF_4^-$ produces *N*-acyliminium ions of type **219** which react with Ph_2Zn in CH_2Cl_2, producing the desired α-substituted amine **220** in 95% yield (d.r. = 98.8:1.2); see Scheme 64[152]. Benzotriazole is an excellent leaving group and the readily available imidazolidin-2-ones of type **221** react with aryl-, alkenyl- or alkylzinc derivatives via an elimination–addition mechanism providing the *trans*-products of type **222** with >99% diastereoselectivity (Scheme 65)[153].

The addition of zinc organometallics to *in situ* generated oxenium ions by the reaction of mixed acetals with TMSOTf[154] allows a highly stereoselective preparation of protected *anti*-1,3-diols of type **223** (Scheme 66). The addition of TMSOTf triggers also the allylic substitution of glycal derivatives, providing the substitution products of type **224** with excellent regio- and diastereoselectivity.

The opening of epoxides with zinc reagents is a difficult reaction. However, activated epoxides such as the glycal epoxides **225** react with diorganozincs in the presence

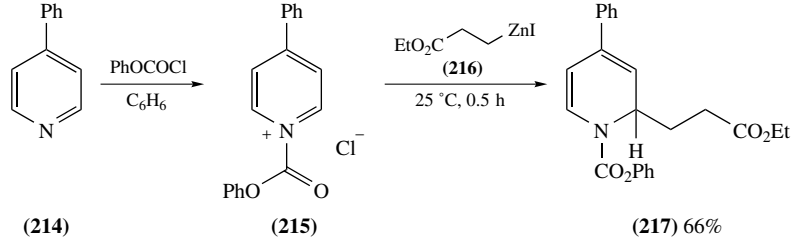

SCHEME 64. Reaction of zinc organometallics with pyridinium derivatives

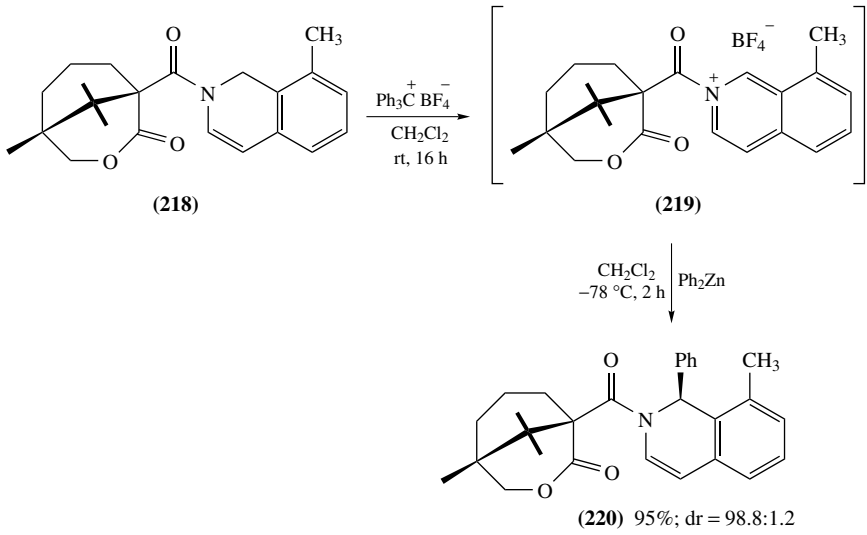

(218) **(219)**

(220) 95%; dr = 98.8:1.2

SCHEME 64. (*continued*)

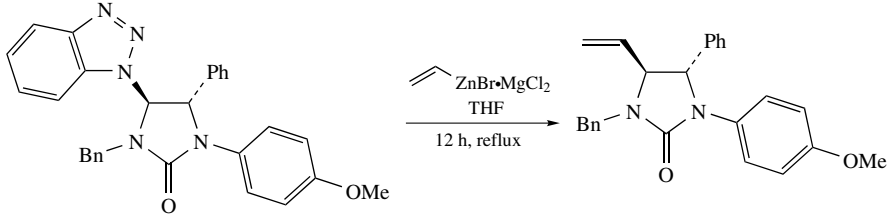

(221) **(222)** 68%; *trans*:*cis* > 99:1

SCHEME 65. Addition of vinylzinc bromide to iminium salts generated from benzotriazole derivatives

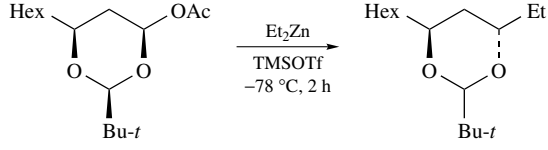

(223) 100%

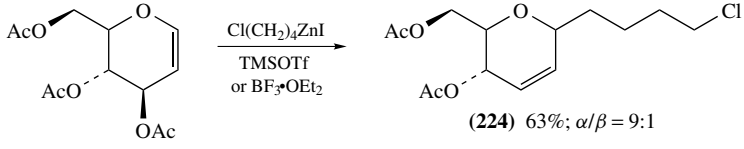

(224) 63%; $\alpha/\beta = 9:1$

SCHEME 66. Reaction of zinc reagents with acetals and related compounds

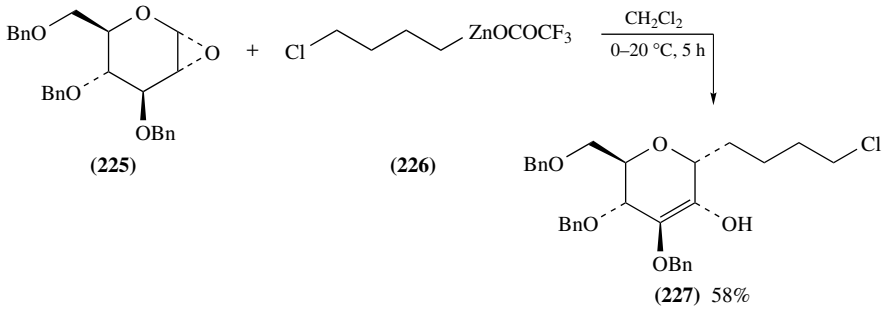

SCHEME 66. (*continued*)

of CF_3CO_2H[155]. Presumably the reaction of R_2Zn with CF_3CO_2H produces the highly Lewis-acidic species $RZnOCOCF_3$ (**226**). This reaction proceeds smoothly in CH_2Cl_2 and furnishes the α-C-glycoside **227** in 58% yield.

Although alkylzinc derivatives add only slowly to aldehydes, alkenylzinc derivatives display a higher reactivity. Thus, the addition of vinylzinc chloride **228** to the aminoaldehyde **229** provides the allylic alcohol **230** in 60% yield[156]. The addition rate can be increased by performing the reaction in the presence of a Lewis acid. Thus, the addition of the homoenolate **216** to the aminoaldehyde **231** provides the aminoalcohol **232** with good diastereoselectivity (Scheme 67)[157]. Reactive benzylic or related zinc reagents, such as **233**, add smoothly to aldehydes providing the allylic alcohol **234** in almost quantitative yield (Scheme 67)[158]. In a non-complexing solvent, such as dichloromethane,

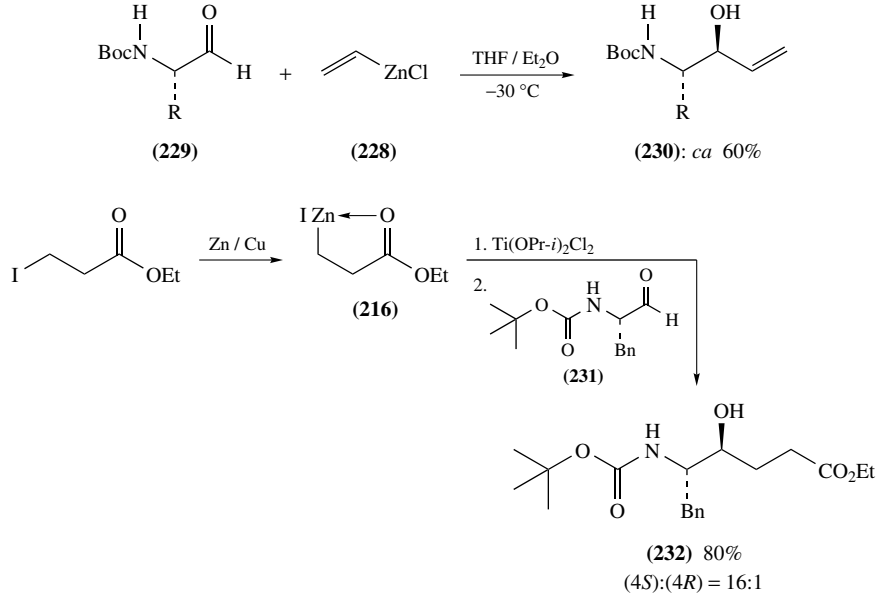

SCHEME 67. Addition of organozinc halides to aldehydes

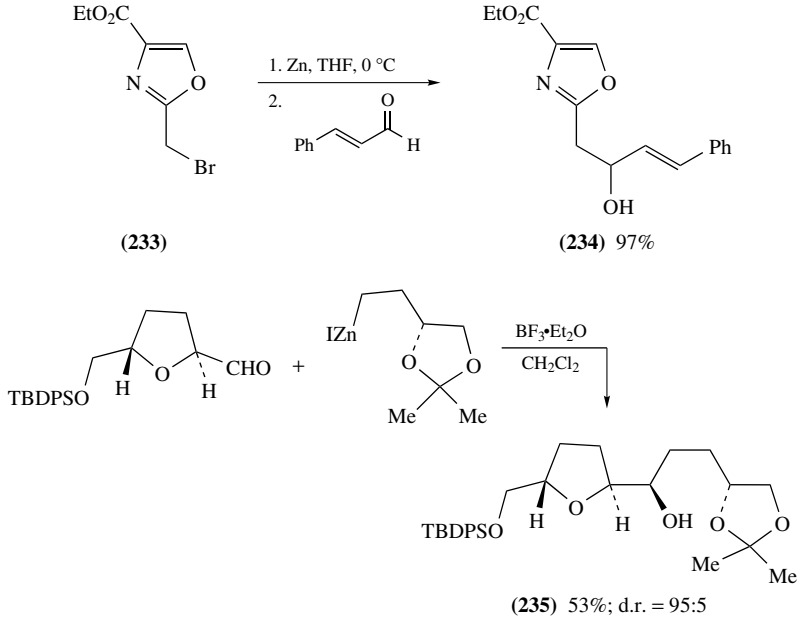

SCHEME 67. (*continued*)

functionalized alkylzinc halides add to α-functionalized aldehydes, leading to the addition product **235** again with a remarkable diastereoselectivity (Scheme 67)[158].

Benzylic acetates are unreactive toward organozinc compounds. However, various ferrocenyl acetates, such as **236**, react with dialkylzinc halides in the presence of $BF_3{\bullet}OEt_2$ with retention of configuration leading to the chiral ferrocenyl derivatives like **237** (Scheme 68)[159].

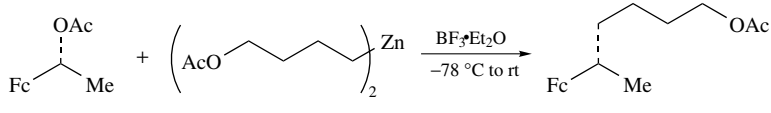

(236) 98% *ee*
Fc = ferrocenyl

(237) 70%, 98% *ee*

SCHEME 68. Substitution with retention on ferrocenyl derivatives

The reactivity of zinc organometallics can be dramatically increased by adding polar solvents like (NMP). Under these conditions various diorganozincs add to a range of Michael acceptors like α,β-unsaturated ketones, aldehydes, nitriles or nitro derivatives (Scheme 69)[160]. The preparation of mixed diorganozincs bearing non-transferable Me_3SiCH_2 groups allows a more efficient transfer of the functionalized group to the Michael acceptor (Scheme 70)[98].

In the case of an intramolecular 1,4-addition, no activation is required[161]. The iodoenone **238** is readily converted into the corresponding alkylzinc iodide, which undergoes an intramolecular addition at 25 °C in THF affording the bicyclic ketone **239** in 65–67%

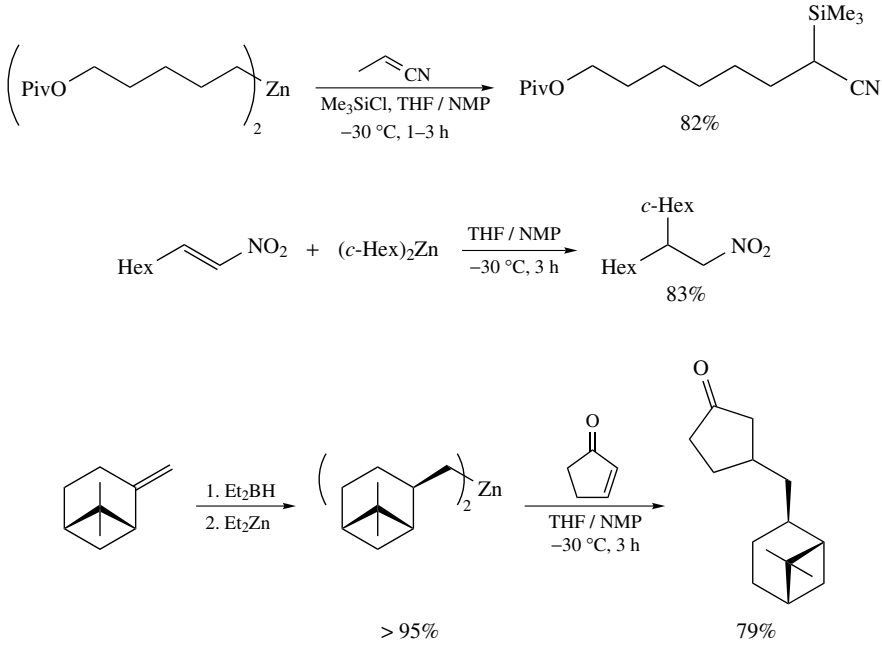

SCHEME 69. NMP promoted Michael additions of diorganozincs

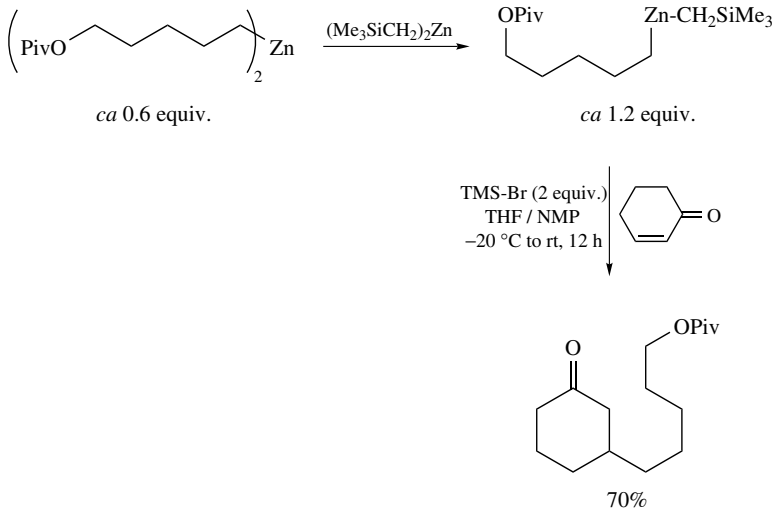

SCHEME 70. Mixed diorganozincs for conjugate addition reactions

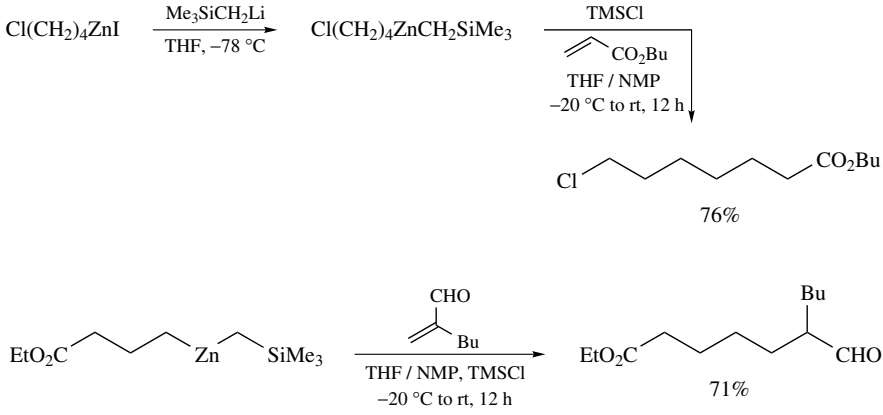

SCHEME 70. (*continued*)

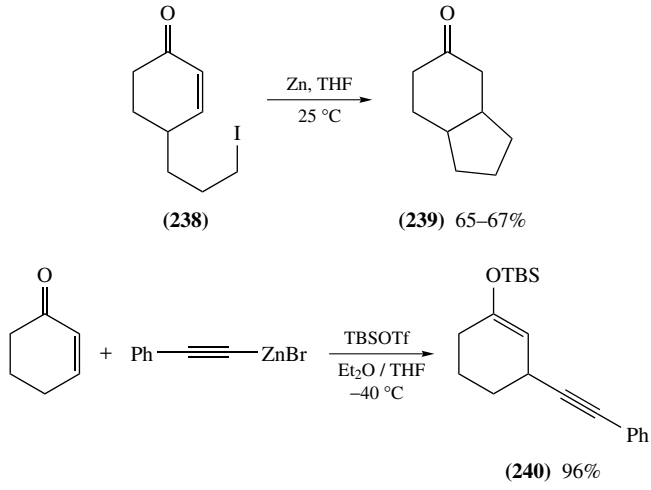

SCHEME 71. Michael addition of organozinc halides

yield.[161]. The addition of alkynylzinc halides to enones is best performed in the presence of *tert*-butyldimethylsilyl triflate. Under these conditions, very high yields of the conjugated adducts, such as **240**, are obtained (Scheme 71)[162].

The addition of the electrophilic silyl reagent strongly activates the enone. It has also been found that Lewis acids, such as $AlCl_3$, accelerate the reaction of dialkylzincs with acid chlorides in CH_2Cl_2[163].

B. Copper(I) Catalyzed Reactions

The moderate intrinsic reactivity of zinc organometallics can be increased by transmetalation with various transition metal salts. Especially useful is the transmetalation of diorganozincs or organozinc halides with the THF-soluble complex of copper(I) cyanide

and lithium chloride (CuCN•2LiCl)[10]. The simple mixing of organozinc compounds with CuCN•2LiCl produces the corresponding copper species tentatively represented as FGRCu(CN)ZnX (**241**). Their reactivity is similar, but somewhat reduced compared to copper species prepared from organomagnesium or lithium compounds[164]. The structure of the mixed copper–zinc reagents is only known by EXAFS spectroscopy, indicating that the cyanide ligand is coordinated to the copper center[165]. In contrast to lithium or magnesium derived organocopper reagents, they display an increased thermal stability and alkylzinc–copper reagents can be heated in 1,2 dimethoxyethane (DME) or DMPU at 60–85 °C for several hours without appreciable decomposition[166]. A wide range of electrophiles reacts very efficiently with the copper–zinc compounds **241** leading to polyfunctional products (Scheme 72)[6].

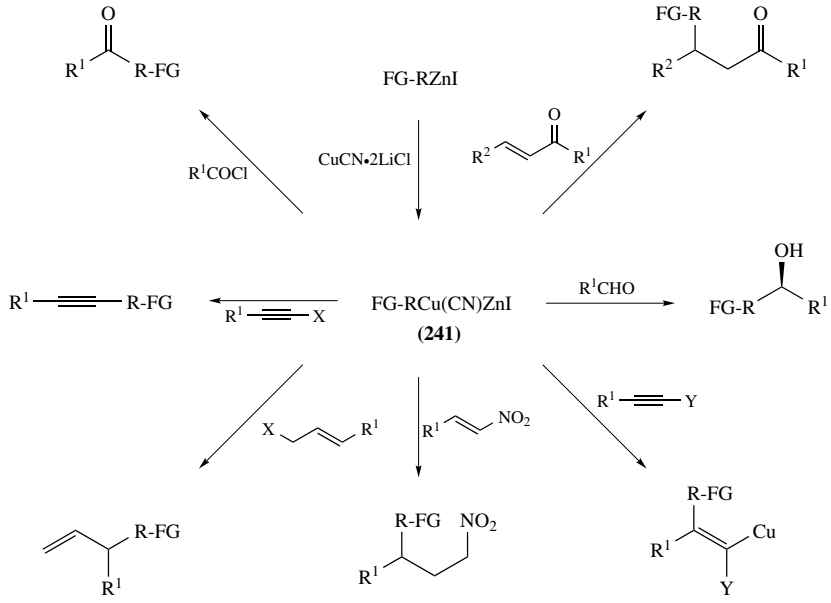

SCHEME 72. General reactivity pattern of zinc–copper reagents

1. Substitution reactions

Substitution reactions of zinc or zinc–copper organometallics with R_3SiCl are usually difficult, but R_3SnCl reacts much more readily. By using DMF as solvent, the heterocyclic zinc reagent **242** reacts with Ph_3SnCl providing the tin derivative **243** in 37% yield[167]. The β-zincated phosphonate **244** provides under mild conditions the expected stannylated product **245** in 81% yield (Scheme 73)[55]. Allylation reactions with zinc organometallics proceed in the presence of copper salts with very high S_N2'-selectivity. This is in contrast to the palladium or nickel catalyzed reactions which proceed via a π-allyl palladium intermediate and afford generally the coupling product at the less substituted end of the allylic system.

Thus, the zincated propionitrile **246**[168] reacts with cinnamyl bromide in the presence of CuCN•2LiCl leading to the S_N2'-substitution product **247**, whereas in the presence of catalytic amounts of $Pd(PPh_3)_4$ the formal S_N2-substitution product **248** is obtained

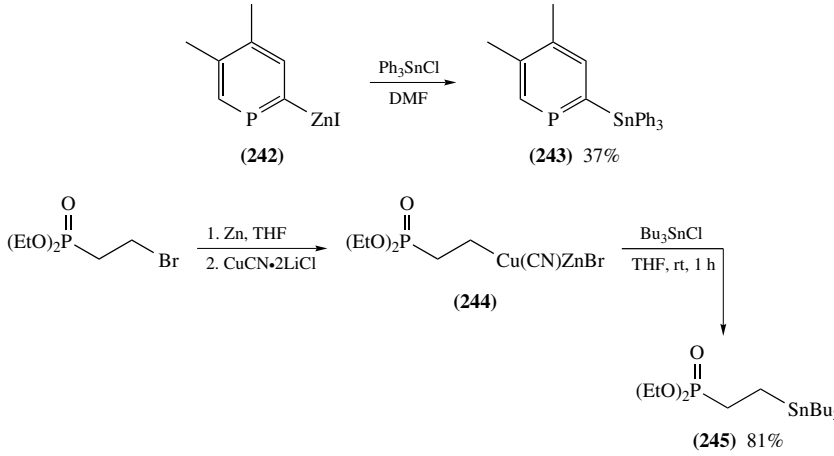

SCHEME 73. Stannylation of zinc–copper reagents

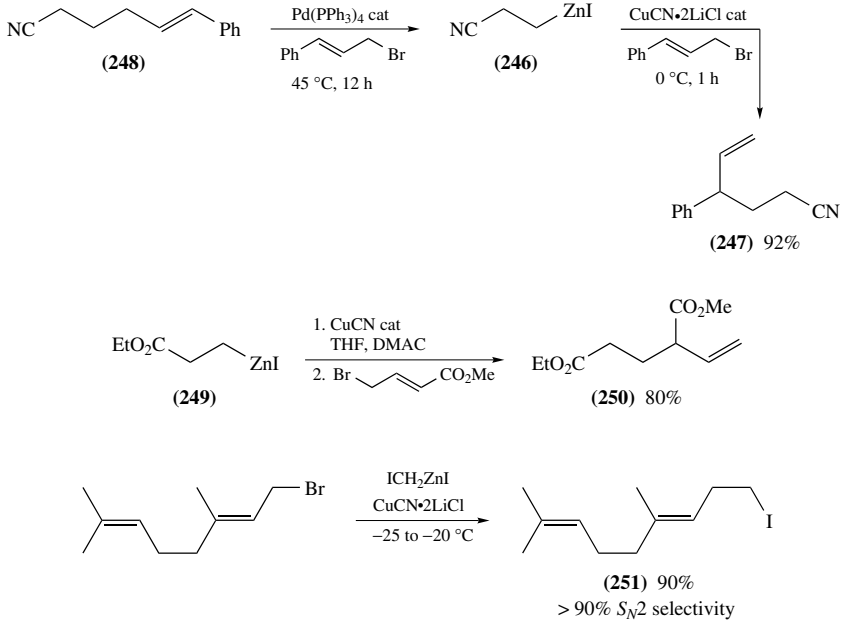

SCHEME 74. Regioselective allylations with zinc–copper reagents

(Scheme 74). The presence of a functional group, such as an ester like in **249**, does not modify this regioselectivity and affords the S_N2'-product **250** in 80% yield (Scheme 74)[168b]. Interestingly, the zinc–copper carbenoid $ICH_2Cu(CN)Znl$ affords as an exception the S_N2-substitution product **251** allowing a homologation of an allylic bromide by a CH_2I unit (Scheme 74)[47b]. A range of polyfunctional zinc–copper reagents are readily allylated[6].

A quinine alkaloid derivative containing a vinyl group, such as **252**, has been hydroborated, undergone a boron–zinc exchange and copper(I) catalyzed allylation, leading to the alkaloid derivative **253**[103b]. A new route to hydrophobic amino acids is possible by using the reaction of the zinc reagent with prenyl chloride in the presence of $CuBr{\bullet}Me_2S$ (0.1 equivalent). Under these conditions, a mixture of S_N2 and S_N2' products (55:45) is obtained. They can be readily separated by taking advantage of the higher reactivity of trisubstituted alkenes compared with terminal alkenes toward MCPBA (Scheme 75)[169].

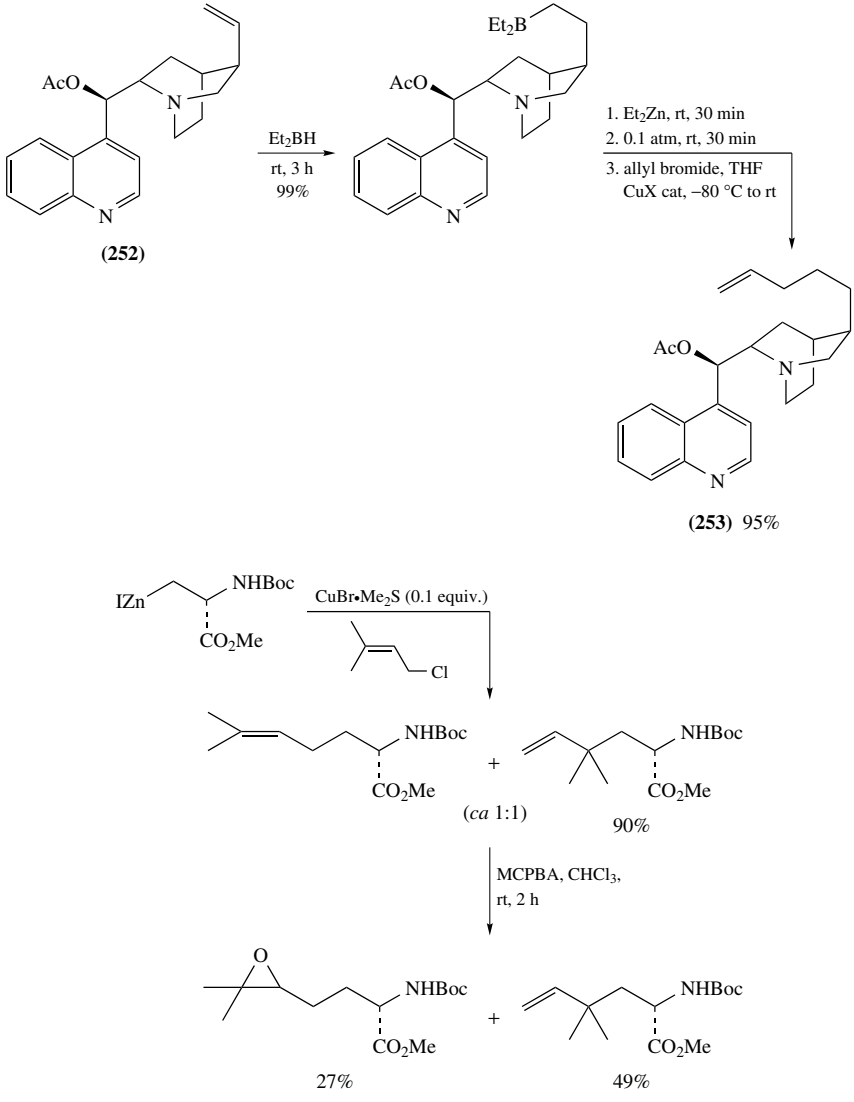

SCHEME 75. Allylic substitutions with zinc–copper reagents

Although zinc–copper reagents do not open epoxides, the more reactive α,β-unsaturated epoxides react readily with various functionalized zinc–copper organometallics[170] or functionalized zinc reagents in the presence of a catalytic amount of MeCu(CN)Li[171]. Thus, the opening of δ-epoxy-α,β-unsaturated esters such as **254** with Me_2Zn•CuCN proceeds with high *anti*-stereoselectivity leading to the allylic alcohol **255** in 96% yield. Also, the opening of the unsaturated epoxide (**256**) affords the allylic alcohol **257** in 98% yield (Scheme 76).

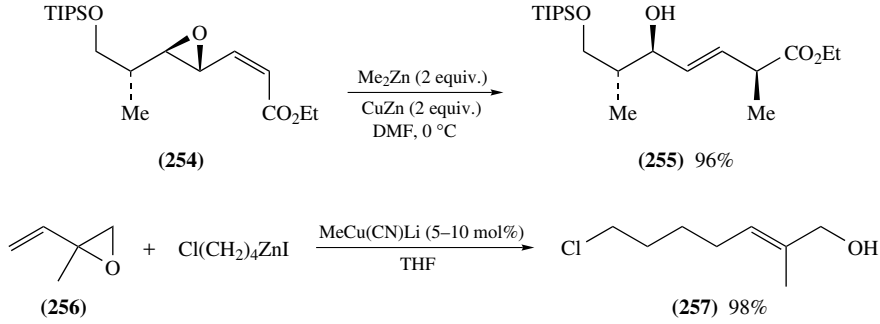

SCHEME 76. Opening of α,β-unsaturated epoxides with copper–zinc reagents

Interestingly, the high S_N2' selectivity of organozinc–copper derivatives allows the performance of multiple allylic substitutions with excellent results. Thus, the reaction of the multi-coupling reagent[172] **258** with an excess of copper–zinc reagent provides the double S_N2'-reaction product **259** in 89% yield (Scheme 77)[48b]. Propargylic halides or

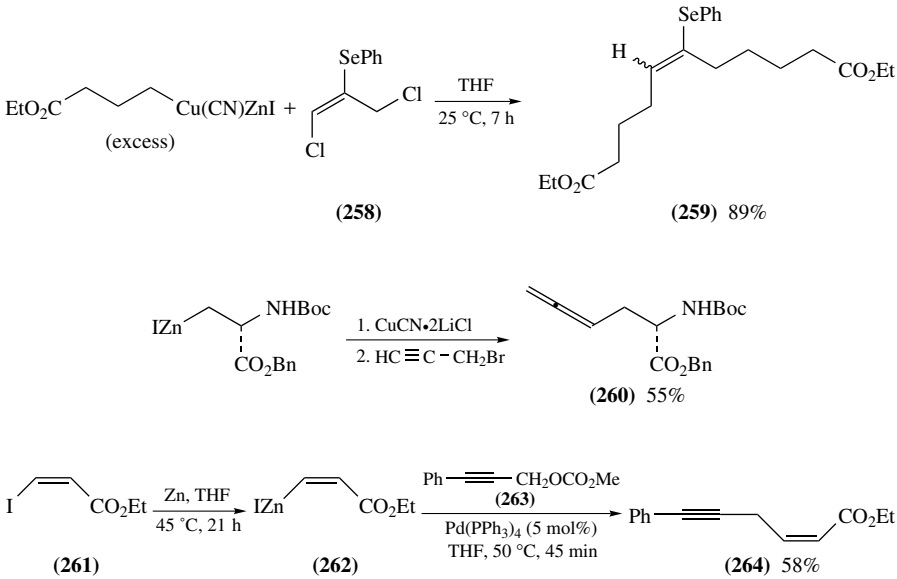

SCHEME 77. Reaction of zinc organometallics with unsaturated halides

sulfonates react with zinc–copper reagents leading to the S_N2'-substitution product like the allenic aminoacid derivative **260**. Interestingly, the regioselectivity is reversed by performing the reaction in the presence of catalytic amounts of palladium(0). Thus, the insertion of zinc powder into the Z-alkenyl iodide **261** is complete in THF at 45 °C within 21 h. The resulting Z-zinc reagent **262** (E:Z > 99:1) reacts with the propargylic carbonate **263** in the presence of $Pd(PPh_3)_4$ (5 mol%) leading formally to the S_N2-substitution product **264** in 58% yield (Scheme 77)[173].

Propargylic mesylates such as fluorine-substituted derivative **265** react with PhZnCl in the presence of $Pd(PPh_3)_4$ (5 mol%) in THF at 0 °C within 2 h to provide the *anti*-S_N2' product in excellent yield and complete transfer of the stereochemistry leading to the allene **266** (Scheme 78)[174]. Copper(I) catalyzed allylic substitutions with functionalized diorganozincs proceed with high S_N2' selectivity. Thus, the reaction of the chiral allylic phosphate **267**[175] with 3-carbethoxypropylzinc iodide in the presence of CuCN•2LiCl (2 equivalents) furnishes the *anti*-S_N2' substitution product **268** in 68% yield. By the addition of *n*-BuLi (1.2 equivalents) and TMSCl (1.5 equivalents), the bicyclic enone **269** is obtained in 75% yield and 93% *ee* (Scheme 79)[176].

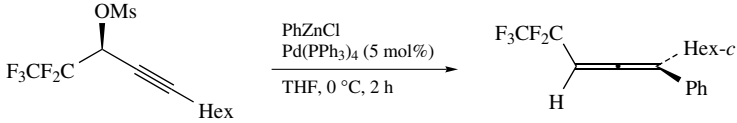

(265) 94% *ee* **(266)** 70%; 94% *ee*

SCHEME 78. Stereoselective propargylic substitution reaction

This reaction can also be extended to open-chain systems. In this case, chiral allylic alcohols have been converted into pentafluorobenzoates which proved to be appropriate leaving groups. Whereas both (E)- and (Z)-allylic pentafluorobenzoates undergo the S_N2' substitution, in the case of (E)-substrates, two conformations **270** and **271** are available for an *anti*-substitution providing, besides the major *trans*-product (*trans*-**272**), also *ca* 10% of the minor product *cis*-**272** (Scheme 79). By using the (Z)-allylic pentafluorobenzoates, only *trans*-substitution products are produced since the conformation **273** leading to a *cis*-product is strongly disfavored due to allylic 1,3-strain[177]. Thus,

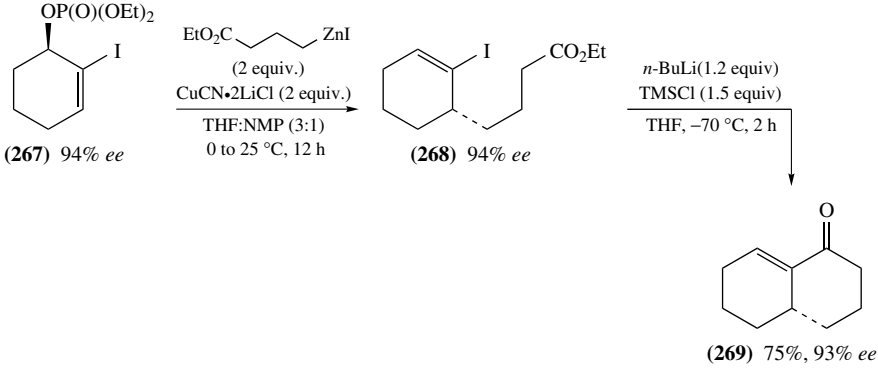

(267) 94% *ee* **(268)** 94% *ee* **(269)** 75%, 93% *ee*

SCHEME 79. Stereoselective *anti*-S_N2'-substitutions

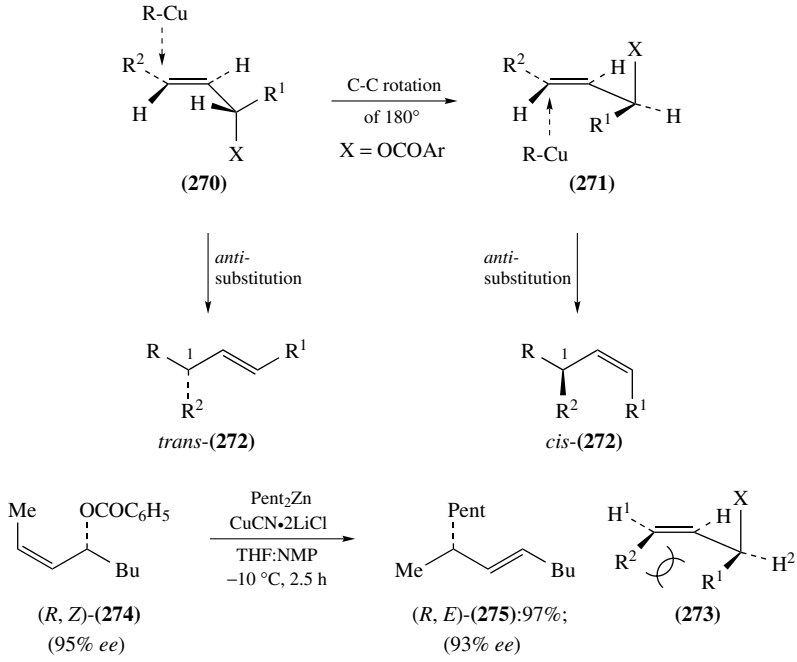

SCHEME 79. (*continued*)

the *cis*-allylic pentafluorobenzoates (*R*,*Z*)-**274** reacts with $Pent_2Zn$ furnishing only the *trans*-S_N2'-substitution product (*R*,*E*)-**275** in 97% yield with 93% *ee* (Scheme 79)[178].

Interestingly, this substitution reaction can be applied to the stereoselective assembly of chiral quaternary centers. The trisubstituted allylic pentafluorobenzoates (*E*)- and (*Z*)-**276** readily undergo a substitution reaction at $-10\,^{\circ}C$ with $Pent_2Zn$ furnishing the enantiomeric products (*S*)- and (*R*)-**277** with 94% *ee*. The ozonolysis of (*R*)-**277** gives, after reductive work-up, the chiral aldehyde (*S*)-**278** in 71% yield with 94% *ee*. The *anti*-selectivity is observed with a wide range of diorganozincs like primary and secondary dialkylzincs, as well as diaryl- and dibenzyl-zinc reagents[178]. It has been applied to an enantioselective synthesis of (+)-ibuprofen **279** (Scheme 80). Even sterically hindered allylic substrates like the allylic phosphonate **280** react with mixed diorganozinc reagents of the type $RZnCH_2SiMe_3$ in the presence of CuCN•2LiCl, providing only the S_N2' substitution product regardless of the presence of the two methyl groups adjacent to the allylic center. The reaction with $EtO_2C(CH_2)_2ZnCH_2SiMe_3$ provides the *anti*-substitution product **281** in 81% with 97% *ee*. It is readily converted in (R)-α-ionone **282** (45%; 97% *ee*). The *ortho*-diphenylphosphanyl ligand orients the S_N2' substitution in a *syn*-manner with high regio- and stereoselectivity to the *cis*-product (Scheme 81)[179,180].

Allylic substitution using organozinc reagents can also be performed using a chiral catalyst[181]. The use of a modular catalyst is an especially versatile strategy and has been applied to the stereoselective preparation of quaternary centers with great success[182]. In the presence of 10 mol% of the modular ligand **283**, highly enantioselective substitutions of allylic phosphates like **284**, leading to the fish deterrent sporochnol (**285**: 82% yield, 82% *ee*), have been performed.

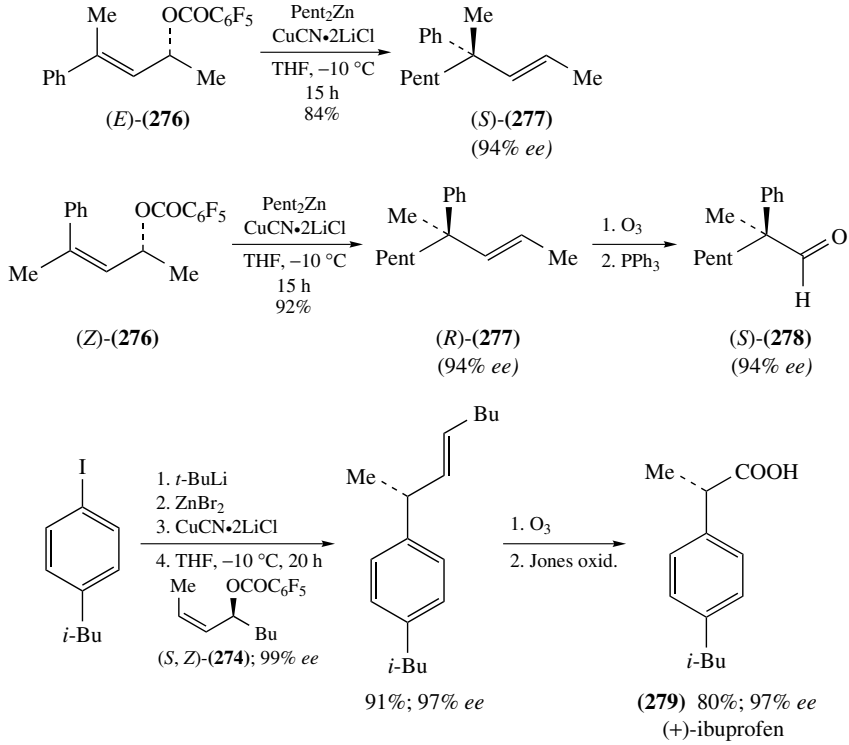

SCHEME 80. Preparation of quarternary chiral centers and (+)-ibuprofen synthesis

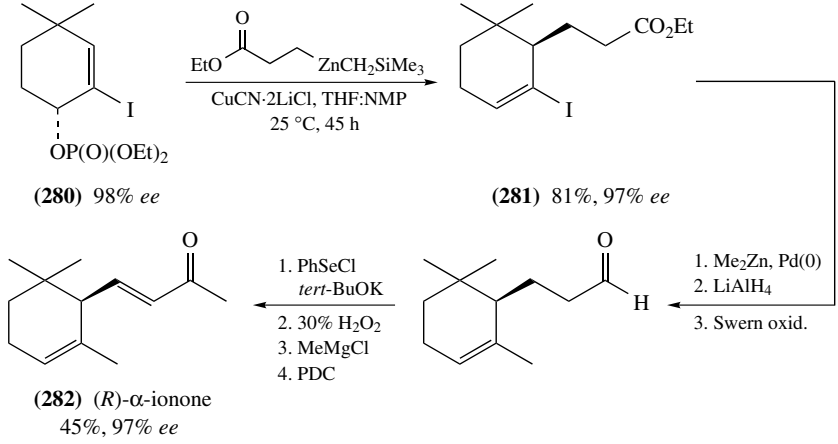

SCHEME 81. Synthesis of (*R*)-α-ionone using a stereoselective *anti*-S_N2'-substitution

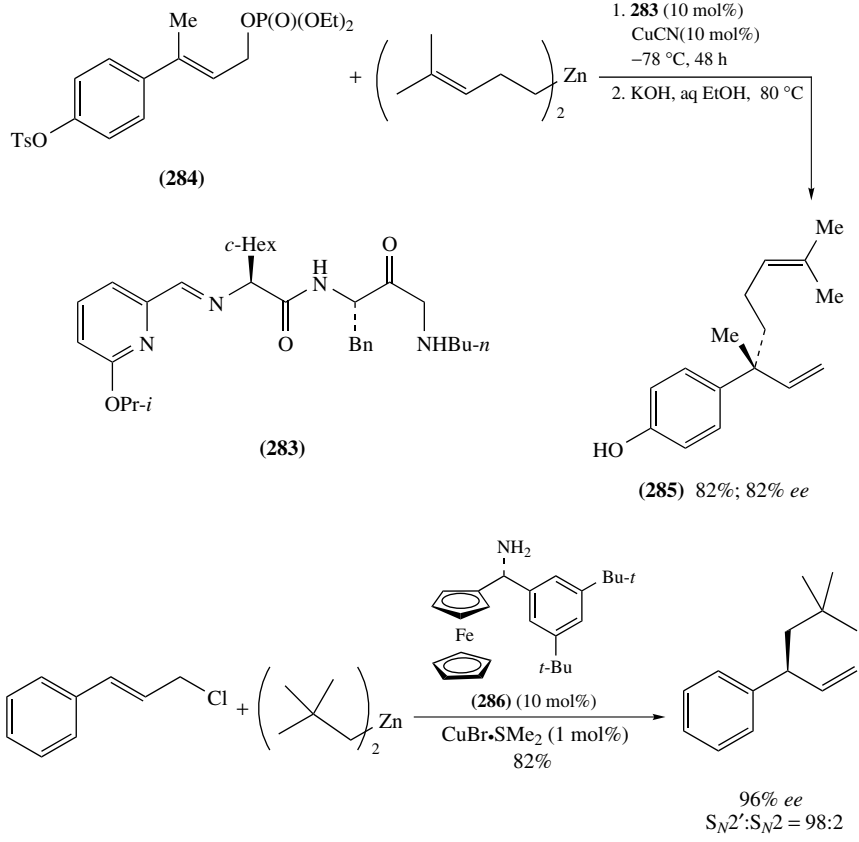

SCHEME 82. Catalytic S_N2'-allylic substitutions

Sterically very hindered diorganozincs like dineopentylzinc react enantioselectively with allylic chlorides in the presence of the chiral ferrocenylamine **286** with up to 98% *ee* (Scheme 82)[183]. The addition of zinc–copper organometallics to unsaturated cationic metal complexes derived, for example, from pentadienyliron and pentadienylmolybdenum cations affords the corresponding dienic complexes. Thus, the addition of a zinc–copper homoenolate to the cationic η^5-cycloheptadienyliron complex **287** leads to the polyfunctional iron–dienic complex **288** in 65% yield[184]. This chemistry has been extensively developed by Yeh and coworkers[185]. The addition of allylic and benzylic zinc reagents to (η^6-arene)-$Mn(CO)_3$ cations of type **289** provides, with excellent stereoselectivity, the neutral (η^5-cyclohexadienyl)$Mn(CO)_3$ complexes such as **290** in 92% yield. Less reactive functionalized alkylzinc compounds show a more complicated reaction pathway due to an isomerization of the organozinc species (Scheme 83)[186]. Rigby and Kirova-Snover[187] have applied these reactions to the synthesis of several natural products. Thus, the alkylation of the cationic tropylium complex **291** with the functionalized zinc reagent **292** furnishes the chromium complex **293**, which was an intermediate for the synthesis of β-cedrene (Scheme 83).

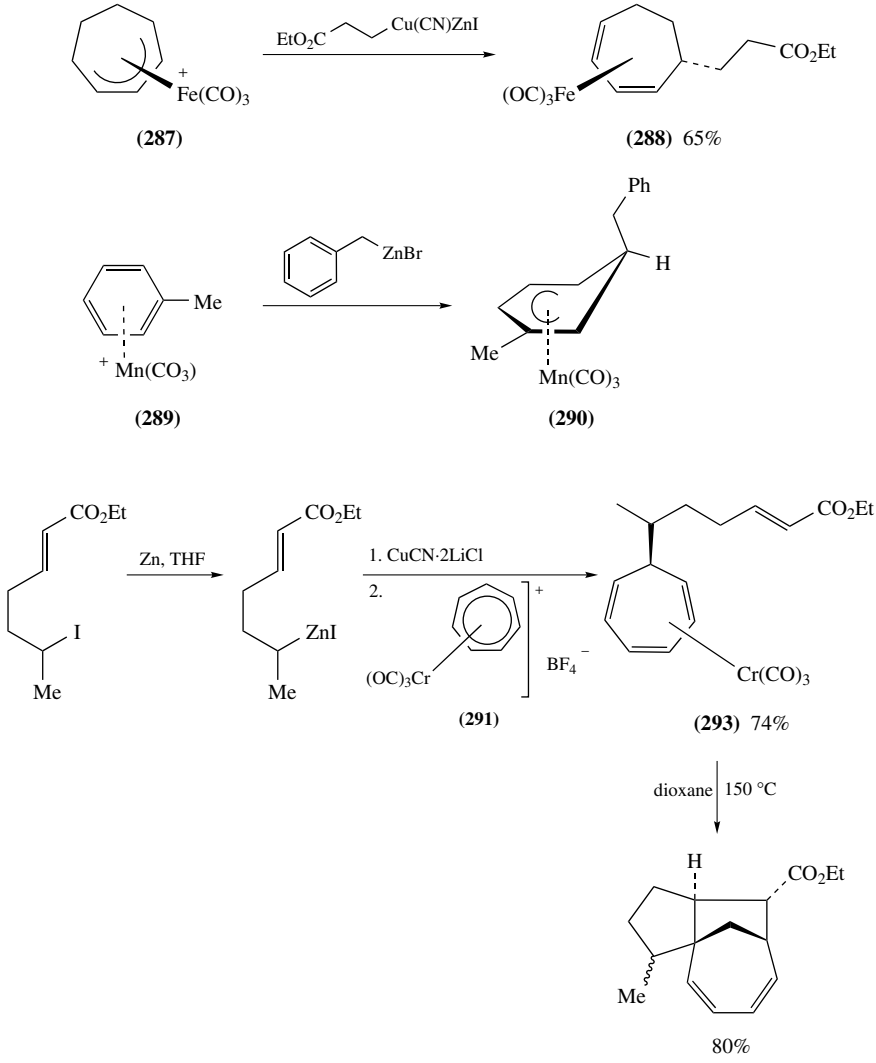

SCHEME 83. Reaction of zinc–copper reagents with cationic transition metal complexes

Yeh and Chuang[49] have shown that such addition reactions provide polyfunctional cationic chromium species, such as **294**, which can be converted to highly functionalized bicyclic ring systems (**295**) that are difficult to prepare otherwise (Scheme 84).

Alkynyl iodides and bromides react smoothly with various zinc–copper organometallics at $-60\,^{\circ}C$ leading to polyfunctional alkynes[48d]. Iodoalkynes, such as **296**[188], react at very low temperature, but lead in some cases to copper acetylides as by-products (I/Cu exchange reaction). 1-Bromoalkynes are the preferred substrates. Corey and Helel[189] have prepared a key intermediate **297** of the side chain of Cicaprost™ by reacting the chiral zinc

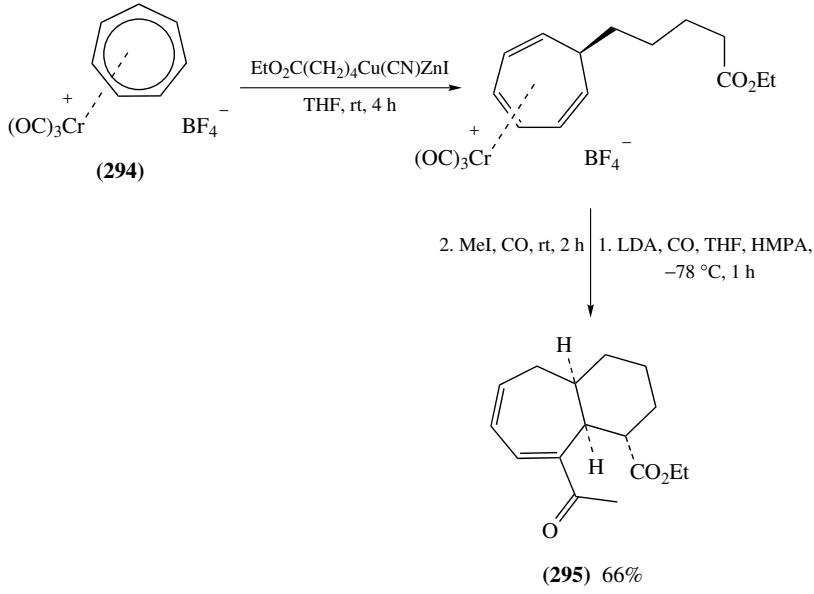

SCHEME 84. Addition of functionalized zinc–copper reagents to cationic chromium complexes and subsequent cyclization

reagent **298** with 1-bromopropyne, leading to the functionalized alkyne **299** (Scheme 85). This cross-coupling has also been used to prepare a pheromone (**300**)[48d].

Substitution at C_{sp^2} centers can also be accomplished as long as the haloalkene is further conjugated with an electron-withdrawing group at β-position. Thus, 3-iodo-2-cyclohexenone reacts with the zinc reagent **301** bearing a terminal alkyne, affording the functionalized enone **302**[11]. Similarly, the stepwise reaction of 3,4-dichlorocyclobutene-1,2-dione (**303**) with two different zinc–copper reagents furnishes polyfunctional squaric acid derivatives, such as **304**[190]. By using mixed diorganozinc reagents of the type FG-RZnMe[191], a catalytic addition–elimination can be performed with a wide range of

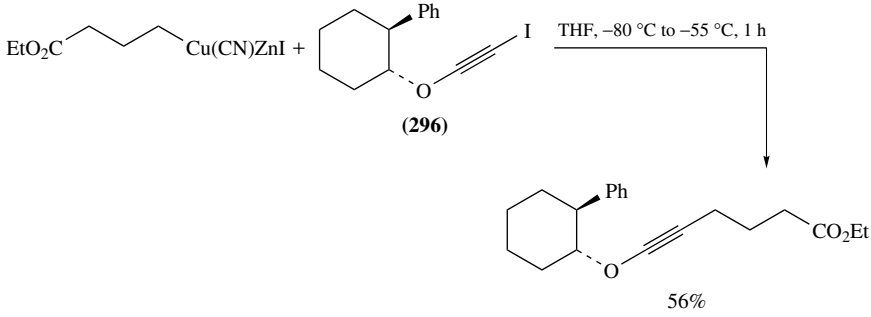

SCHEME 85. Cross-coupling of zinc–copper organometallics with 1-haloalkynes

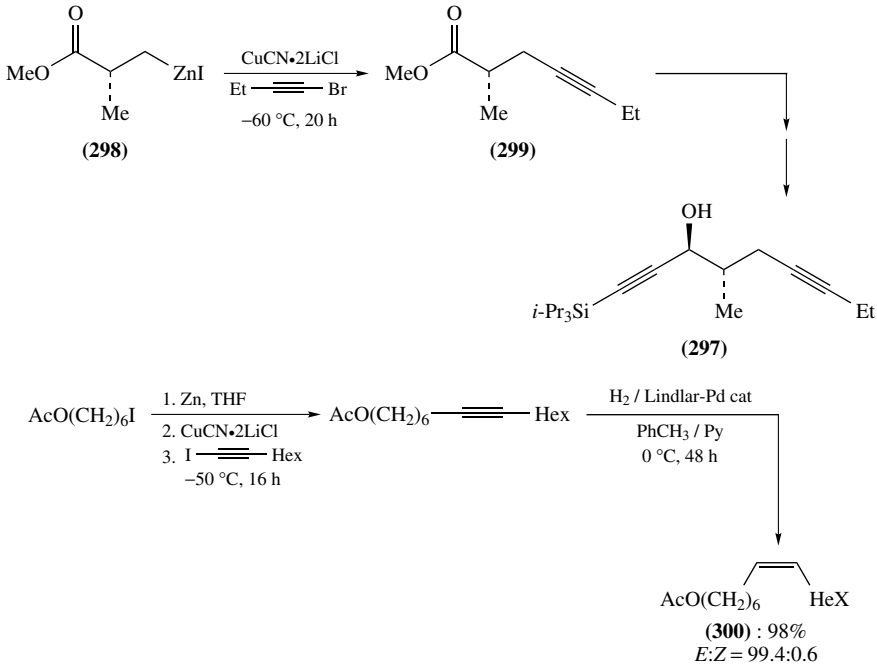

SCHEME 85. (*continued*)

β-ketoalkenyl triflates. Thus, the penicillin derivative **305** reacts with the mixed copper reagent **306**, providing the desired product **307** in excellent yield (Scheme 86)[191].

Functionalized heterocycles such as **308** can be prepared in a one-pot synthesis, in which the key step is the addition–elimination of a functionalized copper–zinc reagent **309** to the unprotected 3-iodoenone **310**, producing the annelated heterocycle **308** in 41% (Scheme 87)[192].

Besides enones, several Michael acceptors having a leaving group in β-position react with zinc–copper reagents. Thus, diethyl[(phenylsulfonyl)methylene]malonate (**311**) reacts with zinc–copper reagent **312** providing the addition substitution product **313** in 90% yield[193]. Similarly, the zinc–copper reagent **314** reacts with 2-phenylsulfonyl-1-nitroethylene (**315**) providing the intermediate triene **316**, which cyclizes on silica gel at 25 °C within 4 h affording the Diels–Alder product **317** in 85% (Scheme 87)[194]. The cross-coupling reaction with unactivated alkenyl iodides requires harsh conditions, but produces the desired products with retention of the double bond configuration[166]. The alkylation of primary alkyl halides and benzylic halides can be readily performed with diorganozincs treated with one equivalent of $Me_2CuMgCl$ in DMPU. This cross-coupling reaction tolerates a range of functionalities (ester, cyanide, halide and nitro group). The methyl group plays the role of a non-transferable group under our reaction conditions. Thus, the reaction of the dialkylzinc **318** with the nitro-substituted alkyl iodide **319** provides the cross-coupling product **320** in 83% yield[195]. A nickel-catalyzed cross-coupling reaction between an arylzinc reagent, such as **321**, and a functionalized alkyl iodide can be successfully achieved using 3-trifluoromethylstyrene **322** as a promoter. The role of this electron-poor styrene will be to coordinate the nickel(II) intermediate

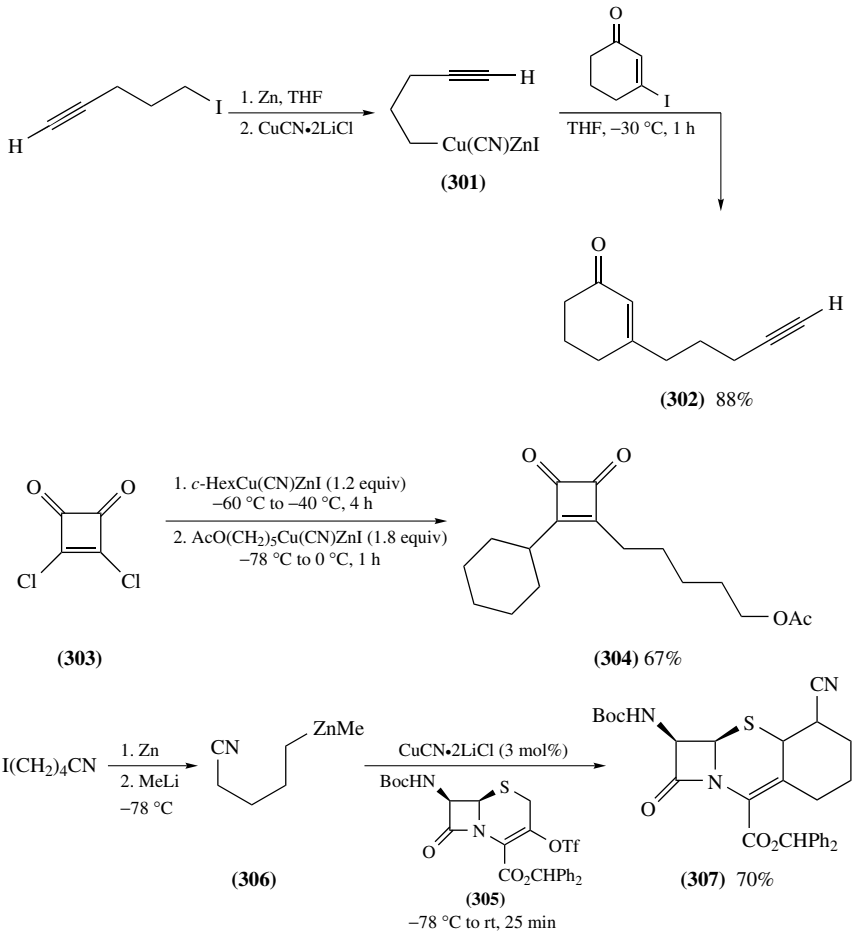

SCHEME 86. Addition–elimination reaction with zinc–copper reagents

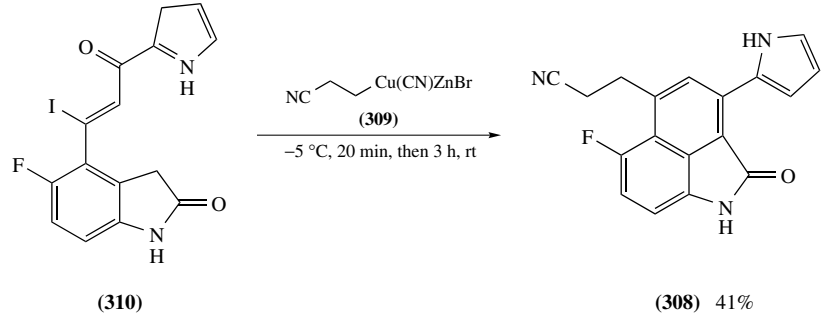

SCHEME 87. Addition–elimination reactions of copper–zinc reagents with various Michael acceptors bearing a leaving group in β-position

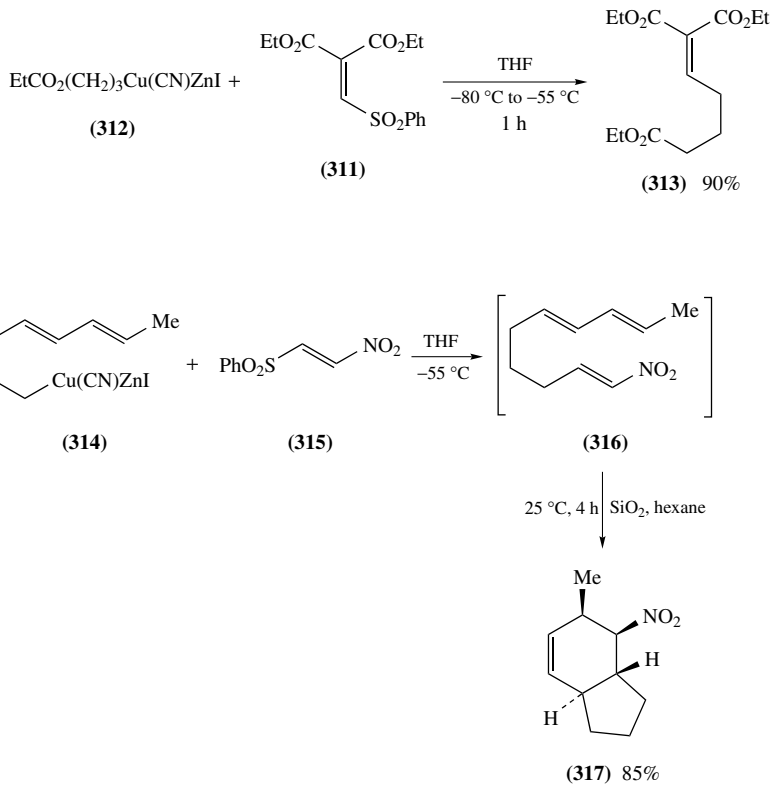

SCHEME 87. (*continued*)

bearing an aryl and an alkyl moiety and to promote the reductive elimination leading to the cross-coupling product **323**[196,197]. Interestingly, this cross-coupling reaction can be readily performed between two C_{sp^3} centers. Thus, the reaction of primary or secondary alkylzinc iodides with various primary alkyl iodides or bromides in the presence of catalytic amount of $Ni(acac)_2$ (10 mol%), Bu_4NI (3 equiv) and 4-fluorostyrene (20 mol%) provides the corresponding cross-coupling products in satisfactory yields[199]. More reactive secondary dialkylzincs and the mixed organozinc compounds $RZnCH_2SiMe_3$ undergo the cross-coupling in the absence of Bu_4NI[198].

Thus, the secondary diorganozinc **324** obtained by the hydroboration of norbornene with Et_2BH and subsequent boron–zinc exchange undergoes a smooth cross-coupling with the iodoketone **325** at $-30\,^{\circ}C$ (16 h reaction time) furnishing stereoselectively the *exo*-ketone **326** in 61% yield. Polyfunctional products, such as **327**, are readily obtained by performing the cross-coupling of functionalized alkylzinc iodides with functionalized alkyl bromides (Scheme 88)[198].

2. Acylation reactions

The uncatalyzed reaction of acid chlorides with organozincs is sluggish and inefficient. It is often complicated by side-reactions and usually leads to low yields of the

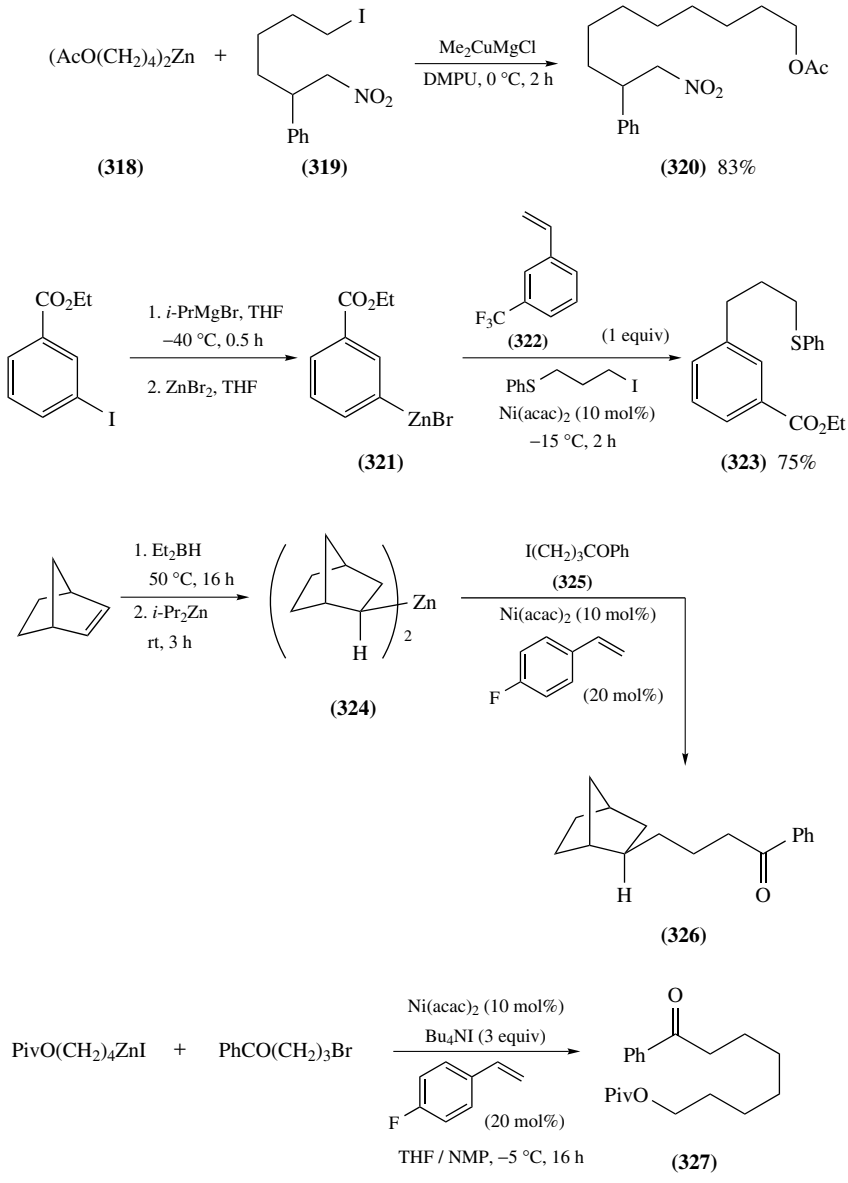

SCHEME 88. Cross-coupling reactions with zinc organometallics

desired acylation products. In contrast, the CuCN•2LiCl mediated acylation of various zinc reagents affords ketones in excellent yields. The zinc–copper reagent **328** obtained by direct zinc insertion to the iodide **329** followed by a transmetalation with CuCN•2LiCl reacts with benzoyl chloride at 25 °C, leading to the ketone **330** in 85% yield[52b]. The functionalized benzylic bromide **331** is converted in the usual way into the zinc–copper

derivative **332**, which is readily acylated leading, after aqueous workup, to the functionalized indole **333** in 73% yield (Scheme 89)[50]. Bis-zinc organometallics, such as **334** and **335**, are also acylated after transmetalation with CuCN•2LiCl, leading to the corresponding diketones **336**[21] and **337**[200].

Allylic zinc reagents are highly reactive and add to acid chlorides and anhydrides. A double addition of the allylic moiety usually occurs, leading to tertiary alcohols[15,20]. The double addition can be avoided by using a nitrile as substrate[201] (Blaise reaction). By

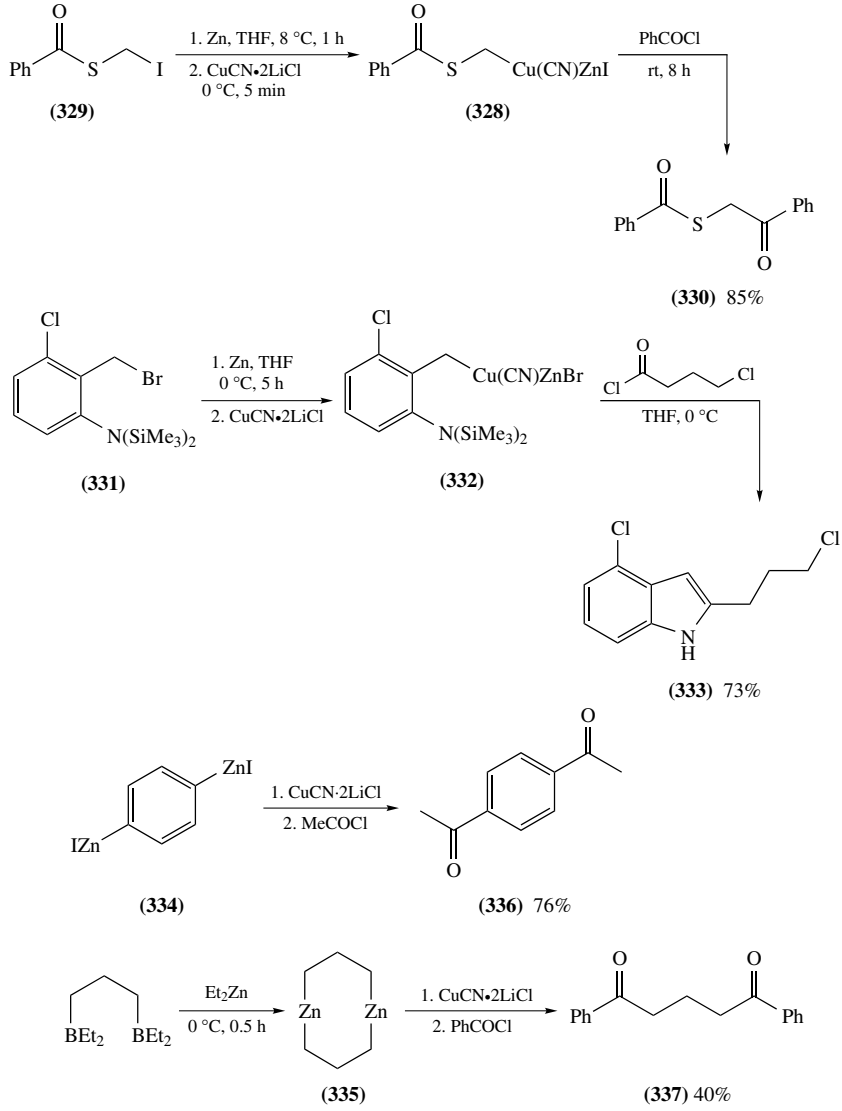

SCHEME 89. Acylation of zinc–copper reagents

using Barbier conditions, it was possible to generate the zinc reagent corresponding to the bromide **338** and to add it to a nitrile. After acidic workup, the unsaturated ketone **339** is obtained in 82% yield (Scheme 90)[202, 203].

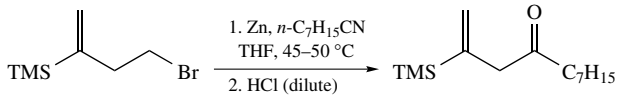

(338) **(339)** 82%

SCHEME 90. Acylation by the addition of an allylic zinc reagent to a nitrile

3. Addition reactions

Allylic and to the same extent propargylic zinc reagents add to aldehydes, ketones and imines under mild conditions[203]. Thus 2-carbethoxyallylzinc bromide (**340**), which is readily prepared by the reaction of ethyl (2-bromomethyl)acrylate[204] with zinc dust in THF (17–20 °C, 0.5 h), adds to a range of aldehydes and imines to provide α-methylene-γ-butyrolactones and lactams[205]. Chiral lactams can be prepared by adding the allylic zinc (**183**) to imines bearing amino alcohol substituents[206]. Functionalized allylic zinc reagents have been used to prepare a range of heterocycles, such as **341**[207]. The addition of propargylic zinc halides to aldehydes or ketones often provides mixtures of homopropargylic and allenic alcohols[208].

Interestingly, silylated propargylic zinc reagents, such as **342**, may be better viewed as the allenic zinc reagent **343** which reacts with an aldehyde via a cyclic transition state, affording only the *anti*-homopropargylic alcohol **344** with 90% yield (Scheme 91)[137]. Alkylzinc halides react only sluggishly with aldehydes or ketones. This reactivity can be

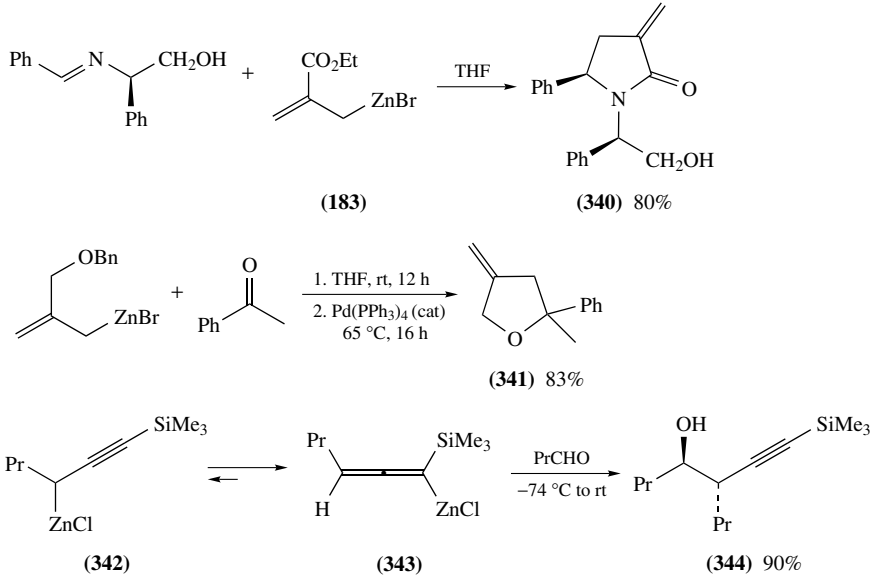

(183) **(340)** 80%

(341) 83%

(342) **(343)** **(344)** 90%

SCHEME 91. Reaction of allenic, propargylic and allylic zinc reagents with carbonyl derivatives

improved by activating the carbonyl derivative with a Lewis acid. Excellent results are obtained with titanium alkoxides[209], Me_3SiCl[210] or $BF_3{\bullet}OEt_2$[48c] (Scheme 92). Depending on the nature of the catalyst, either the 1,2-addition product (**345**) or the 1,4-addition product (**346**) is obtained by the addition of the zinc–copper reagent **347** to cinnamaldehyde[48c].

In a non-complexing solvent like CH_2Cl_2, alkylzinc reagents, such as **348** and *ent*-**348**, react with polyfunctional aldehydes, leading to highly functionalized alcohols, such as

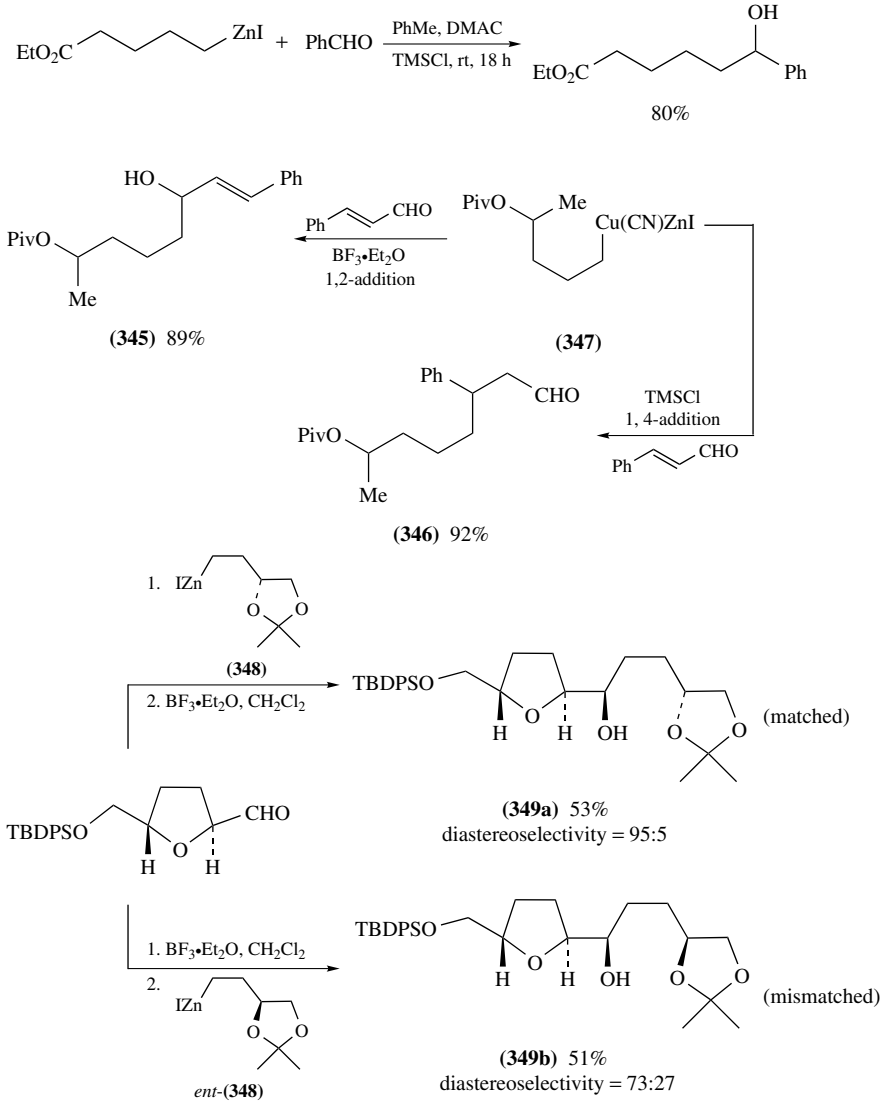

SCHEME 92. Selectivity in the reaction of zinc and zinc–copper reagents with aldehydes

349a and **349b** with high diastereoselectivity in the 'matched' case (Scheme 92)[158,210]. Polyoxygenated metabolites of unsaturated fatty acids have been prepared by the addition of functionalized zinc–copper reagents to unsaturated aldehydes in the presence of $BF_3{\bullet}OEt_2$, providing allylic alcohols of type **350**[211]. Allylic zinc reagents readily add to aldehydes with good stereoselectivity in some cases. Thus, the addition of dicrotylzinc[212a] to the aminoaldehyde **351** furnishes the alcohol **352** as one diastereomer in 82% yield. Interestingly, the corresponding Grignard reagent leads to a mixture of diastereoisomers (Scheme 93)[212b]. The addition of copper–zinc organometallics to imines is difficult. Benzylic zinc reagents display, however, an enhanced reactivity and react directly under well-defined conditions with *in situ* generated imines. A diastereoselective one-pot addition of functionalized zinc organometallics can be realized by performing the reaction in 5M $LiClO_4$ (in ether) in the presence of TMSCl. By using Reformatsky reagents and a chiral amine like (*R*)-phenylethylamine, diastereoselectivities with up to 95% have been obtained. With the benzylic zinc reagent **353**, the secondary amine **354** is obtained in 60% yield and 70% *de*[213].

Mangeney and coworkers[214] have found that alkylzinc reagents add to reactive imine derivatives and have used this property to prepare chiral amino acids (Scheme 94). The

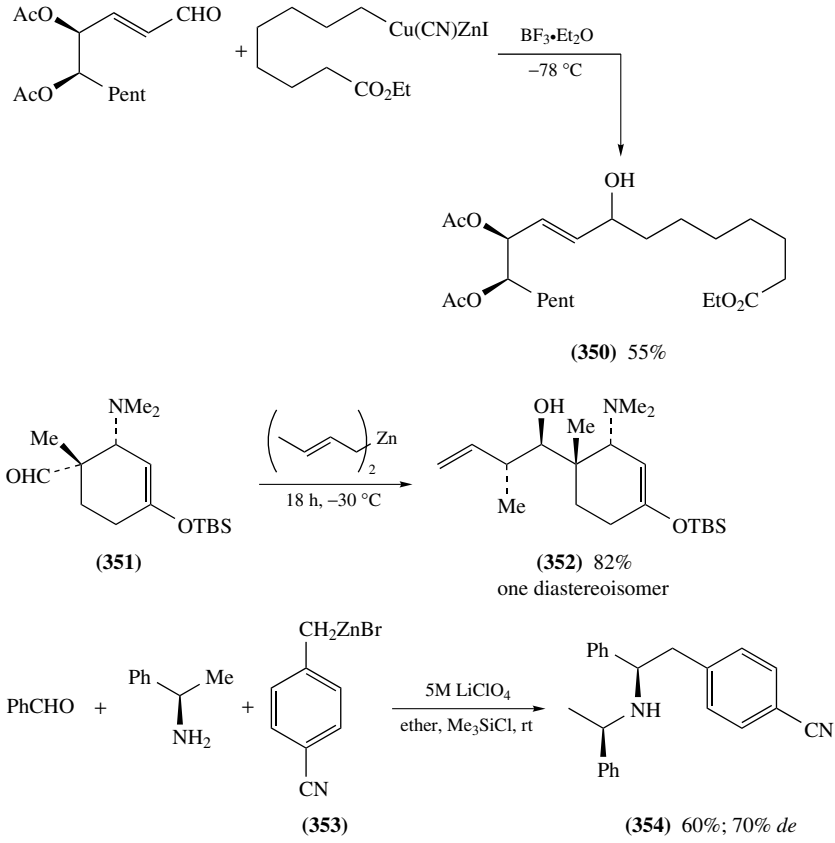

SCHEME 93. Addition reactions of zinc and copper–zinc reagents to carbonyl compounds

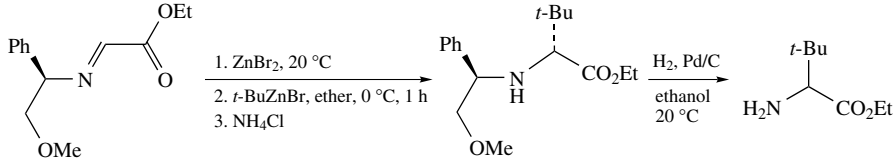

(355) **(356)** 68% (*R*)-**(357)** 100%; 85% *ee*

SCHEME 94. Addition of a tertiary alkylzinc reagent to a chiral iminoester

addition of *tert*-BuZnBr to the chiral α-imino esters **355**, bearing a phenylglycinol unit provides in ether the corresponding adduct **356** with a diastereoselectivity of 96:4. After removal of the chiral inductor by hydrogenolysis, the corresponding amino ester **357** is obtained in 85% *ee*.

Copper–zinc reagents add to various pyridinium salts leading either to the 1,2- or to the 1,4-adduct, depending on the substituent pattern of the pyridine ring (Scheme 95)[150, 215].

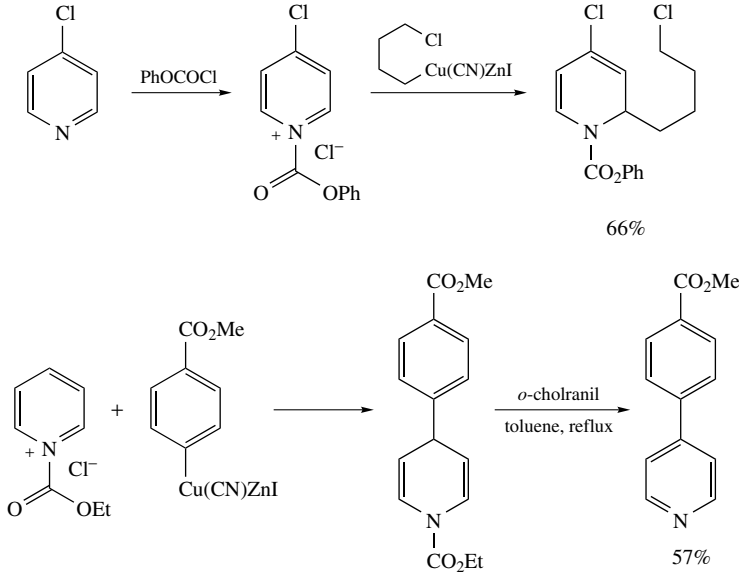

SCHEME 95. Addition of copper–zinc reagents to pyridinium salts

4. Michael additions

Organocopper reagents derived from organolithium or magnesium derivatives add readily to various Michael acceptors[64]. The zinc–copper reagents obtained by reacting organozinc halides with CuCN•2LiCl undergo numerous 1,4-addition reactions with various Michael acceptors. The presence of TMSCl is especially useful and effective[216]. It ensures high yields of the conjugate adducts. Thus, the addition of various polyfunctional zinc–copper reagents with cyclohexenone provides the desired 1,4-addition product **358** in the presence of TMSCl in 97% yield[10, 217]. Sterically hindered enones, such as 3-cyclohexyl-2-cyclohexen-1-one **359**, undergoes a conjugate addition in the

presence of $BF_3{\bullet}OEt_2$, affording the ketone **360** bearing a quaternary center in β-position (Scheme 96)[48a]. Unsaturated copper reagents are best added via alkenylzirconium species, which are readily prepared by hydrozirconation. In the presence of catalytic amounts of $Me_2Cu(CN)Li_2$, they add to various enones affording the unsaturated ketones of type **361** in satisfactory yield (Scheme 96)[21].

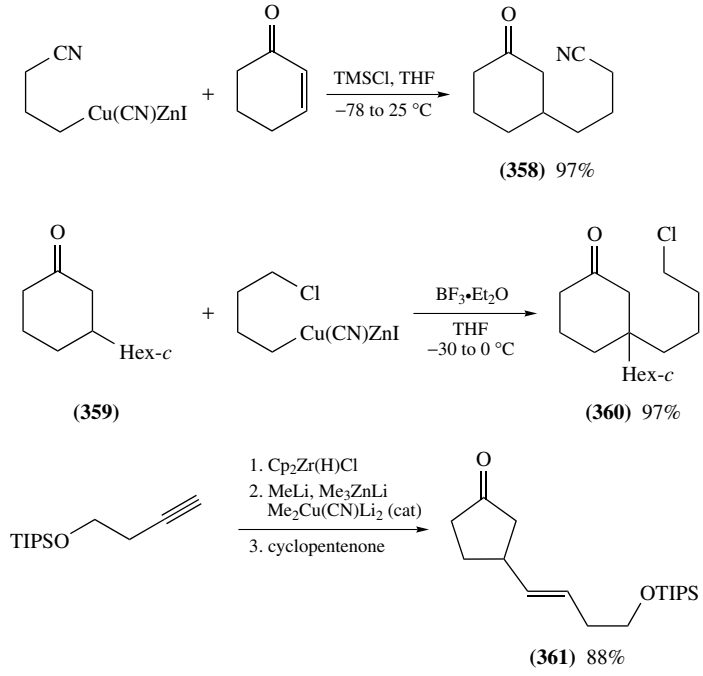

SCHEME 96. Michael addition of zinc–copper reagents to enones

Arylzinc reagents, obtained by the electrochemical reduction of the corresponding aromatic chloride or bromide using a sacrificial zinc electrode, allow the preparation of zinc reagents bearing a keto group[36]. *Exo*-methylene ketones such as **362** add various copper–zinc reagents. This methodology has been applied for the synthesis of various prostaglandines, such as **363**[218]. Enantioselective Michael additions have been pioneered by Feringa[219], Alexakis[220] and coworkers. Remarkably, only a catalytic amount of the chiral ligand **364** (4 mol%) and of $Cu(OTf)_2$ (2 mol%) is required. The 1,4-addition product **365** is obtained with an enantiomeric excess of 93% *ee*[219a]. It has been applied for an enantioselective synthesis of prostaglandin E_1 methyl ester (**366**)[221] and can be used for the performance of a highly regiodivergent and catalytic parallel kinetic resolution[222]. The nature of the copper salt strongly influences the enantioselectivity and copper carboxylates proved to be especially efficient (Scheme 97)[220c]. Hoveyda and Hird have developed a very efficient modular ligand based on various amino acids. The modular ligand **367** has been optimized for the enantioselective addition of Et_2Zn to the oxazolidinone **368**[223]. The resulting products of type **369** can be converted into other carbonyl compounds (ketones, Weinreb amides, carboxylic acids) by standard methods. A stereoselective synthesis of substituted pyrrolidines has been achieved by a sequential domino-Michael addition and intramolecular carbozincation. Thus, the reaction of the acyclic ester **370**

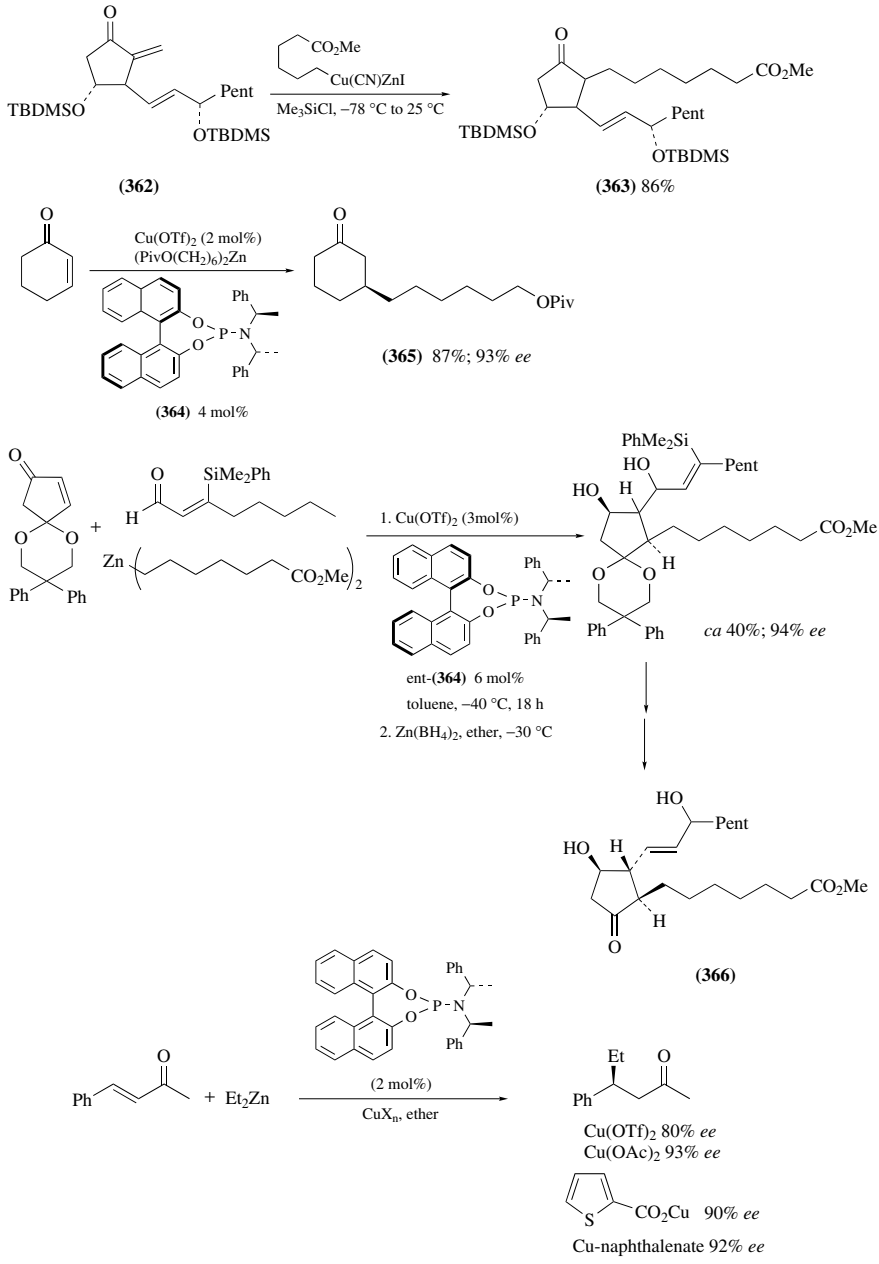

SCHEME 97. Stereoselective Michael addition of zinc reagents to enones

with a copper–zinc reagent such as **371** provides, with high stereoselectivity, the pyrrolidine **372** (d.r. = 95:5); see Scheme 98. The intermediate zinc–copper reagent obtained after cyclization can be trapped with an electrophile such as allyl bromide, providing a product of type **373** in satisfactory yield[224].

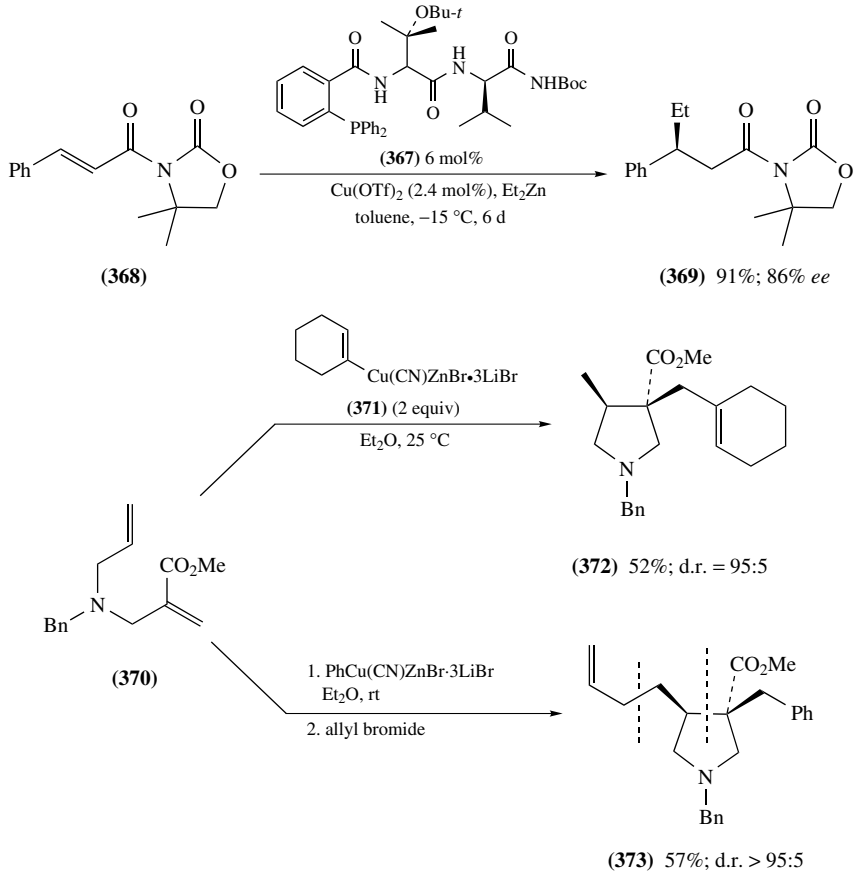

SCHEME 98. Stereoselective additions of zinc–copper reagents to enoates

The addition to α,β-unsaturated esters is usually difficult. However, under appropriate conditions, the 1,4-addition of diorganozincs to enoates is possible[225]. As mentioned above, Michael-addition reactions can also be catalyzed by Ni(II) salts[99]. The 1,4-addition of functionalized organozinc iodides to enones in the presence of $Ni(acac)_2$, a diamine as ligand and TMSCl provides, after hydrolysis, the Michael adducts in satisfactory yields[226].

Nitroolefins are excellent Michael acceptors which react with a broad range of nucleophiles in a Michael fashion. The resulting functionalized nitroalkanes can be readily converted into amines by reduction reactions or to carbonyl compounds by a Nef reaction[227]. The addition of nucleophiles to nitroolefins is complicated by the subsequent addition of the resulting nitronate to remaining nitroolefin. Whereas such a side-reaction is quite fast for lithium and magnesium[228] nitronates, it is slow for zinc

nitronates. Thus, various functionalized zinc–copper reagents add to nitroalkenes leading to Michael adducts, such as **374** in good yields[11,30]. The reaction with 1-acetoxy-2-nitro-2-propene (**375**)[172] and functionalized zinc–copper reagents provides an access to terminal nitroolefins, such as **376**[30]. The highly reactive reagent[229] undergoes the allylic substitution reaction already at −55 °C. Similarly, (2-phenylsulfonyl)nitroethylene (**377**) undergoes an addition–elimination reaction with the copper–zinc species **378** at −60 °C leading to the triene **379** in 92% yield (Scheme 99)[30,229].

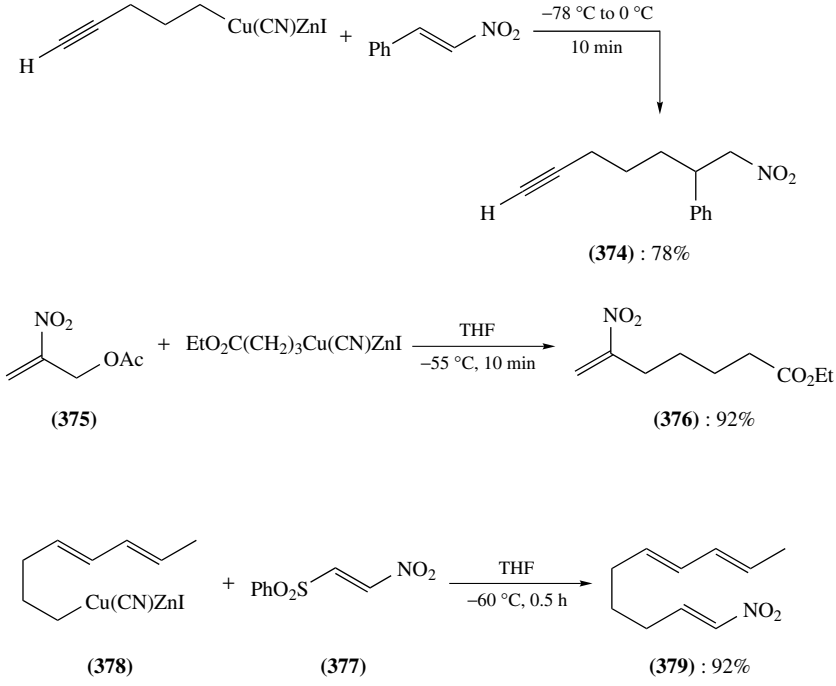

SCHEME 99. Addition of zinc–copper reagents to nitroolefins

Interestingly, bis(methylthio)-1-nitroethylene (**380**) reacts with dimetallic zinc–copper species leading to the corresponding *exo*-methylene cycloalkenes, such as **381** (Scheme 100)[30]. β-Disubstituted nitroolefins are especially difficult to prepare by nitroaldol condensation. The addition of zinc–copper reagents to nitroolefins followed by a reaction with phenylselenyl bromide produces, after H_2O_2 oxidation, *E*/*Z* mixtures of β-disubstituted nitroalkenes, such as **382** (Scheme 100)[230].

It is noteworthy that the intermediate zinc nitronate resulting from the oxidative Nef reaction can be directly prepared leading to a polyfunctional ketone, such as **383** in high yield (Scheme 100)[30]. The addition of copper organometallics to triple bonds (carbocupration)[231] can be realized with copper reagents derived from zinc organometallics. The *syn*-addition of zinc–copper reagents to activated triple bonds, such as acetylenic esters, is especially easy. The carbocupration of ethyl propiolate at −60 °C to −50 °C produces the *syn*-addition product **384** after protonation at low temperature. Interestingly, if the reaction mixture is warmed up in the presence of an excess of TMSCl, an equilibration occurs and the C-silylated unsaturated product **385** is obtained[48d]. The

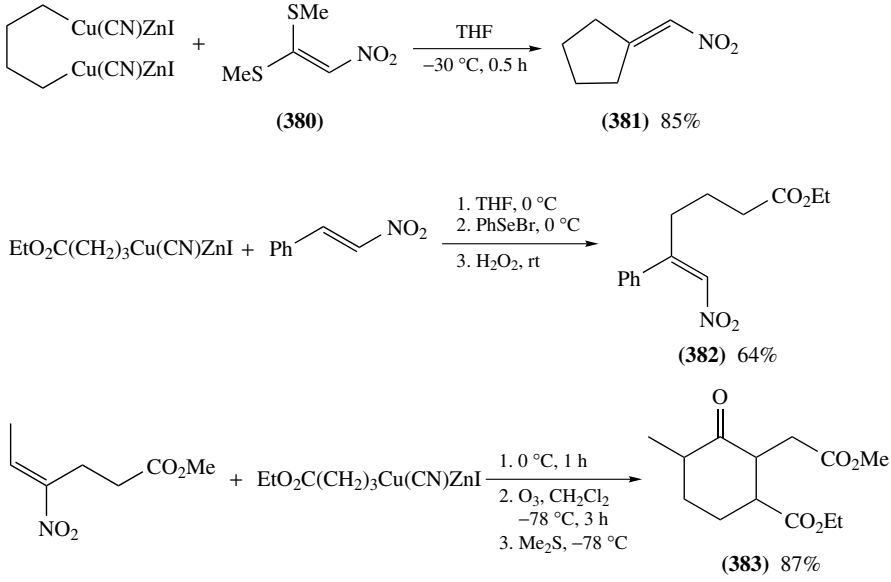

SCHEME 100. Reaction of functionalized zinc–copper reagents with polyfunctional nitroolefins

presence of acidic hydrogens of the amide group does not interfere with the carbocupration reaction. Thus, the unsaturated amide **386** affords after addition the *E*-unsaturated amide **387** in 53% as 10% *E*-isomer (Scheme 101)[11].

A formal [3+2]-cycloaddition can be accomplished by adding bis(2-carbethoxyethyl) zinc to acetylenic esters[232c]. This reaction allows the construction of complex cyclopentenones, such as **388**, which is a precursor of (±)-bilobalide (Scheme 101)[232c]. The allylzincation of trimethylsilylacetylenes can be performed intramolecularly providing a functionalized alkenylzinc which cyclizes in the presence of $Pd(PPh_3)_4$ at 25 °C within 3.5 h, leading to the bicyclic product **389** in 84% yield (Scheme 102)[233]. The addition of allylic zinc halides to various alkynes occurs in the absence of copper salts. The related

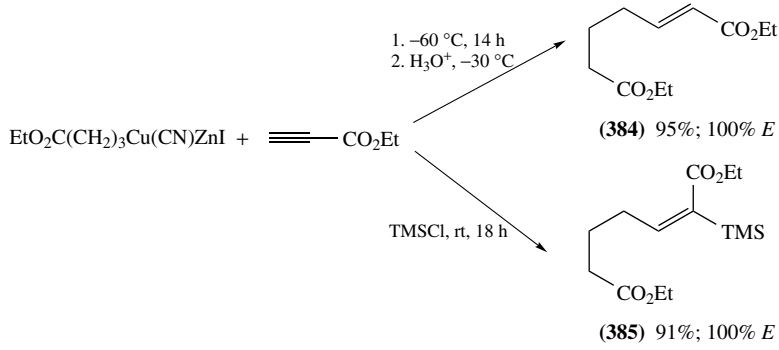

SCHEME 101. Carbocupration of acetylenic carbonyl derivatives

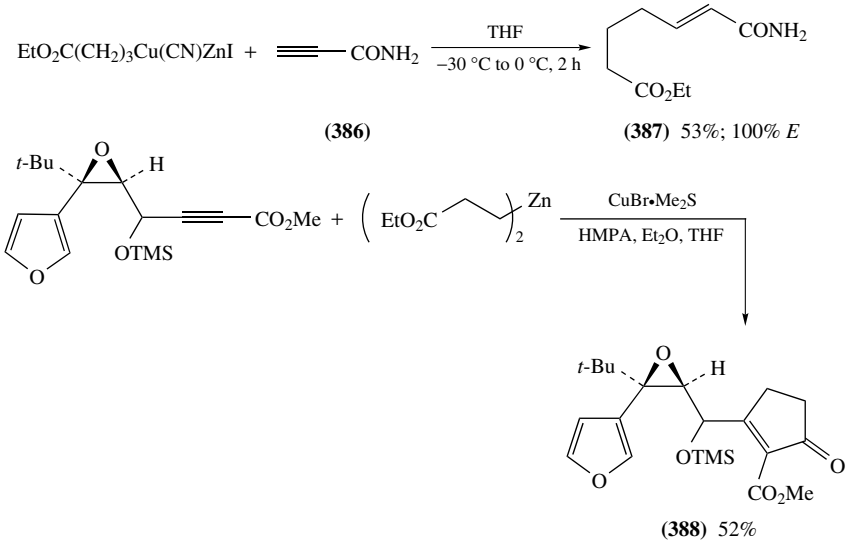

SCHEME 101. (*continued*)

addition to 1-trimethylsilyl alkynes[234], unsaturated acetals[235] and cyclopropenes[236] occurs readily. Functionalized allylic zinc reagents can be prepared by the carbozincation of a dialkoxymethylenecyclopropane **390** with dialkylzincs. Thus, the reaction of **390** with Et_2Zn provides the allylic zinc reagent **391**. After the addition of an electrophile, the desired adduct **392** is obtained in good yield[237].

Allylic zinc reagents are highly reactive reagents which are prone to undergo carbozincation of weakly activated alkenes[143]. Thus, the addition of the mixed methallyl(butyl)zinc **393** with the vinylic boronate **394** provides the intermediate zinc reagent **395**. After the addition of an extra equivalent of $ZnBr_2$, CuCN•2LiCl and allyl bromide, the reaction mixture was worked up oxidatively providing the alcohol **396** in 83% yield[238].

Functionalized allylic zinc reagents can also be generated *in situ*. The direct cyclization of allenyl aldehydes such as **397** with diorganozincs in the presence of $Ni(cod)_2$ (10–20 mol%) provides cyclic homoallylic alcohols such as **398** with good diastereoselectivity[239]. The allylzincation of alkenylmagnesium reagents is a very convenient synthesis of 1,1-bimetallic reagents of magnesium and zinc[240]. Thus, the addition of the ethoxy-substituted allylic zinc reagent (**399**) to the alkenylmagnesium reagent **400** provided, after the addition of Me_3SnCl (1 equiv), the α-stannylated alkylzinc species **401**, which is readily oxidized with O_2 leading to the aldehyde **402** with an excellent transfer of the stereochemistry (Scheme 103)[241].

The activation of primary zinc–copper reagents with $Me_2Cu(CN)Li_2$ allows one to carbocuprate weakly activated alkynes. The carbocupration of the alkynyl thioether **403** leads to the *E*-alkene **404** with high stereoselectivity[242]. Although primary alkylzinc regents do not add to unactivated alkynes, the addition of the more reactive secondary copper–zinc reagents affords the desired product **405** with high *E*-stereoselectivity[242]. The intramolecular carbocupration proceeds also with primary copper organometallics leading, after allylation, to the *exo*-alkenylidencyclopentane derivative **406** in 60% yield (Scheme 104)[242]. The addition of zinc malonates, such as **407**, produces the carbometalation product **408** in 50% yield (Scheme 104)[243].

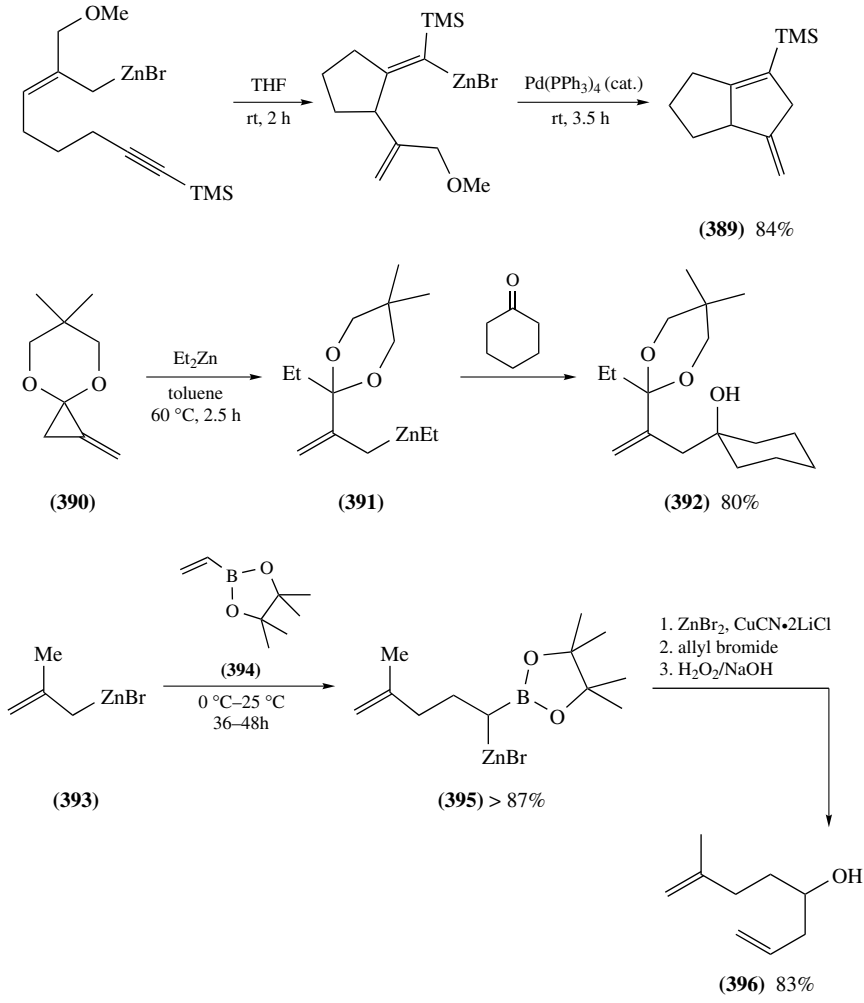

SCHEME 102. Allylzincation of unsaturated compounds

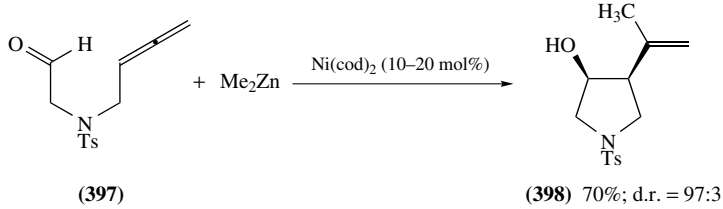

SCHEME 103. Allylzincation reactions

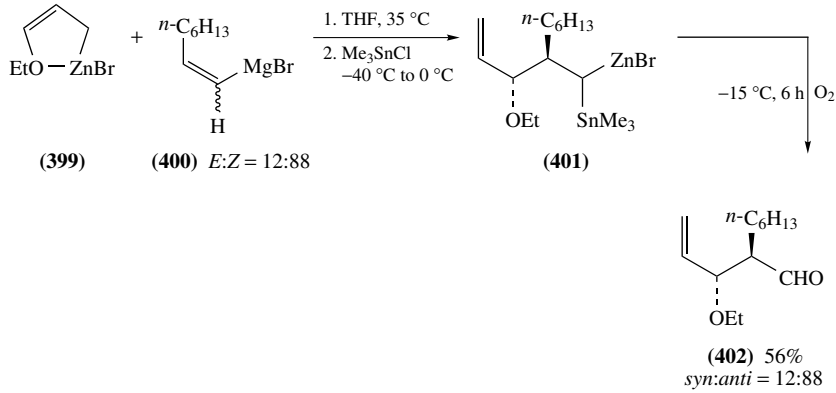

(399) **(400)** *E*:*Z* = 12:88 **(401)**

(402) 56%
syn:*anti* = 12:88

SCHEME 103. (*continued*)

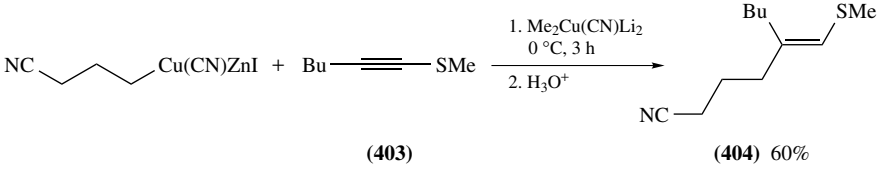

(403) **(404)** 60%

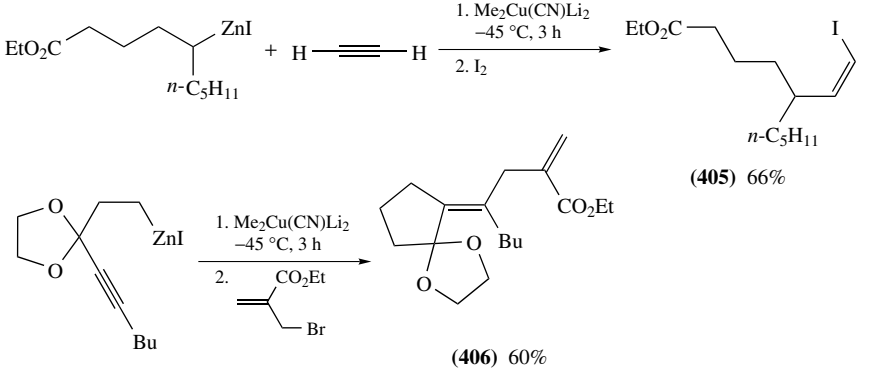

(405) 66%

(406) 60%

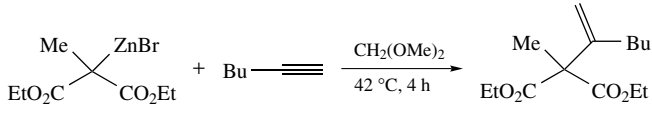

(407) **(408)** 50%

SCHEME 104. Carbozincation and carbocupration of alkynes

C. Palladium and Nickel Catalyzed Reactions

Negishi and coworkers discovered 25 years ago that organozinc halides undergo smooth Pd(0)-catalyzed cross-coupling reactions with aryl, heteroaryl and alkenyl halides as well as acid chlorides[7, 244]. These cross-coupling reactions have a broad scope and have found many applications[7]. They have been performed with a range of polyfunctional organozinc halides[245]. These zinc organometallics may contain a silylated acetylene[246], an alkenylsilane[247], an allylic silane[248], an alkoxyacetylene[249], a polythiophene[250], polyfunctional aromatics[251], heterocyclic rings[252], an ester[21, 253], a nitrile[21, 58], a ketone[254], a protected ketone[252a], a protected aminoester[255], a stannane[256] or a boronic ester[53b]. The cross-coupling reaction with homoenolates proceeds especially well with bis(*tris-o*-tolylphosphine)palladium dichloride[253a] leading to the desired cross-coupling products, such as **409**. Biphenyls, such as **410**, have been often prepared by using $Pd(PPh_3)_4$ as a catalyst[21]. Recently, Fu and Dai[257] have demonstrated that Negishi cross-coupling reactions can be efficiently performed by using the sterically hindered phosphine $(t\text{-}Bu)_3P$ as a ligand, which results in very active catalytic species $(t\text{-}Bu_3P)Pd$. In these cases, the cross-coupling can be performed with aryl chlorides and tolerates the presence of some functionalities. Thus, the cross-coupling between cheap 2-chlorobenzonitrile and *p*-tolylzinc chloride proceeds with exceptionally high turnovers (TON>3000) leading to the biphenyl **411** in 97% yield (Scheme 105)[257].

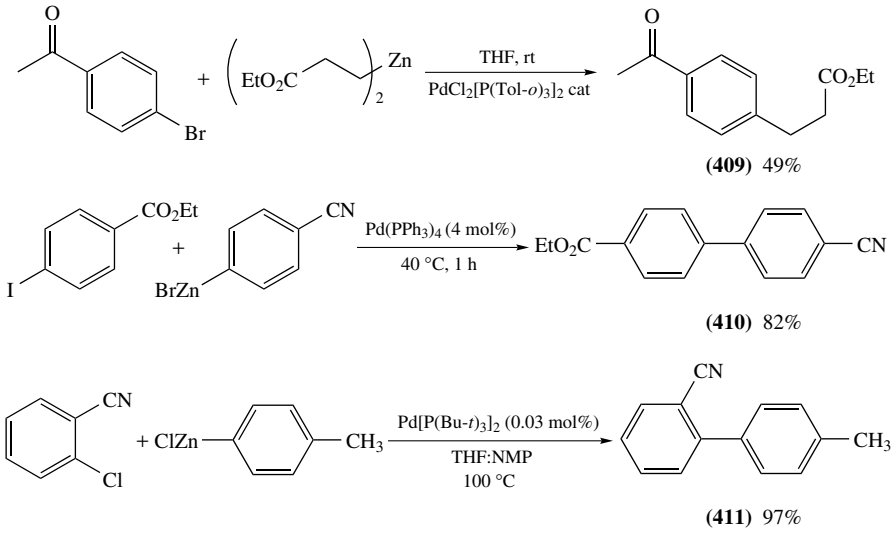

SCHEME 105. Palladium catalyzed cross-coupling reactions

New α-amino acids such as **412** (Scheme 106) have been prepared in high optical purity by using the reaction of pyridyl bromide **413** with Jackson reagent **15**[25e]. Fmoc-protected amino acids are routinely used in automated solid-phase peptide synthesis. The Fmoc-protected zinc reagent **414** is readily prepared from the corresponding alkyl iodide **415**. The Pd-catalyzed cross-coupling with various aryl iodides [Pd_2dba_3 (2.5 mol%), $P(Tol\text{-}o)_3$ (10 mol%)] in DMF at 50 °C furnishes the corresponding arylated amino acid derivatives **416** in 25–59% yield[258]. Removal of the *tert*-butyl ester is readily achieved with Et_3SiH and TFA leading to Fmoc-protected amino acids[259].

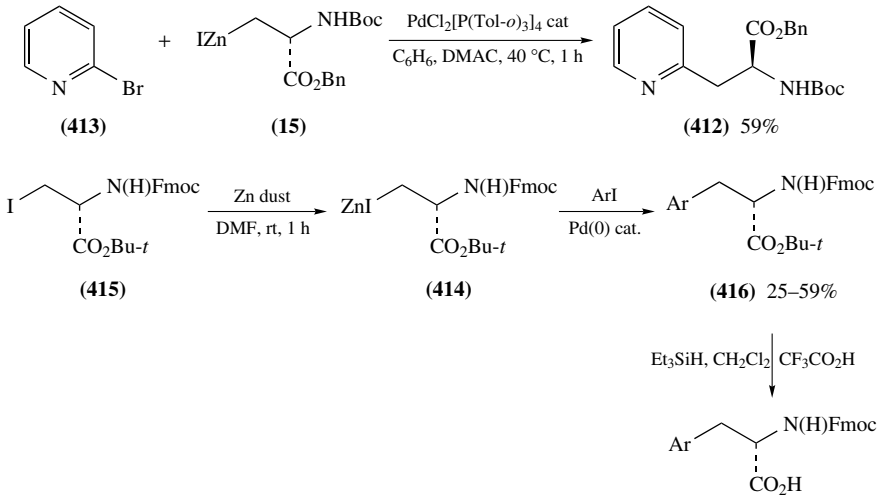

SCHEME 106. Synthesis of α-amino acids by Negishi cross-couplings

The reaction of the zinc homoenolate **417** with ketene acetal triflates such as **418** in the presence of a palladium(0) catalyst ($Pd(PPh_3)_4$, 5 mol%) leads to the corresponding cross-coupling product **419**. This key sequence has been used for the iterative synthesis of polycyclic ethers[260]. A smooth cross-coupling is observed between (2*E*, 4*E*)-5-bromopenta-2,4-dienal **420** and various zinc reagents, leading to dienic aldehydes of type **421** in good to excellent yields and high stereomeric purity. Using the isomeric (2*E*, 4*Z*)-5-bromopenta-2,4-dienal furnishes the corresponding diene with a partial isomerization of the double bonds (Scheme 107)[261]. Negishi cross-coupling reaction can be performed with complex alkenyl iodides such as **422**, leading to the steroid derivative **423** in 88% yield. The palladium(0) catalyst ($Pd(PPh_3)_4$) was generated *in situ* from $Pd(OAc)_2$ (10 mol%) and PPh_3 (40 mol%) (Scheme 107)[262].

Nickel salts are also excellent catalysts; however, the nature of the ligands attached to the nickel metal center is very important and needs often to be carefully chosen to achieve high reaction yields. Interestingly, nickel on charcoal (Ni/C) proved to be an inexpensive heterogeneous catalyst for the cross-coupling of aryl chlorides with functionalized organozinc halides. Thus, the cross-coupling of 4-chlorobenzaldehyde with 3-cyanopropylzinc iodide produces, in refluxing THF, the desired cross-coupling product **424** in 80% yield[263]. Tucker and de Vries developed an alternative homogeneous cross-coupling. Thus, $NiCl_2(PPh_3)_2$ (7.5 mol%) and PPh_3 (15 mol%) was found to be an excellent cross-coupling catalyst for performing the cross-coupling between aryl chlorides such as **425** and functionalized arylzinc bromides like **426**. A complete conversion was obtained at 55 °C after a reaction time of 5 h, affording the cross-coupling product **427** in 75% yield (Scheme 108)[264].

The cross-coupling of alkynylzinc halides or fluorinated alkenylzinc halides with fluorinated alkenyl iodides allows the preparation of a range of fluorinated dienes or enynes[265]. Functionalized allylic boronic esters can be prepared by the cross-coupling of (dialkylboryl)methylzinc iodide **428** with functionalized alkenyl iodides. The intramolecular reaction provides cyclized products, such as **429** (Scheme 109)[53c–e]. In some cases, reduction reactions[266] or halogen–zinc exchange reactions[40] are observed.

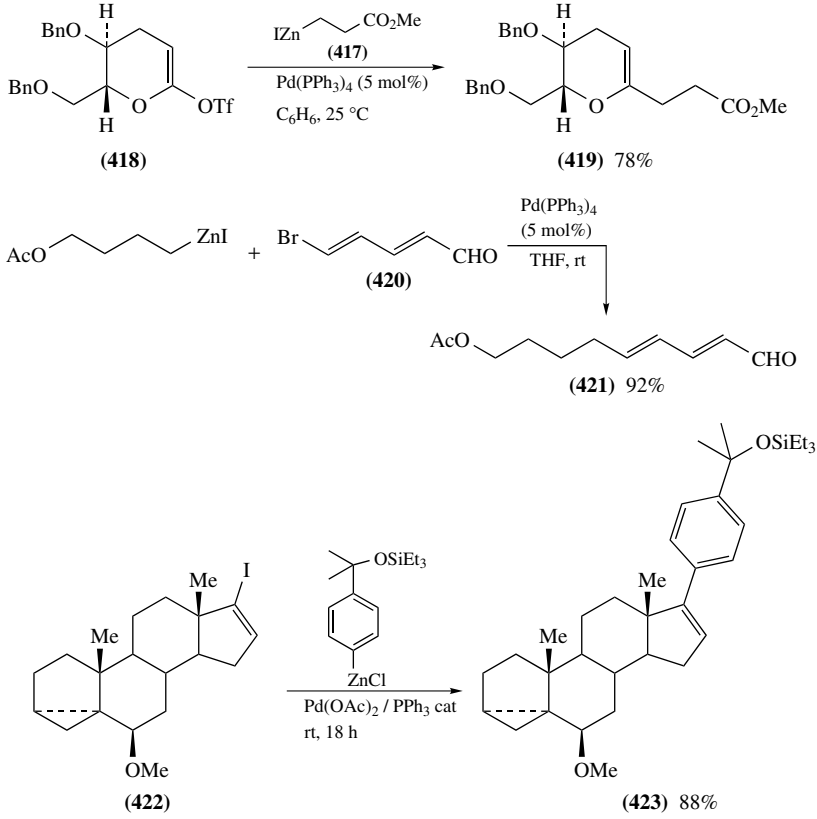

SCHEME 107. Negishi cross-coupling of zinc organometallics with polyfunctional unsaturated derivatives

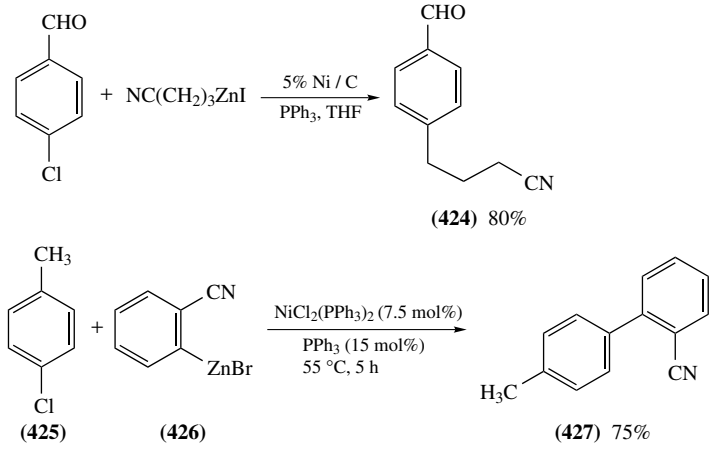

SCHEME 108. Nickel-catalyzed cross-coupling reactions

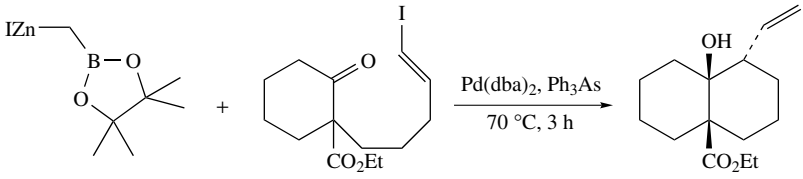

(428) **(429)** 70%

SCHEME 109. *In situ* generation of allylic boronic esters via cross-coupling reactions

Functionalized heterocyclic zinc reagents are very useful building blocks for the preparation of polyfunctional heterocycles, as shown with the pyridylzinc derivative **430** prepared by reductive lithiation followed by a transmetalation with zinc bromide[267]. The cross-coupling of the zinc reagent **430** with a quinolyl chloride provides the new heterocyclic compound **431**. The selective functionalization of positions 4 and 3 of pyridines is possible starting from 3-bromopyridine **432**, which is selectively deprotonated in position 4 by the reaction with LDA in THF at −95 °C followed by a transmetalation with $ZnCl_2$. The resulting zinc species **433** undergoes a Pd-catalyzed cross-coupling with various aryl halides (Ar^1-X) affording products of type **434**. The cross-coupling of **434** with a zinc reagent Ar^2-X in the presence of a Pd(0) catalyst provides 3,4-diarylpyridines of type **435**[268]. The functionalized iodoquinoline **436** reacts with *i*-PrMgCl at −30 °C, providing an intermediate heteroarylmagnesium species which, after transmetalation to the corresponding zinc derivative **437**, undergoes a smooth cross-coupling reaction with ethyl 4-iodobenzoate in the presence of $Pd(dba)_2$ (3 mol%) and tfp (tris(*o*-furyl)phosphan) (6 mol%) in THF at rt providing the desired cross-coupling product **438** in 74% yield (Scheme 110)[269].

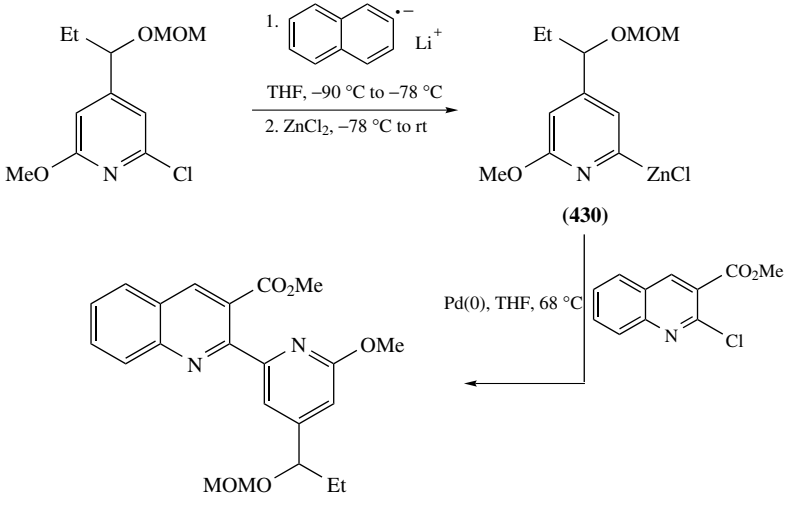

(431) 81%

SCHEME 110. Negishi cross-coupling with heterocyclic zinc reagents

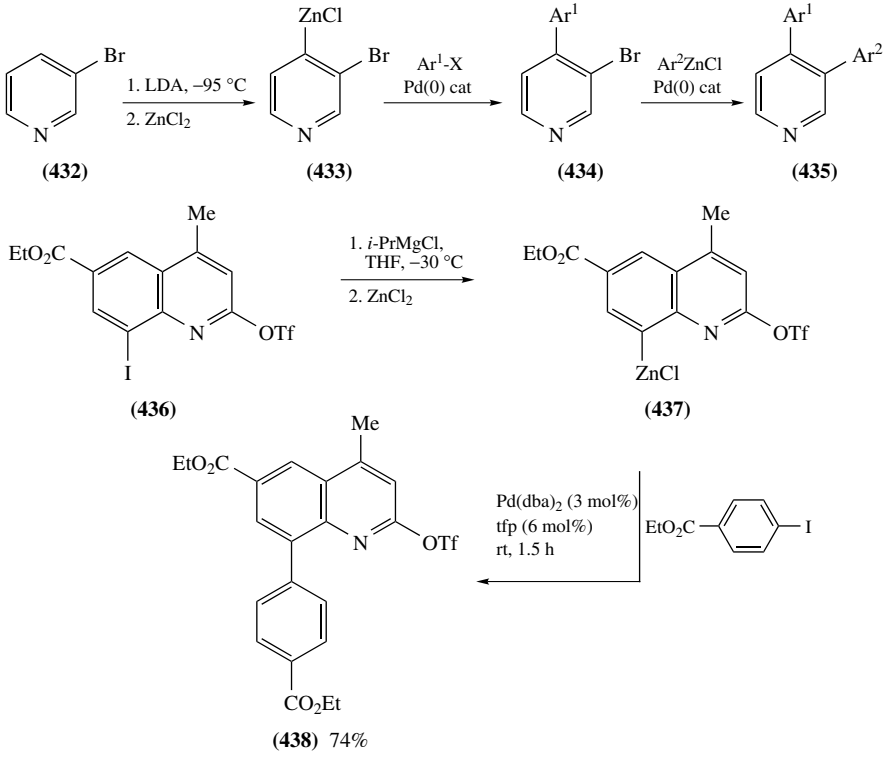

SCHEME 110. (*continued*)

The selective functionalization of heterocycles is an important synthetic goal. Purines display multiple biological activities such as antiviral or cytostatic properties. The synthesis of analogues such as **441** can be achieved by a regioselective cross-coupling of functionalized benzylic zinc reagents such as **440** with the dichloropurine derivative **439** in the presence of $Pd(PPh_3)_4$ (5 mol%)[270]. L-Azatyrosine **442** is an anticancer lead compound, which can be readily prepared using Jackson's reagent **15** and a Negishi cross-coupling reaction with 2-iodo-5-methoxypyridine **443** affording the amino-ester **444** in 59% yield. Its deprotection according to a procedure of Burke and Ye[271] produces L-azatyrosine **442**[272]. Functionalized alkenylzinc species such as **445** can be prepared via an iodine–magnesium exchange followed by a transmetalation with $ZnBr_2$. The Pd-catalyzed cross-coupling reaction with 4-iodobenzonitrile proceeds at 60 °C in THF, leading to the arylated product **446** in 57% yield[273]. 1,1-Dibromo-1-alkenes of type **447** undergo a highly *trans*-selective Pd-catalyzed cross-coupling with alkylzinc reagents using bis(2-diphenylphosphinophenyl) ether (DPE-phos) as a ligand. The use of $Pd(PBu\text{-}t_3)_2$ is crucial for achieving stereospecific methylation with nearly 100% retention of configuration (Scheme 111)[274].

Ferrocenyl groups are useful tools for stereoselective syntheses. Hayashi and coworkers have discovered a novel class of ferrocenyl catalysts allowing the kinetic resolution of benzylic zinc derivatives, such as **448**[275]. The racemic mixture of the benzylic zinc reagent

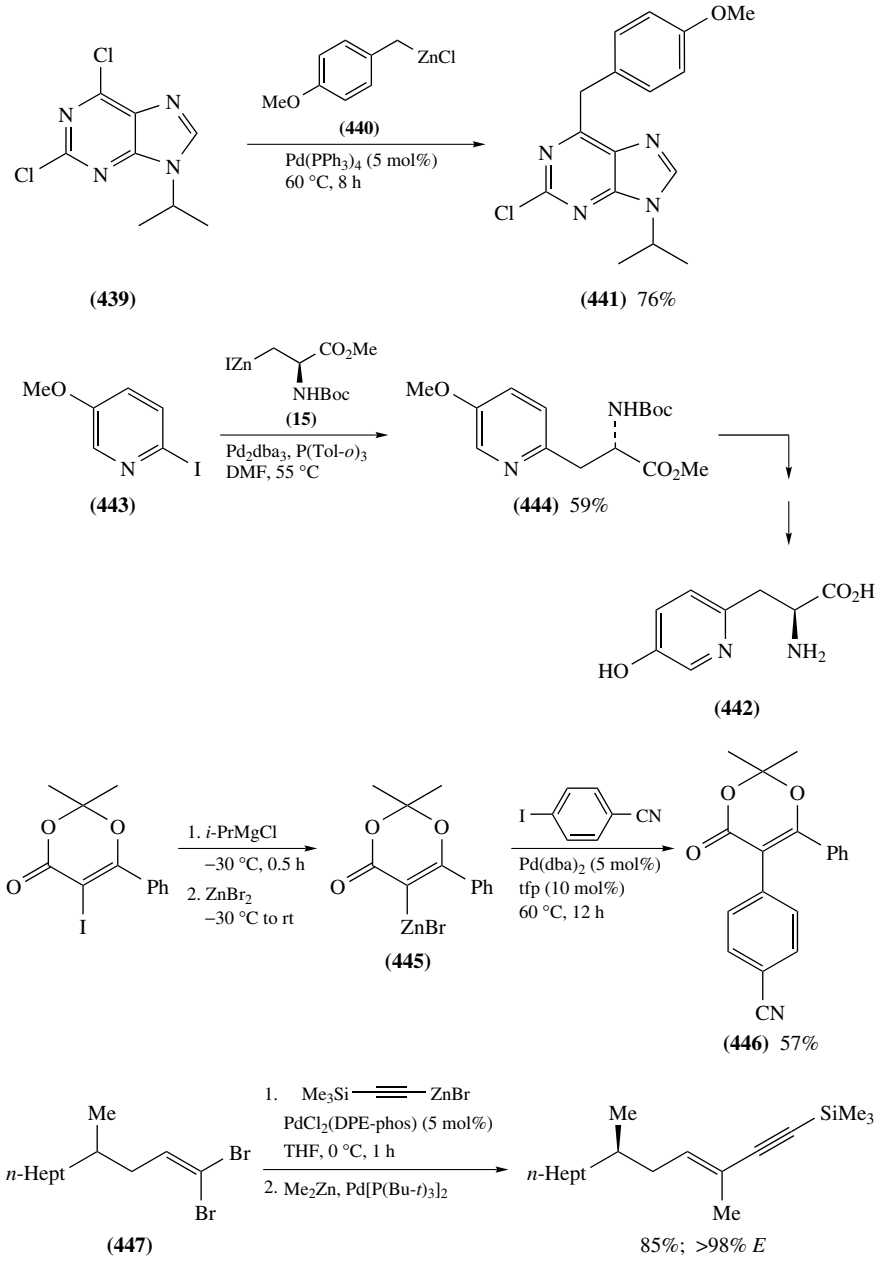

SCHEME 111. Negishi cross-coupling reactions

448 obtained by transmetalation from the corresponding Grignard reagent reacts with vinyl bromide in the presence of a Pd catalyst and the ferrocenyl aminophosphine **449**, leading to the asymmetric cross-coupling product **450** with up to 85–86% *ee*. Complex ferrocenyl derivatives such as **453**, being of interest as molecular materials with large second-order non-linear optical properties (NLO), have been prepared by the cross-coupling of the ferrocenylzinc reagent **452** with 1,3,5-tribromobenzene. The starting zinc reagent has been prepared starting from the chiral ferrocenyl derivative **451**. Selective metalation of **451** with *tert*-BuLi followed by a transmetalation with $ZnCl_2$ furnishes the zinc reagent **452**. Negishi cross-coupling was best performed using $PdCl_2(PPh_3)_2$ (5 mol%) as catalyst (Scheme 112)[276].

Further applications of Negishi's cross-coupling reactions for the synthesis of new chiral ferrocenyl ligands have been reported[277]. Interestingly, cross-coupling reactions can also be performed using triorganozincates, such as **454**[278]. Chloroenyne **455** reacts with various

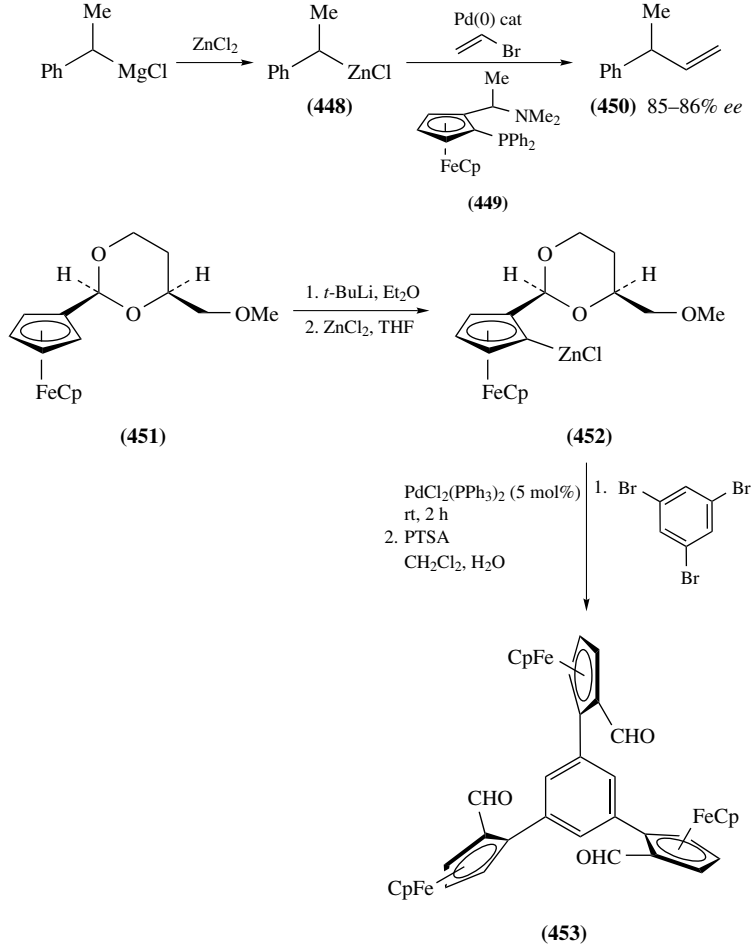

(453)

SCHEME 112. Ferrocenyl groups in cross-coupling reactions

magnesium zincates such as **454** generated *in situ* in the presence of $PdCl_2$(dppf) (5 mol%) in THF at 66 °C, showing that alkenyl chlorides readily insert Pd(0) complexes. Especially easy is the reaction of conjugated chloroenynes such as **455**, leading to the enyne **456** (Scheme 113)[278]. A selective cross-coupling reaction of (Z)-2,3-dibromopropenoate **457** with organozinc compounds allows the preparation of highly functionalized enolates such as **458** (Scheme 113).

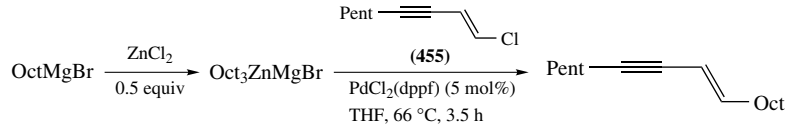

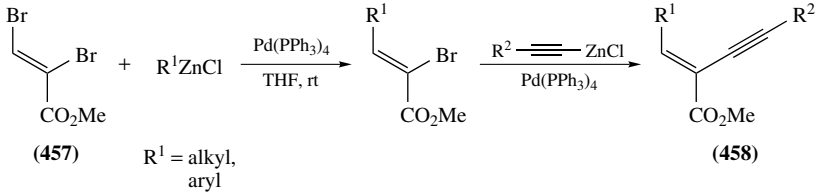

SCHEME 113. Synthesis of enynes using zinc organometallics

A flexible and convergent access to 2,3-disubstituted benzo[*b*]thiophenes, such as **459**, has been developed. The most concise approach involves a sequential coupling of an *o*-bromoiodobenzene, such as **460**, with benzylmercaptan and zinc acetylides, leading to the adduct **461**. Treatment with iodine followed by an iodine/magnesium exchange and acylation provides the polyfunctional benzofuran derivatives like **459**[279]. Negishi and Zeng have recently developed a novel highly selective route to carotenoids and related natural products via Zr-catalyzed carboalumination and Pd-catalyzed cross-coupling of unsaturated zinc reagents. Starting from β-ionone (**462**), the first cross-coupling sequence affords the unsaturated product (**463**) which, by an iterative reaction sequence and dimerization, affords β-carotene (**464**) with high stereoisomeric purity (Scheme 114)[280].

Acylation of organozincs with acid chlorides is efficiently catalyzed by palladium(0) complexes[244c–d,21]. Many functional groups are tolerated in this reaction. The cross-coupling of 3-carbethoxypropylzinc iodide with methacryl chloride provides an expeditive approach to polyfunctional enones, such as **465**[281]. The acylation of serine or glutamic acid-derived zinc species as developed by Jackson and coworkers[25–27] provides chiral γ-keto-α-amino acids in good yields. The acylation of the Jackson reagent with phenyl chloroformate or the direct reaction of an organozinc reagent with carbon monoxide under sonication in the presence of catalytic amounts of $(PPh_3)_2PdCl_2$ leads to the C_2-symmetrical ketone **466**[25k]. In a related reaction, organozinc halides are treated with carbon monoxide and an allylic benzoate in the presence of a catalytic amount of palladium(0) complex and provides *S*-ketoesters (Scheme 115)[282]. The reaction of *syn*- or *anti*-3-iodo-2-methylbutanamide **467** with zinc powder furnishes the zinc reagent **468**, which reacts with benzoyl chloride in the presence of Pd(0) catalyst leading to the *syn*-product **469** (Scheme 115)[283].

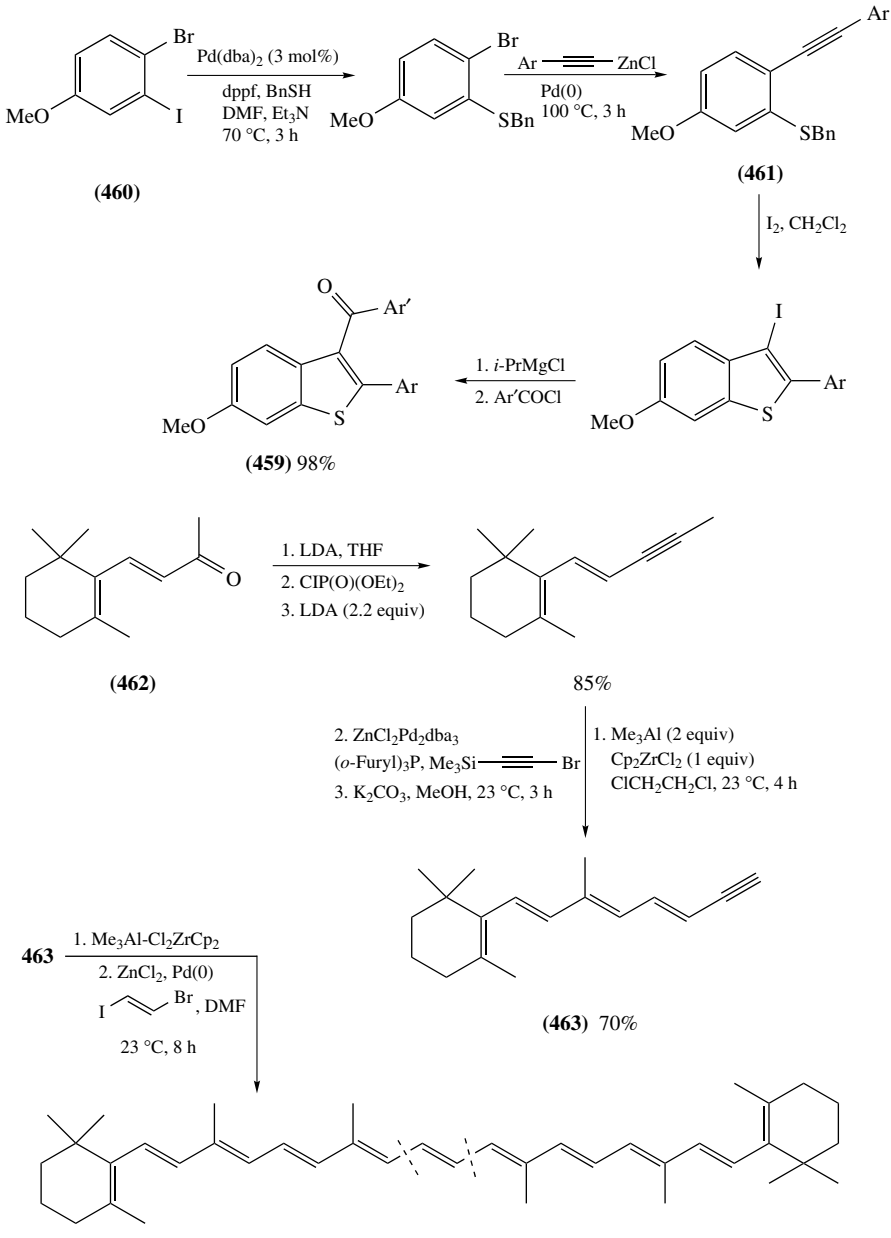

(464) β-carotene 68%; > 99% isomeric purity

SCHEME 114. Further applications of the Negishi cross-coupling reaction

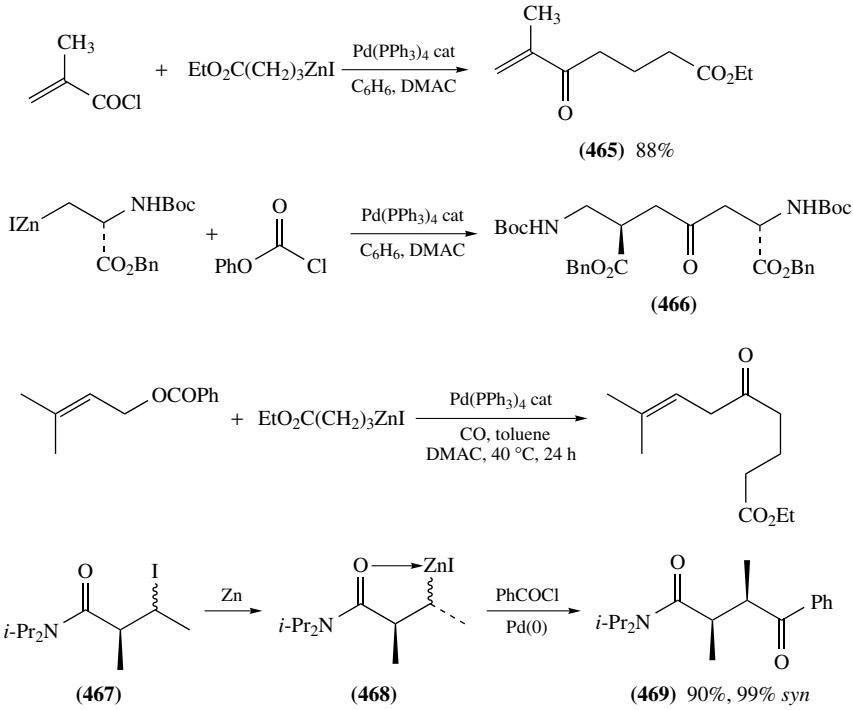

SCHEME 115. Palladium-catalyzed acylation reactions of organozincs

The reaction of thioesters, such as **470**, in the presence of nonpyrophoric $Pd(OH)_2/C$ (Pearlman's catalyst) with various functionalized organozinc halides leads to functionalized unsymmetrical ketones, such as **471**, in high yield (Fukuyama reaction)[284]. This catalyst can also be used for Sonogashira and Suzuki reactions[285]. The $Ni(acac)_2$-catalyzed cross-coupling of the functionalized zinc reagent with various thioesters such as **472** provides, under mild conditions, the acylation product **473** in 74% yield (Scheme 116). Interestingly, the addition of the organometallic zinc species to the thiolactone **474** furnishes, after acidic treatment, the vinylic sulfide **475** in 81% yield. The use of bromine for the activation of zinc dust for the preparation of the zinc reagent was found to be advantageous[286].

D. Reactions Catalyzed by Titanium and Zirconium(IV) Complexes

As mentioned previously, Lewis acids accelerate the addition of zinc organometallics to carbonyl derivatives. Titanium and zirconium(IV) salts are especially efficient catalysts. Oguni and coworkers[287] have shown in pioneer work that various chiral aminoalcohols catalyze the addition of diethylzinc to aldehydes[288]. Yoshioka, Ohno and coworkers have shown that the 1,2-bis-sulfonamide **476** is an excellent ligand for the asymmetric addition of Et_2Zn to various aldehydes[289]. The catalysts of the TADDOL family such as **477a** and **477b**, tolerate many functional groups in the aldehyde as well as in the diorganozinc. These catalysts were discovered by Seebach and have found numerous applications in asymmetric catalysis[290]. The convenient preparation of diorganozincs, starting from

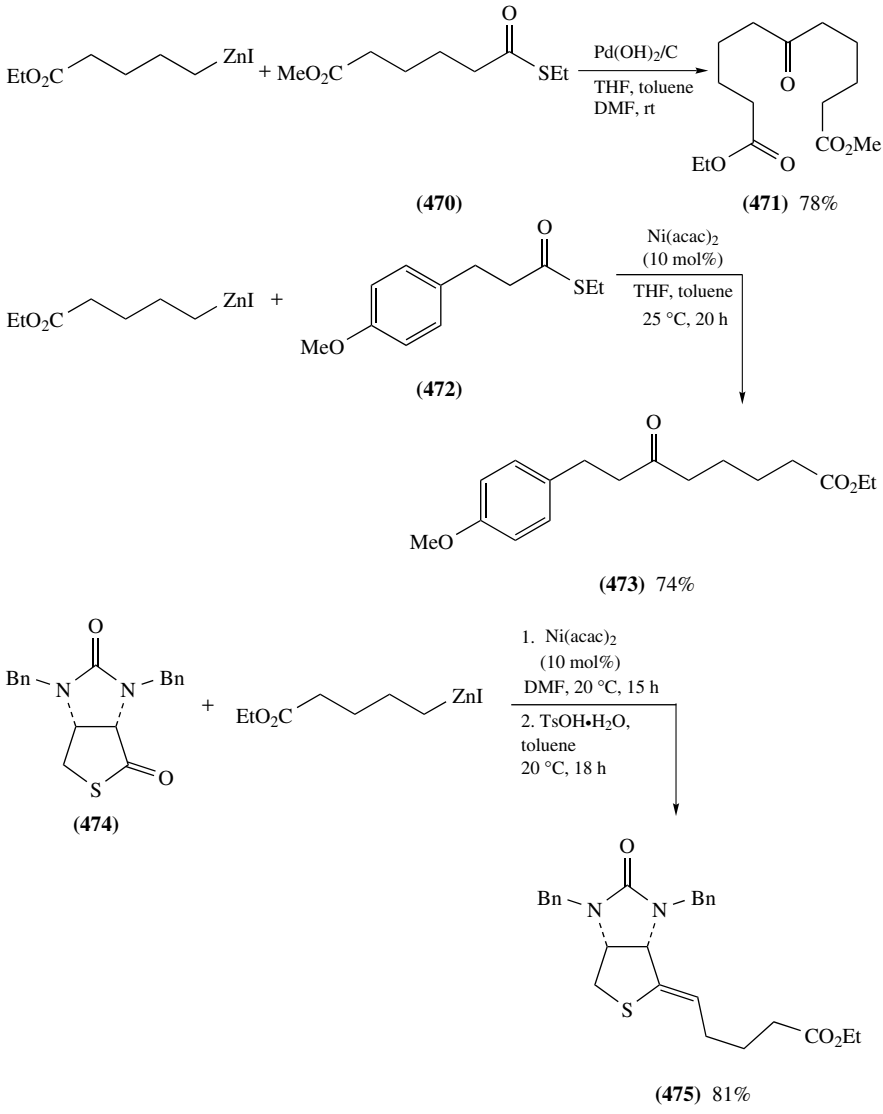

SCHEME 116. Acylation of thioesters with zinc organometallics

alkylmagnesium halides using $ZnCl_2$ in ether as transmetalating reagent followed by the addition of 1,4-dioxane, constitutes a practical method for the enantioselective addition of dialkylzincs[290f]. The enantioselective addition of polyfunctional diorganozincs is especially interesting. Thus, the reaction of the zinc reagent **478** with benzaldehyde in the presence of TADDOL **477a** provides the functionalized benzylic alcohol **479** in 84% *ee*[290f]. The more bulky ligand **477b** allows the addition of diorganozincs such as **480** to acetylenic aldehydes, leading to propargylic alcohols like **481** in 96% *ee* (Scheme 117)[290g].

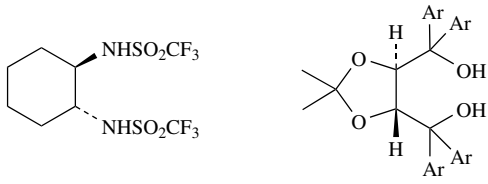

(476) TADDOL **(477a)** Ar = Ph
(477b) Ar = 2-naphthyl

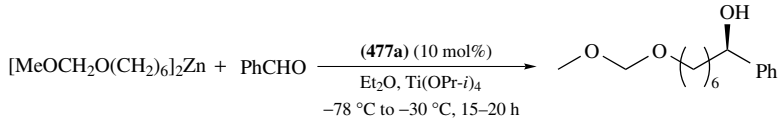

(478) **(479)** 68%, 84% *ee*

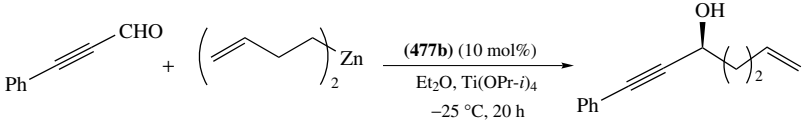

(480) **(481)** 78%, 96% *ee*

SCHEME 117. Enantioselective addition of functionalized diorganozincs to aldehydes catalyzed by TADDOL

This approach has been extended to the conjugate addition of primary dialkylzincs to 2-aryl- and 2-heteroaryl-nitroolefins and allows the preparation of enantioenriched 2-arylamines[291]. Dendric styryl TADDOLS[292, 293] and polymer-bound Ti-TADDOLates[294] have been proven to be very practical chiral catalysts for the enantioselective addition to aldehydes. Likewise, the immobilization of BINOL by cross-linking copolymerization of styryl derivatives has allowed several enantioselective Ti and Al Lewis acid mediated additions to aldehydes[294]. Dialkylzincs obtained via an I/Zn exchange or a B/Zn exchange have also been successfully used for the enantioselective additions to a variety of aldehydes[295]. The use of *trans*-(1R,2R)-bis(trifluoromethanesulfamido)cyclohexane (**476**) is an excellent chiral ligand. The presence of an excess of titanium tetraisopropoxide (2 equivalents) is, however, required[295]. The addition to unsaturated α-substituted aldehydes gives excellent enantioselectivities leading to polyfunctional allylic alcohols, such as **482**[93b]. Replacement of Ti(OPr-*i*)$_4$ with the sterically hindered titanium alkoxide (Ti(OBu-*t*)$_4$) leads to higher enantioselectivities[296].

This enantioselective preparation of allylic alcohols has been applied to the synthesis of the side chain of prostaglandins[297]. The addition to functionalized aldehydes, such as **483**, allows the synthesis of C_2-symmetrical 1,4-diols, such as **484**, with excellent diastereoselectivity and enantioselectivity[93b, 298]. An extension of this method allows the synthesis of C_3-symmetrical diol[299]. Aldol-type products result from the catalytic enantioselective addition of functionalized dialkylzincs to 3-TIPSO-substituted aldehydes, such as **485**, followed by a protection–deprotection and oxidation sequence affording **486** in 70% yield and 91% *ee* (Scheme 118)[300]. The addition to α-alkoxyaldehydes provides a

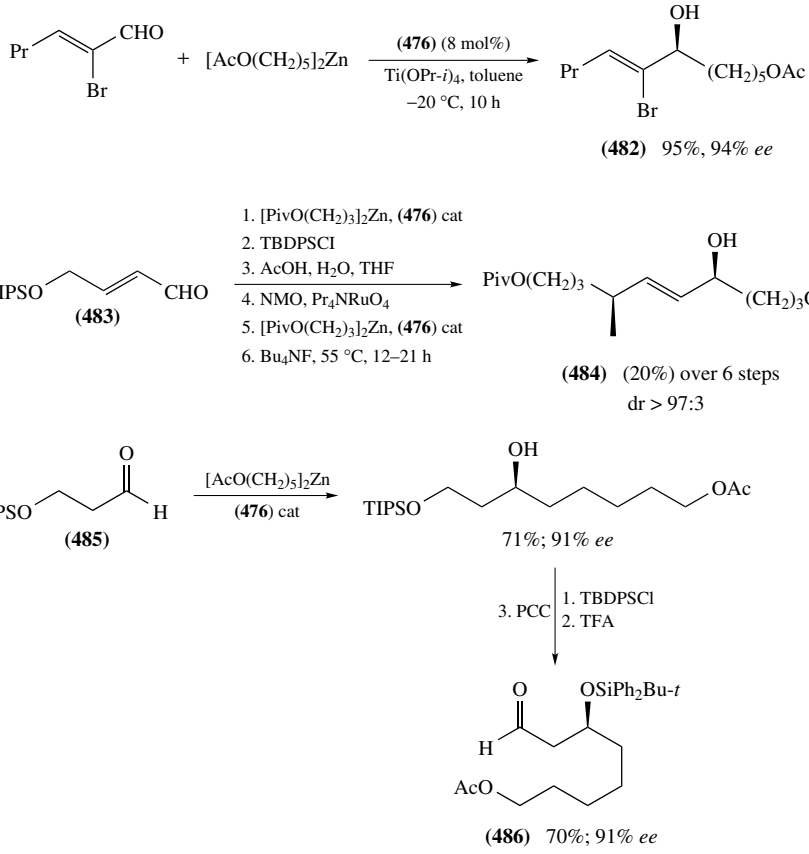

SCHEME 118. Enantioselective addition of functionalized dialkylzincs to functionalized aldehydes

general approach to monoprotected 1,2-diols which can be converted to epoxides, such as **487**, in excellent enantioselectivity[301]. The configuration of the newly chiral center does not depend on the configuration of the ligand **476**. Thus, the reaction of the chiral aldehyde **488** with a functionalized zinc reagent ($[PivO(CH_2)_3]_2Zn$) in the presence of the ligand **476** and **ent-476** gives the two diastereomeric allylic alcohols (**489** and **490**) with high stereoselectivity (Scheme 119)[298a].

Further applications to the preparation of chiral polyoxygenated molecules[302] and to the synthesis of the natural product (−)-mucocin[303] have been reported. The enantioselective addition of the functionalized diorganozinc reagent **491** to dodecanal in the presence of $Ti(OPr\text{-}i)_4$ and the chiral ditriflamide **476** provides the desired chiral alcohol **492** with 99% of diastereomeric excess and 65% yield. The diorganozinc reagent was obtained by treating the alkyl iodide **493** with an excess of Et_2Zn in the presence of CuCN (3 mol%). The chiral building block **492** was used in the total synthesis of cycloviracin B1, of interest for its selective antiviral activity[304]. An elegant synthesis of (*R*)-(−)-muscone has been reported by Oppolzer and coworkers[305]. The alkenylzinc reagent was prepared by hydroboration of the acetylenic aldehyde **494** with $(c\text{-Hex})_2BH$ at 0 °C, followed by a B/Zn exchange with Et_2Zn. The intramolecular addition in the presence of the chiral

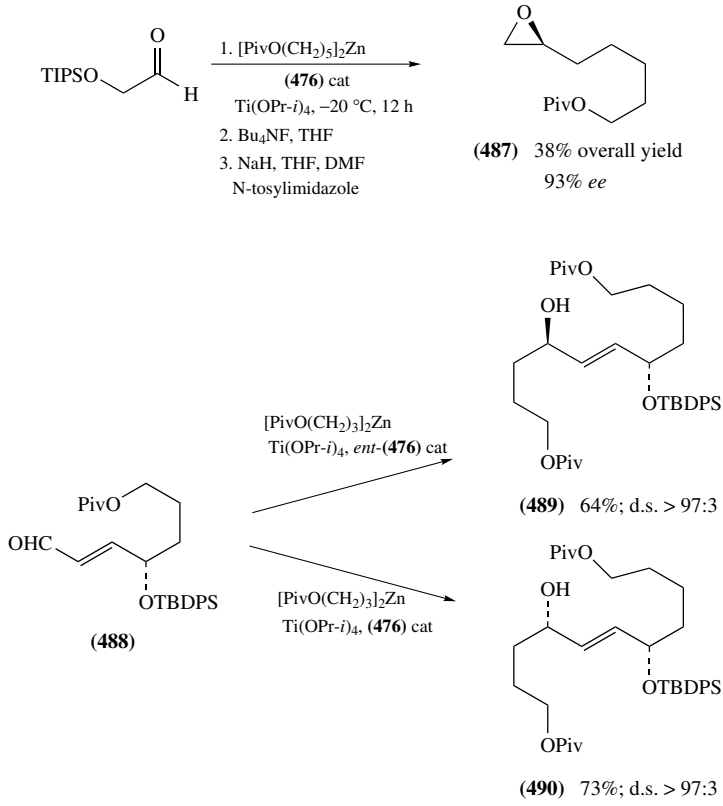

SCHEME 119. Enantioselective additions of functionalized zinc reagents to chiral aldehydes

aminoalcohol **495** provides the allylic alcohol **496** with 72% yield and 92% *ee*[104c,305]. The enantioselective addition of dialkylzincs to aromatic ketones is especially difficult. Yus and coworkers have developed a new chiral ligand **497** allowing the addition of dialkylzincs to various aromatic ketones in good yields. The enantioselective addition is promoted by Ti(OPr-*i*)$_4$ and tolerates the presence of several functional groups. Thus, the addition of Et_2Zn to phenacyl bromide provides the chiral alcohol **498** in 95% yield and 92% *ee* (Scheme 120)[306].

Alkynylzinc species generated *in situ* catalytically add to various aldehydes in very high enantioselectivities using reagent-grade toluene[307]. Chiral propargylic alcohols such as **499** are obtained in this way. As an application, the functionalized alkyne **500** has been added to (*R*)-isopropylidene glyceraldehyde **501** in the presence of $Zn(OTf)_2$ and *N*-methylephedrine providing the propargylic alcohol **502** in 75% and a diastereomeric ratio of 94:6[308]. The asymmetric addition of alkynylzinc reagents to aldehydes and ketones has recently been reviewed[309]. Especially important has been the stoichiometric addition of alkynylzinc derivatives leading to Efavirenz, a new drug for the treatment of AIDS[310]. The reaction of the chiral alkynylzinc reagent **503** obtained by the reaction of the aminoalcohol **504** successively with Me_2Zn, *neo*-PentOH and the alkynyllithium **505** with the activated trifluoromethyl ketone **506** provides the tertiary alcohol **507** in 91% yield and

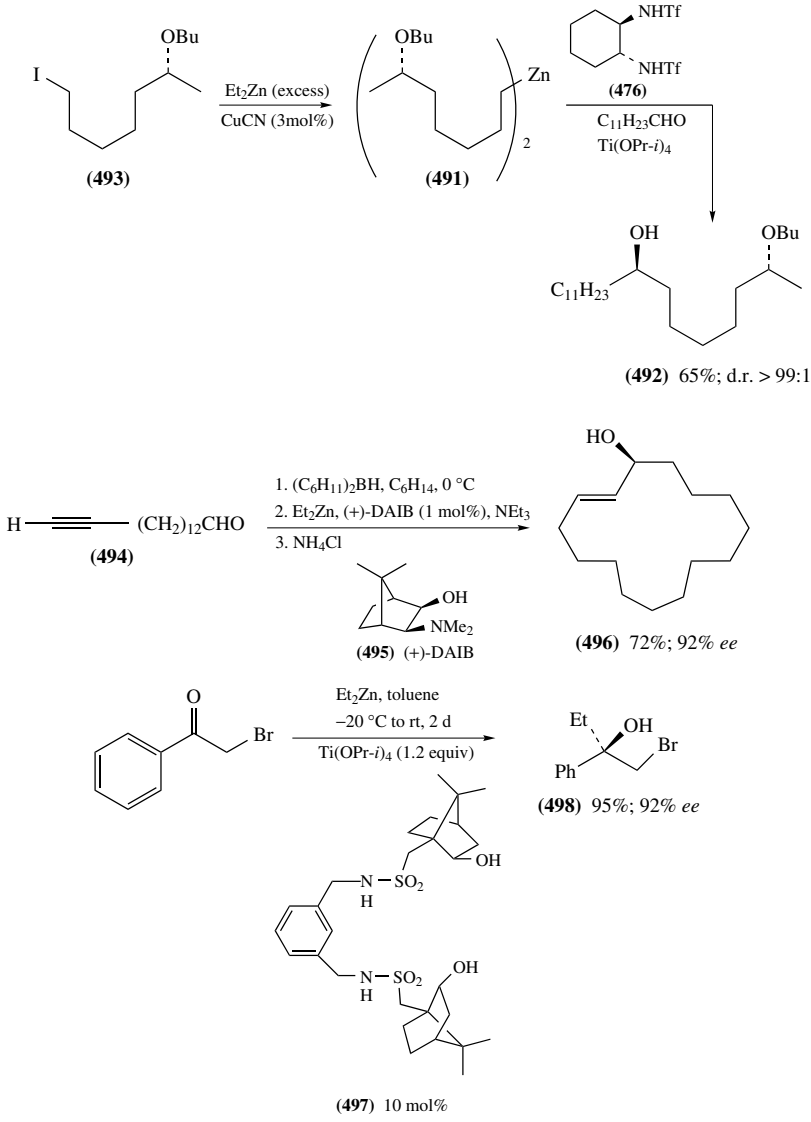

SCHEME 120. Enantioselective additions mediated by titanium salts

97% ee. A catalytic version of this reaction has been described by Carreira and Anand (Scheme 121)[311].

Interestingly, the chiral diamine **508** catalyzes the enantioselective addition of boronic acids to aromatic ketones like acetophenone. The reaction produces interesting tertiary diarylcarbinols such as **509** in up to 93% ee[312]. Bolm and coworkers have shown that this approach can also be used for a simple preparation of chiral diarylcarbinols (such as **510**) in the presence of the chiral ferrocenyl ligand **511** (Scheme 122)[313]. The addition of

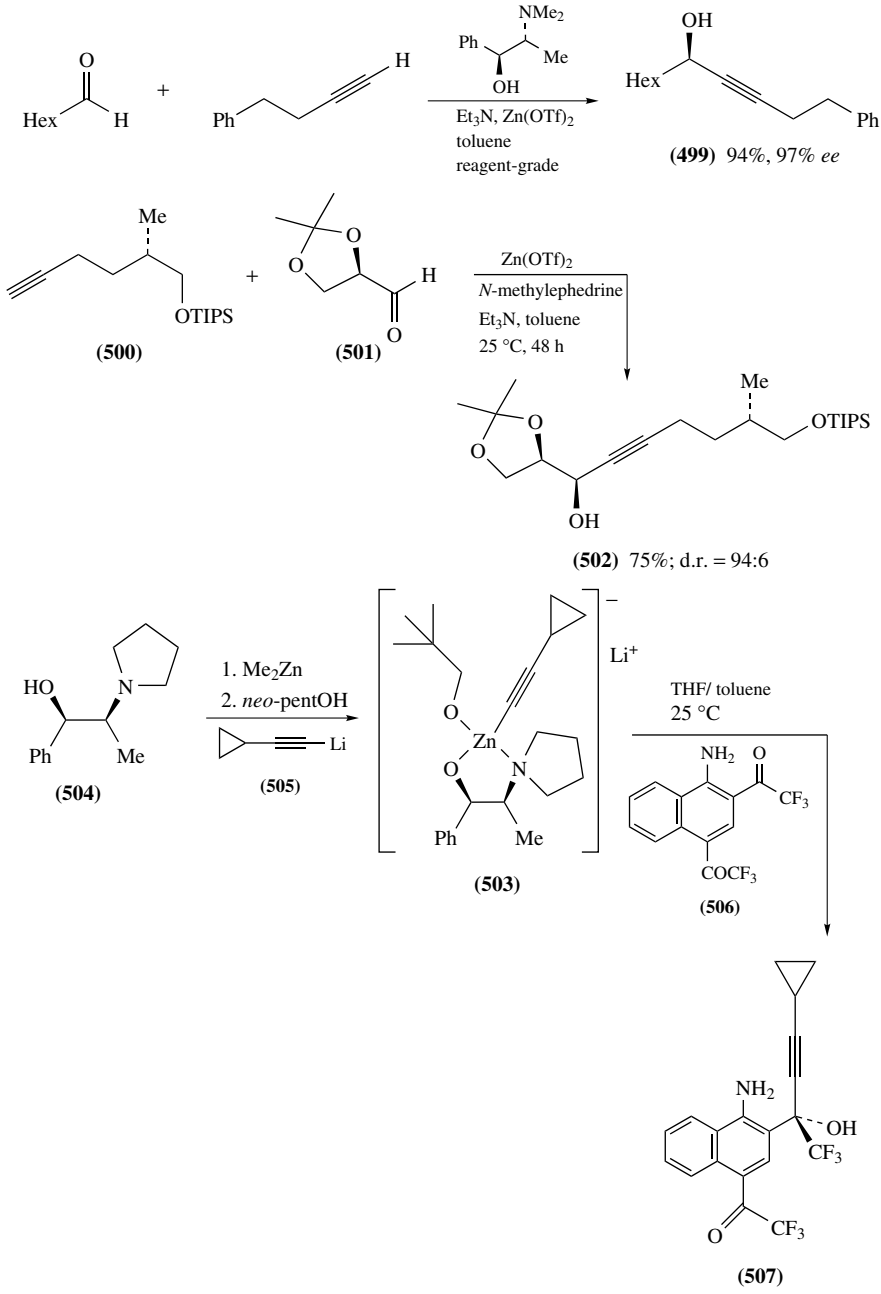

SCHEME 121. Enantioselective preparation of propargylic alcohols

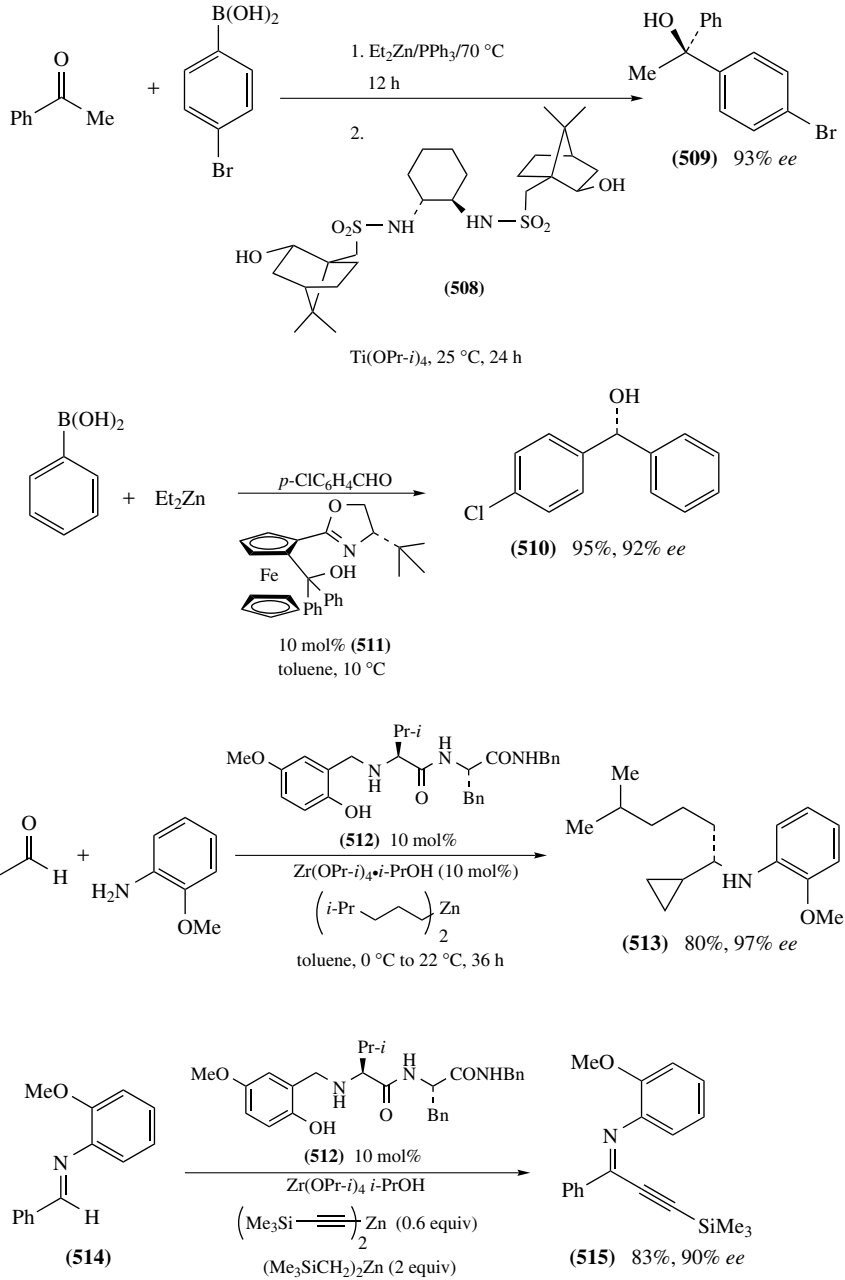

SCHEME 122. Enantioselective additions of diorganozincs to unreactive carbonyl derivatives

diorganozincs to imines is a difficult reaction. However, Hoveyda, Snapper and coworkers have found that the *in situ* generation in the presence of $Zr(OPr\text{-}i)_4$•HOPr-*i*, an excess of a dialkylzinc and a catalytic amount of the aminoacid derivative **512** allows an enantioselective addition, leading to various amines such as **513** with high enantioselectivity. In the presence of the modular catalyst **512** and $Zr(OPr\text{-}i)_4$•HOPr-*i* (11 mol%), the imine **514** reacts with bis-alkynylzincs in the presence of $(Me_3SiCH_2)_2Zn$, which is a zinc reagent with non-transferable Me_3SiCH_2 groups[314]. Under these conditions, an efficient addition reaction proceeds affording the propargylic amine **515** in 83% yield and 90% *ee* (Scheme 122)[315].

E. Reactions of Zinc Organometallics Catalyzed by Cobalt, Iron or Manganese Complexes

The catalysis of reactive main-group organometallics, such as organolithiums or organomagnesiums, by transition metal salts is often complicated by the formation of highly reactive transition metal centered ate-species (R_nMet^-) of transition metal complexes. These are especially prone to undergo β-hydrogen elimination reactions. Consequently, such transmetalations or catalysts have found little application in organic synthesis[316]. Organozinc reagents, due to their lower reactivity, do not have a tendency to produce ate-species (R_nMet^-) of transition metal complexes, therefore the resulting transition metal complexes of the type $RMetX_n$ have much higher thermal stability and a number of alkyl transition metal complexes displaying synthetically useful properties can be accessed in this way. Thus, the reaction of cobalt(II) bromide with dialkylzincs in THF:NMP furnishes blue solutions of organocobalt intermediates that have a half-life of *ca* 40 min at $-10\,^{\circ}C$. Similarly, the reaction of $FeCl_3$ with dipentylzinc produces a gray solution of an organoiron intermediate with a half-life of 2.5 h at $-10\,^{\circ}C$[317]. Interestingly, these new organocobalt(II) species undergo carbonylations at room temperature under mild conditions at rt affording symmetrical ketones, such as **516**, in satisfactory yield[318]. The stoichiometric preparation of organocobalt species is not necessary and catalytic amounts of cobalt(II) salts are sufficient to promote the acylation of diorganozincs[317]. Also, allylic chlorides react with zinc organometallics in a stereoselective manner. Thus, geranyl chloride (**517**) provides the S_N2-substitution product (*E*-**518**) with 90% yield and neryl chloride (**519**) affords the corresponding diene *Z*-**518** in 90% yield (Scheme 123)[317].

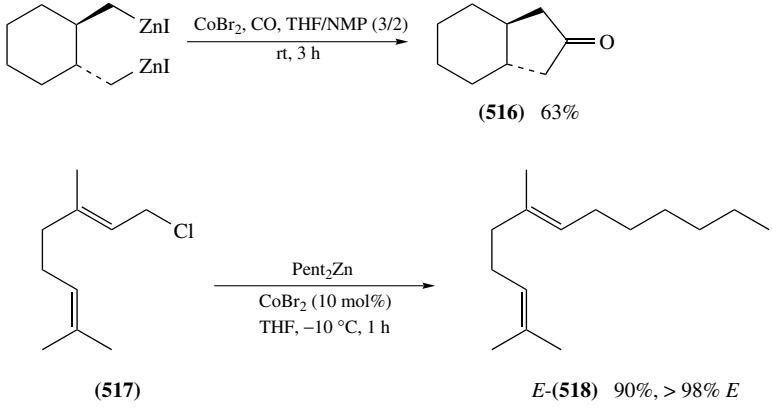

SCHEME 123. Cobalt-mediated reactions of diorganozincs

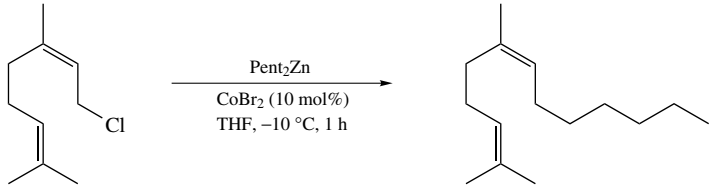

(519) *Z*-**(518)** 90%, > 98% *E*

SCHEME 123. (*continued*)

The reaction of manganese(II) salts with organozinc reagents does not provide the corresponding organomanganese reagents[319]. However, functionalized bromides can be metallated by Et_2Zn in the presence of catalytic amounts of $MnBr_2$[320] leading to a cyclized product, such as **520**, in 82% yield (Scheme 124)[321].

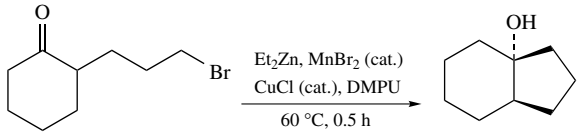

(520) 82%

SCHEME 124. Mn/Cu-mediated reaction of diorganozinc

IV. CONCLUSION

The synthesis of functionalized zinc organometallics can be accomplished with a variety of methods that have been developed in recent years. The intrinsic moderate reactivity of organozinc reagents can be dramatically increased by the use of the appropriate transition metal catalyst or Lewis acid. Furthermore, the low ionic character of the carbon–zinc bond allows the preparation of a variety of chiral zinc organometallics with synthetically useful configurational stability. These properties make organozinc compounds ideal intermediates for the synthesis of complex and polyfunctionalized organic molecules.

V. REFERENCES AND NOTES

1. E. Frankland, *Liebigs Ann. Chem.*, **71**, 171 and 213 (1849).
2. V. Grignard, *Compt. Rend. Acad. Sci. Paris*, **130**, 1322 (1900).
3. (a) S. Reformatsky, *Chem. Ber.*, **20**, 1210 (1887); **28**, 2842 (1895).
   (b) A. Fürstner, *Synthesis*, 571 (1989).
   (c) A. Fürstner, *Angew. Chem., Int. Ed. Engl.*, **32**, 164 (1993).
4. (a) H. E. Simmons and R. D. Smith, *J. Am. Chem. Soc.*, **80**, 5323 (1958).
   (b) H. E. Simmons, T. L. Cairns, A. Vladuchick and C. M. Hoiness, *Org. React.*, **20**, 1 (1972).
   (c) J. Furukawa, N. Kawabata and J. Nishimura, *Tetrahedron Lett.*, **7**, 3353 (1966).
   (d) M. Nakamura, A. Hirai and E. Nakamura, *J. Am. Chem. Soc.*, **125**, 2341 (2003).
   (e) E. Nakamura, K. Sekiya and I. Kuwajima, *Tetrahedron Lett.*, **28**, 337 (1987).
5. H. Hunsdiecker, H. Erlbach and E. Vogt, German patent 722467 (1942); *Chem. Abstr.*, **37**, 5080 (1943).
6. (a) P. Knochel and R. D. Singer, *Chem. Rev.*, **93**, 2117 (1993).
   (b) P. Knochel, *Synlett*, 393 (1995).
   (c) P. Knochel, S. Vettel and C. Eisenberg, *Appl. Organomet. Chem.*, **9**, 175 (1995).

(d) P. Knochel, F. Langer, M. Rottländer and T. Stüdemann, *Chem. Ber.*, **130**, 387 (1997).
(e) P. Knochel, J. Almena and P. Jones, *Tetrahedron*, **54**, 8275 (1998).
(f) P. Knochel and P. Jones, *Organozinc Reagents. A Practical Approach*, Oxford University Press, 1999.
(g) P. Knochel, N. Millot, A. L. Rodriguez and C. E. Tucker, *Org. React.*, **58**, 417 (2001).
(h) A. Boudier, L. O. Bromm, M. Lotz and P. Knochel, *Angew. Chem., Int. Ed.*, **39**, 4415 (2000).
7. (a) E. Negishi, L. F. Valente and M. Kobayashi, *J. Am. Chem. Soc.*, **102**, 3298 (1980).
(b) E. Erdik, *Tetrahedron*, **48**, 9577 (1992).
8. I. Antes and G. Frenking, *Organometallics*, **14**, 4263 (1995).
9. E. Hupe, P. Knochel and K. J. Szabó, *Organometallics*, **21**, 2203 (2002).
10. P. Knochel, M. C. P. Yeh, S. C. Berka and J. Talbert, *J. Org. Chem.*, **53**, 2390 (1988).
11. H. P. Knoess, M. T. Furlong, M. J. Rozema and P. Knochel, *J. Org. Chem.*, **56**, 5974 (1991).
12. S. C. Berk, M. C. P. Yeh, N. Jeong and P. Knochel, *Organometallics*, **9**, 3053 (1990).
13. P. Knochel and C. J. Rao, *Tetrahedron*, **49**, 29 (1993).
14. (a) T. M. Stevenson, B. Prasad, J. R. Citineni and P. Knochel, *Tetrahedron Lett.*, **37**, 8375 (1996).
(b) A. S. B. Prasad, T. M. Stevenson, J. R. Citineni, V. Nyzam and P. Knochel, *Tetrahedron*, **53**, 7237 (1997).
15. M. Gaudemar, *Bull. Soc. Chim. Fr.*, 974 (1962).
16. E. Erdik, *Tetrahedron*, **43**, 2203 (1987).
17. (a) J. K. Gawronsky, *Tetrahedron Lett.*, **25**, 2605 (1984).
(b) G. Picotin and P. Miginiac, *Tetrahedron Lett.*, **28**, 4551 (1987).
18. (a) A. Fürstner, R. Singer and P. Knochel, *Tetrahedron Lett.*, **35**, 1047 (1994).
(b) H. Stadtmüller, B. Greve, K. Lennick, A. Chair and P. Knochel, *Synthesis*, 69 (1995).
19. (a) R. D. Rieke, *Science*, **246**, 1260 (1989).
(b) R. D. Rieke, S.-H. Kim and X. Wu, *J. Org. Chem.*, **62**, 6921 (1997).
(c) L. Zhu and R. D. Rieke, *Tetrahedron Lett.*, **32**, 2865 (1991).
(d) R. D. Rieke, M. S. Sell and H. Xiong, *J. Am. Chem. Soc.*, **117**, 5429 (1995).
(e) R. D. Rieke, P. M. Hudnall and S. T. Uhm, *J. Chem. Soc., Chem. Commun.*, 269 (1973).
(f) R. D. Rieke, P. T.-J. Li, T. P. Burns and S. T. Uhm, *J. Org. Chem.*, **46**, 4323 (1981).
(g) R. D. Rieke and S. T. Uhm, *Synthesis*, 452 (1975).
(h) M. V. Hanson, J. D. Brown and R. D. Rieke, *Tetrahedron Lett.*, **35**, 7205 (1994).
(i) M. V. Hanson and R. D. Rieke, *Synth. Commun.*, **25**, 101 (1995).
(j) R. D. Rieke, M. V. Hanson and J. D. Brown, *J. Org. Chem.*, **61**, 2726 (1996).
(k) A. Guijarro and R. D. Rieke, *Angew. Chem., Int. Ed.*, **37**, 1679 (1998).
20. (a) M. V. Hanson and R. D. Rieke, *J. Am. Chem. Soc.*, **117**, 10775 (1995).
(b) L. Zhu, R. M. Wehmeyer and R. D. Rieke, *J. Org. Chem.*, **56**, 1445 (1991).
21. (a) B. H. Lipshutz and M. R. Wood, *J. Am. Chem. Soc.*, **116**, 11689 (1994).
(b) B. H. Lipshutz and M. R. Wood, *J. Am. Chem. Soc.*, **115**, 12625 (1993).
22. M. V. Hanson, J. D. Brown, R. D. Rieke and O. J. Niu, *Tetrahedron Lett.*, **35**, 7205 (1994).
23. T. Ito, Y. Ishino, T. Mizuno, A. Ishikawa and J. Kobayashi, *Synlett*, 2116 (2002).
24. (a) P. Knochel and J. F. Normant, *Tetrahedron Lett.*, **25**, 4383 (1984).
(b) D. Peters and R. Miethchen, *J. Prakt. Chem.*, **337**, 615 (1995).
(c) T. Kitazume and N. Ishikawa, *J. Am. Chem. Soc.*, **107**, 5186 (1985).
(d) H. Tso, T. Chou and Y. Lai, *J. Org. Chem.*, **54**, 4138 (1989).
(e) J. P. Sestelo, J. L. Mascarenas, L. Castedo and A. Mourino, *J. Org. Chem.*, **58**, 118 (1993).
(f) L. A. Sarandeses, A. Mourino and J. L. Luche, *J. Chem. Soc., Chem. Commun.*, 798 (1992).
25. (a) M. J. Dunn, R. F. W. Jackson, J. Pietruszka, N. Wishart, D. Ellis and M. J. Wythes, *Synlett*, 499 (1993).
(b) R. F. W. Jackson, N. Wishart and M. J. Wythes, *Synlett*, 219 (1993).
(c) M. J. Dunn, R. F. W. Jackson, J. Pietruszka and D. Turner, *J. Org. Chem.*, **60**, 2210 (1995).
(d) C. Malan and C. Morin, *Synlett*, 167 (1996).
(e) R. F. W. Jackson, M. J. Wythes and A. Wood, *Tetrahedron Lett.*, **30**, 5941 (1989).
(f) R. F. W. Jackson, A. Wood and M. J. Wythes, *Synlett*, 735 (1990).
(g) M. J. Dunn and R. F. W. Jackson, *J. Chem. Soc., Chem. Commun.*, 319 (1992).

(h) R. F. W. Jackson, N. Wishart, A. Wood, K. James and M. J. Wythes, *J. Org. Chem.*, **57**, 3397 (1992).
(i) C. S. Dexter and R. F. W. Jackson, *J. Chem. Soc., Chem. Commun.*, 75 (1998).
(j) J. L. Fraser, R. F. W. Jackson and B. Porter, *Synlett*, 379 (1994).
(k) R. F. W. Jackson, W. Neil and M. J. Wythes, *J. Chem. Soc., Chem. Commun.*, 1587 (1992).
26. R. F. W. Jackson, I. Rilatt and P. J. Murray, *Chem. Commun.*, 1242 (2003).
27. R. F. W. Jackson, I. Rilatt and P. J. Murray, *Org. Biomol. Chem.*, **2**, 110 (2004).
28. C. Hunter, R. F. W. Jackson and H. K. Rami, *J. Chem. Soc., Perkin Trans. 1*, 1349 (2001).
29. C. Jubert and P. Knochel, *J. Org. Chem.*, **57**, 5425 (1992).
30. C. Jubert and P. Knochel, *J. Org. Chem.*, **57**, 5431 (1992).
31. S. Huo, *Org. Lett.*, **5**, 423 (2003).
32. (a) B. H. Lipshutz, P. A. Blomgren and S. K. Kim, *Tetrahedron Lett.*, **40**, 197 (1999).
(b) B. H. Lipshutz and P. A. Blomgren, *J. Am. Chem. Soc.*, **121**, 5819 (1999).
(c) C. Dai and G. C. Fu, *J. Am. Chem. Soc.*, **123**, 2719 (2001).
33. (a) H. Blancou and A. Commeyras, *J. Fluorine Chem.*, **20**, 255 (1982).
(b) H. Blancou and A. Commeyras, *J. Fluorine Chem.*, **20**, 267 (1982).
(c) S. Benefice-Malouet, H. Blancou and A. Commeyras, *J. Fluorine Chem.*, **30**, 171 (1985).
34. (a) R. N. Haszeldine and E. G. Walaschewski, *J. Chem. Soc.*, 3607 (1953).
(b) W. T. Miller, E. Bergman and A. H. Fainberg, *J. Am. Chem. Soc.*, **79**, 4159 (1957).
(c) R. D. Chambers, W. K. R. Musgrave and J. Savoy, *J. Chem. Soc.*, 1993 (1962).
(d) D. J. Burton, *Tetrahedron*, **48**, 189 (1992).
(e) D. J. Burton, Z.-Y. Yang and P. A. Morken, *Tetrahedron*, **50**, 2993 (1994).
35. (a) D. J. Burton and D. M. Wiemers, *J. Am. Chem. Soc.*, **107**, 5014 (1985).
(b) D. M. Wiemers and D. J. Burton, *J. Am. Chem. Soc.*, **108**, 832 (1986).
(c) B. Jiang and Y. Xu, *J. Org. Chem.*, **56**, 733 (1991).
(d) P. A. Morken, H. Lu, A. Nakamura and D. J. Burton, *Tetrahedron Lett.*, **32**, 4271 (1991).
(e) P. A. Morken and D. J. Burton, *J. Org. Chem.*, **58**, 1167 (1993).
36. (a) S. Sibille, V. Ratovelomanana, J. Périchon, S. Sibille and M. Troupel, *Synthesis*, 369 (1990).
(b) M. Durandetti, M. Devaud and J. Périchon, *New J. Chem.*, **20**, 659 (1996).
(c) S. Sibille, V. Ratovelomanana, J.-Y. Nédélec and J. Périchon, *Synlett*, 425 (1993).
(d) C. Gosmini, J.-Y. Nédélec and J. Périchon, *Tetrahedron Lett.*, **38**, 1941 (1997).
(e) N. Zylber, J. Zylber, Y. Rollin, E. Dunach and J. Périchon, *J. Organomet. Chem.*, **444**, 1 (1993).
(f) Y. Rollin, S. Derien, E. Dunach, C. Gébéhenne and J. Périchon, *Tetrahedron*, **49**, 7723 (1993).
37. (a) P. Gomes, C. Gosmini and J. Périchon, *Synlett*, **10**, 1673 (2002).
(b) P. Gomes, H. Fillon, C. Gosmini, E. Labbé and J. Périchon, *Tetrahedron*, **58**, 8417 (2002).
(c) H. Fillon, E. Le Gall, C. Gosmini and J. Périchon, *Tetrahedron Lett.*, **43**, 5941 (2002).
(d) C. Gosmini, Y. Rollin, J.-Y. Nédélec and J. Périchon, *J. Org. Chem.*, **65**, 6024 (2000).
38. S. Seka, O. Buriez, J.-Y. Nédélec and J. Périchon, *Chem. Eur. J.*, **8**, 2534 (2002).
39. (a) M. Mellah, E. Labbé, J.-Y. Nédélec and J. Périchon, *New. J. Chem.*, **25**, 318 (2001).
(b) C. Gosmini, J.-Y. Nédélec and J. Périchon, *Tetrahedron Lett.*, **41**, 201 (1999).
40. (a) H. Stadtmüller, R. Lentz, C. E. Tucker, T. Stüdemann, W. Dörner and P. Knochel, *J. Am. Chem. Soc.*, **115**, 7027 (1993).
(b) H. Stadtmüller, A. Vaupel, C. E. Tucker, T. Stüdemann and P. Knochel, *Chem. Eur. J.*, **2**, 1204 (1996).
(c) A. Vaupel and P. Knochel, *J. Org. Chem.*, **61**, 5743 (1996).
41. (a) H. Stadtmüller, C. E. Tucker, A. Vaupel and P. Knochel, *Tetrahedron Lett.*, **34**, 7911 (1993).
(b) A. Vaupel and P. Knochel, *Tetrahedron Lett.*, **35**, 8349 (1994).
42. (a) A. Vaupel and P. Knochel, *Tetrahedron Lett.*, **36**, 231 (1995).
(b) H. Stadtmüller and P. Knochel, *Synlett*, 463 (1995).
43. K. A. Agrios and M. Srebnik, *J. Org. Chem.*, **58**, 6908 (1993).
44. (a) I. Klement, P. Knochel, K. Chau and G. Cahiez, *Tetrahedron Lett.*, **35**, 1177 (1994).
(b) E. Riguet, I. Klement, C. K. Reddy, G. Cahiez and P. Knochel, *Tetrahedron Lett.*, **37**, 5865 (1996).

45. (a) H. Fillon, C. Gosmini and J. Périchon, *J. Am. Chem. Soc.*, **125**, 3867 (2003).
(b) P. Gomes, C. Gosmini and J. Périchon, *Synthesis*, 1909 (2003).
(c) I. Kazmierski, M. Bastienne, C. Gosmini, J.-M. Paris and J. Périchon, *J. Org. Chem.*, **69**, 936 (2004).
(d) I. Kazmierski, C. Gosmini, J. M. Paris and J. Périchon, *Tetrahedron Lett.*, **44**, 6417 (2003).
(e) S. Seka, O. Buriez and J. Périchon, *Chem. Eur. J.*, **9**, 3597 (2003).
46. (a) T. N. Majid and P. Knochel, *Tetrahedron Lett.*, **31**, 4413 (1990).
(b) A. S. B. Prasad and P. Knochel, *Tetrahedron*, **53**, 16711 (1997).
(c) S. C. Berk, P. Knochel and M. C. P. Yeh, *J. Org. Chem.*, **53**, 5789 (1988).
(d) J. J. van der Baan, H. Stichter, G. J. J. Out, F. Bickelhaupt and G. W. Klumpp, *Tetrahedron Lett.*, **29**, 3579 (1988).
(e) J. van der Louw, J. L. van der Baan, H. Stichter, G. J. J. Out, F. J. J. de Kanter, F. Bickelhaupt and G. W. Klumpp, *Tetrahedron*, **48**, 9877 (1992).
(f) J. van der Louw, J. L. van der Baan, G. J. J. Out, F. J. J. de Kanter, F. Bickelhaupt and G. W. Klumpp, *Tetrahedron*, **48**, 9901 (1992).
(g) T. A. van der Heide, J. L. van der Baan, F. Bickelhaupt and G. W. Klumpp, *Tetrahedron Lett.*, **33**, 475 (1992).
(h) G. A. Molander and D. C. Shubert, *J. Am. Chem. Soc.*, **108**, 4683 (1986).
47. (a) C. E. Tucker, S. A. Rao and P. Knochel, *J. Org. Chem.*, **55**, 5446 (1990).
(b) P. Knochel, T. S. Chou, H. G. Chen, M. C. P. Yeh and M. J. Rozema, *J. Org. Chem.*, **54**, 5202 (1989).
(c) T. S. Chou and P. Knochel, *J. Org. Chem.*, **55**, 4791 (1990).
(d) P. Knochel, T. S. Chou, C. Jubert and R. Duddu, *J. Org. Chem.*, **58**, 588 (1993).
48. (a) M. C. P. Yeh, P. Knochel, W. M. Butler and S. C. Berk, *Tetrahedron Lett.*, **29**, 6693 (1988).
(b) H. G. Chen, J. L. Gage, S. D. Barrett and P. Knochel, *Tetrahedron Lett.*, **31**, 1829 (1990).
(c) M. C. P. Yeh, P. Knochel and L. E. Santa, *Tetrahedron Lett.*, **29**, 3887 (1988).
(d) M. C. P. Yeh and P. Knochel, *Tetrahedron Lett.*, **30**, 4799 (1989).
(e) C. Retherford, M. C. P. Yeh, I. Schipor, H. G. Chen and P. Knochel, *J. Org. Chem.*, **54**, 5200 (1989).
49. M. C. P. Yeh and C.-N. Chuang, *J. Chem. Soc., Chem. Commun.*, 703 (1994).
50. H. G. Chen, C. Hoechstetter and P. Knochel, *Tetrahedron Lett.*, **30**, 4795 (1989).
51. M. C. P. Yeh, H. G. Chen and P. Knochel, *Org. Synth.*, **70**, 195 (1991).
52. (a) S. Achyutha Rao, C. E. Tucker and P. Knochel, *Tetrahedron Lett.*, **31**, 7575 (1990).
(b) S. Achyutha Rao, T.-S. Chou, I. Schipor and P. Knochel, *Tetrahedron*, **48**, 2025 (1992).
53. (a) P. Knochel, *J. Am. Chem. Soc.*, **112**, 7431 (1990).
(b) G. Kanai, N. Miyaura and A. Suzuki, *Chem. Lett.*, 845 (1993).
(c) T. Watanabe, N. Miyaura and A. Suzuki, *J. Organomet. Chem.*, **444**, C1 (1993).
(d) T. Watanabe, M. Sakai, N. Miyaura and A. Suzuki, *J. Chem. Soc., Chem. Commun.*, 467 (1994).
54. (a) C. Janakiram Rao and P. Knochel, *J. Org. Chem.*, **56**, 4593 (1991).
(b) P. Knochel and C. Janakiram Rao, *Tetrahedron*, **49**, 29 (1993).
(c) B. S. Bronk, S. J. Lippard and R. L. Danheiser, *Organometallics*, **12**, 3340 (1993).
55. C. Retherford, T.-S. Chou, R. M. Schelkun and P. Knochel, *Tetrahedron Lett.*, **31**, 1833 (1990).
56. W. E. Parham and C. K. Bradsher, *Acc. Chem. Res.*, **15**, 300 (1982).
57. (a) J. F. Cameron and J. M. J. Frechet, *J. Am. Chem. Soc.*, **113**, 4303 (1991).
(b) P. Wiriyachitra, S. J. Falcone and M. P. Cava, *J. Org. Chem.*, **44**, 3957 (1979).
58. C. E. Tucker, T. N. Majid and P. Knochel, *J. Am. Chem. Soc.*, **114**, 3983 (1992).
59. E. M. E. Viseux, P. J. Parsons and J. B. J. Pavey, *Synlett*, 861 (2003).
60. B. A. Anderson and N. K. Harn, *Synthesis*, 583 (1996).
61. S. Superchi, N. Sotomayor, G. Miao, B. Joseph and V. Snieckus, *Tetrahedron Lett.*, **37**, 6057 (1996).
62. (a) E. Lorthiois, I. Marek and J.-F. Normant, *Tetrahedron Lett.*, **38**, 89 (1997).
(b) P. Karoyan and G. Chassaing, *Tetrahedron Lett.*, **38**, 85 (1997).
(c) P. Karoyan, J. Quancard, J. Vaissermann and G. Chassaing, *J. Org. Chem.*, **68**, 2256 (2003).
(d) P. Karoyan and G. Chassaing, *Tetrahedron: Asymmetry*, **8**, 2025 (1997).

(e) P. Karoyan, A. Triolo, R. Nannicini, D. Giannotti, M. Altamura, G. Chassaing and G. E. Perrotta, *Tetrahedron Lett.*, **40**, 71 (1999).
(f) P. Karoyan and G. Chassaing, *Tetrahedron Lett.*, **43**, 253 (2002).
(g) J. Quancard, H. Magella, S. Lavielle, G. Chassaing and P. Karoyan, *Tetrahedron Lett.*, **45**, 2185 (2004).
63. (a) E. Nakamura and K. Kubota, *J. Org. Chem.*, **62**, 792 (1997).
(b) M. Nakamura, T. Hatakeyama, K. Hara and E. Nakamura, *J. Am. Chem. Soc.*, **125**, 6362 (2003).
(c) M. Nakamura, H. Isobe and E. Nakamura, *Chem. Rev.*, **103**, 1295 (2003).
(d) M. Nakamura, T. Inoue, A. Sato and E. Nakamura, *Org. Lett.*, **2**, 2193 (2000).
64. (a) J. P. Gillet, R. Sauvetre and J.-F. Normant, *Synthesis*, 538 (1986).
(b) J.-F. Normant, *J. Organomet. Chem.*, **400**, 19 (1990).
65. (a) T. Shigeoka, Y. Kuwahara, K. Watanabe, K. Satro, M. Omote, A. Ando and I. Kumadaki, *J. Fluorine Chem.*, **103**, 99 (2000).
(b) T. Shigeoka, Y. Kuwahara, K. Watanabe, K. Satro, M. Omote, A. Ando and I. Kumadaki, *Heterocycles*, **52**, 383 (2000).
66. J. M. Bainbridge, S. J. Brown, P. N. Ewing, R. R. Gibson and J. M. Percy, *J. Chem. Soc., Perkin Trans. 1*, 2541 (1998).
67. R. Anilkumar and D. J. Burton, *Tetrahedron Lett.*, **43**, 6979 (2002).
68. J. Ichikawa, M. Fujiwara, H. Nawata, T. Okauchi and T. Minami, *Tetrahedron Lett.*, **37**, 8799 (1996).
69. (a) P. Wipf and W. Xu, *J. Org. Chem.*, **61**, 6556 (1996).
(b) P. Wipf and W. Xu, *Tetrahedron Lett.*, **35**, 5197 (1994).
70. Y. Ni, K. K. D. Amarasinghe and J. Montgomery, *Org. Lett.*, **4**, 1743 (2002).
71. E. Negishi, N. Okukado, A. O. King, D. E. Van Horn and B. I. Spiegel, *J. Am. Chem. Soc.*, **100**, 2254 (1978).
72. R. K. Dieter, R. T. Watson and R. Goswami, *Org. Lett.*, **6**, 253 (2004).
73. E. Frankland and D. Duppa, *Liebigs Ann. Chem.*, **130**, 117 (1864).
74. M. J. Rozema, R. Duddu, C. E. Tucker and P. Knochel, *J. Organomet. Chem.*, **438**, 11 (1992).
75. P. Knochel, W. Dohle, N. Gommermann, F. F. Kneisel, F. Kopp, T. Korn, I. Sapountzis and V. A. Vu, *Angew. Chem., Int. Ed.*, **42**, 4302 (2003).
76. A. E. Jensen and P. Knochel, *J. Organomet. Chem.*, **653**, 122 (2002).
77. (a) D. Seyferth, H. Dertouzos and L. J. Todd, *J. Organomet. Chem.*, **4**, 18 (1965).
(b) D. Seyferth and S. B. Andrews, *J. Organomet. Chem.*, **30**, 151 (1971).
78. (a) P. Knochel, N. Jeong, M. J. Rozema and M. C. P. Yeh, *J. Am. Chem. Soc.*, **111**, 6474 (1989).
(b) P. Knochel and S. Achyutha Rao, *J. Am. Chem. Soc.*, **112**, 6146 (1990).
(c) M. J. Rozema and P. Knochel, *Tetrahedron Lett.*, **32**, 1855 (1991).
(d) M. R. Burns and J. K. Coward, *J. Org. Chem.*, **58**, 528 (1993).
(e) A. Sidduri, M. J. Rozema and P. Knochel, *J. Org. Chem.*, **58**, 2694 (1993).
(f) A. Sidduri and P. Knochel, *J. Am. Chem. Soc.*, **114**, 7579 (1992).
79. P. Knochel, M. J. Rozema, C. E. Tucker, C. Retherford, M. I. Furlong and S. Achyutha Rao, *Pure. Appl. Chem.*, **64**, 361 (1992).
80. (a) E. Negishi and K. Akiyoshi, *J. Am. Chem. Soc.*, **110**, 646 (1988).
(b) E. Negishi, K. Akiyoshi, B. O'Connor, K. Takagi and G. Wu, *J. Am. Chem. Soc.*, **111**, 3089 (1989).
81. T. Katsuhira, T. Harada, K. Maejima, A. Osada and A. Oku, *J. Org. Chem.*, **58**, 6166 (1993).
82. (a) T. Harada, K. Hattori, T. Katsuhira and A. Oku, *Tetrahedron Lett.*, **30**, 6035 and 6039 (1989).
(b) T. Harada, T. Katsuhira, K. Hattori and A. Oku, *J. Org. Chem.*, **58**, 2958 (1993).
(c) T. Harada, T. Katsuhira and A. Oku, *J. Org. Chem.*, **57**, 5805 (1992).
83. J. P. Varghese, I. Zouev, L. Aufauvre, P. Knochel and I. Marek, *Eur. J. Org. Chem.*, 4151 (2002).
84. S. Achyutha Rao and P. Knochel, *J. Org. Chem.*, **56**, 4591 (1991).
85. R. Duddu, M. Eckhardt, M. Furlong, H. P. Knoess, S. Berger and P. Knochel, *Tetrahedron*, **50**, 2415 (1994).
86. (a) M. Sakurai, T. Hata and Y. Yabe, *Tetrahedron Lett.*, **34**, 5939 (1993).

(b) S. Sakami, T. Houkawa, A. Asaoka and H. Takei, *J. Chem. Soc., Perkin Trans. 1*, 285 (1995).
(c) T. Houkawa, T. Ueda, S. Sakami, M. Asaoka and H. Takei, *Tetrahedron Lett.*, **37**, 1045 (1996).
87. C. Darcel, F. Flachsmann and P. Knochel, *Chem. Commun.*, 205 (1998).
88. F. Wang, J. Tang, L. Labaudinière, I. Marek and J.-F. Normant, *Synlett*, 723 (1995).
89. J.-F. Poisson and J. F. Normant, *J. Am. Chem. Soc.*, **123**, 4639 (2001).
90. J.-F. Poisson and J. F. Normant, *Org. Lett.*, **3**, 1889 (2001).
91. I. Wilson and R. F. W. Jackson, *J. Chem. Soc., Perkin Trans. 1*, 2845 (2002).
92. (a) J. Furukawa, N. Kawabata and J. Nishimura, *Tetrahedron Lett.*, **7**, 3353 (1966).
(b) J. Furukawa and N. Kawabata, *Adv. Organomet. Chem.*, **12**, 83 (1974).
93. (a) M. J. Rozema, A. Sidduri and P. Knochel, *J. Org. Chem.*, **57**, 1956 (1992).
(b) M. J. Rozema, C. Eisenberg, H. Lütjens, R. Ostwald, K. Belyk and P. Knochel, *Tetrahedron Lett.*, **34**, 3115 (1993).
94. A. B. Charette, A. Beauchemin and J.-F. Marcoux, *J. Am. Chem. Soc.*, **120**, 5114 (1998).
95. E. Hupe, M. I. Calaza and P. Knochel, *J. Organomet. Chem.*, **680**, 136 (2003).
96. L. Micouin and P. Knochel, *Synlett*, 327 (1997).
97. F. F. Kneisel, M. Dochnahl and P. Knochel, *Angew. Chem., Int. Ed.*, **43**, 1017 (2004).
98. (a) S. Berger, F. Langer, C. Lutz, P. Knochel, T. A. Mobley and C. K. Reddy, *Angew. Chem., Int. Ed. Engl.*, **36**, 1496 (1997).
(b) P. Jones, C. K. Reddy and P. Knochel, *Tetrahedron*, **54**, 1471 (1998).
99. C. Petrier, J. De Souza Barbosa, C. Dupuy and J.-L. Luche, *J. Org. Chem.*, **50**, 5761 (1985).
100. E. J. Corey, J. O. Link and Y. Shao, *Tetrahedron Lett.*, **33**, 3435 (1992).
101. L. I. Zakharin and O. Y. Okhlobystin, *Z. Obshch. Chim.*, **30**, 2134 (1960); *Engl. Trans.*, 2109; *Chem. Abstr.*, **55**, 9319a (1961).
102. (a) K.-H. Thiele and P. Zdunneck, *J. Organomet. Chem.*, **4**, 10 (1965).
(b) K.-H. Thiele, G. Engelhardt, J. Köhler and M. Arnstedt, *J. Organomet. Chem.*, **9**, 385 (1967).
103. (a) F. Langer, J. Waas and P. Knochel, *Tetrahedron Lett.*, **34**, 5261 (1993).
(b) F. Langer, L. Schwink, A. Devasagayaraj, P.-Y. Chavant and P. Knochel, *J. Org. Chem.*, **61**, 8229 (1996).
104. (a) M. Srebnik, *Tetrahedron Lett.*, **32**, 2449 (1991).
(b) W. Oppolzer and R. N. Radinov, *Helv. Chim. Acta*, **75**, 170 (1992).
(c) W. Oppolzer and R. N. Radinov, *J. Am. Chem. Soc.*, **115**, 1593 (1993).
105. R. Köster, G. Griasnow, W. Larbig and P. Binger, *Liebigs Ann. Chem.*, **672**, 1 (1964).
106. A. Devasagayaraj, L. Schwink and P. Knochel, *J. Org. Chem.*, **60**, 3311 (1995).
107. H. C. Brown, A. K. Mandal, N. M. Yoon, B. Singaram, J. R. Schwier and P. K. Jadhav, *J. Org. Chem.*, **47**, 5069 (1982).
108. (a) L. Micouin, M. Oestreich and P. Knochel, *Angew. Chem., Int. Ed. Engl.*, **36**, 245 (1997).
(b) A. Boudier, F. Flachsmann and P. Knochel, *Synlett*, 1438 (1998).
(c) E. Hupe and P. Knochel, *Org. Lett.*, **3**, 127 (2001).
109. E. Hupe and P. Knochel, *Angew. Chem., Int. Ed.*, **40**, 3022 (2001).
110. A. Boudier, E. Hupe and P. Knochel, *Angew. Chem., Int. Ed.*, **39**, 2294 (2000).
111. I. Fleming and N. J. Lawrence, *J. Chem. Soc., Perkin Trans 1*, 3309 (1992).
112. (a) E. Hupe, M. I. Calaza and P. Knochel, *Tetrahedron Lett.*, **42**, 8829 (2001).
(b) E. Hupe, M. I. Calaza and P. Knochel, *Chem. Eur. J.*, **9**, 2789 (2003).
113. K. Burgess and M. J. Ohlmeyer, *J. Org. Chem.*, **56**, 1027 (1991).
114. (a) K. Burgess and M. J. Ohlmeyer, *Chem. Rev.*, **91**, 1179 (1991).
(b) A. H. Hoveyda, D. A. Evans and G. C. Fu, *Chem. Rev.*, **93**, 1307 (1993).
115. (a) D. A. Evans, G. C. Fu and A. H. Hoveyda, *J. Am. Chem. Soc.*, **110**, 6917 (1988).
(b) K. Burgess and M. J. Ohlmeyer, *Tetrahedron Lett.*, **30**, 395 (1989).
116. E. Hupe, M. I. Calaza and P. Knochel, *Chem. Commun.*, 1390 (2002).
117. (a) S. Vettel, A. Vaupel and P. Knochel, *Tetrahedron Lett.*, **36**, 1023 (1995).
(b) S. Vettel, A. Vaupel and P. Knochel, *J. Org. Chem.*, **61**, 7473 (1996).
118. (a) Y. Tamaru, A. Tanaka, K. Yasui, S. Goto and S. Tanaka, *Angew. Chem., Int. Ed. Engl.*, **34**, 787 (1995).
(b) M. Shimizu, M. Kimura, S. Tanaka and Y. Tamaru, *Tetrahedron Lett.*, **39**, 609 (1998).
119. (a) Y. Tamaru, *J. Organomet. Chem.*, **576**, 215 (1999).

(b) M. Kimura, I. Kiyama, T. Tomizawa, Y. Horino, S. Tanaka and Y. Tamaru, *Tetrahedron Lett.*, **40**, 6795 (1999).
(c) M. Kimura, S. Matsuo, K. Shibata and Y. Tamaru, *Angew. Chem., Int. Ed.*, **38**, 3386 (1999).
(d) M. Kimura, T. Tomizawa, Y. Horino, S. Tanaka and Y. Tamaru, *Tetrahedron Lett.*, **41**, 3627 (2000).
(e) K. Shibata, M. Kimura, M. Shimizu and Y. Tamaru, *Org. Lett.*, **3**, 2181 (2001).
(f) M. Kimura, Y. Horino, R. Mukai, S. Tanaka and Y. Tamaru, *J. Am. Chem. Soc.*, **123**, 10401 (2001).
120. (a) P. Jones, N. Millot and P. Knochel, *Chem. Commun.*, 2405 (1998).
(b) P. Jones, N. Millot and P. Knochel, *J. Org. Chem.*, **64**, 186 (1999).
(c) P. Jones and P. Knochel, *Chem. Commun.*, 2407 (1998).
(d) N. Millot and P. Knochel, *Tetrahedron Lett.*, **40**, 7779 (1999).
(e) C. Piazza, N. Millot and P. Knochel, *J. Organomet. Chem.*, **624**, 88 (2001).
121. R. Benn, E. G. Hoffmann, H. Lehmkuhl and H. Nehl, *J. Organomet. Chem.*, **146**, 103 (1978).
122. W. Oppolzer, H. Bienayme and A. Genevois-Borella, *J. Am. Chem. Soc.*, **113**, 9660 (1991).
123. C. Meyer, I. Marek and J.-F. Normant, *Tetrahedron Lett.*, **37**, 857 (1996).
124. (a) W. Tückmankel, K. Oshima and H. Nozaki, *Chem. Ber.*, **119**, 1581 (1986).
(b) R. M. Fabicon, M. Parvez and H. G. Richey, *J. Am. Chem. Soc.*, **113**, 1412 and 6680 (1991).
(c) A. P. Purdy and C. F. George, *Organometallics*, **11**, 1955 (1992).
(d) H. Toshiro, H. Wada and A. Oku, *J. Org. Chem.*, **60**, 5370 (1995).
125. (a) M. Isobe, S. Konda, N. Nagasawa and T. Goto, *Chem. Lett.*, 679 (1977).
(b) R. A. Kjonaas and R. K. Hoffer, *J. Org. Chem.*, **53**, 4133 (1988).
(c) R. A. Kjonaas and E. J. Vawter, *J. Org. Chem.*, **51**, 3933 (1986).
126. (a) J. F. G. A. Jansen and B. L. Feringa, *Tetrahedron Lett.*, **29**, 3593 (1988).
(b) J. F. G. A. Jansen and B. L. Feringa, *J. Chem. Soc., Chem. Commun.*, 741 (1989).
(c) J. F. G. A. Jansen and B. L. Feringa, *J. Org. Chem.*, **55**, 4168 (1990).
127. D. Seebach and W. Langen, *Helv. Chim. Acta*, **62**, 1701 and 1710 (1979).
128. (a) M. Uchiyama, M. Koike, M. Kameda, Y. Kondo and T. Sakamoto, *J. Am. Chem. Soc.*, **118**, 8733 (1996).
(b) Y. Kondo, N. Takazawa, C. Yamazaki and T. Sakamoto *J. Org. Chem.*, **59**, 4717 (1994).
129. (a) Y. Kondo, T. Komine, M. Fujinami, M. Uchiyama and T. Sakamoto, *J. Comb. Chem.*, **1**, 123 (1999).
(b) G. Reginato and M. Taddei, *II Farmaco*, **57**, 373 (2002).
130. T. Harada, T. Kaneko, T. Fujiwara and A. Oku, *J. Org. Chem.*, **62**, 8966 (1997).
131. I. N. Houpis, A. Molina, I. Dorziotis, R. A. Reamer, R. P. Volante and P. J. Reider, *Tetrahedron Lett.*, **38**, 7131 (1997).
132. (a) P. Knochel, in *Comprehensive Organic Synthesis*, Vol. 1 (Eds. B. M. Trost, I. Fleming and S. L. Schreiber), Pergamon, Oxford, 1991, p. 221.
(b) P. Knochel and J.-F. Normant, *Tetrahedron Lett.*, **25**, 1475 (1984).
(c) G. Rousseau and J. Drouin, *Tetrahedron*, **39**, 2307 (1983).
(d) P. Knochel and J.-F. Normant, *Tetrahedron Lett.*, **25**, 4383 (1984).
133. Y. A. Dembélé, C. Belaud, P. Hitchcock and J. Villiéras, *Tetrahedron: Asymmetry*, **3**, 351 (1992).
134. P. Knochel and J.-F. Normant, *J. Organomet. Chem.*, **309**, 1 (1986).
135. H. Yamamoto, in *Comprehensive Organic Synthesis*, Vol. 2 (Eds. B. M. Trost, I. Fleming and S. L. Schreiber), Pergamon, Oxford, 1991, p. 81.
136. (a) J. A. Marshall, *Chem. Rev.*, **100**, 3163 (2000).
(b) J. A. Marshall and M. M. Yanik, *J. Org. Chem.*, **66**, 1373 (2001).
(c) B. W. Gung, X. Xue, N. Katz and J. A. Marshall, *Organometallics*, **22**, 3158 (2003).
137. G. Zweifel and G. Hahn, *J. Org. Chem.*, **49**, 4565 (1984).
138. K. Nützel, in *Methoden der Organischen Chemie, Metallorganische Verbindungen Be, Mg, Ca, Sr, Ba, Zn, Cd*, Vol. 13/2a, Stuttgart, 1973, p. 552.
139. (a) T. Harada and E. Kutsuwa, *J. Org. Chem.*, **68**, 6716 (2003).
(b) T. Harada and A. Oku, in *Organozinc Reagents. A Practical Approach* (Eds. P. Knochel and P. Jones), Chap. 6, Oxford, University Press New York, 1999.
140. J. G. Giess and M. Le Blanc, *Angew. Chem.*, **90**, 654 (1978).

141. (a) I. Klement and P. Knochel, *Synlett*, 1113 (1995).
(b) I. Klement, H. Lütjens and P. Knochel, *Tetrahedron*, **53**, 9135 (1997).
142. I. Klement, K. Lennick, C. E. Tucker and P. Knochel, *Tetrahedron Lett.*, **34**, 4623 (1993).
143. (a) M. Gaudernar, *C. R. Acad. Sci. Paris*, **273**, 1669 (1971).
(b) P. Knochel and J.-F. Normant, *Tetrahedron Lett.*, **27**, 1039, 1043 and 4427 (1986).
(c) I. Marek and J.-F. Normant, *Chem. Rev.*, **96**, 3241 (1996).
(d) I. Marek and J.-F. Normant, *J. Org. Chem.*, **59**, 4154 (1994).
(e) D. Beruben, I. Marek, J.-F. Normant and N. Platzer, *J. Org. Chem.*, **60**, 2488 (1995).
144. (a) F. Langer and P. Knochel, *Tetrahedron Lett.*, **36**, 4591 (1995).
(b) F. Langer, K. Püntener, R. Stürmer and P. Knochel, *Tetrahedron: Asymmetry*, **8**, 715 (1997).
145. A. Longeau, F. Langer and P. Knochel, *Tetrahedron Lett.*, **37**, 2209 (1996).
146. (a) S. J. Greenfield, A. Agarkov and S. R. Gilbertson, *Org. Lett.*, **5**, 3069 (2003).
(b) H. Stadtmüller and P. Knochel, *Organometallics*, **14**, 3163 (1995).
147. N. Millot, C. Piazza, S. Avolio and P. Knochel, *Synthesis*, 941 (2000).
148. N. Gommermann, C. Koradin and P. Knochel, *Synthesis*, 2143 (2002).
149. F. Lamaty, R. Lazaro and J. Martinez, *Tetrahedron Lett.*, **38**, 3385 (1997).
150. (a) D. L. Comins and S. O'Connor, *Tetrahedron Lett.*, **28**, 1843 (1987).
(b) D. L. Comins and M. A. Foley, *Tetrahedron Lett.*, **29**, 6711 (1988).
151. E. Nakamura, S. Aoki, K. Sekiya, H. Oshino and I. Kuwajima, *J. Am. Chem. Soc.*, **109**, 8056 (1987).
152. M. Ludwig, K. Polborn and K. T. Wanner, *Heterocycles*, **61**, 299 (2003).
153. A. R. Katritzky, Z. Luo, Y. Fang and P. J. Steel, *J. Org. Chem.*, **66**, 2858 (2001).
154. (a) S. N. Thorn and T. Gallagher, *Synlett*, 185 (1996).
(b) S. D. Rychnovsky and N. A. Powell, *J. Org. Chem.*, **62**, 6460 (1997).
155. (a) S. Xue, K.-Z. Han, L. He and Q.-X. Guo, *Synlett*, 870 (2003).
(b) J. D. Rainier and J. M. Cox, *Org. Lett.*, **2**, 2707 (2000).
156. W. J. Thompson, T. J. Tucker, J. E. Schwering and J. L. Barnes, *Tetrahedron Lett.*, **31**, 6819 (1990).
157. A. E. Decamp, A. T. Kawaguchi, R. P. Volante and I. Shinkai, *Tetrahedron Lett.*, **32**, 1867 (1991).
158. U. Koert, H. Wagner and U. Pidun, *Chem. Ber.*, **127**, 1447 (1994).
159. J. J. Almena Perea, T. Ireland and P. Knochel, *Tetrahedron Lett.*, **38**, 5961 (1997).
160. (a) C. K. Reddy, A. Devasagayaraj and P. Knochel, *Tetrahedron Lett.*, **37**, 4495 (1996).
(b) M. Kitamura, T. Miki, K. Nakano and R. Noyori, *Tetrahedron Lett.*, **37**, 5141 (1996).
161. B. S. Bronk, S. J. Lippard and R. L. Danheiser, *Organometallics*, **12**, 3340 (1993).
162. S. Kim and J. M. Lee, *Tetrahedron Lett.*, **31**, 7627 (1990).
163. M. Arisawa, Y. Torisawa, M. Kawahara, M. Yamanaka, A. Nishida and M. Nakagawa, *J. Org. Chem.*, **62**, 4327 (1997).
164. (a) G. Posner, *Org. React.*, **19**, 1 (1972).
(b) B. H. Lipshutz, *Synthesis*, 325 (1957).
(c) B. H. Lipshutz and S. Seugepta, *Org. React.*, **41**, 135 (1992).
(d) G. Posner, *Org. React.*, **22**, 253 (1975).
165. T. Stemmler, J. E. Penner-Hahn and P. Knochel, *J. Am. Chem. Soc.*, **115**, 348 (1993).
166. S. Marquais, G. Cahiez and P. Knochel, *Synlett*, 849 (1994).
167. H. T. Teunissen and F. Bickelhaupt, *Tetrahedron Lett.*, **33**, 3537 (1992).
168. (a) M. C. P. Yeh and P. Knochel, *Tetrahedron Lett.*, **29**, 2395 (1988).
(b) H. Ochiai, Y. Tamaru, K. Tsubaki and Z. Yoshida, *J. Org. Chem.*, **52**, 4418 (1987).
(c) M. Arai, T. Kawasuji and E. Nakamura, *J. Org. Chem.*, **58**, 5121 (1993).
(d) E. Nakamura, K. Sekiya, M. Arai and S. Aoki, *J. Am. Chem. Soc.*, **111**, 3091 (1989).
(e) K. Sekiya and E. Nakamura, *Tetrahedron Lett.*, **29**, 5155 (1988).
169. H. J. C. Deboves, U. Grabowska, A. Rizzo and R. F. W. Jackson, *J. Chem. Soc., Perkin Trans. 1*, 4284 (2000).
170. A. Hirai, A. Matsui, K. Komatsu, K. Tanino and M. Miyashita, *Chem. Commun.*, 1970 (2002).
171. B. H. Lipshutz, K. Woo, T. Gross, D. J. Buzard and R. Tirado, *Synlett*, 477 (1997).
172. (a) P. Knochel and D. Seebach, *Tetrahedron Lett.*, **23**, 3897 (1982).
(b) D. Seebach and P. Knochel, *Helv. Chim. Acta*, **67**, 261 (1984).
173. S. Ma and A. Zhang, *J. Org. Chem.*, **67**, 2287 (2002).

174. T. Konno, M. Tanikawa, T. Ishihara and H. Yamanaka, *Collect. Czech. Chem. Commun.*, **67**, 1421 (2002).
175. A. Yanagisawa, Y. Noritake, N. Nomura and H. Yamamoto, *Synlett*, 251 (1991).
176. M. I. Calaza, E. Hupe and P. Knochel, *Org. Lett.*, **5**, 1059 (2003).
177. R. W. Hoffmann, *Chem. Rev.*, **89**, 1841 (1989).
178. N. Harrington-Frost, H. Leuser, M. I. Calaza, F. F. Kneisel and P. Knochel, *Org. Lett.*, **5**, 2111 (2003).
179. D. Soorukram and P. Knochel, *Org. Lett.*, **6**, 2409 (2004).
180. (a) B. Breit and P. Demel, *Adv. Synth. Catal.*, **343**, 429 (2001).
(b) B. Breit and P. Demel, *Tetrahedron*, **56**, 2833 (2000).
181. (a) A. S. E. Karlström, F. F. Huerta, G. J. Meuzelaar and J. E. Bäckvall, *Synlett*, 923 (2001).
(b) G. J. Meuzelaar, A. S. E. Karlström, M. van Klaveren, E. S. M. Persson, A. del Villar, G. van Koten and J.-E. Bäckvall, *Tetrahedron*, **56**, 2895 (2000).
(c) A. Alexakis, C. Malan, L. Lea, C. Benhaim and X. Fournioux, *Synlett*, 927 (2001).
(d) A. Alexakis and K. Croset, *Org. Lett.*, **4**, 4147 (2002).
(e) H. Malda, A. W. van Zijl, L. A. Arnold and B. L. Feringa, *Org. Lett.*, **3**, 1169 (2001).
(f) O. Equey, E. Vrancken and A. Alexakis, *Eur. J. Org. Chem.*, 2151 (2004).
(g) K. Tissot-Croset, D. Polet and A. Alexakis, *Angew. Chem., Int. Ed.*, **43**, 2426 (2004).
182. C. A. Luchaco-Cullis, H. Mizutani, K. E. Murphy and A. H. Hoveyda, *Angew. Chem., Int. Ed.*, **40**, 1456 (2001).
183. (a) F. Dübner and P. Knochel, *Tetrahedron Lett.*, **41**, 9233 (2000).
(b) F. Dübner and P. Knochel, *Angew. Chem., Int. Ed.*, **38**, 379 (1999).
184. W. Blankenfeldt, J.-W. Liao, L.-C. Lo and M. C. P. Yeh, *Tetrahedron Lett.*, **37**, 7361 (1996).
185. (a) M. C. P. Yeh, M.-L. Sun and S.-K. Lin, *Tetrahedron Lett.*, **32**, 113 (1991).
(b) M. C. P. Yeh and S. J. Tau, *J. Chem. Soc., Chem. Commun.*, 13 (1992).
(c) M. C. P. Yeh, C.-J. Tsou, C.-N. Chuang and H.-C. Lin, *J. Chem. Soc., Chem. Commun.*, 890 (1992).
(d) M. C. P. Yeh, B.-A. Shen, H.-W. Fu, S. I. Tau and L. W. Chuang, *J. Am. Chem. Soc.*, **115**, 5941 (1993).
186. M. C. P. Yeh, C.-C. Hwu, A.-T. Lee and M.-S. Tsai, *Organometallics*, **20**, 4965 (2001).
187. J. H. Rigby and M. Kirova-Snover, *Tetrahedron Lett.*, **38**, 8153 (1997).
188. H. Sörensen and A. E. Greene, *Tetrahedron Lett.*, **31**, 7597 (1990).
189. E. J. Corey and C. J. Helel, *Tetrahedron Lett.*, **38**, 7511 (1997).
190. A. Sidduri, N. Budries, R. M. Laine and P. Knochel, *Tetrahedron Lett.*, **33**, 7515 (1992).
191. B. H. Lipshutz and R. W. Vivian, *Tetrahedron Lett.*, **40**, 2871 (1999).
192. J.-J. Liu, F. Konzelmann and K.-C. Luk, *Tetrahedron Lett.*, **44**, 3901 (2003).
193. C. E. Tucker and P. Knochel, *Synthesis*, 530 (1993).
194. C. Retherford and P. Knochel, *Tetrahedron Lett.*, **32**, 441 (1991).
195. C. E. Tucker and P. Knochel, *J. Org. Chem.*, **58**, 4781 (1993).
196. (a) R. Giovannini, T. Stüdemann, G. Dussin and P. Knochel, *Angew. Chem., Int. Ed.*, **37**, 2387 (1998).
(b) A. Devasagayaraj, T. Stüdemann and P. Knochel, *Angew. Chem., Int. Ed. Engl.*, **34**, 2723 (1995).
197. R. Giovannini and P. Knochel, *J. Am. Chem. Soc.*, **120**, 11186 (1998).
198. A. E. Jensen and P. Knochel, *J. Org. Chem.*, **67**, 79 (2002).
199. M. Piber, A. E. Jensen, M. Rottländer and P. Knochel, *Org. Lett.*, **1**, 1323 (1999).
200. (a) H. Eick and P. Knochel, *Angew. Chem., Int. Ed. Engl.*, **35**, 218 (1996).
(b) A. S. Bhanu Prasad, H. Eick and P. Knochel, *J. Organomet. Chem.*, **562**, 133 (1998).
(c) Y. Tamaru, H. Ochiai, F. Sanda and Z. Yoshida, *Tetrahedron Lett.*, **26**, 5529 (1985).
201. (a) K. Soai, T. Suzuki and T. Shono, *J. Chem. Soc., Chem. Commun.*, 317 (1994).
(b) N. El Alami, C. Belaud and J. Villiéras, *J. Organomet. Chem.*, **319**, 303 (1987).
202. (a) P. Knochel and J.-F. Normant, *Tetrahedron Lett.*, **25**, 4383 (1984).
(b) G. Rousseau and J. M. Conia, *Tetrahedron Lett.*, **22**, 649 (1981).
(c) G. Rousseau and J. Drouin, *Tetrahedron*, **39**, 2307 (1983).
203. (a) L. Miginiac, in *The Chemistry of Metal–Carbon Bond*, Vol. 3 (Eds. F. R. Hartley and S. Patai), Wiley, New York, 1985, p. 99.
(b) P. Knochel, in *Comprehensive Organic Synthesis*, Vol. 1 (Eds. B. M. Trost, I. Fleming and S. L. Schreiber), Pergamon, Oxford, 1991, p. 211.

204. (a) J. Villiéras and M. Rambaud, *Synthesis*, 924 (1982).
(b) J. Villiéras and M. Villiéras, *Janssen Chimica Acta*, **11**, 3 (1993).
205. (a) N. E. Alami, C. Belaud and J. Villiéras, *Tetrahedron Lett.*, **28**, 59 (1987).
(b) N. E. Alami, C. Belaud and J. Villiéras, *J. Organomet. Chem.*, **348**, 1 (1988).
206. Y. A. Dembélé, C. Belaud and J. Villiéras, *Tetrahedron: Asymmetry*, **3**, 511 (1992).
207. (a) J. van der Louw, J. L. van der Baan, F. Bickelhaupt and G. W. Klumpp, *Tetrahedron Lett.*, **28**, 2889 (1987).
(b) J. van der Louw, J. L. van der Baan, H. Stieltjes, F. Bickelhaupt and G. W. Klumpp, *Tetrahedron Lett.*, **28**, 5929 (1987).
(c) J. van der Louw and J. L. van der Baan, *Tetrahedron*, **48**, 9877 (1992).
208. (a) J. L. Moreau, in *The Chemistry of Ketenes, Allenes and Related Compounds* (Ed. S. Patai), Wiley, New York, 1980, p. 363.
(b) M. Suzuki, Y. Morita and R. Noyori, *J. Org. Chem.*, **55**, 441 (1990).
209. H. Ochiai, T. Nishihara, Y. Tamaru and Z. Yoshida, *J. Org. Chem.*, **53**, 1343 (1988).
210. J. Berninger, U. Koert, C. Eisenberg-Höhl and P. Knochel, *Chem. Ber.*, **128**, 1021 (1995).
211. P. Quinton and T. Le Gall, *Tetrahedron Lett.*, **32**, 4909 (1991).
212. (a) H. Lehmkuhl, I. Döring, R. McLane and H. Nehl, *J. Organomet. Chem.*, **221**, 1 (1981).
(b) R. L. Soucy, D. Kozhinov and V. Behar, *J. Org. Chem.*, **67**, 1947 (2002).
213. M. R. Saidi and N. Azizi, *Tetrahedron: Asymmetry*, **13**, 2523 (2002).
214. K. P. Chiev, S. Roland and P. Mangeney, *Tetrahedron: Asymmetry*, **13**, 2205 (2002).
215. (a) M.-J. Shiao, K.-H. Liu and L.-G. Lin, *Synlett*, 655 (1992).
(b) W.-L. Chia and M.-J. Shiao, *Tetrahedron Lett.*, **32**, 2033 (1991).
(c) T.-L. Shing, W. L. Chia, M.-J. Shiao and T.-Y. Chau, *Synthesis*, 849 (1991).
(d) M.-J. Shiao, W. L. Chia, T.-L. Shing and T. J. Chow, *J. Chem. Res. (S)*, 247 (1992).
(e) C. Agami, F. Couty, J.-C. Daran, B. Prince and C. Puchot, *Tetrahedron Lett.*, **31**, 2889 (1990).
(f) C. Agami, F. Couty, M. Poursoulis and J. Vaissermann, *Tetrahedron*, **48**, 431 (1992).
(g) C. Andrés, A. González, R. Pedrosa, A. Pérez-Encabo, S. García-Granda, M. A. Salvadó and F. Gómez-Beltrán, *Tetrahedron Lett.*, **33**, 4743 (1992).
(h) J.-L. Bettiol and R.-J. Sundberg, *J. Org. Chem.*, **58**, 814 (1993).
(i) J. Yamada, H. Sato and Y. Yamamoto, *Tetrahedron Lett.*, **30**, 5611 (1989).
216. (a) C. Chuit, J. P. Foulon and J.-F. Normant, *Tetrahedron*, **37**, 1385 (1981); *Tetrahedron*, **36**, 2305 (1980).
(b) M. Bourgain-Commercon, J. P. Foulon and J. F. Normant, *J. Organomet. Chem.*, **228**, 321 (1982).
(c) E. J. Corey and N. W. Boaz, *Tetrahedron Lett.*, **26**, 6015 and 6019 (1985).
(d) A. Alexakis, J. Berlan and Y. Besace, *Tetrahedron Lett.*, **27**, 1047 (1986).
(e) Y. Horiguchi, S. Matsuzawa, E. Nakamura and I. Kuwajima, *Tetrahedron Lett.*, **27**, 4025 (1986).
(f) E. Nakamura, S. Matsuzawa, Y. Horiguchi and I. Kuwajima, *Tetrahedron Lett.*, **27**, 4029 (1986).
(g) M. Bergdahl, E.-L. Lindtstedt, M. Nilsson and T. Olsson, *Tetrahedron*, **44**, 2055 (1988).
(h) M. Bergdahl, E.-L. Lindtstedt, M. Nilsson and T. Olsson, *Tetrahedron*, **45**, 535 (1989).
(i) M. Bergdahl, E.-L. Lindtstedt and T. Olsson, *J. Organomet. Chem.*, **365**, C11 (1989).
(j) M. Bergdahl, M. Nilsson and T. Olsson, *J. Organomet. Chem.*, C19 (1990).
(k) M. Bergdahl, M. Eriksson, M. Nilsson and T. Olsson, *J. Org. Chem.*, **58**, 7238 (1993).
217. Y. Tamaru, H. Tanigawa, T. Yamamoto and Z. Yoshida, *Angew. Chem. Int. Ed. Engl.*, **28**, 351 (1989).
218. (a) H. Tsujiyama, N. Ono, T. Yoshino, S. Okamoto and F. Sato, *Tetrahedron Lett.*, **31**, 4481 (1990).
(b) T. Yoshino, S. Okamoto and F. Sato, *J. Org. Chem.*, **56**, 3205 (1991).
(c) K. Miyaji, Y. Ohara, Y. Miyauchi, T. Tsuruda and K. Arai, *Tetrahedron Lett.*, **34**, 5597 (1993).
219. (a) B. L. Feringa, M. Pineschi, L. A. Arnold, R. Imbos and A. H. M. de Vries, *Angew. Chem., Int. Ed. Engl.*, **36**, 2620 (1997).
(b) E. Keller, J. Maurer, R. Naasz, T. Schader, A. Meetsma and B. L. Feringa, *Tetrahedron: Asymmetry*, **9**, 2409 (1998).

(c) R. Naasz, L. A. Arnold, M. Pineschi, E. Keller and B. L. Feringa, *J. Am. Chem. Soc.*, **121**, 1104 (1999).
(d) R. Imbos, M. H. G. Britman, M. Pineschi and B. L. Feringa, *Org. Lett.*, **1**, 623 (1999).
(e) L. A. Arnold, R. Imbos, A. Mandoli, A. H. M. De Vries, R. Naasz and B. L. Feringa, *Tetrahedron*, **56**, 2865 (2000).
(f) F. Bertozzi, P. Crotti, B. L. Feringa, F. Macchia and M. Pineschi, *Synthesis*, 483 (2001).
220. (a) A. Alexakis, J. Burton, J. Vastra and P. Mangeney, *Tetrahedron: Asymmetry*, **8**, 3987 (1997).
(b) A. Alexakis, G. P. Trevitt and G. Bernadelli, *J. Am. Chem. Soc.*, **123**, 4358 (2001).
(c) A. Alexakis, C. Benhaim, S. Rosset and M. Humann, *J. Am. Chem. Soc.*, **124**, 5262 (2002).
(d) O. Knopff and A. Alexakis, *Org. Lett.*, **4**, 3835 (2002).
(e) A. Alexakis and C. Benhaim, *Eur. J. Org. Chem.*, 3221 (2002).
(f) A. Alexakis and S. March, *J. Org. Chem.*, **67**, 8753 (2002).
221. L. A. Arnold, R. Naasz, A. J. Minnaard and B. L. Feringa, *J. Am. Chem. Soc.*, **123**, 5841 (2001).
222. R. Naasz, L. A. Arnold, A. J. Minnaard and B. L. Feringa, *Angew. Chem., Int. Ed.*, **40**, 927 (2001).
223. A. W. Hird and A. H. Hoveyda, *Angew. Chem., Int. Ed.*, **42**, 1276 (2003).
224. F. Denes, F. Chemla and J. F. Normant, *Eur. J. Org. Chem.*, 3536 (2002).
225. G Cahiez, P. Verregas, C. E. Tucker, T. N. Majid and P. Knochel, *J. Chem. Soc., Chem. Commun.*, 1406 (1992).
226. D. H. Yang, J. X. Wang and Y. Hu, *J. Chem. Res. (S)*, 79 (2002).
227. (a) D. Seebach, E. W. Colvin, F. Lehr and T. Weller, *Chimia*, **33**, 1 (1979).
(b) A. Yoshikoshi and M. Miyashita, *Acc. Chem. Res.*, **18**, 284 (1985).
(c) A. G. M. Barrett and G. G. Graboski, *Chem. Rev.*, **86**, 751 (1986).
(d) R. Tamura, A. Kamimura and N. Ono, *Synthesis*, 423 (1991).
228. (a) S. B. Bowlus, *Tetrahedron Lett.*, 3591 (1975).
(b) A.-T. Hansson and M. Nilsson, *Tetrahedron*, **38**, 389 (1982).
(c) S. Stiver and P. Yates, *J. Chem. Soc., Chem. Commun.*, 50 (1983).
229. C. Retherford and P. Knochel, *Tetrahedron Lett.*, **32**, 441 (1991).
230. S. E. Denmark and L. R. Marcin, *J. Org. Chem.*, **58**, 3850 (1993).
231. J.-F. Normant and A. Alexakis, *Synthesis*, 841 (1981).
232. (a) M. T. Crimmins and P. G. Nantermet, *J. Org. Chem.*, **55**, 4235 (1990).
(b) M. T. Crimmins, P. G. Nantermet, B. W. Trotter, I. M. Vallin, P. S. Watson, L. A. McKerlie, T.-L. Reinhold, A. W.-H. Cheung, K. A. Steton, D. Dedopoulou and J. L. Gray, *J. Org. Chem.*, **58**, 1038 (1993).
(c) M. T. Crimmins, D. K. Jung and J. L. Gray, *J. Am. Chem. Soc.*, **115**, 3146 (1993).
233. J. van der Louw, C. M. D. Komen, A. Knol, F. J. J. de Kanter, J. L. van der Baan, F. Bickelhaupt and G. W. Klumpp, *Tetrahedron Lett.*, **30**, 4453 (1989).
234. (a) E. Negishi and J. A. Miller, *J. Am. Chem. Soc.*, **105**, 6761 (1983).
(b) G. A. Molander, *J. Org. Chem.*, **48**, 5409 (1983).
235. A. Yanagisawa, S. Habane and H. Yamamoto, *J. Am. Chem. Soc.*, **111**, 366 (1989).
236. K. Kubota, M. Nakamura, M. Isaka and E. Nakamura, *J. Am. Chem. Soc.*, **115**, 5867 (1993).
237. (a) M. Nakamura, N. Yoshikai and E. Nakamura, *Chem. Lett.*, 146 (2002).
(b) K. Kubota and E. Nakamura, *Angew. Chem., Int. Ed. Engl.*, **36**, 2491 (1997).
238. M. Nakamura, K. Hara, T. Hatakeyama and E. Nakamura, *Org. Lett.*, **3**, 3137 (2001).
239. (a) J. Montgomery and M. Song, *Org. Lett.*, **4**, 4009 (2002).
(b) S.-K. Kang and S.-K. Yoon, *Chem. Commun.*, 2634 (2002).
240. (a) M. Gaudemar, *C.R. Hebd. Scéances Acad. Sci., Ser. C*, **273**, 1669 (1971).
(b) Y. Frangin and M. Gaudemar, *C.R. Hebd. Scéances Acad. Sci., Ser C*, **278**, 885 (1974).
(c) M. Bellasoued, Y. Frangin and M. Gaudemar, *Synthesis*, 205 (1977).
(d) P. Knochel and J.-F. Normant, *Tetrahedron Lett.*, **27**, 1039 (1986).
(e) P. Knochel and J.-F. Normant, *Tetrahedron Lett.*, **27**, 1043 (1986).
(f) P. Knochel and J.-F. Normant, *Tetrahedron Lett.*, **27**, 4427 (1986).
(g) P. Knochel and J.-F. Normant, *Tetrahedron Lett.*, **27**, 5727 (1986).
(h) D. Beruben, I. Marek, L. Labaudinière and J.-F. Normant, *Tetrahedron Lett.*, **34**, 2303 (1993).
(i) J.-F. Normant and J.-C. Quirion, *Tetrahedron Lett.*, **30**, 3959 (1989).

(j) I. Marek, J.-M. Lefrançois and J.-F. Normant, *Synlett*, 633 (1992).
(k) I. Marek, J.-M. Lefrançois and J.-F. Normant, *Tetrahedron Lett.*, **33**, 1747 (1992).
(l) I. Marek, J.-M. Lefrançois and J.-F. Normant, *Tetrahedron Lett.*, **32**, 5969 (1991).
(m) I. Marek and J.-F. Normant, *Tetrahedron Lett.*, **32**, 5973 (1991).
241. P. Knochel, C. Xiao and M. C. P. Yeh, *Tetrahedron Lett.*, **29**, 6697 (1988).
242. S. A. Rao and P. Knochel, *J. Am. Chem. Soc.*, **113**, 5735 (1991).
243. M. T. Bertrand, G. Courtois and L. Miginiac, *Tetrahedron Lett.*, 1945 (1974).
244. (a) M. Kobayashi and E. Negishi, *J. Org. Chem.*, **45**, 5223 (1980).
(b) E. Negishi, *Acc. Chem. Res.*, **15**, 340 (1982).
(c) E. Negishi, V. Bagheri, S. Chatterjee, F.-T. Luo, J. A. Miller and A. T. Stoll, *Tetrahedron Lett.*, **24**, 5181 (1983).
(d) R. A. Grey, *J. Org. Chem.*, **49**, 2288 (1984).
245. (a) E. Negishi, A. O. King and N. Okukado, *J. Org. Chem.*, **42**, 1821 (1977).
(b) R. Rossi, F. Bellina, A. Carpita and R. Gori, *Synlett*, 344 (1995).
(c) E. Negishi, H. Matsushita, M. Kobayashi and C. L. Rand, *Tetrahedron Lett.*, **24**, 3823 (1983).
(d) J. G. Millar, *Tetrahedron Lett.*, **30**, 4913 (1989).
(e) S. Hyuga, N. Yamashina, S. Hara and A. Suzuki, *Chem. Lett.*, 809 (1988).
(f) R. C. Borner and R. F. W. Jackson, *J. Chem. Soc., Chem. Commun.*, 845 (1994).
(g) T. Sakamoto, Y. Kondo, N. Takazawa and H. Yamanaka, *Tetrahedron Lett.*, **34**, 5955 (1993).
(h) A. Minato, K. Suzuki, K. Tamao and M. Kumada, *Tetrahedron Lett.*, **25**, 2583 (1984).
(i) T. Sakamoto, S. Nishimura, Y. Kondo and H. Yamanaka, *Synthesis*, 485 (1988).
(j) T. Sato, A. Kawase and T. Hirose, *Synlett*, 891 (1992).
246. E. Negishi, H. Matsushita, M. Kobayashi and C. L. Raud, *Tetrahedron Lett.*, **24**, 3823 (1983).
247. S. Hyuga, N. Yamashina, S. Hara and A. Suzuki, *Chem. Lett.*, 809 (1988).
248. A. Minota, K. Suzuki, K. Tamao and M. Kumada, *Tetrahedron Lett.*, **25**, 2583 (1984).
249. A. Löffler and G. Himbert, *Synthesis*, 495 (1992).
250. G. Mignani, F. Leising, R. Meyrueix and H. Samson, *Tetrahedron Lett.*, **31**, 4743 (1990).
251. C. A. Quesnelle, O. B. Familoni and V. Snieckus, *Synlett*, 349 (1994).
252. (a) T. Sakamoto, Y. Kondo, N. Murata and H. Yamanaka, *Tetrahedron Lett.*, **33**, 5373 (1992).
(b) T. Sakamoto, Y. Kondo, N. Takazawa and H. Yamanaka, *Heterocycles*, **36**, 941 (1993).
(c) D. Trauner, J. B. Schwartz and S. J. Danishefsky, *Angew. Chem., Int. Ed.*, **38**, 3543 (1999).
(d) A. S. Bell, D. A. Roberts and K. S. Ruddock, *Synthesis*, 843 (1987).
253. (a) E. Nakamura and I. Kuwajima, *Tetrahedron Lett.*, **27**, 83 (1986).
(b) T. Sakamoto, S. Nishimura, Y. Kondo and H. Yamanaka, *Synthesis*, 485 (1988).
254. Y. Tamaru, H. Ochiai, T. Nakamura and Z. Yoshida, *Angew. Chem., Int. Ed. Engl.*, **99**, 1193 (1987).
255. R. F. W. Jackson, K. James, M. J. Wythes and A. Wood, *J. Chem. Soc., Chem. Commun.*, 644 (1989).
256. T. Sato, A. Kawase and T. Hirose, *Synlett*, 891 (1992).
257. C. Dai and G. C. Fu, *J. Am. Chem. Soc.*, **123**, 2719 (2001).
258. H. J. C. Deboves, C. A. G. N. Montalbetti and R. F. W. Jackson, *J. Chem. Soc., Perkin Trans. 1*, 1876 (2001).
259. A. Mehta, R. Jaouhari, T. J. Benson and K. T. Douglas, *Tetrahedron Lett.*, **33**, 5441 (1992).
260. (a) I. Kadota, H. Takamura, K. Sato and Y. Yamamoto, *J. Org. Chem.*, **67**, 3494 (2002).
(b) Y. Tamaru, H. Ochial, T. Nakamura and Z. Yoshida, *Tetrahedron Lett.*, **27**, 955 (1986).
(c) Y. Tamaru, H. Ochial, T. Nakamura, K. Tsubaki and Z. Yoshida, *Tetrahedron Lett.*, **26**, 5559 (1985).
261. N. Vicart, G.-S. Saboukoulou, Y. Ramondenc and G. Plé, *Synth. Commun.*, **33**, 1509 (2003).
262. A. Przezdziecka, A. Kurek-Tyrlik and J. Wicha, *Collect. Czech. Chem. Commun.*, **67**, 1658 (2002).
263. B. H. Lipshutz and P. A. Blomgren, *J. Am. Chem. Soc.*, **121**, 5819 (1999).
264. (a) J. A. Miller and R. P. Farrell, *Tetrahedron Lett.*, **39**, 6441 (1998).
(b) C. E. Tucker and J. G. de Vries, *Topics in Catalysis*, **19**, 111 (2002).
265. (a) J. P. Gillet, R. Sauvêtre and J.-F. Normant, *Synthesis*, 538 (1986).
(b) J.-P. Gillet, R. Sauvêtre and J.-F. Normant, *Tetrahedron Lett.*, **26**, 3999 (1985).
(c) F. Tellier, R. Sauvêtre and J.-F. Normant, *J. Organomet. Chem.*, **303**, 309 (1986).

(d) F. Tellier, R. Sauvêtre, J.-F. Normant, Y. Dromzee and Y. Jeannin, *J. Organomet. Chem.*, **331**, 281 (1987).
(e) P. Martinet, R. Sauvêtre and J.-F. Normant, *J. Organomet. Chem.*, **367**, 1 (1989).
266. (a) K. Yuan and W. J. Scott, *Tetrahedron Lett.*, **30**, 4779 (1989).
(b) K. Yuan and W. J. Scott, *J. Org. Chem.*, **55**, 6188 (1990).
(c) K. Park, K. Yuan and W. J. Scott, *J. Org. Chem.*, **58**, 4866 (1993).
267. N. Murata, T. Sugihara, Y. Kondo and T. Sakamoto, *Synlett*, 298 (1997).
268. (a) G. Karig, J. A. Spencer and T. Gallagher, *Org. Lett.*, **3**, 835 (2001).
(b) C. G. V. Sharples, G. Karig, G. L. Simpson, J. A. Spencer, E. Wright, N. S. Millar, S. Wonnacott and T. Gallagher, *J. Med. Chem.*, **45**, 3235 (2002).
269. A. Staubitz, W. Dohle and P. Knochel, *Synthesis*, 233 (2003).
270. M. Hocek, I. Votruba and H. Dvoraka, *Tetrahedron*, **59**, 607 (2003).
271. B. Ye and T. R. Burke Jr., *J. Org. Chem.*, **60**, 2640 (1995).
272. A. W. Seton, M. F. G. Stevens and A. D. Westwell, *J. Chem. Res. (S)*, 546 (2001).
273. J. Thibonnet, V. A. Vu, L. Berillon and P. Knochel, *Tetrahedron*, **58**, 4787 (2002).
274. J.-C. Shi, X. Zeng and E. Negishi, *Org. Lett.*, **5**, 1825 (2003).
275. (a) T. Hayashi, T. Hagihara, Y. Katsuro and M. Kumada, *Bull. Chem. Soc. Jpn.*, **56**, 363 (1983).
(b) T. Hayashi, *J. Organomet. Chem.*, **653**, 41 (2002).
276. V. Mamane, T. Ledoux-Rak, S. Deveau, J. Zyss and O. Riant, *Synthesis*, 455 (2003).
277. (a) M. Lotz, G. Kramer and P. Knochel, *Chem. Commun.*, 2546 (2002).
(b) R. J. Kloetzing, M. Lotz and P. Knochel, *Tetrahedron: Asymmetry*, **14**, 255 (2003).
(c) T. Bunlaksananusorn, K. Polborn and P. Knochel, *Angew. Chem., Int. Ed.*, **42**, 3941 (2003).
(d) T. Bunlaksananusorn, A. P. Luna, M. Boniu, L. Micouin and P. Knochel, *Synlett*, 2240 (2003).
278. (a) J.-F. Peyrat, E. Thomas, N. L'Hermite, M. Alami and J.-D. Brion, *Tetrahedron Lett.*, **44**, 6703 (2003).
(b) M. Alami, S. Gueugnot, E. Doingues and G. Linstrumelle, *Tetrahedron*, **51**, 1209 (1995).
279. B. L. Flynn, P. Verdier-Pinard and E. Hamel, *Org. Lett.*, **3**, 651 (2001).
280. F. Zeng and E. Negishi, *Org. Lett.*, **3**, 719 (2001).
281. Y. Tamaru, H. Ochiai, T. Nakamura and Z. Yoshida, *Org. Synth.*, **67**, 98 (1989).
282. (a) Y. Tamaru, K. Yasui, H. Takanabe, S. Tanaka and K. Fugami, *Angew. Chem., Int. Ed. Engl.*, **31**, 645 (1992).
(b) K. Yasui, K. Fugami, S. Tanaka and Y. Tamaru, *J. Org. Chem.*, **60**, 1365 (1995).
283. M. Asaoka, M. Tamaka, T. Houkawa, T. Ueda, S. Sakami and H. Takei, *Tetrahedron*, **54**, 471 (1998).
284. H. Tokuyama, S. Yokoshima, T. Yamashita and T. Fukuyama, *Tetrahedron Lett.*, **39**, 3189 (1998).
285. Y. Mori and M. Seki, *J. Org. Chem.*, **68**, 1571 (2003).
286. (a) T. Shimizu and M. Seki, *Tetrahedron Lett.*, **43**, 1039 (2002).
(b) T. Shimizu and M. Seki, *Tetrahedron Lett.*, **42**, 429 (2001).
(c) M. Kimura and M. Seki, *Tetrahedron Lett.*, **45**, 1635 (2004).
287. (a) N. Oguni, T. Omi, Y. Yamamoto and A. Nakamura, *Chem. Lett.*, 841 (1983).
(b) N. Oguni and T. Omi, *Tetrahedron Lett.*, **25**, 2823 (1984).
(c) N. Oguni, Y. Matsuda and T. Kaneko, *J. Am. Chem. Soc.*, **110**, 7877 (1988).
288. (a) K. Soai and S. Niwa, *Chem. Rev.*, **92**, 833 (1992).
(b) D. A. Evans, *Science*, **240**, 420 (1988).
(c) R. Noyori and M. Kitamura, *Angew. Chem., Int. Ed. Engl.*, **30**, 49 (1991).
289. (a) M. Yoshioka, T. Kawakita and M. Ohno, *Tetrahedron Lett.*, **30**, 1657 (1989).
(b) H. Takahashi, T. Kawakita, M. Yoshioka, S. Kobayashi and M. Ohno, *Tetrahedron Lett.*, **30**, 7095 (1989).
(c) H. Takahashi, T. Kawakita, M. Ohno, M. Yoshioka and S. Kobayashi, *Tetrahedron*, **48**, 5691 (1992).
290. (a) A. K. Beck, B. Bastani, D. A. Plattner, W. Petter, D. Seebach, H. Braunschweiger, P. Gysi and L. VaVecchia, *Chimia*, **45**, 238 (1991).
(b) B. Schmidt and D. Seebach, *Angew. Chem., Int. Ed. Engl.*, **30**, 99 (1991).
(c) D. Seebach, L. Behrendt and D. Felix, *Angew. Chem., Int. Ed. Engl.*, **30**, 1008 (1991).
(d) B. Schmidt and D. Seebach, *Angew. Chem., Int. Ed. Engl.*, **30**, 1321 (1991).

(e) J. L. von dem Bussche-Hünnefeld and D. Seebach, *Tetrahedron*, **48**, 5719 (1992).
(f) D. Seebach, D. A. Plattner, A. K. Beck, Y. M. Wang, D. Hunziker and W. Petter, *Helv. Chim. Acta*, **75**, 2171 (1992).
(g) D. Seebach, A. K. Beck, B. Schmidt and Y. M. Wang, *Tetrahedron*, **50**, 4363 (1994).
291. H. Schafer and D. Seebach, *Tetrahedron*, **51**, 2305 (1995).
292. D. Seebach, A. K. Beck and A. Hechel, *Angew. Chem., Int. Ed.*, **40**, 92 (2001).
293. B. P. Rheiner, H. Sellner and D. Seebach, *Helv. Chim. Acta*, **80**, 2027 (1997).
294. H. Sellner, C. Faber, P. B. Rheiner and D. Seebach, *Chem. Eur. J.*, **6**, 3692 (2000).
295. (a) L. Schwink and P. Knochel, *Chem. Eur. J.*, **4**, 950 (1998).
(b) W. Brieden, R. Ostwald and P. Knochel, *Angew. Chem., Int. Ed. Engl.*, **32**, 582 (1993).
296. S. Nowotny, S. Vettel and P. Knochel, *Tetrahedron Lett.*, **35**, 4539 (1994).
297. (a) R. Noyori and M. Suzuki, *Angew. Chem., Int. Ed. Engl.*, **23**, 847 (1984).
(b) M. Suzuki, A. Yanagisawa and R. Noyori, *J. Am. Chem. Soc.*, **307**, 3348 (1990).
(c) Y. Morita, M. Suzuki and R. Noyori, *J. Org. Chem.*, **54**, 1785 (1989).
(d) R. Noyori, S. Suga, K. Kawai, S. Okada and M. Kitamura, *Pure Appl. Chem.*, **60**, 1597 (1988).
298. (a) S. Vettel and P. Knochel, *Tetrahedron Lett.*, **35**, 5849 (1994).
(b) R. Ostwald, P.-Y. Chavant, H. Stadtmüller and P. Knochel, *J. Org. Chem.*, **59**, 4143 (1994).
(c) W. R. Roush and K. Koyama, *Tetrahedron Lett.*, **33**, 6227 (1992).
299. H. Lütjens and P. Knochel, *Tetrahedron: Asymmetry*, **5**, 1161 (1994).
300. P. Knochel, W. Brieden, M. J. Rozema and C. Eisenberg, *Tetrahedron Lett.*, **34**, 5881 (1993).
301. C. Eisenberg and P. Knochel, *J. Org. Chem.*, **59**, 3760 (1994).
302. A. Fürstner and T. Müller, *J. Org. Chem.*, **63**, 424 (1998).
303. S. Bäurle, S. Hoppen and U. Koert, *Angew. Chem., Int. Ed.*, **38**, 1263 (1999).
304. A. Fürstner, M. Albert, J. Mlynarski, M. Matheu and E. DeClercq, *J. Am. Chem. Soc.*, **125**, 13132 (2003).
305. W. Oppolzer, R. N. Radinov and J. de Bradander, *Tetrahedron Lett.*, **36**, 2607 (1995).
306. M. Yus, D. J. Ramón and O. Prieto, *Tetrahedron: Asymmetry*, **14**, 1103 (2003).
307. D. Boyalli, E. Frantz and E. M. Carreira, *Org. Lett.*, **4**, 2605 (2002).
308. A. Fettes and E. M. Carreira, *Angew. Chem., Int. Ed.*, **41**, 4098 (2002).
309. L. Pu, *Tetrahedron*, **59**, 9873 (2003).
310. L. S. Tan, C. Y. Chen, R. D. Tillyer, E. J. J. Grabowski and P. J. Reider, *Angew. Chem., Int. Ed.*, **38**, 711 (1999).
311. N. K. Anand and E. M. Carreira, *J. Am. Chem. Soc.*, **123**, 9687 (2001).
312. O. Prieto, D. J. Ramon and M. Yus, *Tetrahedron: Asymmetry*, **14**, 1955 (2003).
313. (a) J. Rudolph, T. Rasmussen, C. Bolm and P.-O. Norrby, *Angew. Chem., Int. Ed.*, **42**, 3002 (2003).
(b) J. Rudolph, N. Hermanns and C. Bolm, *J. Org. Chem.*, **69**, 3997 (2004).
(c) C. Bolm and J. Mueller, *Tetrahedron*, **50**, 4355 (1994).
(d) C. Bolm, J. Mueller, G. Schlingloff, M. Zehnder and M. Neuburger, *J. Chem. Soc., Chem. Commun.*, **2**, 182 (1993).
(e) C. Bolm, G. Schlingloff and K. Harms, *Chem. Ber.*, **124**, 1191 (1992).
(f) C. Bolm, N. Hermanns, A. Classen and K. Muniz, *Bioorg. Med. Chem. Lett.*, **12**, 1795 (2002).
314. J. R. Porter, J. F. Traverse, A. H. Hoveyda and M. L. Snapper, *J. Am. Chem. Soc.*, **123**, 10409 (2001).
315. J. F. Traverse, A. H. Hoveyda and M. L. Snapper, *Org. Lett.*, **5**, 3273 (2003).
316. T. Yamamoto, A. Yamamoto and S. Ikeda, *J. Am. Chem. Soc.*, **93**, 3350 (1971).
317. C. K. Reddy and P. Knochel, *Angew. Chem., Int. Ed. Engl.*, **35**, 1700 (1996).
318. A. Devasagayaraj and P. Knochel, *Tetrahedron Lett.*, **36**, 8411 (1995).
319. (a) G. Cahiez, *Actual Chim.*, 24 (1984).
(b) B. Weidmann and D. Seebach, *Angew. Chem., Int. Ed. Engl.*, **22**, 31 (1983).
(c) G. Cahiez and B. Laboue, *Tetrahedron Lett.*, **30**, 3545 (1989).
(d) G. Cahiez and B. Laboue, *Tetrahedron Lett.*, **30**, 7369 (1989).

(e) G. Cahiez and M. Alami, *Tetrahedron*, **45**, 4163 (1989).
(f) G. Cahiez, P.-Y. Chavant and E. Metais, *Tetrahedron Lett.*, **33**, 5245 (1992).
(g) G. Cahiez, B. Figadère and P. Cléry, *Tetrahedron Lett.*, **35**, 3065 (1994).
(h) G. Cahiez, K. Chau and P. Cléry, *Tetrahedron Lett.*, **35**, 3069 (1994).
320. E. Riguet, I. Klement, C. K. Reddy, G. Cahiez and P. Knochel, *Tetrahedron Lett.*, **37**, 5865 (1996).
321. T. Stüdemann, M. Ibrahim-Ouali, G. Cahiez and P. Knochel, *Synlett*, 143 (1998).

CHAPTER 9

Photochemical transformations involving zinc porphyrins and phthalocyanines

MATHIAS O. SENGE and NATALIA N. SERGEEVA

School of Chemistry, Trinity College Dublin, Dublin 2, Ireland
Fax: +353 1 896 8536; e-mail: sengem@tcd.ie

The chemistry of organozinc compounds
Edited by Z. Rappoport and I. Marek

I. ABBREVIATIONS

chl	chlorophyll
D–B–A–	donor–bridge–acceptor systems
ET	electron transfer
MV	methyl viologen
OEP	2,3,7,8,12,13,17,18-octaethylporphyrinato
PET	photoinduced electron transfer
PS	photosensitizer
TPP	5,10,15,20-tetraphenylporphyrinato

II. INTRODUCTION

The photochemistry of true organozinc compounds remains completely unexplored. In fact, a literature search in preparation of this work, to the best of our knowledge, revealed no photochemical studies or reactions of species involving a Zn–C bond (December 2004). Broadening the topic to include the photochemistry of 'organic' compounds containing zinc atoms quickly identifies zinc(II) chelates as an area of active photochemical research. Due to their biological relevance, technical importance and good stability, substituted zinc(II) porphyrins **1**, 5,10,15,20-tetraazaporphyrins (porphyrazines) **2** and phthalocyanines **3** have found significant use as industrial pigments, electron transfer components, photochemical transformations and in photobiotechnology and we will focus on the latter aspects in this review.

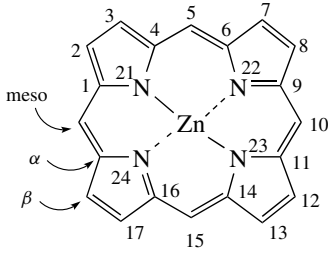

(1)

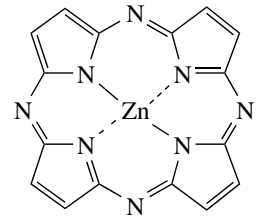

(2)

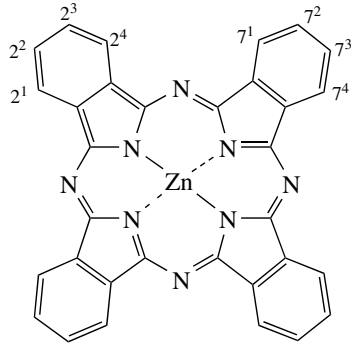

(3)

For practical purposes we have concentrated on the literature of the last decade, focusing on publications that address photochemical transformations involving zinc(II) chelates of porphyrins and 5,10,15,20-tetraazaporphyrins. Nevertheless, even with such a limited approach the body of available literature is significant and we can only use selected examples to highlight the state of the art of this field. A description of syntheses, methodology or electron transfer reactions is outside the purview of this work and the present work can only give a rather selective and personal view on ongoing studies in this area.

III. BASIC PHOTOCHEMISTRY OF PORPHYRINS

A. General Concepts and Theoretical Background

Tetrapyrroles contain an extended π-conjugated system which is responsible for their use in a wide range of applications ranging from technical (pigments, catalysts, photoconductors) to medicinal (photodynamic therapy) uses. The electronic absorption spectra are governed by the aromatic 18π electron system and typically consist of two main bands. In phthalocyanines the Q band around 660–680 nm is the most intense one accompanied by a weaker Soret band near 340 nm[1]. In porphyrins the situation is reversed with an intense Soret band around 380–410 nm and weaker Q bands in the 550–650 nm region. The position and intensity of the absorption bands are affected by the central metal, axial ligands, solvation, substituents and their regiochemical arrangement, and aggregation. The theoretical background has been widely reviewed and established in pioneering works by Gouterman[2], Stillman and Nyokong[3] and Mack and Stillman[4]. Ishii and Kobayashi have recently provided a review on the photophysical properties of phthalocyanines that also describes the theoretical background in excellent detail[5].

The spectral characteristics depend strongly on the substituent pattern. By now almost all possible combinations of electron-donating, electron-withdrawing or sterically demanding groups have been prepared[6–12]. Recent studies have addressed questions of regiochemistry[10], theoretical calculations[12], solubility[13] and the influence of sterically demanding[11,14] or heteroatom-containing substituents[15]. Intriguingly, perdeuteriated (phthalocyanato)zinc(II) shows no differences in the excited state kinetics or quantum yields compared to undeuteriated material[16].

At present, most studies on new photochemically active systems concentrate on polychromophoric, dendritic, supramolecular systems and novel materials. For example, theoretical calculations indicate that the development of related nanotubes will result in materials with excellent electron-acceptor properties and highly red-shifted bands in the near-IR region[17].

Zinc(II) tetrapyrroles behave like most other organic chromophores. Absorption of light will lead to the rapid formation of the lowest excited singlet state by promotion of an electron from the HOMO to the LUMO. The excited state can then either relax to the ground state via radiative (fluorescence) or nonradiative processes (internal conversion of vibrational relaxation). Another possibility is intersystem crossing to form a triplet state which again can relax either via radiative (phosphorescence) or nonradiative processes. In our context, both excited state types can take part in photochemical reactions and, in the presence of donor or acceptor units, energy or electron transfer between the chromophores can compete with these processes. For an excellent review of the basic processes involved in the latter, see the paper by Gust and Moore[18].

Zinc(II) porphyrins and phthalocyanines may form ions upon illumination[19]. For example, using hydrazine as an electron donor, illumination with visible light results in formation of the anion radical of zinc(II) phthalocyanine at RT[20] while use of CBr_4 as electron acceptor resulted in formation of the π-cation radical[21]. These radicals can also undergo further photochemical reactions[22,23].

B. Stability and Degradation

Although porphyrins and especially phthalocyanines are stable compounds, both will undergo photooxidative degradation or photoexcited ET reactions[24–27]. Studies of water-soluble phthalocyanines in aqueous suspensions of TiO_2 showed that naphthalocyanine and porphyrazine derivatives exhibit substantially higher photochemical stability than standard phthalocyanines[28]. The stability of the latter is critically dependent on the presence or absence of electron donors[29]. The photostability can be increased by formation of cyclodextrin inclusion complexes, which also results in higher singlet oxygen quantum yields while the fluorescence quantum yields remained unchanged[30], by introduction of peripheral substituents[31] or by preparation of copolymer conjugates[32]. The determination of their photostability is an important prerequisite for their use as photosensitizers in technical and medicinal applications (*vide infra*)[33].

IV. DONOR–ACCEPTOR COMPOUNDS FOR PET

A. Electron Transfer Studies

Studies on electron transfer present the largest area of photochemical studies on porphyrins and phthalocyanines. This is a result of their importance in photosynthesis, respiration and naturally occurring electron transfer reactions. The available literature is very extensive and it is difficult to distinguish between zinc-containing systems and others. This field has been reviewed repeatedly in recent years and a detailed discussion of the electron transfer properties of porphyrins and phthalocyanines is outside the purview of the present work. In addition, to focus in the context of electron transfer studies solely on zinc(II) derivatives would be an arbitrary restriction. Nevertheless, a multitude of publications deal with zinc(II) chelates of porphyrins. First, zinc derivatives exhibit photochemical properties similar to the natural magnesium derivatives while being more stable and easier to synthesize[34]. Second, the propensity of zinc to act as an acceptor atom is used in many supramolecular approaches and/or for modulation of the chromophore properties via axial ligand binding.

Most electron transfer studies are aimed at the synthesis and investigation of donor–acceptor complexes that mimic the natural processes. Typically, this involves the construction of systems consisting of donor(s), some covalent or noncovalent bridging unit, and acceptor(s) (Figure 1). In an ideal situation all requirements of the natural system would be modeled. These include: (A) unidirectional electron transfer → redox gradient in subunits; (B) rigid linker groups which do not play a role in ET → no heteroatoms, conjugated systems etc.; (C) defined overall geometry with correct relative orientation of the subunits → e.g. special pair model with cofacial orientation of the macrocycles → use of coupling reactions which give products with defined geometry; (D) modeling the protein environment → scaffold, electronic and steric effects/reconstituted pigment–protein systems.

Detailed investigations on the influence of the geometry and spatial arrangement or the reorganization energy are then possible by variation of the individual subunits and/or substituents. Several thousand systems of this general type have been prepared and used for investigation of the photoinduced electron transfer (PET) and numerous reviews have been published in this area, the most comprehensive ones being by Wasielewski[35] and by Gust and Moore[18]. More specialized works have treated emerging trends and contemporary approaches (see below) and a number of reviews dealt with chlorophyll chemistry and related chromophore systems[36,37].

Most of the available literature on ET studies in donor–acceptor compounds focuses on porphyrins. Phthalocyanine building blocks have been used less often[38], a result of their low solubility and (until recently) the lack of appropriate synthetic methodologies to

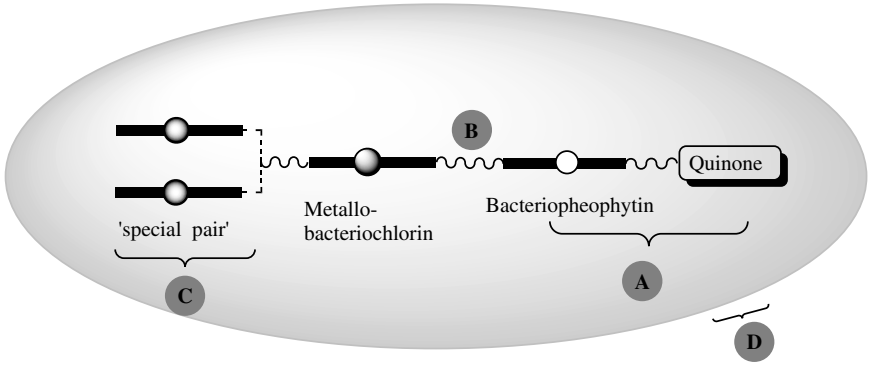

FIGURE 1. Design criteria for modeling photosynthetic reaction centers

selectively introduce functional groups or for the synthesis of unsymmetrically substituted derivatives.

B. Current Trends

Many new concepts have been developed for ET models in recent years. To illustrate the rapid development of this field, a few characteristic examples of current interest will be given below. More and more supramolecular approaches are used for the construction of ET model compounds and supramolecular donor–acceptor complexes were recently reviewed by Otsuki[39]. Especially attractive are rotaxane-based and transition-metal-assembled arrays capable of long-range PET[40–42]. Similarly, many recent studies have concentrated on using fullerene–porphyrin conjugates for studies on electron-transfer[43,44].

1. Electron transfer compounds with novel acceptor groups

Fullerenes are currently enjoying considerable attention as acceptor groups in ET compounds[44,45]. Fullerenes can accept up to six electrons, exhibit small reorganization energies while photoinduced charge-separation is accelerated and charge recombination is slowed. Thus, relatively long-lived charge-separated states are obtained without a special environment such as an apoprotein[46]. A recently described system consisting of a ferrocene, two porphyrins and one C_{60} unit exhibited a lifetime of 1.6 s (!), comparable to bacterial photosynthetic reaction centers. The quantum yields for charge separation in complex biomimetic systems can reach unity.

Fullerenes (mostly C_{60} but also C_{70}[47]) have been incorporated into multicomponent systems with stepwise charge separation[44,45,48–50] and used as core groups for dendrimers with zinc(II) porphyrin donors[51]. By now, C_{60} has also been linked to chlorins and phytochlorin derivatives[52,53] and carotenoid–porphyrin–C_{60} systems are under investigation[54]. Many of these systems utilize a pyrrolidine linkage, but bislactone-[55] or Diels–Alder derived cyclohexene-linked[49,52] systems have also found wide application. Currently, nanostructured systems are emerging[56] and new attention has been focused on combining the utility of fullerene acceptor groups in rotaxane systems[57–60]. Zinc(II) porphyrins have been used in many systems for complexation studies[61] and to modulate the ET properties by using axial coordination effects[62–64] or to construct self-assembled donor–acceptor systems[64–66]. For example, pyridinofullerenes were used as axial ligands

for Zn(II)TPP or Zn(II)OEP; the formation of the noncovalent porphyrin–fullerene dyad was indicated by fluorescence quenching of Zn(II)TPP[67]. This photoinduced electron transfer is an exergonic process[68]. For a related triad (C_{60} + 2 Zn(II) porphyrins), it was shown that the main quenching pathway involved charge-separation from the excited singlet state Zn(II)TPP to the C_{60} unit in noncoordinating solvents and from the triplet excited state of Zn(II)TPP in coordinating solvents[69]. Similar approaches have been used with zinc(II) phthalocyanines[70]. Some of the characteristics of fullerene-containing systems, e.g. recombination to the triplet state, were also observed with specifically designed triads without a fullerene unit[71].

While most studies utilized quinones as acceptor compounds, these studies almost exclusively used *p*-quinones. Nevertheless, the isomeric, but synthetically less accessible porphyrin-*o*-quinones are much better electron acceptors[72]. This results in a higher ΔG_{ET} and thus in a higher efficiency of the electron transfer and several *o*-quinone-containing zinc(II) porphyrin dyads (e.g. **4–6**), triads and tetrads have been prepared[73–75]. In order to achieve a variation of ΔG_{ET}, the general strategy in electron transfer studies generally involves the synthesis of different models via chemical modification of the porphyrin donor or the quinone acceptor. However, this also leads to changes in a number of other variables, such as distance, solvent term and electronic matrix element, resulting in altered electron transfer rates. Here, the utilization of porphyrin-*o*-quinones as electron transfer systems offers an attractive alternative. With them, a facile and simple variation of ΔG_{ET} can be achieved by using the *in situ* formed semiquinones for metal chelatization (Figure 2)[76]. Some of the sterically hindered parent free-base systems (e.g. free base of **6**) can undergo photochemical degradation reactions. However, such side reactions were not observed with the zinc(II) complexes[73,74].

Many other building blocks have been developed for use in photochemically active compounds. Perylene units have attracted attention as energy transfer donors, as they increase the light-harvesting efficiency in the green spectral region (where porphyrins are relatively transparent)[77–79]. A typical example is **7**[80], but larger arrays including some with phthalocyanine units have been described as well[81] and perylene units have been used as bridging units in D–B–A systems[81,82].

Other recently studied acceptor groups (some of which have been used in prior work) encompass mainly imide derivatives[83] and included naphthalenediimide[84,85], pyromellitimide[86] or phthalimides[87]. Using iron(III) porphyrins as acceptors, it was shown

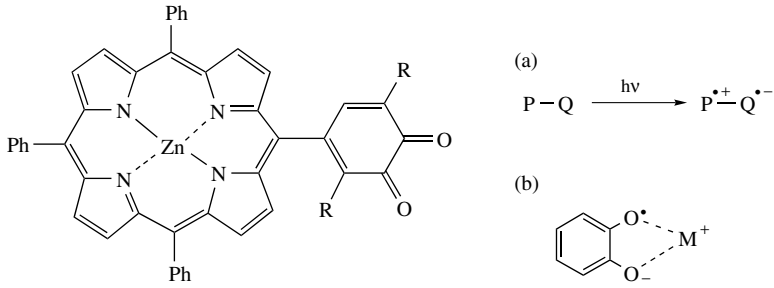

(4) R = Me
(5) R = H
(6) R = *t*-Bu

FIGURE 2. Zinc(II) porphyrin–*o*-quinone dyads and two typical reactions: (a) photoinduced charge separation, (b) chelation of *in situ* formed semiquinone anions. PQ = porphyrin quinine; M = metal

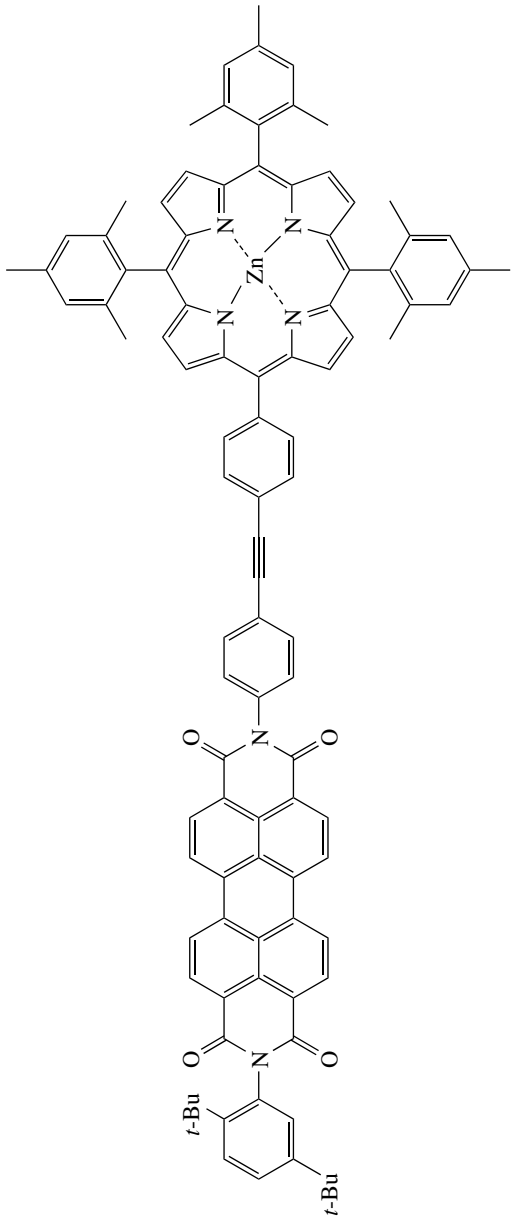

(7)

that with low-spin iron acceptors the deactivation of the excited donor changes from enhanced intersystem crossing (which is observed with high-spin iron species)[88] to electron transfer in systems with π-conjugated bridges[89]. Mataga and coworkers used directly linked zinc(II) porphyrin–imide dyads to observe the whole bell-shaped energy gap law in intramolecular charge-separation from the S_2 excited state[90].

2. Light-harvesting complexes

The propensity of zinc tetrapyrroles for aggregation has been widely used to mimic natural antenna systems of photosynthesis. The best studied system is the chlorosome, where bacteriochlorophylls self-organize *without* the use of a protein scaffold requiring constructing arrays with as many chromophores as possible. Thus, many studies on the self-assembly of bacteriochlorophyll model compounds or dendritic/polymeric approaches have been performed[91,92]. Current studies focus on large aggregates and chirality effects[93].

A typical example involves the perylene monoimide donors described above. They have been used to construct antenna models in which up to eight perylene units were covalently bound to a zinc(II) porphyrin[94]. Osuka and coworkers' windmill porphyrins also present excellent antenna complex building blocks (*vide infra*)[95]. In addition, several 'porphyrin wheel' antenna complexes were prepared by template-assisted synthesis[96,97] or self-aggregation[98]. Intramolecular cyclization of porphyrin dodecamers to a porphyrin wheel has also been achieved[99].

3. Reaction center models

Classic examples for structural models of the photosynthetic reaction center are the cofacial bisporphyrins or bischlorins[100] which model the structural arrangement of the special pair in the reaction center[101–103]. Zinc(II) bisporphyrins with various other geometrical arrangements, e.g. skewed[104], have been prepared as well, including those bearing C_{60} acceptor groups[105]. The important two-tetrapyrrole unit found in the special pair has by now been realized in a multitude of different geometrical arrangements. Depending on the porphyrin–porphyrin or porphyrin–acceptor linkage, *meso–meso*, *meso-*β[106] and $\beta-\beta$[107] linked systems have been prepared. Similar arrangements are also possible using noncovalent self-assembly. Noncovalent binding of substrates at the zinc(II) center can be used to control the PET in such systems[108].

Nowadays, most reaction center models carry suitable antenna pigments and acceptor groups and in effect are photosystem models. A typical example for a state-of-the-art system that incorporates many aspects of a photosystem consisted of a boron dipyrrin covalently linked to a zinc(II) porphyrin, which carried a suitably modified C_{60} derivative as axial ligand. Selective excitation of the boron dipyrrin as antenna pigment resulted in energy transfer to a zinc(II) porphyrin followed by electron transfer to the C_{60} acceptor[109].

4. Current synthetic concepts

Over the years many different synthetic strategies have been employed to construct ET compounds or multiporphyrin systems and the available synthetic repertoire is continuously expanding[110].

One of the most significant breakthroughs in multichromophoric systems was made by Osuka and coworkers in their work on *meso–meso*-linked multiporphyrins[111–113]. Based on their synthesis of directly linked bisporphyrins **8** they were able to prepare zinc(II) porphyrin-based wires (up to the 128mer)[114]. These systems are characterized by large excitonic interactions between the porphyrins resulting in efficient energy transfer along

the wires. Structurally, neighboring porphyrin units are orthogonal to each other, which prevents full electronic delocalization. Lowering the dihedral angle (e.g. via strapping of the porphyrin units) between the porphyrins and increasing the overlap of the π-systems results in a decrease in the intensity of the exciton split Soret band and red-shift of the absorption maxima[115]. This chemistry could be expanded to prepare so-called windmill porphyrins[95,116] combining linear and branched[117] multiporphyrin arrays. Intriguingly, these porphyrin oligomers could be oxidized to flat 'porphyrin-tapes' (**9**). These systems exhibit quite different photochemical properties and have extremely short-lived excited states[118]. Overall, charge-transfer probability calculations showed that the lowest excited states of the tapes resemble a Wannier-type exciton, while the oligomers (**8**) are more like a Frenkel-type exciton.

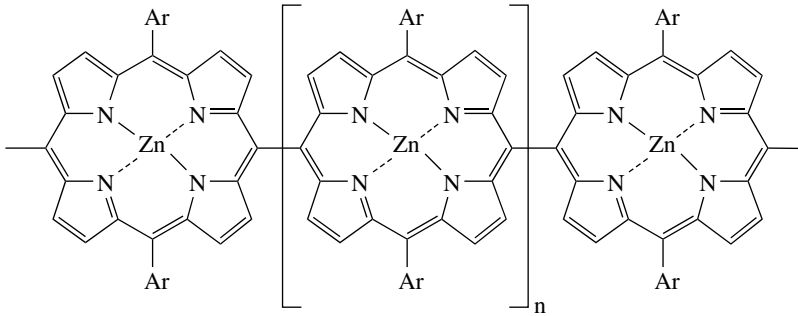

(8)

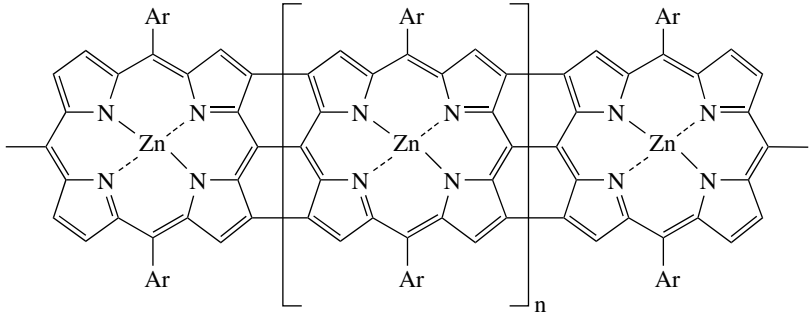

(9)

e.g., Ar = Ph or *p*-Tol

Recent work related to zinc(II) derivatives focused on self-assembly via hydrogen bonding[119], crystal engineering to yield 3D structures[120], calixarene linker groups[121], crown ether conjugates[122], the fullerene systems briefly discussed above and nucleobase derivatives[123,124]. A whole cornucopia of different linker or solubility-enhancing groups[125] has been used in the construction of D–B–A systems. Aryl, alkene, ester, amide and alkyne units have found widespread use and ongoing developments include catecholate[126], phenylethyne[127], imine[128], azo[129], bipyridine[130], (bisdipyrrinato)metal[131], cyclophane[132] and boronate groups[133]. Short diphosphonium bridges were used to $\beta-\beta$ link zinc(II)

porphyrins resulting in significant excitonic interactions[134] while ruthenium(II) trisphenanthroline units[135] or *trans*-substituted Pt(II) derivatives[136] were used to achieve a linear geometry[135]. Similarly, zinc(II) porphyrins covalently linked to rhenium carbonyl groups[137] and to tungsten pentacarbonyl residues were prepared. Nevertheless, only minor photochemical interactions were found between the two units in the latter[138]. Zinc(II) phthalocyanines have been coupled to Ru(II) tris(bipyridine)[139] and Ru(II) terpyridine[140] units as have zinc(II) porphyrins[136, 141].

A typical example for current studies on the influence of the geometry and regiochemical arrangement of linker groups on the ET properties is the comparison of *meso*- and β-linked D–B–A systems. For example, the Zn(II)TPP donor has a relatively slow $S_2 \rightarrow S_1$ IC rate and studies on the competitive ET from S_2 and S_1 states showed that efficient ET from the S_2 state to the pyromellitimide acceptor occurs in both **10** and **11**. However, charge separation from the S_1 state in **10** is 6 times faster than in the β-linked **11**, while the subsequent charge recombination is faster for **10**[142]. The β-positions have also been used to fuse aromatic systems onto the porphyrin to yield systems with extended conjugation[110, 143, 144].

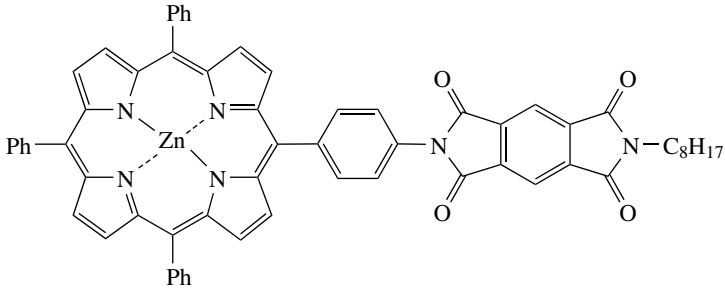

(10)

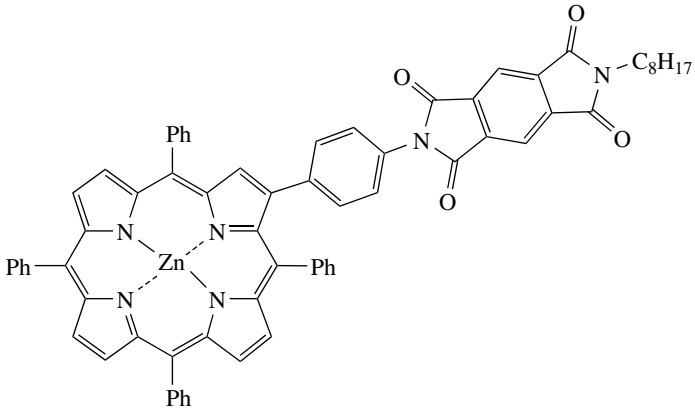

(11)

Most state-of-the-art examples are based on supramolecular approaches using noncovalent interactions[39, 145] or metal chelation[131]. This includes the modulation of the PET

properties in systems where the donor–acceptor excited states are close to each other[141] and simple D–A systems. A typical example is the axial coordination of pyridyl ferrocene acceptors to the zinc center to suppress singlet oxygen generation[146] or the highly selective imidazole recognition found with phenanthroline-strapped zinc porphyrins[147]. A representative phthalocyanine system is **12**, where the PET from the zinc(II) phthalocyanine to a paraquat electron acceptor is enhanced by noncovalent bonding between the crown ether moiety and paraquat through π-donor–acceptor interactions[148]. Zinc(II) phthalocyanine perylenediimide conjugates showed formation of H-type heptameric aggregates with ultrafast ET between neighboring aggregates[149].

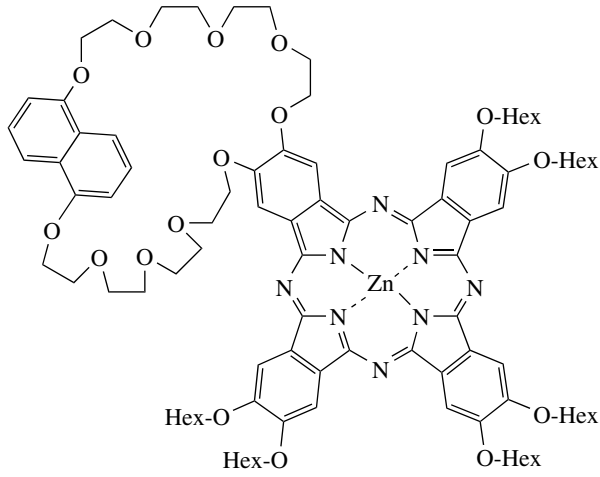

(12)

D–B–A systems may also be constructed using axial coordination and hydrogen-bonding interactions (**13**)[150]. Very attractive are recently described molecular switches, where a photochromic dihydroindolizine moiety was linked to zinc(II) porphyrins. The photochromic acceptor unit could be controlled by light, resulting in a system where the PET could be switched on and off by illumination[151]. Even better, specifically designed tetrad ET systems have been shown to possess logic-gate behavior[152].

Zinc(II) porphyrins have served as core pigments for dendritic systems for some time[153–155]. Such systems have also been used in supramolecular chemistry. For example, a zinc(II) porphyrin with negatively charged aryl ether dendritic branches was noncovalently bound to electron acceptor groups and underwent long-range PET through the dendrimer branches[156]. Nowadays they are also used as repeating building blocks for dendrimers[157] or polymers[158]. Zinc(II) phthalocyanines are increasingly used in dendritic systems or modified with π-conjugated oligomers, too[159, 160]. Depending on the steric crowding induced by the dendritic side chains, significantly red-shifted absorption spectra were obtained[161, 162].

5. Materials and formulations

Most PET or excited state deactivation studies have been performed in solution, although some investigations of Langmuir–Blodgett mono-[163] and multilayer[164] films have been

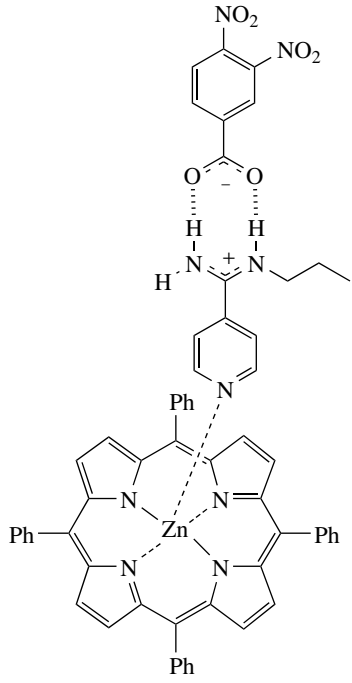

(13)

reported[165, 166]. Other approaches included liquid crystals[167], adsorption on clay surfaces[168], incorporation of Zn(II)TPP in cellulose acetate hollow fiber membranes[169] to generate heterogenous photosensitizers[170, 171], preparation of aqueous silica suspensions containing both zinc(II) porphyrins and tris(2,2′-bipyridyl)ruthenium(II)[172]; or the incorporation in lipid bilayers[173], micelles[174, 175] or vesicles[176, 177]. Most of the current interest is aimed at nanostructured systems. A classic example is the preparation of 'dendritic' nanoclusters, where gold clusters were linked via thio bridges to zinc(II) porphyrins. The porphyrins in such 3D structures exhibited photophysical properties resembling those of porphyrins in solution (e.g. suppressed quenching of fluorescence) in contrast to 2D systems[178]. (5,10,15,20-Tetrakis(perylenediimide)porphyrinato)zinc(II) units have been shown to self-assemble to photofunctional nanoparticles[79]. Self-assembly of the respective donor and acceptor groups can also be used to form so-called nanoaggregates[132].

V. APPLIED PHOTOCHEMISTRY

A. Use as Pigments

Phthalocyanines with various central metals are some of the most widely used pigments and dyes and they have found industrial uses for oil desulfurization, as photoconducting agents in photocopiers, deodorants, germicides, optical computer disks and much more[11, 179, 180]. As outlined below, nowadays attention is focused on semiconductor devices, photovoltaic cells, optical and electrochemical sensing and molecular electronic materials.

B. Photonics

Both porphyrins and phthalocyanines have attracted considerable interest as photonics materials, notably due to their large and fast nonlinear optical responses and because they can exhibit strong reverse saturable absorption[181]. While zinc(II) derivatives have been investigated for two decades, derivatives with closed-shell metal ions are probably superior to simple zinc(II) derivatives[182]. Multiporphyrin arrays constructed by self-assembly have been shown to exhibit excellent properties as third-order nonlinear optical materials. However, the coordination structures tend to dissociate in polar solvents and thus efforts are under way to use covalent tethers to hold the arrays together. Many modern synthetic methods have been used to overcome this problem. For example, olefin metathesis has been used successfully with zinc(II)porphyrins to yield slipped cofacial bisporphyrins[183]. Likewise, many catenane[184,185] and cavitand systems[186] with electronic communication between the building blocks have been developed. Future work will more and more concentrate on using such systems on surfaces for the preparation of hybrid materials. One example is a report on methods to link zinc(II) porphyrins to silicon (Si100)[187].

C. Photosensitization Reactions

1. General principle

The most prominent photochemical reaction of porphyrins involves photosensitization upon absorption of light. This property is of crucial importance in photosynthesis and is the basis for medicinal and industrial uses of tetrapyrroles. A typical example is the reaction of phthalocyanines with oxygen[188]. This involves an efficient energy transfer quenching of the T_1 state by O_2 ($^3\Sigma^-_g$) with $k \sim 10^9$ $M^{-1}s^{-1}$ for metallophthalocyanines to yield singlet molecular oxygen ($^1\Delta_g$) and superoxide which have been thought to be the main toxic reactive intermediates. Mechanistic studies on the reaction of the photoexcited zinc(II) phthalocyanines with hydroperoxides indicate the additional possibility to form oxygen-centered radicals[189]. Modification of the basic phthalocyanine macrocycle, e.g. exchange of the annelated benzene rings to pyridines in tetra-2,3-pyridinoporphyrazines, results in diminished singlet oxygen quantum yields[190].

2. Photovoltaic applications

Solar energy conversion and photovoltaic devices encompass one of the most active applied topics of research in this area[191]. Thus, photoelectrochemical cells based on electrodes (SnO_2, Pt) coated with tetrapyrroles have been studied for a long time[191–194]. Most studies were performed with phthalocyanines due to their stability and wide range of redox potentials and colors and zinc(II) derivatives have featured in such studies[195]. Likewise, many of the new systems described above have been used in dye-sensitized photoelectrochemical solar cells[45,196–198]. These include tyrosine-modified phthalocyanines for near-IR sensitization[199] and liquid crystalline porphyrins[200].

Many photovoltaic systems are aimed at the generation of hydrogen and a multitude of complex systems have been studied[194,201–212]. Typically, such systems are comprised of four components: an electron donor, a photosensitizer, an electron carrier or relay system and a catalyst (A in Figure 3). In analogy to the D–A systems described for ET studies, the photosensitizer and the electron carrier can be combined in one molecule. Several examples with covalently linked porphyrin–viologen systems have been described, wherein the photoexcited singlet and triplet state of the zinc porphyrin are easily quenched by the bonded viologen[213]. Likewise, many attempts have been undertaken to optimize an

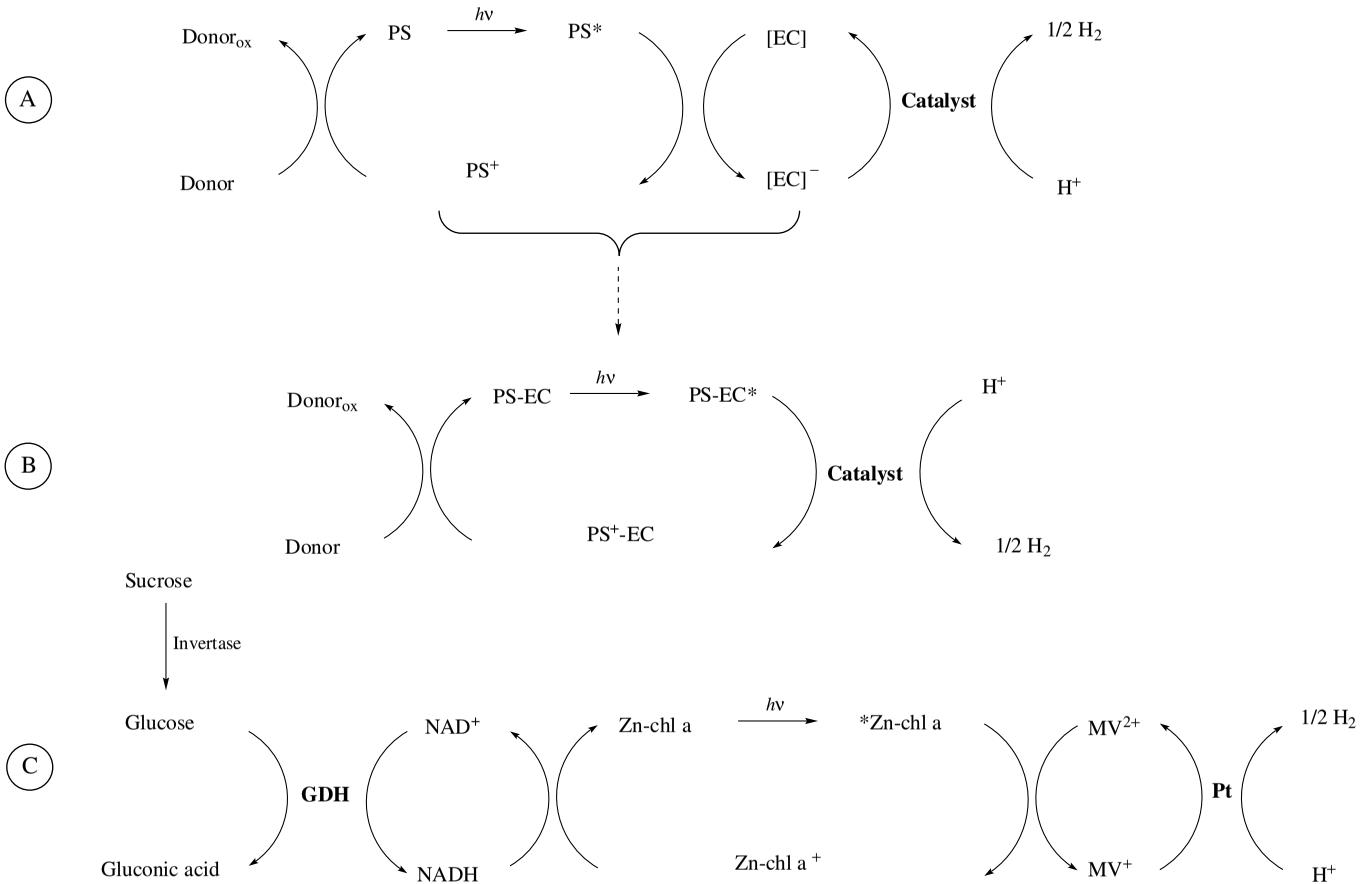

FIGURE 3. Photoinduced hydrogen production systems. PS = photosensitizer, EC = electron carrier, GDH = glucose dehydrogenase

effective charge separation and suppression of back electron transfer either via structural modifications or by using colloidal suspensions[203], liposomes or membrane vesicles[214,215].

While most systems use methylviologen or derivatives thereof as electron carrier, considerable flexibility exists in the choice of catalysts and electron donor. Mostly, either Pt/TiO_2[211,202] or the enzyme hydrogenase[204,205,215,216] are used as catalysts. Experimental systems often use small organic molecules as electron donors. For example, triethanolamine[214,215] and NAD/NADH[213,216] have been used. The latter opens the possibility to develop biotechnological hydrogen production systems using coupled reactions[217,218]. A typical example of potential biohydrogen production systems is shown in Figure 3 (C). Here, a zinc(II) chlorophyll derivative (Zn-chl a) derived from *Spirulina* is used and shows superior photostability and photosensitizing activity compared to the natural magnesium complex. Glucose dehydrogenase (GDH) is used to regenerate NADH, thus ultimately coupling the photochemical reaction and hydrogen production to sucrose as a biomass electron source[219,220].

3. Medicinal use in photodynamic therapy

Tetrapyrroles find increasing use in photomedicine and photodynamic therapy (PDT) presents the one clearly established medicinal application of tetrapyrroles to date[221]. Typically, two different photosensitization processes are discussed. Type I reactions include charge transfer, whereas the type II pathway involves transfer of excitation energy from porphyrin to triplet oxygen. Photodynamic therapy relies on the selective accumulation of a photosensitizer in target tissue where it can be activated with light to produce toxic singlet oxygen resulting in, e.g., tumor necrosis as outlined in Figure 4. This concept is now making its potential felt in oncology, as antiviral and antibacterial PDT, and in the treatment of diseases like age-related macular generation and psoriasis. Several tetrapyrrole-based compounds have been approved for medicinal applications and others are in Phase-2 trials. Although many different derivatives are under investigation, the majority of compounds are free-base derivatives. Only few zinc(II) porphyrins have been investigated in this context due to their lability.

The situation is different for zinc(II) phthalocyanines. A classic study on zinc(II)phthalocyanine **3** shows that it is an efficient photosensitizer for singlet oxygen with a quantum

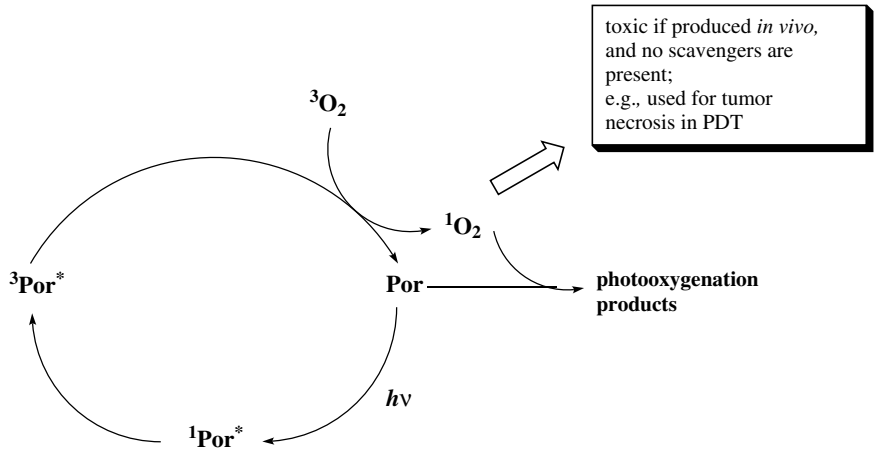

FIGURE 4. Porphyrins as photosensitizers in photodynamic therapy

yield of *ca* 0.4[222]. The efficiency of the photosensitization reaction strongly depends on the macrocycle conformation and substituents pattern[223]. Thus, the quantum yield for singlet oxygen generation for tetrasulfonated zinc(II) phthalocyanines (0.7) is almost three times that of the zinc(II) naphthalocyanines (0.25)[26]. Phthalocyanine derivatives exhibit some photophysical advantages compared to porphyrins: increased Q-band absorption coefficient, red-shifted absorption bands resulting in deeper light tissue penetration[224], high triplet quantum yields, long triplet lifetimes and high singlet oxygen and fluorescence yields[225]. For a specific pattern of substituents, this can result in improved photodynamic activities compared to commercial photosensitizers[224, 226].

A few current examples are shown below and include unsymmetrically substituted derivatives **14**[227], the cationic derivative **15**[228], the neutral derivative **16**[226] and the classic anionic derivative **17**[229, 230], '(tetrabenzoporphyrinato)zinc(II)', an intermediate structure between that of porphyrins and phthalocyanines, and have also been investigated in this respect. However, its quantum yield for singlet oxygen generation (0.023) in liposomes is much lower than that of Photofrin (0.19)[177].

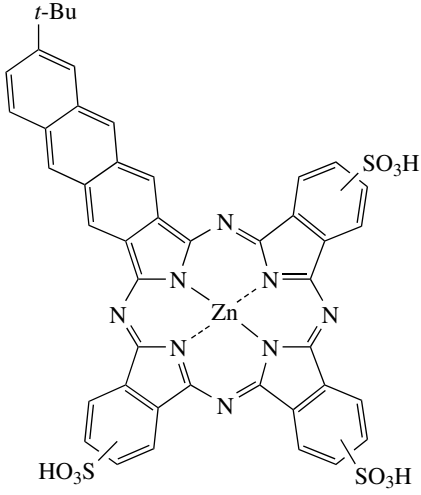

(14)

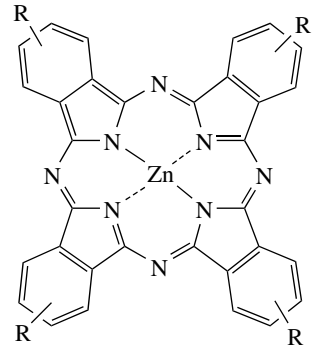

(15) R = $C(CH_3)_2CH_2N(CH_3)_3^+$
(16) R = $SO_2N(C_8H_{17})_2$
(17) R = SO_3^-

Efforts are under way to improve the solubility and localization of such photosensitizers[226, 227, 230]. Thus, water-soluble zinc(II) phthalocyanines[26, 231, 232], cationic (amphiphilic) zinc(II) phthalocyanines[228, 233], perhalogenated zinc(II) phthalocyanines[234–236], sterically hindered[237], polymer appended[32] and dendritic systems[155] have been prepared and new delivery systems investigated[238]. Many of these systems are under scrutiny for their antibacterial action[239]. Note that zinc(II) derivatives are not necessarily the best metal derivatives of phthalocyanines for use in PDT[240]. Taking aspects like tissue clearance and target specific localization into account, porphyrin derivatives will most likely carry the field in this application.

Tetrapyrroles have also found wide use in DNA binding and intercalation studies[241] and type II photosensitized reactions[242] offer an intriguing possibility for site-specific

photoinduced oxidation of DNA. Most studies were performed with free-base porphyrins, but a recent example is the use of a tetraruthenated zinc(II) porphyrin[243] for the specific photooxidation of 2-deoxyguanosine bases to form 8-oxo-2-deoxyguanosines[244].

4. Chemical uses

A number of photosensitization reactions have been described that offer potential use in chemical applications or are of fundamental interest. One of the oldest photochemical reactions involving zinc(II) tetrapyrrole photosensitizers is the photoreduction of methyl viologen[245]. Typically, this involves the generation of the radical anion of the zinc complex which is a strong reducing agent, e.g. by reductive quenching of cysteine. The reaction in solution is often hampered by dimerization and inactivation of the sensitizer. For anionic photosensitizers this can be overcome by incorporation in cationic micelles while neutral chromophores may be solubilized by surfactant solution[176, 246, 247]. For the reaction with triethanolamine it was shown that phthalocyanines with neutral or heavy atom containing substituents were most efficient[248]. The reaction of zinc(II) porphyrins with viologens has also been studied in Langmuir–Blodgett films[249, 250], in covalently-linked systems[251, 252], using reconstituted porphyrin–protein complexes[253], and in the presence of colloidal Pt catalysts[202], platinized zeolites[203] or hydrogenases[204, 205, 216] for potential use in hydrogen production[206–209,212] and for the uphill photooxidation of NADH analogues[254].

The system design for hydrogen production described above (Figure 3) is a rather general setup that can be used in many other ways for chemical transformations[255]. For example, the 'photosynthetic' formic acid production via photoreduction of CO_2 has been developed to a significant level[256, 257]. A typical state-of-the-art system is shown in Figure 5. It consists of a donor (NEt_3), a zinc(II) porphyrin (PS), methyl viologen (MV) as electron carrier and formate dehydrogenase (FDH) from *Saccharomyces cerevisiae* and effects the conversion of CO_2(HCO_3^-) to formic acid in 10.8% yield[258, 259]. In a similar manner, lactic acid production using lactate dehydrogenase and NEt_3 as electron donor has been described[260]. At present, applications such as these together with photovoltaic systems appear to be the most promising areas of practical use for photochemically active zinc(II) tetrapyrroles.

Phthalocyanines play a prominent role in photocatalytic oxidation and reduction reactions[261, 262]. The oxidation rates depend strongly on the oxidation potential of the central metal, and thus zinc(II) derivatives typically take up a middle position. Some selected examples for the use of zinc(II) tetrapyrroles as photosensitizers are the oxidation of isopropyl alcohol[263] or water[264], the photochemical dediazoniation of arene diazonium salts with a zinc(II) phthalocyanine derivative[265], the photocatalytic decomposition of CCl_4[266], trichlorophenol[267], amino acids[26, 268] and of atrazine[269] and have been described. Likewise, reactions with hydroquinone[171], cellulose[270] and the photocatalytic destruction

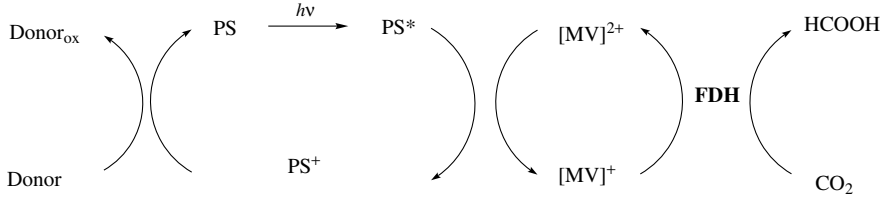

FIGURE 5. Coupled systems for photosynthetic transformations. PS = photosensitizer, MV = methyl viologen, FDG = formate dehydrogenase

of organic matter in effluents from the paper industry[271] were studied. Self-assembled porphyrin systems have been used to study the photoreduction of quinones at liquid/liquid interfaces[272]. Of more theoretical interest are studies on the photoisomerization of stilbene derivatives or valence isomerizations catalyzed by zinc(II) tetrapyrroles[273].

D. Other Applications

A rapidly expanding field is the development of tetrapyrrole-based optical gas sensors. Recently, electron-deficient zinc(II) porphyrins have been under investigation as oxygen sensors based on the stationary-state quenching of the porphyrin triplet–triplet absorption by O_2[274]. Color changes have been described upon binding of NaCN to zinc(II) porphyrin crown ether conjugates, indicating the possibility to develop visible sensing devices based on selective ion-pair recognition[275].

VI. ACKNOWLEDGMENT

The preparation of this chapter was made possible by generous funding from Science Foundation Ireland (Research Professorship—SFI 04/RP1/B482).

VII. REFERENCES

1. T. Nyokong and H. Isago, *J. Porphyrins Phthalocyanines*, **8**, 1083 (2004).
2. M. Gouterman, in *The Porphyrins* (Ed. D. Dolphin), Vol. 3, Academic Press, New York, 1978, p. 1.
3. M. J. Stillman and T. Nyokong, in *Phthalocyanines—Properties and Applications* (Eds. C. C. Leznoff and A. B. P. Lever), Vol. 1, VCH, New York, 1989, pp. 133–291.
4. J. Mack and M. J. Stillman, in *The Porphyrin Handbook* (Eds. K. M. Kadish, K. M. Smith and R. Guilard), Vol. 16, Academic Press, San Diego, CA, 2003, pp. 43–116.
5. K. Ishii and N. Kobayashi, in *The Porphyrin Handbook* (Eds. K. M. Kadish, K. M. Smith and R. Guilard), Vol. 16, Academic Press, San Diego, CA, 2003, pp. 1–42.
6. J. C. Biffinger, H. Sun, A. P. Nelson and S. G. Di Magno, *Org. Biomol. Chem.*, **1**, 733 (2003).
7. A. Ogunsipe, J.-Y. Chen and T. Nyokong, *New J. Chem.*, **28**, 822 (2004).
8. N. A. Kuznetsova, N. S. Gretsova, E. A. Kalmykova, E. A. Makarova, S. N. Dashkevich, V. M. Negrimovskii, O. L. Kaliya and E. A. Luk'yanets, *Russ. J. Gen. Chem. (Engl. Transl.)*, **70**, 133 (2000).
9. N. Kobayashi, M. Togashi, T. Osa, K. Ishii, S. Yamauchi and H. Hino, *J. Am. Chem. Soc.*, **118**, 1073 (1996).
10. N. Kobayashi, H. Ogata, N. Nonaka and E. A. Luk'yanets, *Chem. Eur. J.*, **9**, 5123 (2003).
11. C. C. Leznoff and A. B. P. Lever (Eds.), *Phthalocyanines—Properties and Applications*, Vols. 1–4, VCH, New York, 1989, 1993, 1993, 1996.
12. S. P. Keizer, J. Mack, B. A. Bench, S. M. Gorun and M. J. Stillman, *J. Am. Chem. Soc.*, **125**, 7067 (2003).
13. O. S. Finikova, A. V. Cheprakov, P. J. Carroll and S. A. Vinogradov, *J. Org. Chem.*, **68**, 7517 (2003).
14. M. O. Senge and I. Bischoff, *Tetrahedron Lett.*, **45**, 1647 (2004).
15. K. I. Ozoemena and T. Nyokong, *Inorg. Chem. Commun.*, 1192 (2003).
16. S. M. Bishop, A. Beeby, A. W. Parker, M. S. C. Foley and D. Phillips, *J. Photochem. Photobiol., Part A: Chem.*, **90**, 39 (1995).
17. Y. Yamaguchi, *J. Phys. Chem.*, **120**, 7963 (2004).
18. D. Gust and T. A. Moore, in *The Porphyrin Handbook* (Eds. K. M. Kadish, K. M. Smith and R. Guilard), Vol. 8, Academic Press, San Diego, CA, 2000, pp. 153–190.
19. S. G. Ballard and D. Mauzerall, *Biophys. J.*, **24**, 335 (1978).
20. J. Mack and M. J. Stillman, *J. Am. Chem. Soc.*, **116**, 1292 (1994).
21. T. Nyokong, Z. Gasyna and M. J. Stillman, *Inorg. Chem.*, **26**, 548 (1987).
22. B. Van Vlierberge and G. Ferraudi, *Inorg. Chem.*, **26**, 337 (1987).

23. P. Neta and H. Levanon, *Isr. J. Chem.*, **22**, 107 (1982).
24. S. P. Keizer, W. Han and M. J. Stillman, *Inorg. Chem.*, **41**, 353 (2002).
25. K. Lang, D. M. Wagnerova and J. Brodilova, *J. Photochem. Photobiol., Part A: Chem.*, **72**, 9 (1993).
26. J. D. Spikes, J. E. van Lier and J. C. Bommer, *J. Photochem. Photobiol., Part A: Chem.*, **91**, 193 (1995).
27. R. Slota and G. Dyrda, *Inorg. Chem.*, **42**, 5743 (2003).
28. N. A. Kuznetsova, V. M. Negrimovskii, V. M. Derkacheva, E. A. Makarova, O. L. Kaliya and E. A. Luk'yanets, *Russ. J. Gen. Chem. (Engl. Transl.)*, **67**, 463 (1997).
29. Y. Nishimura, Y. Kaneko, T. Arai, H. Sakuragi, K. Tokumaru, M. Kiten, S. Yamamura and D. Matsunaga, *Chem. Lett.*, 1935 (1990).
30. P. Tau, A. O. Ogunsipe, S. Maree, M. D. Maree and T. Nyokong, *J. Porphyrins Phthalocyanines*, **7**, 439 (2003).
31. P. Matlaba and T. Nyokong, *Polyhedron*, **21**, 2463 (2002).
32. Z. W. Gu, J. D. Spikes, P. Kopeckova and J. Kopecek, *Collect. Czech. Chem. Commun.*, **58**, 2321 (1993).
33. K. Giering, C. Dressler, R. Herter, R. Senz, J. G. Moser and H.-P. Berlien, *Proc. SPIE*, **2625**, 77 (1996).
34. F. Li, S. Gentemann, W. A. Kalsbeck, J. Seth, J. S. Lindsey, D. Holten and D. F. Bocian, *J. Mater. Chem.*, **7**, 1245 (1997).
35. M. R. Wasielewski, *Chem. Rev.*, **92**, 435 (1992).
36. B. D. Berezin, S. V. Rumyantseva, A. P. Moryganov and M. B. Berezin, *Russ. Chem. Rev. (Engl. Transl.)*, **73**, 185 (2004).
37. M. O. Senge and K. M. Smith, in *Anoxygenic Photosynthetic Bacteria* (Eds. R. E. Blankenship, M. T. Madigan and C. E. Bauer), Kluwer, Dordrecht, 1995, pp. 137–151.
38. H. Xu, T. Shen, O. Zhou, S. Shen, J. Liu, L. Li, S. Zhou, X. Zhang, Q. Yu, Z. Bi and X. Xiao, *J. Photochem. Photobiol., Part A: Chem.*, **65**, 267 (1992).
39. J. Otsuki, *Trends Phys. Chem.*, **8**, 61 (2001).
40. J.-C. Chambron, J.-P. Collin, J.-O. Dalbavie, C. O. Dietrich-Buchecker, V. Heitz, F. Odobel, N. Solladié and J.-P. Sauvage, *Coord. Chem. Rev.*, **178–180**, 1299 (1998).
41. A. Harriman and J. P. Sauvage, *Chem. Soc. Rev.*, **25**, 41 (1996).
42. J. P. Collin, A. Harriman, V. Heitz, F. Odobel and J. P. Sauvage, *Coord. Chem. Rev.*, **148**, 63 (1996).
43. D. Gust, T. A. Moore and A. L. Moore, *Res. Chem. Intermed.*, **23**, 621 (1997).
44. H. Imahori, *Org. Biomol. Chem.*, **2**, 1425 (2004).
45. H. Imahori and S. Fukuzumi, *Adv. Funct. Mater.*, **14**, 525 (2004).
46. H. Imahori, K. Tamaki, Y. Araki, T. Hasobe, O. Ito, A. Shimomura, S. Kundu, T. Okada, Y. Sakata and S. Fukuzumi, *J. Phys. Chem. A*, **106**, 2803 (2002).
47. T. Kesti, N. Tkachenko, H. Yamada, H. Imahori, S. Fukuzumi and H. Lemmetyinen, *Photochem. Photobiol. Sci.*,**2**, 251 (2003).
48. H. Imahori, K. Tamaki, Y. Araki, Y. Sekiguchi, O. Ito, Y. Sakata and S. Fukuzumi, *J. Am. Chem. Soc.*, **124**, 5165 (2002).
49. T. D. M. Bell, K. P. Ghiggino, K. A. Jolliffe, M. G. Ranasinghe, S. J. Langford, M. J. Shephard and M. N. Paddon-Row, *J. Phys. Chem. A*, **106**, 10079 (2002).
50. H. Imahori, Y. Sekiguchi, Y. Kashiwagi, T. Sato, Y. Araki, O. Ito, H. Yamada and S. Fukuzumi, *Chem. Eur. J.*, **10**, 3184 (2004).
51. X. Camps, E. Dietel, A. Hirsch, S. Pyo, L. Echegoyen, S. Hackbarth and B. Röder, *Chem. Eur. J.*, **5**, 2362 (1999).
52. S. Fukuzumi, K. Ohkubo, H. Imahori, J. Shao, Z. Ou, G. Zheng, Y. Chen, R. K. Pandey, M. Fujitsuka, O. Ito and K. M. Kadish, *J. Am. Chem. Soc.*, **123**, 10676 (2001).
53. H. Helaja, A. Y. Tauber, Y. Abel, N. V. Tkachenko, H. Lemmetyinen, I. Kilpeläinen and P. H. Hynninen, *J. Chem. Soc., Perkin Trans. 1*, 2403 (1999).
54. G. Kodis, P. A. Liddell, A. L. Moore, T. A. Moore and D. Gust, *J. Phys. Org. Chem.*, **17**, 724 (2004).
55. F.-P. Montforts, I. Vlassiouk, S. Smirnov and M. Wedel, *J. Porphyrins Phthalocyanines*, **7**, 651 (2003).
56. T. Yamaguchi, N. Ishii, K. Tashiro and T. Aida, *J. Am. Chem. Soc.*, **125**, 13934 (2003).

57. N. Watanabe, N. Kihara, Y. Furusho, T. Takata, Y. Araki and O. Ito, *Angew. Chem., Int. Ed.*, **42**, 681 (2003).
58. D. I. Schuster, K. Li, D. M. Guldi and J. Ramey, *Org. Lett.*, **6**, 1919 (2004).
59. K. Li, P. J. Bracher, D. M. Guldi, M. Ángeles Herranz, L. Echegoyen and D. I. Schuster, *J. Am. Chem. Soc.*, **126**, 9156 (2004).
60. K. Li, D. I. Schuster, D. M. Guldi, M. Ángeles Herranz and L. Echegoyen, *J. Am. Chem. Soc.*, **126**, 3388 (2004).
61. D. M. Guldi, C. Luo, A. Schwartz, M. Scheloske and A. Hirsch, *Chem. Commun.*, 1066 (2001).
62. F. D'Souza, G. R. Deviprasad, M. E. El-Khouly, M. Fujitsuka and O. Ito, *J. Am. Chem. Soc.*, **123**, 5277 (2001).
63. F. D'Souza, S. Gadde, M. E. Zandler, A. Klykov, M. E. El-Khouly, M. Fujitsuka and O. Ito, *J. Phys. Chem. A*, **106**, 12393 (2002).
64. F. D'Souza, G. R. Deviprasad, M. E. Zandler, M. E. El-Khouly, M. Fujitsuka and O. Ito, *J. Phys. Chem. B*, **106**, 4952 (2002).
65. F. D'Souza, P. M. Smith, S. Gadde, A. L. McCarty, M. J. Kullman, M. E. Zandler, M. Itou, Y. Araki and O. Ito, *J. Phys. Chem. B*, **108**, 11333 (2004).
66. F. D'Souza, G. R. Deviprasad, M. E. Zandler, M. E. El-Khouly, M. Fujitsuka and O. Ito, *J. Phys. Chem. A*, **107**, 4801 (2003).
67. S. R. Wilson, S. MacMahon, F. T. Tat, P. D. Jarowski and D. I. Schuster, *Chem. Commun.*, 226 (2004).
68. F. D'Souza, G. R. Deviprasad, M. S. Rahman and J. Choi, *Inorg. Chem.*, **64**, 9124 (1999).
69. M. E. El-Khouly, S. Gadde, G. R. Deviprasad, M. Fujitsuka, O. Ito and F. D'Souza, *J. Porphyrins Phthalocyanines*, **7**, 1 (2003).
70. D. M. Guldi, J. Ramey, M. V. Martínez-Díaz, A. de la Escosura, T. Torres, T. Da Ros and M. Prato, *Chem. Commun.*, 2774 (2002).
71. S. L. Gould, G. Kodis, R. E. Palacios, L. de la Garza, A. Brune, D. Gust, T. A. Moore and A. L. Moore, *J. Phys. Chem. B*, **108**, 10566 (2004).
72. K. M. Giangiacomo and P. L. Dutton, *Proc. Natl. Acad. Sci. USA*, **86**, 2658 (1989).
73. M. Speck, M. O. Senge, A. Schäfer and H. Kurreck, *Bioorg. Med. Chem. Lett.*, **7**, 2589 (1997).
74. M. Speck, H. Kurreck and M. O. Senge, *Eur. J. Org. Chem.*, 2303 (2000).
75. M. O. Senge, S. Hatscher, Z. Ökten and M. Speck, *Tetrahedron Lett.*, **44**, 4463 (2003).
76. M. Speck, D. Niethammer and M. O. Senge, *J. Chem. Soc., Perkin Trans. 2*, 455 (2002).
77. R. S. Loewe, K. Tomizaki, J. W. Youngblood, Z. Bo and J. S. Lindsey, *J. Mater. Chem.*, **12**, 3438 (2002).
78. K. Tomizaki, P. Thamyongkit, R. S. Loewe and J. S. Lindsey, *Tetrahedron*, **59**, 1191 (2003).
79. T. van der Boom, R. T. Hayes, Y. Zhao, P. J. Bushard, E. A. Weiss and M. R. Wasielewski, *J. Am. Chem. Soc.*, **124**, 9582 (2002).
80. S. Prathapan, S. I. Yang, J. Seth, M. A. Miller, D. F. Bocian, D. Holten and J. S. Lindsey, *J. Phys. Chem. B*, **105**, 8237 (2001).
81. R. T. Hayes, M. R. Wasielewski and D. Gosztola, *J. Am. Chem. Soc.*, **122**, 5563 (2000).
82. C.-C. You and F. Würthner, *Org. Lett.*, **6**, 2401 (2004).
83. N. Mataga, S. Taniguchi, H. Chosrowjan, A. Osuka and N. Yoshida, *Photochem. Photobiol. Sci.*, **2**, 493 (2003).
84. Y. Mori, Y. Sakaguchi and H. Hayashi, *J. Phys. Chem. A*, **106**, 4453 (2002).
85. K. Okamoto, Y. Mori, H. Yamada, H. Imahori and S. Fukuzumi, *Chem. Eur. J.*, **10**, 474 (2004).
86. N. P. Redmore, I. V. Rubtsov and M. J. Therien, *Inorg. Chem.*, **41**, 566 (2002).
87. N. Mataga, H. Chosrowjan, S. Taniguchi, Y. Shibata, N. Yoshida, A. Osuka, T. Kikuzawa and T. Okada, *J. Phys. Chem. A*, **106**, 12191 (2002).
88. K. Kilså, J. Kajanus, S. Larsson, A. N. Macpherson, J. Mårtensson and B. Albinsson, *Chem. Eur. J.*, **7**, 2122 (2001).
89. K. Pettersson, K. Kilså, J. Mårtensson and B. Albinsson, *J. Am. Chem. Soc.*, **126**, 6710 (2004).
90. N. Mataga, H. Chosrowjan, Y. Shibata, N. Yoshida, A. Osuka, T. Kikuzawa and T. Okada, *J. Am. Chem. Soc.*, **123**, 12422 (2001).
91. R. A. Haycock, A. Yartsev, U. Michelsen, V. Sundstrom and C. A. Hunter, *Angew. Chem., Int. Ed.*, **39**, 3616 (2000).

92. C. Ikeda, Y. Tanaka, T. Fujihara, Y. Ishii, T. Ushiyama, K. Yamamoto, N. Yoshioka and H. Inoue, *Inorg. Chem.*, **40**, 3395 (2001).
93. T. S. Balaban, A. D. Bhise, M. Fischer, M. Linke-Schaetzel, C. Roussel and N. Vanthuyne, *Angew. Chem., Int. Ed.*, **42**, 2140 (2003).
94. K. Tomizaki, R. S. Loewe, C. Kirmaier, J. K. Schwartz, J. L. Retsek, D. F. Bocian, D. Holten and J. S. Lindsey, *J. Org. Chem.*, **67**, 6519 (2002).
95. A. Nakano, A. Osuka, T. Yamazaki, Y. Nishimura, S. Akimoto, I. Yamazaki, A. Itaya, M. Murakami and H. Miyasaka, *Chem. Eur. J.*, **7**, 3134 (2001).
96. K. Tomizaki, L. Yu, L. Wei, D. F. Bocian and J. S. Lindsey, *J. Org. Chem.*, **68**, 8199 (2003).
97. L. Yu and J. S. Lindsey, *J. Org. Chem.*, **66**, 7402 (2001).
98. Y. Kuramochi, A. Satake and Y. Kobuke, *J. Am. Chem. Soc.*, **126**, 8668 (2004).
99. X. Peng, N. Aratani, A. Takagi, T. Matsumoto, T. Kawai, I.-W. Hwang, T. Kyu Ahn, D. Kim and A. Osuka, *J. Am. Chem. Soc.*, **126**, 4468 (2004).
100. W. W. Kalisch, M. O. Senge and K. Ruhlandt-Senge, *Photochem. Photobiol.*, **67**, 312 (1998).
101. J. Brettar, J.-P. Gisselbrecht, M. Gross and N. Solladié, *Chem. Commun.*, 733 (2001).
102. C. Pascard, J. Guilhem, S. Chardon-Noblat and J.-P. Sauvage, *New J. Chem.*, **17**, 331 (1993).
103. J. T. Fletcher and M. J. Therien, *Inorg. Chem.*, **41**, 331 (2002).
104. D. A. Shultz, H. Lee, K. Kumar and K. P. Gwaltney, *J. Org. Chem.*, **64**, 9124 (1999).
105. P. A. Liddell, G. Kodis, L. de la Garza, A. L. Moore, T. A. Moore and D. Gust, *J. Phys. Chem. B*, **108**, 10256 (2004).
106. M. O. Senge, B. Rößler, J. von Gersdorff, A. Schäfer and H. Kurreck, *Tetrahedron Lett.*, **45**, 3363 (2004).
107. Y. Deng, C. K. Chang and D. G. Nocera, *Angew. Chem., Int. Ed.*, **39**, 1066 (2000).
108. S. Yagi, M. Ezoe, I. Yonekura, T. Takagishi and H. Nakazumi, *J. Am. Chem. Soc.*, **125**, 4068 (2003).
109. F. D'Souza, P. M. Smith, M. E. Zandler, A. L. McCarty, M. Itou, Y. Araki and O. Ito, *J. Am. Chem. Soc.*, **126**, 7898 (2004).
110. M. O. Senge and J. Richter, *J. Porphyrins Phthalocyanines*, **8**, 934 (2004).
111. N. Aratani, A. Tsuda and A. Osuka, *Synlett*, 1663 (2001).
112. A. Nakano, Y. Yasuda, T. Yamazaki, S. Akimoto, I. Yamazaki, H. Miyasaka, A. Itaya, M. Murakami and A. Osuka, *J. Phys. Chem. A*, **105**, 4822 (2001).
113. N. Aratani and A. Osuka, *Bull. Chem. Soc. Jpn.*, **74**, 1361 (2001).
114. N. Aratani, A. Osuka, Y. H. Kim, D. H. Jeong and D. Kim, *Angew. Chem., Int. Ed.*, **39**, 1458 (2000).
115. N. Yoshida, T. Ishizuka, A. Osuka, D. H. Jeong, H. S. Cho, D. Kim, Y. Matsuzaki, A. Nogami and K. Tanaka, *Chem. Eur. J.*, **9**, 58 (2003).
116. A. Nakano, A. Osuka, I. Yamazaki, T. Yamazaki and Y. Nishimura, *Angew. Chem., Int. Ed. Engl.*, **37**, 3023 (1998).
117. N. Aratani and A. Osuka, *Org. Lett.*, **3**, 4213 (2001).
118. H. S. Cho, D. H. Jeong, S. Cho, D. Kim, Y. Matsuzaki, K. Tanaka, A. Tsuda and A. Osuka, *J. Am. Chem. Soc.*, **124**, 14642 (2002).
119. X.-B. Shao, X.-K. Jiang, X. Zhao, C.-X. Zhao, Y. Chen and Z.-T. Li, *J. Org. Chem.*, **69**, 899 (2004).
120. M. O. Senge and K. M. Smith, *Chem. Commun.*, 923 (1994).
121. M. Dudič, P. Lhoták, H. Petříčková, I. Stibor, K. Lang and J. Sýkora, *Tetrahedron*, **59**, 2409 (2003).
122. Y. Kubo, Y. Ishii, T. Yoshizawa and S. Tokita, *Chem. Commun.*, 1394 (2004).
123. E. Stulz, *Synlett*, 1579 (2004).
124. X. Li and D. K. P. Ng, *Tetrahedron Lett.*, **42**, 305 (2001).
125. P. Thamyongkit, M. Speckbacher, J. R. Diers, H. L. Kee, C. Kirmaier, D. Holten, D. F. Bocian and J. S. Lindsey, *J. Org. Chem.*, **69**, 3700 (2004).
126. I. Seotsanyana-Mokhosi, S. Maree, M. D. Maree and T. Nyokong, *J. Porphyrins Phthalocyanines*, **7**, 167 (2003).
127. K. Tomizaki, A. B. Lysenko, M. Taniguchi and J. S. Lindsey, *Tetrahedron*, **60**, 2011 (2004).
128. I. V. Sazanovich, A. Balakumar, K. Muthukumaran, E. Hindin, C. Kirmaier, J. R. Diers, J. S. Lindsey, D. F. Bocian and D. Holten, *Inorg. Chem.*, **42**, 6616 (2003).
129. T. E. O. Screen, I. M. Blake, L. H. Rees, W. Clegg, S. J. Borwick and H. L. Anderson, *J. Chem. Soc., Perkin Trans. 1*, 320 (2002).

130. K. F. Cheng, C. M. Drain and K. Grohmann, *Inorg. Chem.*, **42**, 2075 (2003).
131. L. Yu, K. Muthukumaran, I. V. Sazanovich, C. Kirmaier, E. Hindin, J. R. Diers, P. D. Boyle, D. F. Bocian, D. Holten and J. S. Lindsey, *Inorg. Chem.*, **42**, 6629 (2003).
132. A. de la Escosura, M. V. Martinez-Diaz, P. Thordarson, A. E. Rowan, R. J. M. Nolte and T. Torres, *J. Am. Chem. Soc.*, **125**, 12300 (2003).
133. H. Shiratori, T. Ohno, K. Nozaki, I. Yamazaki, Y. Nishimura and A. Osuka, *J. Org. Chem.*, **65**, 8747 (2000).
134. L. Ruhlmann and A. Giraudeau, *Eur. J. Inorg. Chem.*, 3276 (2002).
135. X. J. Salom-Roig, J.-C. Chambron, C. Goze, V. Heitz and J.-P. Sauvage, *Eur. J. Org. Chem.*, 3276 (2002).
136. A. Harriman, M. Hissler, O. Trompette and R. Ziessel, *J. Am. Chem. Soc.*, **121**, 2516 (1999).
137. C. J. Aspley, J. R. Lindsay Smith and R. N. Perutz, *J. Chem. Soc., Dalton Trans.*, 2269 (1999).
138. C. J. Aspley, J. R. Lindsay Smith, R. N. Perutz and D. Pursche, *J. Chem. Soc., Dalton Trans.*, 170 (2002).
139. A. González-Cabello, P. Vázquez, T. Torres and D. M. Guldi, *J. Org. Chem.*, **68**, 8635 (2003).
140. M. Kimura, T. Hamakawa, K. Hanabusa, H. Shirai and N. Kobayashi, *Inorg. Chem.*, **40**, 4775 (2001).
141. K. Araki, P. Losco, F. M. Engelmann, H. Winnischofer and H. E. Toma, *J. Photochem. Photobiol. Part A: Chem.*, **142**, 25 (2001).
142. R. T. Hayes, C. J. Walsh and M. R. Wasielewski, *J. Phys. Chem. A*, **108**, 2375 (2004).
143. K. Tan, L. Jaquinod, R. Paolesse, S. Nardis, C. Di Natale, A. Di Carlo, L. Prodi, M. Montalti, N. Zaccheroni and K. M. Smith, *Tetrahedron*, **60**, 1099 (2004).
144. S. Fukuzumi, K. Ohkubo, W. E, Z. Ou, J. Shao, K. M. Kadish, J. A. Hutchison, K. P. Ghiggino, P. J. Sintic and M. J. Crossley, *J. Am. Chem. Soc.*, **125**, 14984 (2003).
145. S. J. Langford and V.-L. Lau, *Aust. J. Chem.*, **57**, 29 (2004).
146. Y. Kashiwagi, H. Imahori, Y. Araki, O. Ito, K. Yamada, Y. Sakata and S. Fukuzumi, *J. Phys. Chem. A*, **107**, 5515 (2003).
147. D. Paul, J. A. Wytko, M. Koepf and J. Weiss, *Inorg. Chem.*, **41**, 3699 (2002).
148. T. Muto, M. Kimura, K. Hanabusa and H. Shirai, *Tetrahedron Lett.*, **40**, 3199 (1999).
149. X. Li, L. E. Sinks, B. Rybtchinski and M. R. Wasielewski, *J. Am. Chem. Soc.*, **126**, 10810 (2004).
150. J. Otsuki, M. Takatsuki, M. Kaneko, H. Miwa, T. Takido, M. Seno, K. Okamoto, H. Imahori, M. Fujitsuka, Y. Araki, O. Ito and S. Fukuzumi, *J. Phys. Chem. A*, **107**, 379 (2003).
151. Y. Terazono, G. Kodis, J. Andréasson, G. Jeong, A. Brune, T. Hartmann, H. Dürr, A. L. Moore, T. A. Moore and D. Gust, *J. Phys. Chem. B*, **108**, 1812 (2004).
152. M. Andersson, L. E. Sinks, R. T. Hayes, Y. Zhao and M. R. Wasielewski, *Angew. Chem., Int. Ed.*, **42**, 3139 (2003).
153. S. Hecht, N. Vladimirov and J. M. J. Fréchet, *J. Am. Chem. Soc.*, **123**, 18 (2001).
154. C. S. Rajesh, G. J. Capitosti, S. J. Cramer and D. A. Modarelli, *J. Phys. Chem. B*, **105**, 10175 (2001).
155. G.-D. Zhang, N. Nishiyama, A. Harada, D.-L. Jiang, T. Aida and K. Kataoka, *Macromolecules*, **36**, 1304 (2003).
156. R. Sadamoto, N. Tomioka and T. Aida, *J. Am. Chem. Soc.*, **118**, 3978 (1996).
157. M.-S. Choi, T. Aida, T. Yamazaki and I. Yamazaki, *Chem. Eur. J.*, **8**, 2667 (2002).
158. F. Takei, S. Nakamura, K. Onitsuka, A. Ishida, S. Tojo, T. Majima and S. Takashi, *Chem. Lett.*, **32**, 506 (2003).
159. M. Kimura, H. Narikawa, K. Ohta, K. Hanabusa, H. Shirai and N. Kobayashi, *Chem. Mater.*, **14**, 2711 (2002).
160. A. C. H. Ng, X.-Y. Li and D. K. P. Ng, *Macromolecules*, **32**, 5292 (1999).
161. M. Kimura, K. Nakada, Y. Yamaguchi, K. Hanabusa, H. Shirai and N. Kobayashi, *Chem. Commun.*, 1215 (1997).
162. C. Ryppa and M. O. Senge, *Heterocycles*, **63**, 505 (2004).
163. T. Yamazaki, I. Yamazaki and A. Osuka, *J. Phys. Chem. B*, **102**, 7858 (1998).
164. H. Ohkita, T. Ogi, R. Kinoshita, S. Ito and M. Yamamoto, *Polymer*, **43**, 3571 (2002).
165. T. T. H. Tran, J. F. Lipskier, D. Houde, C. Pepin, R. Langlois and S. Palacin, *J. Chem. Soc., Faraday Trans.*, **88**, 2529 (1992).
166. O. Korth, T. Hanke, J. von Gersdorff, H. Kurreck and B. Röder, *Thin Solid Films*, **382**, 240 (2001).

167. A. Berg, Z. Shuali, H. Levanon, A. Wiehe and H. Kurreck, *J. Phys. Chem. A*, **105**, 10060 (2001).
168. S. Takagi, D. A. Tryk and H. Inoue, *J. Phys. Chem. B*, **106**, 5455 (2002).
169. C. C. Wamser, M. Calvin and G. A. Graf, *J. Membrane Sci.*, **28**, 31 (1986).
170. B. A. Gregg, M. A. Fox and A. J. Bard, *Tetrahedron*, **45**, 4707 (1989).
171. F.-R. F. Fan and A. J. Bard, *J. Am. Chem. Soc.*, **101**, 6139 (1979).
172. P. Serguievski, W. E. Ford and M. A. J. Rodgers, *Langmuir*, **12**, 348 (1996).
173. K. Iida, M. Nango, M. Matsuura, M. Yamaguchi, K. Sato, K. Tanaka, K. Akimoto, K. Yamashita, K. Tsuda and Y. Kurono, *Langmuir*, **12**, 450 (1996).
174. M. E. Daraio, P. F. Aramendia and E. San Roman, *J. Photochem. Photobiol., Part A: Chem.*, **77**, 41 (1994).
175. M. E. Daraio, A. Völker, P. F. Aramendia and E. San Roman, *Langmuir*, **12**, 2932 (1996).
176. J. K. Hurst, L. Y. C. Lee and M. Grätzel, *J. Am. Chem. Soc.*, **105**, 7048 (1983).
177. E. Gross, B. Ehrenberg and F. M. Johnson, *Photochem. Photobiol.*, **57**, 808 (1993).
178. H. Imahori, Y. Kashiwagi, Y. Endo, T. Hanada, Y. Nishimura, I. Yamazaki, Y. Araki, O. Ito and S. Fukuzumi, *Langmuir*, **20**, 73 (2004).
179. F. H. Moser and A. H. Thomas, *The Phthalocyanines*, Vols. 1–2, CRC Press, Boca Raton, FL, 1983.
180. H. Shirai and N. Kobayashi, *Phthalocyanines—Chemistry and Functions*, IPC, Tokyo, 1997.
181. W. Blau, H. Byrne, W. M. Dennis and J. M. Kelly, *Opt. Commun.*, **56**, 25 (1985).
182. K. McEwan, K. Lewis, G.-Y. Yang, L.-L. Chng, Y.-W. Lee, W.-P. Lau and K.-S. Lai, *Adv. Funct. Mater.*, **13**, 863 (2003).
183. A. Othashi, A. Satake and Y. Kobuke, *Bull. Chem. Soc. Jpn*, **77**, 365 (2004).
184. M. J. Gunter and S. M. Farquhar, *Org. Biomol. Chem.*, **1**, 3450 (2003).
185. M. J. Gunter, T. P. Jeynes and P. Turner, *Eur. J. Org. Chem.*, 193 (2004).
186. S. D. Starnes, D. M. Rudkevich and J. Rebek Jr., *J. Am. Chem. Soc.*, **123**, 4659 (2001).
187. Z. Liu, A. A. Yasseri, R. S. Loewe, A. B. Lysenko, V. L. Malinovskii, Q. Zhao, S. Surthi, Q. Li, V. Misra, J. S. Lindsey and D. F. Bocian, *J. Org. Chem.*, **69**, 5568 (2004).
188. W. M. Sharman, S. M. Allen and J. E. van Lier, in *Methods in Enzymology* (Eds. L. Packer and H. Sies), Vol. 319, Academic Press, New York, 2000, p. 375.
189. T. G. Gantchev and J. E. van Lier, *Chem. Phys. Lett.*, **369**, 627 (2003).
190. I. Seotsanyana-Mokhosi, N. Kuznetsova and T. Nyokong, *J. Photochem. Photobiol., Part A: Chem.*, **140**, 215 (2001).
191. D. Schlettwein, N. I. Jaeger and T. Oeherman, in *The Porphyrin Handbook* (Eds. K. M. Kadish, K. M. Smith and R. Guilard), Vol. 16, Academic Press, San Diego, CA, 2003, p. 247.
192. I. B. Dmitriev, V. G. Meminushchii, O. S. Nedelina, V. A. Ilatovskii and G. G. Komissarov, *Biofizika*, **34**, 199 (1989); *Chem. Abstr.* **111**, 94022u (1989).
193. V. A. Ilatovskii and G. G. Komissarov, *Zh. Fiz. Khim.*, **65**, 1075 (1991); *Chem. Abstr.* **115**, 37360m (1991).
194. J. Davila, A. Harriman, M. C. Richoux and L. R. Milgrom, *Chem. Commun.*, 525 (1987).
195. P. Leempoel, F.-R. F. Fan and A. J. Bard, *J. Phys. Chem.*, **87**, 2948 (1983).
196. M. E. Milanesio, M. Gervaldo, L. A. Otero, L. Sereno, J. J. Silber and E. N. Durantini, *J. Phys. Org. Chem.*, **15**, 844 (2002).
197. A. F. Nogueira, L. F. O. Furtado, A. L. B. Formiga, M. Nakamura, K. Araki and H. E. Toma, *Inorg. Chem.*, **43**, 396 (2004).
198. M. A. Loi, P. Denk, H. Hoppe, H. Neugebauer, D. Meissner, C. Winder, C. J. Brabec, N. S. Sariciftci, A. Gouloumis, P. Vázquez and T. Torres, *Synthetic Metals*, **137**, 1491 (2003).
199. J. He, G. Benkö, F. Korodi, T. Polivka, R. Lomoth, B. Åkermark, L. Sun, A. Hagfeldt and V. Sundström, *J. Am. Chem. Soc.*, **124**, 4922 (2002).
200. B. A. Gregg, M. A. Fox and A. J. Bard, *J. Phys. Chem.*, **94**, 1586 (1990).
201. I. Okura, *Coord. Chem. Rev.*, **68**, 53 (1985).
202. A. Harriman, G. Porter and M. C. Richoux, *J. Chem. Soc., Faraday Trans. 2*, **78**, 1955 (1982).
203. L. Persaud, A. J. Bard, A. Campion, M. A. Fox, T. E. Mallouk, S. E. Webber and J. M. White, *J. Am. Chem. Soc.*, **109**, 7309 (1987).
204. I. Okura, S. Kusunoki and S. Aono, *Inorg. Chem.*, **22**, 3828 (1983).
205. Y. Amao and I. Okura, *J. Mol. Catal. A,* **145**, 51 (1999).
206. I. Okura, M. Takeuchi and N. Kim-Thuan, *Chem. Lett.*, **9**, 765 (1980).
207. A. J. Abdul-Ghani and S. Abdul-Kareem, *Int. J. Hydrogen Energy,* **14**, 313 (1989).

208. Y. Amao, K. Yamane and I. Okura, *Chem. Lett.*, 871 (1997).
209. G. McLendon and D. S. Miller, *Chem. Commun.*, 533 (1980).
210. K. Kalyanasundaram, *J. Chem. Soc., Faraday Trans. 2,* **79**, 1365 (1983).
211. E. A. Malinka, G. L. Kamalov, S. V. Vodzinskii, V. I. Melnik and Z. I. Zhilina, *J. Photochem. Photobiol., Part A: Chem.*, **90**, 153 (1995).
212. W. Schuhmann, H. P. Josel and H. Parlar, *Angew. Chem., Int. Ed. Engl.*, **26**, 241 (1987).
213. Y. Amao, T. Kamachi and I. Okura, *J. Porphyrins Phthalocyanines,* **2**, 201 (1998).
214. Y. Amao, Y. Tomonou, Y. Ishikawa and I. Okura, *Int. J. Hydrogen Energy,* **27**, 621 (2002).
215. Y. Amao, Y. Tomonou and I. Okura, *Sol. Energy Mater. Sol. Cells,* **79**, 103 (2003).
216. Y. Amao, T. Kamachi and I. Okura, *J. Mol. Catal. A,* **120**, L5 (1997).
217. Y. Saiki and Y. Amao, *Biotechnol. Bioeng.*, **82**, 710 (2003).
218. Y. Saiki, Y. Ishikawa and Y. Amao, *Chem. Lett.*, 218 (2002).
219. J. Woodward, M. Orr, K. Cordray and E. Greenbaum, *Nature,* **405**, 1014 (2000).
220. T. Inoue, S. N. Kumar, T. Kamachi and I. Okura, *Chem. Lett.*, 147 (1999).
221. R. Bonnett, *Chemical Aspects of Photodynamic Therapy,* Gordon and Breach Sci. Publ., Amsterdam, 2000.
222. G. Valduga, S. Nonell, E. Reddi, G. Jori and S. E. Braslavsky, *Photochem. Photobiol.*, **48**, 1 (1988).
223. H. Weitman, S. Schatz, H. E. Gottlieb, N. Kobayashi and B. Ehrenberg, *Photochem. Photobiol.*,**73**, 473 (2001).
224. M. Ochsner, *J. Photochem. Photobiol., Part B: Biol.*, **32**, 3 (1996).
225. I. Rosenthal, *Photochem. Photobiol.*, **53**, 859 (1991).
226. D. J. Ball, S. R. Wood, D. I. Vernon, J. Griffiths, T. M. A. R. Dubbelman and S. B. Brown, *J. Photochem. Photobiol., Part B: Biol.*, **45**, 28 (1998).
227. S. Kudrevich, N. Brasseur, C. La Madeleine, S. Gilbert and J. E. van Lier, *J. Med. Chem.*, **40**, 3897 (1997).
228. D. A. Fernández, J. Awruch and L. E. Dicelio, *J. Photochem. Photobiol., Part B: Biol.*, **41**, 227 (1997).
229. J. Griffiths, J. Cruse-Sawyer, S. R. Wood, J. Schofield, S. B. Brown and B. Dixon, *J. Photochem. Photobiol., Part B: Biol.*, **24**, 195 (1994).
230. J. Griffiths, J. Schofield, M. Wainwright and S. B. Brown, *Dyes and Pigments*, **33**, 65 (1997).
231. U. Drechsler, M. Pfaff and M. Hanack, *Eur. J. Org. Chem.*, 3441 (1999).
232. R. W. Boyle and J. E. van Lier, *Synthesis,* **9**, 1079 (1995).
233. K. Sakamoto, T. Kato, E. Ohno-Okumura, M. Watanabe and M. J. Cook, *Dyes and Pigments*, **64**, 63 (2005).
234. K. Oda, S. Ogura and I. Okura, *J. Photochem. Photobiol., Part B: Biol.*, **59**, 20 (2000).
235. R. Decreau, M.-J. Richard and M. Julliard, *J. Porphyrins Phthalocyanines,* **5**, 390 (2001).
236. K. Fukushima, K. Tabata and I. Okura, *J. Porphyrins Phthalocyanines,* **2**, 219 (1998).
237. B. D. Rihter, M. D. Bohorquez, M. A. J. Rodgers and M. E. Kenney, *Photochem. Photobiol.*, **55**, 677 (1992).
238. M. N. Sibata, A. C. Tedesco and J. M. Marchetti, *Eur. J. Pharm. Sci.*, **23**, 131 (2004).
239. A. Segalla, C. D. Borsarelli, S. E. Braslavsky, J. D. Spikes, G. Roncucci, D. Dei, G. Chiti, G. Jori and E. Reddi, *Photochem. Photobiol. Sci.*, **1**, 641 (2002).
240. G. Canti, D. Lattuada, R. Cubeddu, P. Taroni and G. Valentini, *Medecine Biologie Environment,* **20**, 165 (1992).
241. B. Meunier, *Chem. Rev.*, **92**, 1411 (1992).
242. C. S. Foote, *Photochem. Photobiol.*, **54**, 659 (1991).
243. W. Adam, C. R. Saha-Möller and A. Schönberger, *J. Am. Chem. Soc.*, **119**, 719 (1997).
244. K. Araki, C. A. Silva, H. E. Toma, L. H. Catalani, M. H. G. Medeiros and P. Di Mascio, *J. Inorg. Biochem.*, **78**, 269 (2000).
245. Y. Fujiwara, J. Hamada, T. Aoki, T. Shimizu, Y. Tanimoto, H. Yonemura, S. Yamada, T. Ujiie and H. Nakamura, *Mol. Phys.*, **100**, 1405 (2002).
246. J. R. Darwent, *Chem. Commun.*, 805 (1980).
247. J. R. Darwent, I. McCubbin and G. Porter, *J. Chem. Soc., Faraday Trans. 2*, **78**, 903 (1982).
248. L. M. Gurdzhiyan, V. M. Derkacheva, A. V. Butenin, O. L. Kaliya and E. A. Luk'yanets, *Zh. Obshch. Khim.*, **52**, 1439 (1982); *Chem. Abstr.* **97**, 101557v (1982).
249. M. Vandevyver, A. Ruaudel-Teixier and A. Barraud, *J. Chim. Phys.*, **82**, 707 (1985).
250. H. Yonemura, K. Ohishi and T. Matsuo, *Chem. Lett.*, 661 (1996).

251. Y. Amao, T. Kamachi and I. Okura, *J. Photochem. Photobiol., Part A: Chem.*, **98**, 59 (1996).
252. Y. Amao, T. Kamachi and I. Okura, *Inorg. Chim. Acta,* **267**, 257 (1998).
253. H. Sugimoto, K. Kuramoto and S. Inoue, *J. Chem. Soc., Perkin Trans. 1,* 1826 (2002).
254. S. Fukuzumi, H. Imahori, K. Okamoto, H. Yamada, M. Fujitsuka, O. Ito and D. M. Guldi, *J. Phys. Chem. A,* **106**, 1903 (2002).
255. S. Fukuzumi, in *The Porphyrin Handbook* (Eds. K. M. Kadish, K. M. Smith and R. Guilard), Vol. 8, Academic Press, San Diego, CA, 2000, pp. 115–151.
256. J. R. Premkumar and R. Ramaraj, *Chem. Commun.*, 343 (1997).
257. R. Miyatani and Y. Amao, *J. Mol. Catal. B,* **27**, 121 (2004).
258. R. Miyatani and Y. Amao, *Biotechnol. Lett.*, **24**, 1931 (2002).
259. R. Miyatani and Y. Amao, *J. Jpn. Petrol. Inst.*, **47**, 27 (2004).
260. R. Miyatani and Y. Amao, *Photochem. Photobiol. Sci.*, **3**, 681 (2004).
261. D. Schlettwein and N. I. Jaeger, *J. Phys. Chem.*, **97**, 3333 (1993).
262. D. Schlettwein, M. Kaneko, A. Yamada, D. Wöhrle and N. I. Jaeger, *J. Phys. Chem.*, **95**, 1748 (1991).
263. K. Uchida, M. Soma, T. Onishi and K. Tamaru, *Z. Phys. Chem.*, **106**, 317 (1977).
264. O. V. Gerasimov, S. V. Limar and V. N. Parmon, *J. Photochem. Photobiol., Part A: Chem.*, **56**, 275 (1991).
265. H. G. O. Becker, R. Krueger and R. Schuetz, *J. Prakt. Chem.*, **328**, 729 (1986).
266. R. F. Khairutdinov, E. Kh. Brikenshtein and L. N. Strekova, *Izv. Akad. Nauk SSSR, Ser. Khim.*, **7**, 1504 (1982); *Chem. Abstr.* **97**, 136553t (1982).
267. K. Kasuga, A. Fujita, T. Miyazako, M. Handa and T. Sugimori, *Inorg. Chem. Commun.*, **3**, 634 (2000).
268. X.-F. Zhang and H.-J. Xu, *J. Photochem. Photobiol., Part B: Biol.*, **24**, 109 (1994).
269. V. Héquet, P. Le Cloirec, C. Gonzalez and B. Meunier, *Chemosphere,* **41**, 379 (2000).
270. J. L. Thomas and N. S. Allen, *Dyes and Pigments*, **53**, 195 (2002).
271. A. E. H. Machado, J. A. de Miranda, R. F. de Freitas, E. T. F. M. Duarte, L. F. Ferreira, Y. D. T. Albuquerque, R. Ruggiero, C. Sattler and L. de Oliveira, *J. Photochem. Photobiol., Part A: Chem.*, **155**, 231 (2003).
272. N. Eugster, D. J. Fermin and H. H. Girault, *J. Am. Chem. Soc.*, **125**, 4862 (2003).
273. A. J. Abdul-Ghani, N. O. T. Bashi and S. N. Maree, *J. Sol. Energy Research,* **5**, 53 (1987).
274. K. Mochizuki, N. Asakura, T. Kamachi and I. Okura, *Electrochemistry (Tokyo, Japan),* **70**, 416 (2002).
275. Y.-H. Kim and J.-I. Hong, *Chem. Commun.*, 512 (2002).

CHAPTER **10**

Synthesis and reactions of allenylzinc reagents

JAMES A. MARSHALL

Department of Chemistry, University of Virginia, PO Box 400319, Charlottesville, VA 22904, USA
Fax: +1 434 924 7993; e-mail: jam5x@virginia.edu

I. ZINCATION OF PROPARGYLIC BROMIDES

The earliest studies on allenylzinc reagents were mainly concerned with the regioselectivity of addition reactions to aldehydes and ketones. Moreau and Gaudemar converted

The chemistry of organozinc compounds
Edited by Z. Rappoport and I. Marek

TABLE 1. Additions of allenylzinc bromides to aldehydes and ketones

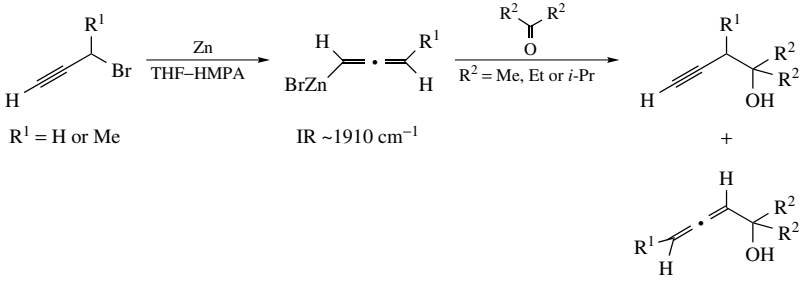

R[1] = H or Me

IR ~1910 cm^{-1}

R[1]	R[2]	Yield (%)	Propargyl:allenyl
H	Me	74	88:12
H	Et	60	75:25
H	*i*-Pr	49	44:56
Me	Me	43	100:0
Me	Et	42	99:1
Me	*i*-Pr	35	60:40

propargyl bromide and 2-bromo-3-butyne to the bromozinc reagents by treatment with zinc in THF–HMPA (Table 1)[1]. The infrared spectra of these reagents were suggestive of the allenyl rather than the alternative propargyl structure, or a mixture of the two. Upon addition to dimethyl, diethyl and diisopropyl ketones, these reagents afforded mixtures of alkynyl and allenyl adducts with the latter isomers becoming increasingly favored with increasing steric requirements of the ketone substrate. The ratio of isomeric adducts from a given reaction was not affected by an increase in reaction times.

II. MECHANISTIC STUDIES

When the alcohol adduct from the allenylzinc reagent and diisopropyl ketone was treated with 80 mol% of allenylzinc bromide in HMPA, a mixture containing 12% of diisopropyl ketone and 88% of recovered alcohol was obtained after 7 days at 'ambient temperatures' (equation 1). Thus, it may be deduced that the allenylzinc additions are reversible. Presumably, the propargyl adducts are intrinsically favored, but steric interactions between the R[1] and R[2] substituents in the propargyl product favors an increased proportion of allenyl adducts in a reversible process (see Table 1). HMPA would expectedly facilitate reversal of the addition by decreasing the ion pairing between the alkoxide anion and ZnBr cation of the adducts. This expectation was subsequently confirmed by a study of solvent effects.

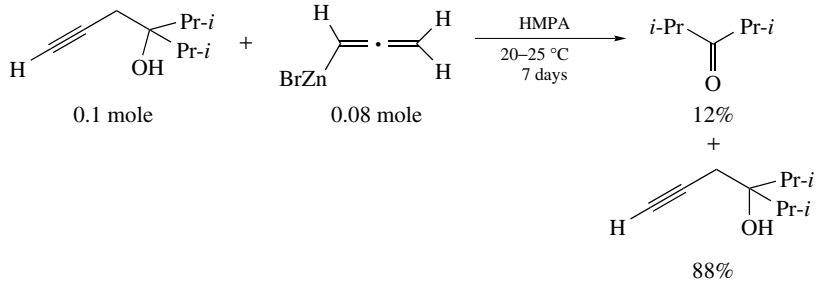

0.1 mole 0.08 mole 12% 88%

(1)

The genesis of the allenyl adduct was a subject of some speculation. Direct addition of the allenylzinc reagent to the carbonyl group of the ketone (equation 2) or isomerization of the propargylic adduct by a [1,3] prototropic shift (equation 3) were two possibilities that were considered. A third possibility would involve an S_E2' addition of a propargylzinc intermediate to the ketone (equation 2). Evidence for the first or third pathways was secured by a deuterium labeling study in which the allenylzinc reagent was prepared from 3-deuterio-1-bromo-2-propyne. Upon addition to diisopropyl ketone, this reagent gave rise to a 40:60 mixture favoring the allenyl adduct. The deuterium distribution in this mixture was consistent with the hypothesis that the allenylcarbinol arises from the propargylic bromozinc reagent or through direct addition of the allenylzinc bromide. The latter pathway would require a facile metallotropic equilibrium in which the minor propargylzinc isomer is more reactive, since the infrared evidence indicated that the allenylzinc isomer greatly predominates. The alternative genesis of the allenylcarbinol through a 1,3-shift could be ruled out based on the labeling pattern in the addition product.

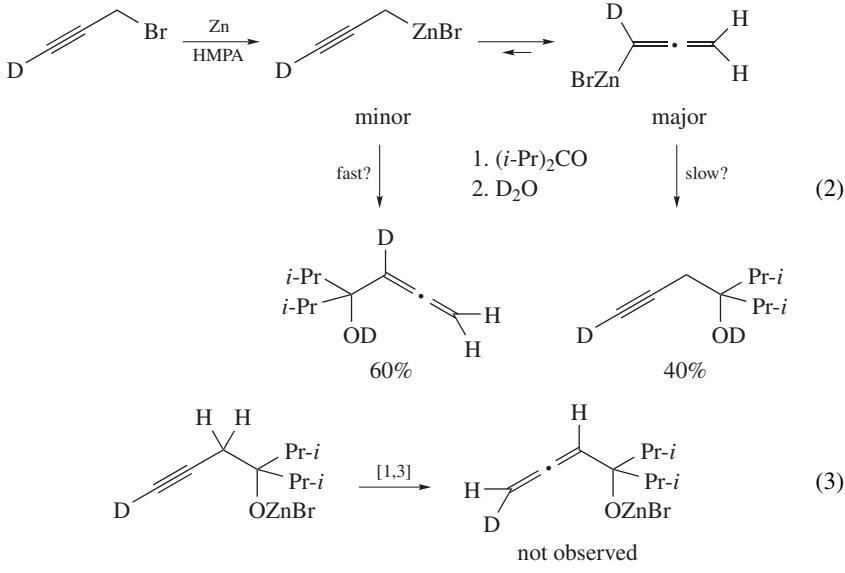

Later work by Barbot and Miginiac[2] and Jones and Knochel[3] showed that additions of allylic zinc reagents to aldehydes are also reversible and occur by S_E2' pathways. In the former case, the mixture of regioisomeric alcohol adducts from prenylzinc bromide and 3-pentanone changed composition in favor of the unbranched isomer with increased reaction times and temperature (equation 4)[2].

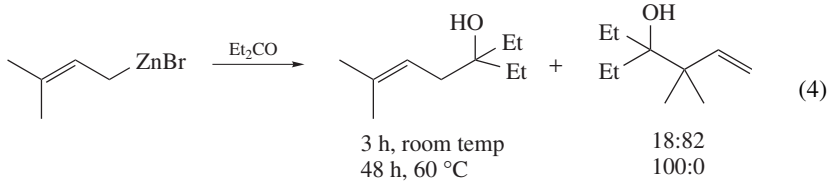

Jones and Knochel found that the adduct of allylzinc bromide and di-*t*-butyl ketone, upon conversion to the bromozinc alkoxide, serves as a source of allylzinc bromide,

which could be trapped with added benzaldehyde thereby confirming the reversibility of the addition (equation 5)[3].

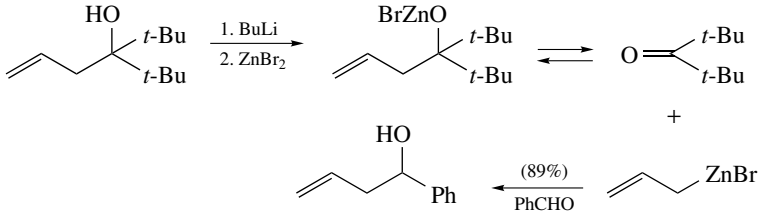

(5)

Further studies of Moreau and Gaudemar revealed that the ratio of propargyl and allenyl adducts was influenced by solvent (Table 2)[4]. Increased amounts of allenic adducts were observed in the dipolar aprotic solvents DMSO and HMPA. This finding supports the presumed greater ease of reversal in the addition reactions, although appropriate control experiments were not carried out.

TABLE 2. Solvent effects in allenylzinc bromide additions

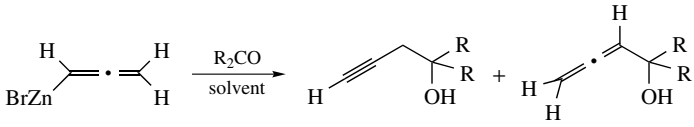

	R = Et	R = *i*-Pr
Solvent	Propargyl:allenyl	Propargyl:allenyl
Dioxane	88:12	77:23
THP	87:13	60:40
THF	82:18	64:36
DME	86:14	62:38
DMSO	78:22	45:55
HMPA	72:28	42:58

TABLE 3. Effect of carbonyl structure on allenylzinc bromide additions

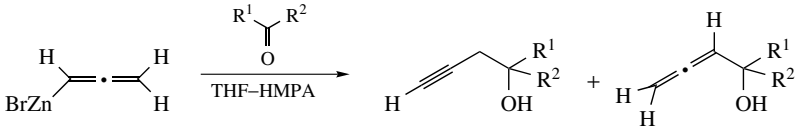

R^1	R^2	Yield (%)	Propargyl:allenyl
CCl_3	H	44	100:0
CH_3	H	75	>95:5
Pr	H	62	95:5
Me	Me	74	88:12
t-Bu	Me	69	80:20
Et	Et	60	75:25
i-Pr	*i*-Pr	49	46:54

III. REGIOCHEMISTRY OF ADDITIONS TO ALDEHYDES AND KETONES

Reactions of allenylzinc bromide reagents with aldehydes afford increased amounts of propargyl adducts compared to analogous additions to ketones (Table 3). Presumably, diminished steric interactions render the aldehyde propargylic adducts more stable than their ketone counterparts. Alternatively, equilibration of the kinetic propargylic adducts with the allenyl isomers is slower for the adducts of aldehydes.

IV. STEREOCHEMISTRY OF ADDITIONS

In their quest for alkynyl-substituted 1,2-diols, Epsztein and coworkers examined additions of alkoxy allenylzinc reagents to aldehydes (Table 4)[5]. The reagents were prepared from various propargylic ethers by lithiation with BuLi followed by addition of ZnI_2. Although exact ratios were not determined, the major propargylic products were surmised to be the *anti* isomers based on spectral data and comparison with authentic samples.

The *anti* stereoisomer was thought to arise from the allenylzinc reagent through a transition state in which the allenyl and aldehyde substituents adopt an *anti* arrangement (equation 6). The alternative transition state leading to the minor *syn* adducts would be disfavored by eclipsing interactions between these two substituents. In the proposed transition states, complexation between the zinc halide and the carbonyl oxygen was not considered.

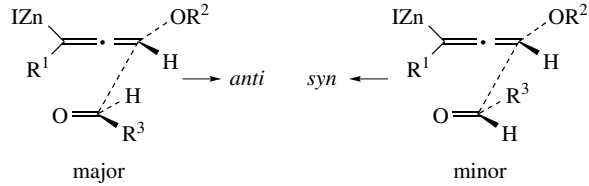

(6)

TABLE 4. Additions of alkoxyallenylzinc iodide reagents to aldehydes

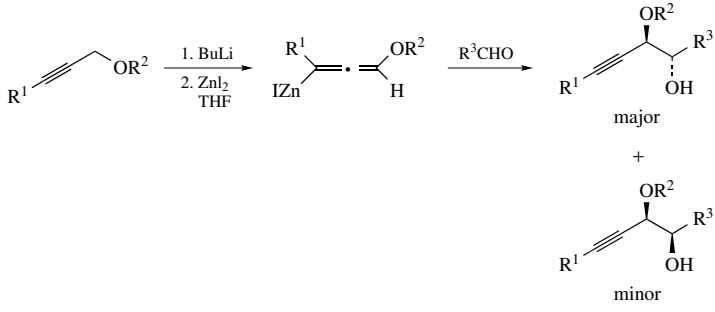

R^1	R^2	R^3	Yield (%)
C_5H_{11}	THP	Ph	60
C_5H_{11}	THP	$C_5H_{11}C{\equiv}C$	80
C_5H_{11}	THP	H	63
C_5H_{11}	Et	Ph	85
C_5H_{11}	Et	Me	90
C_5H_{11}	Et	H	70
TMS	THP	Ph	55
TMS	Et	Ph	80
TMS	Et	$C_5H_{11}C{\equiv}C$	80

Chwastek and coworkers were the first to examine the effect of substrate chirality on the stereochemical outcome of allenylzinc additions to ketones[6]. Thus, treatment of the propargyl ether of TMS propargyl alcohol with BuLi followed by addition of ZnI_2 led to a solution of the racemic allenylzinc iodide (infrared band at ~ or ca. 1900 cm^{-1}). Subsequent addition of dehydroandrosterone acetate afforded a propargyl adduct with the 17*R*, 20*S* configuration (equation 7). A cyclic transition state was proposed for this addition in which attack of the allenylzinc reagent takes place at the less hindered β-face of the C17 carbonyl with an *anti* relationship between the OTHP substituent of the allene reagent and the larger C13 quaternary center of the ketone carbonyl (equation 8).

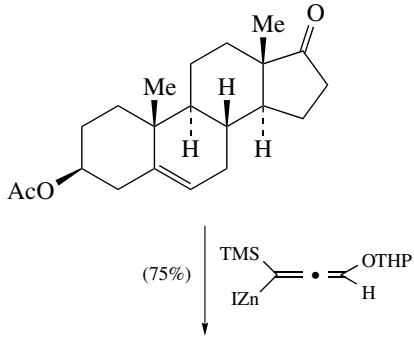

(7)

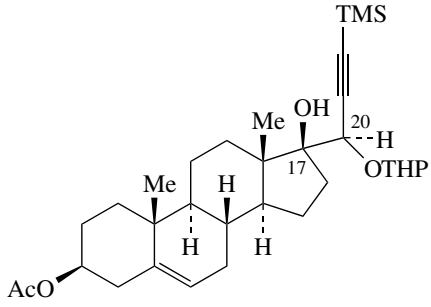

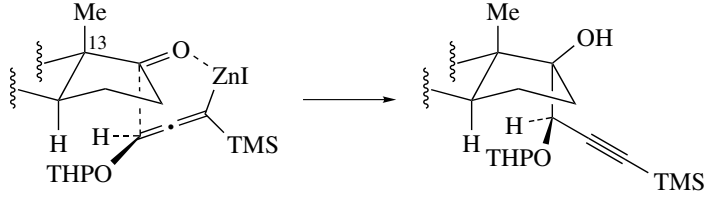

(8)

Zweifel and Hahn found that deprotonation of terminal allenes with *t*-BuLi and subsequent addition of $ZnCl_2$ leads to terminal allenylzinc reagents, which afford *anti* adducts upon addition to various aldehydes (Table 5)[7]. Branching in the aldehyde and allene substituents enhanced the *anti*:*syn* ratio of adducts, in keeping with the previously proposed cyclic transition state for such additions.

TABLE 5. Preparation of allenylzinc chloride reagents from allenes

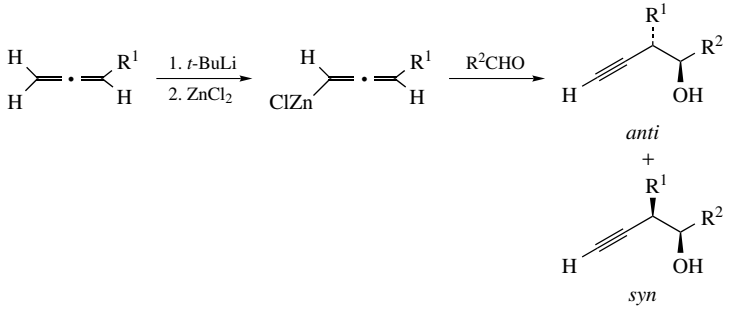

R^1	R^2	Yield (%)	*anti*:*syn*
C_5H_{11}	Et	89	92:8
C_5H_{11}	*i*-Pr	94	97:3
C_5H_{11}	*t*-Bu	86	99:1
C_6H_{13}	Et	95	96:4
C_6H_{13}	*i*-Pr	86	99:1
C_6H_{13}	*t*-Bu	77	99:1
c-C_6H_{11}	Et	80	98:2
t-Bu	Et	69	99:1

It was also found that allenylzinc reagents, derived from TMS alkynes by the foregoing lithiation–transmetallation protocol, afford *anti* adducts in high yield upon treatment with aldehydes (equation 9).

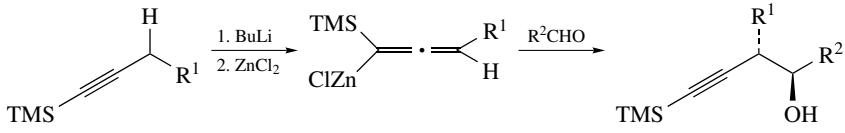

$R^1 = C_6H_{13}$, R^2 = Et, *i*-Pr, *t*-Bu; *anti*:*syn* = 99:1–92:8 (9)

V. TRANSITION STATE CALCULATIONS

The proposed transition state geometry for additions of allenylzinc reagents to aldehydes receives support from a recent computational study[8]. Transition state structures for the reaction of an (*M*)-1,2-butadienylzinc reagent and acetaldehyde were located at the B3LYP/6-31G* level of theory. A tetrahedrally-coordinated zinc atom with a dimethyl ether ligand, a surrogate for the THF solvent, was found to give energy differences that are most consistent with the observed results. The calculated structure shows staggering of the substituents on the bonding allenyl and carbonyl sp^2 carbons (dihedral angle *ca* 30°) and a slightly bent allenyl moiety (Figure 1). A relatively 'late' transition state is proposed for this reaction based on comparisons to *ab initio* transition states for dialkylzinc and allylborane additions. The computational study confirms the assumption that steric interactions between the aldehyde and allene substituents control the diastereoselectivity of the reaction. An unexpected finding was the influence of the chiral zinc atom on

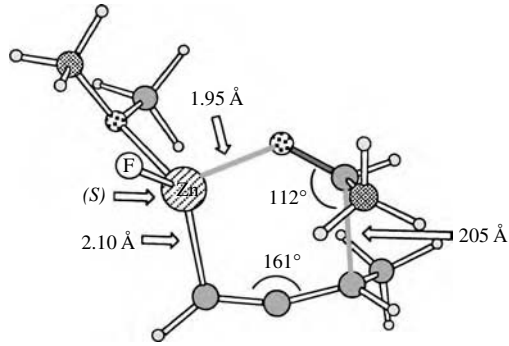

FIGURE 1. Transition state for the addition of (*M*)-1,2-butadienylzinc fluoride, as a dimethyl ether solvate, to acetaldehyde calculated at the B3LPY/6-31G* level of theory

transition state energies. The depicted structure with (*S*) chirality at Zn was found to be 0.47 kcal mol^{-1} lower in energy than the (*R*)-Zn diastereomer. Interestingly, the sterically enforced *anti* arrangement of the allenyl and aldehyde CH_3 substituents requires the Zn to coordinate *syn* to the aldehyde CH_3.

VI. REAGENT REGIOSELECTIVITY

As part of a larger study on reactions of unsaturated organometallic reagents, Miginiac and Mesnard examined additions of several allenylzinc reagents to 2-TMS-2,3-propadienal (equation 10)[9]. Although the unsubstituted and the α-methylated allenic reagents afforded only the propargylic adducts, the γ-methyl reagent yielded the allenic product as the major regioisomer. Presumably, steric interactions between the γ-methyl of the allenylzinc and the α-TMS substituent of the aldehyde direct the regiochemistry of the addition away from the allenic in favor of the propargylic zinc reagent (equation 11).

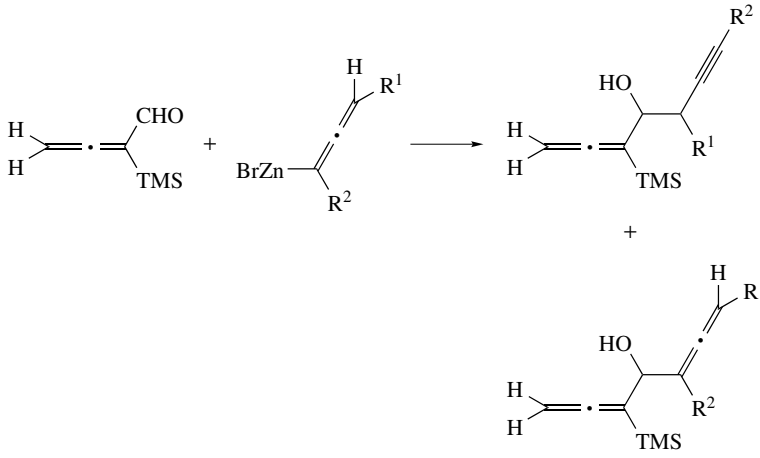

(10)

$R^1 = R^2 = H$; 65% 100:0
$R^1 = H$, $R^2 = Me$; 60% 100:0
$R^1 = Me$, $R^2 = H$; 40% 20:80

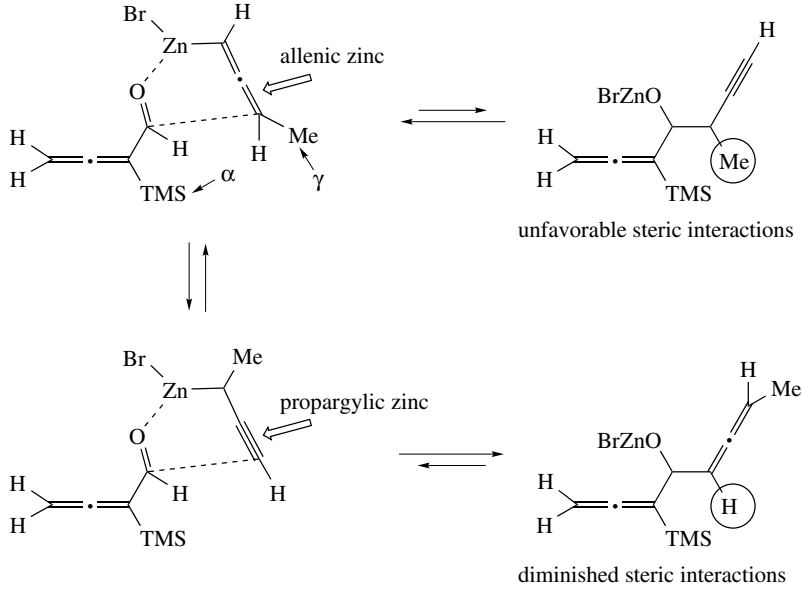

(11)

Interestingly, a second allenyl adduct, isomeric with the major product, was also formed in the latter reaction. This isomer was surmised to arise by a retro reaction of the initial allenyl adduct to form a TMS propargylzinc bromide reagent, which subsequently adds to the liberated aldehyde (equation 12). The regiochemistry of this addition is also thought to be directed by steric effects, again involving the methyl and TMS substituents.

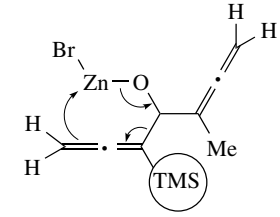

disfavored by steric interactions

(12)

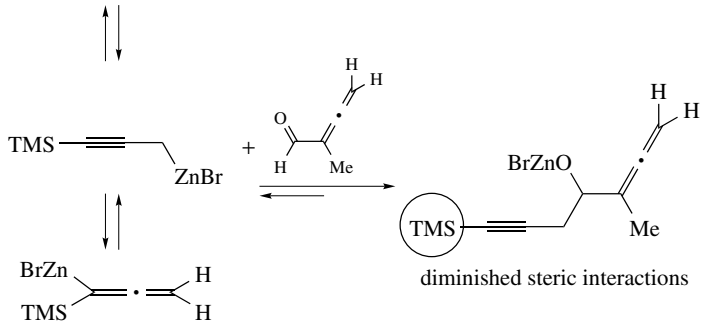

VII. IODOALLENE-DERIVED REAGENTS

In a subsequent study, Miginiac and coworkers examined additions of allenylzinc reagents to an *N*-TMS imine derived from the mono diethyl acetal of acetylene dicarboxaldehyde[10]. These additions afforded the homopropargylic adducts as the free primary amines (equation 13).

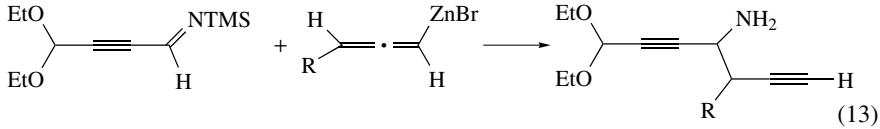

R = H 82%
R = Me 73%

(13)

An alternative route to terminal allenylzinc reagents was explored by Utimoto and coworkers[11]. They found that terminal iodoallenes undergo halogen–metal exchange with diethylzinc to afford allenylzinc intermediates, which yield mainly *anti* homopropargylic alcohol adducts with aldehydes and ketones (Tables 6 and 7). However, the diastereoselectivity of the additions was rather low in comparison to the previously examined allenylzinc halides. This finding is suggestive of competing reaction pathways involving both cyclic and acyclic transition states. The latter process would expectedly favor the *syn* adduct. Alternatively, it could be argued that the allenyl ethylzinc species, a comparatively weaker Lewis acid than its halogen analogs, might form a looser complex with the aldehyde carbonyl, in which case eclipsing interactions in the cyclic transition state that disfavor the *syn* adduct would play a lesser role. Interestingly, addition to acetophenone afforded a greater proportion of the *anti* adduct than the corresponding addition to benzaldehyde.

The related allenylzinc chloride reagents, derived from the foregoing terminal iodoallenes by lithiation and transmetalation, afforded *anti* adducts of aldehydes with excellent selectivity (Table 8).

To probe the nature of the allenyl iodide–diethylzinc exchange process, Utimoto and coworkers monitored the ^{1}H NMR spectrum of a 1:1 mixture of iodoallene and Et_2Zn in C_6D_6[11]. It was found that within 2 hours, the olefinic protons of the allenyl iodide were

TABLE 6. Ethylzincation of allenyl iodides

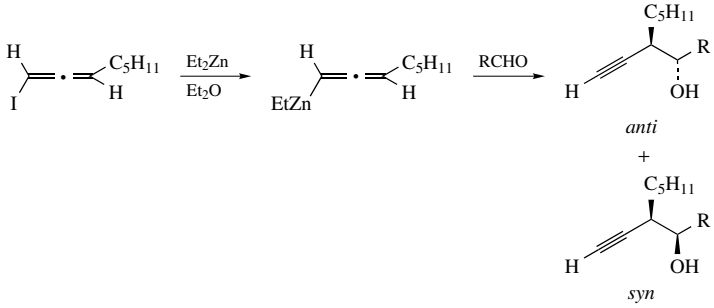

R	Yield (%)	*anti*:*syn*
Ph	58	63:37
Bu	63	87:13
t-Bu	44	>99:1

TABLE 7. Addition of ethylzinc allenyl reagents to ketones

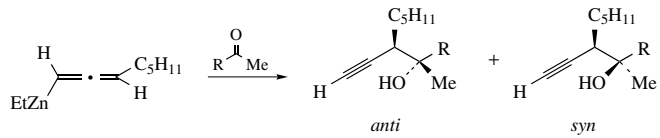

R	Yield (%)	*anti*:*syn*
Ph	61	86:14
Bu	62	52:48

TABLE 8. Preparation of chlorozinc allenyl reagents from iodoallenes

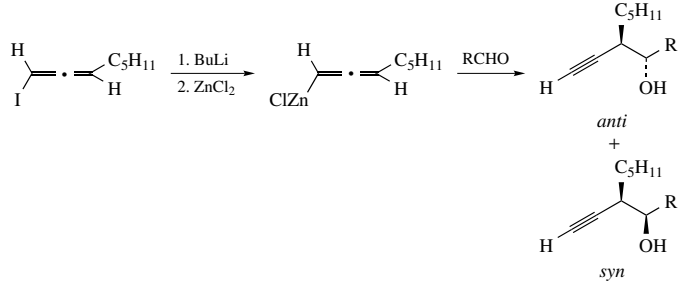

R	Yield (%)	*anti*:*syn*
Bu	72	91:9
C_5H_{11}	72	91:9
t-Bu	65	>99:1

reduced to 60% of their initial intensity and new signals attributable to EtI appeared. The presumed polymeric nature of organozinc halides obscured signals that might be attributed to the allenylzinc reagent. Because no changes in the spectrum were observed after 2 hours, it was assumed that the mixture had reached an equilibrium state. Upon addition of benzaldehyde, the residual allenyl iodide peaks disappeared and the expected homopropargylic alcohol adduct was formed (equation 14). Evidently, the diethylzinc present in the equilibrating mixture does not react with benzaldehyde but simply replenishes the more reactive allenylzinc reagent that is consumed in the reaction.

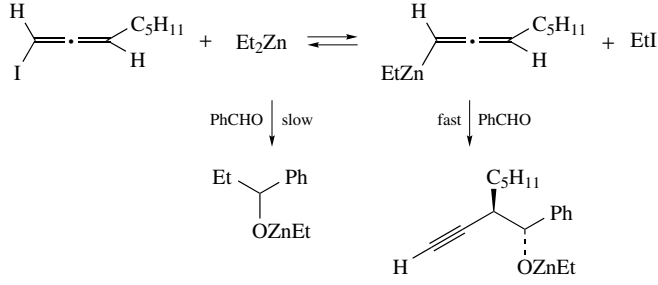

(14)

VIII. CONFIGURATIONAL STABILITY

The Utimoto group was the first to investigate the optical stability of allenylzinc reagents[11]. When (*M*)-1-iodo-1,2-heptadiene of 98% ee was subjected to exchange with diethylzinc at 0 °C followed by addition of benzaldehyde, the homopropargylic alcohol adduct was found to be racemic (equation 15). The proposal was advanced that the allenylzinc reagent racemizes as a result of a rapid interconversion with its enantiomeric propargylic isomers, presumably via a nonselective 1,3-metalotropic transfer (equation 16). It is also possible that a direct iodine zinc exchange might take place through a single-electron transfer process in which a presumed allenyl radical intermediate would racemize by a reversible inversion of the sp^2 center, similar to that proposed for the formation of Grignard reagents (equation 17). A distinction is not possible from this experiment, but subsequent work has shown that certain chiral allenylzinc reagents retain their configuration at temperatures below −10 °C.

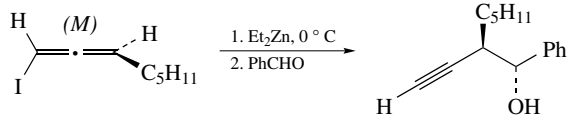

(15)

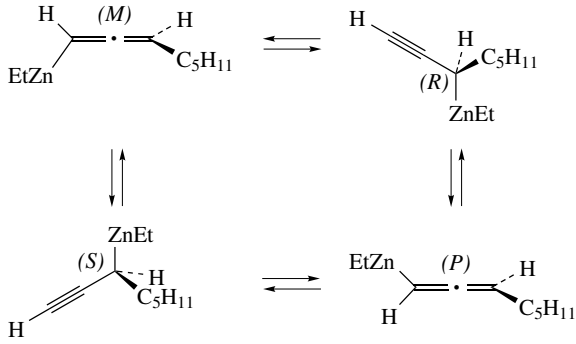

(16)

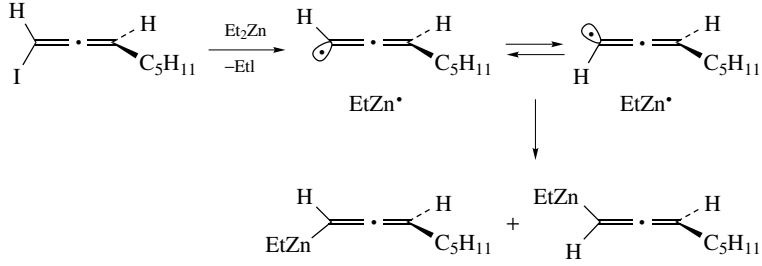

(17)

IX. ALLENYL ALKYLZINC REAGENTS

A novel approach to allenylzinc reagents, reported by Oku and coworkers, employs propargylic mesylates as starting materials[12]. Treatment with triorganozincates, prepared in situ by the reaction of dialkylzinc compounds with organolithium reagents, affords transient allenyl dialkylzinc intermediates. These intermediates were found to react with various

TABLE 9. Trapping of ethylzinc allenyl reagents prepared from propargylic mesylates

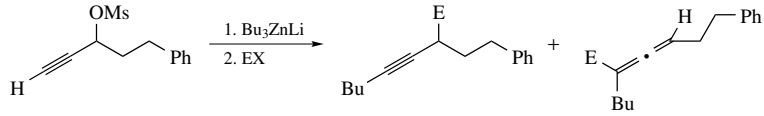

propargyl allenyl

EX	Yield (%)	Propargyl:allenyl
I_2	—	81:6
NCS	—	82:4
TMSCl	90	90:10
DPSCl	86	96:4
DCl	90	0:100

EX	Yield (%)	Propargyl:allenyl
MeCOCl	80	89:11
BuCOCl	90	88:12
t-BuCOCl	91	95:5

TABLE 10. Trapping of allenylzinc reagents with DCl

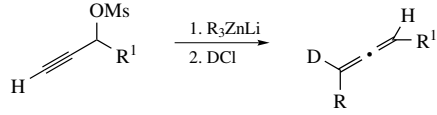

R^1	R	Yield (%)	%D
$PhCH_2CH_2$	Me	96	94
$PhCH_2CH_2$	Bu	97	92
$PhCH_2CH_2$	*s*-Bu	96	94
$PhCH_2CH_2$	*t*-Bu	76	93
$PhCH_2CH_2$	Ph	77	81
C_8H_{17}	Bu	97	92
c-C_6H_{11}	Bu	95	91

TABLE 11. Additions of butylzinc allenyl reagents to aldehydes

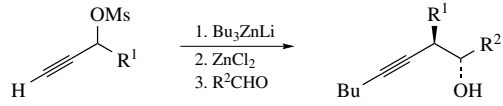

R^1	R^2	Yield (%)	*anti*:*syn*
Me	*i*-Pr	89	98:2
C_8H_{17}	*i*-Pr	85	99:1
C_8H_{17}	$PhCH_2CH_2$	86	95:5
c-C_6H_{11}	Et	89	97:3

electrophiles to afford mainly homopropargylic substitution products, including halides, silanes and ketones (Table 9).

Evidence for an allenylzinc intermediate was obtained through deuteriolysis with DCl, whereupon a deuteriated allene of the expected composition was obtained in high yield (Table 10).

Conversion of the presumptive dialkyl allenylzinc intermediate to the corresponding chlorozinc species could be effected by exposure to $ZnCl_2$. Subsequent addition of various aldehydes led to *anti* homopropargylic alcohols (Table 11). In contrast, reaction of the

presumed allenyl alkylzinc precursor with aldehydes afforded a mixture of regio- and stereoisomers.

A non-terminal propargylic mesylate failed to react with Bu_3ZnLi (equation 18). This finding indicates that a terminal alkynyl hydrogen is an essential feature for the zincation reaction. When the propargylic methyl ether analog of a terminal propargylic ether was treated first with Bu_3ZnLi and then with D_2O-DCl, the isolated alkyne was found to contain 99% of a terminal deuterium, showing that the zinc reagent is sufficiently basic to abstract an alkynyl proton (equation 19).

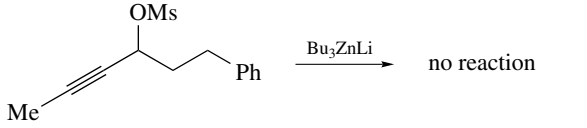

(18)

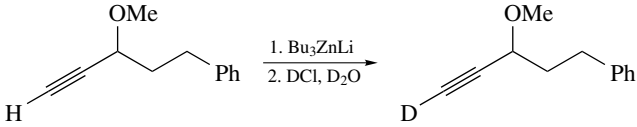

(19)

Taken together, these observations suggest a reaction pathway involving an intermediate dialkyl alkynylzinc species which rearranges to the allenylzinc reagent by alkyl migration from zinc and internal S_N2' displacement of the mesylate (equation 20).

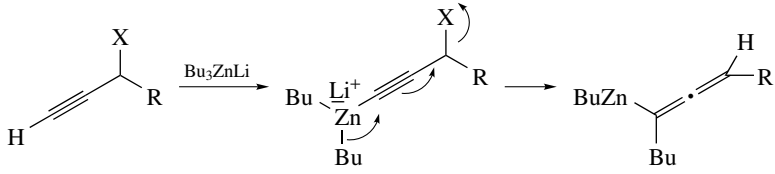

(20)

A variation of this reaction on an alkynyloxirane substrate was employed to prepare a deuteriated allenylcarbinol (equation 21)[13]. The reaction afforded a 70:30 mixture of diastereomeric products, indicating that the presumed internal S_N2' cleavage of the epoxide is not highly diastereoselective.

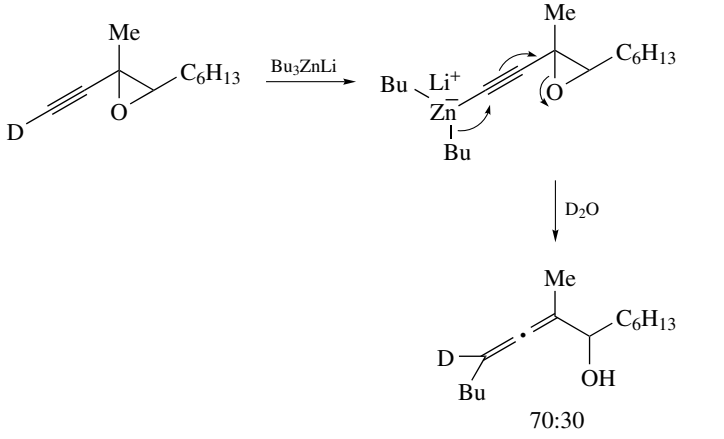

(21)

70:30

TABLE 12. Coupling of allenylzinc bromide reagents with haloarenes

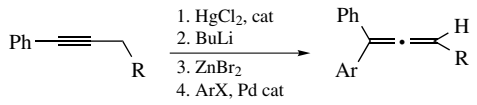

R	Pd cat	ArX	Yield (%)
H	$Pd(PPh_3)_4$	PhI	83
H	$Pd(PPh_3)_4$	*p*-MeC_6H_4I	79
H	$PdCl_2$•$2PPh_3$	*p*-MeC_6H_4I	49
H	$Pd(PPh_3)_4$	*p*-$MeOC_6H_4I$	69
H	$PdCl_2$•$2PPh_3$	*p*-$O_2NC_6H_4Br$	55
Pr	$Pd(PPh_3)_4$	1-iodonaphthalene	79
Pr	$Pd(PPh_3)_4$	PhI	75
Pr	$Pd(PPh_3)_4$	*p*-MeC_6H_4I	68
Pr	$Pd(PPh_3)_4$	*p*-$MeOC_6H_4I$	75
Pr	$Pd(PPh_3)_4$	1-iodonaphthalene	68

X. COUPLING OF ALLENYLZINC BROMIDE REAGENTS WITH ARYL AND VINYL HALIDES

Ma and Zhang studied Pd-catalyzed coupling reactions of allenylzinc bromide reagents with various aryl and vinylic halides (Table 12)[14]. Phenyl-substituted alkynes were converted to these reagents by lithiozincation with BuLi and $ZnBr_2$ catalyzed by mercuric chloride. In a coupling reaction with iodobenzene, the use of $HgCl_2$ in the lithiation step led to a 20% improvement in overall yield. In all cases examined, 1,1-disubstituted allenes were formed as the sole products. $Pd(PPh_3)_4$ proved superior to $PdCl_2$•$2PPh_3$ and bromobenzene failed to react with either catalyst.

TMS alkynes were also examined as precursors to allenylzinc bromides[15]. Pd-catalyzed coupling of these reagents with β-iodo acrylates afforded enynes as sole products (Table 13). However, although *o*-iodotoluene also gave the alkynyl product, both iodobenzene and 1-iodonaphthalene gave rise to mixtures of alkynyl and allenyl adducts. In the latter case, replacement of the TMS substituent with the bulkier TBS resulted in complete conversion to the alkynyl product, no doubt the consequence of a steric directing effect.

XI. PALLADIOZINCATION OF PROPARGYLIC MESYLATES

In an extension of the methodology reported by Tamaru and coworkers for allylic benzoates[16], Marshall and Adams found that propargylic mesylates could be converted to allenylzinc reagents with Pd(0) catalysts and an equivalent of Et_2Zn[17,18]. When this novel palladiozincation reaction was conducted in the presence of aldehydes, *anti* homopropargylic alcohols were produced as the major adducts (Tables 14 and 15).

Reactions employing enantioenriched propargylic mesylates afford adducts with only slight loss of enantiomeric purity. The overall process proceeds with net inversion at the propargylic center. These findings are consistent with a pathway involving conversion of the mesylate to a transient allenylpalladium intermediate by an S_N2' process and subsequent Pd–Zn exchange with retention of configuration. Addition of the allenylzinc reagent to aldehydes must then occur through the accepted cyclic transition state. A catalytic cycle was proposed for this reaction sequence (Figure 2).

TABLE 13. Coupling of allenylzinc bromide reagents with vinylic iodides

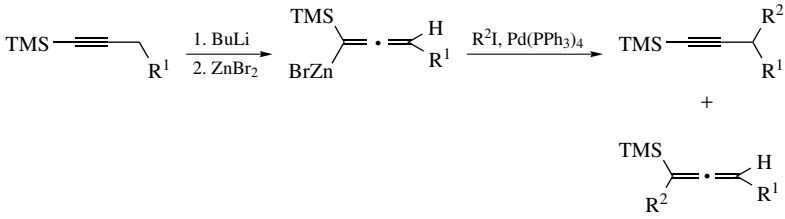

R^1	R^2I	Propargyl:allenyl	Yield (%)
H	(*E*)-ICH=CHCO$_2$Me	100:0	66
H	(*E*)-ICH=CHCO$_2$Et	100:0	96
H	(*Z*)-ICH=CHCO$_2$Et	100:0	60
Pr	(*E*)-ICH=CHCO$_2$Et	100:0	58
H	*o*-MeC$_6$H$_4$I	100:0	52
H	PhI	50:50	47
H	1-Iodonaphthalene	70:30	58
H[a]	1-Iodonaphthalene	100:0	52

[a] 1-TBS-1-propyne.

TABLE 14. Palladiozincation of (*R*)-3-butyn-2-yl mesylate

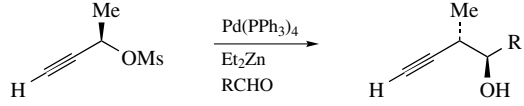

R	Yield (%)	*anti*:*syn*	er
c-C$_6$H$_{11}$	85	95:5	>95:5
C$_6$H$_{13}$	70	88:12	95:5
TBSOCH$_2$CH$_2$	56	86:14	93:7
(*E*)-BuCH=CH	71	77:23	94:6
C$_6$H$_{13}$C≡C	60	68:32	95:5

TABLE 15. Palladiozincation of (*R*)-5-acetoxy-3-pentyn-2-yl mesylate

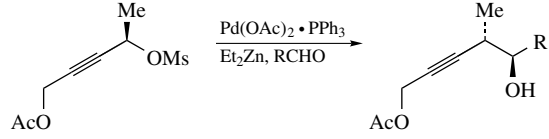

R	Yield (%)	*anti*:*syn*	er
c-C$_6$H$_{11}$	75	95:5	95:5
i-Pr	75	95:5	96:4
C$_6$H$_{13}$	74	88:12	93:7

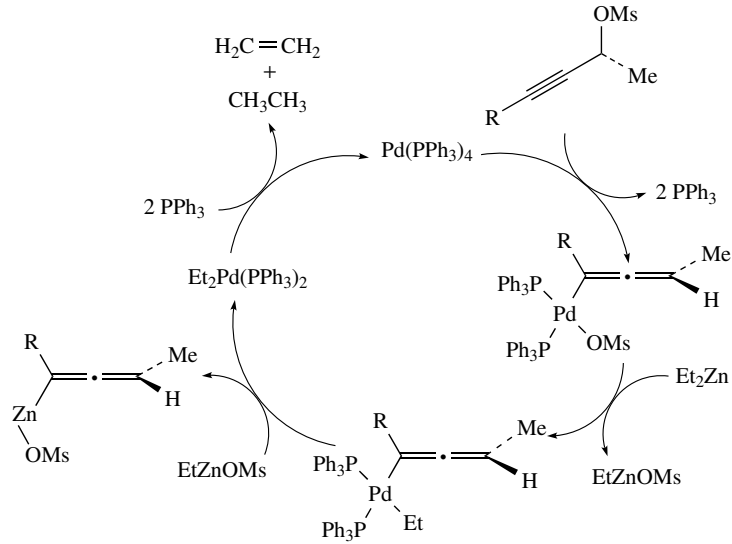

FIGURE 2. Proposed catalytic cycle for palladiozincation of propargylic mesylates

When the palladiozincation was performed in the absence of an aldehyde substrate, two products could be isolated. The major product was the ethyl-substituted allene resulting from reaction of the putative allenylpalladium intermediate with diethylzinc (equation 22). Interestingly, this product is formed in only trace amounts when an aldehyde substrate is present. The second adduct is a dimeric allene, which can be envisioned as arising from coupling of the allenylzinc and allenylpalladium intermediates.

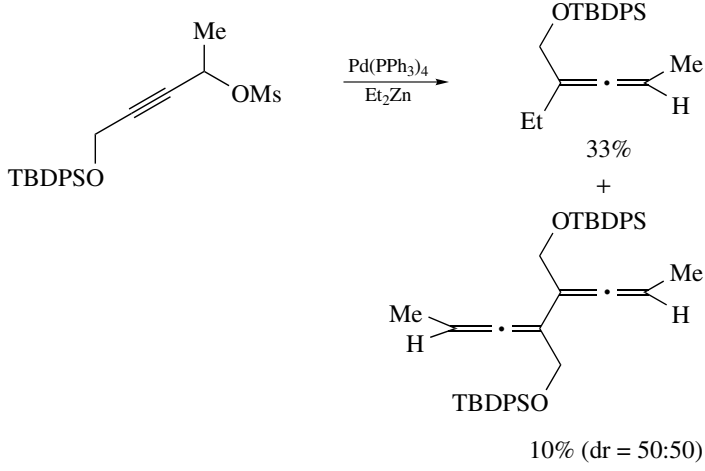

(22)

XII. DOUBLE DIASTEREOSELECTION

Additions of the chiral allenylzinc reagents to enantiomeric α-methyl-β-OBn aldehyde substrates proceeded with a high degree of reagent control to afford *anti*,*syn* or *anti*,*anti* adducts (equations 23 and 24). In these additions, the preferred *anti* orientation of the allenyl methyl and the aldehyde substituents requires the reaction to proceed by the normally less-favored *anti* Felkin–Anh pathway (equation 25).

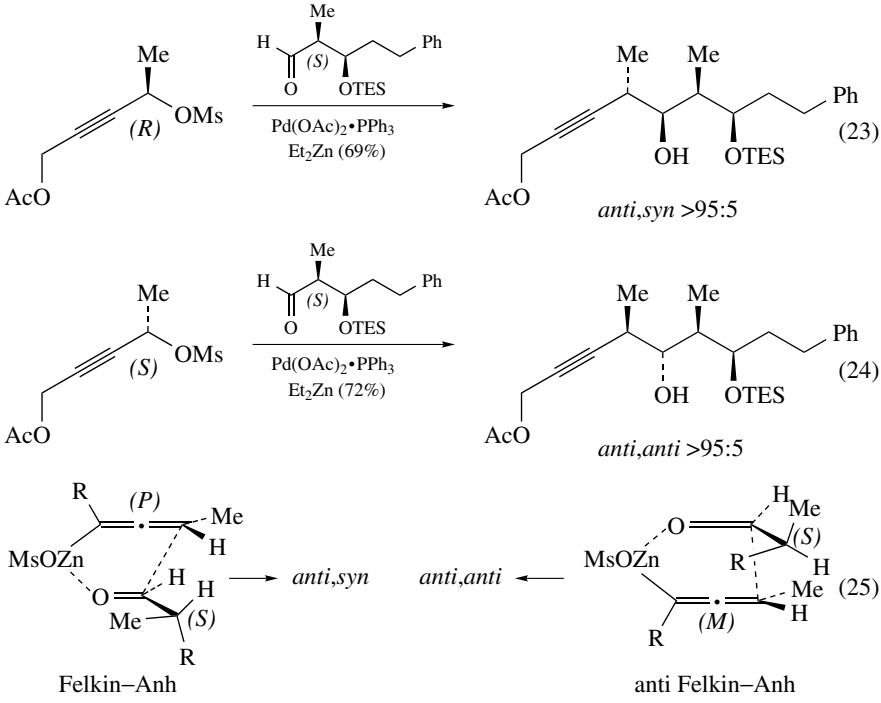

A more extensive investigation of the matching and mismatching characteristics of allenylzinc reactions was conducted by Marshall and Schaaf[19]. The thrust of their studies focused on the effect of a β-OTBS stereocenter on the stereoselectivity of the reactions. The alcohol adducts thus obtained are related to a biologically important family of polyketide natural products. Remarkably, the *syn*,*syn* and *syn*,*anti* aldehyde substrates were converted to the stereopentad adducts with virtually complete diastereoselectivity and no discernable mismatching (equations 26 and 27). The major byproducts, produced in $<$10% yield, resulted from partial racemization of the allenylpalladium and/or allenylzinc intermediates. As expected, all the additions proceed with overall inversion at the propargylic stereocenter.

Additions to the *anti*,*anti* and *anti*,*syn* aldehydes exhibited a more typical matched/mismatched profile (equations 28 and 29). It was concluded that dipole effects of the β-OTBS group must play an important role in the mismatching observed with these latter two aldehydes.

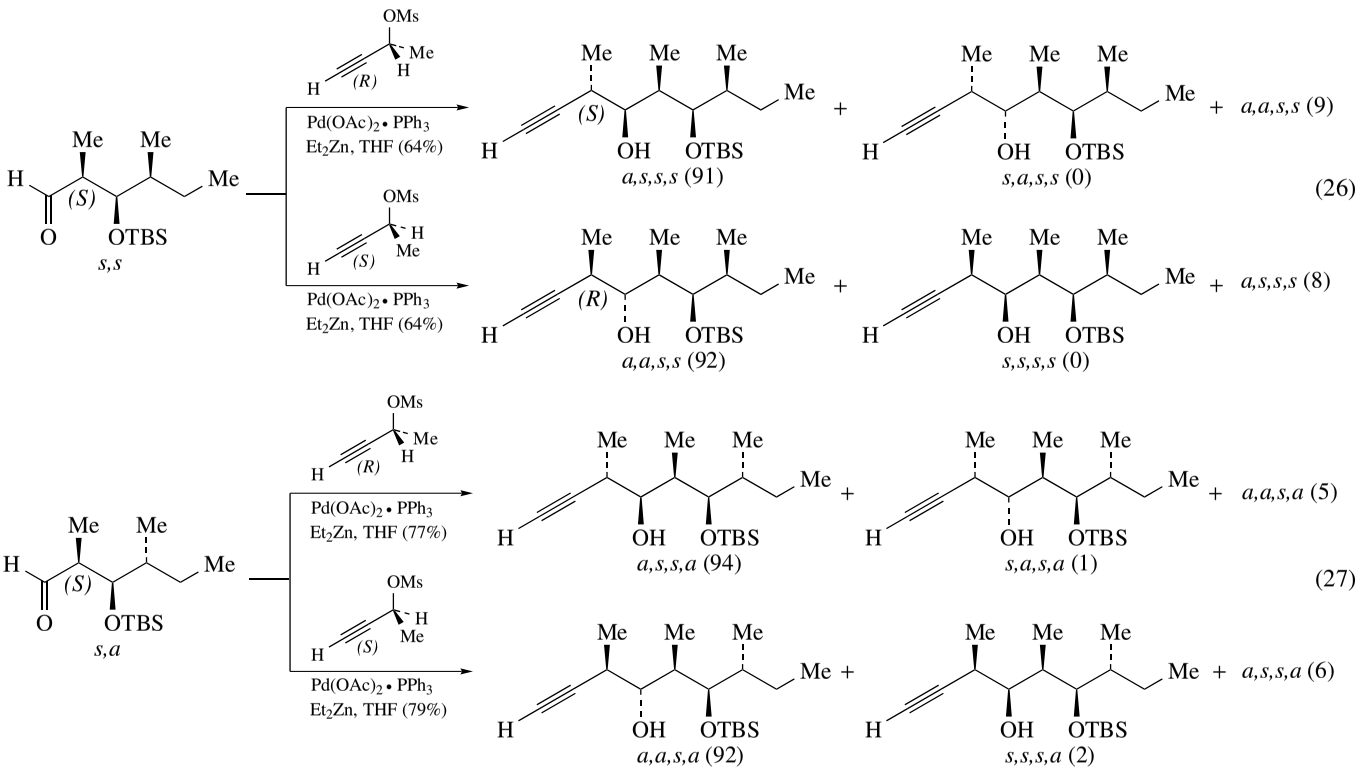
OMs
Me
H
(R)
H
Pd(OAc)2 • PPh3
Et2Zn, THF (64%)
Me
Me
H
(S)
Me
O
OTBS
s,s
OMs
H
Me
(S)
H
Pd(OAc)2 • PPh3
Et2Zn, THF (64%)
Me
Me
Me
(S)
Me
H
OH
OTBS
a,s,s,s (91)
+
Me
Me
Me
Me
H
OH
OTBS
s,a,s,s (0)
+ a,a,s,s (9)
Me
Me
Me
(R)
Me
H
OH
OTBS
a,a,s,s (92)
+
Me
Me
Me
Me
H
OH
OTBS
s,s,s,s (0)
+ a,s,s,s (8)
(26)
OMs
Me
H
(R)
H
Pd(OAc)2 • PPh3
Et2Zn, THF (77%)
Me
Me
H
(S)
Me
O
OTBS
s,a
OMs
H
Me
(S)
H
Pd(OAc)2 • PPh3
Et2Zn, THF (79%)
Me
Me
Me
Me
H
OH
OTBS
a,s,s,a (94)
+
Me
Me
Me
Me
H
OH
OTBS
s,a,s,a (1)
+ a,a,s,a (5)
Me
Me
Me
Me
H
OH
OTBS
a,a,s,a (92)
+
Me
Me
Me
Me
H
OH
OTBS
s,s,s,a (2)
+ a,s,s,a (6)
(27)

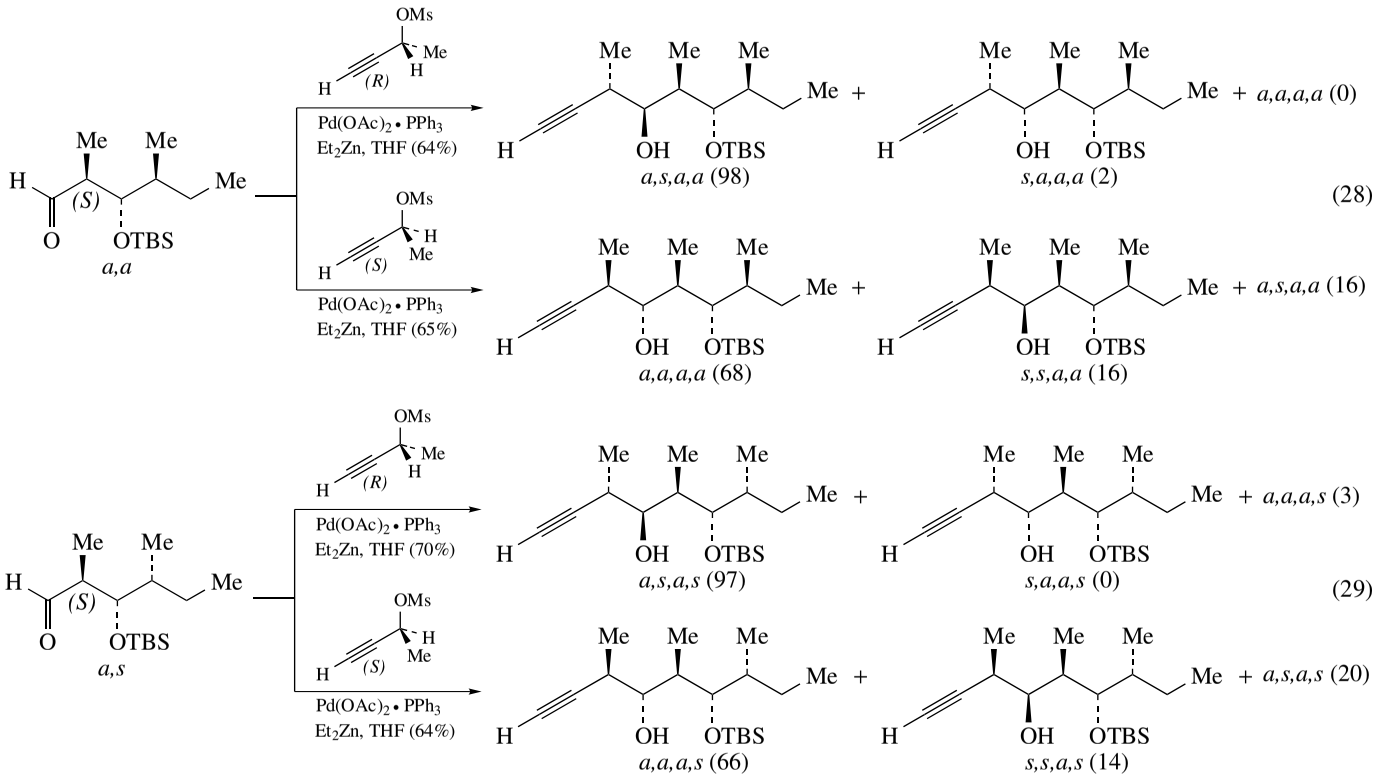
OMs
Me
H
(R)
Pd(OAc)2 • PPh3
Et2Zn, THF (64%)
Me
Me
H
(S)
O
OTBS
a,a
OMs
H
Me
(S)
Pd(OAc)2 • PPh3
Et2Zn, THF (65%)
Me
Me
Me
Me
H
OH
OTBS
a,s,a,a (98)
+
s,a,a,a (2)
+ a,a,a,a (0)
a,a,a,a (68)
s,s,a,a (16)
+ a,s,a,a (16)
(28)
OMs
Me
H
(R)
Pd(OAc)2 • PPh3
Et2Zn, THF (70%)
Me
Me
H
(S)
O
OTBS
a,s
OMs
H
Me
(S)
Pd(OAc)2 • PPh3
Et2Zn, THF (64%)
Me
Me
Me
Me
H
OH
OTBS
a,s,a,s (97)
+
s,a,a,s (0)
+ a,a,a,s (3)
a,a,a,s (66)
s,s,a,s (14)
+ a,s,a,s (20)
(29)

Mismatching is also observed in additions of the chiral allenylzinc mesylate reagents to lactic aldehyde derivatives[20]. Addition of the (*M*)-reagent, derived from the (*S*)-mesylate, to the (*R*)-α-OBn or OTBS aldehyde proceeds by a Felkin–Anh arrangement to afford the *anti*,*anti* adduct (equation 30), whereas reaction with the enantiomeric (*P*)-allenylzinc reagent takes place by way of the less favored *anti*-Felkin–Anh array to yield the *anti*,*syn* adduct as the major product (equation 31). The racemic allenylzinc reagent affords an essentially 1:1 mixture of the diastereomeric *anti* adducts (equation 32). It can therefore be surmised that the additions are largely reagent controlled (equation 33).

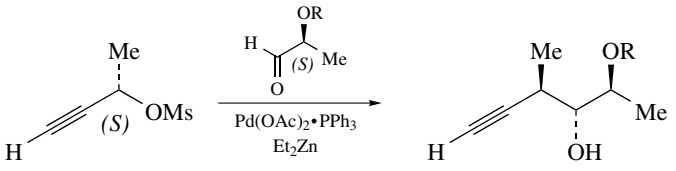

R = Bn (70%, dr = 94:6)
R = TBS (70%, dr = 100:0) (30)

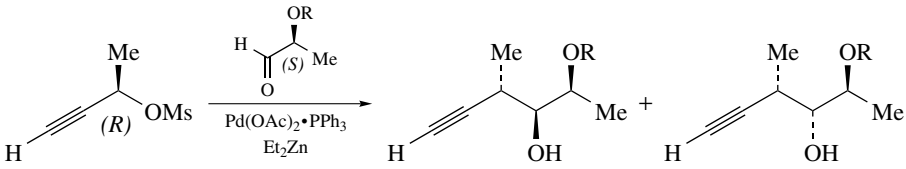

R = Bn (70%, dr = 86:14)
R = TBS (75%, dr = 85:15) (31)

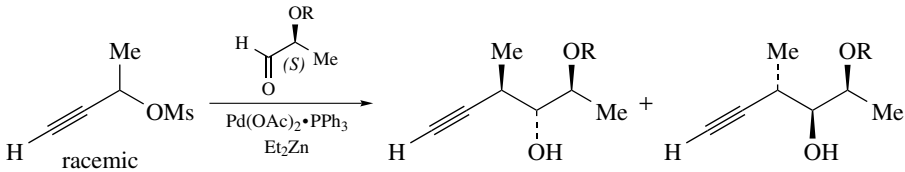

R = Bn (92%, dr = 50:45:5[a])
R = TBS (89%, dr = 50:43:7[a])
[a]*syn* adduct. (32)

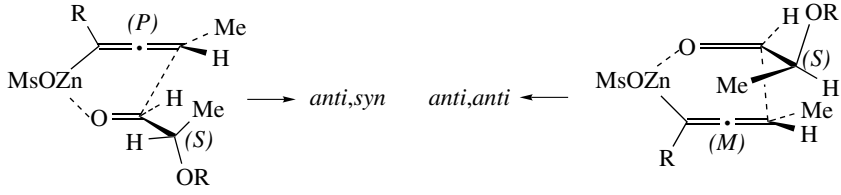

(33)

TABLE 16. Preparation of trifluoromethylallenylzinc reagents from trifluoromethyl-substituted propargylic mesylates

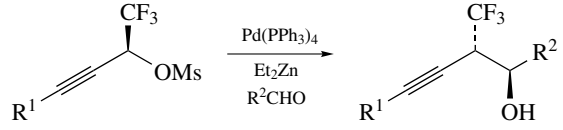

R^1	R^2	Yield (%)	*anti*:*syn*
CH_2OBn	Bu	52	91:9
CH_2OBn	*t*-Bu	43	>91:9
CH_2OBn	(*E*)-PhCH=CH	47	81:19
CH_2OBn	Ph	36	87:13
CH_2OBn	$TBSOCH_2$	33	90:10
Ph	Bu	42[a]	93:7
Pr	Bu	20[b]	93:7

[a] 18% allene.
[b] 12% allene.

Kitazume and coworkers employed the foregoing palladiozincation methodology to prepare anti trifluoromethyl-substituted homopropargylic alcohols from trifluoromethyl propargyl mesylates in the presence of catalytic $Pd(PPh_3)_4$ and Et_2Zn in CH_2Cl_2 (Table 16)[21]. Reactions conducted in THF proceeded in low yield. Addition of the benzyloxymethyl-substituted reagent to 3-pentanone afforded a 60:40 mixture of propargylic and allenic adducts.

Reagents derived from alkynyl CF_3 mesylates could be employed in additions to pentanal, leading to CF_3 alkynyl adducts (equation 34).

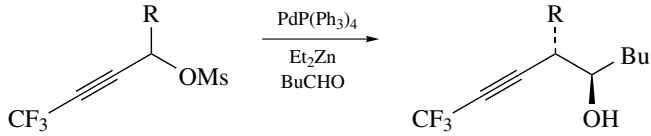

(34)

R = CH_2OBn (43%, dr = 89:11)
R = *t*-Bu (57%, dr = 99:1)

XIII. APPLICATIONS TO NATURAL PRODUCT SYNTHESIS

As previously mentioned, the palladiozincation methodology is applicable to the synthesis of various segments of natural products of the medicinally important polyketide family. The efficiency and convenience of the chiral allenylzinc reagents is demonstrated in the synthesis of subunits of tautomycin (Figure 3)[22], discodermolide (Figure 4)[23], bafilomycin V_1 (Figure 5)[24], leptofuranin (Figure 6)[25] and zincophorin (Figure 7)[26]. In a total synthesis of bafilomycin V_1, for example, seven of the thirteen stereocenters were introduced by means of allenylzinc chemistry. Three of these in the C5–C11 fragment and four in the C15–C25 subunit were constructed from a precursor (*R*)-mesylate and various aldehydes.

A recent synthesis of zincophorin methyl ester by Cossy and coworkers employs allenylzinc methodology to construct a side chain *anti*,*syn* stereotriad (Figure 7)[26].

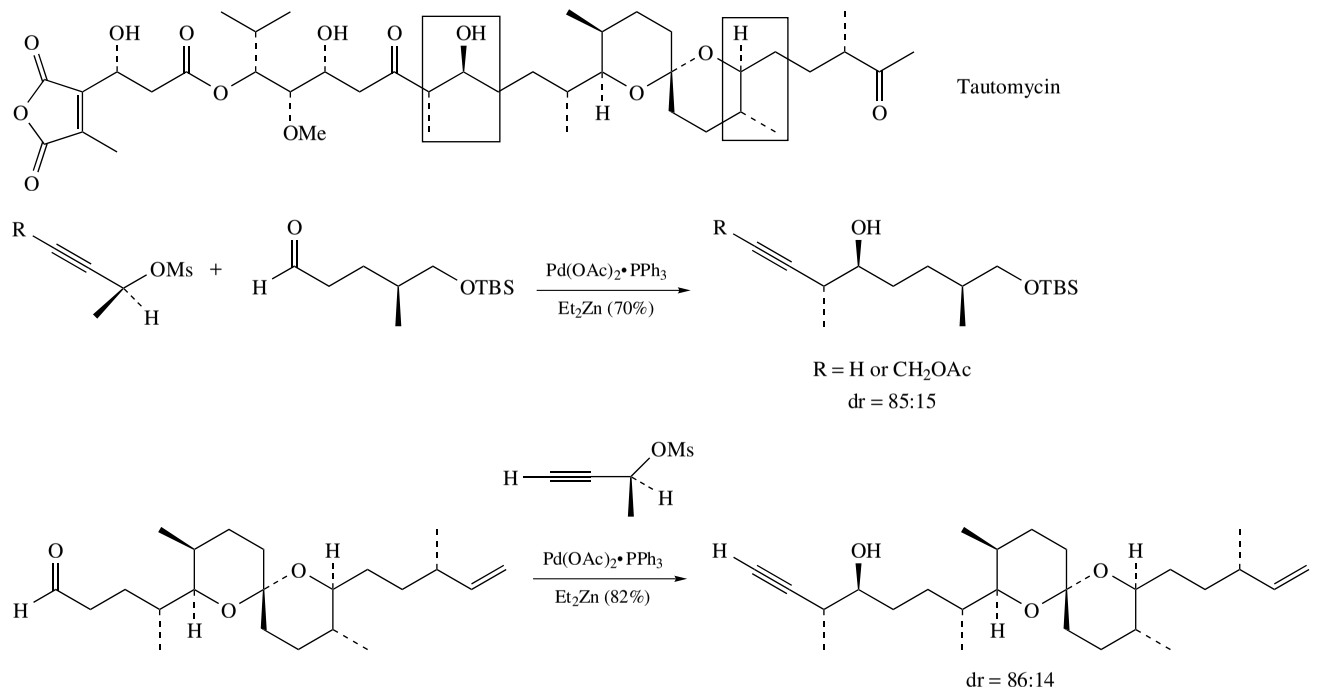

FIGURE 3. Construction of key segments of tautomycin

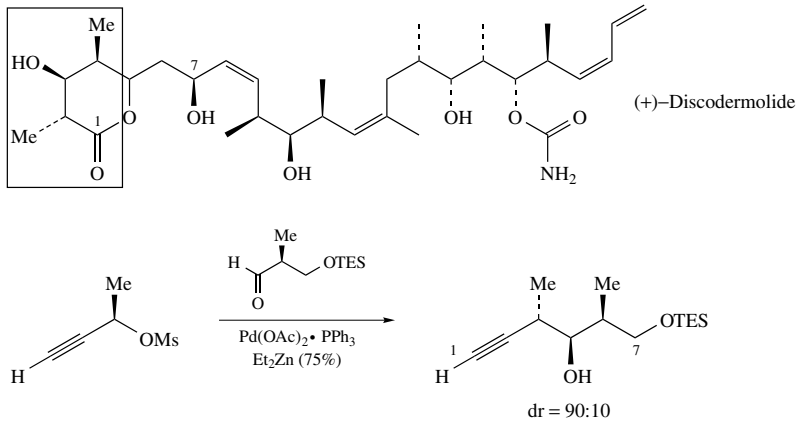

FIGURE 4. Construction of C1–C7 of discodermolide

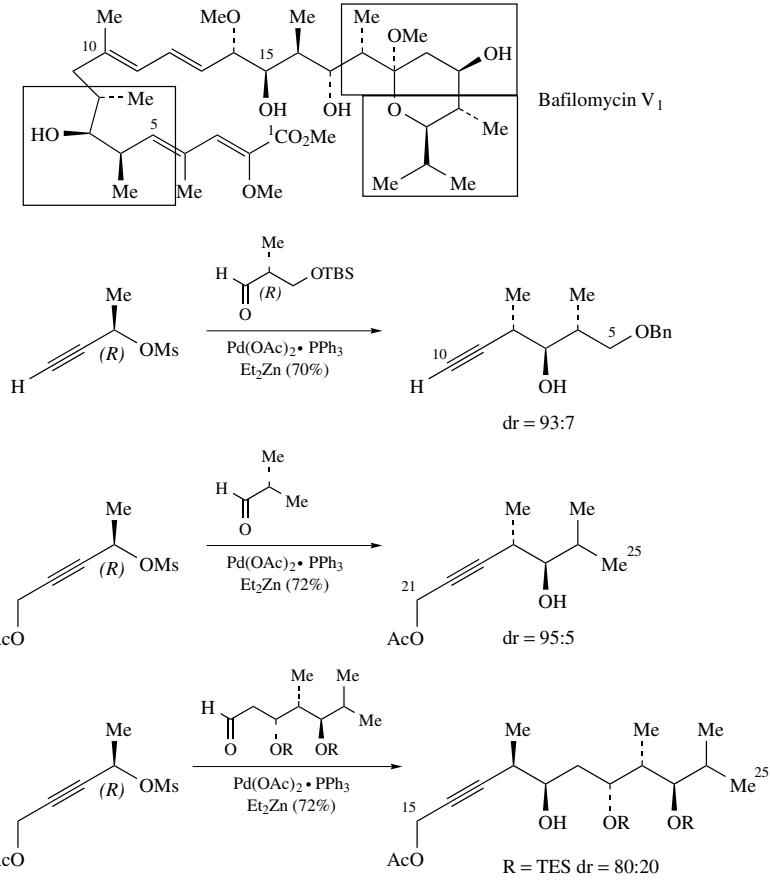

FIGURE 5. Construction of key segments of bafilomycin V_1

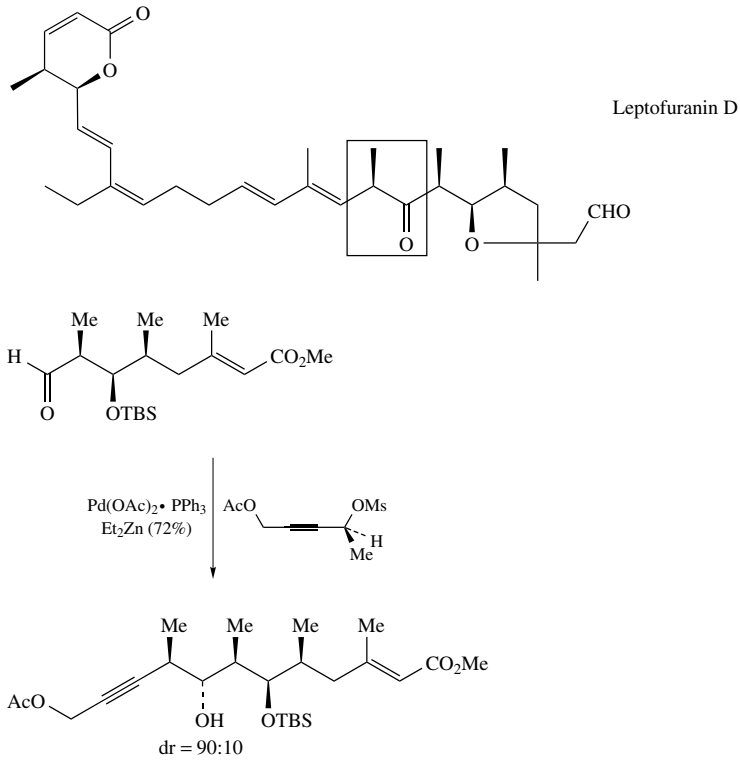

FIGURE 6. Construction of a C1–C12 segment of leptofuranin D

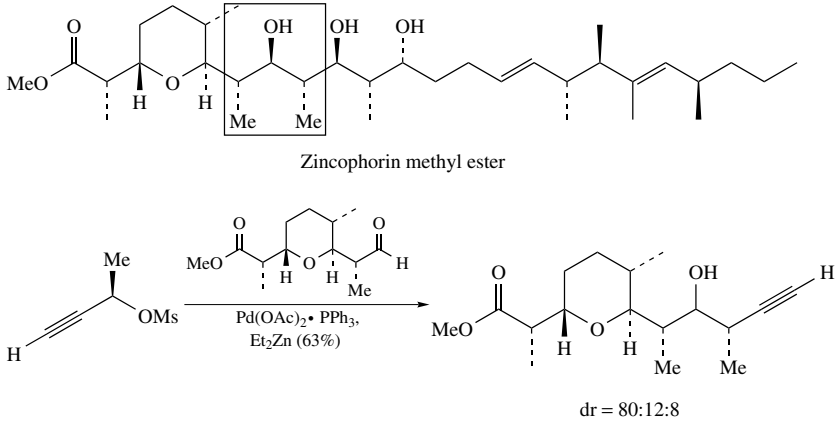

FIGURE 7. Construction of a key segment of zincophorin methyl ester

XIV. ADDITIONS TO IMINES AND ALDEHYDES

Normant and Poisson prepared allenylzinc bromide reagents from TMS acetylenes along the lines of Epsztein and coworkers[5], by sequential lithiation with *s*-BuLi to yield a lithiated species, and subsequent transmetallation with $ZnBr_2$ (equation 35)[27,28]. Additions to racemic β-silyloxy aldehydes proceed with low diastereoselectivity to afford mixtures of the *anti*,*anti* and *anti*,*syn* adducts (Table 17). The latter adducts are formed via an *anti* Felkin–Anh transition state. Additions to the racemic *N*-benzylimine analogs, on the other hand, proceed with nearly complete Felkin–Anh diastereoselectivity to yield the *anti*,*anti* amino alcohol adducts (Table 18).

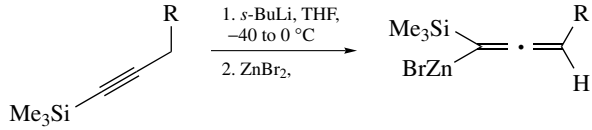

(35)

When they subjected the allenylzinc reagent to the Hoffmann test for configurational stability,[29] Poisson, Chemla and Normant found that at $-50\,^{\circ}C$, racemization does not occur at a significant rate (equation 36)[30,31]. Accordingly, when the racemic allenylzinc reagent was added slowly to the *N*-benzylimine of (R)-mandelic aldehyde at $-50\,^{\circ}C$, a 1:1 mixture of the *anti*,*syn* and *anti*,*anti* adducts was isolated in 65% yield. However, when the addition process was reversed, a 3:1 mixture favoring the matched *anti*,*anti* adduct was formed in 53% yield, suggestive of a partial kinetic resolution.

Addition of an excess of the racemic allenylzinc reagent to the *N*-benzylimine of (*S*)-malic aldehyde TBS ether yielded the matched *anti*,*anti* adduct of >95% enantiomeric purity derived from the (*M*)-enantiomer of the reagent (equation 37)[31].

TABLE 17. Addition of TMS allenylzinc reagents to silyl-protected mandelic aldehydes

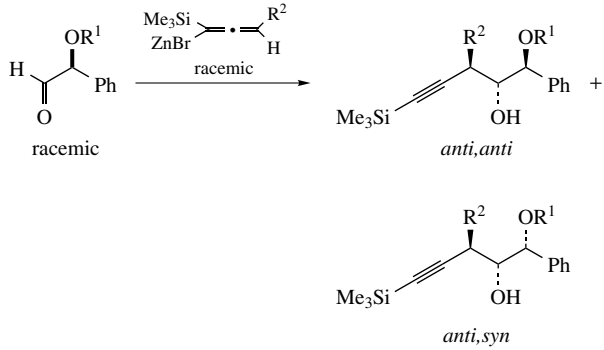

R^1	R^2	Yield (%)	*anti*,*anti*:*anti*,*syn*
TIPS	Me	85	53:47
TBS	Me	90	55:45
TBDPS	Me	97	58:42
TBS	Pr	90	58:42
TBDPS	Pr	90	67:33

TABLE 18. Addition of TMS allenylzinc reagents to silyl-protected mandelic imines

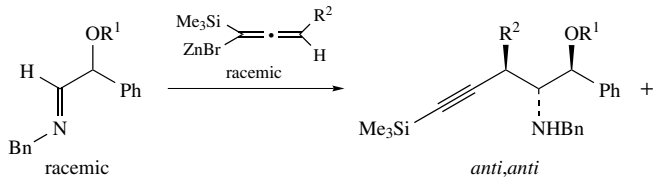

R^1	R^2	Yield (%)	*anti,anti*:*anti,syn*
TIPS	Pr	70	>97:3
TBS	Me	68	>97:3
TBS	Pr	85	>97:3
DPS	Pr	90	93:7

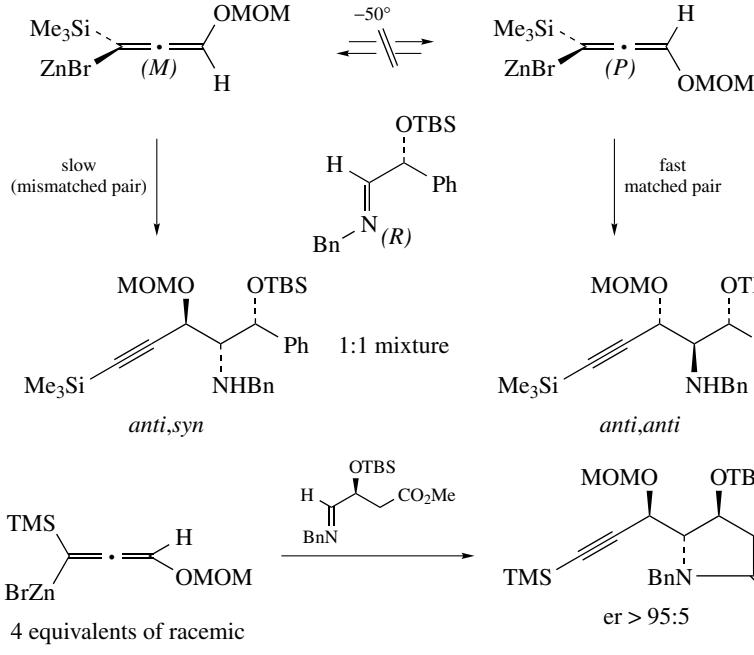

(36)

(37)

XV. KINETIC RESOLUTION OF CHIRAL ALLENYLZINC REAGENTS

The significant rate differences of additions to the silyloxy imines enabled Normant and Poisson to effect a kinetic resolution of the racemic allenylzinc reagent in a reaction with enantiomerically enriched imines[31]. When 0.6 equivalents of the *N*-benzylimine of (*R*)-lactic or mandelic aldehyde was added to the racemic allenylzinc reagent derived from 1-trimethylsilyl-2-hexyne, the matched (*P*)-reagent was consumed rapidly and the mismatched (*M*)-enantiomer was left unchanged at temperatures up to −10 °C (Figure 8). Addition of *t*-BuCHO to the reaction mixture yielded the adduct of the (*M*)-reagent of nearly 100% enantiomeric purity.

Extending the earlier studies of Epsztein and coworkers[5], Normant and Poisson examined additions of the allenylzinc reagent from the MOM ether of TMS propargyl alcohol to *N*-benzylimines of racemic TBS-protected mandelic and lactic aldehydes[28]. The racemic *anti*,*anti* amino derivatives were formed with high diastereoselectivities (equation 38). In contrast, addition of this allenylzinc bromide reagent to racemic TBS-protected mandelic aldehyde afforded a 48:33:19 mixture of three diastereomers (equation 39).

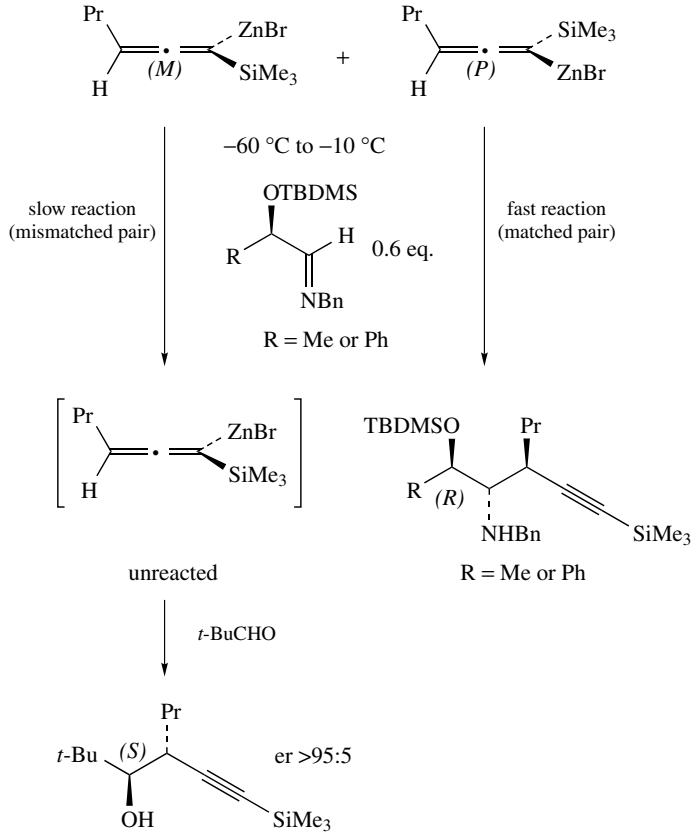

FIGURE 8. Kinetic resolution of an allenylzinc reagent by means of chiral imines

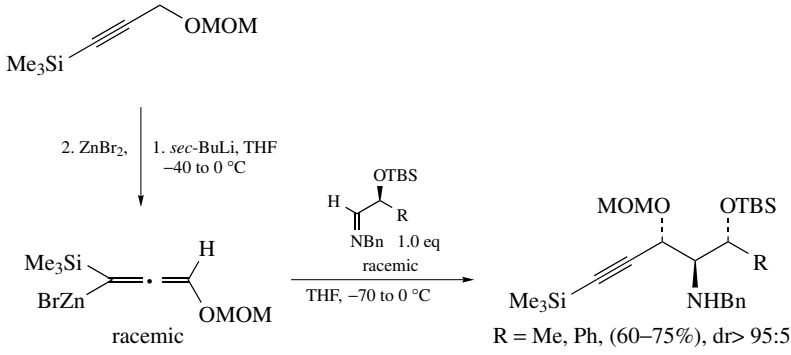

(38)

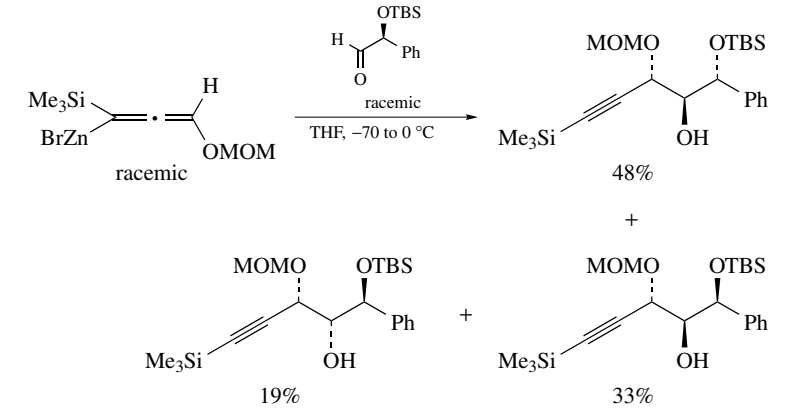

(39)

XVI. AMINE-SUBSTITUTED ALLENYLZINC REAGENTS

Mangeney and coworkers prepared allenylzinc reagents from *N*,*N*-dibenzyl TMS propargylamine by deprotonation with *s*-BuLi and treatment of the intermediate litho derivative with $ZnBr_2$[32]. Subsequent addition of 3-methylbutanal afforded a 90:10 mixture of the *anti* and *syn* amino alcohol adducts (equation 40).

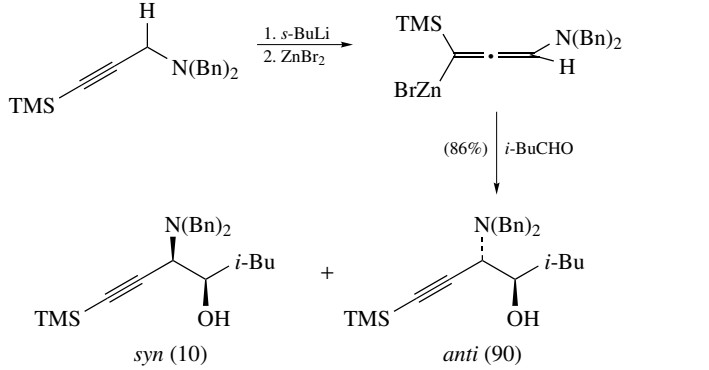

(40)

TABLE 19. Addition of alkylaminoallenylzinc reagents to aldehydes

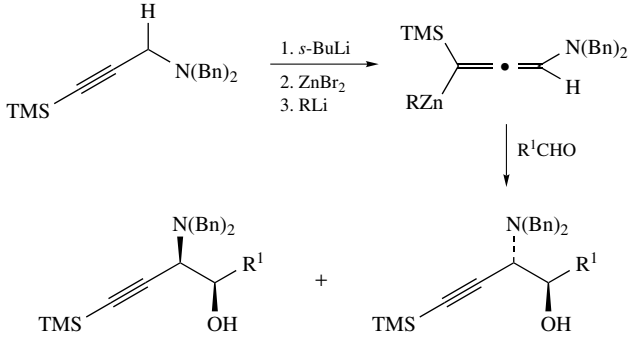

syn *anti*

R	R^1	Yield (%)	*anti*:*syn*
Bu	*i*-Bu	75	82:18
t-Bu	*i*-Bu	72	88:12

TABLE 20. Addition of lithio dialkylaminoallenylzincate reagents to aldehydes

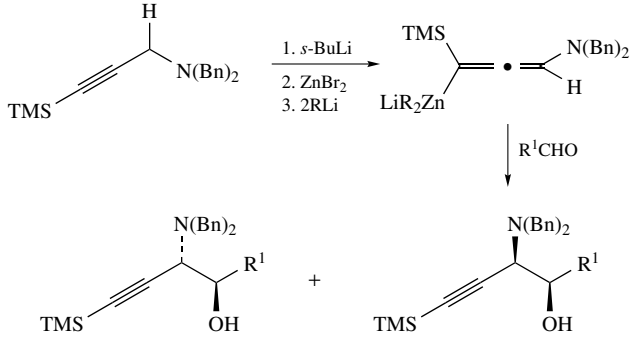

anti *syn*

R	R^1	Yield (%)	*syn*:*anti*
Et	*i*-Bu	72	50:50
Et	*t*-Bu	81	65:35
Et	Ph	82	67:33
Bu	*i*-Bu	77	59:41
Ph	*i*-Bu	75	45:55
t-Bu	*i*-Bu	84	84:16
t-Bu	Bu	78	83:17
t-Bu	*c*-C_6H_{11}	87	82:18
t-Bu	*t*-Bu	81	88:12
t-Bu	Ph	80	85:15

Surmising that the replacement of the Br ligand in the allenylzinc intermediate with an alkyl group would lower the Lewis acidity of the allenylzinc reagent, thereby favoring an acyclic transition state and a resultant increase in the proportion of *syn* adduct, the Mangeney group added BuLi to the intermediate allenylzinc bromide prior to addition of the aldehyde. However, in line with the prior findings of Utimoto and coworkers[11], the *anti* adduct still predominated (Table 19). Furthermore, the use of *t*-BuLi in the ligand exchange reaction slightly increased the proportion of *anti* adduct.

When two equivalents of the organolithium reagent were employed in the ligand exchange, the *syn* adduct was produced in equal or greater amount than the *anti*, depending on the nature of the added RLi reagent (Table 20). It is presumed that under these latter conditions a litho dialkylallenylzincate reagent is formed.

XVII. ADDITIONS TO SULFOXIMINES

Chemla and Ferreira effected lithiozincation of TMS propargyl chloride to prepare chloroallenylzinc bromide reagents (Table 21)[33]. Subsequent reaction of these reagents with *N*-*t*-butyl-substituted sulfoximines yielded the related *trans*-sulfoxinyl aziridines, arising from internal displacement of the chloride substituent of the *anti* sulfinamide adduct. A transition state in which the *t*-BuSO group is eclipsed with the alkynyl (vs R) substituent accounts for the preferred formation of the major *N*-sulfinyl diastereomer (equation 41).

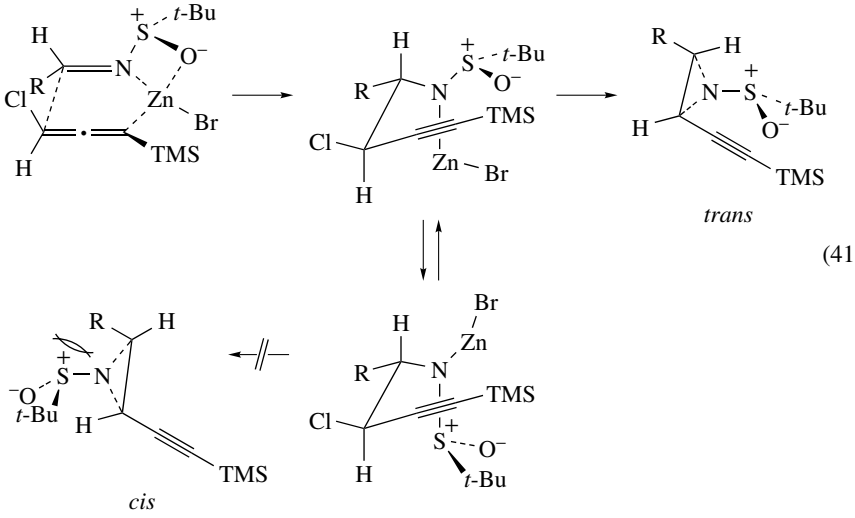

(41)

XVIII. ADDITIONS OF CHLOROALLENYLZINC REAGENTS TO ALDEHYDES AND IMINES

Additions of the foregoing chloroallenylzinc reagent to aldehydes, and *N*-TMS and *N*-benzylimines allowed access to alkynyloxiranes and aziridines[34]. The former result from a two-step process in which the initial *anti* adducts are converted to *trans* alkynyloxiranes upon treatment with DBU or KF (Table 22). The latter conditions effect desilylation as well as cyclization. Interestingly, when the addition to isobutyraldehyde is conducted with

TABLE 21. Addition of chloroallenylzinc bromide reagents to sulfoximines

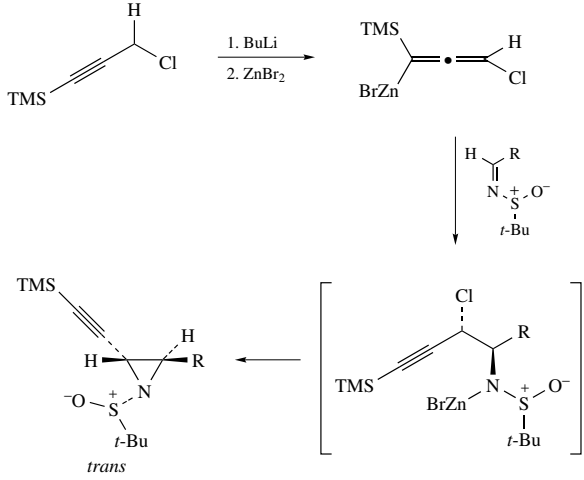

R	Yield (%)	*trans*:*cis*
Me	35	90:10
Pr	70	90:10
i-Pr	64	96:4
c-C_6H_{11}	56	90:10
t-Bu	0	—
Ph	58	91:9
(*E*)-MeCH=CH	67	94:6

TABLE 22. Addition of chloroallenylzinc bromide reagents to aldehydes

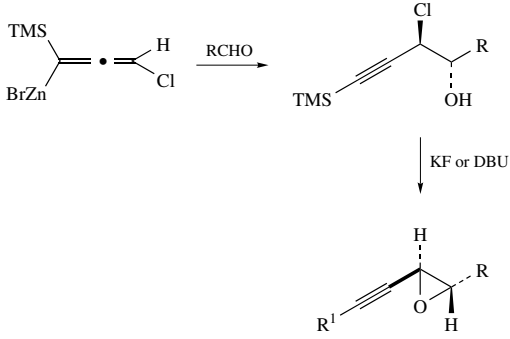

R	Yield (%)	*anti*:*syn*
Bu	81	85:15
i-Pr	75	95:5
t-Bu	82	>98:2
(*E*)-MeCH=CH	82	84:16
(*E*)-PhCH=CH	75	80:20

R	R^1	Yield (%)
i-Pr	H	35
t-Bu	TMS	97
(*E*)-MeCH=CH	TMS	93
(*E*)-PhCH=CH	H	90
(*E*)-PhCH=CH	TMS	98

the bromoallenylzinc bromide reagent, the bromoallene adduct is isolated in 15% yield along with 77% of the propargyl isomer (equation 42).

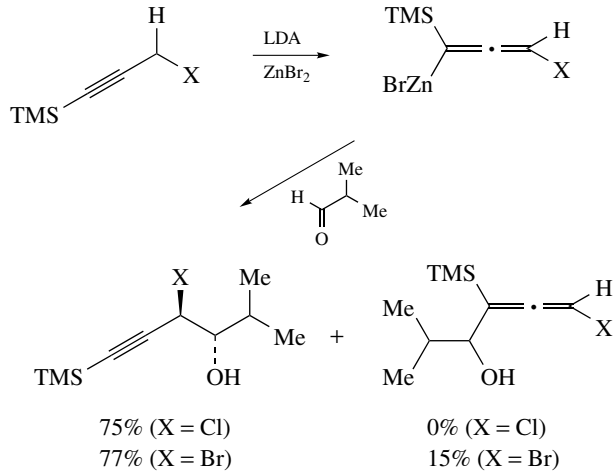

(42)

75% (X = Cl) 0% (X = Cl)
77% (X = Br) 15% (X = Br)

Addition of the chloroallenylzinc chloride reagent to *N*-benzylimines afforded the *trans*-aziridine products directly (Table 23). Evidently the higher nucleophilicity of the *N*-benzyl substituent promotes in situ displacement of the vicinal chloride of the major anti adduct. The *N*-benzyl substituent was assumed to adopt an orientation trans to the R group of the aziridine.

TABLE 23. Addition of chloroallenylzinc bromide reagents to imines

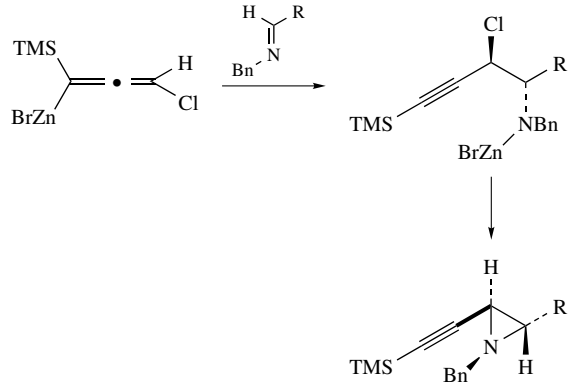

>98:2

R	Yield (%)
Bu	50
c-C_6H_{11}	98
t-Bu	12
Ph	73
(*E*)-PhCH=CH	65

TABLE 24. Addition of chloroallenylzinc bromide reagents to TMS imines

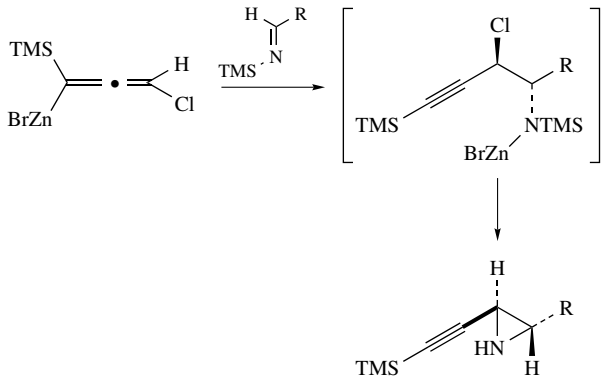

R	Yield (%)
Bu	63
i-Pr	79
t-Bu	40
Ph	62
(*E*)-PhCH=CH	65
(*E*)-MeCH=CH	79

Additions to *N*-TMS imines proceeded analogously, except that the *N*-TMS grouping was cleaved under the reaction conditions (Table 24). The ^{1}H NMR spectra of the NH aziridine products contained broad signals indicative of a mixture of N−H stereoisomers. However, upon N-benzylation, these products were converted to the previously prepared *trans*-aziridines, thereby confirming the expected *anti* selectivity of the addition.

XIX. REFERENCES

1. J. L. Moreau and M. Gaudemar, *Bull. Soc. Chim. Fr.*, 2171 (1970).
2. F. Barbot and P. Miginiac, *Tetrahedron Lett.*, 3829 (1975).
3. P. Jones and P. Knochel, *J. Org. Chem.*, **64**, 186 (1999).
4. J. L. Moreau and M. Gaudemar, *Bull. Soc. Chim. Fr.*, 2175 (1970).
5. F. Mercier, R. Epsztein and S. Holland, *Bull. Soc. Chim. Fr.*, 690 (1972).
6. H. Chwastek, R. Epsztein and N. Le Goff, *Tetrahedron*, **29**, 883 (1973).
7. G. Zweifel and G. Hahn, *J. Org. Chem.*, **49**, 4565 (1984).
8. B. W. Gung, X. Xue, N. Knatz and J. A. Marshall, *Organometallics*, **22**, 3158 (2003).
9. D. Mesnard and L. Miginiac, *J. Organomet. Chem.*, **440**, 277 (1992).
10. G. Cortes, V. Desre and L. Miginiac, *J. Organomet. Chem.*, **570**, 279 (1998).
11. H. Shinokubo, H. Miki, T. Yokoo, K. Oshima and K. Utimoto, *Tetrahedron*, **51**, 11681 (1995).
12. T. Katsuhira, T. Harada, K. Maejima, A. Osada and A. Oku, *J. Org. Chem.*, **58**, 6166 (1993).
13. J. A. Marshall and G. Bartley, *J. Org. Chem.*, **59**, 7169 (1994).
14. S. Ma and A. Zhang, *J. Org. Chem.*, **63**, 9601 (1998).
15. S. Ma and A. Zhang, *J. Org. Chem.*, **67**, 2287 (2002).
16. Y. Tamaru, A. Tanaka, K. Yasui, S. Goto and S. Tanaka, *Angew. Chem., Int. Ed. Engl.*, **34**, 787 (1995).
17. J. A. Marshall and N. D. Adams, *J. Org. Chem.*, **63**, 3812 (1998).
18. J. A. Marshall and N. D. Adams, *J. Org. Chem.*, **64**, 5201 (1999).
19. J. A. Marshall and G. M. Schaaf, *J. Org. Chem.*, **66**, 7825 (2001).

20. J. A. Marshall and H. R. Chobanian, *J. Org. Chem.*, **65**, 8357 (2000).
21. T. Sakamoto, K. Takahashi, T. Yamazaki and T. Kitazume, *J. Org. Chem.*, **64**, 9467 (1999).
22. J. A. Marshall and M. M. Yanik, *J. Org. Chem.*, **66**, 1373 (2001).
23. J. A. Marshall and B. A. Johns, *J. Org. Chem.*, **63**, 7885 (1998).
24. J. A. Marshall and N. D. Adams, *J. Org. Chem.*, **67**, 733 (2002).
25. J. A. Marshall and G. M. Schaaf, *J. Org. Chem.*, **68**, 7428 (2003).
26. M. Defosseux, N. Blanchard, C. Meyer and J. Cossy, *Org. Lett.*, **5**, 4037 (2003).
27. J.-F. Poisson and J. F. Normant, *J. Org. Chem.*, **65**, 6553 (2000).
28. J.-F. Poisson and J. F. Normant, *Org. Lett.*, **3**, 1889 (2001).
29. R. W. Hoffmann, J. Lanz, R. Metternich, G. Tarara and D. Hoppe, *Angew. Chem., Int. Ed. Engl.*, **26**, 1145 (1987).
30. J.-F. Poisson, F. Chemla and J. F. Normant, *Synlett*, 305 (2001).
31. J.-F. Poisson and J. F. Normant, *J. Am. Chem. Soc.*, **123**, 4639 (2001).
32. F. Bernaud, E. Vrancken and P. Mangeney, *Org. Lett.*, **5**, 2567 (2003).
33. F. Chemla and F. Ferreira, *Synlett*, 983 (2004).
34. F. Chemla, N. Bernard, F. Ferreira and J. F. Normant, *Eur. J. Org. Chem.*, 3295 (2001); F. Chemla and F. Ferreira, *Curr. Org. Chem.*, **6**, 539, (2002).

CHAPTER **11**

Palladium- or nickel-catalyzed cross-coupling reactions with organozincs and related organometals

EI-ICHI NEGISHI, QIAN HU, ZHIHONG HUANG, GUANGWEI WANG and NING YIN

Herbert C. Brown Laboratories of Chemistry, Purdue University, 560 Oval Drive, West Lafayette, Indiana 47907-2084, USA
Fax: +1 765 496 3380; e-mail: negishi@purdue.edu

The chemistry of organozinc compounds
Edited by Z. Rappoport and I. Marek

I. INTRODUCTION

Palladium- or nickel-catalyzed cross-coupling as defined by the general equation shown in equation 1 has become over the past thirty years one of the most general and selective methods for carbon–carbon bond formation[1,2]. In this chapter, attention is mainly focused on the Pd-catalyzed cross-coupling reactions of organometals containing Zn along with related reactions of organometals containing Mg, Al, Zr and some others. Brief but due attention is paid to the genesis of the reaction. Many of the results discussed in pertinent books, book chapters and reviews[1–28] will be presented only in a brief summary form with some emphasis on the applications to the syntheses of natural products and other compounds of materials of chemical interest. Comprehensive discussions of general and specific topics of the Pd-catalyzed cross-coupling reported before 2000 may be found in the pertinent chapters indicated in Table 1 and references cited therein. However, the Pd- or Ni-catalyzed cross-coupling has continued evolving vigorously. Consequently, many of the discussions presented in this chapter will be about those recent and significant new developments published over the past several years.

$$R^1M + R^2X \xrightarrow{\text{cat. } PdL_n \text{ or } NiL_n} R^1 - R^2 + MX \quad (1)$$

Discovery of the Pd-catalyzed cross-coupling and early findings. A few years after the discovery of the Ni-catalyzed Grignard cross-coupling, often called the Kumada coupling or Kumada–Tamao–Corriu coupling, in 1972[12,29], a few groups led by Murahashi[30], Negishi[5b,31–39], Fauvarque[40] and Ishikawa[41] seemingly independently reported the Pd-catalyzed cross-coupling[3]. Whereas the groups led by Murahashi[30a], Fauvarque[40a] and Ishikawa[41] initially reported some Pd-catalyzed Grignard cross-coupling reactions, the Negishi group focused its attention on the discovery and development of the cross-coupling reactions of organometals containing various metals including Zn, B, Al, Zr, Sn and others in addition to Mg (Scheme 1). Thus, Negishi was either the first or among the

TABLE 1. Classification of Pd-catalyzed cross-coupling reactions [a]

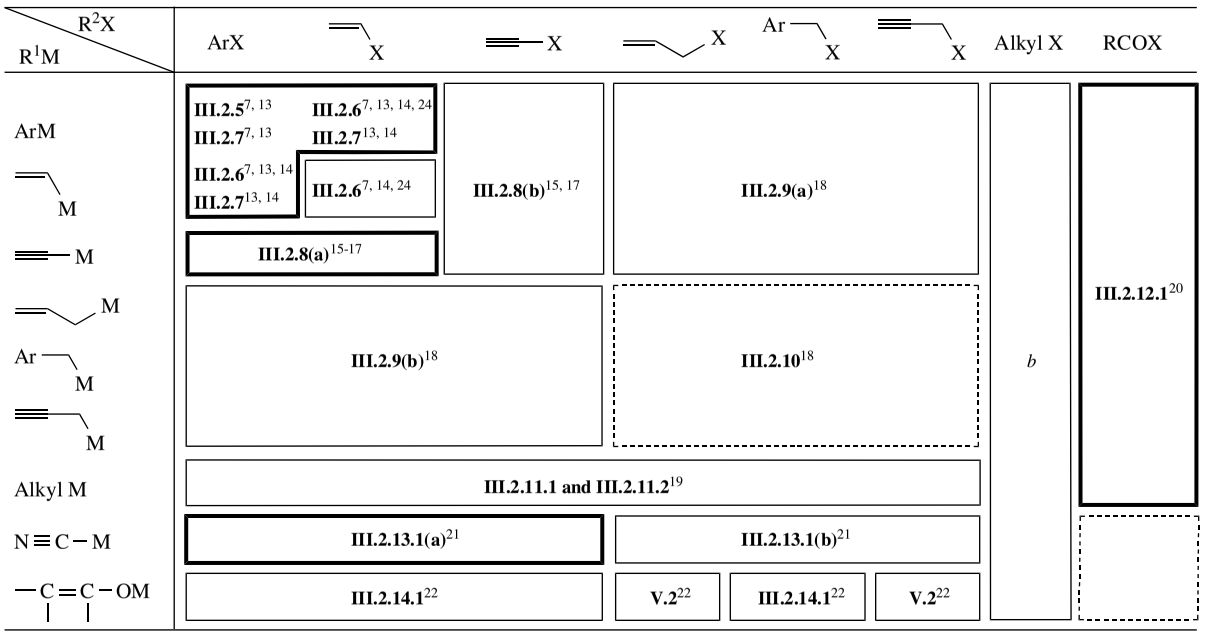

[a] The numbers represented by III.2.*n*, where *n* is 5–14, indicate the corresponding chapter in Reference 1. Bold-line frame: generally favorable; broken-line frame: generally not well-developed; Solid-line frame: others.
[b] Discussed in detail in this review.

first to report the Pd- or Ni-catalyzed cross-coupling reactions of Zn, B, Al and Zr[39]. Some of the prototypical examples of the Pd-catalyzed cross-coupling reactions of organometals containing Al, Zr, Zn and B reported during the 1976–1978 period are shown in Schemes 2–7. The results shown in Schemes 2–5 represent the earliest sets of examples of the Pd- or Ni-catalyzed hydrometallation–cross-coupling[31,32,34,35,37] and carbometallation–cross-coupling[38] tandem reactions. They have also provided, for the first time, the currently most general and highly selective synthesis of conjugated dienes (Schemes 3–5). The results shown in Scheme 6[33–35] represent some of the earliest examples of the Pd- or Ni-catalyzed organozincs, while the reaction of the alkynylborates shown in Scheme 7 is the first satisfactory Pd-catalyzed cross-coupling reaction of organoborons[5b,c].

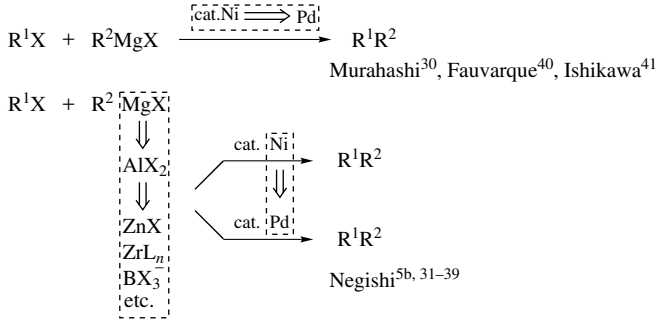

SCHEME 1. Evolutionary discovery and developments of the Pd-catalyzed cross-coupling

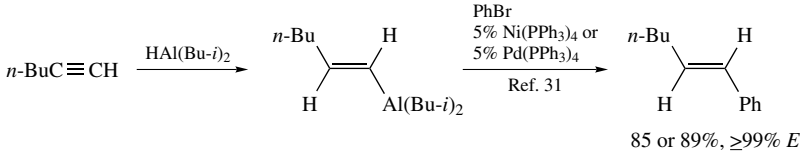

SCHEME 2. Pd- or Ni-catalyzed alkenyl–aryl coupling

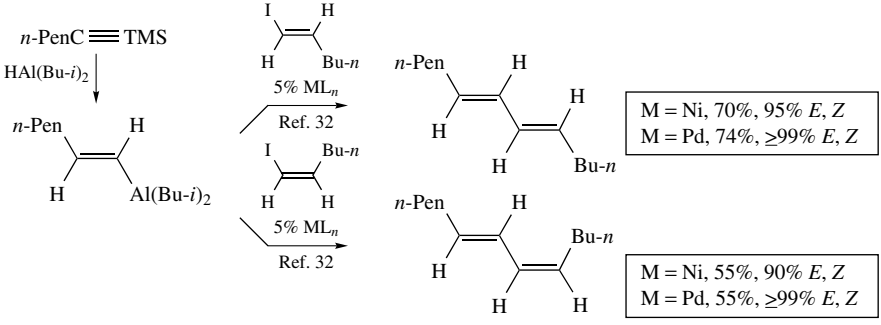

SCHEME 3. Pd- or Ni-catalyzed alkenyl–alkenyl coupling

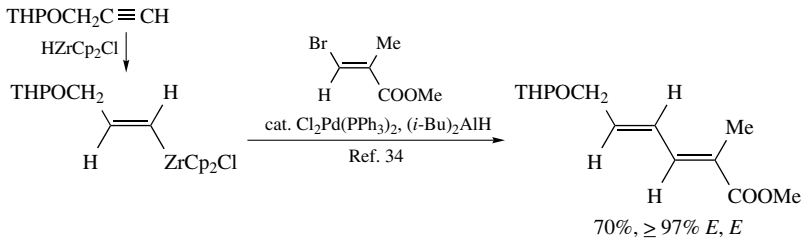

SCHEME 4. Pd-catalyzed hydrozirconation–cross-coupling tandem reaction

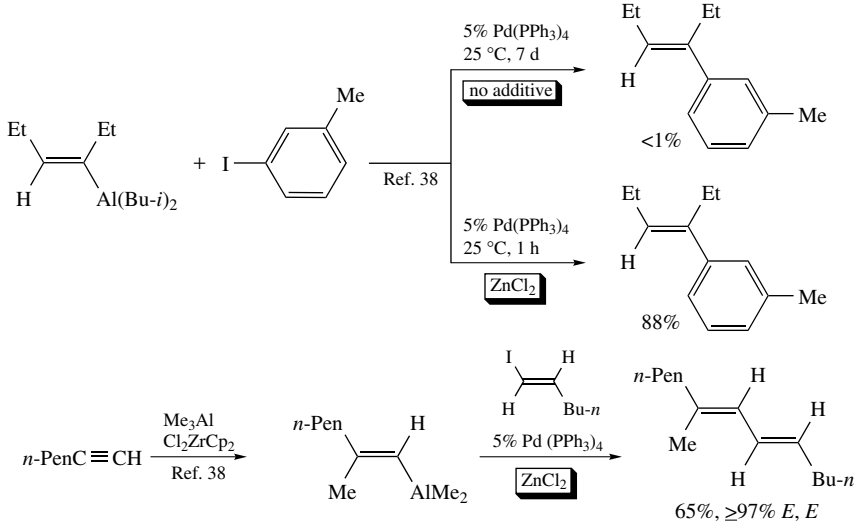

SCHEME 5. Pd- and Zn-cocatalyzed alkenyl–aryl and alkenyl–alkenyl coupling reactions

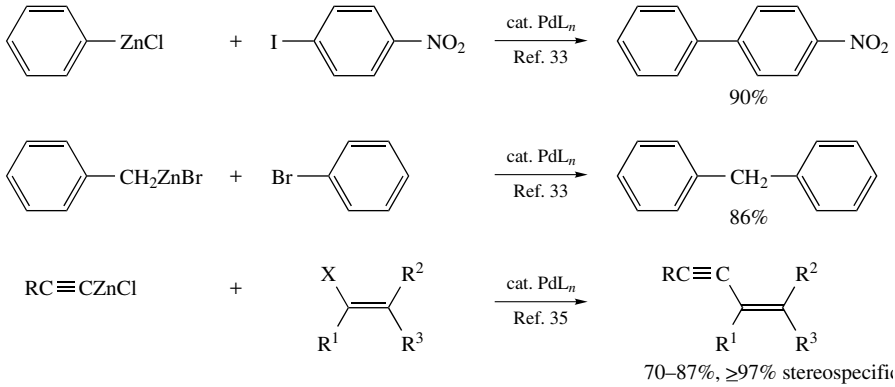

SCHEME 6. Pd-catalyzed reaction of alkynylzincs with alkenyl halides

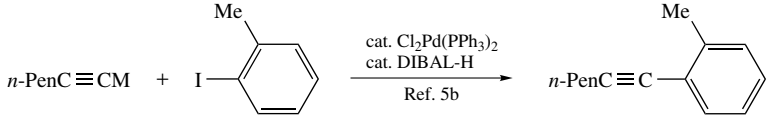

M	Temp (°C)	Time (h)	Yield (%)
ZnCl	25	1	91
BBu_3Li	25	3	10
BBu_3Li	reflux	1	92
$SnBu_3$	25	6	83

SCHEME 7. Pd-catalyzed alkynylation with alkynylmetals containing Zn, B and Sn

Today, Zn and B are two of the most satisfactory and widely used metals. Although the current scope of the Pd-catalyzed cross-coupling with Grignard reagents is considerably more limited than that of organometals containing Zn and B, Grignard reagents may be as satisfactory as or more satisfactory than those containing Zn and B in some cases. Moreover, Grignard reagents, along with organolithiums, often provide by direct metallation the first generation organometals through which other second generation organometals containing Zn, B, Sn and others can be prepared. In such cases, Grignard reagents should be tested first before converting them into the second generation organometals. On the other hand, organometals containing B, Al, Zr, Cu, Si, Sn as well as Mg, Zn and In can be obtained as the first generation organometals via hydrometallation, carbometallation, halometallation and metallometallation (Schemes 8–11). Any advantages associated with each metal can be exploited in developing the most satisfactory procedure for a given task of cross-coupling.

(a) *syn-Hydrometallation* (B, Al, Zr, Zn, Si, Sn etc.)

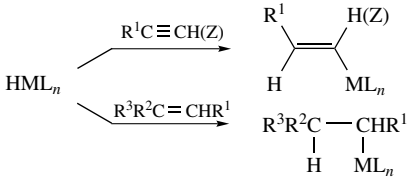

M: B, Al, and Zr --- Three most widely used metals.
Zn, Si, and Sn --- Have so far been less widely used for various different reasons.

(b) *anti-Hydrometallation* (In and others)

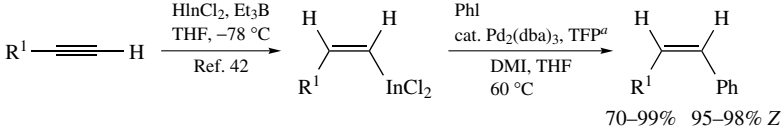

70–99% 95–98% *Z*

[a] TFP = Tris(2-furyl)phosphine

SCHEME 8. Hydrometallation reactions for Pd-catalyzed alkenylation

(a) *Zr-catalyzed syn-carboalumination*[43]

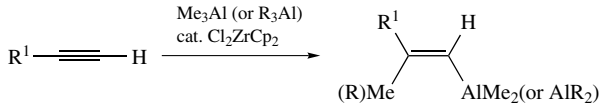

(b) *Zr-catalyzed asymmetric carboalumination of alkenes (ZACA reaction)*[44]

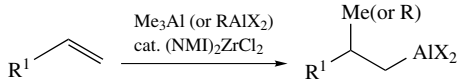

NMI = 1-(neomenthyl)indenyl

(c) *Zr-catalyzed carbomagnesiation*[45] *and carbozincation*[46]

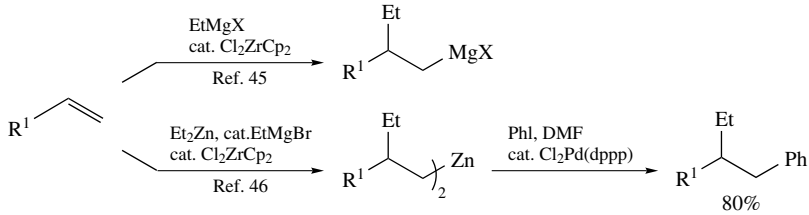

The current scope of these reactions is largely limited to ethylmetallation.

(d) *Carbocupration*[47, 48]

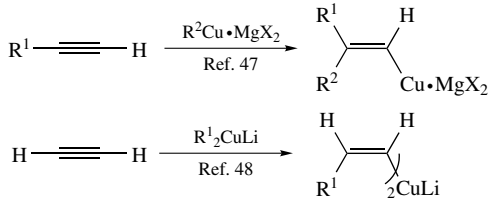

SCHEME 9. Carbometallation reactions for Pd-catalyzed alkenylation

(a) *anti-Halometallation*

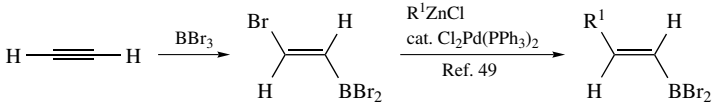

Presumably, *syn*-haloboration is followed by isomerization

(b) *syn-Haloboration*

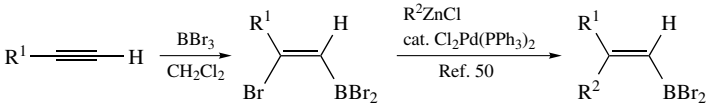

SCHEME 10. Heterometallation reactions for Pd-catalyzed alkenylation

(c) *Diboration and silaboration*

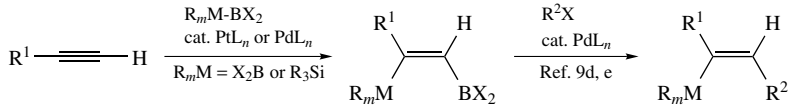

(d) *Distannation*

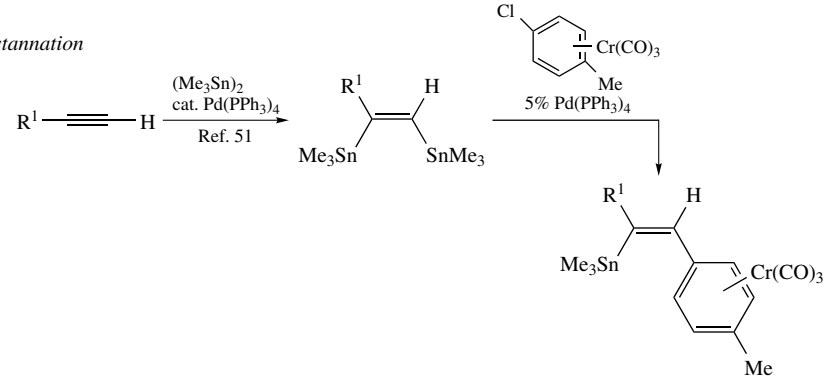

SCHEME 10. (*continued*)

The discovery of the use of Zn salts, e.g. $ZnCl_2$, as cocatalysts for promoting the Pd- or Ni-catalyzed cross-coupling of organometals containing Al and Zr in 1978[38] has proved to be a significant breakthrough. Since active organometallic species in these Zn-cocatalyzed reactions have been shown to be at least in part organozincs, the cocatalysis by Zn salts has effectively expanded the scope of the Pd- or Ni-catalyzed cross-coupling of organozincs. At the same time, the results of the Zn-cocatalyzed cross-coupling, such

(a) *Cyclic anti-hydrometallation*

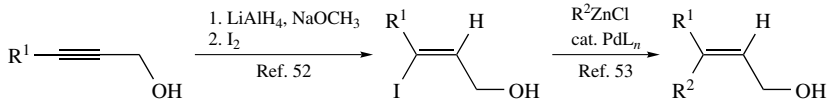

(b) *Cu-catalyzed cyclic anti-carbomagnesation*[54]

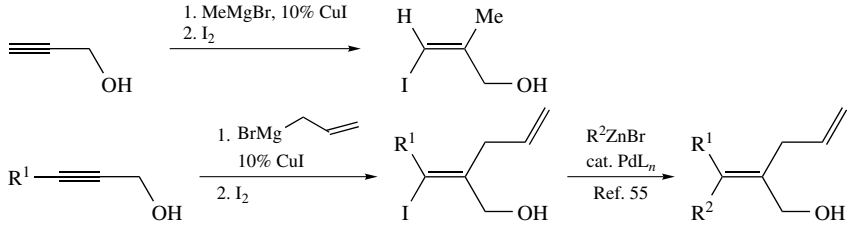

SCHEME 11. Cyclic *anti*-hydrometallation and *anti*-carbometallation reactions for Pd-catalyzed alkenylation

(c) *Zr-catalyzed cyclic anti-carboalumination*[56]

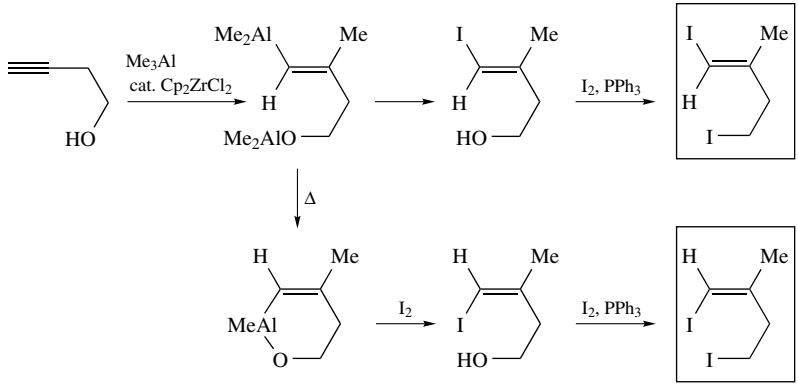

SCHEME 11. (*continued*)

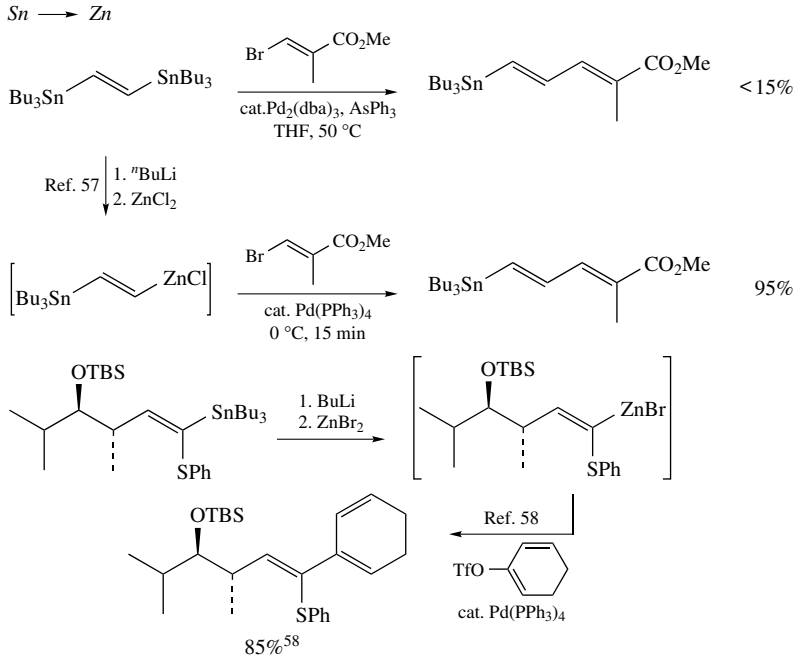

SCHEME 12. Higher reactivities displayed by organozincs relative to those of Sn, B or Cu in Pd-catalyzed alkenylation

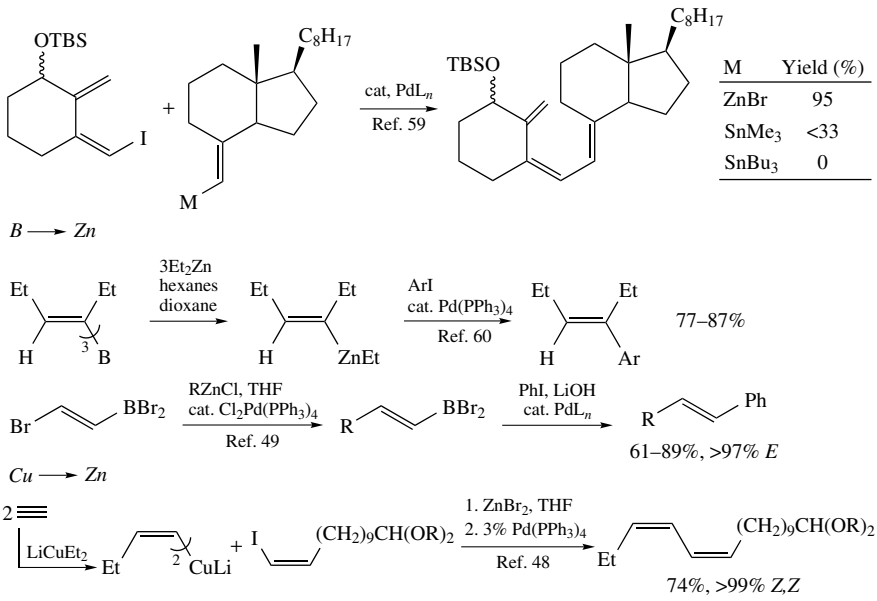

SCHEME 12. (*continued*)

as those shown in Schemes 5 and 12, have repeatedly demonstrated the superior reactivity of organozincs as compared with those containing Al[38], Zr[38], Sn[57–59], B[49,60] and Cu[48]. Recently, the use of organozincs in place of Zn salts as exemplified by one reaction[60] in Scheme 12 has been shown to be effective. This topic will be discussed later in detail.

II. OVERVIEW OF THE Pd- OR Ni-CATALYZED CROSS-COUPLING OF ORGANOZINCS

Inspection of the generic equation of the Pd- or Ni-catalyzed cross-coupling, i.e. equation 1, indicates that there are several changeable parameters to be optimized for a given task of the synthesis of R^1–R^2. The R^1 and R^2 groups are not changeable but are still interchangeable, since the desired product R^1–R^2 may be prepared by the reaction of either R^1M with R^2X or R^1X with R^2M. However, the genuinely changeable parameters for equation 1 are (1) countercations (M), (2) leaving groups (X) and (3) catalysts (PdL_n or NiL_n) including ligands (L). Although not shown in equation 1, cocatalysts or additives and solvents are also important changeable parameters. In short, the key to the successful development or application of the Pd- or Ni-catalyzed cross-coupling is to find an optimal set of parameters for a given task.

A. Countercations (M)

In the introductory section, a brief discussion of some of the ten or so metals used as countercation component as well as of the general superiority of Zn in the Pd-catalyzed cross-coupling was presented. Also discussed was that reactive organozinc species may be generated *in situ* through transmetallation between organometals containing B, Al, Sn, Zr, Cu and so on and Zn salts or alkylzincs. Organozincs have indeed been

prepared by most, if not all, of the ten or a dozen well-known methods of preparation of organometals[61] including (i) transmetallation, (ii) oxidative metallation of organic halides and other electrophiles, (iii) metal–halogen exchange, (iv) metal–hydrogen exchange, (v) hydrometallation and (vi) carbometallation[8a,b,62].

1. Transmetallation

Transmetallation between organometals containing various metals and zinc salts or alkylzincs is by far the most widely used method of preparation of organozincs for Pd- or Ni-catalyzed cross-coupling. In cases where Grignard reagents and organoalkali metals containing Li, Na or K are used as the first generation organometals, transmetallation generally proceeds to completion. Moreover, it can proceed beyond the first transmetallation. Thus, for example, the reaction of organolithiums and zinc salts can give mono-, di- and even triorganylzinc species depending on the reactant ratio and reaction conditions (Scheme 13). In most cases, the organozinc products are indicated as RZnX, R_2Zn and R_3ZnLi, respectively. Except in cases where diorganylzincs (R_2Zn) are isolated as pure compounds, however, the other metals, such as Li and Mg, are present in the organozinc reagent generated *in situ*. Some recent results of the Pd-catalyzed reaction of phenylzincs and (*E*)-1-octenyl halides indicate that there can be significant differences between organozincs derived from organolithiums and those derived from Grignard reagents[63] (Scheme 14). In short, whereas PhZnBr derived from PhMgBr reacts readily with both (*E*)-1-octenyl iodide and bromide, PhZnBr derived from PhLi reacts well with the iodide but not with the bromide. Interestingly, PhMgCl without $ZnBr_2$ reacts well with (*E*)-1-octenyl bromide to give (*E*)-1-phenyl-1-octene in 95% yield, but the yield observed with (*E*)-1-octenyl iodide was only 44% even under reflux for 24 h. It is tempting to interpret these results in terms of the hard and soft acids and bases principle. Irrespective of the precise reason, they could be potentially general and practically important phenomena. It is strongly advisable to indicate the origin of organometals, perhaps in parentheses, as in Schemes 13 and 14.

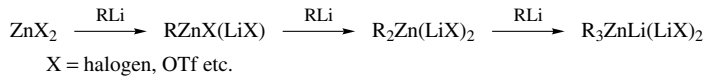

SCHEME 13. A series of transmetallations between an organolithium and a zinc salt

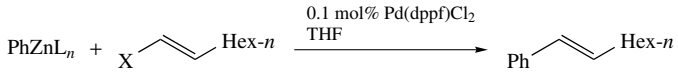

$PhZnL_n$	X	Temp. (°C)	Time (h)	Prod. (%)	Halide (%)	Diene (%)
PhZnBr(LiBr)	I	23	20	99	0	0
PhZnBr(LiBr)	Br	reflux	24	14	74	6
PhZnBr(MgClBr)	I	23	20	96	3	<1
PhZnBr(MgClBr)	Br	23	20	98	2	0

SCHEME 14. Comparison of PhZnBr derived from PhLi and PhMgBr in the Pd-catalyzed alkenylation

Another important class of transmetallation reactions are those involving more electronegative metals than Li and Mg, such as Al and Zr shown in Scheme 5, as well as

B and Cu shown in Scheme 12. In these reactions, the extent of transmetallation has not generally been determined, but it is likely that, in many of these reactions, equilibrium mixtures are obtained. Even so, some remarkably favorable results have been obtained in many cases. In cases where highly volatile organozincs, such as Me_2Zn and Et_2Zn, are used for B-to-Zn transmetallation, highly volatile Me_3B and Et_3B formed as byproducts can be removed under high vacuum[64] (Scheme 15). Since these compounds are highly pyrophoric, due precautions must be taken to prevent fire hazard. Evaporation of boranes, however, is not always necessary, as shown in Scheme 15, where $(i\text{-Pr})_2Zn$ is used as a reagent[65]. It should be noted that, for the Sn-to-Zn transmetallation, a preferred method is to carry out the Sn → Li → Zn double transmetallation, as shown in Scheme 12.

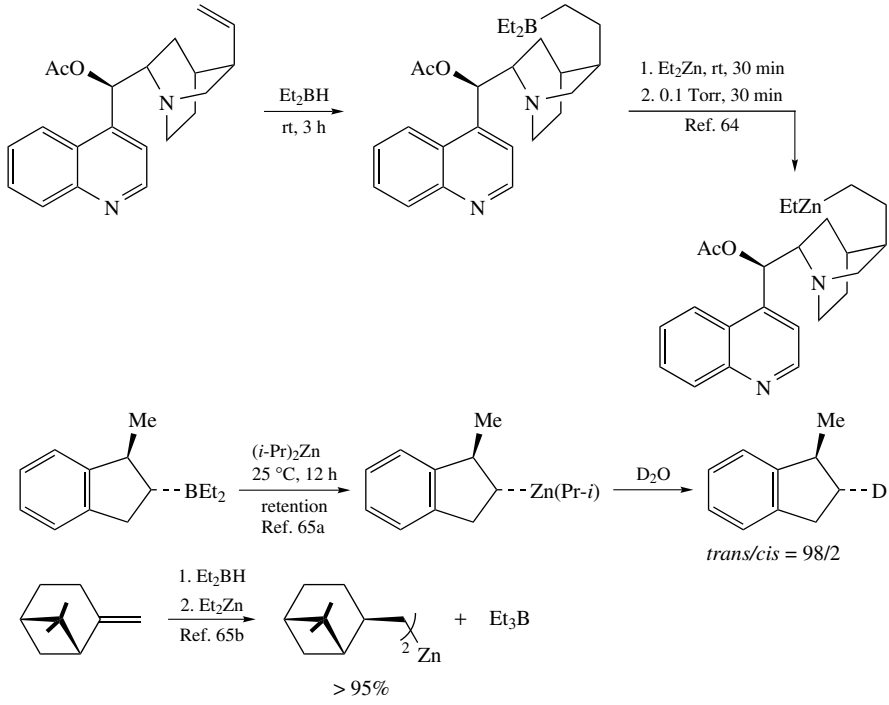

SCHEME 15. B-to-Zn transmetallation with dialkylzincs

2. Oxidative zincation

When the starting organic electrophiles are highly reactive, oxidative zincation is often the method of choice. The preparation of allyl-[66] and benzylzinc[33] derivatives falls into this category (Scheme 16). In contrast with the preparation of the corresponding Li and Mg derivatives which are usually plagued by various unwanted side reactions, such as homodimerization, the zinc reactions are often very clean and usually cleaner than the corresponding Li or Mg reactions.

Formation of the Simmons–Smith reagent, i.e. ICH_2ZnI, and the Furukawa reagent, i.e. ICH_2ZnEt, provide additional examples[62]. For activation of Zn to be used for direct oxidation zincation of more usual organic halides, various methods including washing with dilute HCl and treatment with Me_3SiCl in the presence or absence of $BrCH_2CH_2Br$

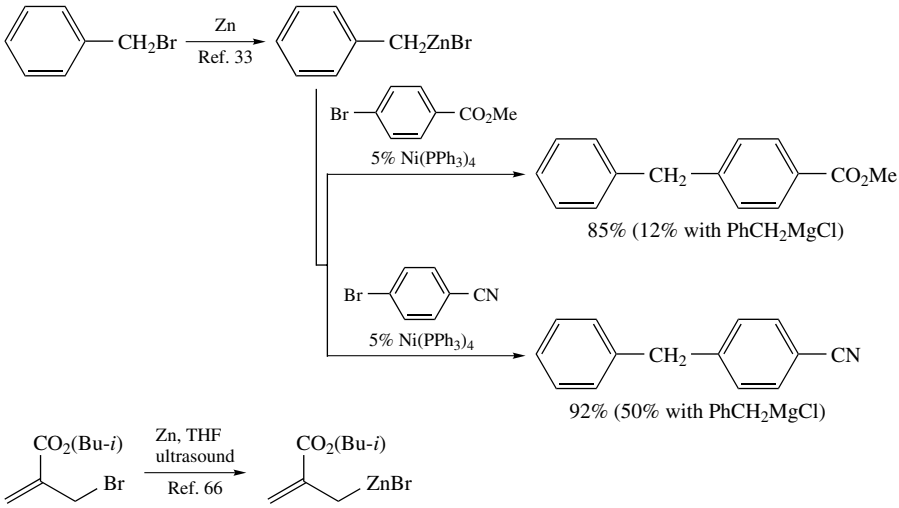

SCHEME 16. Preparation of allyl- and benzylzinc derivatives by oxidative zincation

have been used[62]. More deliberate preparations of active Zn include reduction of $ZnCl_2$ with potassium–graphite[67], i.e. C_8K, and most notably a series of methods developed by Rieke[62, 68]. Somewhat surprisingly, these methods do not appear to have been widely used for the Pd- or Ni-catalyzed cross-coupling in the past. A priori, it might be expected that the direct oxidative zincation method should be synthetically equivalent to other methods, such as the Li-to-Zn or Mg-to-Zn transmetallation method. However, this point may have to be experimentally established. Here again, it is important to remember that organozincs generated by these methods contain Li, K or some other metals.

3. Zn–halogen exchange

Although not widely applicable at this moment, treatment of alkyl iodides with Et_2Zn in the presence of a catalytic amount of CuI or CuCN can provide the corresponding alkylzinc derivatives by a radical process[8a,b].

4. Zn–hydrogen exchange

Treatment of active H-containing compounds, such as terminal alkynes, with organozincs provides a convenient route to organozincs, as exemplified by the generation of alkynylzincs from terminal alkynes with alkylzinc derivatives[62].

5. Hydrozincation

Hydrozincation is not as widely observable as that involving B, Al and Zr. This is one of the main reasons why the indirect hydrometallation–transmetallation procedures shown in Schemes 8 and 12 have been developed and used. It is nevertheless highly desirable to directly generate organozincs to be used for the Pd- or Ni-catalyzed cross-coupling from alkenes and alkynes via hydrozincation. Indeed, such reactions have been developed, as shown in Scheme 17. However, further developments are clearly desirable.

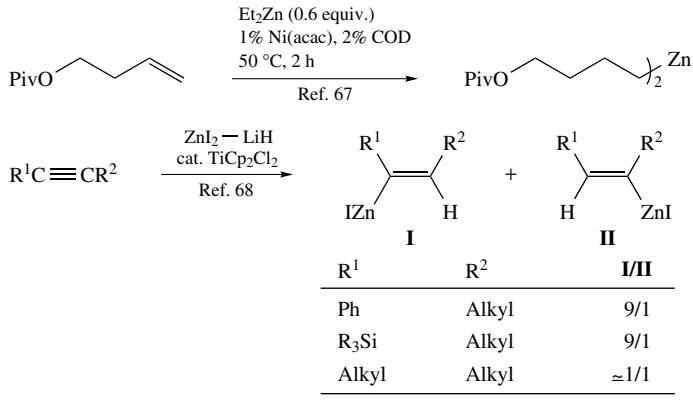

R^1	R^2	**I/II**
Ph	Alkyl	9/1
R_3Si	Alkyl	9/1
Alkyl	Alkyl	≃1/1

SCHEME 17. Hydrozincation of alkenes and alkynes

6. Carbozincation

The Zr-catalyzed carboalumination–Pd-catalyzed cross-coupling tandem process has been extensively developed as a method for the synthesis of trisubstituted alkenes, as discussed later. It is nevertheless desirable to develop direct carbozincation of alkenes and alkynes. Probably the oldest carbozincation is that of allylzinc derivatives[8,62] which generally proceeds with allylic rearrangement, and it is generally believed that this reaction proceeds via 6-centered transition states. Allylzincation of 1-trimethylsilyl-1-alkynes is 100% regioselective, although it is only 85% stereoselective. With crotylzinc bromide, a clean allyl rearrangement is observed. On the other hand, the $ZrCp_2I_2$-catalyzed crotylzincation of 5-decyne proceeds without allylic rearrangement. It is likely that the latter reaction proceeds via a four-centered mechanism[69] (Scheme 18).

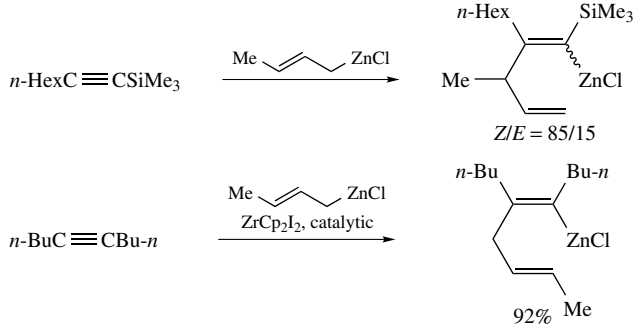

SCHEME 18. Crotylzincation of alkynes

A few alkylzincation reactions of alkenes and alkynes are also known, as shown in Schemes 9 and 19. The ethylzincation of alkenes cocatalyzed by $ZrCp_2Cl_2$ and EtMgBr must be closely related to the Dzhemilev ethylmagnesation[45], but the ethylzincation is cleaner than that with EtMgBr[46]. Just like the Dzhemilev ethylmagnesation, the Zr-catalyzed carbozincation of alkenes also fails to proceed with Me_2Zn. On the other hand, the reaction of dialkylzincs with alkynes in the presence of $ZrCp_2I_2$ (1 equiv.) proceeds with either Me_2Zn or Et_2Zn[70] (Scheme 19).

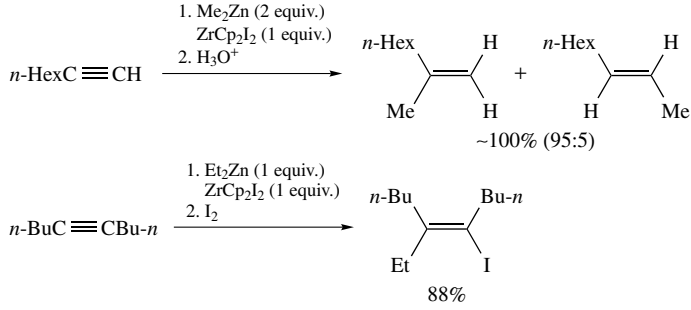

SCHEME 19. Zr-promoted carbozincation of alkynes

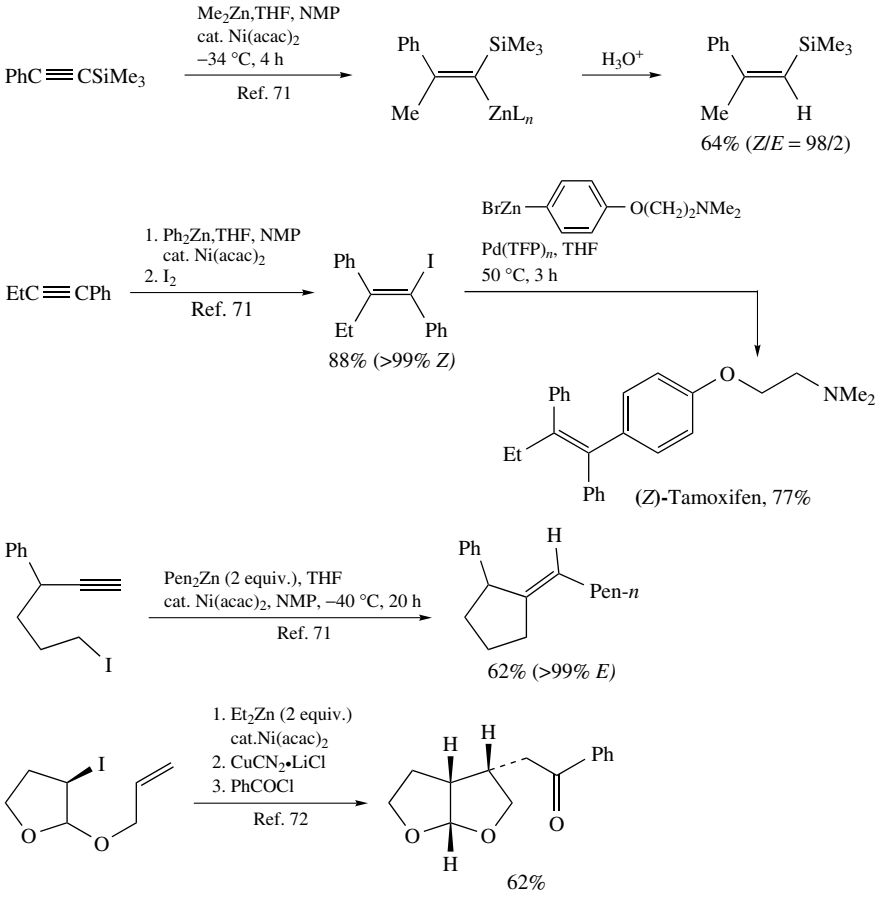

SCHEME 20. Ni-catalyzed carbozincation of alkynes and alkenes

Also promising are both intermolecular and intramolecular carbozincation of alkynes catalyzed by $Ni(acac)_2$ in THF-NMP. The intramolecular cyclic carbozincation has also been observed with ω-iodo-1-alkenes (Scheme 20).

7. Other methods of preparation of organozincs

There are some other methods of preparation of organozincs that are discrete from any of the above-described methods, as shown in Scheme 21.

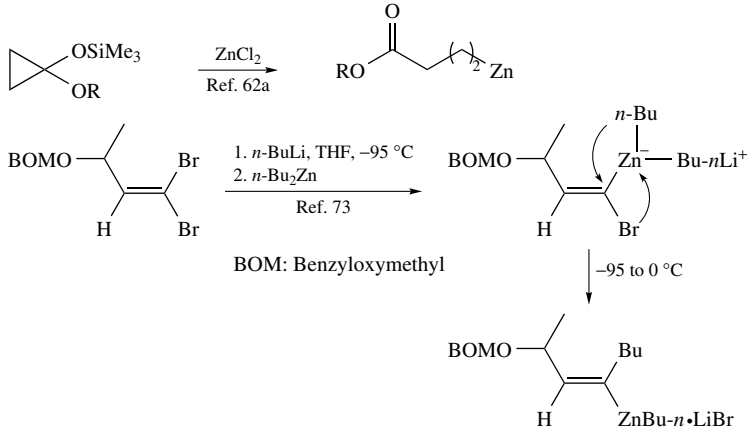

SCHEME 21. Other methods of preparation of organozincs

B. Leaving Groups (X)

In the 1970s, the Pd-catalyzed cross-coupling was mostly performed with organic iodides, and less frequently with bromides. Organic chlorides were rarely used, and fluorides were used even less frequently or perhaps almost never. It is important to realize that, in any Pd- or Ni-catalyzed cross-coupling, the oxidative addition of Pd or Ni to organic halides or related electrophiles may be considered as the initiation step and that coordination or binding of Pd or Ni to the organic moiety of the organic electrophiles is the crucial microstep of the oxidative addition. It is not unreasonable to visualize the mechanisms of oxidative addition of Pd to alkenyl and alkyl electrophiles, as depicted in Scheme 22[74]. These mechanisms may be appropriately modified for the oxidative addition of Ni complexes and for aryl, alkynyl, benzyl and propargyl electrophiles. These mechanisms explain nicely the retention of configuration for the cases of alkenyl electrophiles and the inversion for the reactions of allyl electrophiles. More importantly, these mechanisms clearly indicate that the reactivity of organic electrophiles must depend critically not only on the leaving groups (X) but also on the carbon groups (R^2 in equation 1). As a rule of thumb, the order of reactivity of various C groups is as follows.

$$\boxed{\text{Allyl} \geq \text{Propargyl} > \text{Benzyl, Acyl} > \text{Alkenyl} \geq \text{Alkynyl} > \text{Aryl} >> \text{Alkyl}}$$

With a given C group, the approximate order of reactivity of the leaving group (X) is as follows.

$$\boxed{\text{I} > \text{OTf} > \text{Br} > \text{Cl} > \text{F}}$$

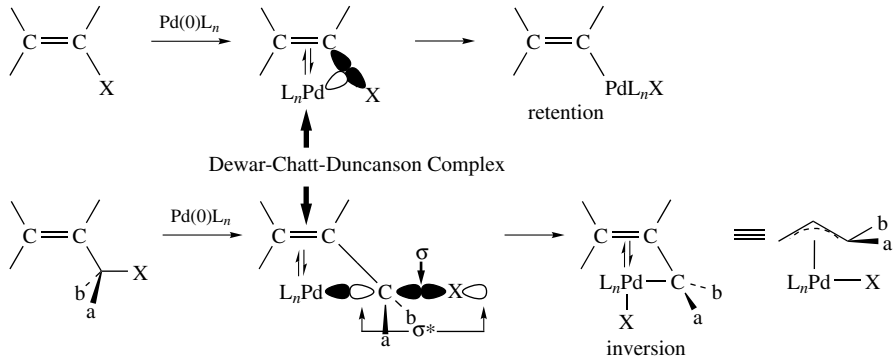

SCHEME 22. Proposed mechanisms for oxidative addition of Pd to alkenyl and allyl electrophiles

Thus, a wide variety of allylic derivatives including those with I, Br, Cl, OAc, $OAlMe_2$, $OPO(OEt)_2$, OSO_2Ph, OSO_2Me and even $OSiMe_3$ as leaving groups can participate in various Pd-catalyzed allylation[75], and most, if not all, of these groups can also serve as leaving groups in the Pd-catalyzed propargylation[76] (Scheme 23).

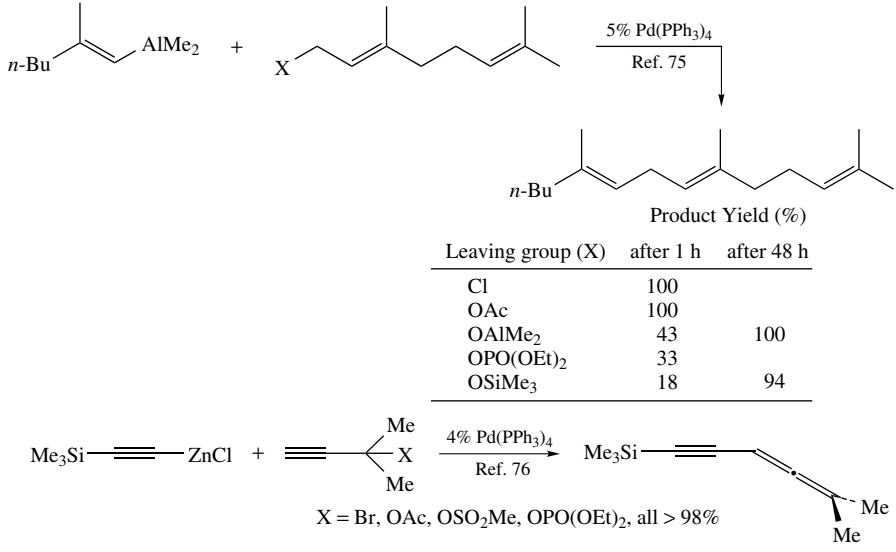

SCHEME 23. Pd-catalyzed allylation and propargylation with various leaving groups

For oxidative addition of Pd to alkenyl, aryl and alkynyl electrophiles, most of the leaving groups listed in Scheme 23 are ineffective. Primarily for economic reasons, intensive investigations have been made to successfully employ bromides and chlorides over the past 10–15 years. This topic is discussed throughout those sections discussing recent developments. Therefore, only a brief discussion of some fundamentally important points will be presented here. In the oxidative addition of Pd(0) complexes, the Pd complexes serve primarily as nucleophiles for their Pd(0)-to-Pd(II) oxidation. This predicts that those

Pd complexes containing electron-rich ligands would be more effective in the oxidative addition of Pd (or Ni). However, the overall cross-coupling process is generally considered to involve transmetallation and reductive elimination or their equivalents and alternatives. In any case, some reductive process must be involved for the entire process to be catalytic in Pd or Ni. In such processes, electron-deficient ligands must be generally favored over electron-rich ligands. Consequently, the effects of ligands in oxidative and reductive steps are generally opposite to each other. On balance, the use of Pd complexes containing arylphosphines has been shown to be a reasonable compromise. In dealing with those electrophiles that are less reactive in oxidative addition, it had long been known that more nucleophilic alkylphosphines would more readily undergo oxidative addition with organic bromides and chlorides, but they were less effective in an overall sense in the Pd- or Ni-catalyzed cross-coupling. This long-standing dilemma was resolved through the use of very bulky alkylphosphines and other electron-donating ligands, such as *N*-heterocyclic carbenes, NHC hereafter. Today, three halogens, i.e. I, Br and Cl, as well as oxygenated leaving groups, such as OTf, OTs and so on, are all widely used, as detailed throughout this chapter.

C. Pd or Ni Catalysts and Ligands (L)

If one considers oxidative addition of Pd or Ni species to organic electrophiles as the initiation step in the Pd- or Ni-catalyzed cross-coupling, Pd or Ni species must be either introduced to the reactor as Pd(0) or Ni(0) species or *in situ* converted to such species. Except in the form of atomic or oligomeric Pd(0) or Ni(0) vapor, metallic Pd(0) or Ni(0) species are polymeric and of insufficient reactivity. Various forms of metallic Pd or Ni including Pd or Ni on carbon or other supports fall into this category. So, essentially all of the Pd or Ni precatalysts including so-called 'ligand-less' complexes are mononuclear or oligonuclear ligand-stabilized complexes, the great majority of which are Pd–phosphine or Ni–phosphine complexes. In many ways, the choice of ligands including their design, preparation and application has played one of the central roles in the development of the Pd- or Ni-catalyzed cross-coupling, especially over the last couple of decades. A brief history of evolution of the catalysts or ligands (L) for the Pd- or Ni-catalyzed cross-coupling of organometals containing Zn along with a limited number of examples involving Mg, Al and Zr is presented below.

1. Triphenylphosphine as an inexpensive and widely applicable prototypical phosphine

In the 1970s, most of the Pd- or Ni-catalyzed cross-coupling reactions were performed with Pd–PPh_3 or Ni–PPh_3 complexes represented by $Pd(PPh_3)_4$, $Ni(PPh_3)_4$, $Pd(PPh_3)_2Cl_2$ and $Ni(PPh_3)_2Cl_2$. As a rule, Pd(0) or Ni(0) complexes tend to be unstable and of relatively short shelf life. In fact, $Ni(PPh_3)_4$ most probably is not commercially available, and it must be generated as needed. Although $Ni(PPh_3)_2Cl_2$ is relatively inexpensive (*ca* \$1,000/mol), $Pd(PPh_3)_4$ and $Pd(PPh_3)_2Cl_2$ are typically ten to twenty times as expensive as $Ni(PPh_3)_2Cl_2$. Some of the least expensive anhydrous Pd(II) salts include $Pd(OAc)_2$, $PdCl_2$ and $PdBr_2$, and the *in situ* generation of $Pd(PPh_3)_2Cl_2$ and $Pd(PPh_3)_4$ as shown in Scheme 24[77,78] may be recommended as one of the most economical, convenient and cleanest procedures for *in situ* generation of these complexes, which can also be applied to the preparation of many other Pd and Ni complexes as well.

Nickel(II) salts, such as $NiCl_2$, $NiBr_2$ and $Ni(acac)_2$, are commercially available in anhydrous form as inexpensive compounds ($\leqslant$\$200–300/mol), and some others, such as $Ni(OAc)_2{\cdot}4H_2O$ and $Ni(NO_3)_2{\cdot}6H_2O$, are also inexpensive but available only as hydrates. Recently, Ni(II) on C was prepared from $Ni(NO_3)_2{\cdot}6H_2O$ and charcoal and used as needed

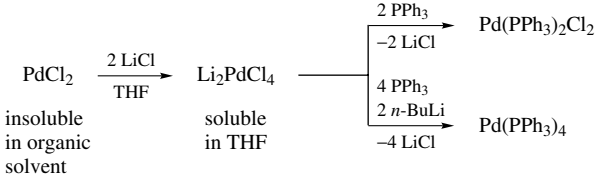

SCHEME 24. Economical and convenient *in situ* generation of $Pd(PPh_3)_2Cl_2$ and $Pd(PPh_3)_4$

by treating it with PPh_3 (4 equiv.) and *n*-BuLi (2 equiv.) in THF[79, 80]. Of all commercially available phosphines, PPh_3 appears to be by far the least expensive one ($33/mol). Therefore, it should be the ligand of choice in cases where it is satisfactory.

2. Sterically and electronically modified monodentate triarylphosphines, such as tris(2-furyl)phosphine and tris(o-tolyl)phosphine

Essentially all triarylphosphines other than PPh_3 are significantly more expensive than PPh_3. Even so, some sterically and electronically modified monodentate triarylphosphines, such as tris(*o*-tolyl)phosphine (TTP)[81a] and tris(2-furyl)phosphine (TFP)[81b], have exhibited catalytic reactivities that are clearly superior to those of PPh_3 in many demanding cases of cross-coupling, such as α-alkenylation of α-haloenones[82].

3. Bidentate bis(α,ω-diphenylphosphino)alkanes, bis(1,1′-diphenylphosphino)ferrocene (dppf), bis(o,o′-diphenylphosphino)phenyl ether (DPEphos) and related chelating phosphines

A series of Pd complexes containing bis(α,ω-diphenylphosphino)alkanes, such as $Pd(dppe)Cl_2$, $Pd(dppp)Cl_2$, $Pd(dppb)Cl_2$, where dppe, dppp, dppb are $Ph_2P(CH_2)_nPPh_3$ with ethylene, trimethylene and tetramethylene tethers, respectively, were reported in the 1960s and 1970s[74]. Another important bidentate ligand introduced in the 1980s[83] is bis(1,1′-diphenylphosphino)ferrocene (dppf) (**1**). Another group of bidentate triarylphosphines that have exhibited superior reactivities include bis(*o*,*o*′-diphenylphosphino)phenyl ether (DPEphos) (**2**)[84]. These chelating ligands, especially **1** and **2**, have proved to be very useful in a wide range of cross-coupling reactions where some widely used monodentate phosphines, such as PPh_3 and TFP, were shown to be less than satisfactory. For example, *trans*-selective monosubstitution of 1,1-dibromo-1-alkenes with alkynyl-[85], aryl-[86] and alkenylzincs[87] has been satisfactorily performed with dppf and DPEphos as ligands, as detailed later.

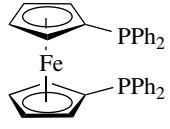

dppf (**1**)

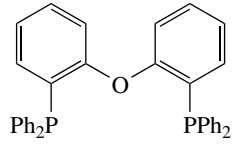

DPEphos (**2**)

Another important, if expected, recent finding with these bidentate ligands is that the catalyst turnover numbers (TON) observable with $Pd(dppf)Cl_2$ and $Pd(DPEphos)Cl_2$ are consistently higher than those observed with Pd catalysts containing monodentate ligands, such as PPh_3 and TFP[63]. In a comparative study using Zn, Mg, B, Al, In, Sn, Zr, Cu and

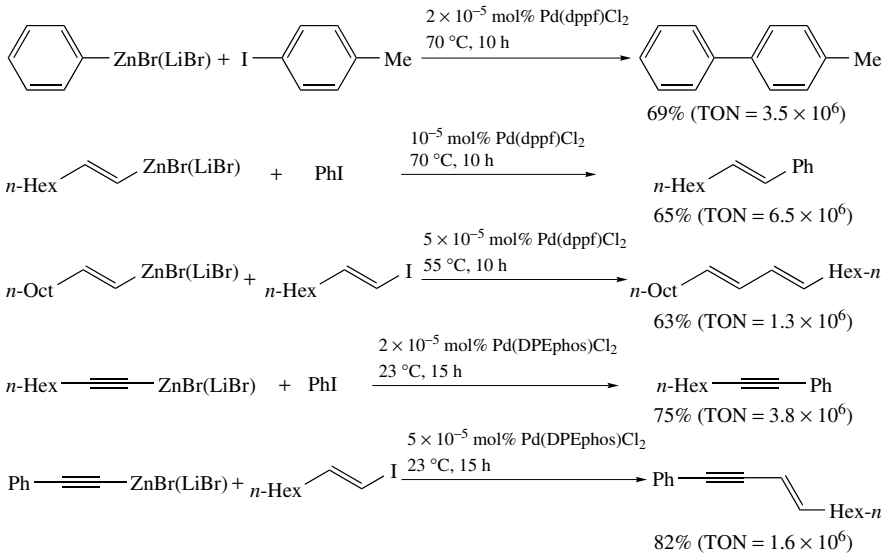

SCHEME 25. High turnover numbers observed in the Pd-catalyzed cross-coupling with $Pd(dppf)Cl_2$ or $Pd(DPEphos)Cl_2$ as a catalyst

Mn, the highest TONs were observable with Zn as the countercation. Some of the high TONs observed in the Pd-catalyzed cross-coupling reactions of organozincs are shown in Scheme 25[63].

4. Bulky trialkyl- and dialkylarylphosphines

Although some bulky trialkylphosphines have been known for a long time, their usefulness in many previously difficult cases of the Pd- or Ni-catalyzed cross-coupling, such as those involving organic bromides and chlorides, especially alkyl bromides and chlorides, and alkylmetals, has been demonstrated mainly within the past several years. Some representative examples of alkyl-containing phosphines are shown in Figure 1.

Pioneering studies with trialkylphosphines by Fu and coworkers[88] and with dialkylarylphosphines by Buchwald and coworkers[89] have provided solutions to many pending problems of the Pd-catalyzed cross-coupling, such as those shown in Scheme 26. Applications of bulky alkyl-containing phosphines are further discussed also in later sections.

5. Non-phosphine ligands

Prior to the development of the Pd-catalyzed alkylation with bulky alkylphosphines as ligands, Knochel and coworkers[90] reported that the reaction of Et_2Zn with 5-bromo-3-butyl-1-pentene catalyzed by Ni(acac)–LiI would give the alkyl–alkyl coupling product in 82% yield, while the corresponding reaction of 1-bromo-3-ethylheptane only produced the corresponding alkylzinc reagent in $\geqslant$85% yield[90] (Scheme 27).

This has led to the discovery of electron-deficient styrenes, such as those shown in Figure 2. As detailed later, these ligands have been shown to be effective for the Ni-catalyzed alkylation of organozincs with primary alkyl iodides and bromides[91]. More recently, Fu[88k] has reported that a catalyst consisting of $Ni(COD)_2$ and *s*-Bu-Pybox (**3**) is satisfactory even for the reaction of primary alkylzincs with secondary alkyl bromides

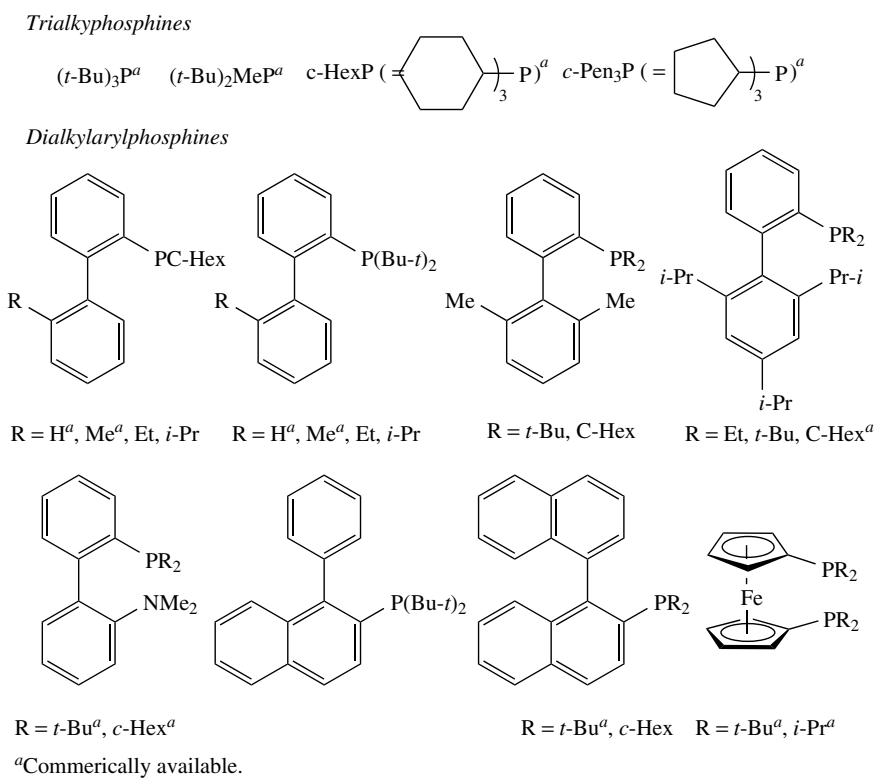

FIGURE 1. Representative examples of trialkyl- and dialkylarylphosphines

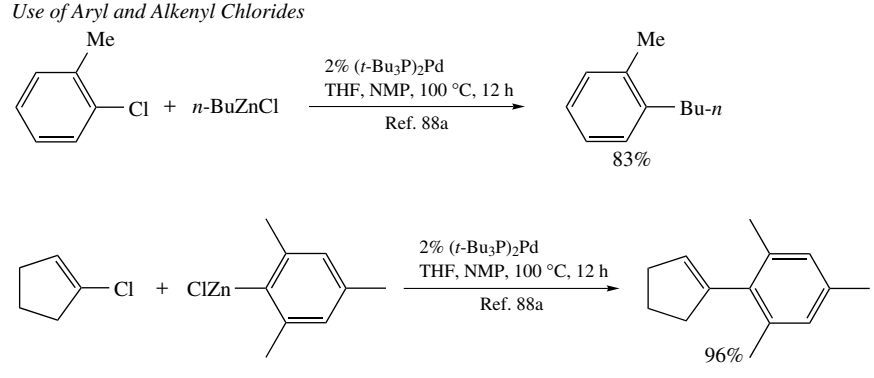

SCHEME 26. Use of bulky trialkylphosphines for Pd-catalyzed alkylation

Use of Alkyl Electrophiles Containing I, Br, Cl, and OTs

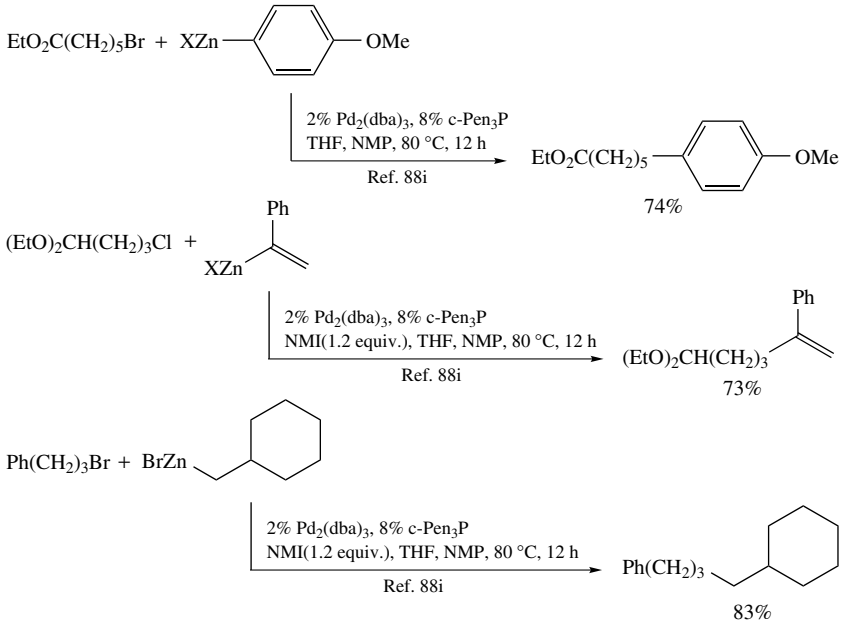

Use of Alkylzincs and 2-Bromo-1,3-dienes, 2-Bromo-1,3-enynes, or α-Bromostyrenes

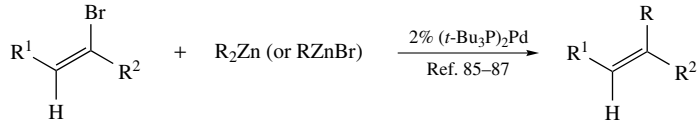

excellent yields, retention of configuration

R^1 = Alkyl, Alkenyl, Aryl, Alkynyl etc. R^2 = Alkenyl, Aryl, Alkynyl

R = Me, Et, Higher Alkyl.

SCHEME 26. (*continued*)

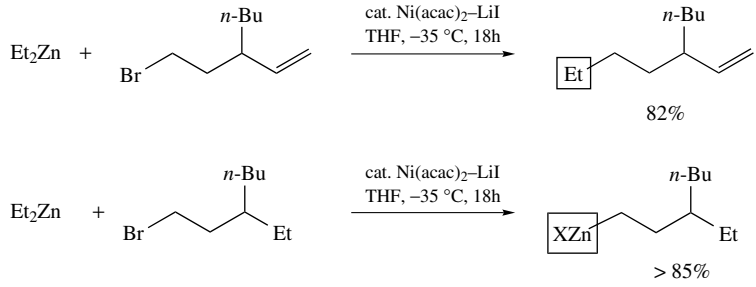

SCHEME 27. Effects of a proximal π-bond in the Ni-catalyzed reaction of Et_2Zn with alkyl bromides

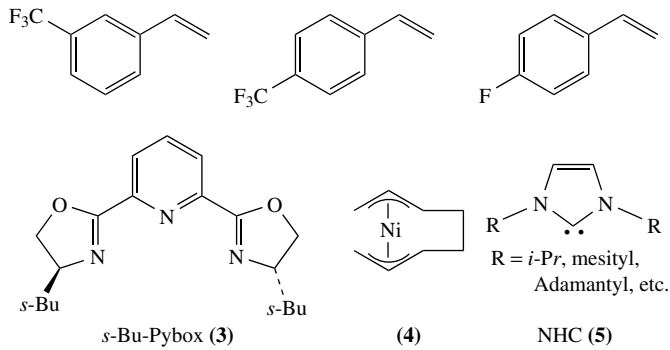

FIGURE 2. Non-phosphine ligands or complexes for Ni-catalyzed alkylation

and iodides. In 2002, Kambe, Terao and their coworkers[92] reported yet another version of the Ni-catalyzed coupling of alkylmagnesium halides with alkyl bromides, tosylates and even fluorides, but not chlorides in the presence of a catalytic amount of $NiCl_2$ and 1,3-butadienes. It has been suggested that the Ni-butadiene dimer complex **4** might be serving as a catalyst. It is possible that the Ni-catalyzed alkylation reactions of Knochel and Kambe share some common structural and mechanistic features. For various Pd- or Ni-catalyzed cross-coupling reactions, *N*-heterocyclic carbenes (NHC, **5**) have also been widely used, as discussed later for specific cases[93].

6. Binary ligand combinations

In view of the opposite electronic requirements for oxidative addition and reductive elimination in a catalytic cycle in the Pd- or Ni-catalyzed cross-coupling, the use of two or more ligands or their complex with Pd or Ni in a given Pd- or Ni-catalyzed cross-coupling reaction may be worth consideration. In attempts to overcome difficulties in achieving clean and high-yielding cross-coupling between alkenyl metals containing Al or Zr and (*E*)-1-iodo-2-bromoethylene, a dozen or more binary combinations of one Pd–phosphine complex and one free phosphine were screened. Also screened were $ZnBr_2$ and $InCl_3$ used as added cocatalysts. Strikingly, only one combination consisting of Pd(DPEphos)Cl_2, DIBAL-H and TFP (Tris(2-furyl)phosphine) in a 1:2:2 molar ratio along with the use of $InCl_3$, but not $ZnBr_2$, as a cocatalyst was satisfactory and by far superior to all of the other combinations tested[94]. Curiously, a complementary combination of Pd(TFP)$_2Cl_2$ and free DPEphos was far inferior to the Pd(DPEphos)Cl_2–TFP combination, thereby negating the initial assumption presented above. So, the results remain unexplained and mysterious. Nonetheless, the results are fully reproducible and the beneficial effects of the Pd(DPEphos)Cl_2–TFP–$InCl_3$ catalyst system appears to be widely and predictably observable.

Many additional new and useful developments will be made concerning catalysts and ligands for the Pd- or Ni-catalyzed cross-coupling in the near future, which will make this generally applicable synthetic methodology even more general. After all, the overall thermodynamics are favorable with few or possibly no exceptions. It is primarily a matter of devising kinetically favorable and selective paths from the starting compounds to the desired products.

D. Cocatalysts or Additives

Since the discovery of favorable effects exerted by $ZnCl_2$, $ZnBr_2$ and other metal salts in 1978[38], a fair number of other cocatalysts or additives have been found mostly for the Pd- or Ni-catalyzed cross-coupling reactions of organometals containing metals, such as B, Si, Sn and so on. Except for some solvents and related compounds, such as NMI, e.g. *N*-methylimidazole[88i], Zn salts including $ZnCl_2$ and $ZnBr_2$ have been the major and generally applicable cocatalysts for the Pd- or Ni-catalyzed cross-coupling with organometals containing Al and Zr. Since these Zn salts have been shown to be effective even in those cross-coupling reactions with B, Sn and Cu, they have been responsible for significantly expanding the synthetic scope of the Zn-based Pd- or Ni-catalyzed cross-coupling (Scheme 28).

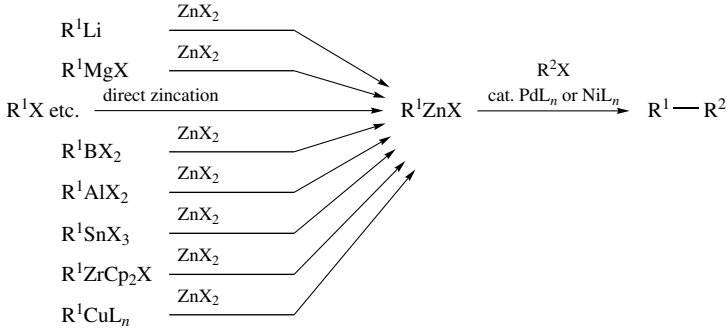

SCHEME 28. Zn-based protocols for the Pd- or Ni-catalyzed cross-coupling

In sharp contrast to the very reliable Pd-catalyzed monosubstitution of (*E*)-1-iodo-2-bromoethene with alkynylzincs[95–97], the corresponding reaction of alkenylmetals containing Al, Zr or Zn proved to be much more demanding, and these cases led to the development of two phosphine-containing catalyst systems[94] discussed in the preceding section. Also found in the same investigation was the unexpected reactivity of $InCl_3$ or $InBr_3$ added as a cocatalyst which was substantially superior to that of $ZnCl_2$ or $ZnBr_2$, as shown in Scheme 29. It should be noted that alkenylzincs generated via the corresponding alkenyllithiums are more reactive than the corresponding alkenylindiums prepared in a similar manner[94]. Some favorable synergistic effects must be operative in the Al–In and Zr–In systems.

E. Solvents

In most, if not all, of the transition metal-catalyzed organometallic reactions including the Pd- or Ni-catalyzed cross-coupling, solvents are not used merely to dissolve and dilute reactants and reagents. They often serve as cocatalysts or promoters and even reactants in a limited number of cases. More than 20 solvents have been used for the Pd- or Ni-catalyzed cross-coupling (Table 2). In the absence of any specific information, it is not unreasonable to choose first THF. Frequently, it is desirable to use one or more cosolvents typically for an increased level of solvent polarity and/or electron-donating ability. One of the most frequently used solvents for this purpose is DMF, but some others, such as NMP, pyridine and NMI (*N*-methylimidazole), have also been used frequently. In some extreme cases,

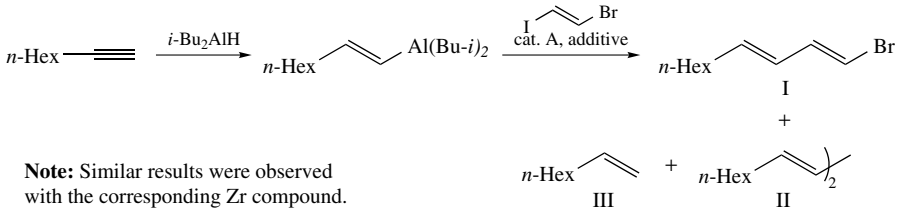

Note: Similar results were observed with the corresponding Zr compound.

Additive mol(%)	Temp. (°C)	Time (h)	I (%)	II (%)	III (%)
None	23	10	5	9	75
$ZnBr_2$ (100)	23	4	34	35	24
$InCl_3$ (10)	0	4	82	2	7

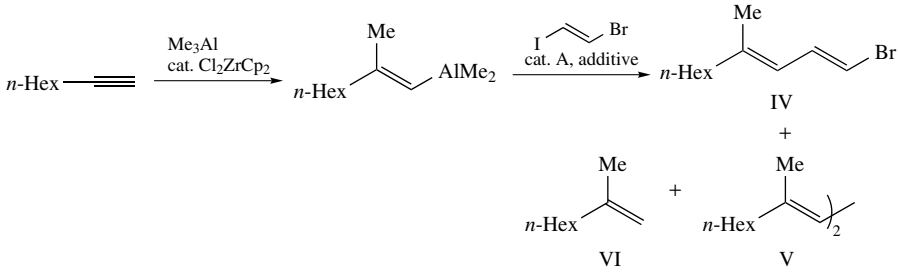

Additive mol(%)	Temp. (°C)	Time (h)	IV (%)	V (%)	VI (%)
None	0	10	4	trace	81
$ZnBr_2$ (100)	0	4	26	42	24
$InCl_3$ (34)	0	4	91	2	6

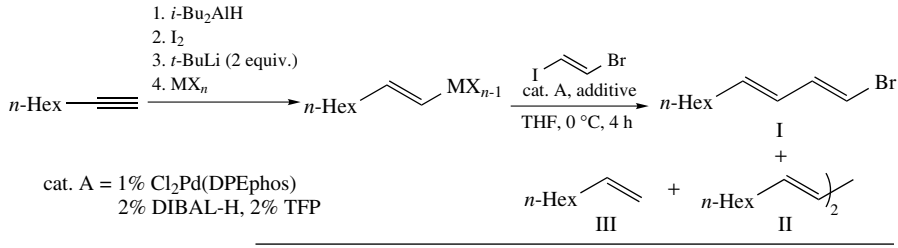

cat. A = 1% Cl_2Pd(DPEphos)
2% DIBAL-H, 2% TFP

MX_n	I (%)	II (%)	III (%)
$ZnBr_2$ (1.0 equiv.)	75	4	10
$InCl_3$ (0.34 equiv.)	67	16	12

SCHEME 29. Pd- and In-cocatalyzed cross-coupling of alkenylalanes with (*E*)-1-iodo-2-bromoethene

it might be desirable to fully replace THF or other less polar solvents for maximizing the effects of highly polar solvents. In some delicate cases, however, it might be more desirable to use less polar solvent for greater discrimination of two or more competing processes. For example, *trans*-selective monosubstitution of 1,1-dichloro-1-octene lacking

TABLE 2. Commonly used solvents for Pd- or Ni-catalyzed cross-coupling

Hydrocarbons	Halogenated hydrocarbons	Ethers	Amines	Nitriles and carbonyl compounds	Polar aprotic solvents	Alcohols and phenols	Water
Toluene Benzene	CH_2Cl_2 $CHCl_3$	**THF** Ether Dioxane	NEt_3 Pyridine NMI	MeCN Acetone EtOAc	DMF DMA DMSO HMPA NMP	MeOH EtOH *t*-BuOH Phenol	H_2O

any unsaturated substituent by using Pd(DPEphos)Cl_2 as a catalyst is a delicate reaction, which was shown to proceed much more selectively in ether than in THF in some cases (Scheme 30)[86].

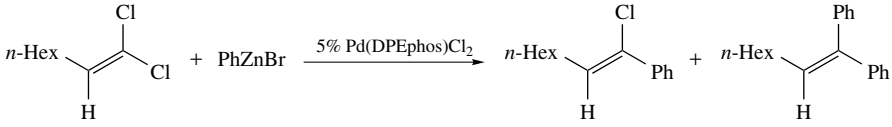

Solvent	Temp. (°C)	**SM**(%)	Yield (%) Mono	Di
THF	50	19	69	11
ether	reflux	2	94	4

SCHEME 30. Use of a less polar solvent for higher selectivity in Pd-catalyzed *trans*-selective monosubstitution of 1,1-dichloro-1-alkenes

III. RECENT ADVANCES IN THE Pd- OR Ni-CATALYZED CROSS-COUPLING WITH ORGANOMETALS CONTAINING Zn, Mg, Al AND Zr

In this section, notable recent advances in the Pd- or Ni-catalyzed cross-coupling between an arylmetal and an alkenyl electrophile is termed the aryl–alkenyl coupling. The complementary reaction of an alkenylmetal with an aryl electrophile that can produce the same cross-coupling products can then be termed the alkenyl–aryl coupling and distinguished from the aryl–alkenyl coupling. The order of discussion below more or less follows that employed in *Handbook of Organopalladium Chemistry for Organic Synthesis*[1].

A. Aryl–Aryl, Aryl–Alkenyl and Alkenyl–Aryl Coupling Reactions

1. Aryl–aryl coupling[13]

The Pd- or Ni-catalyzed aryl–aryl coupling as of several years ago was comprehensively reviewed[13,14]. Some special topics highlighted in these reviews include (a) Pd-catalyzed cross-coupling involving heteroaryl (or hetaryl) compounds[13b], (b) directed *ortho*-metallation–cross-coupling protocol[13c], (c) asymmetric biaryl synthesis[25] and (d) synthesis of naturally occurring biaryls and related compounds[26]. Discussion of those results that have already been presented in the reviews cited above will be kept at a minimum, and the readers are referred to these reviews.

As has often been stated, the Pd- or Ni-catalyzed aryl–aryl coupling can be achieved by using organometals containing ten or so different metals, but it has been most extensively carried out with those containing B, Zn, Mg and Sn, although the inherent toxicity

associated with organotins is an increasingly recognized concern to be dealt with. Arylmetals containing Si and a couple of other metals are promising. Until some such metals emerge as superior counteractions, B and Zn along with Mg should be considered first in most cases. In less demanding cases of aryl–aryl coupling, most, if not all, of ten or so metals will provide comparably satisfactory results. In more demanding cases, however, the superior reactivity, generally high yields and surprisingly high but often underappreciated chemoselectivity are some of the features associated with arylzincs, that will make Zn the metal of choice, while the robustness and ease of handling of areneboronic acids including their tolerance for air and moisture as well as high chemoselectivity represent the superior properties of arylboronic acids in the absence of added strong bases. It should however be noted that, in most cases, arylmetals containing Zn and B, especially the latter, are prepared from organometals containing Li or Mg. Since at least one of the two arylmetals used in the aryl–aryl coupling must be an arylmetal, their chemoselectivity is, in fact, often that of organometals containing Li or Mg. At present, arylzincs may well be more widely available by direct zincation without going through arylmetals containing Li or Mg than arylboronic acids.

a. Heterosubstituted arylzincs. In view of the discussion presented above, it is useful to note that a wide variety of heterofunctional arylzincs (Figure 3) and hetarylzincs (Figure 4) are known[98]. Since those shown in Figures 3 and 4 are excerpted from a table compiled in 1999[98], many more must be known today.

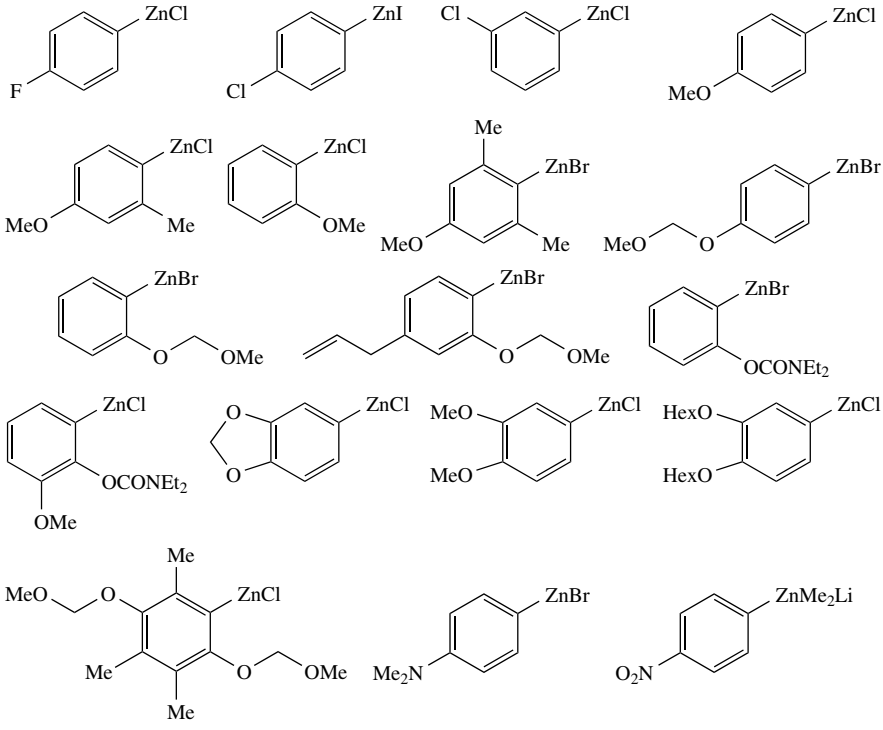

FIGURE 3. Heterofunctionally substituted arylzincs

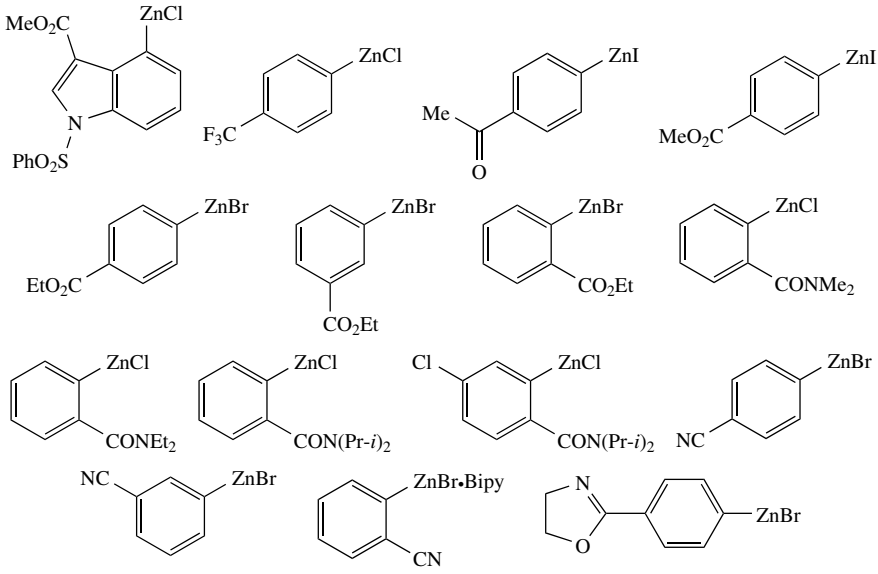

FIGURE 3. (*continued*)

Five-membered Hetarylzincs

• *With One Heteroatom in a Heterocycle*

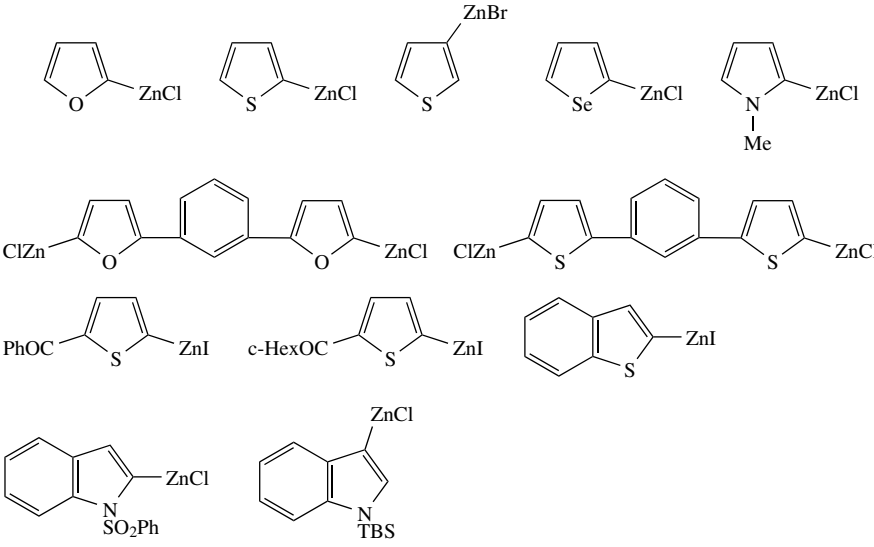

FIGURE 4. Hetarylzincs prepared in or before 1997

•With Two Heteroatoms in a Heterocycle

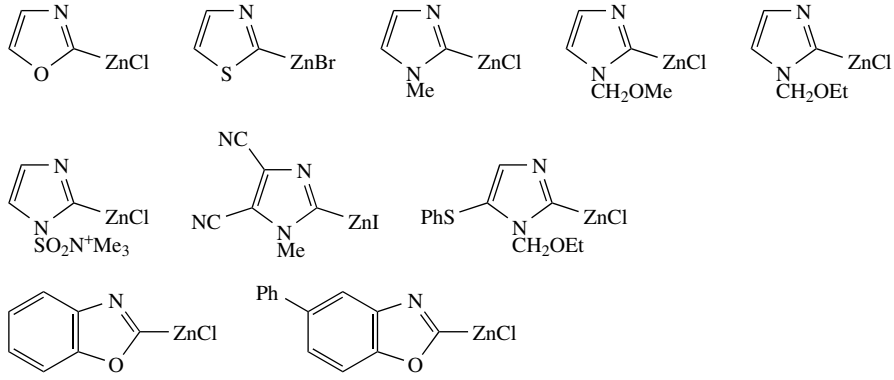

Six-membered Hetarylzincs

•With One Heteroatom in a Heterocycle

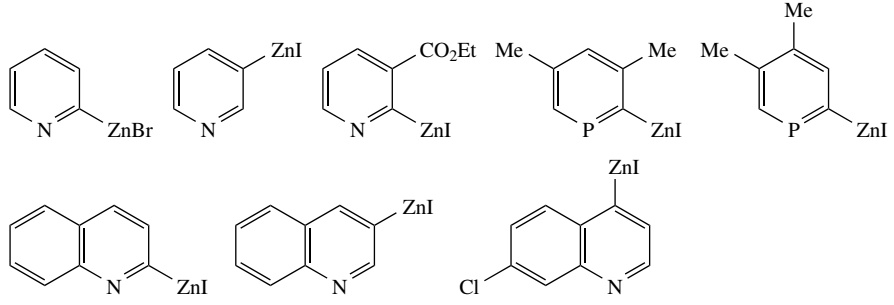

•With Two Heteroatoms in a Heterocycle

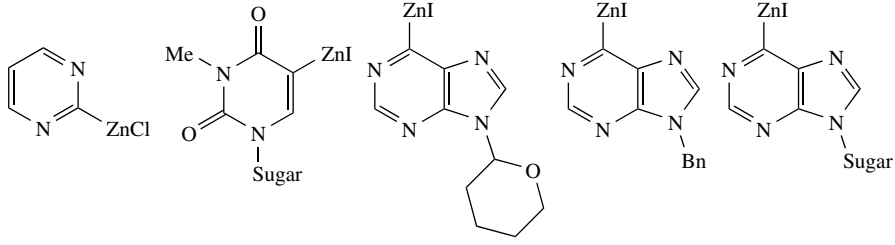

FIGURE 4. (*continued*)

b. Aryl chlorides. The Ni-catalyzed aryl–aryl coupling with arylmagnesiums[41,99] and the Ni- or Pd-catalyzed aryl–aryl coupling with arylzincs[33] have been known since the mid-1970s. Most of the earlier examples employed aryl iodides and bromides. Mainly for economical reasons, the use of aryl chlorides is desirable. Although rare, both Ni and Pd catalysts were successfully used for the reaction of arylmagnesium derivatives with aryl chlorides as early as 1980[100]. Since around 1998, a number of notable developments

have been made on the Pd- or Ni-catalyzed cross-coupling with aryl chlorides. It does appear that, at least for cross-coupling two robust aromatic groups using one aryl chloride, the Ni–Mg combination may well be intrinsically more favorable than others, which may represent another possible manifestation of the hard and soft acids and bases principle. Nonetheless, other metal countercations, notably Zn[101] and B[9e, 102], have also been successfully used in the Ni- or Pd-catalyzed aryl–aryl coupling with aryl chlorides. As discussed earlier, highly reactive hindered trialkylphosphines[88], dialkylarylphosphines[89] and NHC (**5**)[93] have collectively provided solutions to the long-pending problem of how to promote generally slow oxidative addition reactions of aryl chlorides without retarding other microsteps, e.g. reductive elimination, of the Pd- or Ni-catalyzed cross-coupling.

c. Asymmetric synthesis of biaryls[25]. Aryl–aryl coupling of any kind offers an exciting possibility of preparing some of their sterically hindered members as stereoisomerically pure atropisomers. Attempts to synthesize optically active biaryls by the reaction of 2-substituted naphthylmagnesium bromide with the corresponding naphthyl bromide were made as early as 1975[103], but the products displayed disappointingly low enantiomeric excesses of $\leqslant$13%. In the late 1980s, Hayashi and coworkers dramatically improved the enantioselectivity to 95% ee (Scheme 31)[104a]. This study has clearly established the viability of the asymmetric cross-coupling approach to the synthesis of stereoisomerically pure chiral biaryls, even though it should be extensively developed further to establish it as a general and satisfactory method. More recent investigations with arylborons are also known[9e].

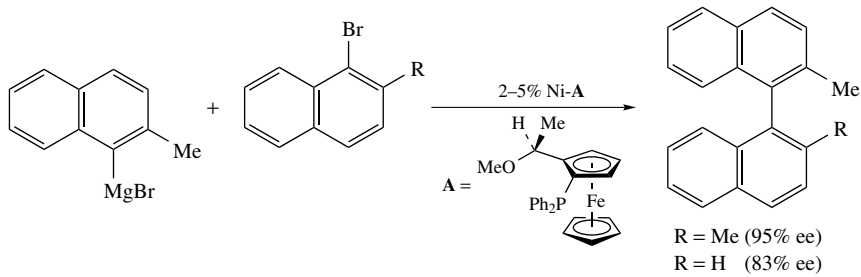

SCHEME 31. Ni-catalyzed asymmetric synthesis of biaryls

Another interesting and promising approach is what has been termed as *enantiopositionselective asymmetric cross-coupling* exemplified in Scheme 32[104b–d]. Owing to statistical enantiomeric amplification through kinetic resolution of monosubstituted isomeric products, a relatively high enantioselectivity range of 90–99% ee was attained along with excellent product yields of $\geqslant$87%, except in one case.

2. Aryl–alkenyl and alkenyl–aryl coupling[7,14,22–24]

Aryl–alkenyl and alkenyl–aryl coupling reactions lie between aryl–aryl and alkenyl–alkenyl coupling reactions. Since these two reactions can give the same cross-coupling products, the task of their synthesis is more flexible and hence somewhat less demanding. In cases where the required alkenylmetals are readily preparable as the first-generation organometals via hydrometallation, carbometallation and other methods, the alkenyl–aryl coupling route may, a priori, be favored. After all, a large number of aryl halides and related electrophiles are commercially available. This fact also favors

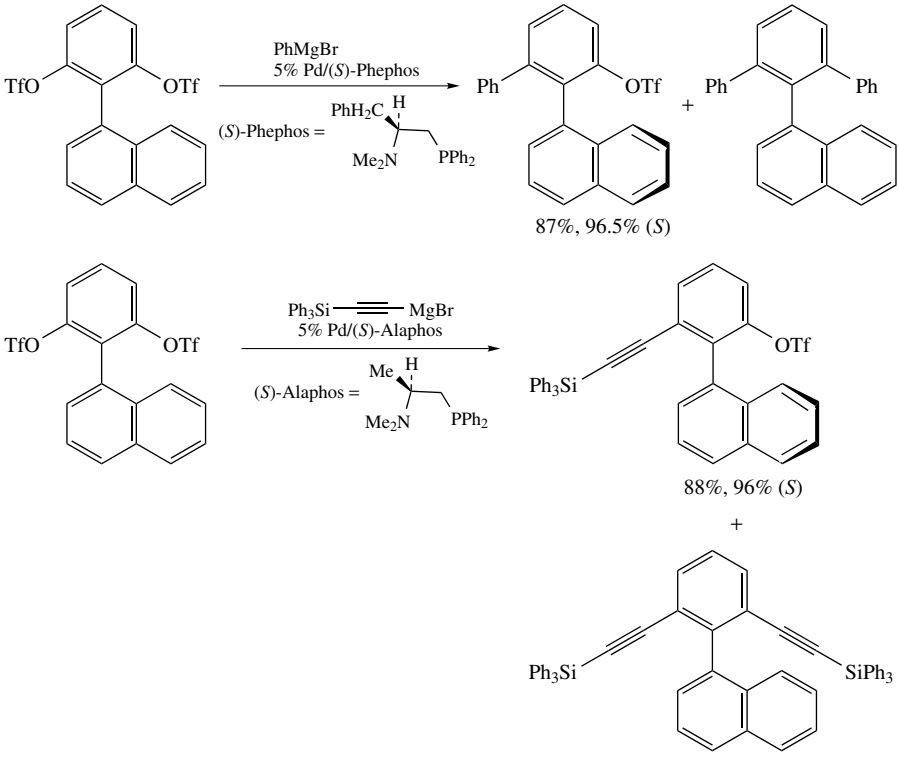

SCHEME 32. Pd-catalyzed enantioposition-selective synthesis of atropisomeric biaryls

the alkenyl–aryl coupling. In many other cases, however, alkenyl halides may be more readily available than the corresponding alkenylmetals. In such cases, the generally higher reactivity of alkenyl halides in their oxidative addition with Ni- or Pd-complexes as compared with that of aryl halides tends to favor the aryl–alkenyl coupling route, although other factors might prove to be also important. Examples of alkenyl halide synthons excerpted from the literature including reviews[7, 14, 22–24] cited above are shown in Figure 5.

Some of the notable recent developments in the Pd- or Ni-catalyzed aryl–alkenyl and alkenyl–aryl coupling reactions include the use of aryl and alkenyl chlorides along the lines of earlier discussions. Just a couple of representative examples of the aryl–alkenyl coupling reaction with alkenyl chlorides are shown in Scheme 33.

In the examples shown in Scheme 33, the main concern was how to elevate the reactivity of organic chlorides in the Pd- or Ni-catalyzed coupling. In the Pd- or Ni-catalyzed selective stepwise double cross-coupling of 1,1-dihalo-1-alkenes containing Br and Cl, on the other hand, the main problem is how to prevent unwanted disubstitution during the first substitution, for at least two reasons. Firstly, 1,1-dihalo-1-alkenes are substantially more reactive than similarly structured monohalo-1-alkenes, since the two geminal halogen atoms mutually activate both carbon–halogen bonds, but the one that is *trans* to the carbon substituent reacts preferentially, presumably for steric reasons. The products of the first substitution, when isolated, are relatively unreactive internal (*Z*)-monohaloalkenes. Mechanistically, however, the initially formed products of the first substitution must be Pd or Ni π-complexes of the (*Z*)-monohaloalkenes that are poised to undergo the second

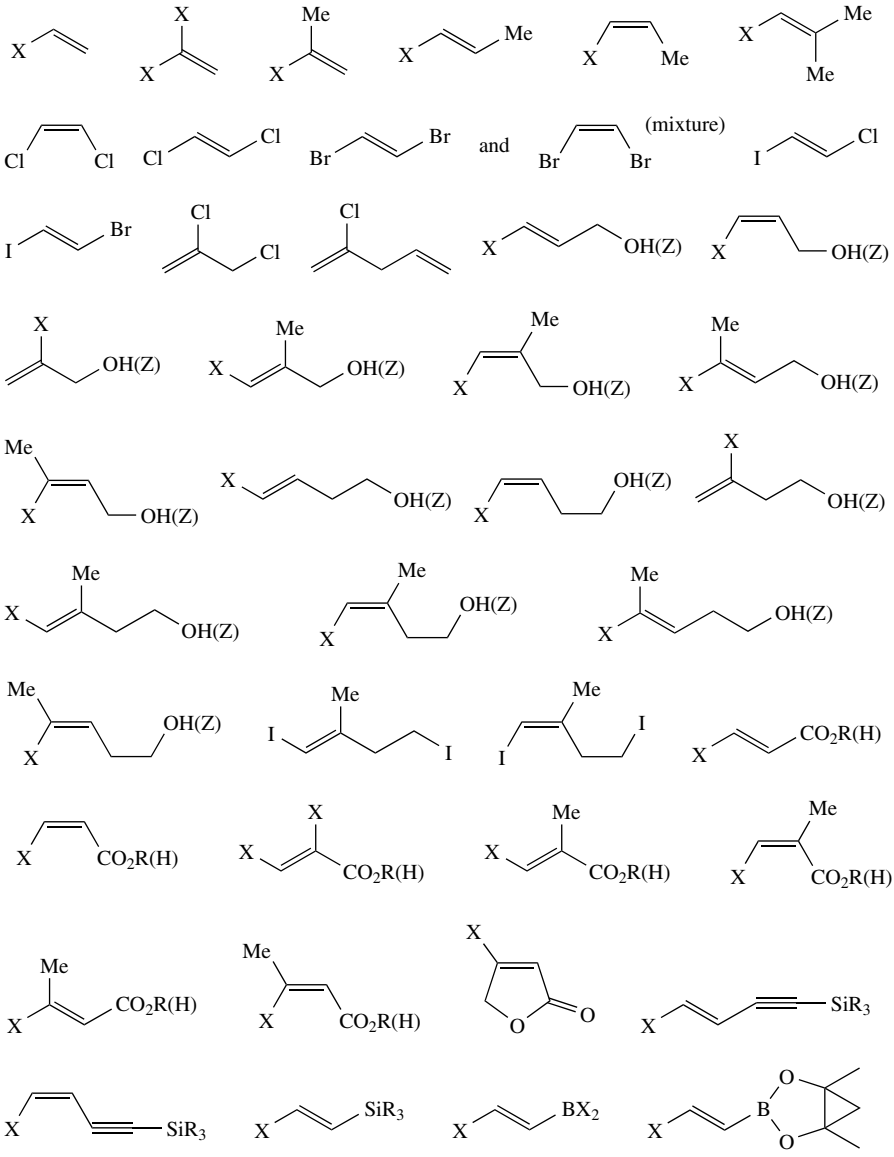

X = I, Br, Cl etc. Z = Hydroxyl-protecting groups. R = Me, Et etc.

FIGURE 5. Alkenyl halide synthons used for Pd- or Ni-catalyzed alkenylation

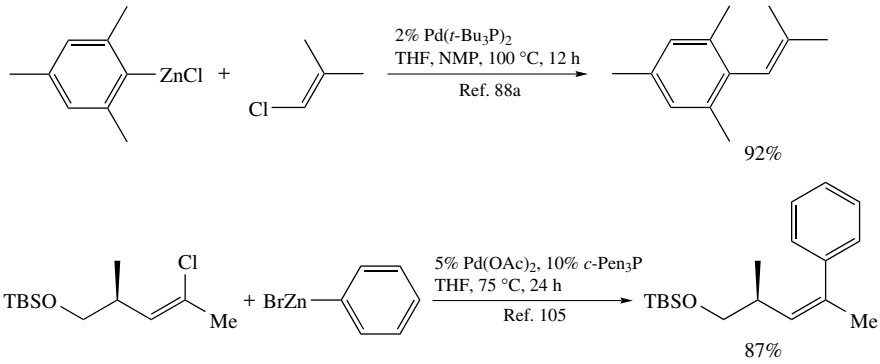

SCHEME 33. Pd-catalyzed aryl–alkenyl coupling reactions with alkenyl chlorides

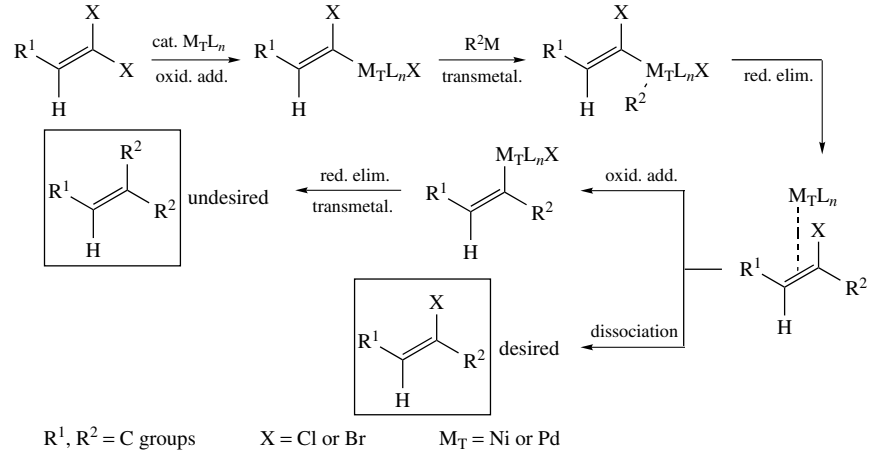

SCHEME 34. Probable mechanistic paths for mono- and disubstitution reactions of 1,1-dihalo-1-alkenes

oxidative addition, which must significantly accelerate the unwanted second substitution that is to be avoided (Scheme 34).

The *trans*-selective monosubstitution and the separate subsequent second substitution with different organometals were investigated by Tamao[106] in 1987 with β,β-dichlorostyrenes. Although many subsequent investigations led to the development of synthetically useful *trans*-selective monosubstitution processes, the unexpectedly intricate second substitution and the overall scope of the mono- and disubstitution of 1,1-dihalo-1-alkenes have been developed and clarified only within the last several years. As the most exciting results pertain to the alkenyl–alkenyl coupling, the detailed discussion will be presented later in the following section.

The Pd-catalyzed aryl–alkenyl and alkenyl–aryl coupling reactions involving Zn, Al and Zr have been applied to the syntheses of a fair number of natural products[26]. Recent examples published in the last several years include the syntheses of UB-165[107] and (−)-diazonamide A[108] (Scheme 35).

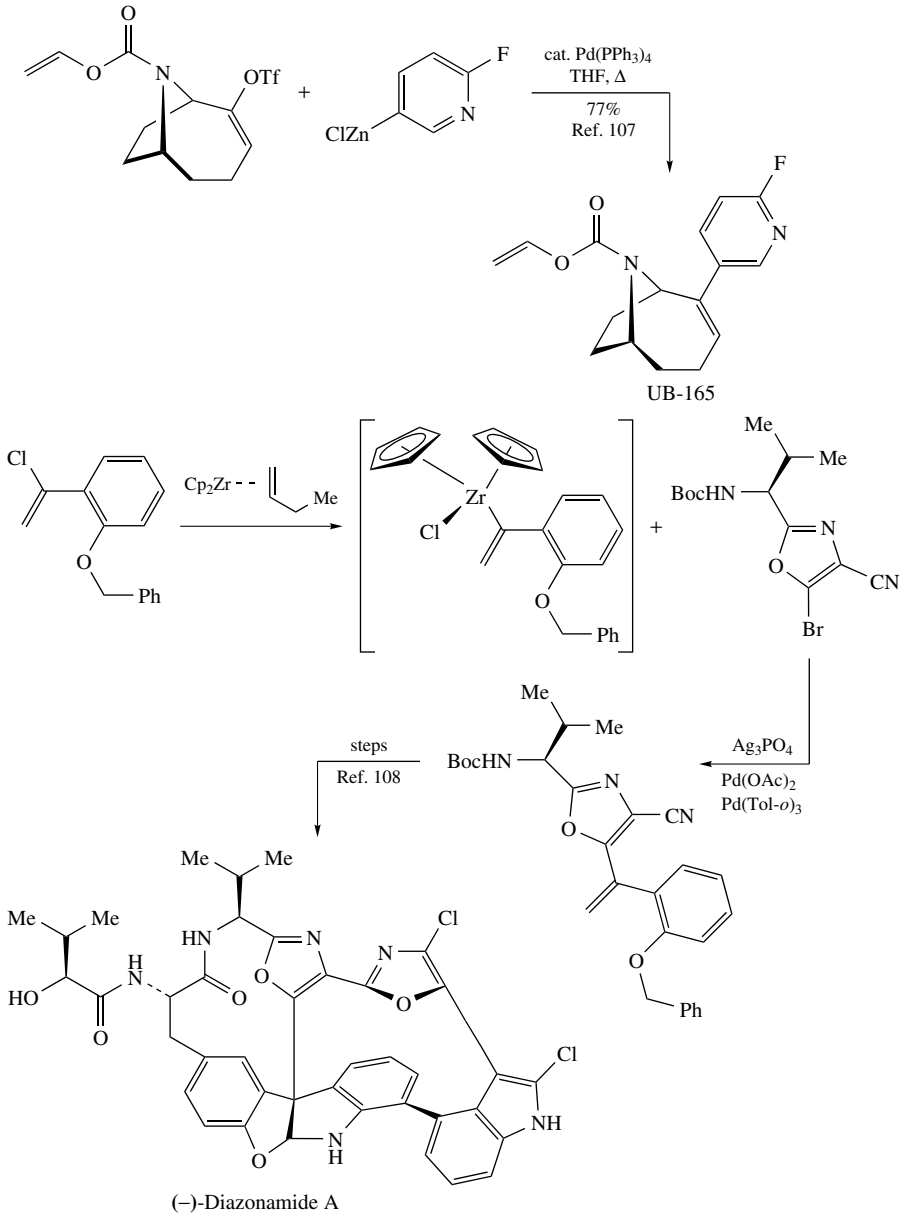

SCHEME 35. Recent syntheses of natural products via Pd-catalyzed aryl–alkenyl or alkenyl–aryl coupling

B. Alkenyl–Alkenyl Coupling[6,7,14,24]

1. Overview

Alkenyl and allyl groups containing olefinic π-bonds represent some of the most reactive groups towards Pd and Ni. With delicate regio- and stereochemical features associated with them, they also represent some of the most intricate functional groups that can lead to many unexpected phenomena. As in other cases, it is important to be able to use relatively inexpensive alkenyl chlorides. However, some other features, such as stereoselectivity, regioselectivity, yields and catalyst turnover numbers, tend to be more important in the alkenyl–alkenyl coupling than in most of the other cross-coupling reactions, and the use of more expensive alkenyl iodides and bromides may readily be justified in many delicate cases of alkenyl–alkenyl coupling. One of the earliest reports of the Pd-catalyzed cross-coupling shown in Schene 3 clearly demonstrated that Pd catalysts can be distinctly superior to Ni catalysts with respect to stereoselectivity[32]. The great majority of the currently known cases of delicate alkenyl–alkenyl coupling have indeed been performed with Pd catalysts rather than their Ni analogues. The generally superior reactivity profile of alkenylzincs as well as the ability of Zn(II) compounds to cocatalyze and promote the Pd-catalyzed alkenylation of those alkenylmetals containing Li, Mg, B, Al, Sn, Zr and Cu reported as early as the 1970s[38] (Schemes 4 and 5) have been widely recognized and applied to the synthesis of dienes (Scheme 12). The *in situ* generation of alkenylmetals by hydro-, carbo- and heterometallation followed by the same-pot cross-coupling also introduced in the 1970s[31,32,34,38] has provided a previously undeveloped, convenient and selective methodology for the synthesis of alkenes, especially conjugated dienes. The Pd-catalyzed alkenyl–alkenyl coupling reaction either with alkenylzincs or with other alkenylmetals containing Al and Zr in the presence of Zn salts has been widely applied to the synthesis of conjugated diene-containing natural products both as their intermediates and as the final targets. Those that have been synthesized since 1995 are summarized in Table 3. The broken lines shown in the target structures indicate the points of cross-coupling. In cases where the nature of alkenyl–alkenyl cross-coupling is not clear, it is elaborated in Scheme 36.

2. Recent advances

Some recent methodological findings that have already been discussed earlier in this chapter include:

(a) the use of Pd complexes with chelating phosphines, such as dppf (**1**) and DPEphos (**2**), in the Pd-catalyzed cross-coupling including alkenyl–alkenyl coupling, for high catalyst TONs of $\geqslant 10^4 - 10^6$ (Scheme 25)[63],
(b) the use of a two-phosphine catalyst system consisting of 1% Pd(DPEphos)Cl_2, 2% DIBAL-H and 2% TFP as well as $InCl_3$ as a cocatalyst in the reaction of alkenylmetals containing Al or Zr with (*E*)-1-iodo-2-bromoethylene (Scheme 29)[94], and
(c) the stepwise double substitution of 1,1-dibromo-1-alkenes and 1,1-dichloro-1-alkenes. This last topic was briefly introduced in Section III.A but not discussed in detail. So, its full discussion is presented below with emphasis on the Pd-catalyzed *trans*-selective monoalkenylation to produce (*Z*)-2-halo-1,3-dienes and their subsequent cross-coupling to give trisubstituted alkenes.

A systematic investigation of the *trans*-selective monosubstitution of a variety of 1,1-dibromo-1-alkenes has established that their reaction with alkenyl-[87], alkynyl-[85] and arylzincs[86] in the presence of 1–5 mol% Pd(DPEphos)Cl_2 provides a generally applicable and satisfactory procedure (Scheme 37). For most cases, THF is a reasonably satisfactory

TABLE 3. Pd-catalyzed alkenyl–alkenyl coupling involving Al, Zr and Zn in the synthesis of natural products

Year	Natural Product	Countercation (cocatalyst)	Major Author	Reference
1995	Papulacandin D	Zr	Barrett, A. G. M.	109
1996	Discodermolides	Zn	Schreiber, S. L.	110
1996	Zaragozic acid C	Zn	Paterson, I.	111
1996	Nakienone B	Zn	Negishi, E.	112
1997	Nakienone A	Zn	Negishi, E.	82b
1997	Gadain and Savinin	Zn	Rossi, R.	113
1998	Okinonellin B	$Al(ZnCl_2)$	Romo, D.	114
1998	(±)-Carbacyclin	Sn→I→Li→Zn	Negishi, E.	82c
1999	Lissoclinolide	Zr	Negishi, E.	115
1999	Reveromycin B	$Zr(ZnCl_2)$	Theodorakis, E. A.	116
2000	Pitiamide A	$Zr(ZnCl_2)$	Wipf, P.	117
2000	Xerulin	$Zr(ZnCl_2)$	Negishi, E.	95
2001	β-Carotene	$Al(ZnCl_2)$	Negishi, E.	97
2001	γ-Carotene	$Al(ZnCl_2)$	Negishi, E.	97
2001	Eunicenone A	$Zr(ZnCl_2)$	Corey, E. J.	118
2001	FR901464 (antitumor antibiotics)	$Zr(ZnCl_2)$	Jacobsen, E. N.	119
2002	Motuporin	$Zr(ZnCl_2)$	Panek, J. S.	120
2004	*cis*- and *trans*-Bupleurynol	Zr	Organ, M. G.	121
2004	(−)-Callystatin A	$Zr(ZnCl_2)$	Panek, J. S.	122
2004	6,7-Dehydrostipiamide	Zn	Negishi, E.	123
2004	Xerulinic acid	Sn → Li → Zn	Brückner, R.	124

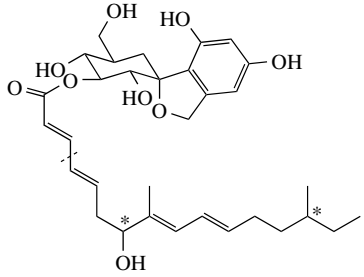

Papulacandin D

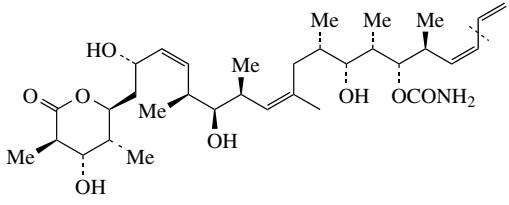

Discodermolides

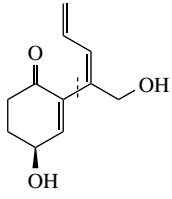

Nakienone B

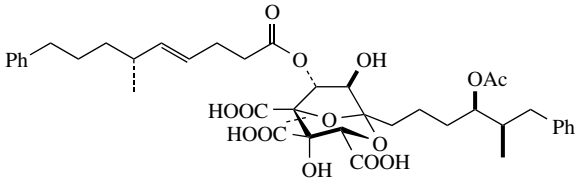

Zaragozic acid C

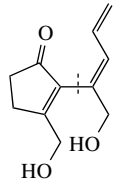

Nakienone A

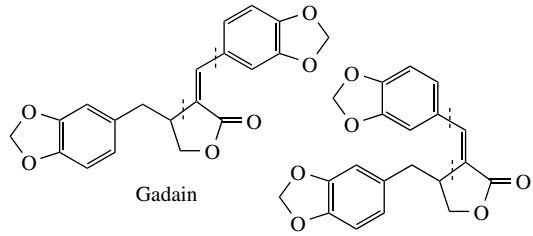

Gadain Savinin

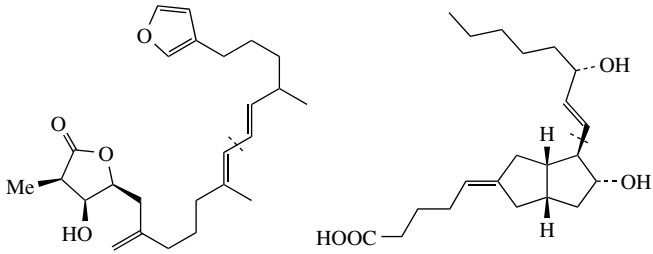

Okinonellin B Carbacyclin

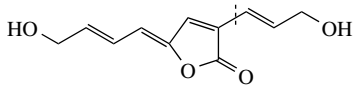

Lissoclinolide

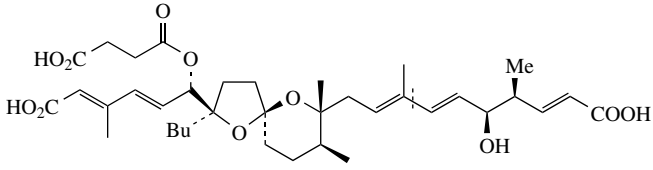

Reveromycin B

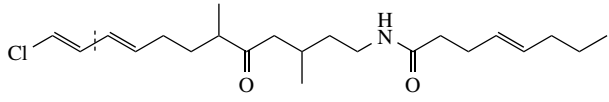

Pitiamide A

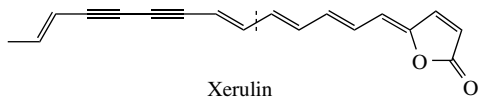

Xerulin

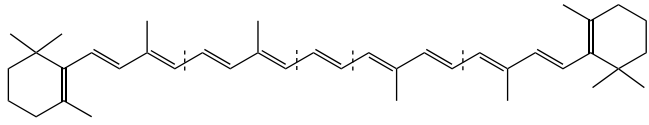

β-Carotene

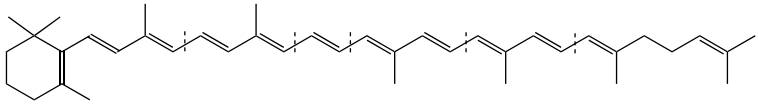

γ-Carotene

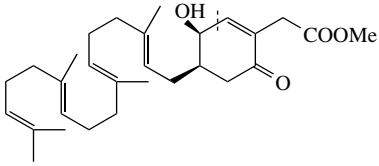

Eunicenone A

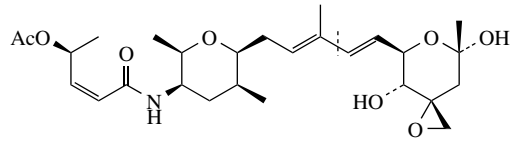

FR901464 (antitumor antibiotics)

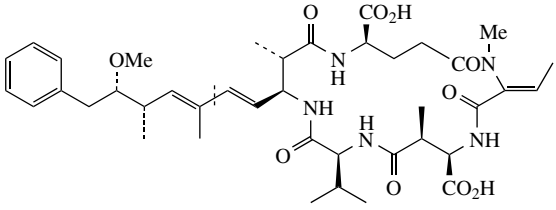

Motuporin

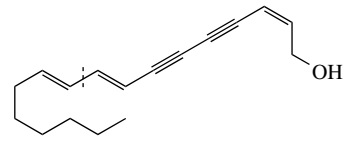

cis-Bupleurynol

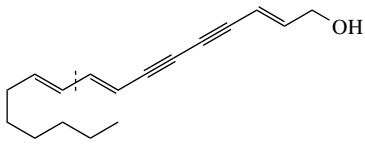

trans-Bupleurynol

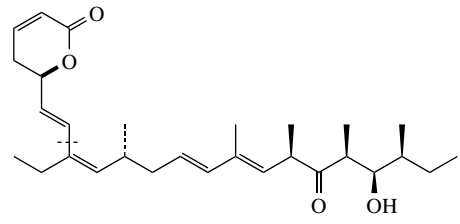

(−)-Callystatin A

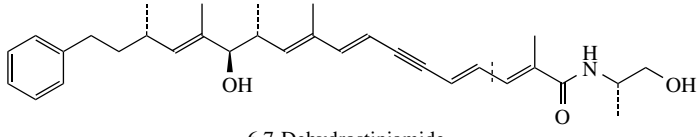

6,7-Dehydrostipiamide

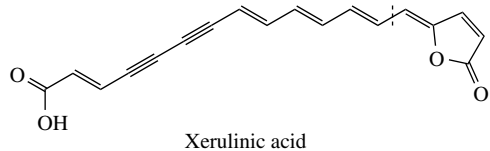

Xerulinic acid

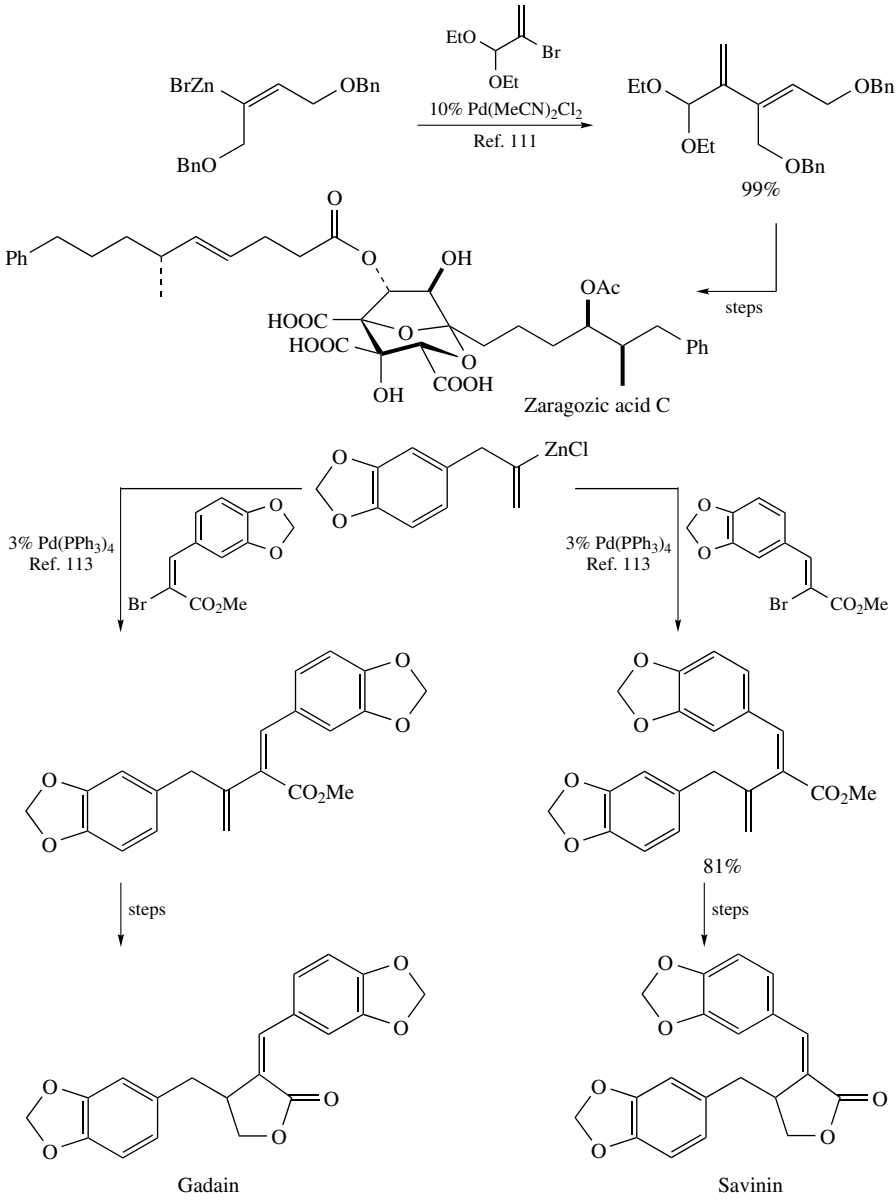

SCHEME 36. Some recent examples of the synthesis of natural products and related compounds by the Pd-catalyzed alkenyl–alkenyl coupling

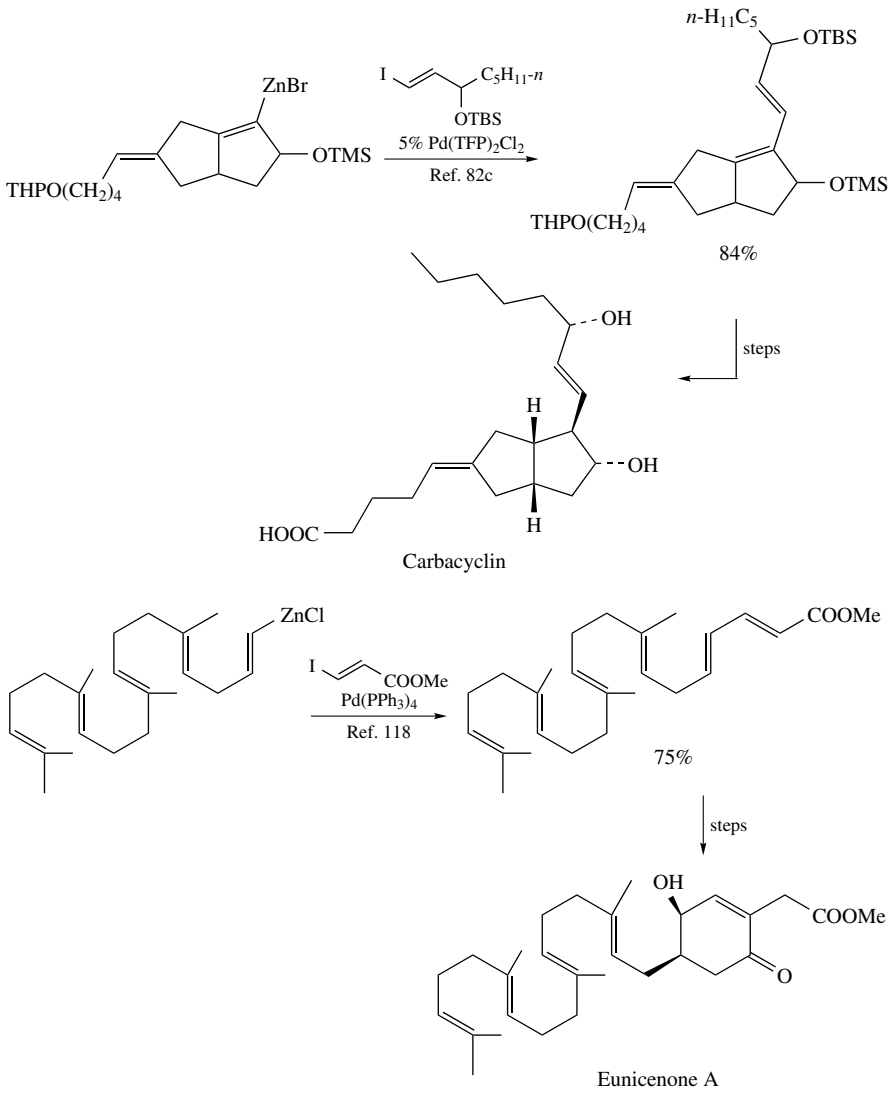

SCHEME 36. (*continued*)

solvent. This procedure is also generally satisfactory for the corresponding reactions of 1,1-dichloro-1-alkenes. As already shown in Scheme 30, ether is more satisfactory than THF for monophenylation of certain 1,1-dichloro-1-alkenes.

The second substitution of 1,1-dibromo-1-alkenes involved the Pd-catalyzed cross-coupling reactions of **6–8** obtained as shown in Scheme 37. Quite unexpectedly, the reaction of **6a** with MeZnBr in the presence of several Pd-phosphine catalysts produced the expected cross-coupling products of $\geqslant$95% stereoisomeric purity in 76–91% yields, but careful 1D NOE analyses have firmly established that the reaction was accompanied

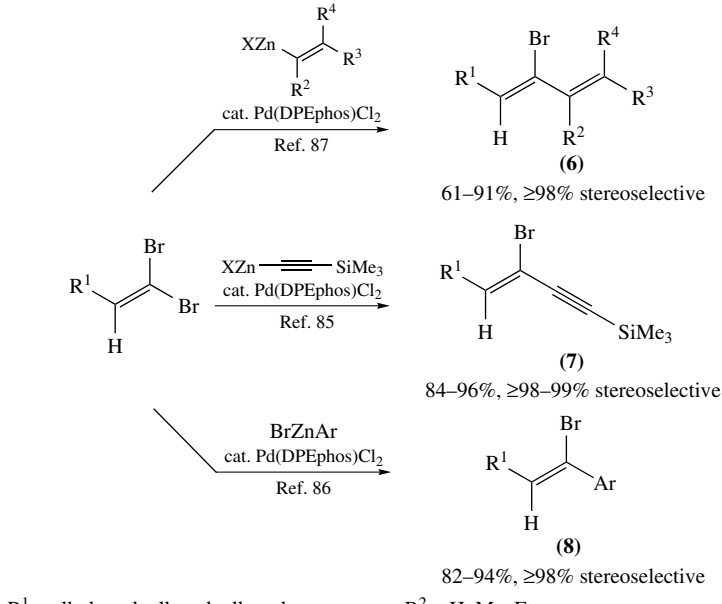

SCHEME 37. *trans*-Monosubstitution of 1,1-dibromo-1-alkenes with alkenyl-, alkynyl- and arylzincs in the presence of Pd(DPEphos)Cl_2 as a catalyst

by clean inversion of configuration. With either Pd(DPEphos)Cl_2 or Pd(dppf)Cl_2 as a catalyst, the products were $\geqslant$97–98% inverted (Scheme 38)[125]. This clean inversion was observable with various R^5ZnX in which R^5 was Me, Et, *n*-Bu, Ph, $H_2C{=}CH$ and $HC{\equiv}C$. It may tentatively be concluded that the observed stereoinversion has little or nothing to do with R^5 and that it is general with respect to R^5. On the other hand, it is inhibited by the presence of an alkenyl or alkynyl group as R^1, while an aryl group in the same position partially inhibits stereoisomerization. As interesting as the stereoinversion reaction is, it is also desirable to prevent it for the production of the stereo-retained conjugated dienes. It has been found that the use of Pd(PBu-t_3)$_2$, other bulky trialkylphosphine-containing Pd catalysts and $Pd_2(dba)_3$–NHC complexes permits full retention ($\geqslant$98%) of configuration (Scheme 38)[87].

A recent synthesis of (−)-callystatin A[122] made use of the methylation of 2-bromo-1,3-dienes with retention of configuration by the use of Pd(PBu-t_3)$_2$ as a catalyst.

Although the mechanism of stereoinversion is not yet clear, the $\pi-\sigma-\pi$ mechanism widely accepted for the stereoisomerization of allylpalladium derivatives cannot operate in this case, since the concerted $\pi-\sigma-\pi$ mechanism should be accompanied by a stereoinversion of the second double bond, which has not been observed. The observed inversion of only the bromine-bearing C=C bond may involve a dipolar mechanism shown in Scheme 39[7]. This mechanism needs to be experimentally supported, however.

The second-stage substitution with retention under the catalytic influence of Pd(PBu-t_3)$_2$ or a related Pd–alkylphosphine complex can also be performed with **7**[85] and **8**[86] in $\geqslant$98% selectivity.

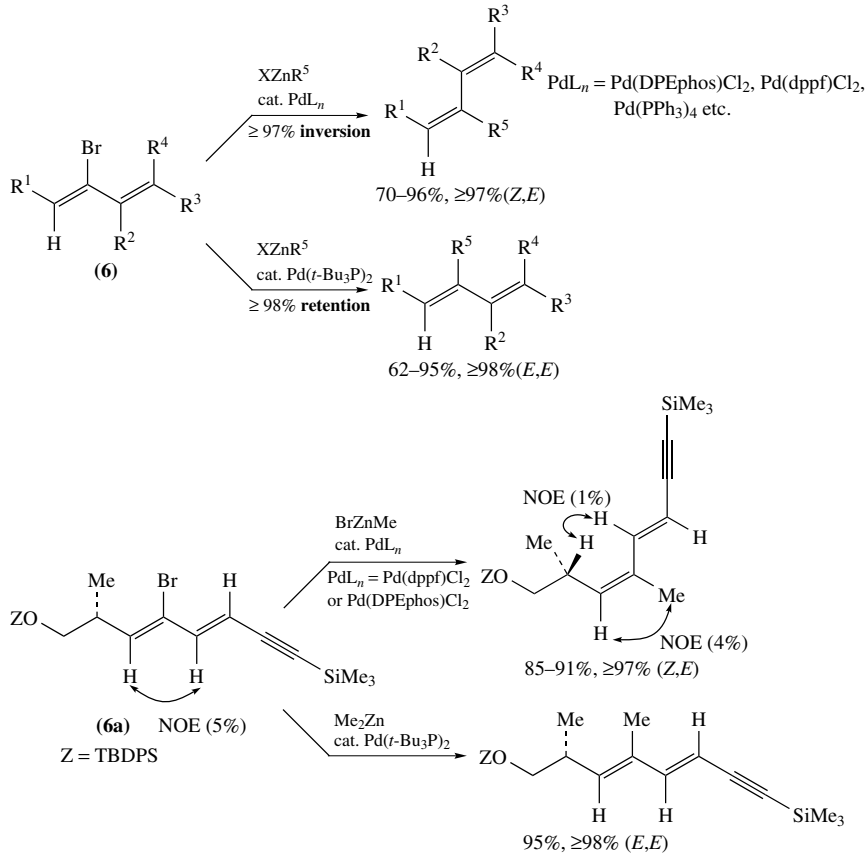

SCHEME 38. Pd-catalyzed coupling reactions of 2-bromo-1,3-dienes with or without stereoinversion

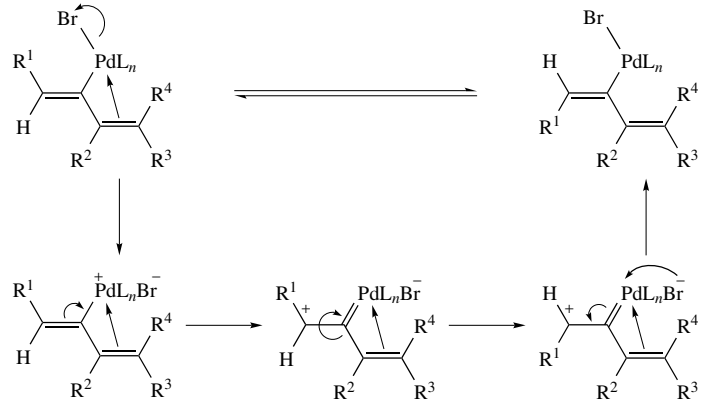

SCHEME 39. A probable mechanism for stereoisomerization of 2-pallada-1,3-dienes

C. Pd-catalyzed Alkynylation

1. General discussion

The Pd-catalyzed alkynylation is one of the most widely used C−C bond formation reactions. It has been thoroughly and extensively reviewed recently[15−17]. So only a brief overview and a discussion of some of the most recent advances will be presented in this section. As in the case of alkenyl−alkenyl coupling, Ni catalysts have rarely been used for alkynylation, even though Ni catalysts do affect the desired alkynylation in some cases. One main reason for disfavoring Ni is that Ni can readily react with alkynes to undergo alkyne cyclooligomerization represented by arene formation. The Pd-catalyzed alkynylation can, in principle, be performed in three discrete manners, as shown in Scheme 40.

Protocol I *Use of Terminal Alkynes*

Heck Alkynylation [15, 126]

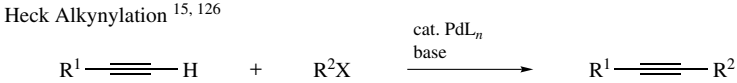

Sonogashira Alkynylation[16]

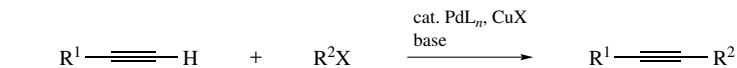

Protocol II *Use of Preformed Alkynylmetals*

M = Zn, Mg, B, Al, In, Si, Sn, Mn, Cu etc.

Protocol III *Use of Alkynyl Halides and Other Electrophiles*

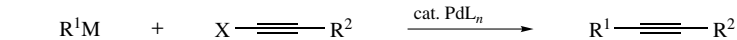

SCHEME 40. Three discrete protocols for Pd-catalyzed alkynylation

a. Comparison of various protocols for Pd-catalyzed alkynylation. Currently, the most widely used is the Sonogashira version of the Heck alkynylation (Protocol I). It combines the operational simplicity of the Heck alkynylation and a wider synthetic applicability stemming from the use of Cu cocatalysts. It should be noted, however, that the Heck alkynylation is just as satisfactory as the Sonogashira version in many cases. It is therefore advisable to initially run both reactions and compare the results. Although both Heck and Sonogashira alkynylation reactions are satisfactory in many less-demanding cases, a number of limitations have also been noted in recent years. In many of these 'more-demanding' cases, the use of preformed organometallic reagents has provided either outright solutions or superior alternatives. This point has not yet been widely recognized, but some of the notable major differences should be noted and taken advantage of.

i. Availability of two complementary protocols. With the use of preformed organometals, alkynes can be prepared through the use of either Protocol II or Protocol III. In a growing number of cases, Protocol III can come to the rescue in cases where Protocol II is fundamentally unsuitable. The Heck−Sonogashira methodology lacks this flexibility. The Pd-catalyzed alkynylation of alkylzincs with IC≡CSiMe$_3$[127] shown in equation 2 exemplifies the advantages of Protocol III. The use of 1-iodo- and 1-bromo-1-alkynes reported

as early as 1978[38] has previously been reported mostly for the Pd-catalyzed aryl–alkynyl and alkenyl–alkynyl coupling reactions[15].

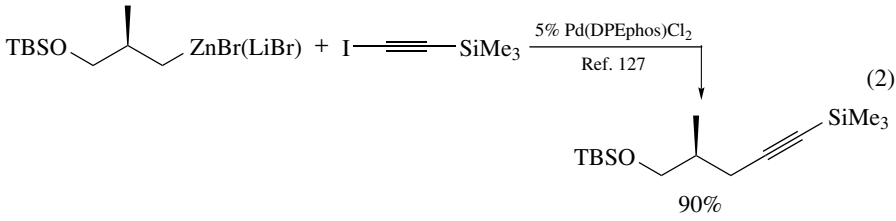

(2)

ii. Direct synthesis of terminal alkynes by the use of ethynylmetals. Direct ethynylation with acetylene by Heck–Sonogashira alkynylation has not been satisfactory due to competitive and extensive disubstitution of acetylene. This difficulty can be readily avoided or minimized by the use of ethynylmetals, especially ethynylzincs[15, 35, 36, 95, 128–130] (Scheme 41).

iii. Pd-catalyzed alkynylation with alkynes containing electron-withdrawing substituents. The Pd-catalyzed alkynylation with alkynes containing electron-withdrawing substituents by Sonogashira alkynylation tends to be unsatisfactory. The corresponding reactions of alkynylzincs have generally proceeded very well[15, 127, 131, 132] (Scheme 41).

iv. Use of alkenyl electrophiles that are prone to side reactions. Whereas monoalkynylation of 1,2-dichloroethylene by the Sonogashira alkynylation is generally satisfactory[15, 133], the corresponding monoalkynylations of (*E*)-1-iodo-2-bromoethylene undergoes mainly alkyne dimerization. Indeed, alkyne dimerization is a rather frequently encountered side reaction in the Sonogashira alkynylation. The use of alkynylzincs can readily circumvent the difficulty[132] (Scheme 41).

The Sonogashira alkynylation of (*Z*)-β-iodoacrylic acid is accompanied by synthetically useful cyclization to produce lactones[134]. In some favorable cases, this has provided an attractive route to (*Z*)-γ-alkylidene-γ-butenolactones, such as (+)-goniobutenolide A[137a], rubrolides A, C, D and E[128], a thiophenelactone from *Chamaemelum nobile L*[129], freelingyne[137b] and xerulin[95]. The synthesis of xerulin was efficiently and selectively achieved by using the Pd-catalyzed alkynylation with alkynylzincs five times, the above-mentioned lactonization by the Sonogashira alkynylation and the Pd-Zn cocatalyzed alkenyl–alkenyl coupling with an alkenylzirconium intermediate in a mere 5 steps in the longest linear sequence in 30% overall yield (Scheme 42).

Despite these favorable results, the Pd-catalyzed lactonization with alkyl-substituted alkynes generally gives unattractive mixtures of five- and six-membered lactones. In marked contrast, the Pd-catalyzed reaction of alkynylzincs with (*Z*)-β-iodoacrylic acid gives only the expected enynoic acids[135], which can then be selectively lactonized to give either five- or six-membered lactones[136] (Scheme 41).

v. Use of sterically hindered, relatively unreactive organic electrophiles. Under comparable reaction conditions, the Pd-catalyzed alkynylation with alkynylzincs tends to be significantly more facile than the corresponding Sonogashira alkynylation, as suggested by the results in Scheme 43[138].

b. Current scope of protocol II involving the use of preformed alkynylmetals. Palladium-catalyzed alkynylation with preformed alkynylmetals has been performed with ten to a

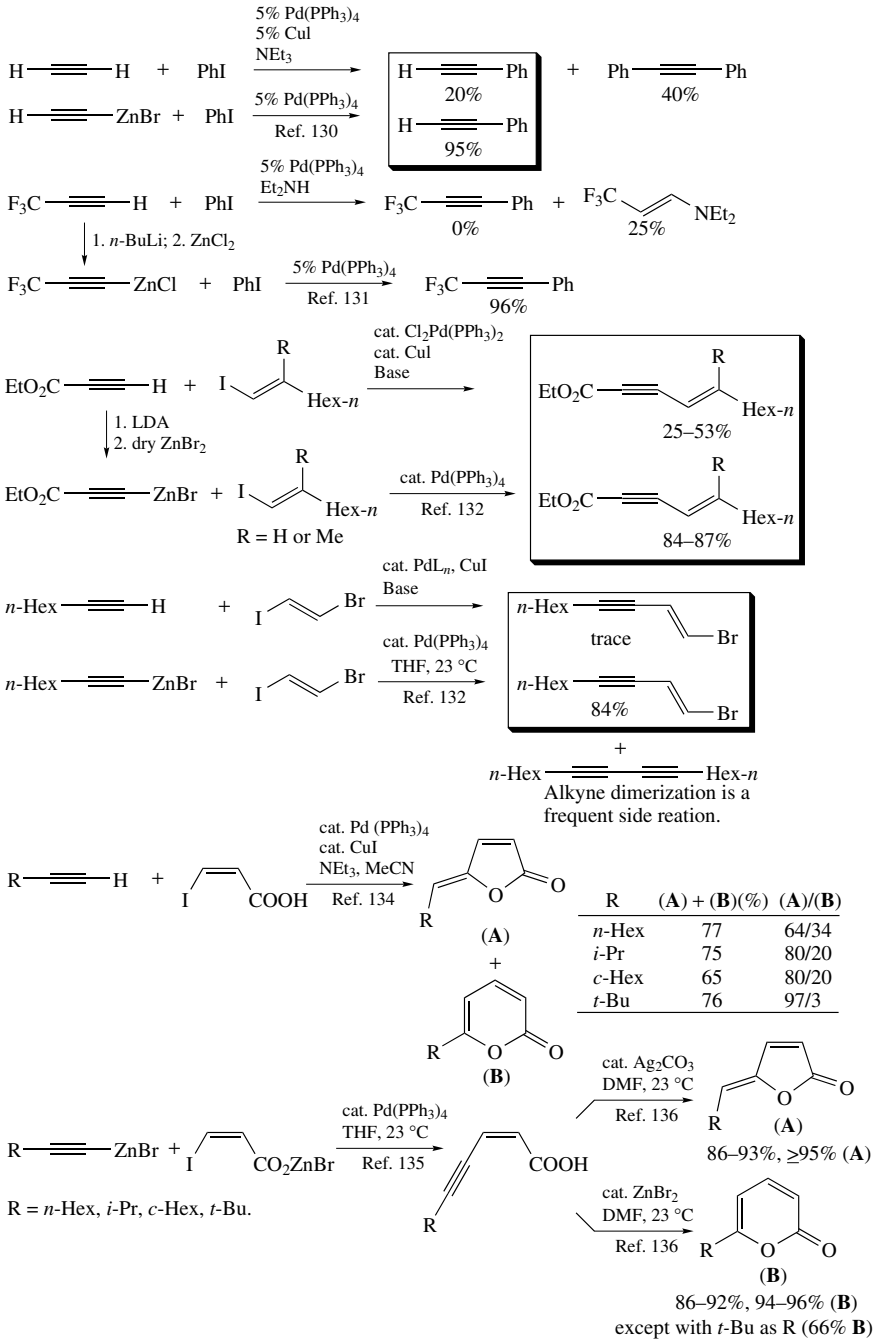

R	(A) + (B)(%)	(A)/(B)
n-Hex	77	64/34
i-Pr	75	80/20
c-Hex	65	80/20
t-Bu	76	97/3

SCHEME 41. Comparison of the Negishi alkynylation and the Sonogashira alkynylation

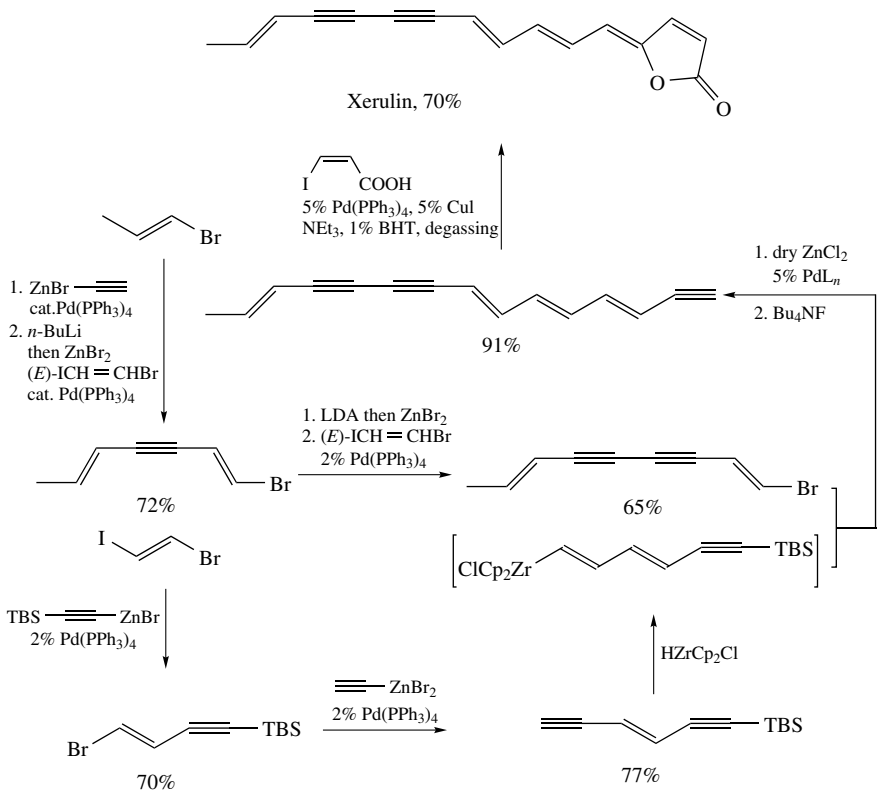

SCHEME 42. Synthesis of xerulin via six Pd-catalyzed alkynylation and one Pd-catalyzed alkenyl–alkenyl coupling[95]

dozen metals. In the first systematic screening of metal countercations, reported in 1978[5b], Zn, B and Sn, namely the three most widely used metals at present, were found to be the three most satisfactory metals. Alkali metals, such as Li, were mostly ineffective, although they were at least as reactive as Zn under the stoichiometric conditions. Catalyst poisoning may be suspected. Although often less satisfactory than alkynylzincs, alkynylmagnesium derivatives can be very satisfactory in less-demanding cases. Several other metals including Al, Si and Mn have also been used. Alkynylsilanes[11] by themselves are quite inert. In fact, some silyl groups have served as effective protecting groups, but they can be activated by various methods, as needed, thereby providing a unique class of alkynylating agents. Yet another metal that has emerged within the past several years is In. Indeed, it is among the several most reactive and nearly as reactive as Zn, although $InCl_3$ is significantly more expensive than $ZnCl_2$ or $ZnBr_2$. In summary, except in some special cases, Zn is generally the metal of choice in almost all respects. In cases alkynylmagnesiums are generated as the first-generation alkynylmetals, they should also be tested for objective comparison.

c. Current scope of Pd-catalyzed alkynylation with alkynylzincs with respect to electrophilic coupling partners. The great majority of the currently known reactions of this

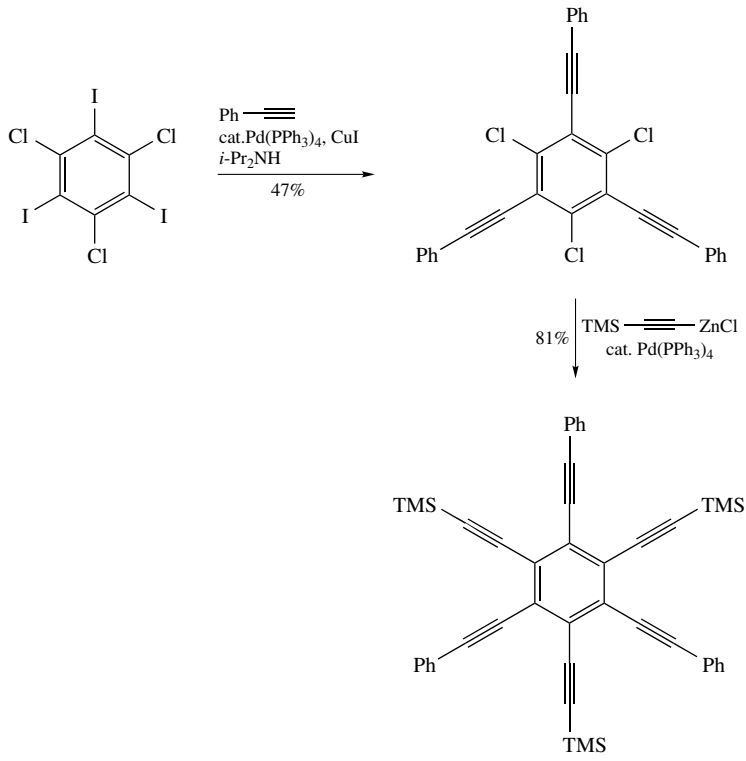

SCHEME 43. Use of the Sonogashira and Negishi alkynylation in the synthesis of a hexaalkynyl benzene

class involve alkynyl–aryl and alkynyl–alkenyl coupling reactions. The examples discussed in this review also pertain to these reactions, especially alkynyl–alkenyl coupling. The current status of the other classes of alkynylation is briefly discussed below.

i. Alkynyl–alkynyl coupling. There have been a fair number of successful examples of the Pd-catalyzed alkynyl–alkynyl coupling[15]. Nevertheless, competitive formation of two possible homo-coupled conjugated diynes is a frequently observed side reaction, the extents of which cannot be readily predicted. Nor can they be readily avoided. Despite some reports claiming successful developments of satisfactory procedures, further fundamental improvements are desirable. In this context, the development of some strictly cross-selective diyne syntheses via alkynyl–alkenyl coupling briefly introduced in Scheme 42 and discussed later in further detail are noteworthy as superior alternatives to both Pd-catalyzed alkynyl–alkynyl coupling and the long known Cadiot–Chodkiewicz reaction[139].

ii. Allyl, benzyl, propargyl and allenyl electrophiles. The Pd-catalyzed alkynyl–propargyl and alkynyl–allenyl coupling reactions with alkynylzincs were investigated systematically as early as 1981[140]. Both of these reactions generally produce allenynes. In this sense, the two reactions are synthetically equivalent. However, the scope of the alkynyl–propargyl

reaction with respect to the leaving group of electrophilic partners is much wider[15,17]. Alkynyl epoxides are also good electrophilic partners[15,17]. In marked contrast, the Pd-catalyzed alkynyl–allyl and alkynyl–benzyl coupling reactions had been mysteriously elusive. A breakthrough was made several years ago by Sarandeses and coworkers[141] with alkynylindiums, but the success appears to be more due to the use of $Pd(dppf)Cl_2$ as a catalyst. More recent studies have clearly shown that both alkynyl–benzyl[142] and alkynyl–allyl[143] coupling reactions are satisfactorily achieved by using alkynylzincs and $Pd(DPEphos)Cl_2$ in THF or DMF, the latter being distinctly superior in the alkynyl–allyl coupling. A detailed comparative study has indicated that $Pd(dppf)Cl_2$ is also satisfactory but less effective, whereas other Pd complexes containing PPh_3, TFP and $(t\text{-}Bu)_3P$ are rather unsatisfactory. The corresponding reactions of alkynylmetals containing In and B are nearly as satisfactory as those of Zn. At low catalyst loading levels, however, B appears to be less satisfactory than Zn and In, and subtle but unmistakable differences in yield–TON profiles and in stereoselectivity indicate that Zn is superior to In. These results are summarized in Table 4[142] and Scheme 44[143].

iii. Alkynyl–acyl coupling. The Pd-catalyzed alkynyl–acyl coupling reaction developed in 1983[144] is generally satisfactory, and it has been satisfactorily applied to the synthesis of modhephene[145] (Scheme 45). Unlike Cu-promoted acylation, the Pd-catalyzed reaction of alkynylzincs with acyl chlorides is not complicated by conjugated addition of ynones formed as the products.

In summary, the Pd-catalyzed alkynylation with alkynylzincs has finally become generally applicable with the exception of the alkynyl–alkyl coupling and often capricious

TABLE 4. Pd-catalyzed alkynyl–benzyl coupling

$$PhC{\equiv}CML_n + BrCH_2Ph \xrightarrow[\text{Ref. 142}]{\text{cat. } PdL_n,\ \text{THF}} PhC{\equiv}CCH_2Ph + PhC{\equiv}C\frac{}{}_2$$

ML_n	PdL_n	Mol%	Temp (°C)	Yield (%) $PhC{\equiv}CCH_2Ph$	Yield (%) $PhC{\equiv}C\frac{}{}_2$	Yield (%) $BrCH_2Ph$
ZnBr	$Pd(dppf)Cl_2$	5	Reflux	96	<1	<1
		10^{-1}	Reflux	80	<1	14
		10^{-3}	Reflux	17	<1	80
ZnBr	$Pd(DPEphos)Cl_2$	5	23	97	<1	<1
		10^{-1}	23	98	<1	<1
		10^{-3}	Reflux	71	<1	24
		10^{-4}	Reflux	53	<1	40
$In(C{\equiv}CPh)_2$	$Pd(DPEphos)Cl_2$	5	23	96	<1	<1
		10^{-1}	23	95	<1	<1
		10^{-3}	Reflux	69	<1	27
		10^{-4}	Reflux	49	<1	50
B-MeO-9-BBN	$Pd(DPEphos)Cl_2$	5	23	90	2	3
		10^{-1}	Reflux	83	<1	9
		10^{-3}	Reflux	31	<1	62
MgBr	$Pd(DPEphos)Cl_2$	5	Reflux	42	23	27
		0	Reflux	2	35	39
$SnBu_3$	$Pd(DPEphos)Cl_2$	5	Reflux	57	<1	<1
$H + CuI, K_2CO_3$	$Pd(DPEphos)Cl_2$	5	Reflux	32	14	18

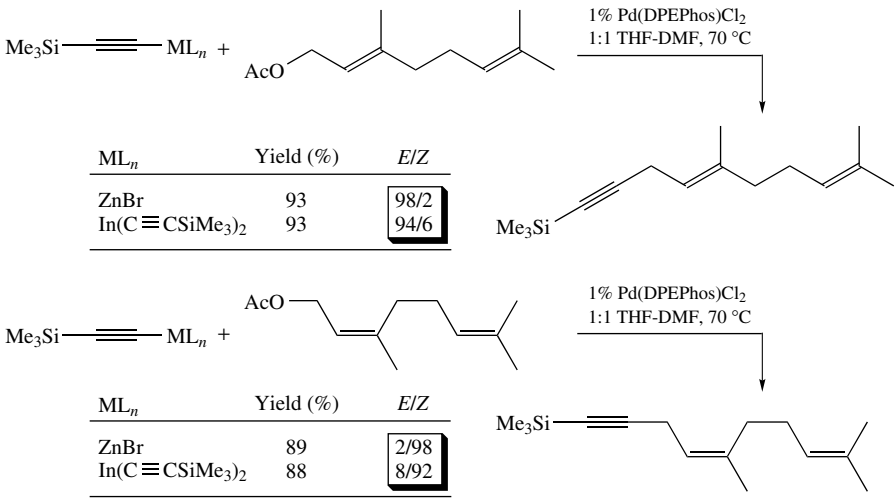

ML_n	Yield (%)	*E*/*Z*
ZnBr	93	98/2
$In(C{\equiv}CSiMe_3)_2$	93	94/6

ML_n	Yield (%)	*E*/*Z*
ZnBr	89	2/98
$In(C{\equiv}CSiMe_3)_2$	88	8/92

SCHEME 44. Comparison of Zn and ln in the Pd-catalyzed reaction of alkynylmetals with geranyl and neryl acetate

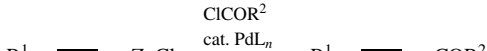

R^1 = *n*-Pent, *n*-Hex

R^2	Yield (%)
Me	81
Ph	73

R^2	Yield (%)
(*E*)-MeCH=CH	81
Ph	73

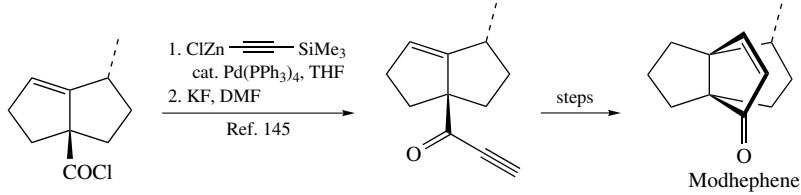

SCHEME 45. Pd-catalyzed reaction of alkynylzincs with acyl chlorides

alkynyl–alkynyl coupling, to which a highly satisfactory alternative has been developed. It is also desirable to be able to develop a satisfactory and general procedure for alkynyl–propargyl (or allenyl) coupling to produce 1,4-diynes.

2. Recent advances in the Pd-catalyzed alkynylation

The Pd-catalyzed reaction of alkynylzincs with alkenyl electrophiles is generally dependable and widely applicable. However, recent studies with 1,1-dihalo-1-alkenes, 1,2-dihaloalkenes, and other alkenyl halides have indicated that the presence of two proximal

halogen atoms can significantly affect the reactivity of these dihaloalkenes and related alkenyl electrophiles, leading to a number of unexpected results.

a. Pd-catalyzed alkynyl–alkenyl coupling with 1,1-dihalo-1-alkenes. Mutual activation of the carbon–halogen bonds of 1,1-dihalo-1-alkenes toward oxidative addition of Pd and potential complication due to competitive double substitution in the Pd-catalyzed *trans*-selective monosubstitution (Scheme 34) were discussed in Section III.A.2. A systematic optimization of reaction parameters was made for the Pd-catalyzed *trans*-selective monoalkynylation of various 1,1-dibromo- and 1,1-dichloro-1-alkenes with both $Me_3SiC{\equiv}CZnX$ (X = Cl or Br) and $Me_3SiC{\equiv}CH$ used under the Sonogashira alkynylation conditions[85, 146]. As summarized in Scheme 37 in Section III.B.2, the combined use of 1,1-dibromo-1-alkenes, $Me_3SiC{\equiv}CZnX$ and Pd(DPEphos)Cl_2 leads to both excellent yields (84–96%) and nearly perfect *trans*-selectivity of ⩾98–99%. Under similar conditions, the Sonogashira reaction with $Me_3SiC{\equiv}CH$ has been comparably satisfactory. The use of Pd(dppf)Cl_2 in these reactions is nearly as satisfactory as that of Pd(DPEphos)Cl_2 in the corresponding reaction of 1,1-dichloro-1-alkenes. However, the alkynylzinc reaction has been distinctly superior to the Sonogashira alkynylation, as exemplified in Scheme 46.

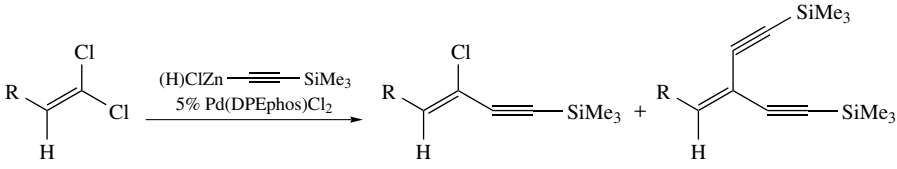

Mono Di

R	Protocol	Mono (%)	Di (%)
Ph	Negishi	84	13
Ph	Sonogashira	56	4
n-Hex	Negishi	65	8
n-Hex	Sonogashira	26	2

SCHEME 46. Comparison of the Negishi and Sonogashira reations in the Pd-catalyzed alkynylation of 1,1-dichloro-1-alkenes

The previously problematic second substitution after the *trans*-selective monoalkynylation can now be achieved selectively (⩾98% selective with retention) and in high yields. The use of alkylzincs and most critically alkylphosphines such as $(t\text{-Bu})_3P$, as ligands, was the key to the development of the satisfactory procedure (Scheme 47)[85]. Conventional arylphosphines, such as PPh_3, TFP and DPEphos, as well as the use of Ni catalysts in conjunction with alkylmetals containing Mg[106] and Zn led to low yields and/or extensive and synthetically unattractive stereoisomerization[85].

This reaction has recently been applied to the synthesis of the side chains of mycolactones A and B[147] (Scheme 48).

b. Pd-catalyzed alkynyl–alkenyl coupling with 1,2-dihaloethylenes. 1,2-Dihaloethylenes are potentially attractive but often capricious two-carbon synthons for Pd- or Ni-catalyzed cross-coupling. Of the six such compounds containing Cl, Br and/or I, each of which

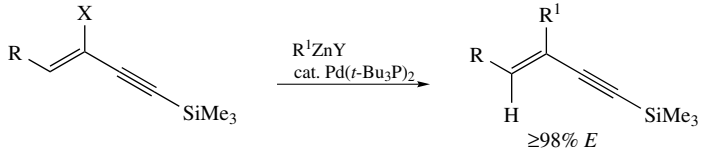

R	X	R^1	Y	Product (%)
n-Nonyl	Br	Me	Me or Cl	93–95
n-Hex	Br	Et	Et	93
Ph	Cl	Me	Me	>95
Me_3Si—≡	Cl	Me	Me	94
$TBSOCH_2CH(Me)CH_2$	Br	Me	Me	95
$TBSOCH_2CH(Me)CH_2$	Br	Et	Et	99

SCHEME 47. Alkylation of (*Z*)-3-halo-1-trimethylsilyl-3-en-1-ynes with alkylzincs in the presence of Pd(*t*-$Bu_3P)_2$

can exit as *E* and *Z* isomers, (*E*)- and (*Z*)-1,2-dichloroethylene and (*E*)-1-iodo-2-bromoethylene are commercially available. Also available is an *E* and *Z* mixture of 1,2-dibromoethylene. Although not commercially available at present, (*E*)-1-iodo-2-choloroethylene[96, 148] has been shown to be synthetically useful. Selective monoalkynylation of either (*E*)- or (*Z*)-1,2-dichloroethylene by the Sonogashira alkynylation was shown to be satisfactory provided that 5 molar equivalents of 1,2-dichloroethylene were used[133]. In cases where the recovery of the unreacted 1,2-dichloethylene and the subsequent reactions of chloroethylene do not offer serious problems, this would be a relatively economical and satisfactory option. A more selective synthesis of (*E*)-chloroenynes[96, 148] can be achieved by the Pd-catalyzed reaction of alkynylzincs with (*E*)-1-iodo-2-chloroethylene. When more reactive (*E*)-bromoenynes are needed, the Pd-catalyzed reaction of alkynylzincs with (*E*)-1-iodo-2-bromoethylene[96, 97] provides a generally satisfactory procedure (Scheme 49). Difficulties encountered in the Pd-catalyzed alkenyl–alkenyl coupling with (*E*)-1-iodo-2-bromoethylene[94] (Scheme 29) have not been observed in the alkynyl–alkenyl coupling. As shown in Scheme 41, the Sonogashira reaction with (*E*)-1-iodo-2-bromoethylene leads to alkyne homodimerization without producing the desired (*E*)-bromoenynes in useful yields. Terminally silylated enynes, such as (*E*)-$Me_3SiC{\equiv}CCH{=}CHBr$ (**9**)[97] and (*E*)-$TBSC{\equiv}CCH{=}CHBr$ (**10**)[95], have been prepared by this method and used as useful four-carbon synthons, as already shown in a highly efficient synthesis of xerulin[95] (Scheme 42).

The bromoenynes, such as **9** and **10**, have been shown to be useful mainly in two discrete manners. One is to use them as four-carbon synthons for the synthesis of conjugated oligoenes[149] (Scheme 50), carotenoids and retinoids[97] (Scheme 51) and conjugated enynes[123] (Scheme 52). In these cases, these reagents including **9** and **10** are used as alkenylating agents. The other is to use haloenynes as conjugated diyne equivalents[96] (Scheme 53). In principle, this method can be readily extended to the selective synthesis of oligoynes of the prespecified degree of oligomerization[150]. The strictly 'pair-selective' synthesis of conjugated diynes provides, in many cases, a distinct advantage over the Cadiot–Chodkiewicz reaction[139] and the capricious and similarly

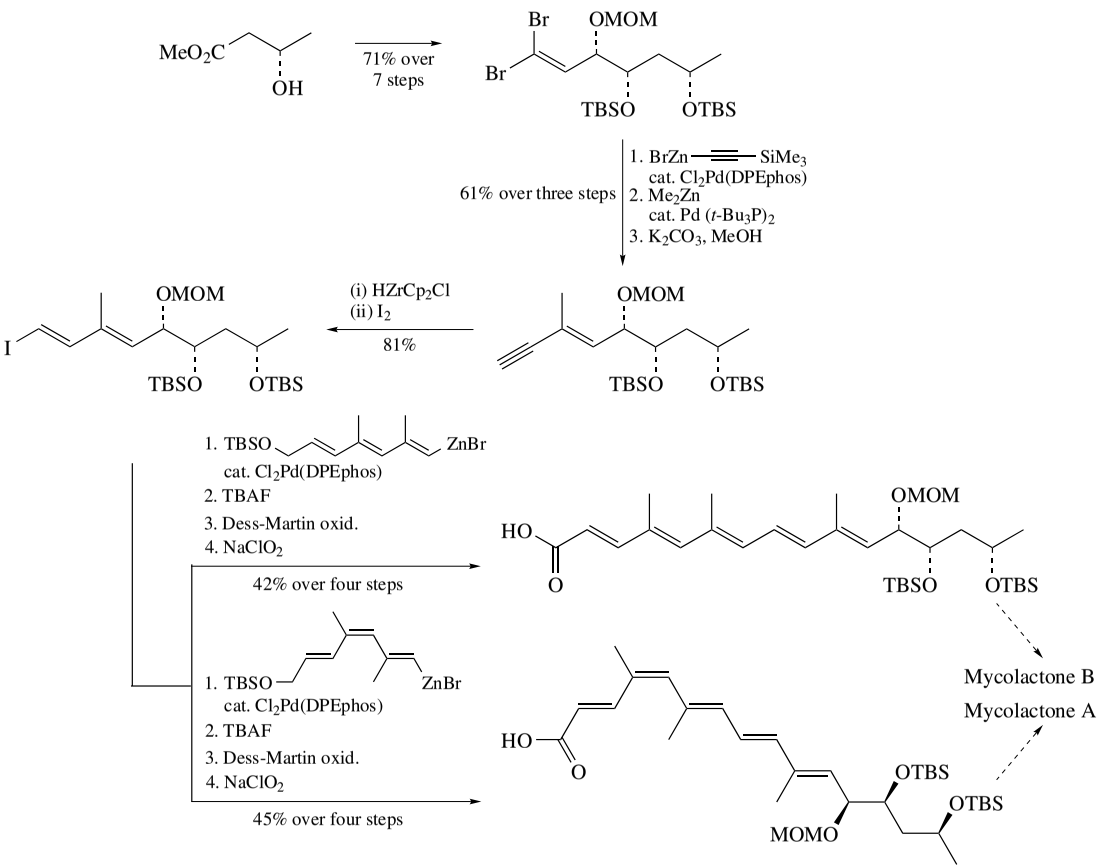

SCHEME 48. Synthesis of the side chains of mycolactones A and B via Pd-catalyzed stepwise double substitution

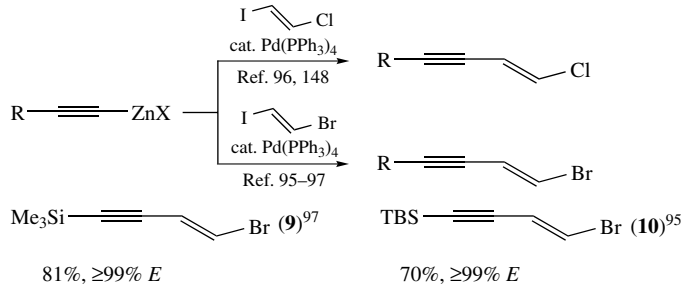

SCHEME 49. Pd-catalyzed cross-coupling of alkynylzincs with (*E*)-ICH=CHCl and (*E*)-ICH=CHBr

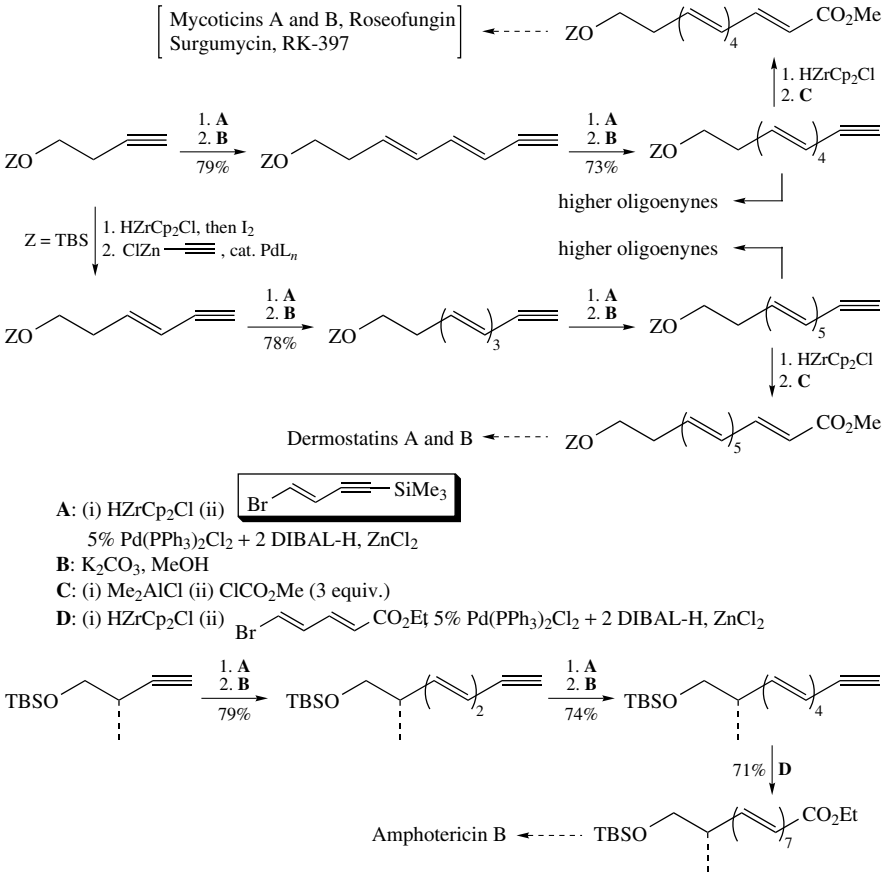

SCHEME 50. Synthesis of conjugated oligoenes via an iterative hydrozirconation–cross-coupling tandem process[149]

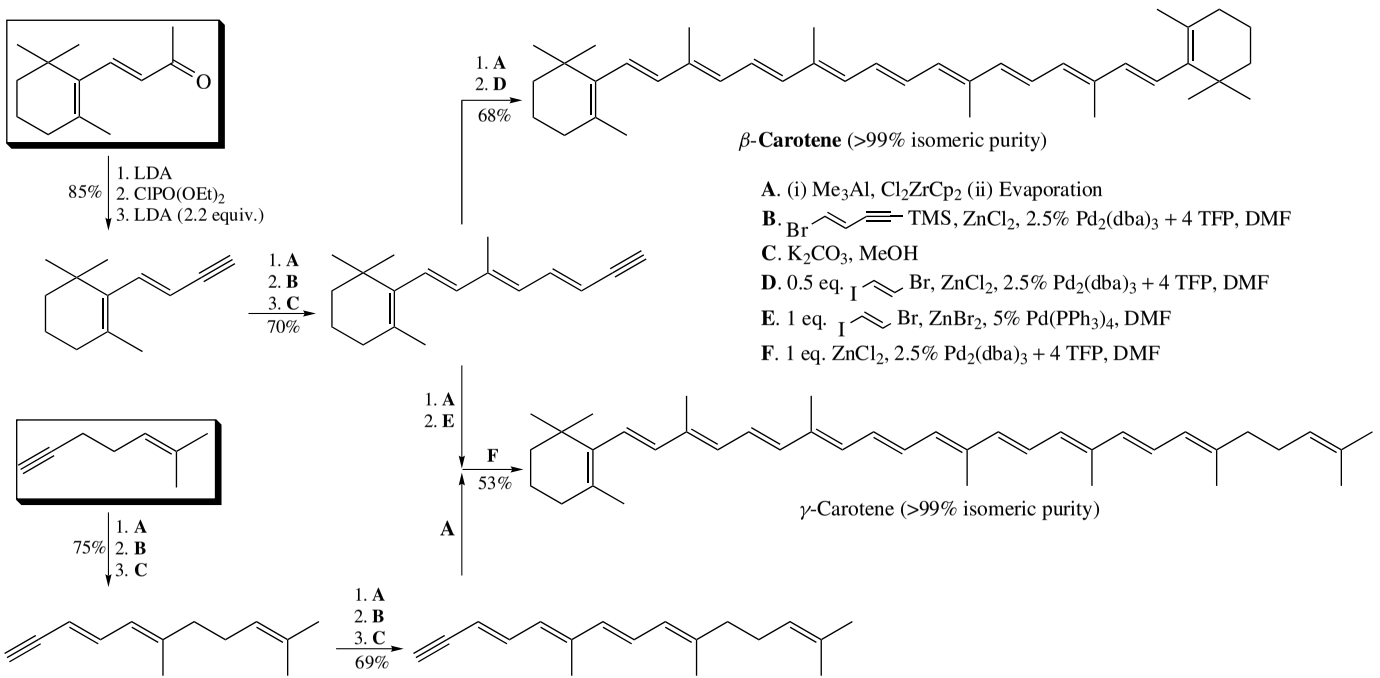

SCHEME 51. Synthesis of β- and γ-carotenes via an iterative carboalumination–cross-coupling tandem process[97]

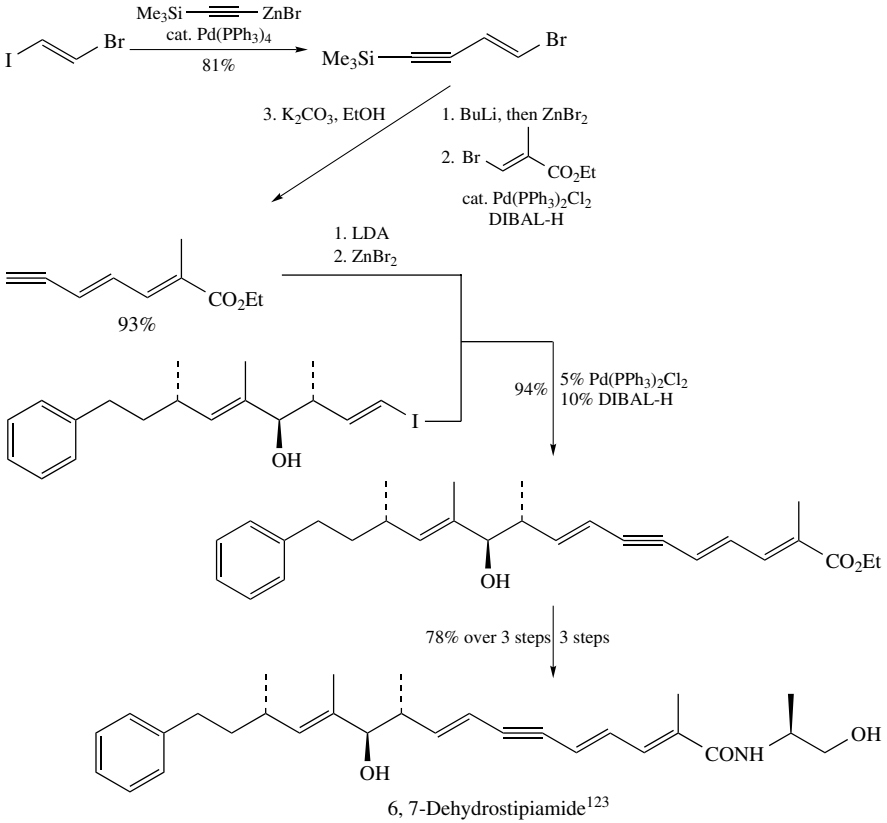

SCHEME 52. Pd-catalyzed alkynylation–alkenylation of (*E*)-1-bromo-2-iodoethylene via (*E*)-$Me_3SiC{\equiv}CCH{=}CHZnBr$

unpredictable Pd-catalyzed alkynyl–alkynyl coupling. It is also noteworthy that the use of much less expensive vinylidene chloride can further economize the synthesis of conjugated diynes[151] (Scheme 54). For satisfactory monoalkynylation of vinylidene chloride, a large excess, typically five-fold excess of vinylidene chloride is used under the Sonogashira conditions[152]. Further optimization is very desirable.

A recent synthesis of a conjugated triendiyne, *trans*-bupleurynol, exemplifies the use of the conjugated diyne synthesis developed above to the synthesis of natural products[121, 153] (Scheme 55).

c. Pd-catalyzed α-alkynylation of α-haloenones and related electrophiles. α-Substitution of carbonyl compounds via their enolates is one of the most fundamental and widely used methods for carbon–carbon bond formation. In its original form, however, its applicability was limited only to the alkylation with certain classes of alkyl electrophiles. Two discrete but complementary approaches to overcome various long-pending limitations have been developed through the use of transition metal catalysts. They may be

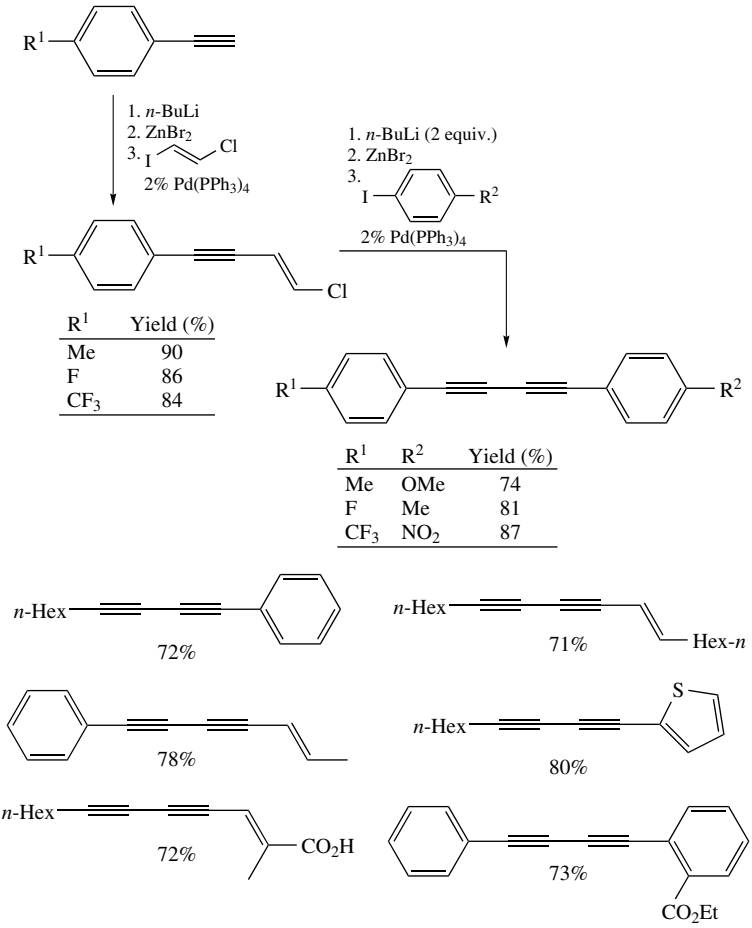

R^1	Yield (%)
Me	90
F	86
CF_3	84

R^1	R^2	Yield (%)
Me	OMe	74
F	Me	81
CF_3	NO_2	87

SCHEME 53. Synthesis of conjugated diynes via Pd-catalyzed alkynylation of 1,2-dihaloethylenes[96]

shown schematically as in Scheme 56. Since one of the preferred methods of controlling the regioselectivity of enolate alkylation involves conjugate reduction of enones for the generation of regiodefined enolates, a scheme starting with enones is shown for a fair comparison of the two complementary protocols. Both the direct α-substitution protocol (Protocol I)[154] and the α-haloenone protocol (Protocol II)[155] catalyzed by Pd and Ni catalysts have been extensively developed. For simpler cases where generation of one of the two or more possible enolates is not a serious issue, α-arylation and α-alkenylation according to Protocol I may be more convenient. In highly demanding cases where regioselectivity and other delicate issues are critically important, however, Protocol II may be preferred or even necessary. Since it is not practical to discuss this vast topic, the readers are referred to some of the pertinent references cited above. In this section, only the Pd-catalyzed α-alkynylation of α-haloenones to produce **11** is discussed. In principle, **11**

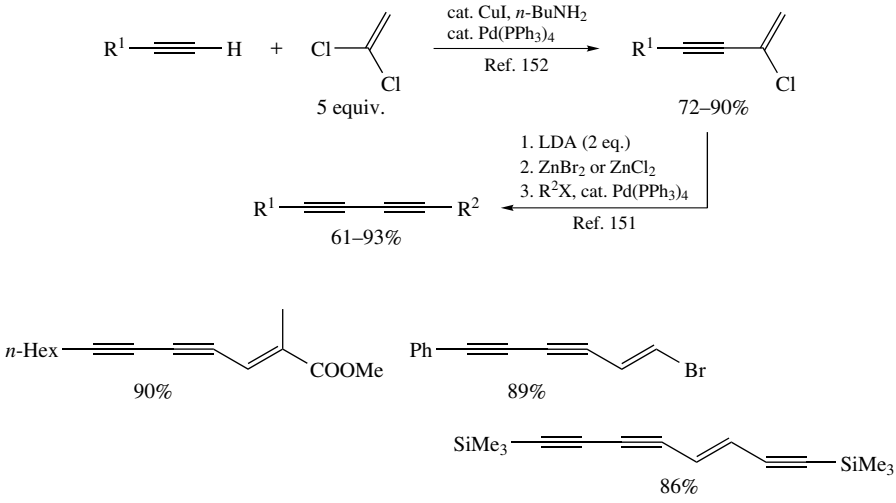

SCHEME 54. Pd-catalyzed strictly 'pair-selective' two-step synthesis of unsymmetrically substituted conjugated diynes

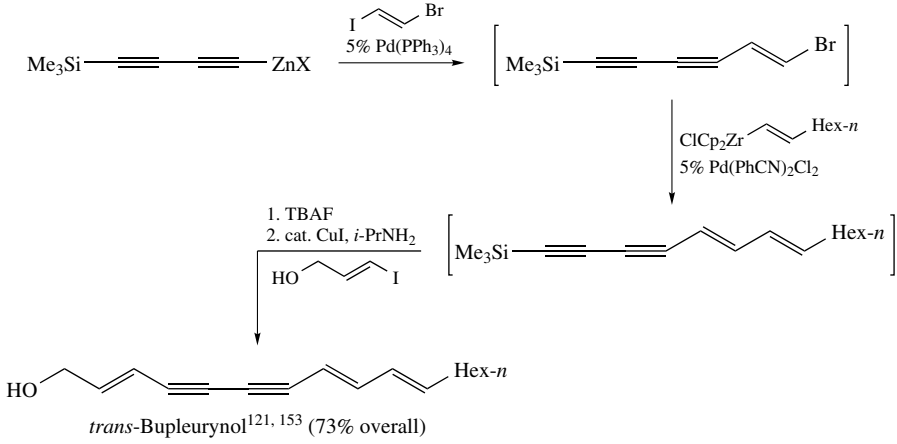

SCHEME 55. Pd-catalyzed dialkynylation and alkynylation–alkenylation of (*E*)-1-bromo-2-iodoethylene

containing an alkynyl group as R may be convertible to **12**, but this does not appear to have been demonstrated. Similarly, the transition metal-catalyzed direct α-alkynylation of enolate to produce **12** containing an alkynyl group as R appears to be unknown.

Three methods for the Pd-catalyzed α-alkynylation of enones according to Protocol II have been developed and applied to the synthesis of harveynone and tricholomenyn

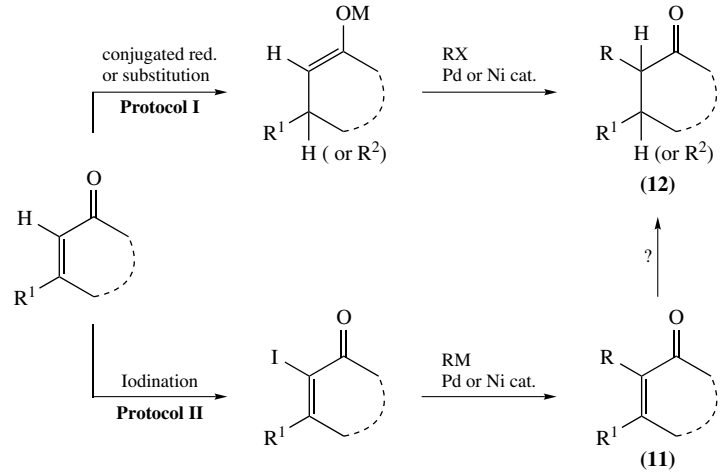

SCHEME 56. Two complementary protocols for Pd- or Ni-catalyzed α-substitution of carbonyl compounds

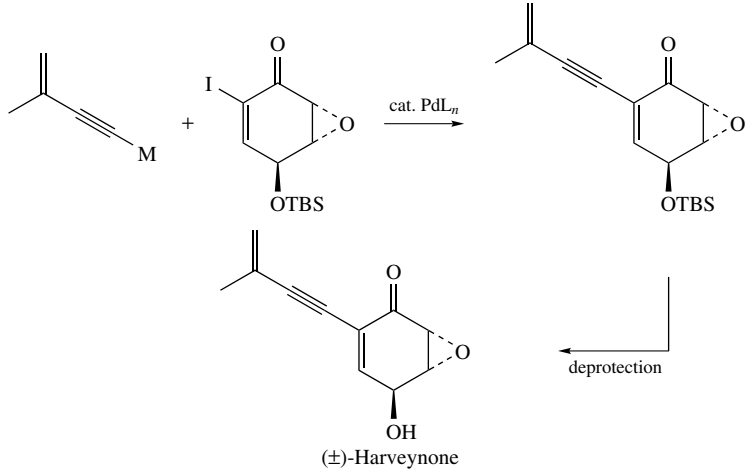

(±)-Harveynone

M	PdL_n	Cond.	Yield (%)	Reference
Zn	$Pd(dba)_2$, TFP	DMF	73	155
Sn	$Cl_2Pd(PPh_3)_2$	cat. CuI, NMP	82	156b
H	$Cl_2Pd(PPh_3)_2$	cat. CuI, *i*-Pr_2NH	52	157

SCHEME 57. Pd-catalyzed α-alkenylation and α-alkynylation of α-iodo-α,β-unsaturated carbonyl compounds

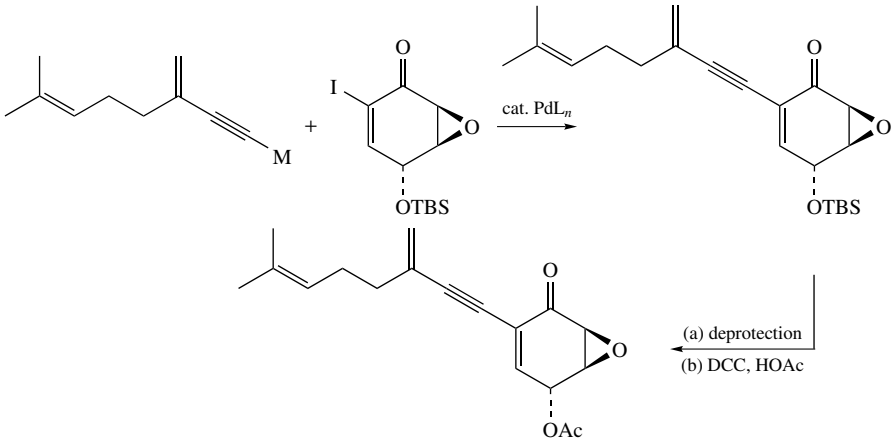

(−)-Tricholomenyn A

M	PdL$_n$	Cond.	Yield (%)	Reference
Zn	Pd(dba)$_2$, TFP	DMF	80	155
Sn	$Cl_2Pd(PPh_3)_2$	cat. CuI, NMP	39	156a
H	$Cl_2Pd(PPh_3)_2$	cat. CuI, *i*-Pr_2NH	54	157

SCHEME 57. (*continued*)

A[155–157]. While all of the three methods provided the desired products, the alkynylzinc route appears to be the most dependable and satisfactory (Scheme 57).

d. Synthesis of natural products via Pd-catalyzed alkynylation with alkynylmetals containing Zn or Mg. Natural products synthesized since 1996 using the Pd-catalyzed alkynylation of alkenyl electrophiles with alkynylmetals containing Zn or Mg are listed in Table 5.

D. Pd- or Ni-catalyzed Allylation, Benzylation and Propargylation (Allenylation)[18]

1. Overview

In Table 1 containing 72 (= 9×8) classes of cross-coupling reactions, 42 of them, nearly 60% of the total, involve the use of at least one allyl, benzyl or propargyl (or allenyl) reagent as a cross-coupling partner. They can be divided into five categories corresponding to the five blocks in Table 1, as shown below.

Category I (9 classes)

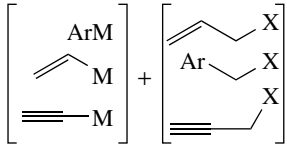

Category II (9 classes)

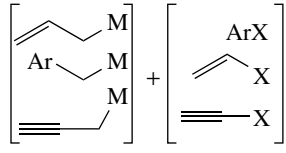

Category III (9 classes)

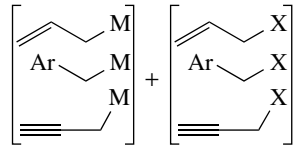

Category IV (9 classes)

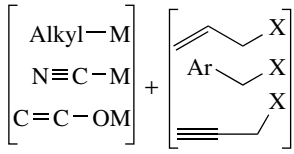

Category V (6 classes)

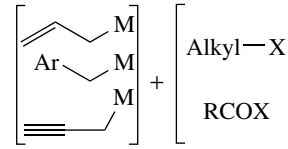

TABLE 5. Natural products synthesized since 1996 by using the Pd-catalyzed alkynylation of alkenyl electrophiles with alkynylmetals containing Zn or Mg

Year	Natural Products	Metal	Halogen	Catalyst	Major Author	Reference
1997	Freelingyne	Mg	I	$Pd(PPh_3)_4$	E. Negishi	137b
2000	Xerulin	Zn	I and Br	$Pd(PPh_3)_4$	E. Negishi	95
2000	(±)-Harveynone	Zn	I	$Pd(dba)_2$, TFP	E. Negishi	155
2000	(−)-Tricholomenyn A	Zn	I	$Pd(dba)_2$, TFP	E. Negishi	155
2001	(−)-Salicylihalamides A and B	Zn	I	$Pd(PPh_3)_4$	A. Fürstner	158
2004	Ant venom	Zn	I	$Pd(PPh_3)_4$	M. G. Organ	153a
2004	*cis*- and *trans*-Bupleurynol	Zn	I	$Pd(PPh_3)_4$	M. G. Organ	121
2004	6,7-Dehydrostipiamide	Zn	I	$Pd(PPh_3)_2Cl_2$, DIBAL-H	E. Negishi	123
2005	Side chains of mycolactones A and B	Zn	I	$Pd(DPEphos)Cl_2$	E. Negishi	147

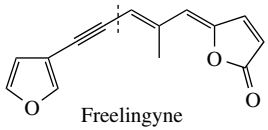

Freelingyne

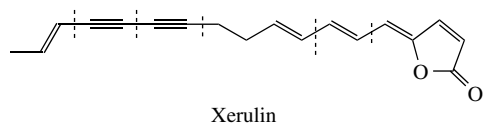

Xerulin

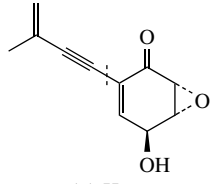

(±)-Harveynone

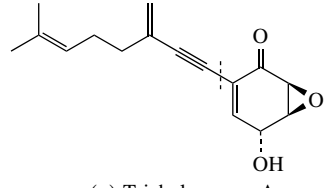

(−)-Tricholomenyn A

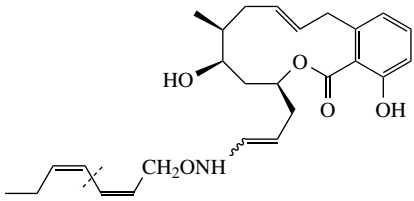

(–)-Salicylihalamides A and B

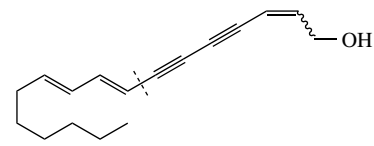

cis- and *trans*-Bupleurynols

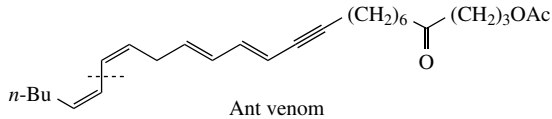

Ant venom
(13*E*, 15*E*, 18*Z*, 20*Z*)-4-Oxopentacosa-
13, 15, 18, 20-tetraen-11-yn-1-yl acetate

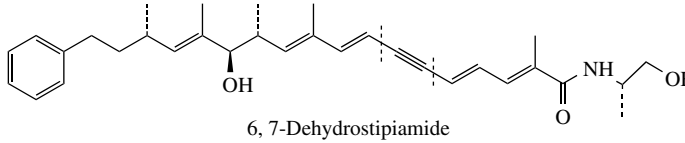

6, 7-Dehydrostipiamide

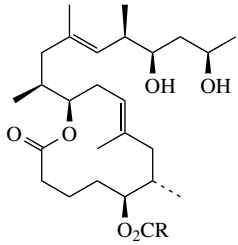

Mycolactones B and A

side chain of Mycolactone B

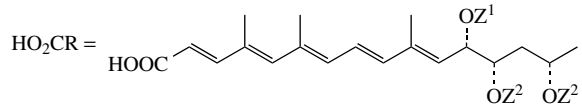

side chain of Mycolactone A

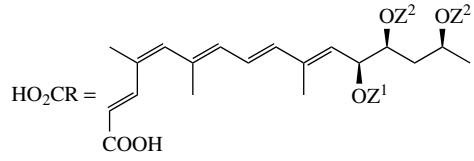

Compound	Z^1	Z^2
Natural Product	H	H
Intermediate	MOM	TBS

Propargylmetals and propargyl electrophiles are in most cases either equivalent or readily interconvertible to allenylmetals and allenyl electrophiles. For the sake of simplicity, they are all represented as propargylmetals and propargyl electrophiles in the classification shown above.

Although any generalizations suffer from exceptions, the following may be presented as the current overview of the Pd- or Ni-catalyzed allylation, benzylation and propargylation (or allenylation)

a. Allyl electrophiles. There are nine different classes of allylation with allyl electrophiles in Table 1. Allyl electrophiles are generally very reactive, presumably due to a

combination of facile formation of Pd–alkene π-complexes and subsequent intramolecular displacement of the leaving group, as proposed in Scheme 22. At the same time, allyl electrophiles are among the most capricious and unpredictable. Thus, they are prone to regioisomerization through allylic rearrangement and attendant stereoisomerization. Aside from these delicate issues, however, both aryl–allyl and alkenyl–allyl coupling reactions with Pd or Ni catalysts are generally facile and high-yielding reactions[18].

Somewhat mysteriously, the Pd-catalyzed alkynyl–allyl and alkynyl–benzyl coupling reactions had until recently been elusive. This limitation has been overcome[142, 143] over the last several years, as discussed in Section III.C.1.c.

Although not discussed in this chapter, the Tsuji–Trost reaction[159] is undoubtedly the most extensively investigated Pd-catalyzed allylation with allyl electrophiles. There have also been some uncatalyzed and Cu-catalyzed reactions of allyl electrophiles with alkyl metals and metal cyanides. On the other hand, the Pd- or Ni-catalyzed reactions of allyl electrophiles with organometals containing allyl-, benzyl-, propargyl- and other alkylmetals do not appear to have been extensively investigated.

b. Benzyl electrophiles. The Pd-catalyzed reaction of arylzincs with benzyl halides appears to be generally facile and satisfactory[18]. Although the Pd- or Ni-catalyzed alkenyl–benzyl coupling involving alkenylmetals containing B, Al and Sn is known[18], relatively little is known about the Pd- or Ni-catalyzed reactions of alkenylzincs with benzyl halides. Just like the Pd-catalyzed alkynyl–allyl coupling, the Pd-catalyzed alkynyl–benzyl coupling had until recently been essentially unknown. Following a breakthrough made with alkynylindiums[141], a systematic investigation was performed[142]. The results summarized in Table 4 indicate that the Pd-catalyzed reactions of both alkynylzincs and alkynylindiums with benzyl bromide catalyzed by Pd(DPEphos)Cl_2 or Pd(dppf)Cl_2 are very satisfactory.

c. Propargyl and allenyl electrophiles. A series of systematic investigations of the Pd-catalyzed reactions of aryl-[160], alkenyl-[76, 161], alkynyl-[76, 161] and allenylzincs[76, 161] with propargyl and allenyl bromides and related electrophiles by Vermeer and coworkers in the 1980s demonstrated that these reactions were generally favorable. In all cases reported in these studies, allenes rather than propargyl derivatives were the products, as shown in Scheme 58.

d. Allylzincs and related allylmetals. Surprisingly, little is known about the Pd- or Ni-catalyzed allylation with allylmetals. In view of the generally high reactivity of allyl electrophiles, difficulties observed with the corresponding allylzincs and related allylmetals are somewhat puzzling. One possible explanation might be that Pd-bound allyl group are bidentate ligands and that they can serve as catalyst poisons. Whereas the molar ratio of such an allyl group to Pd in the reaction of allyl electrophiles is typically 1, the molar ratio of an allylmetal to Pd under catalytic conditions is typically 20–100 or even higher. Less reactive and less coordinating allylmetals might therefore be less poisoning. Indeed, most of the Pd-catalyzed reactions of allylmetals reported in the literature have been observed with allyltins[18b].

e. Benzylzincs. Unlike allylzincs, benzylzincs are generally excellent cross-coupling partners in the Pd- or Ni-catalyzed cross-coupling. The aromatic and sterically demanding nature of the aryl group might be responsible for minimizing the putative catalyst poisoning effect. A number of favorable examples of the Pd- or Ni-catalyzed benzyl–aryl[18a, 33], benzyl–alkenyl[18a, 162] and even benzyl–allyl[163] as well as benzyl–benzyl[163] coupling reactions have been reported.

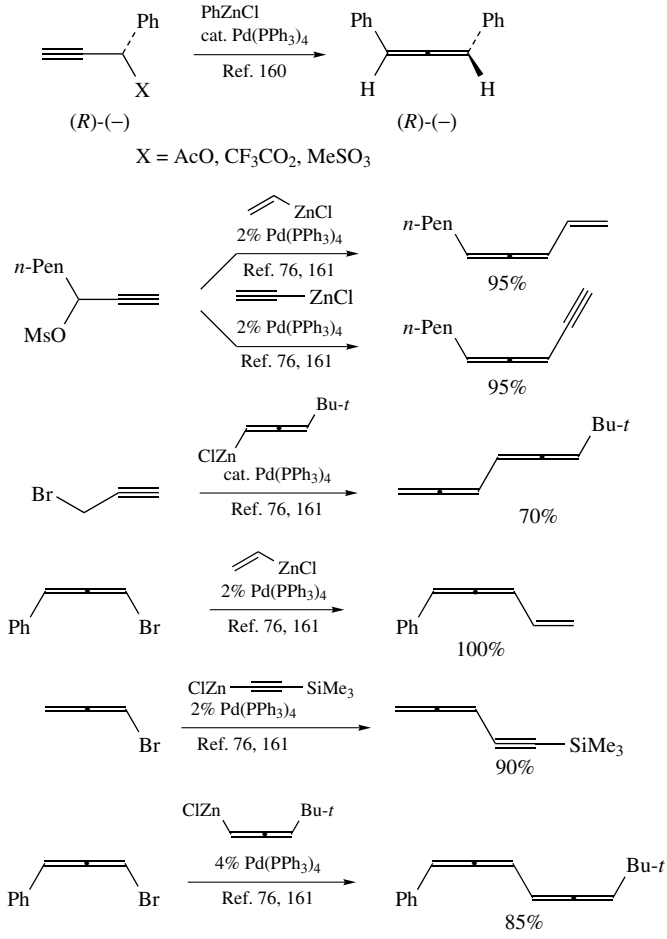

SCHEME 58. Pd-catalyzed propargylation and allenylation

f. Propargylzincs or allenylzincs. Propargyl- and allenylzincs are normally considered to represent the two resonance structures of the same species. Their reactivity profile more closely resembles that of alkenylzincs than that of allylzincs. Their Pd-catalyzed reactions with either propargyl or allenyl halides give allenylallenes in high yields (Scheme 58). Although relatively little is known about their other cross-coupling reactions, it does appear that they might prove to be generally satisfactory cross-coupling partners.

2. Recent advances

a. Pd-catalyzed alkynyl–allyl and alkynyl–benzyl coupling reactions. One of the notable methodological advances over the last several years is the development of satisfactory and widely applicable procedures for the Pd-catalyzed alkynyl–allyl and alkynyl–benzyl coupling reactions discussed in some detail in Section III.C.1.c. These

procedures have provided the long-missing pieces for rounding out the Category I reactions consisting of nine classes of Pd- or Ni-catalyzed cross-coupling.

b. Pd-catalyzed propargyl (or allenyl)–aryl and propargyl (or allenyl)–allyl coupling reactions. As shown in Scheme 58, the Pd-catalyzed cross-coupling of both propargyl and allenyl electrophiles produced exclusively or predominantly allene derivatives. In a limited number of cases, organozincs derived from propargyl electrophiles also selectively produced allenes. A series of extensive studies of the Pd-catalyzed reaction of organozincs generated by lithiation–zincation of 2-alkynes have led to a couple of complementary procedures providing either allenes or propargylated arenes (Scheme 59)[164a]. In the formation of propargylated arenes, however, the C≡C bond undergoes regioisomerization via double 1,3-lithium shifts and the Pd-catalyzed C–C bond formation actually involves an alkynyl–aryl coupling (Scheme 59). Earlier, it was also reported that addition of 1.5 mol% of $HgCl_2$ would alter the course of reaction from allene formation to that of propargylated arenes[164b].

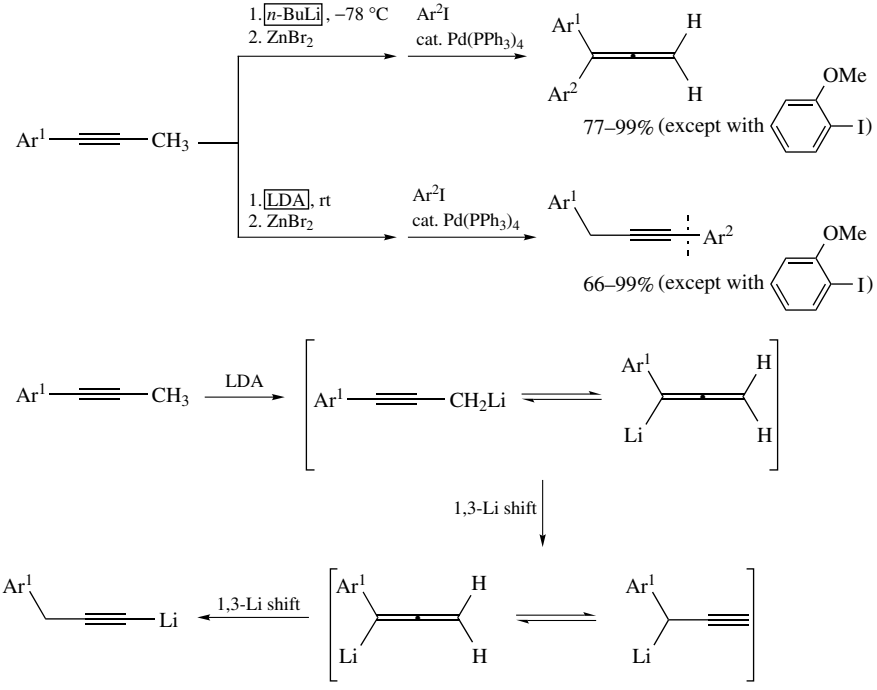

SCHEME 59. The Pd-catalyzed reactions of organozincs obtained via lithiation–zincation of 1-aryl-1-propynes with aryl iodides

In the proposed mechanism shown in Scheme 59, possible involvement of five organolithium species is considered. According to this scheme, formation of not one but two allenes should be possible. It has indeed been demonstrated that either of the two possible allenes can be obtained selectively from the same starting compounds by choosing either *n*-BuLi or LDA as a base[165] (Scheme 60). The use of LDA promotes the 1,3-Li shift. Promotion of the 1,3-Li shift can also be realized by using HMPA as an additive[166].

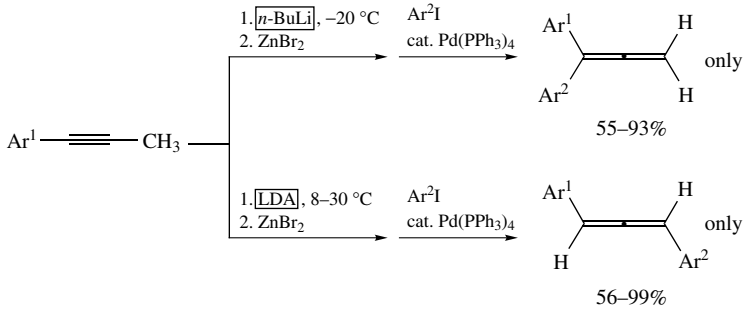

SCHEME 60. Selective formation of either of the two possible regioisomers of allenes via Pd-catalyzed allenylation of aryl iodides

Yet another propargylation–allenylation dichotomy was observed with β-halo-α,β-unsaturated esters[167], which could also be used either as electrophiles or as nucleophiles via zincation with Zn, $BrCH_2CH_2Br$ and Me_3SiCl in THF[62]. A series of studies has led to a fine-tunable protocol involving alkenyl–propargyl (or allenyl) coupling[167d] (Scheme 61). Although the great majority of examples involve the use of β-zinco-α,β-unsaturated esters, this protocol is also applicable to the arylation of propargyl electrophiles. In short, the use of PPh_3 as a ligand favors the formation of 5-yn-2-enoic esters, while the allenylated products can be obtained selectively ($\geqslant$95% regioselectivities) by using 2-diphenylphosphino-2′-hydroxy-1,1′-binaphthalene (**13**).

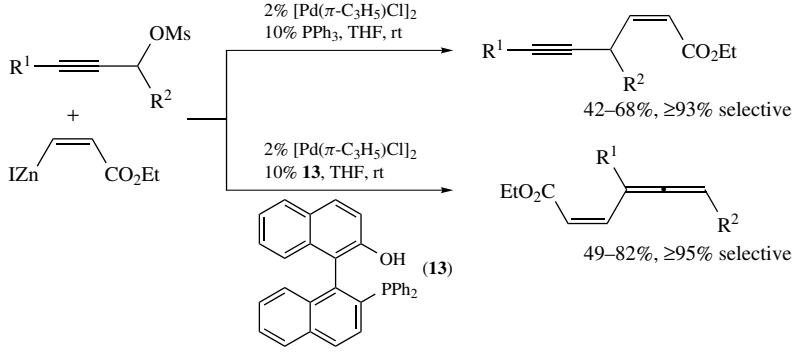

SCHEME 61. A fine-tunable protocol for Pd-catalyzed alkenyl–propargyl or alkenyl-allenyl coupling

Despite delicate selectivity issues discussed above, these recent studies have made the Pd-catalyzed propargylation or allenylation with propargyl–allenyl organozincs potentially useful in a predictable manner. Along with the previously developed benzyl–aryl[33] and benzyl–alkenyl[168] coupling reactions, the Pd-catalyzed propargyl (or allenyl)–aryl and propargyl (or allenyl)–alkenyl cross-coupling reactions make four out of nine classes of Category II cross-coupling synthetically attractive. The corresponding reactions of alkynyl halides, namely benzyl–alkynyl and propargyl (or allenyl)–alkynyl coupling reactions, may be expected to be favorable. In the meantime, the remaining three classes of Pd-catalyzed allylation with allylmetals in Category II as well as most of the Category III cross-coupling reactions still remain largely unexplored.

c. Synthesis of natural products. Although the use of Pd-catalyzed allylation in the synthesis of natural products was reported as early as 1981 for the case of α-farnesene via Pd-catalyzed alkenyl–allyl coupling[169], the number of applications of the Pd-catalyzed allylation, benzylation and propargylation (or allenylation) to the synthesis of natural products is still relatively modest. In the synthesis of hennoxazole via Pd-catalyzed alkenyl–allyl coupling, the use of an alkenylzinc derivative led to a significantly higher yield than that realized in the corresponding alkenyltin reaction[170] (Scheme 62).

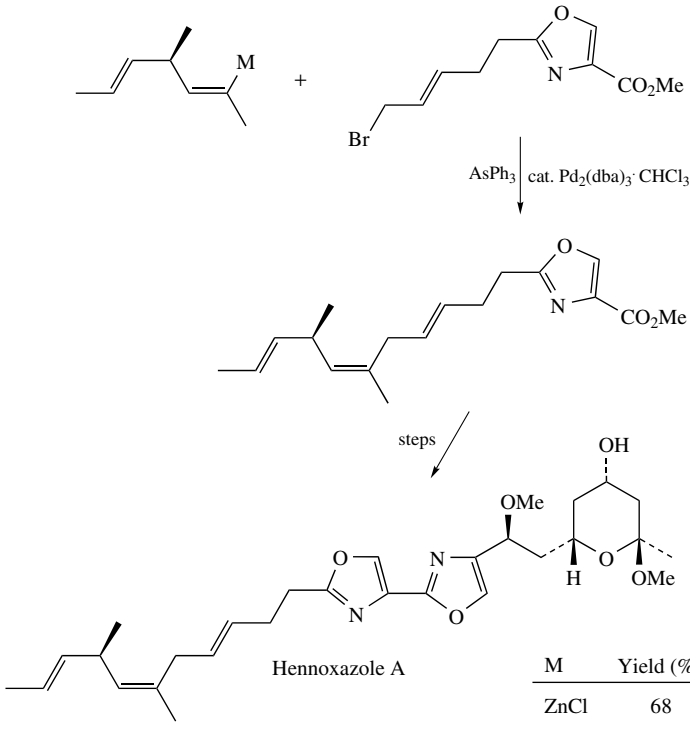

M	Yield (%)	Reference
ZnCl	68	170a
$SnBu_3$	47	170b

SCHEME 62. Synthesis of hennoxazole A via Pd-catalyzed alkenyl–allyl coupling

In the original investigation of the Pd- or Ni-catalyzed alkenyl–benzyl and benzyl–alkenyl coupling reactions[168], both Pd- and Ni-phosphine catalysts were shown to be effective. In some Ni-catalyzed reactions, however, double-bond migration to produce styrene derivatives was observed as a side reaction[169]. Nonetheless, both Pd- and Ni-catalyzed procedures have been successfully applied to the synthesis of various coenzymes Q_n, where n is $\leqslant 10$, and related menaquinones (Scheme 63)[171, 172].

d. Heterocycles. Figure 6 shows the diarylmethanes containing hetaryl groups that have been synthesized by using either Pd-catalyzed aryl–benzyl or benzyl–aryl coupling reactions over the last decade or so.

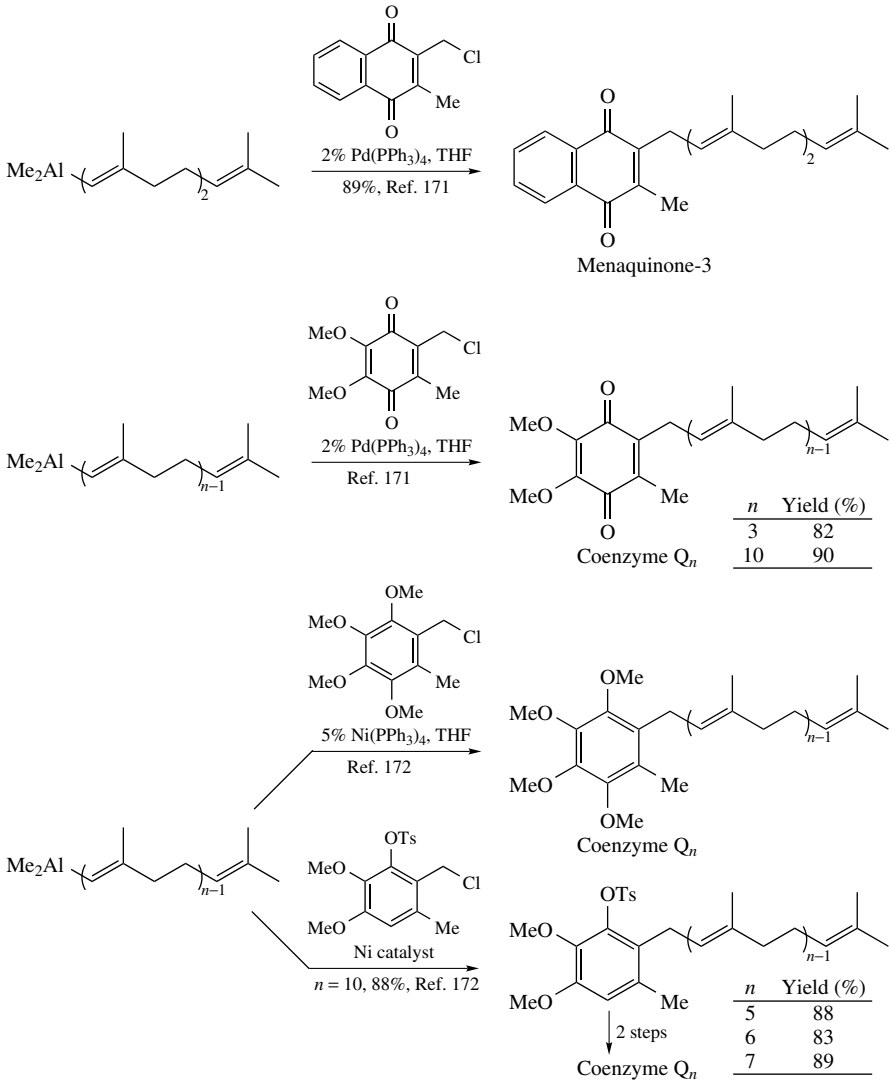

SCHEME 63. Synthesis of coenzyme $Q_n (n \leqslant 10)$ and menaquinone-3 via Pd- or Ni-catalyzed alkenyl–benzyl coupling with alkenylalanes

E. Pd- or Ni-catalyzed Alkylation[19]

1. General discussion

Whereas allyl, benzyl and propargyl electrophiles are among the most reactive towards Pd, Ni and other transition metals, 'ordinary' alkyl halides and related alkyl electrophiles that are not β,γ-unsaturated are among the least reactive carbon electrophiles with respect to oxidative addition to Pd or Ni. Most of the alkyl derivatives are also associated

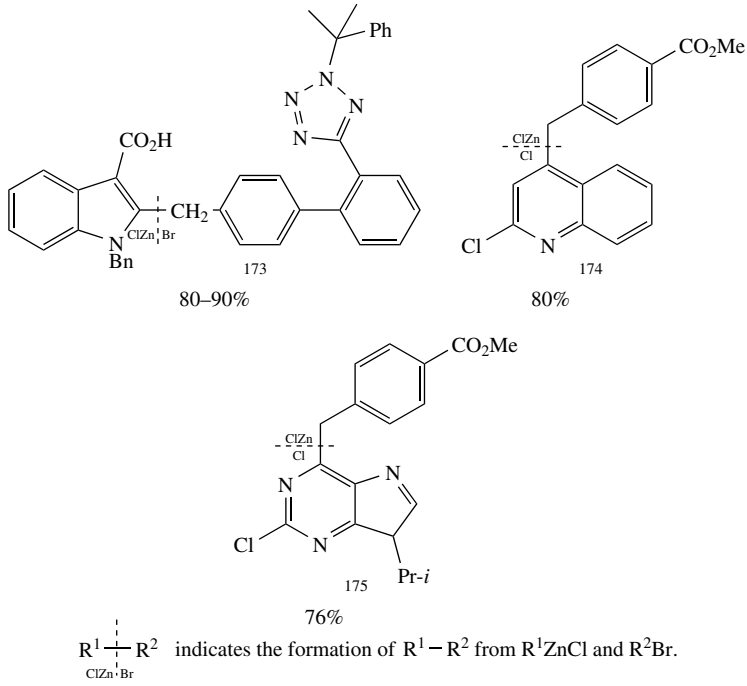

FIGURE 6. Diarylmethanes containing hetaryl groups synthesized by Pd-catalyzed aryl–benzyl or benzyl–aryl coupling

with another fundamental difficulty to be avoided or overcome. In cases where alkyl groups contain one or more β-hydrogen atoms, their transition metal derivatives can often undergo facile β-dehydrometallation in which β-agostic interaction (or hyperconjugation) is thought to play a key role. This reaction can seriously interfere with Pd- or Ni-catalyzed cross-coupling with alkyl derivatives, as indicated in Scheme 64.

a. Discovery and early development of the Pd-catalyzed alkylation. Despite the potential difficulties discussed above, two independent studies on Pd-catalyzed alkylation with alkylzincs were disclosed at the ACS meeting in 1979 and published within a year[176]. It is noteworthy that homoallyl-, homopropargyl- and homobenzylzincs containing relatively acidic β-hydrogen atoms can be employed without the complication due to β-dehydrometallation[176b]. This reaction was soon applied to the synthesis of some terpenoids including farnesol[176b], dendrolasin[178] and mokupalide[178] in a strictly regio- and stereoselective manner. On the other hand, the use of secondary and tertiary alkylzincs is accompanied by β-elimination and regioisomerization to varying extents[176a, 177]. Despite this limitation, the Pd- or Ni-catalyzed alkylation with alkylzincs or alkylmagnesiums has become one of the most generally applicable and reliable methods for alkylation of aryl, alkenyl, alkynyl and acyl derivatives along with its subsequently developed analogues[19c, 178]. Several other metals including Sn and Al have also been used. At present, the Pd- or Ni-catalyzed alkylation with alkyltins is of limited scope, as compared with those with Zn and B[179]. On the other hand, the Pd- or Ni-catalyzed alkylation with alkylalanes is more facile and more widely applicable, although it is still generally less

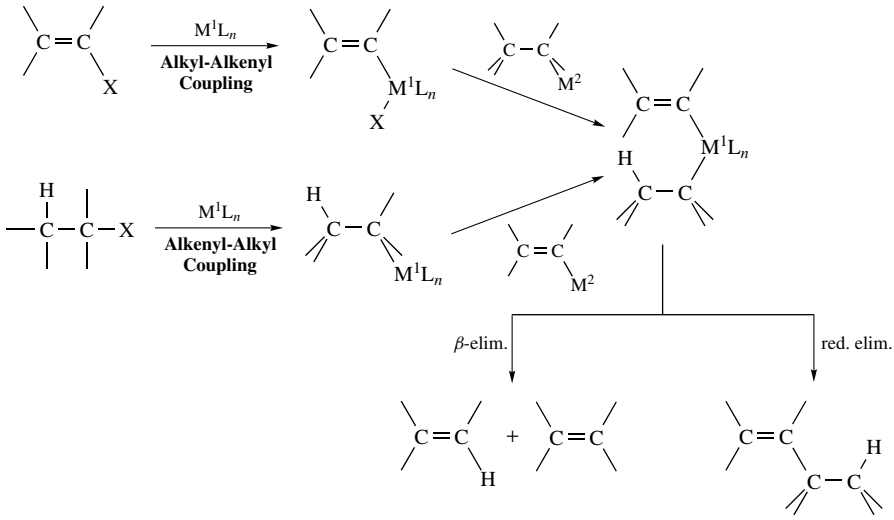

SCHEME 64. Pd- or Ni-catalyzed alkyl–alkenyl and alkenyl–alkyl coupling reactions

satisfactory than those with Zn or B. Nonetheless, *in situ* generation of alkylalanes via hydrometallation and carbometallation followed by Pd- or Ni-catalyzed cross-coupling in one pot is an attractive notion that has been realized recently[180a], as detailed later.

b. Pd- or Ni-catalyzed alkylation with alkyl electrophiles. Until recently, little or nothing had been known about the Pd-catalyzed alkylation with alkyl electrophiles. As briefly mentioned in Section II.C, both Pd- and Ni-catalyzed alkylation with alkyl halides, including not only iodides, bromides and chlorides, but also fluorides, have been developed over the past decades.

In the following two sections, recent advances in the Pd- or Ni-catalyzed alkylation with alkylmetals (Section III.E.2) and with alkyl electrophiles (Section III.E.3) will be discussed.

2. Recent advances in the Pd- or Ni-catalyzed alkylation with alkylmetals

a. Metal countercations, leaving groups and catalysts. Alkylmetals containing Zn and B have been the two most satisfactory classes of nucleophilic partners for Pd- or Ni-catalyzed alkylation. Some unique advantages associated with Al and Mg have recently been noted. The *in situ* generation of isoalkylalanes via hydroalumination or carboalumination of alkenes followed by their Pd- or Ni-catalyzed cross-coupling was a difficult transformation to achieve. As a consequence, a three-step procedure shown in Scheme 65 had been used until recently[180b]. However, a 'one-pot' procedure also shown in Scheme 65 was developed[180a] to make the hydroalumination– or carboalumination–cross-coupling tandem process practically attractive. A different but related carbozincation–cross-coupling tandem process has also been developed (Scheme 66).

With relatively reactive classes of organic halides, such as haloenynes, even chloro derivatives are sufficiently reactive, and their reactions with alkylzincs have been satisfactorily achieved by using $Pd(dppf)Cl_2$[181]. With less reactive classes of organic chlorides, however, it is often desirable or even necessary to use bulky alkylphosphines or NHCs.

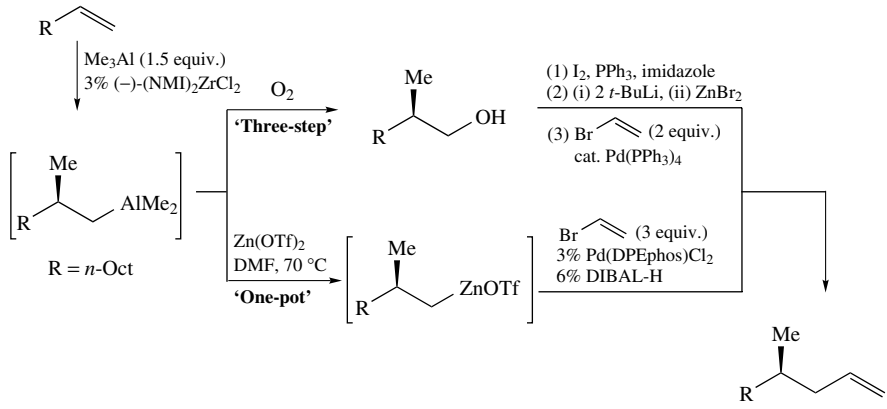

SCHEME 65. The Zr-catalyzed asymmetric carboalumination–Pd-catalyzed vinylation tandem processes

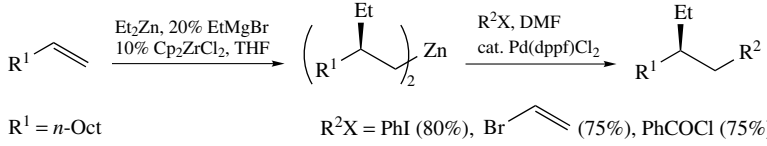

SCHEME 66. The Zr-catalyzed ethylzincation–Pd-catalyzed cross-coupling tandem processes

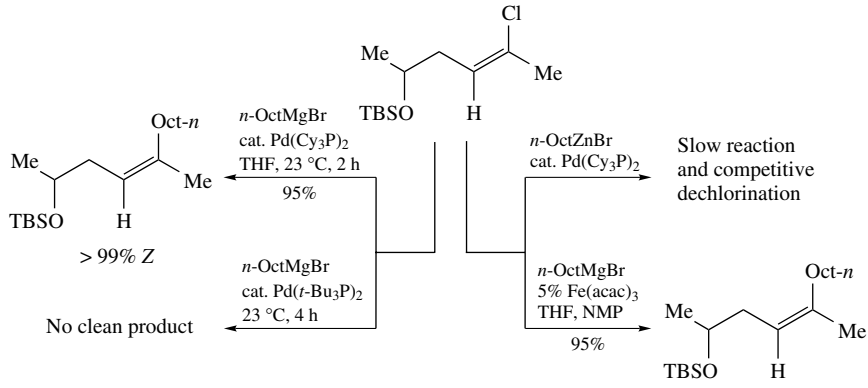

SCHEME 67. Alkylation of alkenyl chlorides with alkylmagnesiums in the presence of Pd catalysts

Moreover, the use of alkylmagnesium derivatives has been shown to be more satisfactory in some cases, as exemplified by the results shown in Scheme 67[105].

The results shown in Scheme 67 as well as those presented in Sections II.C.4 and II.C.5 (Schemes 26 and 27) and Section III.B.2 (Scheme 37) indicate that optimization of reaction parameters for highly demanding cases of the Pd- or Ni-catalyzed cross-coupling must take into consideration synergistic effects among metal countercations, leaving groups, transition metals at the active site of catalysts and their ligands. Thus,

attempts to change the leaving group from expensive I to Br or Cl, in particular, may be aided by concerted shifts involving: (1) arylphosphines-to-alkylphosphines and other non-phosphine ligands and (2) Pd-to-Ni, Fe or Cu. In addition to those new developments shown in Schemes 26, 37 and 67, some others shown in Scheme 68 are also noteworthy.

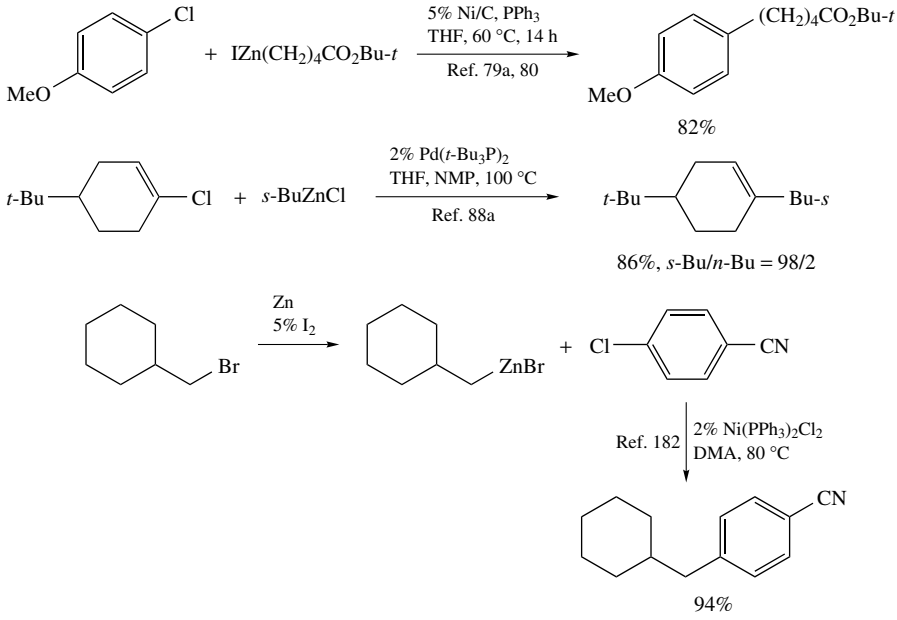

SCHEME 68. Pd- or Ni-catalyzed alkylation of aryl and alkenyl chlorides with alkylzincs

b. Synthesis of natural products via Pd- or Ni-catalyzed alkylation with alkylmetals containing Zn or Mg. In the synthesis of complex natural products, the cost of halogen is often not very important, and the use of organic halides displaying the highest reactivity in the Pd-catalyzed cross-coupling in most cases continues to be dominant. For various reasons including chemoselectivity, the Zn−I−Pd combination appears to be optimal in most cases, although the B−I−Pd combination has also been frequently used[19c, 179]. As repeatedly discussed earlier, moderation, rather than promotion, of reactivity can be of crucial importance. In such cases, the use of organic bromides (Schemes 34, 37 and 38) or chlorides (Scheme 67) may become practically mandatory.

Natural products synthesized via Pd-catalyzed alkylation since 1995 are listed in Table 6, and representative schemes including some crucial cross-coupling steps are shown in Schemes 69–72.

3. Pd- or Ni-catalyzed alkylation with alkyl halides and related electrophiles

Until recently, the Pd- or Ni-catalyzed alkylation with alkyl halides and related electrophiles had represented one of the last bastions to be conquered. Although uncatalyzed cross-coupling reactions of alkyl electrophiles with organolithiums or Grignard reagents have long been known[202], they are of limited synthetic utility. Both promotion of the desired cross-coupling and suppression of undesired side reactions, such as halogen–metal exchange, cross-homo scrambling and β-elimination, have been achieved through the use

TABLE 6. Natural products synthesized via Pd-catalyzed alkylation, homopropargylation and homobenzylation

Year	Name of Natural Product	Metal (M)	Halogen (X)	Major Author	Reference
1995	(+)-Discodermolide	Zn	I	A. B. Smith, III	183
1998	(+)-Amphidinolide J	Zn	I	D. R. Williams	184
1999	Brevetoxin A	Zn	I	K. C. Nicolaou	185
1999	(−)-Epothilone B	Zn	I	D. Schinzer	186
1999	(+)-Pumiliotoxins A & B	Zn	I	C. Kibayashi	187
2001	(*E*)- & (*Z*)-γ-Bisabolene	Zn	I	E. Negishi	188
2001	(−)-4a,5-Dihydrostreptazolin	Zn	I	J. Cossy	189
2001	Mycolactones A & B	Zn	I	Y. Kishi	190
2002	Coenzyme Q_3 & Q_{10}	Zn	I	E. Negishi	171
2002	*trans*-Epothilone A	Zn	I	K. H. Altmann	191
2002	(2*E*, 6*Z*)-Farnesol	Zn	I	E. Negishi	171
2002	(2*Z*, 6*Z*)-Farnesol	Zn	I	E. Negishi	171
2002	(2*Z*, 6*E*)-Farnesol	Zn	I	E. Negishi	171
2002	(2*E*, 6*Z*, 10*E*)-Geranylgeraniol	Zn	I	E. Negishi	171
2002	Menaquinone-3	Zn	I	E. Negishi	171
2002	Oleandolide	Zn	OTf	J. S. Panek	192
2002	Sphingofungin F	Zn	I	W.-H. Ham	193
2003	Borrelidin	Zn	I	J. P. Morken	194
2003	Delactonmycin	Zn	I	R. A. Pilli	195
2004	(−)-Callystatin A	Zn	Br & I	J. S. Panek	122
2004	Capensifuranone	Zn	I	D. R. Williams	196
2004	(+)-Murisolin	Zn	I	D. P. Curran	197
2004	Scyphostatin	Zn	I	E. Negishi	198
2004	Scyphostatin	Zn	I	T. Katoh	199
2004	Siphonarienal	Zn	Br	E. Negishi	200
2004	Siphonarienolone	Zn	Br	E. Negishi	200
2004	Siphonarienone	Zn	Br	E. Negishi	200
2005	Ionomycin (intermediate)	Al(Zn)	Br	E. Negishi	180a
2005	Borrelidin (intermediate)	Al(Zn)	Br	E. Negishi	180a
2005	Preen gland wax of graylag goose *Anser anser*	Al(Zn)	Br	E. Negishi	127
2005	Mycolactone A (side chain)	Zn	I	E. Negishi	201

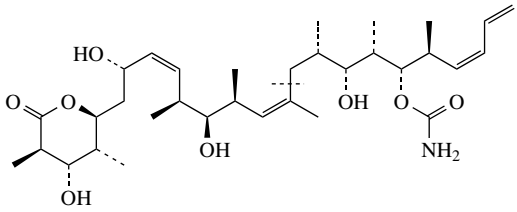

(+)-Discodermolide

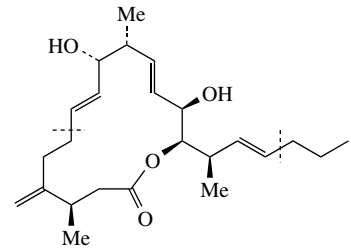

(+)-Amphidinolide J

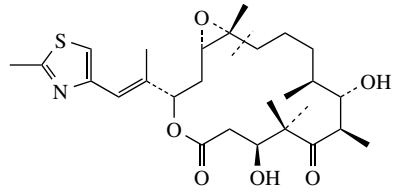

Epothilone B

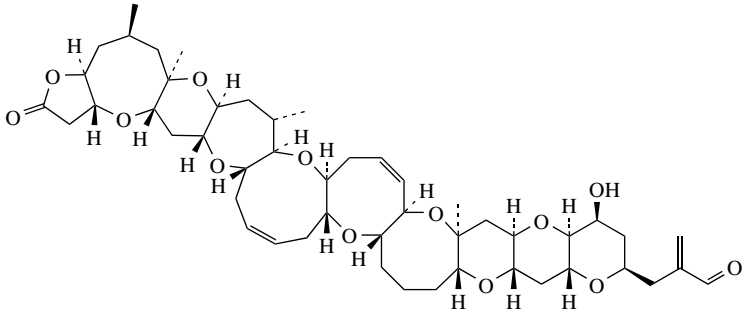

Brevetoxin A

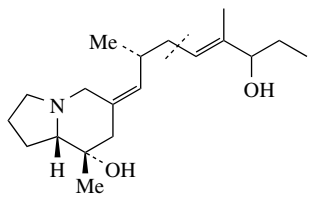

(+)-Pumiliotoxin A

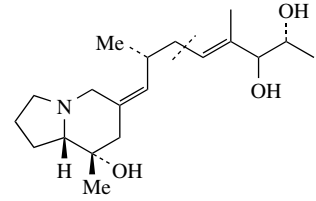

(+)-Pumiliotoxin B

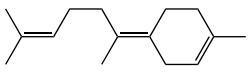

(*E*)-γ-Bisabolene

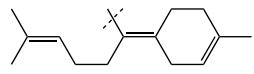

(*Z*)-γ-Bisabolene

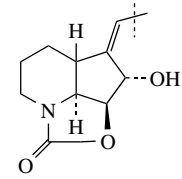

(−)-4a, 5-Dihydrostreptazolin

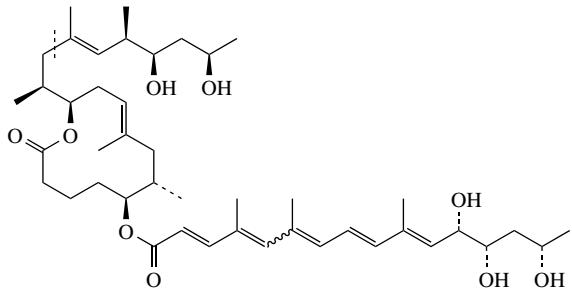

Mycolactones A and B

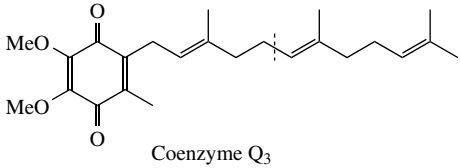

Coenzyme Q_3

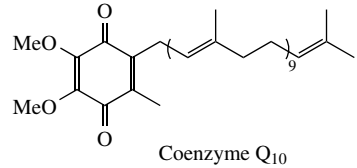

Coenzyme Q_{10}

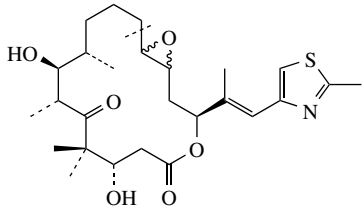

Epothilone A

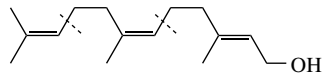

(2*E*, 6*Z*)-Farnesol

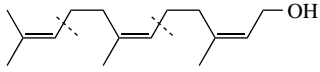

(2*Z*, 6*Z*)-Farnesol

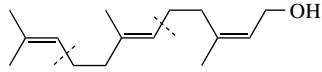

(2*Z*, 6*E*)-Farnesol

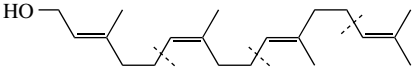

(2*E*, 6*Z*, 10*E*)-Geranylgeraniol

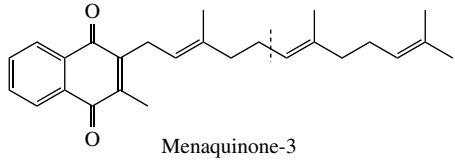

Menaquinone-3

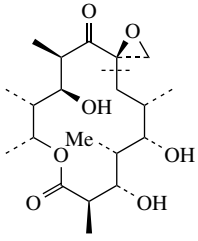

Oleandolide

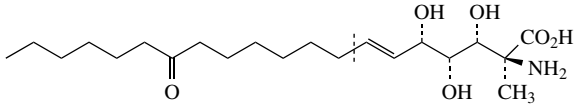

Sphingofungin F

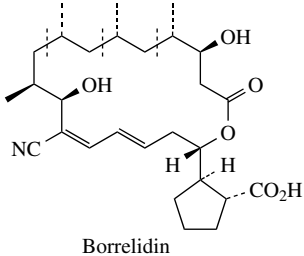

Borrelidin

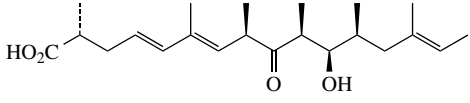

Delactonmycin

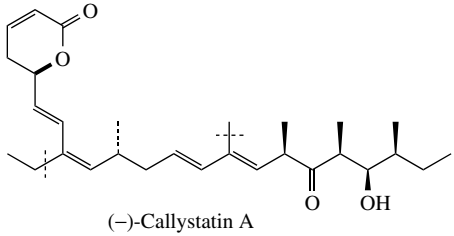

(−)-Callystatin A

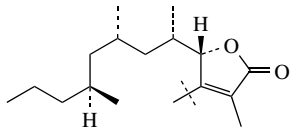

Capensifuranone

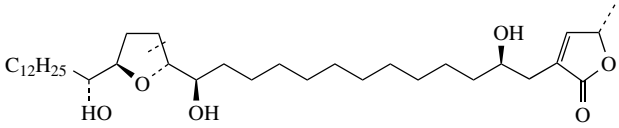

Murisolin

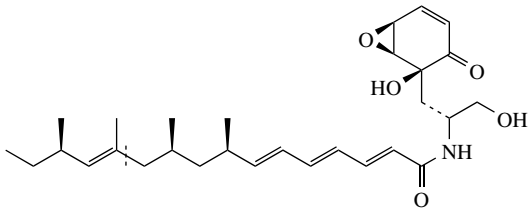

Scyphostatin

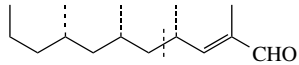

Siphonarienal

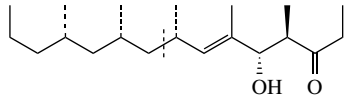

Siphonarienolone

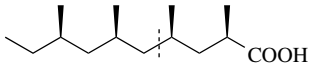

Preen gland wax of
graylag goose *Anser anser*

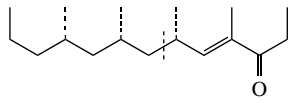

Siphonarienone

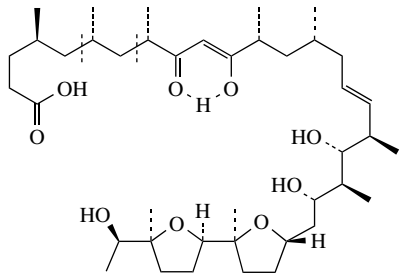

Ionomycin

of either stoichiometric or catalytic amounts of Cu compounds[203]. The reaction of Grignard reagents with alkyl halides and sulfonates in the presence of a catalytic amount (typically $\leqslant 1-5$ mol%) of Li_2CuCl_4[204, 205] is widely applicable and generally dependable, representing the current benchmark against which any new methods must be compared. As for the Pd- or Ni-catalyzed alkylation with alkyl electrophiles, little had been known before 1992. The reproducibility of the final report that dealt with primary and secondary alkyl iodides in the presence of $Pd(dppf)Cl_2$ and DIBAL-H[206] was questioned by other workers[207]. According to these workers, only those reactions that involved the use of neopentylic iodides, alkyl- and arylmagnesium derivatives and $Ni(dppf)Cl_2$ were satisfactory[207]. It is noteworthy that the same group also noted that addition of $ZnCl_2$ (1.5 equiv.) generally lead to 10–30% higher yields[207] (Scheme 73).

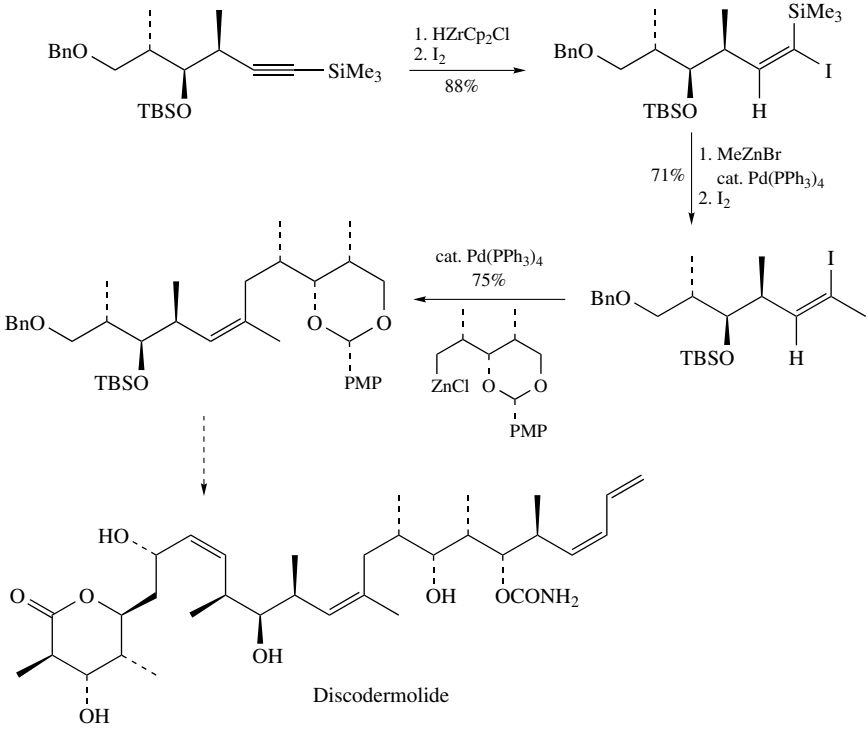

SCHEME 69. Pd-catalyzed dialkylation of 1-sila-1-zircona-1-alkenes via iodinolysis and its application to the synthesis of discodermolide[183]

Following a report in 1992 on the reaction of β-hydrogen-containing alkyl iodides with alkyl-, aryl- and alkenyl-9-BBN derivatives in the presence of $Pd(PPh_3)_4$ and K_3PO_4[208], Knochel and coworkers made an interesting and potentially important observation on the effect of proximal π-bonds shown in Scheme 27[90]. This may have paved the way to their subsequent discovery of the Ni-catalyzed reaction of alkylzincs with primary alkyl iodides in the presence of an electron-deficient styrene or acetophenone[90, 91] (Scheme 74)

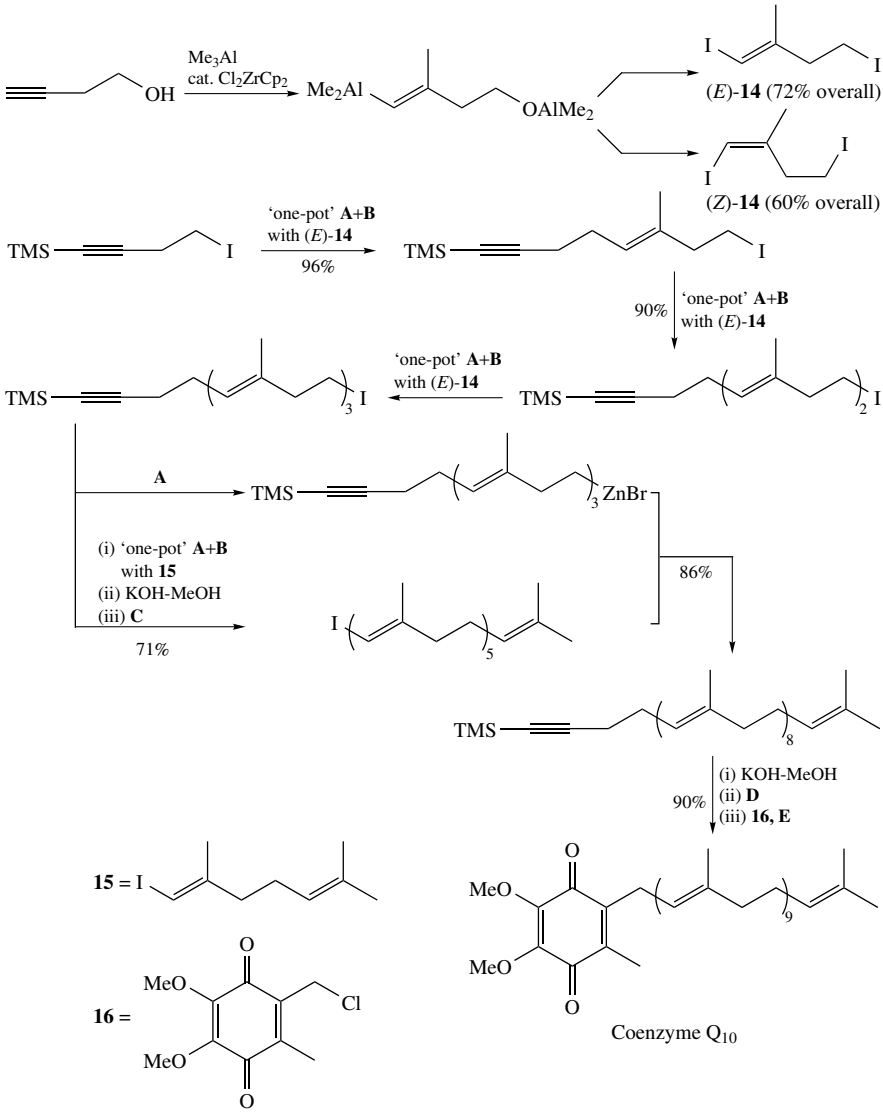

A = (i) *t*-BuLi (2.2 eq.) in Et_2O, –78 °C, 0.5 h. (ii) dry $ZnBr_2$, THF, –78 °C to 0 °C.
B = 2% $Pd(dppf)Cl_2$, THF, 23 °C.
C = (i) Me_3Al (1.5 eq.), Cl_2ZrCp_2 (0.25 eq.), $(CH_2Cl)_2$, 23 °C, 8 h.
(ii) I_2 (1.2 eq.), THF, –78 °C to 23 °C.
D = (i) Me_3Al (1.5 eq.), Cl_2ZrCp_2 (0.25 eq.), $(CH_2Cl)_2$, 23 °C, 8 h.
(ii) Solvent evaporation, extraction with hexanes, evaporation and addition of THF.
E = 4% $Ni(PPh_3)_2Cl_2$, 8% *n*-BuLi, 8% PPh_3, THF, 23 °C.

SCHEME 70. Iterative 'one-pot' homologation of terpenoids containing 1,5-diene units with (*E*)- and (*Z*)-1,4-diiodo-2-methyl-1-butenes and its application to the synthesis of coenzyme Qs, farnesol, and geranylgeraniols[171]

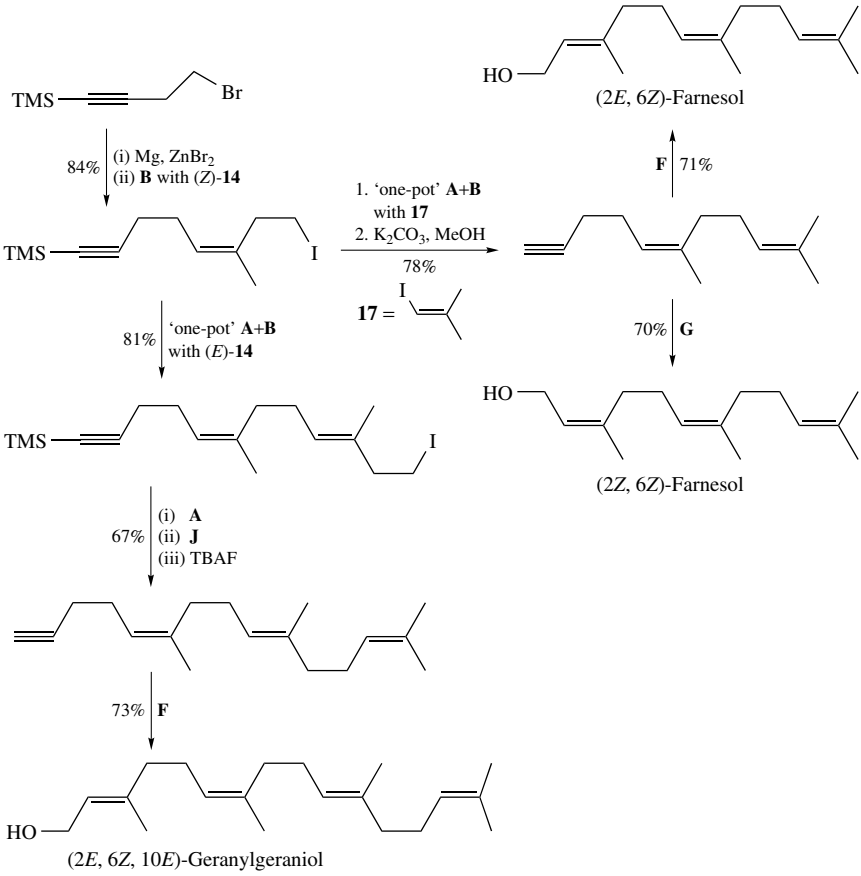

F = (i) Me_3Al (1.5 eq.), Cl_2ZrCp_2 (0.25 eq.), $(CH_2Cl)_2$, 23 °C, 8 h.
(ii) Solvent evaporation, extraction with hexanes. (iii) *n*-BuLi, –30 °C.
(iv) $(CH_2O)_n$, THF, 23 °C, 3 h.
G = (i) *n*-BuLi, THF, –78 °C to 0 °C. (ii) $(CH_2O)_n$ (2 eq.), 23 °C, 3 h.
(iii) *i*-BuMgCl (2.4 eq.), Cl_2TiCp_2 (0.1 eq.), Et_2O, 0 to 23 °C, 2 h.
(iv)THF, MeI, 0 to 23 °C, 2 h.
J = **4**, 2.5% $Pd_2(dba)_3$, 10% TFP, THF, 23 °C, 3 h.

SCHEME 70. (*continued*)

and Kambe and coworkers' discovery of the reaction of alkylmagnesium derivatives with primary alkyl tosylates, bromides and fluorides, but not chlorides, in the presence of a Ni–butadiene dimer complex[92] (Scheme 75).

Another major approach to the Pd- or Ni-catalyzed alkylation with alkyl electrophiles is to use bulky and highly nucleophilic trialkylphosphines to promote slow oxidative addition. Screening of several trialkylphosphines as well as several widely used triarylphosphines for the Pd-catalyzed reaction of *n*-BuZnBr with $Br(CH_2)_3OBn$ led to the following results: Firstly, most of the conventional triarylphosphines including PPh_3, TFP

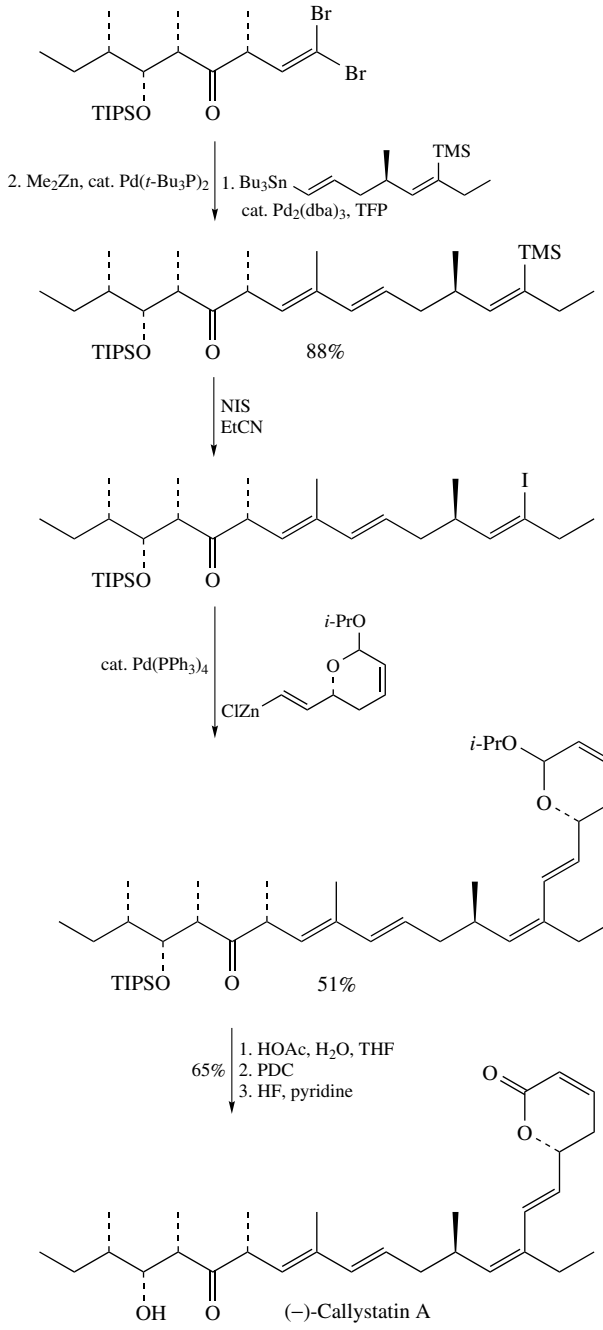

SCHEME 71. Synthesis of (−)-callystatin A via Pd-catalyzed stepwise disubstitution of a 1,1-dibromo-1-alkene[122]

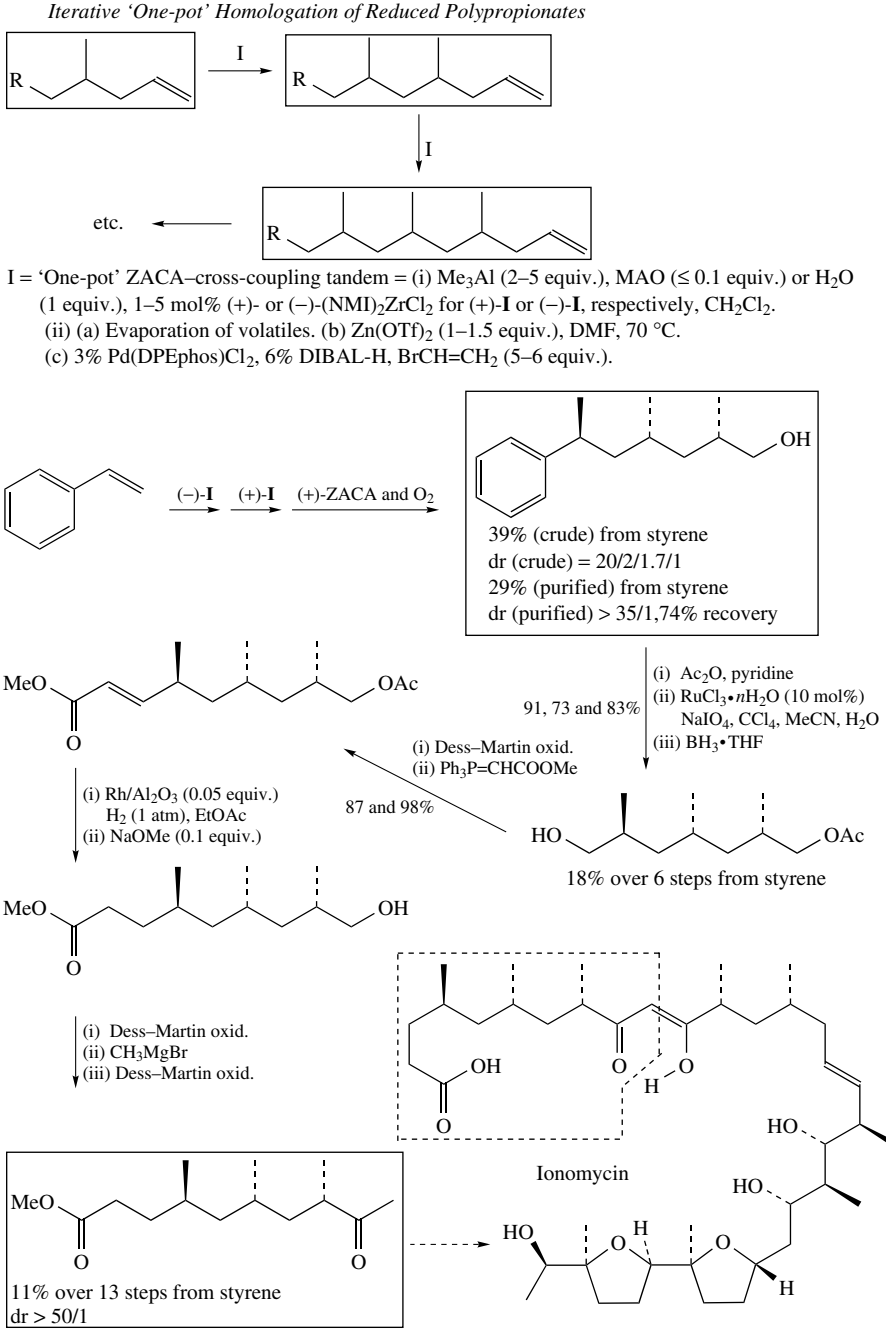

SCHEME 72. Iterative 'one-pot' homologation of reduced polypropionates via ZACA–Pd-catalyzed vinylation and its application to highly efficient catalytic and asymmetric synthesis of key intermediates of ionomycin and borrelidin

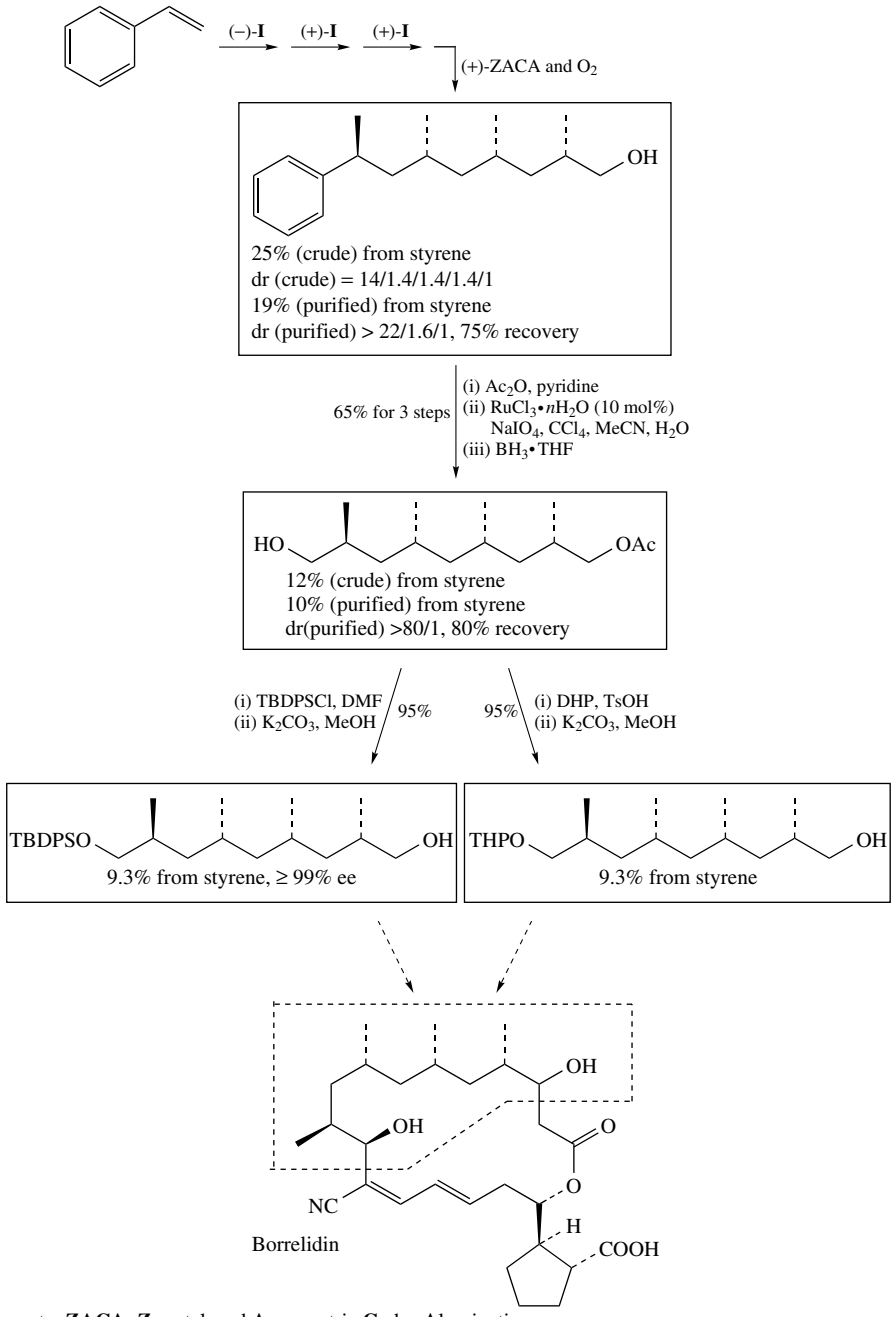

note: **ZACA**: **Z**r-catalyzed **A**symmetric **C**arbo-**A**lumination.

SCHEME 72. (*continued*)

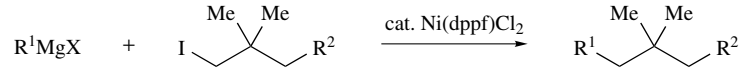

R^1MgX	R^2	Yield (%)
MeMgCl	Ph	77
$MeZnCl•MgCl_2$	Ph	92
o-TolMgCl	Ph	71
o-$TolZnCl•MgCl_2$	Ph	83
1-NaphMgBr	H	57
1-NaphZnBr•MgClBr	H	88

SCHEME 73. Ni-catalyzed reaction of Grignard reagents or organozincs with neopentyl-type iodides

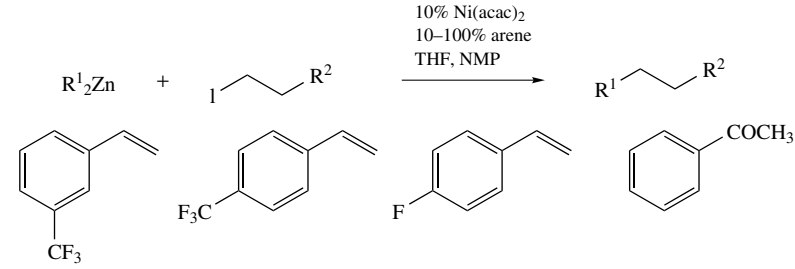

R^1	R^2	Arene	Yields (%)	Reference
n-Pentyl	H_2COC—C₆H₄—CN	MTMS	81	91a
t-$BuCO_2(CH_2)_3$	H_2COC—(2-thienyl)	AcPh	70	91a
NC—C₆H₄—	OC—N(pyrrolidin-2-one)	PTMS	71	91b
C₆H₅—CH_2	$(CH_2)_2O_2CBu$-*t*	PFS	81	91d
cyclohexyl	OC—N(pyrrolidin-2-one)	PFS	63	91g

SCHEME 74. Ni-catalyzed reaction of organozincs with primary alkyl iodides promoted by electron-deficient styrenes or acetophenone

and TTP gave the desired product in less than 5% yields. Secondly, whereas *n*-Bu_3P and *t*-Bu_3P were ineffective, *c*-Pen_3P (70%), *c*-Hex_3P (65%), *i*-Pr_3P (59%) and *t*-Bu_2MeP (55%) were effective, the product yields being indicated in parentheses[88i]. Thirdly, the use of *N*-methylimidazole (NMI) as a promoter and a 2:1 THF–NMP mixture as the solvent was found to be optimal. Primary alkyl electrophiles containing I, Br, Cl and OTs undergo cross-coupling with alkyl, aryl and alkenylzinc derivatives, as summarized in Scheme 76[88i].

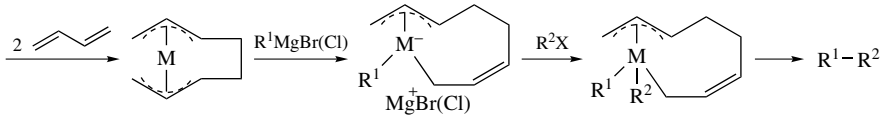

M	R^1	R^2X	R^1-R^2 (%)	Reference
Ni	Et	$Ph(CH_2)_2OTs$	87	92a
Ni	*n*-Bu	*n*-OctCl	96	92a
Ni	*i*-Pr	*n*-OctBr	72	92a
Pd	*n*-Bu	*n*-HexOTs	93	92b
Pd	*s*-Bu	*n*-HexOTs	71	92b
Pd	*n*-Bu	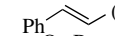	77	92b
Ni (or Cu)	*n*-Pr	*n*-OctBr	97	92c
Ni (or Cu)	*n*-Pr	*n*-OctCl	3	92c
Ni (or Cu)	*n*-Pr	*n*-OctF	94	92c

SCHEME 75. Alkyl–alkyl coupling catalyzed with Ni, Pd or Cu complexes with butadiene dimer

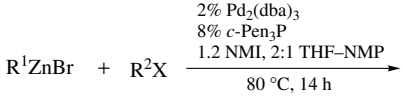

R^1	R^2X	R^1-R^2 (%)
n-Bu	*n*-Oct I	87
$EtO_2C(CH_2)_5$	$NC(CH_2)_6Br$	65
n-Bu	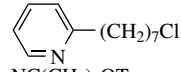	77
$Me_2C(CN)(CH_2)_4$	$NC(CH_2)_5OTs$	64
$CH_2=C(Me)$	*n*-Dec I	93

SCHEME 76. Pd-catalyzed alkylation of organozincs with primary alkyl electrophiles

Rather unexpectedly, the reaction product of alkenylzirconocene chlorides can be alkylated with primary alkyl bromides under the influence of a catalyst–solvent system consisting of 2.5% $Pd(acac)_2$, 2 equiv. LiBr and 1:1 THF–NMP without any phosphine and NMI used above[88l] (Scheme 77).

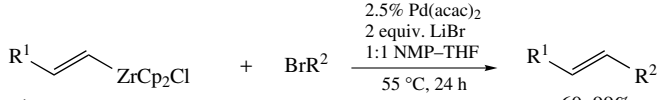

R^1 = *n*-Hex, *t*-Bu, $PhCH_2$, EtO, $THP(OCH_2)_2$ etc.

R^2Br = Primary alkyl bromides

SCHEME 77. Pd-catalyzed alkylation of alkenylzirconocene chlorides with primary alkyl bromides

Although chemoselectivity-related limitations cast a potentially serious concern, Pd- or Ni-catalyzed alkylation with alkyl chlorides may well proceed more satisfactorily with Grignard reagents than with organozincs. A systematic screening of various reaction parameters has led to two kinds of catalyst–solvent systems, one consisting of $Pd(OAc)_2$, *c*-Hex_3P and NMP[209a] and the other consisting of Pd–*N*-heterocyclic

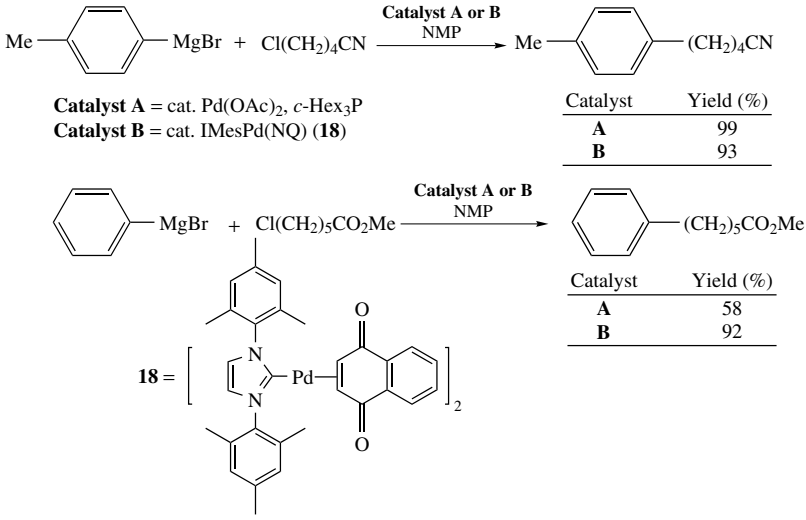

SCHEME 78. Pd-catalyzed reactions of arylmagnesium derivatives with alkyl chlorides

carbene–naphthoquinone complexes, such as IMesPd(NQ) (**18**), and NMP[209b]. Some representative results are shown in Scheme 78.

All of the alkyl electrophiles shown in Schemes 73–78 are primary alkyl derivatives. On the other hand, cross-coupling of primary alkylzincs with secondary alkyl iodides and bromides was shown to be feasible with 4% $Ni(COD)_2$, 8% *s*-Bu-Pybox (**3**) and DMA(N,N-Dimethylacetamide)[88k] (Scheme 79). More recently, a modification of this procedure through the use of *i*-Pr-Pybox and 7:1 DMI/THF, where DMI is 1,3-dimethyl-2-imidazolidinone, in place of *s*-Bu-Pybox (**3**) and DMA has been shown to permit enantioselective alkylation of racemic secondary α-bromoamides with organozincs[210] (Scheme 79).

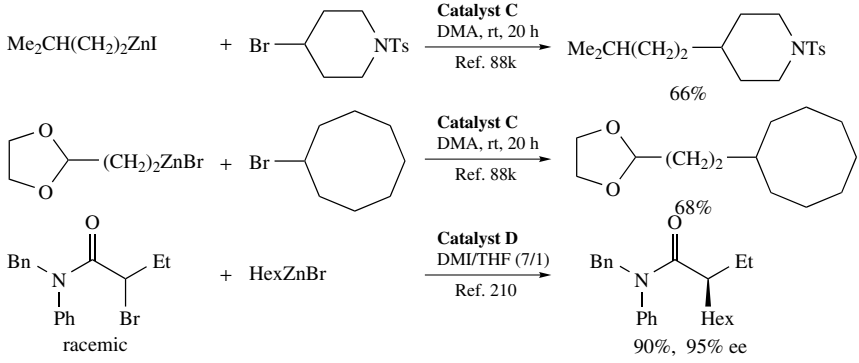

Catalyst C = 4% $Ni(COD)_2$, 8% *s*-Bu-Pybox (**3**)
Catalyst D = 10% Ni-glyme, 13% (*R*)-*i*-Pr-Pybox

SCHEME 79. Ni-catalyzed reaction of primary alkylzincs with secondary alkyl bromides

Although it is outside the scope of this review, some Fe-catalyzed alkylation reactions of organozincs[211] and Grignard reagents[212] with alkyl halides including secondary alkyl bromides and chlorides appear to be highly promising, as indicated by the results shown in Scheme 80[212]. It should be noted that, in cases where secondary alkyl halides are stereodefined at the halogen-bearing carbon center, stereoisomerization at that center is observed. The reaction most likely involved a radical process.

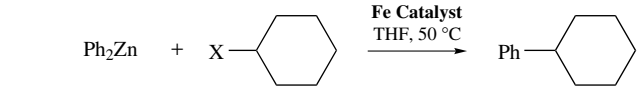

Fe Catalyst = 5% $FeCl_3$, TMEDA (1.5 equiv.)

X	Yield (%)
I	98
Br	97
Cl	88

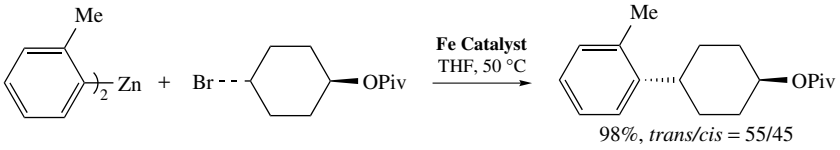

98%, *trans/cis* = 55/45

SCHEME 80. Fe-catalyzed alkylation of organozincs with secondary alkyl halides

F. Acylation and Other Carbon–Carbon Bond Forming Reactions Catalyzed by Pd or Ni

Inspection of Table 1 indicates that acylation, cyanation and enolate substitution represent the other classes of Pd- or Ni-catalyzed cross-coupling. The vast topic of Pd-catalyzed enolate α-substitution including the Tsuji–Trost reaction and other α-substitution reactions[22] is not discussed in this chapter, and the readers are referred to pertinent reviews including that cited above. The other topics are very briefly discussed below.

1. Pd- or Ni-catalyzed acylation of organozincs[20]

The Pd-catalyzed acylation of organozincs was reported in 1983[144], and it has since been widely employed as one of the most satisfactory methods of acylation of organometals[20]. Even in cases where α,β-unsaturated carbonyl compounds are the products, their subsequent conjugate addition reactions do not appear to be competitive. Among recent examples of its application to the synthesis of natural products, the synthesis of amphidinolides T1, T3, T4 and T5 by Fürstner and coworkers[213] is particularly noteworthy (Scheme 81).

A few interesting variants of the Pd-catalyzed acylation of organozincs have been developed. In one such variant, thiol esters are employed in place of acyl chlorides[214]. Another is the Ni-catalyzed reaction of organozincs with cyclic anhydrides[215] shown in Scheme 82. If this desymmetrization reaction can be made highly enantioselective, it would become a significant tool for asymmetric synthesis.

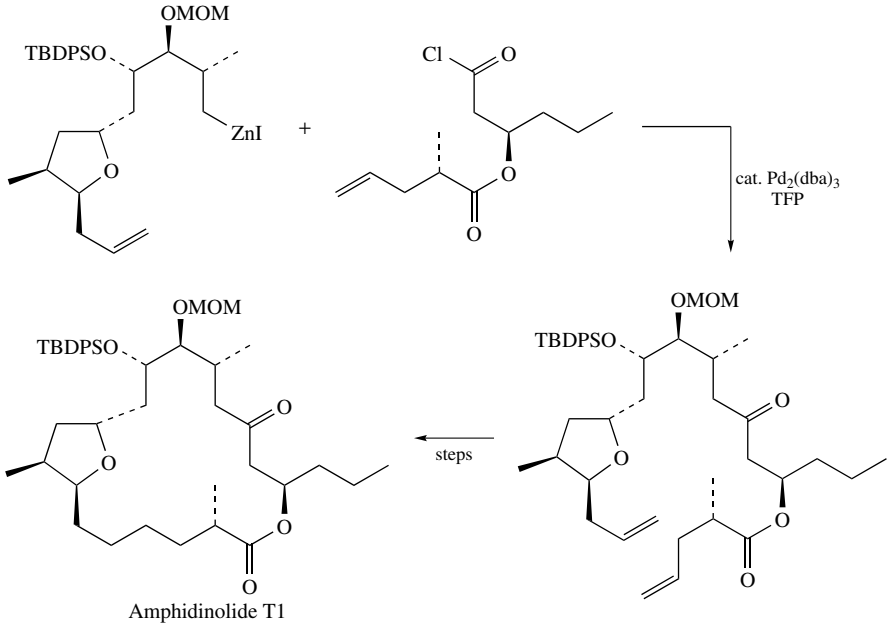

SCHEME 81. Synthesis of amphidinolide T1 via Pd-catalyzed acylation of an alkylzinc derivative

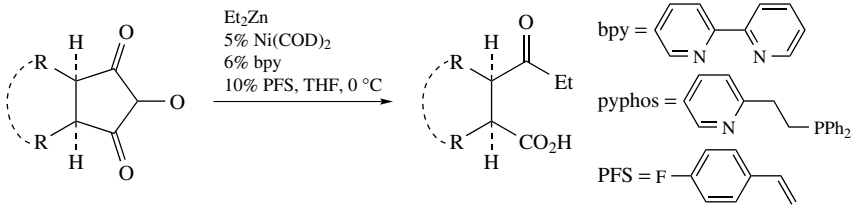

Anhydride		Yield(%)	Anhydride		Yield(%)
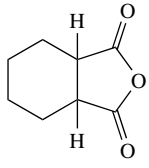	*cis* *trans*	95 87	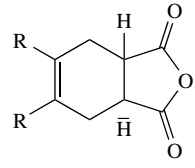	R = H R = Me	95 90
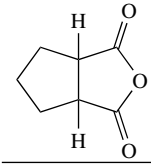		71	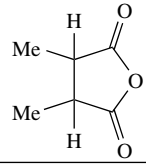		93

SCHEME 82. Ni-catalyzed reaction of alkylzincs with cyclic anhydrides

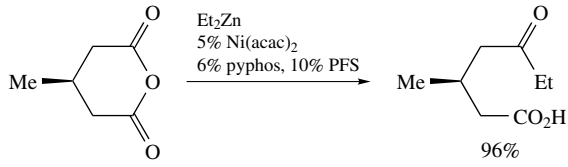

SCHEME 82. (*continued*)

ArX + $Zn(CN)_2$	cat. PdL_n, DMF, 80 °C	ArCN
ArX	cat. PdL_n	ArCN (%) Reference
PhI	2% $Pd(PPh_3)_4$	92 216a
PhBr	6% $Pd(PPh_3)_4$	94 216a
p-$MeOC_6H_4Br$	2–6% $Pd(PPh_3)_4$	95 216a
p-$O_2NC_6H_4Br$	2–6% $Pd(PPh_3)_4$	92 216a
19	4% $Pd(PPh_3)_4$	78 216b
20	4% $Pd(PPh_3)_4$	39 216c
21	2% $Pd(PPh_3)_4$ 16% dppf	92 216d

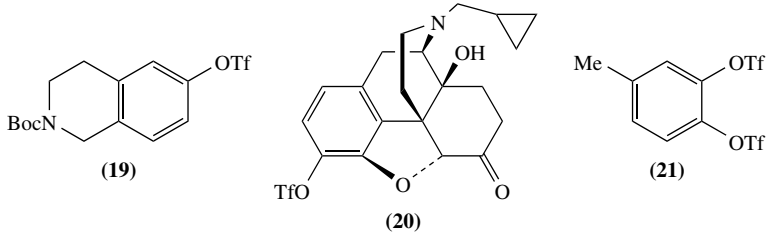

SCHEME 83. Pd-catalyzed cyanation of aryl electrophiles with $Zn(CN)_2$

2. Pd- or Ni-catalyzed cyanation[21a]

Until recently, the Pd- or Ni-catalyzed cyanation had been performed most frequently with metal cyanides containing alkali metals, such as Na and K[21a]. More recently, however, the use of $Zn(CN)_2$ in conjugation with DMF has been reported to be a useful alternative[216] (Scheme 83). Further delineation of the relative merits and demerits among various metal countercations appears to be desirable.

IV. ACKNOWLEDGMENT

The authors thank the National Science Foundation, the National Institutes of Health (GM36792) and Purdue University for support of research in the area covered in this chapter.

V. REFERENCES

1. E. Negishi, in *Handbook of Organopalladium Chemistry for Organic Synthesis*, 2 Vols. (Ed. E. Negishi), Wiley-Interscience, New York, 2002, 3179 pp. For Pd-catalyzed cross-coupling, see: Part III, pp. 215–1119.
2. A. de Meijere and F. Diederich (Eds.), *Metal-Catalyzed Cross-Coupling Reactions*, 2nd edn., 2 Vols., Wiley-VCH, Weinheim, 2004, 916 pp.
3. K. Tamao, T. Hiyama and E. Negishi (Eds.), '30 Years of the Cross-Coupling Reactions', *J. Organomet. Chem.*, **653**, 1–291 (2002).
4. For a listing of earlier reviews of the Negishi, Suzuki, Stille, Sonogashira and other Pd-catalyzed cross-coupling reactions, see: E. Negishi, in Chap. III.1 of Reference 1, pp. 215–227.
5. For an earlier overview of the Negishi coupling, see:
   (a) E. Negishi, in Chap. III.2.1 of Reference 1, pp. 229–247.
   (b) E. Negishi, in *Aspects of Mechanism and Organometallic Chemistry* (Ed. J. H. Brewster), Plenum Press, New York, 1978, pp. 285–317.
   (c) E. Negishi, *Acc. Chem. Res.*, **15**, 340 (1982).
   (d) E. Negishi, in *Current Trends in Organic Synthesis* (Ed. H. Nozaki), Pergamon Press, New York, 1983, pp. 269–280.
   (e) E. Negishi and F. Liu, in *Metal-Catalyzed Cross-Coupling Reactions* (Eds. F. Diederich and P. J. Stang), Wiley-VCH, Weinheim, 1998, pp. 1–47.
   (f) For more recent overviews of the Negishi coupling, see References 5–8.
6. E. Negishi, X. Zeng, Z. Tan, M. Qian, Q. Hu and Z. Huang, Chap. 15 of Reference 2, pp. 815–889.
7. E. Negishi, Q. Hu, Z. Huang, M. Qian and G. Wang, *Aldrichimica Acta*, **38**, 71 (2005).
8. (a) P. Knochel, in *Metal-Catalyzed Cross-Coupling Reactions* (Eds. F. Diederich and P. J. Stang), Wiley-VCH, Weinheim, 1998, pp. 387–419.
   (b) P. Knochel, M. I. Calaza and E. Hupe, Chap. 11 of Reference 2, pp. 619–670.
   (c) P. Knochel, I. Sapountzis and N. Gommermann, Chap. 12 of Reference 2, pp. 671–698.
9. For reviews of the Suzuki coupling, see:
   (a) A. Suzuki, Chap. III.2.2 of Reference 1, pp. 249–262.
   (b) N. Miyaura and A. Suzuki, *Chem. Rev.*, **95**, 2457 (1995).
   (c) A. Suzuki, in *Metal-Catalyzed Cross-Coupling Reactions* (Eds. F. Diederich and P. J. Stang), Wiley-VCH, Weinheim, 1998, pp. 49–97.
   (d) A. Suzuki, *J. Organomet. Chem.*, **576**, 147 (1999).
   (e) A. Suzuki and H. C. Brown, *Organic Syntheses via Borane, Vol. 3: Suzuki Coupling*, Aldrich Chem. Co., Milwaukee, 2003, 314 pp.
   (f) N. Miyaura, Chap. 2 of Reference 2, pp. 41–123.
   (g) F. Bellina, A. Carpita and R. Rossi, *Synthesis*, 2419 (2004).
10. For reviews of the Stille coupling, see:
   (a) M. Kosugi and K. Fugami, Chap. III.2.3 of Reference 1, pp. 263–283.
   (b) J. K. Stille, *Angew. Chem., Int. Ed. Engl.*, **25**, 508 (1986).
   (c) V. Farina, V. Krishnarmonthy and W. J. Scott, *Org. React.*, **50**, 1–652 (1997).
   (d) T. N. Mitchell, in *Metal-Catalyzed Cross-Coupling Reactions* (Eds. F. Diederich and P. J. Stang), Wiley-VCH, Weinheim, 1998, pp. 167–202.
   (e) T. N. Mitchell, Chap. 3 of Reference 2, pp. 125–161.
11. For reviews of the Pd- or Ni-catalyzed cross-coupling reactions of organometals containing Si, Ge, In and other metals see:
   (a) T. Hiyama and E. Shirakawa, Chap. III.2.4 of Reference 1, pp. 285–309.
   (b) T. Hiyama, in *Metal-Catalyzed Cross-Coupling Reactions* (Eds. F. Diederich and P. J. Stang), Wiley-VCH, Weinheim, 1998, pp. 421–453.
   (c) S. E. Denmark and R. F. Sweis, *Acc. Chem. Res.*, **35**, 835 (2002).
   (d) S. E. Denmark and M. H. Ober, *Aldrichimica Acta*, **36**, 75 (2003).
   (e) S. E. Denmark and R. F. Sweis, Chap. 4 of Reference 2, pp. 163–216.
12. For reviews of the Ni-catalyzed cross-coupling reactions of organometals containing Mg, see:
   (a) K. Tamao, in *Comprehensive Organic Synthesis* (Eds. B. M. Trost, I. Fleming and G. Pattenden), Vol. 3, Pergamon Press, Oxford, 1991, pp. 819–887.
   (b) See also Reference 8c.

13. For reviews of Pd-catalyzed aryl–aryl coupling, see:
(a) L. Anastasia and E. Negishi, Chap. III.2.5 of Reference 1, pp. 311–334.
(b) K. Undheim, Chap. III.2.7 of Reference 1, pp. 409–492.
(c) E. J.-G. Anctil and V. Snieckus, Chap. 14 of Reference 2, pp. 761–813. See also A. D. Schlüter and Z. Bo, Chap. III.2.17.2 of Reference 1, pp. 825–861.
14. For reviews of Pd-catalyzed alkenylation, see:
(a) S. Huo and E. Negishi, Chap. III.2.6 of Reference 1, pp. 335–408.
(b) B. H. Lipshutz, Chap. III.2.17.1 of Reference 1, pp. 807–823. See also Reference 7.
15. For reviews of Pd-catalyzed alkynylation in general, see:
(a) E. Negishi and L. Anastasia, *Chem. Rev.*, **13**, 1979 (2003).
(b) J. A. Marsden and M. M. Haley, Chap. 6 of Reference 2, pp. 317–394.
16. For reviews of the Sonogashira coupling, see:
(a) K. Sonogashira, *Comp. Org. Synth.*, **3**, 521 (1991).
(b) K. Sonogashira, in *Metal-Catalyzed Cross-Coupling Reactions* (Eds. F. Diederich and P. J. Stang), Wiley-VCH, Weinheim, 1998, pp. 203–229.
(c) K. Sonogashira, Chap. III.2.8.1 of Reference 1, pp. 493–529.
(d) See also Reference 15.
17. For reviews of the Pd-catalyzed alkynylation with preformed alkynylmetals, see:
(a) E. Negishi and C. Xu, Chap. III.2.8.2 of Reference 1.
(b) See also Reference 16.
18. For reviews of Pd-catalyzed allylation, benzylation and propargylation, see:
(a) E. Negishi and F. Liu, Chap. III.2.9 of Reference 1, pp. 551–589.
(b) E. Negishi and B. Liao, Chap. III.2.10 of Reference 1, pp. 591–596.
(c) J. Tsuji and T. Mandai, in *Metal-Catalyzed Cross-Coupling Reactions* (Eds. F. Diederich and P. J. Stang), Wiley-VCH, Weinheim, 1998, pp. 455–489.
19. For reviews of the Pd-catalyzed alkylation, see:
(a) E. Negishi and S. Gagneur, Chap. III.2.11.1 of Reference 1, pp. 597–618.
(b) E. Negishi and F. Zeng, Chap. III.2.11.2 of Reference 1, pp. 619–633.
(c) S. R. Chemler, D. Trauner and S. J. Danishefsky, *Angew. Chem., Int. Ed.*, **40**, 4544 (2001).
(d) M. R. Netherton and G. C. Fu, *Adv. Synth. Catal.*, **346**, 1525 (2004).
(e) A. C. Frisch and M. Beller, *Angew. Chem., Int. Ed.*, **44**, 674 (2005).
20. For reviews of the Pd-catalyzed acylation and other cross-coupling reactions with α-hetero-substituted organic electrophiles, see:
(a) T. Sugihara, Chap. III.2.12.1 of Reference 1, pp. 635–647.
(b) T. Sugihara, Chap. III.2.12.2 of Reference 1, pp. 649–655.
21. For reviews of the Pd-catalyzed cross-coupling involving α-hetero-substituted organometals, see:
(a) K. Takagi, Chap. III.2.13.1 of Reference 1, pp. 657–672.
(b) F.-T. Luo, Chap. III.2.13.2 of Reference 1, pp. 673–691.
22. For reviews of the Pd-catalyzed α-substitution reactions of enolates, see: E. Negishi, Chap. III.2.14.1 of Reference 1, pp. 693–719. For reviews of the Tsuji–Trost and related reactions, see: Part V of Reference 1, pp. 1663–2117.
23. For reviews of the Pd-catalyzed cross-coupling involving β-hetero-substituted compounds, see:
(a) E. Negishi and A. Alimardanov, Chap. III.2.14.2 of Reference 1, pp. 721–766.
(b) E. Negishi, *J. Organomet. Chem.*, **576**, 179 (1999).
24. For reviews of the Pd-catalyzed conjugate substitution, see: E. Negishi and Y. Dumond, Chap. III.2.15 of Reference 1, pp. 767–806.
25. For reviews of the Pd-catalyzed asymmetric cross-coupling, see:
(a) T. Hayashi, Chap. III.2.16 of Reference 1, pp. 791–806.
(b) M. Ogasawara and T. Hayashi, in *Catalytic Asymmetric Synthesis*, 2nd edn. (Ed. I. Ojima), Wiley-VCH, New York, 2000, pp. 651–674.
26. For reviews of the synthesis of natural products via Pd-catalyzed cross-coupling, see: Z. Tan and E. Negishi, Chap. III.2.18 of Reference 1, pp. 863–942.
27. For reviews of the mechanism of Pd-catalyzed cross-coupling, see:
(a) C. Amatore and A. Jutand, Chap. III.2.19 of Reference 1, pp. 943–972.
(b) A. M. Echavarren and D. J. Cárdenas, Chap. 1 of Reference 2, pp. 1–40.
(c) J. K. Stille and K. S. Y. Lau, *Acc. Chem. Res.*, **10**, 434 (1977).

(d) E. Negishi, T. Takahashi and K. Akiyoshi, in *Catalysis of Organic Reactions* (Eds. P. N. Rylander, H. Greenfield and R. L. Augustine), Marcel Dekker, New York, 1998, pp. 381–407.
28. For reviews of the Pd-catalyzed homo-coupling, see: M. Kotora and T. Takahashi, Chap. III.2.20 of Reference 1, pp. 973–993.
29. (a) K. Tamao, K. Sumitani and M. Kumada, *J. Am. Chem. Soc.*, **94**, 4374 (1972).
(b) R. J. P. Corriu and J. P. Masse, *J. Chem. Soc., Chem. Commun.*, 144 (1972).
(c) K. Tamao, *J. Organomet. Chem.*, **653**, 23 (2002).
30. (a) M. Yamamura, I. Moritani and S. I. Murahashi, *J. Organomet. Chem.*, **91**, C39 (1975).
(b) S. I. Murahashi, M. Yamamura, K. I. Yanagisawa, N. Mita and K. Kondo, *J. Org. Chem.*, **44**, 2408 (1979).
(c) S. I. Murahashi, *J. Organomet. Chem.*, **653**, 27 (2002).
31. E. Negishi and S. Baba, *J. Chem. Soc., Chem. Commun.*, 596 (1976).
32. S. Baba and E. Negishi, *J. Am. Chem. Soc.*, **98**, 6729 (1976).
33. E. Negishi, A. O. King and N. Okukado, *J. Org. Chem.*, **42**, 1821 (1977).
34. E. Negishi and D. E. Van Horn, *J. Am. Chem. Soc.*, **99**, 3168 (1977).
35. A. O. King, N. Okukado and E. Negishi, *J. Chem. Soc., Chem. Commun.*, 683 (1977).
36. A. O. King, E. Negishi, F. J. Villani, Jr. and A. Silveira, Jr., *J. Org. Chem.*, **43**, 358 (1978).
37. N. Okukado, D. E. Van Horn, W. L. Klima and E. Negishi, *Tetrahedron Lett.*, 1027 (1978).
38. E. Negishi, N. Okukado, A. O. King, D. E. Van Horn and B. I. Spiegel, *J. Am. Chem. Soc.*, **100**, 2254 (1978).
39. E. Negishi, *J. Organomet. Chem.*, **653**, 34 (2002).
40. (a) J. F. Fauvarque and A. Jutand, *Bull. Soc. Chim. Fr.*, 765 (1976).
(b) J. F. Fauvarque and A. Jutand, *J. Organomet. Chem.*, **132**, C17 (1977).
41. A. Sekiya and N. Ishikawa, *J. Organomet. Chem.*, **118**, 349 (1976).
42. K. Takami, H. Yorimitsu and K. Oshima, *Org. Lett.*, **4**, 2993 (2002).
43. (a) D. E. Van Horn and E. Negishi, *J. Am. Chem. Soc.*, **100**, 2252 (1978).
(b) E. Negishi, D. E. Van Horn and T. Yoshida, *J. Am. Chem. Soc.*, **107**, 6639 (1985).
44. (a) D. Y. Kondakov and E. Negishi, *J. Am. Chem. Soc.*, **117**, 10771 (1995).
(b) D. Y. Kondakov and E. Negishi, *J. Am. Chem. Soc.*, **118**, 1577 (1996).
45. U. M. Dzhemilev, O. S. Vostrikova and R. M. Sultanov, *Izv. Akad. Nauk SSSR, Ser. Khim.*, 218 (1983); *Engl. Trans.: Bull. Acad. Sci. USSR, Division of Chem. Scien.*, **32**, 193 (1983).
46. S. Gagneur, J. L. Montchamp and E. Negishi, *Organometallics*, **19**, 2417 (2000).
47. (a) J. F. Normant and M. Bourgain, *Tetrahedron Lett.*, 2583 (1971).
(b) For a review, see: J. F. Normant and A. Alexakis, *Synthesis*, 841 (1981).
48. (a) N. Jabri, A. Alexakis and J. F. Normant, *Tetrahedron Lett.*, **22**, 959 (1981).
(b) N. Jabri, A. Alexakis and J. F. Normant, *Tetrahedron Lett.*, **23**, 1589 (1982).
49. S. Hyuga, Y. Chiba, N. Yamashine, S. Hara and A. Suzuki, *Chem. Lett.*, 1757 (1987).
50. A. Satoh and A. Suzuki, *Tetrahedron Lett.*, **29**, 1811 (1988).
51. For applications of distannation, see:
(a) T. N. Mitchell, A. Amamria, H. Killing and D. Rutschow, *J. Organomet. Chem.*, **304**, 257 (1986).
(b) T. N. Mitchell, K. Kwetkat, D. Rutschow and V. Schneider, *Tetrahedron*, **45**, 969 (1989).
52. (a) E. J. Corey, J. A. Katzenellenbogen and G. H. Posner, *J. Am. Chem. Soc.*, **89**, 4245 (1967).
(b) S. E. Denmark and T. K. Jones, *J. Org. Chem.*, **47**, 4595 (1982).
53. E. Negishi, M. Ay, Y. V. Gulevich and Y. Noda, *Tetrahedron Lett.*, **34**, 1437 (1993).
54. J. G. Duboudin and B. Jousseaume, *J. Organomet. Chem.*, **168**, 1 (1979).
55. L. Anastasia, Y. R. Dumond and E. Negishi, *Eur. J. Org. Chem.*, 3039 (2001).
56. S. Ma and E. Negishi, *J. Org. Chem.*, **62**, 784 (1997).
57. P. M. Pihko and A. M. P. Koskinen, *Synlett*, 1966 (1999).
58. A. Pimm, P. Kocienski and S. D. A. Street, *Synlett*, 886 (1992).
59. A. M. Garćia and A. Mascareño, *Tetrahedron Lett.*, **36**, 5413 (1995).
60. K. A. Agrios and M. Srebnik, *J. Organomet. Chem.*, **444**, 15 (1993).
61. E. Negishi, in *Organometallics in Organic Synthesis*, Wiley-Interscience, New York, 1980, 532 pp.
62. For reviews of the preparation of organozincs other than References 8a and 8b, see:
(a) E. Nakamura, in *Organometallics in Synthesis: A Manual*, 2nd edn. (Ed. M. Schlosser), Chap. V, Wiley, Chichester, 2002, pp. 579–664.

(b) E. Erdik, *Organozinc Reagents in Organic Synthesis*, CRC Press, Boca Raton., 1996, 411 pp.
(c) P. Knochel and P. Jones (Eds.), *Organozinc Reagents*, Oxford University Press, Oxford, 1999, 354 pp.
63. Z. Huang, M. Qian, D. J. Babinski and E. Negishi, *Organometallics*, **24**, 475 (2005).
64. M. J. Dunn and R. F. W. Jackson, *J. Chem. Soc., Chem. Commun.*, 319 (1992).
65. (a) L. Micouin, M. Oestreich and P. Knochel, *Angew. Chem., Int. Ed. Engl.*, **36**, 245 (1997).
(b) C. K. Reddy, A. Devasarayaraj and P. Knochel, *Tetrahedron Lett.*, **37**, 4495 (1996).
66. P. Knochel and J. F. Normant, *Tetrahedron Lett.*, **25**, 1475 (1984).
67. S. Vettel, A. Vaupel and P. Knochel, *J. Org. Chem.*, **61**, 7473 (1996).
68. Y. Gao, K. Harada, T. Hata, H. Urabe and F. Sato, *J. Org. Chem.*, **60**, 290 (1995).
69. E. Negishi and J. A. Miller, *J. Am. Chem. Soc.*, **105**, 6761 (1983).
70. E. Negishi, D. E. Van Horn, T. Yoshida and C. L. Rand, *Organometallics*, **2**, 563 (1983).
71. T. Stüdemann and P. Knochel, *Angew. Chem., Int. Ed. Engl.*, **36**, 93 (1997).
72. A. Vaupel and P. Knochel, *Tetrahedron Lett.*, **35**, 8349 (1994).
73. T. Harada, T. Katsuhira, D. Hara, Y. Kotani, K. Maejima, R. Kaji and A. Oku, *J. Org. Chem.*, **58**, 4897 (1993).
74. E. Negishi, Chap. II.3.1 of Reference 1, pp. 127–145.
75. E. Negishi, S. Chatterjee and H. Matsushita, *Tetrahedron Lett.*, **22**, 3737 (1981).
76. H. Kleijn, J. Meijer, G. C. Overbeek and P. Vermeer, *Recl. Trav. Chim. Pays-Bas*, **101**, 97 (1982).
77. D. Choueiry and E. Negishi, Chap. II.2.3 of Reference 1, pp. 47–65.
78. E. Negishi, T. Takahashi and K. Akiyoshi, *J. Chem. Soc., Chem. Commun.*, 1338 (1986).
79. (a) B. H. Lipshutz and P. A. Blomgren, *J. Am. Chem. Soc.*, **121**, 5819 (1999).
(b) B. H. Lipshutz, S. Tasler, W. Chrisman, B. Spliethoff and B. Tesche, *J. Org. Chem.*, **68**, 1177 (2003).
80. B. H. Lipshutz, *Adv. Synth. Catal.*, **343**, 313 (2001).
81. (a) R. F. Heck, *Acc. Chem. Res.*, **12**, 146 (1979).
(b) V. Farina and B. Krishnan, *J. Am. Chem. Soc.*, **113**, 9585 (1991).
82. (a) E. Negishi, Z. R. Owczarczyk and D. R. Swanson, *Tetrahedron Lett.*, **32**, 4453 (1991).
(b) M. Pour and E. Negishi, *Tetrahedron Lett.*, **38**, 525 (1997).
(c) E. Negishi, M. Pour, F. E. Cederbaum and M. Kotora, *Tetrahedron*, **54**, 7057 (1998).
83. T. Hayashi, M. Konishi, Y. Kobori, M. Kumada, T. Higuchi and K. Hirotsu, *J. Am. Chem. Soc.*, **106**, 158 (1984).
84. M. Kranenburg, Y. E M. van der Burgt, P. C. J. Kamer, P. W. N. M. van Leeuwen, K. Goubitz and J. Fraarje, *Organometallics*, **14**, 3081 (1995).
85. J. Shi, X. Zeng and E. Negishi, *Org. Lett.*, **5**, 1825 (2003).
86. J. Shi and E. Negishi, *J. Organomet. Chem.*, **687**, 518 (2003).
87. X. Zeng, M. Qian, Q. Hu and E. Negishi, *Angew. Chem., Int. Ed.*, **43**, 2259 (2004).
88. (a) C. Dai and G. C. Fu, *J. Am. Chem. Soc.*, **123**, 2719 (2001).
(b) M. R. Netherton, C. Dai, K. Neuschütz and G. C. Fu, *J. Am. Chem. Soc.*, **123**, 10099 (2001).
(c) J. H. Kirchhoff, C. Dai and G. C. Fu, *Angew. Chem., Int. Ed.*, **41**, 1945 (2002).
(d) M. R. Netherton and G. C. Fu, *Angew. Chem., Int. Ed.*, **41**, 3910 (2002).
(e) J. H. Kirchhoff, M. R. Netherton, I. D. Hills and G. C. Fu, *J. Am. Chem. Soc.*, **124**, 13662 (2002).
(f) A. F. Littke and G. C. Fu, *Angew. Chem., Int. Ed.*, **41**, 4176 (2002).
(g) K. Meuzel and G. C. Fu, *J. Am. Chem. Soc.*, **125**, 3718 (2003).
(h) J. Y. Lee and G. C. Fu, *J. Am. Chem. Soc.*, **125**, 5616 (2003).
(i) J. Zhou and G. C. Fu, *J. Am. Chem. Soc.*, **125**, 12527 (2003).
(j) M. Eckhardt and G. C. Fu, *J. Am. Chem. Soc.*, **125**, 13642 (2003).
(k) J. Zhou and G. C. Fu, *J. Am. Chem. Soc.*, **125**, 14726 (2003).
(l) S. L. Wiskur, A. Korte and G. C. Fu, *J. Am. Chem. Soc.*, **126**, 82 (2004).
89. (a) J. P. Wolfe, H. Tomori, J. P. Sadighi, J. Yin and S. L. Buchwald, *J. Org. Chem.*, **65**, 1158 (2000).
(b) J. Yin, M. P. Rainka, X.-X. Zhang and S. L. Buchwald, *J. Am. Chem. Soc.*, **124**, 1162 (2002).

(c) T. Hamada, A. Chieffi, J. Ahman and S. L. Buchwald, *J. Am. Chem. Soc.*, **124**, 1261 (2002).
90. A. Devasagayaraj, T. Stüdemann and P. Knochel, *Angew. Chem., Int. Ed. Engl.*, **34**, 2723 (1995).
91. (a) R. Giovannini, T. Stüdemann, G. Dussin and P. Knochel, *Angew. Chem., Int. Ed.*, **37**, 2387 (1998).
(b) R. Giovannini and P. Knochel, *J. Am. Chem. Soc.*, **120**, 11186 (1998).
(c) R. Giovannini, T. Stüdemann, A. Devasagayaraj, G. Dussin and P. Knochel, *J. Org. Chem.*, **64**, 3544 (1999).
(d) M. Piber, A. E. Jensen, M. Rottländer and P. Knochel, *Org. Lett.*, **1**, 1323 (1999).
(e) A. Boudier, C. Darcel, F. Flachomann, L. Micouin, M. Oestreich and P. Knochel, *Chem. Eur. J.*, **6**, 2748 (2000).
(f) A. Boudier, E. Hupe and P. Knochel, *Angew. Chem., Int. Ed.*, **39**, 2294 (2000).
(g) A. E. Jensen and P. Knochel, *J. Org. Chem.*, **67**, 79 (2002).
92. (a) J. Terao, H. Watanabe, A. Ikumi, H. Kuniyasu and N. Kambe, *J. Am. Chem. Soc.*, **124**, 4222 (2002).
(b) J. Terao, Y. Naitoh, H. Kuniyasu and N. Kambe, *Chem. Lett.*, **32**, 890 (2003).
(c) J. Terao, A. Ikumi, H. Kuniyasu and N. Kambe, *J. Am. Chem. Soc.*, **125**, 5646 (2003).
93. For reviews of the use of NHCs in the Pd-catalyzed cross-coupling, see:
(a) A. C. Hillier and S. P. Nolan, *Platinum Met. Rev.*, **46**, 50 (2002).
(b) W. A. Herrmann, K. Öfele, D. V. Preysing and S. K. Schneider, *J. Organomet. Chem.*, **689**, 229 (2003).
94. M. Qian, Z. Huang and E. Negishi, *Org. Lett.*, **6**, 1531 (2004).
95. E. Negishi, A. Alimardanov and C. Xu, *Org. Lett.*, **2**, 65 (2000).
96. E. Negishi, M. Hata and C. Xu, *Org. Lett.*, **2**, 3687 (2000).
97. F. Zeng and E. Negishi, *Org. Lett.*, **3**, 719 (2001).
98. A. Vaupel, F. Langer, V. Malakov and P. Knochel, Chap. A1 in Reference 62c, pp. 325–346.
99. For the Ni-catalyzed Grignard aryl–aryl coupling producing special classes of biaryls, see:
(a) K. Tamao, A. Minato, N. Miyake, T. Matsuda, Y. Kiso and M. Kumada, *Chem. Lett.*, 133 (1975).
(b) R. L. Cough, P. Mison and J. D. Roberts, *J. Org. Chem.*, **41**, 2252 (1976).
100. (a) A. Minato, K. Tamao, T. Hayashi, K. Suzuki and M. Kumada, *Tetrahedron Lett.*, **21**, 845 (1980).
(b) G. S. Reddy and W. Tam, *Organometallics*, **3**, 630 (1984).
(c) T. Katayama and M. Umeno, *Chem. Lett.*, 2073 (1991).
101. J. A. Miller and R. P. Farrell, *Tetrahedron Lett.*, **39**, 6441 (1998).
102. (a) S. Saito, S. Oh-tani and N. Miyaura, *J. Org. Chem.*, **62**, 8024 (1997).
(b) For more recent developments of the Ni- or Pd-catalyzed reactions of arylboron compounds with aryl chlorides, see Reference 9e.
103. K. Tamao, H. Yamamoto, H. Matsumoto, N. Miyake, T. Hayashi and M. Kumada, *Tetrahedron Lett.*, 1389 (1977).
104. (a) T. Hayashi, K. Hayashizaki, T. Kiyoi and Y. Ito, *J. Am. Chem. Soc.*, **110**, 8153 (1988).
(b) T. Hayashi, S. Niizuma, T. Kamikawa, N. Suzuki and Y. Uozumi, *J. Am. Chem. Soc.*, **117**, 9101 (1995).
(c) T. Kamikawa, Y. Uozumi and T. Hayashi, *Tetrahedron Lett.*, **37**, 3161 (1996).
(d) T. Kamikawa and T. Hayashi, *Tetrahedron*, **55**, 3455 (1999).
105. Z. Tan and E. Negishi, *Angew. Chem., Int. Ed.*, **45**, 762 (2006).
106. A. Minato, K. Suzuki and K. Tamao, *J. Am. Chem. Soc.*, **109**, 1257 (1987).
107. A. Sutherland, T. Gallagher, C. G. V. Sharples and S. Wonnacott, *J. Org. Chem.*, **68**, 2475 (2003).
108. J. Li, S. Jeong, L. Essen and P. G. Harran, *Angew. Chem., Int. Ed.*, **40**, 4765 (2001).
109. (a) A. G. M. Barrett, M. Pena and J. A. Willardsen, *J. Chem. Soc., Chem. Commun.*, 1145 (1995).
(b) A. G. M. Barrett, M. Pena and J. A. Willardsen, *J. Org. Chem.*, **61**, 1082 (1996).
110. D. T. Hung, J. B. Nerenberg and S. L. Schreiber, *J. Am. Chem. Soc.*, **118**, 11054 (1996).
111. I. Paterson, K. Febner, M. R. V. Finlay and M. F. Jacobs, *Tetrahedron Lett.*, **37**, 8803 (1996).
112. M. Pour and E. Negishi, *Tetrahedron Lett.*, **37**, 4679 (1996).
113. R. Rossi, F. Bellina, C. Bechini and L. Mannina, *Synthesis*, 1061 (1997).

114. W. D. Schmitz, N. B. Messerschmidt and D. Romo, *J. Org. Chem.*, **63**, 2058 (1998).
115. E. Negishi and C. Xu, *Tetrahedron Lett.*, **40**, 431 (1999).
116. K. E. Drouet and E. A. Theodorakis, *J. Am. Chem. Soc.*, **121**, 456 (1999).
117. S. Ribe, R. K. Kondru, D. N. Beratan and P. Wipf, *J. Am. Chem. Soc.*, **122**, 4608 (2000).
118. T. W. Lee and E. J. Corey, *J. Am. Chem. Soc.*, **123**, 1872 (2001).
119. (a) C. F. Thompson, T. F. Jamison and E. N. Jacobsen, *J. Am. Chem. Soc.*, **122**, 10482 (2000).
    (b) C. F. Thompson, T. F. Jamison and E. N. Jacobsen, *J. Am. Chem. Soc.*, **123**, 9974 (2001).
120. (a) J. S. Panek and T. Hu, *J. Org. Chem.*, **62**, 4914 (1997).
    (b) J. S. Panek and T. Hu, *J. Org. Chem.*, **64**, 3000 (1999).
    (c) T. Hu and J. S. Panek, *J. Am. Chem. Soc.*, **124**, 11368 (2002).
121. H. Ghasemi, L. M. Antunes and M. G. Organ, *Org. Lett.*, **6**, 2913 (2004).
122. N. F. Langille and J. S. Panek, *Org. Lett.*, **6**, 3203 (2004).
123. X. Zeng, F. Zeng and E. Negishi, *Org. Lett.*, **6**, 3245 (2004).
124. A. Sorg and R. Brückner, *Angew. Chem., Int. Ed.*, **43**, 4523 (2004).
125. X. Zeng, Q. Hu, M. Qian and E. Negishi, *J. Am. Chem. Soc.*, **125**, 13636 (2003).
126. H. A. Dieck and F. R. Heck, *J. Organomet. Chem.*, **93**, 259 (1975).
127. B. Liang, T. Novak, Z. Tan and E. Negishi, *J. Am. Chem. Soc.*, **128**, 2770 (2006).
128. M. Kotora and E. Negishi, *Synthesis*, 121 (1997).
129. E. Negishi, C. Xu, Z. Tan and M. Kotora, *Heterocycles*, **46**, 209 (1997).
130. E. Negishi, M. Kotora and C. Xu, *J. Org. Chem.*, **62**, 8957 (1997).
131. N. Yoneda, A. Matsuoka, N. Miyaura, T. Fukuhara and A. Suzuki, *Bull. Chem. Soc. Jpn.*, **63**, 2124 (1990).
132. E. Negishi, M. Qian, F. Zeng, L. Anastasia and D. Babinski, *Org. Lett.*, **5**, 1597 (2003).
133. V. Ratovelomanana and G. Linstrumelle, *Tetrahedron Lett.*, **22**, 315 (1981).
134. X. Lu, X. Huang and S. Ma, *Tetrahedron Lett.*, **34**, 5963 (1993).
135. (a) M. Abarbri, J. L. Parrain and A. Duchêne, *Tetrahedron Lett.*, **36**, 2469 (1995).
    (b) M. Abarbri, J. C. Cintiat, J. L. Parrain and A. Duchêne, *Synthesis*, 82 (1996).
136. L. Anastasia, C. Xu and E. Negishi, *Tetrahedron Lett.*, **43**, 5673 (2002).
137. (a) M. Kotora and E. Negishi, *Tetrahedron Lett.*, **37**, 9041 (1996).
    (b) F. Liu and E. Negishi, *J. Org. Chem.*, **62**, 8591 (1997).
138. M. Sonoda, A. Inaba, K. Itahashi and Y. Tobe, *Org. Lett.*, **3**, 2419 (2001).
139. P. Cadiot and W. Chodkiewicz, in *Chemistry of Acetylene* (Ed. H. G. Viehe), Marcel Dekker, New York, 1969, pp. 597–647.
140. K. Ruitenberg, H. Kleijn, C. J. Elsevier, J. Meijer and P. Vermeer, *Tetrahedron Lett.*, **22**, 1451 (1981).
141. (a) I. Pérez, J. Pérez Sestelo and L. A. Sarandeses, *Org. Lett.*, **1**, 1267 (1999).
    (b) I. Pérez, J. Pérez Sestelo and L. A. Sarandeses, *J. Am. Chem. Soc.*, **123**, 4155 (2001).
142. M. Qian and E. Negishi, *Tetrahedron Lett.*, **46**, 2927 (2005).
143. M. Qian and E. Negishi, *Synlett*, 1789 (2005).
144. E. Negishi, V. Bagheri, S. Chatterjee, F. T. Luo, J. A. Miller and A. T. Stoll, *Tetrahedron Lett.*, **24**, 5181 (1983).
145. C. P. Jasperse and D. P. Curran, *J. Am. Chem. Soc.*, **112**, 5601 (1990).
146. For a related study with alkynylzincs reporting significantly different results, see:
    (a) M. Ogasawara, H. Ikeda, K. Ohtsuki and T. Hayashi, *Chem. Lett.*, 776 (2000).
    (b) M. Ogasawara, H. Ikeda, K. Ohtsuki and T. Hayashi, *Angew. Chem., Int. Ed.*, **39**, 1042 (2000).
    For a related study of the Sonogashira alkynylation reporting significantly different results, see:
    (a) J. Uenishi and K. Matsui, *Tetrahedron Lett.*, **42**, 4353 (2001).
    (b) J. Uenishi, K. Matsui and H. Ohmiya, *J. Organomet. Chem.*, **653**, 141 (2002).
147. N. Yin, G. Wang and E. Negishi, *Angew. Chem., Int. Ed.*, **45**, 2916 (2006).
148. E. Negishi, N. Okukado, S. F. Lovich and F. T. Luo, *J. Org. Chem.*, **49**, 2629 (1984).
149. F. Zeng and E. Negishi, *Org. Lett.*, **4**, 703 (2002).
150. Unpublished results obtained by E. Metay and E. Negishi.
151. M. Qian and E. Negishi, *Org. Process Res. Dev.*, **7**, 412 (2003).
152. V. Ratovelomanana, A. Hammond and G. Linstrumelle, *Tetrahedron Lett.*, **28**, 1649 (1987).
153. (a) M. G. Organ, H. Ghasemi and C. Valente, *Tetrahedron*, **60**, 9453 (2004).
    (b) M. G. Organ and H. Ghasemi, *J. Org. Chem.*, **69**, 695 (2004).
154. For a review, see: D. A. Culkin and J. F. Hartwig, *Acc. Chem. Res.*, **36**, 234 (2003).

155. E. Negishi, Z. Tan, S. Y. Liou and B. Liao, *Tetrahedron*, **56**, 10197 (2000).
156. (a) T. Kamikulo and K. Ogasawara, *Chem. Commun.*, 1679 (1996).
(b) T. Kamikulo and K. Ogasawara, *Heterocycles*, **47**, 69 (1998).
157. M. W. Miller and C. R. Johnson, *J. Org. Chem.*, **62**, 1582 (1997).
158. A. Fürstner, T. Dierkes, O. R. Thiel and G. Blanda, *Chem. Eur. J.*, **7**, 5286 (2001).
159. For extensive reviews with pertinent references, see:
(a) Reference 1, Part V.2, pp. 1163–2117.
(b) J. Tsuji (Ed.), *Palladium Reagents and Catalysis*, Wiley, Chichester, 1995, 560 pp.
160. (a) C. J. Elsevier, P. M. Stehouwer, H. Westmijze and P. Vermeer, *J. Org. Chem.*, **48**, 1103 (1983).
(b) C. J. Elsevier, H. Kleijn, J. Boersma and P. Vermeer, *Organometallics*, **5**, 716 (1986).
161. (a) K. Runtenberg, H. Kleijn, H. Westmijze, J. Meijer and P. Vermeer, *Recl. Trav. Chim. Pays-Bas*, **101**, 405 (1982).
(b) H. Kleijn, H. Westmijze, J. Meijer and P. Vermeer, *Recl. Trav. Chim. Pays-Bas*, **102**, 378 (1983).
162. E. Negishi, H. Matsuzhita and N. Okukedo, *Tetrahedron Lett.*, **22**, 2715 (1981).
163. D. L. Minsker, A. G. Ibragimov and U. M. Dzhemilev, *Zh. Org. Khim.*, **20**, 959 (1984); C.A. No.:101:230040.
164. (a) S. Ma, Q. He and X. Zhang, *J. Org. Chem.*, **70**, 3336 (2005).
(b) S. Ma and A. Zhang, *J. Org. Chem.*, **63**, 9601 (1998).
165. S. Ma and Q. He, *Angew. Chem., Int. Ed.*, **43**, 988 (2004).
166. S. Ma, Q. He and X. Jin, *Synlett*, 514 (2005).
167. (a) S. Ma and L. Wang, *J. Org. Chem.*, **63**, 3497 (1998).
(b) S. Ma, A. Zhang, Y. Yu and W. Xia, *J. Org. Chem.*, **65**, 2287 (2000).
(c) S. Ma and A. Zhang, *J. Org. Chem.*, **67**, 2287 (2002).
(d) S. Ma and G. Wang, *Angew. Chem., Int. Ed.*, **42**, 4215 (2003).
168. E. Negishi, H. Matsushita and N. Okukado, *Tetrahedron Lett.*, **22**, 2715 (1981).
169. H. Matsushita and E. Negishi, *J. Am. Chem. Soc.*, **103**, 2882 (1981).
170. (a) P. Wipf and S. Lim, *Chimia*, **50**, 157 (1996).
(b) P. Wipf and S. Lim, *J. Am. Chem. Soc.*, **117**, 558 (1995).
171. E. Negishi, S. Y. Liou, C. Xu and S. Huo, *Org. Lett.*, **4**, 261 (2002).
172. (a) B. H. Lipshutz, G. Bulow, F. Fernandez-Lazaro, S. K. Kim, R. Lowe, P. Mollard and K. L. Stevens, *J. Am. Chem. Soc.*, **121**, 11664 (1999).
(b) B. H. Lipshutz, P. Mollard, S. S. Pfeiffer and W. Chrisman, *J. Am. Chem. Soc.*, **124**, 14282 (2002).
173. L. E. Fisher, S. S. Labadie, D. C. Reuter and R. D. Clark, *J. Org. Chem.*, **60**, 6224 (1995).
174. T. Shiota and T. Yamamoto, *J. Org. Chem.*, **64**, 453 (1999).
175. M. Hoak, I. Votzuba and H. Dovozakova, *Tetrahedron*, **59**, 607 (2003).
176. (a) T. Hayashi, M. Konishi and M. Kumada, *Tetrahedron Lett.*, 1871 (1979).
(b) E. Negishi, L. F. Valante and M. Kobayashi, *J. Am. Chem. Soc.*, **102**, 3298 (1980).
177. T. Hayashi, M. Konishi, K. Yokota and M. Kumada, *Chem. Lett.*, 767 (1980).
178. M. Kobayashi and E. Negishi, *J. Org. Chem.*, **45**, 5223 (1980).
179. N. Miyaura, T. Ishiyama, M. Ishikawa and A. Suzuki, *Tetrahedron Lett.*, **27**, 6369 (1986).
180. (a) T. Novak, Z. Tan, B. Liang and E. Negishi, *J. Am. Chem. Soc.*, **127**, 2838 (2005).
(b) E. Negishi, Z. Tan, B. Liang and T. Novak, *Proc. Natl. Acad. Sci. U.S.A.*, **101**, 5782 (2004).
181. J.-F. Peyrat, E. Thomas, N. L'Hermite, M. Alami and J.-D. Brion, *Tetrahedron Lett.*, **44**, 6703 (2003).
182. S. Huo, *Org. Lett.*, **5**, 423 (2003).
183. (a) A. B. Smith, III., Y. Qiu, D. R. Jones and K. Kobayashi, *J. Am. Chem. Soc.*, **117**, 12011 (1995).
(b) A. B. Smith, III., T. J. Beauchamp, M. J. LaMarche, M. D. Kaufman, Y. Qiu, H. Arimoto, D. R. Jones and K. Kobayashi, *J. Am. Chem. Soc.*, **122**, 8654 (2000).
(c) For a review on the synthesis of discodermolide, see: I. Paterson and G. J. Florence, *Eur. J. Org. Chem.*, 2193 (2003).
184. D. R. Williams and W. S. Kissel, *J. Am. Chem. Soc.*, **120**, 11198 (1998).
185. (a) K. C. Nicolaou, Z. Yang, G. Shi, J. L. Gunzner, K. A. Agrios and P. Gartner, *Nature*, **392**, 264 (1998).

(b) K. C. Nicolaou, M. E. Bunnage, D. G. McGarry, S. Shi, P. K. Somers, P. A. Wallace, X. Chu, K. A. Agrios, J. L. Gunzner and Z. Yang, *Chem. Eur. J.*, **5**, 599 (1999).
(c) K. C. Nicolaou, P. A. Wallace, S. Shi, M. A. Ouellette, M. E. Bunnage, J. L. Gunzner, K. A. Agrios, G. Shi, P. Gartner and Z. Yang, *Chem. Eur. J.*, **5**, 618 (1999).
(d) K. C. Nicolaou, G. Shi, J. L. Gunzner, P. Gartner, P. A. Wallace, M. A. Ouellette, S. Shi, M. E. Bunnage, K. A. Agrios, C. A. Veale, C. Hwang, J. Hutchinson, C. V. C. Prasad, W. W. Ogilvie and Z. Yang, *Chem. Eur. J.*, **5**, 628 (1999).
(e) K. C. Nicolaou, J. L. Gunzner, G. Shi, K. A. Agrios, P. Gartner and Z. Yang, *Chem. Eur. J.*, **5**, 646 (1999).
186. D. Schinzer, A. Bauer and J. Schieber, *Chem. Eur. J.*, **5**, 2492 (1999).
187. S. Hirashima, S. Aoyagi and C. Kibayashi, *J. Am. Chem. Soc.*, **121**, 9873 (1999).
188. L. Anastasia, Y. R. Dumond and E. Negishi, *Eur. J. Org. Chem.*, 3039 (2001).
189. J. Cossy, I. Pevet and C. Meyer, *Eur. J. Org. Chem.*, 2841 (2001).
190. A. B. Benowitz, S. Fidanze, P. L. C. Small and Y. Kishi, *J. Am. Chem. Soc.*, **123**, 5128 (2001).
191. K. H. Altmann, G. Bold, G. Garavatti, D. Denni, A. Flörsheimer, A. Schmidt, G. Rihs and M. Wartmann, *Helv. Chim. Acta*, **85**, 4086 (2002).
192. T. Hu, N. Takenaka and J. S. Panek, *J. Am. Chem. Soc.*, **124**, 12806 (2002).
193. K.-Y. Lee, C.-Y. Oh and W.-H. Ham, *Org. Lett.*, **4**, 4403 (2002).
194. M. O. Duffey, A. LeTiran and J. P. Morken, *J. Am. Chem. Soc.*, **125**, 1458 (2003).
195. I. R. Corrêa, Jr. and R. A. Pilli, *Angew. Chem., Int. Ed.*, **42**, 3017 (2003).
196. D. R. Williams, A. L. Nold and R. J. Mullins, *J. Org. Chem.*, **69**, 5374 (2004).
197. Q. Zhang, H. Lu, C. Richard and D. P. Curran, *J. Am. Chem. Soc.*, **126**, 36 (2004).
198. Z. Tan and E. Negishi, *Angew. Chem., Int. Ed.*, **43**, 2911 (2004).
199. M. Inoue, W. Yokota, M. G. Murugesh, T. Izuhara and T. Katoh, *Angrew. Chem., Int. Ed.*, **43**, 4207 (2004).
200. M. Magnin-Lachaux, Z. Tan, B. Liang and E. Negishi, *Org. Lett.*, **6**, 1425 (2004).
201. N. Yin and E. Negishi, unpublished.
202. For reviews, see:
(a) E. Negishi, in *Organometallics in Organic Synthesis*, Chap. 4, Wiley-Interscience, New York, 1980, pp. 91–285.
(b) M. Schlosser, in *Organometallics in Synthesis*, 2nd edn. (Ed. M. Schlosser), Chap. 1, Wiley, Chichester, 2002, pp. 1–352.
203. For reviews, see:
(a) G. H. Posner, *Org. React.*, **22**, 253 (1975).
(b) B. H. Lipshutz, in *Organometallics in Synthesis*, 2nd edn. (Ed. M. Schlosser), Chap. 6, Wiley, Chichester, 2002, pp. 665–815.
204. M. Tamura and J. K. Kochi, *J. Organomet. Chem.*, **42**, 205 (1972).
205. G. Cahiez, C. Charboche and M. Jezequel, *Tetrahedron*, **56**, 2733 (2000).
206. P. L. Castle and D. A. Widdowson, *Tetrahedron Lett.*, **27**, 6013 (1986).
207. (a) K. Yuan and W. J. Scott, *Tetrahedron Lett.*, **30**, 4779 (1989).
(b) K. Yuan and W. J. Scott, *J. Org. Chem.*, **55**, 6188 (1990).
(c) K. Yuan and W. J. Scott, *Tetrahedron Lett.*, **32**, 189 (1991).
(d) K. Park, K. Yuan and W. J. Scott, *J. Org. Chem.*, **58**, 4866 (1993).
208. T. Ishiyama, S. Abe, N. Miyaura and A. Suzuki, *Chem. Lett.*, 691 (1992).
209. (a) A. C. Frisch, N. Shaikh, A. Zapf and M. Beller, *Angew. Chem., Int. Ed.*, **41**, 4056 (2002).
(b) A. C. Frisch, F. Ratagoul, A. Zapf and M. Beller, *J. Organomet. Chem.*, **687**, 403 (2003).
210. C. Fischer and G. C. Fu, *J. Am. Chem. Soc.*, **127**, 4594 (2005).
211. M. Nakamura, S. Ito, K. Matsuo and E. Nakamura, *Synlett*, 1794 (2005).
212. (a) T. Nagano and T. Hayashi, *Org. Lett.*, **6**, 1297 (2004).
(b) M. Nakamura, K. Matsuo, S. Ito and E. Nakamura, *J. Am. Chem. Soc.*, **126**, 3686 (2004).
(c) R. Martin and A. Fürstner, *Angew. Chem., Int. Ed.*, **43**, 3955 (2004).
213. (a) A. Fürstner, C. Aïssa, R. Riveiros and J. Ragot, *Angew. Chem., Int. Ed.*, **41**, 4763 (2002).
(b) C. Aïssa, R. Riveiros, J. Ragot and A. Fürstner, *J. Am. Chem. Soc.*, **125**, 15512 (2003).
214. (a) T. Fukuyama, S. C. Lin and L. Li, *J. Am. Chem. Soc.*, **112**, 7050 (1990).
(b) H. Tokuyama, S. Yokoshima, T. Yamashita and T. Fukuyama, *Tetrahedron Lett.*, **39**, 3189 (1998).
(c) For a review, see: T. Fukuyama and H. Tokuyama, *Aldrichimica Acta*, **37**, 87 (2004).

215. E. A. Bercot and T. Rovis, *J. Am. Chem. Soc.*, **127**, 247 (2005).
216. (a) D. M. Tschaen, R. Desmond, A. O. King, M. C. Fortin, B. Piric, S. King and T. R. Verhoeven, *Synth. Commun.*, **24**, 887 (1994).
(b) H. G. Schnick, G. R. Smith and A. J. Tehhen, *Synth. Commun.*, **25**, 3255 (1995).
(c) H. Kulota and K. C. Rice, *Tetrahedron Lett.*, **39**, 2907 (1998).
(d) U. Drecholer and M. Hanack, *Synlett*, 1207 (1998).

CHAPTER **12**

Enantioselective addition of organozinc compounds

KENSO SOAI and TSUNEOMI KAWASAKI

Department of Applied Chemistry, Faculty of Science, Tokyo University of Science, Kagurazaka, Shinjuku-ku, Tokyo 162-8601, Japan
Fax: +81 33 235 2214; e-mail: soai@rs.kagu.tus.ac.jp and tkawa@rs.kagu.tus.ac.jp

and

ITARU SATO

Department of Chemistry, School of Science and Technology, Kwansei Gakuin University, Sanda, Hyogo 669–1337, Japan
Fax: +81 79 565 9077; e-mail: isato@ksc.kwansei.ac.jp

The chemistry of organozinc compounds
Edited by Z. Rappoport and I. Marek

I. INTRODUCTION

Chirality plays a central role in the chemical, biological, pharmaceutical and material sciences. Owing to the recent advances in asymmetric catalysis, catalytic enantioselective synthesis has become one of the most efficient methods for the preparation of enantiomerically enriched compounds. An increased amount of enantiomerically enriched product can be obtained from an asymmetric reaction using a small amount of an asymmetric catalyst. Studies on the enantioselective addition of dialkylzincs to aldehydes have attracted increasing interest. After the chiral amino alcohols were developed, highly enantioselective and reproducible C−C bond forming reactions have become possible.

Nowadays, this chemistry includes a wide range of applications. The organozinc compounds employed in the enantioselective addition include dialkylzincs, dialkenylzincs, dialkynylzincs, diarylzincs and the related unsymmetrical diorganozincs. Electrophiles have been expanded to aldehydes, ketones and imines. Asymmetric amplification has been observed in the enantioselective addition of organozincs. Recently, asymmetric autocatalysis, i.e. automultiplication of chiral compounds, has been created in organozinc addition to aldehydes.

In this chapter, we deal with these topics with an emphasis on the results from our group. However, it is beyond the scope of this chapter to include all of the papers regarding the enantioselective addition of organozinc compounds. Readers are encouraged to refer to the excellent reviews on these topics[1].

II. THE MECHANISM OF CATALYSIS FOR DIORGANOZINC ADDITION TO CARBONYL COMPOUNDS

The mechanism for the addition of dialkylzincs to aldehydes has been studied. Without any activation, addition of dialkylzincs to aldehydes scarcely proceeds. Thus, how to activate dialkylzinc and/or aldehyde should be considered. There are two ways of catalyzing the addition of diorganozinc to carbonyl compounds. One is activation by Lewis base catalyst (equation 1).

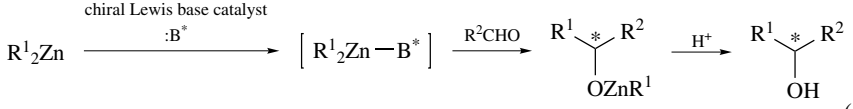

(1)

Lewis bases coordinate to the zinc atom of dialkylzinc. Donation of electrons from the Lewis base weakens the Zn−C bond, and thus enhances the nucleophilicity of the alkyl

groups. Mukaiyama, Soai and coworkers reported that diethylzinc adds to benzaldehyde in the presence of a β-amino alcohol[2]. Thus, the coordination of nitrogen and oxygen atoms to the zinc atom activates dialkylzincs to add to aldehydes. To date, Lewis base catalysis has been greatly expanded, as shown in the following sections. The other mechanism of catalysis is activation of the aldehyde by a Lewis acid catalyst (equation 2). The Lewis acid coordinates to the carbonyl oxygen atom of aldehydes and enhances the electrophilicity of the carbonyl carbon atom.

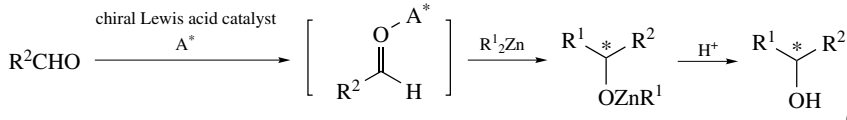

(2)

A. Enantioselective Addition of Dialkylzincs to Aldehydes using Lewis Base Catalysts

As described in the preceding section, β-amino alcohols are strong activators of dialkylzincs. By using a chiral β-amino alcohol, enantioselective addition of dialkylzincs to aldehydes has been reported. *N*,*N*-Dibutylnorephedrine (DBNE, **1**) catalyzes the enantioselective addition of diethylzinc to benzaldehyde and gives chiral 1-phenylpropanol in 90% ee (equation 3)[3]. Addition to aliphatic aldehydes proceeds in a more enantioselective manner (up to 93% ee)[3]. Moreover, addition of α-branched dialkylzinc is effectively catalyzed by DBNE catalyst (up to 98% ee in the addition of diisopropylzinc)[4]. Diphenyl(1-methylpyrrolidin-2-yl)methanol (DPMPM, **2**) catalyzes the addition of diethylzinc to aromatic aldehydes to afford nearly enantiopure (99% ee) *sec*-alcohols[5]. 3-*exo*-(Dimethylamino)isoborneol (DAIB, **3**)[6] and chiral β-amino alcohol **4**[7] also work as highly enantioselective catalysts. Aziridine-based amino alcohol **5**[8], a cyclic amino alcohol screened by using a parallel library **6**[9], aminonaphthol **7**[10] and an iminophenol with [2.2]paracyclophane structure **8**[11] are also known catalysts. The conformationally constrained 1,4-amino alcohol **9**[12] and the lithium amide of piperazine **10**[13] show high catalytic activity as well as high enantioselectivity (92% ee for piperazine lithium amide **10**). Chiral bipyridinedialkanol **11**[14], bis(oxazoline) **12**[15], tetra-coordinated zinc complex **13**[16] and tri-coordinatable pyrazole ligand **14**[17] work as highly enantioselective catalysts. As a Lewis base catalyst with other than hydroxyl group functionality, oxazaborolidine **15**[18], aminothiolate **16**[19], amino disulfide **17**[20], amino thioester **18**[21] and amino diselenide **20**[22] have been reported. The enantioselectivity of a thio analogue **19** of DPMPM **2** is moderate, but the addition of a catalytic amount of metal alkoxide dramatically improves the enantioselectivity[23]. Chiral catalysts derived from ferrocene **21**[24] and **22**[25] exhibit high enantioselectivity.

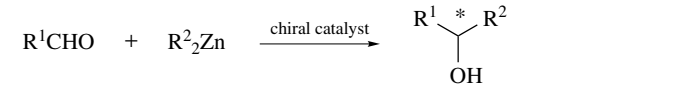

(3)

chiral catalysts

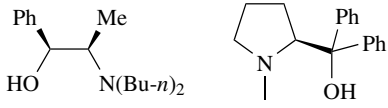

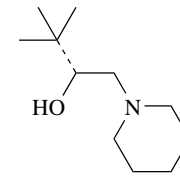

(1*S*, 2*R*)-DBNE (**1**) (*S*)-DPMPM (**2**) DAIB (**3**) (**4**)

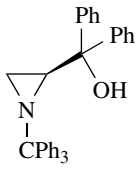

(5)

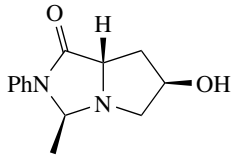

(6)

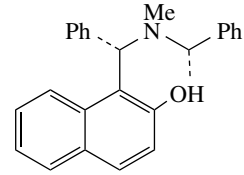

(7)

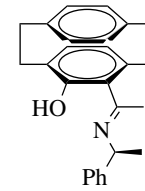

(8)

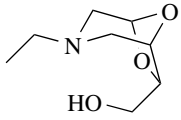

(9)

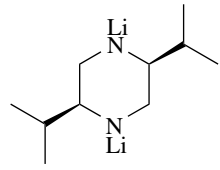

(10)

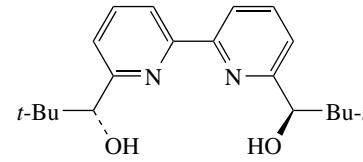

(11)

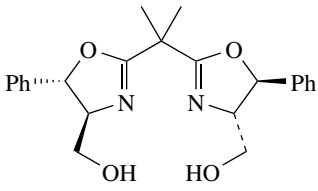

(12)

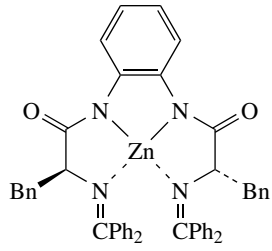

(13)

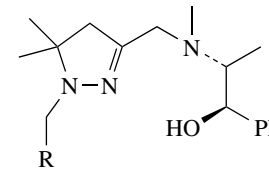

(14), R = 1-naphthyl, 9-anthryl

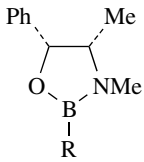

(15)

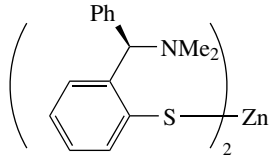

(16)

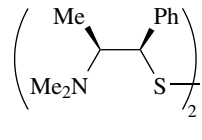

(17)

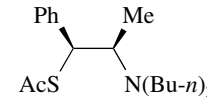

(18)

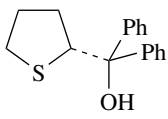

(19)

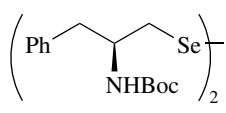

(20)

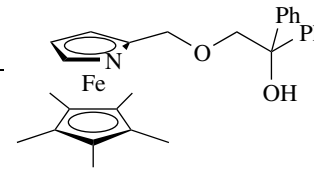

(21)

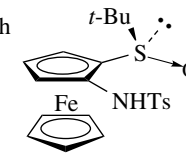

(22)

B. Enantioselective Addition of Dialkylzincs using Lewis Acid Catalysts

The combination of titanium tetraisopropoxide [Ti(OPr-*i*)$_4$] and a chiral ligand has been used to form Lewis acid catalysts. Ohno and coworkers reported the enantioselective addition of diethylzinc to aldehydes using Ti(OPr-*i*)$_4$/C_2-symmetric bis(sulfonamide) **23**[26]. Seebach carried out a comprehensive study using a chiral diol (TADDOL, **24**) as a chiral ligand in combination with Ti(OPr-*i*)$_4$[27]. BINOL[28a, 29] and bis(2-indanol) **25**[28b] are capable of acting as chiral ligands. The tridentate chiral ligand **26** was recently reported[30].

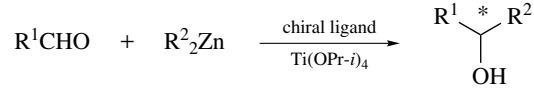

(4)

chiral ligands

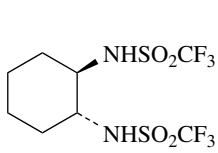

(23)

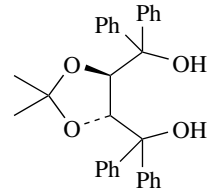

TADDOL (**24**)

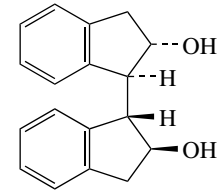

(25)

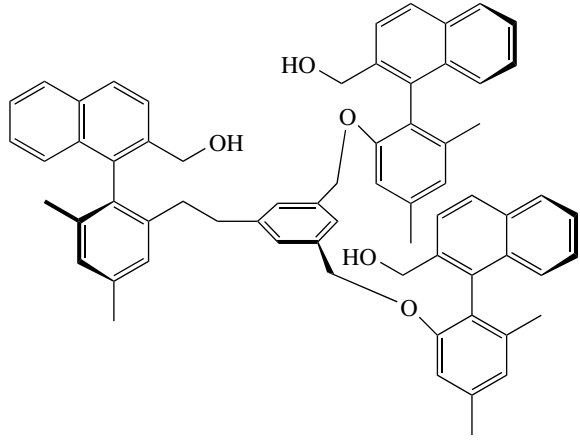

(26)

On the other hand, Soai and coworkers found that chiral thiophosphoramidate **27** formed a complex with Ti(OPr-*i*)$_4$ and that the chiral complex catalyzed the enantioselective addition of dialkylzincs to aldehydes to afford enantioenriched *sec*-alcohols in high enantiomeric excess[31]. In particular, the addition of dicyclopropylzinc exhibits very high enantioselectivity (up to 97% ee)[32].

The simple hydroxycarboxylic acid **28** has been reported as an efficient chiral ligand in combination with Ti(OPr-*i*)$_4$[33].

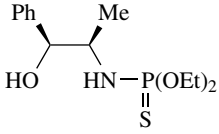

(27)

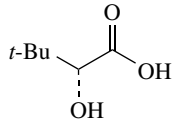

(28)

III. ENANTIOSELECTIVE ADDITION OF ORGANOZINCS TO CARBONYL COMPOUNDS

A. Asymmetric Addition of Dialkylzincs and Functionalized Diorganozincs

A wide variety of dialkyl function of dialkylzincs used in enantioselective alkylation is available[34]. Most of the dialkylzincs can be easily prepared by a metal exchange reaction from the corresponding Grignard reagents (equation 5). After mixing zinc halide and two equivalents of Grignard reagent, distillation affords the corresponding dialkylzinc[34]. Another method is *in situ* formation of dialkylzincs by removing magnesium halide as an insoluble complex with 1,4-dioxane (equation 6)[35, 36].

$$2\ RMgBr \xrightarrow{ZnBr_2} R_2Zn + 2MgBr_2 \xrightarrow{\text{distillation}} R_2Zn \qquad (5)$$

$$2\ RMgX \xrightarrow{ZnCl_2} R_2Zn + 2MgCl(X) \xrightarrow{\text{1,4-dioxane}} R_2Zn + MgCl(X)\bullet\text{dioxane} \qquad (6)$$

Knochel and Singer reported the preparation of functionalized diorganozincs[37] and the enantioselective addition of functionalized diorganozincs to aldehydes. An iodine-zinc exchange reaction provides dialkylzinc reagents with halogen, acyloxy and sulfonamide functions in their ω-positions. The chiral bis(sulfonamide)-titanium complex **29** derived from **23** catalyzed the enantioselective addition to give γ-silylated or γ-stannylated chiral alcohols with high ee (equation 7)[38]. They also reported two methods for the convenient preparation of functionalized diorganozincs from olefins. The former is by the hydroboration of an olefin followed by a zinc-boron exchange reaction (equation 8)[39]. The latter is by hydrozincation catalyzed by a nickel catalyst (equation 9)[40]. The addition of functionalized zinc reagents to aldehydes proceeds enantioselectively in the presence of chiral catalyst **29**[39, 40].

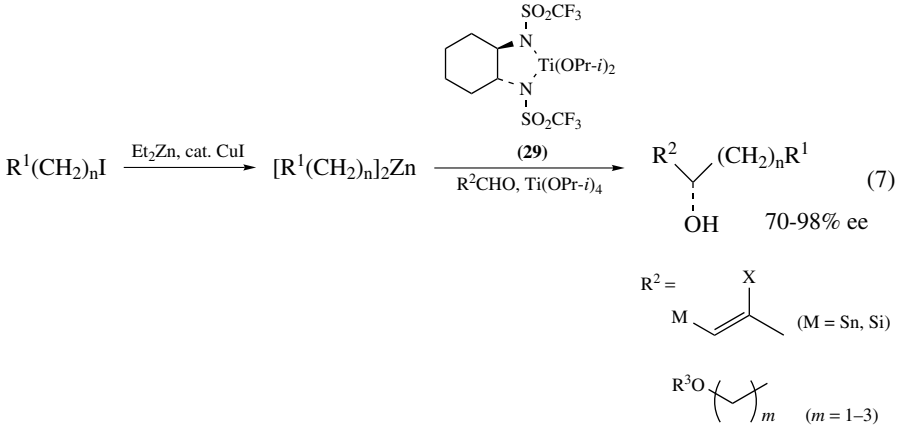

(7)

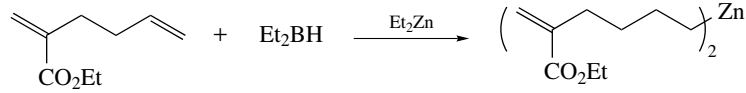

(8)

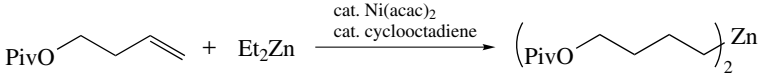

(9)

Unsymmetrical dialkylzincs have also been synthesized by hydroboration and the subsequent zinc-boron exchange reaction[41]. Unsymmetrical dialkylzinc possessing a trimethylsilylmethyl group as a non-transferable group has been developed[42]. By using alkyl(trimethylsilyl)zinc, unlike dialkylzincs, the waste of one equivalent of the valuable alkyl groups is avoided (equations 10 and 11).

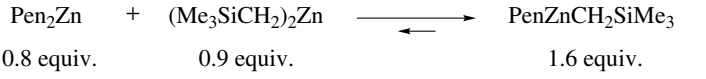

(10)

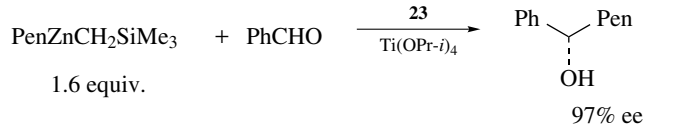

(11)

B. Enantioselective Addition of Diorganozincs to Ketones

Compared with aldehydes, ketones and esters are less reactive electrophiles in the addition of dialkylzincs. This makes it possible to perform a unique reaction that cannot be done with alkyllithium or Grignard reagents, which are too reactive nucleophiles. For example, Watanabe and Soai reported enantio- and chemoselective addition of dialkylzincs to ketoaldehydes and formylesters using chiral catalysts, affording enantiomerically enriched hydroxyketones **30** (equation 12)[43] and hydroxyesters **31** in 91–96% ee, respectively (equation 13). The latter are readily transformed into chiral lactones **32**[44].

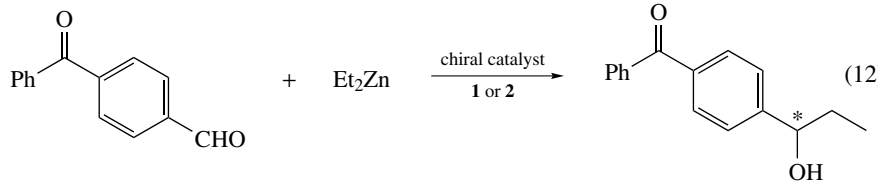

(30)

(12)

chiral catalyst

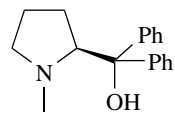

(*S*)-DPMPM (**2**)
96% ee

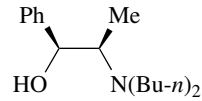

(1*S*, 2*R*)-DBNE (**1**)
91% ee

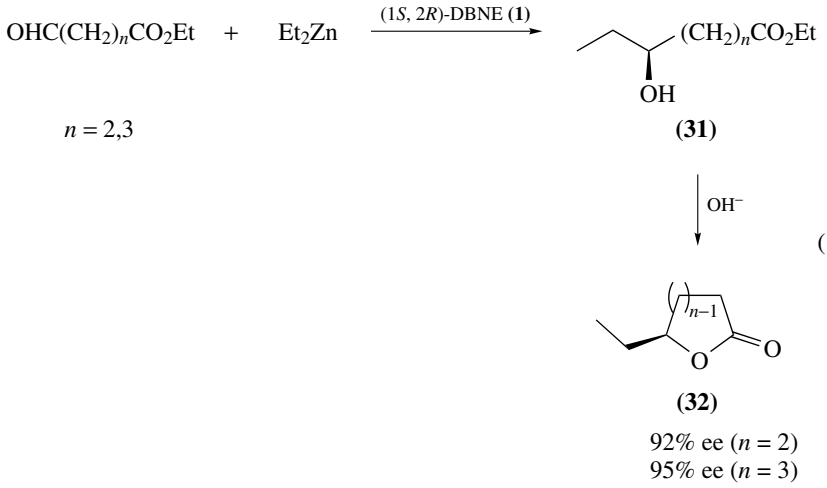

(13)

On the other hand, in the presence of Lewis acid, addition of dialkylzinc to ketones occurs (equation 14)[45]. A stoichiometric amount of Ti(OPr-*i*)$_4$ and a catalytic amount of camphorsulfonamide **33** enable an enantioselective addition of dialkylzincs to ketones[46]. Later, bis(sulfonamide) ligand **34** was found to be a more enantioselective catalyst in this system[47,48].

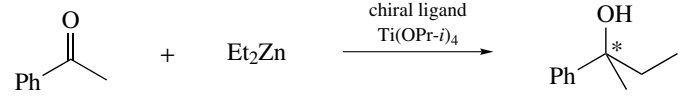

(14)

chiral ligands

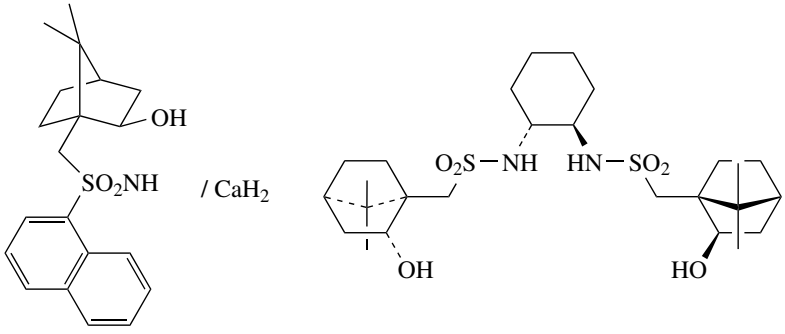

(33)
84% ee

(34)
98% ee

Meanwhile, addition to α-ketoester has been studied (equation 15). The chiral salen-Ti(OPr-*i*)$_2$ catalyst **35**[49] and an amino alcohol derived from hydroxyproline **36**[50] catalyze

the enantioselective addition of diethylzinc and dimethylzinc, respectively, to afford α-hydroxy esters in 78 and 81% ee, respectively.

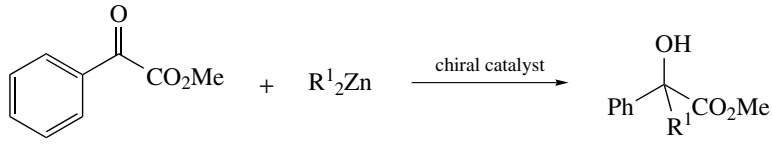

(15)

chiral catalysts

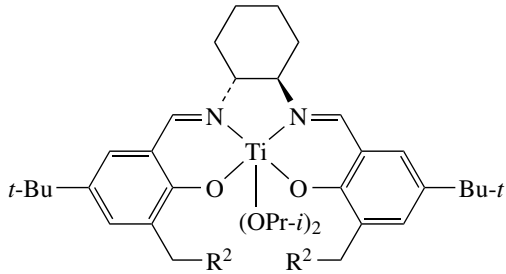

(35)

78% ee (R^1 = Et, R^2 = *c*-NC_5H_{10})

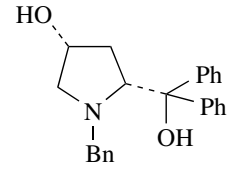

(36)

81% ee (R^1 = Me)

C. Enantioselective Alkenylation of Aldehydes and Ketones

Enantioselective alkenylation was first reported by Oppolzer and Nadinov. Divinylzinc adds to aldehydes in the presence of the chiral diamino alcohol catalyst **37** with high enantioselectivity (>96% ee) (equation 16)[51]. Alkenylzinc bromide adds to aldehydes in the presence of the lithium alkoxide of *N*-methylephedrine (>98% ee)[52]. Ti-TADDOL is also an effective chiral catalyst in the addition of divinylzinc[53].

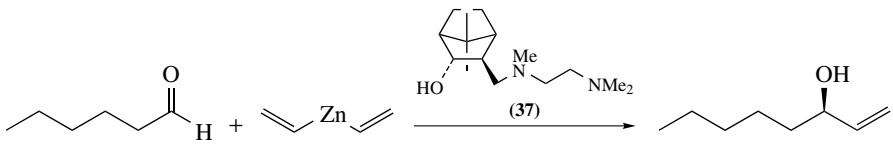

>96% ee

(16)

Oppolzer and Nadinov also reported the synthetic protocol of alkenylalkylzinc from a terminal alkyne (equation 17)[54]. Hydroboration of the alkyne forms a vinylborane, and the subsequent addition of dialkylzinc promotes the zinc-boron exchange reaction to form a mixed zinc reagent, i.e. (*E*)-alkenylalkylzinc. Enantioselective addition of this reagent to aldehydes in the presence of a chiral amino alcohol catalyst proceeds with high enantioselectivity[54]. They used this protocol in an asymmetric macrocyclization from an ω-alkynal[55]. This protocol has also been used by others[56] in the synthesis of amino acids[56b,c] and an immobilized catalyst system[56d]. Soai and Takahashi reported

enantioselective 1,2-addition of an alkenylalkylzinc to an enal to afford enantioenriched diallyl alcohols[57].

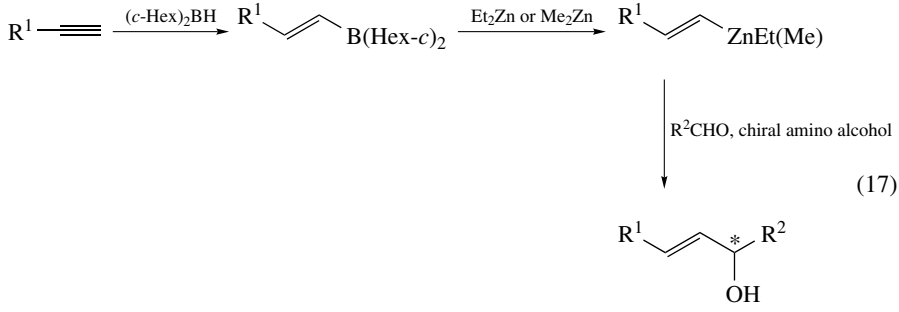

(17)

Another protocol was reported by Wipf and Xu. The hydrozirconation of terminal alkynes followed by the addition of dimethylzinc forms (*E*)-alkenylmethylzinc (equation 18)[58]. The chiral amino thiol **38** has been employed as a catalyst for this reaction[59]. Li and Walsh found that ketones as well as aldehydes are alkenylated by alkenylzinc using the chiral catalyst **34**[60].

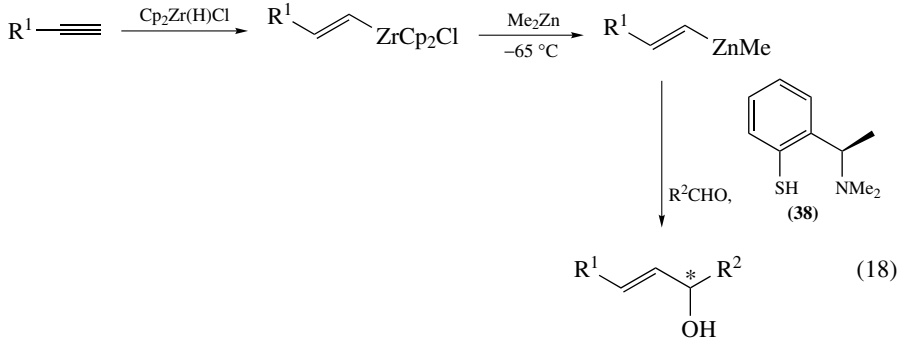

(18)

99% ee
(R^1 = 3-hexyne, R^2 = Ph)

Recently, Soai and coworkers reported an enantioselective addition of diisopropenylzinc and an α-branched vinylzinc reagent to aldehydes (equation 19)[61].

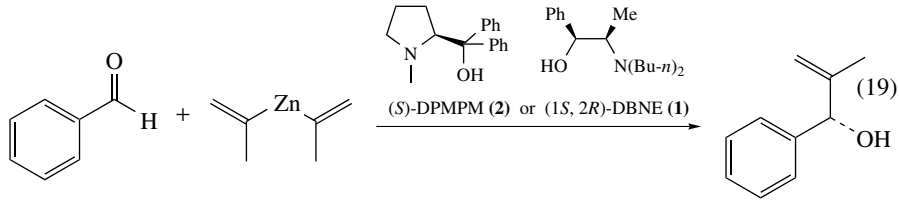

(19)

88–90% ee

D. Enantioselective Addition of Alkynylzincs to Aldehydes and Ketones

Enantioselective addition of alkynyl groups to aldehydes and ketones afford enantioenriched alkynyl alcohols[62]. Early approaches to the catalytic enantioselective addition of dialkynylzincs and alkynylalkylzincs to aldehydes employed catalytic amounts of chiral amino alcohol[63] and amino pyridine[64]. Stoichiometric enantioselective addition of alkynylzinc halide is reported using the lithium alkoxide of *N*-methylephedrine[65].

By using a mixed zinc reagent that is prepared from a terminal alkyne and dialkylzinc (equation 20)[63], catalytic and highly enantioselective (up to 95% ee) addition of alkynylalkylzinc is reported using a chiral pyridyl alcohol[66]. Several series of chiral amino alcohols[67,68], disulfide-oxazolidine[69], BINOL and its derivatives[70], *N*,*O*-ferrocene[71], [2.2]paracyclophane[72] and oxazoline[73] are known to work as chiral catalysts in the enantioselective addition of mixed alkynylalkylzinc reagents.

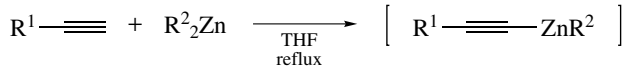

(20)

On the other hand, Lewis acid catalyzed addition to aldehydes has been reported. Chan and coworkers reported that the mixed chiral catalyst Ti(OPr-*i*)$_4$/BINOL/chiral sulfonamide alcohol **39** catalyzes the enantioselective addition of alkynylmethylzinc to aldehyde with up to >99% ee (equation 21)[74]. It was later found that Ti(OPr-*i*)$_4$/chiral sulfonamide alcohol **40**, without using BINOL, also works as a suitable catalyst[75]. Pu and coworkers and Chan and coworkers found that the combination Ti(OPr-*i*)$_4$/BINOL[76,77] and its derivatives[78] are effective catalysts for enantioselective alkynylation with alkynylalkylzinc. Cinchona alkaloids[79], camphorsulfonamide[80] and Boc-L-proline[81] have also been reported as chiral catalysts.

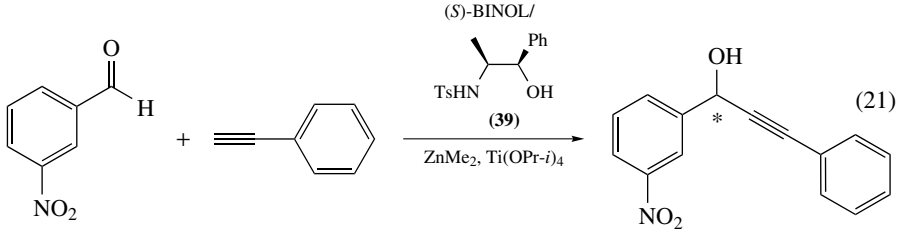

(21)

>99% ee

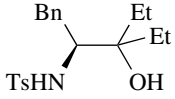

(40)

Chiral Zn(salen) catalyzed enantioselective alkynylation of ketones has been examined by Cozzi[82] and by Saito and Katsuki[83]. Camphorsulfonamide/Cu(OTf)$_2$[84], Ti(O-*i*-Pr)$_4$/BINOL[85] and Et$_3$Al/cinchona alkaloid[86] systems have also been reported. Chiral β-amino alcohols work as chiral catalysts without an additional Lewis acid component[87].

Meanwhile, Carreira and coworkers introduced enantioselective addition of a terminal alkyne to an aldehyde in the presence of $Zn(OTf)_2$, Et_3N and *N*-methylephedrine **41** (equation 22)[88]. The amounts of $Zn(OTf)_2$ and Et_3N were later reduced to a catalytic amount[88b]. This catalytic system has been employed by another group[89] and the enantioselective alkynylation of α-ketoesters has been examined[90].

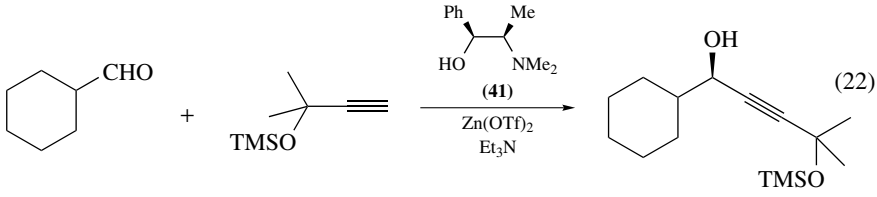

(22)

99% ee

E. Asymmetric Aryl Transfer Reaction to Carbonyl Compounds

Diphenylzinc is an analogue of dialkylzinc. However, the number of reports is limited on the asymmetric phenyl transfer reactions to aldehydes[91]. In 1991, Soai and coworkers reported an enantioselective addition of diphenylzinc to aldehydes (equation 23). In this report, diphenylzinc was prepared from phenyl Grignard reagent and zinc chloride *in situ*. In the presence of a stoichiometric amount of DBNE (**1**), the phenyl transfer reaction proceeds with up to 82% ee[92]. In Seebach's Ti-TADDOL catalyst system, diphenylzinc, which is prepared from phenyl Grignard reagent and zinc chloride, adds to heptanal in 62% ee[53]. Fu and coworkers reported that planar chiral **42** serves as a chiral catalyst in the phenyl transfer reaction to aldehydes using Ph_2Zn[93]. Later, DPMPM **(2)**[94] and binaphthyl-based amino alcohol **43**[95] were found to work as highly enantioselective catalysts for aryl transfer reactions to aldehydes.

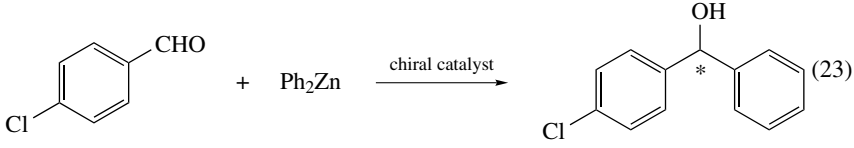

(23)

chiral catalysts

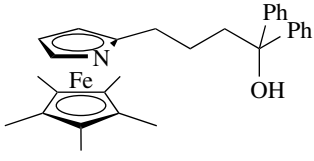

(42)

57% ee

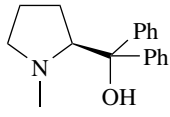

(*S*)-DPMPM **(2)**

93% ee

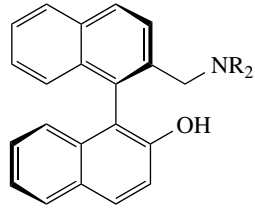

(43)

(NR_2=NMe_2, NBu_2, 1-pyrrolidinyl, 1-piperidinyl, morpholino)

87–95% ee

Recently, Pu's and Bolm's groups reported independently the catalytic and highly enantioselective phenyl transfer reactions using the Ph_2Zn/Et_2Zn mixed reagent (equation 24). Pu's binaphthyl-based catalyst **44** gives the chiral benzhydryl product with up to 94% ee in the aryl transfer reaction to aldehydes[96]. Bolm's chiral ferrocenyl hydroxy oxazoline **45**[97] and chiral η_5-cyclopentadienylrhenium tricarbonyl complex **46**[98] afford the products with 97 and 98% ee, respectively. Arylboronic acids and triphenylboron have also been employed as efficient aryl sources instead of Ph_2Zn[99].

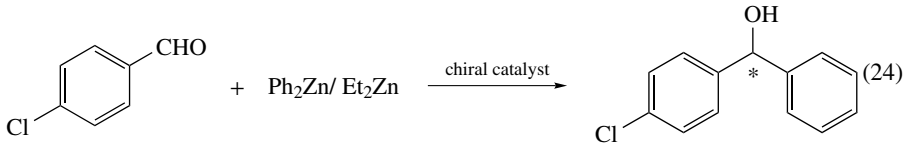

(24)

chiral catalysts

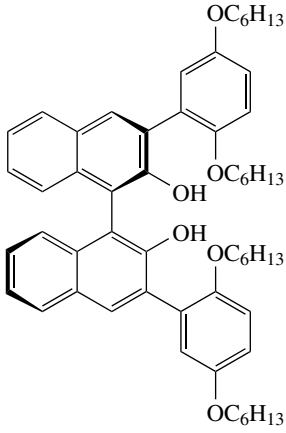

(44)
94% ee

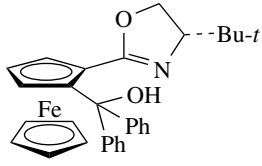

(45)
97% ee

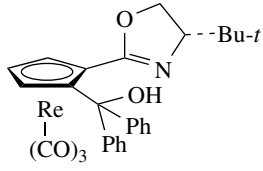

(46)
98% ee

Dosa and Fu reported the first catalytic enantioselective phenyl transfer reaction to ketones (equation 25)[100]. In the presence of 1.5 equivalents of MeOH, the chiral tertiary alcohol was produced in good yield and with high enantioselectivity. Walsh and coworkers recently reported the $Ti(OPr\text{-}i)_4$/chiral dihydroxybis(sulfonamide) catalyst **34** system, whereby enones have been converted to enantioenriched allyl alcohols[101].

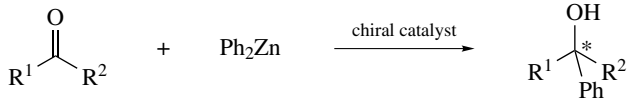

(25)

DAIB (**3**)/ MeOH

91% ee (R^1 = 3-BrC_6H_4, R^2 = Et)

(**34**)/ $Ti(OPr\text{-}i)_4$

96% ee (R^1 = 2-Naphthyl, R^2 = Me)

F. Enantioselective Conjugate Addition of Dialkylzincs to Enones

A catalytic and enantioselective conjugate addition of diethylzinc has been achieved by the combination of a catalytic amount of nickel complex. In 1988, Soai and coworkers reported highly enantioselective conjugate addition of diethylzinc to chalcones in the presence of a catalytic amount of DBNE (**1**) with nickel acetylacetonate $[Ni(acac)_2]$[102–105]. The ee value of the product is as high as 90% ee. The presence of achiral ligands such as Ph_3P increases the ee of the product up to 90% ee. Chiral bipyridinediol (**47**)[106], β-hydroxysulfoximine (**48**)[107], 1-pentyl-2-anilinomethylpyrrolidine[108] and DAIB (**3**)[109] have also been used as chiral catalysts in the presence of $Ni(acac)_2$. Feringa reported that $Co(acac)_2$ catalyzes the conjugate addition[110].

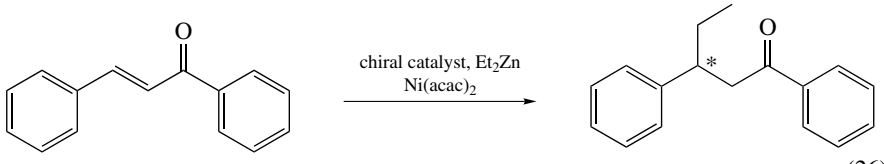

(26)

chiral catalysts

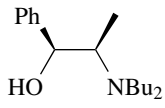

DBNE (**1**)

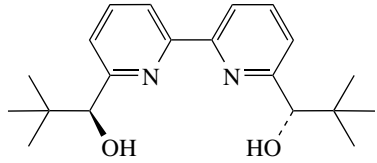

(**47**)

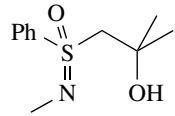

(**48**)

Meanwhile, copper salt catalyzed asymmetric conjugate addition of dialkylzincs has been developed. Alexakis and coworkers reported the catalytic addition of diethylzinc to cyclohexenone using copper salt[111]. Feringa and coworkers developed a marvelous phosphoramidite (**49**)[112]. In the presence of **49** and $Cu(OTf)_2$, diethylzinc adds to cyclohexenone in >98% ee. Recently, asymmetric addition of diphenylzinc using **49** has been reported[113]. Nowadays, compounds **50**[114], **51**[115], **52**[116], **53**[117] and **54**[118] are known as highly enantioselective catalysts.

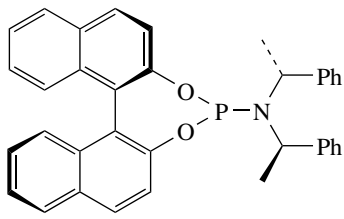

(**49**)

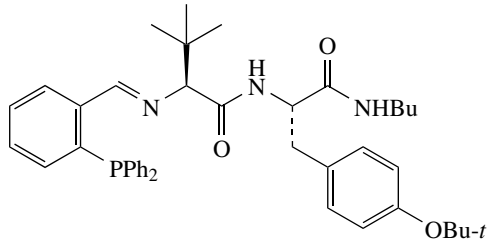

(**50**)

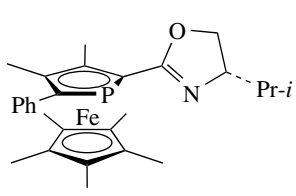

(51)

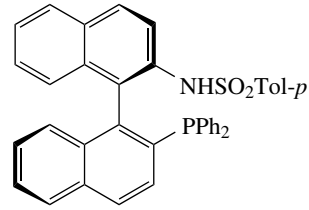

(52)

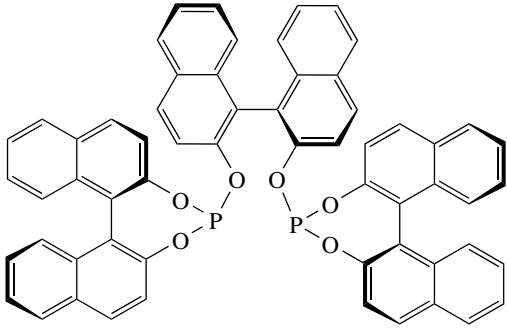

(53)

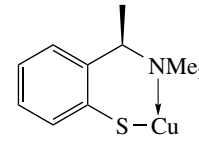

(54)

IV. ENANTIOSELECTIVE ADDITION OF DIORGANOZINCS TO IMINE DERIVATIVES

The carbon-nitrogen double bond (C=N) is an analogue of the carbon-oxygen double bond (C=O). The diastereoselective addition of organometallics to chiral imines and their derivatives has been developed[119]. However, enantioselective addition of organometallics to imines has not been well examined compared with the enantioselective addition to carbonyl groups, probably due to 1) the strong coordination of the formed amines in the reaction and 2) instability of imines. In 1992, Katritzky and Harris reported the enantioselective reaction of *N*-(1-benzotriazoyl)-1-phenylmethyl acetamide and diethylzinc[120]. The substrate is considered to form an acyl imine *in situ* and diethylzinc adds to the acylimine enantioselectively in the presence of DBNE (**1**) (equation 27).

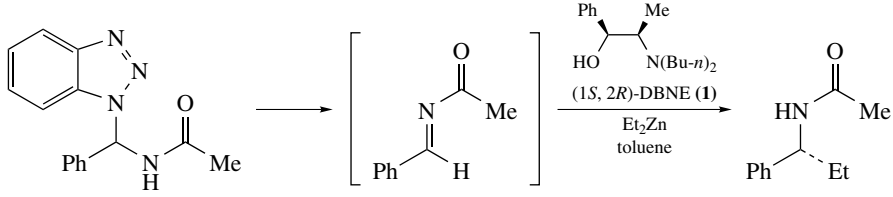

76% ee (27)

Also in 1992, Soai and coworkers reported the enantioselective addition of dialkylzincs to *N*,*N*-diphenylphosphinylimines using DBNE (**1**) and its analogue **55** as chiral ligands

(equation 28)[121]. In addition, asymmetric amplification has also been observed in this system[122]. It may be noted that the *N*,*N*-diphenylphosphinylimines are stable enough to handle without special care. Several groups have reported the enantioselective addition of diorganozincs to *N*,*N*-diphenylphosphinylimines using chiral amino alcohols **56**[123], **57**[124], **58**[125] and the **59**/*i*-Pr_3SiCl system[126]. The copolymerized[127] and dendrimer bound[128] amino alcohols **60** have been found to be efficient chiral ligands.

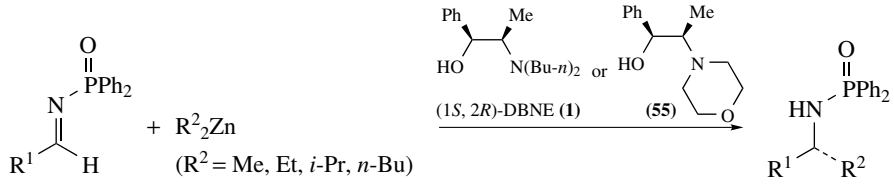

up to 97% ee (28)

chiral catalysts

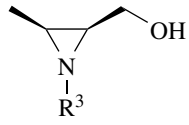

(56) (R^3 = Bn, *i*-Pr)

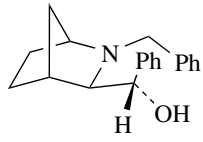

(57)

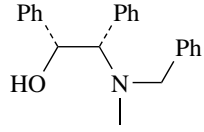

(58)

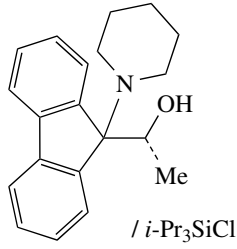

(59)

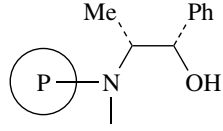

(60)

Addition of an allylic zinc reagent to cyclic aldimines has been reported[129]. Lithiated bisoxazoline **61** and allylzinc reagent form the reactive species, which adds to a cyclic aldimine enantioselectively with up to 97.5% ee (equation 29)[129].

On the other hand, approaches to the use of catalytic amounts of chiral ligands have been developed. Thus, the use of a sub-stoichiometric amount (50 mol%) of DBNE (**1**) affords *N*,*N*-diphenylphosphinylamine with 85% ee in 69% yield[121a]. Similarly, 25 mol% of chiral aziridinyl alcohol **56** (R = *i*-Pr) affords *N*,*N*-diphenylphosphinylamine with 65% ee in 60% yield[123]. In the enantioselective addition reaction of diethylzinc to a nitrone, 20 mol% of the metal alkoxide of diisopropyl tartrate **62** catalyzed the formation of a

hydroxyl amine with up to 94% ee (equation 30)[130]. In the enantioselective addition of diethylzinc to *N*,*N*-diphenylphosphinylimine, 20 mol% of amino alcohol **63** works as a chiral catalyst in the presence of 1 equivalent of i-Pr_3SiCl (equation 31)[131].

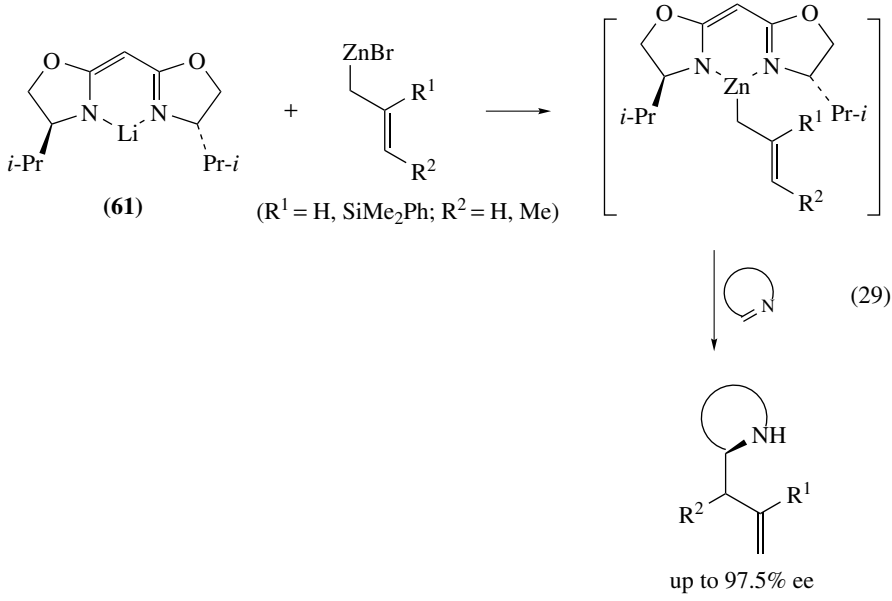

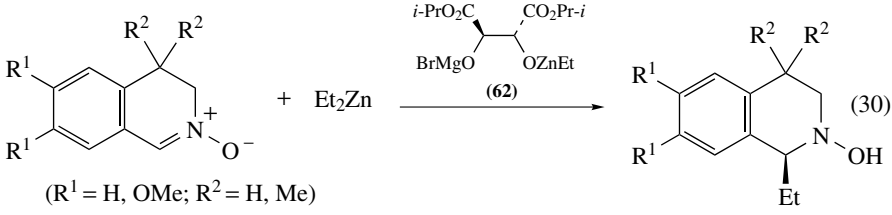

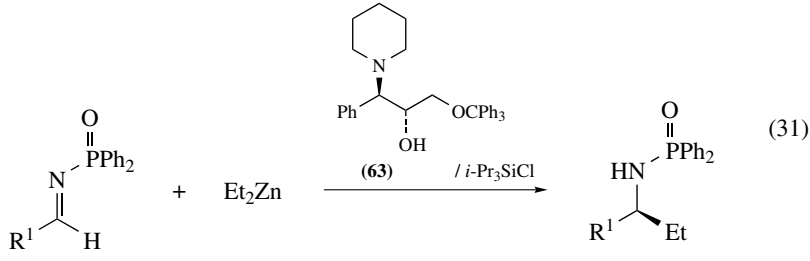

In 2000, a catalytic enantioselective addition was reported using a chiral Lewis acid–ligand system. Tomioka and coworkers reported the enantioselective addition of

diethylzinc to *N*-sulfonylimines in high enantioselectivities (90–94% ee) using $Cu(OTf)_2$ (1–8 mol%)/amidophosphine **64** (1.3–10.4 mol%) as the chiral catalyst (equation 32)[132].

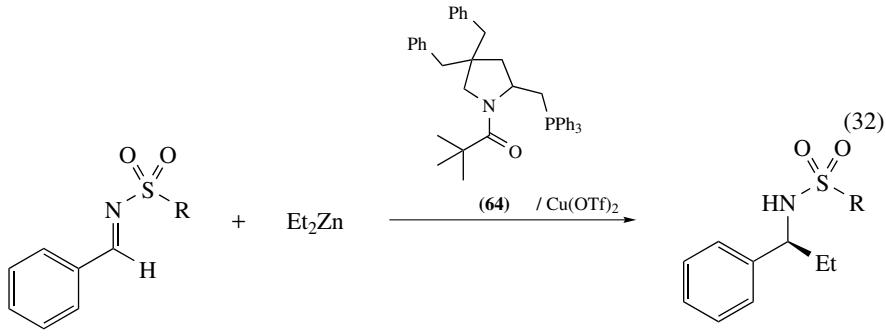

(32)

Hoveyda and coworkers reported that $Zr(OPr\text{-}i)_4 \cdot i\text{-PrOH}$ (0.1–20 mol%)/peptide-derived ligand **65** (0.1–10 mol%) catalyzes the enantioselective addition to aryl amine (equation 33)[133]. Aryl amine can be generated *in situ* from the corresponding aldehyde and *o*-anisylamine[133b].

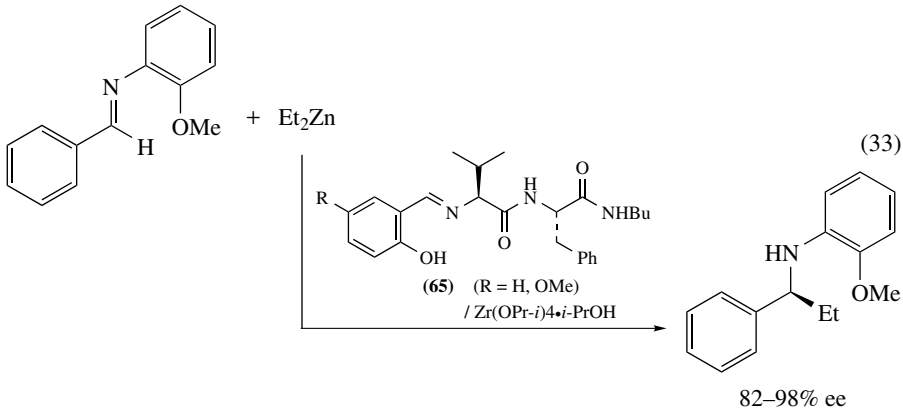

(33)

A Lewis base ligand has been developed as the chiral catalyst. Dahmen, Bräse and coworkers reported that the [2.2]paracyclophane-based chiral *N*,*O*-ligand **8** (2 mol%) affords *N*-formylamine with 84–95% ee (equation 34)[134]. In this system, the phenyl transfer reaction also proceeds in a catalytic manner[134b].

As another approach, Carreira and coworkers reported the alkynylation of a nitrone using a terminal alkyne and catalytic amounts of $Zn(OTf)_2$ and amine[135]. In the presence of a chiral ligand, the reaction proceeds enantioselectively to give hydroxyamine with 88% ee.

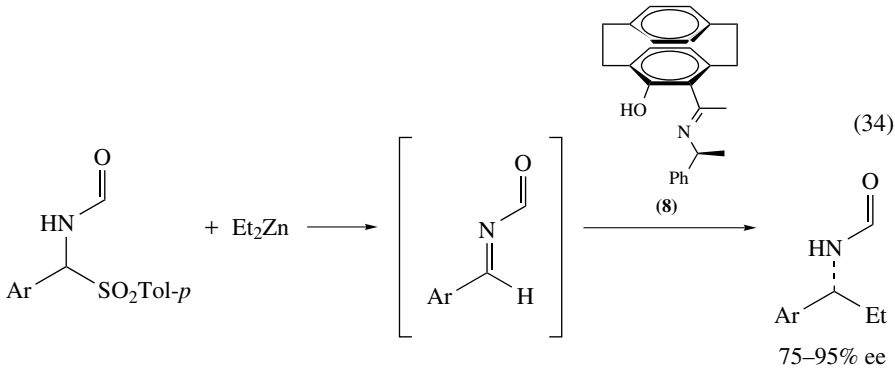

(34)

V. ASYMMETRIC AMPLIFICATION

Much attention has been paid to asymmetric amplification where the enantiomeric excess (ee) of the product is higher than that of the chiral catalyst (equation 35)[136]. The first experiment on asymmetric amplification was reported by Kagan and coworkers in the Katsuki-Sharpless asymmetric epoxidation of allyl alcohols[137]. Asymmetric amplification has also been studied in the asymmetric addition of dialkylzincs to carbonyl compounds.

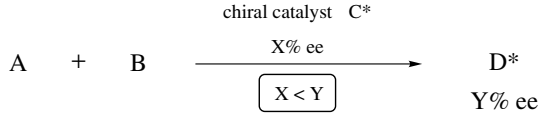

(35)

In the enantioselective addition of diethylzinc to benzaldehyde, a wide variety of chiral catalysts **3**, **4**, **16**, **23**, **47**, **66**–**73** exhibits asymmetric amplification (equation 36 and Table 1).

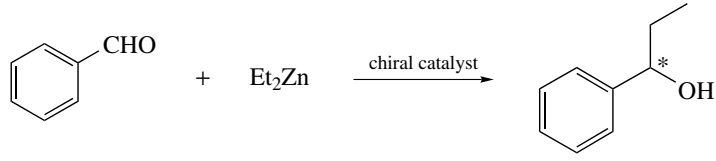

(36)

Mechanistic studies of asymmetric amplification using a chiral amino alcohol catalyst have continued to date[1b, 151–155]. In the case of the chiral titanium complex, the observed asymmetric amplification was influenced by the method of preparation of the catalyst[153]. Asymmetric amplification is also observed in the catalytic addition of diphenylzinc to ketones[100].

TABLE 1. Asymmetric amplification in the enantioselective addition of diethylzinc to benzaldehyde

Chiral ligand (chiral catalyst)			Product		
	mol %	ee (%)	yield (%)	ee (%), (config.)	Reference
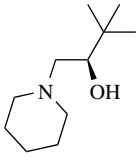 **(4)**	2	10.7	96%	82 (*R*)	138
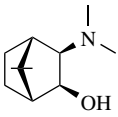 **(3)**	2	20	87%	98 (*S*)	139
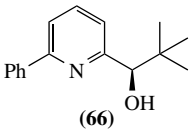 **(66)**	5	30.8	84%	88 (*R*)	140
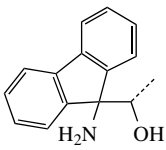 **(67)**	6	16.8	—	83.5 (*S*)	141
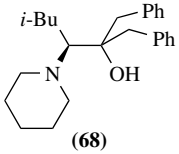 **(68)**	—	20	—	93 (*R*)	142
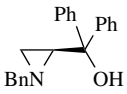 **(69)**	5	40	—	78	143
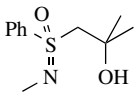 **(47)**	10	23	70%	64	144
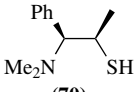 **(70)**	5	50	—	81 (*R*)	145

TABLE 1. (*continued*)

Chiral ligand (chiral catalyst)			Product		
	mol %	ee (%)	yield (%)	ee (%), (config.)	Reference
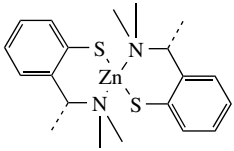 **(71)**	2	40	—	72 (*S*)	146
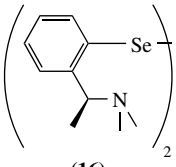 **(16)**	1	51	—	76 (*R*)	147
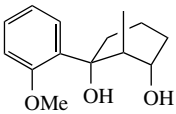 **(72)**	10	52		92 (*R*)	148
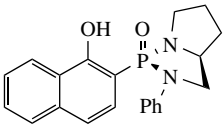 **(73)**	5	50		82 (*R*)	149
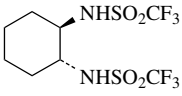 **(23)**	2	50		88	150

In the asymmetric addition of diethylzinc to *N*,*N*′-diphenylphosphinylimine, (1*R*,2*S*)-2-morpholino-1-phenylpropanol with 58% ee promotes the reaction to afford *N*,*N*′-diphenylphosphinylamine with 85% ee (equation 37)[122].

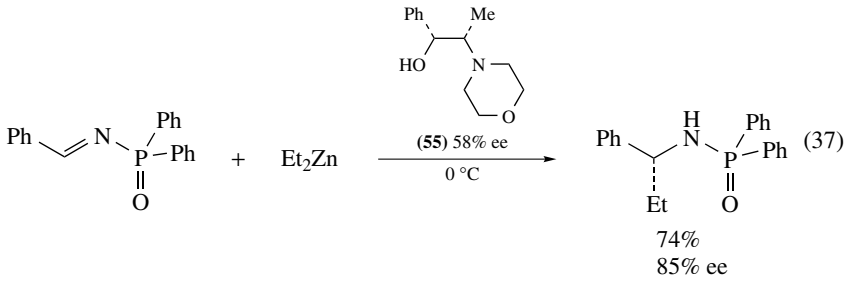

(37)

Enantioselective conjugate addition of diethylzinc proceeds in the presence of Ni(II) complex[104]. Asymmetric amplification was observed in reactions using chiral ligand **1**[156], **66**[157], **47**[107] and **3** (equation 38)[109].

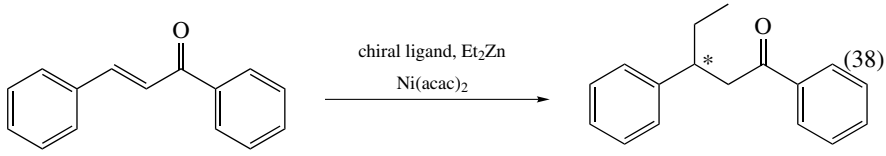

(38)

chiral ligands

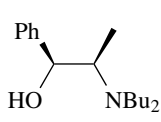

DBNE (**1**)

chiral ligand: 20% ee
product: 74% ee (*R*)

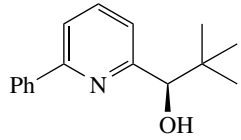

(**66**)

chiral ligand: 16% ee
product: 52% ee (*R*)

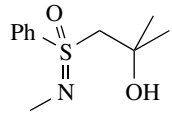

(**47**)

chiral ligand:18% ee
product: 22% ee (*R*)

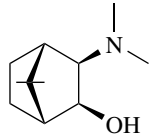

(**3**)

chiral ligand: 25% ee
product: 34% ee (*R*)

VI. ASYMMETRIC AUTOCATALYSIS IN THE ASYMMETRIC ADDITION OF DIALKYLZINCS TO ALDEHYDES

A. Asymmetric Autocatalysis with High Enantioselectivity

Asymmetric autocatalysis is defined as an enantioselective synthesis in which the chiral product acts as an asymmetric catalyst for its own production (equation 39). Asymmetric autocatalysis is an efficient method for the catalytic enantioselective automultiplication of a chiral molecule without the need for any other chiral auxiliary[158].

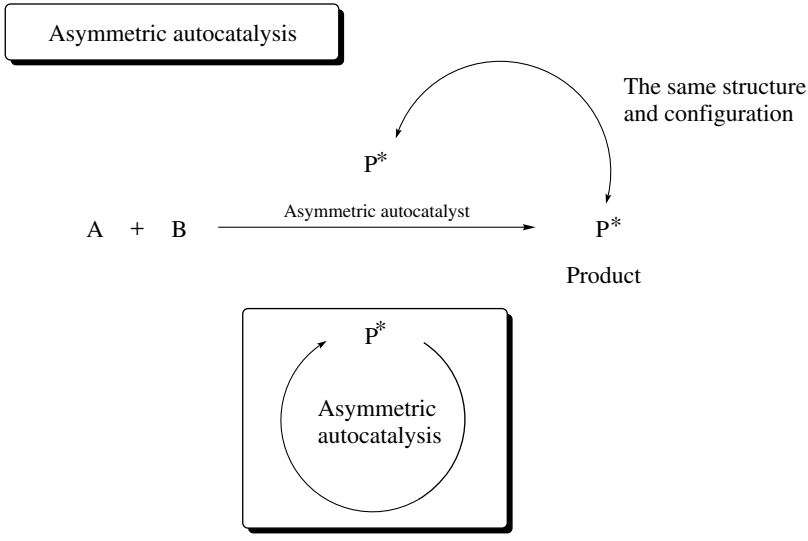

(39)

The first experimental asymmetric autocatalysis was discovered in 1990 in the 3-pyridyl alkanol catalyzed asymmetric addition of dialkylzincs to pyridine-3-carbaldehyde[159]. In the presence of (*S*)-3-pyridyl alkanol **76** (86% ee), i.e. an asymmetric autocatalyst, enantioselective addition of diisopropylzinc to **74** proceeds and (*S*)-3-pyridyl alkanol **76** of the same structure as the asymmetric autocatalyst was obtained in a 67% yield with 35% ee. Moreover, introduction of a carbamoyl group at the 5-position of the pyridine ring enhances the enantioselectivity dramatically[160]. Pyridyl alkanol **77**, which possesses two isopropyl substituents on the nitrogen atom of the carbamoyl group, automultiplies with as high as 86% ee in the asymmetric isopropylation of the corresponding pyridine-3-carbaldehyde **75** (equation 40).

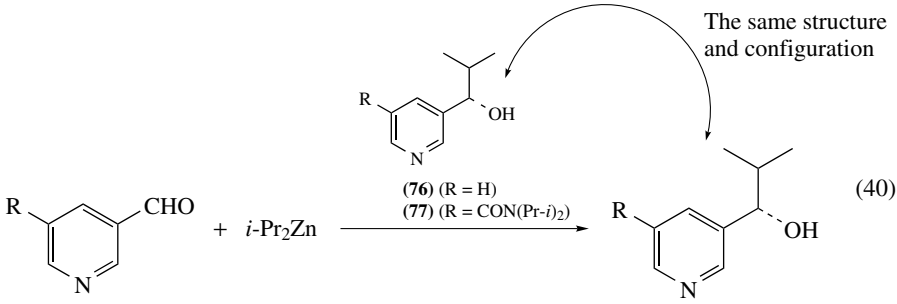

(40)

(74) (R = H)
(75) (R = CON(Pr-*i*)$_2$)

(76) (R = H) 35% ee
(77) (R = CON(Pr-*i*)$_2$) 86% ee

Various compounds such as ferrocenyl alkanol **78**[161], chiral diol **79**[162], 5-pyrimidyl alkanols **80**–**83**[163–165] and 3-quinolyl alkanols **84**–**86**[166, 167] have been found to act as asymmetric autocatalysts. Among them, 5-pyrimidyl alkanols **80**–**83** and 3-quinolyl alkanols **84**–**86** exhibit very high enantioselectivity as asymmetric autocatalysts. In the enantioselective addition of diisopropylzinc to pyrimidine-5-carbaldehyde using (*S*)-5-pyrimidyl alkanol **80** (R = H) as an asymmetric autocatalyst, (*S*)-alkanol **80** with 88% ee possessing the same structure and absolute configuration as the catalyst is obtained. A methyl substituent on the 2-position of the 5-pyrimidyl alkanol increases the enantioselectivity as an asymmetric autocatalyst. The ee of the produced 5-pyrimidyl alkanol **81** reaches 98% when nearly enantiopure catalyst **81** is used[163]. When the substituent at the 2-position of the pyrimidine ring is changed to the *t*-butylethynyl group, practically perfect asymmetric autocatalysis is realized[164]. Thus, in the presence of (*S*)-2-*t*-butylethynyl-5-pyrimidyl alkanol **82** with >99.5% ee as asymmetric autocatalyst, the enantioselective addition of diisopropylzinc to 2-*t*-butylethynylpyrimidine-5-carbaldehyde **87** gives nearly enantiopure (>99.5% ee) (*S*)-2-*t*-butylethynyl-5-pyrimidyl alkanol **82** in near quantitative yield (>9%) (equation 41). The high yield and the high enantioselectivity have been maintained during the ten consecutive asymmetric autocatalytic reactions, in which the obtained product (*S*)-**82** is used as an asymmetric autocatalyst for the next run. During the ten consecutive reactions, the initial (*S*)-5-pyrimidyl alkanol **82** has automultiplied by a factor of about 6×10^7[164].

On the other hand, (*S*)-3-quinolyl alkanol **84** with 94% ee catalyzes enantioselective isopropylation of quinoline-3-carbaldehyde to give the (*S*)-3-quinolyl alkanol **84** itself with 94% ee[166]. The substituent at the 7-position increases the enantiomeric excess to 97% ee[167].

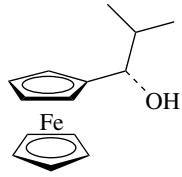

(78)

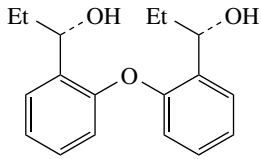

(79)

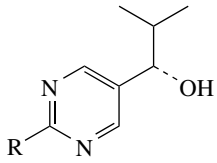

(80) (R = H) 90% ee
(81) (R = Me) 98% ee
(82) (R = C≡C-Bu-*t*) >99.5% ee
(83) (R = (*E*)-CH=CH-Bu-*t* 99% ee

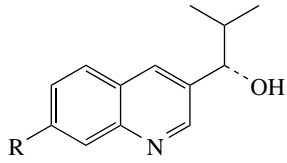

(84) (R = H) 94% ee
(85) (R = OMe) 97% ee
(86) (R = Ph) 97% ee

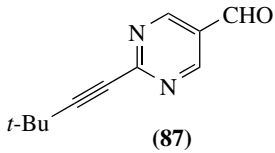

(87)

+ *i*-Pr_2Zn

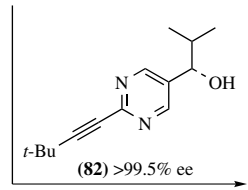

Obtained alkanol is used as an autocatalyst for the next round.

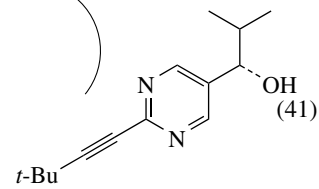

(41)

(82)

1st round:	>99%, >99.5% ee
2nd round	>99%, >99.5% ee
:	:
10th round:	>99%, >99.5% ee

B. Asymmetric Autocatalysis with Amplification of Chirality

As described in the preceding section, asymmetric amplification has been reported in the non-autocatalytic enantioselective addition of dialkylzincs. In asymmetric autocatalysis, amplification of ee has a more significant role, because the product of the asymmetric autocatalysis itself is capable of acting as the asymmetric autocatalyst. Once the product, i.e. the asymmetric autocatalyst with an enhanced ee, is formed in the asymmetric autocatalytic reaction, the product catalyzes the formation of itself with higher ee. From the viewpoint of the molecule, an asymmetric autocatalyst with dominant absolute configuration catalyzes

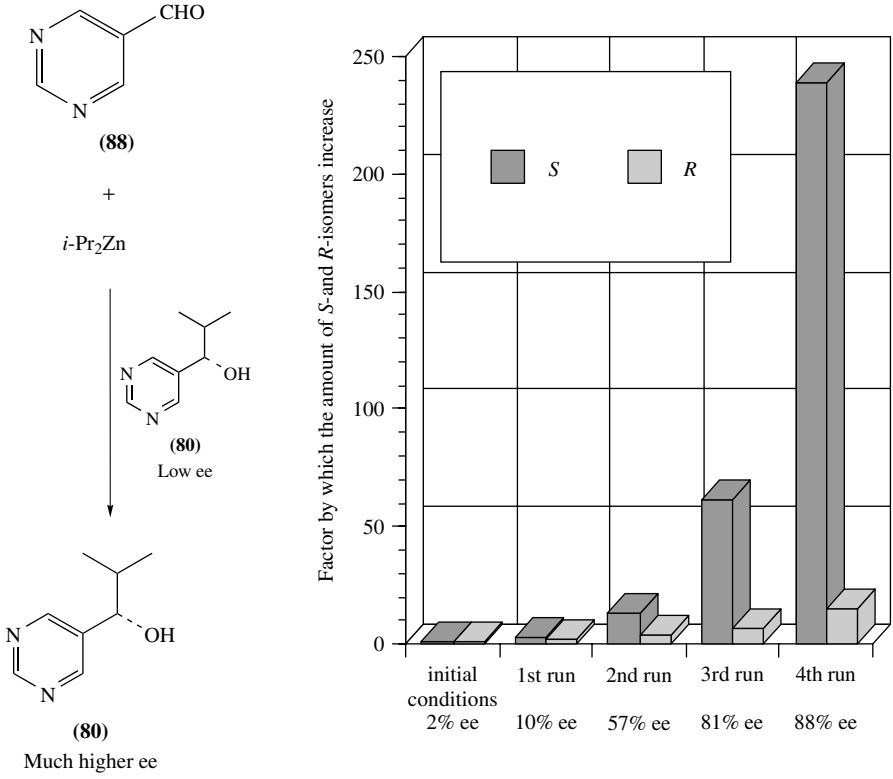

FIGURE 1

the production of itself with the same configuration. During the reaction, the amount of the chiral molecule with the predominant configuration increases significantly. The process provides an analogous prebiotic realization of chiral homogeneity of biomolecules such as L-amino acids[168].

The first asymmetric autocatalysis with amplification of ee was observed in the automultiplication of a 5-pyrimidyl alkanol **80** (Figure 1)[169]. When (*S*)-5-pyrimidyl alkanol **80** with as low as 2% ee is used as the asymmetric autocatalyst for enantioselective addition of diisopropylzinc to pyrimidine-5-carbaldehyde **88**, the ee of the produced pyrimidyl alkanol (and the initial asymmetric autocatalyst) **80** increases to 10% ee (Figure 1, 1st run). Consecutive asymmetric autocatalyses using 5-pyrimidyl alkanol **80** with 10% ee have increased its ee to 57%, 81% and 88% ee, successively. During the reactions, the major (*S*)-enantiomer in the initial asymmetric autocatalyst has automultiplied by a factor of 238, while the slightly minor (*R*)-enantiomer has automultiplied by a factor of only 16.

The asymmetric autocatalysis of 2-*t*-butylethynyl-5-pyrimidyl alkanol **82** starting from extremely low ee has been reported[170]. When (*S*)-2-*t*-butylethynyl-5-pyrimidyl alkanol **82** with only *ca* 0.00005% ee (*S* isomer : *R* isomer = *ca* 50.000025:49.999975) is used as an initial asymmetric autocatalyst, the first round of reaction gives pyrimidyl alkanol **82** with an increased ee of 57% ee (Figure 2). The product is used as an asymmetric autocatalyst for the second run, affording the pyrimidyl alkanol **82** with an enhanced ee

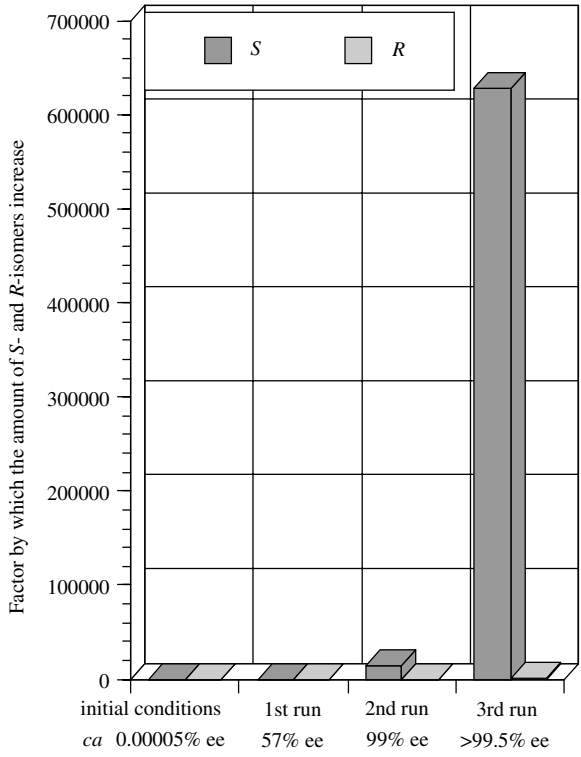

FIGURE 2

of 99%. The third asymmetric autocatalysis using pyrimidyl alkanol **82** with 99% ee as an asymmetric autocatalyst gives nearly enantiopure (>99.5% ee) **82**. During the three consecutive asymmetric autocatalyses, the automultiplication factor of the initially dominant (*S*)-enantiomer reaches to *ca* 630 000 times. On the other hand, the automultiplication factor of the minor (*R*)-isomer is suppressed to less than 1000 times.

The mechanism of the asymmetric autocatalysis with amplification of ee has been examined experimentally by us[171] and other groups[172]. It is basically understood that the aggregation of the isopropylzinc alkoxide of 5-pyrimidyl alkanol is involved in the reaction. Kinetic analysis of the reaction shows that the reaction is second order in the isopropylzinc alkoxide of 5-pyrimidyl alkanol[171].

Meanwhile, asymmetric autocatalysis of 3-quinolyl alkanol **84**–**86**[167, 173] and 5-carbamoyl-3-pyridyl alkanol **77**[174] also proceed with amplification of ee. Quinolyl alkanols **84** with 9% ee increases its ee to 88%[173] and the ee of 5-carbamoyl-3-pyridyl alkanol **77** increased from 14% to 87%[174].

C. Asymmetric Autocatalysis using Chiral Initiators

Chiral compounds can be used as chiral initiators of asymmetric autocatalysts. In the presence of a chiral initiator, an enantiomeric imbalance is induced in the initially formed

zinc alkoxide of pyrimidyl alkanol in the addition of diisopropylzinc to pyrimidine-5-carbaldehyde. The induced enantiomeric imbalance, even when it is extremely small, is enhanced significantly by the subsequent asymmetric autocatalysis of pyrimidyl alkanol with an amplification of ee[175].

When enantioselective addition of diisopropylzinc to pyrimidine-5-carbaldehyde **89** was examined, simple 2-butanol with low (*ca* 0.1%) ee induces a tiny chirality in the initially produced alkanol **81** and the ee value of the finally obtained alkanol becomes higher (73–76%) due to the asymmetric autocatalysis (Table 2). Note that the ee value can be further amplified by subsequent asymmetric autocatalysis, as described in the preceding section. Various chiral compounds have been proved to act as chiral initiators.

Examples of chiral initiators include methyl mandelate[175], amino acids such as leucine and valine[175–177], α-deuteriated chiral primary alcohols[178], [2.2]paracyclophanes[179a,b], [6] and [5]helicenes[180], 1,1′-disubstituted allene[181], 1,1′-binaphthyl[182], chiral epoxides[183], chiral olefins[184] and topologically chiral metal complexes[185].

In place of the above-mentioned chiral organic compounds, chiral inorganic substrates have been examined as chiral initiators. Quartz (SiO_2) exhibits both dextrorotatory (*d*) and levorotatory (*l*) enantiomorphs that exist in nature. Quartz is considered as one of the origins of chirality of organic compounds[186].

As shown in Table 3, the asymmetric autocatalysis using *d*- and *l*-quartz as chiral inducers affords (*S*)- and (*R*)-pyrimidyl alkanol **82** with 95% and 97% ee, respectively[187]. These results stand as the first asymmetric synthesis of highly enantioenriched organic compound using chiral inorganic crystals. Chiral ionic crystals of *d*- and *l*-sodium chlorate ($NaClO_3$) initiate asymmetric autocatalysis to afford (*S*)- and (*R*)-pyrimidyl alkanol **82** with 98% ee, respectively[188a,b]. It should be noted that *d*-$NaClO_3$ and *l*-sodium bromate ($NaBrO_3$) have the same crystal structure. Thus, both *d*-$NaClO_3$ and *l*-$NaBrO_3$ afford (*S*)-pyrimidyl alkanol **82**[188a,b].

Helical silica, which is artificially produced, works as a chiral initiator of asymmetric autocatalysis. Left-handed helical silica induced the production of (*R*)-alkanol **82** with 97% ee and right-handed helical silica gave (*S*)-alkanol **82** with 96% ee[189]. Moreover, inorganic-organic hybrid materials also work as chiral initiators of asymmetric autocatalysis[190,191]. Asymmetric autocatalysis induced by chiral organic cocrystals formed from two achiral organic compounds have been employed as chiral initiators in asymmetric autocatalysis[192].

D. Asymmetric Autocatalysis using Circularly Polarized Light as a Sole Chiral Factor

Right- or left-circularly polarized light (CPL) is a chiral physical force. CPL is one of the proposed origins of chirality of organic compounds. It is known that the asymmetric photolysis of racemic leucine[193], photosynthesis of [6]helicene[194] or photoequilibrium of chiral olefin[195] with CPL induces slight imbalances of chirality. However, the ee values of organic compounds induced by CPL have been very low (<2% ee) in asymmetric photolysis and asymmetric synthesis. To the best of our knowledge, these low ee values of organic compounds have not been correlated with the high ee values of organic compounds. By using these compounds as chiral initiators, the chemical process that correlates chirality of CPL as a source of chirality of organic compounds with high ee has been realized[175,180,184]. Recently, Soai and coworkers reported a straightforward process that correlates the chirality of CPL with that of the organic compound by using asymmetric autocatalysis[196]. Thus, irradiation of the racemic pyrimidyl alkanol **82** with *r*-CPL and the subsequent asymmetric autocatalysis affords nearly enantiopure (>99.5%

TABLE 2. Asymmetric autocatalysis initiated by various organic and metal complex chiral initiators

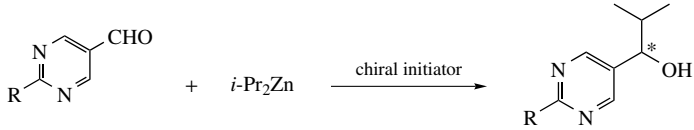

(89) R = Me
or
(87) R = *t*-BuC≡C

(81) or **(82)**

Aldehyde	Chiral initiator	Config. (ee, %)	Alkanol ee (%), (Config.)	Reference
89		*S* (*ca* 0.1) *R* (*ca* 0.1)	73 (*R*) 76 (*S*)	175
89	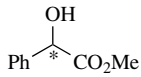	*S* (*ca* 0.1) *R* (*ca* 0.1)	68 (*R*) 70 (*S*)	175
89	leucine	L (*ca* 2) D (*ca* 2)	23 (*R*) 26 (*S*)	175
87		L (>99.5) D (>99.5)	95 (*S*) 95 (*R*)	177
89	valine	L (*ca* 1) D (*ca* 1)	51 (*R*) 47 (*S*)	175
87		L (>99.5) D (>99.5)	82 (*S*) 93 (*R*)	177
87	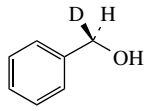	*S* (>95) *R* (>95)	96 (*R*) 95 (*S*)	178
87	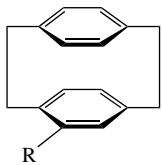 (R = CO_2H)	*S* (99) *R* (93)	95 (*R*) 97 (*S*)	179a
87	(R = Et)	*S* (94) *R* (88)	98 (*S*) 96 (*R*)	179b
87	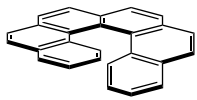	*P* (*ca* 0.13) *M* (*ca* 0.54)	56 (*S*) 62 (*R*)	180
87	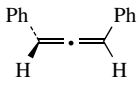	*S* (>99.5) *R* (>99.5)	97 (*R*) 98 (*S*)	181

TABLE 2. (*continued*)

Aldehyde	Chiral initiator	Config. (ee, %)	Alkanol ee (%), (Config.)	Reference
87	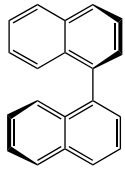	*S* (80) *R* (77)	94 (*R*) 96 (*S*)	182
87		*S* (2) *R* (3)	74 (*R*) 79 (*S*)	183
87		*S* (5) *R* (5)	80 (*R*) 80 (*S*)	183
87	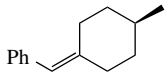	*S* (99) *R* (98)	96 (*R*) 95 (*S*)	184
87	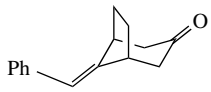	+(1.3) −(1.8)	95 (*S*) 97 (*R*)	184
87	$K[Co(edta)]\cdot 2H_2O$	$(+)_{546}$-(>99) $(-)_{546}$-(>99)	91 (*S*) 95 (*R*)	185
87	$K[Co(trdta)]\cdot 2H_2O$	$(+)_{546}$-(>99) $(-)_{546}$-(>99)	85 (*S*) 88 (*R*)	185

ee) (*R*)-pyrimidyl alkanol **82** (equation 42). On the other hand, irradiation with *l*-CPL followed by asymmetric autocatalysis gives (*S*)-pyrimidyl alkanol **82** with >99.5% ee.

E. Stochastic Production of *S*- and *R*-Enantiomers without Adding a Chiral Source by Asymmetric Autocatalysis: Spontaneous Absolute Asymmetric Synthesis

In the absence of any chiral factors, the probability of the formation of *S*- and *R*-enantiomers is 1 to 1. However, the numbers of the resulting two enantiomers are not exactly the same in almost all cases. Mislow[197] described the inevitability of small enantiomeric enrichment in absolute asymmetric synthesis. According to the statistics, it is expected that a fluctuation in the ratio of the *S*- and *R*-enantiomers becomes more and more likely as the numbers in the enantiomer mixture become smaller[198]. Thus, if the asymmetric autocatalysis is initiated without adding any chiral substance, small fluctuations of enantiomers produced in the initial stage could be enhanced by consecutive asymmetric autocatalytic reaction of pyrimidyl alkanol with amplification of chirality.

Indeed, the reaction of pyrimidine-5-carbaldehydes and $i\text{-}Pr_2Zn$ without the addition of any chiral substance and the subsequent asymmetric autocatalysis with amplification of

TABLE 3. Asymmetric autocatalysis in reaction of **87** initiated by chiral inorganic crystals, inorganic–organic hybrid materials and chiral cocrystals of achiral compounds

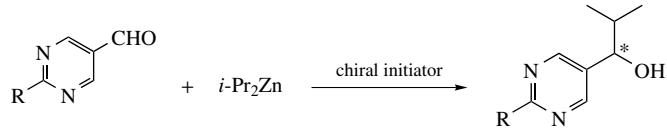

(87) **(82)**

Chiral initiator		Alkanol	
	Config.	ee (%), (Config.)	Reference
Quartz	*d*	97 (*S*)	187
	l	97 (*R*)	
$NaClO_3$	*d*	98 (*S*)	188a
	l	98 (*R*)	
$NaBrO_3$	*d*	98 (*R*)	188a,b
	l	98 (*S*)	
Helical silica	Left-handed	97 (*R*)	189
	Right-handed	96 (*S*)	
Silsesquioxane	(*R*,*R*)	93 (*R*)	190
	(*S*,*S*)	95 (*S*)	
Ephedrine–silica hybrid	(1*R*,2*S*)	97 (*R*)	191
	(1*S*,2*R*)	95 (*S*)	
Chiral cocrystal of tryptamine/*p*-chlorobenzoic acid	*P*	96 (*R*)	192
	M	95 (*S*)	
Chiral cocrystal of 3-indolepropionic acid/phenanthridine	*P*	92 (*S*)	192
	M	97 (*R*)	

ee affords pyrimidyl alkanols with ee above the detection level (15–91% ee, Figure 3)[199]. When the reaction of pyrimidine-5-carbaldehyde **87** with *i*-Pr_2Zn in a mixed solvent of diethyl ether and toluene was carried out 37 times, the absolute configurations of the produced pyrimidyl alkanol **82** showed an approximate stochastic distribution (19 times formation of *S* and 18 times formation of *R*). Other solvents, such as a mixture of ether-toluene, dibutyl ether alone and a mixture of diethyl ether-dibutyl ether, also enable the stochastic formation of (*S*)- and (*R*)-**82**[199c]. It should be noted that these results satisfy one of the necessary conditions of spontaneous absolute asymmetric synthesis.

VII. CONCLUSION

As described, the enantioselective addition of organozincs to aldehydes, ketones, enones and imines has been developed, and the methods for the preparation of enantioenriched alcohols, substituted ketones and imines with high enantiomeric excesses have been provided. In most cases, the reactions proceed in a catalytic manner. Asymmetric amplification has been observed in the dialkylzinc addition to carbonyl compounds. Asymmetric autocatalysis of nitrogen-containing alcohols such as pyrimidyl alkanol has been realized for the first time in dialkylzinc addition to nitrogen-containing aldehydes such as pyrimidine-5-carbaldehyde. Asymmetric autocatalysis exhibits significant amplification of chirality, which enables correlation of the origins of chirality with homochirality of biomolecules. Thus, the enantioselective addition reactions of organozincs have become

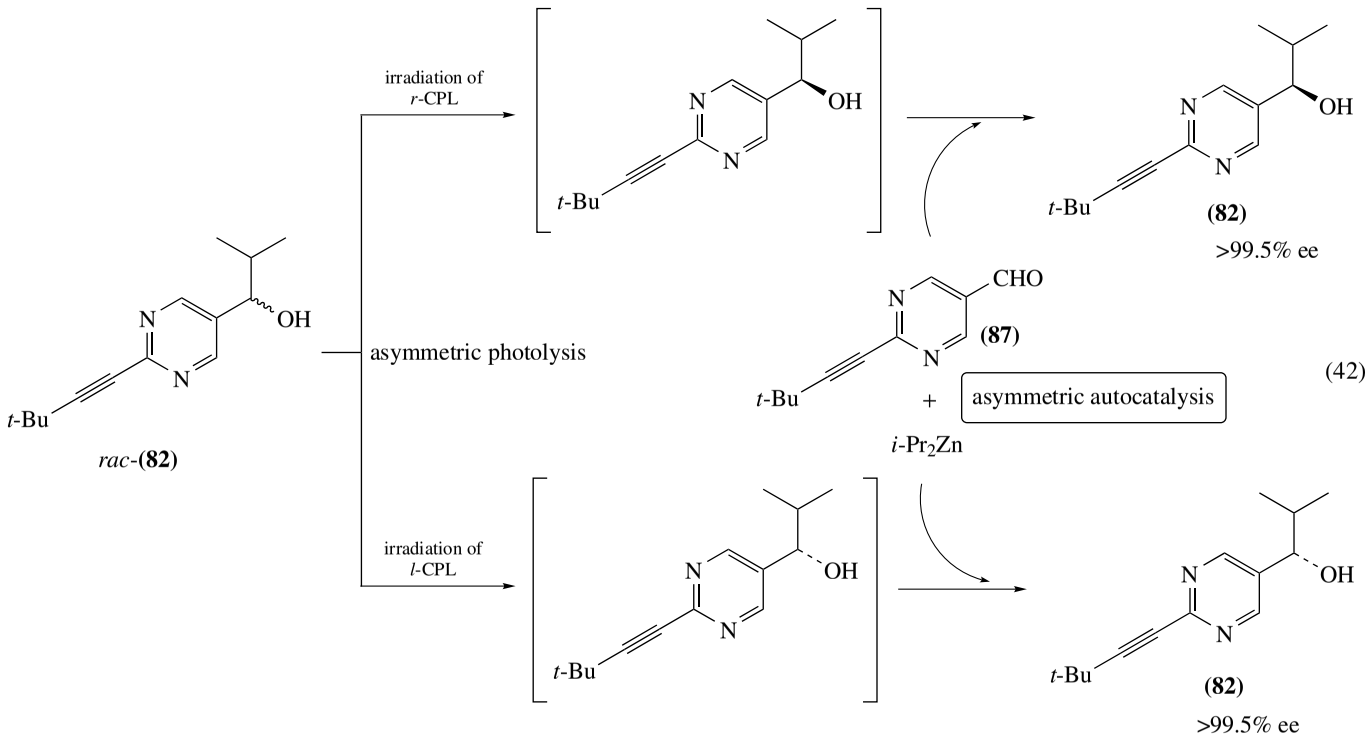
irradiation of
r-CPL
irradiation of
l-CPL
asymmetric photolysis
rac-(82)
t-Bu
OH
N
(87)
CHO
+
asymmetric autocatalysis
i-Pr2Zn
(82)
>99.5% ee
(42)

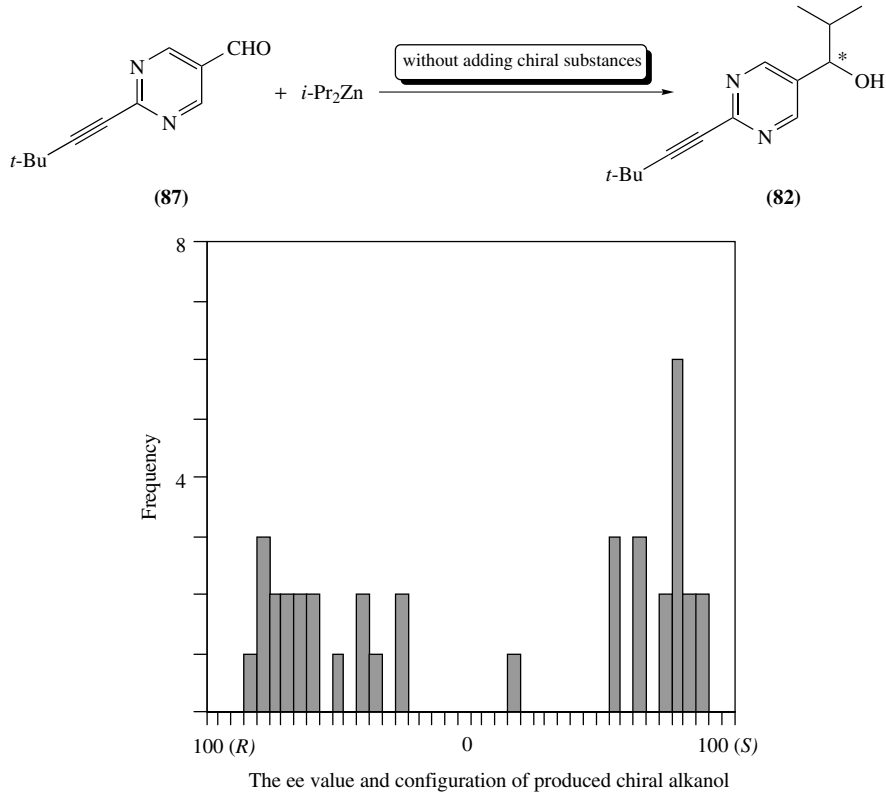

FIGURE 3

not only an efficient asymmetric synthesis but also a powerful tool in clarifying the origin of homochirality of biomolecules.

VIII. ACKNOWLEDGMENT

This work was supported by a Grant-in-Aid for Scientific Research from The Ministry of Education, Culture, Sports, Science and Technology (MEXT). T. K. thanks Nissan Chemical Industries Award in Synthetic Organic Chemistry.

IX. REFERENCES

1. (a) K. Soai and S. Niwa, *Chem. Rev.*, **92**, 833 (1992).
   (b) R. Noyori and M. Kitamura, *Angew. Chem., Int. Ed. Engl.*, **30**, 49 (1991).
   (c) L. Pu and H.-B. Yu, *Chem. Rev.*, **101**, 757 (2001).
2. T. Mukaiyama, K. Soai, T. Sato, H. Shimizu and K. Suzuki, *J. Am. Chem. Soc.*, **101**, 1455 (1979).
3. (a) K. Soai, S. Yokoyama, K. Ebihara and T. Hayasaka, *J. Chem. Soc., Chem. Commun.*, 1690 (1987).
   (b) K. Soai, S. Yokoyama and T. Hayasaka, *J. Org. Chem.*, **56**, 4264 (1991).
4. K. Soai, T. Hayase, K. Takai and T. Sugiyama, *J. Org. Chem.*, **59**, 7908 (1994).

5. (a) K. Soai, A. Ookawa, K. Ogawa and T. Kaba, *J. Chem. Soc., Chem. Commun.*, 467 (1987).
   (b) K. Soai, A. Ookawa, T. Kaba and K. Ogawa, *J. Am. Chem. Soc.*, **109**, 7111 (1987).
6. M. Kitamura, S. Suga, K. Kawai and R. Noyori, *J. Am. Chem. Soc.*, **108**, 6071 (1986).
7. N. Oguni, Y. Matsuda and T. Kaneko, *J. Am. Chem. Soc.*, **110**, 7877 (1988).
8. C. F. Lawrence, S. K. Nayak, L. Thijs and B. Zwanenburg, *Synlett*, 1571 (1999).
9. Y. Uozumi, K. Mizutani and S. Nagai, *Tetrahedron Lett.*, **42**, 407 (2001).
10. D. X. Liu, L. C. Zhang, Q. Wang, C. S. Da, Z. Q. Xin, R. Wang, M. C. K. Choi and A. S. C. Chan, *Org. Lett.*, **3**, 2733 (2001).
11. S. Dahmen and S. Bärse, *Chem. Commun.*, 26 (2002).
12. D. Scarpi, F. Lo Galbo, E. G. Occhiato and A. Guarna, *Tetrahedron: Asymmetry*, **15**, 1319 (2004).
13. S. Niwa and K. Soai, *J. Chem. Soc., Perkin Trans. 1*, 2717 (1991).
14. C. Bolm, G. Schlingloff and K. Harms, *Chem. Ber.*, **125**, 1191 (1992).
15. M. Shinnerl, M. Seitz, A. Kaiser and O. Reiser, *Org. Lett.*, **3**, 4259 (2001).
16. B. D. Dangel and R. Polt, *Org. Lett.*, **2**, 3003 (2000).
17. M. P. Sibi and L. M. Stanley, *Tetrahedron: Asymmetry*, **15**, 3353 (2004).
18. N. N. Joshi, M. Srebnik and H. C. Brown, *Tetrahedron Lett.*, **30**, 5551 (1989).
19. E. Rijinberg, J. T. B. H. Jastrzebski, M. D. Janssen, J. Boersma and G. van Koten, *Tetrahedron Lett.*, **35**, 6521 (1994).
20. R. P. Hof, M. A. Poelert, N. C. M. W. Peper and R. M. Kellogg, *Tetrahedron: Asymmetry*, **5**, 31 (1994).
21. M.-J. Jin, S.-J. Ahn and K.-S. Lee, *Tetrahedron Lett.*, **37**, 8767 (1996).
22. A. L. Braga, M. W. Paixão, D. S. Lüdtke, C. C. Silveira and O. E. D. Rodrigues, *Org. Lett.*, **5**, 2635 (2003).
23. I. Shiina, K. Konishi and Y. Kuramoto, *Chem. Lett.*, 164 (2002).
24. P. I. Dosa, J. C. Ruble and G. C. Fu, *J. Org. Chem.*, **62**, 444 (1997)
25. J. Priego, O. G. Mancheno, S. Cabrera and J. C. Carretero, *Chem. Commun.*, 2026 (2001).
26. (a) M. Yoshioka, T. Kawakita and M. Ohno, *Tetrahedron Lett.*, **30**, 1657 (1989).
    (b) H. Takahashi, T. Kawakita, M. Yoshioka, S. Kobayashi and M. Ohno, *Tetrahedron Lett.*, **30**, 7095 (1989).
    (c) H. Takahashi, T. Kawakita, M. Ohno, M. Yoshioka and S. Kobayashi, *Tetrahedron*, **48**, 5691 (1992).
27. (a) D. Seebach, *Angew. Chem., Int. Ed. Engl.*, **29**, 1320 (1990).
    (b) B. Schmidt and D. Seebach, *Angew. Chem., Int. Ed. Engl.*, **30**, 99 (1991).
    (c) D. Seebach, A. K. Beck, B. Schmidt and Y. M. Wang, *Tetrahedron*, **50**, 4363 (1994).
28. (a) F.-Y. Zhang, C.-W. Yip, R. Cao and A. S. C. Chan, *Tetrahedron: Asymmetry*, **8**, 585 (1997).
    (b) D. X. Liu, L. C. Zhang, Q. Wang, C. S. Da, Z. Q. Xin, R. Wang, M. C. K. Choi and A. C. S. Chan, *Org. Lett.*, **3**, 2733 (2001).
29. M. Mori and T. Nakai, *Tetrahedron Lett.*, **38**, 6233 (1997).
30. G. Bringmann, R.-M. Pfeifer, C. Rummey, K. Hartner and M. Breuning, *J. Org. Chem.*, **68**, 6859 (2003).
31. (a) K. Soai, Y. Hirose and Y. Ohno, *Tetrahedron: Asymmetry*, **4**, 1473 (1993).
    (b) K. Soai, Y. Ohno, Y. Inoue, T. Tsuruoka and Y. Hirose, *Recl. Trav. Chim. Pays-Bas.*, **114**, 145 (1995).
32. T. Shibata, H. Tabira and K. Soai, *J. Chem. Soc., Perkin Trans. 1*, 177 (1998).
33. (a) T. Bauer and J. Tarasiuk, *Tetrahedron Lett.*, **43**, 687 (2002).
    (b) T. Bauer and J. Gajewiak, *Tetrahedron*, **60**, 9163 (2004).
34. P. Knochel, P. Jones and F. Langer, in *Organozinc Reagents* (Eds. P. Knochel and P. Jones), Chap. 5, Oxford Univ. Press, New York, 1999, pp 77–99.
35. D. Seebach, L. Behrendt and D. Felix, *Angew. Chem., Int. Ed. Engl.*, **30**, 1008 (1991).
36. J. L. Bussche-Hünnefeld and D. Seebach, *Tetrahedron*, **48**, 5719 (1992).
37. P. Knochel and R. D. Singer, *Chem. Rev.*, **93**, 2117 (1993).
38. (a) W. Brieden, R. Ostwald and P. Knochel, *Angew. Chem., Int. Ed. Engl.*, **32**, 582 (1993).
    (b) C. Eisenberg and P. Knochel, *J. Org. Chem.*, **59**, 3760 (1994).
    (c) R. Ostwald, P.-Y. Chavant, H. Stadtmüller and P. Knochel, *J. Org. Chem.*, **59**, 4143 (1994).
39. L. Schwink and P. Knochel, *Tetrahedron Lett.*, **35**, 9007 (1994).

40. S. Vettel, A. Vaupel and P. Knochel, *Tetrahedron Lett.*, **36**, 1023 (1995).
41. (a) L. Micouin, M. Ostreich and P. Knochel, *Angew. Chem., Int. Ed. Engl.*, **36**, 245 (1997).
    (b) F. Langer, L. Schwink, P.-Y. Chavant, A. Devasagayaraj and P. Knochel, *J. Org. Chem.*, **61**, 8229 (1996).
42. S. Berger, F. Langer, C. Lutz, P. Knochel, T. A. Mobley and C. K. Reddy, *Angew. Chem., Int. Ed. Engl.*, **36**, 1496 (1997).
43. M. Watanabe and K. Soai, *J. Chem. Soc., Perkin Trans. 1*, 3125 (1994).
44. K. Soai, S. Yokoyama, T. Hayasaka and K. Ebihara, *Chem. Lett.*, 843 (1988).
45. Review: D. J. Ramón and M. Yus, *Angew. Chem., Int. Ed.*, **43**, 284 (2004).
46. (a) D. J. Ramón and M. Yus, *Tetrahedron Lett.*, **39**, 1239 (1998).
    (b) D. J. Ramón and M. Yus, *Tetrahedron*, **54**, 5651 (1998).
47. (a) C. García, L. K. LaRochelle and P. J. Walsh, *J. Am. Chem. Soc.*, **124**, 10970 (2002).
    (b) S.-J. Jeon and P. J. Walsh, *J. Am. Chem. Soc.*, **125**, 9544 (2003).
    (c) C. A. de Parrodi and P. J. Walsh, *Synlett*, 2417 (2004).
48. (a) M. Yus, D. J. Ramón and O. Prieto, *Tetrahedron: Asymmetry*, **13**, 2291 (2002).
    (b) M. Yus, D. J. Ramón and O. Prieto, *Tetrahedron: Asymmetry*, **14**, 1103 (2003).
49. (a) E. F. DiMauro and M. C. Kozlowski, *Org. Lett.*, **4**, 3781 (2002).
    (b) E. F. DiMauro and M. C. Kozlowski, *J. Am. Chem. Soc.*, **124**, 12668 (2002).
50. K. Funabashi, M. Jachmann, M. Kanai and M. Shibasaki, *Angew. Chem., Int. Ed.*, **42**, 5489 (2003).
51. W. Oppolzer and R. N. Nadinov, *Tetrahedron Lett.*, **29**, 5645 (1988).
52. W. Oppolzer and R. N. Nadinov, *Tetrahedron Lett.*, **32**, 5777 (1991).
53. J. L. dem Bussche-Hünnefeld and D. Seebach, *Tetrahedron*, **48**, 5719 (1992).
54. W. Oppolzer and R. N. Nadinov, *Helv. Chim. Acta*, **75**, 170 (1992).
55. (a) W. Oppolzer, R. N. Nadinov and E. El-Sayed, *J. Org. Chem.*, **66**, 4766 (2001).
    (b) W. Oppolzer and R. N. Nadinov, *J. Am. Chem. Soc.*, **115**, 1593 (1993).
56. (a) S. Dahmen and S. Bräse, *Org. Lett.*, **3**, 4119 (2001).
    (b) Y. K. Chen, A. E. Lurain and P. J. Walsh, *J. Am. Chem. Soc.*, **124**, 12225 (2002).
    (c) A. E. Lurain and P. J. Walsh, *J. Am. Chem. Soc.*, **125**, 10677 (2003).
    (d) C. M. Sprout, M. L. Richmond and C. T. Seto, *J. Org. Chem.*, **69**, 6666 (2004).
    (e) J.-X. Ji, L.-Q. Qiu, C. W. Yip and A. S. C. Chan, *J. Org. Chem.*, **68**, 1589 (2003).
57. K. Soai and K. Takahashi, *J. Chem. Soc., Perkin Trans. 1*, 1257 (1994).
58. P. Wipf and W. Xu, *Tetrahedron Lett.*, **35**, 5197 (1994).
59. (a) P. Wipf and S. Ribe, *J. Org. Chem.*, **63**, 6454 (1998).
    (b) P. Wipf, N. Jayasuriya and S. Ribe, *Chirality*, **15**, 208 (2003).
60. H. Li and P. J. Walsh, *J. Am. Chem. Soc.*, **126**, 6538 (2004).
61. T. Shibata, K. Nakatsui and K. Soai, *Inorg. Chim. Acta*, **296**, 33 (1999).
62. Reviews: (a) L. Pu, *Tetrahedron*, **59**, 9873 (2003).
    (b) A. S. C. Chan, G. Lu and X. Li, in *Methodologies in Asymmetric Catalysis* (Ed. S. V. Malhotra), ACS Symp. Ser. 880, Washington DC, 2004, pp. 103–115.
63. S. Niwa and K. Soai, *J. Chem. Soc., Perkin Trans. 1*, 937 (1990).
64. G. Chelucci, S. Conti, M. Falorni and G. Giacomelli, *Tetrahedron*, **47**, 8251 (1991).
65. G. M. R. Tombo, E. Didier and B. Loubinoux, *Synlett*, 547 (1990).
66. M. Ishizaki and O. Hoshino, *Tetrahedron: Asymmetry*, **5**, 1901 (1994).
67. Z. Li, V. Upadhyay, A. E. DeCamp, L. DiMichel and P. J. Reider, *Synthesis*, 1453 (1999).
68. (a) G. Lu, X. Li, Z. Zhou, W. L. Chan and A. S. C. Chan, *Tetrahedron: Asymmetry*, **12**, 2147 (2001).
    (b) Y.-F. Kang, L. Liu, R. Wang, W.-J. Yan and Y.-F. Zhou, *Tetrahedron: Asymmetry*, **15**, 3155 (2004).
69. A. L. Braga, H. R. Appelt, C. C. Silveira, L. A. Wessjohann and P. H. Schneider, *Tetrahedron*, **58**, 10413 (2002).
70. (a) M.-H. Xu and L. Pu, *Org. Lett.*, **4**, 4555 (2002).
    (b) Z.-B. Li and L. Pu, *Org. Lett.*, **6**, 1065 (2004).
    (c) G. Gao, R.-G. Xie and L. Pu, *Proc. Natl. Acad. Sci. U. S. A.*, **101**, 5417 (2004).
    (d) L. Liu and L. Pu, *Tetrahedron*, **60**, 7427 (2004).
71. M. Li, X.-Z. Zhu, K. Yuan, B.-X. Cao and X.-L. Hou, *Tetrahedron: Asymmetry*, **15**, 219 (2004).
72. S. Dahmen, *Org. Lett.*, **6**, 2113 (2004).

73. Y.-F. Kang, R. Wang, L. Liu, C.-S. Da, W.-J. Yan and Z.-Q. Xu, *Tetrahedron Lett.*, **46**, 863 (2005).
74. X. Li, G. Lu, W. H. Kwok and A. S. C. Chan, *J. Am. Chem. Soc.*, **124**, 12636 (2002).
75. Z. Xu, R. Wang, J. Xu, C.-S. Da, W.-J. Yan and C. Chen, *Angew. Chem., Int. Ed.*, **42**, 5747 (2003).
76. (a) D. Moore and L. Pu, *Org. Lett.*, **4**, 1855 (2002).
    (b) G. Gao, D. Moore, R.-G. Xie and L. Pu, *Org. Lett.*, **4**, 4143 (2002).
77. G. Lu, X. Li, G. Chen, W.-L. Chan and A. S. C. Chan, *Tetradedron: Asymmetry*, **14**, 449 (2003).
78. Q.-Z. Liu, N.-S. Xie, Z.-B. Luo, X. Cui, L.-F. Cun, L.-Z. Gong, A.-Q. Mi and Y.-Z. Jiang, *J. Org. Chem.*, **68**, 7921 (2003).
79. R. M. Kamble and V. K. Singh, *Tetrahedron Lett.*, **44**, 5347 (2003).
80. Z. Xu, C. Chen, M. Miao, W. Yan and R. Wang, *Org. Lett.*, **6**, 1193 (2004).
81. Y.-F. Zhou, R. Wang, Z.-Q. Xu. W.-J. Yan, L. Liu, Y.-F. Gao and C.-S. Da, *Tetrahedron: Asymmetry*, **15**, 589 (2004).
82. P. G. Cozzi, *Angew. Chem., Int. Ed.*, **42**, 2895 (2003).
83. B. Saito and T. Katsuki, *Synlett*, 1557 (2004).
84. G. Lu, X. Li, X. Jia, W. L. Chan and A. S. C. Chan, *Angew. Chem., Int. Ed.*, **42**, 5057 (2003).
85. Y. Zhou, R. Wang, Z. Xu, W. Yan, L. Liu, Y. Kang and Z. Han, *Org. Lett.*, **6**, 4147 (2004).
86. L. Liu, R. Wang, Y.-F. Kang, C. Chen, Z.-Q. Xu, Y.-F. Zhou, M. Ni, H.-Q. Cai and M.-Z. Gong, *J. Org. Chem.*, **70**, 1084 (2005).
87. L. Liu, Y.-F. Kang, R. Wang, Y.-F. Zhou, C. Chen, M. Ni and M.-Z. Gong, *Tetrahedron: Asymmetry*, **15**, 3757 (2004).
88. (a) D. E. Frantz, R. Fässler and E. M. Carreira, *J. Am. Chem. Soc.*, **122**, 1806 (2000).
    (b) N. K. Anand and E. M. Carreira, *J. Am. Chem. Soc.*, **123**, 9687 (2001).
    (c) E. El-Sayed, N. K. Anand and E. M. Carreira, *Org. Lett.*, **3**, 3017 (2001).
    (d) H. Sasaki, D. Boyall and E. M. Carreira, *Helv. Chim. Acta*, **84**, 964 (2001).
    (e) D. Boyall, D. E. Frantz and E. M. Carreira, *Org. Lett.*, **4**, 2605 (2002).
89. (a) B. Jiang, Z. Chen and W. Xiong, *Chem. Commun.*, 1524 (2002).
    (b) Z. Chen, W. Xiong and B. Jiang, *Chem. Commun.*, 2098 (2002).
90. B. Jiang, Z. Chen and X. Tang, *Org. Lett.*, **4**, 3451 (2002).
91. Review: C. Bolm, J. P. Hildebrand, K. Muñiz and N. Hermann, *Angew. Chem., Int. Ed.*, **40**, 3284 (2001).
92. K. Soai, Y. Kawase and A. Oshio, *J. Chem. Soc., Perkin Trans. 1*, 1613 (1991).
93. P. I. Dosa, J. C. Ruble and G. C. Fu, *J. Org. Chem.*, **62**, 444 (1997).
94. G. Zhao, X.-G. Li and X.-R. Wang, *Tetrahedron: Asymmetry*, **12**, 399 (2001).
95. D.-H. Ko, K. H. Kim and D.-C. Ha, *Org. Lett.*, **4**, 3759 (2002).
96. (a) W.-S. Huang and L. Pu, *J. Org. Chem.*, **64**, 4222 (1999).
    (b) W.-S. Huang, Q.-S. Hu and L. Pu, *J. Org. Chem.*, **64**, 7940 (1999).
    (c) W.-S. Huang and L. Pu, *Tetrahedron Lett.*, **41**, 145 (2000).
97. (a) C. Bolm and K. Muñiz, *Chem. Commun.*, 1295 (1999).
    (b) C. Bolm, N. Hermanns, J. P. Hildebrand and K. Muñiz, *Angew. Chem., Int. Ed.*, **39**, 3465 (2000).
98. C. Bolm, M. Kesselgruber, N. Hermanns, J. P. Hildebrand and G. Raabe, *Angew. Chem., Int. Ed.*, **40**, 1488 (2001).
99. (a) C. Bolm and J. Rudolph, *J. Am. Chem. Soc.*, **124**, 14850 (2002).
    (b) J. Rudolph, N. Hermanns and C. Bolm, *J. Org. Chem.*, **69**, 3997 (2004).
100. P. I. Dosa and G. C. Fu, *J. Am. Chem. Soc.*, **120**, 445 (1998).
101. (a) C. García and P. J. Walsh, *Org. Lett.*, **5**, 3641 (2003).
    (b) H. Li, C. García and P. J. Walsh, *Proc. Natl. Acad. Soc. U. S. A.*, **101**, 5425 (2004).
102. K. Soai, T. Hayasaka, S. Ugajin and S. Yokoyama, *Chem. Lett.*, 1571 (1988).
103. K. Soai, S. Yokoyama, T. Hayasaka and K. Ebihara, *J. Org. Chem.*, **53**, 4148 (1988).
104. K. Soai, T. Hayasaka, S. Ugajin and S. Yokoyama, *J. Chem. Soc., Chem. Commun.*, 516 (1989).
105. K. Soai, M. Okudo and M. Okamoto, *Tetrahedron Lett.*, **32**, 95 (1991).
106. C. Bolm and M. Ewald, *Tetrahedron Lett.*, **31**, 5011 (1990).
107. C. Bolm, M. Felder and J. Müller, *Synlett*, 439 (1992).
108. M. Asami, K. Usui, S. Higuchi and S. Inoue, *Chem. Lett.*, 297 (1994).

109. A. H. M. de Vries, J. F. G. A. Jansen and B. L. Feringa, *Tetrahedron*, **50**, 4479 (1994).
110. A. H. M. de Vries and B. L. Feringa, *Tetrahedron: Asymmetry*, **8**, 1377 (1997).
111. A. Alexakis, J. Frutos and P. Mangeney, *Tetrahedron: Asymmetry*, **4**, 2427 (1993).
112. (a) B. L. Feringa, *Acc. Chem. Res.*, **33**, 346 (2000).
(b) A. H. M. de Vries, A. Meetsma and B. L. Feringa, *Angew. Chem., Int. Ed. Engl.*, **35**, 2374 (1996).
113. D. Peña, F. López, S. R. Harutyunyan, A. J. Minnaard and B. L. Feringa, *Chem. Commun.*, 1836 (2004).
114. H. Mizutani, S. J. Degrado and A. H. Hoveyda, *J. Am. Chem. Soc.*, **124**, 779 (2002).
115. R. Shintani and G. C. Fu, *Org. Lett.*, **4**, 3699 (2002).
116. T. Morimoto, N. Mochizuki and M. Suzuki, *Tetrahedron Lett.*, **45**, 5717 (2004).
117. M. Yan, L.-W. Yang, K.-Y. Wong and A. S. C. Chan, *Chem. Commun.*, 11 (1999).
118. A. M. Arink, T. W. Braam, R. Keeris, J. T. B. H, Jastrzebski, C. Benhaim, S. Rosset, A. Alexakis and G. van Koten, *Org. Lett.*, **6**, 1959 (2004).
119. Reviews: (a) S. E. Denmark and O. J.-C. Nicaise, in *Comprehensive Asymmetric Catalysis* (Eds. E. N. Jacobsen, A. Pfaltz and H. Yamamoto), Chap. 26.2, Springer-Verlag, Berlin, 1999, pp. 923–965.
(b) K. Hatanaka and H. Yamamoto, in *Comprehensive Asymmetric Catalysis Supplement 1* (Eds. E. N. Jacobsen, A. Pfaltz and H. Yamamoto). Chap. 26.2, Springer-Verlag, Berlin, 2004, pp. 107–116.
(c) S. E. Denmark and O. J.-C. Nicaise, *Chem. Commun.*, 999 (1996).
(d) D. Enders and U. Reinhold, *Tetrahedron: Asymmetry*, **8**, 1895 (1997).
(e) R. Bloch, *Chem. Rev.*, **98**, 1407 (1998).
120. A. R. Katritzky and P. A. Harris, *Tetrahedron: Asymmetry*, **3**, 437 (1992).
121. (a) K. Soai, T. Hatanaka and T. Miyazawa, *J. Chem. Soc., Chem. Commun.*, 1097 (1992).
(b) T. Hayase, Y. Inoue, T. Shibata and K. Soai, *Tetrahedron: Asymmetry*, **7**, 2509 (1996).
122. I. Sato, R. Kodaka and K. Soai, *J. Chem. Soc., Perkin Trans. 1*, 2912 (2001).
123. P. G. Andersson, D. Guijarro and D. Tanner, *J. Org. Chem.*, **62**, 7364 (1997).
124. (a) P. Brandt, C. Hedberg, K. Lawonn, P. Pinho and P. G. Andersson, *Chem,. Eur. J.*, **5**, 1692 (1999).
(b) P. Pinho and P. G. Andersson, *Tetrahedron*, **57**, 1615 (2001).
125. X. Zhang, L. Gong, A. Mi, X. Cui, Y. Jiang, M. C. K. Choi and A. S. C. Chan, *Tetrahedron Lett.*, **42**, 6369 (2001).
126. C. Jimeno, K. S. Reddy, L. Solà, A. Moyano, M. A. Pericàs and A. Riera, *Org. Lett.*, **2**, 3157 (2000).
127. T. Suzuki, N. Narisada, T. Shibata and K. Soai. *Tetrahedron: Asymmetry*, **7**, 2519 (1996).
128. (a) T. Suzuki, Y. Hirokawa, K. Ohtake, T. Shibata and K. Soai, *Tetrahedron: Asymmetry*, **8**, 4033 (1997).
(b) I. Sato, R. Kodaka, T. Shibata, Y. Hirokawa, N. Shirai, K. Ohtake and K. Soai, *Tetrahedron: Asymmetry*, **11**, 2271 (2000).
(c) I. Sato, K. Hosoi, R. Kodaka and K. Soai, *Eur. J. Org. Chem.*, 3115 (2002).
(d) K. Soai and I. Sato, *C. R. Chimie*, **6**, 1097 (2003).
129. M. Nakamura, A. Hirai and E. Nakamura, *J. Am. Chem. Soc.*, **118**, 8489 (1996).
130. Y. Ukaji, Y. Shimizu, Y. Kenmoku, A. Ahmed and K. Inomata, *Chem. Lett.*, 59 (1997).
131. C. Jimeno, A. Vidal-Ferran, A. Moyano, M. A. Pericàs and A. Riera, *Tetrahedron Lett.*, **40**, 777 (1999).
132. H. Fujihara, K. Nagai and K. Tomioka, *J. Am. Chem. Soc.*, **122**, 12055 (2000).
133. (a) J. R. Porter, J. F. Traverse, A. H. Hoveyda and M. L. Snapper, *J. Am. Chem. Soc.*, **123**, 984 (2001).
(b) J. R. Porter, J. F. Traverse, A. H. Hoveyda and M. L. Snapper, *J. Am. Chem. Soc.*, **123**, 10409 (2001).
134. (a) S. Dahmen and S. Bräse, *J. Am. Chem. Soc.*, **124**, 5940 (2002).
(b) N. Hermanns, S. Dahmen, C. Bolm and S. Bräse, *Angew. Chem., Int. Ed.*, **41**, 3692 (2002).
135. (a) D. E. Frantz, R. Fässler, C. S. Tomooka and E. M. Carreira, *Acc. Chem. Res.*, **33**, 373 (2000).
(b) D. E. Frants, R. Fässler and E. M. Carreira, *J. Am. Chem. Soc.*, **121**, 11245 (1999).
136. Reviews: (a) C. Girard and H. B. Kagan, *Angew. Chem., Int. Ed.*, **37**, 2923 (1998).
(b) D. R. Fenwick and H. B. Kagan, *Top. Stereochem.*, **22**, 257 (1999).

(c) K. Mikami, M. Terada, T. Korenaga, Y. Matsumoto, M. Ueki and R. Angelaud, *Angew. Chem., Int. Ed.*, **39**, 3532 (2000).
(d) M. Avalos, R. Babiano, P. Cintas, J. L. Jimenez and J. C. Palacios, *Tetrahedron: Asymmetry*, **8**, 2997 (1997).
137. (a) C. Puchot, O. Samuel. E. Duñach, S. Zhao, C. Agami and H. B. Kagan, *J. Am. Chem. Soc.*, **108**, 2353 (1986).
(b) C. Agami and C. Puchot, *J. Mol. Catal.*, **38**, 341 (1986).
138. N. Oguni, Y. Matsusa and T. Kaneko, *J. Am. Chem. Soc.*, **110**, 7877 (1988).
139. M. Kitamura, S. Okada and R. Noyori, *J. Am. Chem. Soc.*, **111**, 4028 (1989).
140. C. Bolm, G. Schlingoff and K. Harms, *Chem. Ber.*, **125**, 1191 (1992).
141. K. S. Reddy, L. Solà, A. Moyano, M. A. Pericàs and A. Riera, *Synthesis*, 165 (2000).
142. T. Ohga, S. Umeda and Y. Kawanami, *Tetrahedron*, **57**, 4825 (2001).
143. P. C. B. Page, S. M. Allin, S. J. Maddocks and M. R. J. Elsegood, *J. Chem. Soc., Perkin Trans. 1*, 2827 (2002).
144. C. Bolm, J. Müller, G. Schlingoff, M. Zehnder and M. Neuburger, *J. Chem. Soc., Chem. Commun.*, 182 (1993).
145. K. Fitzpatrick, R. Hulst and R. M. Kellogg, *Tetrahedron: Asymmetry*, **6**, 1861 (1995).
146. E. Rijnberg, N. J. Hjovestad, A. W. Kleij, J. T. B. H. Jastrebski, J. Boersma, M. D. Janssen, A. L. Spek and G. van Koten, *Organometallics*, **16**, 2847 (1997).
147. T. Wirth, K. J. Kulicke, G. Fragale, *Helv. Chim. Acta*, **79**, 1957 (1996).
148. I. Sarvary, Y. Wan and T. Frejd, *J. Chem. Soc., Perkin Trans. 1*, 645 (2002).
149. O. Legrand, J.-M. Brunel and G. Buono, *Tetrahedron Lett.*, **41**, 2105 (2000).
150. T. O. Luukas, D. R. Fenwick and H. B. Kagan, *C. R. Chimie*, **5**, 487 (2002).
151. M. Yamakawa and R. Noyori, *J. Am. Chem. Soc.*, **117**, 6327 (1995).
152. M. Kitamura, S. Suga, H. Oka and R. Noyori, *J. Am. Chem. Soc.*, **120**, 9800 (1998).
153. D. G. Blackmond, *Acc. Chem. Res.*, **33**, 402 (2000).
154. Y. K. Chen, A. M. Costa and P. J. Walsh, *J. Am. Chem. Soc.*, **123**, 5378 (2001).
155. F. Buono, P. J. Walsh and D. G. Blackmond, *J. Am. Chem. Soc.*, **124**, 13652 (2002).
156. T. Hayasaka, Master Degree Thesis, Tokyo University of Science (1990).
157. (a) C. Bolm, *Tetrahedron: Asymmetry*, **2**, 701 (1991).
(b) C. Bolm, M. Ewald and M. Felder, *Chem. Ber.*, **125**, 1205 (1992).
158. Reviews: (a) K. Soai, T. Shibata and I. Sato, *Acc. Chem. Res.*, **33**, 382 (2000).
(b) K. Soai and T. Shibata, in *Catalytic Asymmetric Synthesis*, 2nd edn. (Ed. I. Ojima), Wiley, New York, 2000, p. 699.
(c) K. Soai and T. Shibata, *Yuki Gosei Kagaku Kyokai Shi* (*J. Synth. Org. Chem. Jpn.*), **55**, 994 (1997); *Chem. Abstr.*, **128**, 3325 (1998).
(d) K. Soai and T. Shibata, in *Advances in Biochirality* (Eds. G. Pályi, C. Zucchi and L. Caglioti), Chap. 11, Elsevier, Amsterdam, 1999, pp. 125–136.
(e) K. Soai, T. Shibata and I. Sato, *Nippon Kagaku Kaishi* (*J. Chem. Soc. Jpn., Chem. Ind. Chem.)*, 141 (2001); *Chem. Abstr.*, **134**, 366365 (2001).
(f) K. Soai, I. Sato and T. Shibata, *Chem. Record*, **1**, 321 (2001).
(g) K. Soai and I. Sato, *Chirality*, **14**, 548 (2002).
(h) K. Soai, in *Fundamentals of Life* (Eds. G. Pályi, C. Zucchi and L. Caglioti), Elsevier, Paris, 2002, pp. 427–435.
(i) K. Soai, I. Sato and T. Shibata, *Yuki Gosei Kagaku Kyokai Shi* (*J. Synth. Org. Chem. Jpn.*), **60**, 668 (2002); *Chem. Abstr.*, **138**, 122561 (2003).
(j) K. Soai and I. Sato, *Viva Origino*, **30**, 186 (2002); *Chem. Abstr.*, **139**, 69168 (2003).
(k) C. Bolm, F. Bienewald and A. Seger, *Angew. Chem., Int. Ed. Engl.*, **35**, 1657 (1996).
(l) M. Avalos, R. Babiano, P. Cintas, J. L. Jiménez and J. C. Palacios, *Chem. Commun.*, 887 (2000).
(m) H. Buschmann, R. Thede and D. Heller, *Angew. Chem., Int. Ed.*, **39**, 4033 (2000).
(n) M. H. Todd, *Chem. Soc. Rev.*, **31**, 211 (2002).
(o) K. Soai, T. Shibata and I. Sato, *Bull. Chem. Soc. Jpn.*, **77**, 1063 (2004).
(p) K. Mikami and M. Yamanaka, *Chem. Rev.*, **103**, 3369 (2003).
(q) K. Soai, I. Sato and T. Shibata, in *Methodologies in Asymmetric Catalysis* (Ed. S. V. Malhotra), ACS Symp. Ser. 880, Washington DC, 2004, pp. 85–102.
(r) K. Soai, in *Progress in Biological Chirality* (Eds. G. Pályi, C. Zucchi and L. Caglioti), Chap. 29, Elsevier, Amsterdam, 2004, pp. 355–364.

159. (a) K. Soai, H. Hori and S. Niwa, *Heterocycles*, **29**, 2065 (1989).
(b) K. Soai, S. Niwa and H. Hori, *Chem. Commun.*, 982 (1990).
160. T. Shibata, H. Morioka, S. Tanji, T. Hayase, Y. Kodaka and K. Soai, *Tetrahedron Lett.*, **37**, 8783 (1996).
161. K. Soai, T. Hayase and K. Takai, *Tetrahedron: Asymmetry*, **6**, 637 (1995).
162. K. Soai, T. Hayase, C. Shimada and K. Isobe, *Tetrahedron: Asymmetry*, **5**, 789 (1994).
163. T. Shibata, H. Morioka, T. Hayase, K. Choji and K. Soai, *J. Am. Chem. Soc.*, **118**, 471 (1996).
164. T. Shibata, S. Yonekubo and K. Soai, *Angew. Chem., Int. Ed.*, **38**, 659 (1999).
165. I. Sato, T. Yanagi and K. Soai, *Chirality*, **14**, 166 (2002).
166. T. Shibata, K. Choji, H. Morioka, T. Hayase and K. Soai, *J. Chem. Soc., Chem. Commun.*, 751 (1996).
167. I. Sato, T. Nakao, R. Sugie, T. Kawasaki and K. Soai, *Synthesis*, 1419 (2004).
168. (a) B. L. Feringa and R. A. van Delden, *Angew. Chem., Int. Ed.*, **38**, 3418 (1999).
(b) C. Girard and H. B. Kagan, *Angew. Chem., Int. Ed.*, **37**, 2922 (1998).
(c) A. Eschenmoser, *Science*, **284**, 2118 (1999).
(d) H. Zepik, E. Shavit, M. Tang, T. R. Jensen, K. Kjaer, G. Bolbach, L. Leiserowitz, I. Weissbuch and M. Lahav, *Science*, **295**, 1266 (2002).
(e) M. M. Green, J.-W. Park, T. Sato, A. Teramoto, S. Lifson, R. L. B. Selinger and J. V. Selinger, *Angew. Chem., Int. Ed.*, **38**, 3138 (1999).
(f) W. A. Bonner, *Orig. Life Evol. Biosphere*, **25**, 175 (1995).
(g) D. K. Kondepudi and K. Asakura, *Acc. Chem. Res.*, **34**, 946 (2001).
(h) J. S. Siegel, *Chirality*, **10**, 24 (1998).
(i) S. Mason, *Chem. Soc. Rev.*, **17**, 347 (1988).
(j) L. Keszthelyi, *Q. Rev. Biophy.*, **28**, 473 (1995).
(k) V. Avetisov and V. Goldanskii, *Proc. Natl. Acad. Sci., U. S. A.*, **93**, 11435 (1996).
(l) M. Avalos, R. Babiano, P. Cintas, J. L. Jimenez and J. C. Palacios, *Tetrahedron: Asymmetry*, **11**, 2845 (2000).
169. K. Soai, T. Shibata, H. Morioka and K. Choji, *Nature (London)*, **378**, 767 (1995).
170. I. Sato, H. Urabe, S. Ishiguro, T. Shibata and K. Soai, *Angew. Chem., Int. Ed.*, **42**, 315 (2003).
171. (a) I. Sato, D. Omiya, K. Tsukiyama, Y. Ogi and K. Soai, *Tetrahedron: Asymmetry*, **12**, 1965 (2001).
(b) I. Sato, D. Omiya, H. Igarashi, K. Kato, Y. Ogi, K. Tsukiyama and K. Soai, *Tetrahedron: Asymmetry*, **14**, 975 (2003).
172. (a) T. Buhse, *Tetrahedron: Asymmetry*, **14**, 1055 (2003)
(b) I. D. Gridnev, J. M. Serafimov and J. M. Brown, *Angew. Chem., Int. Ed.*, **43**, 4884 (2004).
(c) D. G. Blackmond, *Proc. Natl. Acad. Sci. U. S. A.*, **101**, 5732 (2004).
(d) Y. Saito and H. Hyuga, *J. Phys. Soc. Jpn.*, **73**, 33 (2004).
(e) G. Lente, *J. Phys. Chem. A*, **108**, 9475 (2004).
173. T. Shibata, K. Choji, T. Hayase, Y. Aizu and K. Soai, *Chem. Commun.*, 1235 (1996).
174. S. Tanji, Y. Kodaka, A. Ohno, T. Shibata, I. Sato and K. Soai, *Tetrahedron: Asymmetry*, **11**, 4249 (2000).
175. T. Shibata, J. Yamamoto, N. Matsumoto, S. Yonekubo, S. Osanai and K. Soai, *J. Am. Chem. Soc.*, **120**, 12157 (1998).
176. K. Soai and I. Sato, *Enantiomer*, **6**, 189 (2001).
177. H. Igarashi, D. Omiya, Y. Ohgo, I. Sato and K. Soai, The 81st Annual Meeting of Chem. Soc. Jpn., Abstract 4GZ-17, March, 2002, Tokyo.
178. I. Sato, D. Omiya, T. Saito and K. Soai, *J. Am. Chem. Soc.*, **122**, 11739 (2000).
179. (a) S. Tanji, A. Ohno, I. Sato and K. Soai, *Org. Lett.*, **3**, 287 (2001).
(b) I. Sato, A. Ohno, Y. Aoyama, T. Kasahara and K. Soai, *Org. Biomol. Chem.*, **1**, 244 (2003).
180. I. Sato, R. Yamashima, K. Kadowaki, J. Yamamoto, T. Shibata and K. Soai, *Angew. Chem., Int. Ed.*, **40**, 1096 (2001).
181. I. Sato, Y. Matsueda, K. Kadowaki, S. Yonekubo, T. Shibata and K. Soai, *Helv. Chim. Acta.*, **85**, 3383 (2002).
182. I. Sato, S. Osanai, K. Kadowaki, T. Sugiyama, T. Shibata and K. Soai, *Chem. Lett.*, 168 (2002).
183. T. Kawasaki, M. Shimizu, K. Suzuki, I. Sato and K. Soai, *Tetrahedron: Asymmetry*, **15**, 3699 (2004).

184. I. Sato, R. Sugie, Y. Matsueda, Y. Furumura and K. Soai, *Angew. Chem., Int. Ed.*, **43**, 4490 (2004).
185. I. Sato, K. Kadowaki, Y. Ohgo, K. Soai and H. Ogino, *Chem. Commun.*, 1022 (2001).
186. A. G. Cairns-Smith, *Ber. Dtsch. Chem. Ges.*, 559 (1886).
187. K. Soai, S. Osanai, K. Kadowaki, S. Yonekubo, T. Shibata and I. Sato, *J. Am. Chem. Soc.*, **121**, 11235 (1999).
188. (a) I. Sato, K. Kadowaki and K. Soai, *Angew. Chem., Int. Ed.*, **39**, 1510 (2000).
(b) I. Sato, K. Kadowaki, Y. Ohgo and K. Soai, *J. Mol. Catal. A*, **216**, 209 (2004).
189. I. Sato, K. Kadowaki, H. Urabe, J. Hwa Jung, Y. Ono, S. Shinkai and K. Soai, *Tetrahedron Lett.*, **44**, 721 (2003).
190. T. Kawasaki, K. Ishikawa, H. Sekibata, I. Sato and K. Soai, *Tetrahedron Lett.* **45**, 7939 (2004).
191. I. Sato, M. Shimizu, T. Kawasaki and K. Soai, *Bull. Chem. Soc. Jpn.*, **77**, 1587 (2004).
192. T. Kawasaki, K. Jo, H. Igarashi, I. Sato, M. Nagano, H. Koshima and K. Soai, *Angew. Chem., Int. Ed.*, **44**, 2774 (2005).
193. (a) J. J. Flores, W. A. Bonner and G. A. Massey, *J. Am. Chem. Soc.*, **99**, 3622 (1977).
(b) H. Nishino, A. Kosaka, G. A. Hembury, F. Aoki, K. Miyauchi, H. Shitomi, H. Onuki and Y. Inoue, *J. Am. Chem. Soc.*, **124**, 11618 (2002).
194. (a) A. Moradpour, J. F. Nicoud, G. Balavoine, H. Kagan and G. Tsoucaris, *J. Am. Chem. Soc.*, **93**, 2353 (1971).
(b) W. J. Bernstein, M. Calvin and O. Buchardt, *J. Am. Chem. Soc.*, **94**, 494 (1972).
195. (a) M. Suarez and G. B. Schuster, *J. Am. Chem. Soc.*, **117**, 6732 (1995).
(b) Y. Zhang and G. B. Schuster, *J. Org. Chem.*, **60**, 7192 (1995).
(c) Y. Inoue, H. Tsuneishi, T. Hakushi, K. Yagi, K. Awazu and H. Onuki, *Chem. Commun.*, 2627 (1996).
(d) N. P. M. Huck, W. F. Jager, B. de Lange and B. L. Feringa, *Science*, **273**, 1686 (1996).
196. T. Kawasaki, M. Sato, S. Ishiguro, T. Saito, Y. Morishita, I. Sato, H. Nishino, Y. Inoue and K. Soai, *J. Am. Chem. Soc.*, **127**, 3274 (2005).
197. (a) K. Mislow, *Collect. Czech. Chem. Commun.*, **68**, 849 (2003).
(b) J. S. Siegel, *Nature*, **419**, 346 (2002).
198. W. H. Mills, *Chem. Ind.*, 750 (1932).
199. (a) K. Soai, K. T. Shibata and Y. Kowata, *Japan Kokai Tokkyo Koho* 9268179 (1997). (Application date: February 1, 1996 and April 18, 1996.) An abstract of JP9268179 is available from the European Patent Office (http://ep.espacenet.com).
(b) K. Soai, I. Sato, T. Shibata, S. Komiya, M. Hayashi, Y. Matsueda, H. Imamura, T. Hayase, H. Morioka, H. Tabira, J. Yamamoto and Y. Kowata, *Tetrahedron: Asymmetry*, **14**, 185 (2003).
(c) S. Komiya, M. Hayashi, Y. Matsueda, H. Imamura, K. Jo, T. Hayase, H. Morioka, H. Tabira, J. Yamamoto, Y. Kowata, T. Shibata, I. Sato and K. Soai, The 83rd Annual Meeting of Chem. Soc. Jpn., Abstract 1H5-07, March, 2003, Tokyo.
(d) For non-stochastic formation of pyrimidyl alkanol, D. A. Singleton and L. K. Vo, *J. Am. Chem. Soc.*, **124**, 10010 (2002).

CHAPTER 13

Rearrangements of organozinc compounds

VARINDER K. AGGARWAL and KNUT SOMMER

School of Chemistry, University of Bristol, Cantock's Close, Bristol, BS8 1TS, United Kingdom
Fax: +44 117 929 8611; e-mail: v.aggarwal@bristol.ac.uk

The chemistry of organozinc compounds
Edited by Z. Rappoport and I. Marek

I. 1,2-METALLATE REARRANGEMENTS

A. Introduction

The most important class of rearrangement reactions of organozinc compounds involves a 1,2-migration of an R^1 group from a (formally) negatively charged zinc atom of a zincate complex **1** to an α-carbon with loss of a leaving group X^- and formation of a new organozinc species **2**. In most cases, the leaving group is directly attached to the α-carbon (equation 1).

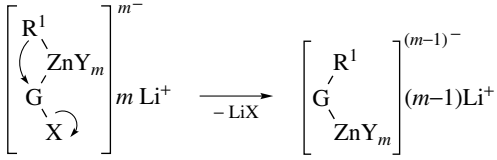

(1)

(1) **(2)**

G = $R^2(R^3)C{=}C$, R^2CH, *cyclo*-(R^2CHCH_2C); Y = R^1 or OR^4;
X^- = leaving group, usually halide anion; m = 1 or 2.

Early[1] examples for this type of reaction were reported by Negishi and coworkers in the late 1980s[2]. α-Haloorganolithium carbenoids **4** were shown to react with a large variety of organometallics L_mMR **3** to give the products of a formal carbene insertion into the metal–carbon bond (**5**) after hydrolysis (equation 2).

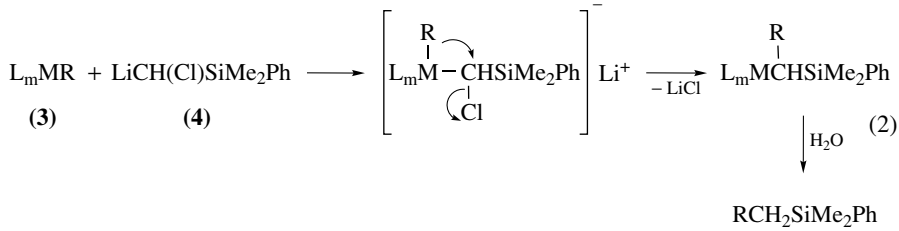

(2)

M = Al, Mg, **Zn**, Cd, Ti, Zr, Hf, V, Cr, Mn, Fe, Co, Ni, Cu. **(5)**

In the case of $(n\text{-Bu})_2Zn$ as the organometallic reagent (R = L = n-Bu; m = 1), the product (n-Bu)CH_2SiMe_2Ph (**5a**) was formed in 61% yield. A 1,2-migration mechanism was proposed on the basis of kinetic data and NMR experiments. Following Negishi's pioneering work, many other examples of related reactions were reported, the most important of which are described below.

B. Reactions of 1,1-Dihalo Compounds with Triorganozincates

The reaction of 1,1-dihalo derivatives (**6**) with triorganozincates (prepared from $ZnCl_2$ and three equivalents of a suitable organolithium or Grignard reagent in THF at 0 °C) at low temperature furnishes, through zinc–halide exchange, 1-halozincates (**7**) which,

upon warming, undergo a rearrangement with loss of the second halide to give a new organozinc **8** (equation 3)[3,4,7,9,11–13].

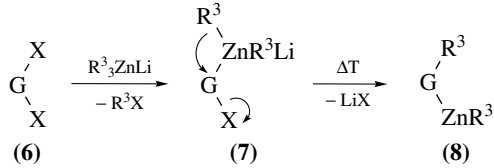

(6) (7) (8) (3)

G = $R^1(R^2)CH_2{=}C$, *cyclo*-(R^1CHCH_2C), R^1CH, X = Br, I

1. 1,1-Dihaloalkenes

Shortly after Negishi's original work, Oku and coworkers described reactions of triorganozincates with 1,1-dibromoalkenes **9**, which gave different products upon protonolysis depending on the reaction temperature (equations 4 and 5)[3].

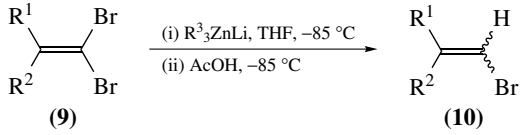

(9) (10) (4)

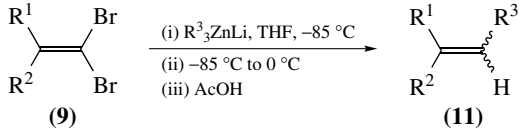

(9) (11) (5)

For example, 2-phenyl-3-octene (**11a**) was formed from 1,1-dibromo-3-phenyl-1-butene (**9a**, R^1 = Ph(Me)CH, R^2 = H) and (n-Bu)$_3$ZnLi upon protonolysis with acetic acid after warming the reaction mixture to 0 °C in 61% yield in an $(E)/(Z)$ ratio of 35/65. In contrast, protonolysis at −85 °C produced 1-bromo-3-phenyl-1-butene (**10a**, equation 4) in 82% yield and 72/28 $(E)/(Z)$ ratio. The $(E)/(Z)$ ratio has obviously been reversed, indicating that the rearrangement takes place with inversion of configuration at the α-carbon. Further investigations[4] revealed that the bromine–zinc exchange reaction proceeds stereospecifically with retention of configuration of the carbenoid atom and preferentially at the sterically more hindered bromine atom (although selectivities are moderate). These results can be rationalized in terms of a linear transition state (either of an ate-complex[5] or an S_N2-type reaction[6]) of the bromine–zinc exchange whereby bond elongation of the carbon–bromine bond leads to a relief of steric strain which is greatest at the more hindered position.

A number of specific examples of the rearrangement reaction are given in Table 1 to provide an indication of the scope of the methodology[7]. Yields are generally good to high, with the sterically demanding t-butyl group giving consistently lower yields compared to other alkyl groups. A drawback of the method is undoubtedly the moderate $(E)/(Z)$ selectivity which is strongly dependent on the steric interactions between the substituents R^1, R^2 and the migrating group R^3. It has been observed that the migration can become non-stereospecific when severe steric repulsion occurs between the zincate group and the *cis* substituent[7].

The alkenylzinc compounds **12** prepared by the described methodology can be used in palladium-catalysed cross coupling reactions using $Pd(PPh_3)_2$ (prepared *in situ* by

TABLE 1. Reactions of 1,1-dibromoalkenes with triorganozincates (equation 5)

Entry	R^1	R^2	R^3	Time[a] (h)	Yield (%)	$(E)/(Z)$
1	PhCH(Me)	H	*n*-Bu	0	83	1/2.3
2	PhCH(Me)	H	*s*-Bu	3	83	1.2/1
3	PhCH(Me)	H	*t*-Bu	1	42	9.2/1
4	Cy	H	*n*-Bu	0	86	1/2.9
5	Ph	Et	*n*-Bu	0	92	1.8/1
6	Ph	$MeOCH_2$	*n*-Bu	0	96	1/1.3
7	Ph	$MeOCH_2$	*s*-Bu	0	95	1/1.2
8	Ph	$MeOCH_2$	*t*-Bu	0	84	1/1.5
9	Ph	$MeOCH_2$	Me	0	90	1/1.3
10		Me	*n*-Bu	0.5	71	1/2.9

[a] The reaction mixture was stirred at −85 °C for the time indicated before gradually being warmed to 0 °C.

reduction of $PdCl_2(PPh_3)_2$ with DIBAH) or $PdCl_2(PPh_3)_2$ as catalyst (equation 6)[7,8]. A few representative examples are given in Scheme 1, the bold-faced substituents indicating the electrophilic group introduced at the end of the reaction sequence. Yields of compounds **13** are moderate to good but $(E)/(Z)$ selectivities are poor in most cases.

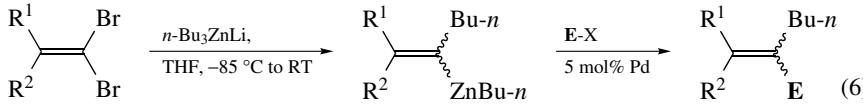

(9) **(12)** **(13)** (6)

E-X = acid chlorides, aryl bromides, vinyl bromides

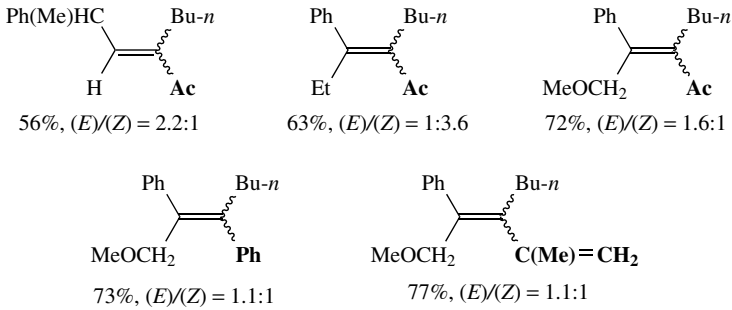

SCHEME 1

2. 1,1-Dihalocyclopropanes

Following the report on reactions of 1,1-dibromoalkenes **9** with triorganozincates, the same group reported reactions of 1,1-dibromocyclopropanes **14** (equation 7)[9].

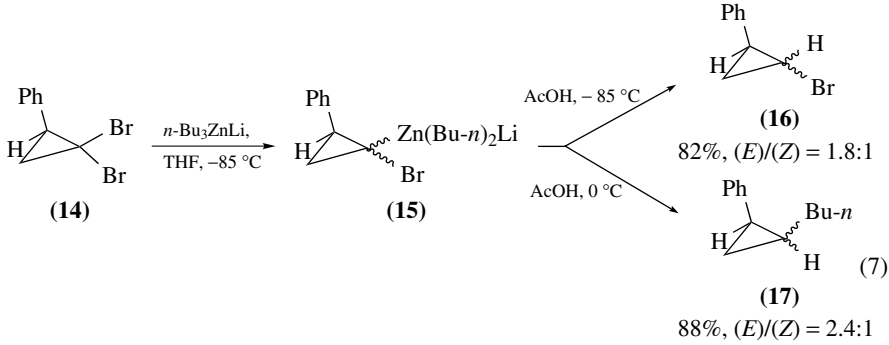

(7)

Addition of lithium tributylzincate to 1,1-dibromo-2-phenylcyclopropane (**14**) at −85 °C produced intermediate zincate carbenoid **15**, which was stable at low temperatures, giving the retained hydrolysis product **16**, but rearranged with inversion of configuration of the carbenoid atom upon warming just as in the case of the alkenyl compounds (see above). More conveniently, the alkylation product **17** was obtained directly in high yield if the addition was carried out at 0 °C (*method A*). Various other alkyl groups could also be transferred, such as *s*- and *t*-butyl and methyl, whereas the transfer of aryl or alkenyl groups failed. As before, the method produces the alkylation products in high yields (78–95%), but with poor (*E*)/(*Z*) selectivities.

To solve this problem, the authors prepared the zinc carbenoid **15** via the corresponding lithium carbenoid which is known to be formed stereoselectively[10] (*method B*, equation 8)[9].

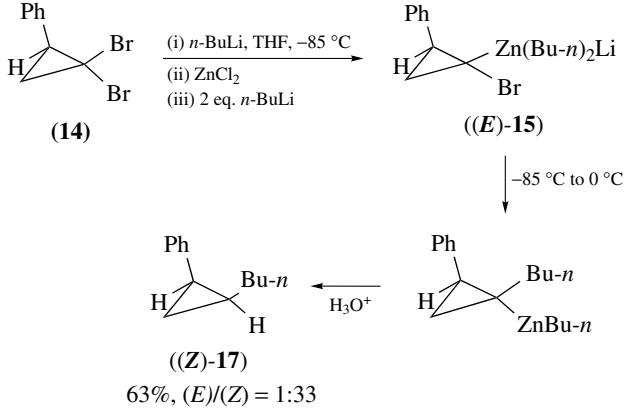

(8)

Although the yield was lower as compared to the original protocol, very high (*Z*) selectivity was observed this time. Generally, the reaction sequence via lithium carbenoids gives somewhat lower yields but significantly improved selectivities. A variant of this method was developed whereby only one equivalent of butyllithium was employed in the second step producing a neutral butyl cyclopropyl zinc species. This dialkylzinc species did not rearrange but addition of two equivalents of metal alkoxides produced a higher order zincate $R^1(R^2)Zn(OR^3)_2Li_2$ which readily underwent the rearrangement[11a].

To obtain (*E*) products, the 1,1-dibromo compounds **14** were first lithiated stereoselectively as described and then transformed into the corresponding 1-bromo-1-chloro

cyclopropanes **18**. The latter reacted with triorganozincates preferentially at the bromine atom giving, after rearrangement and acidic workup, alkylated (*E*)-cyclopropanes with good to high selectivities (*method C*, equation 9)[9,11].

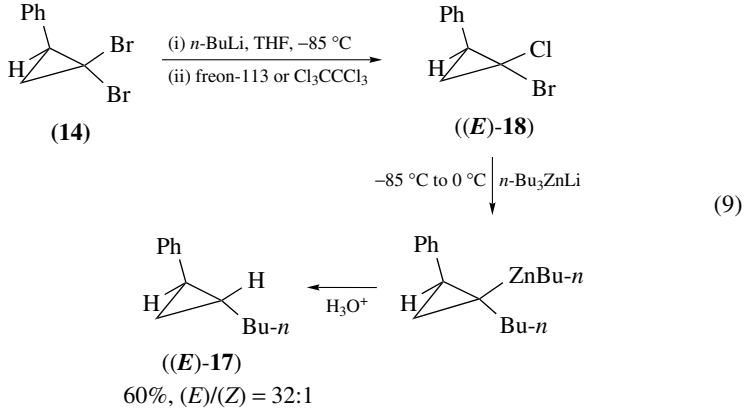

(**14**) ((***E***)-**18**) ((***E***)-**17**)

60%, (*E*)/(*Z*) = 32:1 (9)

Again, the cyclopropylzinc species **17** prepared by the described methods can be reacted under Pd catalysis (10 mol% $Pd(PPh_3)_2$) with various carbon electrophiles **E**-X such as acid chlorides, aryl bromides or vinyl bromides[11]. Representative examples applying methods A–C are given in Scheme 2, the bold-faced substituents indicating the electrophilic group introduced at the end of the reaction sequence[11a].

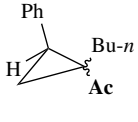

A: 76%, (E)/(Z) = 1:1.9
B: 74%, (E)/(Z) = 16:1
C: 50%, (E)/(Z) = 1:7.0

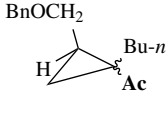

A: 96%, (E)/(Z) = 2.4:1
B: 65%, (E)/(Z) = 5.7:1
C: 52%, (E)/(Z) = 1:21

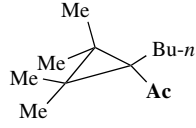

A: 64%

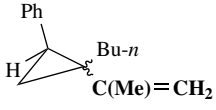

A: 82%, (E)/(Z) = 1:2.7
B: 60%, (E)/(Z) = 9.1:1
C: 68%, (E)/(Z) = 1:16

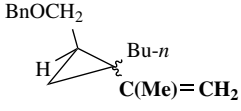

A: 78%, (E)/(Z) = 2.0:1
B: 70%, (E)/(Z) = 9.1:1
C: 47%, (E)/(Z) = 1:>40

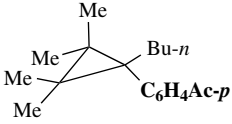

A: 48%

SCHEME 2

3. 1,1-Dihaloalkanes

The above reactions can be extended to encompass 1,1-dibromo*alkanes* **19**, although the latter exhibit significantly lower reactivity than 1,1-dibromoalkenes **9** and the corresponding cyclopropanes **14**[12]. To solve this problem, the triorganozincate was employed in five-fold excess. This methodology gives access to secondary organozinc reagents **20**

which are very useful in organic synthesis[8]. They can be reacted in palladium-catalysed cross-coupling reactions with various carbon electrophiles to give the corresponding alkylation products **21**–**23** in satisfactory yields (equation 10).

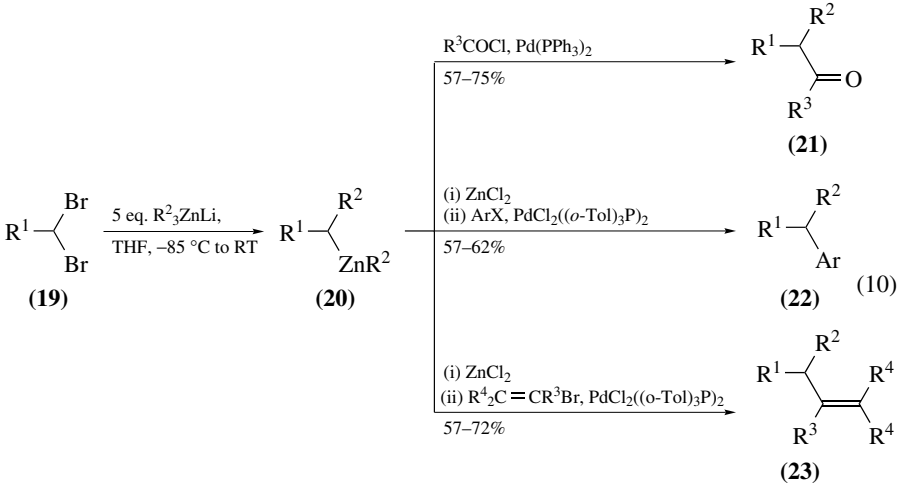

(10)

R^1 = octyl, $PhCH_2CH_2$, $THPO(CH_2)_4$; R^2 = Me, *n*-Bu, *s*-Bu, *t*-Bu; R^3 = Ac, Ph, *t*-Bu;

$R^4 = Me_2C{=}CH$, $CH_2{=}C(Me)$; Ar = Ph, *p*-AcC_6H_4.

More recently, an improved methodology for the preparation of secondary organozincs was introduced by Marek, Knochel and coworkers[13]. Reaction of a 1,1-diiodoalkane **24** with diethylzinc (1.2 equivalents) at −50 °C in a mixture of THF and *N*-methylpyrrolidinone (NMP) and warming to room temperature produced a new secondary organozinc **26** which could be trapped with various electrophiles to give a range of compounds **27** (equation 11).

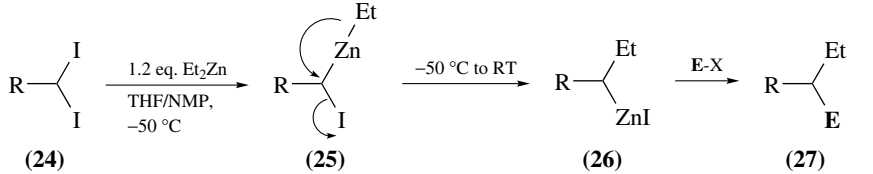

R = $PhCH_2$, *n*-Bu (11)

The presence of NMP was necessary for the rearrangement to occur[14]. It is therefore likely that the structure drawn for the intermediate **25** is oversimplified (it is well-established that a zinc*ate* species is necessary for the rearrangement to occur; see, for example, Section I.B.2 and Reference 11). Representative examples outlining the scope of the methodology are given in Scheme 3.

It was also reported that these reactions proceed equally well in pure THF when two equivalents of LiBr are added[13]. Alternatively, the diorganozinc can be prepared reacting $ZnBr_2$ with two equivalents of RLi or RMgBr, thus producing LiBr or $MgBr_2$, respectively *in situ*. Obviously, LiBr and polar cosolvents such as NMP increase the reactivity of intermediates like **25**[15, 16].

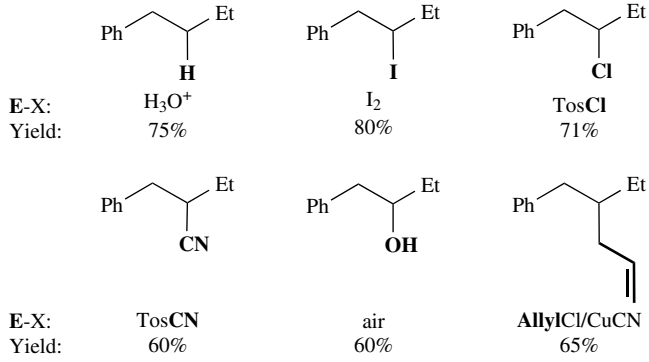

SCHEME 3

C. 1,2-Migrations with Loss of a Leaving Group Attached to a Remote Carbon

1. Propargylic and homopropargylic substrates

The leaving group does not necessarily have to be attached directly to the α-carbon. When employing propargylic substrates **28** the 1,2-migration leads to a three-carbon homologation which can be utilized to prepare allenic zinc reagents **29** (equation 12)[17]. This contrasts the behaviour of organocuprates $R^3{}_2CuLi$ which, on reaction with propargylic derivatives $X(R^1)(R^2)CC{\equiv}CH$, produce allenes $R^1R^2C{=}C{=}C(R^3)H$[18], probably via an S_N2' nucleophilic attack of the Cu(I) atom followed by reductive elimination of the resulting Cu(III) intermediate[19].

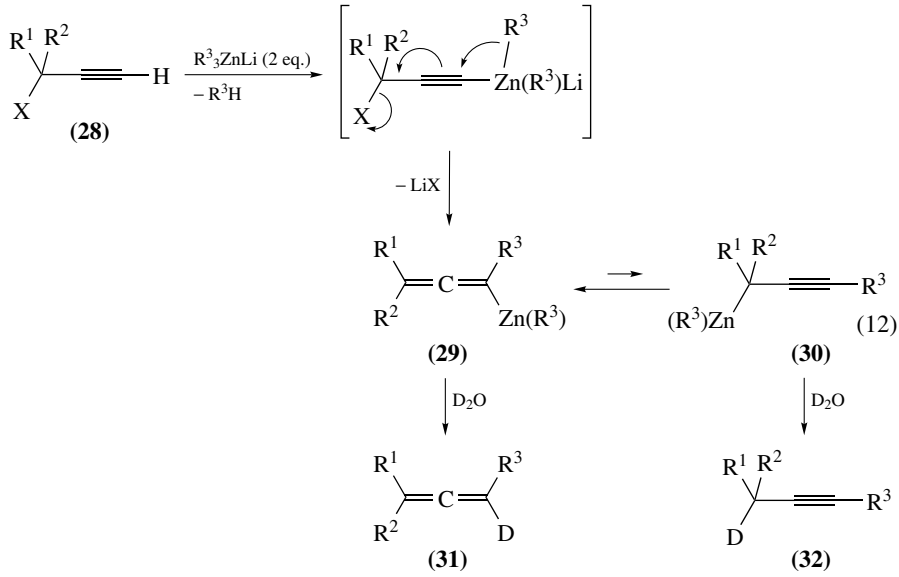

X = OMs, Cl, $OP(O)(OEt)_2$, $OCONPh_2$, $OCONEt_2$

The allenic zinc species formed through the 1,2-migration (**29**) is in equilibrium with a propargylic species **30**. When using simple triorganozincates, alkyne formation is usually negligible (<3%). In the case of sterically demanding zincates such as (*s*-Bu)$_3$ZnLi or (*t*-Bu)$_3$ZnLi however, alkynes can become minor products. For example, the reaction of Ph(CH$_2$)$_2$(MsO)CHC≡CH (**28a**) and (*t*-Bu)$_3$ZnLi followed by quenching with D$_2$O gave the allene Ph(CH$_2$)$_2$CH=C=C(Bu-*t*)D (**31a**) and alkyne Ph(CH$_2$)$_2$(D)CHC≡C(Bu-*t*) (**32a**) in 60 and 16% yield, respectively[17c]. A range of zincate species can be used, including trialkyl, vinyl and aryl zincates.

It has been reported that quenching of the zinc intermediates with electrophiles E-X rather than simple deuteriolysis gives alkynes **33** selectively, thus providing a one-pot protocol for the introduction of a nucleophile (R^3) and an electrophile (E) in the 1- and 3-positions of the propargylic substrate **28** (equation 13).

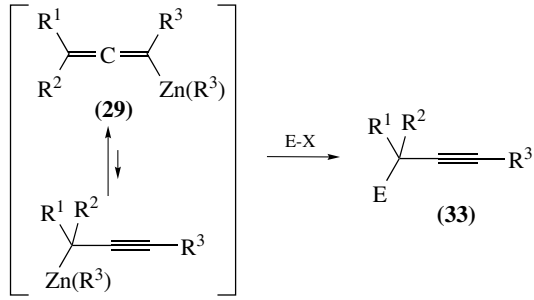

(13)

A range of electrophiles has been applied successfully, including I$_2$, NCS, TMSCl, acid chlorides and aldehydes. The use of the latter allows the stereoselective synthesis of homopropargylic alcohols **34** (equation 14).

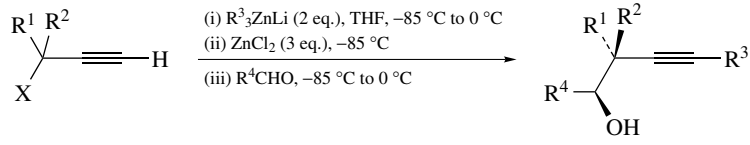

(28) (34)

(14)

X = OMs or Cl; R^1 = alkyl or H; R^2 = H;

R^3 = Me, *n*-Bu, *s*-Bu, *t*-Bu, Ph, CH$_2$=C(Me); R^4 = Ph, alkyl

Treatment of the intermediate allenylic zinc species with an excess of ZnCl$_2$ turned out to be necessary to achieve good diastereoselectivities. A few representative examples are given in Scheme 4[17c].

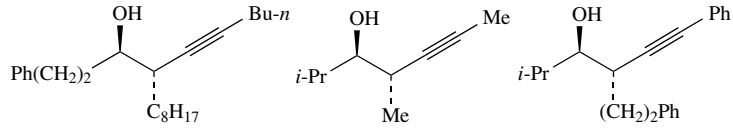

Yield:	83%	66%	56%
anti/syn:	96:4	99.3:0.7	99.1:0.9

SCHEME 4

The process can also be utilized for the synthesis of cyclopropanes when *homo*propargylic substrates **35** are employed (equation 15)[20].

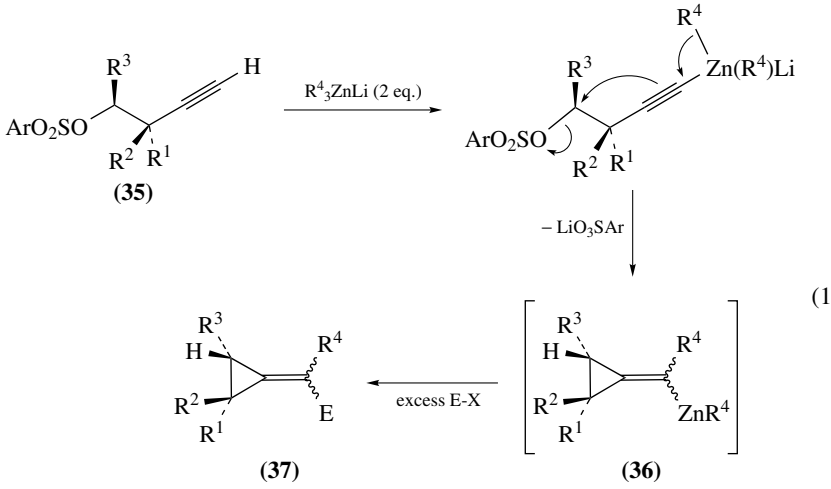

(15)

R^1 = alkyl, H; R^2 = alkyl, H; R^3 = alkyl, H; R^4 = *n*-Bu, *s*-Bu, *t*-Bu, Me, $TMSCH_2$;
E-X = H_2O, D_2O, I_2, TMSCl, TosCN, $ClCO_2Et/PdCl_2(PPh_3)_2$ (5 mol%);
n-BuCOCl/$PdCl_2(PPh_3)_2$) (5 mol%); $Ph(CH_2)_2CHO$

Initial experiments with $(ArSO_2O)CH_2CH(CH_2Ph)C{\equiv}CH$ ($R^1 = PhCH_2$, $R^2 = R^3 =$ H, **35a**) and $(n\text{-Bu})_3ZnLi$ using D_2O as the quenching agent revealed that, depending on the reaction temperature and nature of the leaving group (i.e. Ar), varying amounts of an alkyne $DCH_2CH(CH_2Ph)C{\equiv}C(Bu\text{-}n)$ were obtained in addition to the cyclopropane **37a** ($R^1 = PhCH_2$, $R^2 = R^3 = H$). This was rationalized by a ring-opening reaction of the intermediate **36a** ($R^1 = PhCH_2$, $R^2 = R^3 = H$) leading to a homopropargylic zinc reagent $(R^4)ZnCH_2CH(CH_2Ph)C{\equiv}C(Bu\text{-}n)$ which, upon deuteriolysis, gave an alkyne. Alkyne formation can be retarded by proper choice of the leaving group (strongly electron-withdrawing, such as $p\text{-}ClC_6H_4OSO_2$) and working at low temperature ($\leqslant 0\,^\circ C$). The scope of the methodology is outlined in Table 2[20].

2. Benzylic substrates

The principle outlined above can be applied to the synthesis of benzyl zinc reagents via an interesting 1,2-migration/isomerization sequence (equation 16)[21].

TABLE 2. Representative examples of the formation of cyclopropanes (equation 15, $R^1 = PhCH_2$, $R^2 = R^3 = H$, $R^4 = n$-Bu)

Entry	E-X	Catalyst	Yield (%)	(*E*)/(*Z*)
1	**D**$_2$O	none	93 (95% D)	2.4/1
2	**I**$_2$	none	77	1/2.3
3	**TMS**Cl	none	56	1/1.3
4	Tos**CN**	none	73	1/2.1
5	Cl**CO**$_2$**Et**	5 mol% $PdCl_2(PPh_3)_2$	65	1/3.4

TABLE 3. Representative examples of the formation of benzylic compounds p-$RC_6H_4CH_2E$ (equation 16)

Entry	E-X	R	Product	Yield (%)
1	**Ph(CH$_2$)$_2$CHO**	*n*-Bu	*p*-*n*-BuC$_6$H$_4$CH$_2$**CH(OH)(CH$_2$)$_2$Ph**	80
2	***i*-PrCHO**	*n*-Bu	*p*-*n*-BuC$_6$H$_4$CH$_2$**CH(OH)(Pr-*i*)**	72
3	***i*-PrCHO**	*s*-Bu	*p*-*s*-BuC$_6$H$_4$CH$_2$**CH(OH)(Pr-*i*)**	62
4	***i*-PrCHO**	*t*-Bu	*p*-*t*-BuC$_6$H$_4$CH$_2$**CH(OH)(Pr-*i*)**	56
5	***n*-BuCO**Cl	*n*-Bu	*p*-*n*-BuC$_6$H$_4$CH$_2$**CO(Bu-*n*)**	61
6	Tos**CN**	*n*-Bu	*p*-*n*-BuC$_6$H$_4$CH$_2$**CN**	58

The benzyl zinc reagents **38** can be reacted with various electrophiles E-X including aldehydes (or ketones) and acid chlorides, thus providing access to secondary (or tertiary) alcohols and benzylic ketones, respectively. Examples are given in Table 3[21].

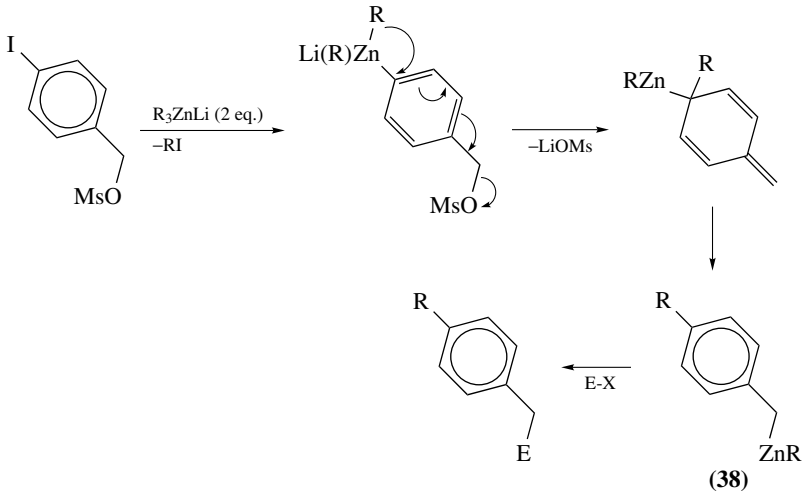

(16)

(38)

R = *n*-Bu, *s*-Bu, *t*-Bu; E-X = aldehydes, ketones, acid chlorides, TosCN, $PhMe_2SiCl$

D. Methylene Homologations

1. Methylene homologations of organometallic reagents using organozincs

This topic has been reviewed elsewhere[22] extensively and is thus only covered briefly in this chapter. Methylene homologations of organometallic reagents with organozincs can be achieved via two different mechanisms: an intramolecular reaction involving a 1,2-metallate rearrangement step (**41**, equation 17a), or an intermolecular S_N2-type reaction between an organometallic species **39** and a zinc carbenoid **40** (equation 17b). Only the former process involves a rearrangement of an organic zinc compound. Since both mechanisms give the same final product **42** it can be difficult to distinguish between the two.

An elegant application of the homologation reaction was reported by Knochel and coworkers[23]. Reactions of organocopper species **43** with (iodomethyl)zinc iodide (**40**)

produce homologated mixed copper–zinc reagents **44** which can be trapped with various electrophiles E-X (equation 18).

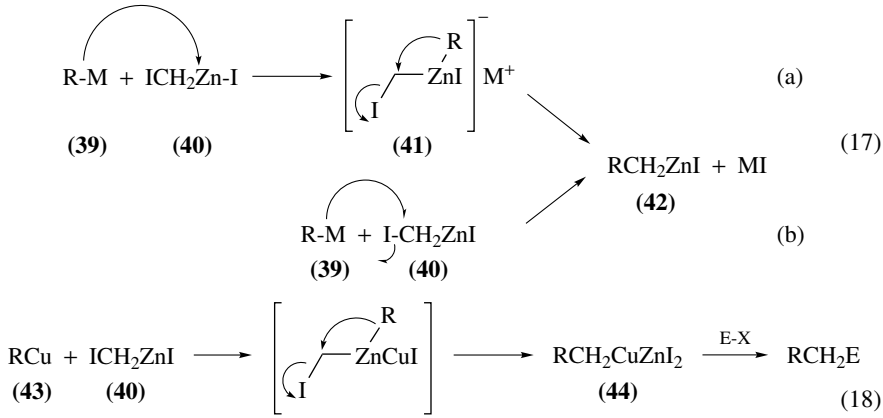

To be synthetically useful, the reactivity of the newly generated organometallic species **44** has to be substantially lower than the reactivity of the starting material **43** in order to avoid polyhomologation. If, on the other hand, RCu (**43**) itself is substantially less reactive than **44**, the homologation can be conveniently carried out in the presence of the electrophile so that all of the homologated organometallic species **44** that is generated is trapped immediately. An example of this strategy is the methylene homologation of alkenylcopper reagents **43a** (prepared by carbocupration of alkynes) to give very reactive allylic organometallic species **44a** which can be reacted with various electrophiles, including aldehydes and ketones (equation 19).

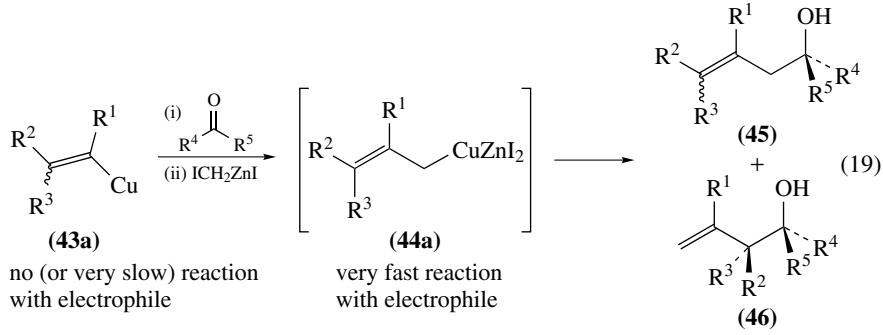

The products are generally obtained in good to very high yields (64–96%) and in most cases with good to excellent selectivities in favour of **46** over **45**[23]. For an asymmetric variant of this process see Section I.D.3.

2. Methylene homologations in allene and olefin synthesis

The process of methylene homologation can be applied to allene and olefin synthesis if the homologated organometallic species has a suitable leaving group Y^- in the β-position. Rather than trapping the newly generated organometallic with an electrophile,

TABLE 4. Representative examples of the formation of allenes $(R^1)(R^2)C{=}C{=}CH_2$ (equation 20)

Entry	R^1	R^2	n	Yield (%)
1	*n*-Hex	Me	1	75
2	*n*-Hex	*n*-Bu	1	80
3	*n*-Hex	*i*-Pr	1	65
4	*n*-Hex	*t*-Bu	1	50
5	*n*-Hex	Ph	1	95
6	*n*-Bu	*n*-Oct	1	80
7	*n*-Bu	*n*-Oct	2	85

spontaneous β-elimination of L_nMY produces allenes or olefins, respectively, depending on the nature of the starting materials. Especially in the case of allene synthesis this new approach constitutes a significant advantage over classical protocols which often lead to mixtures of allenes and alkynes, necessitating tedious separation procedures[24].

The first practical approach applying this strategy consisted of a carbocupration of an alkynyl sulfoxide **47** followed by methylene homologation of **48** with a zinc carbenoid and β-elimination (equation 20)[25]. Yields of 1,1-disubstituted allenes **50** are good to high as outlined in Table 4.

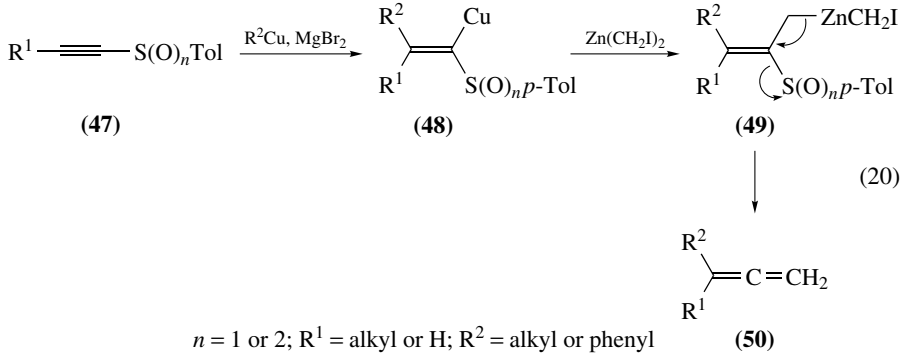

This methodology can be extended to encompass the synthesis of 1,1,3-trisubstituted allenes **51** if substituted organozinc carbenoids are employed as outlined in equation 21[25].

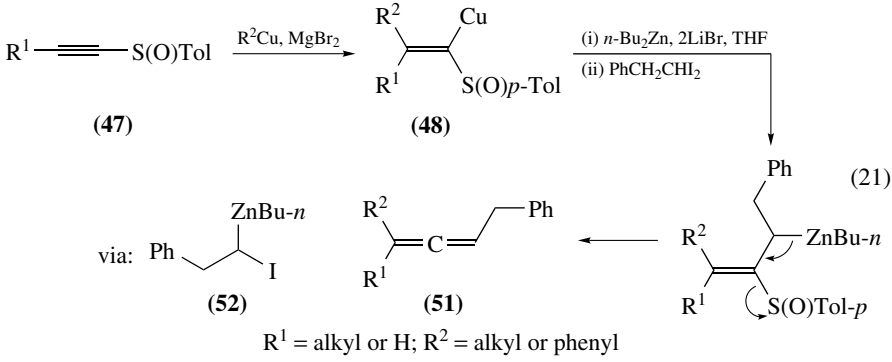

TABLE 5. Representative examples of the formation of allenes $R^1R^2C{=}C{=}CHCH_2Ph$ (equation 21)

Entry	R^1	R^2	Yield (%)
1	*n*-Hex	Et	90
2	*n*-Hex	Ph	84
3	*n*-Hex	*n*-Bu	85
4	*n*-Bu	Et	80

The secondary zinc carbenoid **52** is trapped immediately by the organocopper before it can undergo a rearrangement of the type described in Section I.B.3. This methodology gives 1,1,3-trisubstituted allenes **51** in high yields as shown in Table 5[25].

For the β-elimination to occur smoothly the reaction mixtures must be warmed to room temperature; otherwise the intermediate allylic organometallic **49** undergoes a second homologation (equation 22).

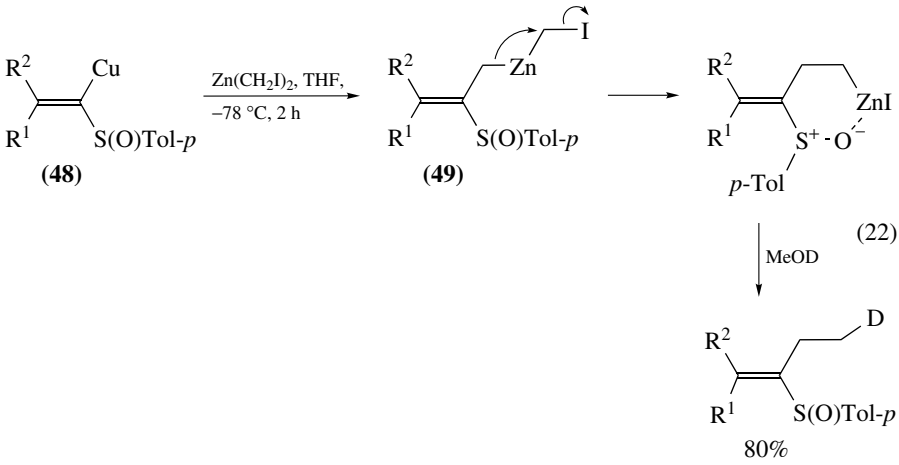

(22)

The allene synthesis strategy outlined in equation 21 can be rendered asymmetric if non-racemic sulfoxides such as **47a** are employed[26]. The diastereoselective step is an equilibration of the sp^3-allylic organometallic species **53** before the β-elimination step (equation 23).

The chiral sulfoxide **47a** was reacted with butyl copper to give an alkenyl copper reagent **48a**, which was transformed into the allylic zinc species **53** by reaction with 1,1-diiodopentane and $(n\text{-Bu})_2Zn$, 2 MgBr (prepared from $ZnBr_2$ and two equivalents of *n*-BuMgBr). The reaction mixture was stirred for 30 minutes at 0–5 °C to allow the equilibration of the sp^3 organometallic centre to occur. The absolute configurations of **47a** and **54** suggest that the intermediate allylic organometallic **53** epimerizes into the more stable configuration with the butyl and tolyl groups being *trans* to each other.

The β-elimination strategy was recently extended to olefin synthesis[27]. Secondary α-sulfinyl organocopper species **55** (prepared from the corresponding lithium compounds via transmetallation with CuBr) react with $Zn(CH_2I)_2$ to give monosubstituted alkenes **56** (equation 24). α,α-Disubstituted alkenes **59** are obtained via a 1,2-metallate rearrangement of a higher-order zincate **58** (equation 25).

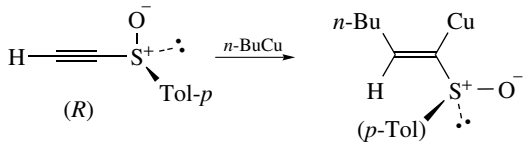

(47a) **(48a)**

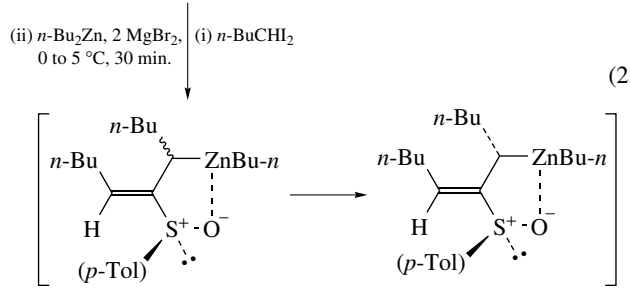

(23)

(53)
diastereomeric mixture of sp^3 secondary organometallics

(53)
thermodynamic equilibration: diastereoenriched sp^3 secondary organometallic

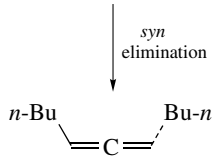

75%, 65% ee (*R*)
(54)

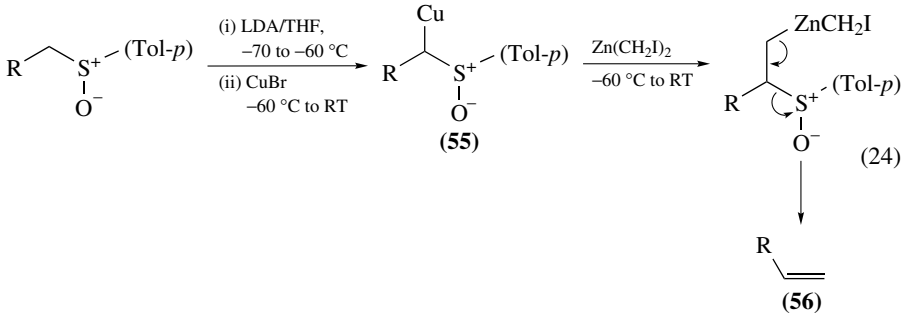

(24)

(55) **(56)**

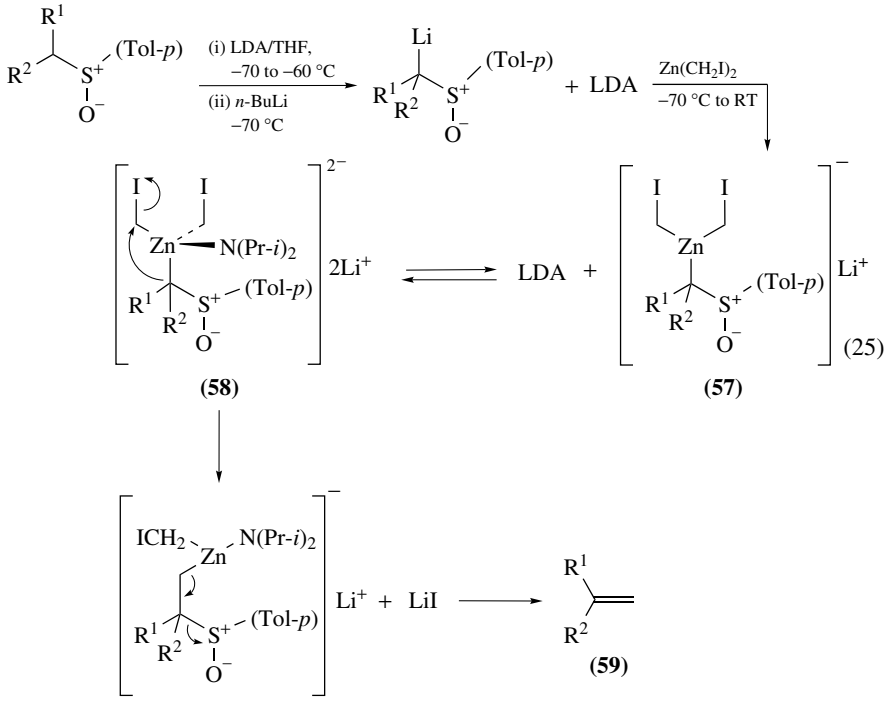

The strategy outlined in equation 24 cannot be applied to the synthesis of α,α-disubstituted alkenes **59** because the intermediate tertiary organocopper is thermally highly unstable, resulting in low yields (<30%) of alkenes. Therefore, the alternative approach via an intramolecular 1,2-zincate rearrangement was developed. It turned out that the addition of butyllithium to regenerate LDA was necessary because otherwise the diisopropylamine formed protonated the zincate intermediate **57**. It is likely that the crucial rearrangement step proceeds via a 'higher order' zincate **58** (i.e. a species in which the zinc atom formally has *two* negative charges)[28]. A few representative examples outlining the utility of the methodology are given in Table 6[27].

TABLE 6. Representative examples of the formation of alkenes $R^1R^2C{=}CH_2$ (equations 24 and 25)

Entry	R^1	R^2	Method described in equation	Yield (%)
1	*n*-$C_{11}H_{23}$	H	24	77
2	$Ph(CH_2)_3$	H	24	70
3	Ph	H	24	50[a]
4	*p*-$MeOC_6H_4$	H	24	65
5	*n*-$C_{11}H_{23}$	*n*-Bu	25	65
6	Ph	$CH_2CH{=}CH_2$	25	67

[a] The low yield of stryrene was attributed to its volatility.

3. Asymmetric reactions of homologated organozincs with aldehydes and imines

In 1996, McWilliams and coworkers described a very interesting tandem asymmetric transformation whereby an asymmetric 1,2-migration from a higher-order zincate **60** was coupled with a stereoselective homoaldol reaction (equation 26)[29].

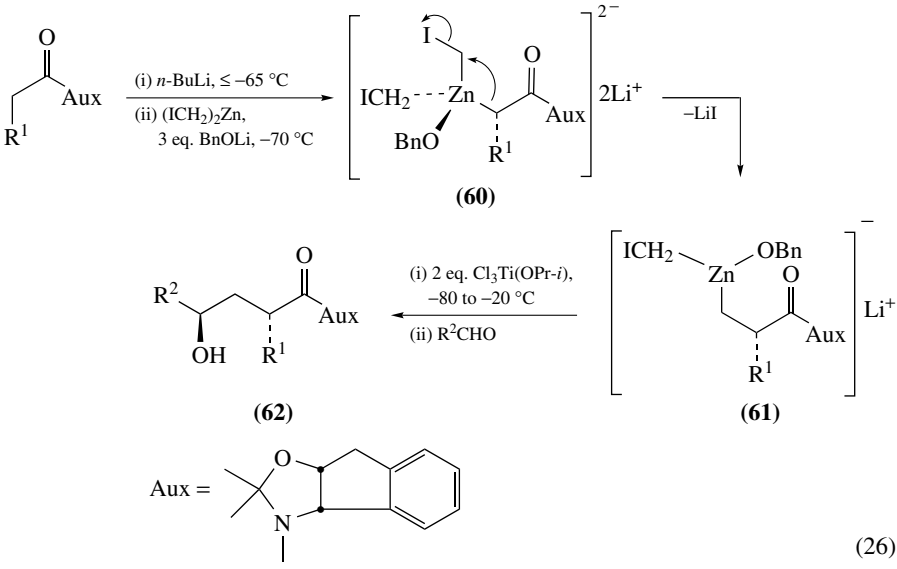

(26)

Several experiments on the influence of the order of addition of reagents and *in situ* IR spectroscopic studies revealed that a 'higher order' zincate **60** is necessary for the rearrangement step to proceed smoothly; the 'normal' zincate species $[(ICH_2)_2ZnCH(R^1)(COAux)]^-Li^+$ turned out to be unreactive. The formation of such a higher-order zincate was ensured by addition of an excess of lithium alkoxides, with BnOLi proving to be the most efficient. The zinc homoenolates **61** were transmetallated with $Cl_3Ti(O\text{-}Pr\text{-}i)$ and reacted with aldehydes to give *anti*-γ-hydroxyamides **62** as outlined in Table 7. The chiral auxiliary can be removed under mild conditions; for example, treatment with *p*-toluenesulfonic acid monohydrate induces cyclization to the lactones in good yields.

TABLE 7. Representative examples of the formation of *anti*-γ-hydroxyamides 62 (equation 26)

Entry	R^1	R^2	de %	Yield (%)
1	Bn	Ph	82	50
2	Me	Ph	80	44
3	Bn	Cy	86	55
4	Me	Cy	86	41
5	Bn	L-(BocNH)(Bn)CH	⩾99	59
6	Me	L-(BocNH)(Bn)CH	82	58

More recently, an elegant strategy for the creation of chiral quaternary centres was reported by Marek and coworkers (equation 27)[30].

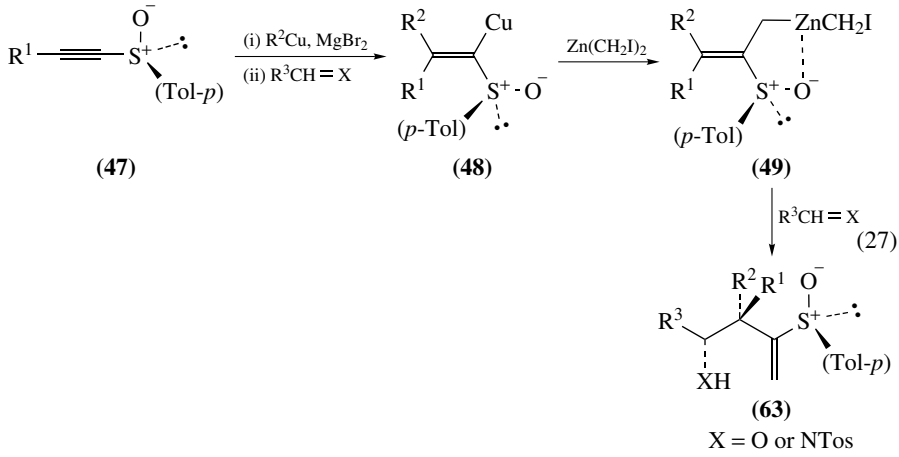

(27)

Carbocupration of chiral alkynylsulfoxides **47** in a regio- and stereospecific manner produces alkenyl organocopper **48**, which is subsequently reacted with bis(iodomethyl) zinc in the presence of aldehydes or imines. The zinc carbenoid homologation step leads to **49**, the conformation of which is controlled by intramolecular chelation; **49** reacts with the aldehyde or imine before it can undergo a β-elimination (cf. equation 20). The final product **63** is generally obtained with high diastereoselectivity and in good overall yield (Table 8).

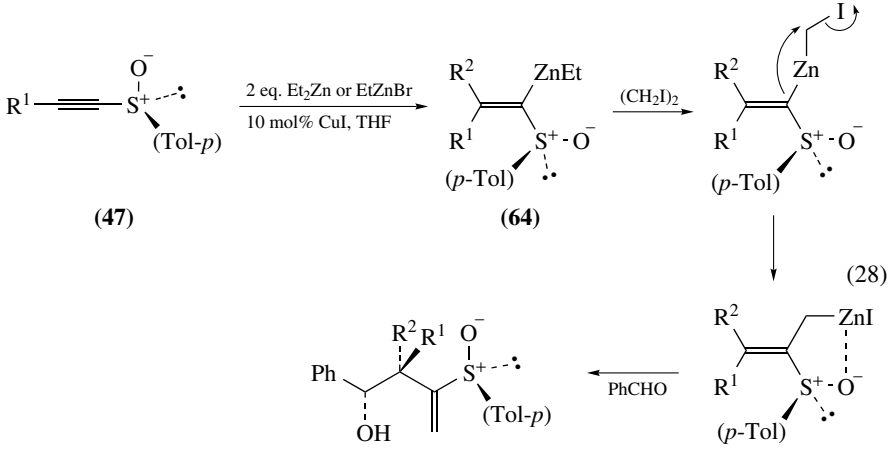

(28)

TABLE 8. Representative examples of the diastereoselective formation of aldehydes and amines (equation 27)

Entry	R^1	R^2	R^3	X	dr	Yield (%)
1	*n*-Bu	Et	Ph	O	>99/1	78
2	*n*-Bu	Et	Ph	NTos	>99/1	72
3	H	Et	Ph	O	4/1	78
4	*n*-Bu	Me	Ph	O	28/1	75
5	*n*-Bu	Et	*n*-Bu	O	30/1	60
6	Et	Me	*n*-Bu	O	30/1	58

The high diastereoselectivity observed is remarkable, particularly in view of the fact that addition of substituted allylzinc halides to aldehydes usually occurs without diastereoselectivity[31]. The high level of stereoselectivity in the allylation reaction was rationalized by a Zimmermann–Traxler chair-like transition state[30].

Furthermore, the authors succeeded in developing a variant *catalytic in copper* (equation 28).[30]

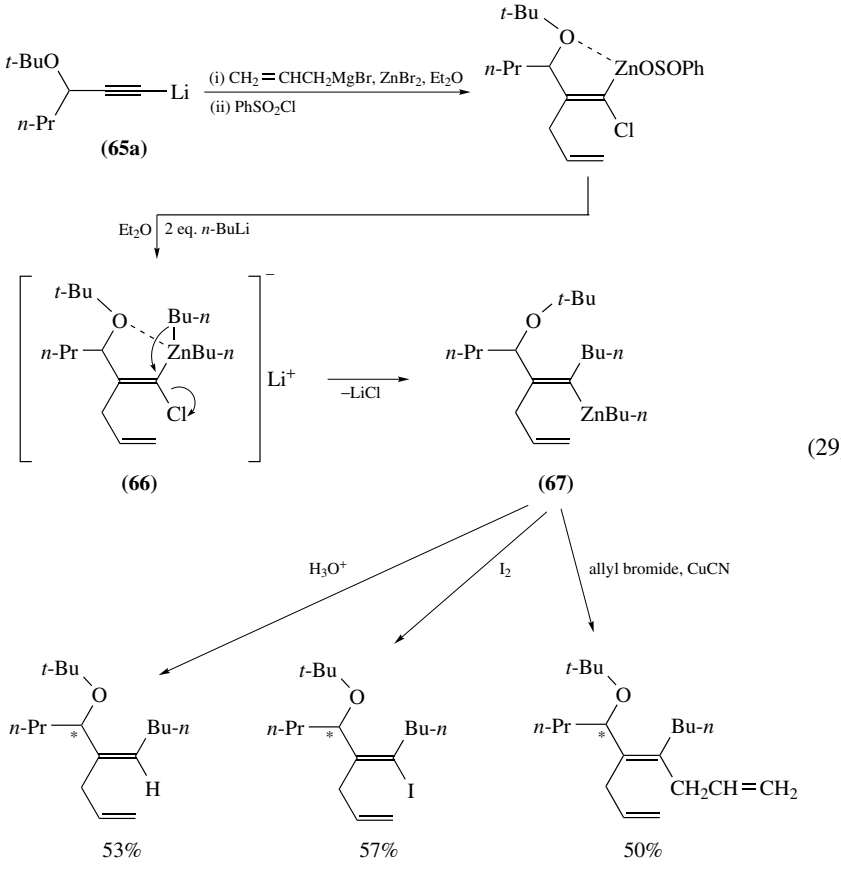

(29)

In this strategy a copper-catalysed carbozincation[32] is employed, leading to organozinc **64** which, upon reaction with diiodomethane, undergoes a methylene homologation. Note the excellent diastereoselectivity even for two groups as similar as methyl and methyl-D_3!

E. Reactions Involving 1,1-Dimetallic Species

In the mid-1990s Normant, Marek and coworkers described a protocol for the synthesis of stereodefined tri- and tetrasubstituted double bonds via allylzincation of lithiated alkynes **65**[33]. The 1,1-dimetallated olefins R(allyl)C=C(M^1)M^2 formed (for details concerning the preparation of 1,1-dimetallic species, see the following Section II.A) can be reacted with two different electrophiles in a selective manner provided that the R group is capable of coordinating to the metal located *cis* to it. Chlorination of the dimetallated species with $PhSO_2Cl$ and subsequent treatment with two equivalents of *n*-BuLi produce a zincate carbenoid **66**, which undergoes a 1,2-metallate rearrangement to give **67** as proven by quenching with various electrophiles (equation 29)[33a].

II. OTHER TYPES OF REARRANGEMENTS

A. Allylmetallation of Alkenyl and Alkynyl Metals

1. Allylmetallation of alkenyl metals

Gaudemar reported in 1971 that allylzinc bromide is able to add to various vinyl Grignard reagents in THF at 35 °C in fair to moderate yields (35–60%)[34]. This reaction type has been substantially developed since then[35]. In the 1980s, Knochel, Normant and coworkers demonstrated the synthetic usefulness of 1,1-dimetallic reagents **70**[36] obtained from reactions of alkenyl organometallics **68** with allylic zinc species **69** (easily formed, for example, from allylmagnesium bromide and $ZnBr_2$) (equation 30)[37].

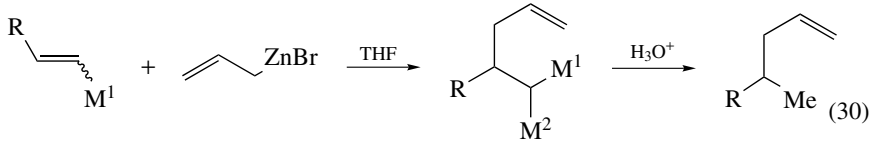

(30)

(68) **(69)** **(70)**

M^1 = Li, MgBr, ... M^2 = Li, MgBr, ZnBr ...

Two main mechanistic hypotheses were considered for this reaction type[38], a 'zinca ene'[39] reaction and a 'metallo-Claisen' rearrangement (equations 31 and 32). **70** and **71**[#] are drawn as monomers for the sake of simplicity. The former probably exists in oligomeric form (see Section II.A.3), whereas the transition state of the 'metallo-Claisen' rearrangement may involve two molecules of **71**[38]. Since the simplified structures are perfectly suitable to rationalize the selectivity and reactivity of these reactions, they are used throughout this chapter.

In the absence of more physical data, the authors considered the second hypothesis (equation 32) to be the more plausible one, because it can easily explain the stereochemical outcome of many reactions (see examples below). These reactions could thus be seen as metal variants of the well-known Cope and Claisen rearrangements[40]. The original

mechanistic assumptions were modified later[41] on the basis of computational studies (see the more detailed mechanistic discussion in Section II.A.3). However, since formulations like **71**#, although oversimplified, are very helpful in rationalizing the diastereoselectivity observed in these reactions, they will be used throughout this chapter.

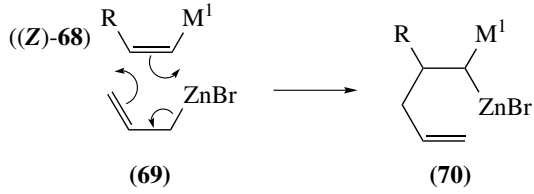

(31)

(69) **(70)**

'zinca ene' reaction

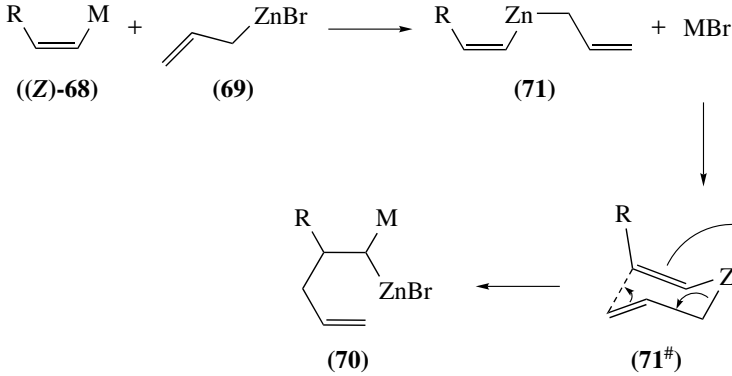

(32)

(70) **(71#)**

'metallo-Claisen'-rearrangement

Geminal bismetallic reagents **70** can be coupled with a variety of electrophiles[37a–e], oxidized to ketones or aldehydes[37f,g], and utilized in the synthesis of functionalized olefins[37h]. It should be noted that *two different electrophiles* can be used to quench **70**, providing an elegant way for functionalization. The scope of this methodology is outlined by examples given in Scheme 5, the bold-faced substituents indicating the electrophilic groups introduced at the end of the reaction sequence[37d].

If the allylic system is substituted, several isomeric products can be formed. Assuming a chair-like transition state, the stereochemical outcome of a 'metallo-Claisen' rearrangement is controlled by the geometries of the vinyl and allyl moieties, so that, if the vinyl part **68** is stereochemically pure, three different products, ***syn/anti*-73** or **74**, can be formed, depending on the exact nature of the active allylic part **72** (Scheme 6)[38].

For a vinylmetal system **68** with a given geometry, the selectivity of the reaction should thus depend on the metallotropic equilibrium of the substituted allylic system **72**. The magnitude of diastereoselectivity in 'metallo-Claisen' reactions is strongly dependent on the nature of substituents on the allyl and vinyl moiety, temperature and solvent[42]. For example, with 1-lithio-*n*-octene and crotylzinc bromide (i.e. $R' = Me$), diastereoselection in THF at 0 °C was found to be poor[43]. However, switching the solvent to ether results in a significant rate enhancement, thereby allowing one to lower the temperature

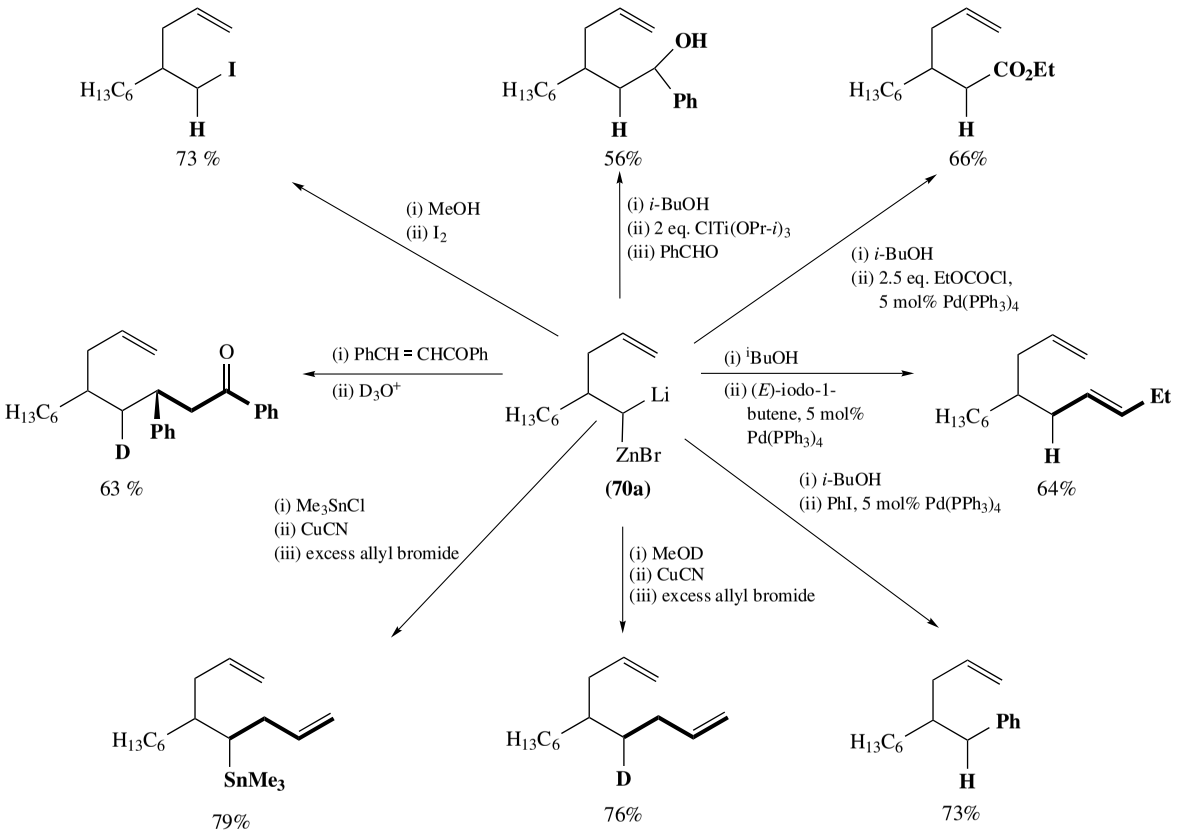
H13C6
I
H
73 %
(i) MeOH
(ii) I2
H13C6
OH
Ph
H
56%
(i) i-BuOH
(ii) 2 eq. ClTi(OPr-i)3
(iii) PhCHO
H13C6
CO2Et
H
66%
(i) i-BuOH
(ii) 2.5 eq. EtOCOCl,
5 mol% Pd(PPh3)4
H13C6
O
Ph
Ph
D
63 %
(i) PhCH = CHCOPh
(ii) D3O+
H13C6
Li
ZnBr
(70a)
(i) iBuOH
(ii) (E)-iodo-1-
butene, 5 mol%
Pd(PPh3)4
H13C6
Et
H
64%
(i) Me3SnCl
(ii) CuCN
(iii) excess allyl bromide
(i) MeOD
(ii) CuCN
(iii) excess allyl bromide
(i) i-BuOH
(ii) PhI, 5 mol% Pd(PPh3)4
H13C6
SnMe3
79%
H13C6
D
76%
H13C6
Ph
H
73%

SCHEME 5

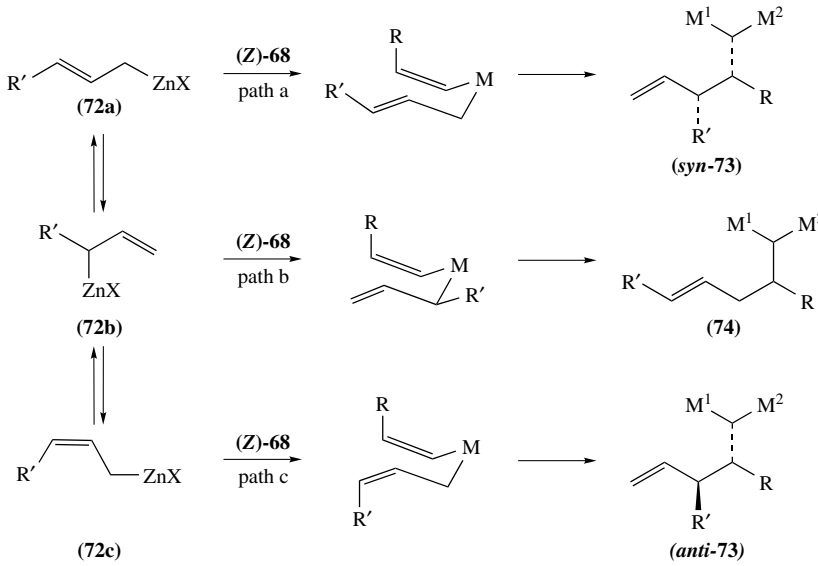

SCHEME 6

to $-50\,^{\circ}C$[42]. Under these conditions, even crotylzinc bromide gives very good diastereoselection (equation 33).

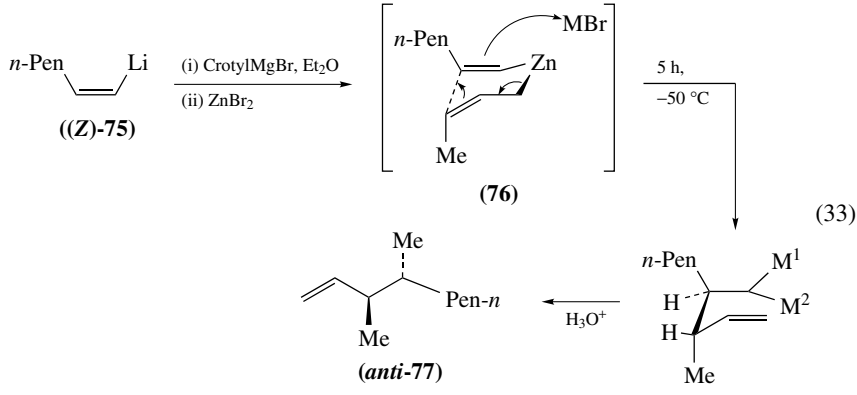

(33)

87%, dr = 98/2

When the pure (*E*) isomer of the vinyl lithium **75** is used as starting material, ***syn*-77** is obtained in 81% yield and with 95/5 dr. This diastereoselection can be accounted for by a kinetically favoured (*Z*) configuration of the crotylzinc species in a chair-like transition state **76** (cf. path c, Scheme 6). However, the metallo ene pathway cannot be ruled out completely and was used sometimes to rationalize the experimental results[44]. This methodology can also be applied to more functionalized molecules as shown in equation 34.[42]

The intramolecular chelation between the ether oxygen and the zinc atom shown in equation 34 can be utilized to create stereocontrol as demonstrated in equation 35[45].

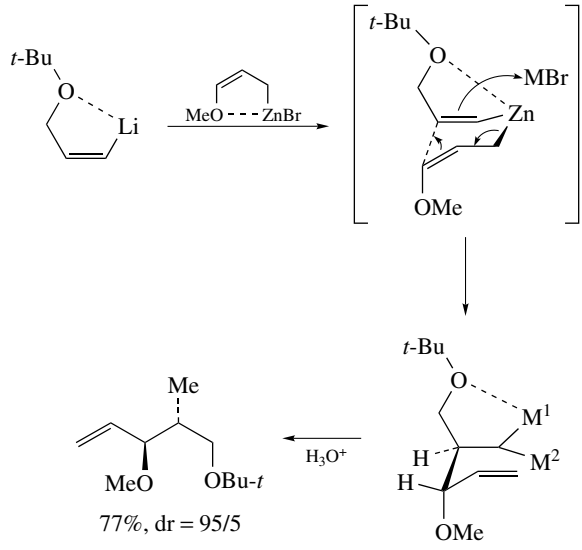

(34)

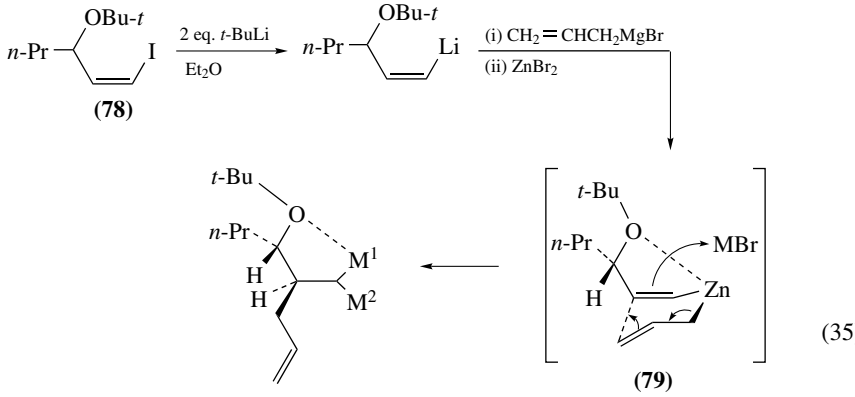

(35)

The position of the propyl group in **79** is fixed by intramolecular chelation between the ether oxygen and the zinc atom, and the allyl part approaches the vinyl moiety *anti* to the propyl group. High diastereoselectivity can also be achieved by chelation in a six-membered ring[44a].

When the *t*-butyl group in **78** is replaced by a methoxymethyl (MOM) group, the dimetallic intermediate **80** undergoes a 1,3-elimination to give a cyclopropane **82** (equation 36)[46].

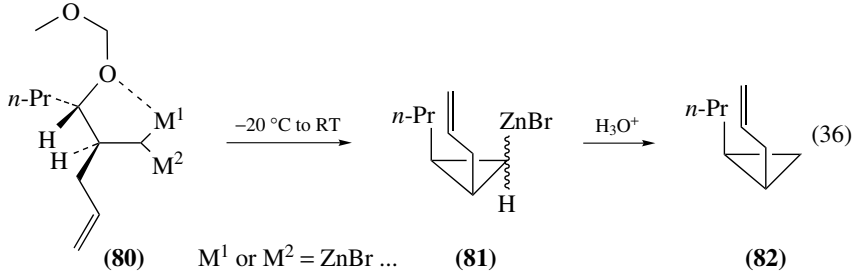

(36)

(80) M^1 or M^2 = ZnBr ... **(81)** **(82)**

To determine the stereochemical relationship between the allyl group and ZnBr in intermediate **81**, the reaction was performed with the more simple substrate **83**, and the intermediate metallated cyclopropane **85** was quenched with allyl bromide after transmetallation to an organocopper (equation 37).

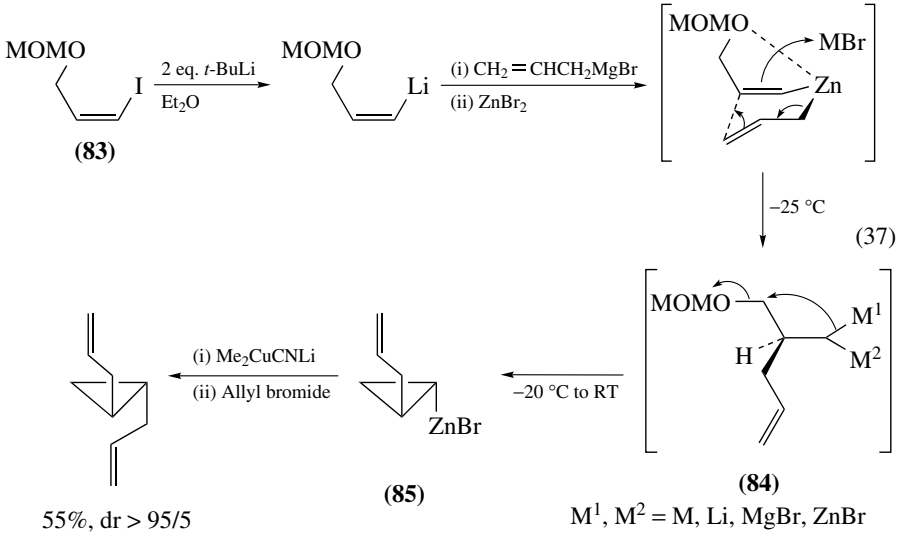

(37)

(83) **(85)** **(84)**

55%, dr > 95/5

M^1, M^2 = M, Li, MgBr, ZnBr

Assuming that the transmetallation and subsequent reaction with allyl bromide do not alter the configuration of the carbon–zinc bond[47], the stereochemistry of the intermediate is that shown for **85**. Hence it follows that one of the two carbon–metal bonds in **84** has

been involved in the elimination *stereoselectively*. The authors proposed an elimination process which proceeds from a W-shaped conformer **86** with inversion at both centres (reaction 38)[46].

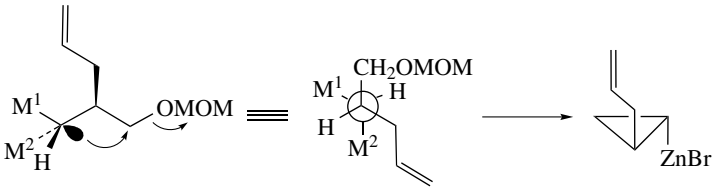

(38)

(86) **(85)**

The stereochemical outcome of these reactions is strongly dependent on the precise nature of the substrates; a detailed discussion would go beyond the scope of this chapter. It should merely be noted that stereoselectivity is generally very high as outlined by examples given in Scheme 7 (the bold-faced substituents indicate the electrophile introduced in the last step).

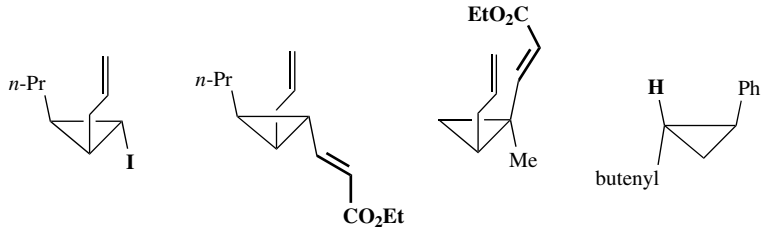

Yield:	65%	72%	82%	90%
dr:	>95/5	>95/5	>95/5	95/5

SCHEME 7

Apart from ethers as chelating groups, facial selectivity through chelation by nitrogen and sulfur has also been reported[48]. A few representative examples are given in Scheme 8 (all reactions were quenched with acid).

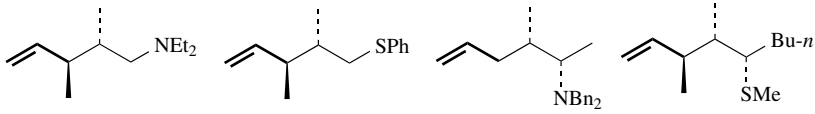

Yield:	65%	56%	75%	62%
dr:	91/9	95/5	>98/2	>95/5

SCHEME 8

Not only heteroatoms but also double bonds can be used as chelating groups via π-interaction (equation 39)[49].

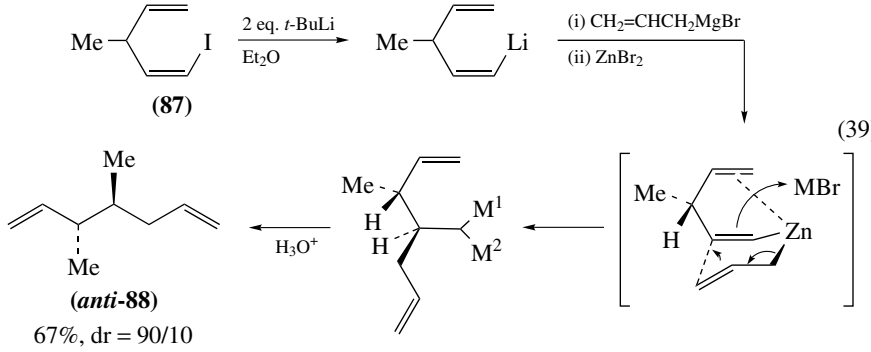

(39)

For unsubstituted allylic systems some kind of intramolecular chelation is necessary to obtain diastereoselection. If the ethylene moiety in **87** is replaced by an ethyl group, diastereoselectivity is lost completely (72% yield, dr = 50/50). The *syn* isomer of **88** can be obtained if the methyl substituent is not attached to the vinyl but to the allyl moiety (equation 40), taking advantage of the selectivity arising from a crotyl system (cf. Scheme 6).

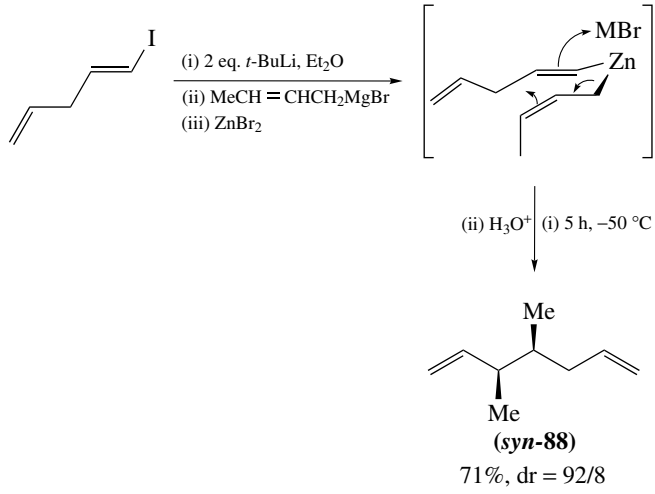

(40)

If the facial selectivity created by intramolecular chelation is combined with the selectivity arising from substitution at the allylic system, the relative stereochemistry of three stereogenic centres can be controlled (equation 41)[49].

The first diastereoselective carbometallation of vinyl metals bearing a chiral auxiliary was reported in 1998 (equation 42)[44b].

A π-stacking interaction (cf. equation 39) between the naphthyl and vinyl zinc moieties is crucial in order to obtain high diastereoselection. If naphthyl is substituted by phenyl, the dr drops to 80/20 and is completely lost with cyclohexyl.

Diastereoselective 'metallo-Claisen' reactions can be used to prepare aldol-type products if the 1,1-dimetallic reagents **91** obtained are oxidized to aldehydes or ketones (equation 43)[37f].

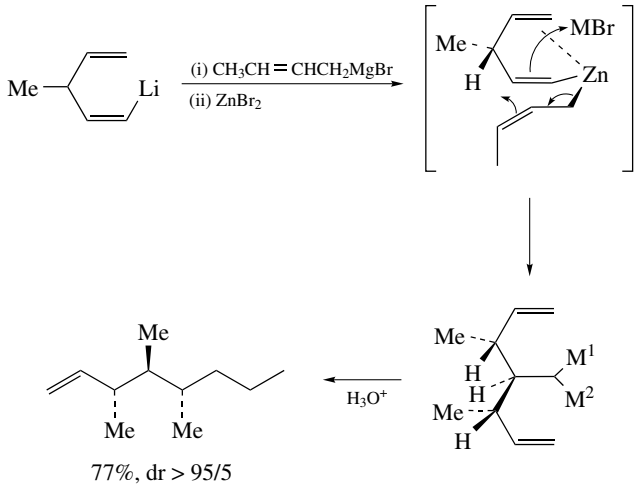

77%, dr > 95/5 (41)

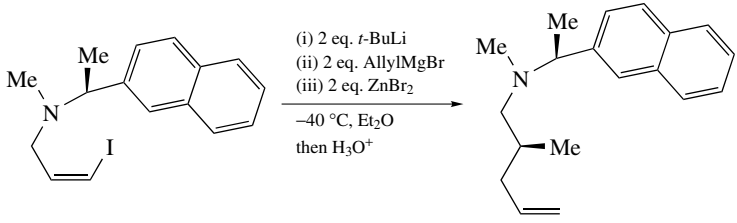

(*S*,*S*), 76%, dr = 96/4 (42)

The stereochemistry of the Grignard reagent **89** is completely transferred into the aldehydes **92** and this can be easily rationalized if one assumes that the rearrangement proceeds via transition states ***(Z)-*** and ***(E)-*****90**, in which the configuration of both starting

TABLE 9. Representative examples of the formation of aldehydes and ketones 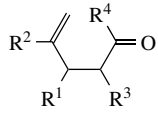

(equation 43)

Entry	R^1	R^2	R^3	R^4	dr	Yield (%)
1	H	Me	H	Ph	—	85
2	Me	H	H	Ph	—	57
3	H	*n*-Bu	H	Ph	—	91
4	H	*n*-Bu	*n*-Hex [a]	H	—	66
5	Me	H	*n*-Hex [a]	H	75/25 [b]	78

[a] A 88/12 (*Z*)/(*E*) mixture of 1-octenylmagnesium bromide was used.
[b] Diastereoisomers are not assigned in Reference 37f.

organometallics is maintained (the zincated allylic ether is most stable in the (*Z*) configuration due to internal chelation[50]). A few more examples indicating the utility of the oxidation methodology are given in Table 9.

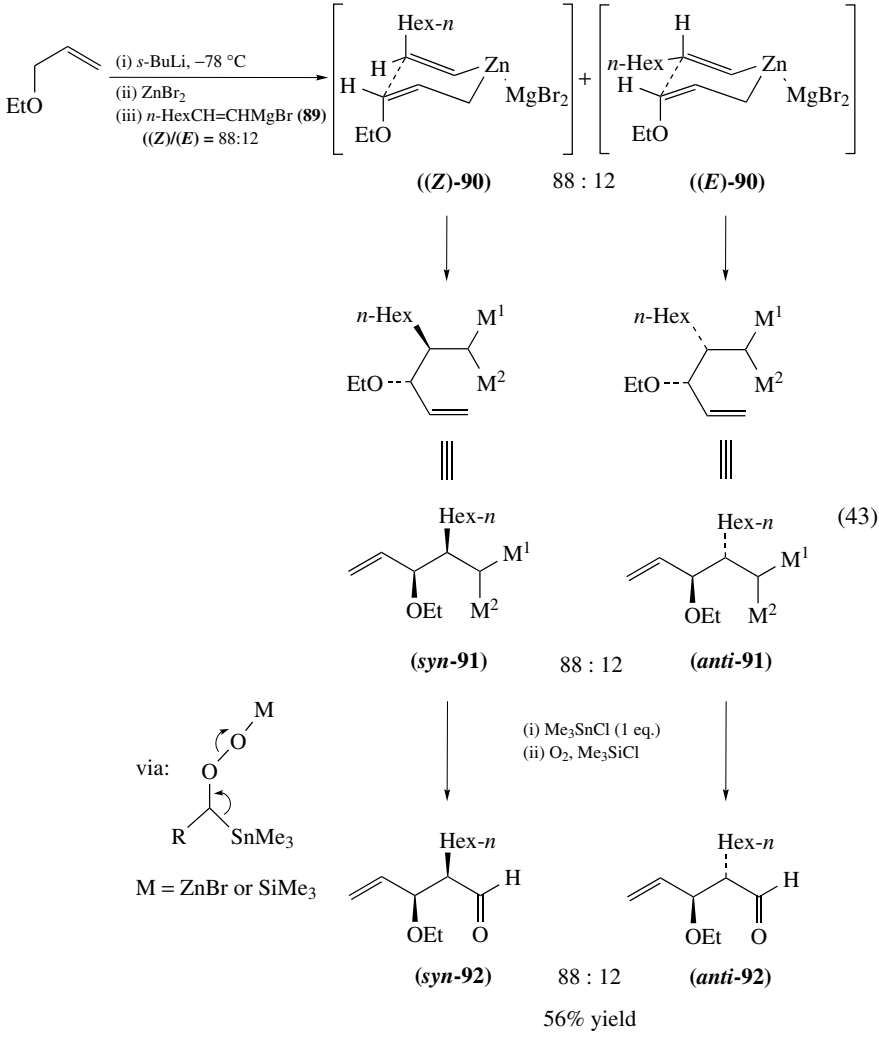

(43)

2. Allylmetallation of alkynyl metals

The allylmetallation of *alkynyl* metals such as **65a** leads to 1,1-dimetallated *alkenes* such as **94a** (equation 44 and Table 10)[33]. Quenching with electrophiles provides access to stereodefined polysubstituted olefins (see also Section I.E).

The coordination of the ether oxygen to M^1 in **94a** decreases the reactivity of the M^1–carbon bond towards electrophiles so that E^1 is introduced selectively *trans* to the ether moiety. Reactions of alkynyl lithiums without coordinating substituents lead to stereorandom products.

TABLE 10. Representative examples of the formation of stereodefined polysubstituted olefins (equation 44)

Entry	E^1-X	E^2-X	Yield (%)
1	Tos**Cl**	**H**Cl	87
2	Tos**CN**	**H**Cl	63
3	Tos**Br**	**H**Cl	63
4	**Me**SSO_2Me	**H**Cl	42
5	**Ph**SSO_2Ph	**H**Cl	88
6	Tos**Cl**	$\mathbf{I}_2$	63
7	Tos**CN**	N**B**S	60
8	Tos**Br**	N**C**S	60

The allylmetallation of propargylic ethers[51] and amines[52] can be carried out diastereoselectively. For example, the reaction of the MEM-protected propargylic alcohol **93b** with crotylzinc bromide gave the product **96b** (via **95b**) with high diastereoselectivity, whereas the *tert*-butyl derivative **93a** gave significantly lower selectivity (equation 45).

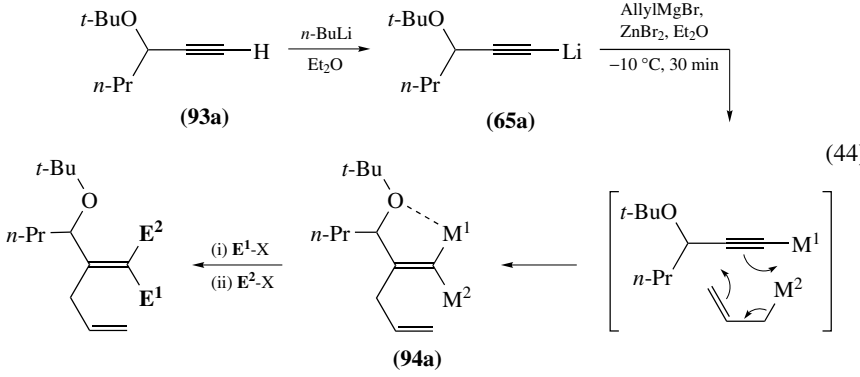

(44)

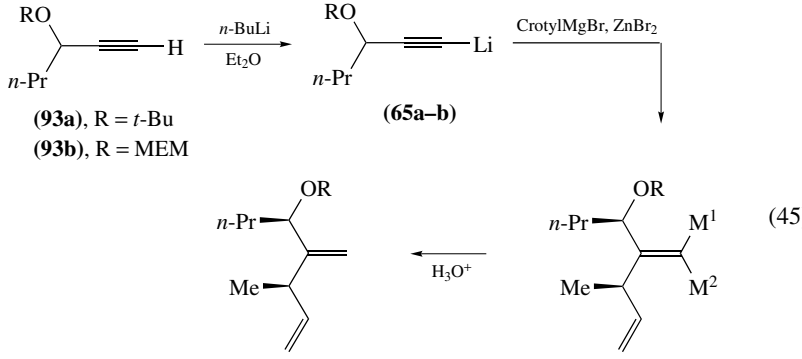

(45)

(**93a**), R = *t*-Bu
(**93b**), R = MEM

R = *t*-Bu (**96a**): 75%, dr = 70/30
R = MEM (methoxyethoxymethyl) (**96b**): 60%, dr = 92/8

(**95a–b**)

TABLE 11. Optimization of diastereoselectivity in the formation of **99** (equation 46)

Entry	Stereochemistry of **97**	Equivalents CrotylMgBr	Equivalents $ZnBr_2$	de of **99**(%)
1	*rac.*	1.5	1	20
2	*rac.*	3	2	40
3	*rac.*	3	3	30
4	*rac.*	2	3	40
5	(*R*)	2	3	76 (62% yield)

It was then reasoned that reactions of enantiopure propargylic amines should lead to the nitrogen analogs of **96** in non-racemic form[52]. First, the de was optimized using racemic starting material **97** (equation 46 and Table 11, entries 1–4)[52].

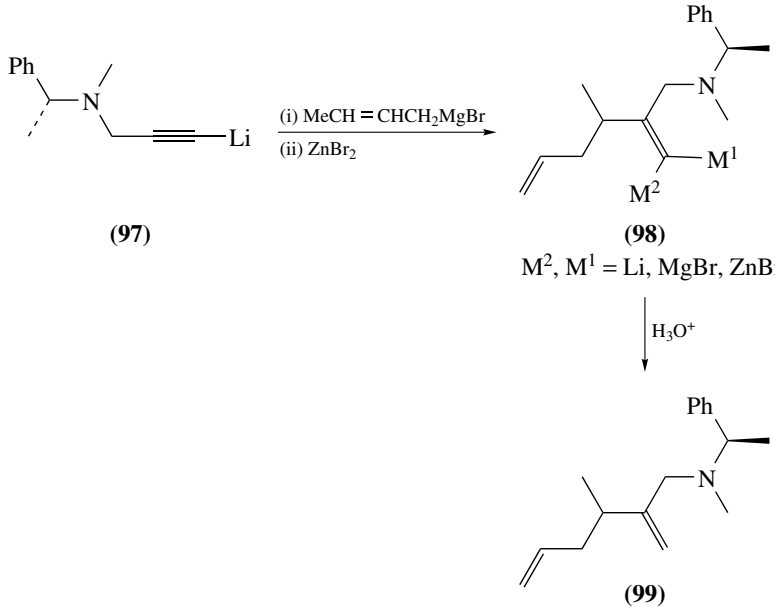

(97) **(98)** **(99)** (46)

The diastereoselectivity is obviously strongly dependent on the amount of zinc and magnesium salts present in the reaction mixture. Having optimized the de using ***rac*-97**, a significant improvement was observed when switching to non-racemic **97** (Table 11, entry 5). This was rationalized by the assumption that the bismetallic intermediate **98** is in fact a di-, tri- or tetramer. The carbozincation process being reversible[34g], it was assumed that a homochiral tri- or tetramer was better matched than one of its diastereomers.

When the above reaction was carried out using the (*S*)-(+)-methyl*cyclohexyl*amine derivative of **97**, the yield was similar (69%), but the de dropped to 0%. This was rationalized by the assumption that π-stacking between the arene moiety and the Zn atom is crucial for facial selectivity as was postulated earlier[44b] for analogous reactions. The de could be further increased by changing the methyl substituent on nitrogen to ethyl (equations 47 and 48). The stereochemistry of **100** was proven by X-ray analysis of its

hydrochloride. Electron-withdrawing groups on nitrogen (N-Boc or N-Tos) lead to almost complete loss of stereoselectivity.

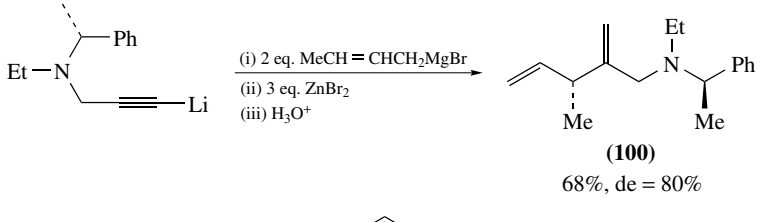

(100)

68%, de = 80% (47)

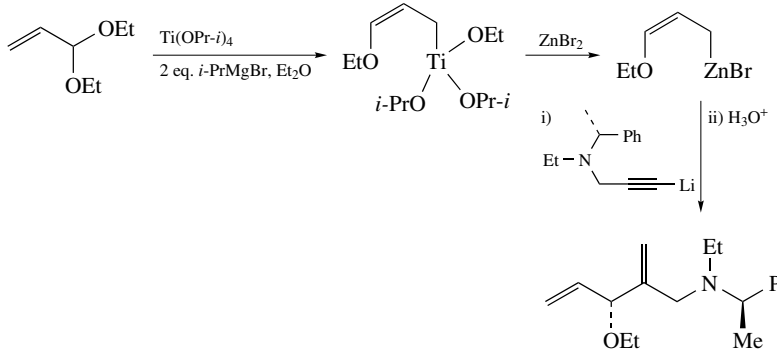

60%, de = 86% (48)

3. Computational results on the reaction mechanism

As mentioned at the beginning of this Section, computational analyses[41,53] have lead to a deeper understanding of the reaction mechanism (equation 49).

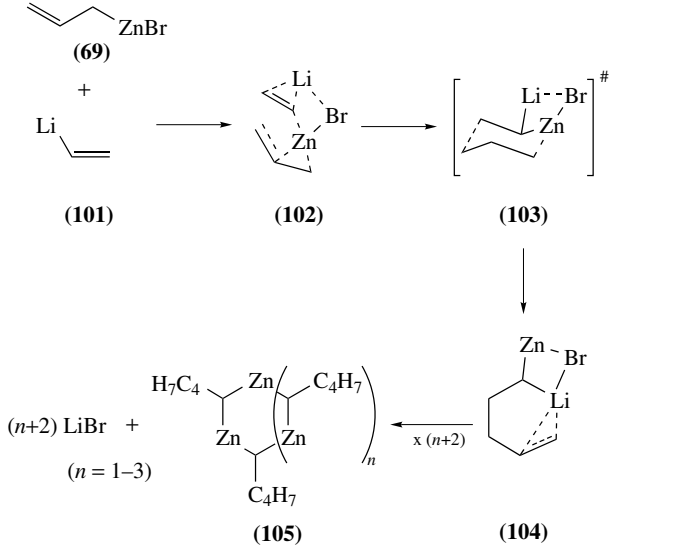

(49)

The initial reaction between allylzinc bromide (**69**) and vinyllithium (**101**) gives a stable complex **102**. In the next step this intermediate forms, via transition state **103**, the lithio zinc adduct **104**, which then oligomerizes to give very stable **105**.

Computational results were also able to account for the observed selectivity in reactions of crotylzinc reagents, which were found to react preferentially in a *cisoid* form (see previous examples). This could be accounted for by the energetic difference of the respective transition states **106** and **107** (equation 50).

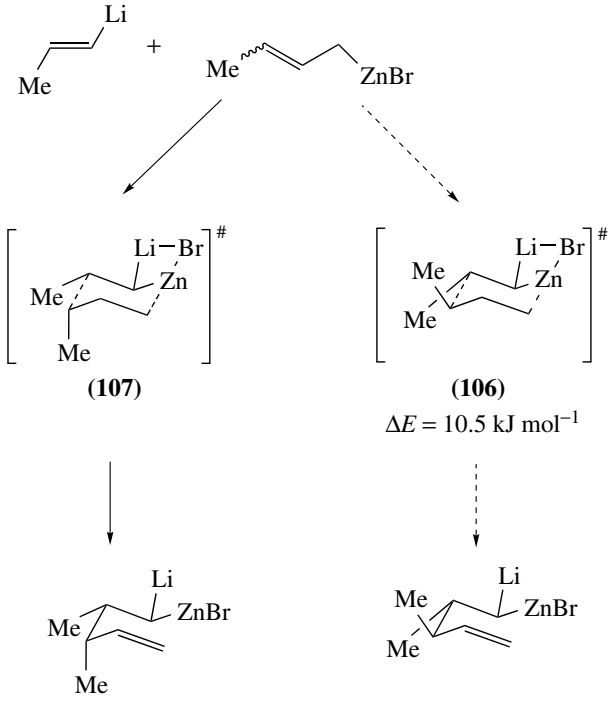

(50)

B. The Reformatsky Reaction

The oldest reaction involving a rearrangement of an organozinc compound is probably the Reformatsky reaction[54,55]. It took one hundred years until its key step could be classified as a [3,3]-sigmatropic shift ('metallo-Claisen' rearrangement) on the basis of computational studies (equation 51)[56].

The rate-determining step was found to be not the [3,3]-sigmatropic shift but rather the conversion of the Reformatsky reagent **108** into its enolate form **109**.

C. Fritsch–Buttenberg–Wiechell Rearrangement[57]

1,1-Dimetallic reagents of the vinylidene type (Section II.A.2), in which the reactivity of one metal is lowered by intramolecular chelation, can be selectively chlorinated to

give zinc carbenoids such as **110** (see also equation 29). The latter are prone to undergo a Fritsch–Buttenberg–Wiechell (FBW) rearrangement (equation 52)[41,51,58].

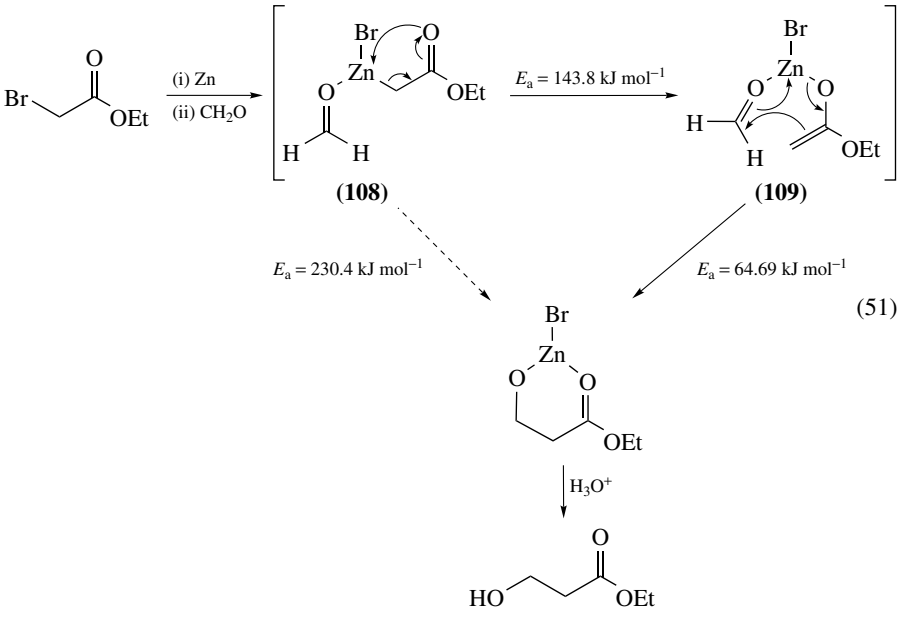

(51)

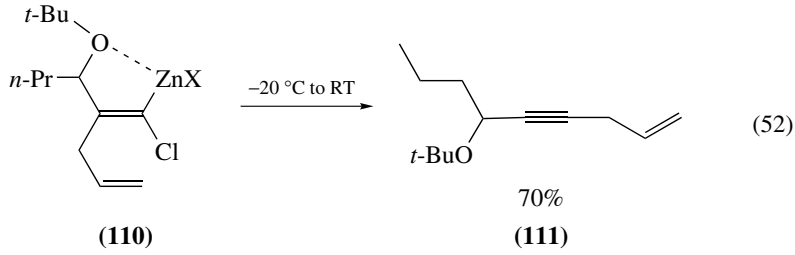

(52)

When the same reaction was performed with the corresponding lithium carbenoid, a complex mixture of products was obtained and the yield of **111** was less than 10%[51]. ^{13}C-labeling experiments revealed that the alkoxyalkyl moiety migrated exclusively (equation 53)[58].

When the alkoxymethine group was replaced by other groups, mixtures of compounds of the type **112a** and **112b** were obtained. It was shown that this was not due to the position of the migrating group in the intermediate chloro carbenoid (*cis* or *trans* to chlorine), but rather reflected different migratory aptitudes. The following order of decreasing migrating aptitude was found:

alkoxymethine > *n*-octyl > allyl > 2-butenyl > cyclohexyl

The FWB rearrangements of zinc carbenoids occur with complete chirality transfer (equation 54)[51].

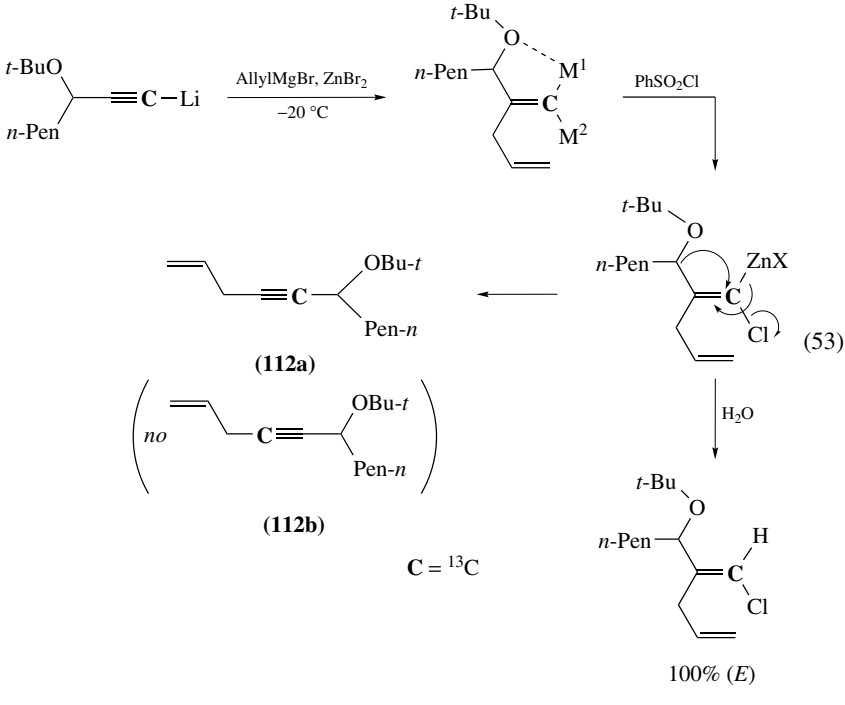

(53)

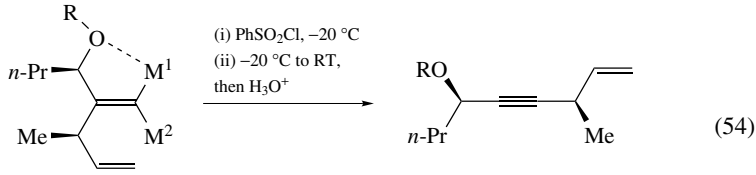

(54)

(95a) R = *t*-Bu, dr = 70/30
(95b) R = MEM, dr = 92/8

(113a) dr = 70/30, 71% yield
(113b) dr = 92/8, 52% yield

The stereochemical purity of the dimetallated species **95** (determined from the corresponding hydrolysed compounds **96**, see equation 45) was completely transferred into the alkynes **113**. It could furthermore be shown that the rearrangement occurs with complete retention of configuration at the migrating carbon. It should be noted that the yield of **113b** is significantly lower than that of **113a**. This was attributed to a stronger chelation resulting in higher stability of the chloro carbenoid intermediate which is thus less likely to rearrange[52]. The chloro carbenoids derived from propargylic amines give the FWB products only in low yield (20%)[52].

D. Zinca-Ene-Allene and Zinc-Enolate Cyclizations

Zinca-ene-allene and related reactions constitute an elegant way for the synthesis of five-membered carbo-[59] and heterocycles[60]. In these reactions, a propargylic lithium species **115-Li** with a double (or triple) bond in the 5-position undergoes, *after*

transmetallation with $ZnBr_2$, a smooth cyclization reaction to form a five-membered ring with perfect diastereoselectivity (equation 55). **115-Li** itself or the magnesium analogue **115-MgBr** are unreactive. Quenching with various electrophiles gives functionalized cyclopentanes **117**–**119** in good yields.

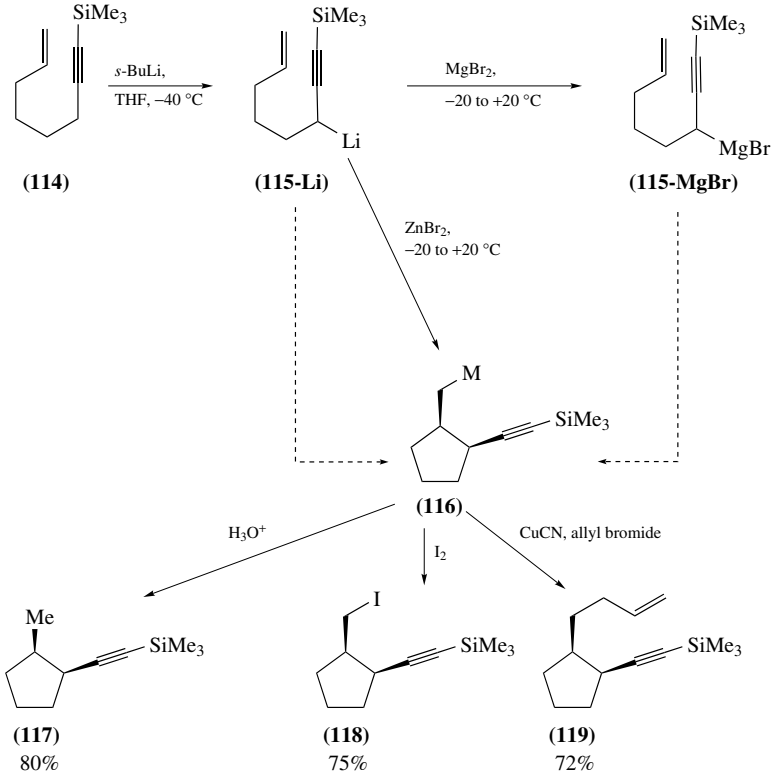

(55)

The perfect diastereoselectivity observed in these reactions lead to the assumption that they do not proceed via a simple anionic intramolecular cyclization (i.e. carbozincation) as was proposed in earlier[61] publications. Cyclizations of non-propargylic substrates[15,62] were shown to proceed with significantly lower diastereoselectivity (*cis*/*trans* typically 75/25). Thus, in the case of propargylic compounds, e.g. **114**, a simple carbozincation process is unlikely to be operative. It was therefore reasoned that the active species in these reactions is not **115-ZnBr** but rather its allenic isomer **120**, which undergoes a 'metallo-ene-allene' reaction in a chair-like transition state as depicted in equation 56[59a].

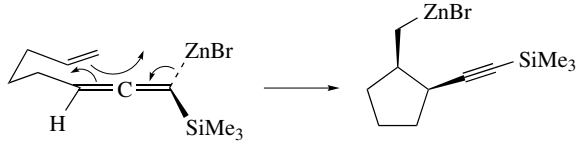

(56)

The methodology can be applied to propargylic ether derivatives, alkyl-substituted propargylic derivatives and substituted allylic derivatives. Quenching of the intermediate **116-ZnBr** with electrophiles provides access to various functionalized cyclopentanes. α,β-Disubstituted olefins do not undergo the cyclization reaction[59a]. The same principle can also be applied to *ω-acetylenic* silylated propargylic derivatives giving functionalized exomethylene cyclopentanes as products[61b]. Representative examples are given in Scheme 9. It should be noted that all products were obtained as single diastereomers.

A very interesting application of the above methodology is the synthesis of heterocycles[60]. Thus, substituted tetrahydrofurans **121**–**123** are obtained easily with perfect diastereoselectivities (equation 57)[60a].

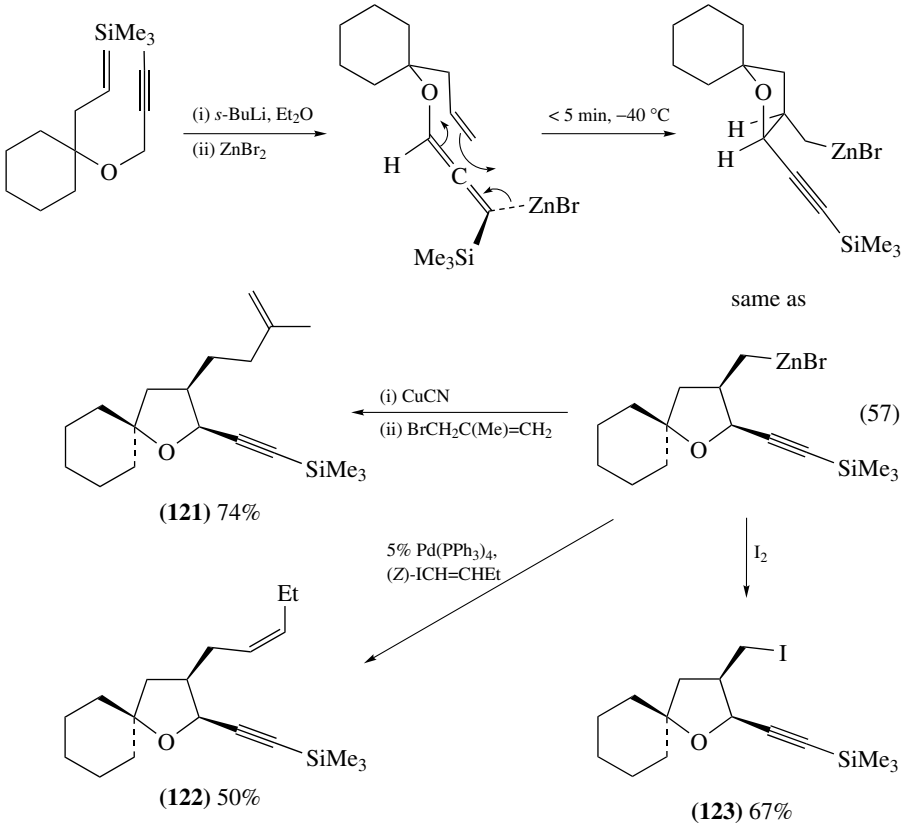

When a new stereogenic centre is added, diastereoselection is no longer perfect but still quite high (Scheme 10)[60a].

The phenyl or butyl substituent preferentially occupies a pseudo-equatorial position in the chair-like transition state which accounts for the observed diastereoselectivity. Since this extra stereogenic centre is quite far from the reacting centres diastereoselection is no longer complete.

The methodology could be further extended to encompass polysubstituted pyrrolidines as outlined in equation 58[60c].

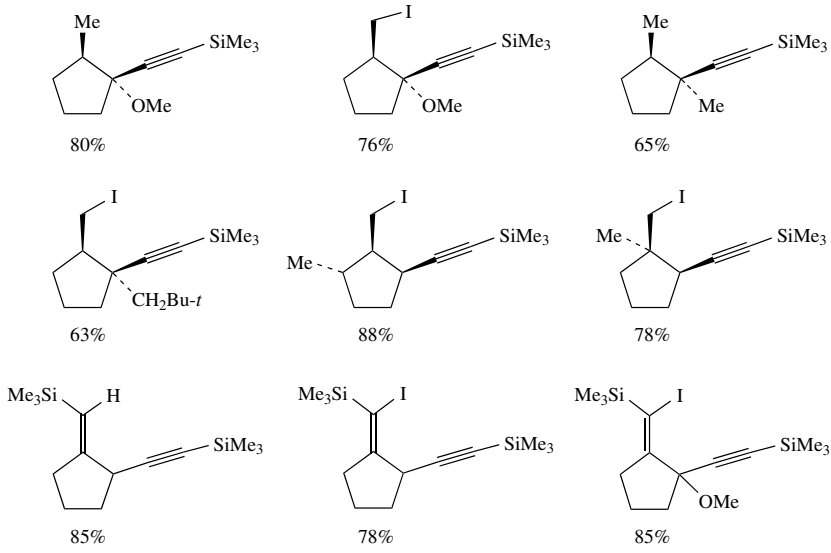

SCHEME 9

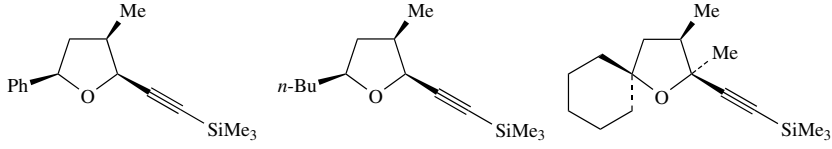

SCHEME 10

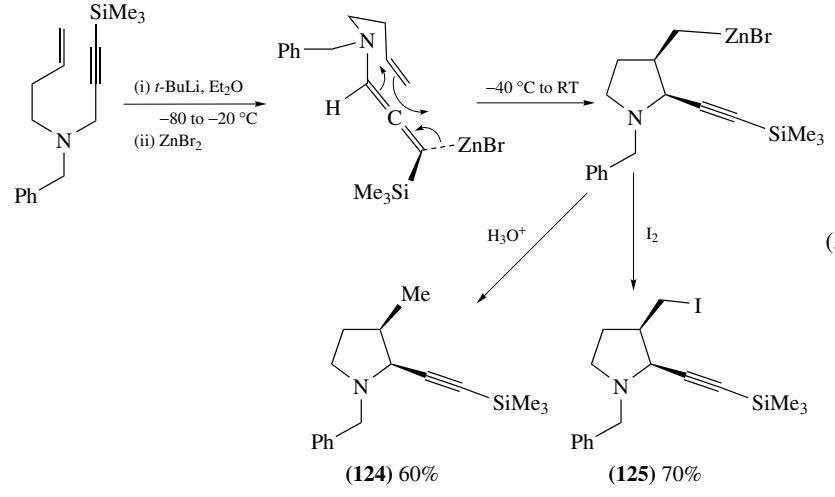

(58)

Again, the products **124** and **125** are obtained as single diastereomers. As in the case of the tetrahydrofurans (see Scheme 10), introduction of a substituent in the 5-position of the heterocycle results in lower diastereoselectivities (dr = 85/15 for cyclohexyl).

An interesting variation of this methodology was developed whereby zinc *enolates* **127** were employed giving 2-ester-substituted pyrrolidines **128**–**130**[60c]. The enolates **127** were obtained via transmetallation of lithium ester enolates **126** with $ZnBr_2$ (equation 59).

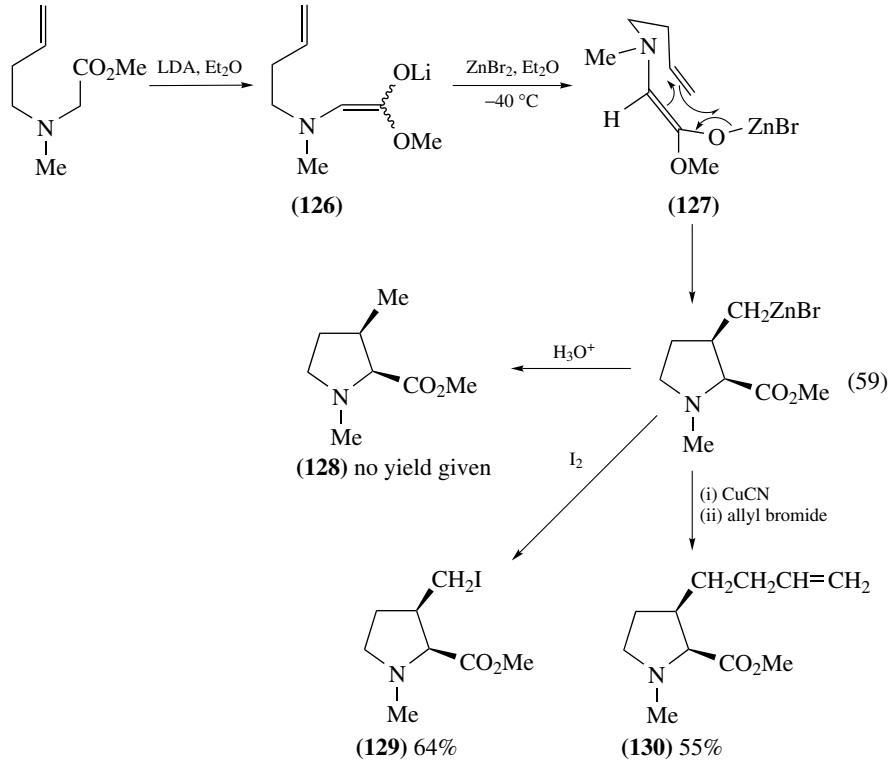

(59)

The *cis* relative configuration was accounted for by a chair-like transition state in which the zinc enolate and the olefin moiety are coplanar as described in **127**. Using *chiral* amines as starting materials, pyrrolidines were obtained with complete diastereoselectivity and excellent enantiomeric excess (equation 60)[60c, d, 63].

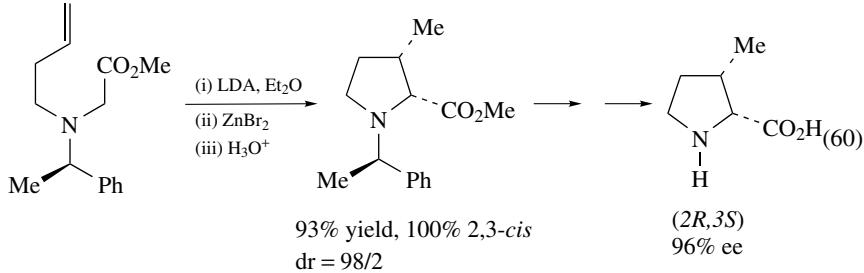

(60)

E. The Rearrangement of 1-Trimethylsilyl-2-propenylzinc Reagents

In 1993, the rearrangement of a 1-trimethylsilyl-2-propenylzinc species (**131**) to the corresponding 2-trimethylsilyl-1-propenylzinc (**132**) was reported. This rearrangement was found to be strongly temperature-dependent (equation 61 and Table 12)[64].

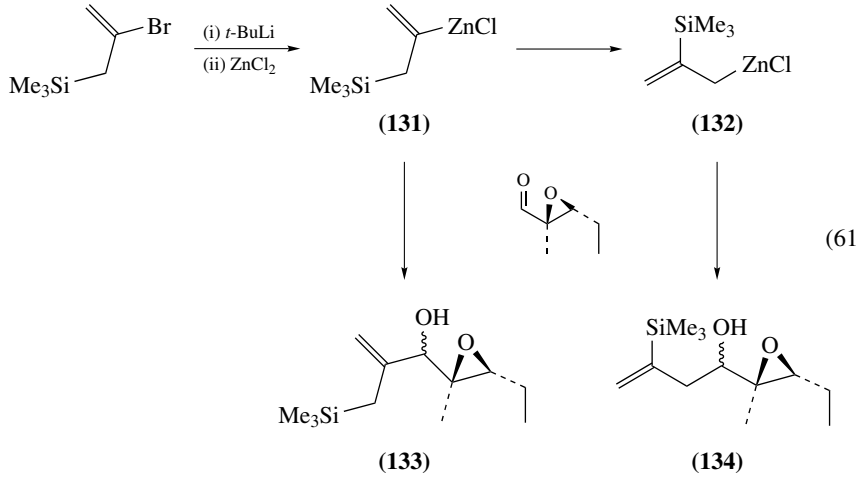

(61)

The rearrangement is incomplete at −100 °C and −50 °C, but warming to 0 °C or room temperature leads to exclusive formation of **134**. The zinc species generated can be coupled with a range of electrophiles as outlined by examples given in Table 13.

Interestingly, the catalyst not only influences reactivity but can also determine whether the product is (formally) derived from **131** or **132** (cf. entries 3 and 4). Several possible mechanisms were considered for these reactions (equations 62 and 63)[64c].

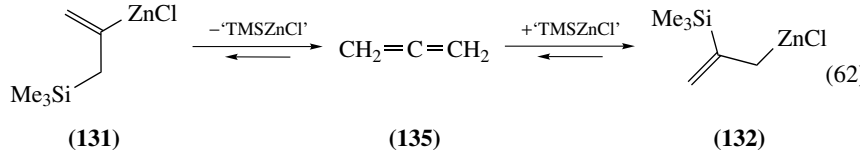

(62)

TABLE 12. The formation of **133** and **134** under different temperature conditions (equation 61)

Entry	Temperature Conditions	Yield **133**(%)	dr **133** (*anti/syn*)	Yield **134**(%)	dr **134** (*anti/syn*)
1	−70 °C to 0 °C	0	—	65	74/26
2	−70 °C to RT, then re-cool to −70 °C	0	—	77	75/25
3	−70 °C to −50 °C	38	66/34	12	58/42
4	−100 °C	60	17/83	16	62/38

TABLE 13. Representative examples of reactions of 1-trimethylsilyl-2-propenylzinc reagents (equation 61)

Entry	Electrophile	Catalyst	Product	Yield (%)
1	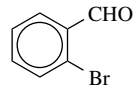	none	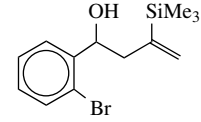	90
2	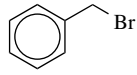	none	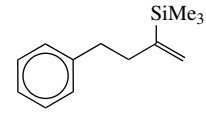	86
3	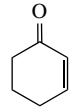	BF_3•OEt_2	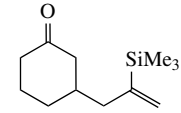	34
4	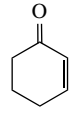	$Ni(acac)_2$	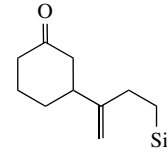	80
5	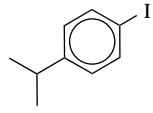	$Pd(PPh_3)_4$	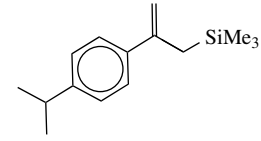	88

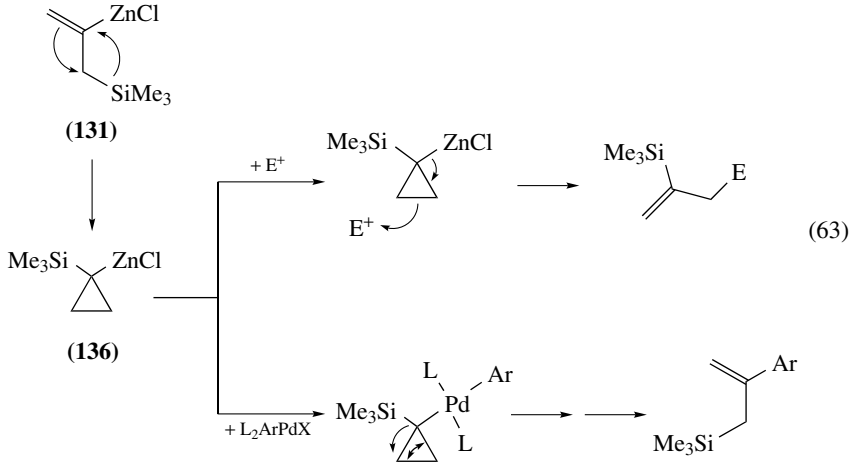

(63)

A mechanism via an allene intermediate **135** was considered (equation 62), whereby elimination and re-addition of 'TMSZnCl' could account for the rearrangement. Alternatively, a cyclopropylzinc intermediate **136** was proposed which, depending on the electrophile, could undergo different reactions (equation 63). This could account for the observed dependence of the product distribution on the electrophile (see entries 2 and 5 in Table 11).

III. CONCLUSIONS

This review demonstrates that rearrangement processes of organozinc compounds provide access to new organometallic species which can be trapped with a range of electrophiles to give highly functionalized products in good overall yields. Many reactions proceed via cyclic transition states leading to excellent diastereoselectivities. The methodologies described herein allow the synthesis of complex products which are difficult to obtain by alternative methods.

IV. REFERENCES AND NOTES

1. Perhaps the earliest example was published in 1969 by Whitlock and Overman, who described angular methylation of a cyclic lithium enolate with Simmons–Smith reagent. H. W. Whitlock, Jr. and L. E. Overman, *J. Org. Chem.*, **34**, 1962 (1969). However, since the mechanism of this reaction is not clear, it is not included in this review.
2. (a) E. Negishi and K. Akiyoshi, *J. Am. Chem. Soc.*, **110**, 646 (1988).
   (b) E. Negishi, K. Akiyoshi, B. O'Connor, K. Takagi and G. Wu, *J. Am. Chem. Soc.*, **111**, 3089 (1989).
3. T. Harada, D. Hara, K. Hattori and A. Oku, *Tetrahedron Lett.*, **29**, 3821 (1988).
4. (a) T. Harada, T. Katsuhira and A. Oku, *J. Org. Chem.*, **57**, 5805 (1992).
   (b) T. Harada, T. Katsuhira, K. Hattori and A. Oku, *Tetrahedron*, **50**, 7987 (1994).
5. (a) H. J. S. Winkler and H. J. Winkler, *J. Am. Chem. Soc.*, **88**, 964 (1966).
   (b) H. J. S. Winkler and H. J. Winkler, *J. Am. Chem. Soc.*, **88**, 969 (1966).
   (c) H. R. Rogers and K. Houk, *J. Am. Chem. Soc.,* **104**, 522 (1982).
6. (a) H. J. Reich, N. H. Philips and I. L. Reich, *J. Am. Chem. Soc.*, **107**, 4101 (1985).
   (b) H. J. Reich, D. P. Green and N. H. Philips, *J. Am. Chem. Soc.*, **111**, 3444 (1989).
7. T. Harada, T. Katsuhira, D. Hara, Y. Kotani, K. Maejima, R. Kaji and A. Oku, *J. Org. Chem.*, **58**, 4897 (1993).
8. For general reviews on organozinc-mediated reactions see:
   (a) P. Knochel and R. D. Singer, *Chem. Rev.*, **93**, 2117 (1993).
   (b) P. Knochel, J. J. A. Perea and P. Jones, *Tetrahedron*, **54**, 8275 (1998).
9. (a) T. Harada, K. Hattori, T. Katsuhira and A. Oku, *Tetrahedron Lett.*, **30**, 6035 (1989).
   (b) T. Harada, T. Katsuhira, K. Hattori and A. Oku, *Tetrahedron Lett.*, **30**, 6039 (1989).
10. (a) K. Kitatani, T. Hiyama and H. Nozaki, *Bull. Chem. Soc. Jpn.*, **50**, 1600 (1977).
    (b) D. Seyferth, R. L. Lambert, Jr. and M. Massol, *J. Organomet. Chem.*, **88**, 255 (1975).
11. (a) T. Harada, T. Katsuhira, K. Hattori and A. Oku, *J. Org. Chem.,* **58**, 2958 (1993).
    (b) T. Harada, T. Katsuhira, K. Hattori and A. Oku, *Tetrahedron*, **50**, 7987 (1994).
12. T. Harada, Y. Kotani, T. Katsuhira and A. Oku, *Tetrahedron Lett.*, **32**, 1573 (1991).
13. A. Shibli, J. P. Varghese, P. Knochel and I. Marek, *Synlett*, 818 (2001).
14. For examples of the rate-increasing effect of NMP in 1,4-addition reactions of R_2Zn to enones, see:
    (a) P. Jones, C. K. Reddy and P. Knochel, *Tetrahedron*, **54**, 1471 (1998).
    (b) C. K. Reddy, A. Devasagayaraj and P. Knochel, *Tetrahedron Lett.*, **37**, 4495 (1996).
    (c) P. Jones and P. Knochel, *J. Chem. Soc., Perkin Trans. 1*, 3117 (1997).
15. It is known that lithium halides modify the Lewis acidic character of the zinc atom: C. Meyer, I. Marek, G. Courtemanche and J. F. Normant, *Tetrahedron*, **50**, 11665 (1994).
16. The formation of zincates from diorganozincs and salts has been studied:
    (a) K. H. Kubas and D. F. Schriver, *J. Am. Chem. Soc.*, **92**, 1949 (1970).
    (b) D. F. Schriver, G. J. Kubas and J. A. Marshall, *J. Am. Chem. Soc.*, **93**, 5076 (1971).

(c) E. C. Ashby and R. G. Beach, *Inorg. Chem.*, **10**, 2486 (1971).
(d) E. C. Ashby and J. J. Watkins, *Inorg. Chem.*, **12**, 2493 (1973).
(e) R. M. Fabicon, A. Pagerski and H. G. Richey Jr., *J. Am. Chem. Soc.*, **113**, 6680 (1991).
17. (a) T. Katsuhira, T. Harada, K. Maejima, A. Osada and A. Oku, *J. Org. Chem.*, **58**, 6166 (1993).
(b) T. Harada, A. Osada and A. Oku, *Tetrahedron Lett.*, **36**, 723 (1995).
(c) T. Harada, T. Katsuhira, A. Osada, K. Iwazaki, K. Maejima and A. Oku, *J. Am. Chem. Soc.*, **118**, 11377 (1996).
18. (a) S. R. Landor, *The Chemistry of the Allenes*, Academic Press, New York, 1982.
(b) H. F. Schuster and G. M. Coppola, *Allenes in Organic Chemistry*, Wiley, New York, 1984.
19. (a) J. M. Dollat, J. L. Luche and P. Crabbe, *J. Chem. Soc., Chem. Commun.*, 761 (1977).
(b) A. Alexakis, I. Marek, P. Mangeney and J. F. Normant, *J. Am. Chem. Soc.*, **112**, 8042 (1990).
20. T. Harada, H. Wada and A. Oku, *J. Org. Chem.*, **60**, 5370 (1995).
21. T. Harada,, T. Kaneko, T. Fujiwara and A. Oku, *J. Org. Chem.*, **62**, 8966 (1997).
22. I. Marek, *Tetrahedron*, **58**, 9463 (2002).
23. A. Sidduri, M. J. Rozema and P. Knochel, *J. Org. Chem.*, **58**, 2694 (1993).
24. (a) M. H. Nantz, D. M. Bender and S. Janaki, *Synthesis*, 577 (1993).
(b) M. P. Doyle, V. Bagheri and E. E. Claxton, *J. Chem. Soc., Chem. Commun.*, 46 (1990).
(c) P. Crabbe, E. Barrerio, J. M. Dollat and J. L. Luche, *J. Chem. Soc., Chem. Commun.*, 183 (1976).
(d) J. Tsuji, T. Sugiura and I. Minami, *Synthesis*, 603 (1987).
(e) A. G. Myers and B. Zheng, *J. Am. Chem. Soc.*, **118**, 4492 (1996).
(f) T. Satoh, Y. Kuramochi and Y. Inoue, *Tetrahedron Lett.*, **40**, 8815 (1999).
(g) R. S. Brinkmeyer and T. MacDonald, *J. Chem. Soc., Chem. Commun.*, 876 (1978).
25. J. P. Varghese, P. Knochel and I. Marek, *Org. Lett.*, **2**, 2849 (2000).
26. J. P. Varghese, I. Suev, L. Aufauvre, P. Knochel and I. Marek, *Eur. J. Org. Chem.*, 4151 (2002).
27. A. Abramovitch, J. P. Varghese and I. Marek, *Org. Lett.*, **6**, 621 (2004).
28. For an excellent overview of various zincate species see: M. Uchiyama, M. Kameda, O. Mishima, N. Yokohama, M. Koike, Y. Kondo and T. Sakamoto, *J. Am. Chem. Soc.*, **120**, 4934 (1998) and references cited therein.
29. J. C. McWilliams, J. D. Armstrong, III., N. Zheng, M. Bhupathy, R. P. Volante and P. J. Reider, *J. Am. Chem. Soc.*, **118**, 11970 (1996).
30. G. Sklute, D. Amsallem, A. Shabli, J. P. Varghese and I. Marek, *J. Am. Chem. Soc.*, **125**, 11776 (2003).
31. S. R. Wilson and M. E. Guazzaroni, *J. Org. Chem.*, **54**, 3087 (1989).
32. N. Maezaki, H. Sawamoto, R. Yoshigami, T. Suzuki and T. Tanaka, *Org. Lett.*, **5**, 1345 (2003).
33. (a) I. Creton, I. Marek and J. F. Normant, *Tetrahedron Lett*., **36**, 7451 (1995).
(b) I. Creton, I. Marek and J. F. Normant, *Synthesis*, 1499 (1996).
34. (a) M. Gaudemar, *C. R. Acad. Sci. Paris, Série C*, **273**, 1669 (1971).
(b) Y. Frangin and M. Gaudemar, *C. R. Acad. Sci. Paris, Série C*, **278**, 885 (1974).
(c) M. Bellassued, Y. Frangin and M. Gaudemar, *Synthesis*, 205 (1977).
(d) J. Auger, G. Courtois and L. Miginiac, *J. Organomet. Chem.*, **133**, 285 (1977).
(e) G. Courtois and L. Miginiac, *C. R. Acad. Sci. Paris, Série C*, **285**, 207 (1977).
(f) F. Bernardou and L. Miginiac, *C. R. Acad. Sci. Paris, Série C*, **280**, 1473 (1975).
(g) F. Bernardou and L. Miginiac, *Tetrahedron Lett.*, 3083 (1976).
(h) M. T. Bertrand, G. Courtois and L. Miginiac, *Tetrahedron Lett.*, 1945 (1974).
(i) M. T. Bertrand, G. Courtois and L. Miginiac, *Tetrahedron Lett.*, 3147 (1975).
35. I. Marek and J. F. Normant, in *Metal-Catalyzed Cross-coupling Reactions* (Eds. P. J. Stang and J. Diederich), Wiley-VCH, Weinheim 1998, pp. 271–337.
36. For general reviews on *gem*-dimetallic reagents see:
(a) I. Marek and J. F. Normant, *Chem. Rev.*, **96**, 3241 (1996).
(b) I. Marek, *Chem. Rev.*, **100**, 2887 (2000) [sp^2].
37. (a) P. Knochel and J. F. Normant, *Tetrahedron Lett.*, **27**, 1039 (1986).
(b) P. Knochel and J. F. Normant, *Tetrahedron Lett.*, **27**, 1043 (1986).
(c) P. Knochel and J. F. Normant, *Tetrahedron Lett.*, **27**, 4427 (1986).
(d) P. Knochel and J. F. Normant, *Tetrahedron Lett.*, **27**, 4431 (1986).

(e) P. Knochel and J. F. Normant, *Tetrahedron Lett.*, **27**, 5727 (1986).
(f) P. Knochel, C. Xiao and M. C. P. Yeh, *Tetrahedron Lett.*, **29**, 6697 (1988).
(g) P. Knochel, M. C. P. Yeh and C. Xiao, *Organometallics*, **8**, 2831 (1989).
(h) C. E. Tucker, S. A. Rao and P. Knochel, *J. Org. Chem.*, **55**, 5446 (1990).
38. I. Marek, J.-M. Lefrançois and J. F. Normant, *J. Org. Chem.*, **59**, 4154 (1994).
39. A 'zinca ene' reaction is by definition (M. B. Smith and J. March, *Advanced Organic Chemistry—Reactions, Mechanisms, and Structure*, 5th edition, Wiley, New York, 2001, p. 1377) not a rearrangement, because it involves two different molecules. Nevertheless, reactions of the type described in equation 30 are included in this review regardless whether the authors rationalized them by a 'metallo-ene' or 'metallo-Claisen' pathway. This is justified since the original mechanistic assumptions were modified later (see Section II.A.3).
40. For reviews see:
(a) R. K. Hill, in *Asymmetric Synthesis* (Ed. J. D. Morrison), Wiley, New York, 1984, p. 503.
(b) J. W. ApSimon and T. L. Collier, *Tetrahedron*, **42**, 5157 (1986).
(c) H. Ito and T. Taguchi, *Chem. Soc. Rev.*, **28**, 43 (1999).
(d) S. M. Allin and R. D. Baird, *Curr. Org. Chem.*, **5**, 395 (2001).
(e) M. Hiersemann and L. Abraham, *Eur. J. Org. Chem.*, 1461 (2002).
(f) U. Nubbemeyer, *Synthesis*, 961 (2003).
41. J. F. Normant, *Acc. Chem. Res.*, **34**, 640 (2001) and references cited therein.
42. I. Marek, J.-M. Lefrançois and J. F. Normant, *Synlett*, 633 (1992).
43. P. Knochel and J. F. Normant, unpublished results, cited in Reference 42.
44. See for example:
(a) A. Bähr, I. Marek and J. F. Normant, *Tetrahedron Lett.*, **37**, 5873 (1996).
(b) D. Brasseur, H. Rezaei, A. Fuxa, A. Alexakis, P. Mangeney, I. Marek and J. F. Normant, *Tetrahedron Lett.*, **39**, 4821 (1998).
45. (a) I. Marek, J.-M. Lefrançois and J. F. Normant, *Tetrahedron Lett.*, **32**, 5969 (1991).
(b) I. Marek and J. F. Normant, *Tetrahedron Lett.*, **32**, 5973 (1991).
46. D. Beruben, I. Marek, J. F. Normant and N. Platzer, *J. Org. Chem.*, **60**, 2488 (1995).
47. The configurational stability of cyclopropyllithiums has been established:
(a) H. M. Walborsky, F. J. Impastato and A. E. Young, *J. Am. Chem. Soc.*, **86**, 3283 (1964).
(b) H. M. Walborsky and R. B. Banks, *Bull. Soc. Chim. Belg.*, **89**, 849 (1980).
(c) H. M. Walborsky and C. Zimmerman, *J. Am. Chem. Soc.*, **114**, 4996 (1992).
(d) H. M. Walborsky and C. Hamdouchi, *J. Org. Chem.*, **58**, 1187 (1993) and references cited therein.
48. D. Brasseur, I. Marek and J. F. Normant, *Tetrahedron*, **52**, 7235 (1996).
49. I. Marek, D. Beruben and J. F. Normant, *Tetrahedron Lett.*, **36**, 3695 (1995).
50. (a) D. A. Evans, G. C. Andrews and B. Buckwalter, *J. Am. Chem. Soc.*, **96**, 5560 (1974).
(b) W. C. Still and T. L. MacDonald, *J. Am. Chem. Soc.*, **96**, 5561 (1974).
51. I. Creton, H. Rezaei, I. Marek and J. F. Normant, *Tetrahedron Lett.*, **40**, 1899 (1999).
52. H. Rezaei, I. Marek and J. F. Normant, *Tetrahedron*, **57**, 2477 (2001).
53. (a) I. Marek, P. R. Schreiner and J. F. Normant, *Org. Lett.*, **1**, 929 (1999).
(b) A. Hirai, M. Nakamura and E. Nakamura, *J. Am. Chem. Soc.*, **121**, 8665 (1999).
54. S. N. Reformatsky, *Chem. Ber.*, **20**, 1210 (1887).
55. For reviews see:
(a) M. T. Crimmins and P. G. Nantermet, *Org. Prep. Proced. Int.*, **25**, 41 (1993).
(b) F. Orsini and G. Sello, *Curr. Org. Synth.*, **1**, 111 (2004).
56. M. J. S. Dewar and K. M. Merz, Jr., *J. Am. Chem. Soc.*, **109**, 6553 (1987).
57. (a) P. Fritsch, *Liebigs Ann. Chem.*, **272**, 319 (1894).
(b) W. P. Buttenberg, *Liebigs Ann. Chem.*, **272**, 324 (1894).
(c) H. Wiechell, *Liebigs Ann. Chem.*, **272**, 337 (1894).
(d) G. Köbrich, *Angew. Chem., Int. Ed. Engl.*, **4**, 49 (1965).
58. H. Rezaei, S. Yamanoi, F. Chela and J. F. Normant, *Org. Lett.*, **2**, 419 (2000).
59. (a) C. Meyer, I. Marek, G. Courtemanche and J. F. Normant, *J. Org. Chem.*, **60**, 863 (1995).
(b) C. Meyer, I. Marek and J. F. Normant, *Tetrahedron Lett.*, **37**, 857 (1996).
60. (a) E. Lorthiois, I. Marek, C. Meyer and J. F. Normant, *Tetrahedron Lett.*, **36**, 1263 (1995).
(b) P. Karoyan and G. Chassaing, *Tetrahedron Lett.*, **38**, 85 (1997).
(c) E. Lorthiois, I. Marek, C. Meyer and J. F. Normant, *Tetrahedron Lett.*, **38**, 89 (1997).

(d) E. Lorthiois, I. Marek and J. F. Normant, *J. Org. Chem.,* **63**, 2442 (1998).
(e) P. Karoyan and G. Chassaing, *Tetrahedron Lett.*, **43**, 1221 (2002).
61. (a) G. Courtemanche and J. F. Normant, *Tetrahedron Lett.*, **32**, 5317 (1991).
(b) C. Meyer, I. Marek and J. F. Normant, *Tetrahedron Lett.*, **35**, 5645 (1994).
62. (a) C. Meyer, I. Marek, G. Courtemanche and J. F. Normant, *Synlett*, 266 (1993).
(b) C. Meyer, I. Marek, G. Courtemanche and J. F. Normant, *Tetrahedron Lett.*, **34**, 6053 (1993).
63. For the synthesis of polysubstituted piperidines see: E. Lorthiois, I. Marek and J. F. Normant, *J. Org. Chem,.* **63**, 566 (1998).
64. (a) J. J. Eshelby, P. C. Crowley and P. J. Parsons, *Synlett*, 277 (1993).
(b) J. J. Eshelby, P. C. Crowley and P. J. Parsons, *Synlett*, 279 (1993).
(c) J. J. Eshelby, P. J. Parsons and P. J. Crowley, *J. Chem. Soc., Perkin Trans. 1*, 191 (1996).

CHAPTER **14**

1,1-Bismetallated species

SEIJIRO MATSUBARA

Department of Material Chemistry, Graduate School of Engineering, Kyoto University, Kyoudai-katsura, Nishikyo, Kyoto 606-8501, Japan
Fax: +81 75 383 2438; e-mail: matsubar@orgrxn.mbox.media.kyoto-u.ac.jp

I. INTRODUCTION

A small package of a molecular model made of resinous balls and sticks, which we had bought for the fundamental organic chemistry class, was so impressive that it gave us the feeling that we could prepare any kind of organic compounds. However, we learned the difference between a model and a real molecule, as soon as we began to study an organic reaction. The parts of the model for sp^3 carbon atom are black small balls with

The chemistry of organozinc compounds
Edited by Z. Rappoport and I. Marek

two halls and two projections, that make free connection possible between the parts. If one gives such ability to real carbon atoms, this allows us to build a perfect molecule. For this purpose, to one carbon atom we should add a functionality that makes possible multiplex C−C bond formation. An attempt at such a method is to use *gem*-dimetallic reagent. *Gem*-dimetal species containing various metal atoms have been already reported. From all varieties, *gem*-dimetal species containing zinc have been the most frequently used in organic synthesis due to their highest stability. In this chapter, the preparation of sp^3-geminated organozinc reagents will be introduced first, followed by their reactions. The chemistry of sp^2-geminated organozinc species will also be shown[1,2].

II. PREPARATION OF sp^3-GEMINATED ORGANODIZINC REAGENTS

The preparation of sp^3-geminated organodimetal compounds has been achieved mainly by one of the following three methods: 1) Double deprotonation of a methyl or methylene carbon, connected to an anion-stabilizing groups, by alkylmetal, 2) halogen–metal exchange of *gem*-dihaloalkane, and 3) regioselective carbometallation of alkenylmetal compounds (Scheme 1). Many organodilithium compounds carrying anion stabilizing groups have been prepared by double deprotonation using alkyllithium or lithium amide as a base. Considering the low basicity of organozinc compounds, however, the deprotonation procedure is not appropriate for the preparation of the corresponding dizinc compounds. The simple method would be a direct reduction of 1,1-dihaloalkane with zinc metal (Scheme 1). Major works by Fried[3] and Miyano[4] and their coworkers demonstrated that treatment of dihalomethane with excess zinc gives *gem*-dizinc species in their Wittig-type methylenation reaction. Since then, the reduction of dihalomethane has been investigated by Nysted[5], Takai, Oshima, and Nozaki[6], Eisch[7], Lombardo[8] and their coworkers for the methylenation of carbonyl compounds. A wide range of reactions using this *gem*-dizinciomethane reagent has been shown by Matsubara, Utimoto and coworkers[9]. The preparation of *gem*-dimetal compounds via carbometallation (Scheme 1) was found by Gaudemar[10]. He has shown that the addition of allylzinc halide to alkenylmagnesium reagents leads to the *gem*-dimetal compounds. More practical and deeper mechanistic studies have further been developed by Normant, Knochel, Marek and Nakamura[1a,c,11–13]. While various metal atoms can be used in the alkenyl metal moiety (Mtl^1 in Scheme 1), zinc metal is indispensable in Mtl^2 as an allylic zinc compound or an additive. It was also shown by Nakamura that a zincated hydrazone also adds to vinyl Grignard reagent to give functionalized sp^3-geminated organodimetal species[14].

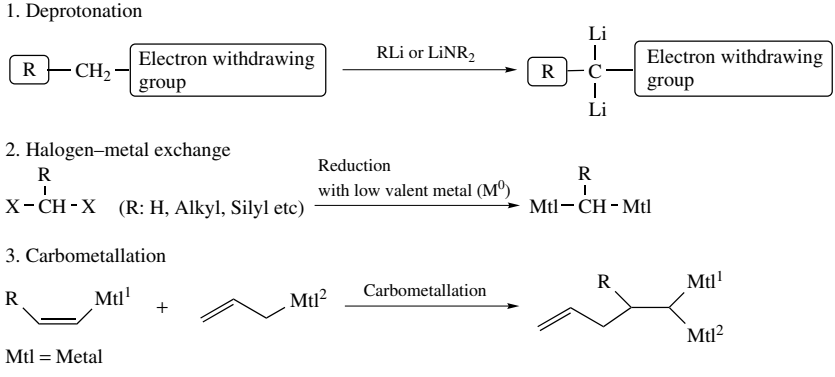

SCHEME 1

A. By Dihalomethane and Zinc

A direct reduction of dihalomethane with zinc may be considered to be the easiest way to prepare methylene dizinc compound, but is also well known as the classical preparation of halomethylzinc, namely the Simmons–Smith reagent[15]. The typical procedure to prepare the Simmons–Smith reagent is to treat diiodomethane with a zinc–copper couple in ether as solvent. When this procedure is performed in THF as solvent, *gem*-dizinc species is formed to some extent. The electrophilic Simmons–Smith carbenoid reacts with alkenes but does not attack carbonyl compounds. On the other hand, the nucleophilicity of *gem*-dizinc species, which was formed via a further reduction of the Simmons–Smith reagent, should be enhanced by doubly substituted electropositive zinc atoms. Once *gem*-dimetal species adds to a carbonyl group, the pathway may lead to a Wittig-type olefination reaction. In 1966, Fried and coworkers used the *gem*-dizinc species, which was prepared from diiodomethane and a zinc–copper couple in THF, for the methylenation of a steroid derivative (equation 1)[3,16]. In this substrate, the hydroxyl group at the α-position of the ketone plays an important role. A chelation enhanced the nucleophilicity of the dizinc species[17]. Methylenation of aldehyde was also examined under the same condition by Miyano and coworkers in 1966 (equation 2)[4]. They supposed that the *gem*-dizinc compound was formed *in situ*, but did not try to investigate its structure.

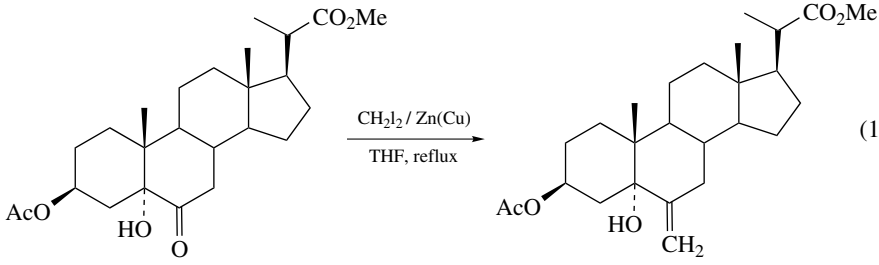

(1)

$$\mathrm{PhCHO} \xrightarrow[\mathrm{THF,\ 35\,^{\circ}C}]{\mathrm{CH_2I_2/Zn(Cu)}} \underset{54\%}{\mathrm{PhCH{=}CH_2}} \qquad (2)$$

Not only a zinc–copper couple, but also a zinc-lead couple forms a *gem*-dimetal species from diiodomethane, according to the 1975 Nysted patent[5]. He also insisted that treatment of dibromethane with a zinc–lead couple in THF at 80 °C forms a characteristic *gem*-dizinc species **1** (equation 3). However, there was no further evidence concerning the structure except ^{1}H NMR data, which was not enough for the complete structural determination. The obtained compound was definitely a *gem*-dizinc species, but the written structure **1** was not fully characterized. The white solid **1** is obtained as a dispersion in THF, and does not dissolve in DMF and DMI (1,3-dimethyl-2-imidazolidinone). This THF dispersion is commercially available from Aldrich Co. as Nysted reagent. Nysted also showed that this dizinc compound is effective for the methylenation of α-hydroxy ketone moiety in steroid derivatives[5].

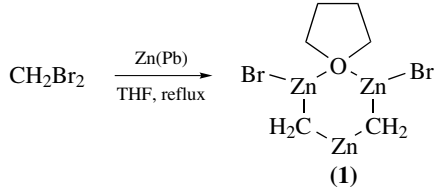

(1) (3)

Nozaki, Oshima, Takai and coworkers reported in 1978 that the reagent prepared from diiodomethane, zinc and titanium(IV) chloride is effective for the methylenation of ketones[6a]. In their procedure, the reagent was prepared by mixing diiodomethane (3.0 eq), zinc powder (9.0 eq) and titanium(IV) chloride (1.0 eq) in THF for 30 min at 25 °C. A ketone (1.0 eq) was added to the prepared reagent. Instead of titanium(IV) chloride, other metal halides were also examined (equation 4) and were less effective. Methylenation of highly enolizable ketones, such as α- and β-tetralone, were performed by the reagent system. Treatment of these ketones with methylenetriphenylphosphorane does not give any methylenated product[6b].

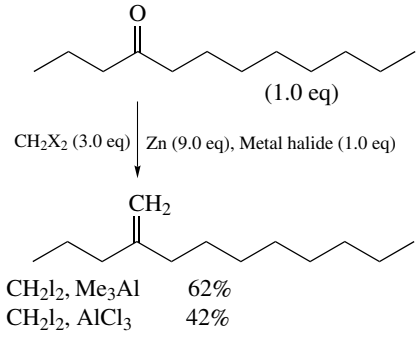

(4)

In these reports, the zinc powder which had been used by Nozaki, Oshima and Takai was pyrometallurgy zinc, which contained originally 0.04–0.07% of lead (Pb). This catalytic amount of lead played an important role in the acceleration of the further reduction of Simmons–Smith reagent into *gem*-dizinc species, according to Takai, Utimoto and coworkers' report[18]. The effect of lead is consonant with Nysted's result[5]. In other words, the aging period for the preparation of dizinc reagent would be much longer when pure zinc (without lead) is used for this purpose.

Eisch and Piotrowski reported the preparation of *gem*-dizinc compounds from diiodomethane and zinc powder in the titanocene chloride mediated methylenation of ketones in 1983 (equation 5)[7]. In this case, it was not mentioned that they had used pyrometallurgy zinc. The Tebbe-type reagent **2** was shown as an intermediary species. Before addition of titanocene chloride, the amount of methane was measured after hydrolysis of the reaction mixture to determine the formation of *gem*-dizinc species[7].

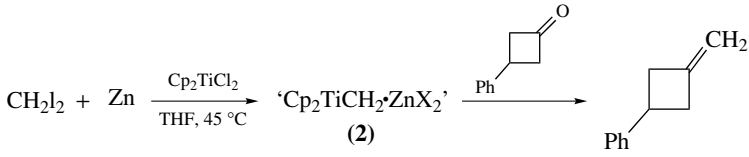

(5)

In 1998, Matsubara, Utimoto and coworkers reported a general procedure for the preparation of bis(iodozincio)methane, which was obtained as a THF solution (equation 6)[9]. The detailed structural study of the solution by SANS (small angle neutron scattering), AXS (anomalous X-ray scattering) and EXAFS (extended X-ray absorption fine structure) implied that the *gem*-dizinc species prepared from diiodomethane and zinc is the monomeric bis(iodozincio)methane (**3**). Formation of polymethylene zinc **4** via Schlenk

equilibrium is not observed under the condition in equation 7[19]. A solution of **3** in THF can be kept unchanged for at least a month in a sealed vessel. Starting from the reagent **3**, various synthetic transformations have been developed[2a–c].

$$\mathrm{I{-}CH_2{-}I + Zn} \xrightarrow[\mathrm{THF,\ 0\ ^\circ C}]{\text{cat. } \mathrm{PbCl_2}} \underset{(\mathbf{3})(50\%\ \text{yield})}{\mathrm{IZn{-}CH_2{-}ZnI}} \tag{6}$$

$$\mathrm{IZn{-}CH_2\text{-}ZnI} \rightleftharpoons \underset{(\mathbf{4})}{\mathrm{IZn}\left(\mathrm{CH_2Zn}\right)_n\mathrm{I}} + n\,\mathrm{ZnI_2} \tag{7}$$

B. By Dihaloalkane and Zinc

Following the procedure for the preparation of bis(iodozincio)methane (**3**), 1,1-dihaloalkane may be converted into the corresponding *gem*-dizinc species. Treatment of 1,1-diiodoethane with zinc in the presence of lead gives *gem*-dizincioethane species (equation 8). A ^{1}H NMR analysis showed the formation of sp^3-geminated organodizinc species, but the existence of Schlenk equilibrium (see equation 7) had not been excluded[9]. Computational studies by Nakamura and coworkers have determined the structure of 1,1-dizincioethane as being oligomeri(9)c[13].

$$\mathrm{CH_3CHI_2} \xrightarrow[\mathrm{THF,\ 25\ ^\circ C,\ 1\ h}]{\mathrm{Zn/cat.PbCl_2}} \underset{50\%}{\mathrm{CH_3CH(ZnL_n)_2}} \tag{8}$$

$\mathrm{L_n}$: -I or $-(\mathrm{CH_2Zn})_n\mathrm{I}$

In general, the preparation of *gem*-dizincioalkane via the treatment of 1,1-dihaloalkane with zinc is more difficult than the preparation of *gem*-dizinciomethane. The reduction of *gem*-dihaloalkanes carrying β-hydrogens may suffer from β-hydride elimination and result in the formation of alkenes. In addition, depending on the substrate, the intermediary α-haloalkylzinc compound is less stable than α-halomethylzinc towards the α-elimination (Scheme 2).

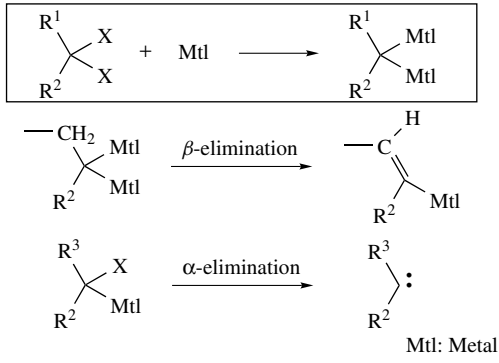

SCHEME 2

These side reactions, however, can be suppressed by addition of TMEDA. As shown in equations 9–11, several types of *gem*-dizinc compounds are prepared in the presence of

TMEDA. These dizinc species (equations 9–11) are, however, less stable that bis(iodozincio)methane (**3**) in solution[9].

$$CH_3CH_2CHI_2 \xrightarrow[\text{THF, 40 °C, 1 h}]{\text{Zn/cat.PbCl}_2\text{, TMEDA}} CH_3CH_2CH(ZnL_n)_2 \quad 30\% \tag{9}$$

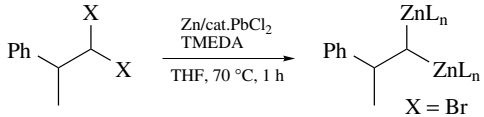

$X = Br \quad 40\%$ (10)

L_n: -Br or $-(CH_2Zn)_{\overline{n}}Br$

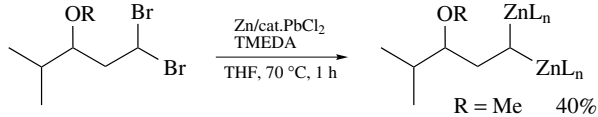

$R = Me \quad 40\%$
$R = MOM \quad 40\%$ (11)

L_n: -Br or $-(CH_2Zn)_{\overline{n}}Br$

In the above procedures, the preparation of 1,1-dihaloalkanes is indispensable, but it often contains some synthetic difficulties. Several efficient methods have been reported for their preparations. Halogen-exchange reaction is one of the most commonly used (Scheme 3)[20]. Selective reduction of 1,1-dihaloalkene with diazene also gives 1,1-dihaloalkane[21].

$$CH_3CHCl_2 + C_2H_5I \xrightarrow{AlCl_3} CH_3CHI_2$$

$$RCHO \xrightarrow{Tf_2O} RCH(OTf)_2 \xrightarrow{MgI_2} R\text{-}CHI_2$$

SCHEME 3

C. By Heteroatom-substituted Dihaloalkane and Zinc

Treatment of trimethylsilyldibromomethane with pyrometallurgy zinc in THF affords the corresponding dizinc compound in good yield (equation 12)[22]. When pure zinc (without lead) is used, a catalytic amount of $PbCl_2$ should be added. The silyl group may promote the reduction of the C−Br bond by stabilization of the radical species. The obtained *gem*-dizinc is fairly stable, as it has no β-hydrogen. There is no information to determine the detailed structure of the silyl-substituted *gem*-dizinc species in solution; it may form oligomers. Raston and coworkers prepared trimethylsilyl(2-pyridyl)dizinciomethane from the corresponding antimony compound and isolated the tetrameric crystal **5**[23]. In the same way, *gem*-dizinc species carrying a germyl and boryl group on the α-position are also prepared in good yields (equations 13 and 14)[24, 25].

$$RMe_2SiCHBr_2 \ (1.0\ eq) \xrightarrow[60\,^\circ C,\ 6\ h,\ THF]{\text{Zn (2.5 eq)}\ \text{cat. PbCl}_2} RMe_2SiCH(ZnL_n)_2 \tag{12}$$

$R = Me \quad 72\%$
$R = Ph \quad 72\%$
$R = p\text{-}MeOC_6H_4 \quad 80\%$

L_n: -Br or $-(CH_2Zn)_{\overline{n}}Br$

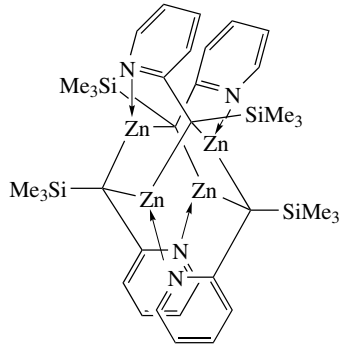

(5)

$$Et_3GeCHBr_2 \xrightarrow[60\,^{\circ}C,\ 6\ h,\ THF]{Zn\ (2.5\ eq),\ cat.\ PbCl_2} Et_3GeCH(ZnL_n)_2 \quad (13)$$

(1.0 eq) 40%

L_n: -Br or $-(CH_2Zn)_n-Br$

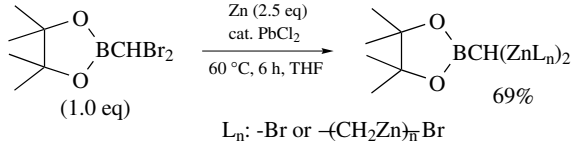

(1.0 eq) 69% (14)

L_n: -Br or $-(CH_2Zn)_n-Br$

D. Via Carbometallation

As described above, preparation of sp^3-geminated organodizinc compounds by insertion of zinc metal into a carbon–halogen bond may lead to some difficulties when applied to 1,1-dihaloalkane[9]. A totally different synthetic route, however, solves these problems. The route is based on the carbometallation reaction of allylzinc to alkenylmetal. In 1971, Gaudemar found that allylzinc halide adds to vinyl Grignard reagents[10a]. Normant and Knochel further developed this reaction as a practical method for the preparation of sp^3-geminated organodimetal compounds (equation 15)[11].

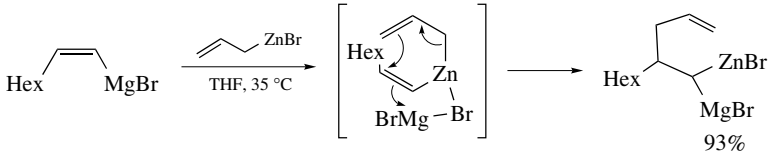

93% (15)

This process seems to be contra-intuitive, since two nucleophiles lead to a third nucleophile, but is much easier than the allylzincation of simple alkenes. The reaction is profiled by *ab initio* calculations, and the energy diagram in Scheme 4 explains the rapid reaction of alkenyl metal with allylzinc halide[12]. A detailed and advanced computational study for this process by Nakamura and coworkers shows the existence of two possible pathways. One is the metalo-ene pathway whereas the second one corresponds to a metala-Claisen reaction (Scheme 5)[13]. In both cases, allylzinc and vinyl metal react via a six-membered transition state.

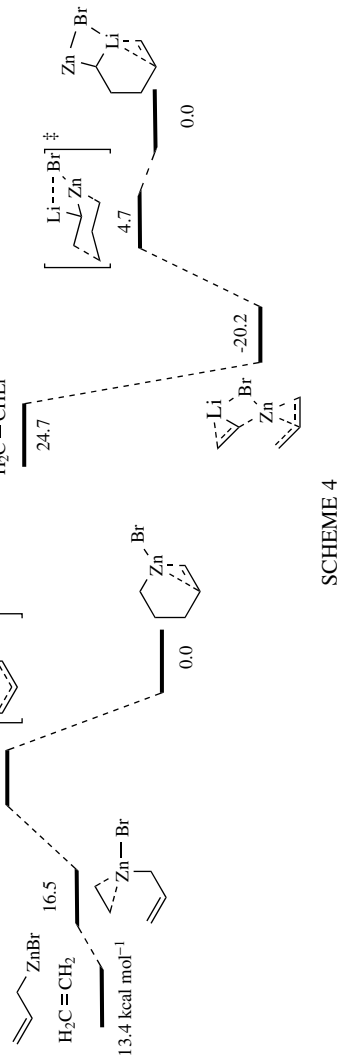
ZnBr
H2C=CH2
13.4 kcal mol−1
16.5
Zn — Br
28.0
Zn
Br
‡
0.0
ZnBr
H2C=CHLi
24.7
Li
Br
Zn
-20.2
Li---Br
Zn
‡
4.7
Zn — Br
Li
0.0

SCHEME 4

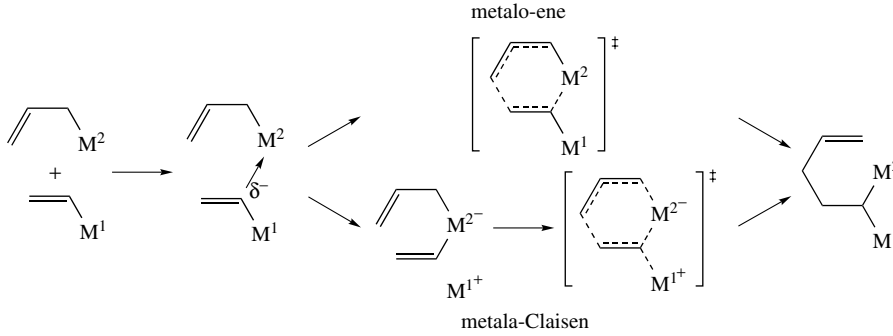

SCHEME 5

As shown in Scheme 6, the addition forms two stereogenic centers via the favorable chair-like transition state. The diastereoselective construction of stereogenic centers has been studied extensively by Marek and Normant[1a]. For the control of stereochemistry, one should think about the configuration of allylzinc compounds and the alkenyl metal. Interestingly, a comparison of four possible transition states (Scheme 7) by calculation concludes that *Z*-crotylzinc bromide is the most favorable transition state. This means that it is not necessary to think about the stereochemistry of crotylzinc bromide as its configuration changes via 1,3-transposition of the zinc atom (Scheme 6)[12].

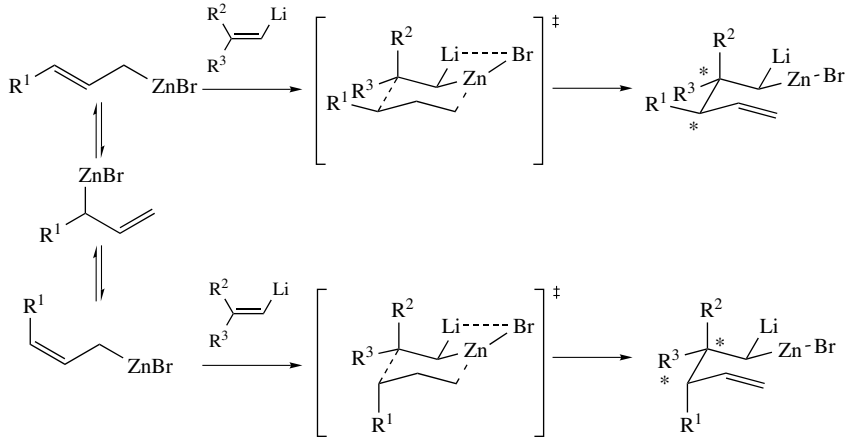

SCHEME 6

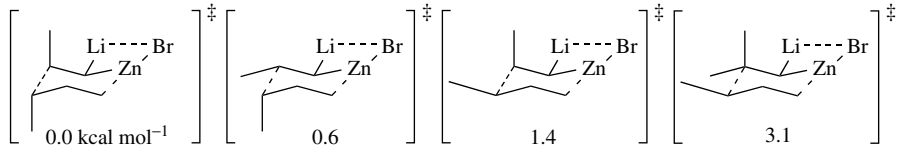

SCHEME 7

Based on these investigations, stereochemically defined alkenyllithium is treated with stereochemically undefined crotylzinc to give the adduct diastereoselectively (equation 16)[26]. Many types of stereoselective reactions will be shown in Section III.

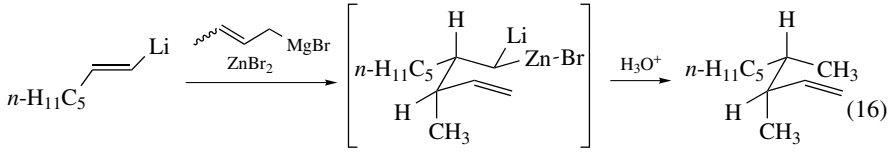

81% (*syn*/*anti* = 95/5)

III. REACTION OF sp^3-GEMINATED ORGANODIZINC REAGENTS

There are many useful transformations using organozinc reagents. Although these reagents are fairly stable as compared to the corresponding magnesium or lithium reagents, the reaction of organozinc derivatives have to be realized by appropriate activation. In the case of sp^3-geminated organodizinc reagent, the nucleophilicity should be increased compared with a simple organomonometal species, as the carbon is substituted with a pair of electropositive metal atoms. In addition, their unique structure should lead to unique specific transformations. The classical reactions of sp^3-geminated organodizinc reagent are summarized in Scheme 8.

1. Olefination

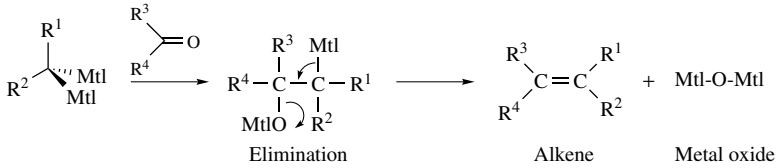

2. Sequential Reaction with Two Electrophiles

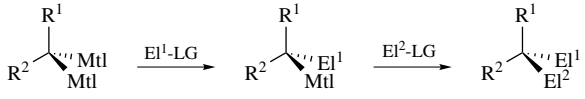

Intermediary organomonometal

El^1-LG, El^2-LG: electrophiles (LG = leaving group)

3. Nucleophilic Cyclopronation

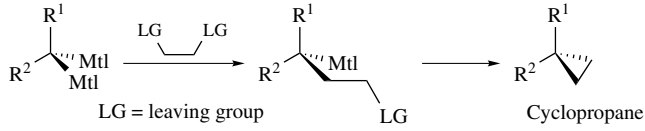

4. As Lewis Acid

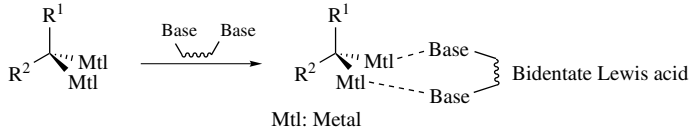

SCHEME 8

A. Methylenation

The olefination reaction of carbonyl compounds may be performed in various ways. For this purpose, the Wittig reaction has been frequently used[27]. The control of stereochemistry in the product had also been well studied by Schlosser. Both the *E* and *Z* isomers in the product can be obtained with excellent selectivity by Schlosser's modified method[28]. Despite the usefulness of the Wittig reaction, some drawbacks exist. For instance, ylide is usually basic enough to lead to an enolization of the starting carbonyl compound. At the same time, it often suffers from low nucleophilicity. For example, treatment of α-tetralone with methylenetriphenylphosphorane does not give the olefin, as a deprotonation reaction occurs to form the enolate. Treatment of esters with an ylide often ends with recovery of the starting ester, due to low nucleophilicity of the ylide. These facts lead to a new interest in organobimetallic compounds[2b, c, 29]. As shown previously (equations 1 and 2), a methylenation reaction of α-alkoxyketones and aldehydes was performed with a mixture of a zinc–copper couple and dihalomethane. The Nysted reagent was also effective for the same transformation (equation 3)[5]. Those methods, containing a *gem*-dizinc species as a reactive species, showed an attractive substitute for the Wittig reaction. The scope of the reaction was extended dramatically by addition of titanium salt (equation 4). This method was developed by Nozaki, Oshima, Takai and coworkers in 1981[6a]. Their protocol was modified by Lombardo in 1982[8]. According to Lombardo's report, the aging period for the preparation of the reagent should be three days, while in the original method the aging time was only 30 min (equation 17). Lombardo had applied the original procedure to the methylenation of gibberellin derivative and observed only decomposition of the substrate. Takai, Utimoto and coworkers also reported that lead (Pb), which is contained in the commercially available pyrometallurgy zinc, played an important role in the acceleration of further reduction of the Simmons–Smith reagent into *gem*-dizinc species[18]. This effect of lead is consonant with Nysted's result[5]. In other words, the aging period for the preparation of dizinc reagent should be much longer than 30 min when pure zinc (without lead) is used. The point about the aging period for preparation of reactive species, argued by Lombardo, should not be attributed only to the formation of *gem*-dizinc species, as titanium(IV) chloride is also reduced with zinc powder[30]. A subtle difference in reduction of titanium(IV) with Zn may lead to the problem of the reproducibility of the methylenation reaction. Therefore, Matsubara, Utimoto and coworkers studied again the effect of titanium salt, using a solution of bis(iodozincio)methane (**3**) in THF. This study gave a clear procedure for the methylenation reaction[9].

$$\text{Zn (440 mmol)} + \text{CH}_2\text{Br}_2\,\text{(144 mmol)} + \text{TiCl}_4\,\text{(103 mmol)} \xrightarrow[\text{THF (250 ml)}]{\text{3 days, 5 °C}} \text{[active species]}$$

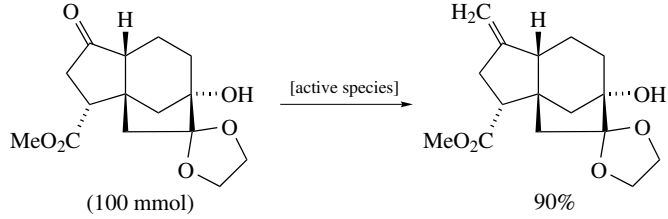

(100 mmol) 90% (17)

Aldehydes are methylenated by bis(iodozincio)methane (**3**) without the mediation of titanium salt. Commercially available Nysted reagent **1** is also effective for this transformation; in this case, the addition of a catalytic amount of $BF_3{\bullet}OEt_2$ improved the yield (Table 1)[31a, c].

TABLE 1. Methylenation of aldehydes with bis(iodozincio)methane (**3**) and Nysted reagent (**1**)[a]

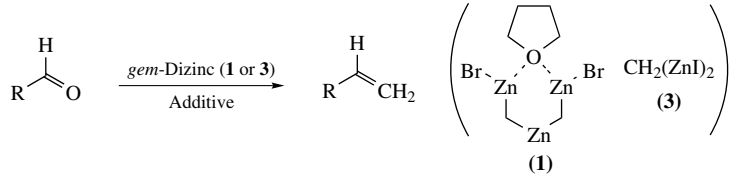

Entry	R−CHO (1.0 mmol)[b]	Dizinc	Additive	Alkene (%)
1	$CH_3(CH_2)_{10}CHO$	**3** (1.0 mmol)	none	74
2		**3** (2.0 mmol)	none	96
3		**1** (1.0 mmol)[a]	none	68
4		**1** (1.0 mmol)[a]	BF_3•OEt_2 (0.1 mmol)	83
5	$PhCH_2CH_2CHO$	**3** (1.0 mmol)	none	46
6	(*E*)-PhCH=CHCHO	**3** (1.0 mmol)	none	47
7	(*E*)-PhCH=CHCHO	**1** (1.0 mmol)	BF_3•OEt_2 (0.1 mmol)	69
8	(*S*)-$PhCH(CH_3)CHO$	**3** (1.0 mmol)	none	64[c]

[a] Nysted reagent was weighed according to the structure **1**, shown in the original patent[9].
[b] RCHO (1.0 mmol), dizinc (1.0 or 2.0 mmol) and additive were mixed in THF.
[c] No epimerization was observed.

The nucleophilic attack of the organometallic reagents on the carbonyl group is enhanced by the presence of heteroatom at the α-position which generates a chelate intermediate[17]. As shown by Fried (equation 1), α-alkoxyketones can be transformed into alkenes by a mixture of diiodomethane and a zinc–copper couple[3]. In equations 18 and 19, ketones carrying an oxygen atom at the α-position are converted into methylenated products with bis(iodozincio)methane (**3**) without[31b,32] any additives. Not only ketones carrying an oxygen atom at the α-position but also those carrying a nitrogen atom at the same position are also easily converted into allylamine derivatives with **3** (equation 20)[32].

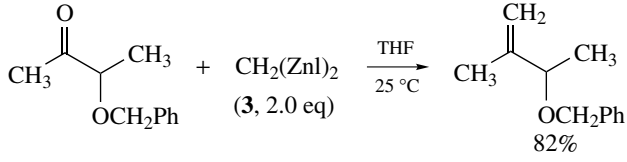

(18)

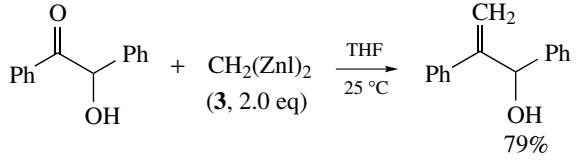

(19)

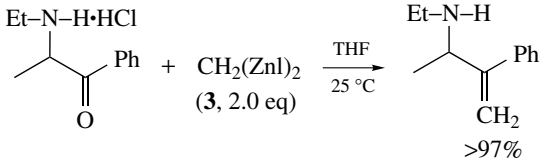

(20)

TABLE 2. Titanium salt mediated methylenation of ketones with bis(iodozincio) methane (**3**)

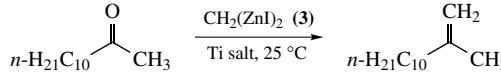

Entry	Ti salt [a]	**3** (eq)	Alkene (%) [b]	Recovery (%)
1	None	1	15	10
2	$TiCl_4$	1	26	<5
3	$TiCl_4$	2	78	<5
4	$3TiCl_3 \bullet AlCl_3$	2	43	33
5	α-$TiCl_3$	1	<5	72
6	β-$TiCl_3$	1	83	<5
7	β-$TiCl_3$	2	87	<5
8	$TiCl_2$	2	<5	86

[a] $3TiCl_3 \bullet AlCl_3$ (Aldrich), α-$TiCl_3$ (Aldrich) and $TiCl_2$(Aldrich).
[b] Isolated yields.

As shown in Table 2, a ketone such as 2-dodecanone can be methylenated when it is treated with bis(iodozincio)methane (**3**) in the presence of various titanium salts[33]. Without titanium salt, the methylenation does not proceed. As a source of titanium chloride, β-$TiCl_3$, which is prepared from titanium(IV) chloride and hexamethyldisilane following Girolami's procedure[2c,34], is shown to be the most effective. An equimolar mixture of **3** and β-$TiCl_3$ gives the most reactive reagent for the methylenation. As described before, for the methylenation procedure described by Takai or Lombardo, a mixture of diiodomethane, zinc and titanium(IV) chloride was used. In these procedures, titanium(IV) chloride would be reduced into low-valent titanium species. The oxidation state of titanium is crucial for the reproducibility of the reaction. The higher the valent titanium is, the better the Lewis acid. Hence the combination of bis(iodozincio)methane (**3**) solution and β-$TiCl_3$, which is not easily reduced with zinc, is very desirable[9]. $TiCl_4$ is also a possible mediator with 2 equivalents of **3**, as the dizinc reagent also immediately reduces $TiCl_4$ into $TiCl_3$.

The preparation of β-$TiCl_3$ was performed according to Girolami's report[9,35]. This report corrected the errors originally described by Naula and Sharma, who had reported that $TiCl_2$ was formed from the reaction of titanium(IV) chloride and hexamethyldisilane (Scheme 9)[36]. Girolami pointed out that hexamethyldisilane cannot reduce titanium(III) chloride into titanium(II) or (I) chloride regardless of the stoichiometry. Matsubara, Utimoto and coworkers used the titanium chloride prepared from titanium(IV) chloride and hexamethyldisilane in their olefination reaction according to Naula and Sharma's report[37]. In these series of reports, the salt was written as $TiCl_2$. It should be β-$TiCl_3$, according to Girolami's correction in 1998, although all procedures and results in Matsubara's previous olefination reactions are correct.

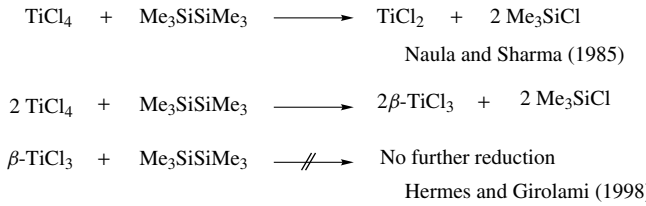

SCHEME 9

In Scheme 10, the results of the reactions of various ketones with *gem*-dizinc **3** and β-$TiCl_3$ are shown[9]. Although the yields are not excellent, the highly enolizable ketones. α- and β-tetralones are also transformed into alkenes. As shown in Scheme 11, Nysted reagent **1** is also applicable with the use of β-$TiCl_3$. When using Nysted reagent (**1**), the titanium mediated methylenation works better in the presence of $BF_3{\bullet}OEt_2$[31a].

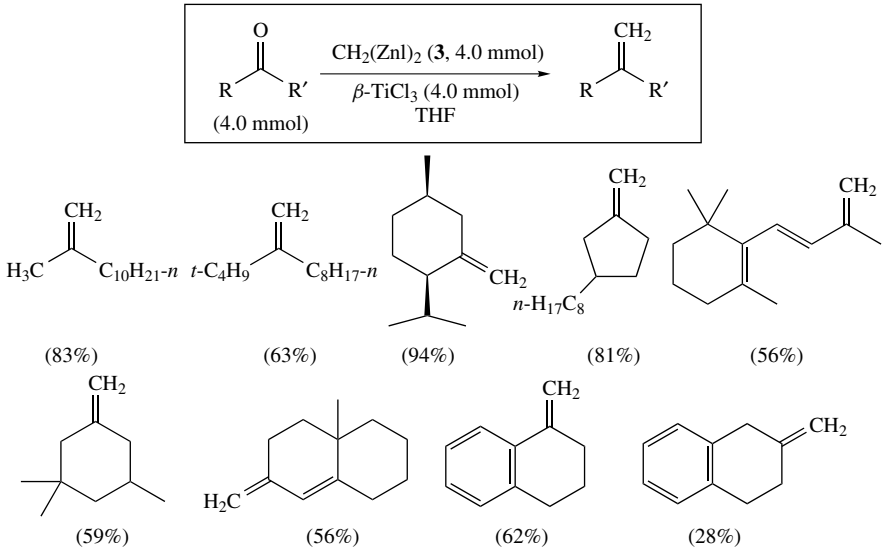

SCHEME 10

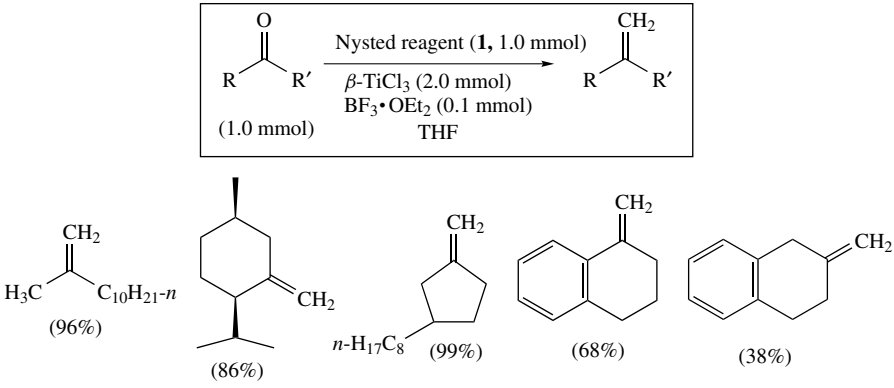

SCHEME 11

The methylenation reaction of ester gives vinyl ether. As shown in Scheme 12, the addition of TMEDA is necessary for the desired methylenation[38].

As shown in equation 21, the methylenation of polyketone is performed with bis(iodozincio)methane (**3**) and β-$TiCl_3$[39]. With these substrates, the Wittig reagent and the

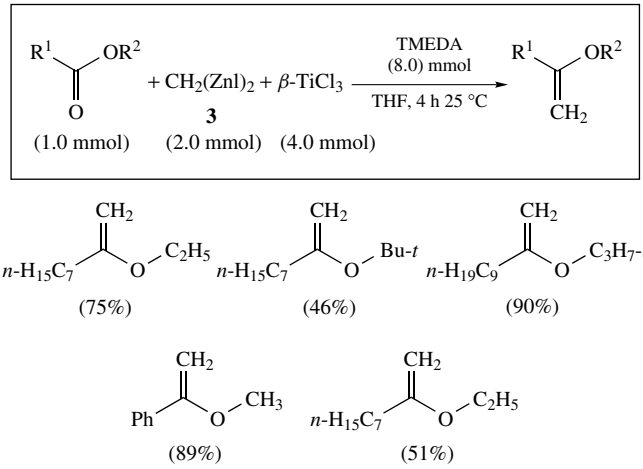

SCHEME 12

Tebbe reagent as well as Zn-CH_2X_2-$TiCl_4$ did not give satisfactory results. However, the combination of **3** and β-$TiCl_3$ gave fully methylenated products without racemization.

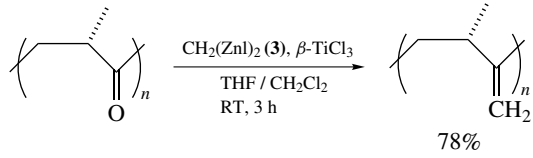

(21)

The role of titanium salt is to activate the carbonyl compounds as Lewis acid. As described above, bis(iodozincio)methane (**3**) is nucleophilic enough to attack the carbonyl group of aldehydes or α-alkoxyketones. In the reaction with simple ketones or esters, however, the addition of titanium salt is necessary to facilitate the nucleophilic attack. Instead of this Lewis acid activator, simple heating may induce the nucleophilic attack. Treatment of 2-dodecanone with **3** without titanium salt at higher temperature, however, does not improve the yield of alkene (Scheme 13). The reason for the low reactivity of **3** at higher temperature comes from the structural change of **3** into the polymeric methylene zinc **4** through the Schlenk equilibrium shown in equation 7[40].

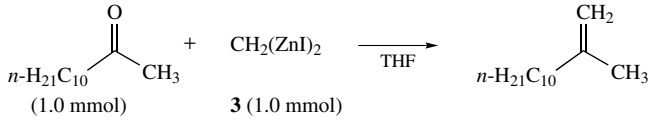

Reaction condition	Alkene (%)	Recovery (%)
25 °C, 15 h	15	10
60 °C, 6 h	26	43
β-$TiCl_3$ (1.2 mmol), 25 °C, 0.5 h	84	<3

SCHEME 13

TABLE 3. Methylenation of 2-dodecanone with **3** in the presence of additive

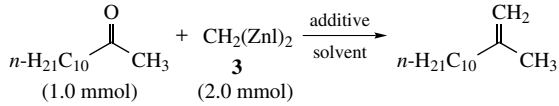

Entry	Solvent	Condition	Additive	Yield (%)
1	THF (3.0 ml)[a]	25 °C/15 h	none	15
2	THF (3.0 ml)[a]	60 °C/6 h	none	43
3	THF (3.0 ml)[a]	60 °C/6 h	THT (0.5 ml)[c]	86
4	THF (3.0 ml)[a]	60 °C/6 h	[bmim][PF_6][c] (0.1 ml)[d]	56
5	THF (2.0 ml)/hexane (1.0 ml)[b]	60 °C/6 h	[bmim][PF_6][c] (0.1 ml)[e]	81

[a] Ketone (1.0 mmol), **3** (0.5 M THF solution, 2.0 mmol) and THF (1.0 ml) were used.
[b] Ketone (1.0 mmol), **3** (0.5 M THF solution, 2.0 mmol) and hexane (1.0 ml) were used.
[c] THT: tetrahydrothiophene. [bmim]: 1-butyl-3-methylimidazolinium.
[d] The reaction mixture was monophasic.
[e] The reaction mixture was biphasic.

This structural change is suppressed by the addition of tetrahydrothiophene (THT)[19b]. It prevents the formation of polymethylene zinc, i.e. $(-CH_2Zn-)_n$. Without THT, a solution of **3** in THF yields polymethylene zinc at 60 °C. Monomeric bis(iodozincio)methane (**3**) is much more active for methylenation as compared to polymethylene zinc. As shown in Table 3 (entry 3), the addition of THT to the reaction mixture at 60 °C improved the yield of the alkene dramatically. Practically, however, its stinking property makes the experimental procedure in large scale uncomfortable. Fortunately, an ionic liquid, 1-butyl-3-methylimidazolium hexafluorophosphate ([bmim][PF_6]), plays the same role. Ionic liquid also stabilizes the monomeric structure of **3** even at 60 °C and maintains it during the reaction at the same temperature. The method can be applied to various ketones as shown in Scheme 14.[4]

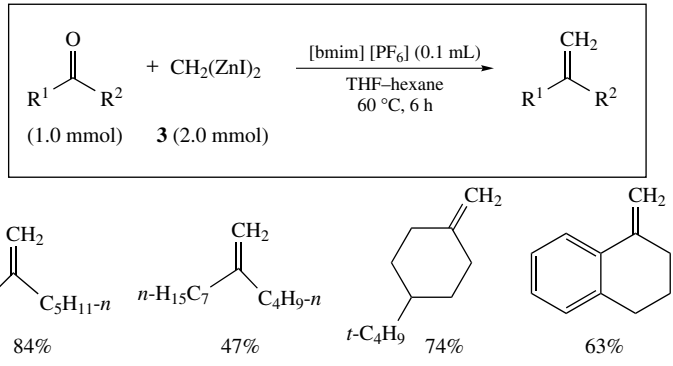

SCHEME 14

Diverse activation methods of bis(iodozincio)methane (**3**) for the methylation reactions lead to chemoselective transformations. For instance, the α-keto group is methylated selectively by **3** in the presence of a simple ketone (equation 22)[32]. The opposite selectivity is observed in the reaction using **3** and β-$TiCl_3$ (equation 23)[32]. Aldehyde is methylenated selectively by **3** in the presence of simple ketone (equation 24)[9]. Both aldehyde

and ketone are methylenated by **3** and β-$TiCl_3$ (equation 25)[9]. Ketone is methylenated selectively by **3** and ionic liquid in the presence of ester (equation 26)[40].

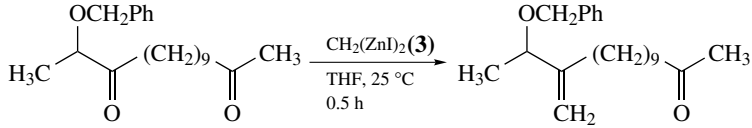

(22)

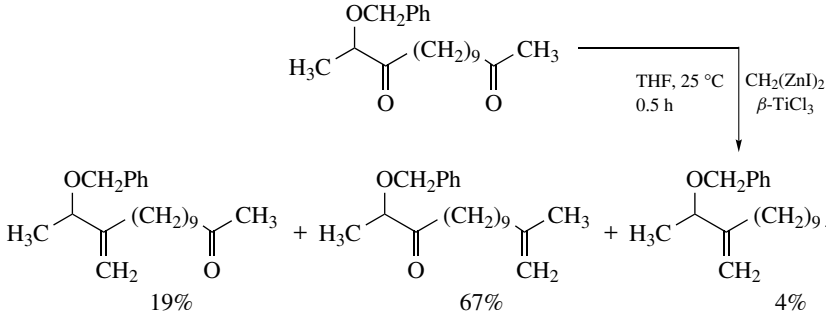

(23)

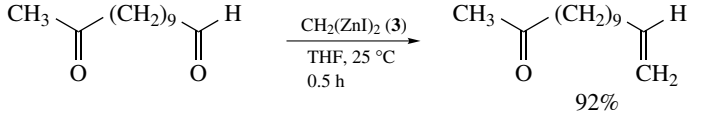

(24)

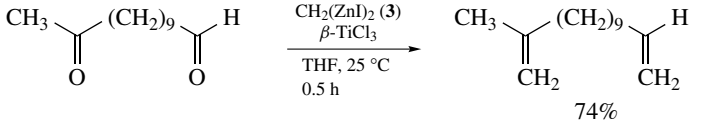

(25)

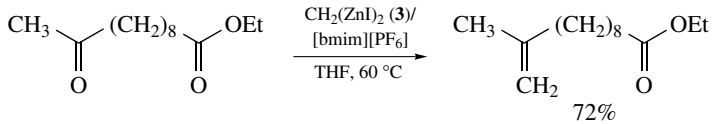

(26)

B. Alkylidenation

As described in Section II, the preparation of 1,1-dizincioalkane can be achieved not only by reduction of 1,1-dihaloalkane, but also by allylzincation of alkenyl metal compounds. The reaction of allylzinc with alkenyl Grignard reagent, which is followed by the addition of aldehydes, gives dienes as shown in Scheme 15[11,41].

Treatment of ketones with 1,1-dizincioethane, prepared from 1,1-diiodoethane and zinc, gives the corresponding alkenes under the action of β-$TiCl_3$, as shown in Scheme 16.

Alkylidenation of esters by treatment with a mixture of Zn (containing 0.04–0.07% of lead), $RCHBr_2$, $TiCl_4$ and TMEDA works well (Scheme 17). The reaction requires a large excess of reagent. It should be noted that zinc powder in this procedure is also a pyrometallurgy zinc. When pure zinc without lead is used, a catalytic amount of $PbCl_2$

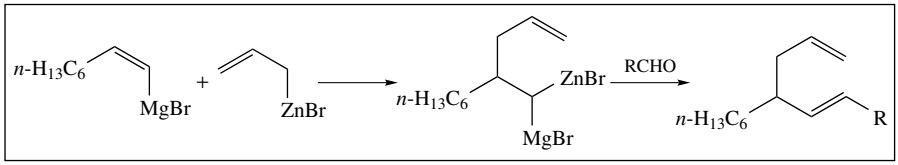

PhCHO — 78% (*E*/*Z* = 99/1)

C_2H_5CHO — 61% (*E*/*Z* = 95/5)

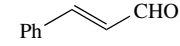

58% (*E*/*Z* = 92/8)

SCHEME 15

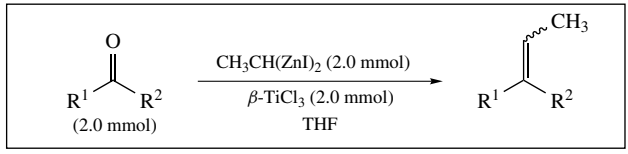

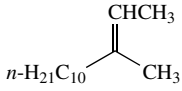

62% (*E*/*Z* = 1/1)

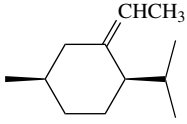

13% (*E*/*Z* = 1/1)

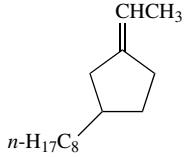

48% (*E*/*Z* = 1/1)

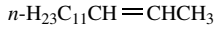

63% (*E*/*Z* = 67/33)

SCHEME 16

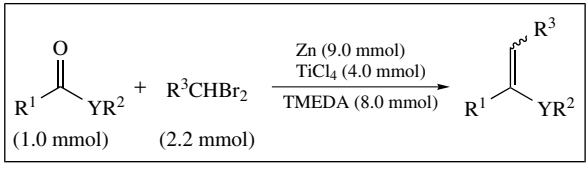

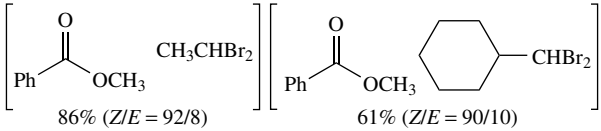

86% (*Z*/*E* = 92/8)

61% (*Z*/*E* = 90/10)

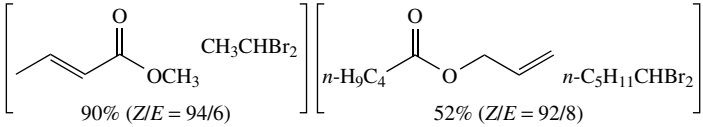

90% (*Z*/*E* = 94/6)

52% (*Z*/*E* = 92/8)

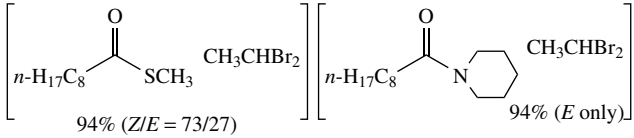

94% (*Z*/*E* = 73/27)

94% (*E* only)

SCHEME 17

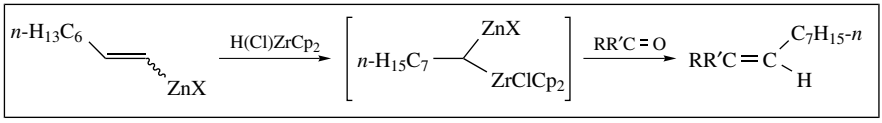

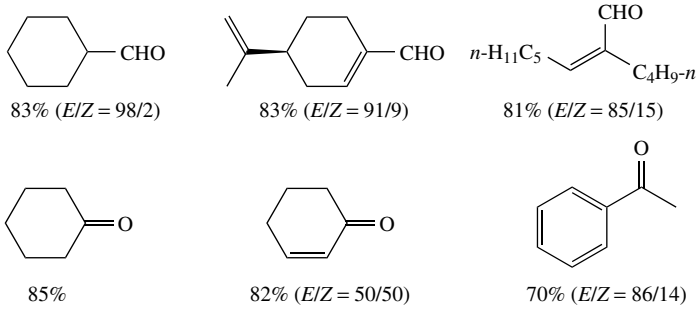

SCHEME 18

should be added. Good stereoselectivities are observed. The major products are the *Z*-isomers. This reagent can also undergo the ethylidenation of thioester and amide[42].

A dimetal species, obtained by treatment of vinylzinc with Schwartz's reagent, leads to a very effective alkylidenation reaction as shown in Scheme 18[43].

C. Synthesis of Alkenyl-silane, -germane and -borane

Silyl-[22], germyl-[24] and boryl-substituted[25] *gem*-dizinciomethanes are prepared by the direct reduction of the corresponding *gem*-dibromethane derivatives with pyrometallurgy zinc. When pure zinc without lead is used, a catalytic amount of $PbCl_2$ should be added. Reactions of carbonyl compounds with these *gem*-dizinc species in the presence of titanium salt give the corresponding heteroatom substituted alkenes. As shown in Table 4, β-$TiCl_3$ is used except for the reaction of α-boryl-substituted *gem*-dizinc. Titanium(IV) chloride ($TiCl_4$) is used for the reaction in the case of α-boryl reagent. This boryl-substituted dizinc reagent would not reduce $TiCl_4$ (entries 6–8).

D. Sequential Reaction with Two Electrophiles

Bis(iodozincio)methane (**3**), which possesses two nucleophilic sites on a single carbon, has the possibility to react sequentially with two different electrophiles. It will act as a molecular hinge which connects two electrophiles. It was found that the reactivity of the first C–Zn bond of **3** is much higher than that of the resulting methylzinc in the reaction with water or iodine (equation 27). These results indicate that it is possible to use these two C–Zn bonds individually[44].

$$CH_2(ZnI)_2 + D_2O \xrightarrow[-35\,^\circ C]{THF} CHD(ZnI) \xrightarrow[0\,^\circ C]{D_2O/THF} CHD_2 \qquad (27)$$

Knochel and Normant investigated the reactivity of *gem*-dimetal species, prepared by the Gaudemar/Normant procedure. As shown in Scheme 19, the *gem*-dimetal

TABLE 4. Reactions of carbonyl compounds with α-heteroatom-substituted dizinc species[a]

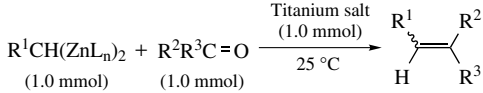

Entry	R^1	R^2	R^3	Titanium salt	Yield (%)[b]	*E*/*Z*
1	Me_3Si	*n*-$C_{11}H_{23}$	H	β-$TiCl_3$	92	89/11
2		$PhCH_2CH_2$	H	β-$TiCl_3$	78	90/10
3		(*E*)-PhCH=CH	H	β-$TiCl_3$	55	68/32
4		Ph	CH_3	β-$TiCl_3$	54	61/39
5	$PhMe_2Si$	*n*-$C_{11}H_{23}$	H	β-$TiCl_3$	86	87/13
6		$PhCH_2CH_2$	H	$TiCl_4$	70	74/26
7		*n*-$C_{11}H_{23}$	H	$TiCl_4$	58	74/26
8		*n*-$C_{10}H_{21}$	CH_3	$TiCl_4$	71	59/41
9	Et_3Ge	$PhCH_2CH_2$	H	β-$TiCl_3$	79	74/26
10		Ph	CH_3	β-$TiCl_3$	63	65/35

[a] These dizinc species were prepared as shown in equations 12–14[22, 24, 25].
[b] Isolated yields.

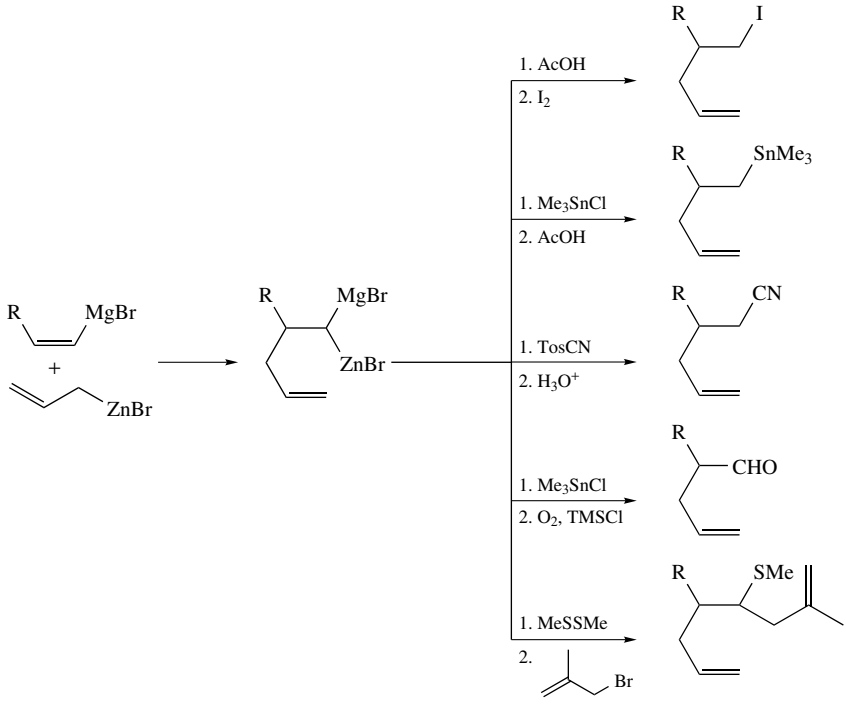

SCHEME 19

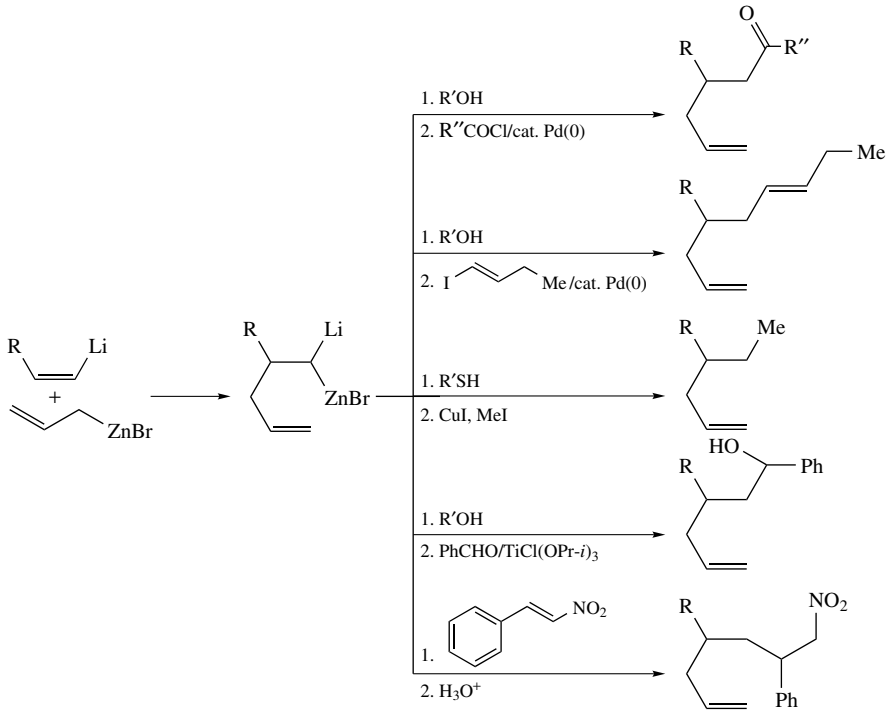

SCHEME 20

species prepared from allylzinc and alkenyl Grignard reagent was treated with various electrophiles[11a,45].

They also showed that the *gem*-dimetal species from allylzinc and alkenyllithium lead to selective reactions with electrophiles as shown in Scheme 20[11b,46].

The attractive feature of *gem*-dimetal species is the formation of two C−C bonds simultaneously. For example, Knochel and Normant converted the *gem*-dimetal species into a copper reagent and treated with various electrophiles. As shown in Scheme 21, bisallylation and bismethylation are now possible[11b].

To make the transformation even more useful, different carbon electrophiles should be connected sequentially in a stepwise manner. For this purpose, a transition-metal-catalyzed cross-coupling reaction opened the way. As shown in Scheme 22, cinnamyl chloride is treated with bis(iodozincio)methane (**3**) in the presence of palladium catalyst with various phosphine ligands. Phosphine ligands, having an electron-withdrawing group, such as tris[3,5-bis(trifluoromethyl)phenyl]phosphine and tris(2-furanyl)phosphine, show excellent results[47].

Instead of quenching with deuterium chloride, the intermediary organomonozinc compound can be used as a new nucleophile. Not only allylic halide but also alkenyl or aryl halide can be used as the first electrophile with bis(iodozincio)methane (**3**). In Scheme 23, examples for sequential coupling are summarized. In the case of coupling with bromoalkene, a nickel catalyst is more effective than a palladium catalyst.

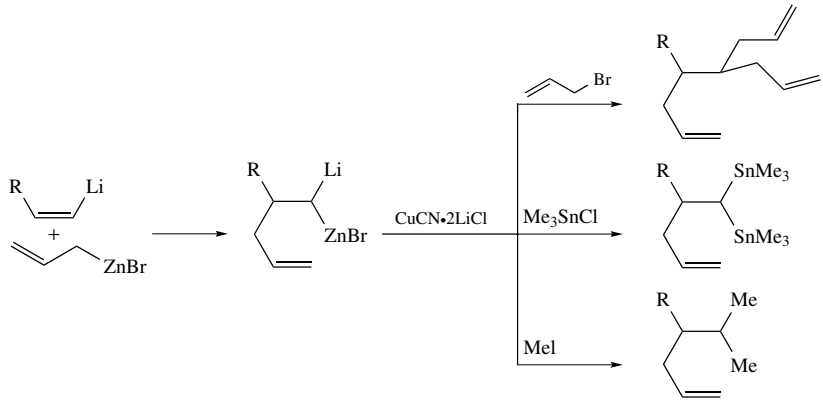

SCHEME 21

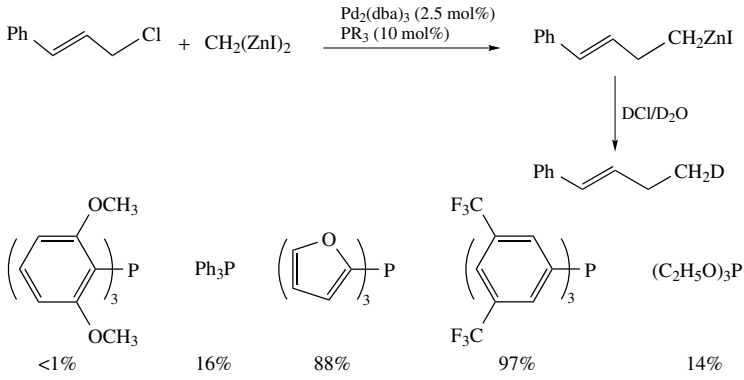

SCHEME 22

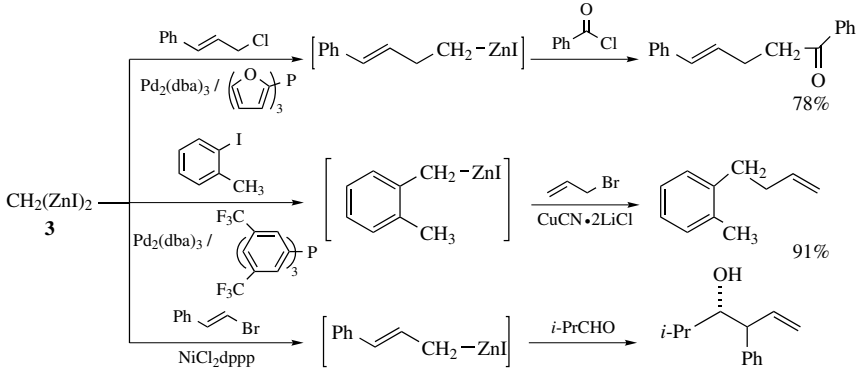

dba: *trans*,*trans*-dibenzylideneacetone
dppp: 1,2-bis(diphenylphosphino)propane

SCHEME 23

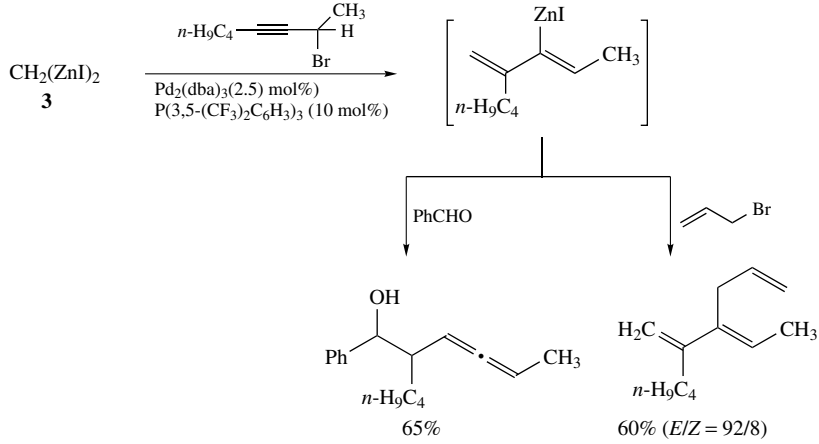

SCHEME 24

A conjugated dienyl zinc reagent is easily obtained from propargyl bromide and **3** as shown in Scheme 24. The species reacted with allyl bromide as a dienylzinc, and with benzaldehyde as an allenylzinc species[48].

As for the preparation of 1,3-diene, the reaction of **3** with the propargyl ether, described in Scheme 25, was also developed. This reaction is a convenient way to prepare aryl substituted 1,3-butadiene[49].

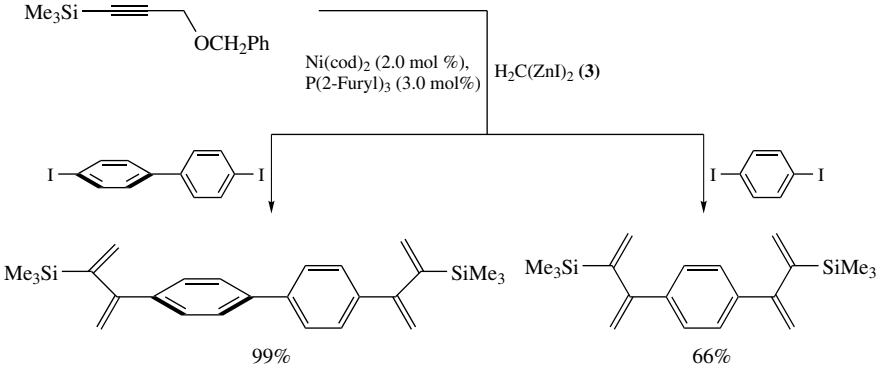

SCHEME 25

As described in the former section, silyl-, boryl- and germyl-substituted *gem*-dizinc reagents are easily prepared. These dizinc reagents also perform the sequential coupling reaction as shown in Scheme 26[22, 24, 25].

The sequential coupling reactions may be applied to the formation of an optically active organozinc compound. Chiral organometallic compounds, which are generated in enantiomerically enriched form, will give a direct way to construct asymmetric carbon in optically active form[50, 51]. As shown in equation 28, the reaction gives chiral monozinc compound via desymmetrization after the first coupling reaction. The whole reaction can be expected as follows: 1) Oxidative insertion of palladium(0) to RX; 2) transmetallation

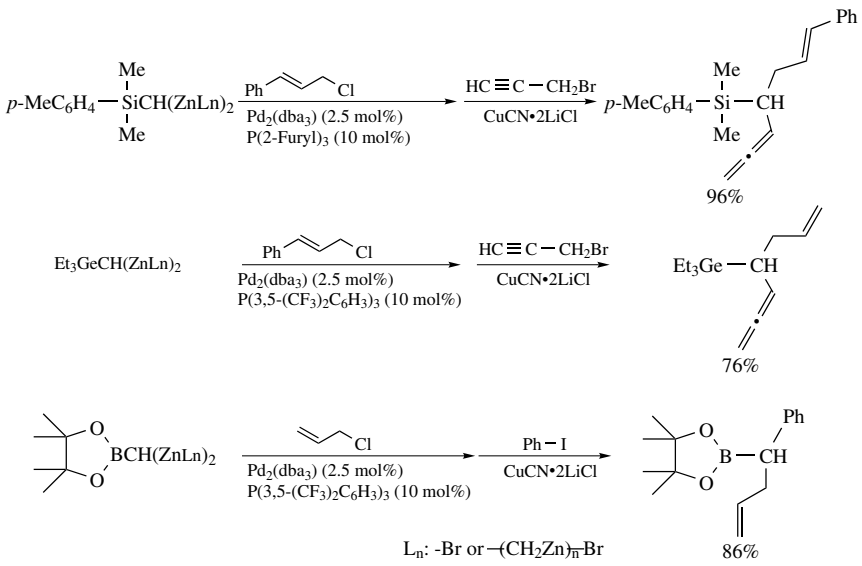

SCHEME 26

of *gem*-dizinc compound to the palladium complex via desymmetrization; 3) formation of configurationally stable organic monozinc compound, after reductive elimination. The transmetallation step is crucial for the asymmetric induction.

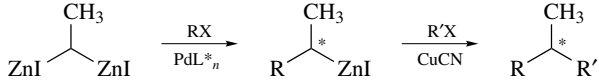

(28)

L*: chiral phosphine ligand

As shown in equation 29, 1,1-bis(iodozincio)ethane was reacted with cinnamyl carbonates in the presence of Pd(0) catalyst with chiral phosphine ligand, MOP[51,52]. The formed organozinc intermediate was treated with propargyl bromide under the mediation of copper salt. The observed asymmetric induction reached up to 33% ee.

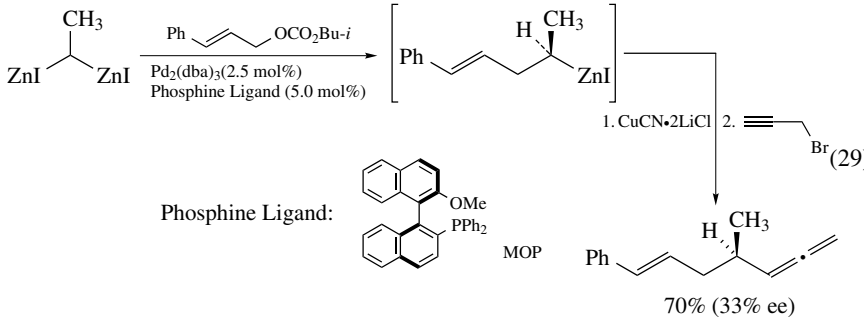

(29)

Sequential reaction of *gem*-dizinc reagent with acyl cyanide affords 1,3-diketone, as shown in Scheme 27. Benzoyl chloride and bis(iodozincio)methane (**3**), however, did not

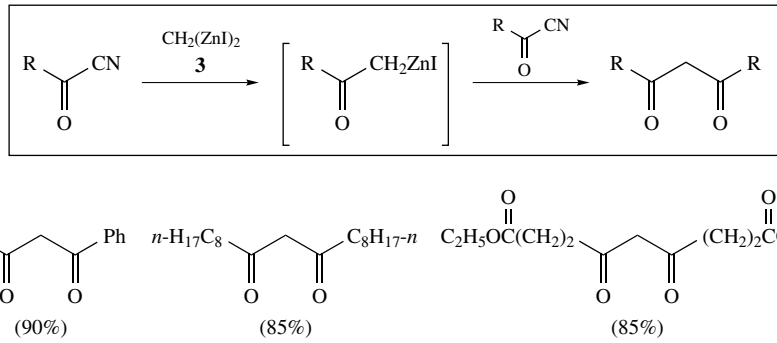

SCHEME 27

give the corresponding 1,3-diketone[53], but rather the THF ring opening (equation 30). Therefore, acyl chlorides react faster with THF than with the solution of **3** containing zinc(II) iodide. While palladium catalyst helps the formation of 1,3-diketones from acyl chloride and **3**[53], the activation of **3** with tetrahydrothiophene (THT) has also a positive effect (Scheme 28)[19]. The addition of THT activates the reagent **3** and makes its addition to acyl chloride faster.

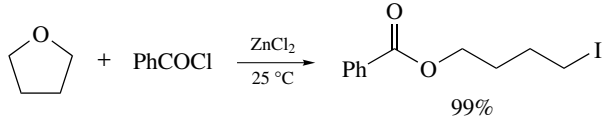

(30)

The conjugate addition of bis(iodozincio)methane to α,β-unsaturated carbonyl compound gives γ-zincio substituted enolate. As shown in equation 31, bis(iodozincio)methane reacts with *s*-cis α,β-unsaturated ketone in the presence of chlorotrimethylsilane to afford the silyl enol ether carrying a C−Zn bond. These zinc-substituted silyl enolates can be used for further coupling reactions (equation 32)[54].

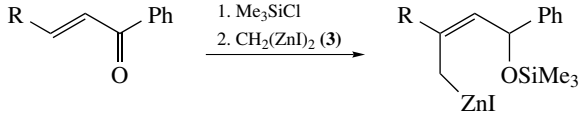

(31)

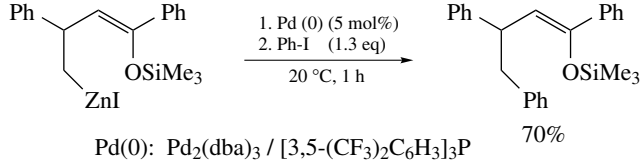

(32)

The conjugate addition of 1,1-bis(iodozincio)ethane to α,β-unsaturated ketone raises the question of diastereoselectivities. As shown in Scheme 29, the diastereoselective 1,4-addition of 1,1-bis(iodozincio)ethane leads to the diastereomerically enriched secondary organozinc reagent[55].

The above 1,4-additions were performed with *s-cis* enones. In the case of the reaction with *s-trans* enone such as cyclohexenone, bis(iodozincio)methane (**3**) should

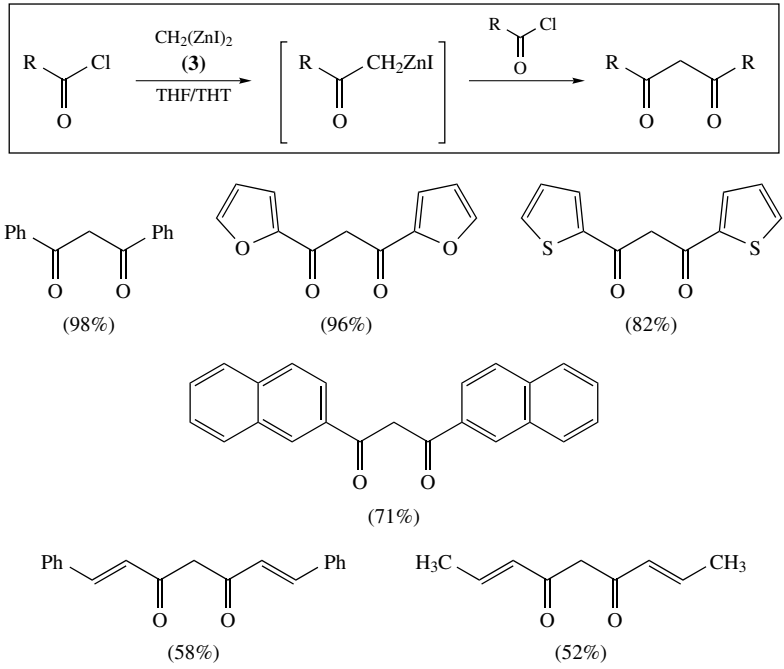

SCHEME 28

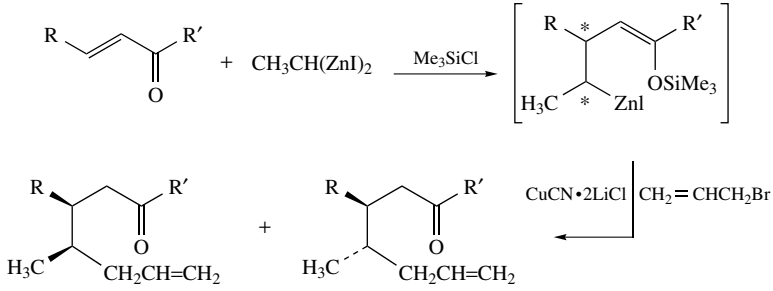

R = Ph,	R′ = Ph	86%	(98/2)
= Me,	= Ph	81%	(>95/<5)
= Ph,	= Me	44%	(71/29)
= Ph,	= *t*-Bu	75%	(95/5)

SCHEME 29

be converted into the corresponding copper reagent for the effective 1,4-addition. As shown in Scheme 30, the copper reagent reacts with cyclohexenone in the presence of chlorotrimethylsilane to give γ-zincio silyl enol ether[54].

The 1,4-addition of sp^3-geminated organodimetal compounds, prepared by the Gaudemar/Normant coupling reaction, to alkylidenemalonate gives *Z*-alkene selectively through elimination of the malonate moiety (equation 33)[56,57].

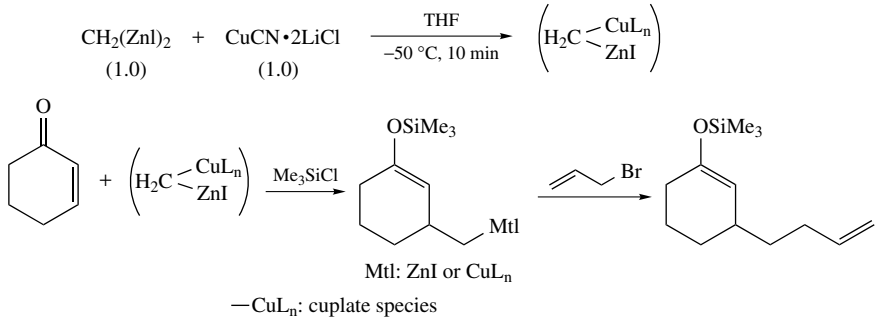

SCHEME 30

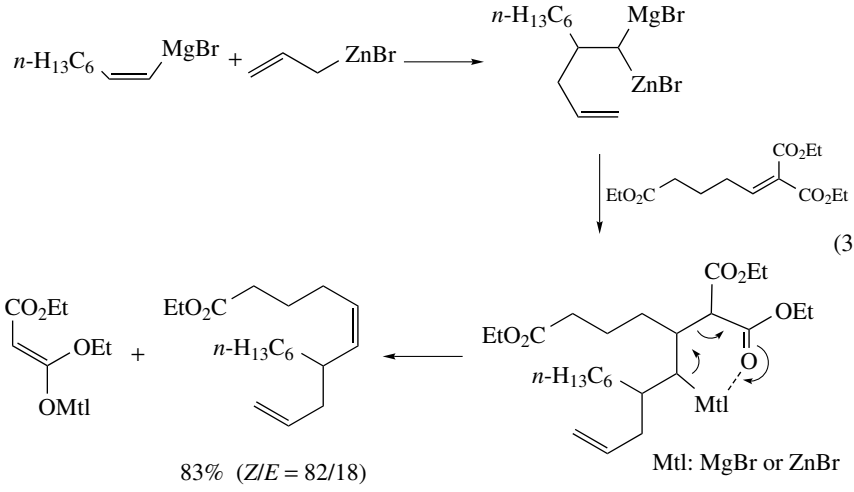

(33)

E. Diastereoselective Construction of Carbon Skeleton by the Gaudemar/Normant Coupling

As shown previously in Scheme 6, an important method for the preparation of sp^3-geminated organodimetal compounds is the Gaudemar/Normant coupling reaction. This reaction leads to excellent diastereoselectivity due to the proximate effect in the transition state (equation 34)[12, 13, 41, 58, 59].

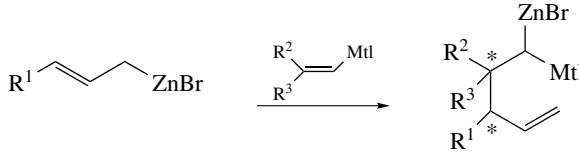

(34)

Indeed, as shown in Scheme 31, highly diastereoselective crotylzincation of *t*-butoxy-substituted *Z*-alkenyl lithium affords sp^3-geminated organodimetal compound with high diastereoselectivity[41]. Once the alkenyllithium has a secondary allylic substituent, three

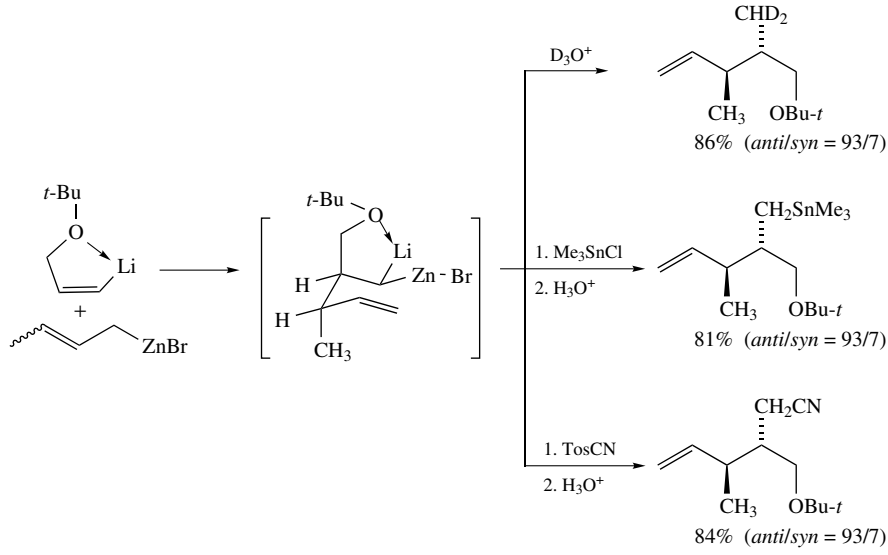

SCHEME 31

stereogenic centers are created (equation 35)[60]. A chelation in the allylzinc reagent did not interfere and highly diastereoselective addition occurs (equation 36). A 1,3-diol derivative is also obtained diastereoselectively (equation 37)[61].

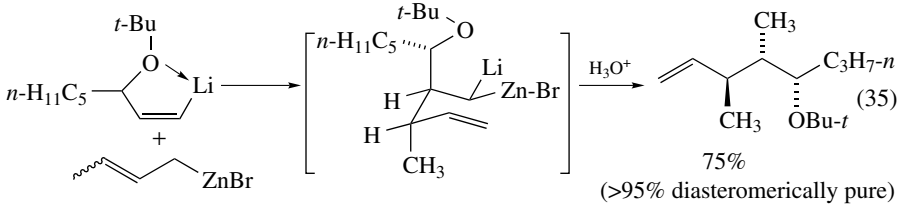

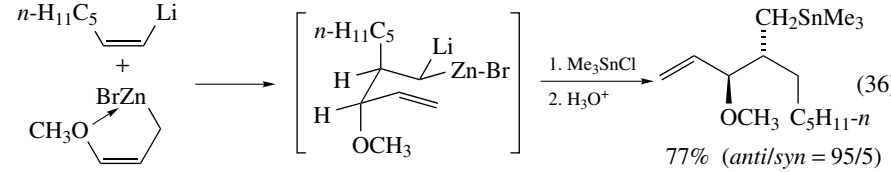

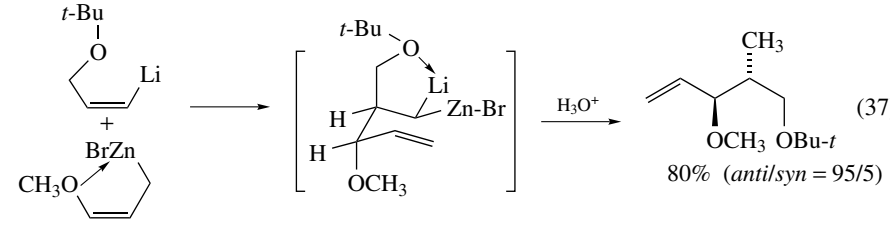

These highly diastereoselective transformations lead the way to asymmetric induction by means of chiral auxiliaries. As shown in equations 38 and 39, the use of chiral amines induces the chirality transfer in the Gaudemar/Normant coupling reaction[62,63].

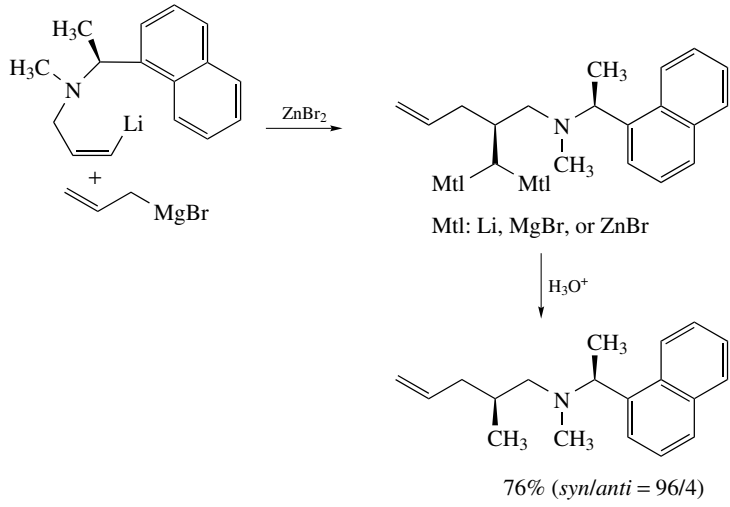

(38)

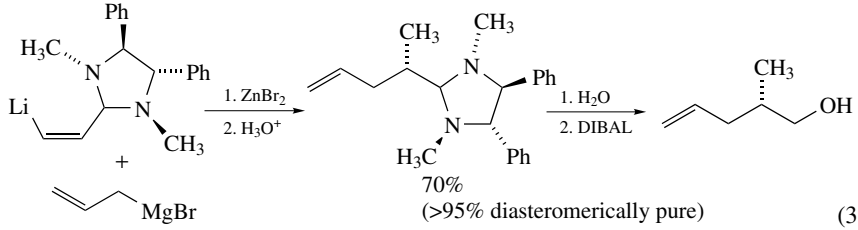

(39)

A formal synthesis of Serricornin was perfomed by a diastereoselective Gaudemar/Normant coupling reaction between (*Z*)-γ-alkoxyalkenyllithium and trimethylsilyl-substituted allyllithium under the mediation of zinc(II) bromide (Scheme 32)[64].

Allenylzinc reagent also adds to alkenyl metal to afford sp^3-geminated organodimetal compounds. In equation 40, the alkynyl group was introduced diastereoselectively[61].

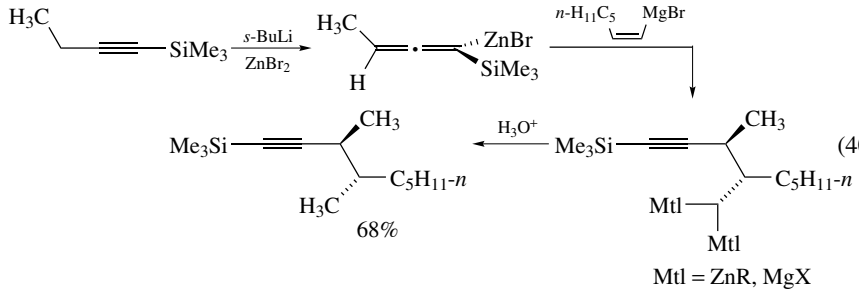

(40)

Allenyl metal compounds also act as an acceptor of allylzinc reagent. As shown in Scheme 33, the obtained allylic bismetal species reacted sequentially. A terminal allene

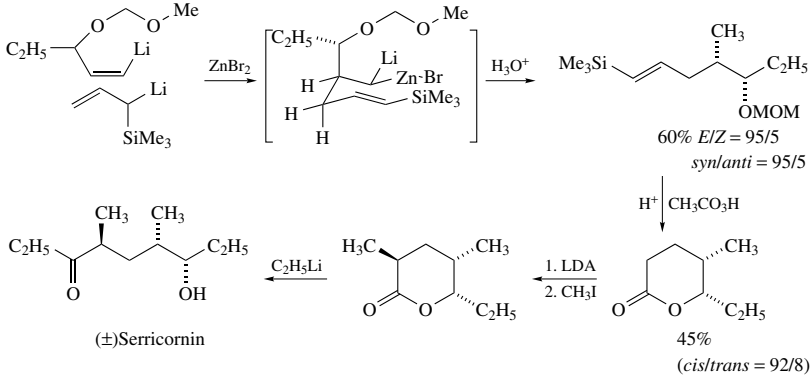

SCHEME 32

gave a reactive allenyl metal, which reacts with allylzinc to give a cyclohexane derivative via a sequential allylzincation reaction (equation 41)[65].

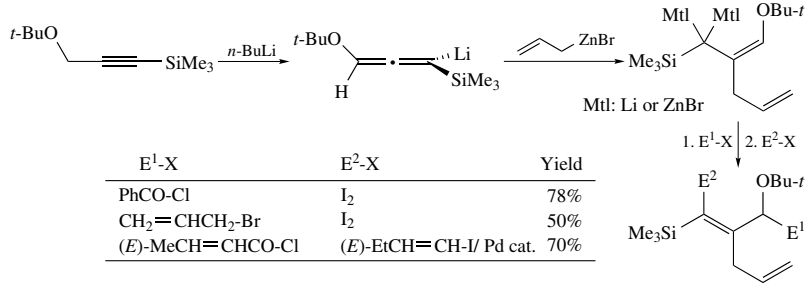

E^1-X	E^2-X	Yield
PhCO-Cl	I_2	78%
CH_2═$CHCH_2$-Br	I_2	50%
(*E*)-MeCH═CHCO-Cl	(*E*)-EtCH═CH-I/ Pd cat.	70%

SCHEME 33

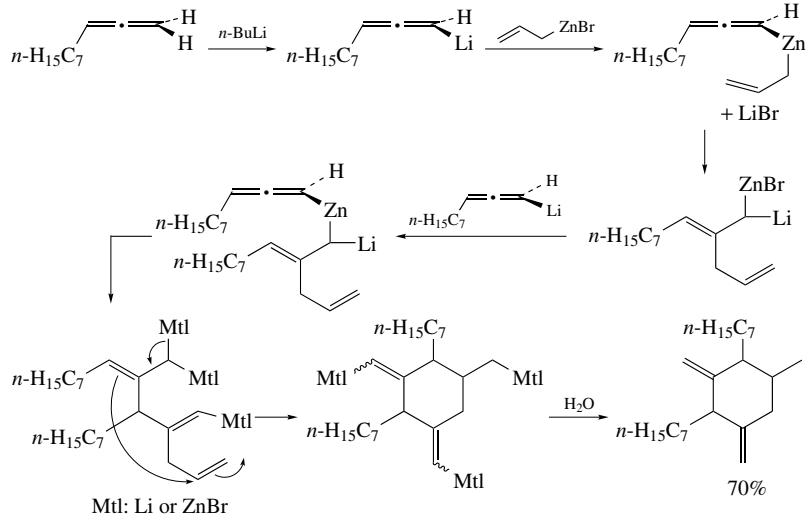

(41)

When butyllithium was added to thioethyl-substituted enyne, a carbolithiation reaction occurs to give the allenyllithium species, which may further react with allylzinc (equation 42). This reaction affords thioalkyl-substituted *gem*-dimetal[66].

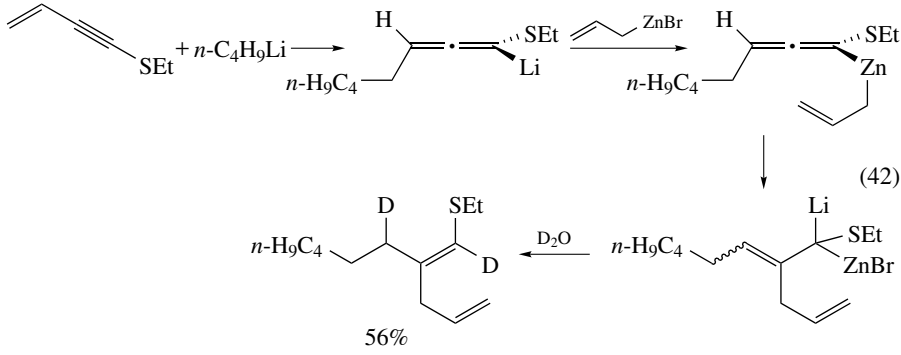

F. Nucleophilic Cyclopropanation

The most common method to prepare cyclopropenyl derivatives is the reaction between an electrophilic carbenoid and an alkene. On the other hand, sp^3-geminated organodimetal compounds possess two nucleophilic sites on the same carbon, so should lead to nucleophilic [2 + 1] reaction with 1,2-diketones. Indeed, the reaction of bis(iodozincio)methane (**3**) with 1,2-diketones shows a novel [2 + 1] reaction to form *cis*-cyclopropanediol diastereoselectively as shown in Scheme 34[67].

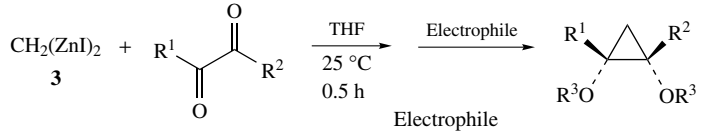

	Electrophile	
$R^1 = R^2 = Ph$	Ac_2O	69% ($R^3 = Ac$)
$R^1 = R^2 = Ph$	Me_3SiCl	78% ($R^3 = Me_3Si$)
$R^1 = Ph$, $R^2 = CH_3$	H_3O^+	80% ($R^3 = H$)
$R^1 = R^2 = CH_3CH_2$	Ac_2O	59% ($R^3 = Ac$)

SCHEME 34

The reaction pathway of **3** and 2,3-dioxobutane was profiled by *ab initio* calculation. It was rationalized that the initial complex of this transformation was a face-to-face complex. The sequential attack of **3** on 1,2-diketone proceeds in *s*-cis fixed conformation. In this complex, **3** worked as a bidentate Lewis acid. The detailed structural information determined by calculation of the initial complex is shown in Scheme 35. The dihedral angle O(1)−C(1)−C(2)−O(2) is 47.7°. The distortion from a flat configuration (i.e. dihedral angle = 0 or 180°) suppresses the deprotonation of the methyl group that should have lead to the unfavorable enolization of the diketone[68].

The same type of reaction between **3** and α-ketoimime is also known to give *cis*-α-aminocyclopropanol, as shown in Scheme 36. The reaction proceeds also with high diastereoselectivity[69].

Epoxyketone is also a good electrophile for the reagent **3** to form the cyclopropane ring. The first step of the reaction is the diastereoselective attack of the ketone by **3**, followed by

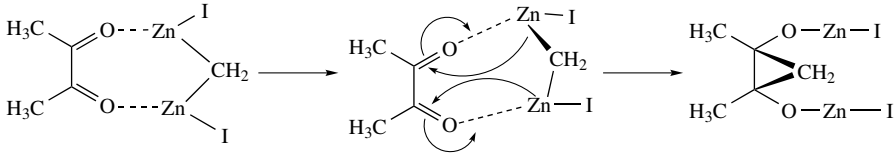

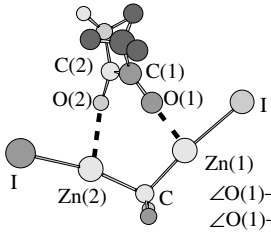

SCHEME 35

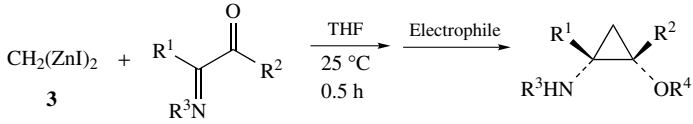

	Electrophile	
$R^1 = R^2 = Ph$, $R^3 = Ts$	H_3O^+	97% ($R^4 = H$)
$R^1 = R^2 = Ph$, $R^3 = Ts$	Me_3SiCl	>99% ($R^4 = Me_3Si$)
$R^1 = R^2 = R^3 = Ph$	H_3O^+	>99% ($R^4 = H$)
$R^1 = R^2 = 2$-Naphtyl, $R^3 = Ts$	Me_3SiCl	>99% ($R^4 = Me_3Si$)

SCHEME 36

a stereospecific reaction of the remaining alkylzinc halide to the epoxide with inversion. As shown in equation 43, an optically active substrate afforded a cyclopropanol derivative in an optically active form without any loss of optical purity[70].

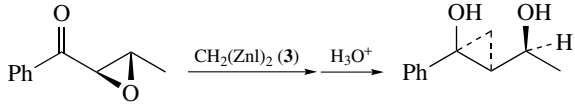

(43)

Reaction of bis(iodozincio)methane (**3**) with β-acylcrotonate also afforded cyclopropane derivative (equation 44). As shown in equation 45, the cyclopropane ring in this product opens and reacts with an imine to give β-aminoalkanol derivatives diastereoselectively[71].

An alkoxy group at the γ-position induces a cyclopropanation reaction of the dimetallic species as shown in equation 46. The formation of the *gem*-dimetal species proceeded diastereoselectively as described above. The ring closure proceeds with inversion of configuration to form stereospecifically the cyclopropane ring. An alkoxy substituent at the γ-position of the allylzinc reagent also induces the cyclopropanation reaction (equation 47)[61a, 72].

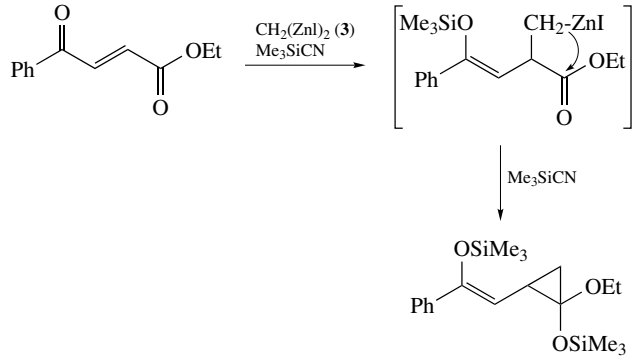

(44)

99% (*Z*-only)

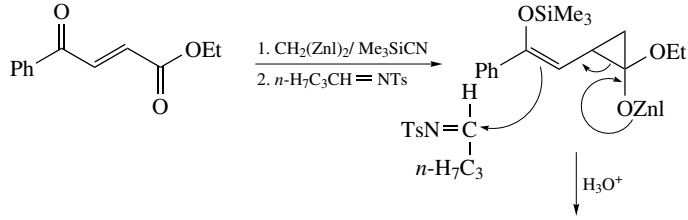

(45)

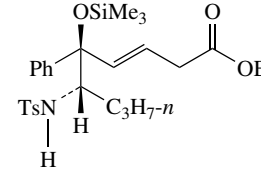

92%
Single diastereomer

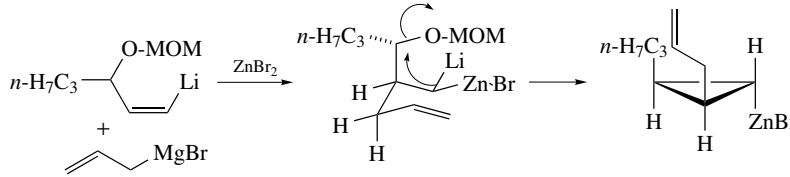

(46)

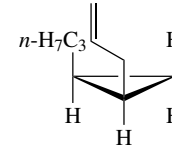

70%

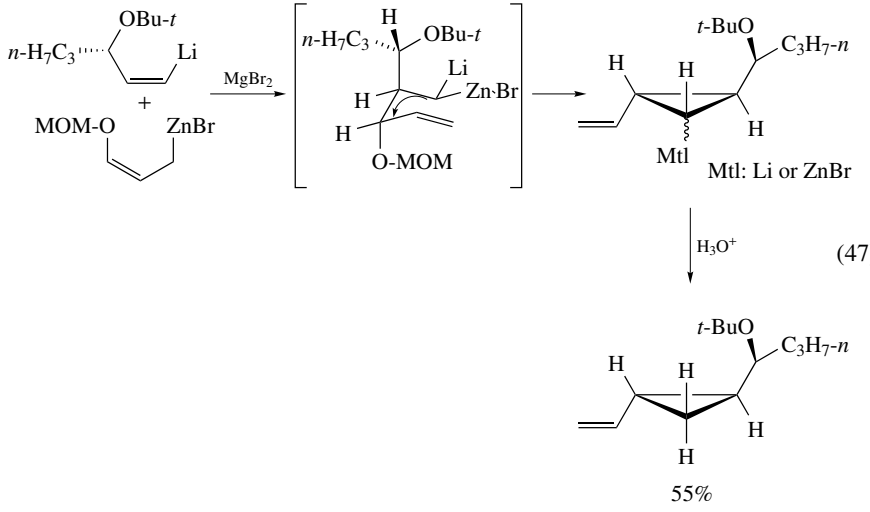

(47)

In these examples, the obtained cyclopropylmetal derivatives were protonolyzed. As shown in equation 48, further C−C bond formation is also possible via a copper transmetallation followed by addition of electrophiles[73].

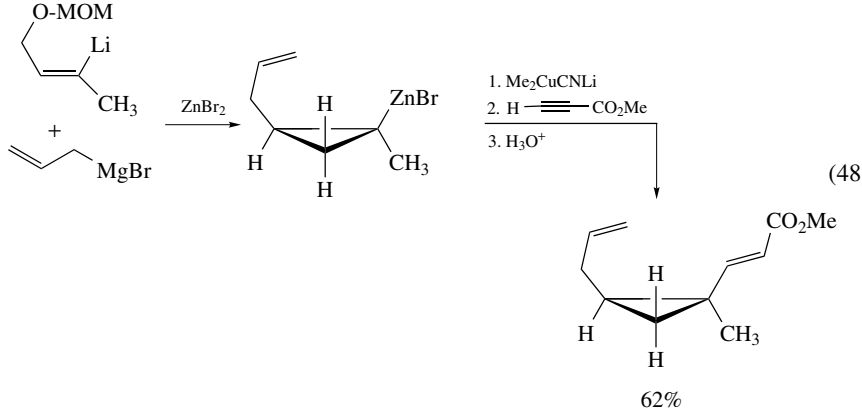

(48)

G. Pinacolone Rearrangement with Unusual Diastereospecificity

Treatment of 2,3-epoxyalkanol with bis(iodozincio)methane (**3**) gave homoallylic alcohol derivatives (equation 49). The formation can be explained via a pinacolone rearrangement followed by methylenation reaction (equation 50)[74]. The rearrangement is induced by the presence of bis(iodozincio)methane (**3**).

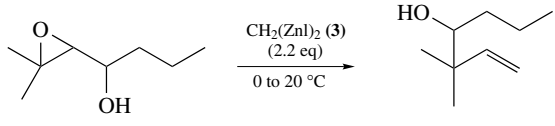

(49)

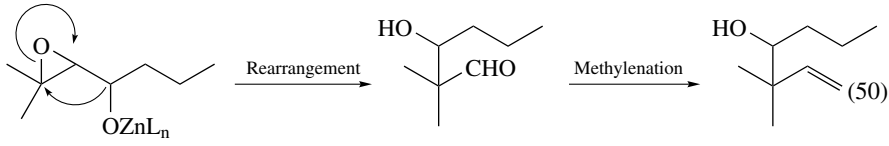

L_n: -I or -CH_2ZnI

When an optically active epoxide is treated with bis(iodozincio)methane **3**, the homoallylic alcohol is obtained with a slight loss of enantiomeric purity (equation 51). The absolute configuration of the product showed that the migrating hydroxymethyl group comes from the front side of the C−O group. The migration occurs with retention of configuration[74–76].

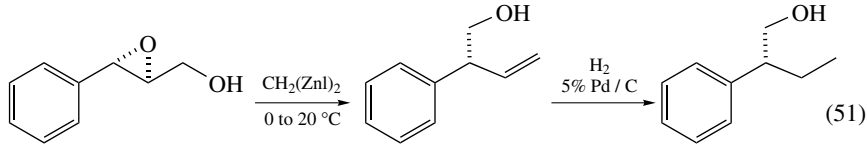

75%

(2*S*, 3*S*/2*R*, 3*R* = 99.5/0.5) (*S*/*R* = 4/96) $[\alpha]^{23}_D$ −15.0 ± 2.5 ($CHCl_3$, *c* 1.00)

H. 1,1-Dimetal Species from Zincated Hydrazone and Alkenylmetal

Nakamura and coworkers showed that the addition reaction of zincated hydrazone to vinylmagnesium halide as electrophile gives the sp^3-geminated organodimetal reagent (Scheme 37). The reaction pathway can be considered as a metalla-aza-Claisen-type

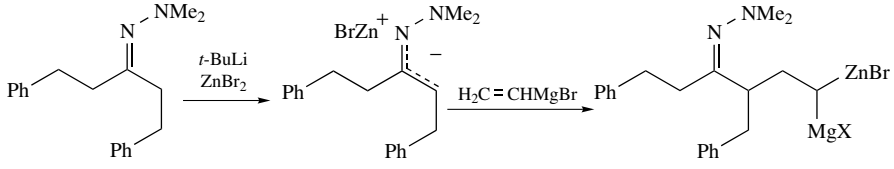

Electrophile[1]	Electrophile[2]	R^1	R^2	Yield(%)
t-BuOH	methyl vinyl ketone/CuCN	-H	-$CH_2CH_2COCH_3$	33
t-BuOH	Allyl bromide/CuCN	-H	-CH_2CH=CH_2	82
MeSSMe	Allyl bromide	-SMe	-CH_2CH=CH_2	84

1. Electrophile[1]
2. Electrophile[2]

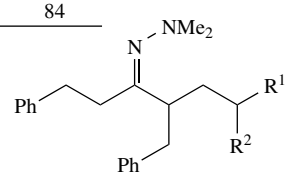

SCHEME 37

rearrangement. The obtained *gem*-dimetal species can be used for further transformation. As shown in equation 52, treatment of the prepared *gem*-dimetal species with aldehyde gives *E*-alkene diastereoselectively[14, 77].

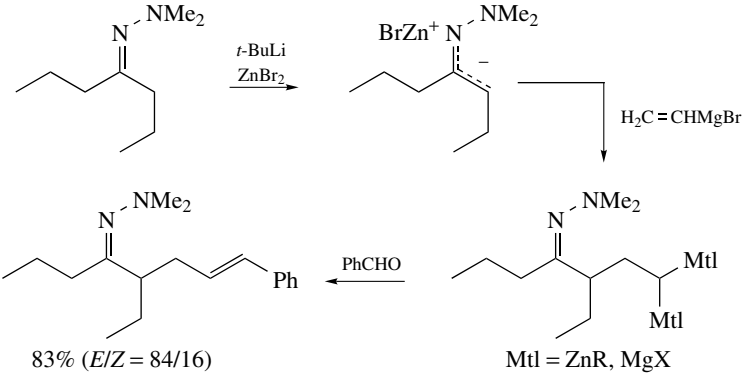

(52)

As shown in equation 53, when the zincated hydrazone, prepared from hydrazone by treatment with 2 equivalents of *t*-butyllithium and zinc(II) bromide, is treated with alkenylborane, the α-borylorganozinc is obtained with high diastereoselectivity. This pseudo-*gem*-dimetal species reacts with allyl halide stereospecifically. Through the transformation, three stereogenic centers are constructed diastereoselectively[77].

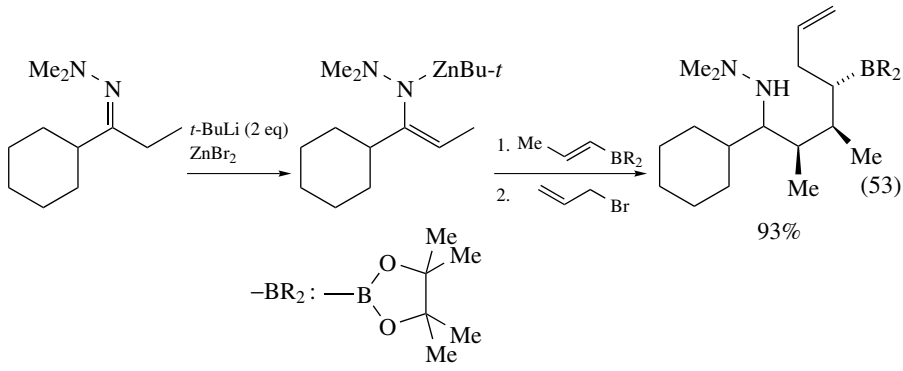

(53)

I. *gem*-Dizincio Reagent Working as Carbenoid

Bis(iodozincio)iodomethane was prepared from diethylzinc and iodoform as shown in equation 54 by Charette and coworkers[78]. This prepared bis(iodozincio)iodomethane possesses both a carbenoid and a *gem*-dimetal species, and therefore reacts as a zinciomethyl carbenoid.

(54)

As shown in equation 55, when the benzyl ether of *cis*-2-buten-1,4-diol is treated with bis(iodozincio)iodomethane, the cyclopropylzinc intermediate is obtained and reacts with various electrophiles. The obtained cyclopropyl derivative has all-*cis* configuration. In this reaction, zinc halide, which is present in the solution, plays an important role[79].

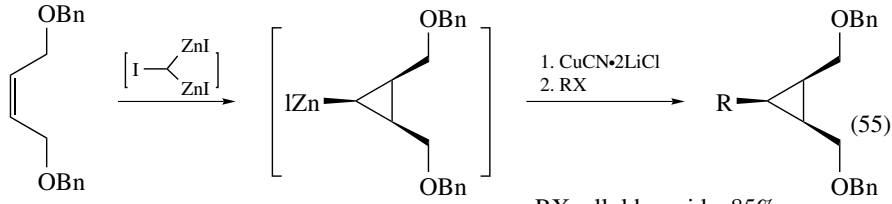

(55)

RX: allyl bromide 85%
benzoyl chloride 84%

IV. PREPARATION AND REACTION OF sp^2-GEMINATED ORGANODIZINC REAGENTS

The preparation and reaction of sp^2-geminated organodizinc reagents is an attractive topic of research, since these species should be an important precursor for stereoselective synthesis of alkene[1b, 80]. One method was based on the hydrometallation or carbometallation reaction of metal acetylide. As terminal alkyne is easily converted into the corresponding zinc acetylide, the hydrozirconation of such species gives sp^2-geminated organodimetal compound, which reacts with aldehyde to afford allene (equation 56)[81]. Titanocene dichloride catalyzed the addition of trimethylaluminum to the zinc acetylide to give the sp^2-geminated organodimetal species via a carbometallation reaction (equation 57)[82].

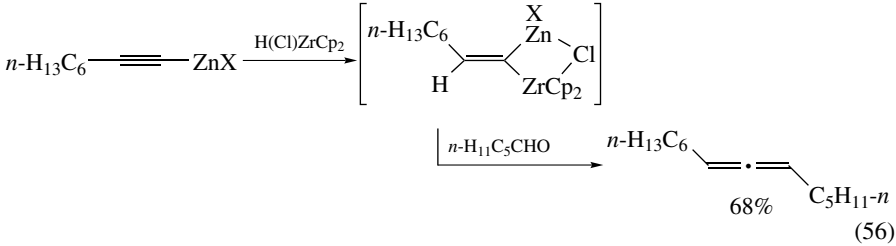

(56)

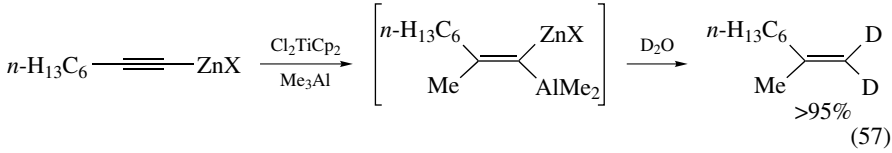

(57)

Zinc(II) halide mediated Gaudemar/Normant-type allylmetallation to metal acetylide is also an efficient route. As shown in Scheme 38, the obtained sp^2-geminated organodizinc reagent reacts with various electrophiles[83].

In the dimetal species described in Scheme 38, one of the two C−metal bonds can react selectively with a source of Cl^+ to give the corresponding sp^2-carbenoid species.

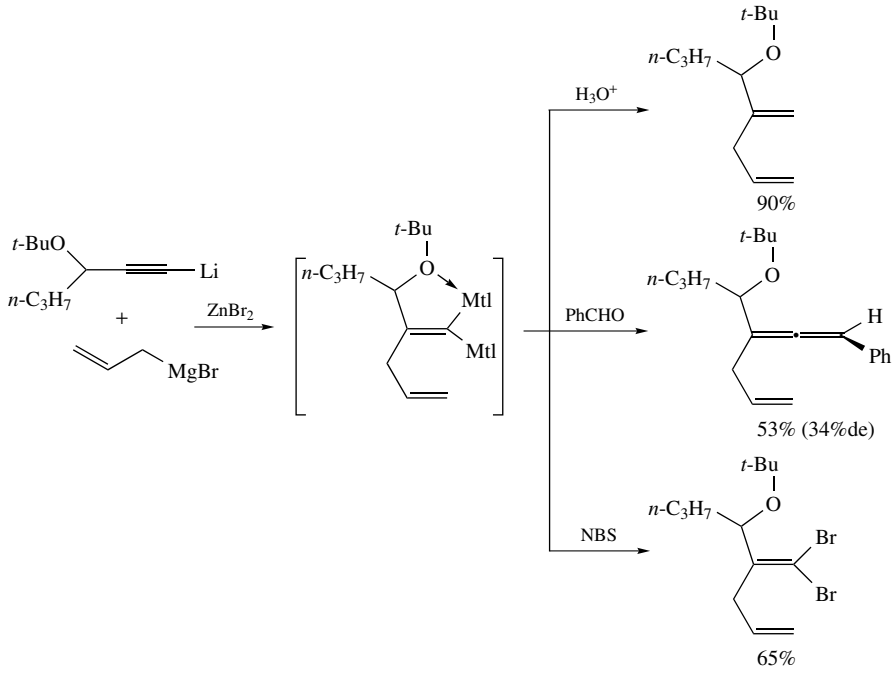

SCHEME 38

This carbenoid undergoes a Fritsch–Buttenberg–Wiechell rearrangement[84] when warmed at room temperature, to give the internal acetylene derivative (equation 58)[85].

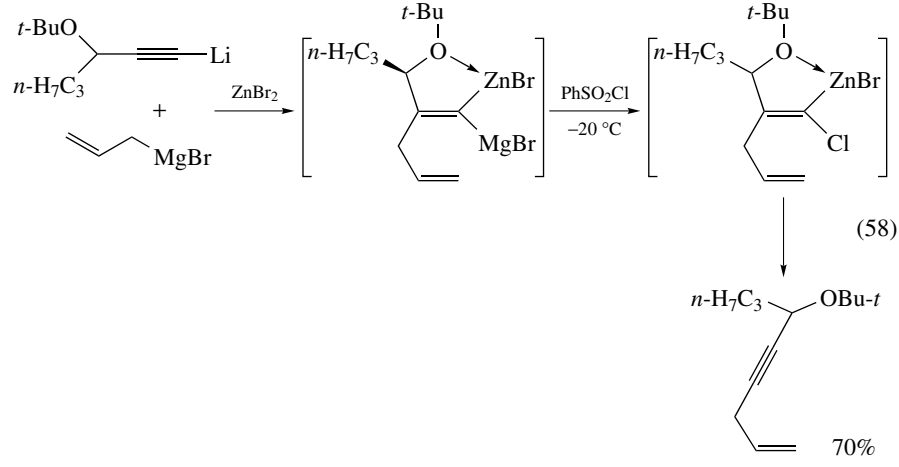

(58)

This Gaudemar/Normant type allylmetallation proceeds diastereoselectively when crotylmagnesium bromide is used. As shown in equation 59, the allyl alcohol can be obtained diastereoselectively via the corresponding sp^2-geminated organodimetal.

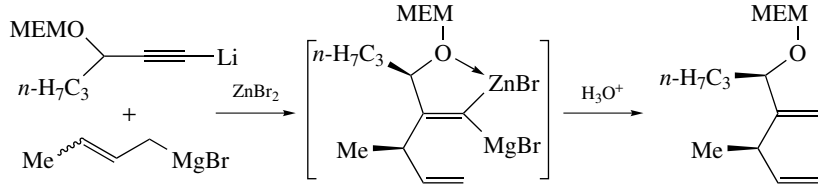

(59)

60% (*syn*/*anti* = 92/8)

The intermediary formed sp^2-geminated organodimetal in equation 59 also undergoes the Fritsch–Buttenberg–Wiechell rearrangement, once transformed into alcohol, to give diastereomerically enriched alkynol (equation 60)[85].

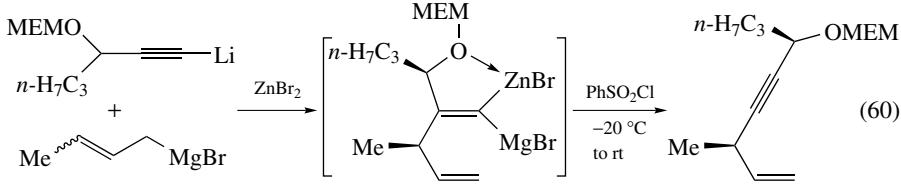

(60)

52% (*syn*/*anti* = 92/8)

Intramolecular nucleophilic reaction of sp^2-geminated organodimetal species gives cycloalkyl metal derivative, which can be converted into the corresponding alkenyl iodide. The iodide can be used for further transition-metal-catalyzed cross-coupling reaction (equations 61 and 62)[86].

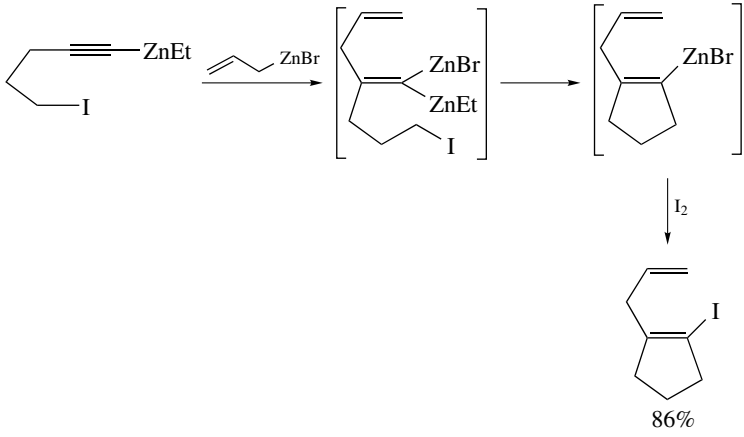

(61)

86%

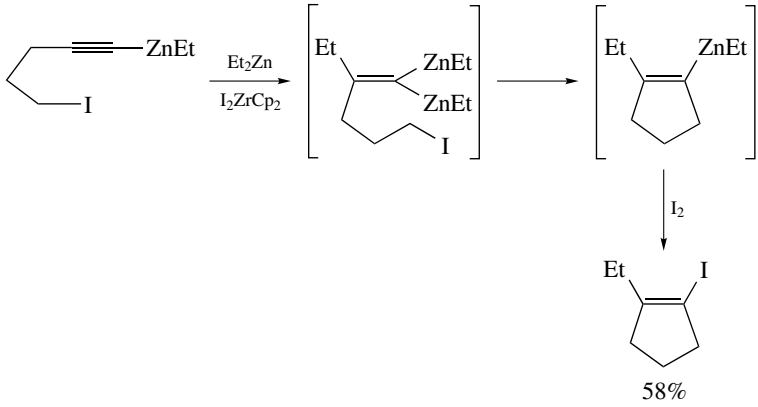

(62)

V. CONCLUSION

As shown here, 1,1-bismetallated species reagents containing zinc atom have been widely used for highly chemo- and diastereoselective molecular transformation. Not only zinc derivatives, but also magnesium, lithium and chromium derivatives present high potentials in organic synthesis. Although new synthetic transformations have been elegantly developed in the last decade, the application to enantioselective synthesis is still in its infancy. This fascinating research will, without any doubt, see a tremendous evolution in the next few years.

VI. REFERENCES

1. (a) I. Marek and J. F. Normant, *Chem. Rev.*, **96**, 3241 (1996).
   (b) I. Marek, *Chem. Rev.*, **100**, 2887 (2000).
   (c) J. F. Normant, *Acc. Chem. Res.*, **34**, 640 (2001).
   (d) P. Knochel, in *Handbook of Grignard Reagents* (Eds. G. S. Silverman and P. E. Rakita), Marcel Dekker, New York, 1996, p. 633.
   (e) J. F. K. Müller, *Eur. J. Inorg. Chem.*, 789 (2000).
2. (a) S. Matsubara, K. Oshima and K. Utimoto, *J. Organomet. Chem.*, **617–618**, 39 (2001).
   (b) S. Matsubara and K. Oshima, *Proc. Jpn. Acad.*, **79**, 71 (2003).
   (c) S. Matsubara and K. Oshima, in *Modern Carbonyl Olefination* (Ed. T. Takeda), Chap. 5, Wiley-VCH, Weinheim, 2004.
   (d) I. Marek and J. F. Normant, in *Organozinc Reagents* (Eds. P. Knochel and P. Jones), Chap. 30, Oxford University Press, New York, 1999.
3. P. Turnbull, K. Syoro and J. H. Fried, *J. Am. Chem. Soc.*, **88**, 4764 (1966).
4. (a) H. Hashimoto, M. Hida and S. Miyano, *Kogyo Kagaku Zasshi*, **69**, 174 (1966); *Chem. Abstr.*, **65**, 20492 (1966).
   (b) H. Hashimoto, M. Hida and S. Miyano, *J. Organomet. Chem.*, **10**, 518 (1967).
5. The Nysted reagent [L. N. Nysted, US Patent 3 865 848 (1975); *Chem. Abstr.*, **83**, 10406q (1975)] is commercially available from Aldrich Co.
6. (a) K. Takai, Y. Hotta, K. Oshima and H. Nozaki, *Tetrahedron Lett.*, **27**, 2417 (1978).
   (b) J.-I. Hibino, T. Okazoe, K. Takai and H. Nozaki, *Tetrahedron Lett.*, **26**, 5579 and 5581 (1986).
7. J. J. Eisch and A. Piotrowski, *Tetrahedron Lett.*, **24**, 2043 (1983).
8. (a) L. Lombardo, *Tetrahedron Lett.*, **23**, 4293 (1982).
   (b) L. Lombardo, *Org. Synth.*, **65**, 81 (1987).
9. S. Matsubara, T. Mizuno, T. Otake, M. Kobata, K. Utimoto and K. Takai, *Synlett*, 1369 (1998).

10. (a) M. Gaudemar, *C. R. Acad. Sci. Paris*, **273**, 1669 (1971).
(b) M. Bellassoued, Y. Frangin and M. Gaudemar, *Synthesis*, 205 (1977).
11. (a) P. Knochel and J. F. Normant, *Tetrahedron Lett.*, **27**, 1039 and 1043 (1986).
(b) P. Knochel and J. F. Normant, *Tetrahedron Lett.*, **27**, 4427 and 4431 (1986).
12. I. Marek, P. R. Schreiner and J. F. Normant, *Org. Lett.*, **1**, 929 (1999).
13. (a) A. Hirai, M. Nakamura and E. Nakamura, *J. Am. Chem. Soc.*, **121**, 8665 (1999).
(b) A. Hirai, M. Nakamura and E. Nakamura, *J. Am. Chem. Soc.*, **122**, 11791 (2000).
14. E. Nakamura, K. Kubota and G. Sakata, *J. Am. Chem. Soc.*, **119**, 5457 (1997).
15. (a) H. E. Simmons and R. D. Smith, *J. Am. Chem. Soc.*, **80**, 5323 (1958).
(b) A. B. Charette and J. F. Marcoux, *Synlett*, 1197 (1995).
16. P. T. Harrison, R. J. Rawson, P. Turnbull and J. H. Fried, *J. Org. Chem.*, **36**, 3515 (1971).
17. (a) X. Chen, E. R. Hortelano, E. L. Eliel and S. V. Frye, *J. Am. Chem. Soc.*, **114**, 1778 (1992).
(b) K. Utimoto, A. Nakamura and S. Matsubara, *J. Am. Chem. Soc.*, **112**, 8189 (1990).
18. K. Takai, T. Kakiuchi, Y. Kataoka and K. Utimoto, *J. Org. Chem.*, **59**, 2668 (1994).
19. (a) S. Matsubara, K. Oshima, H. Matsuoka, K, Matsumoto, K. Ishikawa and E. Matsubara, *Chem. Lett.*, **34**, 952 (2005).
(b) S. Matsubara, Y. Yamamoto and K. Utimoto, *Synlett*, 1471 (1998).
20. (a) J. A. Miller and M. J. Nunn, *Tetrahedron Lett.*, **15**, 2691 (1974).
(b) R. L. Letsinger and C. W. Kammeyer, *J. Am. Chem. Soc.*, **73**, 4476 (1951).
(c) M. E. Jung, A. B. Mossman and M. A. Lyster, *J. Org. Chem.*, **43**, 3698 (1978).
(d) A. Garcia Martinez, A. Herrera Fernandez, R. Martinez Alvarez, A. Garcia Fraile, J. Bueno Calderon and J. Barcina, *Synthesis*, 1076 (1986).
(e) L. Aufauvre, P. Knochel and I. Marek, *Chem. Commun.*, 2207 (1999).
(f) C. C. Gonzalez, A. R. Kennedy, E. I. Leon, C. Riesco-Fagundo and E. Suarez, *Angew. Chem., Int. Ed.*, **40**, 2326 (2001).
21. J.-M. Cloarec and A. B. Charette, *Org. Lett.*, **6**, 4731 (2004).
22. S. Matsubara, Y. Otake, T. Morikawa and K. Utimoto, *Synlett*, 1315 (1998).
23. P. C. Andrews, C. L. Raston, B. W. Skelton and A. H. White, *Organometallics*, **17**, 779 (1998).
24. S. Matsubara, H. Yoshino, K. Utimoto and K. Oshima, *Synlett*, 495 (2000).
25. S. Matsubara, Y. Otake, Y. Hashimoto and K. Utimoto, *Chem. Lett.*, 747 (1999).
26. I. Marek, J. M. Lefrançois and J. F. Normant, *J. Org. Chem.*, **59**, 4154 (1994).
27. (a) A. Maercker, *Org. React.*, **14**, 270 (1965).
(b) B. E. Maryanoff and A. B. Reits, *Chem. Rev.*, **89**, 863 (1989).
28. (a) M. Schlosser, *Top. Stereochem.*, **5**, 1 (1970).
(b) B. Schaub, T. Jenny and M. Schlosser, *Tetrahedron Lett.*, **25**, 4097 (1984).
29. F. Z. Dörwart, in *Metal Carbenes in Organic Synthesis*, Wiley-VCH, Weinheim, 1999.
30. T. Mukaiyama, T. Sato and J. Hanna, *Chem. Lett.*, 1041 (1973).
31. (a) S. Matsubara, M. Sugihara and K. Utimoto, *Synlett*, 313 (1998).
(b) W. Tochtermann, S. Bruhn, M. Meints, C. Wolff, E.-M. Peters, K. Peters and H. G. von Schnering, *Tetrahedron*, **51**, 1623 (1995).
(c) R. Gleiter, T. Herb and J. Hofmann, *Synlett*, 987 (1996).
32. K. Ukai, D. Arioka, H. Yoshino, H. Fushimi, K. Oshima, K. Utimoto and S. Matsubara, *Synlett*, 513 (2001).
33. S. Matsubara and Y. Yokota, unpublished results.
34. A. R. Hermes and G. S. Girolami, *Inorg. Synth.*, **32**, 309 (1998).
35. S. Matsubara, Y. Hashimoto, T. Okano and K. Utimoto, *Synlett*, 1411 (1999).
36. S. P. Naula and H. K. Sharma, *Inorg. Synth.*, **24**, 181 (1985).
37. Y. Hashimoto, U. Mizuno, H. Matsuoka, T. Miyahara, M. Takakura, M. Yoshimoto, K. Oshima, K. Utimoto and S. Matsubara, *J. Am. Chem. Soc.*, **123**, 1503 and 4869 (2001).
38. S. Matsubara, K. Ukai, T. Mizuno and K. Utimoto, *Chem. Lett.*, 825 (1999).
39. K. Nozaki, N. Kosaka, V. M. Graubner and T. Hiyama, *Macromolecules*, **34**, 6167 (2001).
40. H. Yoshino, M. Kobata, Y. Yamamoto, K. Oshima and S. Matsubara, *Chem. Lett.*, **33**, 1224 (2004).
41. I. Marek, J. M. Lefrançois and J. F. Normant, *J. Org. Chem.*, **59**, 4154 (1994).
42. (a) T. Okazoe, K. Takai, K. Oshima and K. Utimoto, *J. Org. Chem.*, **52**, 4410 (1987).
(b) K. Takai, O. Fujimura, Y. Kataoka and K. Utimoto, *Tetrahedron Lett.*, **30**, 211 (1989).

43. C. E. Tucker and P. Knochel, *J. Am. Chem. Soc.*, **113**, 9888 (1991).
44. S. Matsubara, *J. Org. Synth. Soc. Jpn.*, **58**, 118 (2000).
45. I. Klement, K. Lennick, C. E. Tucker and P. Knochel, *Tetrahedron Lett.*, **34**, 4623 (1993).
46. P. Knochel, C. Xiao and M. C. P. Yeh, *Tetrahedron Lett.*, **29**, 6697 (1988).
47. (a) K. Utimoto, N. Toda, T. Mizuno, M. Kobata and S. Matsubara, *Angew. Chem., Int. Ed. Engl.*, **36**, 2804 (1997).
    (b) H. Yoshino, N. Toda, M. Kobata, K. Ukai, K. Oshima, K. Utimoto, and S. Matsubara, *Chem. Eur. J.*, **12**, 721 (2005).
48. S. Matsubara, K. Ukai, N. Toda, K. Utimoto and K. Oshima, *Synlett*, 995 (2000).
49. Z. Ikeda, K. Oshima, and S. Matsubara, Org. Lett., 7, 4859 (2005).
50. (a) D. Hoppe and T. Hense, *Angew. Chem., Int. Ed. Engl.*, **36**, 2282 (1997).
    (b) P. Beak, A. Basu, D. J. Gallagher and Y. S. Park, *Acc. Chem. Res.*, **29**, 552 (1996).
    (c) V. Schulze and R. W. Hoffmann, *Chem. Eur. J.*, **54**, 337 (1999).
    (d) C. D. Graf and P. Knochel, *Tetrahedron*, **55**, 8801 (1999).
    (e) E. Hupe and P. Knochel, *Org. Lett.*, **3**, 127 (2001).
51. S. Matsubara, N. Toda, M. Kobata and K. Utimoto, *Synlett*, 987 (2000).
52. Y. Uozumi and T. Hayashi, *J. Am. Chem. Soc.*, **113**, 9585 (1991).
53. S. Matsubara, K. Kawamoto and K. Utimoto, *Synlett*, 267 (1998).
54. S. Matsubara, D. Arioka and K. Utimoto, *Synlett*, 1411 (1999).
55. S. Matsubara, H. Yamamoto, D. Arioka, K. Utimoto and K. Oshima, *Synlett*, 1202 (2000).
56. C. E. Tucker, S. A. Rao and P. Knochel, *J. Org. Chem.*, **55**, 5446 (1990).
57. C. E. Tucker and P. Knochel, *Synthesis*, 530 (1993).
58. N. Chinkov, G. Sklute, H. Chechik, A. Abramovitch, D. Amsallem, J. Varghese, S. Majumdar and I. Marek, *Pure Appl. Chem.*, **76**, 517 (2004).
59. G. Sklute, D. Amsallem, A. Shabli, J. P. Varghese and I. Marek, *J. Am. Chem. Soc.*, **125**, 11776 (2003).
60. I. Marek and J. F. Normant, *Tetrahedron Lett.*, **32**, 5973 (1991).
61. (a) D. Brasseur, I. Marek and J. F. Normant, *Tetrahedron*, **52**, 7235 (1996).
    (b) A. Bähr, I. Marek and J. F. Normant, *Tetrahedron Lett.*, **37**, 5873 (1996).
62. D. Brasseur, H. Rezaei, A. Fuxa, A. Alexakis, P. Mangeney, I. Marek and J. F. Normant, *Tetrahedron Lett.*, **39**, 4821 (1998).
63. D. Brasseur, I. Marek and J. F. Normant, *C. R. Acad. Sci. Paris*, **1**(IIC), 621 (1998).
64. F. Ferreira and J. F. Normant, *Eur. J. Org. Chem.*, 3581 (2000).
65. (a) J. F. Normant, J. C. Quirion, A. Alexakis and Y. Masuda, *Tetrahedron Lett.*, **30**, 3955 (1989).
    (b) J. F. Normant and J. C. Quirion, *Tetrahedron Lett.*, **30**, 3959 (1989).
66. L. Labaudinière and J. F. Normant, *Tetrahedron Lett.*, **33**, 6139 (1992).
67. K. Ukai, K. Oshima and S. Matsubara, *J. Am. Chem. Soc.*, **122**, 12047 (2000).
68. S. Matsubara, K. Ukai, H. Fushimi, Y. Yokota, H. Yoshino, K. Oshima, K. Omoto, A. Ogawa, Y. Hioki and H. Fujimoto, *Tetrahedron*, **58**, 8255 (2002).
69. K. Nomura, K. Oshima and S. Matsubara, *Tetrahedron Lett.*, **45**, 5957 (2004).
70. K. Nomura and S. Matsubara, *Angew. Chem., Int. Ed.*, **44**, 5860 (2005).
71. T. Hirayama, K. Oshima and S. Matsubara, *Angew. Chem., Int. Ed.*, **44**, 3293 (2005).
72. D. Beruben, I. Marek, J. F. Normant and N. Platzer, *J. Org. Chem.*, **60**, 2488 (1995).
73. D. Beruben, I. Marek, J. F. Normant and N. Platzer, *Tetrahedron Lett.*, **34**, 7575 (1993).
74. S. Matsubara, H. Yamamoto and K. Oshima, *Angew. Chem., Int. Ed.*, **41**, 2837 (2002).
75. (a) K. Maruoka, T. Ooi, S. Nagahara and H. Yamamoto, *Tetrahedron*, **47**, 6983 (1991).
    (b) M. E. Jung and K. L. Anderson, *Tetrahderon Lett.*, **38**, 2605 (1997).
76. A. Job, C. F. Janeck, W. Bettray, R. Peters and D. Enders, *Tetrahedron*, **58**, 2253 (2002).
77. M. Nakamura, T. Hatakeyama, K. Hara, H. Fukudome and E. Nakamura, *J. Am. Chem. Soc.*, **126**, 14344 (2004).
78. (a) A. B. Charette, A. Gagnon and J. F. Fournier, *J. Am. Chem. Soc.*, **124**, 386 (2002).
    (b) J. F. Fournier and A. B. Charette, *Eur. J. Org. Chem.*, 1401 (2004).
79. C. Zhao, D. Wang and D. L. Phillips, *J. Am. Chem. Soc.*, **124**, 12903 (2002).
80. I. Creton, I. Marek and J. F. Normant, *Synthesis*, 1499 (1996).
81. (a) J. Schwartz and D. Hart, *J. Am. Chem. Soc.*, **96**, 8115 (1974).
    (b) C. E. Tucker and P. Knochel, *J. Am. Chem. Soc.*, **113**, 9888 (1991).

82. D. E. Van Horn, L. F. Valente, M. J. Idacavage and E. Negishi, *J. Organomet. Chem.*, **156**, C20 (1978).
83. I. Creton, I. Marek and J. F. Normant, *Tetrahedron Lett.*, **36**, 7451 (1995).
84. (a) P. Fritsch, *Liebigs Ann. Chem.*, **272**, 319 (1894).
(b) W. P. Buttenberg. *Liebigs Ann. Chem.*, **272**, 324 (1894).
(c) H. Wiechell, *Liebigs Ann. Chem.*, **272**, 337 (1894).
85. I. Creton, H. Rezaei, I. Marek and J. F. Normant, *Tetrahedron Lett.*, **40**, 1899 (1999).
86. E. Negishi, H. Sawada, J. M. Tour and Y. Wei, *J. Org. Chem.*, **53**, 913 (1988).

CHAPTER **15**

The chemistry of organozincate compounds

TOSHIRO HARADA

Department of Chemistry and Materials Technology, Kyoto Institute of Technology, Matsugasaki, Sakyo-ku, Kyoto 606-8585, Japan
Fax: +81 75 724 7580; e-mail: harada@chem.kit.ac.jp

I. INTRODUCTION

Since a diorganozinc compound has two vacant $4p$ orbitals on the zinc atom, it can accommodate two or four electrons from organometallic derivatives to form a tri- or tetracoordinated ate complex (**1** or **2**), called an organozincate. Organozincates have been known since 1858, when Wanklyn prepared Et_3ZnNa and Et_3ZnK from a reaction between Et_2Zn and the alkali metal[1]. In 1951, Wittig and coworkers reported that Ph_3ZnLi metalates fluorene and adds to benzophenone[2]. However, very little has been reported before the initial work of Isobe, Goto, and coworkers in 1977 on their use in organic synthesis for the conjugate addition of trialkylzincates to cyclic enones[3]. Now, organozincates constitute a useful class of organozinc reagents with characteristic reactivities.

The chemistry of organozinc compounds
Edited by Z. Rappoport and I. Marek

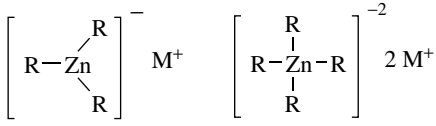

(1) **(2)**

Organozincates are generally more reactive than organozinc halides and diorganozincs. Like Grignard reagents, zincates add to ketone carbonyl groups and lead to ring-opening of epoxides without the aid of catalysts or promoters. Zincates are reactive enough to undergo halogen–zinc exchange with organic halides. In spite of these reactivities, zincates exhibit compatibility with some functional groups. One of the characteristic features in their synthetic application is that they can be used for the creation of multiple carbon–carbon bonds in a one-pot reaction. For example, conjugate addition to α,β-unsaturated ketones and the subsequent reaction of the resulting zinc enolates with electrophiles furnish three-component coupling products (equation 1). Zincates bearing a leaving group at a proper position rearrange with 1,2-migration of the ate ligand to give homologated organozincs, which can subsequently be trapped with electrophiles (equation 2).

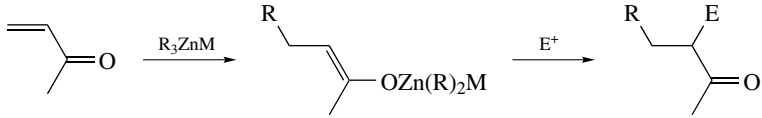

(1)

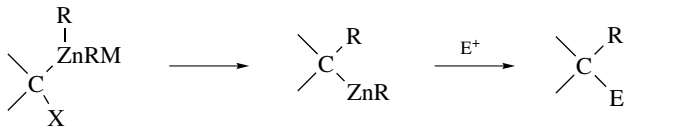

(2)

The solid state structures of a variety of zincates have been characterized by X-ray crystallographic analysis. These include not only homoleptic tri- and tetraorganozincates R_3ZnM (M = Li[4], MgX_5, Na, K[6]), $[R_3Zn]_2M$ (M = Ca[7], Ba[8], Mg[9]) and R_4ZnLi_2[4a, 10], but also mixed zincates $R^1(R^2)_2ZnM$ (M = Li[11], K[6]) and $R_2(Y)ZnLi$ (Y = RO[12], R_2N[11, 13]). In general, tri- and tetraorganozincates show trigonal and tetrahedral geometry of zinc atoms, respectively. The structures of zincates in solution, on the other hand, are difficult to be characterized and relatively more elusive[14]. This chapter describes the chemistry of organozincates with emphasis on their synthetic application and they are often represented by stoichiometric formulation. Preparative aspects of the topic have been reviewed[15]. An extensive review covering early publications has appeared[16].

II. PREPARATION OF ZINCATES

A. Preparation of Zincates by Ate-Complex Formation

Triorganozincates are prepared by the reaction of diorganozincs with organolithium or Grignard reagents (equation 3). More conveniently, a variety of zincates (R = alkyl, alkenyl, aryl, silyl) can be prepared by transmetalation of Zn^{II} salts such as $ZnCl_2$[17] and $ZnBr_2$ with three equivalents of the organometallic reagents (equation 4). Despite concurrent metal salt formation (LiCl, MgX_2), zincates prepared by this method can be used in many reactions without any differences in reactivity compared to salt-free zincates.

Mixed zincates $R^1(R^2)_2ZnLi$ are prepared either from $(R^2)_2Zn$ and R^1Li or by successive addition of R^2Li (2 equiv) and R^1Li (1 equiv) to ZnX_2. Sodium and potassium zincates are prepared from diorganozinc according to Wanklyn's procedure (equation 5)[1].

$$R_2Zn + \underset{M = Li, MgX}{RM} \xrightarrow[THF, ether]{} R_3ZnM \quad (3)$$

$$\underset{X = Cl, Br}{ZnX_2} + \underset{M = Li, MgX}{3\ RM} \xrightarrow[THF, ether]{} R_3ZnM + 2\ MX \quad (4)$$

$$R_2Zn + \underset{M = Na, K}{2/3\ M} \xrightarrow[benzene]{} 2/3\ R_3ZnM + 1/3\ Zn \quad (5)$$

Treatment of Me_3ZnLi with MeLi generates Me_4ZnLi_2 in equilibrium[14d], which, in turn, reacts with Me_3SiCN and Me_3SiNCS to give $Me_3Zn(CN)Li_2$ and $Me_3Zn(SCN)Li_2$, respectively (equations 6 and 7)[18]. These tetracoordinated zincates exhibit higher reactivity in comparison with the tricoordinated counterparts (*vide infra*).

$$Me_3ZnLi + MeLi \underset{THF}{\rightleftharpoons} Me_4ZnLi_2 \quad (6)$$

$$Me_4ZnLi_2 + \underset{Y = CN, SCN}{Me_3SiY} \xrightarrow[THF]{} \underset{Y = CN, SCN}{Me_3Zn(Y)Li_2} \quad (7)$$

B. Preparation of Mixed Zincates by Metalation

Zincates are reactive enough to metalate certain acidic hydrogens to give the corresponding mixed zincates. Common lithium triorganozincates react readily with terminal alkynes to generate alkynylzincates (equation 8)[19]. *o*-Functionalized arylzincates can be prepared by directed metalation with sterically hindered TMP-zincate **3**, generated by treatment of t-Bu_2Zn with lithium tetramethylpiperidide (equation 9)[20]. The metalation tolerates reactive functionalities such as ester and cyano groups. Lithiation of isoquinoline is difficult due to the reaction of the resulting α-lithio species with isoquinoline leading to dimer formation[21]. On the other hand, electron deficient heteroaromatics such as pyridine and isoquinoline are successfully metalated by **3** at the α position to give heteroarylzincates **4a** and **4b**. Regiochemistry in the zincation of bromopyridines is influenced significantly by the choice of amino-zincates (Scheme 1)[22]. TMP-zincate **3** reacts preferentially at the 6-position of 2-bromopyridine whereas a diisopropylaminozincate regioselectively metalates at the 3-position. The two aminozincates also show complementary selectivity toward 3-bromopyridine.

$$R^1{-}{\equiv}{-}H + (R^2)_3ZnLi \xrightarrow[THF]{} R^1{-}{\equiv}{-}Zn(R^2)_2Li \quad (8)$$

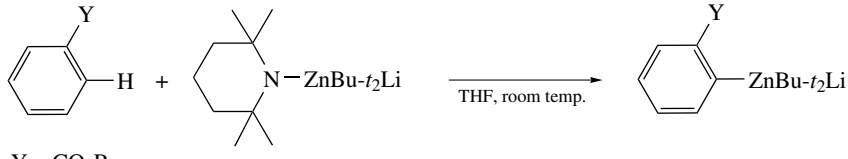

Y = CO_2R, $CONR_2$, CN

(3)

(9)

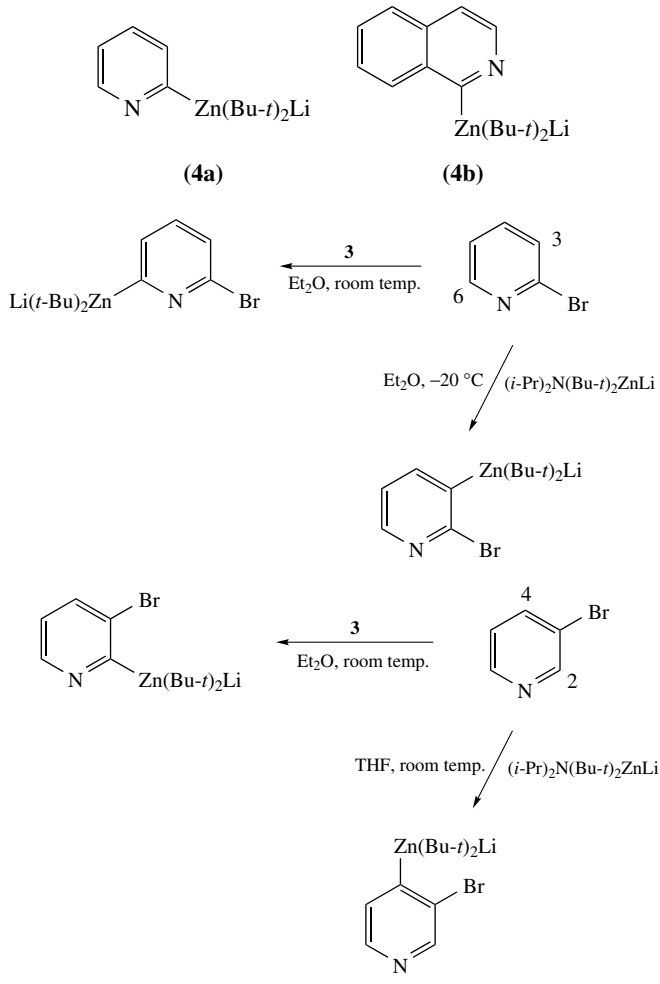

SCHEME 1

C. Preparation of Mixed Zincates by Halogen–Zinc Exchange Reaction

Lithium trialkylzincates undergo facile halogen–zinc exchange reaction with organic bromides, such as *gem*-dibromo and -bromochloro compounds, and bromoalkynes to give the corresponding mixed zincates (equation 10)[22–25,19]. For example, the exchange reaction of *gem*-dibromoalkenes is accomplished within 0.5 h at $-85\,^{\circ}C$ except for Me_3ZnLi, which requires higher temperature (equation 11)[23b]. The reactivity of zincates decreases roughly in the order *n*-Bu $\cong$ *s*-Bu > *t*-Bu > Me. No reaction was observed for Ph_3ZnLi. A preferential trend was observed for the exchange of the more sterically hindered bromine atom as shown by the selectivity described in Chart 1[26]. The corresponding lithium alkylidenecarbenoids [$R^1(R^2)C{=}C(Br)Li$], especially those with $R^2 = H$, are known to be unstable even at low temperature, undergoing a Fritsch–Buttenberg–Wiechell rearrangement

to alkynes ($R^1C{\equiv}CR^2$)[27]. Zincate carbenoids generated in equation 11 are stable enough to be used in further transformations (*vide infra*).

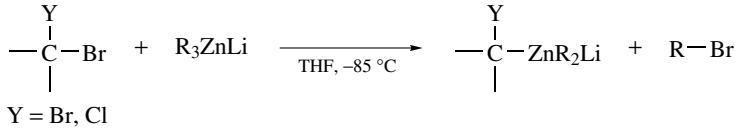

(10)

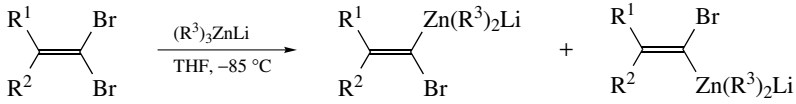

(11)

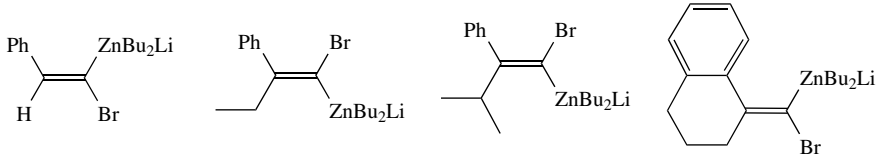

CHART 1. The ratio corresponds to that of major (shown) and minor zinates

Aryl iodides undergo facile exchange reaction at low temperature to give mixed arylzincates (equation 12)[28–30]. Reactions using Me_3ZnLi and *t*-Bu_3ZnLi tolerate reactive functionalities. Iodine–zinc exchange reaction of primary and secondary alkyl iodides also proceeds with *t*-Bu_3ZnLi at room temperature[29]. The trialkylzincates are not reactive toward aryl bromides. Generation of arylzincates from the bromides is possible by using more reactive tetracoordinated zincates. Me_4ZnLi_2 and $Me_3Zn(L)Li_2$ (L = CN, SCN) undergo facile and clean bromine–zinc exchange between 0 °C and room temperature (equation 13)[18]. The tetracoordinated zincates also undergo a tellurium–zinc exchange reaction (equation 14)[18c].

(12)

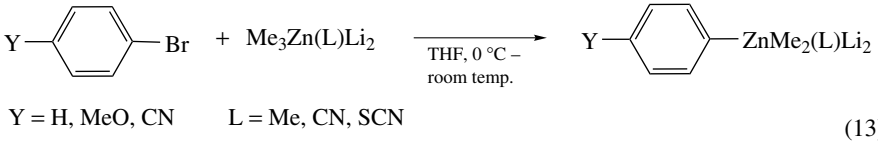

(13)

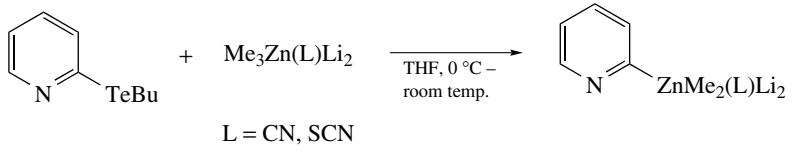

(14)

III. REACTION OF ZINCATES

A. Carbonyl Addition and Ring Opening of Epoxides

o-Functionalized arylzincates and heteroarylzincates prepared by metalation (equation 9) or by halogen–zinc exchange (equations 12–14) react with benzaldehyde to give the corresponding carbinols in high yields. The reactivity order of the ligands is an important factor when mixed zincates are used. The approximate order of Bu ≅ Ph > Me > *t*-Bu has been reported based on results shown in equation 15[29].

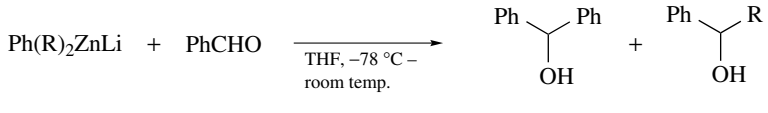

R = Bu	21:79
R = Me	93:7
R = *t*-Bu	100:0

(15)

An arylzincate, generated by iodine–zinc exchange of **5** with Me_3ZnLi, undergoes selective 6-*endo*-cyclization to give **6** (equation 16)[18c]. Tetracoordinated zincates exhibit an opposite regioselectivity leading to the formation of 5-*exo*-cyclization product **7**. The intermolecular ring-opening reaction of styrene oxide, however, is non-regioselective irrespective of the structure of zincates.

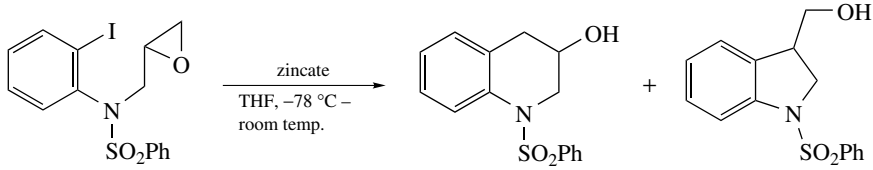

(5) **(6)** 6-*endo* **(7)** 5-*exo*

Zincate	**6**:**7**
Me_3ZnLi	96:4
Me_4ZnLi_2	13:87
$Me_3Zn(SCN)Li_2$	3:97
$Me_3Zn(CN)Li_2$	20:80

(16)

B. Conjugate Addition to α,β-Unsaturated Compounds

Triorganozincates react with unhindered α,β-unsaturated ketones, such as cycloalkenones and vinyl ketones, in a 1,4-fashion[3, 31, 32]. For the reaction with lithium zincates, prepared from RLi and $ZnCl_2$ (usually as its TMEDA complex), 1,4-addition takes place exclusively. On the other hand, the reaction of magnesium zincates derived from Grignard reagents is often accompanied by a minor formation of 1,2-adducts. The approximate reactivity order obtained from the product distribution using mixed zincates is $Me_3CCH_2 \ll Me_3C$, Me < Ph, Me_2CHCH_2 < Et, Bu, Me_2CH, $CH{:}CH_2 \ll Me_2PhSi$[32]. Therefore, mixed dimethylzincates, $R(Me)_2ZnM$ (M = Li, MgX), are used for the selective transfer of the R group when R is *n*- or *sec*-alkyl, Ph, vinyl or silyl (equation 17). This sequence differs from that exhibited by mixed cuprates, which transfer neopentyl and

t-butyl groups more easily than the corresponding zincates[33]. Chiral aza-enolate **8** undergoes stereoselective conjugate addition in the form of mixed zincate **9** (equation 18)[34]. Hydrolysis of the adduct gives rise to enantiomerically enriched 1,5-diketones **10**. Conjugate addition of a mixed zincate **12** ($n = 2$) derived from α,β-dianion **11** leading to 1,6-diketone **13** has been reported (equation 19)[35]. The methyl transfer competes in the reaction with dimethylzincate **12** ($n = 1$).

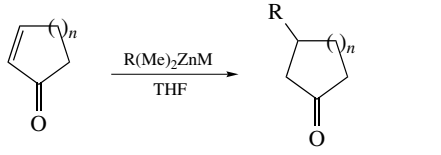

(17)

R = *n*- or *sec*-alkyl, phenyl, vinyl, silyl
M = Li, MgX

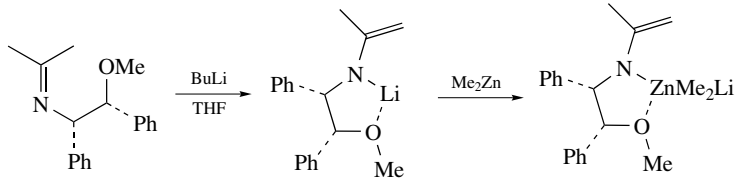

(8) **(9)**

(18)

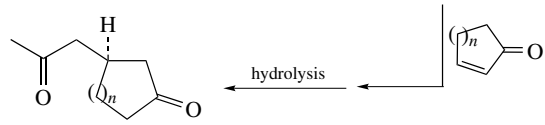

(10)

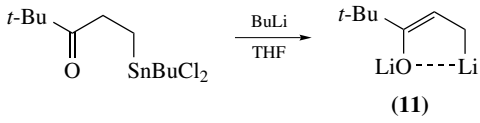

(11)

$n = 1$; Me_2Zn

$n = 2$; 1. $ZnCl_2$ (0.5 equiv), 2. MeLi (0.5 equiv)

(19)

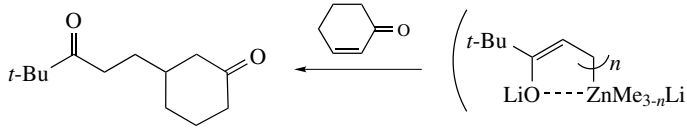

(13) **(12)**

While zincates are less reactive than cuprates in conjugate addition, the resulting zincate enolates show higher reactivity and can be used in subsequent carbonyl addition and alkylation[36]. Noyori's three-component coupling synthesis of prostaglandins, first developed by using an organocopper(I) reagent as nucleophile[37], was later improved by the advantageous use of mixed zincate reagents[38,39]. For example, zincate enolate intermediate **14** reacts with allyl iodide **15** efficiently to give the three-component coupling product **16** (equation 20)[40]. The limitation of enones in the initial conjugate addition could

be overcome by the use of $Me_2Cu(CN)Li_2$ as a catalyst[41]. As shown in equation 21, cuprate-induced transmetalation of alkenylzirconium **18**, prepared from alkyne **17** by hydrozirconation with the Schwartz' reagent [$Cp_2Zr(H)Cl$], and subsequent delivery of this alkenyl ligand to the poorly reactive β-substituted enone **19** generate a copper enolate, which is converted to reactive zinc enolate **20**[42] in situ by Me_3ZnLi, thereby recycling the cuprate[41a]. Reaction of **20** with an aldehydo-ester gives **21**.

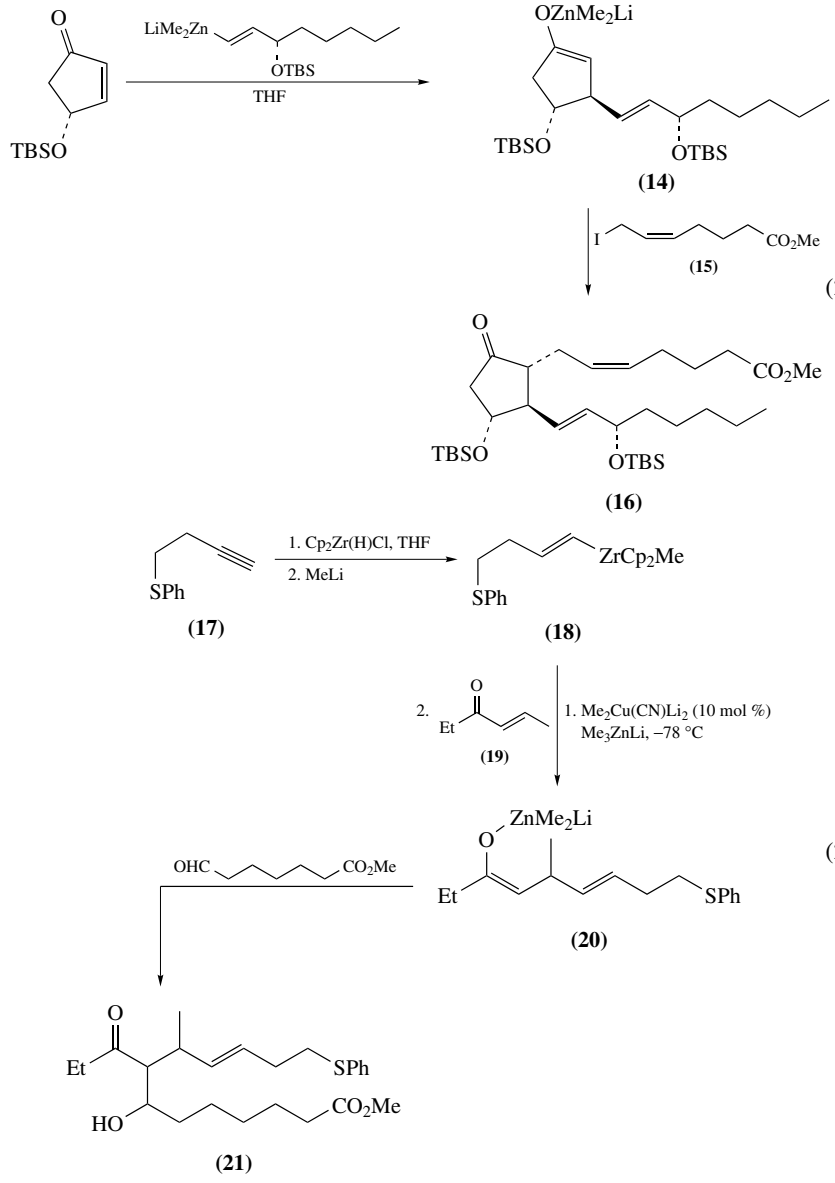

Few examples have been reported for the conjugate addition of zincates to α,β-unsaturated esters[43]. Tetracoordinated zincates generated from iodo-enoates **22** undergo intramolecular conjugate addition to give **23** in moderate yields (equation 22)[18c]. No cyclization was observed when Me_3ZnLi was used in this reaction. A reagent formulated as $[Bn(TMS)N]_3ZnLi$ was prepared from Bn(TMS)NLi and $ZnCl_2$•TMEDA[44]. The amino-zincate reacts with dimenthyl ester **24** to give diastereoselectively the cyclization product **25** via a tandem conjugate addition (equation 23).

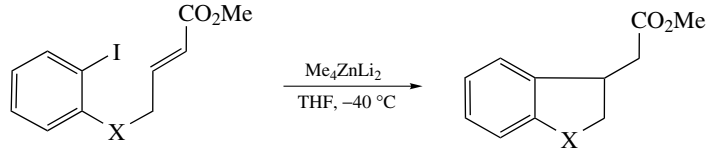

(22)

(22) X = O, NSO_2Ph **(23)**

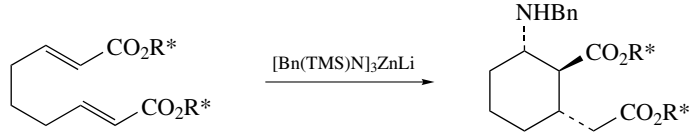

(23)

R* = (–)-menthyl

(24) **(25)**

Mixed silylzincate [$(Me_2PhSi)R_2ZnLi$; R = Me, Et] adds to a variety of α,β-unsaturated carbonyl compounds including less reactive esters and amides to give the corresponding β-silyl carbonyl compounds **26** (equation 24)[45]. The silylzincates generally give better yields of products than silylcuprate, $(PhMe_2Si)_2Cu(CN)Li_2$. A combined reagent of the silyllithium and substoichiometric amount (>10 mol%) of Me_2Zn can be employed as well for the reaction of relatively reactive substrates[46]. Tandem 1,4-addition/alkylation sequence furnishes *anti* product **27** with high stereoselectivity (equation 25)[45a]. Selective delivery of the stannyl group is also observed for a mixed zincate derived from a stannyllithium and Et_2Zn (equation 26)[47]. The stannylzincate reacts with unsaturated ester **28** with a high facial selectivity opposite that observed for the stannyllithium to give *syn*-**29**.

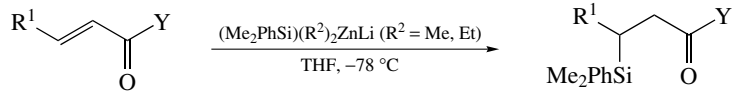

(24)

Y = H, alkyl, aryl, OR, NR'_2 **(26)**

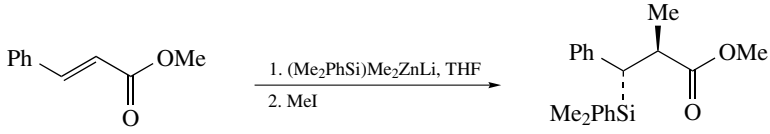

(25)

97:3

(27)

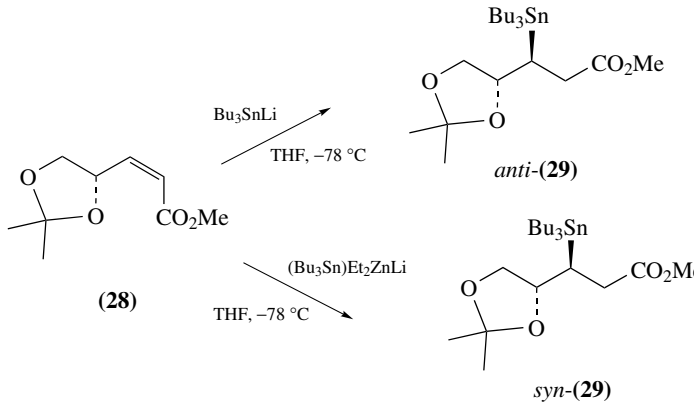

(26)

C. 1,2-Migration of Zincate Carbenoids

1,2-Migration or 1,2-migratory insertion is one of the most fundamental patterns for carbon–carbon and carbon–heteroatom bond formation. Indeed, the majority of carbon–carbon bond-forming reactions of organoboron compounds proceed via 1,2-migration[48]. A zincate bearing a leaving group at the α carbon, or zincate carbenoid **31**, also rearranges with 1,2-migration of the alkyl ligand (R) to give organozinc **32** with carbon–carbon bond formation (Scheme 2)[49]. The initial report of the 1,2-migration reaction of zincates has been described in the reaction of $LiCH(Cl)SiMe_2Ph$ with Bu_2Zn leading to the alkylated product, $BuCH_2SiMe_2Ph$, after hydrolysis[50]. The homologated organozinc **32** is not only protonated to give **33** (E = H) but also can be utilized in the second carbon–carbon bond formation with a variety of electrophiles. Since zincate carbenoids **31** are prepared from *gem*-dihalo derivatives **30a–c**, the overall reaction sequence is regarded as a tandem carbon–carbon bond-forming reaction with a nucleophile (R) and an electrophile (E)[23–25].

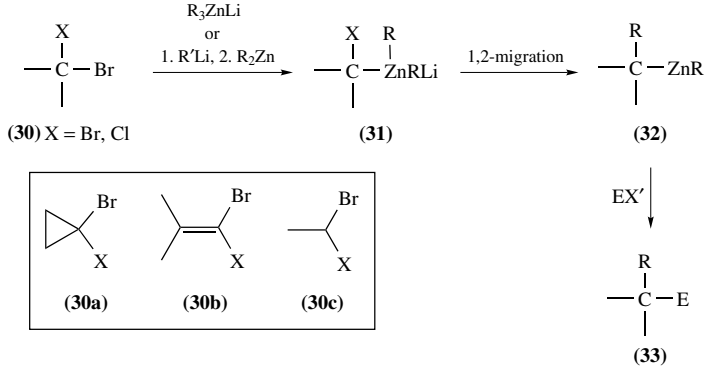

SCHEME 2

Treatment of *gem*-dibromocyclopropane **34** with Bu_3ZnLi from −85 to 0 °C generates 1-butylcyclopropylzinc **36** via the 1,2-migration of the zincate carbenoid **35** (equation 27)[24]. Subsequent Pd^0-catalyzed cross-coupling reactions afford cyclopropane

37 as a mixture of the stereoisomers. It is known that 1,2-alkyl migrations of boronates[51,48] and alanates[52] proceed with inversion of configuration at the carbon bearing a leaving group. A similar stereochemical outcome was reported for 1-halocyclopropylzincates (Scheme 3)[24]. Under the thermodynamically controlled conditions, bromine–lithium exchange reaction of dibromocyclopropane **38** gives *trans*-1-bromocyclopropyllithium **39**[26]. Zincate *cis*-**40**, generated by treatment of **39** with a dialkylzinc, rearranges on warming to afford the homologated cyclopropylzinc *trans*-**41** stereoselectively. Chlorination of **39** followed by bromine–zinc exchange of the resulting bromochlorocyclopropane **42** with a trialkylzincate generates *trans*-zincate **43**, which rearranges to give cyclopropylzinc *cis*-**41**. The cross-coupling of *trans*- and *cis*-**41** proceeds without loss of the stereochemical integrities. Therefore, one can obtain the desired stereoisomer of substituted cyclopropanes by a one-pot reaction as illustrated in equations 28 and 29.

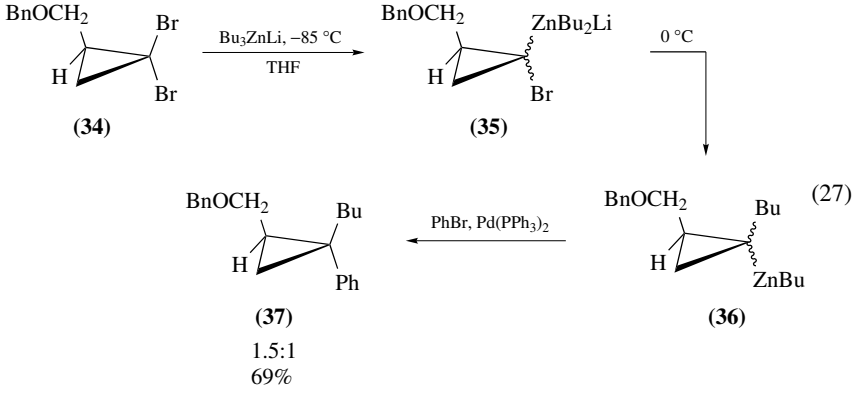

(27)

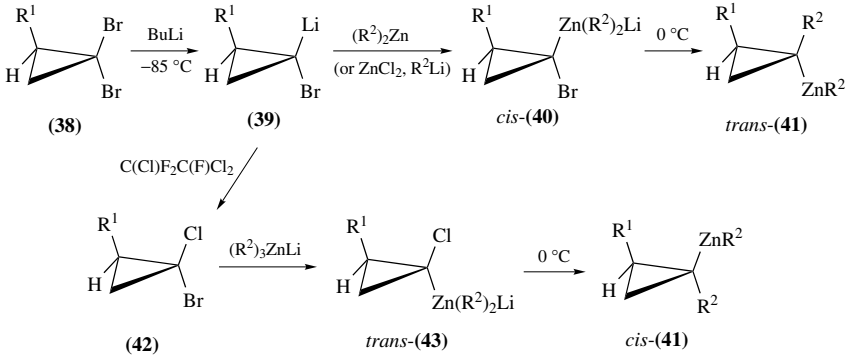

SCHEME 3

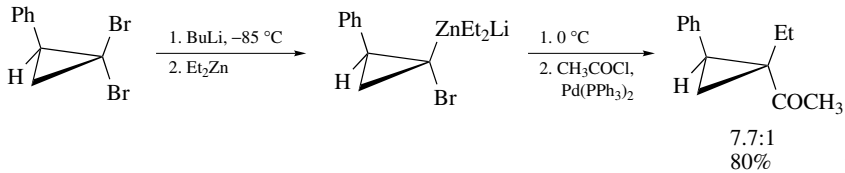

(28)

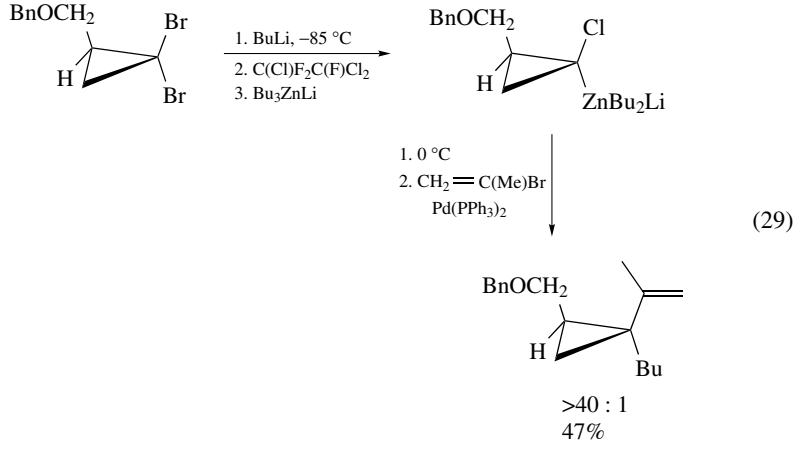

(29)

Stereospecific inversion is also observed in the 1,2-migration of trisubstituted 1-haloalkenylzincates (Scheme 4)[23b]. Upon warming up to 0 °C, (*Z*)-**44** and (*E*)-**46** rearrange to give alkylation product (*Z*)- and (*E*)-**45**, respectively, with high stereoselectivity. On the other hand, the 1,2-migration of tetrasubstituted 1-haloalkenylzincates (*Z*)-**47** and (*E*)-**49** is less stereoselective (Scheme 5). While the butyl group migration proceeded with some selectivity with inversion of configuration, preferential migration with retention was observed for the sterically demanding *t*-butyl group. The timing of the carbon–halogen bond breaking and the carbon–carbon bond formation has been proposed to be important in determining the stereochemical course of the 1,2-migration to (*E*)- and (*Z*)-**48**. Without unfavorable steric constraint, invertive migration to *Z*-**48** takes place synchronously with the breaking of the carbon–halogen bond. When the migration becomes sterically less feasible, the bond breaking may precede and, in the extreme case, the alkyl migration may proceed non-stereospecifically in a stepwise manner via intermediate **50**.

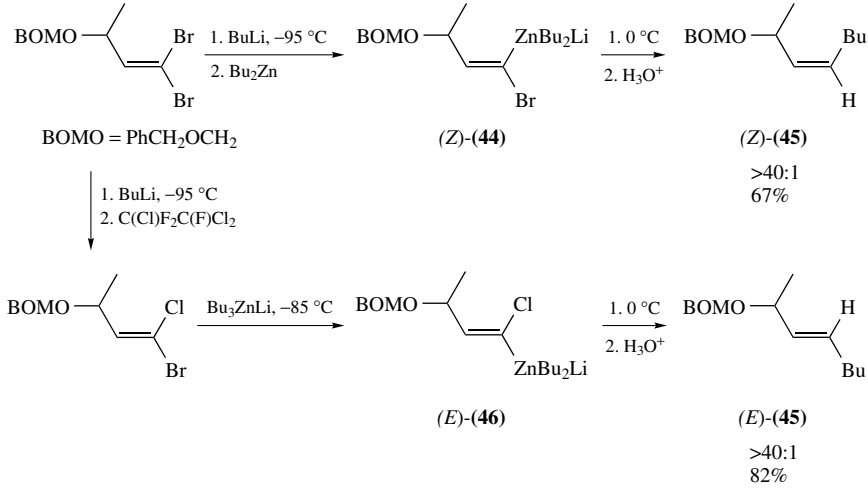

SCHEME 4

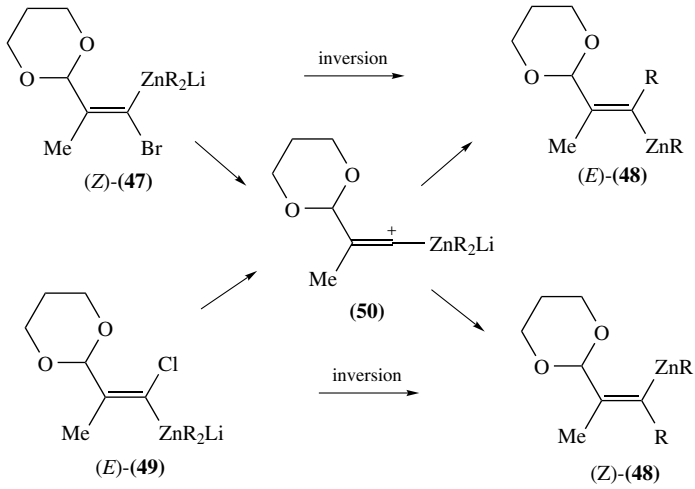

R	(*E*)-**48**:(*Z*)-**48**	
	from (*Z*)-**47**	from (*E*)-**49**
Bu	2.9:1	1:20
s-Bu	1.2:1	1:4.0
t-Bu	1:6.4	1:1.4

SCHEME 5

Treatment of 1,1-dibromoalkanes **51** with trialkylzincates at temperatures from −85 °C to room temperature gives homologated secondary alkylzinc species **53**, which undergo subsequent cross-coupling reaction with organyl halides catalyzed by the Pd[(*o*-tol)$_3$P]$_2$ to give **54a–c** in a single flask operation (equation 30)[25]. The intermediate 1-bromoalkylzincates **52** cannot be trapped by hydrolysis because the bromine–zinc exchange of **51** requires higher temperature (> −40 °C) and the resulting zincate carbenoids **52** undergo 1,2-migration at those temperatures. In order to ensure a complete transformation, a large excess (5 equiv) of the zincate needs to be used.

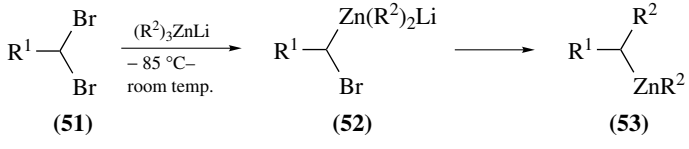

(51) **(52)** **(53)**

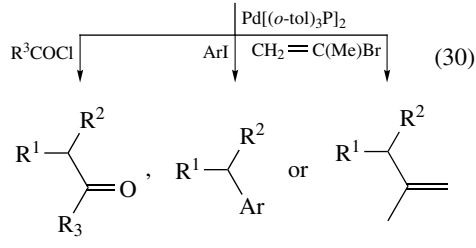

(30)

(54a) **(54b)** **(54c)**

Carbomagnesiation of alkenyllithium with allylmagnesium bromide gives rise to *gem*-bismetallic derivatives **55**[53]. Chlorination of **55** with benzenesulfonyl chloride and treatment with alkyllithium (2 equiv) afford the alkylation product **57** in good overall yield (equation 31)[54]. A mechanism involving 1,2-migration of the formed intermediate zincate carbenoids **56** has been proposed for this reaction.

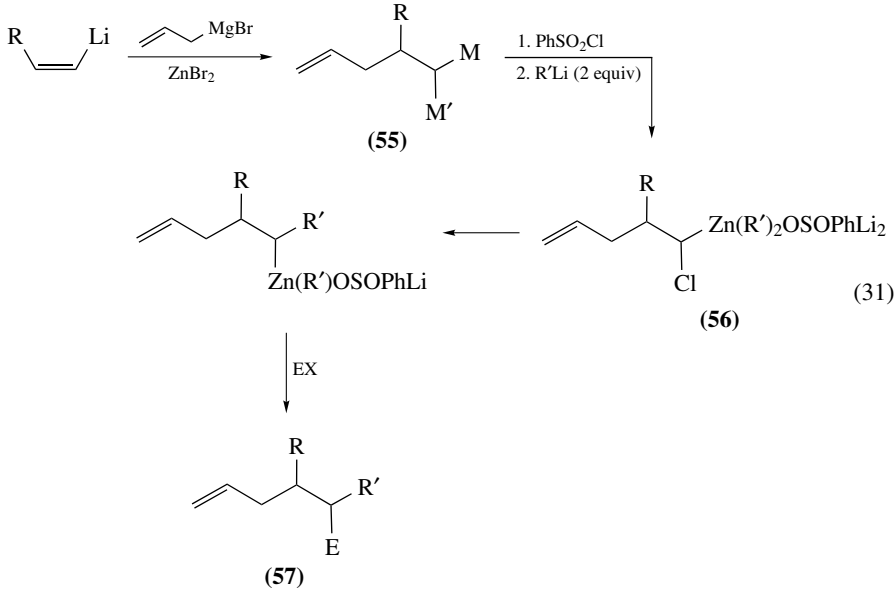

Homologation reaction of lithium enolates with bis(iodomethyl)zinc (**58**) yields a homoenolate, namely the organozinc derivatives bearing a carbonyl group at the β position (Scheme 6)[55]. Treatment of the lithium enolate of cyclohexanone, generated from the silyl

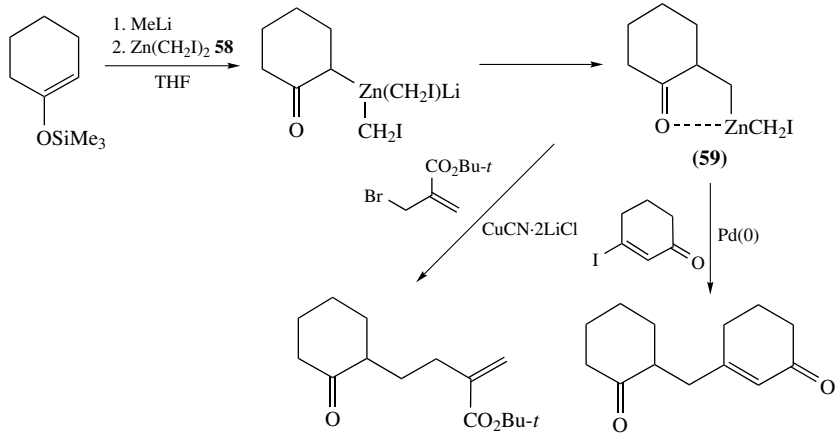

SCHEME 6

enol ether, with **58** affords homoenolate **59**, which can be used in the subsequent allylation or cross-coupling reaction. A chiral auxiliary-based approach has been reported for the stereoselective generation of homoenolate **62** (equation 32)[56]. By treatment with **58** and lithium benzyloxide, a lithium enolate generated from chiral amide **60** is transformed to **61** with high diastereoselectivity. The alkoxide is indispensable to the efficient 1,2-migration, suggesting that the reaction proceeds through tetracoordinated zincate **61**. The involvement of tetracoordinated alkoxyzincates has been also implicated in the 1,2-migration of 1-bromocyclopropyl carbenoids[24c]. Transmetalation of **62** with (i-PrO)$TiCl_3$ followed by the reaction with aldehydes gives the homoaldol product **63** diastereoselectively. Treatment of **63** with p-toluenesulfonic acid induces cyclization to the optically pure lactones **64**.

Aryl sulfoxides **65** are transformed to alkenes **68** via homologation of the corresponding α-lithiosulfoxides (equation 33)[57]. Tetracoordinated zincate **66**, generated by treatment of the carbanion with **58** in the presence of LDA, rearranges to give β-zinciosulfoxide **67**, which undergoes elimination to give **68**.

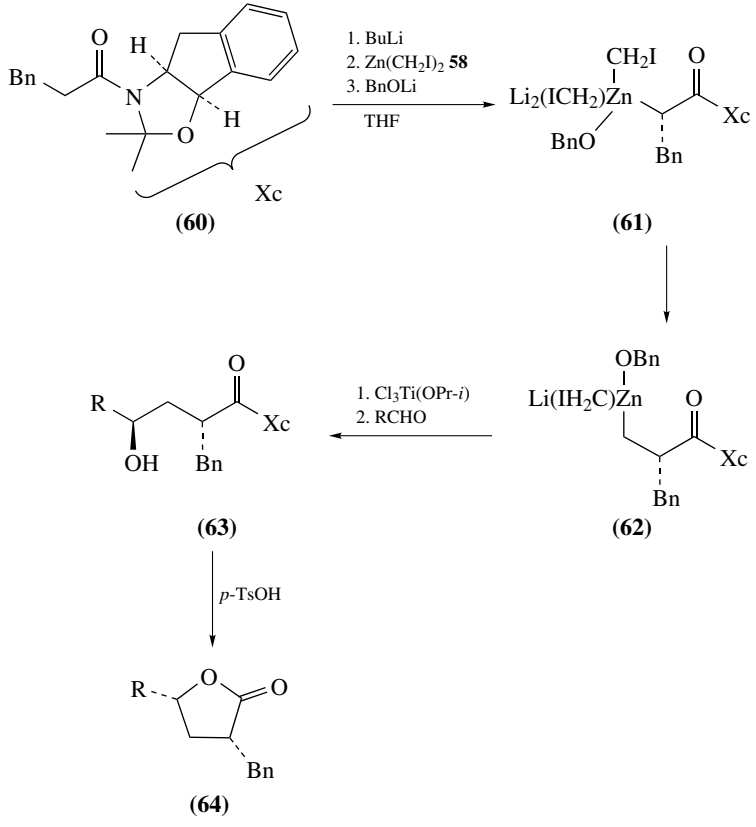

(32)

D. 1,2-Migration of Alkynylzincates and Arylzincates

Cuprates are known to react with propargylic derivatives to give allenes[58]. The allene formation is also observed in the reaction with zincates (equation 34). However, the reaction course is different. As demonstrated by deuterium incorporation in D_2O quench

experiments, the reaction of zincates produces homologated allenic zincs **71**. The reaction proceeds through a mechanism involving initial metalation of the terminal alkynes followed by 1,2-migration of the resulting alkynylzincates **70**. Since allenic zincs **71** can be utilized further in the reaction with electrophiles, the overall reaction serves as a synthetically versatile three-component coupling of propargylic substrates, zincates and electrophiles (Scheme 7)[19].

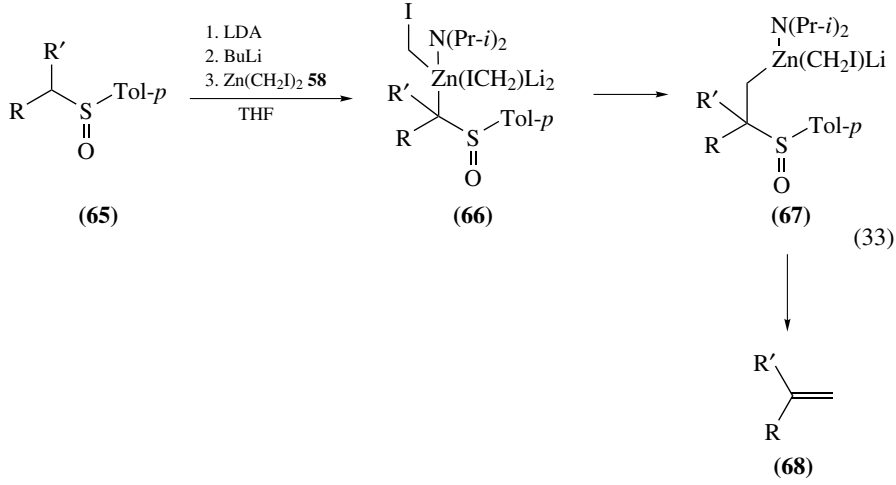

(33)

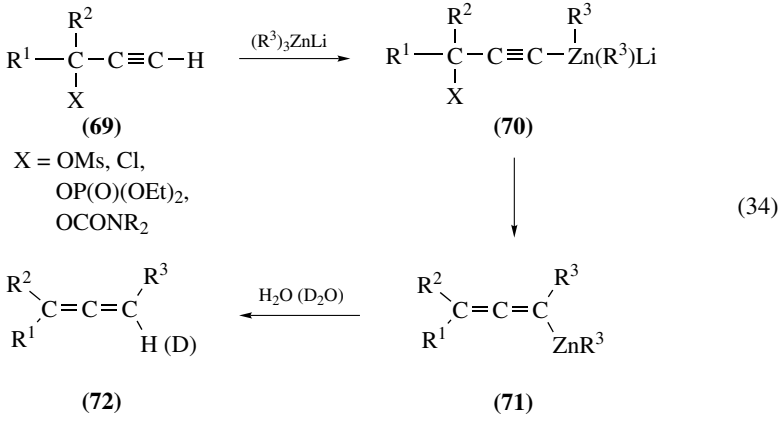

(34)

Reactions are generally carried out by using two equivalents of zincates in THF at temperature varying from −85 to 0 °C. Lithium or chloromagnesium trialkylzincates can be used for preparing the corresponding allenic zinc **71**. Allenic zinc bearing alkenyl and aryl groups can be prepared by using the corresponding lithium zincates. Secondary mesylates (**69**; X = OMs) and tertiary chlorides (**69**; X = Cl) are common propargylic substrates while phosphates (**69**; X = $OP(O)R_2$) and carbamates (**69**; X = $OCONR_2$) can be used as well. For the less reactive zincate such as Me_3ZnLi and $(TMSCH_2)_3ZnLi$, better results are obtained by using the carbamates. The nature of the leaving group X in **69** influences both the rate of the initial zincation step and the subsequent 1,2-migration. The metalation is the rate-determining step for mesylates and proceeds nicely at −60 °C.

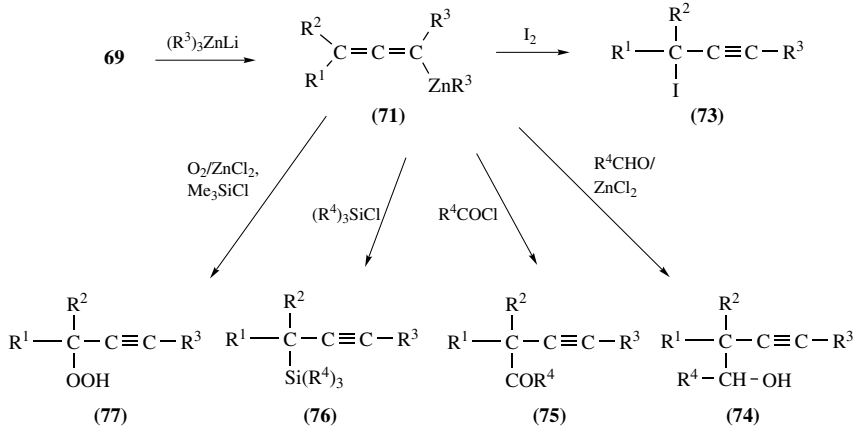

SCHEME 7

The resulting alkynylzincates **70** (X = OMs) rearrange to give allenic zincs **71** at this temperature, which give **72** by reaction with water. On the other hand, the 1,2-migration is the rate-determining step for the carbamate derivatives. The zincation step requires higher temperature (−15 °C) and the corresponding zincates **70** (X = $OCONR_2$) undergo 1,2-migration during warming up to room temperature. Propargylic chlorides exhibit an intermediate reactivity.

Successive treatment of the homologated allenic zincs **71** with electrophiles regioselectively furnishes propargylic products **73–77** (Scheme 7)[19c]. As the carbon–zinc bond of the allenic moiety of **71** reacts preferentially, excess electrophiles are not required except for iodination reaction. Equations 35 and 36 illustrate the utility of the reaction for the preparation of propargylsilanes and alkynones, respectively. Direct reaction of the resulting allenic zincs **71** with aldehydes gives *anti*- and *syn*-adducts **74** without selectivity. Nonetheless, one can obtain *anti*-**74** with high selectivity (>95:5) when **71** is converted to allenic chlorozinc **78** by treatment with $ZnCl_2$ (equation 37). According to this protocol, a wide range of *anti*-homopropargylic alcohols can be stereo- and regioselectively prepared from various propargylic substrates, zincates and aldehydes in a convergent manner. The allenic zincs **71** also react with molecular oxygen to give propargyl hydroperoxides **77**[59]. In this reaction, the use of $ZnCl_2$ and chlorotrimethylsilane as additives is essential to convert **71** into more reactive chlorozinc species.

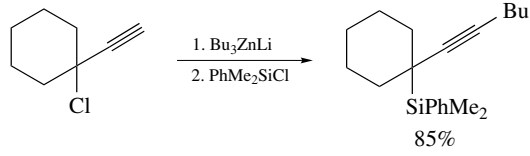

85%

(35)

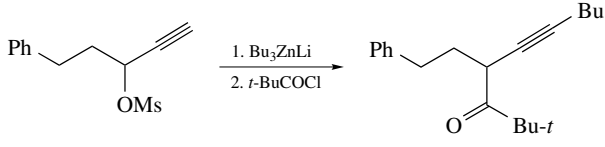

86%

(36)

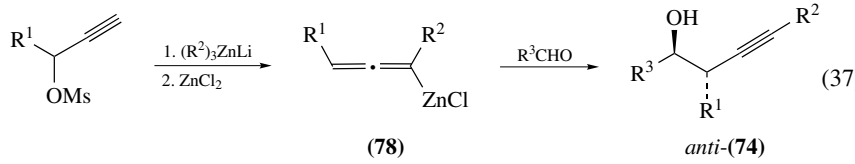

(78) *anti*-(74) (37)

In contrast to other organozincates, silylzincates react with propargylic substrates **69** in a S_N2' fashion and give the α-silylallenes **79** instead of the corresponding allenic zinc species, accompanied by a minor amount of the silylalkyne **80** (equation 38)[19c]. On the other hand, the bromine–zinc exchange reaction of bromopropargylic mesylate **81** generates the alkynylzincate intermediate **82**, which rearranges to give the α-sillylallenic zinc **83** in metallotropic equilibrium with its propargylic zinc counterpart **84** (equation 39). Although propargylic zinc **84** is the predominant species in the equilibrium, the mixture exhibits a regioselectivity similar to the classical other homologated allenic zinc species (equation 40).

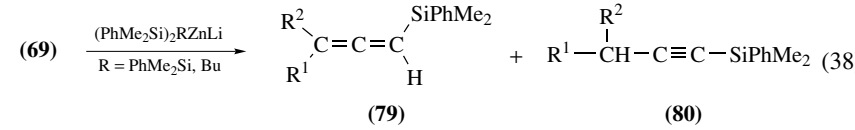

(79) (80) (38)

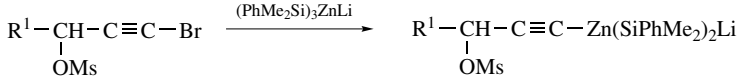

(81) (82)

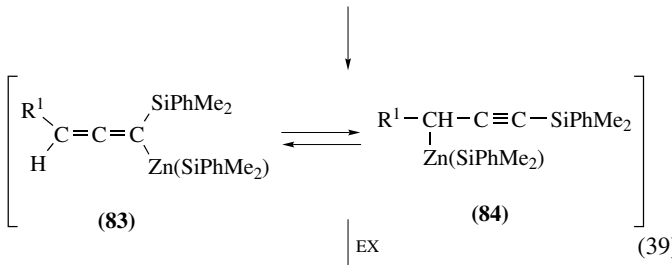

(83) (84) (39)

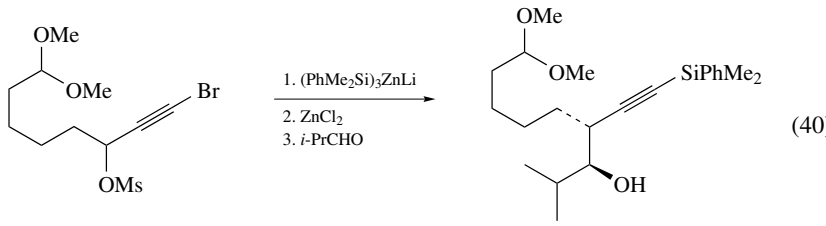

58% (40)

1,2-Migration has been also reported for an alkynylzincate bearing a leaving group at the homopropargylic position[60]. Alkynylzincate **86** generated by treatment of sulfonate **85** with $(R^3)_3ZnLi$ (R^3 = alkyl, aryl) undergoes 1,2-migration with simultaneous cyclization at temperature between −20 and −10 °C to give the 1-(cyclopropylidene)alkylzinc derivatives **87** (equation 41). At higher temperature (*ca* 0 °C), **87** undergoes a ring-opening to the homopropargylic zinc **88**. In the 1,2-migration/cyclization, two bonds are formed preferentially, but not exclusively, at the same face of the triple bond (equation 42). Formation of the *cis*-adduct **90** in the reaction of *anti* homopropargylic sulfonate **89** demonstrates that the cyclization proceeds with inversion of stereochemistry at the electrophilic carbon. Organozinc reagents **87**, thus generated, are used successively in the reaction with electrophiles, such as I_2, TMSCl, TsCN, RCOCl and aldehydes, to furnish a variety of functionalized (methylene)cyclopropanes **91** (equation 43).

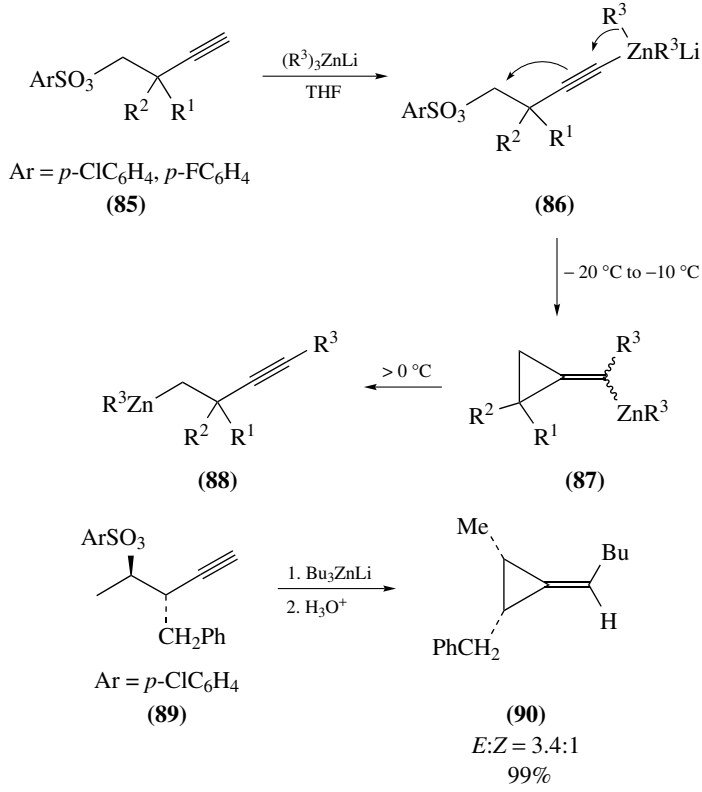

(41)

(42)

Similar 1,2-migration/cyclization is observed in the reaction of 5-hexynyl tosylate **92a** with zincates (equation 44)[61]. In addition to the *exo*-cyclization leading to (alkylidene)cyclopentane **93a**, *endo*-cyclization occurs competitively to give cyclohexene **94a**, which is a major product in the reaction with Ph_3ZnLi. In the reaction of the phenyl-substituted derivative **92b**, two *endo*-cyclization products **94b** and **94′** (1:1) were obtained as well as *exo*-cyclization product **93b**. A unified mechanism in which the π-electrons of the alkynylzincate **95** participate in *exo*- and *endo*-cyclization (Scheme 8) has been proposed to rationalize these observations. The intermediacy of cyclohexyne **96** was verified

by the formation of the Diels–Alder adduct **97** with 1,3-diphenylisobenzofuran. While homologous 6-heptynyl sulfonate **98** ($n = 3$) exhibits analogous reactivity, no cyclization was observed for 4-pentynyl sulfonate **98** ($n = 1$) (Scheme 9).

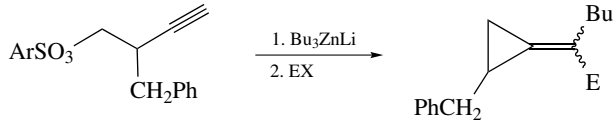

Ar = *p*-ClC_6H_4 **(91)**

EX	E
I_2	I
Me_3SiCl	Me_3Si
TsCN	CN
RCOCl, $Pd(PPh_3)_2$	COR
RCHO	CH(OH)R

(43)

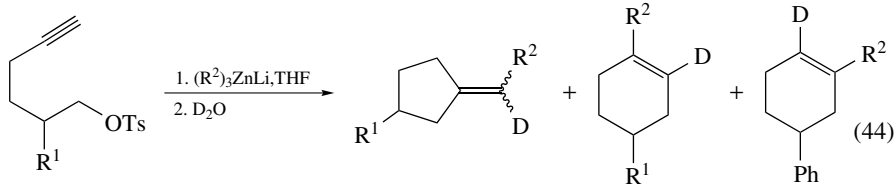

(44)

(92a) R^1 = H
(92b) R^1 = Ph

(93a) **(93b)** **(94a)** **(94b)** **(94′)**

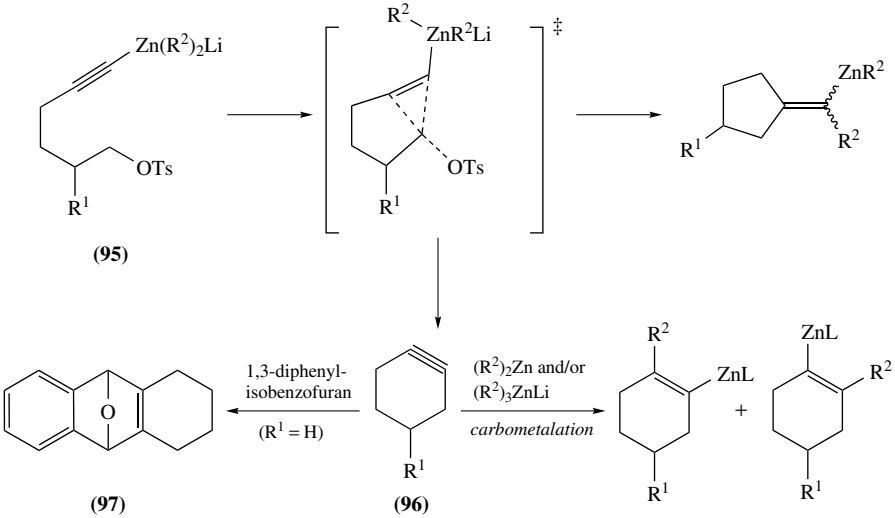

SCHEME 8

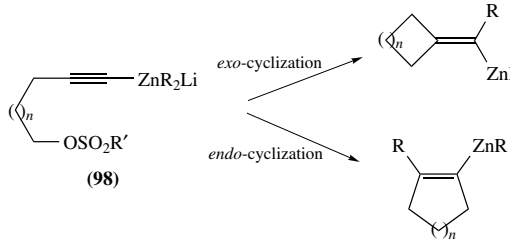

n	*exo*	*endo*
0	yes	yes
1	no	no
2	yes	yes
3	yes	yes

SCHEME 9

Arylzincates **100** bearing a leaving group at the benzylic position rearrange with carbon–carbon bond formation to generate homologated benzylzinc **102** via 4-methylene-2,5-cyclohexadienylzinc **101** (Scheme 10)[62]. Although the 1,2-migration of **100** leading to the cross-conjugated intermediate **101** suffers from a loss of aromatic stabilization, the reaction proceeds smoothly at −40 °C. While the *m*-analogue **104** is stable under similar conditions, the *o*-analogue **105** rearranges to give a mixture of benzylzinc **106** (via 1,2-migration) and arylzinc **107** (via intramolecular alkylation). Arylzincates **100** are prepared from 4-iodobenzyl derivatives **99a** and **99b**. The resulting benzylzincs **102** react with a variety of electrophiles without the aid of palladium(0) or other catalysts to give **103**. The overall reaction provides a unique method for three-component coupling in which nucleophiles and electrophiles are introduced at the remote positions of benzylic substrates. An epoxide ring also serves as a leaving group. The reaction of *p*-iodostyrene oxide with Bu_3ZnLi yields *p*-butylstyrene through benzylzinc **108** (equation 45).

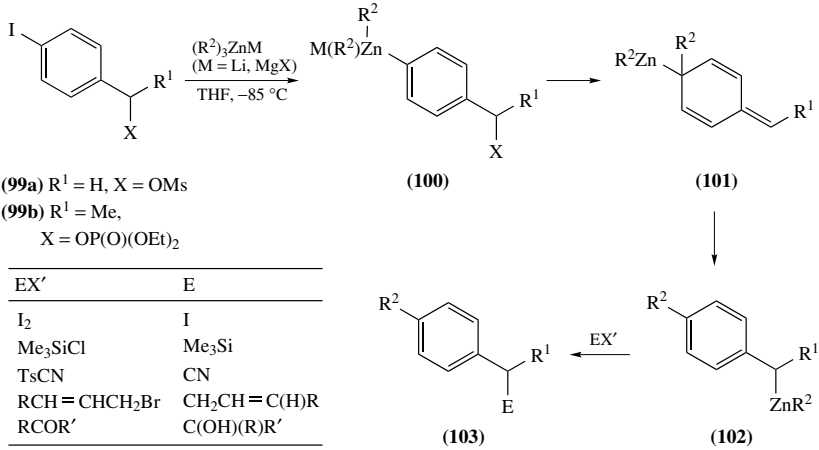

(99a) R^1 = H, X = OMs
(99b) R^1 = Me, X = $OP(O)(OEt)_2$

(100) **(101)** **(102)** **(103)**

EX′	E
I_2	I
Me_3SiCl	Me_3Si
TsCN	CN
$RCH{=}CHCH_2Br$	$CH_2CH{=}C(H)R$
RCOR′	C(OH)(R)R′

SCHEME 10

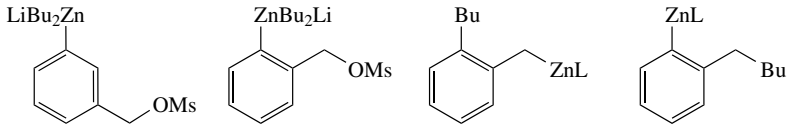

(104) **(105)** **(106)** **(107)**

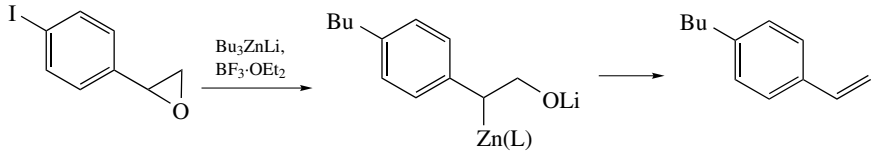

(108) 47% (45)

E. Generation of Benzynes

Treatment of *o*-iodophenyl triflate **109a** with Bu_3ZnLi (2 equiv) at $-85\,^{\circ}C$ generates benzyne **111** ($R^1 = Me$), which undergoes a carbozincation reaction to give a mixture of arylzincs **112** and **112′** (Scheme 11)[63]. When tosylate **109b** is used with Bu_3ZnLi, benzyne formation from the arylzincate intermediate **110** ($R^1 = Me$, $R^2 = Bu$) requires higher temperature such as $0\,^{\circ}C$. *o*-Bromoarylzincate **110** ($R^1 = H$, $R^2 = t$-Bu), generated by treatment of 1,3-bromoiodobenzene (**109c**) with t-Bu_3ZnLi, is more stable and does not lead to benzyne formation at $0\,^{\circ}C$. On the other hand, the reaction of **109c** with Me_3ZnLi provides a clean generation of benzyne without concomitant carbozincation, as demonstrated by high-yield formation of the 1,3-diphenylisobenzofuran adduct **113**[64]. Directed zincation of *m*-bromoarenes **114** by aminozincate **115** can be used in the regioselective generation of functionalized benzynes **116** (equation 46)[64]. By virtue of the high

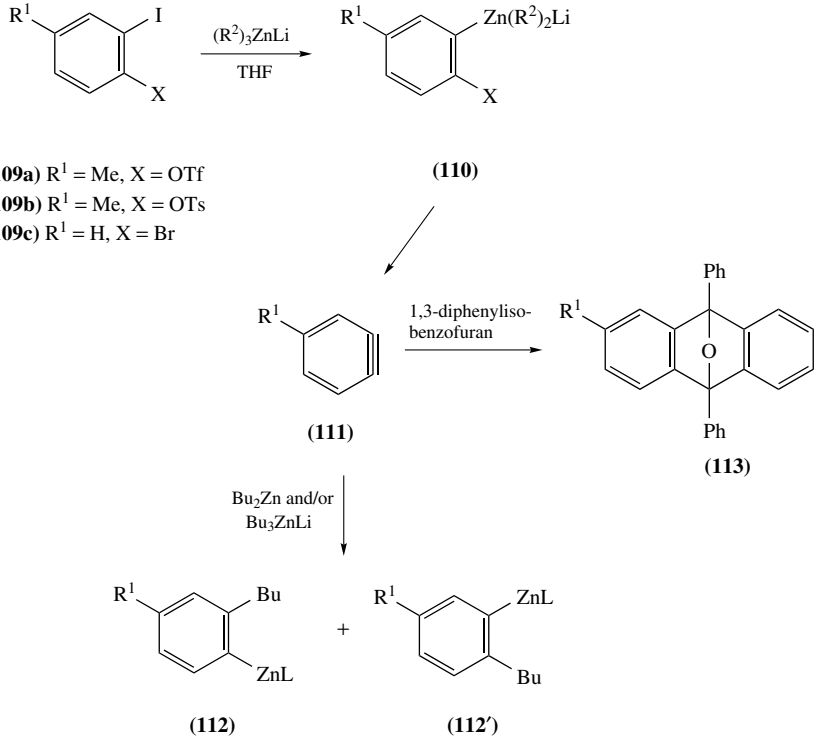

SCHEME 11

regioselectivity and functional group compatibility, the method may find a wide synthetic applicability.

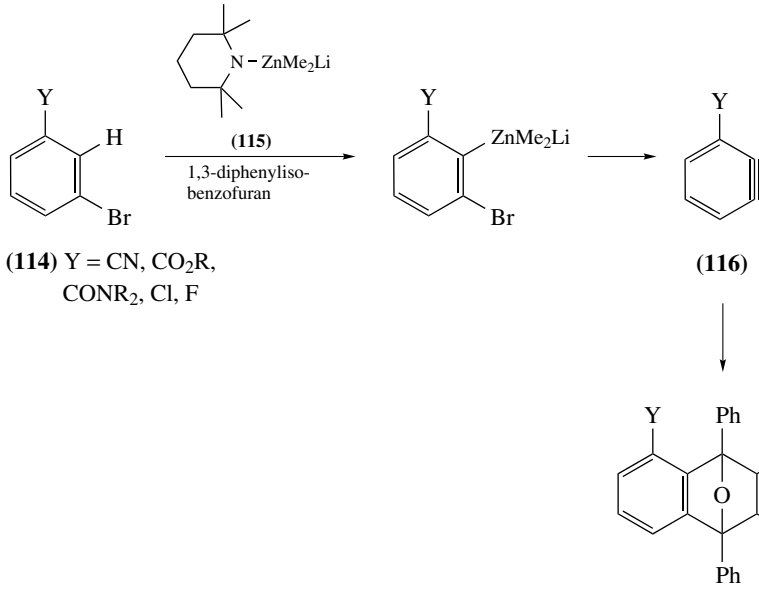

(114) Y = CN, CO_2R, $CONR_2$, Cl, F

(116)

(46)

3-Iodo-4-methoxyphenyl triflate **117** reacts with Bu_3ZnLi at room temperature to give **118** and then the butylation products **120** and **120′** (equation 47)[63]. Intermediacy of *m*-benzyne **119** has been proposed for this reaction. Products derived from *p*-benzyne were not obtained in the reaction of *p*-iodophenyl triflate with the zincate.

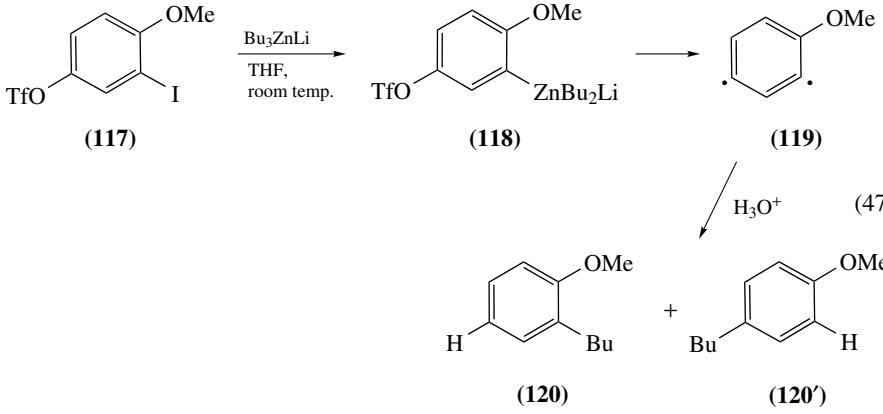

(117) **(118)** **(119)**

(47)

(120) **(120′)**

F. Cross-coupling Reaction

Like other organozinc reagents[65], zincates are excellent nucleophiles in the transition metal catalyzed cross-coupling reaction. Tri- and tetra-arylzincates are reported to

transfer all aryl groups in the Pd^0-catalyzed cross-coupling reaction[66]. In the reaction of 2-furyllithium **121** and 2-chloropyridine, $ZnCl_2$ stoichiometry can be reduced to 1:3–4 to achieve high-yield formation of the coupling product **122** (equation 48). Most recently, the utility of zincates as nucleophiles in iron-catalyzed cross-coupling reaction of aryl chlorides has been reported[67].

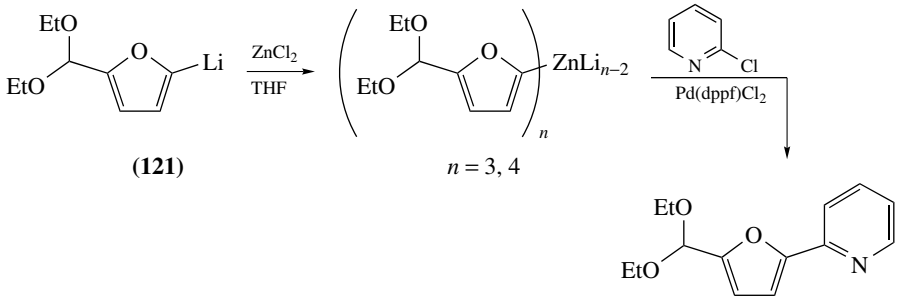

(121) $n = 3, 4$

(122) (48)

The oxovanadium(V)-induced cross-coupling of two ligands on mixed zincates has been reported[68]. Arylzincate **124** (which is formed from **123**) is oxidized by $V(O)(OEt)Cl_2$ to give the cross-coupling products **125** (equation 49). A minor formation of the homo-coupling product **126** is observed when zincate **124** is prepared by the reaction of an aryllithium and a diorganozinc. The undesirable pathway is completely suppressed by using halogen–zinc exchange reaction with Me_3ZnLi (for ArI) or Me_4ZnLi_2 (for ArBr) for the preparation of the zincate[68b]. The oxidative cross-coupling of zincates has been exploited in vicinal dialkylation of cyclic enones (equation 50)[69]. Conjugate addition of Bu_3ZnLi to cycloalkenones followed by the oxidation of the resulting zinc enolate **127** with $V(O)(OEt)Cl_2$ gives the 2,3-dibutylcycloalkanone **128** (R^1, R^2 = Bu) in good yields. The reaction of 2-cyclohexenone with $BuMe_2ZnLi$ regioselectively affords 2-methyl-3-butylcyclohexanone (**128**; $n = 1$, R^1 = Bu, R^2 = Me).

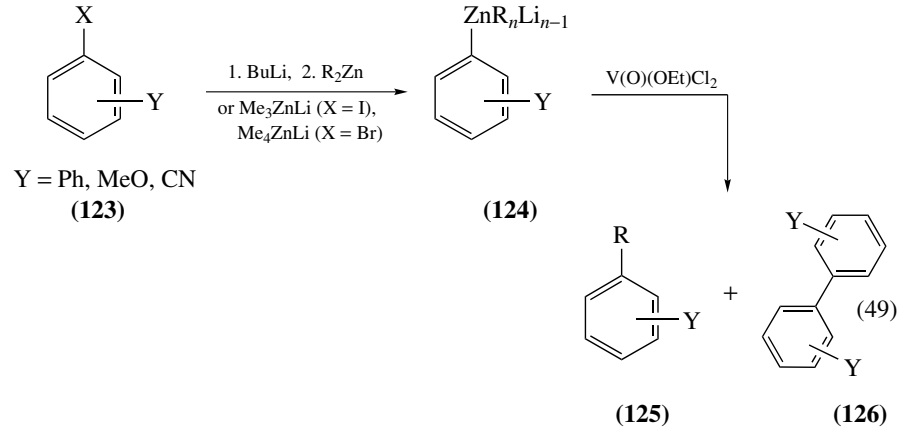

Y = Ph, MeO, CN

(123) **(124)** (49)

(125) **(126)**

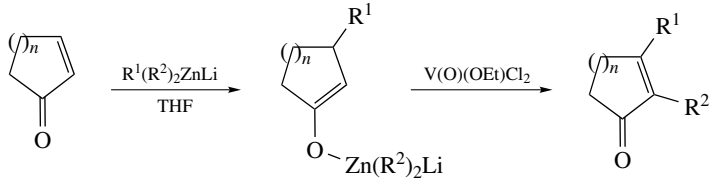

(50)

(127) **(128)**

IV. CONCLUDING REMARKS

Organozincates exhibit a wide range of reactivities as a most reactive class of organozinc reagents. Of these, the homologation of zincates via 1,2-migration and the tandem conjugate addition/alkylation sequence represent their utility in convergent construction of complex molecular frameworks. Recent studies have revealed that their reactivity can be tuned by controlling the steric and electronic nature of ate ligands and by choosing a tri- or tetra-coordination state. Despite these advances, some fundamental chemistry of organozincates has not yet been fully clarified. For example, disproportionation of a certain mixed zincate to form homoleptic zincates has been observed by ^{1}H NMR analysis[4b] whereas such a process seems to be less feasible judging from the successful use of mixed zincates in many synthetic reactions. Not much attention has been paid to the theoretical treatment of the reactivity of organozincates[33]. It is reasonable to anticipate that their scope and synthetic utility will be further exploited and expanded by the fruitful cooperation of chemists working in broader area.

V. REFERENCES

1. (a) J. A. Wanklyn, *Proc. R. Soc. London*, 341 (1858).
   (b) J. A. Wanklyn, *Justus Liebigs Ann. Chem.*, 67 (1858).
2. G. Wittig, F. J. Meyer and G. Lange, *Ann.*, **571**, 167 (1951).
3. M. Isobe, S. Kondo, N. Nagasawa and T. Goto, *Chem. Lett.*, 679 (1977).
4. (a) K. Thiele, H. Goerls and W. Seidel, *Z. Anorg. Allg. Chem.*, **624**, 555 (1998).
   (b) E. Rijnberg, J. T. B. H. Jastrzebski, J. Boersma, H. Kooijman, N. Veldman, A. L. Spek and G. van Koten, *Organometallics*, **16**, 2239 (1997).
   (c) H.-O. Fröhlich, B. Kosan, B. Müller and W. Hiller, *J. Organomet. Chem.*, **441**, 177 (1992).
5. G. G. Matthias, K. Harms, J. Merle and W. D. K. Werner, *Z. Anorg. Allg. Chem.*, **624**, 1387 (1998).
6. A. P. Purdy and C. F. George, *Organometallics*, **11**, 1955 (1992).
7. M. Westerhausen, C. Gückel, H. Piotrowski and M. Vogt, *Anorg. Allg. Chem.*, **628**, 735 (2002).
8. M. Westerhausen, C. Gückel and P. Mayer, *Angew. Chem., Int. Ed.*, **40**, 266 (2001).
9. (a) E. Rijnberg, J. T. B. H. Jastrzebski, J. Boersma, H. Kooijman, A. L. Spek and G. van Koten, *J. Organomet. Chem.*, **541**, 181 (1997).
   (b) A. J. Edwards, A. Fallaize, P. R. Raithby, M.-A. Rennie, A. Steiner, K. L. Verhorevoort and D. S. Wright, *J. Chem. Soc., Dalton Trans.*, 133 (1996).
10. (a) E. Weiss and R. Wolfrum, *Chem. Ber.*, **101**, 35 (1968).
    (b) H.-O. Fröhlich, B. Kosan, B. Undeutsch and H. Görls, *J. Organomet. Chem.*, **472**, 1 (1994).
11. M. Westerhausen, B. Bernd; W. Schwarz and S. Henkel, *Z. Naturforsch., B: Chem. Sci.*, **49**, 199 (1994).
12. R. M. Fabicon, M. Parvez and H. G. Richey, Jr., *J. Am. Chem. Soc.*, **113**, 1412 (1991).
13. (a) M. A. Putzer, B. Neumuller and K. Dehnicke, *Z. Anorg. Allg. Chem.*, **623**, 539 (1997).
    (b) S. R. Boss, R. Haigh, D. J. Linton, P. Schooler, G. P. Shields and A. E. H. Wheatley, *Dalton Trans.*, 1001 (2003).

14. For NMR study, see:
(a) L. M. Seitz and T. L. Brown, *J. Am. Chem. Soc.*, **88**, 4140 (1966).
(b) L. M. Seitz and T. L. Brown, *J. Am. Chem. Soc.*, **89**, 1602 (1967).
(c) L. M. Seitz and B. F. Little, *J. Organomet. Chem.*, **18**, 227 (1969).
(d) T. A. Mobley and S. Berger, *Angew. Chem., Int. Ed.*, **38**, 3070 (1999).
(e) F. Kaufmann, A. Geaudelle, B. Kaempf, F. Schue, A. Deluzarche and A. Maillard, *J. Organomet. Chem.*, **24**, 13 (1970).
15. T. Harada and A. Oku, in *Organozinc Reagents* (Eds. P. Knochel and P. Jones), Chap. 6, Oxford University Press, Oxford, 1999, p. 101.
16. K. Nützel, in *Methoden der Organischen Chemie (Houben-Weyl)*, Vol. 13, part 2a, 4th edn., Thieme, Stuttgart, 1973, p. 197.
17. Non-hygroscopic $ZnCl_2$-TMEDA (tetramethylethylenediamine) complex[3] is often used.
18. (a) M. Uchiyama, M. Koike, M. Kameda, Y. Kondo and T. Sakamoto, *J. Am. Chem. Soc.*, **118**, 8733 (1996).
(b) M. Uchiyama, Y. Kondo, T. Miura and T. Sakamoto, *J. Am. Chem. Soc.*, **119**, 12372 (1997).
(c) M. Uchiyama, M. Kameda, O. Mishima, N. Yokoyama, M. Koike, Y. Kondo and T. Sakamoto, *J. Am. Chem. Soc.*, **120**, 4934 (1998).
19. (a) T. Katsuhira, T. Harada, K. Maejima, A. Osada and A. Oku, *J. Org. Chem.*, **58**, 6166 (1993).
(b) T. Harada, T. Katsuhira, A. Osada, K. Iwazaki, K. Maejima and A. Oku, *J. Am. Chem. Soc.*, **118**, 11377 (1996).
20. Y. Kondo, M. Shirai, M. Uchiyama and T. Sakamoto, *J. Am. Chem. Soc.*, **121**, 3539 (1999).
21. A. J. Clarke, S. McNamara and O. Meth-Cohn, *Tetrahedron Lett.*, 2373 (1974).
22. T. Imahori, M. Uchiyama, T. Sakamoto and Y. Kondo, *Chem. Commun.*, 2450 (2001).
23. (a) T. Harada, D. Hara, K. Hattori and A. Oku, *Tetrahedron Lett.*, **29**, 3821 (1988).
(b) T. Harada, T. Katsuhira, D. Hara, Y. Kotani, K. Maejima, R. Kaji and A. Oku, *J. Org. Chem.*, **58**, 4897 (1993).
24. (a) T. Harada, K. Hattori, T. Katsuhira and A. Oku, *Tetrahedron Lett.*, **30**, 6035 (1989).
(b) T. Harada, K. Hattori, T. Katsuhira and A. Oku, *Tetrahedron Lett.*, **30**, 6039 (1989).
(c) T. Harada, T. Katsuhira, K. Hattori and A. Oku, *J. Org. Chem.*, **58**, 2958 (1993).
25. T. Harada, Y. Kotani, T. Katsuhira and A. Oku, *Tetrahedron Lett.*, **32**, 1573 (1991).
26. T. Harada, T. Katsuhira, K. Hattori and A. Oku, *Tetrahedron*, **50**, 7987 (1994).
27. R. Knorr, *Chem. Rev.*, **104**, 3795 (2004).
28. Y. Kondo, N. Takazawa, C. Yamazaki and T. Sakamoto, *J. Org. Chem.*, **59**, 4717 (1994).
29. Y. Kondo, M. Fujinami, M. Uchiyama and T. Sakamoto, *J. Chem. Soc., Perkin Trans. 1*, 799 (1997).
30. (a) T. Harada, T. Kaneko, T. Fujiwara and A. Oku, *J. Org. Chem.*, **62**, 8966 (1997).
(b) T. Harada, T. Kaneko, T. Fujiwara and A. Oku, *Tetrahedron*, **54**, 9317 (1998).
31. (a) R. A. Kjonaas and E. J. Vawter, *J. Org. Chem.*, **51**, 3993 (1986).
(b) R. A. Watson and R. A. Kjonaas, *Tetrahedron Lett.*, **27**, 1437 (1986).
(c) R. A. Kjonaas and R. K. Hoffer, *J. Org. Chem.*, **53**, 4133 (1988).
32. W. Tuckmantel, K. Oshima and H. Nozaki, *Chem. Ber.*, **119**, 1581 (1986).
33. For the correlation of reactivities of zincates and cuprates with *d*-orbital energies of the ate complexes, see; S. Mori, A. Hirai, M. Nakamura and E. Nakamura, *Tetrahedron*, **56**, 2805 (2000).
34. K. Yamamoto, M. Kanoh, N. Yamamoto and J. Tsuji, *Tetrahedron Lett.*, **28**, 6347 (1987).
35. I. Ryu, M. Ikebe, N. Sonoda, S. Yamato, G. Yamamura and M. Komatsu, *Tetrahedron Lett.*, **41**, 5689 (2000).
36. Y. Morita, M. Suzuki and R. Noyori, *J. Org. Chem.*, **54**, 1785 (1989).
37. R. Noyori and M. Suzuki, *Angew. Chem., Int. Ed. Engl.*, **23**, 847 (1984).
38. (a) M. Suzuki, H. Koyano, Y. Morita and R. Noyori, *Synlett*, 22 (1989).
(b) M. Suzuki, Y. Morita, H. Koyano, M. Koga and R. Noyori, *Tetrahedron*, **46**, 4809 (1990).
39. (a) T. Takahashi, M. Nakazawa, M. Kanoh and K. Yamamoto, *Tetrahedron Lett.*, **31**, 7349 (1990).
(b) T. Takahashi, T. Shimayama, M. Miyazawa, M. Nakazawa, H. Yamada, K. Takatori and M. Kajiwara, *Tetrahedron Lett.*, **33**, 5973 (1992).
(c) T. Takahashi, M. Nakazawa, K. Takatori, S. Nishimura and K. Yamamoto, *Natural Product Letters*, **1**, 263 (1993).

40. For three-component coupling approach in natural product syntheses, see:
(a) A. B. Smith, III, T. A. Rano, N. Chida, G. A. Sulikowski and J. L. Wood, *J. Am. Chem. Soc.*, **114**, 8008 (1992).
Silylzincate;
(b) A. G. M. Barrett, J. Head, M. J. Smith, N. S. Stock, A. J. P. White and D. J. Williams, *J. Org. Chem.*, **64**, 6005 (1999).
41. (a) B. H. Lipshutz and M. R. Wood, *J. Am. Chem. Soc.*, **116**, 11689 (1994).
(b) B. H. Lipshutz, M. R. Wood and R. Tirado, *J. Am. Chem. Soc.*, **117**, 6126 (1995).
(c) B. H. Lipshutz, T. Gros, D. J. Buzard and R. Tirado, *J. Chin. Chem. Soc.*, **44**, 1 (1997).
(d) B. H. Lipshutz, *Acc. Chem. Res.*, **30**, 277 (1997).
42. B. H. Lipshutz and M. R. Wood, *Tetrahedron Lett.*, **35**, 6433 (1994).
43. F. Denes, F. Chemla and J. F. Normant, *Eur. J. Org. Chem.*, 3536 (2002).
44. N. Shida, T. Uyehara and Y. Yamamoto, *J. Org. Chem.*, **57**, 5049 (1992).
45. (a) R. A. N. C. Crump, I. Fleming and C. J. Urch, *J. Chem. Soc., Perkin Trans. 1*, 701 (1994).
(b) A. Vaughan and R. D. Singer, *Tetrahedron Lett.*, **36**, 5683 (1995).
46. B. L. MacLean, K. A. Hennigar, K. W. Kells and R. D. Singer, *Tetrahedron Lett.*, **38**, 7313 (1997).
47. A. Krief, L. Provins and W. Dumont, *Angew. Chem., Int. Ed.*, **38**, 1946 (1999).
48. H. C. Brown, *Organic Synthesis via Borane*, Wiley-Interscience, New York, 1975.
49. For review, see: I. Marek, *Tetrahedron*, **58**, 9463 (2002).
50. E. Negishi and K. Akiyoshi, *J. Am. Chem. Soc.*, **110**, 646 (1988).
51. R. L. Danheiser and A. C. Savoca, *J. Org. Chem.*, **50**, 2401 (1985).
52. J. A. Miller *J. Org. Chem.*, **54**, 998 (1989).
53. I. Marek and J. F. Normant, *Chem. Rev.*, **96**, 3241 (1996).
54. F. Chemla, I. Marek and J. F. Normant, *Synlett*, 665 (1993).
55. (a) S. Achyutha Rao and P. Knochel, *J. Org. Chem.*, **56**, 4591 (1991).
(b) P. Knochel, M. J. Rozema, C. E. Tucker, C. Retherford, M. Furlong and S. AchyuthaRao, *Pure Appl. Chem.*, **64**, 361 (1992).
56. J. C. McWilliams, J. D. Armstrong, III, N. Zheng, M. Bhupathy, R. P. Volante and P. J. Reider, *J. Am. Chem. Soc.*, **118**, 11970 (1996).
57. A. Abramovitch, J. P. Varghese and I. Marek, *Org. Lett.*, **6**, 621 (2004).
58. (a) J. M. Dollat, J. L. Luche and P. J. Crabbe, *J. Chem. Soc., Chem. Commun.*, 761 (1977).
(b) A. Alexakis, I. Marek, P. Mangeney and J. F. Normant, *J. Am. Chem. Soc.*, **112**, 8042 (1990).
59. T. Harada and E. Kutsuwa, *J. Org. Chem.*, **68**, 6716 (2003).
60. T. Harada, H. Wada and A. Oku, *J. Org. Chem.*, **60**, 5370 (1995).
61. T. Harada, T. Otani and A. Oku, *Tetrahedron Lett.*, **38**, 2855 (1997).
62. (a) T. Harada, T. Kaneko, T. Fujiwara and A. Oku, *J. Org. Chem.*, **62**, 8966 (1997).
(b) T. Harada, T. Kaneko, T. Fujiwara and A. Oku, *Tetrahedron*, **54**, 9317 (1998).
63. T. Harada, M. Chiba and A. Oku, *J. Org. Chem.*, **64**, 8210 (1999).
64. M. Uchiyama, T. Miyoshi, Y. Kajihara, T. Sakamoto, Y. Otani, T. Ohwada and Y. Kondo, *J. Am. Chem. Soc.*, **124**, 8514 (2002).
65. (a) K. Oshima, 'Transition Metal Catalyzed Reactions of Organozinc Compounds', in *Advances in Organometallic Chemistry* (Ed. L. S. Liebiskind), Vol. 2, JAI Press, London, 1991, p. 101.
(b) E. Erdik, *Tetrahedron*, **48**, 9577 (1992).
66. D. R. Gauthier, Jr., R. H. Szumigala, Jr., P. G. Dormer, J. D. Armstrong, III, R. P. Volante and P. J. Reider, *Org. Lett.*, **4**, 375 (2002).
67. (a) A. Fuerstner and A. Leitner, *Angew. Chem., Int. Ed.*, **41**, 609 (2002).
(b) A. Fuerstner, A. Leitner, M. Mendez and H. Krause, *J. Am. Chem. Soc.*, **124**, 13856 (2002).
68. (a) T. Hirao, T. Takada and A. Ogawa, *J. Org. Chem.*, **65**, 1511 (2000).
(b) T. Takada, H. Sakurai and T. Hirao, *J. Org. Chem.*, **66**, 300 (2001).
69. T. Hirao, T. Takada and H. Sakurai, *Org. Lett.*, **2**, 3659 (2000).

CHAPTER **16**

Fluorinated organozinc reagents

CHARLES R. DAVIS

Sigma-Aldrich, 6000 N. Teutonia Avenue, Milwaukee, WI 53209, USA
Fax: +1 414 298 4224; e-mail: cdavis1@sial.com

and

DONALD J. BURTON

Department of Chemistry, University of Iowa, Iowa City, IA 52242, USA
Fax: +1 319 335 1270; e-mail: donald-burton@uiowa.edu

The chemistry of organozinc compounds
Edited by Z. Rappoport and I. Marek

I. INTRODUCTION

Fluorinated zinc reagents have been utilized as replacements for many of the unstable fluorinated lithium or magnesium reagents. This chapter details methodology for the synthesis of a wide variety of fluorinated zinc reagents and specific applications of these reagents in functionalization processes. The chapter is divided into sections based on the type of fluorinated group attached to the zinc. The coverage is designed as a general overview of each type of functionalized zinc reagent and is not intended to be a comprehensive review of every fluorinated zinc reagent reported in the chemical literature. Our goal is to acquaint the reader with the general types of fluorinated zinc reagents available, their preparation and specific examples of their functionalization, so as to inform the reader of the current state of knowledge of this class of organometallic reagents and how these types of organometallic compounds can be used effectively in their own research. There are many reports of zinc(II) fluorophores as sensors in apoptosis, gene expression or protein structure and functions. Since the preparation and utility of these fluorophores is straightforward and not unique to fluorinated zinc reagents, this particular application of zinc reagents will not be covered in this chapter.

II. FLUOROALKENYLZINC REAGENTS

The synthetic utility of fluorine-containing vinyllithium and Grignard reagents has been limited by the low thermal stability of many of these reagents. Fluorinated vinylzinc reagents were one of the alternative organometallic reagents selected to overcome this limitation, and indeed most of the fluorinated vinylzinc reagents exhibited superior thermal stability. Unfortunately, the increased thermal stability (>RT) is accompanied by a lower nucleophilicity, and many of these fluorinated vinylzinc reagents do not readily react with carbonyl functionality (aldehydes, ketones etc.). However, the use of these fluorinated vinylzinc reagents has been shown to be very efficient for coupling reactions under the influence of palladium catalysis (the Negishi reaction)[1].

Fluorinated vinylzinc reagents can be prepared by three methods: (1) capture of the corresponding vinyllithium reagents at low temperatures with a zinc salt; (2) capture of the corresponding vinyllithium reagent *in situ* with a zinc salt at ambient temperatures; or (3) direct insertion of zinc into the carbon–halogen bond of a fluorinated vinyl halide.

A. Method (1): Capture of Vinyllithium Reagents at Low Temperatures

The first method reported in the literature was initiated and developed by Normant, Sauvetre and coworkers[2]. The methodology involves generation of the fluorinated vinyllithium at low temperatures (−80 to −110 °C) via selective metallation or metal/halogen exchange from the corresponding hydrofluoroalkene or fluorinated vinyl halide[2,3]. Addition of a zinc halide to the lithium reagent solution (at low temperature) gives the stable (>RT) fluorinated vinylzinc reagents in excellent yields. The reaction temperatures are a function of the thermal stability of the particular fluorinated vinyllithium reagents. Some specific examples are illustrated in equations 1–8.

$$F_2C{=}CFCl \xrightarrow[\substack{THF/Et_2O\\ -110\,^\circ C}]{BuLi} [F_2C{=}CFLi] \xrightarrow[-100\,^\circ C]{ZnCl_2} F_2C{=}CFZnCl^{4} \qquad (1)$$

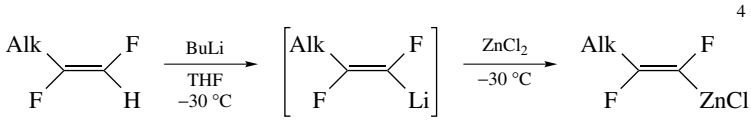

(2)

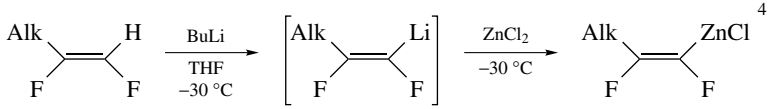

(3)

$$F_2C{=}CH_2 \xrightarrow[\substack{\text{THF}\\-110\,^\circ\text{C}}]{s\text{-BuLi}} [F_2C{=}CHLi] \xrightarrow[-100\,^\circ\text{C}]{\text{ZnCl}} F_2C{=}CHZnCl^{4} \qquad (4)$$

$$\underset{Z/E\,=\,2/98}{\text{AlkCF}{=}\text{CClH}} \xrightarrow[\substack{\text{THF/Et}_2\text{O}\\-110\,^\circ\text{C}}]{s\text{-BuLi}} [\text{AlkCF}{=}\text{CClLi}] \xrightarrow[-100\,^\circ\text{C}]{ZnCl_2} \underset{Z/E\,=\,98/2}{\text{AlkCF}{=}\text{CClZnCl}^{4}} \qquad (5)$$

$$CF_3CH{=}CF_2 \xrightarrow[\substack{\text{THF}\\-78\,^\circ\text{C}}]{t\text{-BuLi}} [CF_3C(Li){=}CF_2] \xrightarrow[-78\,^\circ\text{C}]{ZnCl_2} CF_3C(ZnCl){=}CF_2{}^{5} \qquad (6)$$

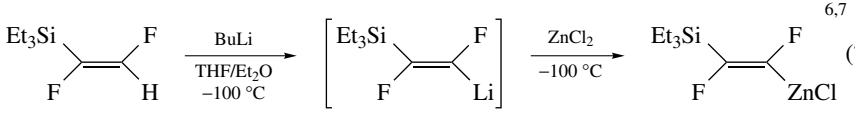

(7)

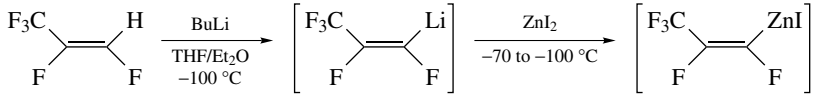

(8)

The synthetic protocol for many of these reagents is detailed elsewhere[9]. Note that stereochemistry in *E*/*Z* alkenes is preserved in the formation of both the fluorinated vinyllithium and the fluorinated vinylzinc reagents, and that hindered bases permit selective metallation vs. metal/halogen exchange.

The zinc reagents described above have shown extensive utility in coupling reactions with palladium catalysis. For example, coupling with heterocyclic iodides provides the corresponding fluorinated vinyl derivatives, as illustrated in equations 9–11.

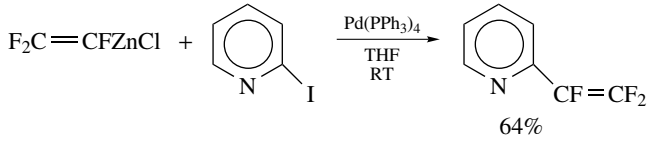

(9)

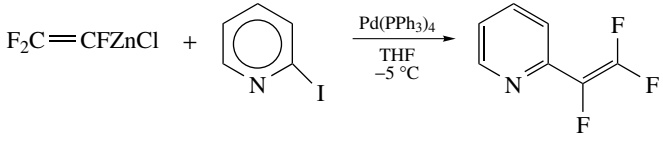

(10)

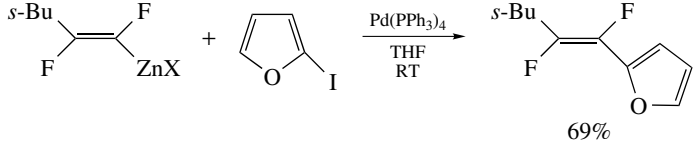

(11)

Similarly, palladium-catalyzed acylation provides a stereospecific entry to the α,β-unsaturated esters or ketones[10], as shown in equations 12–16.

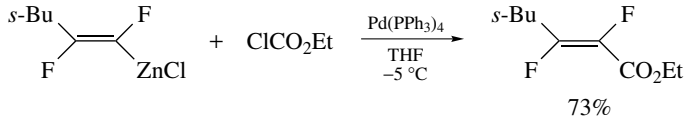

(12)

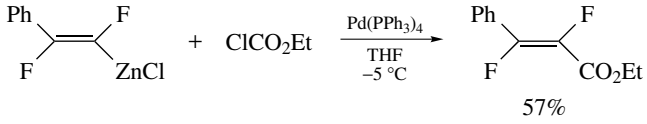

(13)

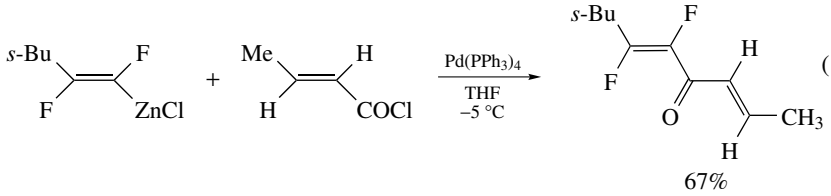

(14)

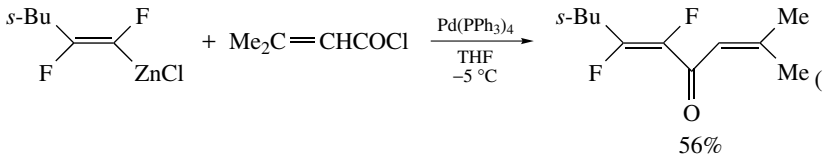

(15)

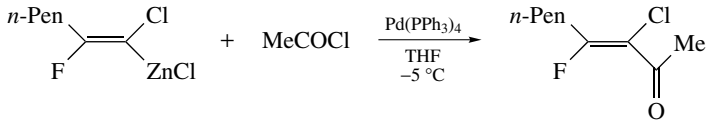

(16)

Related methodology has been utilized to prepare fluoroenynes either by coupling fluorinated vinyl halides with an acetylenic zinc reagent or via coupling of a fluorinated vinylzinc reagent with 1-iodo-1-alkynes[2,11], as illustrated in equations 17–21.

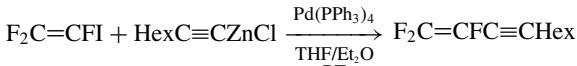

(17)

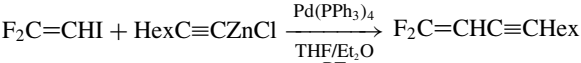

(18)

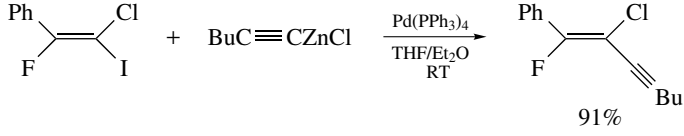

(19)

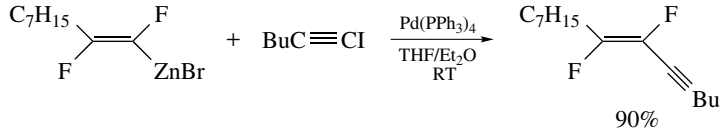

(20)

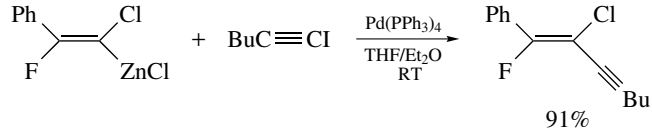

(21)

The preparation of fluorinated dienes is particularly advantageous via the palladium catalyzed coupling protocol. By proper selection of the appropriate vinylzinc reagent and vinyl iodide, a wide variety of fluorinated dienes can be stereospecifically prepared, as illustrated in equation 22.

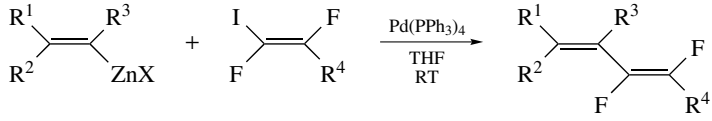

(22)

Typical examples of this synthetic protocol[12] are illustrated in equations 23–26.

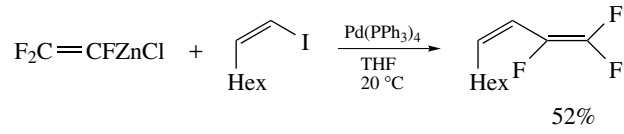

(23)

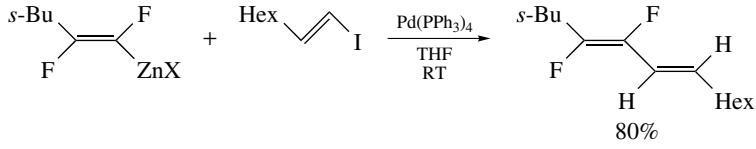

(24)

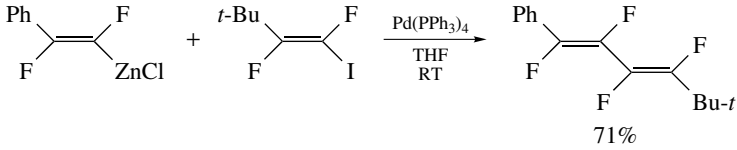

(25)

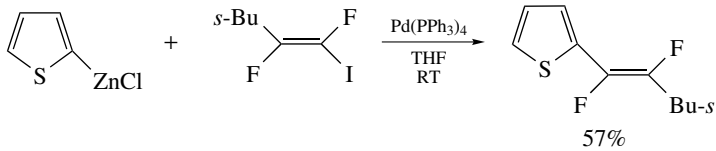

(26)

This methodology has been adapted to the preparation of fluorinated polyenes, as described in equation 27.

Similarly, the fluorinated analog of the codlemone phenomone has been synthesized by application of this coupling methodology[13], as illustrated in equation 28.

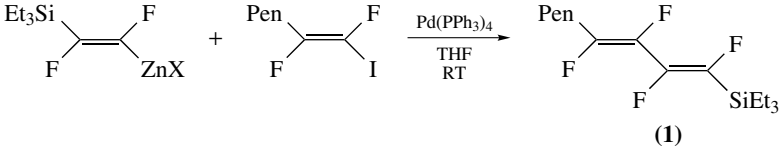

(1)

(2) (27)

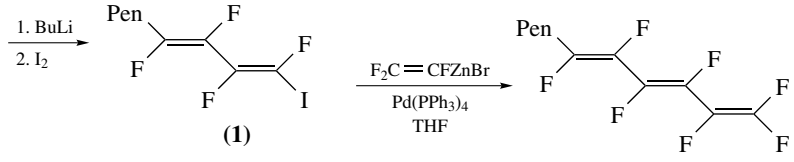

(1) 75%

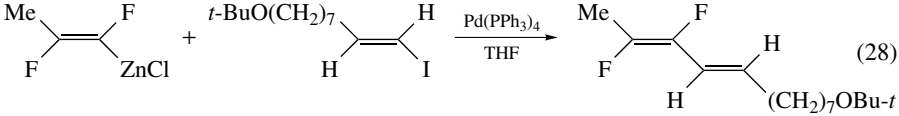

(28)

(from $F_2C{=}CFCl$) 85%

B. Method (2): *In Situ* Capture of Vinyllithium Reagents at Ambient Temperatures

The most recent methodology for the preparation of fluorinated vinylzinc reagents involves the *in situ* capture of the corresponding vinyllithium reagents with an anhydrous zinc salt. In this protocol, the base utilized to generate the vinyllithium reagent can also react with the zinc halide (equation 29). Therefore, one must develop reaction conditions that favor reaction of the base selectively with the organic substrate and not with the zinc halide. This dilemma has not been easy to solve and until recently impeded this approach to fluorinated vinylzinc reagents. In addition, if one wishes to carry out this procedure at ambient temperatures, capture of the unstable fluorinated vinyllithium reagent must be faster than β-elimination of the vinyllithium intermediate.

$$F_2C{=}CFH \xrightarrow[ZnCl_2]{RLi} [F_2C{=}CFZnCl] \text{ and/or } R_2Zn \tag{29}$$

Kumadaki and coworkers[14,15] reacted $F_2C{=}CHCl$ with *s*-BuLi in the presence of zinc chloride at $-60\,^{\circ}C$ in ether/cyclohexane (equation 30).

$$F_2C{=}CHCl \xrightarrow[\substack{ZnCl_2\\ether/cyclohexane\\-60\,^{\circ}C}]{s\text{-BuLi}} [F_2C{=}CClZnCl] \tag{30}$$

The intermediate vinyllithium reagent is presumably trapped *in situ* by the zinc chloride to form the 1-chloro-2,2-difluorovinylzinc reagent. Subsequent coupling of this reagent with 3,8-diiododeuterioporphoryrin derivatives gives the 3,8-bis(1-chloro-2,2-difluorovinyl) deuterioporphoryrins. The overall yield (based on zinc reagent) was <30%, and a large excess of zinc reagent was necessary to achieve significant amounts of the coupled product. There has also been some question concerning the assignment of the ^{19}F NMR spectrum of the presumed zinc reagent[16]. Also, this work (at $-60\,^{\circ}C$) did not solve the problem of low-temperature reactions. Kumadaki and coworkers recently reported the use of $CF_3CHClBr$ (Halothane) as a precursor to $[F_2C{=}CClZnCl]$ (equation 31); however, the yield of the zinc reagent was not reported[17]. Although Kumadaki reports reasonable yields of coupled products employing Halothane as a precursor, this precursor in our hands did not cleanly give high yields of the zinc reagent (equation 32)[18].

$$CF_3CHClBr \xrightarrow[\substack{ZnCl_2\\THF\\-60\,^{\circ}C}]{s\text{-BuLi}} [F_2C{=}CClZnCl] \xrightarrow[\substack{Pd(PPh_3)_4\\THF\\RT}]{ArI} F_2C{=}CClAr^{17} \tag{31}$$

$$CF_3CHClBr + Base \xrightarrow[15 \text{ or } -78\,^{\circ}C]{ZnCl_2} F_2C{=}CClZnCl + F_2C{=}CHBr + CF_2{=}CHCl + CF_3CHClBr^{18} \tag{32}$$

Bases: BuLi, *t*-BuLi, LDA, LTMP

The first practical application of this *in situ* protocol was reported by Anilkumar and Burton in 2002[19]. These workers examined the reaction of a wide variety of organolithium bases with the cheap, commercially available CF_3CFH_2 (HFC-134a) in the presence of anhydrous zinc salts. They established that LDA and anhydrous zinc chloride could effectively react with CF_3CFH_2 to produce good yields of the trifluorovinylzinc reagent at ambient temperatures[19,20] (15–20 °C) (equation 33). The *in situ* production of trifluorovinylzinc from CF_3CFH_2 was based on previous reports by Coe and coworkers[21–23]. In the presence of the diisopropylamine formed in the metallation reactions, the vinyllithium reagents could effectively compete for the zinc halide to produce the trifluorovinylzinc reagent[20].

$$CF_3CFH_2 \xrightarrow[\substack{ZnCl_2\\THF\\RT}]{LDA} [F_2C{=}CFH] + i\text{-}Pr_2NH + LiF \xrightarrow{LDA} [F_2C{=}CFLi] + i\text{-}Pr_2NH \xrightarrow{ZnCl_2} [F_2C{=}CFZnCl] + LiCl \quad (73\%) \tag{33}$$

The *in situ* formed vinylzinc reagent could subsequently be coupled (with palladium catalysis) with aryl iodides, as illustrated in equation 34. 1-Iodonaphthalene and

2-iodothiophene give 83 and 59%, respectively, of the trifluorovinyl derivative. Thus, this work represents the first, efficient, commercially viable route to 1,2,2-trifluorostyrenes[24], an industrially important co-monomer.

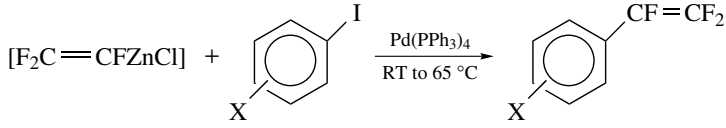

(34)

X = H (69%); X = *p*-F (64%); X = *m*-F (63%); X = *o*-F (74%); X = *p*-NO_2 (37%); X = *m*-NO_2 (61%); X = *p*-CF_3 (66%); X = *m*-CF_3 (67%); X = *o*-CF_3 (61%); X = *p*-OMe (82%); X = *m*-OMe (85%); X = *o*-$CH(CH_3)_2$ (86%); X = *m*-Cl (70%); X = *p*-Cl (82%); X = *p*-Br (75%); X = *p*-I (71%, bis adduct).

Extension of this methodology to other CF_3CH_2X (X = Cl, Br, I) derivatives demonstrated the generality of this protocol as a general, useful entry to zinc reagents of the type [F_2C=CXZnCl], where X = F, Cl, Br, I. Coupling of these *in situ* room-temperature-generated vinylzinc reagents provides a useful ambient, high yield, one-flask preparation of α-halo-β,β-difluorostyrenes. Typical examples of this class of styrenes, where X = Cl, are cited in equation 35[16, 18]. Disubstituted analogs could also be prepared, as illustrated in equations 36–38.

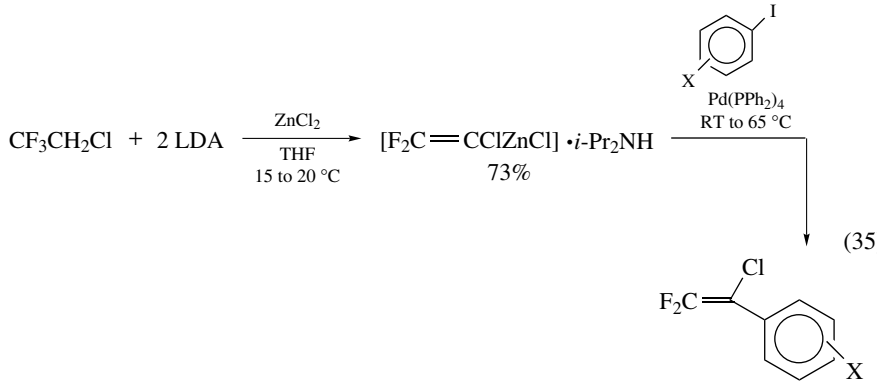

(35)

X = H (77%); X = *p*-F (81%); X = *p*-Me (83%); X = *p*-CO_2Et (70%); X = *m*-NO_2 (77%); X = *m*-OMe (79%); X = *m*-CF_3 (67%); X = *o*-$CH(CH_3)_2$ (75%); X = *p*-Cl (700%); X = *p*-Br (85%).

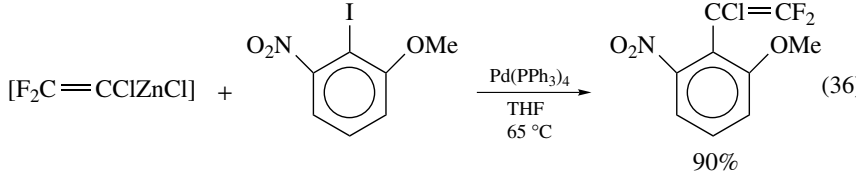

(36)

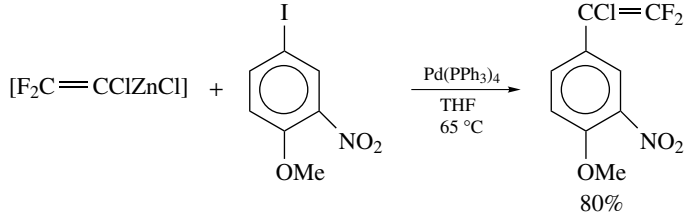

(37)

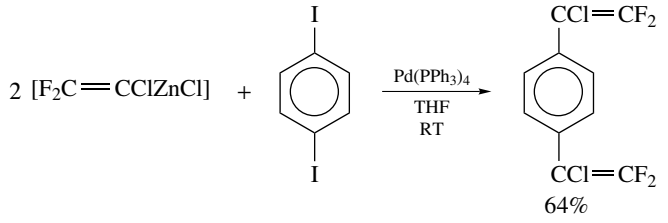

(38)

With either CF_3CH_2Br or $F_2C{=}CHBr$, this *in situ* protocol yielded $[F_2C{=}CBrZnCl]$ in high yield, which on coupling (with palladium catalysis) with aryl iodides gave the corresponding α-bromo-β,β-difluorostyrenes in high yields (equation 39)[25].

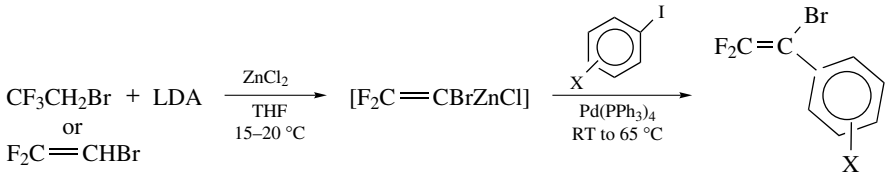

X = H (76%); X = *p*-F (75%); X = *p*-Cl (82%); X = *o*-Me (86%); X = *m*-NO_2 (75%); X = *p*-OMe (82%); X = *o*-CF_3 (74%); *p*-I (69%, bis adduct); 2-thienyl (64%). (39)

Similarly, CF_3CH_2I provided the α-iodovinylzinc reagent, as outlined in equation 40[26].

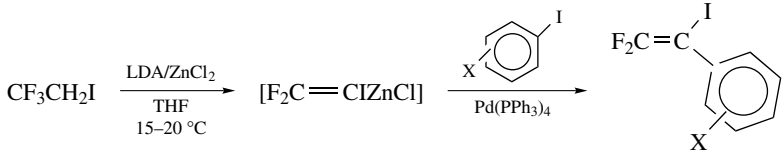

(40)

X = H (79%); X = *p*-F (71%); X = *m*-F (73%); X = *p*-Cl (78%); X = *o*-OMe (72%); X = *m*-NO_2 (78%); X = *m*-OMe (80%); X = *p*-I (62%, bis adduct).

Thus, this *in situ* protocol provides a general entry to $[F_2C{=}CXZnCl]$ reagents (where X = F, Cl, Br, I). It avoids the use of low temperatures (−60 to −100 °C) and is easier to scale-up. The precursors (CF_3CH_2X) are commercially available, cheap or moderately priced, and in some cases (X = F) is a cost-effective entry to commercially useful compounds. The α-bromo- and α-iodostyrenes also provide useful precursors to 1,1-difluoromethylene olefins via subsequent Suzuki couplings[27], as outlined in

equation 41. Many other precursors can be utilized in this *in situ* approach and this newer route should find many useful applications in the future.

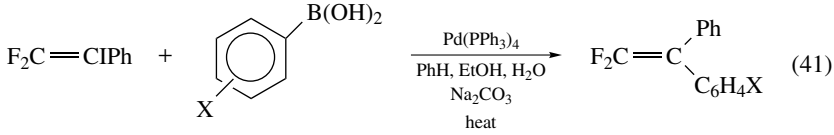

(41)

C. Method (3): Insertion of Zn° into The Carbon–Halogen Bond

The third method for the preparation of fluorinated vinylzinc reagent does not involve the use of the unstable fluorinated vinyllithium reagents, but employs the direct reaction of fluorovinyl bromides or iodides with activated zinc[28]. This route avoids the low-temperature problems associated with the limited thermal stability of fluorovinyllithium reagents and utilizes direct insertion of Zn° into the carbon–halogen bond (equation 42). The insertion reaction can be carried out in a variety of solvents, such as DMF, DMAC, THF, glymes and acetonitrile[28,29]. Though the vinyl halide required is more expensive than the precursors utilized in methods 1 and 2 above, the procedure is straightforward and is more readily scaled-up due to the avoidance of low temperatures. In general, fluorinated vinyl bromides required more polar solvents than the corresponding fluorinated vinyl iodides. It has also been reported that a less polar solvent can be employed if a strongly coordinating ligand, such as TMEDA, is used (equation 43)[30,31].

$$\underset{X = I,\ Br}{R_FFC{=}CFX} + Zn^{\circ} \xrightarrow[RT]{\text{solvent}} R_FFC = CFZnX + (R_FFC{=}CF)_2Zn + ZnX_2 \qquad (42)$$

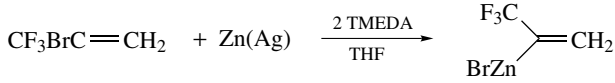

(43)

The zinc reagents are formed as a mono/bis mixture, and the mono/bis ratio varied with the structure of the vinyl halide and the solvent[28]. However, this ratio was inconsequential in palladium catalyzed coupling processes with aryl or vinylic halides. The zinc reagents produced by this method exhibit exceptional thermal stability, and a large batch of the zinc reagent can be prepared and utilized over an extended period of time in a variety of synthetic reactions without any significant loss of activity of the stock solution[28]. Note (Table 1) that the stereochemical integrity of the *E*/*Z* vinyl halides is preserved at all times in the formation of the fluorinated vinylzinc reagent. These zinc reagents are slightly moisture-sensitive and can be hydrolyzed to $R_FCF{=}CFH$. These zinc reagents also readily react with halogens, such as I_2 or Br_2, and allow the more accessible F-vinyl bromides to be conveniently converted to the F-vinyl iodides[9,32–34] (equations 44 and 45).

$$F_2C{=}CFBr \xrightarrow[DMF,\ RT]{Zn} [F_2C{=}CFZnBr] \xrightarrow{I_2} F_2C{=}CFI \qquad (44)$$

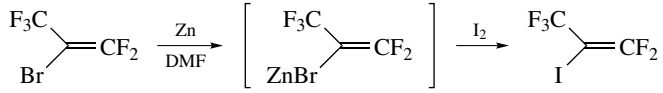

(45)

TABLE 1. Preparation of vinyl zinc reagents via Zn° insertion into F-vinyl halides

$$R_FFC{=}CFX + Zn^\circ \xrightarrow[RT-80\,^\circ C]{solvent} R_FFC{=}CFZnX$$

Halide	Solvent	Zn reagent	Yield (%)	References
$F_2C{=}CFI$	DMF	$F_2C{=}CFZnI$	79	28
$F_2C{=}CFI$	TG (triglyme)	$F_2C{=}CFZnI$	95	28
$F_2C{=}CFBr$	DMF	$F_2C{=}CFZnBr$	72	9, 28
Z-$CF_3FC{=}CFI$	DMF	*Z*-$CF_3FC{=}CFZnI$	100	28
E-$CF_3FC{=}CFI$	TG	*E*-$CF_3FC{=}CFZnI$	100	28
Z-$CF_3CF_2FC{=}CFI$	TG	*Z*-$CF_3CF_2FC{=}CFZnI$	90	28
$F_2C{=}CBr_2$	DMF	$F_2C{=}CBrZnBr$	97	28, 35
E-$CF_3HC{=}CFI$	TG	*E*-$CF_3HC{=}CFZnI$	89	28
E-$CF_3FC{=}C(CF_3)I$	TG	*E*-$CF_3FC{=}C(CF_3)ZnI$	75	28
Z-$CF_3(CF_2)_4FC{=}CFBr$	DMF	*Z*-$CF_3(CF_2)_4FC{=}CFZnBr$	77	28
Z-$HFC{=}CFI$	DMAC	*Z*-$HFC{=}CFZnI$	76	36
E-$HFC{=}CFI$	DMF	*E*-$HFC{=}CFZnI$	63	37, 38
$F_2C{=}CHI$	DMF	$F_2C{=}CHZnI$	70	39
$(CF_3)_2C{=}CBr_2$	DMF	$(CF_3)_2C{=}C(ZnBr)_2$	61	40
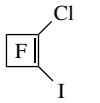	DMF	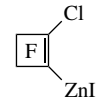	>90	41
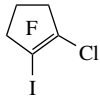	DMF	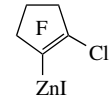	96	42
E-$FClC{=}CFI$	DMF	*E*-$FClC{=}CFZnI$	93	43
Z-$FClC{=}CFI$	DMF	*Z*-$FClC{=}CFZnI$	92	43
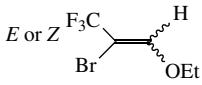	THF/TMEDA	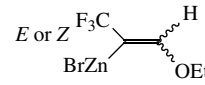	80–85	44

Typical examples of fluorovinylzinc reagents prepared by the direct insertion method are summarized in Table 1.

Little mechanistic work has been reported on the direct reaction of F-vinyl halides with Zn°. Jairaj and Burton have studied the mechanistic details of the reaction between *Z*-1-iodopentafluoropropene with Zn° and have presented mechanistic evidence consistent with the formation of a vinyl carbanion that is captured *in situ* by zinc halide to form the vinylzinc reagent[45]. Their mechanism is presented in Scheme 1.

The solvated vinylzinc reagent does not add to benzaldehyde; however, under Barbier conditions, the reaction of Zn°, *Z*-$CF_3CF{=}CFI$ in DMF stereospecifically gives the *E*-allyl alcohol consistent with trapping of the carbanion intermediate (Scheme 2).

The 2-pentafluoropropenylzinc reagent was prepared by Morken, Burton and coworkers via a novel one-pot reaction of $CF_3CBr_2CF_3$ with two equivalents of zinc in DMF (equation 46)[34]. The initially formed dehalogenation product, $CF_3BrC{=}CF_2$, reacted rapidly with the second equivalent of zinc to give the insertion product. Similarly, $CF_3CF_2CBr_2CF_3$ reacted with two equivalents of zinc in DMF to give the analogous internal 2-butenylzinc reagent as a mixture of *E*/*Z* isomers (equation 47)[46]. No terminal zinc reagent was detected. Thus, either vinyl halides can be directly reacted with zinc to

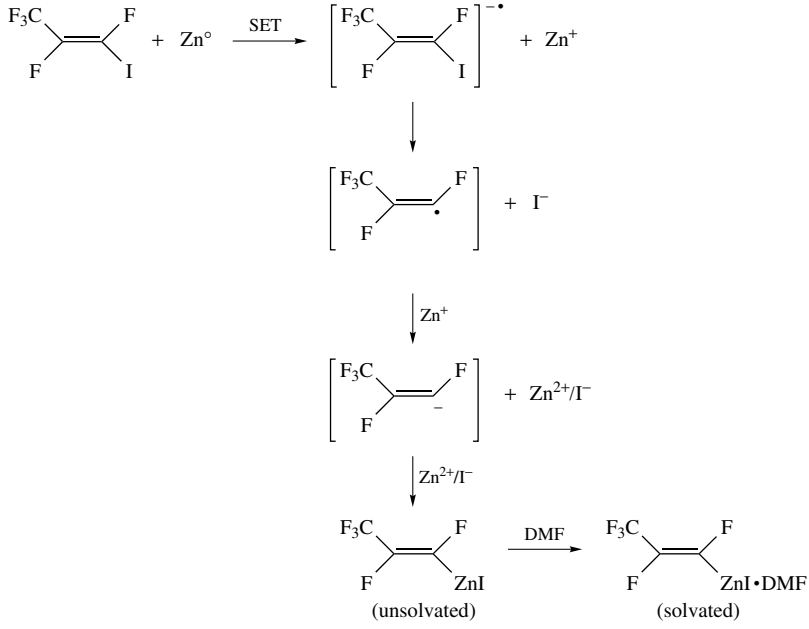

SCHEME 1

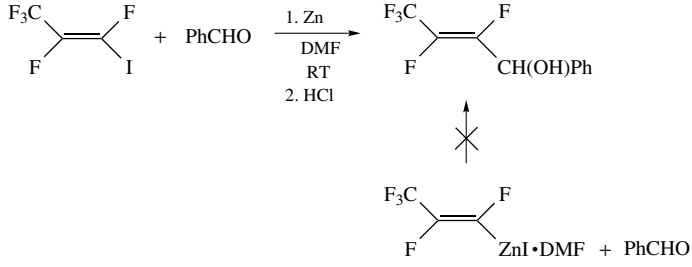

SCHEME 2

give the insertion product, or the requisite vinyl halide can be generated *in situ* followed by a subsequent zinc insertion to produce the fluorinated vinylzinc reagent.

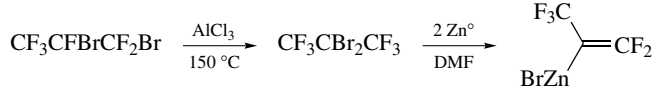

(46)

(47)

The fluorinated vinylzinc reagents formed via direct insertion of zinc into the carbon–halogen bond of a vinyl halide have served as useful synthons for the stereospecific synthesis of a wide variety of fluorinated compounds. Some illustrative examples of some of the synthons developed are summarized in the following sections.

1. Stereospecific preparation of fluorinated styrenes

Heinze and Burton reported the first practical synthesis of α,β,β-trifluorostyrenes via the palladium-catalyzed coupling of the trifluorovinylzinc reagent with aryl iodides[29] (equation 48). This methodology avoided the low temperatures in the earlier tetrafluoroethylene route[47], avoided side products (stilbenes) and/or multi-step procedures that plagued earlier reports of this important olefin[29].

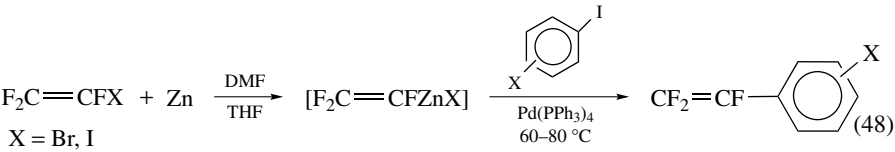

(48)

X = H (74%); X = *p*-OMe (61%); X = *m*-NO_2 (94%); X = *o*-NO_2 (73%); X = *m*-CF_3 (89%); X = *m*-CH_3 (85%); X = *o*-$CH(CH_3)_2$ (70%); X = *o*-Br (76%); X = *o*-CF_3 (73%); X = *p*-Cl (77%).

Similar methodology with Z-$CF_3FC{=}CFI$ and *E*-$CF_3FC{=}CFI$ stereospecifically gives the corresponding 1-arylperfluoropropenes[29].

The stereospecific preparation of *Z*-α,β-difluorostyrenes was accomplished by Davis and Burton via modification of the Heinze methodology, as illustrated in equation 49[37,38]. The *Z*-α,β-difluorostyrenes could be readily converted to other synthons, such as *E*-α,β-difluoro-β-iodostyrenes (*E*-FIC=CFPh) and *E*-α,β-difluoro-β-tributylstannanes (*E*-$PhFC{=}CFSnBu_3$), by known literature reactions[38], and which could be utilized as synthons in other coupling reactions.

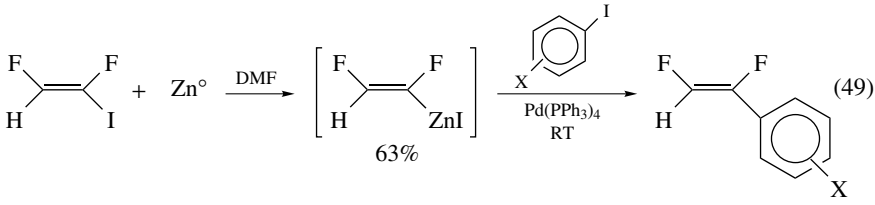

(49)

X = H (65%); X = *p*-CH_3 (85%); X = *p*-NO_2 (66%); X = *o*-NO_2 (78%); X = *p*-CH_3 (72%); X = *p*-CO_2Et (93%); X = *p*-$CH_3C(O)$ (71%); X = *m*-Cl (60%); X = *p*-CF_3 (70%); X = *o*-$CH(CH_3)_2$ (55%).

The corresponding *E*-α,β-difluorostyrenes were stereospecifically prepared by an analogous coupling process from *Z*-HFC=CFI, as illustrated in equation 50[36]. In contrast to the analogous *E*-vinylzinc reagent, the palladium-catalyzed coupling reaction was sluggish and incomplete; however, the use of Cu(I)Br as a co-catalyst accelerated the coupling reactions and most reactions went to completion in 1–2 h time to give good yields of the *E*-α,β-difluorostyrenes.

This insertion methodology was also adapted to the preparations of α-halo-β,β-difluorostyrenes by Nguyen, as illustrated in equation 51[35]. This methodology complements

the similar preparation of α-bromo-β,β-difluorostyrenes from CF_3CH_2Br (described in method 2, part B)[25].

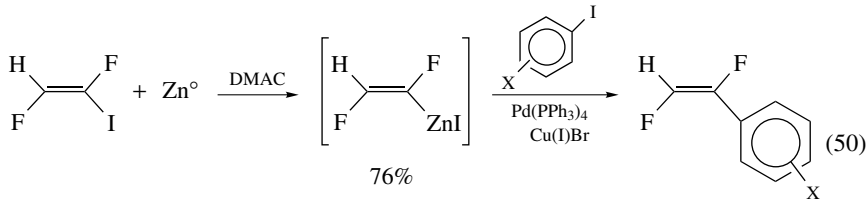

(50)

X = *p*-F (89%); X = H (74%); X = *p*-Br (94%); X = *p*-I (94%, bis adduct); X = *p*-Cl (95%); X = *p*-OMe (94%); X = *m*-CF_3 (84%); X = *p*-NO_2 (87%); X = *m*-NO_2 (93%).

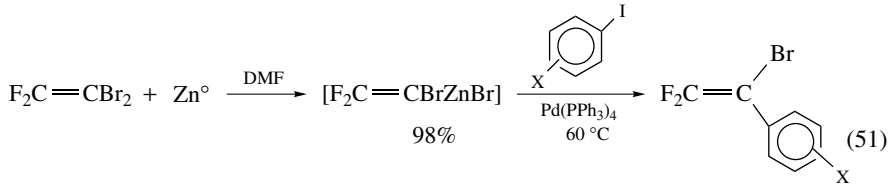

(51)

X = H (87%); X = *o*-CH_3 (81%); X = *p*-OMe (93%); X = *m*-NO_2 (96%); X = *m*-CH_3 (93%); X = *o*-CF_3 (83%); X = *p*-CH_3 (77%); X = *p*-I (84%, bis adduct).

Nguyen and Burton also reported a practical route to 2,2-difluorostyrenes via the palladium-catalyzed coupling of 1-iodo-2,2-difluoroethylene with aryl iodides, as outlined in equation 52[39]. Surprisingly, $F_2C{=}CHBr$ does not work well in this reaction. The initially formed vinylzinc reagent undergoes a novel acid–base reaction (with unreacted olefin) and both [$F_2C{=}CHZnBr$] and [$F_2C{=}CBrZnBr$] are formed, as well as $F_2C{=}CH_2$ (Scheme 3). Thus, $F_2C{=}CHI$ is necessary to achieve selective formation of only the 2,2-difluorostyrene derivative.

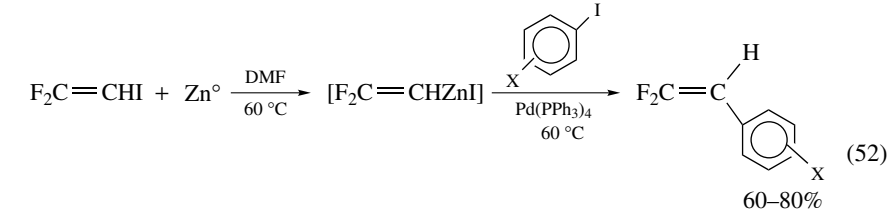

(52)

60–80%

X = H (87%); X = *o*-OCH_3 (71%); X = *m*-OMe (88%); X = *m*-CH_3 (78%); X = *o*-F (69%); X = *p*-$CH_3C(O)$ (78%); X = *m*-NO_2 (92%); X = *p*-CH_3 (75%); X = *p*-NO_2 (86%); X = *m*-CF_3 (80%); X = *p*-CF_3 (80%).

Morken and Burton extended this methodology to the synthesis of β,β-difluoro-α-(trifluoromethyl)styrenes, as illustrated in equation 53[34]. The steric hindrance presented by

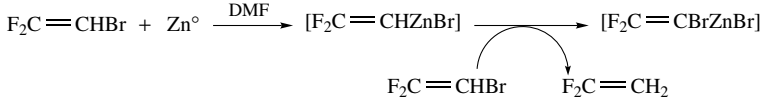

SCHEME 3

the α-CF_3 group required higher temperatures than the simple synthons, but the coupling process generally works well.

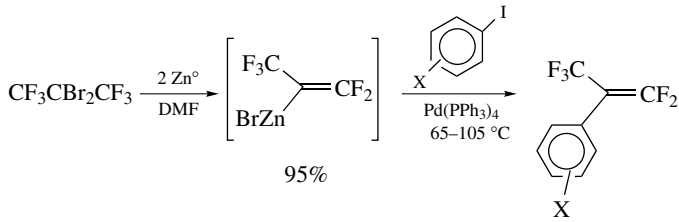

(53)

X = H (62%); X = *p*-NO_2 (75%); X = *m*-NO_2 (72%); X = *p*-OMe (68%); X = *p*-Br (64%); X = *m*-Cl (45%); X = *p*-CO_2Et (73%); X = *p*-CH_3 (66%); X = *o*-F (64%).

2. Preparation of 1,1,2-trifluoro-2-trimethylsilylethylene

A key starting material for the preparation of fluorine-containing vinylzinc synthons is $F_2C{=}CFSiMe_3$, which can be readily prepared via reaction of trifluorovinyllithium with Me_3SiCl (equation 54). However, separation of the vinylsilane from solvent and halogen exchange by-products has hindered this route to this key starting material. As an alternative, silyl derivatives, such as Et_3SiCl and $PhSiMe_2Cl$, have been utilized to facilitate isolation of the vinylsilane. However, the use of these alternative silanes significantly increases the cost of this key material. Jairaj and Burton have solved this dilemma by the development of the Cu(I)Br-catalyzed silylation of the 1,1,2-trifluoroethenylzinc reagent with the cheap Me_3SiCl[48] (equation 55). This reaction protocol is easily scaled up and isolation of the trifluorovinylsilane is facile. The synthetic protocol is described in detail in this report.

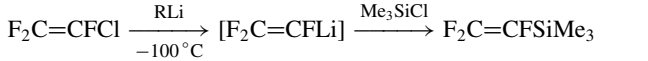

(54)

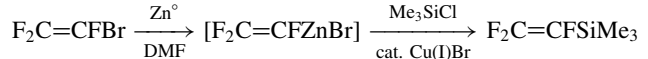

(55)

3. Stereospecific preparation of fluorinated dienes

Heinze, MacNeil and coworkers developed the first methodology for the preparation of isomerically pure *E*- and *Z*-perfluoro-1,3-pentadienes, as described in equations 56 and 57[49,50]. Similar methodology was employed for the preparation of related perfluoro-3,5-octadiene systems[49]. These dienes were key components for studying the kinetic and thermodynamic electrocyclic interconversions of perfluorinated dienes and cyclobutenes,

and unambiguously established that an electronic component, as well as a steric component, controlled these interconversions[49].

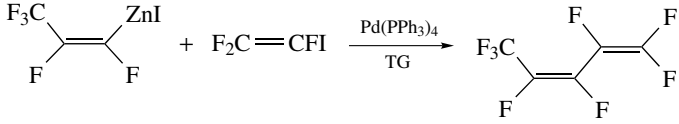

50% (56)

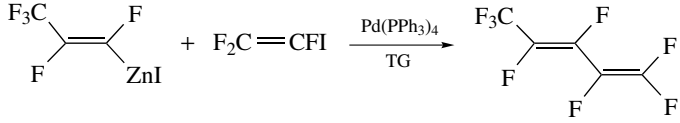

80% (57)

Fluorinated vinylzinc reagents undergo coupling with $CuBr_2$ or $FeCl_3$ to give symmetrical dienes (equations 58 and 59)[51,52].

$$F_2C{=}CFZnX + CuBr_2 \xrightarrow[\text{vacuum}]{-25\text{ to }-15\,^\circ C} \underset{97\%}{F_2C{=}CFCF{=}CF_2} \quad (58)$$

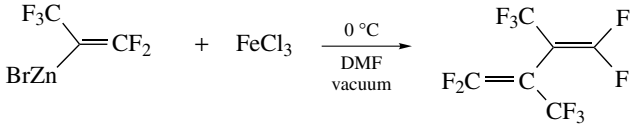

85% (59)

Fluorinated α-halovinylzinc reagents (halogen = Cl, Br, I), when treated with a catalytic amount of CuBr, provides a useful entry to fluorinated 1,2,3-cumulenes (equation 60)[53,54]. The *E*- and *Z*-cumulenes were readily separated by silica gel chromatography and pure multigram quantities of pure cumulenes were easily synthesized by this methodology. The mechanism of this novel reaction was elucidated by Morken and coworkers[54].

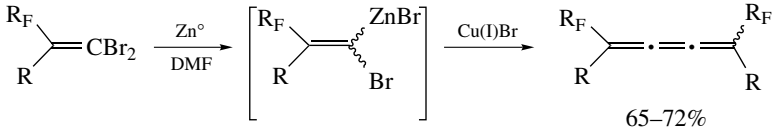

65–72% (60)

$R_F = CF_3, C_2F_5, C_3F_7$
R = Ph, C_6F_5

Dolbier and coworkers have utilized similar coupling with 1,2-diiodonaphthalene and 9-iodo-10-nitrophenanthrene to introduce two trifluorovinyl groups onto the aromatic

substrate (equations 61 and 62)[55]. Sprague and coworkers employed similar methodology in the preparation of a complex fluorinated styrene derivative[56].

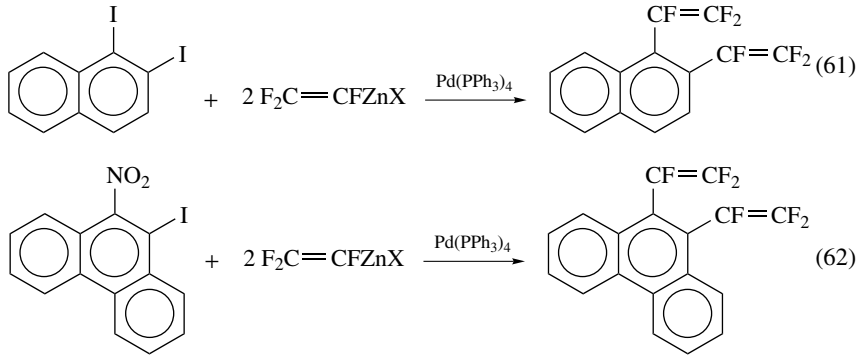

4. Allylation

Fluorinated vinylzinc reagents readily react (particularly with Cu(I)X catalysis) with allyl halides at room temperature (equation 63)[57]. With a substituted allyl halide, the 2-propenyl reagent gave products of both α- and γ-attack. The predominant product is derived from attack at the less hindered position (equation 64)[5].

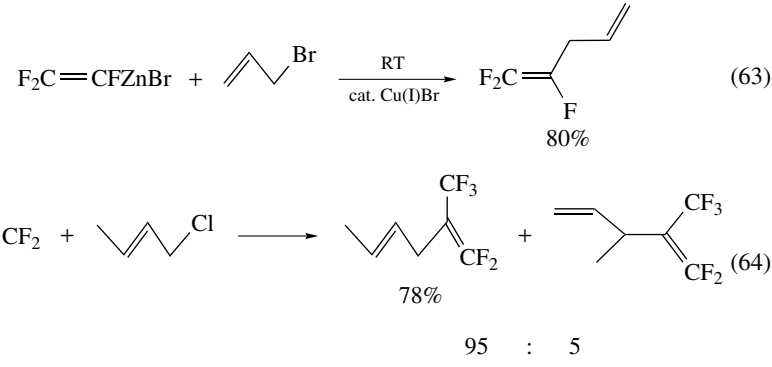

5. Acylation

Spawn and Burton investigated the reactions of the trifluorovinylzinc reagent with acyl halides. The reactions were sluggish and gave low yields of the trifluorovinyl ketones. However, with Cu(I)Br catalysis, the acylation occurred rapidly and gave excellent yields of the trifluorovinyl ketones (equation 65)[58].

$$F_2C{=}CFZnX + RC(O)Cl \xrightarrow[\text{glyme, RT}]{\text{Cu(I)Br}} F_2C{=}CFC(O)R \qquad (65)$$

R = Me (76%); R = Et (83%); R = Pr (73%); R = *i*-Pr (87%); R = *t*-Bu (81%); R = Pen (67%); R = C(O)OEt (50%); R = CH_2Cl (44%); R = $CH_2CH_2C(O)OMe$ (44%).

The 2-perfluoropropenyl zinc reagent reacted similarly to give the corresponding ketone (equation 66)[51].

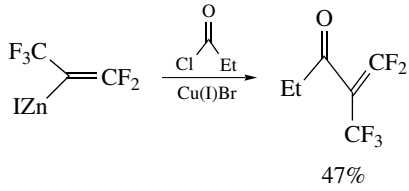

(66)

6. Preparation of functionalized CF_3-containing compounds

The partially fluorinated vinylzinc reagent, reported by Shi and coworkers, has been utilized to prepare the fluoro analog of Naproxen and for the key intermediate for a novel synthetic pyrethroid (equations 67 and 68)[44].

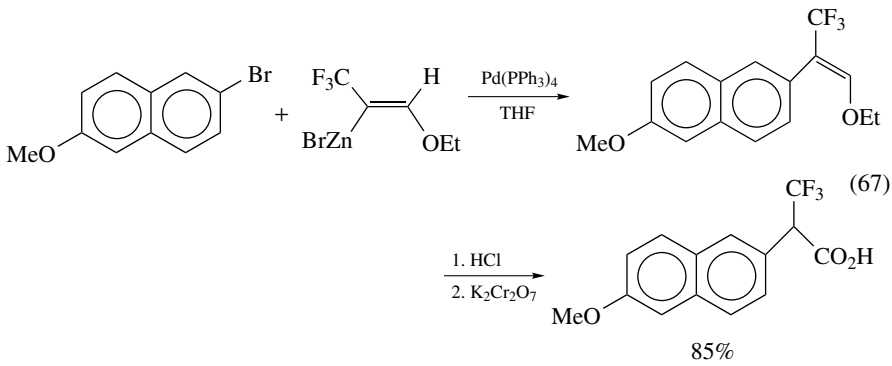

(67)

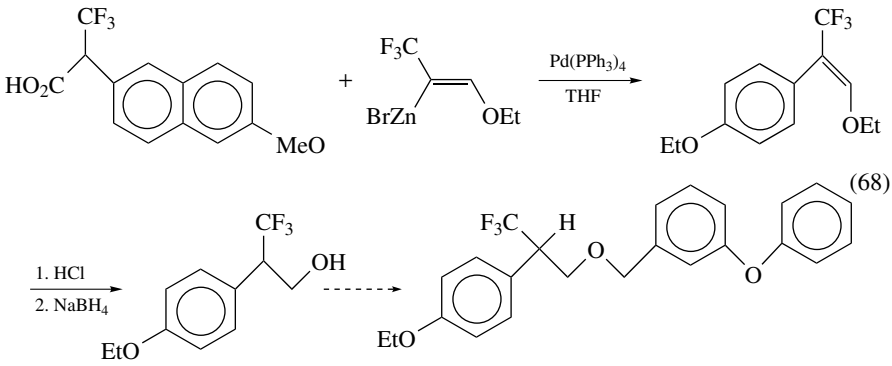

(68)

7. Allene formation

An improved route to tetrafluoroallene was developed by Lu and coworkers based on the preparation of 2-bromopentafluoropropene from the pentafluoropropen-2-ylzinc reagent (equation 69)[59].

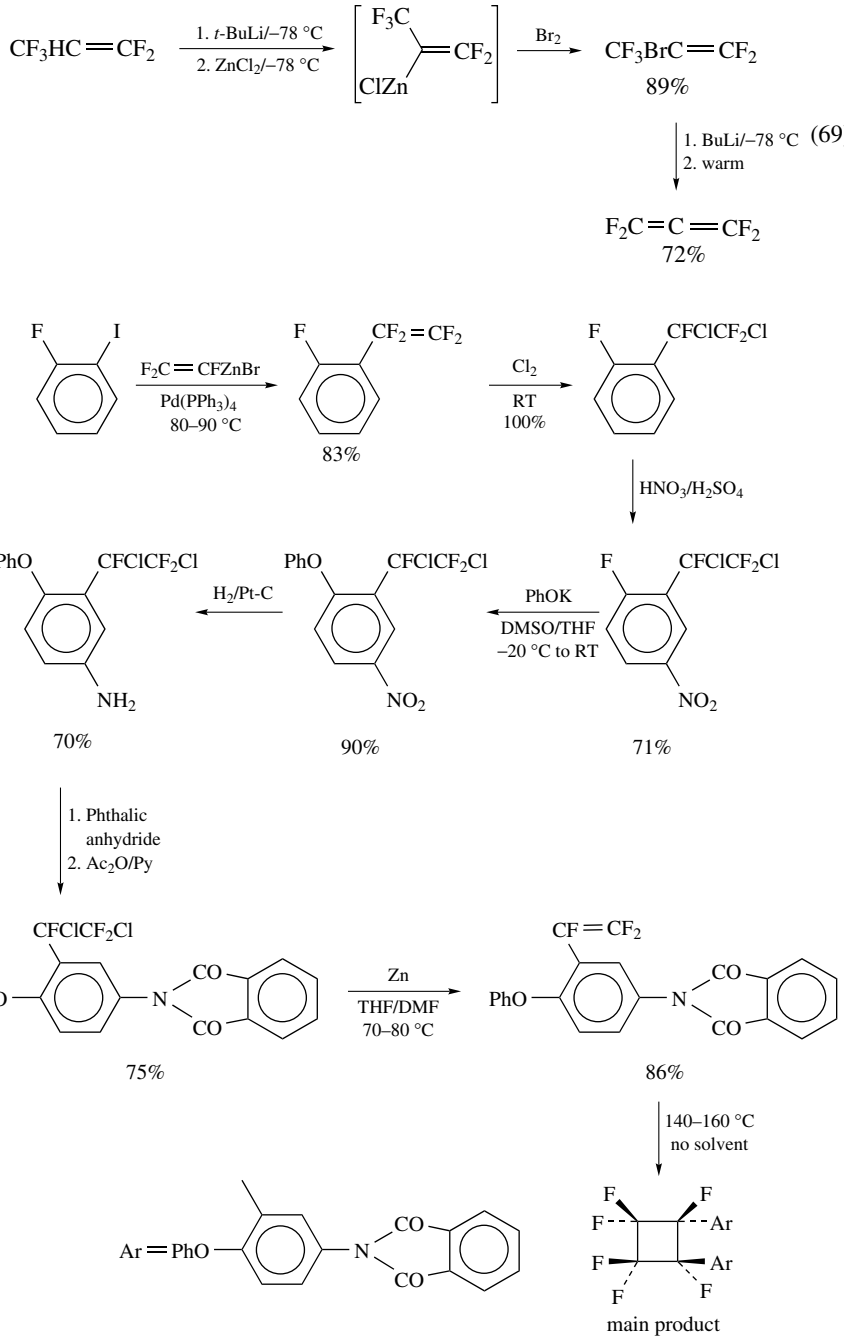
CF3HC=CF2
1. t-BuLi/–78 °C
2. ZnCl2/–78 °C
F3C
CF2
ClZn
Br2
CF3BrC=CF2
89%
1. BuLi/–78 °C
2. warm
(69)
F2C=C=CF2
72%
F
I
F2C=CFZnBr
Pd(PPh3)4
80–90 °C
F
CF2=CF2
83%
Cl2
RT
100%
F
CFClCF2Cl
HNO3/H2SO4
F
CFClCF2Cl
NO2
71%
PhOK
DMSO/THF
–20 °C to RT
PhO
CFClCF2Cl
NO2
90%
H2/Pt-C
PhO
CFClCF2Cl
NH2
70%
1. Phthalic anhydride
2. Ac2O/Py
CFClCF2Cl
PhO
N
CO
CO
75%
Zn
THF/DMF
70–80 °C
CF=CF2
PhO
N
CO
CO
86%
140–160 °C
no solvent
Ar=PhO
N
CO
CO
F
F
F
Ar
F
Ar
F
F
main product

SCHEME 4

8. Preparation of polymer precursor

Yamamoto and coworkers utilized the resultant product from the palladium catalyzed reaction of 1-fluoro-2-iodobenzene with the trifluorovinylzinc reagent to prepare a trifluorovinylimide, which on thermal dimerization at 140–160 °C gave predominantly the *E*-cyclobutane, whose structure was established by X-ray crystallography (Scheme 4)[60].

Modification of Scheme 4 allowed the preparation of a trifluorovinyl-containing polyimide. Related types of trifluorovinyl precursors (which can undergo 2 + 2 thermal cycloaddition) have been investigated in recent years by Dennis Smith and coworkers at Clemson University[61–63].

III. PERFLUOROARYL ZINC REAGENTS

In contrast to the extensive investigation of fluorovinylzinc reagents and their synthetic utility, only limited literature exists on fluorinated arylzinc reagents. Bis(pentafluorophenyl) zinc can be prepared by the reaction of zinc chloride with either pentafluorophenyllithium or pentafluorophenylmagnesium bromide (equation 70)[64, 65]. An alternative route is via decarboxylation of zinc bis(pentafluorobenzoate) (equation 71)[65].

$$\underset{\text{M = Li, MgX}}{ZnCl_2 + 2\ C_6F_5M} \longrightarrow (C_6F_5)_2Zn + MCl_2 \tag{70}$$

$$Zn(OCOC_6F_5)_2 \xrightarrow[10^{-2}\text{Torr}]{220\,^\circ\text{C}} \underset{62\%}{(C_6F_5)_2Zn} \tag{71}$$

Several forms of bis(pentafluorophenyl)zinc have been observed[65]. The high temperatures employed in the decarboxylation route illustrate the thermal stability of the aryl zinc reagents. 1:1 Metal complexes, such as 2,2′-bipyridine and 1,10-phenanthroline, are readily formed by these zinc reagents[66, 67].

Similar to the zinc insertion methodology for the preparation of fluorinated vinylzinc reagents (Section II.C), zinc reacts quantitatively with bromo- and iodopentafluorobenzene in coordinating solvents such as THF, Et_2O, DME, DG (diglyme), DMF, DMAC and DMSO to give bis(pentafluorophenyl)zinc (equation 72)[68]. These workers also obtained equilibrium constants for the Schlenk equilibrium between the mono/bis species via ^{19}F NMR spectra.

$$2\ C_6F_5I + Zn^\circ \xrightarrow[\text{solvent}]{\text{coordinating}} (C_6F_5)_2Zn \tag{72}$$

The decarboxylation route has also been employed by Sartori and Adelt for the preparation of bis(tetrafluoropyridyl)zinc (equation 73)[69].

$$Zn(OCOC_5F_4N) \xrightarrow{300\,^\circ\text{C}} \underset{76\%}{(C_5F_4N)_2Zn} \tag{73}$$

More recently, Lange and Naumann have described a new exchange method for the preparation of bis(perfluoroorgano)zinc compounds, which involves the reaction of iodopentafluorobenzene with a dialkylzinc in the presence of a Lewis acid (equation 74)[70].

$$2\ C_6F_5I + Et_2Zn \xrightarrow[20\,^\circ\text{C}]{\text{Py•DG}} \underset{\text{quant.}}{(C_6F_5)_2Zn} + 2\ EtI \tag{74}$$

A novel approach to perfluoroarylzinc reagents was recently reported by Miller, Platonov and coworkers. This route involves direct insertion of zinc into carbon–fluorine bonds in the presence of metal salts, such as $SnCl_2$, $CuCl_2$ and $ZnBr_2$. These reactions are accelerated by ultrasound (equation 75)[71]. The reaction rate decreased in THF or if $ZnBr_2$ or $CuCl_2$ were used.

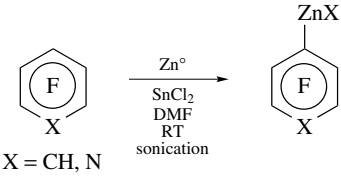

(75)

The reaction failed without addition of the salts. The range of substrate reactivity formed was:

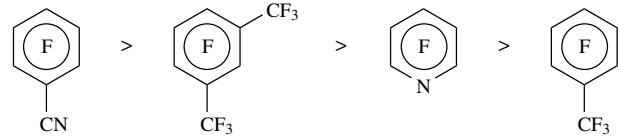

Hexafluorobenzene and perfluoro-*o*-xylene failed to react under these conditions. Reaction of these zinc reagents with H_3O^+, Br_2 and $CuCl_2$ gave the expected hydro and bromo compounds and the corresponding biphenyl in good yields (equations 76–78).

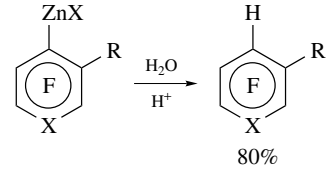

(76)

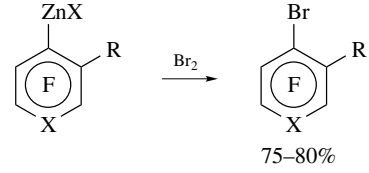

(77)

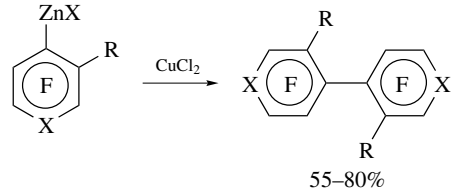

(78)

IV. FLUORINATED ALLYL AND PROPARGYLZINC REAGENTS

The formation of a stable, detectable fluorinated allylic or propargylic zinc reagent has not yet been accomplished by synthetic chemists. When perfluoroallyl iodide was reacted with zinc in DMF, only a low yield (*ca* 10%) of the presumed zinc reagent was detected

by ^{19}F NMR; the major product of this reaction was the coupled product, perfluoro-1,5-hexadiene (equation 79)[72]. In contrast to this observation, the corresponding cadmium reagent, prepared by reaction of perfluoroallyl iodide with Cd° in DMF was formed in 73% yield[72].

$$F_2C{=}CFCF_2I + Zn^\circ \xrightarrow{DMF} \underset{48-77\%}{F_2C{=}CF(CF_2)_2FC{=}CF_2} \tag{79}$$

Although stable fluorinated allyl or propargyl zinc reagents have not yet been prepared, the *in situ* capture of fluorine-containing allyl or propargyl derivatives via reaction of an allylic halide or propargylic halide with zinc has been utilized by synthetic chemists to introduce these moieties into organic substrates. For example, Yang and Burton utilized the reaction of 3-bromo-3,3-difluoropropene with zinc powder in THF in the presence of aldehydes and ketones to provide a useful route to *gem*-difluoroallylic alcohols (equation 80)[73,74]. Aromatic and aliphatic aldehydes and ketones worked well in this transformation. With α,β-unsaturated aldehydes and ketones, exclusive formation of the 1,2-addition product was observed; no 1,4-addition product was detected—even in the presence of Cu(I)I (equation 81)[74]. Similar allylation had previously been reported by Seyferth and coworkers[75] utilizing the *gem*-(difluoroallyl)lithium reagent, generated by lithium exchange between BuLi and $H_2C{=}CHCF_2Br$ at $-95\,^\circ C$ or via an *in situ* reaction between BuLi and $Me_3SnCH_2CH{=}CF_2$ at $-95\,^\circ C$ (equations 82 and 83)[76] or via preparation of the allyl tin reagent via reaction of β-trimethylstannylethylidenetriphenylphosphorane with chlorodifluoromethane (equation 84)[77].

$$PhCHO + H_2C{=}CHCF_2Br + Zn^\circ \xrightarrow[0\,^\circ C \text{ to RT}]{THF} \underset{67\%}{H_2C{=}CHCF_2CH(OH)Ph} \tag{80}$$

$$PhHC{=}CHCHO + H_2C{=}CHCF_2Br \xrightarrow[0\,^\circ C \text{ to RT}]{Zn^\circ,\ THF} \underset{75\%}{H_2C{=}CHCF_2CH(OH)HC{=}CHPh} \tag{81}$$

$$H_2C{=}CHCF_2Br + BuLi \xrightarrow[-95\,^\circ C]{THF} [H_2C{=}CHCF_2]^-Li^+ \xrightarrow{PhCHO} \underset{78\%}{H_2C{=}CHCF_2CH(OH)Ph} \tag{82}$$

$$Me_3SnCH_2HC{=}CF_2 + BuLi \xrightarrow[-95\,^\circ C]{THF} [F_2C{=}CHCH_2]^-Li^+ \xrightarrow{PhC(O)Me} \underset{78\%}{PhMeC(OH)CF_2HC{=}CH_2} \tag{83}$$

$$2\ Ph_3P{=}CHCH_2SnMe_3 + HCF_2Cl \longrightarrow Me_3SnCH_2HC{=}CF_2 \tag{84}$$

Hiyama and coworkers produced the same allylation compounds via the *in situ* reaction of 1,1-difluoro-3-(dimethylphenylsilyl)propene and aldehydes with catalytic tris(diethylamino)sulfonium difluorotrimethylsilicate (TASF) or potassium *t*-butoxide (equation 85)[78,79].

$$F_2C{=}CHCH_2SiMe_2Ph + PhCHO \xrightarrow[\substack{HMPA\\RT}]{TASF} \underset{68-93\%}{H_2C{=}CHCF_2CH(OH)Ph} \tag{85}$$

The isomeric 3,3-difluoro-3-(dimethylphenylsilyl)propene gave exclusively the same product (equation 86)[79].

$$H_2C{=}CHCF_2SiMe_2Ph + PhCHO \xrightarrow[\substack{DMPU\\RT}]{TASF} \underset{58\%}{H_2C{=}CHCF_2CH(OH)Ph} \qquad (86)$$

Note that in all three routes described above, the exclusive product formed is the isomer that results from CF_2 terminus attack on the carbon atom of the carbonyl group. In the Seyferth modification, the reactions utilize the unstable allyllithium intermediate and must be conducted at low temperatures. In the Hiyama approach, the method necessitated the prior preparation of the requisite (difluoroallyl)silanes. The Yang route utilizes an available precursor, avoids unstable intermediates, exhibits a wider range of substrate reactivity and can be routinely done at room temperature. The regiochemical results noted above are in agreement with Tonachini and Canopa's theoretical description[80] and can be rationalized in terms of the more nucleophilic α-carbon of the *gem*-difluoroallyl intermediate[74].

Ishihara and coworkers have reported that the reaction of 2-[(trimethylsilyl)methyl]-3-chloro-3,3-difluoropropene couples regioselectively with a variety of carbonyl compounds in the presence of zinc–copper(I) chloride or silver acetate to give 2,2-difluoro-3-(trimethylsilyl)methyl-3-buten-1-ol derivatives (equation 87)[81]. Note again that the difluoroallyl zinc species generated *in situ* reacts exclusively on the difluoromethylene terminus.

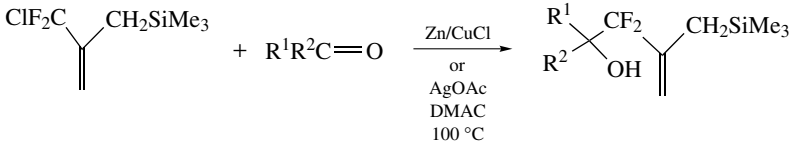

(87)

Recently, Zhu and coworkers have investigated the reaction of the zinc reagent from ethyl 3-bromodifluoromethyl-3-benzyloxyacrylate. The exclusive zinc reagent formed in DMF was the γ-carbon metallated product (equation 88)[82]. These workers utilized this reaction to prepare α-difluorovinyl substituted β-hydroxyesters in high yields and high regioselectivity via the reactions of aldehydes mediated by zinc (equation 89)[82].

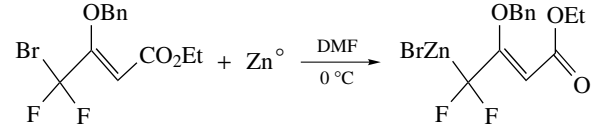

(88)

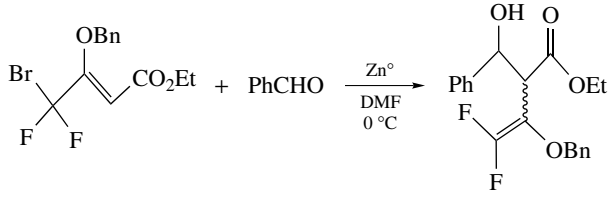

(89)

95%
syn/anti = 41/54

When similar reactions were carried out with tetrakis(dimethylamino)ethylene (TDAE) in THF or DMF, the *gem*-difluorinated δ-hydroxy esters were obtained (equation 90)[82].

Fried and coworkers prepared fluorine-containing propargylic halides via reaction of alkynyllithium reagents with CF_2BrCl (equation 91)[83]. These workers utilized these propargylic halides for the total synthesis of 7,7- 10,10- and 13,13-difluoroarachidonic acids. Sham and Betebenner subsequently employed these propargyl-type fluoro precursors to design a synthesis of 3-fluoro-2,5-disubstituted furans (equation 92)[84]. The 2-substituent can be readily varied by choice of the appropriate aldehyde as the starting material.

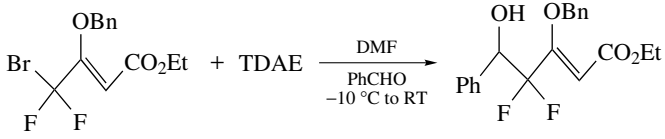

48% (90)

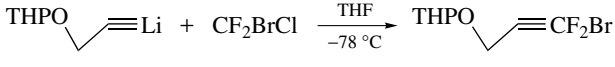

52% (91)

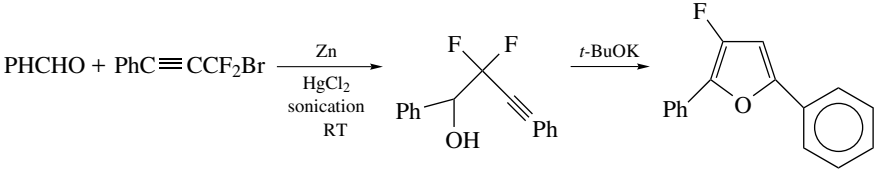

98% (92)

V. PERFLUOROALKYNYLZINC REAGENTS

Perfluoroalkynylzinc reagents have been prepared by three methods:

(a) Dehalogenation of 1,1,1,2,2-pentachloroperfluoroalkanes in DMF[85].
(b) Capture of perfluoroalkynyllithium reagents with $ZnCl_2$ in THF[86].
(c) Direct reaction of 1-iodoperfluoro-1-alkynes with zinc in DMF or TG[87,88].

The resultant perfluoroalkynylzinc reagents exhibit good thermal stability. For example, $C_4F_9C{\equiv}CZnX$ in DMF showed only a 4% loss of activity after 36 days at room temperature[87]. Decomposition occurred upon heating to 100 °C. Comparatively, perfluoroalkynyllithium reagents are typically generated at −70 °C, although significant decomposition is generally not observed until exposure to temperatures above 0 °C[89–91]. The corresponding perfluoralkynylmagnesium reagents show increased stability vs. the lithium reagents as the magnesium reagents tolerate reflux conditions in ether[92–94]. Thus, the significant margin of thermal stability generally observed between fluorinated zinc reagents and their lithium and magnesium counterparts is somewhat lessened in this comparison. This is not unexpected as there are no β-fluorines and a β-elimination decomposition pathway is unavailable.

Finnegan and Norris first reported trifluoropropynylzinc by dehalogenation of 3,3,3-trifluorotrichloropropene to give a mixture of mono and bis(trifluoropropynyl)zinc (equation 93)[95]. Addition of water to the zinc reagent solution gave trifluoropropyne. The zinc reagent underwent oxidative coupling to form perfluoro-2,4-hexadiyne[96].

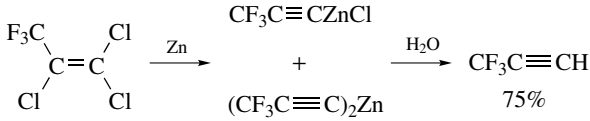

(93)

The higher acetylenic homologues have been prepared by Burton and Spawn from 1,1,1,2,2-pentachloroperfluoroalkanes and Zn in DMF (equation 94). The pentachloro precursors were obtained from the corresponding commercially available 1,1,2-trihydroperfluoro-1-alkenes. Acid hydrolysis of these zinc reagents gave the perfluoroalkynes in good yield[85].

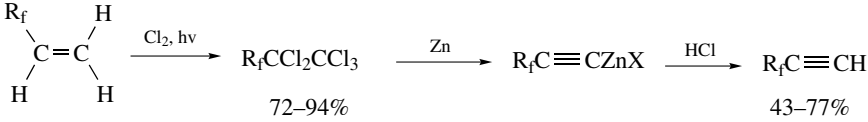

$R_f = C_3F_7, C_4F_9, C_6F_{13}, C_8F_{17}, C_{10}F_{21}$ (94)

Metallation of perfluoroalkynyllithiums with $ZnCl_2$ in THF provides an alternative route to perfluoroalkynylzinc reagents[86]. A notable difference is that the zinc reagents prepared by this approach exhibited greater reactivity toward Pd-catalyzed coupling reactions. Bunch and Bumgardner reported that trifluoropropynylzinc chloride coupled with aryl iodides in the presence of $Pd(PPh_3)_4$ gives aryl trifluoroacetylene in high yields (equation 95)[86]. In contrast, the zinc reagent prepared directly from 1,1,2-trichloro-3,3,3-trifluoropropene gave the coupled products in less than 40% yields[86].

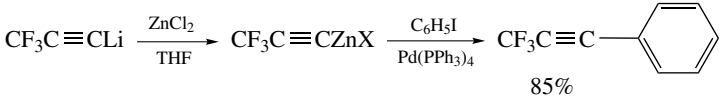

(95)

Longer perfluoroalkyl chain alkynylzinc reagents have also been reported by Yoneda and coworkers to undergo coupling with aryl iodides (Scheme 5)[97]. However, the reaction with heteroaromatic iodides was sluggish and attempted coupling with bromobenzene gave only traces of product. Vinyl iodides and bromides also coupled with the zinc reagents in presence of the Pd catalyst to yield the corresponding enynes with retention of configuration.

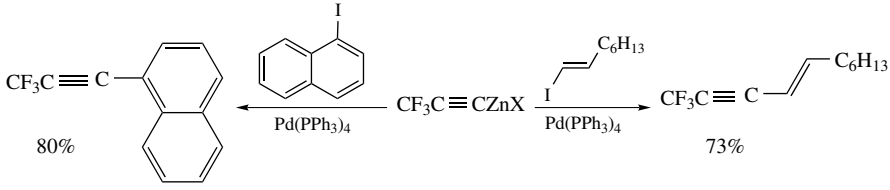

SCHEME 5

Burton and coworkers developed the direct metallation of 1-iodoperfluoro-1-alkynes for the preparation of perfluoroalkynylzinc reagents[87]. When 1-iodoperfluoro-1-alkynes

were treated with zinc in TG (triglyme) or DMF at room temperature, the zinc reagents were formed in excellent yields as a mixture of mono and bis(perfluoroalkynyl) species (equation 96). The mono and bis reagents were readily distinguishable by ^{19}F NMR based on enhancement of the signal for the mono species upon addition of zinc iodide.

$$R_fC{\equiv}CI \xrightarrow[TG \text{ or } DMF]{Zn} R_fC{\equiv}CZnI + (R_fC{\equiv}C)_2Zn \qquad (96)$$

Perfluoroalkynylzinc reagents do not generally undergo direct acylation or allylation. One exception, however, is reaction of bis(trifluoropropynyl)zinc with benzoyl chloride, without catalyst, to give the aroyltrifluoromethyl acetylene (equation 97)[98].

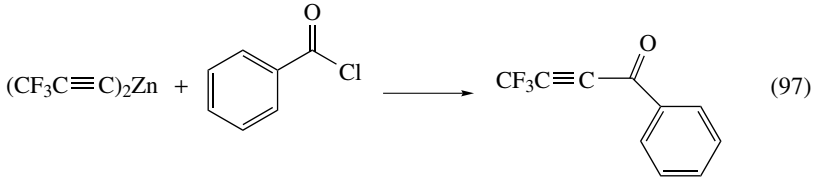

(97)

The synthetic utility of perfluoroalkynylzinc reagents is extended via quantitative transmetallation with Cu(I) halides in DMF to give versatile perfluoroalkynylcopper reagents[87]. The pre-generated copper reagents are thermally stable from room temperature to 65 °C, although perfluorohexynylcopper has been utilized at significantly higher temperatures. Typical coupling reactions of the copper reagents with aryl iodides, vinyl iodides, allyl halides and 1-iodoperfluoroalkynes are outlined below (Scheme 6)[87].

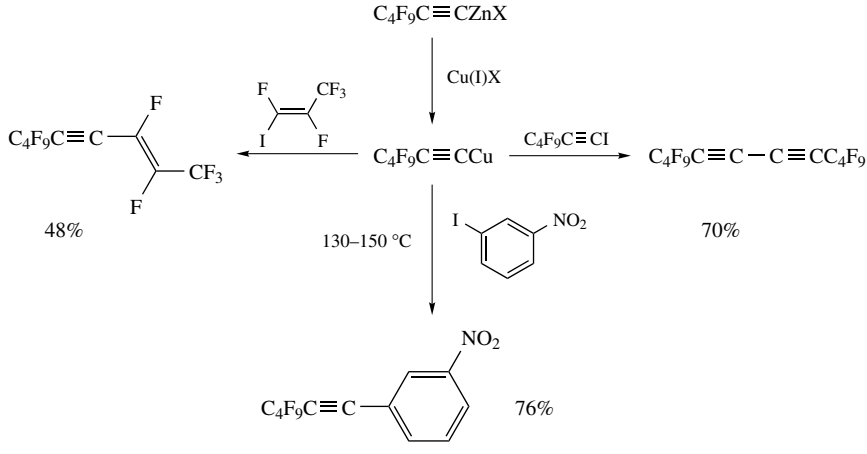

SCHEME 6

VI. PERFLUOROALKYLZINC REAGENTS

Solvated perfluoroalkylzinc reagents are formed by reaction of perfluoroalkyl iodides with zinc in ethereal solvents[99, 100]. Yields are dependent on substrate concentration and

temperature. For example, n-C_3F_7I gives an optimum yield of zinc reagent at 0 °C in dilute dioxane solution (equation 98), whereas higher temperatures led to increased levels of the n-perfluorohexane dimer.

$$n\text{-}C_3F_7I \xrightarrow[\text{dioxane}]{\text{Zn}} \underset{50-75\%}{n\text{-}C_3F_7ZnI} \tag{98}$$

Similarly, the method could be extended to $(CF_3)_2CFI$ and $CF_3(CF_2)_4I$ substrates[100, 101] but CF_3I failed to give the organozinc reagent under these conditions[100]. Generally, the protocol requires peroxide-free solvents to avoid significant formation of R_fH and dilute solutions to limit dimerization.

Conditions favoring dimerization have been applied independently by Keller and Tarrant[102, 103] as well as Henne and Postelneck[104] in homologous coupling of chlorofluorocarbon iodides to generate α,ω-perfluorodiene precursors (equation 99). Attempts to cross-couple chlorofluorocarbon iodides, however, yielded mixtures and limited the utility of this reaction[105].

$$CF_2ClCFClI + Zn \xrightarrow[CH_2Cl_2]{Ac_2O} \underset{51\%}{CF_2ClCFClCFClCF_2Cl} \tag{99}$$

In DMSO, DMF and HMPA solvents, reaction of perfluoroalkyl iodides with Zn–Cu couple and KSCN gives mainly isomeric fluoroolefins[106].

Recently, Naumann and coworkers reported solvated bis(perfluoroalkyl)zinc reagents by reaction of Et_2Zn and perfluoroalky liodides in hexane followed by solvent exchange (equation 100)[107]. Two-dimensional NMR $^{19}F,^{19}F$ and $^{13}C,^{19}F$ correlation spectroscopy experiments provided an independent and unambiguous method for characterization of the constitution of perfluoroalkyl groups in these zinc reagents[108].

$$Et_2Zn + 2\ R_fI \xrightarrow[\text{2. Solvent, } -20\,^\circ\text{C, 15 min}]{\text{1. hexane, } -78\,^\circ\text{C}} \underset{51-95\%}{(R_f)_2Zn\bullet 2Solvent} + 2\ EtI \tag{100}$$

$$R_f = C_2F_5,\ n\text{-}C_3F_7,\ (CF_3)_2CF,\ n\text{-}C_4F_9,\ n\text{-}C_6F_{13},\ n\text{-}C_7F_{15},\ n\text{-}C_8F_{17}$$

$$\text{Solvent} = \text{MeCN, THF, DMSO}$$

The above solvent-exchange method is complementary to a related earlier report wherein bis(trifluoromethyl)zinc could be formed quantitatively by reaction of CF_3I with R_2Zn in a Lewis base solvent (equation 101). This method was not general in scope, however, as C_2F_5I and $(CF_3)_2CFI$ substrates did not yield the respective zinc reagents cleanly[109].

$$Et_2Zn + 2\ CF_3I \longrightarrow \underset{\text{quantitative}}{(CF_3)_2Zn} + 2\ EtI \tag{101}$$

Solvated trifluoromethylzinc has also been prepared by ligand exchange reaction of dialkylzincs with bis(trifluoromethyl)mercury or cadmium (equation 102)[110, 111]. Varying the reactant ratios led to mixed alkylperfluoroalkylzincs.

$$(CH_3)_2Zn + (CF_3)_2M \xrightarrow{\text{solvent}} (CF_3)_2Zn\bullet Solvent + (CH_3)_2M \tag{102}$$
$$M = Cd,\ Hg$$

Burton and Weimers reported the preparation of trifluoromethylzinc from dihalodifluoromethane and zinc in DMF (equation 103)[112].

$$\underset{X = Br,\ Cl}{2CF_2X_2 + Zn} \xrightarrow[RT]{DMF} \underset{80-85\%}{CF_3ZnX + (CF_3)_2Zn} \tag{103}$$

Remarkably, DMF functions both as a solvent and reactant; inhibition and trapping experiments support a SET mechanism producing difluorocarbene, which on further reaction with fluoride, generated by reaction of difluorocarbene with DMF, eventually leads to the trifluoromethylzinc reagent (Scheme 7).

$$CF_2X_2 + Zn \longrightarrow Zn^+ + [CF_2X_2]^{\bullet -}$$

$$[CF_2X_2]^{\bullet -} + Zn^+ \longrightarrow Zn^{+2} + [CF_2X]^- + X^-$$

$$[CF_2X]^- \rightleftharpoons [:CF_2] + X^-$$

$$[:CF_2] + Me_2NCHO \longrightarrow Me_2NCF_2H + CO$$

$$Me_2NCF_2H + [:CF_2] \longrightarrow [CF_3]^- + Me_2\overset{+}{N}{=}CFH$$

$$[CF_3]^- + [ZnX]^+ \longrightarrow CF_3ZnX$$

SCHEME 7

Klabunde and coworkers reported preparation of unsolvated CF_3ZnI by reaction of zinc and CF_3I[113]. The unsolvated reagent exhibited lower stability and higher reactivity as compared to solvated forms and decomposed at temperatures above $-100\,^{\circ}C$.

Naumann and coworkers observed high thermal decomposition temperatures for solvated perfluoroalkylzinc reagents (Table 2)[107]. Though more reactive, perfluoroalkyllithium and magnesium reagents are comparatively less stable; C_2F_5Li, for example, has been reported to have a half-life of 8 hours at $-78\,^{\circ}C$[114, 115]. Perfluoroalkylmagnesium reagents are typically generated at -50 to $0\,^{\circ}C$[116], and consequently are often used under Barbier conditions.

Generally, the high stability of solvated perfluoroalkylzincs places a limitation on their synthetic utility. For example, C_3F_7ZnX in DMF is unreactive toward the electrophilic Bu_3SnCl[117], and dioxane solutions of C_3F_7ZnI are unreactive toward aldehydes, ketones and non-fluorinated acyl chlorides, and give low yields of perfluoroketones with perfluoroacyl chlorides[100]. Sekiya and Ishikawa, however, demonstrated high yield acylations of benzoyl halides and anhydrides with perfluoroisopropylzinc in the presence of pyridine

TABLE 2. Thermal decomposition (°C) of bis(perfluoroalkylzinc) complexes

R_f	C_2F_5	$(CF_3)_2CF$	n-C_3F_7	n-C_4F_9
$Zn(R_f)_2$•2 MeCN	147	121	143	139
$Zn(R_f)_2$•2 THF	159		152	149
$Zn(R_f)_2$•2 DMSO	162			

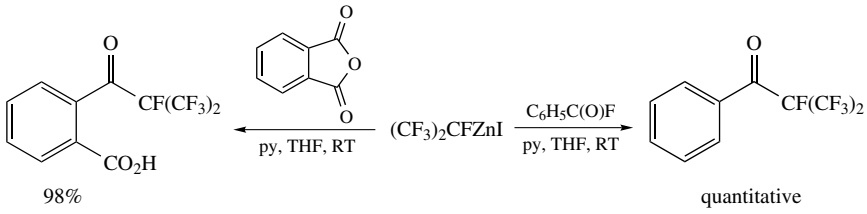

SCHEME 8

(Scheme 8)[118]. *n*-Heptafluoroisopropylzinc was unreactive under similar conditions and lower yields were realized with aliphatic acyl fluorides and chlorides.

The unique route to CF_3ZnX, reported by Burton and Wiemers, is also applicable to preparation of CF_3CdX[112]. Notably, the zinc reagent undergoes metathesis with Cu(I) salts only slowly at room temperature. In contrast, the corresponding cadmium reagent readily exchanges at $-40\,^{\circ}C$, leading to a useful, pregenerative route to CF_3Cu[119]. Thus, it is the cadmium variation of this protocol, followed by metathesis to generate CF_3Cu, which most readily results in a method highly applicable to the industrially important process of aryl trifluoromethylation (Scheme 9)[120–122].

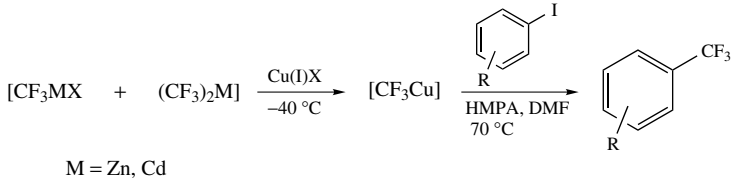

SCHEME 9

Despite the lower reactivity of solvated perfluoroalkylzinc reagents, perfluoroalkyl iodides undergo synthetically useful zinc-mediated reactions under Barbier conditions which often employ ultrasound and co-catalysts. Under these conditions, the zinc reagents are not well characterized and radical intermediates and SET mechanisms are proposed in some cases. Representative examples are presented below and include the ultrasound-promoted, zinc-mediated perfluoroalkylation of various substrates as reported by Ishikawa and coworkers (Scheme 10)[123–126]. Yields of carbinols could be improved by use of Ti(II) co-catalyst. Ultrasound promoted the coupling of perfluoroalkyl iodides with vinyl and allyl halides in the presence of Pd co-catalysts.

CF_3Br has been reported by Wakselman and coworkers to react with aldehydes and zinc, facilitated by peroxide, to give carbinols in modest to good yields[127–129]. Perfluoroalkylation of aldehydes has also been achieved utilizing Pd and Ni co-catalysts in DMF, though similar reactions with ketones, acetal, epoxides and acid chlorides were unsuccessful[130]. Methyl viologen, MV^+, has also served as an electron mediator in addition of perfluoroalkyl iodides to aldehydes[131]. Typical examples from these methods are indicated in equations 104–106.

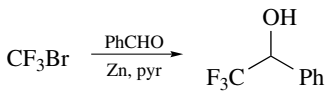

(104)

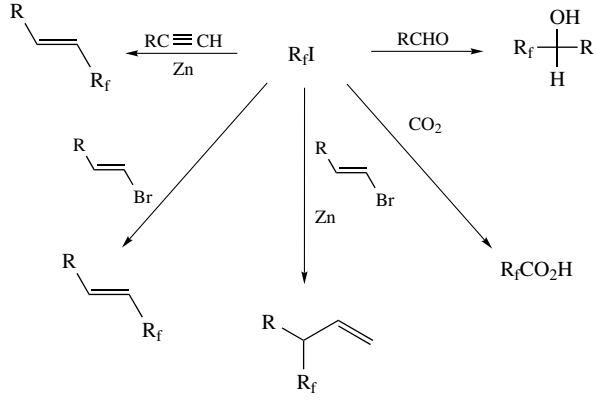

SCHEME 10

$$R_fI + RCHO \xrightarrow[Zn]{M(PPh_3)_2Cl_2} \underset{R_f}{\overset{OH}{\diagup\!\diagdown}}R \qquad M = Pd, Ni \tag{105}$$

$R_f = CF_3, C_2F_5, i\text{-}C_3F_7, C_4F_9, C_6F_{13}, C_8F_{17}$

$$R_fI + RCHO \xrightarrow[MV^{2+}]{Zn} \underset{R_f}{\overset{OH}{\diagup\!\diagdown}}R \quad 48\text{–}68\% \qquad MeCN, rt \tag{106}$$

Employment of Zn−Cu couple is representative of another approach. For example, reaction of perfluoroalkyl iodides with carbonates gives fluorocarboxylic esters (equation 107)[132]. Similarly, reaction of perfluoroalkyl iodides with Zn−Cu couple and CO_2 or SO_2 in DMSO affords the perfluorocarboxylic acids and sulfonyl chlorides, respectively[133]. A double methylene inserted product is formed when dibromomethane is used as a substrate (equation 108)[134].

$$R_fI + \underset{EtO}{\overset{O}{\diagup\!\diagdown}}OEt \xrightarrow[2.\ H^+]{1.\ Zn/Cu} R_fCO_2Et \quad 50\text{–}70\% \tag{107}$$

$$C_6F_{13}I + Zn/Cu \xrightarrow{CH_2Br_2} C_6F_{13}CH_2CH_2I \quad 50\% \tag{108}$$

Although the perfluoroalkyllithium and magnesium reagents are more reactive vs. the corresponding zinc reagents, application of the zinc-mediated methods, when either can be utilized, avoids the low temperatures necessary for the former approach.

1,1-dichlorotrifluoroethylzinc chloride, CF_3CCl_2ZnCl, has received significant attention due to its ease of preparation and utility in synthesis of industrially important compounds. Posta and Paleta first reported this reagent by reaction of trichlorotrifluoroethane with

zinc in ethereal solvents[135]. Lang and coworkers prepared the DMF complex by direct reaction of CF_3CCl_3 with zinc in DMF or by ligand exchange from the diethyl ether complex (Scheme 11)[136].

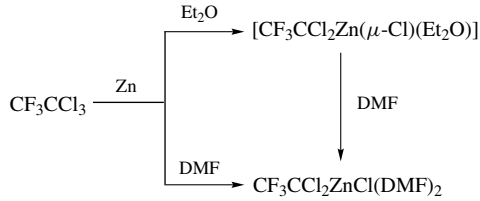

SCHEME 11

Although the pregenerated reagent does undergo addition to aldehydes, it adds most efficiently under Barbier conditions to aldehydes[137–139], α-keto esters and α,β-unsaturated aldehydes[140], but not to ketones, to give carbinols in good yields (Scheme 12). CF_3CCl_2ZnCl also reacts with DMF in the presence of chlorosilane to give α-siloxy-*N*,*N*-dimethylamine, which undergoes acid hydrolysis to give the aldehydes in good yield[137]. Unlike alkylzinc reagents, reaction of CF_3CCl_2ZnCl, in combination with optically active ligands and aldehydes, gave no optically pure alcohols[141].

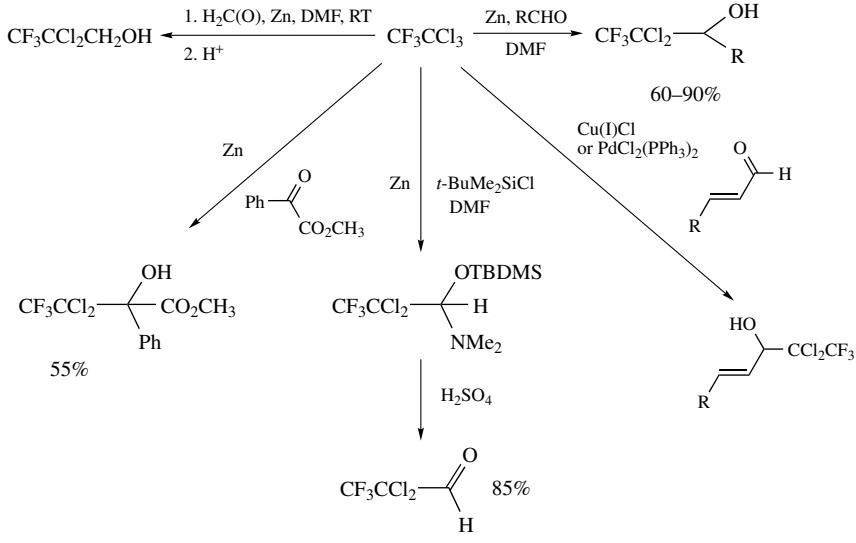

SCHEME 12

CF_3CCl_3 reacts with aldehydes in the presence of excess zinc and Ac_2O to stereoselectively form (*Z*)-alkenes (Scheme 13)[142]. Lewis acids such as $TiCl_4$ and $SiCl_4$ were used in the method. A similar protocol in the presence of $AlCl_3$, however, results in a different course and produces propenols in good yield[142,143]. These compounds had previously been prepared by addition of the labile $F_2C{=}CClLi$ to carbonyls below $-100\,^{\circ}C$. This $CF_3CCl_3/Zn/AlCl_3$ method avoids this difficult reaction.

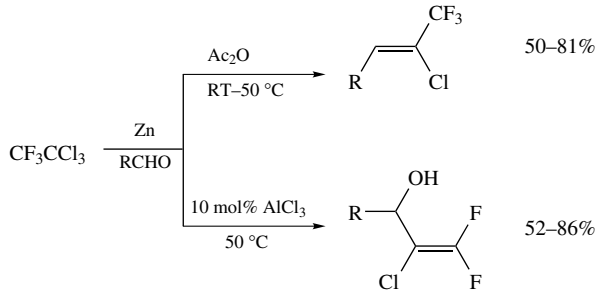

SCHEME 13

The method has been applied successfully to synthesis of artificial pyrethroids bearing the HC=C(Cl)CF_3 moiety[143, 144].

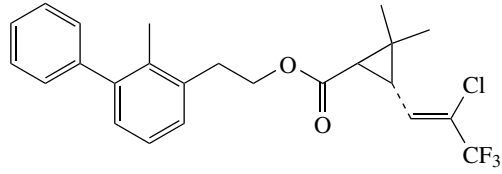

Similarly, new synthetic routes to fluorinated alkenes and aryl trifluoropropynes have also been enabled by modification of the addition or addition–elimination products (Scheme 14)[145, 146].

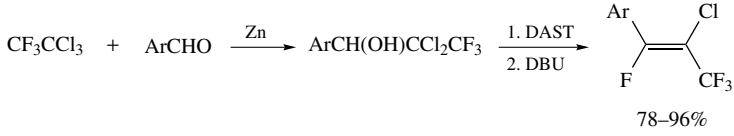

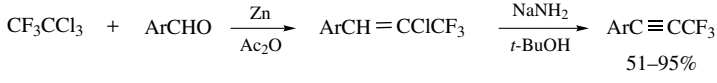

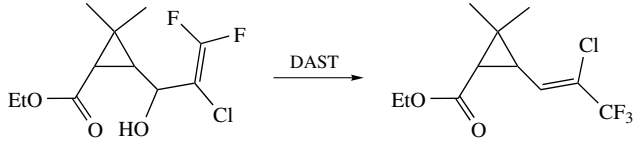

SCHEME 14

VII. DIALKOXYPHOSPHINYLDIFLUOROMETHYLZINC REAGENTS

Introduction of the dialkoxyphosphinyldifluoromethyl moiety into organic compounds has attracted attention due to the biological properties exhibited by these derivatives

as compared to their non-fluorinated analogues[147]. Dialkoxyphosphinyldifluoromethylzinc reagents provide a useful entry into compounds containing this biologically important group.

Treatment of dialkyl bromodifluoromethylphosphonates with zinc gives the dialkoxyphosphinyldifluoromethylzinc reagents in good yields (equation 109)[148]. A variety of solvents can be employed.

$$\underset{\text{R = Et, } i\text{-Pr, } n\text{-Bu}}{(RO)_2P(O)CF_2Br} + Zn \xrightarrow[RT-60^\circ C]{\text{solvent}} (RO)_2P(O)CF_2ZnBr \qquad (109)$$

Solvent = dioxane, THF, DME, TG

The thermal stability of these zinc reagents parallel their fluorinated vinyl and alkynyl counterparts[148]. For example, only 49% of $(BuO)_2P(O)CF_2ZnX$ decomposed on heating to 100 °C for 4 hours and homogeneous solutions of the zinc reagents can be stored at room temperature for months without change. Although the dialkoxyphosphinyldifluoromethylzinc reagent is not as reactive as the corresponding lithium reagent, it is the method of choice when either of the reagents can be employed, particularly on larger scales, as low temperatures are avoided. The reactivity of the zinc reagents is enhanced by addition of copper(I) halides, as the intermediate dialkoxyphosphinyldifluoromethylcopper reagents are more readily trapped by electrophiles. Representative examples are illustrated in Scheme 15[149–151].

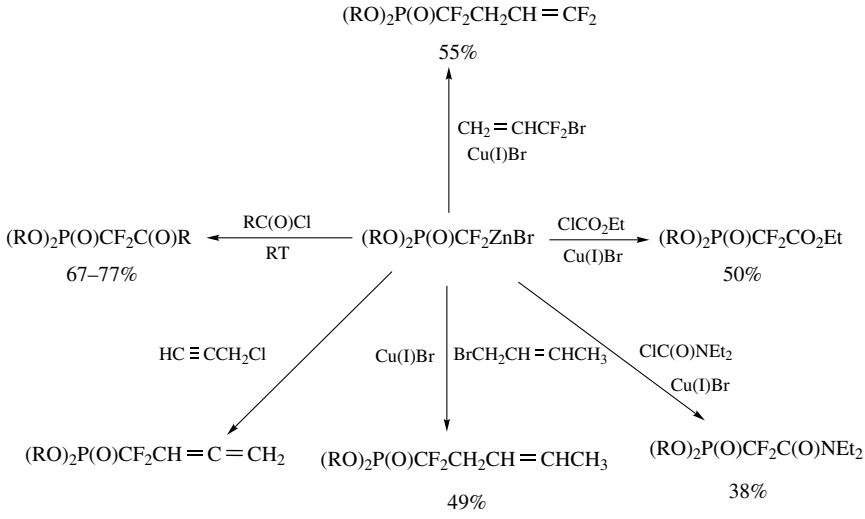

SCHEME 15

Lindell and Turner have subsequently applied the methodology to the synthesis of difluoromethylene phosphonates for evaluation as inhibitors of aspartate transcarbamoylase (equation 110)[152]. Similarly, Chambers and coworkers utilized this method in the preparation of 2-amino-1,1-difluoroethylphosphonic acid, a phosphate mimic (equation 111)[153].

The zinc reagent reacts with 1-bromoalkynes in presence of Cu(I)Br to give α,α-difluoropropargylphosphonates (equation 112)[154]. These compounds had previously been

prepared utilizing an α-ketophosphonate of limited stability and a large excess of DAST fluorinating agent[155].

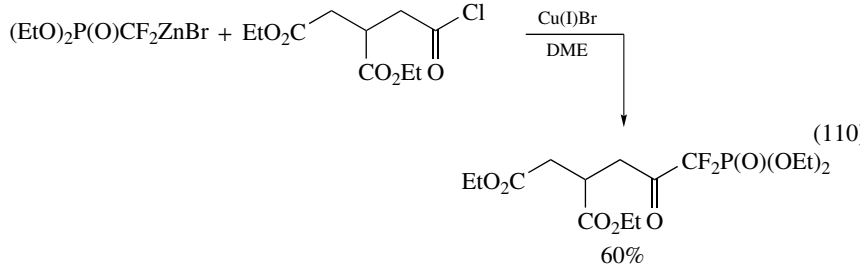

(110)

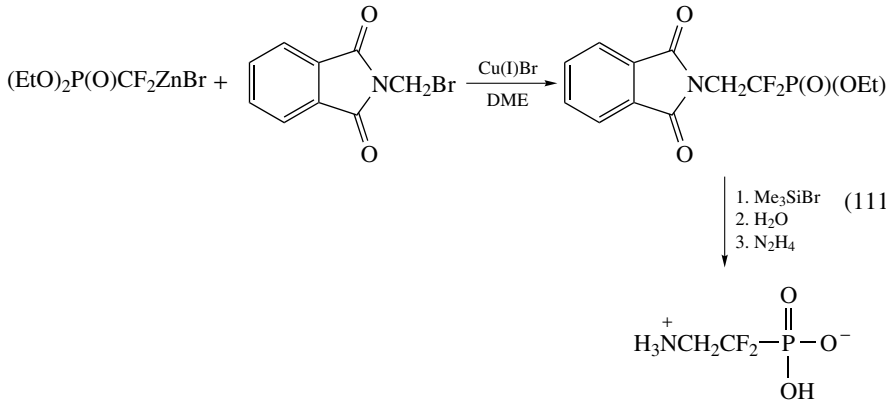

(111)

$$(EtO)_2P(O)CF_2ZnBr \xrightarrow[<5\,^\circ C,\ THF]{Cu(I)Br} \xrightarrow[<5\,^\circ C-RT]{RC\equiv CBr} RC\equiv CCF_2P(O)(OEt)_2 \qquad (112)$$

Qiu and Burton reported that both the cadmium and zinc reagents couple with aryl iodides in the presence of Cu(I)Cl (equation 113)[156].

$$\underset{M = Cd,\ Zn}{(EtO)_2P(O)CF_2MBr} \xrightarrow[CuCl]{ArI} \underset{(65-88\%)}{(EtO)_2P(O)CF_2Ar} \qquad (113)$$

Similarly, Shibuya and coworkers demonstrated Cu(I)Br-catalyzed coupling of the zinc reagent with alkenyl halides (equation 114)[157].

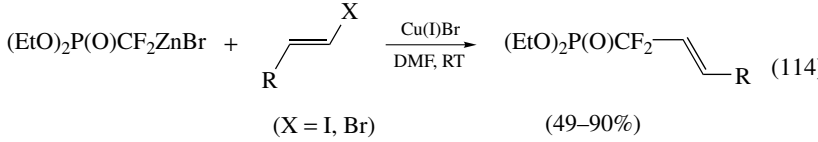

(114)

Recently, the copper(I) halide-catalyzed arylation procedure has been successfully utilized to incorporate the $(EtO)_2P(O)CF_2$ moiety into a variety of biologically active targets.

Representative examples include the synthesis of phosphonothioic acids for evaluation as inhibitors of protein tyrosine phosphatases (equation 115)[158].

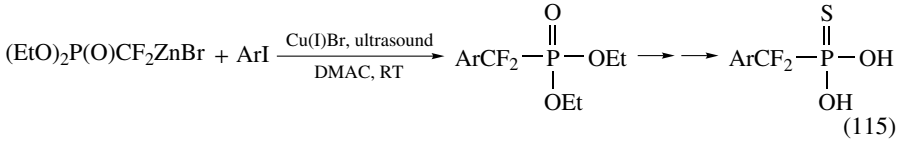

(115)

Intermediates[159, 160] were similarly prepared via the arylation procedure enroute to non-hydrolyzable phosphothreonine derivatives and phosphotyrosine analogue, respectively.

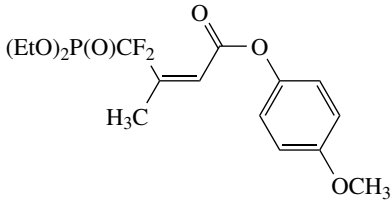

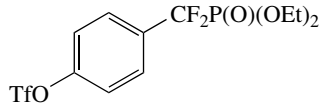

In the absence of a trapping electrophile and in a poor coordinating solvent, copper(I) halide-mediated reactions of $(EtO)_2P(O)CF_2ZnBr$ give *E*- and *Z*-1,2-difluoroethenediyl-bisphosphonates[161]. The bisphosphonates are presumably formed via dimerization of dialkoxyphosphinylfluoromethyl carbene or dialkoxyphosphinyldifluoromethylcopper carbenoid. Attempts to trap a carbene with alkenes were unsuccessful.

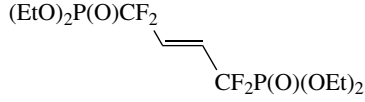

Although the α,α-difluorophosphates have been widely investigated over the last 20 years, recent experimental and theoretical reports have indicated that α-fluorophosphonates could be an improved mimic for phosphates[162–164]. Recently, the organometallic reagent $(EtO)_2P(O)CFHZnBr$ was generated in excellent yields via the reaction of $(EtO)_2P(O)CFHBr$ with zinc metal (Scheme 16)[165]. The zinc reagent underwent direct reaction with electrophiles such as allyl halides and ethyl chloroformate. Metathesis with Cu(I)Br gave a more reactive copper reagent and allowed further functionalization with vinyl, alkynyl and aryl halides.

The α-fluorophosphonate moiety has previously been introduced utilizing thermally unstable organolithium reagents[166, 167] and fluorinating agents such as DAST[168]. $(EtO)_2P(O)CFHZnBr$ is thermally stable, scalable and avoids the use of expensive and hazardous fluorination reagents.

VIII. CARBOALKOXYDIFLUOROMETHYLENEZINC REAGENTS

The reaction of halodifluoroacetates with carbonyl compounds in the presence of zinc gives α,α-difluoro-β-hydroxyesters and was first reported by Fried and coworkers

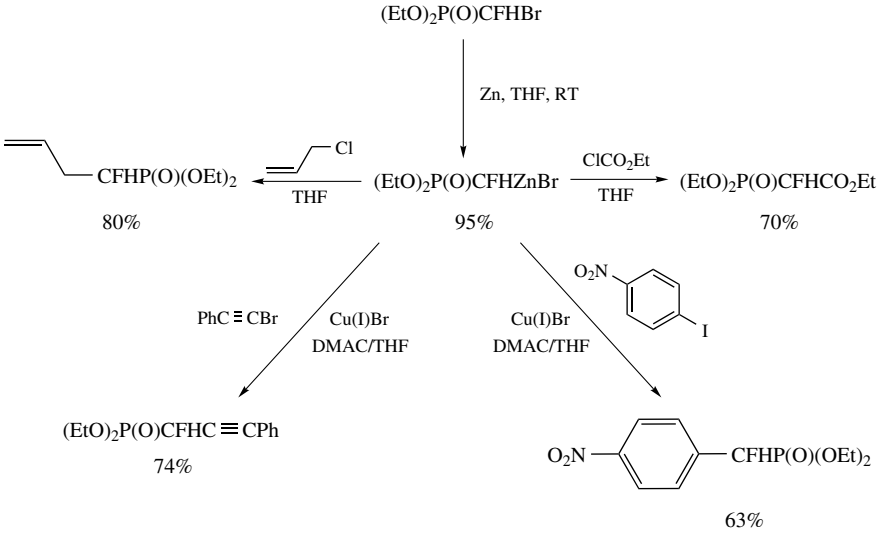

SCHEME 16

(equation 116)[169]. The intermediate Reformatsky reagents are typically stable in solution but generally trapped *in situ* with electrophiles (Barbier conditions)[169, 170].

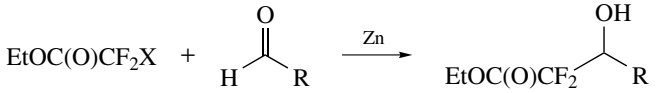

(116)

X = I, Br

When Zn(Hg) amalgam was used to generate the zinc reagent in triglyme, the reagent was characterized by ^{19}F and ^{13}C NMR and found to be carbon-metallated[171]. When the intermediate zinc reagent is generated from iododifluoroacetates, a variety of solvents may be employed (THF, dioxane, DMF, DME and MeCN) although best results are generally obtained with MeCN[172]. THF has been used extensively, however, with bromodifluoroacetates[173, 174]. Lang and Schaub demonstrated that the cheapest precursor, ethyl chlorodifluoroacetate, could also be converted to the Reformatsky reagent in DMF though ethereal solvents were ineffective[175]. The zinc reagent was generated *in situ* and underwent addition to aryl and aliphatic aldehydes in good yields (equation 117).

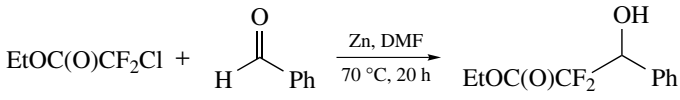

(117)

The α,α-difluoro Reformatsky reagent has been applied extensively to preparation of compounds containing the $-CF_2C(O)-$ group and its derivatives since this functionality often confers enhanced biological activity. Typical examples include the preparation of

selectively fluorinated thromboxane A_2 analogues[173] (equation 118) and the preparation of 1-(2-deoxy-2,2-difluororibofuranosyl)pyrimidine nucleosides (equation 119)[174].

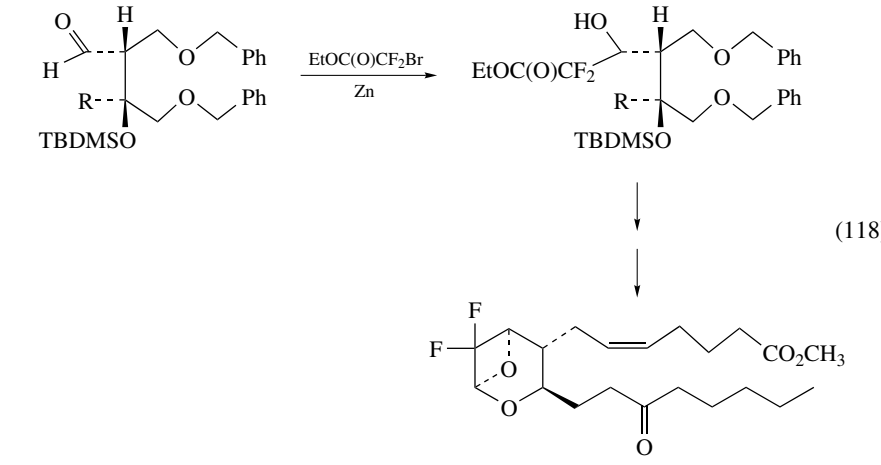

(118)

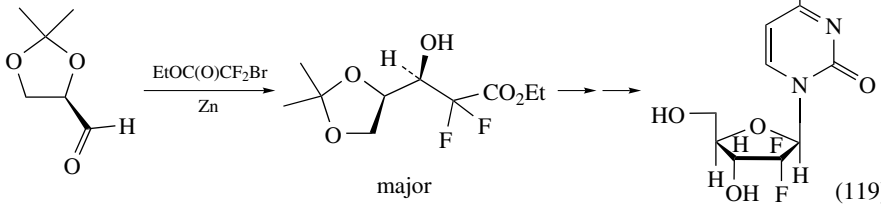

(119)

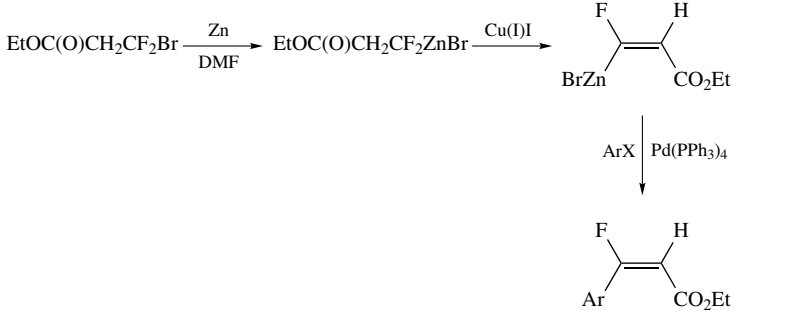

SCHEME 17

Recently a one-carbon homologue of $XZnCF_2CO_2Et$ was analogously prepared by treatment of $XZnCF_2CH_2CO_2Et$ with zinc in DMF to give a stable zinc reagent characterized by ^{19}F NMR[176]. Mechanistic studies suggested that, in the presence of Cu(I)I and $Pd(PPh_3)_4$, the zinc reagent underwent stereoselective elimination to an alkenyl zinc, which subsequently cross-coupled with aryl and alkenyl halides to give *E*- and *Z*-β-fluoro-α,β-unsaturated esters (Scheme 17).

Other α-fluorinated carboethoxy substrates have been utilized in Reformatsky reactions. Treatment of ethyl dibromofluoroacetate with aldehydes or ketones in presence of zinc and Et_2AlCl gave diastereomeric α-bromo-α-fluoro-β-hydroxyalkanoic esters in good yield (49–77%) (equation 120)[177]. Use of 2 equivalents each of RCHO, Zn and Et_2AlCl gave the double coupled products in good yield.

Recently, Ishihara and coworkers demonstrated that zinc-mediated reaction of 2-bromo-2,3,3,3-tetrafluoropropanoate with chiral imines afforded *threo*- and *erythro*-isomers of α-fluoro-α-(trifluoromethyl)-β-amino esters in good yields with high diastereomeric excess (equation 121)[178].

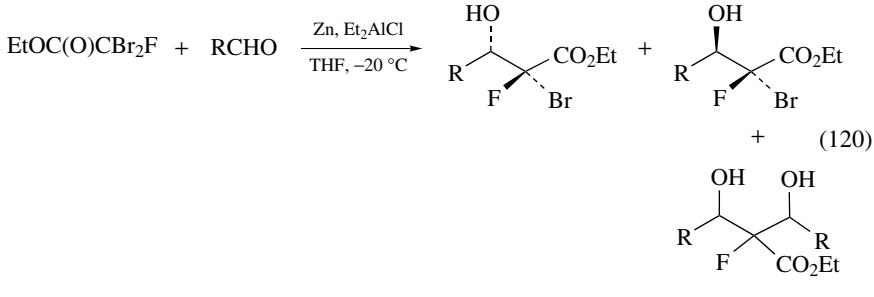

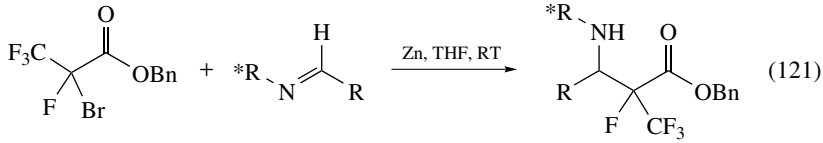

IX. REFERENCES

1. E. Negishi and F. Liu, in *Metal-Catalyzed Cross-Coupling Reactions* (Eds. F. Diederich and P. J. Stang), Wiley-VCH, Weinheim, 1998, p. 1.
2. J. F. Normant, *J. Organomet. Chem.*, **400**, 19 (1990).
3. S. Martin, R. Sauvetre and J. F. Normant, *J. Organomet. Chem.*, **264**, 155 (1984).
4. J.-P. Gillet, R. Sauvetre and J. F. Normant, *Tetrahedron Lett.*, **26**, 3999 (1985).
5. P. A. Morken, H. Lu, A. Nakamura and D. J. Burton, *Tetrahedron Lett.*, **32**, 4271 (1991).
6. P. Martinet, R. Sauvetre and J. F. Normant, *J. Organomet. Chem.*, **367**, 1 (1989).
7. P. Martinet, R. Sauvetre and J. F. Normant, *Bull. Soc. Chim Fr.*, **127**, 86 (1990).
8. D. J. Burton, T. D. Spawn, P. L. Heinze, A. R. Bailey and S. Shin-Ya, *J. Fluorine Chem.*, **44**, 167 (1989).
9. C. R. Davis and D. J. Burton, in *Organozinc Reagents, A Practical Approach* (Eds. P. Knochel and P. Jones), Oxford, New York, 1999, p. 57.
10. J. P. Gillet, R. Sauvetre and J. F. Normant, *Synthesis*, 538 (1986).
11. F. Tellier, R. Sauvetre and J. F. Normant, *J. Organomet. Chem.*, **328**, 1 (1987).
12. F. Tellier, R. Sauvetre and J. F. Normant, *J. Organomet. Chem.*, **292**, 19 (1985).
13. F. Tellier, R. Sauvetre and J. F. Normant, *J. Organomet. Chem.*, **364**, 17 (1989).
14. T. Shigeoka, Y. Kuwahara, K. Watanabe, K. Sato, M. Omote, A. Ando and I. Kumadaki, *J. Fluorine Chem.*, **103**, 99 (2000).
15. A. Ando and I. Kumadaki, *J. Fluorine Chem.*, **100**, 135 (1999).
16. R. Anilkumar and D. J. Burton, *Tetrahedron Lett.*, **43**, 6979 (2002).
17. M. Nishihara, Y. Nakamura, N. Maruyama, K. Sato, M. Omote, A. Ando and I. Kumadaki, *J. Fluorine Chem.*, **122**, 247 (2003).
18. R. Anilkumar and D. J. Burton, *J. Fluorine Chem.*, **126**, 835 (2005).
19. R. Anilkumar and D. J. Burton, *Tetrahedron Lett.*, **43**, 2731 (2002).

20. A. Raghavanpillai and D. J. Burton, *J. Org. Chem.*, **69**, 7083 (2004).
21. J. Burdon, P. L. Coe, I. B. Haslock and R. L. Powell, *J. Chem. Soc., Commun.*, 49 (1996).
22. J. Burdon, P. L. Coe, I. B. Haslock and R. L. Powell, *J. Fluorine Chem.* **85**, 151 (1997).
23. J. Burdon, P. L. Coe, I. B. Haslock and R. L. Powell, *J. Fluorine Chem.*, **99**, 127 (1999).
24. C. Stone, T. J. Peckham, D. J. Burton and R. Anilkumar, U.S. Patent 6,653,515 (2003).
25. R. Anilkumar and D. J. Burton, *J. Fluorine Chem.*, **125**, 561 (2004).
26. R. Anilkumar and D. J. Burton, *J. Fluorine Chem.*, **126**, 457 (2005).
27. R. Anilkumar and D. J. Burton, University of Iowa, unpublished results.
28. S. W. Hansen, T. D. Spawn and D. J. Burton, *J. Fluorine Chem.*, **35**, 415 (1987).
29. P. L. Heinze and D. J. Burton, *J. Org. Chem.*, **53**, 2714 (1988).
30. B. Jiang and Y. Xu, *J. Org. Chem.*, **56**, 7336 (1991).
31. B. Jiang and Y. Xu, *Tetrahedron Lett.*, **33**, 511 (1992).
32. P. L. Heinze, Ph.D. Thesis, University of Iowa, 1986.
33. C. Lim, D. J. Burton and C. A. Wesolowski, *J. Fluorine Chem.*, **119**, 21 (2003).
34. P. A. Morken and D. J. Burton, *J. Org. Chem.*, **58**, 1167 (1993).
35. B. V. Nguyen and D. J. Burton, *J. Org. Chem.*, **63**, 1714 (1998).
36. Q. Liu and D. J. Burton, *Tetrahedron Lett.*, **41**, 8045 (2000).
37. C. R. Davis and D. J. Burton, *Tetrahedron Lett.*, **37**, 7237 (1996).
38. C. R. Davis and D. J. Burton, *J. Org. Chem.*, **62**, 9217 (1997).
39. B. V. Nguyen and D. J. Burton, *J. Org. Chem.*, **62**, 7758 (1997).
40. P. C. Bachand, M.S. Thesis, University of Iowa, 1986.
41. S. K. Shin and S. K. Choi, *J. Fluorine Chem.*, **43**, 439 (1989).
42. S. K. Choi and Y. T. Jeong, *J. Chem. Soc., Chem. Commun.*, 1478 (1988).
43. C. Lim, University of Iowa, unpublished results.
44. G. Q. Shi, X. H. Huang and F. Hong, *J. Org. Chem.*, **61**, 3200 (1996).
45. V. Jairaj and D. J. Burton, *J. Fluorine Chem.*, **111**, 233 (2001).
46. P. A. Morken, R. F. Campbell and D. J. Burton, *J. Fluorine Chem.*, **66**, 81 (1994).
47. S. Dixon, *J. Org. Chem.*, **21**, 400 (1956).
48. V. Jairaj and D. J. Burton, *J. Fluorine Chem.*, **121**, 75 (2003).
49. W. R. Dolbier, Jr., H. Koroniak, D. J. Burton, P. L. Heinze, A. R. Bailey, G. S. Shaw and S. W. Hansen, *J. Am. Chem. Soc.*, **109**, 219 (1987).
50. K. B. MacNeil, Ph.D. Thesis, University of Iowa, 1991.
51. P. A. Morken, Ph.D. Thesis, University of Iowa, 1992.
52. S. W. Hansen, Ph.D. Thesis, University of Iowa, 1984.
53. P. A. Morken, N. C. Baenziger, D. J. Burton, P. C. Bachand, C. R. Davis, S. D. Pedersen and S. W. Hansen, *J. Chem. Soc., Chem. Commun.*, 566 (1991).
54. P. A. Morken, P. C. Bachand, D. C. Swenson and D. J. Burton, *J. Am. Chem. Soc.*, **115**, 5430 (1993).
55. W. R. Dolbier, Jr., K. Palmer, H. Koroniak, H. Q. Zhang and V. L. Goedkin, *J. Am. Chem. Soc.*, **113**, 1059 (1991).
56. L. G. Sprague, A. W. Snow and J. R. Griffith, *J. Fluorine Chem.*, **52**, 301 (1991).
57. J. Mohtasham, G. L. Gard, Z. Y. Yang and D. J. Burton, *J. Fluorine Chem.*, **50**, 31 (1990)
58. T. D. Spawn and D. J. Burton, *Bull. Soc. Chim. Fr.*, 1 (1986).
59. H. Lu, H. B. Friedrich and D. J. Burton, *J. Fluorine Chem.*, **75**, 83 (1995).
60. M. Yamamoto, D. C. Swenson and D. J. Burton, *Macromol. Symp.*, **82**, 125 (1994).
61. D. W. Smith, Jr., J. Ji, S. Narayan-Sarathy, R. Neilson and D. Babb, *ACS Symp. Ser.* (Ed. S. Carlson), **729**, 308 (1999).
62. D. W. Smith, Jr., D. A. Babb, H. V. Shah, A. Hoeglund, R. Traiphol, D. Perahia, H. W. Boone, C. Langhoff and M. Radler, *J. Fluorine Chem.*, **104**, 109 (2000).
63. D. W. Smith, Jr., S. Chen, S. Kumar, J. Ballato, H. Shah, C. Topping and S. Foulger, *Adv. Mater.*, **14**, 1585 (2002).
64. J. G. Noltes and J. W. G. Van Den Hurk, *J. Organomet. Chem.*, **1**, 377 (1964).
65. P. Sartori and M. Weidenbruch, *Chem. Ber.*,**100**, 3016 (1967).
66. J. G. Noltes and J. W. G. Van Den Hurk, *J. Organomet. Chem.*, **3**, 222 (1965).
67. S. C. Cohen and A. G. Massey, *Advances in Fluorine Chemistry*, *Vol. 6* (Eds. J. C. Tatlow, R. D. Peacock, H. H. Hyman and M. Stacey), CRC Press, Boca Raton, 1970, p. 133.
68. D. F. Evans and R. F. Phillips, *J. Chem. Soc., Dalton Trans.*, 978 (1973).
69. P. Sartori and H. Adelt, *J. Fluorine Chem.*, **3**, 275 (1973/74).

70. H. Lange and D. Naumann, *J. Fluorine Chem.*, **26**, 435 (1984).
71. A. Miller, V. I. Krasnov, D. Peters, V. E. Platonov and R. Miethchen, *Tetrahedron Lett,,* **41**, 3817 (2000).
72. D. J. Burton, Y. Tarumi and P. L Heinze, *J. Fluorine Chem.*, **50**, 257 (1980).
73. Z. Y. Yang and D. J. Burton, *J. Fluorine Chem.*, **44**, 339 (1989).
74. Z. Y. Yang and D. J. Burton, *J. Org. Chem.*, **56**, 1037 (1991).
75. D. Seyferth, R. M. Simon, D. J. Sepelak and H. A. Klein, *J. Am. Chem. Soc.*, **105**, 4634 (1983).
76. D. Seyferth, R. M. Simon, D. J. Sepelak and H. A. Klein, *J. Org. Chem.*, **45**, 2273 (1980).
77. D. Seyferth and K. R. Wursthorn, *J. Organomet. Chem.*, **182**, 455 (1979).
78. T. Hiyama, M. Obayashi and M. Sawahata, *Tetrahedron Lett.*, **24**, 4113 (1983).
79. M. Fujita, M. Obayashi and T. Hiyama, *Tetrahedron*, **44**, 4135 (1988).
80. G. Tonachini and C. Canopa, *Tetrahedron*, **45**, 5163 (1989).
81. T. Ishihara, S. Miwatashi, M. Kuroboshi and K. Utimoto, *Tetrahedron Lett.*, **32**, 1069 (1991).
82. W. Peng, P. He, S. Zhu and Z. Li, *Tetrahedron Lett.*, **45**, 3677 (2004).
83. P. Y. Kwok, F. W. Muellner, C. K. Chen and J. Fried, *J. Am. Chem. Soc.*, **109**, 3684 (1987).
84. H. Sham and D. A. Betebenner, *J. Chem. Soc., Chem. Commun.*, 1134 (1991).
85. D. J. Burton and T. D. Spawn, *J. Fluorine Chem.*, **38**, 119 (1988).
86. J. E. Bunch and C. L. Bumgardner, *J. Fluorine Chem.*, **36**, 313 (1987).
87. T. D. Spawn, Ph.D. Thesis, University of Iowa, 1987.
88. D. J. Burton, Presented at the ACS 10th Winter Fluorine Conference, St. Petersburg, FL, January 1991, Abstract No. 16.
89. F. G. Drakesmith, O. J. Stewart and P. Tarrant, *J. Org. Chem.*, **33**, 280 (1968).
90. L. Sibous and A. E. Tipping, *J. Fluorine Chem.*, **62**, 39 (1993).
91. A. L. Johnson, *J. Med. Chem.*, **15**, 854 (1972).
92. A. L. Henne and M. Nager, *J. Am. Chem. Soc.*, **74**, 650 (1952).
93. M. I. Bruce, D. A. Harbourne, F. Waugh and F. G. A. Stone, *J. Chem. Soc. A*, 356 (1968).
94. W. R. Cullen and M. C. Waldman, *J. Fluorine Chem.*, **1**, 41 (1971/72).
95. W. G. Finnegan and W. P. Norris, *J. Org. Chem.*, **28**, 1139 (1963).
96. W. P. Norris and W. G. Finnegan, *J. Org. Chem.*, **31**, 3292 (1966).
97. N. Yoneda, S. Matsuoka, N. Miyaura, T. Fukuhara and A. Suzuki, *Bull. Chem. Soc. Jpn.*, **63**, 2124 (1990).
98. C. L. Bumgardner, J. E. Bunch and M. H. Whangbo, *J. Org. Chem.*, **51**, 4082 (1986).
99. R. N. Haszeldine and E. G. Waldschewski, *J. Chem. Soc.*, 3607 (1953).
100. W. T. Miller, Jr., E. Bergman and A. H. Fainberg, *J. Am. Chem. Soc.*, **79**, 4159 (1957).
101. R. D. Chambers, W. K. R. Musgrave and J. Savory, *J. Chem. Soc.*, 1993 (1962).
102. T. M. Keller and P. Tarrant, *J. Fluorine Chem.*, **6**, 105 (1975).
103. T. M. Keller and P. Tarrant, *J. Fluorine Chem.*, **6**, 297 (1975).
104. A. L. Henne and W. Postelneck, *J. Am. Chem. Soc.*, **77**, 2334 (1955).
105. K. C. Eapen and C. Tamborski, *J. Fluorine Chem.*, **35**, 421 (1987).
106. H. Blancou, P. Moreau and A. Commeyras, *Tetrahedron*, **33**, 2061 (1977).
107. D. Naumann, C. Schorn and W. Tyrra, *Z. Anorg. Allg. Chem.*, **625**, 827 (1999).
108. C. Schorn, D. Naumann, H. Scherer and J. Hahn, *J. Fluorine Chem.*, **107**, 159 (2001).
109. H. Lange and D. Naumann, *J. Fluorine Chem.*, **26**, 435 (1984).
110. E. K. S. Liu and L. B. Asprey, *J. Organomet. Chem.*, **169**, 249 (1979).
111. E. K. S. Liu, *Inorg. Chem.*, **19**, 266 (1980).
112. D. J. Burton and D. M. Wiemers, *J. Am. Chem. Soc.*, **107**, 5014 (1985).
113. K. J. Klabunde, M. S. Key and J. Y. F. Low, *J. Am. Chem. Soc.*, **94**, 999 (1972).
114. P. G. Gassman and N. J. O'Reilly, *Tetrahedron Lett.*, **26**, 5243 (1985).
115. P. G. Gassman and N. J. O'Reilly, *J. Org. Chem.*, **52**, 2481 (1987).
116. R. N. Haszeldine, *J. Chem. Soc.*, 3423 (1952).
117. D. J. Burton and V. Jairaj, *J. Fluorine Chem.*, **125**, 673 (2004).
118. A. Sekiya and N. Ishikawa, *Chem. Lett.*, 81 (1977).
119. D. M. Weimers and D. J. Burton, *J. Am. Chem. Soc.*, **108**, 832 (1986).
120. D. M. Weimers, University of Iowa, unpublished results.

121. T. S. Chou, Ph.D. Thesis, University of Iowa, 1987.
122. V. Nair and G. S. Buenger, *J. Am. Chem. Soc.*, **111**, 8502 (1989).
123. N. Ishikawa, M. Takahashi, M. Sato and T. Kitazume, *J. Fluorine Chem.*, **22**, 585 (1983).
124. T. Kitazume and N. Ishikawa, *Chem. Lett.*, 1453 (1982).
125. T. Kitazume and N. Ishikawa, *Chem Lett.*, 137 (1982).
126. T. Kitazume and N. Ishikawa, *J. Am. Chem. Soc.*, **107**, 5186 (1985).
127. C. Francese, M. Tordeux and C. Wakselman, *J. Chem. Soc., Chem. Commun.*, 642 (1987).
128. M. Tordeux, C. Francese and C. Wakselman, *J. Chem. Soc., Perkin Trans. 1*, 1951 (1990).
129. C. Francese, M. Tordeux and C. Wakselman, *Tetrahedron Lett.*, **29**, 1029 (1988).
130. N. J. O'Reilly, M. Maruta and N. Ishikawa, *Chem. Lett.*, 517 (1984).
131. T. Kitazume and T. Ikeya, *J. Org. Chem.*, **53**, 2349 (1988).
132. S. Benefice, H. Blancou and A. Commeyras, *Tetrahedron*, **40**, 1541 (1984).
133. H. Blancou, P. Moreau and A. Commeyras, *J. Chem. Soc., Chem. Commun.*, 885 (1976).
134. H. Blancou and A. Commeyras, *J. Fluorine Chem.*, **20**, 255 (1982).
135. A. Posta and O. Paleta, *Collect. Czech. Chem. Commun.*, **37**, 3946 (1972).
136. D. Bellus, B. Klingert, R. W. Lang and G. Rihs, *J. Organomet. Chem.*, **339**, 17 (1988).
137. R. W. Lang, *Helv. Chim. Acta*, **71**, 369 (1988).
138. R. W. Lang, *Helv. Chim. Acta*, **69**, 881 (1986).
139. M. Fujita, T. Morita and T. Hiyama, *Tetrahedron Lett.*, **27**, 2135 (1986).
140. M. Fujita and T. Hiyama, *Bull. Chem. Soc. Jpn.*, **60**, 4377 (1987).
141. A. Solladie-Cavallo and S. Quazzotti, *J. Fluorine Chem.*, **46**, 221 (1990).
142. M. Fujita and T. Hiyama, *Tetrahedron Lett.*, **27**, 3655 (1986).
143. M. Fujita, K. Kondo and T. Hiyama, *Bull. Chem. Soc. Jpn.*, **60**, 4385 (1987).
144. M. Fujita, T. Hiyama and K. Kondo, *Tetrahedron Lett.*, **27**, 2139 (1986).
145. M. Kuroboshi and T. Hiyama, *Chem. Lett.*, 1607 (1990).
146. T. Hiyama, K. Sato and M. Fujita, *Bull. Chem. Soc. Jpn.*, **62**, 1352 (1989).
147. G. M. Blackburn, *Chem. Ind. (London)*, 134 (1981).
148. D. J. Burton, T. Ishihara and M. Maruta, *Chem. Lett.*, 755 (1982).
149. D. J. Burton, L. G. Sprague, D. J. Pietrzyk and S. H. Edelmuth, *J. Org. Chem.*, **49**, 3438 (1984).
150. D. J. Burton and L. G. Sprague, *J. Org. Chem.*, **53**, 1523 (1988).
151. D. J. Burton and L. G. Sprague, *J. Org. Chem.*, **54**, 613 (1989).
152. S. D. Lindell and R. M. Turner, *Tetrahedron Lett.*, **31**, 5381 (1990).
153. R. D. Chambers, D. O'Hagan, R. B. Lamont and S. C. Jain, *J. Chem. Soc., Chem. Commun.*, 1053 (1990).
154. X. Zhang and D. J. Burton, *Tetrahedron Lett.*, **41**, 7791 (2000).
155. F. Benayoud and G. B. Hammond, *J. Chem. Soc., Chem. Commun.*, 1447 (1996).
156. W. Qiu and D. J. Burton, *Tetrahedron Lett.*, **37**, 2745 (1996).
157. T. Yokomatsu, K. Suemune, T. Murano and S. Shibuya, *J. Org. Chem.*, **61**, 7207 (1996).
158. T. Yokomatsu, H. Takechi, T. Murano and S. Shibuya, *J. Org. Chem.*, **65**, 5858 (2000).
159. A. Otaka, E. Mitsuyama, T. Kinoshita, H. Tamamaru and N. Fujii, *J. Org. Chem.*, **65**, 4888 (2000).
160. G. S. Cockerill, H. J. Easterfield and J. M. Percy, *Tetrahedron Lett.*, **40**, 2601 (1999).
161. D. J. Burton, L. G. Sprague, R. D. Guneratne and W. E. Bennett, *J. Fluorine Chem.*, **49**, 75 (1990).
162. D. O'Hagan and H. S. Rzepa, *J. Chem. Soc., Chem. Commun.*, 645 (1997).
163. G. R. J. Thatcher and A. S. Campbell, *J. Org. Chem.*, **58**, 2272 (1993).
164. J. Nieschalk, A. S. Batsanov, D. O'Hagan and J. A. K. Howard, *Tetrahedron*, **52**, 165 (1996).
165. X. Zhang, W. Qiu and D. J. Burton, *Tetrahedron Lett.*, **40**, 2681 (1999).
166. G. M. Blackburn and A. Rashid, *J. Chem. Soc., Chem. Commun.*, 317 (1988).
167. R. Waschbuch, J. Carran, A. Morinetti and P. Savignac, *Synthesis*, **7**, 727 (1997).
168. F. Benayoud, L. Chen, G. A. Moniz, A. J. Zopato and G. B. Hammond, *Tetrahedron*, **54** 15541 (1998).
169. J. Fried, E. A. Hallinan and M. J. Szwedo, *J. Am. Chem. Soc.*, **106**, 3871 (1984).
170. E. A. Hallinan and J. Fried, *Tetrahedron Lett.*, **25**, 2301 (1984).

171. D. J. Burton and J. C. Easdon, *J. Fluorine Chem.*, **38**, 125 (1988).
172. O. Kitigawa, T. Taguchi and Y. Kobayashi, *Tetrahedron Lett.*, **29**, 1803 (1988).
173. J. Fried, M. J. Szwedo, C. Chen, C. O'Yang, T. A. Morinelli, A. K. Okwu and P. V. Halushka, *J. Am. Chem. Soc.*, **111**, 4510 (1989).
174. L. W. Hertel, J. S. Kroin, J. W. Misner and J. M. Tustin, *J. Org. Chem.*, **53**, 2406 (1988).
175. R. W. Lang and B. Schaub, *Tetrahedron Lett.*, **29**, 2943 (1988).
176. S. Peng, F. Qing, Y. Li and C. Hu, *J. Org. Chem.*, **65**, 694 (2000).
177. T. Ishihara, T. Matsuda, K. Imura, H. Matsui and H. Yamanaka, *Chem. Lett.*, 2167 (1994).
178. T. Sekiguchi, K. Sato, T. Ishihara, T. Konno and H. Yamanaka, *Chem. Lett.*, **33**, 666 (2004).

CHAPTER **17**

Electrochemical generation and reaction of zinc reagents

JACQUES PÉRICHON, CORINNE GOSMINI and OLIVIER BURIEZ

C.N.R.S. UMR 7582, Laboratoire d'Electrochimie Catalyse et Synthése Organique, Université Paris XII, 2-8 rue H. Dunant, F-94320 Thiais, France
Fax: +33 14 978 1148; e-mail: perichon@glvt-cnrs.fr; gosmini@glvt-cnrs.fr; olivier.buriez@ens.fr

The chemistry of organozinc compounds
Edited by Z. Rappoport and I. Marek

I. INTRODUCTION

The formation of organozinc compounds by reaction of zinc metal with organic halides often requires both the activation of Zn metal by various treatments, and the use of reactive organic halides such as iodides or activated bromides. Moreover, the alternative transmetallation methods between a zinc halide and an organomagnesium or lithium compound are, in many cases, incompatible with the presence of sensitive functional groups on the organic moiety inasmuch as very low temperature is required[1]. Consequently, the electrochemical approach may offer a useful alternative to the conventional chemical routes. Indeed, the electroreduction of a zinc salt at between −0.8 and −1.4 V/SCE (saturated calomel electrode), depending on the nature of the organic solvent, produces a divided nascent zinc at the cathode surface. However, this electrolytic zinc, Zn*, only reacts with reactive organic halides such as α-bromoesters, allyl or benzyl bromides (equation 1).

$$Zn^{2+} + 2e \xrightarrow{\text{organic solvent}} Zn^* \xrightarrow{RX} RZnX \qquad (1)$$

The reactivity of these organozinc compounds depends on the experimental protocol. The coupling reaction of these compounds with various substrates is thus more efficient when the organozinc compound is prepared in the presence of the substrate. This suggests the formation of an 'R−Zn' intermediary species which would be more reactive than the classical organozinc compound RZnX.

The zinc(II) ions can be produced by the oxidation of a plate, or of a zinc rod concomitantly to the reduction process (Scheme 1).

This corresponds to the well-known sacrificial anode process that has been widely developed to achieve electrosyntheses reactions in undivided cells[2]. This allows the *in situ* preparation of zinc(II) ions, thus avoiding the use of hygroscopic zinc halides.

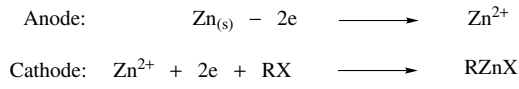

SCHEME 1

The electrochemical way can also be used to activate massive zinc being under plates or rod forms. First, the electrooxidation of the zinc anode by a catalytic amount of electricity allows one to strip the surface similarly to an acidic treatment. Second, the electrolytic deposit of a small amount of zinc on a massive zinc surface also leads to the activation of the metal according to a process which is not understood yet.

The above-mentioned various zinc-based electrochemical processes lead necessarily to a transient organozinc species of the type 'R−Zn' which can evolve, in some cases, to a stable organozinc compound RZnX (Scheme 2).

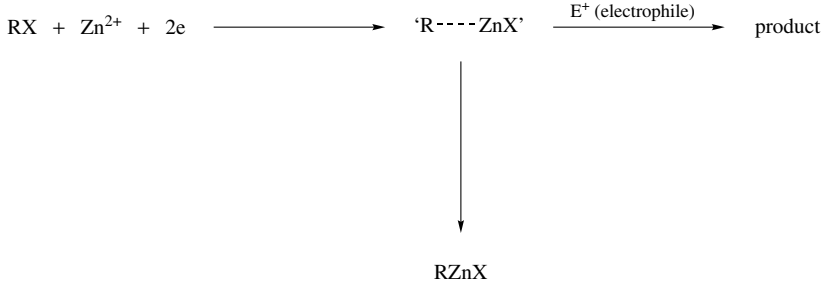

SCHEME 2

Another approach, recently described, consists in the electrochemical preparation of a very active zinc with the use of a mediator[3]. This zinc is able to react with low reactive organic halides. This electrochemical process is analogous to the chemical reaction developed by Rieke in which the naphthalene anion radical is used to activate metals such as zinc[4].

Finally, over the last decade, it has been shown that combination of electrochemistry and homogeneous catalysis in the presence of nickel complexes[5], or of simple cobalt salts[6], allowed the preparation of organozinc compounds from aromatic halides (iodide, bromide or chloride), hetero-aromatics, and aliphatic compounds bearing electron-donating or electron-withdrawing functional groups. Aryldizinc compounds were also prepared by the same method from the corresponding organic dihalides[7].

The main advantage of this procedure is that reactions occur at relatively high potential values, thus allowing the presence of sensitive functional groups on the starting material. In the presence of a nickel complex as catalyst, the process can be summarized as depicted in Scheme 3.

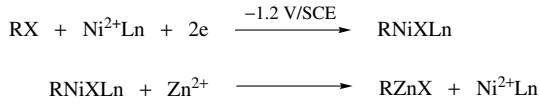

SCHEME 3

The reactions occur at a redox potential value close to that of the $Ni^{2+}Ln/Ni^{0}Ln$ couple. The real catalyst is the $Ni^{0}Ln$ species which reacts by oxidative addition with

RX, thus affording the corresponding RNiX compounds. In the presence of zinc(II) ions, this intermediate would undergo a transmetallation reaction to produce the organozinc compound RZnX. Note that zinc(II) ions can be brought either by addition of a zinc salt ($ZnBr_2$ or $ZnCl_2$) in the solution or by oxidation of a zinc anode.

Regarding the cobalt-catalyzed reactions, the electrochemical analyses of the involved processes allowed the discovery of a chemical way for the synthesis of these organozinc compounds. This chemical way will be evoked in this chapter.

A number of electrochemical reactions involving organic halides have been carried out in the presence of both a catalytic amount of a transition metal, M_t (M_t = Ni, Co), and zinc(II) ions (generally formed by oxidation of a sacrificial zinc anode). Though the presence of zinc(II) ions has, probably, an effect on the reactions progress, the formation of a transient organozinc species could be put forward. In this case, the responsible species for the success of the reactions is, very likely, the organometallic derivative of the transition metal RM_tX which is obtained according to equation 2.

$$RX + M_t^{2+} + 2e \longrightarrow RM_tX \qquad (2)$$

II. ELECTROCHEMICAL GENERATION OF A REACTIVE ZINC FOR THE FORMATION OF STABLE OR TRANSIENT ORGANOZINC REAGENTS AND THEIR REACTIVITY

A. Electrochemical Formation of Reactive Zinc

Various electrochemical routes[8] have been considered to make a reactive zinc, from zinc(II) ions, capable of reacting with halogenated substrates, RX, which can react with electrophilic derivatives E^+. Reactions can be concerted or sequenced as depicted in Scheme 4.

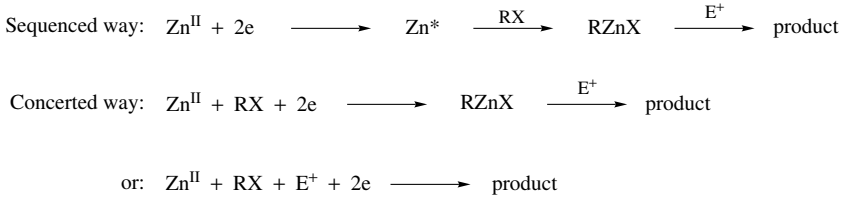

SCHEME 4

The zinc(II) ions can either be introduced in the reaction mixture before running the experiment (from commercially available $ZnBr_2$ or $ZnCl_2$), or generated *in situ*, in an undivided electrochemical cell, by oxidation of a zinc anode in the presence of 1,2-dibromoethane (Scheme 5).

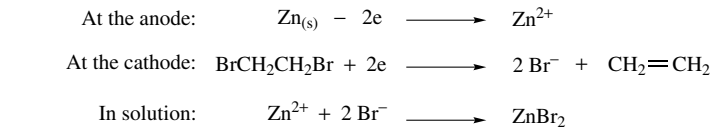

SCHEME 5

This last procedure allows the preparation of anhydrous zinc bromide in the solvent used (CH_3CN, DMF etc.). Note that, simultaneously to the electroreduction of dibromoethane,

$ZnBr_2$ can also be partially reduced ($-1.4 < E < -1$ V/SCE), thus affording an electrolytic zinc.

In solution, and especially in acetonitrile, $ZnBr_2$, and likely $ZnCl_2$, exists under a slow equilibrium mixture of several species more or less halogenated[9]: Zn^{2+}, $ZnBr^+$, $ZnBr_2$, $ZnBr_3^-$, $ZnBr_4^{2-}$. Dissolution of $ZnBr_2$ in acetonitrile leads to roughly 20–30% of Zn^{2+}, which is the most readily reducible species (-1 V/SCE).

An active zinc can also be prepared in the absence of bromide ions. In this case, the zinc(II) ions electrogenerated by oxidation of a zinc anode are concomitantly reduced at the cathode surface (Scheme 6).

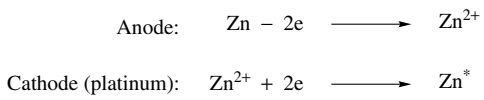

SCHEME 6

The reactions are conducted under inert atmosphere, at room temperature, in DMF as solvent, and in the presence of NEt_4ClO_4 as the supporting electrolyte. A divided black zinc is thus obtained. The specific surface area of this zinc (24 to 56 m^2/g) is all the larger as the current density applied (usually 60 mA/cm^2) during the electrochemical process is low[10].

Alternatively to this procedure, the reaction can be conducted in the presence of naphthalene[11]. However, the reaction has to be performed at $-10\,^{\circ}C$ in this case. Though naphthalene is more difficult to reduce (-2.5 V/SCE) than zinc(II) ions, the authors plead the following process (equation 3).

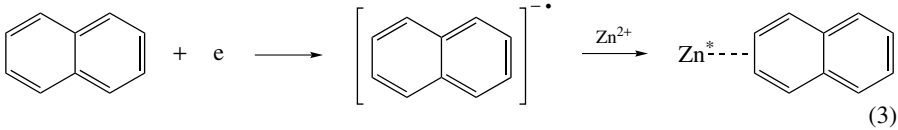

(3)

This mechanism is absolutely possible since a high current density is applied at the cathode surface.

This activated zinc would be an aggregation of very fine zinc particles dispersed in the DMF solution. The size of these particles is smaller than that obtained in the previous process, which was performed in the absence of naphthalene[12]. This electrochemical method is comparable to the chemical Rieke procedure in which the activated zinc is prepared by reduction of zinc halide with alkali metal naphthalenide in THF[13].

Other electrochemical ways have been attempted to generate an activated zinc surface from massive zinc (rod or plate). Two types of activation have been developed. In the first one, a low current density is applied on the massive zinc, which is used as the anode. The electroscoring of the zinc surface makes it reactive towards organic halides that are easily reducible. These reactions are catalytic in electricity. This electroscoring, which is all the more efficient as the applied current density is low, is equivalent to an acidic treatment of the surface.

In the second one, a catalytic amount of ZnX_2 (X = Cl, Br) is reduced at the zinc surface to be activated. As described below, this activation gives excellent and reproducible results with organic halides that are relatively easily reducible.

However, the mechanisms involved in these reactions have not been elucidated yet. Nevertheless, we can advance the formation of an organozinc compound able to reduce oxide-type impurities being at the zinc surface.

B. Synthesis of Stable or Transient Organozinc Species and their Reactivity

1. From electrolytic zinc

The activated zinc obtained by electrochemical reduction of Zn^{2+} in dimethylformamide has been used for the isoprenylation of aldehydes and ketones. This has been reported by Tokuda and coworkers (equation 4)[10].

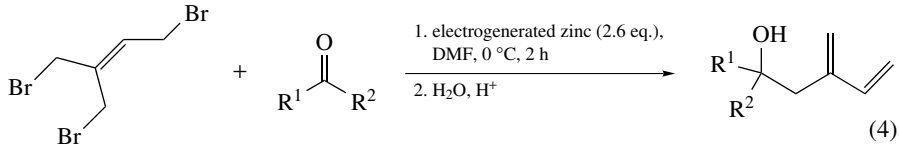

(4)

The isoprenylation of isovaleraldehyde led to the product in 68% isolated yield, higher than with a conventional procedure using zinc dust in DMF, or refluxing THF. The same procedure was used for the coupling reaction of allylic bromides with aldehydes and ketones, via the preliminary formation of organozinc compounds coming from the reaction between the electrolytic zinc and allylic bromides[12].

The same group also achieved the regioselective propargylation of aldehydes and ketones affording the corresponding homopropargyl alcohols (equation 5)[14].

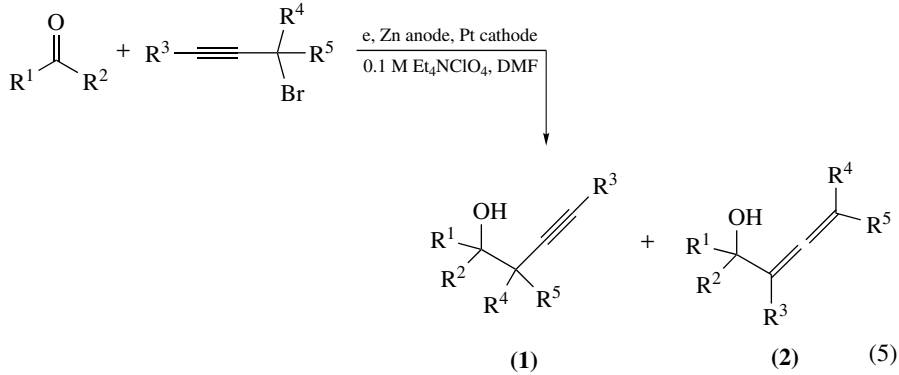

(1) **(2)** (5)

In all cases, the reaction led exclusively, or preferentially, to the homopropargyl alcohols (isomer ratios **1/2** from 100/0 to 69/31). The electrochemical propargylation using a zinc anode probably proceeds via the formation of an intermediate organozinc compound. This is supported by the fact that the reaction of benzaldehyde with propargyl bromide, in the presence of electrochemically generated reactive zinc in a DMF solution, resulted in the formation of propargylzinc bromide, and finally gave homopropargyl (**1**) and allenyl alcohol (**2**) in 72% yield (**1**/**2** = 96/4), i.e. slightly lower than that obtained when the reaction is concerted (90%).

Tokuda and coworkers have also synthesized organozinc compounds of alkyl iodides by the reaction of iodides (**3**, **4**, **5**, **6**) with an electrogenerated reactive zinc[15].

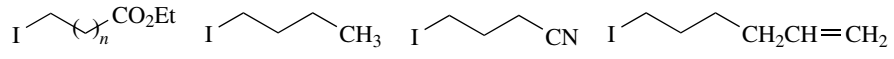

n = 1 to 3

(3) **(4)** **(5)** **(6)**

The synthesis of these organozinc compounds is fast (10 min) and leads to high yields, in DMF, at temperatures between 0 °C and room temperature. These organozincs can successfully be utilized for the palladium-catalyzed ($Pd[P(Tol\text{-}o)_3]_2Cl_2$, 5 mol%) cross-coupling reaction with aryl halides. This reaction, which is carried out in THF, gives the corresponding cross-coupled products in moderate to high yields (equation 6).

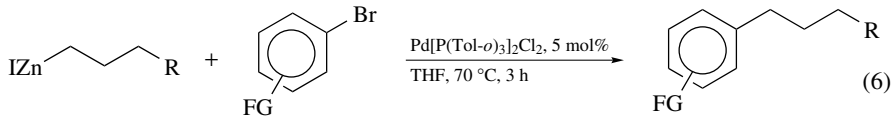

(6)

FG = 4-OCH_3, 4-$COCH_3$, H — 48–98% isolated yield

In addition, the organozinc compound obtained from ethyl 4-bromobutanoate reacts under similar conditions to those described previously, with 4-bromoacetophenone, to give the corresponding product in good yield[15]. The preparation of organozinc compounds and their cross-coupling with aryl halides can be carried out in one step (equation 7).

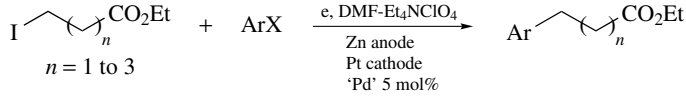

(7)

In this case, however, the yields are lower than those obtained by the two-step procedure (21–59% isolated yields). This is likely due to the occurrence of several competing reduction steps. The Pd(0) species generated by a two-electron reduction may thus react with the alkyl iodide by oxidative addition preferentially to the aryl halide.

The electrolytic zinc prepared in the presence of naphthalene at −20 °C appears more reactive than that prepared in the absence of a mediator, as observed in equation 8.

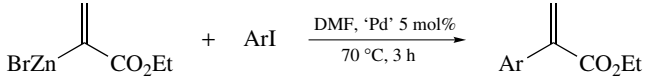

(8)

The corresponding cross-coupled products are obtained in excellent yields (98%) when the reactivate zinc is prepared in the presence of naphthalene. Interestingly, the yield falls down to 19% in the absence of mediator whereas no product was obtained from commercial zinc activated by an acidic solution.

The organozinc bromide prepared from ethyl 2-bromoacrylate in the presence of naphthalene can be used for a coupling reaction with a variety of aromatic iodides in quasi-quantitative yields. However, the use of $Pd[P(Tol\text{-}o)_3]_2Cl_2$ as catalyst is required for reactions carried out in the presence of aromatic bromides non substituted or substituted by electron-donating or electron-withdrawing groups. In this case, reactions are performed under reflux in THF.

These cross-coupling reactions were successfully applied to a synthesis of the precursor of naproxen and cicloprofen, non-steroidal anti-inflammatory agents[11].

Recently, this electrogenerated reactive zinc prepared in the presence of naphthalene has been successfully used for the synthesis of organozinc compounds from alkyl bromides $Br(CH_2)_nR$ ($n = 3$ or 5, R = CH_3, CO_2Et, CN, ...). These organozinc compounds, which are prepared in DMF solution, react in THF with various aromatic bromides in the presence of $Pd[P(Tol\text{-}o)_3]_2Cl_2$ as catalyst. In this case, the cross-coupling products are obtained in high yields[16].

The sacrificial zinc anode process has also been used to perform the electrochemical cyclopropanation of alkenes from dibromomethane or bromochloromethane in CH_2Cl_2/

DMF mixture[17]. The reaction is carried out either in the absence or in the presence of zinc salt ($ZnBr_2$), added before running the electrolysis. The presence of zinc salts allows one to reduce or suppress an induction period, which is observed otherwise (equation 9).

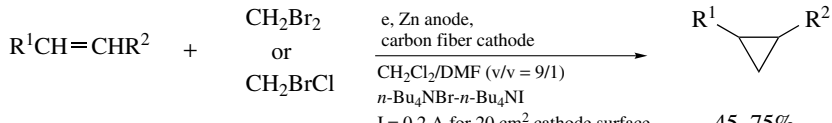

1 eq. 2.2 to 7 eq. 45–75% (9)

$R^1 = CH_3$, Ar
$R^2 = CH_2OH$

Cyclopropanes are obtained in moderate to good yields (45–75%) with allylic alcohols, cyclic olefins, geraniol etc. The yields are lower with styrene, and olefins activated by the presence of an electron-withdrawing group (e.g. 2-cyclohexen-1-one). No cyclopropanation was observed with vinyl chloride. The olefins, which give good yields in the presence of CH_2Br_2, lead also to moderate to good results when the electrosynthesis is carried out in the presence of $(CH_3)_2CBr_2$, $PhCHBr_2$ or $PhCHCl_2$. Many similarities may be observed between the electrochemical Zn-based system and the classical Zn-promoted Simmons–Smith reaction[18]. It has been inferred that the electrolytic process involved a zinc carbenoid as intermediate, which was accumulated during electrolysis, especially when the reaction with alkene was slow. Indeed, the electrolysis of a CH_2Br_2 solution and subsequent addition of crotyl alcohol gave the expected cyclopropane. In addition, iodonolyses of solutions show the presence of diiodomethane, or a mixture of diiodomethane and bromoiodomethane, indicating the formation of an organozinc intermediary.

The electrochemical reduction of bromotrifluoromethane (CF_3Br) in DMF in a cell fitted with a sacrificial zinc anode and a stainless steel or nickel cathode is a typical case where the organometallic compound formation can be realized according to two different processes, and where a transient species having a different reactivity compared to usual organometallics can be produced.

When the electrochemical reaction is carried out in DMF solution[19], in the presence of a zinc anode and at a low current intensity, the organozinc compounds CF_3ZnBr and $(CF_3)_2Zn$ are produced with faradaic yields higher than 100%. Interestingly, the lower the current density, the higher the faradaic yield.

In a divided cell and under low current intensity, the organozinc compounds are almost only produced in the anodic compartment. This can be explained by an attack process of the zinc anode by anodic electroscoring of the latter. This electroscoring generates an active zinc surface which chemically reacts with CF_3Br (equation 10).

$$Zn_{anode} - 2e \xrightarrow{DMF} Zn^* + Zn^{2+} \xrightarrow[CF_3Br(p = 1\ bar)]{DMF,\ RT} CF_3ZnBr + (CF_3)_2Zn \qquad (10)$$

Under a high electrolysis current intensity, the zinc(II) ions electroformed in the active zinc vicinity prevent the chemical reaction from becoming the major process. In an undivided cell and under a high electrolysis current intensity, the anodic scoring of zinc is negligible. In this case, the organozinc compounds are produced after reaction of the electrolytic zinc with CF_3Br (Scheme 7).

What is the reactivity of these organozinc compounds? In both cases they are unreactive towards carbonyl compounds such as aldehydes or ketones. Conversely, if reactions

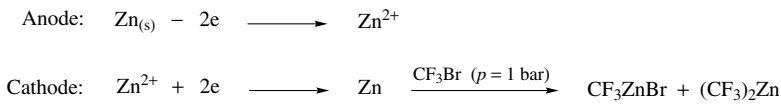

SCHEME 7

are concerted, i.e. if the zinc activation is performed in the presence of aldehydes, the corresponding alcohols are produced in high yields[20]. The overall reaction is shown in equation 11 and results are summarized in Table 1.

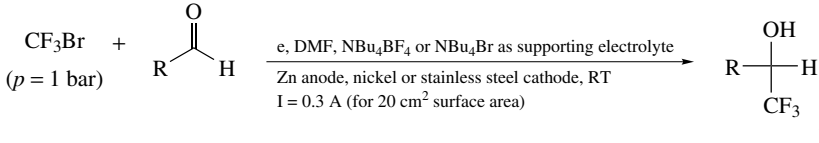

(11)

This sacrificial anode process compares favorably with Wakselman's classical Barbier procedure which requires activated zinc powder, and CF_3Br under pressure, leading to lower yields with benzaldehyde (52% in DMF)[21]. These good results compared to those obtained from a mixture of CF_3ZnBr and $(CF_3)_2Zn$ allow one to illustrate the formation of a transient organozinc compound of the type 'CF_3-Zn', which would be the really active species. This prompts the following question: does the reduction of Zn^{2+} in Zn

TABLE 1. Electroreductive coupling between CF_3Br and aldehydes

Aldehyde	Alcohol	Isolated yield (%)
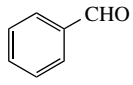	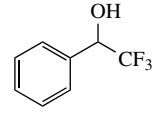	95
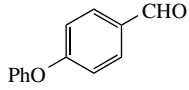	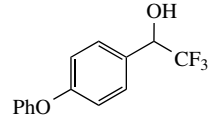	90
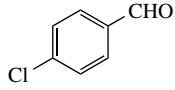	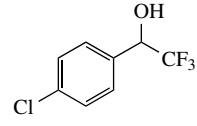	90
$(CH_3)_3CCHO$	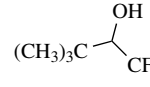	80
n-$C_6H_{13}CHO$	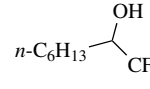	80
n-$C_6H_{13}CHO$	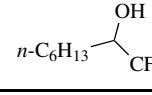	70

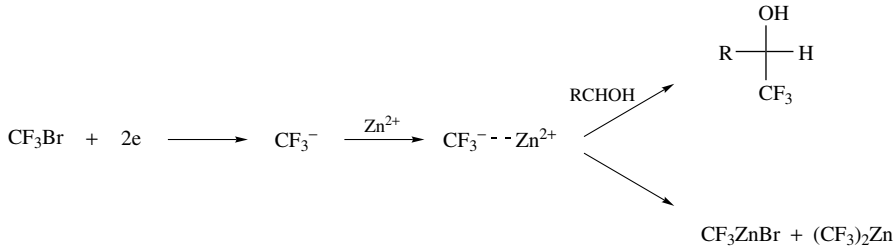

SCHEME 8

(at −1.4 V/SCE) occur before that of CF_3Br in CF_3^-? According to the results, CF_3Br would be reduced first (Scheme 8).

The good results obtained with aldehydes prompted us to extend this process to ketones. The yields into trifluoromethyl alcohols are lower into this case. As a matter of fact, the reaction works well (30 to 57% in yield) only with non-enolizable ketones such as benzophenone or fluorenone. Moreover, the yields into alcohols are around 5% from cyclohexanone or acetophenone and CF_3H is mainly produced. Scheme 9 may be depicted with $PhCOCH_3$.

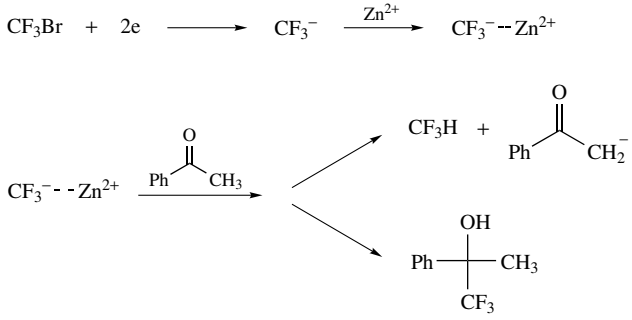

SCHEME 9

The use of tetramethylethylenediamine (TMEDA) improves the yields which, however, remain low (37 and 20% of isolated alcohol yields in the presence of acetophenone and cyclohexanone, respectively).

The aminoalcoholate $CF_3CH(O^-)NMe_2$ is also formed in low amount in the trifluoromethylation procedure described above[22]. This suggests a reaction between DMF with the transient species CF_3^-- -Zn^{2+} which would occur at the cathode. Indeed, CF_3CHO is produced if preparative electrolyses are carried out in pure DMF. This CF_3CHO was isolated as its diacetate equivalent $CF_3CH(OCOCH_3)_2$. Moreover, CF_3CHO is obtained in a faradaic yield of 23% along with the stable organozinc compounds CF_3ZnBr and $(CF_3)_2Zn$ (Scheme 10).

Interestingly[22], the isolated yield of CF_3CHO can be increased up to 75% if the reaction is performed in the presence of a sacrificial aluminum anode and of an additive such as $AlCl_3$, or BF_3. Et_2O.

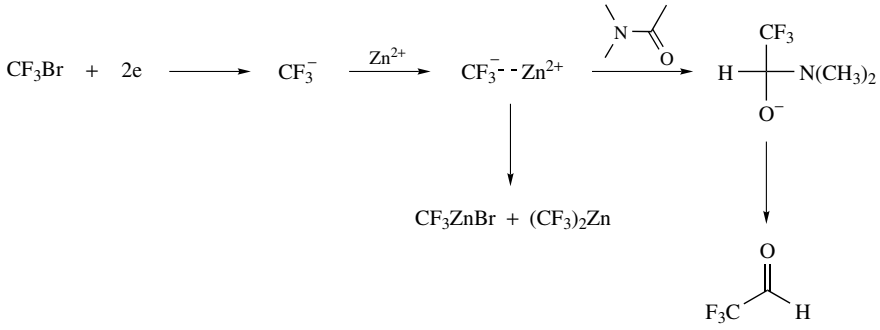

SCHEME 10

2. From activation of massive zinc

The massive zinc (rod or plate) reacts spontaneously with activated bromides provided the preliminary electroreduction of a catalytic amount of zinc salt ($ZnBr_2$ or $ZnCl_2$) occurs. Reactions are carried out in nitrile solvents (CH_3CN, PhCN, ...) or their mixture with dichloromethane. An undivided cell fitted with a zinc anode and an indifferent cathode (gold, nickel, carbon, zinc, ...) is used. As observed with benzylic bromides, the activation leads to an organozinc compound able to react with either the nitrile solvent or an electrophile reagent. The process is depicted in equation 12.

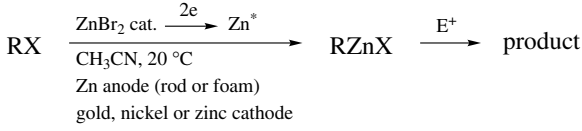

(12)

The reactions of massive zinc with the organic halides are relatively fast. Moreover, the rate of the reaction can be increased with a low current intensity being applied during the process between the cathode and the anode.

Once the process has started, if the crude solution is transferred into another cell containing a nitrile solvent, an organic halide and massive zinc, the reaction keeps going until total consumption of the halide. The mechanism of this activation process, which is reproducible, simple and mild, has not been elucidated yet. However, we can consider that the electrolytic zinc coming from the reduction of $ZnBr_2$ reacts with RX to produce the corresponding organozinc compound RZnX, which would be able to reduce the impurities at the massive zinc surface. This would generate active sites for further reactions with organic halides.

Anyway, this massive zinc activation process has been successfully used to achieve a number of reactions which usually require more delicate and uncertain zinc activation processes.

a. Synthetic applications to the Blaise reaction[23]. The activated zinc prepared as described previously has been used for the coupling reaction of α-bromoesters with nitriles $CH_3(CH_2)_nCN$ with $n = 1$ or 4, $CH_2{=}C(CH_3)CN$ and $Cl(CH_2)_3CN$ in acetonitrile, benzonitrile or dichloromethane as solvents. The reaction is fast (20 min to 2 h) and affords

corresponding β-ketoesters in good to excellent yields (50–95%) after an acidic treatment (equation 13).

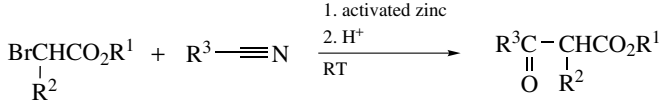

$$BrCHCO_2R^1 + R^3{-}{\equiv}N \xrightarrow[RT]{\text{1. activated zinc; 2. } H^+} R^3C(=O)CHCO_2R^1 \quad (13)$$

R^2

$R^1 = CH_3$, tC_4H_9 and $R^3 = CH_3$, C_6H_5
($R^2 = H$, CH_3)

Dichloromethane has been found to be an efficient solvent for the activation and for subsequent coupling reactions. Indeed, in dichloromethane, these reactions can be carried out at room temperature in the presence of nitriles and α-bromoesters taken in the same molar ratio, and lead to β-ketoesters in good yields (40–60%). Conversely, in dimethylformamide, and even with an excess of nitrile, only very low yields of ketoester could be obtained (<20%).

b. Reformatsky-type reactions[24]. In acetonitrile, the coupling reaction between α-bromoesters with various ketones (aromatic and alkyl), or aldehydes in the presence of an activated massive zinc, leads to good and reproducible yields of β-hydroxyesters (50–90%) in a time reaction of 30 min to 2 h (equation 14).

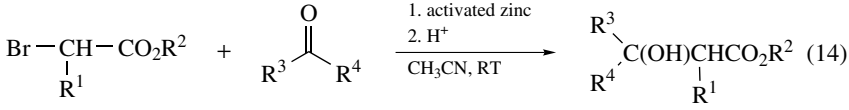

$$Br{-}CH(R^1){-}CO_2R^2 + R^3C(=O)R^4 \xrightarrow[CH_3CN,\ RT]{\text{1. activated zinc; 2. } H^+} R^3R^4C(OH)CH(R^1)CO_2R^2 \quad (14)$$

Unlike usual processes, the coupling reaction does not need any excess of halide (the carbonyl compound and the α-bromoester are used in the same molar ratio), or, most remarkably, any excess of zinc as reducing agent, which is also consumed stoichiometrically.

The method is also applicable to the coupling of α-bromoesters with anhydrides as depicted in equation 15.

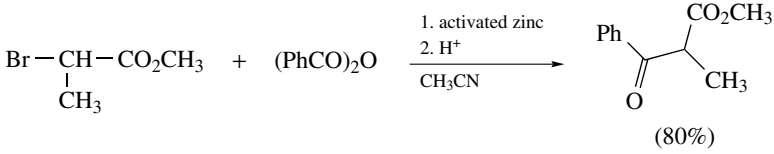

$$Br{-}CH(CH_3){-}CO_2CH_3 + (PhCO)_2O \xrightarrow[CH_3CN]{\text{1. activated zinc; 2. } H^+} \text{(80\%)} \quad (15)$$

c. Allylation of carbonyl compounds. The coupling reaction of allylic bromides with carbonyl compounds such as aromatic and aliphatic aldehydes as well as ketones leads to the corresponding allylic alcohol in good yields (54–85%) and with high regioselectivity (see, for instance, equation 16)[25].

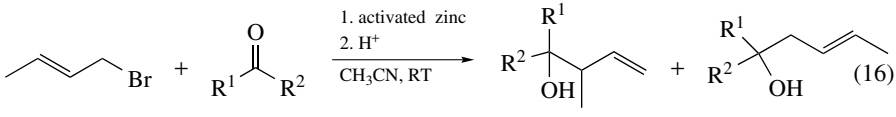

(16)

In all cases, the ratio of branched (**7**) to linear alcohols (**8**) was 95/5 or higher. The homoallylic alcohols were formed in 1–2 h at room temperature. In addition to the homoallylic alcohol, it has illustrated the formation of an unsaturated ketone coming from the reaction of the organozinc intermediary with the solvent acetonitrile (equation 17)

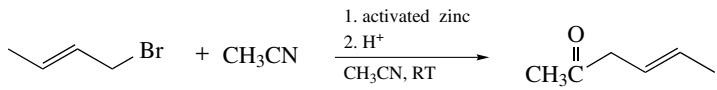

(17)

This ketone was usually obtained in 10–20% yield, except with a sterically hindered ketone such as 3,3-dimethyl-2-butanone. In this last case, the main product was the unsaturated ketone isolated in 75% whereas the expected alcohol was formed in less than 20% yield.

Moreover, no aldol or pinacol-type dimerization of the carbonyl compound was observed, even in the case of easily reducible benzophenone or benzaldehyde derivatives. As observed previously, the nature of the solvent is an important factor for the success of the reaction. Indeed, no homoallylic alcohols were formed in DMF.

The process has been applied successfully for the synthesis of α-methylene-γ-lactones from functionalized allyl bromides (equation 18)[25].

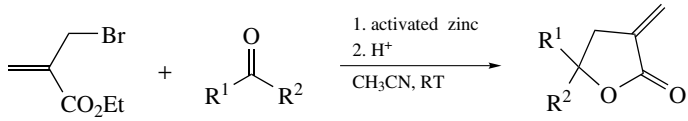

(18)

Both aldehydes and ketones afforded good yields (60–90%) of lactones, the reaction being very sensitive to the steric hindrance of the carbonyl group. Thus, benzophenone was converted in only 10%.

The good results obtained for the synthesis of homoallylic alcohols led us to study a similar reaction in the presence of a trifluorinated analog of prenyl bromide[26]. The conversion of this substrate into the corresponding organozinc compound was not described, and attempts to synthesize it by the common zinc activation methods were unsuccessful. Nevertheless, the zinc activation using an electrochemical process, based on the cathodic reduction of a catalytic amount of zinc bromide in the presence of a zinc anode, allowed the coupling reaction of a trifluoroprenyl bromide with carbonyl compounds giving alcohols (**9**) and (**10**) as depicted in equation 19.

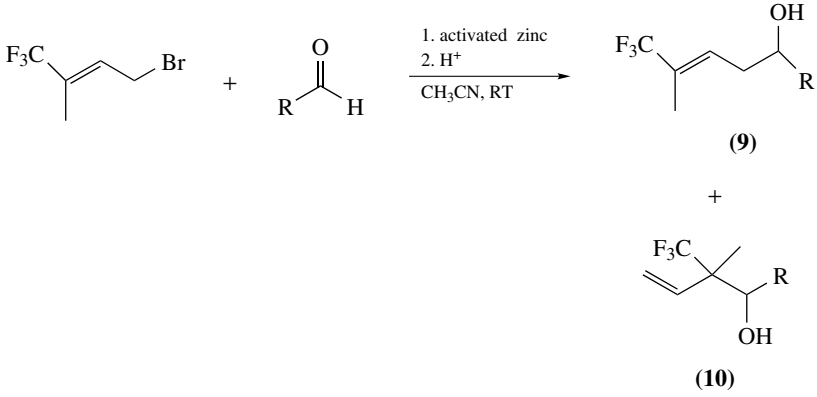

(19)

TABLE 2. Allylation of aldehydes with trifluoroprenyl bromide

RCHO	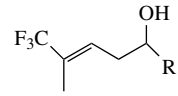 (9)	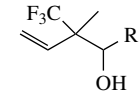 (10)
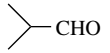	13%	—
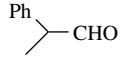	46%	—
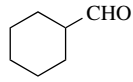	42%	21%
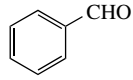	—	70%
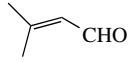	—	57%
n-$C_8H_{17}CHO$	—	79%

Several examples of addition to aldehydes are mentioned in Table 2.

Except in the case of isobutyraldehyde, where the non-optimized poor yield may be due to the high volatility of the resulting product, the alcohols are formed in good yields. When the aldehyde is sterically hindered (entries 1–2), α-allylation is observed. Conversely, branched alcohols result from unhindered or aromatic aldehydes (entries 4 to 6). Starting from 3-methyl-2-butenal (entry 5), a fluorinated analog of Artemisia alcohol is formed in one step[27].

Allylic zinc bromides also generally couple with ketones and acid anhydrides. In the case of trifluoroprenyl bromide, the attempts were only successful with ethyl pyruvate. However, it appears that this reaction provides the transposition product in 50% yield (equation 20).

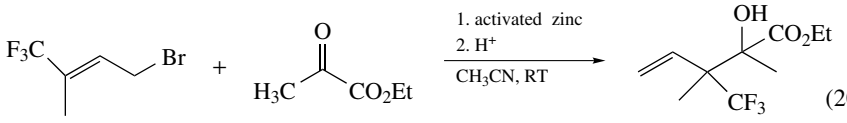

(20)

As for the above-mentioned reactions, the reaction rate can be accelerated if a low additional reduction current is applied after the electrochemical zinc activation.

d. Synthesis of benzylic zinc species and their reactivity towards aldehydes[28]. Unlike the above-mentioned results where the zinc derivative could not be isolated, it is noteworthy that benzylic zinc compounds, obtained from the corresponding bromide derivative, are generated in over 80% yield with 2 to 4 h of reaction time (equation 21).

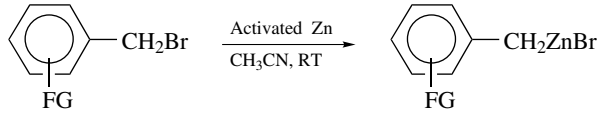

(21)

The reactions lead to a low amount of bibenzyl, except when the aromatic ring is substituted by a methyl substituent in *ortho* or *para* position. The benzylic zinc species exhibit a high stability in acetonitrile and solutions can be stored for several days, at room temperature under argon atmosphere with no detectable damage of the organozinc. Despite this stability, these organozinc species can react with aromatic aldehyde and 3-thiophene aldehyde provided use is made of chlorotrimethylsilane, which is known to activate the carbonyl function (equation 22)[29].

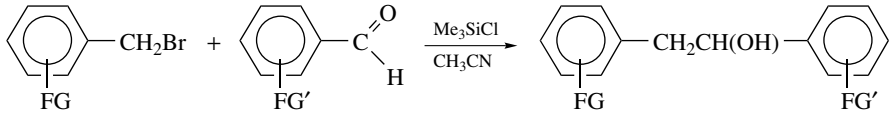

(22)

Whatever the functional groups FG (H, 2-CN, 3-CN, 4-CN, 4-CF_3) and FG′ (electron donating or electron withdrawing), reactions are fast and lead to good yields (60 to 77%) with respect to the starting benzylic bromide. In all cases, there is no reaction with the functional group borne by the aldehyde even if FG′ is a reactive group (CN, CO_2R).

On the other hand, the coupling of *ortho*-methylbenzyl bromide with *ortho*-methoxybenzaldehyde leads to the alcohol with a low yield (10%). No explanation has been found yet for this result.

e. Conclusion. Owing to its simplicity and reproducibility, the electrochemical zinc activation is an interesting procedure. However, in terms of substrate activation its range is limited. Indeed, no results have been obtained with aromatic halides or activated organic chlorides.

III. ELECTROCHEMICAL PREPARATION OF ORGANOZINC REAGENTS USING NICKEL OR COBALT CATALYSIS

A. Introduction

The synthesis of organozinc compounds by electrochemical processes from either low reactive halogenated substrates (alkyl chlorides) or pseudo-halogenated substrates (phenol derivatives, mesylates, triflates etc.) remains an important challenge. Indeed, as mentioned above, the use of electrolytic zinc prepared from the reduction of a metal halide or from zinc(II) ions does not appear to be a convenient method. However, recent work reported by Tokuda and coworkers would suggest that the electroreduction of a zinc(II) species in the presence of naphthalene leads to the formation of a very active zinc capable of reacting even with low reactive substrates (equation 23)[11].

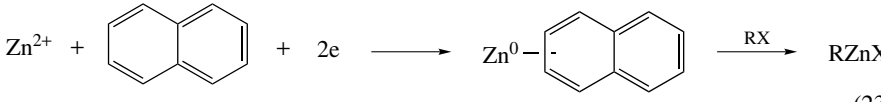

(23)

Nevertheless, this electrochemical zinc activation procedure, which looks like the chemical activation developed by Rieke, does not appear to be very convenient for the electrochemical synthesis of organozinc compounds in one step (equation 24) without preparation of the active zinc in a preliminary step[4, 13].

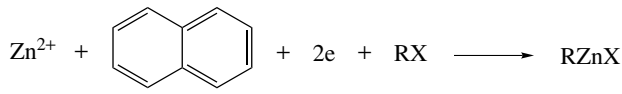

(24)

Indeed, the three involved species in this process have reductive potential values in the following order: $Zn^{2+} > RX >$ naphthalene.

Notably, Zn^{2+} ions are more easily reduced than naphthalene. This indicates that the electroreduction of the latter is very likely achieved on a recovered electrolytic zinc cathode. What happens under these conditions? So far, no data allow us to answer this question. The only information is the experimental observation of a characteristic transient color of the naphthalene anion radical indicating the reduction of this hydrocarbon, simultaneously with the reduction of Zn^{2+}, owing likely to a too high current density set at the cathode[11]. Moreover, the presence of an alkyl halide under such conditions would lead to its reduction on the zinc deposit, and this reduction would occur more easily than the reduction of naphthalene according to complex processes (equation 25).

$$RX + e \longrightarrow RX^{-\bullet} \longrightarrow R^{\bullet} + X^{-} \xrightarrow{e} R^{-} + X^{-} \tag{25}$$

As a consequence, there is no chance to synthesize organozinc compounds in good yields under these conditions. Taking into account the above remarks, the reduction or the activation of organic halides must thus occur at a more positive value than the reduction of zinc(II) ions. Recently, it has been reported that stable nickel(0) complexes, obtained by reduction of nickel salts (especially nickel halides) in the presence of various ligands, reacts with most of the organic halides by oxidative addition to give organonickel compounds from which a number of coupling reactions with electrophiles have been performed (equation 26)[30].

$$Ni^{2+}Ln \xrightarrow{\text{reduction}} Ni^{0}Ln \xrightarrow{RX} RNi^{II}X(Ln) \xrightarrow{E^{+}} RE^{+} + Ni^{II}Ln + X^{-} \tag{26}$$

The production of a stable or a transient intermediary of the type RNiXLn proves the activation of the organic halide RX.

Over the past few years, it has been shown that the electroreduction of NiLn complexes is feasible in various solvents (DMF, acetonitrile, THF, ...) at potential values depending on the nature of both solvent and ligand. The electroformed species reacts by oxidative addition with halogenated derivatives including organic halides (iodide, bromide, chloride) (equation 27).

$$RX + Ni^{II}Ln + 2e \longrightarrow RNiX(Ln) \tag{27}$$

In all events, the activation/reduction of RX occurs at potential values higher than that observed for the $Zn^{II}/Zn_{(s)}$ couple. As a consequence, the electrochemical synthesis of organozinc compounds can be achieved by nickel-catalyzed processes.

The results will be reported in the following part (see Section III.B), in addition to the properties of aromatic and hetero-aromatic organozinc compounds which have been prepared according to this process.

Recently[31,32], it has been shown that the electrochemical reduction of a cobalt halide CoX_2 (X = Cl or Br) in the absence or presence of a ligand leads to a cobalt(I) species able to react with aromatic halides. This can be achieved in DMF or acetonitrile (equation 28).

$$CoX_2 + e \longrightarrow Co^{I}X + X^{-} \xrightarrow{RX} RCo^{III}X_2 \tag{28}$$

This reaction leads to an organocobalt complex, $RCo^{III}X_2$, which is reduced to the corresponding $RCo^{II}X$. Owing to the low stability of the cobalt(I) species, the reaction proceeds in one step (equation 29).

$$RX + CoX_2 + e \longrightarrow RCo^{III}X_2 \tag{29}$$

As observed in the presence of nickel complexes, these reactions occur at potential values higher than that observed for the $Zn^{II}/Zn_{(s)}$ couple.

This activation permits one to develop a number of cobalt-catalyzed coupling reactions with various substrates E^+ (equation 30)[33–38].

$$RX + E^+ + 2e \xrightarrow{Co^{II}\ cat.} RE^+ \tag{30}$$

This activation has also been used to successfully develop an electrochemical process for the preparation of organozinc compounds. Results, mechanisms and reactivity of organozinc compounds are reported in the next part (see Section III.B).

B. Electrochemical Preparation of Organozinc Compounds using Nickel as Catalyst

1. From aromatic halides[5,39,40]

The electroreduction of aromatic chlorides or bromides in dimethylformamide (DMF) as solvent, containing *n*-Bu_4NBr as supporting electrolyte, and in the presence of $NiBr_2(bpy)_3$ (7% with respect to ArX) as catalyst, affords the corresponding organozinc species in good yields. The electrolyses are performed at room temperature, in a cell fitted with both a sacrificial zinc anode and a carbon fiber cathode (20 cm^2). A constant intensity of 0.15 A (around 7.5 mA cm^{-2}) was applied until 2 F mol^{-1} of halide have been passed. Iodine titration of the resulting solution indicated 60–70% conversion of ArX to ArZnX. Less than 10% was recovered as biaryl and around 30% as ArH. A part of the required zinc(II) ions is generated *in situ* from the zinc rod oxidation. The overall reaction can be summarized as in equation 31.

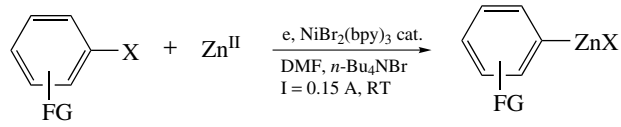

(31)

The organozinc species are produced in good yield in the absence or in the presence of electron-withdrawing or electron-donating functional groups.

The excellent compatibility of the process can be especially underlined with electron-withdrawing groups which are reknowed as being very reactive. On the other hand, no results were obtained with halogenated nitrobenzene since, in this case, the electrogenerated Ni^0 more easily reduces the NO_2 group than it reacts with the carbon–halide bond. Interestingly, the addition of both dried $ZnBr_2$ (0.5 molar equivalent with respect to ArX) and 2,2′-bipyridine ligand (two extra molar equivalents with respect to Ni) leads to an increase in the organozinc species yields (75–80% with respect to the starting ArX). The crucial role of the bipyridine ligand on the reaction progress will be reported later. Under the conditions just described, the biaryl formation is almost completely suppressed. Conversely, biaryl becomes the main product of this electrochemical reaction in the presence of only one molar equivalent of 2,2′-bipyridine ligand per nickel center.

Other classical ligands such as triphenylphosphine or 1,2-diphenylphosphinoethane have been considered. However, no good results were obtained under these conditions since a mixture of ArH and ArAr was produced. Moreover, the use of acetonitrile as solvent does not lead to positive results. In addition to the above-described general case, some particular cases have been examined, such as in the presence of bromothiophene.

2. From bromothiophene

The 2-thienylzinc bromide compound was prepared according to the same process described above in a 45% yield (equation 32)[39]. However, a different procedure has been used for the preparation of the 3-thienylzinc bromide compound[41].

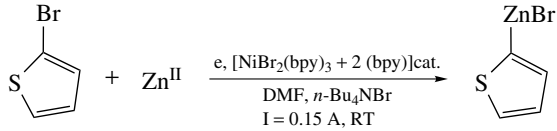

(32)

Interestingly, Rieke's zinc cannot afford this synthesis from 3-bromothiophene into one step. Indeed, the substrate has to be first transformed in the corresponding 3-iodothiophene, which is more reactive than the bromide analogue (equation 33)[42].

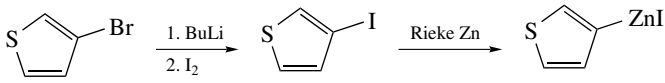

(33)

This last electrochemical process is carried out in an undivided electrolysis cell fitted with a sacrificial magnesium anode and a nickel foam as cathode. The reaction is conducted in dimethylformamide in the presence of both $NiBr_2$(bpy) as the catalyst and dried $ZnBr_2$ (1.1 molar equivalents with respect to bromothiophene), which is used both as supporting electrolyte and as a zinc(II) ion source. The other conditions are the same as those described in the section concerning the aromatic halides. The yield of 3-thienylzinc bromide was roughly 80%, as determined by GC analysis after treatment with iodide (equation 34).

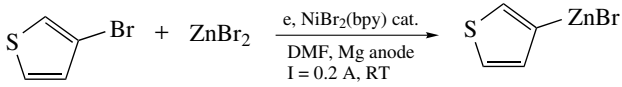

(34)

Despite the use of $NiBr_2$(bpy), bithiophene is not produced during the reaction. The use of excess bipyridine in the general case suggests the formation of a thienyl nickel intermediate associated to zinc(II) which would evolve towards 3-thienylzinc bromide along with regeneration of the catalyst. The formation of an organomagnesium intermediate (owing to the use of a magnesium rod as anode) can be ruled out, since no organometallic was detected in the absence of zinc salt. In addition, no product coming from a possible reaction between magnesium and DMF was detected.

The electrochemical conversion of 2,5-dibromo-3-substituted thiophenes to the corresponding thienylzinc species has been achieved by a similar method in an undivided cell fitted with a zinc sacrificial anode using catalytic amounts of $NiBr_2$(bpy) as the catalyst[43]. The overall reaction giving (**11**) and (**12**) is presented in equation 35. The results are reported in Table 3.

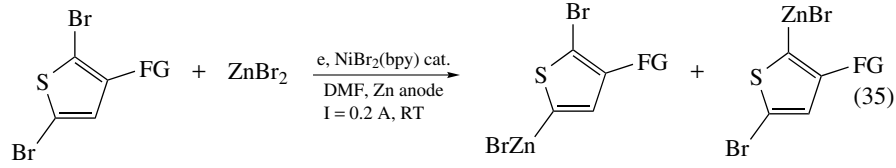

(35)

(11) **(12)**

TABLE 3. Yields and regioselectivity for the conversion of 3-substituted 2-dihalothiophenes into thienylzinc species

FG	Overall yield of **11** + **12** (%)	Regioselectivity **11** + **12**
H	30	—
CH_3	75	100:0
n-C_6H_{13}	76	100:0
$CH_2CO_2C_2H_5$	90	70:30
$CH(CH_3)CO_2CH_3$	80	60:40
$CH_2C_6H_5$	60	80:20
C_6H_5	65	70:30
p-$C_6H_4CO_2C_2H_5$	45	72:28
$COCH_3$	45	100:0

The yields are moderate to excellent. In most cases, the yields are affected by the formation of the corresponding oligo/polythiophenes. For all substrates, only traces of hydrogenated products were detected. Concerning the 2,5-dibromo-3-hexylthiophene substrate, its consumption follows the expected, theoretical, 2 Faradays per mole slope during the major part of the electrolysis. However, if the electrolysis is carried out at room temperature, the yield decreases from 76 to 60%, and a suspension of brown solid particles corresponding to likely oligomers is observed at the end of the electrolysis. The regioselectivity of the reaction has been studied. For the phenyl- or benzyl-substituted thiophenes, the proportion of the two regioisomers is similar to that reported by Chen and Rieke[44]. Yet, the electrochemical method allows a higher regioselectivity for a thiophene ring substituted with an hexyl group.

The formation of 2,5-di(bromozincio)thiophenes is never observed in significant yields (<5%), even if the electrolysis is continued to a charge corresponding to 4 Faradays per mol.

3. Mechanism of the electrochemical conversion of aryl halides to arylzinc compounds by nickel catalysis[5,45]

The potential for the electroreduction of $NiBr_2$(bpy), in the absence or presence of additional 2,2′-bipyridine ligands, in DMF containing tetra-*n*-butylammonium tetrafluoroborate, at a gold electrode ranges between −1.15 and −1.25 V/SCE (equation 36).

$$NiBr_2(bpy)_n + 2e \overset{\text{DMF, RT}}{\rightleftharpoons} Ni^0(bpy)_n + 2\ Br^- \tag{36}$$

The bi-electronic reduction of this nickel compound generates a zero-valent nickel complex which is stable on the time scale of cyclic voltametry, provided at least three bipyridine ligands per nickel center are present.

Under the same conditions, the reduction of $ZnBr_2$ involves several steps. The first one, which leads to solid zinc, is well defined and occurs at −1.4 V/SCE (equation 37).

$$Zn^{2+} + 2e \longrightarrow Zn_{(s)} \tag{37}$$

The oxidation of solid zinc deposited at the electrode surface is mainly observed at −0.9 V/SCE. The second one, which occurs at about −2 V/SCE, is not well resolved. It corresponds to the reduction of both $ZnBr_2$ and $ZnBr_3^-$ in solid zinc, $Zn_{(s)}$. As a matter

of fact, only a small amount of Zn^{2+} (*ca* 12%) is reduced at −1.4 V/SCE owing to the following slow equilibrium (equation 38)[9].

$$\underset{64\%}{3\ ZnBr_2} \rightleftharpoons \underset{12\%}{Zn^{2+}} + \underset{24\%}{2\ ZnBr_3^-} \tag{38}$$

For the same concentration, the current intensity observed at −1.4 V for a $ZnBr_2$-containing solution is consequently smaller than that obtained from a solution containing the bipyridine ligand and $NiBr_2$ (bpy/Ni = 1/3).

The addition of one molar equivalent of bipyridine with respect to $ZnBr_2$ leads to a positive shift of the original reduction process located at −1.4 V/SCE and, more importantly, the signal intensity increases. Under these conditions, indeed, half of the zinc(II) species becomes electroactive and exists under bipyridine complexes[9] **13**, **14**, **15**, **16** and **17**.

$ZnBr_2(bpy)$	$Zn(bpy)^{2+}$	$Zn(bpy)_2{}^{2+}$	$Zn(bpy)_3{}^{2+}$	$ZnBr(bpy)^+$
(**13**)	(**14**)	(**15**)	(**16**)	(**17**)

The electroreduction of $NiBr_2(bpy)$ in the presence of an aromatic halide makes the signal irreversible. In this case, the electroreduction occurs at about −1.2 V/SCE (equation 39).

$$NiBr_2(bpy) + ArX + 2e \longrightarrow ArNiX(bpy) \tag{39}$$

This overall reaction is the combination of both the electrochemical reaction (equation 39) and the oxidative addition of the aryl halide, ArX, to the electrogenerated nickel(0) (equation 40).

$$Ni^0(bpy) + ArX \longrightarrow ArNiX(bpy) \tag{40}$$

The electrochemical analysis allowed the determination of kinetic constants for this reaction[46]. Thus, in the presence of bromobenzene, the rate constant for the oxidative addition was found to be equal to about 70 $M^{-1}\,s^{-1}$. The σ-arylnickel complexes are unstable, except those obtained from *o*-tolyl or mesityl bromide as starting substrates. In these particular cases, the arylnickel complexes can be prepared by electrolysis from an ArBr/$NiBr_2$(bpy) equimolar ratio. However, the exhaustive electrolysis of an aromatic iodide in the presence of $ZnBr_2$, in DMF and at −1.4 V/SCE, leads to the corresponding arylzinc compound but the yield remains low (<20%). Indeed, the aryl iodide is mainly converted to ArH according to, very likely, a radical process (Scheme 11).

SCHEME 11

Several attempts were made with higher concentrations in ArI (up to 0.1 M) but failed. The major part of zinc is deposited at the electrode surface. These results match well those described in the first part of this chapter (see Section II). Indeed, in DMF, it has been clearly shown that the electrolytic zinc reacts only with activated alkyl halides.

The addition of excess $ZnBr_2$ to a $Ni(bpy)_3{}^{2+}$-containing solution (Zn/Ni = 10/1) does not lead to a color change of the solution. The complexes obtained from a mixture of Ni^{2+} and 2,2′-bipyridine are more stable than those obtained in the presence of zinc[9]. However, studies by cyclic voltametry of nickel–bpy complexes show several changes in

the cyclic voltammograms obtained after addition of zinc(II) ions. In summary, this work shows bpy exchange reactions between zinc(II) ions and the electrogenerated $Ni^0(bpy)_3$. More pronounced modifications were obtained with the addition of bpy (bpy/Zn(II) < 1). In conclusion, the bi-electronic reduction of the zinc(II) species at about −1.4 V would involve a complex of the type $ZnBr_y(bpy)_x^{(2-y)+}$, which would be formed by reaction of $ZnBr_2$ with both the added bipyridine and $Ni^0(bpy)_3$. Moreover, the $Ni^0(bpy)_3$ complex would be successively converted to $Ni^0(bpy)_2$, $Ni^0(bpy)$ and Ni as the added amount of $ZnBr_2$ increases.

The addition of bromobenzene in a solution containing both $ZnBr_2$, bpy and $Ni(bpy)_3^{2+}$ leads to a large increase in the current intensity of the nickel(II) reduction signal, indicating a nickel catalytic process. Interestingly, the current intensity of the zinc(II) reduction is hardly affected. Additionally, the signal corresponding to the oxidation of solid zinc, generated after reduction of the zinc(II) species, disappears in the presence of a large excess of bromobenzene. The addition of excess bipyridine leads to a decrease in the catalytic effect (reduction of Ni^{II}). Similar phenomena are observed with 4-bromoanisole as the aryl halide.

The most important point of this electrochemical study is the presence of a catalytic process depending on the aromatic halide concentration (increase of the reduction signal) and which occurs at the same potential at which the σ-arylnickel complex is produced. This suggests a metal-exchange reaction between ArNiX and Zn(II) to give Ni(II) and an organozinc species, RZnX (equation 41).

$$Ni^{II} + ArX + 2e \longrightarrow ArNiX \xrightarrow{Zn^{II}} ArZnX + Ni^{II} \tag{41}$$

To confirm this assumption, exhaustive preparative electrolyses of *o*-tolyl bromide in the presence of $NiCl_2(bpy)$ (Ni/ArBr = 1/5) have been carried out in the presence of a sacrificial aluminum or magnesium anode, and at the potential corresponding to the Ni^{II}/Ni^0 couple. After a charge of two electrons per mole of Ni(II) was passed, a characteristic orange solution of *o*-$MeC_6H_4NiCl(bpy)$ was obtained. No reaction was observed with the addition of a stoichiometric amount of $ZnBr_2$. Conversely, the *o*-tolylZnBr complex, prepared from the corresponding organomagnesium complex, reacts with $NiCl_2(bpy)$, thus affording the *o*-$MeC_6H_4NiCl(bpy)$ compound. This clearly shows the occurrence of a transmetallation reaction under these conditions (equation 42).

$$ArZnX + NiCl_2(bpy) \longrightarrow ArNiX(bpy) + ZnCl_2 \tag{42}$$

In agreement with this, the chemical reduction by activated zinc powder of a solution containing $NiCl_2(bpy)$ and PhBr produces an orange solution containing PhNiBr(bpy) and $ZnCl_2$. However, the *o*-tolylZnX complex does not react with $Ni(bpy)_3^{2+}$ whereas, conversely, the *o*-MeC_6H_4NiBr complex reacts with $ZnBr_2$ in the presence of excess bipyridine. In accordance with the above-proposed process, it can be concluded that the transmetallation reaction occurs in the Ni → Zn direction in the presence of excess bipyridine (equation 43).

$$ArNiX(bpy) + ZnX_2 \xrightarrow{\text{(bpy) excess}} ArZnX + Ni(bpy)_3^{2+} + 2\ X^- \tag{43}$$

As a matter of fact, it has been suggested that the presence of free bipyridine is required to allow the formation of a mixed complex in which the Zn^{II} species and the σ-arylnickel compound are close to each other (Scheme 12). This process, which occurs at the potential of the Ni^{II}/Ni^0 transition, has been proposed to give an account of the arylzinc

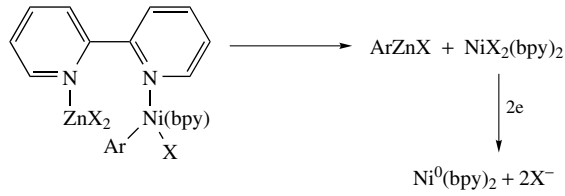

SCHEME 12

compounds electrosynthesis from relatively reactive organic bromides and catalyzed by $NiX_2(bpy)_n$ complexes.

In the presence of low reactive aromatic substrates such as *o*-tolyl chloride, it has been shown that production of the aromatic zinc occurs only at the potential at which the zinc(II) bipyridine is reduced, i.e. at about −1.4 V/SCE. Furthermore, the nickel(II) complex is also reduced at this potential value. In this case, the formation of either a bi-metallic species, or a cluster (**18**), intermediary combining Ni(0) and Zn(0) via the bipyridine ligand is suggested. This complex would react with the aromatic chloride to produce the corresponding ArZnCl along with the regeneration of the nickel catalyst.

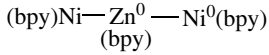

(18)

4. Reactivity of electrochemically prepared arylzinc compounds via a nickel catalysis

Arylzinc species prepared via the sacrificial anode process and from aryl halides in the presence of a nickel 2,2′-bipyridine, as already reported in Section III.B.1, were found totally unreactive towards common electrophiles such as aldehydes, carboxylic anhydrides or activated alkyl halides. However, they react with some electrophiles when they are activated by the presence of a catalytic amount of copper salts (10 mol% CuI) together with tetramethylethylene diamine (TMEDA) as described by Knochel and Singer on the ArZnX−CuCN metal exchange[47] or when the reaction is catalyzed by palladium complex.

a. Reaction with cyclohex-2-en-1-one[5]. Conjugate addition to cyclohex-2-en-1-one was readily achieved in the presence of an excess of chlorotrimethylsilane (2 eq. vs cyclohex-2-en-1-one) added dropwise at room temperature or with slight heating (30–40 °C). Isolated yields based on initial ArX are moderate to good (30 to 63%) (equation 44).

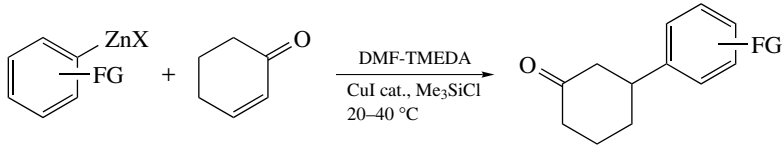

(44)

FG = CO_2Me, CN, OMe, CF_3, COMe
X = Br, Cl

b. Reaction with allyl halides[5]. Though allyl bromides react instantaneously with arylzinc species in the presence of a catalytic amount of copper salt together with

TMEDA, coupling with allyl chlorides requires slight heating over a period of two hours (equation 45).

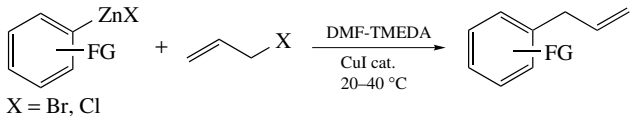

(45)

The yields based on the starting aryl halides depend on the nature of the functional group on the aromatic nucleus (41 to 63%).

c. With trifluoroacetic anhydrides[5]. Trifluoromethyl ketones were obtained from reaction between electrogenerated arylzinc species and trifluoroacetic anhydride. In this case, the use of CuBr−MeS_2 complex in catalytic amount was preferable to the TMEDA−CuI complex (equation 46) as described in Section III.B.4.a.

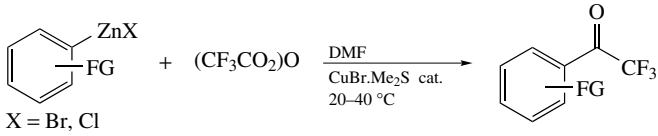

(46)

Good yields are obtained ranging from 32 to 52% vs. initial aryl halides.

d. With aryl halides: synthesis of unsymmetrical biaryls[39]. It would have been simpler to take advantage of the presence of the nickel complex in the reaction mixture to carry on the cross-coupling of ArZnX with Ar′X by subsequent addition of the last reagent. Unfortunately, this overligated nickel was unable to make the cross-coupling with Ar′X. However, the use of another catalyst such as bis(triphenyl)dichloropalladium was found quite convenient to catalyze the expected cross-coupling to prepare unsymmetrical biaryls. For example, the palladium complex $PdCl_2(PPh_3)_2$ was able to catalyze the cross-coupling reaction in 65% yield from 4-bromobenzonitrile and 4-trifluoromethylchlorobenzene as the source for the organozinc reagent formed, as described in Section III.B.1. In the last coupling reactions, the formation of side products, notable ArH and Ar-Ar, could have been a severe limitation to this coupling. Careful investigations aimed at studying the nature of the catalyst provided clear-cut evidence for the key role of the 2,2′-bipyridine ligand. Indeed, no more than 10% of homocoupling occurred when reactions were performed in the presence of $Ni(BF_4)_2(bpy)_3$ instead of $NiBr_2(bpy)$, whereas it was totally suppressed when running the reaction of arylzinc species formation in the presence of added $ZnBr_2$ and extra 2,2′-bipyridine (2 eq. vs $Ni(BF_4)_2(bpy)_3$). Under these conditions, the yields of arylzincs, as measured by iodine titration, were 75–80% in DMF regardless of the substituent on the aromatic ring. Additionally, the use of bis(triphenylphosphine)dichloropalladium (0.5–2%) catalysis affords the expected cross-coupling in better yields according to equation 47. Results are reported in Table 4.

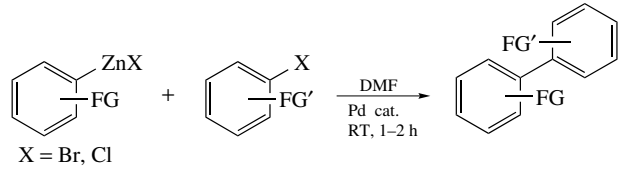

(47)

TABLE 4. Palladium-catalyzed coupling of electrogenerated arylzinc species with various aryl halides

ArZnX	Ar′X	ArAr′ (Yield %)
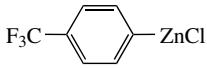	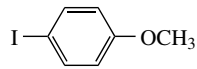	83
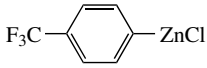	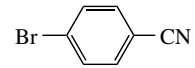	83
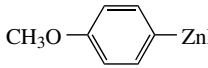	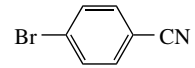	90
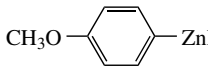	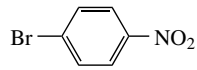	84
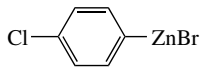	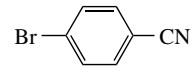	59
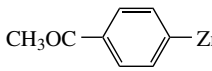	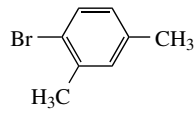	48
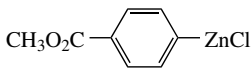	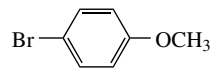	84
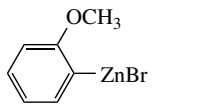	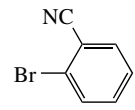	65
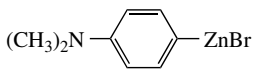	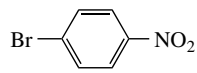	84
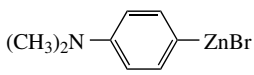	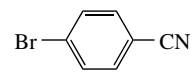	83
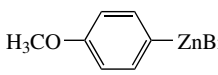	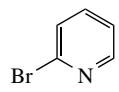	49

The slow addition of the arylzinc compound to a solution containing both an aryl halide, Ar′X, and the palladium complex furnished the biaryl in good to excellent yields. The very reactive Pd(0) complex was likely formed *in situ* by reduction of the starting palladium(II) complex by ArZnX. The reactions were very rapid (*ca* 1 or 2 h) compared to most usual Pd-catalyzed reactions involving ArZnX (*ca* 24 h). The reduction of Pd(II) could account for the formation of a small amount of Ar-Ar (2–5%) in the last non-electrochemical step while no homocoupling of Ar′X occurred.

3-Thienylzinc bromide prepared under mild conditions by electroreduction of a DMF solution containing 3-bromothiophene, zinc bromide and a catalytic amount of nickel–bipyridine complex, using a magnesium rod as the sacrificial anode as described in

Section III.B.2, was then coupled with aryl halides[41] using this palladium catalysis according to equation 48.

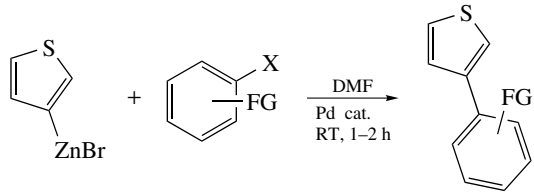

(48)

The coupling product occurred in high yield with iodobenzene (80% vs 3-bromothiophene). With aryl bromides, an electron-withdrawing group was required to achieve the coupling reaction (with FG = *p*-CN and *o*-MeOCO, yields are 47% and 40%, respectively, vs 3-bromothiophene). Conversely, no coupling product was observed in the presence of electron-donor substituents. In this last case, the deactivated aryl bromide is certainly unreactive towards zero-valent palladium.

e. Polymerization of 3-methylthiophene[48]. The preparation of 3-substituted polythiophenes is carried out through the electrochemical synthesis of intermediate thienylzinc species and their consecutive palladium-catalyzed coupling according to equation 49.

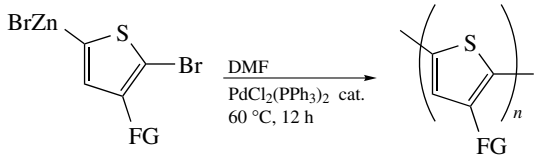

(49)

These thienylzinc intermediates were formed from the nickel-catalyzed electrochemical conversion of 2,5-dibromo-3-substituted thiophenes, as described in Section III.B.2. Yields, calculated vs. original 2,5-dihalothiophene based on the mass of solid recovered, are moderate (30% with FG = *p*-$EtO_2CC_6H_4-$) to good (80% with FG = Me). The structural properties of polythiophenes were characterized by several techniques, including ^{1}H-NMR, UV-vis spectrophotometry and MALDI-TOF-MS. For instance, these techniques showed that poly(3-hexylthiophene) is regioregular and presents a mass of *ca* 4000, which corresponds to 24 monomer units. Even though the direct nickel-catalyzed electroreductive polymerization of 3-substituted 2,5-dihalothiophenes is a much more straightforward route to prepare the corresponding polythiophenes (equation 50), the two-step electrochemical preparation of 3-substituted polythiophene involving organozinc species is significantly higher than the one-step process (equation 50).

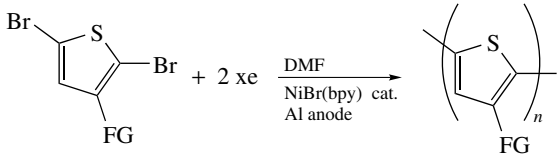

(50)

In this last reaction, the resulting polymers are much more polydispersed and/or regiorandom.

f. With 2-halogenopyridine[40]. Arylzinc compounds prepared from aryl bromides or chlorides by the electrochemical method using a nickel catalyst, stoichiometric zinc ions and a magnesium anode in a DMF solution can be coupled with 2-chloropyridine. The reaction is carried out at room temperature for *para*- and *meta*-substituted organozinc compounds whereas a temperature of 60 °C was required with *ortho*-substituted derivatives (equation 51).

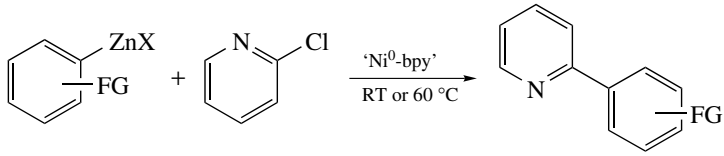

(51)

As described in Section III.B.4.d, a palladium catalyst was required to couple ArZnX with Ar′X. Indeed, the remaining nickel(II) complex in the medium was unable to catalyze this coupling reaction even if it was reduced to the corresponding zero-valent nickel complex. In contrast, with 2-chloropyridine as the heteroaryl halide added in the second stage, the coupling reaction was efficiently catalyzed by Ni^0(bpy). 2-Arylpyridine compounds were obtained in good yields. Results are reported in Table 5.

TABLE 5. Nickel-catalyzed electrochemical arylation of 2-chloropyridine via the formation of an arylzinc intermediate

FG-C_6H_4-ZnX	Coupling product	Isolated yield (%) Based on starting FG-C_6H_4-ZnX
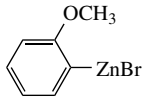	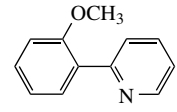	55
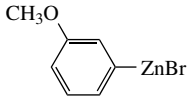	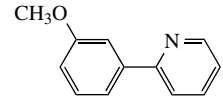	60
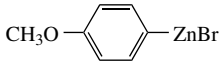	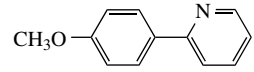	55
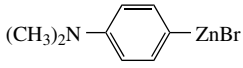	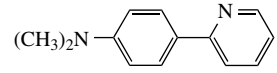	60
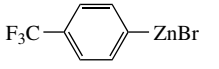	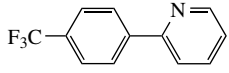	40
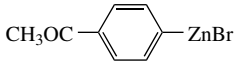	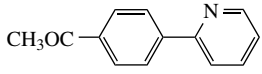	40
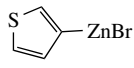	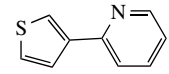	50

Yields versus aryl halides are moderate to good. Other nitrogen heterocycles such as 2-chloro-5-trifluoromethylpyridine or 2-chloropyrimidine were also coupled with *p*-$MeOC_6H_4ZnBr$ in 33% and 54% yields, respectively. Under the same conditions, no coupling product was observed with 3-chloropyridine. This specific behavior of 2-chloropyridine as compared to aryl halides can be explained by the presence of the nitrogen atom close to the carbon−halogen bond.

It has been reported that the electroreductive coupling between aryl halides and 2-chloro- or 2-bromopyridines in the presence of $NiBr_2$(bpy) as the catalyst led to the cross-coupling product in better yields (55−80%) (equation 52)[49].

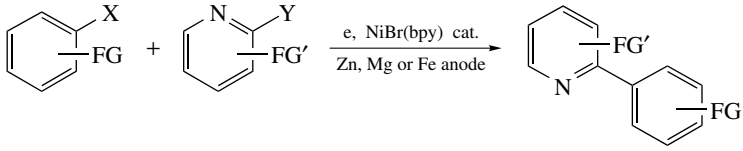

(52)

In a former study, the reaction was carried out in an undivided cell fitted with a magnesium or zinc rod. However, the use of a zinc anode was preferable in the case of aryl bromides substituted with an electron-withdrawing group since zinc(II) ions, formed by anodic oxidation of the zinc rod, allowed the cathode potential to remain higher than −1.6 V/SCE and to thus prevent the direct reduction of the aryl halide. Conversely, when the substituents on the aryl halide was an electron-donating group, the use of a zinc or magnesium anode gave the same yields. Therefore, coupling product yields were improved when iron was used instead of zinc or magnesium as the anode. On the basis of these observations, it can be noted that the success of this reaction was not due to the formation of a transitory intermediate organozinc species but to the presence of a σ-arylnickel intermediate. This assumption is confirmed by the fact that nickel(0) must react faster with the aryl halide than with the 2-halogenopyridine compound for an efficient coupling.

Importantly, the choice of either 2-chloro- or 2-bromo-pyridine depends on the reactivity of the aryl halide.

These results indicate that zinc ions formed by oxidation of the anode do not play a part or only have side effects in the direct electroreductive carbon−carbon bond formation carried out with a zinc anode and a nickel catalyst. In these reactions, a nickel organometallic is involved.

C. Electrochemical Preparation of Organozinc Compounds using Cobalt Halides as Catalysts

The electrochemical preparation of organozinc compounds obtained from the corresponding aromatic halides and with the use of a nickel complex as catalyst is only efficient in dimethylformamide as solvent. Moreover, in most cases and as described previously, the reaction requires the presence of excess 2,2′-bipyridine (five molar equivalents with respect to nickel) to achieve the transmetallation reaction leading to the organozinc compound and to avoid the formation of biaryl, Ar-Ar (equation 53).

$$ArNiX + Zn^{2+} \rightleftharpoons ArZnX + Ni^{2+} \qquad (53)$$

This led us to find new catalytic systems able to turn the electrochemical process to the synthesis of organozinc compounds. In this context, a simple cobalt halides salt can be used advantageously[6]. As a matter of fact, the work devoted to the study of the

electrochemical properties of cobalt halide salts either in mixed solvent (DMF- or MeCN-pyridine (v/v = 9/1)) or in pure acetonitrile furnished good results, and provided further insight to the mechanisms involved in these processes. A general view of these works will be given in the following.

1. Electrochemical behavior of cobalt halides CoX_2 (X = Br, Cl)

a. In a DMF–or a MeCN–pyridine (v/v = 9/1) mixture. In a dimethylformamide/pyridine (v/v = 9/1) mixture, it has been shown by cyclic voltametry that the reduction of CoX_2 (X = Br, Cl) performed at a platinum disk electrode leads to a cobalt(I) species which is stable on the short time scale of cyclic voltammetry, provided the scan rate is higher than (10 V s^{-1}). Under these conditions the reduction process is reversible (equation 54)[31].

$$CoX_2 + e \overset{\text{DMF/pyridine (v/v = 9/1)}}{\rightleftharpoons} Co^{I}X + X^{-} \tag{54}$$

At lower scan rates the reduction of CoX_2 leads to the inactive solid cobalt, $Co_{(s)}$, by disproportionation of Co^{I}, despite the presence of pyridine (Scheme 13).

$$Co^{II}X_2 + e \rightleftharpoons Co^{I}X + X^{-}$$

$$Co^{I}X \longrightarrow 1/2\ Co_{(s)} + 1/2\ Co^{II}X_2$$

$$1/2\ Co^{II}X_2 + 1/2\ e \longrightarrow 1/2\ Co^{I}X + 1/2\ X^{-}$$

Etc.

SCHEME 13

The disproportionation rate constant of Co^{I} has been determined and found equal to $(2 \pm 0.5)\ 10^3\ M^{-1}\ s^{-1}$ (equation 55).

$$2\ Co^{I}X \longrightarrow Co_{(s)} + Co^{II}X_2 \tag{55}$$

When the electroreduction of CoX_2 is carried out in the presence of an aromatic halide (FG-C_6H_4X), a reaction occurs between the electrogenerated cobalt(I) species and the aryl halide (equation 56).

$$Co^{I}X + FG{-}C_6H_4X \longrightarrow FG{-}C_6H_4Co^{III}X_2 \tag{56}$$

The rate constants for this oxidative addition depend on both the halogen atom, in the order I > Br > Cl, and the nature of the functional group (FG).

As expected, for the same halogen atom the reaction is faster in the presence of an electron-withdrawing group than in the presence of an electron-donating group on the aromatic ring. The FG-$C_6H_4Co^{III}X_2$ complexes are also electroreducible at the same potential (−1.40 V/SCE) at which CoX_2 is reduced into $Co^{I}X$ (equation 57).

$$FG{-}C_6H_4Co^{III}X_2 + e \overset{-1.4\ \text{V/SCE}}{\longrightarrow} FG{-}C_6H_4Co^{II}X + X^{-} \tag{57}$$

Controlled-potential ($E = -1.40$ V/SCE) preparative electrolyses of FG-C_6H_4X carried out in the presence of a catalytic amount of CoX_2 indicate competition between the disproportionation of Co^I and the oxidative addition. For instance, the latter is preponderant when X=Br and FG = CO_2Et. The aromatic halide is thus reduced into a mixture of ArH and Ar-Ar. The origin of ArH can be explained by the process shown in Scheme 14.

$$ArCo^{II}X \longrightarrow Ar^{\bullet} + Co^{I}X$$

$$Ar^{\bullet} + \text{solvent} \longrightarrow ArH + \text{solvent}(-H)^{\bullet}$$

SCHEME 14

The biaryl formation is likely the result of more complex processes, involving probably intermediary species such as $ArCo^I$ coming from the reduction of $ArCo^{II}X$ (equation 58).

$$ArCo^{II}X + e \longrightarrow ArCo^{I} + X^{-} \tag{58}$$

All the above-mentioned processes are similar in a CH_3CN–pyridine (v/v = 9/1) mixture[32]. However, the disproportionation rate of Co^I which is electrogenerated at −1.30 V/SCE and its oxidative addition rate to various arylhalides are divided by a factor of two compared to the rate constants determined in DMF–pyridine. It has also been shown that the use of vinyl acetate stabilizes Co^I species. Under these conditions, the disproportionation rate constant is divided by a factor of seven whereas the oxidative addition rate constants are not much affected.

In DMF–pyridine, it has been established that the presence of $ZnBr_2$ (electrochemically *in situ* prepared) leads to a more stable cobalt(I) species (the disproportionation rate is as much as four-times smaller) without altering the oxidative addition rate whatever the aryl halides, ArX (X = Cl, Br)[50]. In addition, the presence of this salt, $ZnBr_2$, leads to a significant increase in the intensity of the cathodic process. This phenomenon has been ascribed to the regeneration of the cobalt(II) salt and not to the reduction of the added $ZnBr_2$, since the latter is reduced at a more negative potential value (−1.7 V/SCE). A transmetallation reaction has been shown between the σ-arylcobalt(II) complex and zinc(II) ions (equation 59).

$$ArCo^{II}X + ZnBr_2 \longrightarrow ArZnX + CoBr_2 \tag{59}$$

In agreement with this, the preparative-scale electrolysis of chlorobenzene carried out in DMF–pyridine, at a constant intensity in a cell fitted with a sacrificial zinc anode and in the presence of both $ZnBr_2$ and $CoBr_2$ as catalyst, affords the formation of the organozinc compound in yields varying from 25 to 60% with respect to the starting PhCl. The yield of the organozinc compound is better when the amount of $ZnBr_2$ increases.

This result clearly shows that the $ZnBr_2$ initially present in solution is essential to both stabilize Co^I, which can react with PhCl, and to produce the corresponding organozinc compound (equation 60).

$$PhCl + ZnBr_2 \xrightarrow[\text{RT, } E = -1.4 \text{ V/SCE}]{\substack{\text{DMF/pyridine (v/v = 9/1)} \\ CoBr_2,\ \text{Zn anode}}} PhZnCl \tag{60}$$

The process is depicted in Scheme 15.

Identical results have been obtained in an acetonitrile/pyridine (v/v = 9/1) mixture.

b. In acetonitrile[51]. In acetonitrile, it has been shown that $CoBr_2$ exists under an equilibrium mixture of several cobalt(II) species which are more or less brominated ($CoBr^+$,

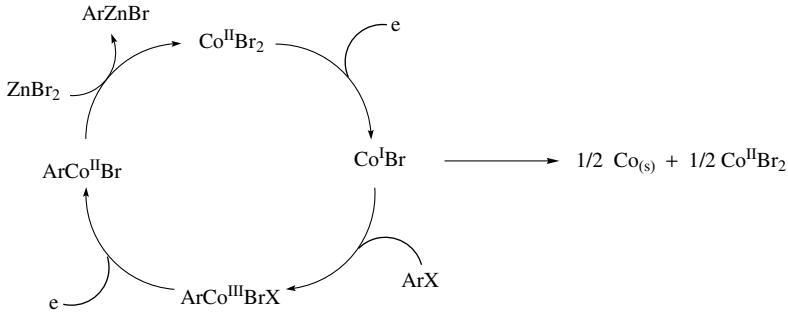

SCHEME 15

$CoBr_2$, $CoBr_3^-$, $CoBr_4^{2-}$, Co^{2+}), where Co^{2+} is the most easily reducible. The reduction of Co^{2+} which occurs at -0.86 V/SCE leads to solid cobalt. The cobalt(I) intermediary, Co^+, could not be detected even at high scan rate (200 $V\,s^{-1}$).

The electrogenerated Co^+ species must therefore undergo a faster disproportionation reaction than that observed in the presence of pyridine and which partially stabilizes the cobalt(I) species.

This assumption is confirmed by the cyclic voltammograms which are not modified by the presence of a reactive aromatic halide (p-$BrC_6H_4CO_2Et$). The Co^+ species disproportionates much more rapidly than a possible reaction with the aryl halide. This behavior is drastically modified when $ZnBr_2$ is added into a $CoBr_2$-containing solution. First, this zinc salt acts as a Lewis acid towards brominated forms of Co^{II}, thus leading to the Co^{2+} species, which becomes the main species. This is observed provided $ZnBr_2$ or Zn^{2+} (brought by addition of the electrochemically formed $Zn(BF_4)_2$) is added in sufficient amounts. Equation 61 illustrates this bromide ion exchange.

$$(Co^{II}Br_x)^{(x-2)-} + Zn^{2+} \rightleftharpoons Co^{2+} + (Zn^{II}Br_x)^{(x-2)-} \qquad (61)$$

Second, the electroreduction of Co^{2+} (at -0.86 V/SCE) which is initially irreversible becomes reversible in the presence of zinc salts. Under these conditions, the electrogenerated Co^+ species has a life-time estimated at several seconds. Consequently, it is more stable towards the disproportionation reaction than the cobalt(I) species generated in the presence of pyridine used as ligand.

This cobalt(I) species formed in the presence of zinc(II) reacts by oxidative addition with aromatic halides (X=I, Br) bearing electron-withdrawing or electron-donating groups, thus affording arylcobalt(III) complexes which are reducible in the corresponding arylcobalt(II) compounds at the same potential at which Co^{2+} is reduced. Conversely to what was stated in the presence of pyridine, it does not react with aromatic chlorides. This was observed even in the presence of substrates activated by an electron-withdrawing group. As already observed in the presence of pyridine, the addition of zinc(II) ions in excess induces an increase in the current intensity, corresponding to the reduction of Co^{2+} (equation 62).

$$ArX + Co^{2+} + 2e \longrightarrow ArCo^{II}X \qquad (62)$$

This is also in agreement with the fact that a transmetallation reaction leading to the organozinc compound and the regeneration of Co^{2+} occurs (equation 63).

$$ArCo^{II}X + Zn^{2+} \longrightarrow ArZnX + Co^{2+} \qquad (63)$$

The electrochemical preparation of organozinc compounds in the presence of CoX_2 as catalyst is thus feasible from the corresponding iodides or bromides, provided ZnX_2 (X = Cl, Br) or Zn^{2+} ($Zn(BF_4)_2$) is present before running the electrosynthesis. Under these conditions, Scheme 16 can be proposed.

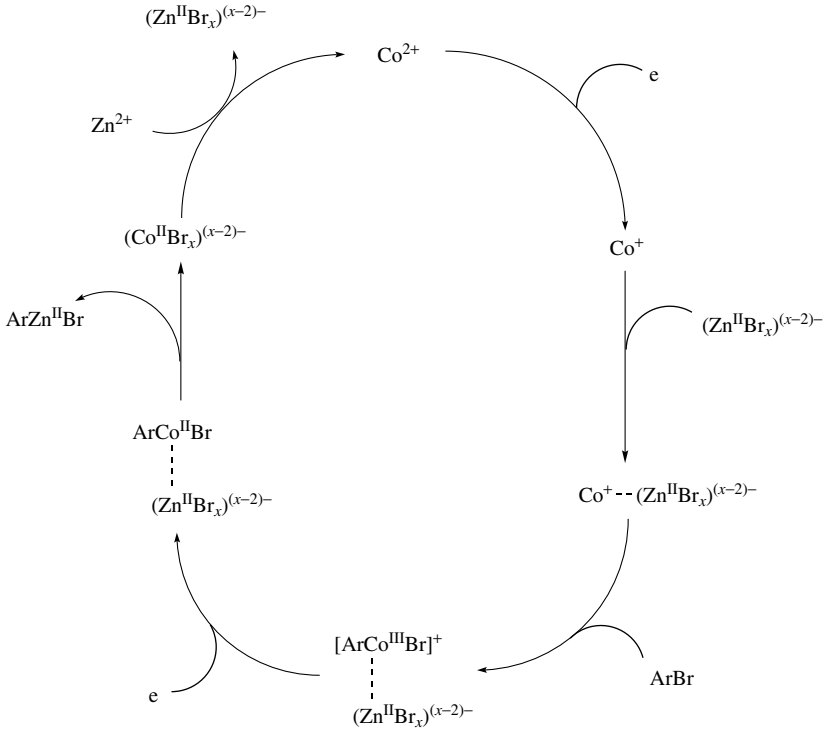

$1 \leq x \leq 4$

SCHEME 16

The gradual disappearance of the catalyst precursor by formation of species $(Co^{II}Br_x)^{(x-2)-}$, which become more and more difficult to reduce as x increases, is highly counterbalanced by the *in situ* generation of Zn^{2+} ions coming from the sacrificial zinc anode. It allows one to dehalogenate the cobalt(II) species and to restore the cobalt catalyst into its initial form Co^{2+}.

2. Electrosynthesis of aryl- or heteroarylzinc compounds

Aryl- or heteroarylzinc species have been successfully synthesized from the corresponding aryl or heteroaryl bromides or chlorides in high yields, on the laboratory scale (10 mmoles of substrate). The use of cobalt as catalyst allowed the synthesis of organozinc reagents using the sacrificial anode process with a wide variety of solvents.

Electrosyntheses are conducted in a one-compartment cell already described[2], fitted with a sacrificial zinc anode and either a nickel foam or a stainless steel cathode. The presence of a supporting electrolyte is unnecessary, the ionic conductivity of the medium

being ensured by a small amount of zinc bromide added into the solution. Electrolyses are run at a constant current intensity of 0.2 A (0.01A cm^{-2}) at room temperature and under inert atmosphere of argon. The oxidation of zinc anode with the concomitant reduction reactions generates zinc ions, which are required for the formation of arylzinc compounds.

a. In DMF/pyridine or CH_3CN/pyridine as solvent[6]. The standard reaction conditions leading to arylzinc compounds are summarized in equation 64. Under these conditions, arylzinc species are obtained in high yields (60–90%) from phenyl bromides substituted by electron-donating substituents until a typical charge of 2.1 Faradays per mol of halide is passed. Even bromoaniline can be converted without protecting the amino group. However, bromophenol is acidic enough to divert the formation of the corresponding arylzinc halide and is recovered unchanged after the workup. For the other cases, the only by-product of the electrolysis is the reduced product ArH, likely formed by decomposition of the arylcobalt intermediate $ArCo^{II}Br$. On the other hand, low yields are obtained from the corresponding aryl chlorides, which are not consumed even when an excess of faradaic charge is engaged. This indicates a too slow reaction of Co(I) with aryl chlorides. When the benzene ring is substituted by an electron-withdrawing group, the yields of the corresponding arylzinc halide, obtained from corresponding bromo or chloro compounds, in the standard reaction conditions, are good to high except when the functional group is COMe or CN. Results are reported in Table 6.

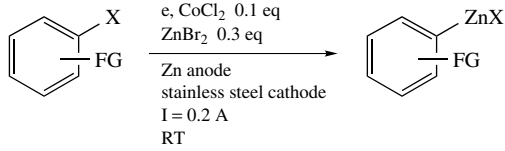

(64)

In the presence of COMe or CN as substituents, poor results are obtained in the standard reaction conditions. The starting compounds, either chloride or bromide, are mostly converted into ArH. This can be explained by the low cathode potential (−2 V/SCE) corresponding to the reduction potential of the halide, indicating a catalyst loss. Indeed, the formation of the arylzinc intermediates occurs at *ca* −1.3 V/SCE, corresponding to the potential at which the catalytic cobalt(I) species is electrogenerated from $CoCl_2$. However, the yields can be increased with the use of a higher amount of the catalyst and/or a higher amount of the initial zinc bromide. Under these last conditions, yields become good to excellent (50–75%).

This method can also be applied to the formation of heteroarylzinc compounds in DMF–pyridine in the standard reaction conditions. Results are reported in Table 7.

TABLE 6. Preparation of arylzinc compounds substituted by electron-withdrawing groups

FG	X	% ArZnX	% ArX recovered
p-$MeSO_2$	Cl	90	0
p-EtOCO	Br	85	0
o-EtOCO	Br	58	19
p-CF_3	Br	70	0
p-Cl	Br	60	0
p-F	Br	79	0
p-MeCO	Br	25	0
o- or *m*- or *p*-CN	Br or Cl	<1	0

TABLE 7. Preparation of arylzinc halides from heteroaryl halides

ArX	% ArZnX
2-Cl-pyridine	50
2-Br-thiophene	67
3-Br-thiophene	25

Also, from 3-thienyl bromide, yields can be increased by modifying the standard conditions (58%).

Under these standard reaction conditions, the acetonitrile/pyridine mixture can replace the DMF/pyridine one. This solvent mixture is also quite convenient for running the preparation of arylzinc halides. Yields are good to excellent (60–90%) and even higher than those obtained in DMF. However, with bromophenol, no organozinc species was formed in acetonitrile as observed in DMF. The formation of arylzinc species is also effective in a mixture of solvents of acetonitrile–DMF–pyridine (8/1/1) in the presence of $CoCl_2$ (13%) as the catalyst precursor and zinc bromide (30%). This method has also been applied to the formation of organozinc halides from alkyl and alkenyl halides. So far, only low yields have been obtained using the standard reaction conditions in DMF–pyridine. Results are reported in Table 8.

The acetonitrile–pyridine mixture solvent has also been used to synthesize diorganozinc compounds[52] from either dibromobenzene or activated dichlorobenzene according to equation 65.

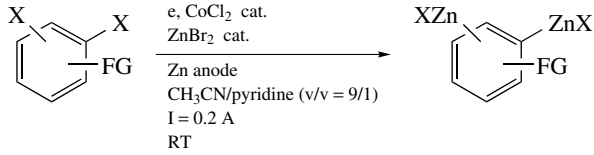

(65)

The reaction conditions are similar to those described for the monohalides, except that the amount of cobalt is doubled. When X = Br, only the dizinc species is obtained at 4 F per mol with good yields except in the case of *o*-dibromobenzene, where the yield is poor. Results are reported in Table 9.

At 2 F mol^{-1}, the mono- and dizinc compounds are obtained simultaneously in variable amounts. 2,5-Dibromothiophene behaves basically like the corresponding benzene reagent. At 4 F mol^{-1}, only the dizinc compound is obtained but the yield is not satisfactory (28%).

On the contrary, dichlorobenzene reagents give a mixture of mono- and dizinc compounds at 4 F mol^{-1}. In fact, the monozinc compound is the main product at 2 F mol^{-1} whereas at more than 2 F mol^{-1} the reaction does not proceed further, even when all the starting reagent is not consumed in the case of non-activated dichlorobenzenes.

TABLE 8. Preparation of arylzinc halides from alkyl and alkenyl halides

R–Br	%RZnBr
1-Bromodecane	30
$Br(CH_2)_3CO_2Et$	42
β-Bromostyrene	45

TABLE 9. Formation of dizinc species from dibromobenzenes

Reagent	$BrZnC_6H_4ZnBr$
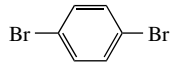	86
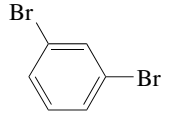	51
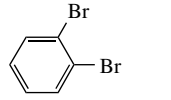	16
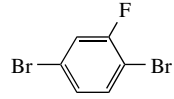	73
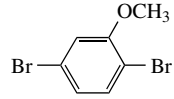	44

2,5-Dichlorothiophene gives mostly the monozinc species at 2 F mol^{-1} (mono/di = 10) and the starting reagent is not totally consumed. With an extra charge, there is no evolution, as observed with dichlorobenzene. In this case, only 40% of dichlorothiophene is converted. On the other hand, with *p*-bromochlorobenzene, only the monozinc compound $BrZnC_6H_4Cl$ shows up at 2 F mol^{-1} and a part of this is transformed into dizinc species at 4 F mol^{-1}.

In conclusion, the electrosynthesis of diarylzinc or diheteroaryl zinc species can be achieved with good yields to the reaction conditions described above to the presence of 10 or 20% of catalyst and using the corresponding dibromides or sometimes dichloride reagents.

These organozinc compounds electrosyntheses have been extrapolated on a larger scale (up to 1 L of solvent) and realized in an electrolysis flow cell, which is supplied continuously. In view of the preceding results, the solvent was a mixture of acetonitrile/pyridine (v/v = 9/1) and electrosyntheses were conducted in the presence of 4-bromoanisole. Results are similar to those obtained with a cell of 50 mL, until 70% of the starting reagent is consumed. Then, the formation of the arylzinc species is stopped. It was demonstrated that this stop is due to the loss of the catalyst via the disproportionation of the Co^I species. This behavior is not surprising, considering electroanalytical studies of the conversion of aryl halides to arylzinc compounds by cobalt catalysis. In fact, it has been shown that the electrochemical reduction of $CoBr_2$ leads to a Co(I) species that leads either to an arylcobalt(III) intermediate (precursor of ArZnX) in the presence of aryl halides or competes with the disproportionation reaction of Co^I into Co^{II} and solid cobalt, Co(s) (see Section III.C.1). Furthermore, the $ArCo^{II}X$ compound obtained by reduction of the corresponding $ArCo^{III}X_2$ complex might evolve to $Ar^\bullet$ and Co^IX, but no data are reported. This species is certainly the principal cause of the reduction product formation as by-product of electrosyntheses. As a result of the electrochemical studies that have

indicated a stabilization of the electrogenerated Co^I species in the presence of zinc ions in pure acetonitrile, a versatile organozinc electrochemical synthesis was developed from aryl bromides in acetonitrile without using pyridine in a cell containing 40 mL of solvent. The presence of a stoichiometric amount of zinc bromide, which was either electrogenerated or introduced from commercial $ZnBr_2$ in the medium, was necessary to have a very promising effect on the Co^I life.

Furthermore, the presence of pyridine in electrosynthesis reaction mixtures can disturb some coupling reactions, its nucleophilic properties being in some cases a drawback when electrophilic species are added to an electrolysis mixture.

b. In pure acetonitrile[53]. All the reactions were carried out under the conditions described in equation 66. Under these conditions, 76% of organozinc species was obtained starting from ethyl 4-bromobenzoate; the by-products were the hydro-dehalogenation product of the starting aromatic halide (ArH = 17%) and the dimerization product (Ar-Ar = 7%).

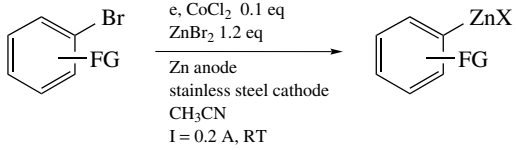

(66)

The main point to note is that the use of an additional ligand such as adiponitrile, vinyl acetate or methyl vinyl ketone is useless; similar yields were obtained. Considering the fact that the presence of an additional ligand did not raise the reaction yields and could have negative effects if the optimal amount is not present in the reaction mixture, it was decided to work without any ligand. The use of dimethylformamide or dimethylacetamide instead of acetonitrile did not lead to organozinc species formation when these solvents were used without addition of pyridine.

According to the results previously described in the electroanalytical studies (see Section III.C.1), aryl chlorides proved to be unreactive to zincation in the absence of pyridine. However, aryl bromides bearing an electron-donating (FG = *p*-MeO) or electron-withdrawing (FG = *p*-EtOCO, *m*-CF_3, *p*-F, *o*-, *m*- or *p*-CN, *p*-MeCO) group are converted to the related organozinc species in fairly good yields, the by-products being ArH (4 to 24%) and Ar-Ar (0 to 7%). Curiously, *p*-fluorobromobenzene led to a 43% yield, 63% of this compound remaining unconsumed after a charge of 2 F per mol of substrate was passed. This fact remains unexplained. For all the other reagents, a charge of 2 faradays is sufficient to totally convert the organozinc compounds according to the mechanism described in Scheme 16.

It can be pointed out that results are not reproducible, depending on the quality of the cobalt salt used and particularly of the $ZnBr_2$. This last species should be produced preferably by cathodic reduction of 1,2-dibromoethane combined with the anodic oxidation of a zinc anode according to Scheme 5 (see Section II.A).

After the electrochemical preparation of $ZnBr_2$ and the introduction of both $CoBr_2$ and aryl halide, it was seen that arylzinc compounds were detected in small amounts without engaging electricity. This phenomena was interpreted as follows: the zinc stemming from electroreduction of $ZnBr_2$ can reduce cobalt(II) halide to form low-valent cobalt Co(I), which can activate aryl bromides to form arylzinc compounds via $ArCo^{II}X$. The mechanism would be similar to that proposed by the electrochemical approach. In this case, the reduced zinc becomes reactive and can replace electricity. From this electrochemical

process, a new chemical reaction was developed aimed at preparing aromatic zinc species from corresponding aryl bromides or iodides using a chemical reducing agent[54, 55, 56].

3. Reactivity of electrochemically prepared arylzinc compounds via a cobalt catalysis

Arylzinc species prepared from aryl halides using cobalt catalysis and a sacrificial anode process present a similar reactivity to those prepared via nickel catalysis or by classical chemical methods. However, the electrochemical synthesis of organozinc reagents using simple cobalt complexes is very easy to activate aryl halides is very easy with reactive functionalized groups under mild conditions, allowing the study of their reactivity. Moreover, it was brought to the fore that cobalt salts did not only catalyze the preparation of arylzinc compounds, but also contribute to increase the reactivity of arylzinc species. In fact, cobalt salts also catalyze some cross-coupling reactions between arylzinc species and electrophilic compounds. To date, studies are in progress to try and get further insights about quantitative interpretation of the processes which occur.

a. Cross-coupling reaction with aryl halide. Electrogenerated arylzinc halides formed either in pure acetonitrile or in the presence of pyridine can be coupled with reactive aromatic halides[6] (for example, PhI) in the same medium using classical catalysis by $PdCl_2(PPh_3)_2$ or $Pd(PPh_3)_4$. Under these conditions, the resulting dissymmetric products (Ar-Ar′) have been isolated in excellent yield.

The cross-coupling between electrogenerated aryldizinc species and iodobenzene can be achieved using the same procedure, leading to a mixture of trimer and dimer (equation 67)[52].

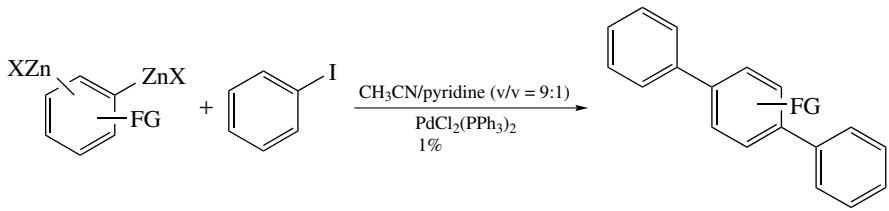

45% vs $ArBr_2$
with FG = H or F (67)

+

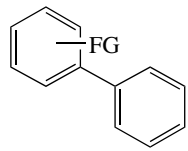

27% with FG = H
17% with FG = F

b. Synthesis of alternating π-conjugated copolymers. The synthesis of alternating π-conjugated copolymers based on this electrochemical preparation of the above-mentioned aryldizinc intermediates was obtained by their subsequent cross-coupling with unsaturated

dihalogenated compounds using a palladium catalysis. Alternating π-conjugated copolymers from benzene and mono- or di-substituted benzene rings were prepared in two steps according to equation 68[57].

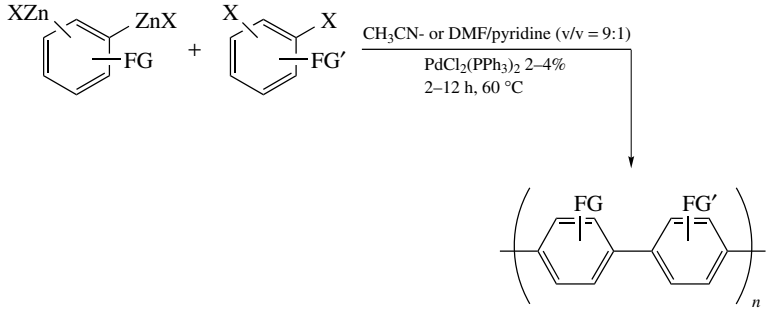

(68)

Since the aryldizinc species are formed in good yields (50–70%), the values reported in Table 10 are most likely affected by losses during the purification steps and depend on the vinyl dihalide, 1,4-dihalobenzene or 2,5-dihalothiophene introduced. In the case of PPVs, the original configuration of the vinyl substrates seems to be retained within the polymer structure.

c. Synthesis of functionalized 4-phenylpyridines[58]. As various functionalized organozinc species are synthesized in high yields using mild reaction conditions in a mixture of CH_3CN/DMF/pyridine (v/v/v = 8/1/1), the convenient one-pot procedure to couple these electrogenerated phenylzinc compounds with pyridinium salts was investigated allowing the synthesis of 4-phenylpyridines, as described in equation 69.

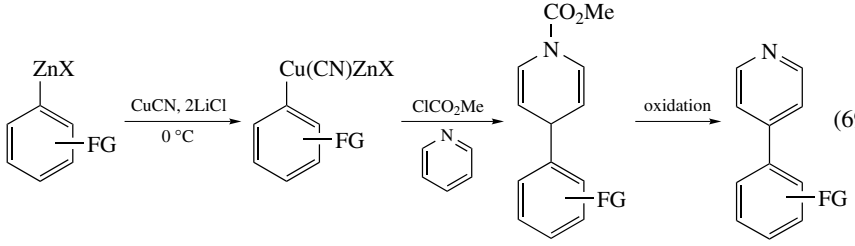

(69)

Thus, after completion of the formation of arylzinc halides, they are converted into mixed copper–zinc organometallic species. Considering the fact that this reaction sequence involves the formation of a pyridinium ion and that during the first step pyridine was present in the electrolysis medium, a simple addition of methyl chloroformate to the solution of mixed copper–zinc organometallic species led to the 4-substituted 1,4-dihydropyridine. Then, this last product was oxidized without being isolated, using silica gel and oxygen or using hydrogen peroxide and acetic acid to afford the desired 4-phenylpyridines. Results are reported in Table 11.

It should be noted that yields are based on starting aryl bromides. Moderate to good overall yields are obtained from aryl bromides substituted by an electron-donating group (35 to 69%).

d. Synthesis of aromatic ketones. Functionalized organozinc species can be transmetallated into organocopper in order to react with acid chlorides[4,47]. However, arylzinc

TABLE 10. Two-step preparation of various π-conjugated copolymers

Polymer	Yield (%)
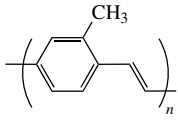	78
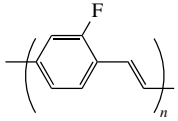	20
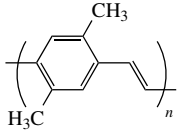	15
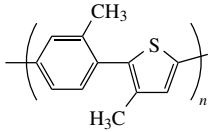	54
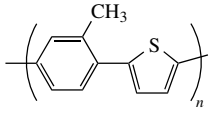	64
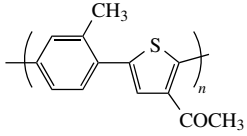	16
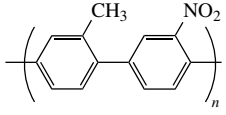	90

species formed by electrochemical methods in acetonitrile could not be activated using a mixture of cuprous cyanide and lithium chloride to form aromatic ketones. Furthermore, they are not coupled with aryl chlorides without catalyst. Then, these compounds undergo coupling in quantitative yields using a palladium catalyst (equation 70).

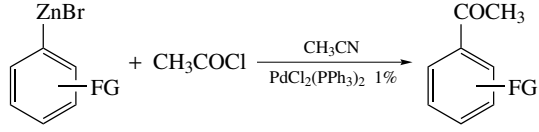

(70)

64–76% vs initial ArBr

TABLE 11. Preparation of functionalized 4-phenylpyridines from various electrochemically prepared organozinc reagents

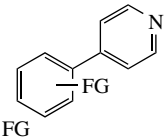

FG	Yield (%)
p-CO_2Et	45
m-CO_2Et	50
p-COMe	39
m-COMe	56
p-CN	43
p-CF_3	44
m-CF_3	47
p-F	55
m-Cl	66

Based on Knochel's work[59], which has employed cobalt halides as catalyst for the acylation of dialkylzinc reagents into ketones, this catalyst has been investigated for the coupling reaction of electrochemical arylzinc compounds formed in acetonitrile (equation 71)[60].

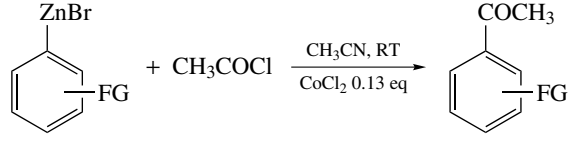

(71)

The overall yields vs initial aromatic bromides are moderate to good, ranging from 26 to 77%, and an electron donating or electron withdrawing group on the aryl bromide does not affect the yield in the coupling reaction. However, acylation of the electrochemically prepared arylzinc species requires the addition of a fresh quantity of CoX_2, although the medium already contained cobalt from the preparation of arylzinc derivatives. The hypothesis is that the electrogenerated Co(I) disproportionates too rapidly into solid cobalt in spite of the presence of zinc bromide.

e. Arylation of activated olefins[61]. It has been shown that $CoBr_2(bpy)_2$ is very efficient when performing conjugated addition of electrochemically arylzinc compounds prepared via cobalt catalysis in an acetonitrile/pyridine mixture (equation 72).

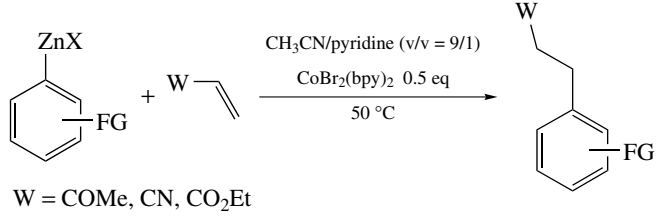

(72)

The amount of cobalt complex in this step influences the reaction rate, but not the yields. Indeed, with only 0.3 equivalent of cobalt catalyst, the arylzinc compound is consumed after 24 h instead of 10 h when 1 equivalent was used. An excess of the activated olefin is required to optimize the yield of the conjugate addition. Under these conditions, this process has been studied with various aryl halides (X = Br, Cl) and activated olefins. Yields range from 40 to 80%.

With a substituent such as a methyl group on the double bond of the olefin, conjugate addition products are isolated in satisfactory yields (equation 73).

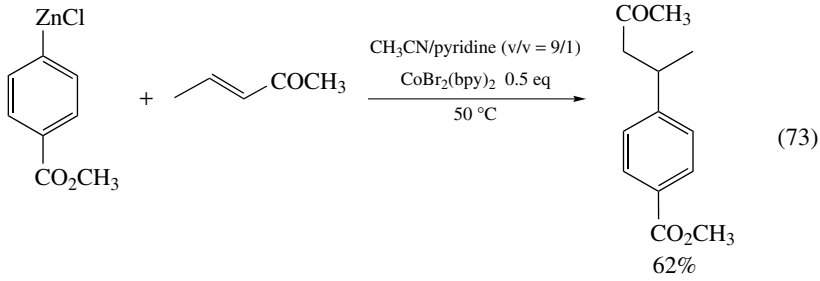

(73)

To date, the role of $CoBr_2(bpy)_2$, which is essential in the coupling reaction with activated olefins, has not been clarified yet.

IV. CONCLUSION

Over the past decade, a variety of electrochemical approaches have been successfully developed to prepare both activated zinc metal and organozinc compounds. Some of these procedures come from the adaptation of chemical methods. In such cases, the chemical reducing agent is replaced by the electrons that are generated at a cathode.

Conversely, other processes are totally original. This is especially encountered when the electrochemical act is associated with a transition metal complex catalysis. These methods have the advantage of affording the organozinc compound synthesis under simple and mild conditions that are compatible with the presence of reactive functional groups on the substrate. Importantly, these procedures are reproducible and can be run by any chemist. Besides, the preparation from a few millimoles to tens of millimoles of the organometallic compound is easy at the laboratory scale.

What happens on a higher scale, and particularly at the industrial scale? To our knowledge, there is no answer yet. Several attempts have been made at preparing a hundred millimoles of organozinc compounds by extrapolating the laboratory processes, but they were not fruitful. The reasons for these failures have been studied and analyzed. This work could be helpful in overcoming the problems encountered. Yet, the use of electrochemistry at a higher scale than that of the laboratory have lead to a number of technical problems that, so far, have not or have only been partially solved. This is particularly true with electrolysis devices using the sacrificial anode process and which can be considered as the only possible system in non-aqueous media. However, this slightly negative statement regarding general interest in organic electrosynthesis must be moderated. Indeed, molecular electrochemistry and especially the use of transient electrochemical methods allows one to obtain valuable information on the mechanisms occurring during electrosyntheses. This general statement applies well to the reactions that have been mentioned in this chapter.

The cross-checking information originating from both electrosynthesis reactions and molecular electrochemistry has allowed one to introduce unambiguous and important

information to a number of significant points concerning the role of the solvent nature, of the ligand, etc., into transition metal catalyzed reactions.

More importantly, the association of synthesis and molecular electrochemistry has allowed one to discover new and original chemical approaches in the preparation of organozinc compounds as well as to develop original chemical reactions concerning the selective activation of functionalized substrates[54–56].

V. REFERENCES

1. C. E. Tucker, T. N. Majid and P. Knochel, *J. Am. Chem. Soc.*, **114**, 3983 (1992).
2. J. Chaussard, J.-C. Folest, J.-Y. Nédélec, J. Périchon, S. Sibille and M. Troupel, *Synthesis*, 369 (1990).
3. A. A. Jalil, N. Kurono and M. Tokuda, *Synthesis*, 2681 (2002)
4. L. Zhu, R. M. Wehmeyer and R. D. Rieke, *J. Org. Chem.*, **56**, 1445 (1991).
5. S. Sibille, V. Ratovelomanana and J. Périchon, *J. Chem. Soc., Chem. Commun.*, 283 (1992).
6. C. Gosmini, Y. Rollin, J.-Y. Nédélec and J. Périchon, *J. Org. Chem.*, **65**, 6024 (2000).
7. H. Fillon, C. Gosmini, J.-Y. Nédélec and J. Périchon, *Tetrahedron Lett.*, **42**, 3843 (2001).
8. P. Knochel and P. Jones, Chap. 8 in *Organozinc Reagents, A Practical Approach* (Eds. L. M. Harwood and C. J. Moody), Oxford University Press, Oxford, 1999, p. 139.
9. S. Ishiguro, M. Miyauchi and K. Ozutumi, *J. Chem. Soc., Dalton Trans.*, 2035 (1990).
10. M. Tokuda, N. Mimura, T. Karasawa, H. Fujita and H. Suginome, *Tetrahedron Lett.*, **34**, 7607 (1993).
11. A. A. Jalil, N. Kurono and M. Tokuda, *Tetrahedron*, **58**, 7477 (2002).
12. M. Tokuda, N. Kurono and N. Mimura, *Chem. Lett.*, **12**, 1091 (1996).
13. R. D. Rieke, *Aldrichimica Acta*, **33**, 52 (2000).
14. N. Kurono, K. Sugita and M. Tokuda, *Tetrahedron*, **56**, 847 (2000).
15. N. Kurono, K. Sugita, S. Takasugi and M. Tokuda, *Tetrahedron*, **55**, 6097 (1999).
16. M. Tokuda, N. Kurono, S. Takasugi and A. A. Jalil, *Proceedings—Electrochemical Society*, 80 (2000).
17. S. Durandetti, S. Sibille and J. Périchon, *J. Org. Chem.*, **56**, 3255 (1991).
18. H. E. Simmons and R. D. Smith, *J. Am. Chem. Soc.*, **81**, 4256 (1959).
19. J. M. Paratian, E. Labbé, S. Sibille, J.-Y. Nédélec and J. Périchon, *J. Organomet. Chem.*, **487**, 61 (1995).
20. S. Sibille, S. Mcharek and J. Périchon, *Tetrahedron*, **45**, 1423 (1989).
21. C. Francèse, M. Tordeux and C. Wakselman, *J. Chem. Soc., Chem. Commun.*, 642 (1987).
22. J. M. Paratian, E. Labbé, S. Sibille, J.-Y. Nédélec and J. Périchon, *Denki Kagaku*, **62**, 1129 (1994) CAN 122:172562.
23. N. Zylber, J. Zylber, Y. Rollin, E. Duñach and J. Périchon, *J. Organomet. Chem.*, **444**, 1 (1993).
24. Y. Rollin, C. Gébéhenne, S. Dérien, E. Duñach and J. Périchon, *J. Organomet. Chem.*, **461**, 9 (1993).
25. Y. Rollin, S. Dérien, E. Duñach, C. Gébéhenne and J. Périchon, *Tetrahedron*, **49**, 7723 (1993).
26. C. Gosmini, Y. Rollin, J. Périchon, C. Wakselman, M. Tordeux and L. Marival, *Tetrahedron*, **53**, 6027 (1997).
27. J. F. Ruppert and J. D. White, *J. Org. Chem.*, **41**, 550 (1976).
28. C. Gosmini, Y. Rollin, C. Gébéhenne, E. Lojou, V. Ratovelomanana and J. Périchon, *Tetrahedron Lett.*, **35**, 5637 (1994).
29. E. Nakamura, S. Aoki, K. Sekiya, H. Oshino and I. Kuwajima, *J. Am. Chem. Soc.*, **109**, 8056 (1987)
30. J.-Y. Nédélec, J. Périchon and M. Troupel, in *Topics in Current Chemistry*, Vol. 185 (Ed. E. Steckhan), Springer-Verlag, Berlin, 1997, pp. 141–173.
31. O. Buriez, C. Cannes, J.-Y. Nédélec and J. Périchon, *J. Electroanal. Chem.*, **495**, 57 (2000).
32. O. Buriez, J.-Y. Nédélec and J. Périchon, *J. Electroanal. Chem.*, **506**, 162 (2001).
33. P. Gomes, C. Gosmini, J.-Y. Nédélec and J. Périchon, *Tetrahedron Lett.*, **41**, 3385 (2000).
34. E. Le Gall, C. Gosmini, J.-Y. Nédélec and J. Périchon, *Tetrahedron Lett.*, **42**, 267 (2001).
35. P. Gomes, C. Gosmini, J.-Y. Nédélec and J. Périchon, *Tetrahedron Lett.*, **43**, 5901 (2002).
36. P. Gomes, H. Fillon, C. Gosmini, E. Labbé and J. Périchon, *Tetrahedron*, **58**, 8417 (2002).

37. P. Gomes, C. Gosmini and J. Périchon, *J. Org. Chem.*, **68**, 1142 (2003).
38. P. Gomes, C. Gosmini and J. Périchon, *Tetrahedron*, **59**, 2999 (2003).
39. S. Sibille, V. Ratovelomanana, J. Y. Nédelec and J. Périchon, *Synlett*, 425 (1993).
40. C. Gosmini, S. Lasry, J. Y. Nédelec and J. Périchon, *Tetrahedron*, **54**, 1289 (1998).
41. C. Gosmini, J.-Y. Nédélec and J. Périchon, *Tetrahedron Lett.*, **38**, 1941 (1997).
42. X. Wu and R. D. Rieke, *J. Org. Chem.*, **60**, 6658 (1995).
43. M. Melhah, E. Labbé, J.-Y. Nédélec and J. Périchon, *New. J. Chem.*, **25**, 318 (2001).
44. T. A. Chen and R. D. Rieke, *J. Am. Chem. Soc.*, **114**, 10087 (1992).
45. M. Devaud and J. Périchon, unpublished results.
46. M. Durandetti, M. Devaud and J. Périchon, *New. J. Chem.*, **20**, 659 (1996).
47. P. Knochel and R. D. Singer, *Chem. Rev.*, **93**, 2117 (1993).
48. M. Melhah, E. Labbé, J.-Y. Nédélec and J. Périchon, *New. J. Chem.*, **26**, 207 (2002).
49. C. Gosmini, J.-Y. Nédélec and J. Périchon, *Tetrahedron Lett.*, **41**, 5039 (2000).
50. S. Seka, O. Buriez, J.-Y. Nédélec and J. Périchon, *Chem. Eur. J.*, **8**, 2534 (2002).
51. S. Seka, O. Buriez and J. Périchon, *Chem. Eur. J.*, **9**, 3597 (2003).
52. H. Fillon, C. Gosmini, J.-Y. Nédélec and J. Périchon, *Tetrahedron Lett.*, **42**, 3843 (2001).
53. H. Fillon, E. Le Gall, C. Gosmini and J. Périchon, *Tetrahedron Lett.*, **43**, 5941 (2002).
54. H. Fillon, C. Gosmini and J. Périchon, *J. Am. Chem. Soc.*, **125**, 3867 (2003).
55. I. Kazmiersky, C. Gosmini, J.-M. Paris and J. Périchon, *Tetrahedron Lett.*, **44**, 6417 (2003).
56. J. Périchon, C. Gosmini and H. Fillon, Patent Application 01/08880, France, July 4 (2001).
57. C. Cécile, M. Melhah, E. Labbé, J.-Y. Nédélec and J. Périchon, *New. J. Chem.*, **26**, 787 (2002).
58. E. Le Gall, C. Gosmini, J.-Y. Nédélec and J. Périchon, *Tetrahedron*, **57**, 1923 (2001).
59. C. K. Reddy and P. Knochel, *Angew. Chem., Int. Ed. Engl.*, **35**, 1700 (1996).
60. H. Fillon, C. Gosmini and J. Périchon, *Tetrahedron*, **59**, 8199 (2003).
61. P. Gomes, C. Gosmini and J. Périchon, *Synlett*, **10**, 1673 (2002).

CHAPTER **18**

The chemistry of zinc enolates

MARCO LOMBARDO and CLAUDIO TROMBINI

Department of Chemistry ''G. Ciamician'', University of Bologna, via Selmi 2, I-40126 Bologna, Italy
Fax: +39 051 209 9456; e-mail: claudio.trombini@unibo.it/marco.lombardo@unibo.it

I. GENERAL AND THEORETICAL ASPECTS

In this chapter the term 'zinc enolate' refers both to molecules like **A**, containing a carbon–zinc bond at the α position of an electron-withdrawing group, and to species **B** which contain an oxygen–zinc bond (Figure 1).

The chemistry of organozinc compounds
Edited by Z. Rappoport and I. Marek

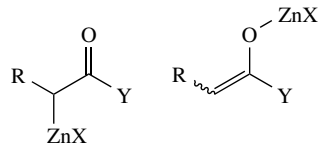

(A) **(B)**

Y = alkyl, alkoxy, dialkylamino, etc.

FIGURE 1

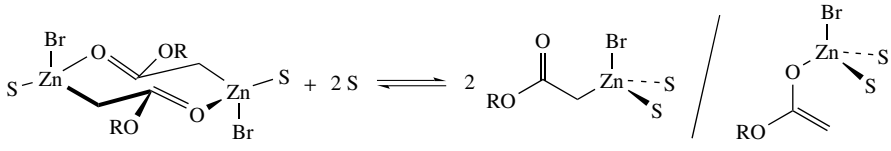

(C) **(D)** **(E)**

S = solvent

FIGURE 2

The most popular zinc enolates are the Reformatsky reagents, formally zinc enolates of esters, which have been the object of structural investigations[1]. NMR studies[2], EXAFS investigations in solution[3] and X-ray structure determinations in the solid state[4] indicate that the structures of the Reformatsky reagents are best represented by the dimeric species **C** and the monomeric *C*-metallated structure **D**, which are in equilibrium as shown in Figure 2. The equilibrium depends on solvent polarity.

On the other hand, the *O*-metallated structure **E** is also observed, for example when a zinc enolate is prepared by transmetallation of a lithium enolate with a Zn(II) salt[5].

Three approaches to zinc enolates are commonly adopted; the process associated to the classical Reformatsky reaction is based on the insertion of Zn(0) into the carbon−halogen bond of an α-haloester. Two additional routes involve (i) transmetallation of a lithium enolate with a Zn(II) salt (Section V.A) and (ii) the transition-metal-catalysed conjugate addition of diethylzinc to Michael acceptors (Section V.B).

Zinc enolates are exploited in a variety of synthetic applications where they are trapped by suitable electrophiles, particularly by carbonyl compounds.

The reaction profile of the addition of zinc enolates to model carbonyl compounds has been computed. The minimum energy reaction path for the addition of the Reformatsky derivative of ethyl bromoacetate to formaldehyde (MNDO implemented by the AMPAC program[6]) was calculated to correspond first to a rate-determining conversion of adduct **F**, deriving from the monomeric *C*-metallated species **D** and formaldehyde, into adduct **G**, followed by a fast [3,3]-sigmatropic shift to give the adduct **H** (Figure 3). An alternative transition state (TS) involving an adduct between the dimeric enolate **C** and two molecules of formaldehyde was also located, but was found to be higher by more than 15 kcal mol^{-1} with respect to the previous TS leading from **F** to **G**.

A successive refinement (MNDO-PM3) of the reaction of the Reformatsky derivative of methyl bromoacetate with both formaldehyde and methanimine was carried out including coordinated THF molecules. It identified a twist-boat transition structure as the most stable TS for the transformation of **G** into **H**[7].

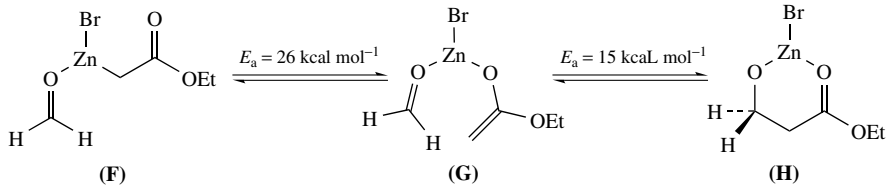

FIGURE 3

In this chapter attention will be focused on the different protocols recently developed to prepare zinc enolates, and on the most significant applications of these reactive intermediates in the field of organic synthesis.

II. THE REFORMATSKY REACTION

A. Introduction

Even though the first olefin–metal complex $K[PtCl_3(C_2H_4)]\bullet H_2O$[8] was reported by Wilhelm Christopher Zeise in 1827[9], the birth of organometallic chemistry is generally associated with the pioneering work of Edward Frankland, who first synthesized organozinc compounds (R_2Zn) by reacting alkyl halides with zinc metal[10]. The insertion of zinc metal into the carbon–halogen bond had found a second outstanding application in the XIX century in the Sergei Nikolaevich Reformatsky (1860–1934) work on α-haloesters **1**[11]. The classic Reformatsky reaction involves the addition of an α-halo ester **1** to a carbonyl compound in the presence of zinc metal to give β-hydroxy esters[12]; when azomethine derivatives are used as electrophiles, β-amino esters (the Gilman–Speeter reaction[13]) are obtained (equation 1).

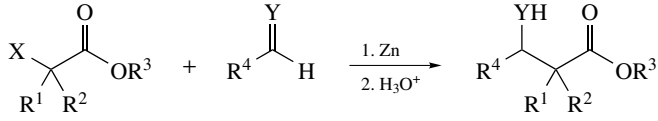

(1)

The Reformatsky reactions are run following two basic procedures: (i) a two-step Grignard-type protocol which first involves the formation of an organometallic zinc enolate derivative followed by addition of the electrophile, and (ii) a Barbier-type protocol where the bromoester and the electrophile are simultaneously exposed to the action of zinc metal.

In the typical old-fashioned Reformatsky protocol[12a–d], a mixture of α-bromoester, carbonyl compound and zinc powder is heated in a solvent, generally benzene, for several hours. Under these conditions, the chemical yields often suffer from the concurrence of side-reactions, such as self-condensation of enolizable aldehydes, Claisen condensation of bromoesters or crotonization of the Reformatsky products. However, ever since the outset of Reformatsky studies, chemists have been aware about the need to activate the zinc surface in order to get higher reaction rates and shorter induction times before the process starts, with lower by-product formation. Thus, it became common practice to

pre-activate the zinc metal with small amounts of an oxidizing agent ($HgCl_2$[14], iodine[15], 1,2-dibromoethane[16] etc.) or by cleaning the surface of the metal with HCl[17] or mineral acids[18]; the latter procedures must be completed by an abundant washing of the metal first with water, then with organic solvents, to completely remove all traces of acids and water.

To better compare modern protocols for the Reformatsky reactions, hereinafter discussed in this section, it is interesting to read, as an example, the experimental procedure reported by R. B. Woodward and coworkers in 1956 for the synthesis of the Lysergic acid precursor **3** (equation 2)[14]. The procedure adopted was a Barbier-like protocol, involving the addition of Zn and of methyl bromoacetate (**1a**) in three portions to a solution of **2** in hot benzene.

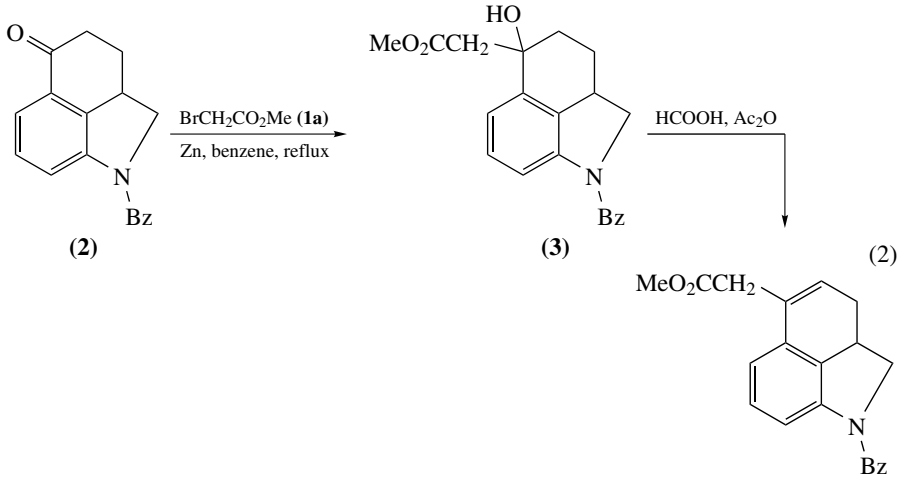

(2)

We read in the experimental section: '*A mixture of 300 g of 1-benzoyl-5-keto-1,2,2a,3,4,5-hexahydrobenz[cd]indole (***2***), 300 g of activated zinc, 1.0 g of mercuric chloride, 6 L of dry benzene and 90 g of methyl bromoacetate (* **1a***) was prepared in a 12 L, 3-neck flask fitted with a stirrer, reflux condenser and heating mantle. The mixture was heated under reflux and stirred, and after an induction period of 10–30 minutes the reaction started, and the solution became cloudy. After 3.5 hours 90 g of methyl bromoacetate and 20 g of zinc were added, and after five hours, 75 g of the bromoester and 60 g of zinc were added. Refluxing and stirring were maintained for a total of six hours, after which the reaction mix was allowed to cool and stand overnight*'.

Section II.B will go through recent achievements on the Reformatsky reaction, with reference to:

(i) new physical and chemical techniques for metal activation[19];

(ii) new halogenated substrates, (α-haloketones[20], α-halonitriles[21], α-halonitro derivatives[22] etc.);

(iii) new reaction conditions (metals alternative to zinc, technical solutions such as continuous flow reactors which limit side-product formation[23], solvent-free conditions[24] etc.), including a wide choice of solvents such as diethyl ether, THF, 1,4-dioxane, dimethoxymethane, acetonitrile, DMF, DMSO, HMPTA, ionic liquids[25] and water[26].

B. Activation Techniques for Zinc Metal

Whenever metallic zinc is to be used in oxidative addition processes, results are affected by the metal surface activity. Two strategies for the production of active zinc metal surfaces can be adopted: (i) chemical or physical activation of commercial zinc powders, or (ii) *in situ* production of highly reactive metal powders by reduction of a zinc salt with a suitable reducing agent.

1. Chemical or physical activation of commercial zinc powders

When zinc is exposed to air at 25 °C, a film of zinc oxide (thickness may range from 5 to 20 Å) is rapidly formed, as confirmed by Auger electron spectroscopy[27]. Thus, when commercial zinc powder is used, grain size and purity are not the only factors limiting the available reactive surface area, but ageing and storage conditions play a fundamental role in determining metal reactivity, too. Since the active metal atoms which start the reaction (defects of the metal surface such as edges, corners and dislocations where not fully coordinated zinc atoms are present) can be partially covered by a passivated layer, surface pre-treatment by physical or chemical methods is a crucial step. Acidic cleaning may be simply achieved by adding to the suspension of the metal in an ethereal solvent a small amount (1–2%) of trimethylsilyl chloride (TMSCl)[27] (which, if not immediately purified before use, always contains traces of 'anhydrous' HCl[28]) or of trifluoroacetic acid (TFA)[29]. The addition of $BF_3 \bullet Et_2O$ to a stirred suspension of bromoester, aliphatic aldehyde and Zn in wet THF (2% H_2O) has been also reported to afford excellent yields of the expected adducts, while benzoyl hydroperoxide is required as supplementary activator in the case of aromatic aldehydes under aqueous conditions[30]. Ammonium chloride works too, and with this metal activator a solvent-free solid-phase Reformatsky reaction has been developed by grinding in a mortar an aromatic ketone, ethyl bromoacetate, zinc powder and NH_4Cl and keeping the mixture at room temperature for 2–3 h. Yields in the 83–99% range were reported[31].

An alternative strategy to improve the efficiency of Reformatsky reactions makes use of freshly prepared metal couples, particularly the Zn–Cu couple[32] and the Zn–Ag couple[33] in THF as solvent.

Sonochemistry offers an important physical tool for metal activation: when an intense ultrasonic wave propagates in a medium, the liquid phase can be torn apart leaving small bubbles (cavitation) filled with vapour and gas. During the compression/decompression cycles of the propagating wave, bubbles grow during decompression and contract, or even implode, during the compression phase, to give hot spots of high temperature (thousands of degrees) and pressure (hundreds of bars). When the cavitational implosive collapse takes place close to a liquid–solid interface an important erosion ensues, likely promoted by particle–particle collisions associated to shockwaves and turbulent flow due to cavitation.

Changes in particle morphology are observed by SEM microscopy, and zinc activation is thought to take place via formation of a high concentration of active metal sites[34]. The solvent of choice for ultrasound-promoted Reformatsky reactions is 1,4-dioxane; reaction rates increase dramatically using normal sonicators[35] or, better, high intensity ultrasonic (HIU) processors working at 20 KHz and 600 W[34,36]. Under HIU irradiation, the cage dione **4** effectively reacted with ethyl bromoacetate (**1b**) and ethyl bromodifluoroacetate (**1c**) to give adducts **5a** and **5b** (equation 3)[37]. In a further example, **1b** and **1c** efficiently react with sym-(keto)dibenzo-16-crown-5 (**6**) under the same experimental conditions to give **7a** and **7b**[38] (equation 4). As a further example of HIU-promoted reaction, fully aromatic Schiff bases have been reported to react with ethyl 2-bromo-2-methylpropanoate

(**1d**) in the presence of unactivated zinc in dioxane at 20 °C in 5 min, to give β-aminoesters or β-lactams in 80–95%[39] (see Section III).

(3)

(4) **(1b)** R = H **(5a)** 75%
(1c) R = F **(5b)** 89%

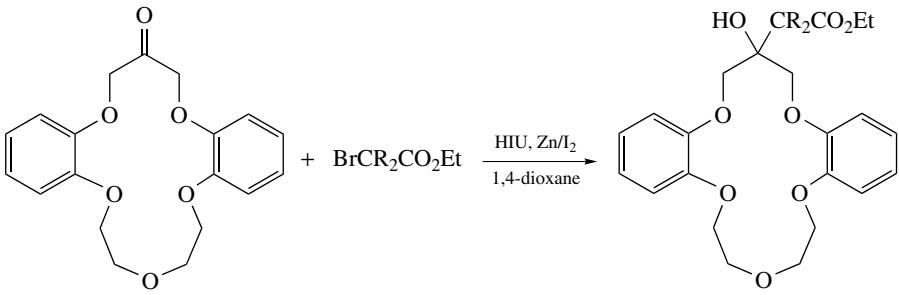

(6) **(1b)** R = H **(7a)** 79%
(1c) R = F **(7b)** 85% (4)

Microwave dielectric heating is a further tool in the hands of synthetic chemists to speed up chemical reactions[40]. From a qualitative point of view, the larger the dielectric constant of a molecule, the greater is its interaction with microwaves; thus, chemicals participating in a reaction do not interact equally with microwaves and selective and fast heating may be achieved. Microwave-assisted solid-state reactions have been the object of several studies: there are examples in which a microwave active reagent is supported on an inactive or poorly active material (e.g. silica, alumina), others in which inactive reagents are supported on an active material. When metal powders are exposed to microwave fields (2450 MHz, 650 W), hot spots up to 1000 °C are rapidly created with a heating rate up to 100 °C s^{-1}; under these conditions, reaction rates significantly increase[41]. For example, a microwave-promoted Reformatsky reaction may be efficiently carried out in the solid state by irradiation of a mixture of activated zinc metal powder, solid NH_4Cl, ethyl bromoacetate (**1b**) and a carbonyl compound in the absence of solvent[42].

2. Preparation of highly reactive forms of zinc metal

Rieke reported in the early 1970s the preparation of highly reactive metal forms by the reduction of metal halides with alkali metals[19]. In the original work, anhydrous $ZnBr_2$ in dry THF was refluxed for 4 h with potassium affording a finely divided slurry of an air-sensitive reactive metal, denoted as Zn* (equation 5)[43].

$$ZnBr_2 + 2\ K \longrightarrow Zn^* + 2\ KBr \quad (5)$$

In the early 1980s, an analogous route to active metals in the form of highly dispersed metals on the graphite surface (M-Gr) was developed. To get M-Gr, the required metal halide (MX_n) was reacted with the graphite lamellar compound potassium-graphite (C_8K) in THF under argon, according to equation 6[44]. Zn-Gr, prepared by the C_8K reduction of $ZnCl_2$, found excellent application in Reformatsky reactions at 0 °C and in Barbier allylations at 20 °C[45].

$$MX_n + n\,C_8K \longrightarrow M\text{-}Gr + n\,KX \qquad (6)$$

Even more reactive was then found to be Zn/Ag-Gr, prepared by the reduction of a $ZnCl_2$/AgOAc mixture (0.1 molar ratio) with C_8K; with this powder Reformatsky reactions could be run at −78 °C[12f,46].

A number of alternative reduction procedures of $ZnCl_2$ are nowadays available, for example using Na naphthalenide in THF[47], Li in dry glyme in the presence of a catalytic amount of naphthalene as electron carrier[48], Na in THF containing liquid NH_3 (10–20% v/v)[49], or high surface alkali metals deposited on various supports such as NaCl, glass powder and polymers (PE, PP and PS/DVB)[50]. Reduction of $Zn(CN)_2$ by means of Li naphthalenide[51] was claimed to afford an even more reactive Zn* species. Ultrasounds accelerate these reductions; a specimen of Zn* powder produced in 40 min at room temperature using Li and ultrasounds displayed the same reactivity in Reformatsky reactions of Zn* produced in refluxing THF for 4 h using K[52].

Electrochemistry offers alternative routes to the preparation of active zinc for the Reformatsky reactions, for instance exploiting the cathodic reduction (−0.8 V *vs* SCE) of $ZnBr_2$ in acetonitrile containing $Bu_4N^+BF_4^-$ as supporting electrolyte[53].

More recently, a pulsed sonoelectrochemical technique was developed to produce a suspension of fine Zn* powder which can be directly used in Reformatsky reactions; $ZnCl_2$ and NH_4Cl (supporting electrolyte) in diluted HCl are subjected to a pulsed electrical current (current density = 10^4 Am^{-2}; pulse duration = 300 ms) and to ultrasound for 1 h[54].

3. Electrochemical Reformatsky reaction promoted by sacrificial anodes

Carbon−carbon bond-forming reactions based on the electrochemical reduction of organic halides in aprotic solvents in the presence of electrophiles became, in the last two decades, standard procedures in electroorganic synthesis[55]. Three examples of electrochemically promoted Reformatsky reactions using sacrificial zinc anodes will be discussed. In the first study, ethyl 2-bromo-2-methylpropanoate (**1d**) was electrolysed in DMF containing Bu_4NBr as supporting electrolyte and succinic anhydride as the electrophile. The mechanism is shown in Figure 4. The zinc anode frees Zn^{2+} ions into the solution, while at the cathode **1d**, the most easily reducible species present in solution, is reduced to a formal enolate **8**; recombination of **8** with Zn^{2+} affords a zinc enolate which eventually adds to succinic anhydride[56].

The authors observed that the applied quantity of electricity (0.2–0.5 F) was always lower than the expected quantity on the basis of Zn consumed (1 g atom). This difference reflects the concurrence of two processes at the anode surface, where the electrochemically promoted reaction (Figure 4) coexists with a classic zinc metal-promoted Reformatsky reaction. Indeed, the electrochemical process produces at the working anode a perfectly clean zinc metal surface, very reactive towards the α-bromoester.

In the second study, the electrochemically promoted Reformatsky reaction is carried out by electrolysing a DMF solution of Bu_4NBr, $ZnBr_2$ (catalytic), $Ni(bipy)_3(BF_4)_2$ (catalytic),

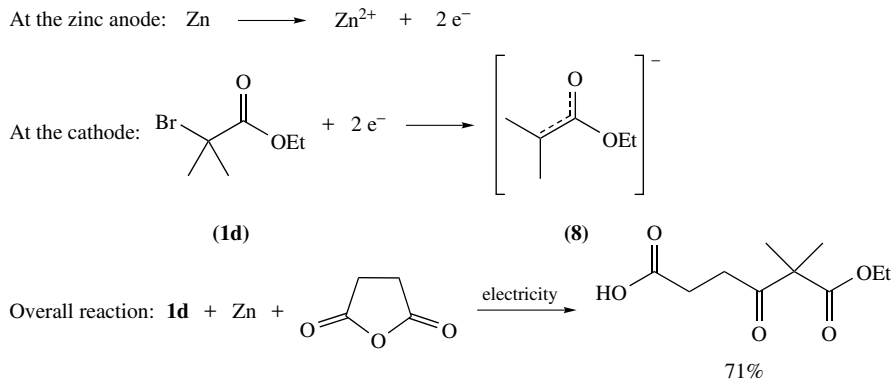

FIGURE 4

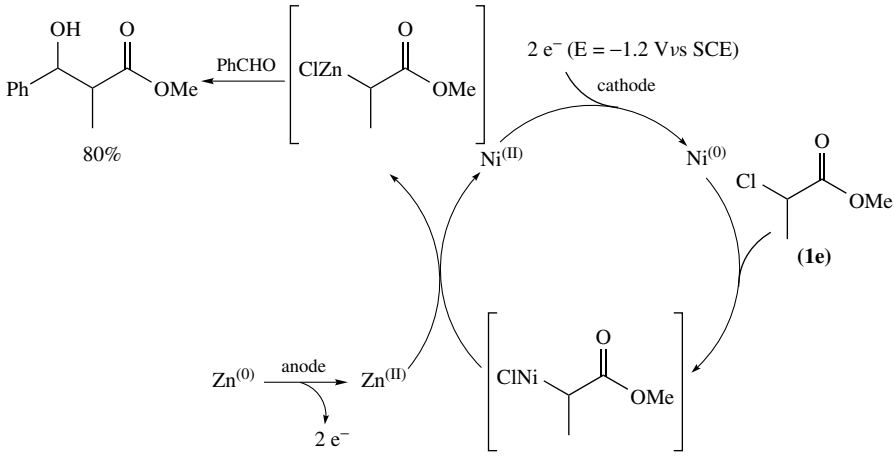

FIGURE 5

containing either a α-chloroester or α-chloronitrile or methyl α,α-dichloroacetate and an aldehyde or ketone. In this solution, $Ni(bipy)_3(BF_4)_2$ is the most readily reducible species and the overall reaction mechanism may be described by the catalytic cycle depicted in Figure 5. A Ni(0) species adds oxidatively to α-chloropropanoate (**1e**) to give a Ni(II) enolate-type complex which undergoes transmetallation by $ZnBr_2$ affording the usual Reformatsky enolate[57].

An analogous non-electrochemical Ni(0)-catalysed process, exploited in a Mannich/Reformatsky multicomponent process[58], will be discussed in Section III (equation 41). In the third study, the α-bromoester **1d** is simply electrolysed in the presence of a carbonyl compound in DMF/THF in a 1:2 ratio using both indium and zinc rods as sacrificial anodes. While aldehydes afford the expected 3-hydroxyesters in high yield, aliphatic, aromatic and cyclic ketones, with the exception of acetone, directly afford β-lactones,

again in very good yields. Similar results are obtained by running classical Reformatsky experiments using zinc and indium powder (equation 7)[59].

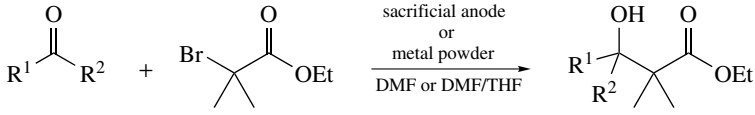

(1d)

favoured when $R^2 = H$

+

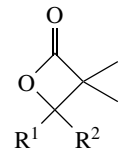

favoured when $R^2 \neq H$ (7)

4. Alternative metals for the Reformatsky reaction

A number of low-valent or zero-valent metals are able to promote Reformatsky-type reactions of α-bromoesters with carbonyl compounds and related electrophiles[60]. Starting with calcium and moving rightward along the fourth row of the periodic table, the following metal species have been reported to promote Reformatsky-type reactions:

(i) Ca atom–THF co-condensates[61].
(ii) $TiCl_2$/Cu or $TiCl_2$/NaI[62], Cp_2TiCl_2/Mn[63].
(iii) $[V_2Cl_3(THF)_6]_2$ $[Zn_2Cl_6]$[64].
(iv) $CrCl_2$/LiI[65]. With this metal, chiral non-racemic α-bromoacetyl oxazolidinone **9a** reacts with 2-methylpropanal to give adduct **10a** in high yield and diastereofacial selectivity[65d] (equation 8).

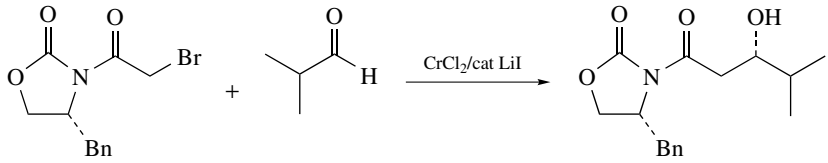

(9a) **(10a)** 91%, 92% d.e. (8)

(v) Mn/TMSCl (cat) or Mn/Et_2AlCl (cat)[66], Mn/$ZnCl_2$ (cat)[67], Li_2MnCl_4/Mg[68], Rieke-Mn*[69].
(vi) $FeBr_2$/bipy, Fe sacrificial anode[70].
(vii) $Co(PMe_3)_4$ or $Co(PPh_3)_4$[71].
(viii) GeI_2/K. With Rieke Ge*, optically active oxazolidinone **9b** affords *syn* adduct **10b** in high facial diastereoselectivity, as shown in equation 9[72].

Among fifth-row metals, a Reformatsky-type reaction of trichloronitromethane with aldehydes has been documented to be promoted by $SnCl_2$[22]. Furthermore, indium thrived

in the 1990s as one of the most appealing alternatives for zinc, mainly in Barbier and Reformatsky reactions[73].

'Exotic' metals of the sixth row have been also reported to promote Reformatsky reactions: for example Rieke-barium[74], which reacts efficiently with α-chloroketones, low-valent tantalum[75] prepared from $TaCl_5$ and Zn(0), and low-valent bismuth[76] prepared from $BiCl_3$ and Al(0), which works in water as solvent.

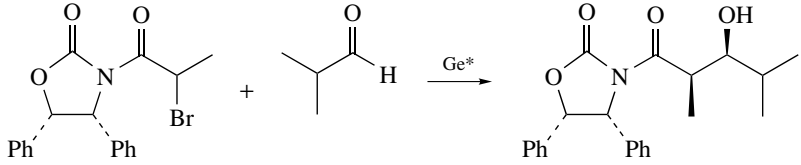

(9)

(9b) **(10b)** 79%, 92% d.e.

At last, among lanthanides, SmI_2 emerged as a powerful promoter of Reformatsky reactions. Two examples are reported here: (i) the addition of chiral non-racemic α-bromoacetyl-2-oxazolidinones **9a,c–f** to prochiral aldehydes takes place in high yield and high diastereoselectivity (d.e. up to 99%) (equation 10)[77]; (ii) the addition of optically active α-bromo-α'-sulphinyl ketone **11** to aldehydes affords *syn*-adducts **12** with a good control of simple diastereoselectivity and high facial selectivity, as shown in equation 11[78].

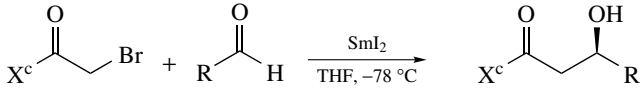

(9a, c–f) 60–95%, 64–99% d.e.

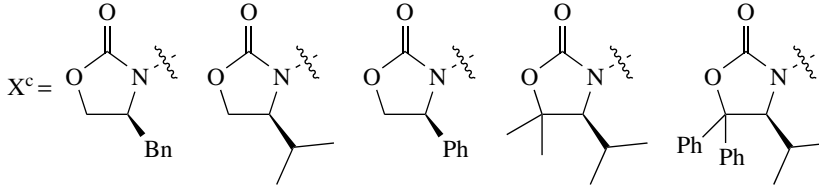

(10)

(9a) **(9c)** **(9d)** **(9e)** **(9f)**

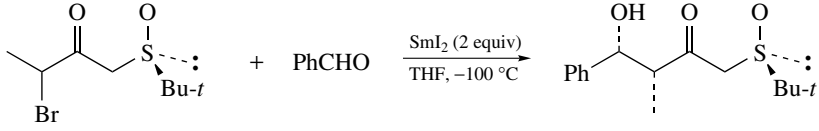

(11) **(12)** 61%, 43% d.e. (11)

Even more interesting turned out to be the SmI_2-promoted intramolecular Reformatsky reaction. It opens a route to medium and large ring systems, as shown by the examples reported in Table 1[79a–e].

TABLE 1. Examples of medium/large ring construction via the SmI_2-promoted intramolecular Reformatsky-type reaction (the new C−C bond is highlighted by the disconnection curve)

Starting material	Reformatsky adduct	Reference
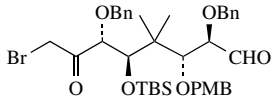	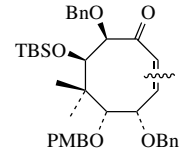	79a
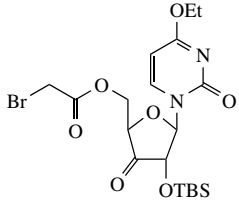	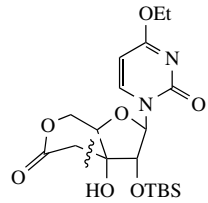	79b
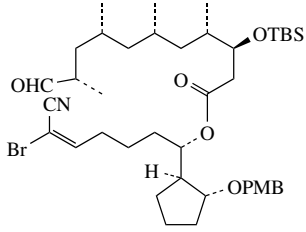	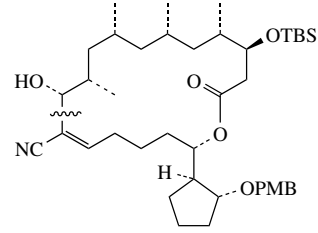	79c
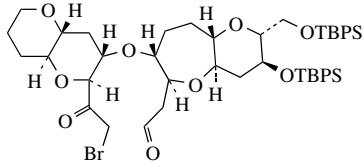	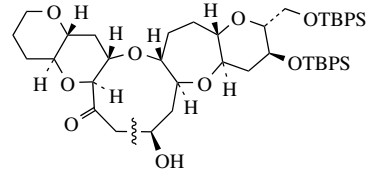	79d
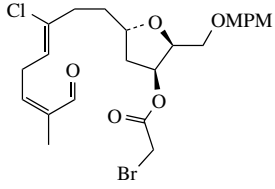	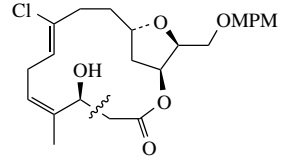	79e

However, a major drawback in the use of a stoichiometric amount of SmI_2 is associated with its cost; to overcome this limitation, a catalytic protocol has been proposed. A Reformatsky reaction can be run with catalytic quantities of SmI_2 if a second metal, able to regenerate Sm(II), is present. An alloy of light lanthanides, called mischmetall, cheaper than samarium and able to quickly reduce Sm(III) to Sm(II), was found to play the role of the required stoichiometric reducing agent, thus improving the economy and the development of samarium chemistry[80].

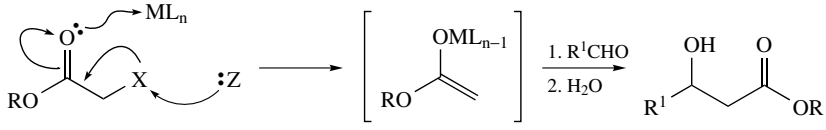

Examples:	X = I	$Z = I^-$	$ML_n = TiI_4$
	X = I	Z = LiI	$ML_n = Bu_2SnI_2$
	X = Br	$Z = Ph_3P$	$ML_n = GeCl_4$
	X = Br	$Z = (o\text{-Tol})_3P$	$ML_n = TiCl_4$

FIGURE 6

For the sake of completion, besides metals in low oxidation state, a Reformatsky-like reaction between an α-bromoester (or α-bromoketone) and an aldehyde may also be promoted by a halophilic agent Z, such as iodide ion[81, 82], Ph_3P[83] or $(o\text{-Tol})_3P$[84] combined with a suitable Lewis acid ML_n. The concerted interaction of the Lewis acid with the carbonyl oxygen atom and the S_N2-type attack of the halophilic species on the α-halogen atom leads to the formation of an intermediate metal enolate; examples are shown in Figure 6.

C. Recent Applications of the Reformatsky Reaction

1. Racemic reactions

In order to testify to the versatility of the Reformatsky reaction, two examples of three-component processes are presented: the synthesis of 3-aryl-4,4-dimethyl-2-oxaspiro[5.5] undecane-1,5-diones **14**[85] (equation 12), and the coupling of two molecules of methyl 2-bromo-2-methyl propanoate (**1f**) with an oxoaryl acetaldehyde **15** to afford 3a-aryl-3,3,6,6-tetramethyl-tetrahydrofuro[3,2-b]furan-2,5-dione **16**[86] (equation 13).

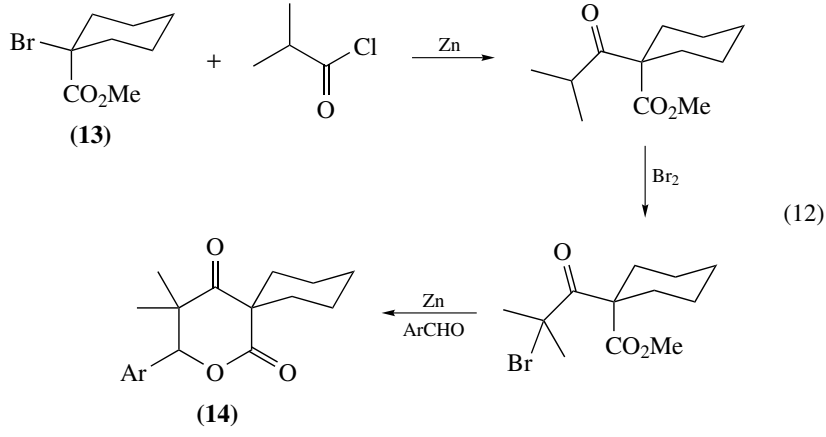

(12)

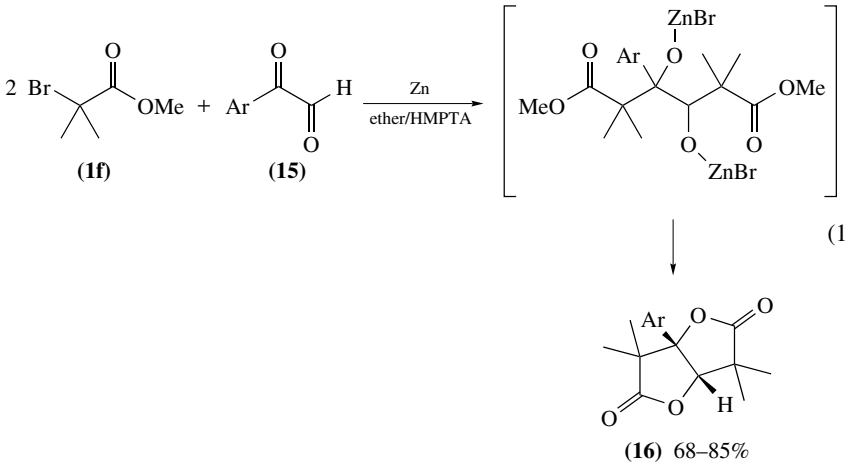

(1f) **(15)** **(16)** 68–85%

(13)

The great impact exerted on bioactive molecules by the selective introduction of fluorine atoms[87] prompted the flourishing of a variety of fluorination techniques in the last two decades[88]. Reformatsky reagents deriving from α,α-difluoro-α-bromoesters were recognized as efficient fluorinated nucleophilic synthons for the introduction of a CF_2 group into a target molecule[88]. Recent applications of α,α-difluoro-α-bromoesters are reported in perfumery chemistry for the synthesis of terpene-derived 1,3-ketoamide **17** (equation 14)[89], in insecticide chemistry for the synthesis of nornicotines **18** (equation 15)[90] and in bioorganic chemistry for the synthesis of 1,1-difluoroalkenes **19**, used as isosters of the carbonyl group in peptidomimetics (equation 16)[91].

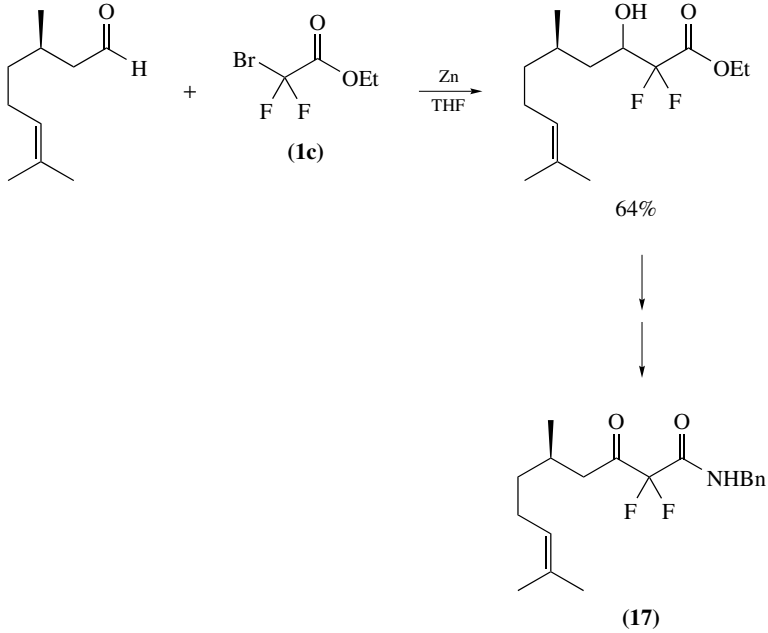

(1c) **(17)**

(14)

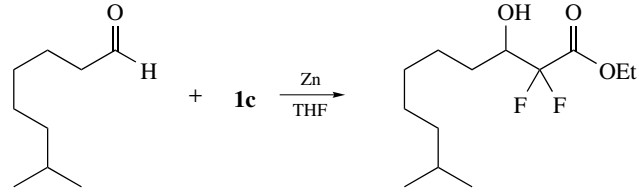

91%

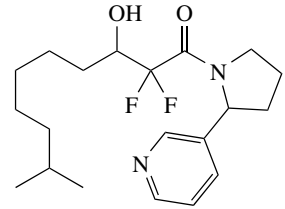

(18) (15)

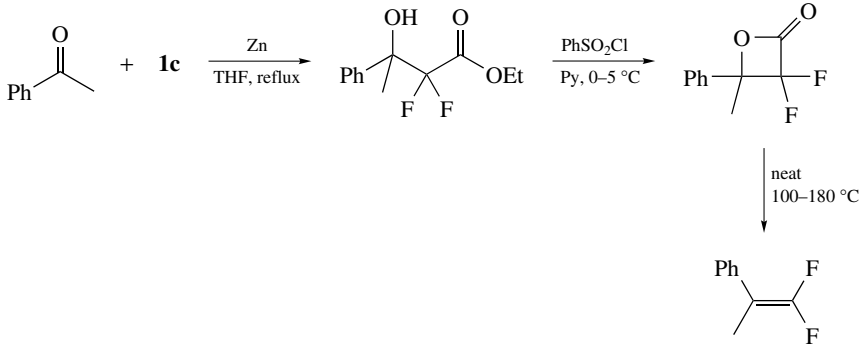

(19) (16)

Further fluorinated synthons **20** (equation 17)[92] and **21** lead to Reformatsky intermediates which are synthetic equivalents of a formal 4,4-difluoroacetoacetate dianion and of a carbalkoxy trifluoromethyl carbene, respectively. The latter has been exploited in a synthesis of *E*-**22** and *Z*-**22**, both inhibitors of GABA aminotransferase (equation 18)[93].

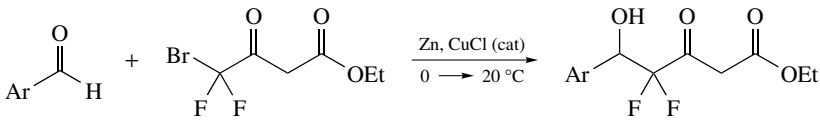

(20) 80–90% (17)

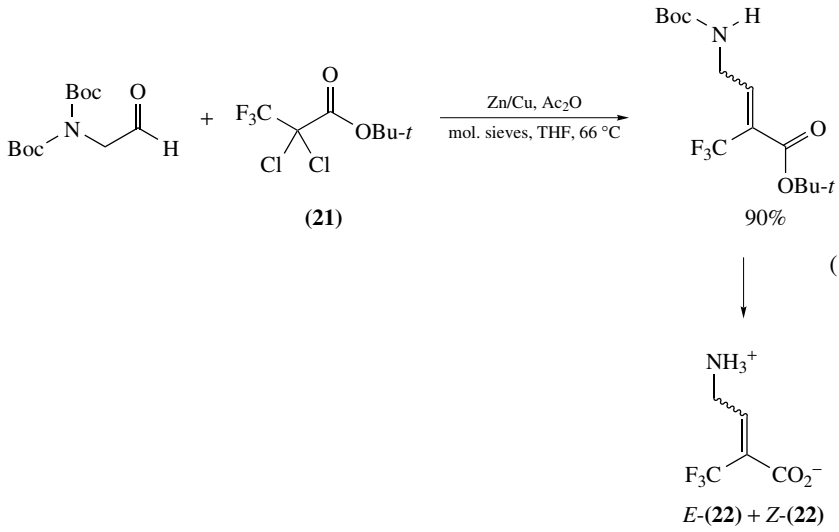

(**21**) 90%

(18)

E-(**22**) + *Z*-(**22**)

On the way to fluorinated target molecules, a CF_2 group may be also incorporated in the ketone framework; in this case drastic conditions are required to promote the Reformatsky reaction with ethyl bromoacetate (**1b**). The example reported in equation 19 was carried out on 100 g scale and was directed to the synthesis of a fluoro analogue **23** of the anticancer drug chlorambucil[94].

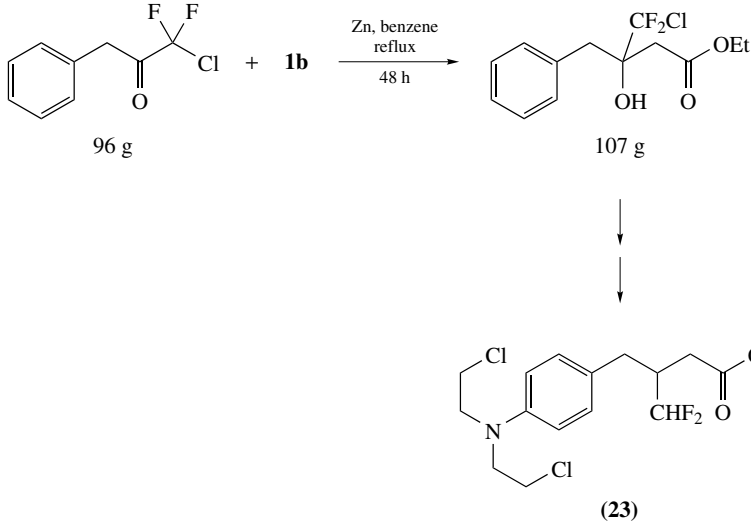

96 g 107 g

(19)

(**23**)

2. Enantioselective reactions

One of the most effective catalytic asymmetric carbon−carbon bond-forming reactions developed in the last decades is represented by the addition of dialkylzinc derivatives

R_2Zn to carbonyl compounds. This reaction is exceptionally sluggish, but, when a suitable protic or aprotic chiral ligand L^* is added to the reaction mixture in catalytic amount, a new species $RZnL^*$ is formed which may display an outstanding higher reactivity, accompanied by a high control of absolute stereochemistry[95]. We refer in this reaction to ligand accelerated catalysis, of paramount interest from an economic point of view, which is made possible in this case by the very low reactivity of R_2Zn with aldehydes. Unfortunately, Reformatsky reagents display a remarkable reactivity towards aldehydes and, as a consequence, asymmetric versions of the Reformatsky reaction developed so far require the use of substoichiometric amounts of chiral ligands ($\geqslant$25% with respect to the haloester), only partially enjoying the effect of ligand acceleration on reaction kinetics. Of course, the addition of the enantiopure ligand generates a chiral Reformatsky reagent whose diastereotopic faces partially discriminate between the enantiotopic faces of a prochiral carbonyl compound. Recent examples of enantioselective Reformatsky reactions promoted by chiral aminoalcohols are collected in Table 2[96a–i].

The most promising results are offered by trifluoromethyl aminoalcohols as chiral ligands (entry 10). Cinchona alkaloids in the presence of pyridine (entry 7) and cinchona-derived surfactants (entry 6), which provide an asymmetric micellar microenvironment in aqueous solvents, are also worthy of note.

3. Diastereoselective reactions

A main drawback of the Reformatsky reaction resides in the poor control of simple diastereoselectivity, resulting in variable ratios of *syn* and *anti* β-hydroxyesters (equation 20)[12f,g].

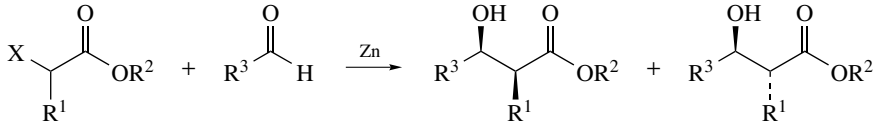

(1) (20)

Slightly better results have been recorded in Reformatsky reactions promoted by different metals and, to this purpose, the reader is directed to Section II.B.4 and references therein. For example, *anti*-selective reactions are reported using chromium[65c] and titanocene(III) enolates[63], while germanium[72], cobalt[71e] and titanium[62] enolates display a remarkable *syn*-stereopreference.

Conversely, acceptable or excellent levels of π-facial diastereoselectivity are obtained in Reformatsky reactions involving a chiral non racemic haloderivative.

An example of a sugar-derived chiral α-haloketone is offered by **24**. When ulosyl bromide **24** is coupled to acetaldehyde in a Grignard-type process, a mixture of isomeric adducts is formed, where the 50% is represented by **25**, possessing the (*R*) configuration at the hydroxyethyl substituent (equation 21). The same protocol is applied in an efficient nucleophilic *C*-glycosidation reaction of **24** with galactose-derived aldehyde **26** to give **27** (equation 22)[20].

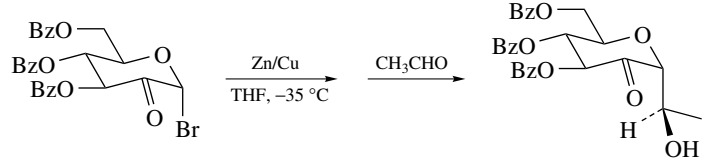

(24) **(25)** 50% (21)

TABLE 2. Chiral ligand-promoted enantioselective Reformatsky reactions

Entry	Chiral ligand L*	Halo-derivative **1** (Solvent, *T*)	RCOR′ (L*/**1**/RCOR′)	e.e % (configuration)	Reference
1	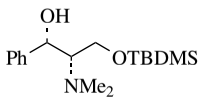	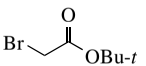 **(1g)** (THF, 0 °C)	PhCHO (1:3:1)	65 % (*S*)	96a
2	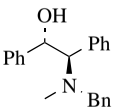	**1b** (THF, reflux)	PhCHO (1:3:1)	65 % (*S*)	96b
3	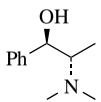	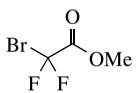 **(1h)** (THF, 0 °C)	PhCHO (2:3:1)	84 % (*S*)	96c
4	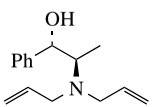	**1g** (THF, toluene, 0 °C)	$PhCOCH_3$	74 % (*S*)	96d
5	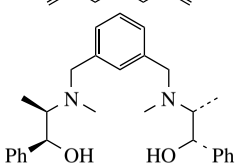	**1g** THF, 0 °C) (1:3:1)	PhCHO (1:6:2)	80 % (*R*)	96e

(*continued overleaf*)

TABLE 2. (*continued*)

Entry	Chiral ligand L*	Haloderivative **1** (Solvent, *T*)	RCOR′ (L*/**1**/RCOR′)	e.e % (configuration)	Reference
6	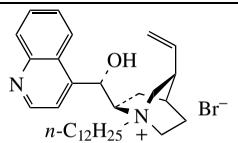	**1g** (H_2O/THF 1:8, 0 °C)	PhCHO (1:4:1)	34 % (*S*)	96f
7	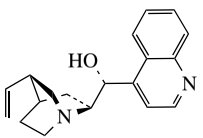	**1g** (THF, pyridine, 0 °C)	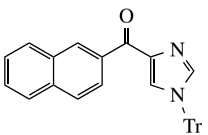 (1.5:4:1)	66 % (*R*)	96g
8	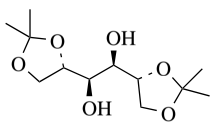	**1b** (THF, reflux)	PhCHO (1:3:1)	30 % (*R*)	96h
9	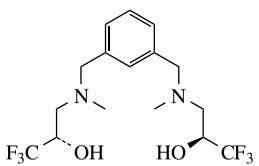	**1b** (THF, reflux)	PhCHO (1:5:2)	68 % (−)	96i
10	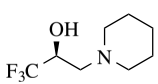	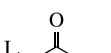 **(1i)** (THF, 20 °C)	PhCHO (3:5:2)	90 % (−)	96i

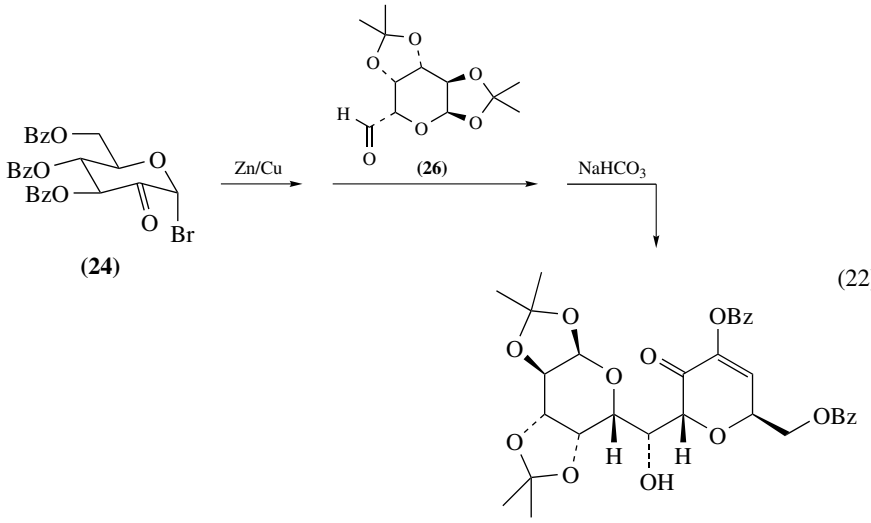

(24)

(22)

(27) 73%, 80% d.e.

Chemists from the Sankyo Co. reported the use of 6-bromopenicillanate **28**, easily obtained from 6-aminopenicillanic acid, in a multistep synthesis of (3*R*,4*R*)-4-acetoxy-3-[(*R*)-1′-((*t*-butyldimethylsilyl)oxy)ethyl]-2-azetidinone (**31**)[97], a pivotal intermediate for the synthesis of 1-β-methyl carbapenem antibiotics (equation 23)[98]. After cleavage of the thiazolidine ring of **28** with trimethyloxonium tetrafluoroborate, the intermediate **29** was subjected to a Reformatsky condensation with acetaldehyde, catalysed by diethylaluminium chloride. The 8-(*S*) stereocentre in **30**, formed in 50% d.e., was inverted under Mitsunobo conditions to approach the target molecule **31**.

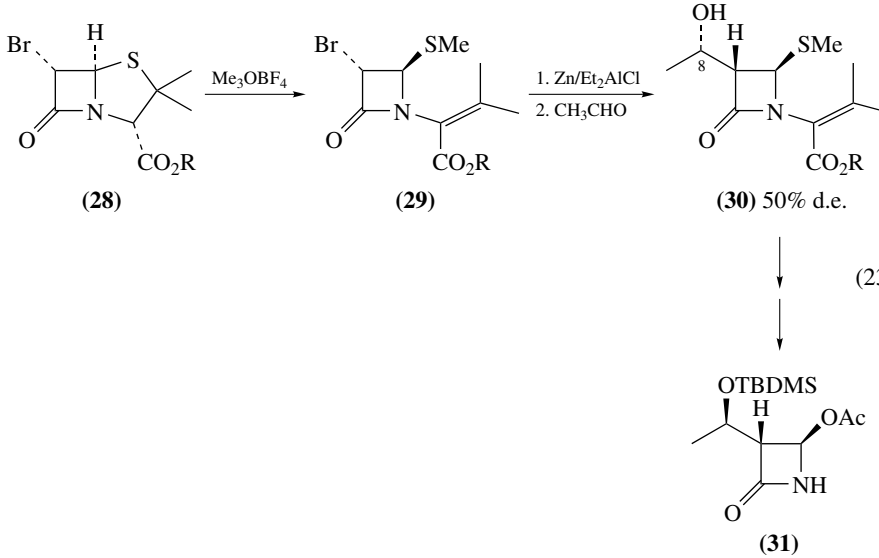

(28) (29) **(30)** 50% d.e.

(23)

(31)

Considerable efforts have been addressed to the use of chiral non-racemic carbonyl compounds in π-face diastereodifferentiating Reformatsky reactions.

L-Glyceraldehyde acetonide (**32**), a classical reference material for testing diastereofacial selectivity in organometallic nucleophilic additions[99], reacts with ethyl bromodifluoroacetate (**1c**) to give the *anti* adduct **33**, as expected on the basis of the most commonly observed stereochemical trends in the addition of organometallic reagents to **32**[99].

Adduct **33** has been exploited in the synthesis of the antiretroviral agent **34**[100] (equation 24), while *ent*-**33**, obtained from D-glyceraldehyde acetonide (*ent*-**32**), was converted into **35**, a fluoro analogue of 2-deoxyribonolactone, a DNA lesion product[101] (equation 25).

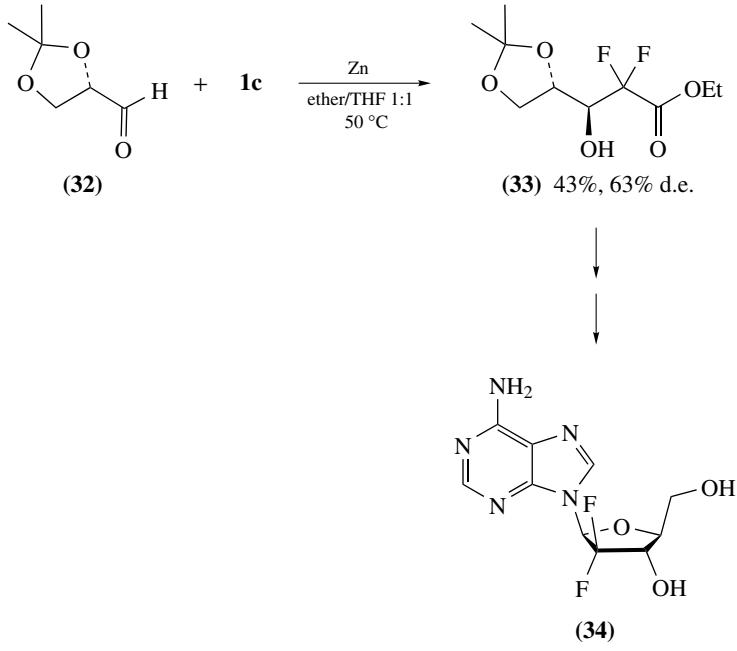

(32) **(33)** 43%, 63% d.e. **(34)** (24)

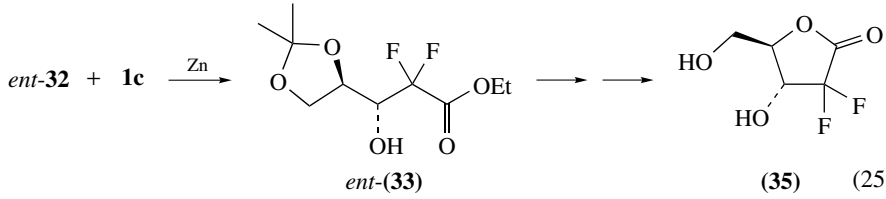

ent-(**33**) **(35)** (25)

A synthesis of a higher sugar, 2-deoxy-4-octulose, has been carried out using, as the key step, the Reformatsky reaction of methyl bromoacetate (**1a**) with the β-D-arabino-hexos-2-ulopyranose derivative **36**, which affords the manno-derivative **37** in good d.e. (equation 26)[102]. The same authors developed analogous diastereoselective syntheses of 4-octulose derivatives, centred on the use of bromoacetonitrile, either in the presence of Zn/Cu couple in dioxane or in the presence of indium powder and TMSCl in THF[21b].

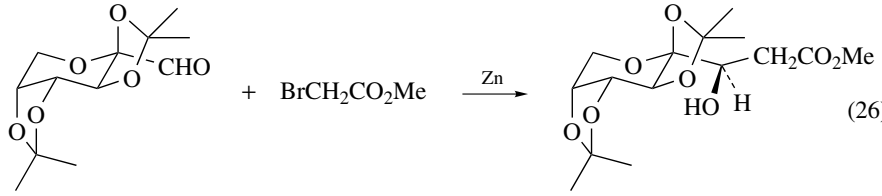

(36) **(1a)** **(37)** 82% d.e. (26)

Working on sugar structures, facial diastereoselectivity is likely to approach 100% if the carbonyl unit is part of a ring, thus taking advantage of conformational rigidity. Indeed, ketosugar **38** reacts with **1b** to give adduct **39** as a single product (equation 27)[103].

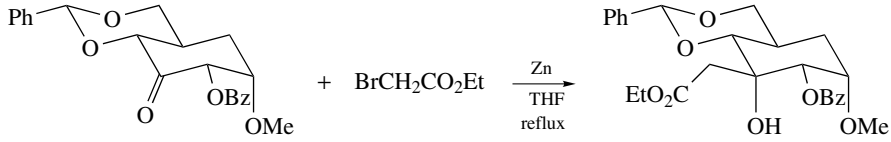

(38) **(1b)** **(39)** single product (27)

In a short synthesis of L-4,4-difluoroglutamic acid, the serinal-protected derivative **40** reacts with both **1b** and **1c** in THF at room temperature to give the adduct **41** and **42**, respectively, in a fairly high *anti*-stereoselectivity (equation 28)[104].

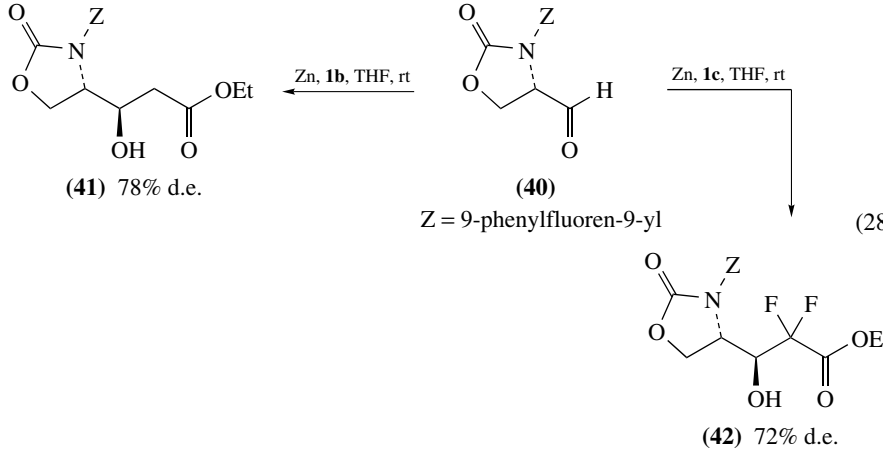

(41) 78% d.e. **(40)**
Z = 9-phenylfluoren-9-yl (28)
(42) 72% d.e.

Attachment of a side carbon chain at C-7 of abietic acid has been carried out via Reformatsky reaction of ketone **43** with zinc and **1b** (equation 29)[105].

On the way to prepare metabolites of equine norethandrolone, a Reformatsky reaction has been applied to epiandrosterone acetate **44** in refluxing benzene; the authors succeeded

in the not easy task of forcing **1b** to react with the sterically congested carbonyl group of the 17-ketosteroid **44** (equation 30)[106].

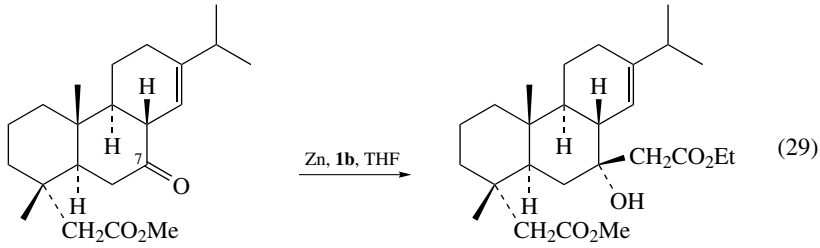

(29)

(43) 81%, 65% d.e.

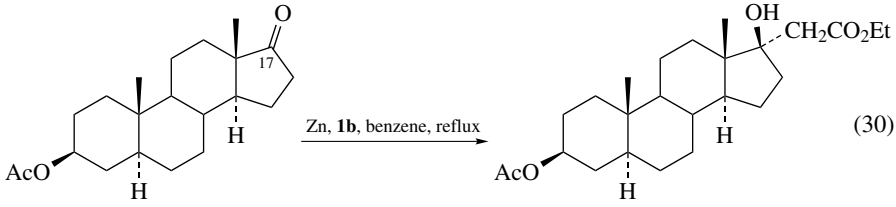

(30)

(44) 84%, 72% d.e.

Very limited are applications of classical Reformatsky protocols in macrocyclisation reactions, where samarium(II) is the most widely used metal, as shown in Table 1. Vedejs succeeded in cyclizing **45** by using Rieke zinc; unfortunately, the intermediate adduct underwent spontaneous dehydration and the isolated product was **46** (equation 31)[107].

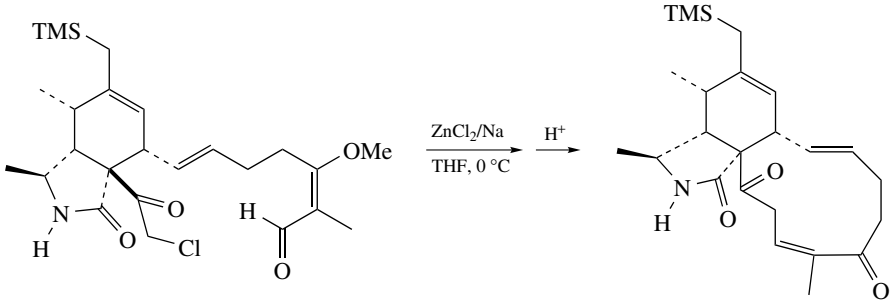

(45) **(46)** 67% (31)

A pretty good diastereocontrol was achieved in the six-membered ring cyclization of **47**, where diethylaluminium chloride and a catalytic amount of $CuBr_2 \bullet SMe_2$ were used to promote the internal attack of the Reformatsky centre to the sterically hindered carbonyl unit to give **48a** and **48b** (equation 32)[108].

In analogy to silyl enol ethers, Reformatsky reagents react with acetals in the presence of Lewis acids such as $TiCl_4$ or $BF_3 \bullet Et_2O$, to give β-alkoxy esters[109]. The reaction is carried out following a two-step Grignard protocol, which involves preliminary formation of the Reformatsky reagent in CH_2Cl_2 by means of the Zn/Cu couple, followed by addition at

−78 °C of the acetal and the Lewis acid. Enantiomerically pure cyclic acetals **49** deriving from chiral diols open a route to adducts **50**, which can be successively elaborated to chiral β-hydroxyesters upon oxidation of the alcoholic group followed by alkaline elimination (equation 33).

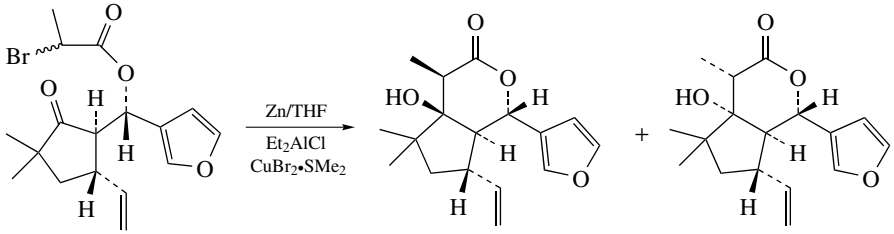

(47) **(48a)** **(48b)**

overall yield 60%, **48a/48b** = 1:20 (32)

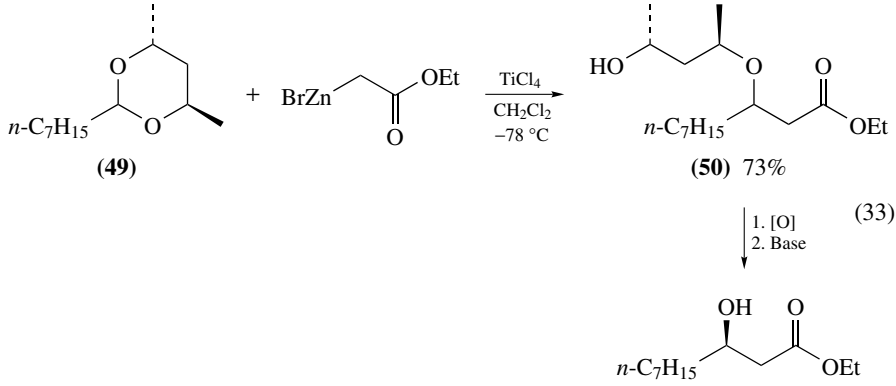

(49) **(50)** 73% (33)

84% e.e.

2-Acyloxytetrahydropyrans and furans (e.g. **51**) similarly react with Reformatsky reagents produced *in situ* in CH_2Cl_2 at 40 °C, as outlined in the example reported in equation 34[110].

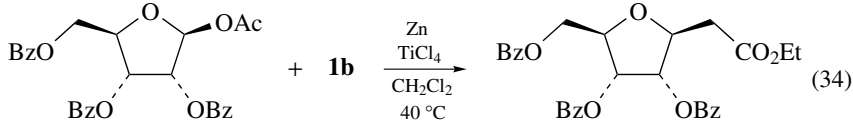

(51) 84% (34)

III. THE GILMAN–SPEETER REACTION

The addition of Reformatsky reagents to aldimines leads to amino-zinc intermediates **52**, which may be protonated to give the corresponding β-amino ester **53** or undergo ring closure to β-lactam **54**, as first reported by Gilman and Speeter (Figure 7)[13]. The **54/53** ratio mainly depends on the nature of the imine substituent R^5 and on temperature[39, 111], as

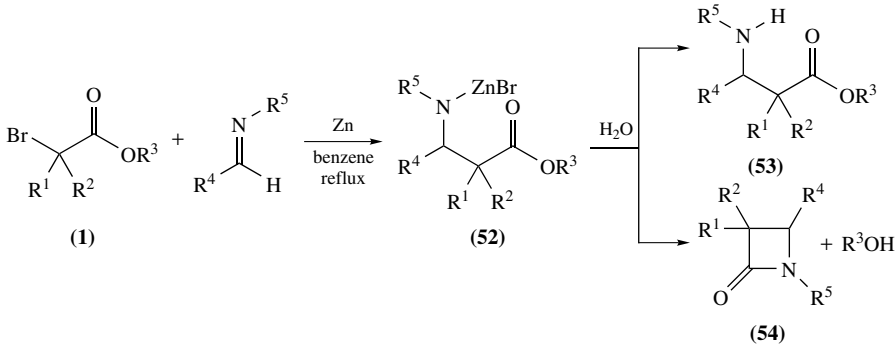

FIGURE 7

outlined by Gaudemar and coworkers[112] and more recently by van Koten and coworkers[113]. In this last work, an ester zinc enolate, prepared by a Li/Zn transmetallation protocol, reacted with a 2-pyridyl *N*-α-methylphenylethyl imine at $-78\,^{\circ}C$ in THF to give **53**, while temperature had to be adjusted at $-20\,^{\circ}C$ to achieve a spontaneous ring closure to **54**.

An electron-withdrawing group R^5 is supposed to inhibit ring closure by lowering the charge density on the nitrogen atom of **52**; an example is offered by Petrini, who makes use of α-amidoalkyl phenyl sulphones **55** as precursors of *N*-acylimines **56**. The reaction of ethyl bromoacetate (**1b**) with **55** in the presence of Zn/Cu couple in CH_2Cl_2 at room temperature affords the corresponding β-amino ester **57** in 75% yield (equation 35)[114]. α-Bromoketones behave similarly in the reaction with **55** deriving both from aromatic and aliphatic aldehydes, thus opening a route to β-aminoketones in good yields[115]. Excellent *anti* facial selectivity (d.e. = 90%) was obtained in the reaction of methyl bromoacetate **1a** with glyceraldehyde-derived α-amidoalkyl phenyl sulphones[116].

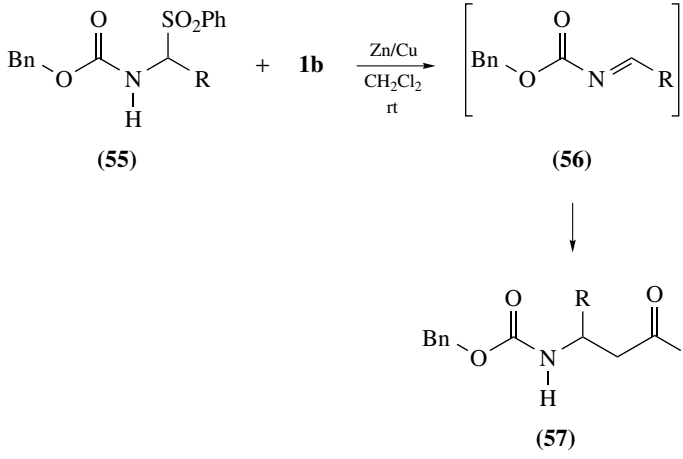

(35)

The *N*-sulphinyl group in Davis sulphinimines **58a** and **58b**[117], in analogy to the alkoxycarbonyl group in **56**, hampers ring closure to β-lactam, as independently reported by Staas and coworkers[118] (equation 36) and Soloshonok and coworkers[119] (equation 37).

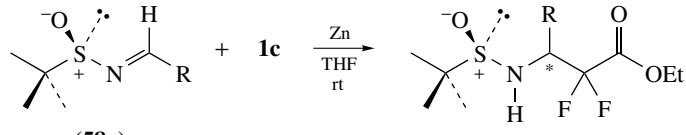

(36)

(58a)

R = alkyl, aryl

50–80%; 60–90% d.e.

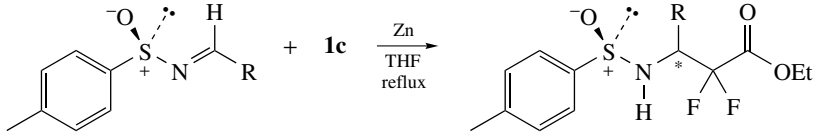

(37)

(58b)

R = alkyl, aryl

60–85%; 76–98% d.e.

In a solid-phase synthesis of α,α-difluoro-β-amino acids (equation 38), supported *N*-(α-aminoalkyl)benzotriazole **59** is reacted with **1c** and zinc to give adducts **60** in d.e. values which depended on the steric bulkiness of the R^1 group, ranging from 0 (R^1 = H) to 88% (R^1 = 2-methylpropyl)[120].

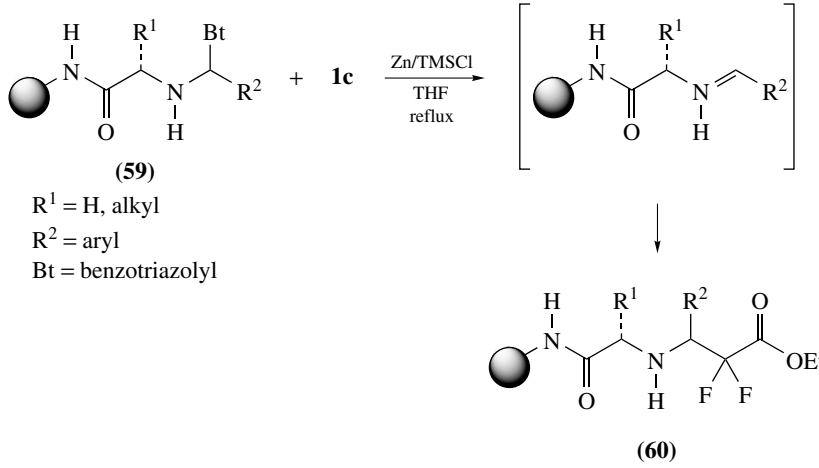

(38)

(59)

R^1 = H, alkyl

R^2 = aryl

Bt = benzotriazolyl

(60)

Inspired by a bright report from Katritzky and coworkers on the use in Reformatsky reactions of a variety of benzotriazolyl aminals[121], which in solution are in equilibrium with the corresponding imines, the formaldehyde aminal **61**[122] was reacted with **1c**, Zn and TMSCl to give adducts **62** (equation 39), which can be successively converted into β-lactams upon treatment with *t*-BuMgCl.

Equations 36–39 suggest that fluorine substituents at the α position of the ester enolate play a role in favouring the formation of β-amino esters. This conclusion is supported by the condensation of the Reformatsky reagent deriving from **20** with imines, the only product being the open-chain adduct **63** (equation 40)[123].

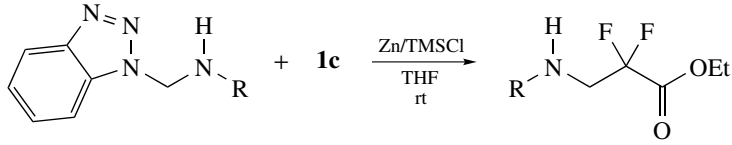

(39)

(61) **(62)**

R = aryl, benzyl

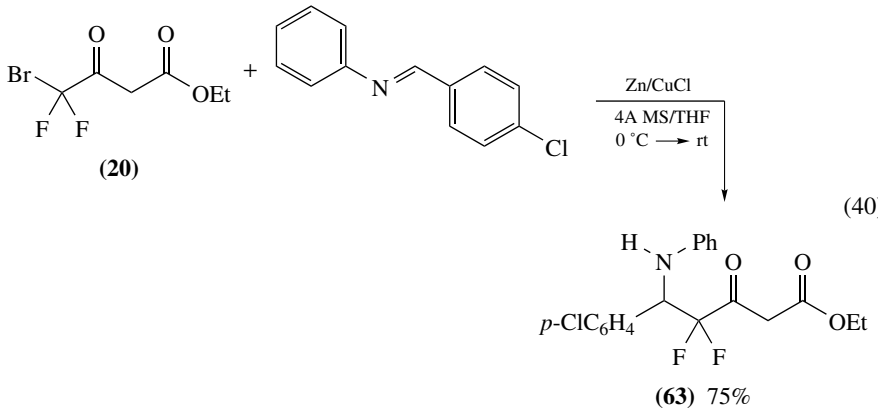

(40)

(20) **(63)** 75%

Working in the field of angiogenesis, a key process in tumour growth, chemists from Pfizer Co. described a fully diastereoselective imino-Reformatsky route to a $\alpha_v\beta_3$ integrin antagonist, in a process suitable for development to the pilot plant. Phenyl glycinol is used as stereochemical control element in imine **65** (Figure 8); the Reformatsky reagent is prepared from *t*-butyl bromoacetate (**1g**) and Zn in THF and added to a *N*-methylpyrrolidone solution of imine **65** in a typical two-step procedure. The authors were able to produce 7.7 kg of **66** in 99% e.e. and in 57% overall yield from starting material **64**[124].

A nickel-catalysed electro-Reformatsky reaction has been previously presented (Section II.B.3, Figure 5)[57]. Based on a formally related catalytic cycle, a nickel-catalysed 3-component route to β-amino esters and amides has been proposed (equation 41). To a CH_2Cl_2 solution of an aldehyde and an aromatic amine are successively added dimethylzinc, methyl bromoacetate (**1a**) and bistriphenylphosphine nickel dichloride. After 1–3 h at rt, products were isolated in very high yield, and this procedure was exploited for the preparation of a chemical library of 64 members, using 4 aldehydes, 4 α-haloesters and 4 substituted anilines[58].

The electron-poor aromatic ring of 1-acylpyridinium ions is known to easily undergo nucleophilic addition by carbon nucleophiles; an example was proposed by Comins and coworkers, who exploited the addition of zinc enolate **68** to enantiopure **67** ($R^* = trans$-2-(α-cumyl)cyclohexyl) in a total synthesis of (+)-cannabisativine (equation 42)[125].

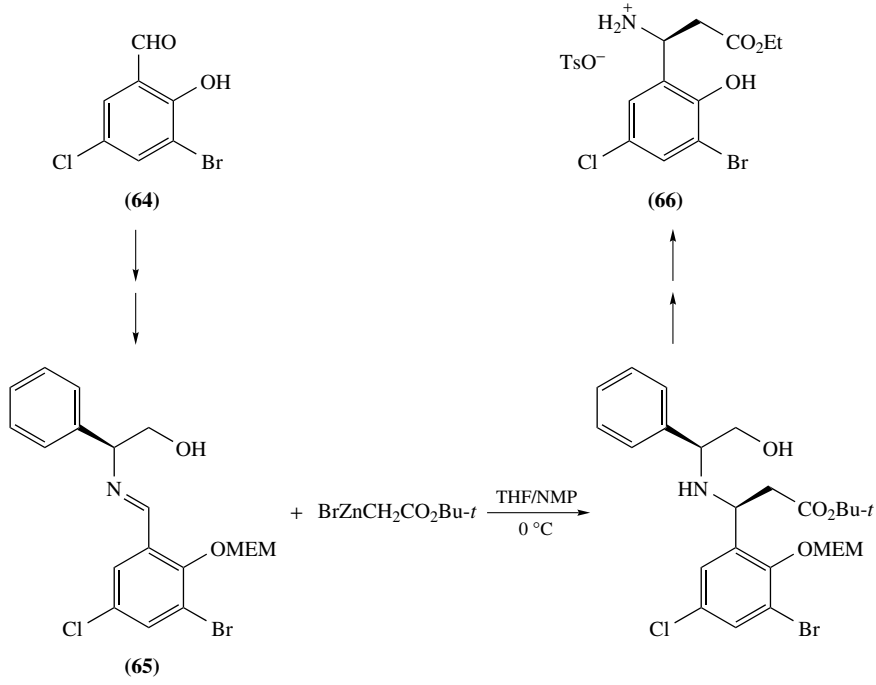

FIGURE 8

The technique of chiral auxiliaries was exploited in a synthesis of cholesterol absorption inhibitors, based on an imino-Reformatsky reaction between bromoacetates of chiral alcohols (e.g. **69a** and **69b**) and imine **70**. Virtual complete asymmetric induction was found with (−)-*trans*-2-phenylcyclohexanol and (−)-phenyl substituted menthol derived chiral auxiliaries (equation 43)[126].

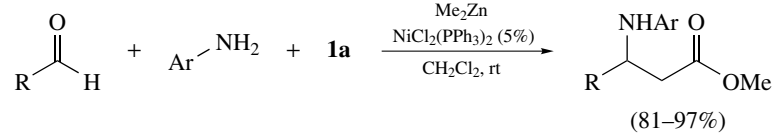

(41)

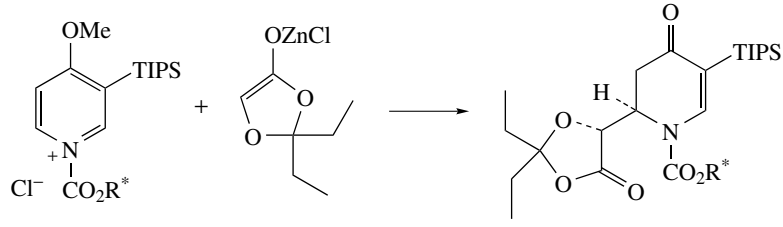

(42)

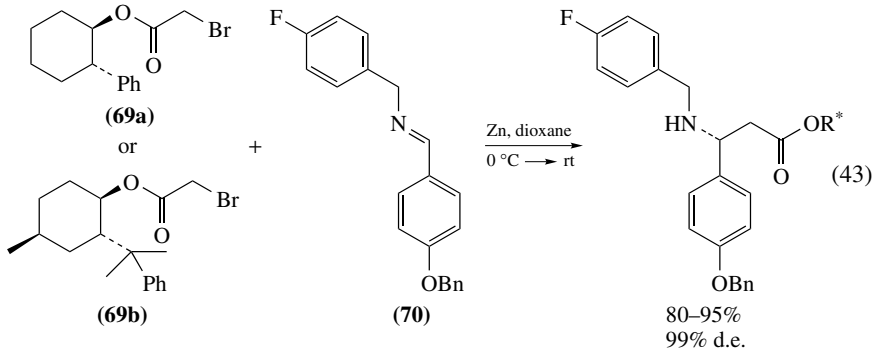

(43)

A further chiral auxiliary-based tactic exploited tricarbonyl(η^6-arene)chromium complexes of aromatic imines **71**, which reacted under ultrasound (US) irradiation with α-bromoesters in a predictable stereochemical course to give comparable amounts of β-aminoesters and β-lactams, as outlined in equation 44[127]. Chromium decomplexation is eventually achieved by photochemical oxidation under air.

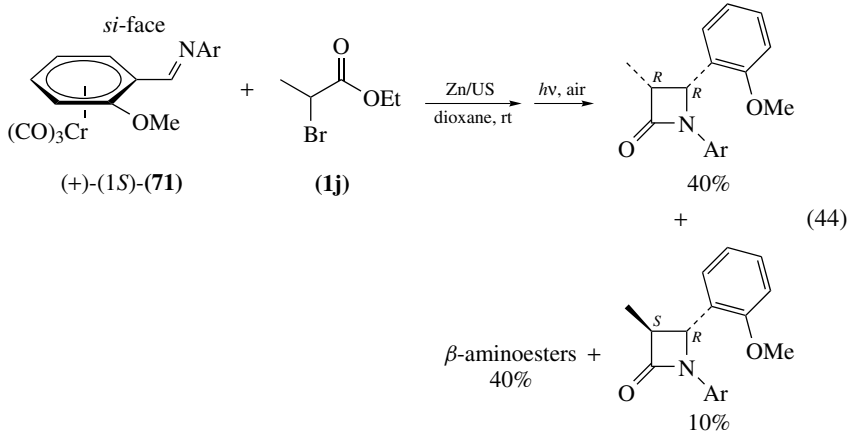

(44)

An efficient asymmetric synthesis of β-lactams, reported by van Koten and coworkers[128], was based on α-aminoesters as chiral auxiliaries and on the preformed imine–$ZnCl_2$ complex (e.g. structure **72** in equation 45), which was then added to the glycine zinc enolate **73**. The presence of $ZnCl_2$ as Lewis acid was essential to ensure complete lactamization.

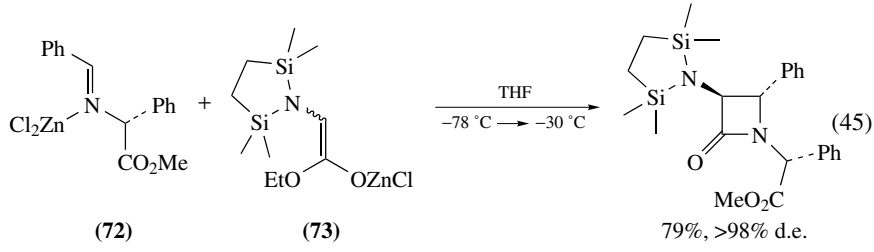

(45)

The influence of a Lewis acid in favouring the ring closure was confirmed by the use of a catalytic amount of Cp_2TiCl_2 in imino-Reformatsky reactions with α-bromoesters, γ-bromocrotonates and α-bromomethylacrylates; the corresponding *cis* β-lactams were obtained in excellent yields in THF at rt[129].

An interesting class of synthetic equivalents of imines is represented by cyclic α-amino ethers, which undergo ring-chain tautomerism under the action of nucleophiles, bases or acids. An example was offered by 1,3-oxazolidines (e.g. **74**), which have been reported to smoothly react with the Reformatsky reagents to produce *in situ* and at room temperature under sonication the corresponding open-chain adducts **75** (equation 46)[130]. The obvious extension to chiral 1,3-oxazolidines was made by Quirion and coworkers: (*R*)-phenyl glycinol-based 1,3-oxazolidines **76**, in equilibrium with the corresponding imino alcohol, reacts with **1c** (3.5 equivalents) in the presence of activated Zn dust affording 3,3-difluoroazetidin-2-ones **77** as the major products (equation 47)[131]. The role of *N*-substituent in controlling the β-aminoester/β-lactam ratio in the last two examples is noteworthy: when the *N*-substituent is a phenyl group, as in **74**, the product is the open-chain adduct **75**; when the *N*-substituent is H, as in **76**, only β-lactam **77** is formed.

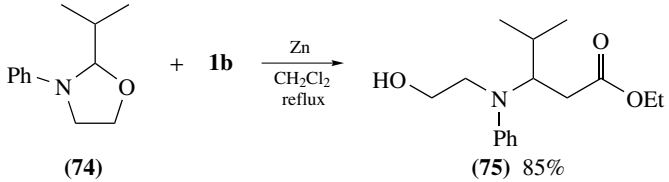

(46)

(74) **(75)** 85%

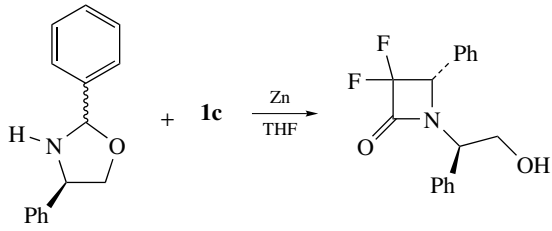

(47)

(76) **(77)** 65%, 99% d.e.

One of the most studied imine precursors in the reaction with organometallic compounds is (3*R*,4*R*)-4-acetoxy-3-[(*R*)-1′-((*t*-butyldimethylsilyl)oxy)ethyl]-2-azetidinone (**31**) (equation 23)[97].

En route to 1-β-methyl carbapenem antibiotics, the reaction of **31** with Reformatsky reagents **78** has been explored; it likely involves preliminary formation of the intermediate **79**, which then undergoes nucleophilic addition to give 2-(4-oxoazetidin-2-yl)-propanoic acid derivatives **80** (equation 48).

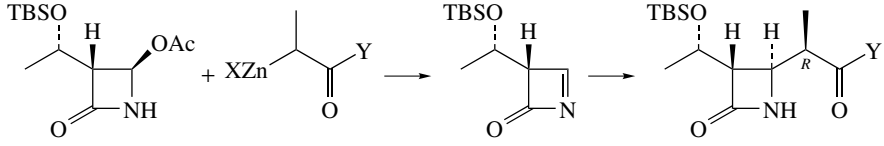

(31) **(78)** **(79)** **(80)** (48)

Table 3[132a–d] collects a few representative examples; the main stereochemical feature of these reactions, namely the ratio between (*R*) and (*S*) epimers at the 2′ position, is reported in terms of the β-methyl/α-methyl (β/α) ratio.

TABLE 3. Reactions of (3*R*,4*R*)-4-acetoxy-3-[(*R*)-1′-((*t*-butyldimethylsilyl)oxy)ethyl]-2-azetidinone (**31**) with 2-halopropanoic acid derivatives **78**

Enolate precursor	Conditions	**80** Yield(%)	β/α	Reference
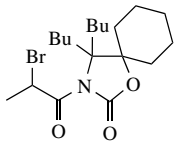 **(78a)**	Zn dust	86	23:1	132a
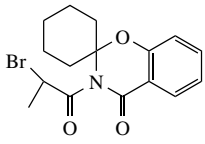 **(78b)**	Zn powder	80	92:8	132b
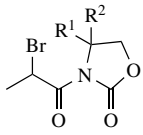 **(78c)**	Zn dust $R^1 = R^2 = Me$ $R^1 = R^2 = H$ $R^1 = H, R^2 = i\text{-Pr}$	94 97 99	79:21 45:55 91:9	132c
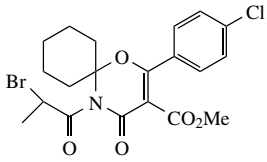 **(78d)**	Zn dust THF, reflux	88	97:3	132d

α-Tertiary aminonitriles **81a** and **81b** are also exploitable as synthetic equivalents of imines. These compounds, when reacted with α-bromoesters in the presence of an excess of zinc, of TMSCl as metal activator and in dimethoxymethane (DMM) as solvent, cleanly undergo replacement of the cyano unit, as shown in equations 49 and 50[133].

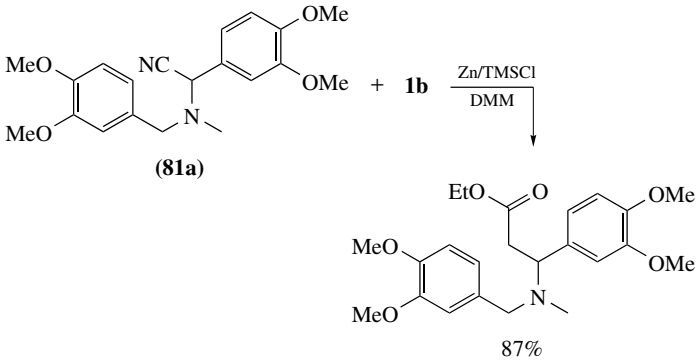

(49)

(81b) 89% (50)

The nitrone functionality has also found a number of applications as acceptor of nucleophilic addition, as recently reviewed[134]. The reaction of nitrone **82** with **1d** directly affords isoxazolidin-5-ones **83**, as shown in equation 51[135].

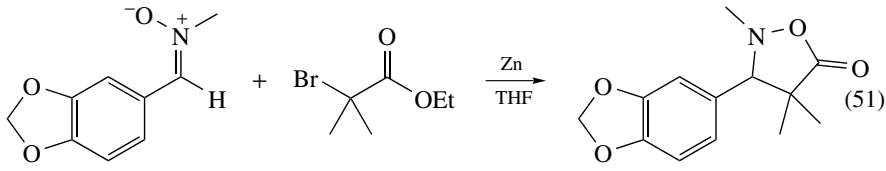

(82) (1d) (83) 52% (51)

IV. FURTHER ELECTROPHILES FOR REFORMATSKY REAGENTS

A. Carboxylic Acid Derivatives

With the aim to prepare α-substituted ulosonic acids, a class of bioactive compounds possessing antibiotic and cytotoxic properties, all the four isomeric forms of bromoester **84** deriving from (+)- and (−)-menthol were synthesized, and each ester was added to D-*mannono*-1,4-lactone **85** in the presence of active metals on graphite, precisely Mg-Gr and Zn/Ag-Gr, to give **86** (equation 52). In all cases, adducts were obtained with a *R*-configured C(2′) stereocentre. Conversely, the opposite asymmetric induction on C(2′) was observed in the Zn/Ag-Gr mediated addition to **85** of a variety of methyl and *t*-butyl esters of benzoic acid, phenylacetic acid and of branched-chain aliphatic acids, as well as of methyl and ethyl α,α-difluorobromoacetate[136]. With reference to the sugar acetalic centre, the α product is obtained with all the Reformatsky reagents tested. The authors believe that the organozinc complex attacks the less hindered *re* face of the lactone (opposite to the dioxolane rings) affording a β product, which rapidly epimerizes to the more stable α-anomer.

Ring-chain tautomerism of intermediate lactols is also exploited in a conversion of Reformatsky adducts **87** into enamines **88** *via* mesylation followed by reaction with aliphatic amines in CH_2Cl_2 at room temperature and in the presence of molecular sieves (equation 53)[137].

Esters are rarely used as electrophiles in Reformatsky reactions. An example was reported by Atkins and coworkers: the quinoline ester **89** failed to react with butanoic acid esters in classical Claisen condensation conditions, but was found to smoothly react with *t*-butyl ester **90** in the presence of zinc in good yield (equation 54)[138].

The reaction of Reformatsky reagents with nitriles, the Blaise reaction[139], found interesting applications in the case of enantiomerically pure *O*-protected cyanohydrins. Among different stereocontrolled approaches[140], the asymmetric enzymatic synthesis of cyanohydrins from aldehydes and HCN can be achieved in both configurations using (*R*) oxynitrilase (available from almond flour) or the (*S*) oxynitrilase (available from *Sorghum*

bicolour), respectively, in ethyl acetate. The subsequent reaction of *O*-TMS cyanohydrins **91** with **1j** in THF at reflux affords, after acidic hydrolysis, enantiomerically enriched tetronic acids **92**, as shown in equation 55[141].

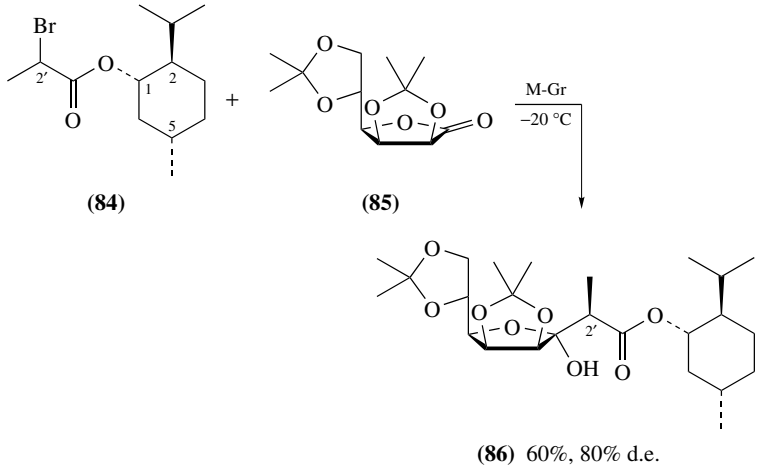

(52)

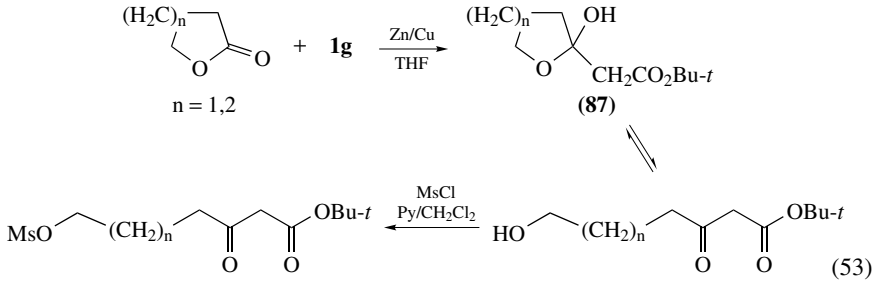

(53)

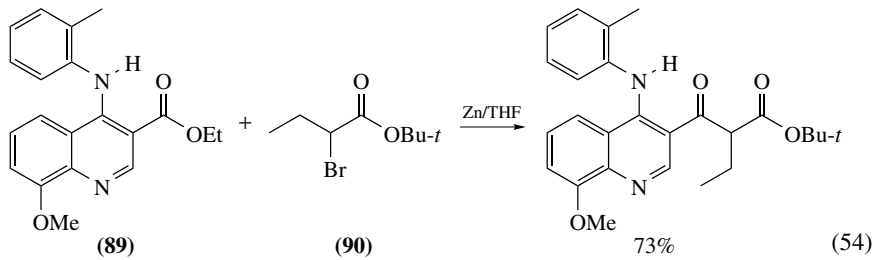

(54)

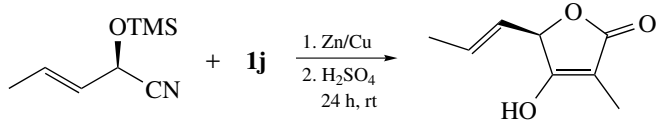

(55)

(91) **(92)** 30%, 97% e.e.

On the other hand, if quenching is carried out with aq NH_4Cl at $-30\,^{\circ}C$, enantiomerically enriched enamino esters **93** can be isolated in high yield (equation 56)[142].

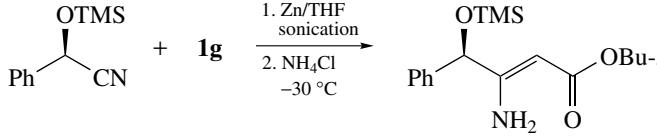

(56)

(93) 80%, 94% e.e.

When α,β-unsaturated esters are the target molecules, the use of a thioaldehyde or thioketone is advisable for the easy elimination of H_2S from the intermediate thiol adduct. This strategy has been applied to thiolactams **94a** and to thionolactones **94b**, opening a route to vinylogous carbamates **95a**[143] and carbonates **95b**[144](equation 57).

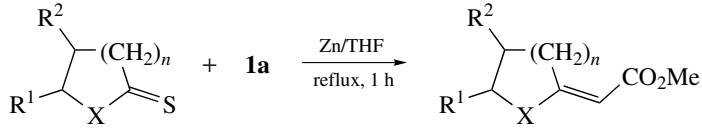

(57)

(94a) X = *N*-Boc
(94b) X = O
n = 1–3

(95a, b)

A closely related reaction between 1-arylpyrrolidine-2-thiones **96** and diethyl bromomalonate **97** under Reformatsky conditions afforded 1-arylpyrrolidin-2-ylidene malonates **98**, which, upon polyphosphoric acid (PPA) induced cyclization, opened a route to pyrrolo[1,2-a] quinolones **99**[145], tricyclic analogues of quinolone antibiotics (equation 58).

Following a similar strategy, the synthesis of tetracyclic models of aziridinomitosenes, bioactive degradation products of mitomycins, was based on the Reformatsky reaction of thiolactam **100**, as shown in equation 59. The synthetic plan and reagent design were directed to the use of an intramolecular Heck reaction of **101** to complete the target skeleton[146].

B. Electron-poor Carbon–Carbon Double Bonds

The most reactive Michael acceptors, such as alkylidene malonates, *gem*-dicyanoalkenes and nitroalkenes, react with α-halozinc esters in a conjugate fashion. Beautiful examples were offered by two stereocontrolled conjugate additions to piperidinone **102** and pyrrolidinone **104** leading to optically active bicyclic lactams **103**[147] (equation 60) and **105** (equation 61)[148]. With these electron-poor alkenes a Grignard two-step protocol is to be adopted in order to avoid the single electron transfer reactions from the metal to the Michael acceptor, which should afford olefin dimers. The best solvent is found to be a

THF/DMPU mixture. The attack of the Reformatsky reagent from the less hindered *exo* face dictates the overall stereochemical outcome.

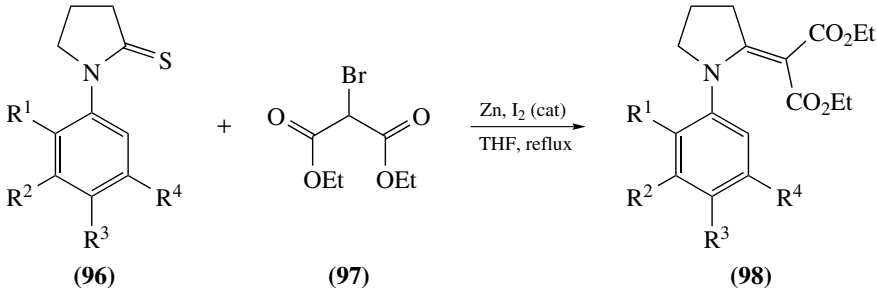

(96) **(97)** **(98)**

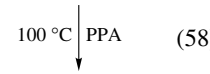

(58)

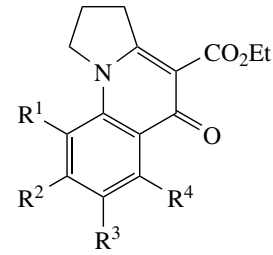

(99) 50–70% from **96**

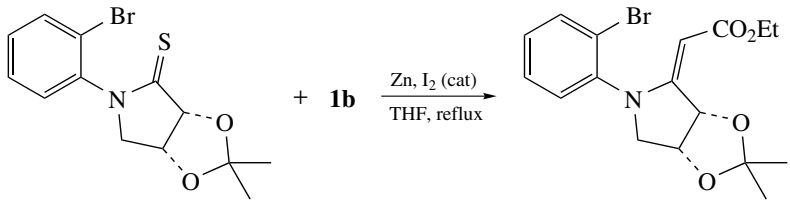

(100) **(101)** 92%

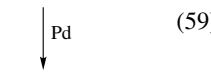

(59)

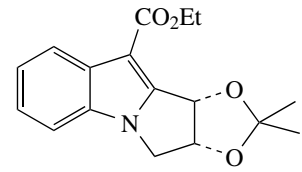

99%

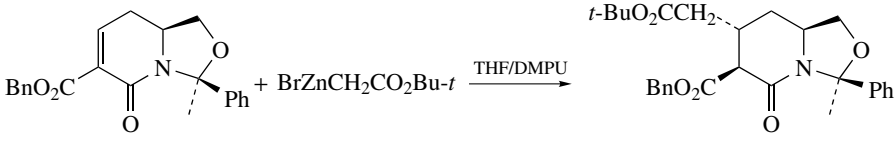

(102) **(103)** 76% (60)

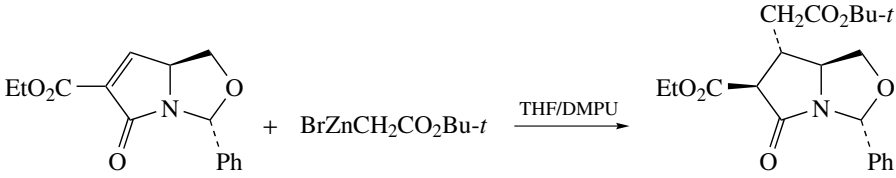

(104) **(105)** 73% (61)

1,1-Dicyanoalkene **106** also reacts in a 1,4-fashion; experimental evidence (ESR techniques, free-radical traps, quenching experiments) proved that the reaction follows a radical pathway, triggered by a single electron transfer from the Reformatsky reagent to **106** (equation 62)[149]. The reaction is speeded up by the presence of Cp_2TiCl_2.

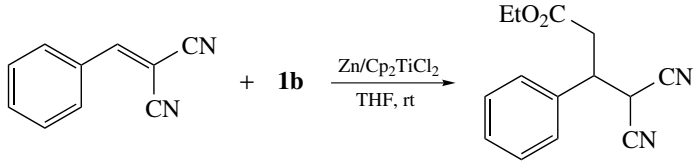

(62)

(106) 82%

As a consequence of the strong electron-withdrawing properties of the nitro group, conjugated nitroalkenes behave as powerful Michael acceptors. An example of conjugate addition of Reformatsky reagents to (2-nitrovinyl)arenes **107** is given in equation 63[150].

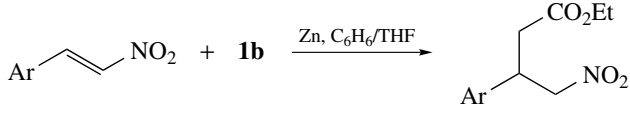

(63)

(107) 50–90%

Using 1-(2-nitrovinyl)pyrrolidines **108** or **111** as Michael acceptors, the addition of the Reformatsky reagent is followed by amine elimination. A formal vinylic substitution ensues, which can take advantage of the presence of stereocenters in the pyrrolidine moiety, affording new chiral nitroolefins **110**[151] and **113**[152], as reported in equations 64 and 65, respectively. In both cases, zinc enolates **109** and **112** are prepared by lithiation/transmetallation of the parent ester.

[60]Fullerene (**114**) also acts as an electrophile towards the Reformatsky reagents. When **114** is stirred with an excess of ethyl bromoacetate (**1b**) and zinc under solvent-free

conditions, after 20 min at rt a 40% conversion into four products is observed, the major one representing the expected addition product **115**[153] (equation 66).

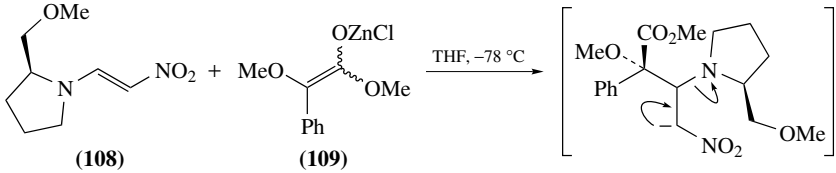

(108) **(109)**

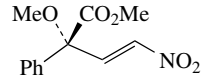

(110) 96%, 69% e.e.

(64)

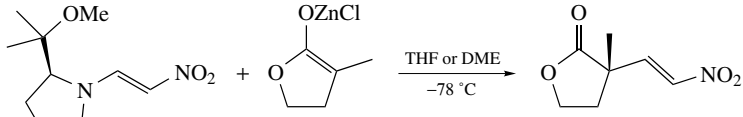

(111) **(112)** **(113)** 98%, 95% e.e.

(65)

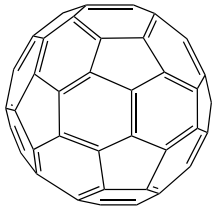

(114)

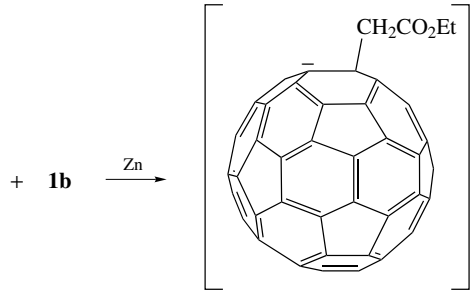

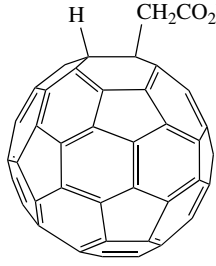

(115) 62% based on converted C_{60}

(66)

C. Phosphorus electrophiles

The introduction of a heteroelement Z on the α-position of an ester functionality is possible by trapping an enolate with a suitable Z−Cl compound, namely via nucleophilic substitution at the Z atom. The heteroelement Z could correspond to Si, B, P, S etc.

Two examples are reported here based on the reaction of Reformatsky reagents with phosphorus(III) electrophiles. In equations 67 and 68, a dichlorophosphine or a monochlorophosphine is reacted with 2 or 1 equivalents of **1a** in the presence of zinc in refluxing benzene. Quenching of the crude unstable tertiary phosphine with H_2O_2 allows one to isolate phosphino oxides **116** and **117** in good yields, generally as stable solid compounds[154].

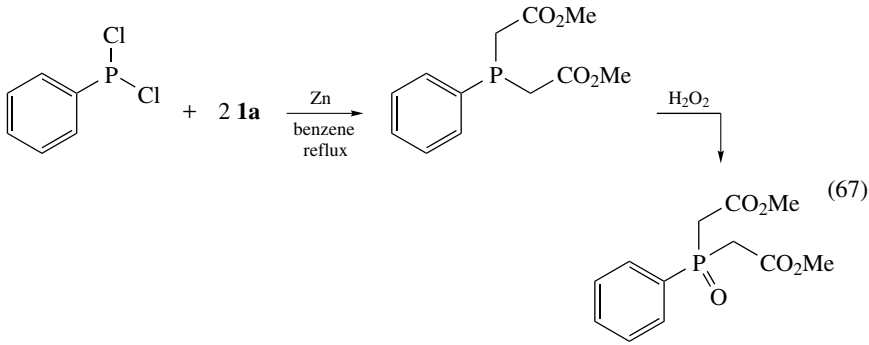

(67)

(116) 64%

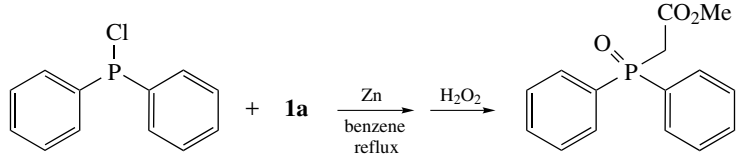

(68)

(117) 63%

In the search for viable antisense oligodeoxynucleotides analogues, critical is the choice of the phosphorylated internucleotide linkage: among other properties, it must be resistant towards the action of nucleases, it should contain an anionic centre to enhance hydrophilicity, it must hybridize to RNA and activate RNase H. All these characteristics seem to belong to phosphonoacetate **118** and thiophosphonoacetate-modified oligodeoxynucleotides **119** (**B** = nucleotide base)[155]. A common P(III) precursor **120** was devised for both **118** and **119**, as outlined in Figure 9. Construction of the phosphinoacetate linkage in **120** was possible by using **121**, which easily undergoes displacement of the amino group by alcohols such as suitably protected 2′-deoxynucleosides. The bis-amidite **121** was accessible in high yield by trapping the preformed Reformatsky reagent **122** with the (*N*,*N*-dialkylamino)chlorophosphine **123** in THF.

D. Transition metal-catalysed coupling reactions

Organozinc reagents, including the Reformatsky reagents, are extensively used in transition metal catalysed coupling reactions with aryl halides or triflates, vinyl halides, and allylic halides or acetates, as reviewed by Erdik[156]. Nickel and palladium complexes are

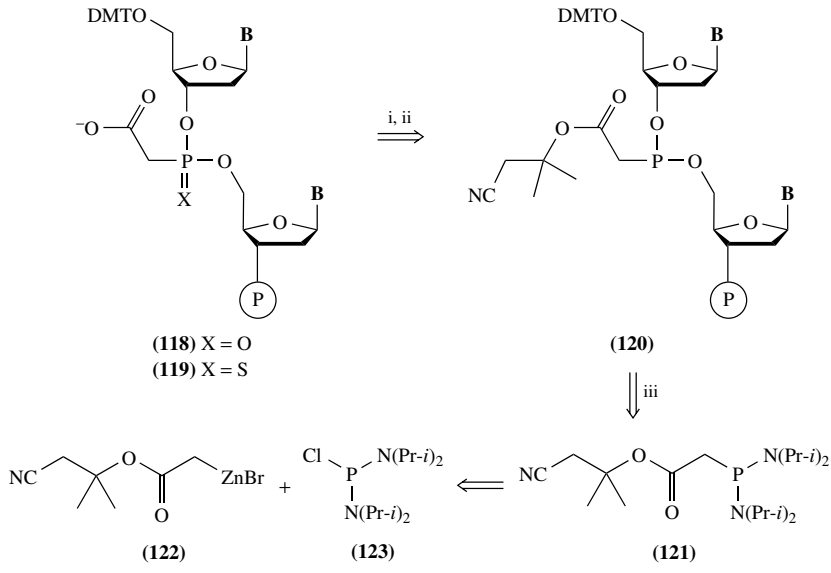

FIGURE 9

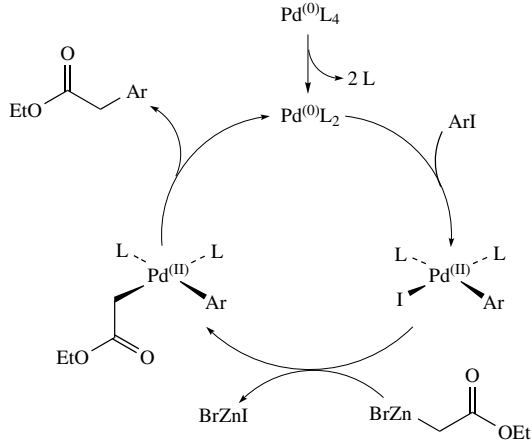

FIGURE 10

the most widely used catalysts with Reformatsky reagents, and highly polar solvent mixtures such as HMPTA/dimethoxymethane and HMPTA/THF have been reported to be necessary for arylation reactions with aryl halides and triflates, respectively[157], as well as with vinyl halides or triflates[158]. A typical catalytic cycle for the cross-coupling reaction is depicted in Figure 10.

In recent contributions, milder conditions have been developed to catalyse the arylation of α-halozinc esters and amides **124** with aryl bromides **125**. Reactions are conducted either under microwave irradiation[159], or at rt in THF or dioxane in conjunction with 1% of $Pd(dba)_2$ and 1% of Q-phos (equation 69)[160].

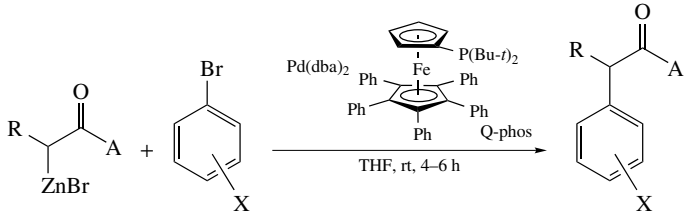

(69)

(124) **(125)**

R = H, Me X = electron-withdrawing
A = OBu-*t*, NEt_2 or electron-donating group

A synthesis of the monomeric unit **128** of a peptide nucleic acid analog (PNA) offers an example of stereospecific cross-coupling of a Reformatsky reagent with (*Z*)-vinylic iodide **126**. The coupling reaction of the preformed Reformatsky reagent prepared in dimethoxymethane (methylal) with **126** is carried out using 8% of $Pd(PPh_3)_4$ in DMPU as the solvent at 65 °C to afford **127** (equation 70)[161].

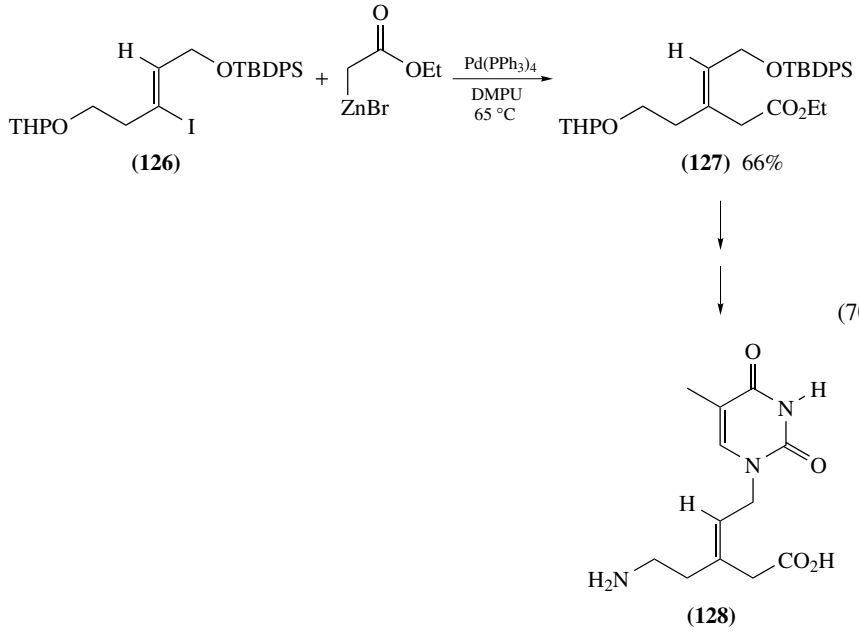

(126) **(127)** 66%

(70)

(128)

Allylic substitution reactions affording γ, δ-unsaturated esters have been also reported; for example, Reformatsky reagents react with allylic halides in the presence of 5% $Cu(acac)_2$ in Et_2O/DMSO mainly affording S_N2-type products (equation 71)[162].

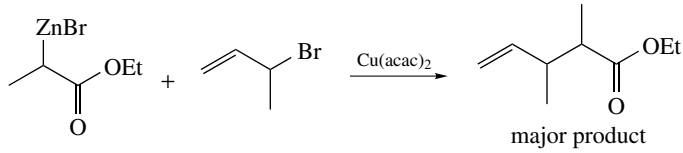

(71)

On the other hand, when preformed Reformatsky reagents are reacted with allylic acetates in the presence of Pd(0) catalysts, substitution takes place regioselectivity at the less substituted allylic terminus (equation 72)[163].

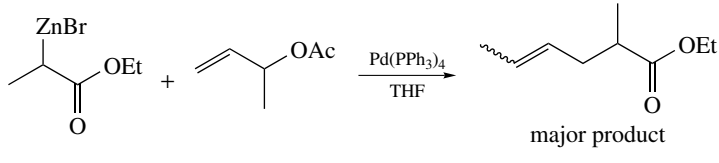

(72)

Zinc dibenzyl malonate complex **129**, prepared by the action of Et_2Zn on dibenzyl malonate, was found to be superior to alkali metal dibenzyl malonates, in terms of enantiomeric control, in the allylic substitution with (±)-**130** catalysed by an *in situ* prepared Pd-(*R*)-BINAP complex (equation 73)[164].

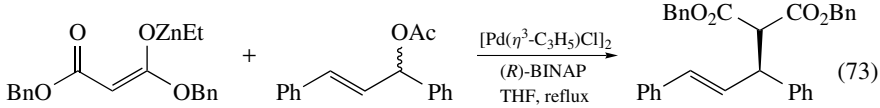

(73)

(129) **(130)** 81%, 95% e.e.

High regioselectivity and asymmetric induction using enantiomerically pure allylic carbonates **132** and **133** was reported in the reaction with the zinc enolate **131** (equations 74 and 75)[165]. Carbonates proved to be the best leaving groups to ensure high values of regioselectivity (the styryl product is always obtained), and of chirality transfer, since they react at a temperature low enough to avoid *syn/anti* isomerization of the intermediate Pd π-complexes.

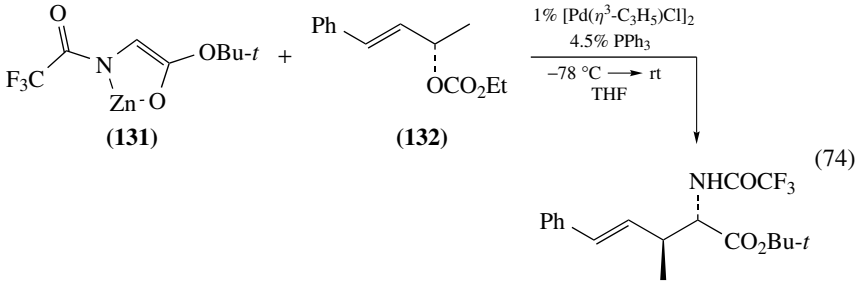

(74)

(131) **(132)** 73%, 91% d.e., 96% e.e.

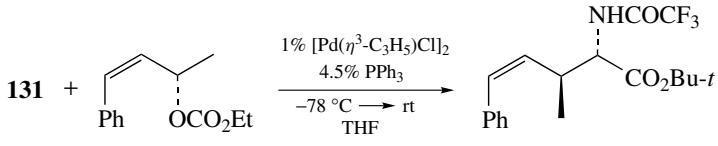

(133) 69%, 98% d.e., 97% e.e. (75)

V. ALTERNATIVE ROUTES TO ZINC ENOLATES

A. Lithiation/Transmetallation Protocols

The most general route to transition metal enolates involves lithiation of an enolisable substrate followed by transmetallation with a proper metal halide; several reports are available in the literature where zinc enolates are prepared via lithium/zinc exchange, and selected examples are discussed henceforth.

The first example (equation 76) deals with an enantioface differentiating protonation of zinc enolate **134** by means of the chiral γ-hydroxyselenoxide **135**. Zinc plays a critical role in determining enantiocontrol by conferring rigidity to the transition state thanks to a simultaneous coordination to the hydroxyl oxygen, to the selenoxide oxygen and, of course, to the enolate oxygen[166].

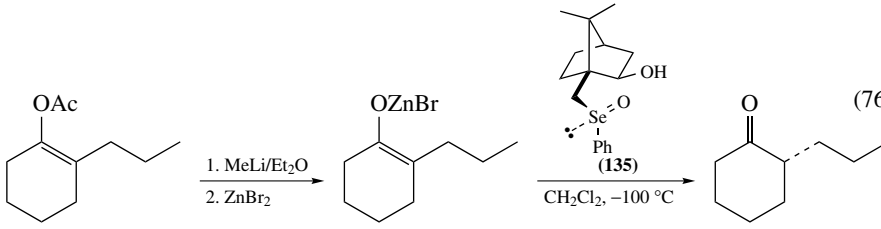

(134) 76%, 88% e.e. (76)

Zinc bisenolate **136** (Figure 11) is prepared by the transmetallation of propiophenone lithium enolate with 0.5 equivalents of $ZnBr_2$; **136** reacts with aldehydes, both aliphatic and aromatic, in a domino aldol reaction which mimics the action of aldolases[167]. The first aldol reaction between **136** and the aldehyde produces zinc aldolate **137**, which then undergoes a second intramolecular aldol addition to adduct **138**. Spontaneous hemiacetalization affords **139**, where all large substituents occupy equatorial positions[168].

In the reaction of a simple ketone enolate with a chiral aldehyde, the use of a zinc enolate may offer advantages in terms of facial selectivity with respect to the use of a lithium enolate. This is exactly the result recorded in the condensation of the kinetic enolate of 2-undecanone **140** with **141**, the key step in a total synthesis of (+)-preussin **142**, a fermentation product with antifungal and antibacterial activity (equation 77)[169]. While 2-undecanone Li enolate did not display stereocontrol when added to **141**, an acceptable *syn* diastereoselectivity was displayed by the Zn enolate **140**.

Dendrimers, among other applications, are generating interest as soluble supports thanks to the following intrinsic characteristics: (i) the well-defined molecular composition of a dendrimer provides a support with a precisely defined arrangement of the reactive sites, (ii) a high loading of reactive sites is achieved on the dendrimer surface and (iii) nanofiltration techniques are available to separate the dendritic support from products. Dendrimer **143**, based on a carbosilane core, possesses 12 ester functionalities on

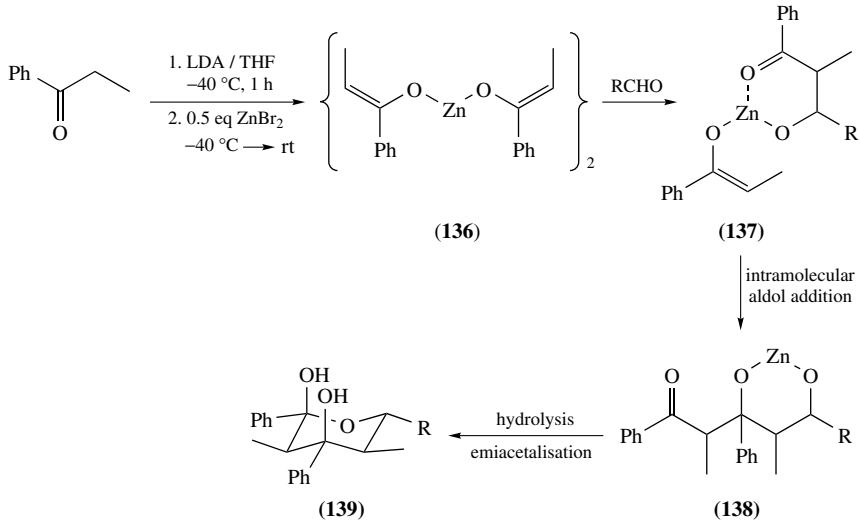

FIGURE 11

its surface; each ester terminus can be deprotonated and transmetallated to give a soluble poly zinc enolate **144**. The usual intermolecular aggregation which characterizes zinc enolates in THF is not possible when enolate sites are bound to the dendrimer surface, and this could confer a different reactivity to **144**. Dendrimer **144** is *in situ* reacted with *N*-silylimine **145**; the initially formed β-aminoester, still bound to the dendrimer framework, undergoes ring closure to *trans*-**146** with concomitant cleavage from the carbosilane support **147**, which ultimately acts as a leaving group (equation 78)[170].

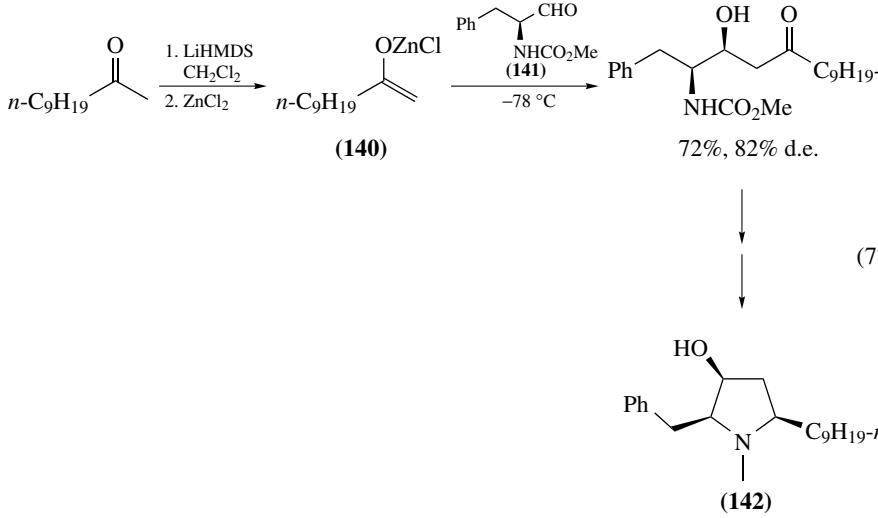

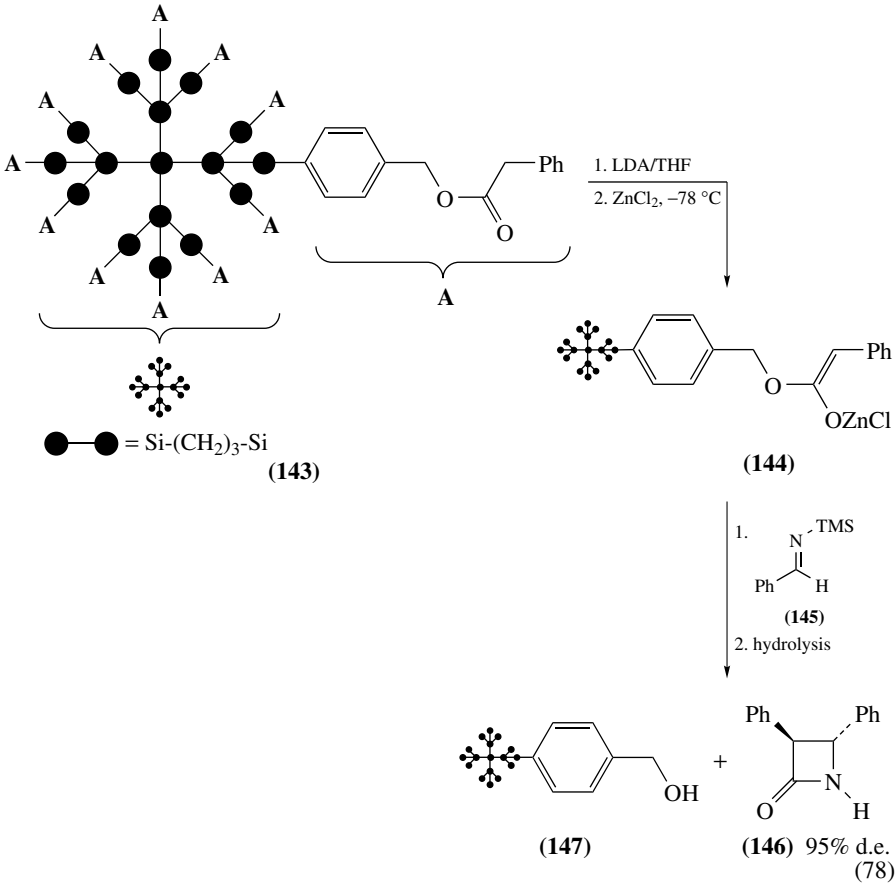

(78)

Allylic glycine ester enolate **148**, when subjected to the lithiation/transmetallation protocol at −78 °C, cleanly undergoes [3,3]-sigmatropic rearrangement on warming up to rt; the resulting α-aminoacid **150**, an interesting non-proteinogenic amino acid, contains a quaternary β-carbon stereocentre (equation 79)[171]. The high level of diastereocontrol is determined by the chelated structure of the zinc-enolate **149**, which favours a well-defined chair-like transition state. Interestingly, the adduct (±)-**150** is obtained also from the *Z*-configured isomer of **148**, by applying the same protocol depicted in equation 79; in this case the Claisen rearrangement is supposed to involve a boat-like transition state.

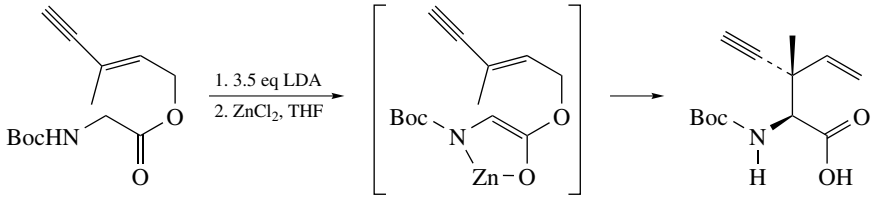

(148) **(149)** (±)-**(150)** (79)

Zinc enolates, besides adding to carbonyl compounds, cleanly add to unactivated alkenes, in a carbozincation process[172]. An intermolecular example is offered by the addition of hydrazone zinc enolates **151** to vinylsilane **152**, which proceeds in high yield and with perfect regioselectivity, provided a 'dummy' non-migrating butyl ligand on the zinc atom is used (equation 80). The intermediate zinc derivative **153** could be trapped by a suitable electrophile to give silane **154**[173], thus opening a route to multicomponent coupling protocols.

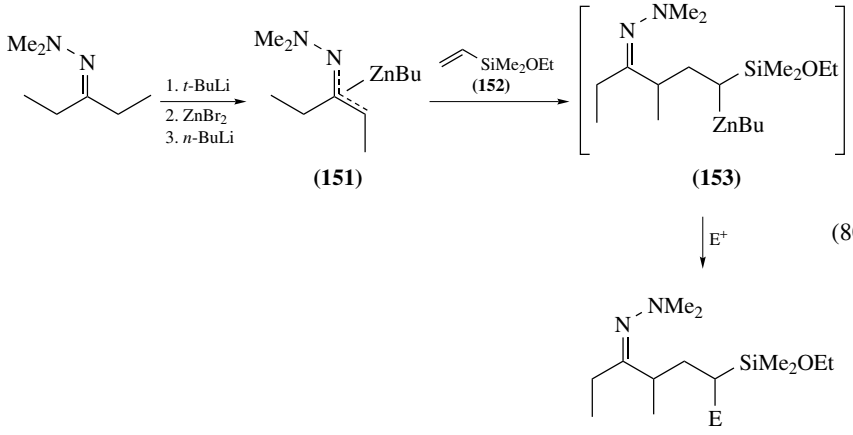

(151) (153)

(80)

(154) 73% for E = H

The addition of zinc enolates to alkenes in the intramolecular version finds several examples in recent literature. Thus, hydrazone **155**, subjected to the same treatment reported for **151** (equation 80), undergoes diastereoselective *5-exo-trig* ($n = 1$) or *6-exo-trig* ($n = 2$) carbocyclization to yield *cis*-**156**, which on reaction with the electrophile E^+ gives **157** (equation 81)[174].

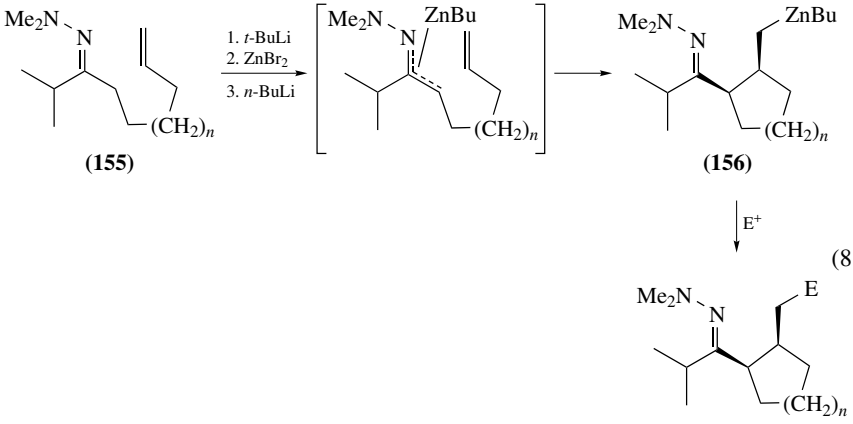

(155) (156)

(81)

(157) E = H
n = 1:90%, 88% d.e.
n = 2:83%, 91% d.e.

Two groups studied independently[175, 176] the intramolecular carbozincation reaction of unsaturated zinc enolates deriving from α-amino acids. *N*-Homoallyl glycine **158** afforded, after lithiation/transmetallation at low temperature, an intermediate *cis*-organozinc species **160**, easily elaborated into different functionalized derivatives (equation 82). To account for the *cis* selectivity, the transition state **159** has been postulated, where zinc simultaneously interacts with the carbon−carbon double bond, the enolate oxygen and the nitrogen atom[175a]. Both R^1 and R^2 groups have been exploited in order to introduce a chirality control element and develop asymmetric syntheses of proline derivatives **161**. Besides, to be 100% diastereoselective, (2*R*,3*S*)-**161** (E = H) was obtained in 96% e.e. using $R^1 = \alpha$-phenylethylamine and $R^2 = Me$[176a].

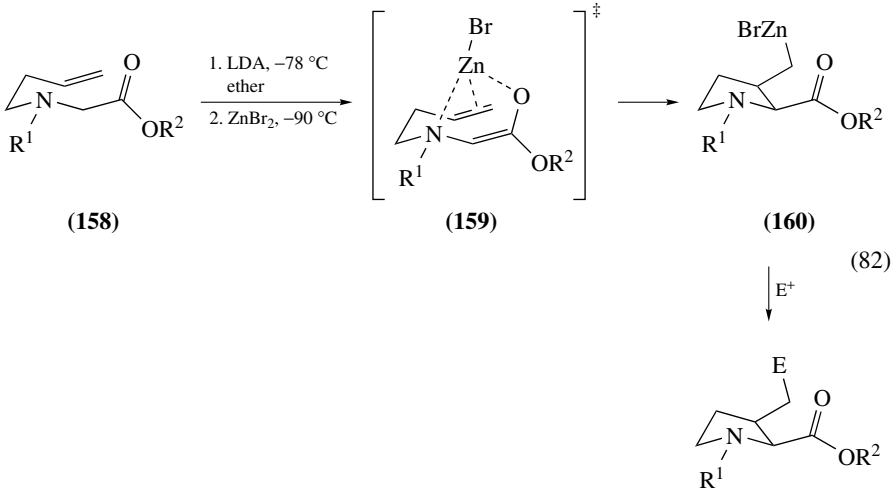

(158) **(159)** **(160)** (82)

(161) E = H, I

The reaction can be also carried out on a solid support such as the Wang resin, compatible with LDA and Zn salts derivatives[175c].

Among other transformations, the following electrophiles have been applied to **161**: (i) TsCN/CuCN, in a synthesis of enantiopure 3-prolinoglutamic acid[175d]; (ii) I_2, in a synthesis of enantiopure 3-iodomethyl prolines[175c]; (iii) MeS-SO_2Me, in a synthesis of enantiopure 3-prolinomethionines[175b]; (iv) allyl bromide/CuCN, in a C-3 chain elongation of prolines[176c].

The perfect diastereocontrol of ring closures of substituted homoallylic glycines[176c] (e.g. **162**) and bishomoallylic glycines[176b] (e.g. **164**) has been also reported, leading to substituted pyrrolidines **163** or piperidines **165** (equations 83 and 84).

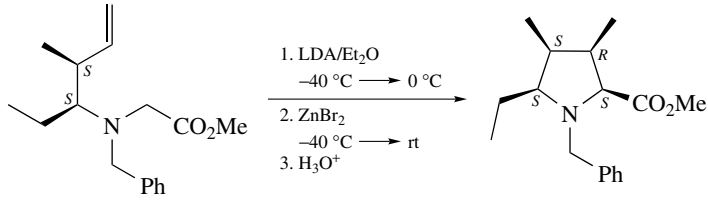

(162) d.r. = 96/4 **(163)** 62%, d.r. = 95/5 (83)

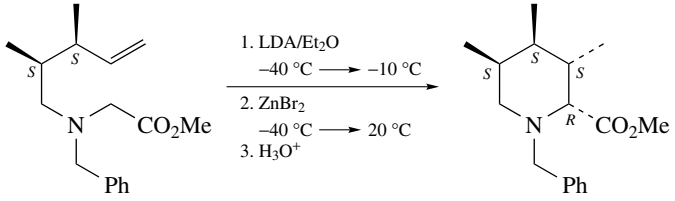

(84)

(164) d.r. = 91/9 **(165)** 68%, d.r. = 90/10

B. Zinc Enolates from Diethylzinc as Metal Source

Several approaches to zinc enolates have been developed in which a dialkylzinc derivative, generally Et_2Zn (**166**), is used as the zinc source, following a variety of reaction mechanisms and processes.

The propensity of **166** to undergo Zn−C bond cleavage by alcohols with formation of ethane and a zinc alkoxide has been brightly exploited in a catalytic asymmetric cross aldol reaction between aryl methyl ketones and aldehydes; 10% of **166** combined with the chiral ligand **167** and $Ph_3P{=}S$ as co-catalyst fosters a catalytic cycle based on zinc enolate **168**. Two proximal zinc atoms are present in the catalyst, the first affording the zinc enolate, the second providing a suitable acidic site able to coordinate the aldehyde. The final aldols **169** are produced in 24–79% yield and with e.e. values ranging from 56 to 99% (Figure 12)[177].

The use of **166** to address zinc carbenoids (e.g. $EtZnCH_2I$) upon reaction with CH_2I_2 has been applied to the preparation of zinc enolates **170** starting from β-ketoesters[178a]. A tandem process has been developed consisting of a Simmons–Smith reaction/cyclopropane ring opening/aldol addition, which allowed one to synthesize aldols **171** in 60–95% yield and with excellent *syn* diastereoselectivity (equation 85)[178b].

The propensity of Et_2Zn (**166**) to undergo metal/iodine exchange upon reaction with activated alkyl iodides opened also a direct route to zinc enolates by simply exposing α-iodoketones[179] or α-iodoesters[180] to **166** or $i\text{-}Pr_2Zn$ in hexane or hexane/ether as solvent at 0–25 °C. A classical two-step procedure can be developed in which the enolate is preformed and then trapped by the carbonyl compound. Interestingly, the intermediate zinc enolate (e.g. **172**) may be also trapped with an *in situ* formed zinc carbenoid, eventually leading to cyclopropanol **173** (equation 86)[181].

Polymetallic chiral aggregates obtained by combining the bis(bromomagnesium) salt **174** with an excess of **166** and iodoacetate allow the asymmetric addition of the resulting Reformatsky reagent to 3,4-dihydroisoquinoline *N*-oxide (**175**)[182a] and to 2-aminophenol imines **176**[182b] (equations 87 and 88). Surprisingly, to reach the best enantioselectivity, 0.8 equivalents of H_2O were necessary with the latter substrates.

Unlike α-iodoesters, α-bromoesters do not interact with **166**. However, the corresponding zinc enolates become accessible if a proper low-valent transition metal is used as catalyst. The Wilkinson's catalyst, $RhCl(PPh_3)_3$, performs particularly well in promoting zinc enolate formation. According to the catalytic cycle depicted in Figure 13, Rh(I) oxidatively adds to the carbon−bromine bond of the haloester affording a Rh(III) enolate **177**, which then undergoes transmetallation by **166** to free the zinc enolate **178**.

Such a catalytic cycle closely resembles that promoted by $NiCl_2(PPh_3)_2$, quoted in Section III (equation 41[58]), where the same oxidative addition/transmetallation sequence is in action.

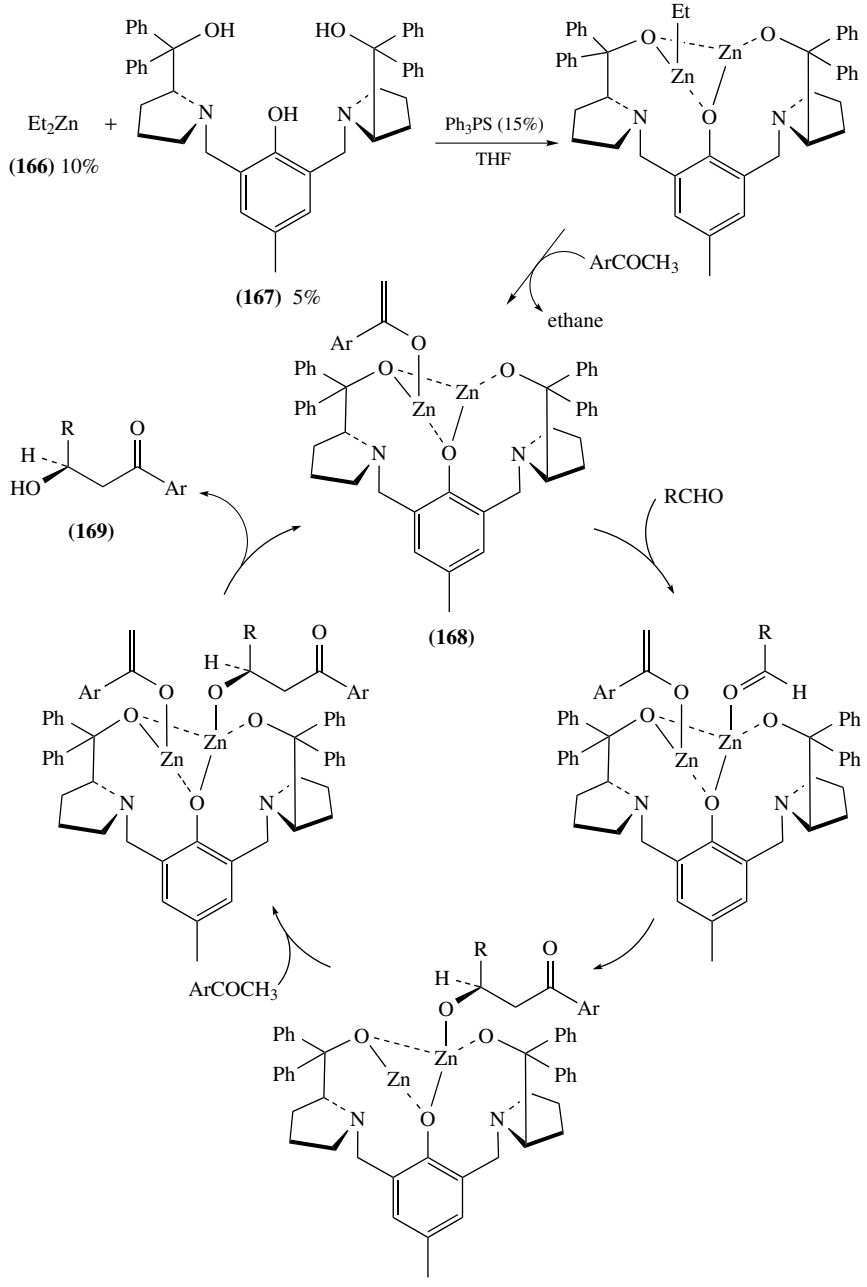
Et2Zn +
(166) 10%
(167) 5%
Ph3PS (15%)
THF
ethane
ArCOCH3
RCHO
(168)
(169)
ArCOCH3

FIGURE 12

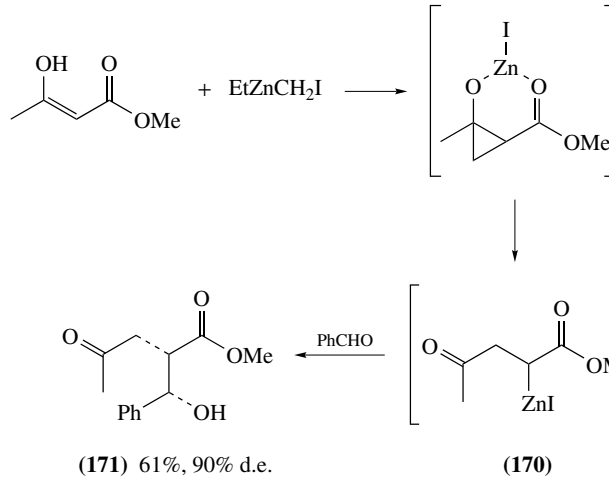

(85)

(171) 61%, 90% d.e. **(170)**

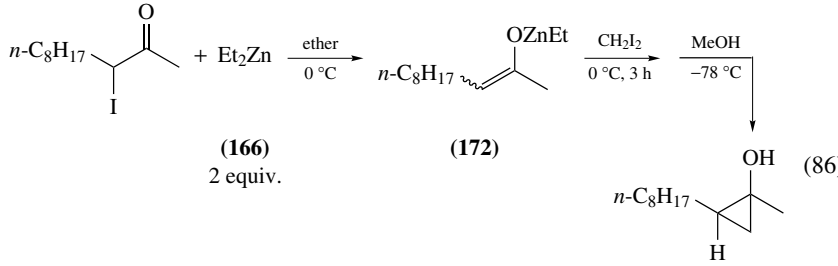

(166)
2 equiv.

(172)

(86)

(173) 82%
cis/*trans* = 93:7

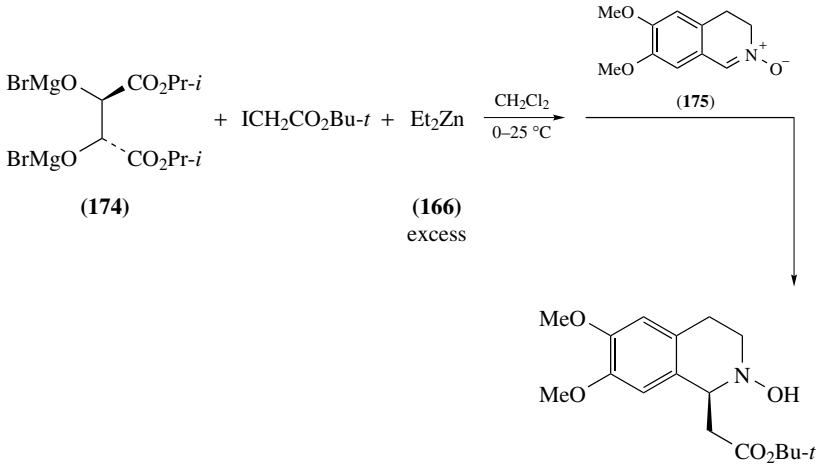

(174)

(166)
excess

(175)

40–90%
up to 82% e.e.

(87)

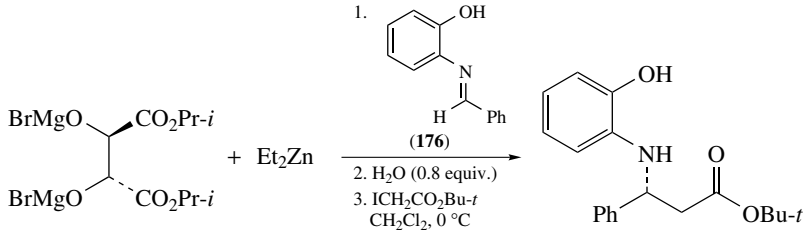

(88)

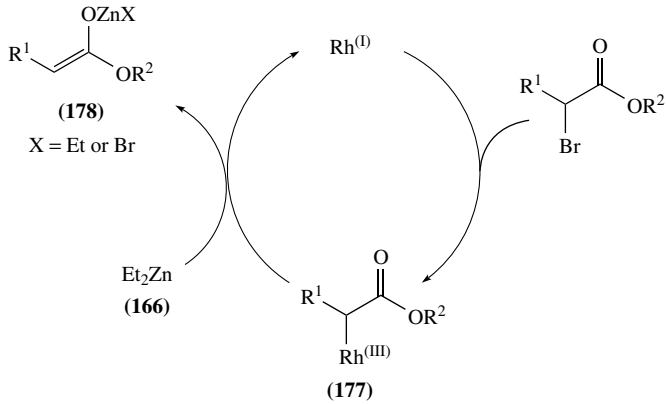

FIGURE 13

If a carbonyl compound is present, the classical addition product is obtained; unfortunately, with propanoic acid derivatives the addition is not diastereoselective (equation 89). Several intramolecular examples have also been reported[183].

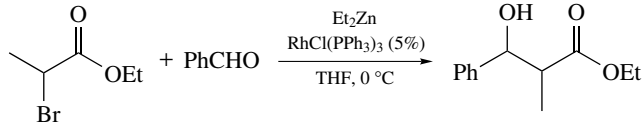

(89)

The rhodium-catalysed Reformatsky protocol has also been applied to aldimines; the selective formation either of β-aminoesters or of β-lactams[184a] is achievable by a proper choice of solvent and temperature, as outlined in equation 90.

The imine may be also prepared *in situ* in a one-pot procedure. Thus, to a crude THF solution of the *in situ* produced (*R*)-phenyl glycinol derived imine **179** are successively added the Wilkinson's catalyst, **1b** and **166**. The enantiomerically pure **180** was isolated in 85% yield (equation 91)[184b].

Ethyl bromodifluoroacetate **1c** was also used in the rhodium-catalysed Reformatsky protocol; the reaction was optimized in acetonitrile as solvent and worked particularly

well with ketones, thus successfully competing with the classical Reformatsky protocol discussed in Section II.B.1 (equations 14–16)[185].

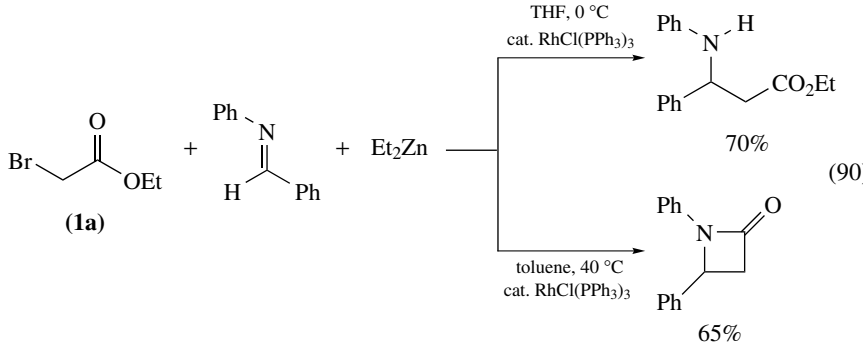

(90)

(**1a**)

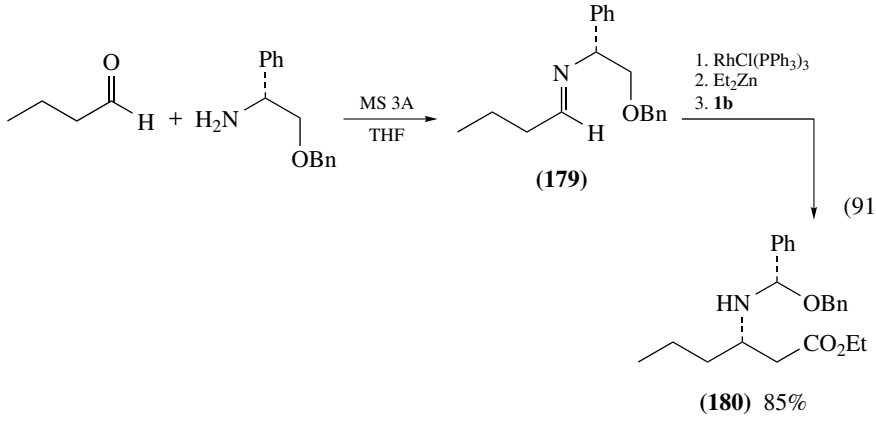

(**179**)

(91)

(**180**) 85%

Dialkylzinc derivatives are inert towards conjugated enones (e.g. **181**) in hydrocarbon or ethereal solvents. The discovery that a conjugate addition can be promoted by Cu(I) salts in the presence of suitable ligands L (e.g. sulphonamide **182**) opened a new route to zinc enolates (e.g. **183**), and hence to the development of three-component protocols, such as the tandem 1,4-addition/aldol addition process outlined in equation 92[186]. If the addition of the aldehyde is carried out at −78 °C, the single adduct **184** is formed, among four possible diastereomeric products. The presence of sulphonamide is fundamental in terms of reaction kinetics; its role is supposed to be in binding both Cu(I) and Zn(II) and forming a mixed metal cluster compound which acts as the true 1,4-addition catalyst.

The presence of a supplementary ligand inspired the design of asymmetric catalytic processes[187]. A breakthrough in the field of copper-catalysed dialkylzinc 1,4-additions was given by phosphoramidite ligands, developed by Feringa and coworkers[188]. One of them, **185**, incorporates two 'matched' chiral substructures, namely the (*S*)-2,2′-binaphthol and the (*R*,*R*)-bis(1-phenylethyl)amine units; the catalyst is simply prepared by mixing **185** and $Cu(OTf)_2$, which was found more efficient than Cu(I) salts, even though the actual catalyst is a Cu(I) complex. Two examples of conjugate addition/enolate trapping reactions, catalysed by the copper complex of **185**, are reported in equations 93[188a] and 94[189].

The latter example shows that in selecting the matched pair *ent*-**185** and acetal **186**, an astonishing high level of double stereodifferentiation can be obtained, affording **187** as a single product. A Lewis acid (TMSOTf) is necessary to activate the acetal functionality.

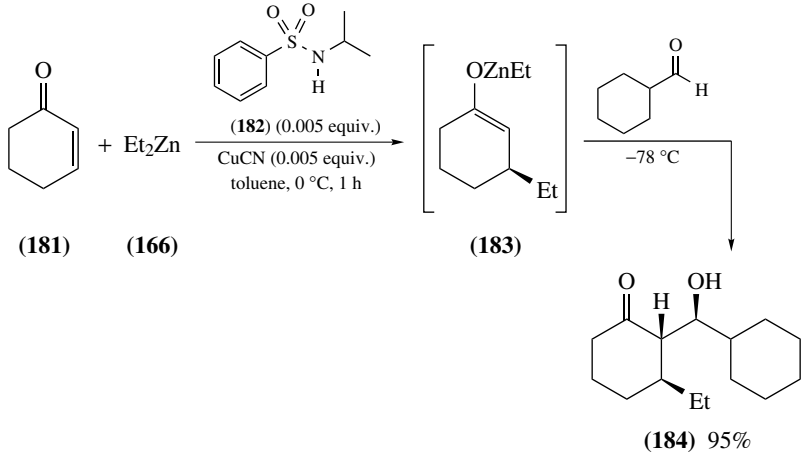

(92)

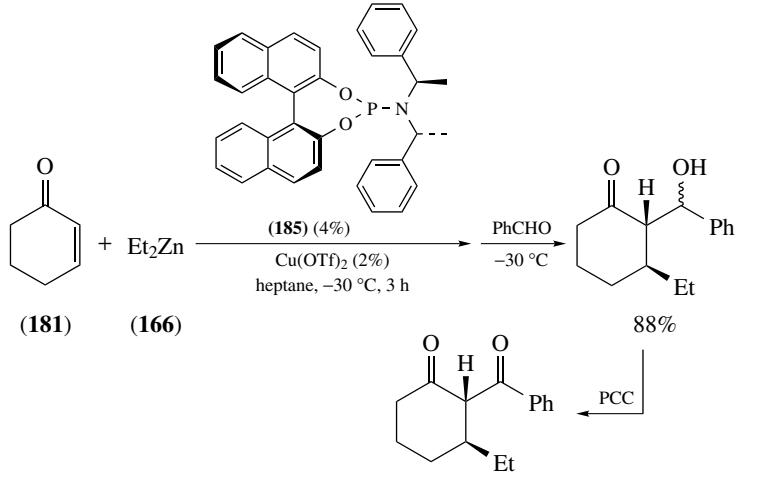

(93)

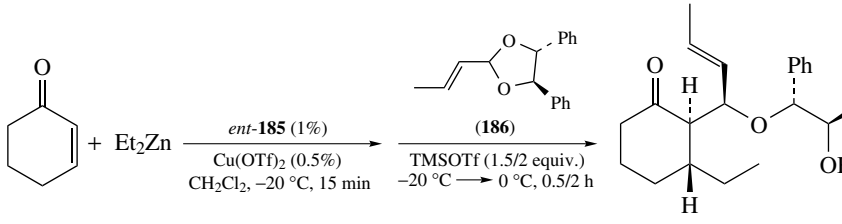

(94)

The opportunity offered by peptides as chelators for both zinc and copper, combined with their easy preparation from readily available starting materials, urged Hoveyda and coworkers to check peptide-based phosphine ligands for the copper-catalysed 1,4 addition of dialkylzinc derivatives. Efficient and enantioselective procedures based on iminophosphines (e.g. **188**) were developed, where critical is the choice of the amino acid pair in terms of reaction rates and in terms of maximum cooperation between the two amino acidic building blocks in determining enantiocontrol (equation 95)[190]. Iminophosphine **189**, with a single amino acid residue, allows one to get exceptionally high enantiocontrol, too. In equation 96, the asymmetric conjugate addition is followed by the alkylation of the intermediate enolate[190b].

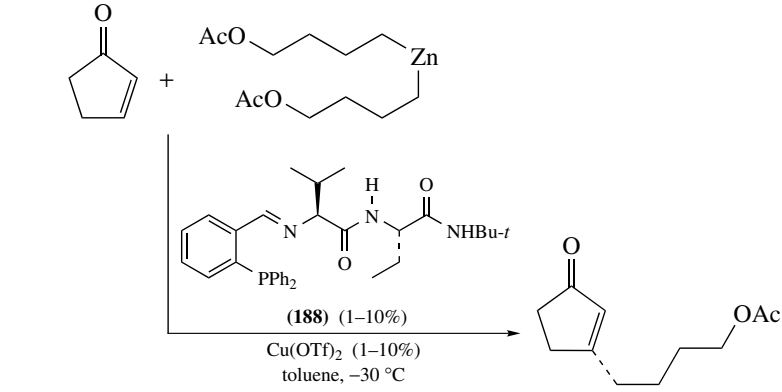

(95)

55%, 98% e.e.

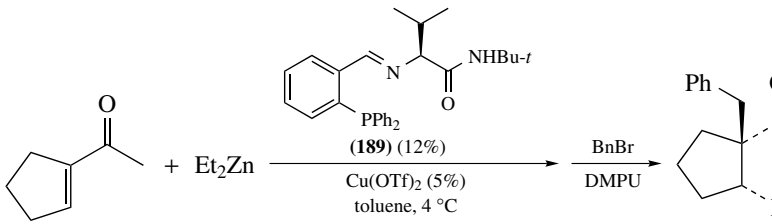

(96)

(166) 70%, 90% d.e.

VI. ZINC DIENOLATES

A major challenge in the chemistry of dienolates is the control of regiochemistry. A number of factors determine the final regiochemical outcome (α *vs* γ attack) of the reaction between **190** and an electrophile E^+ (equation 97).

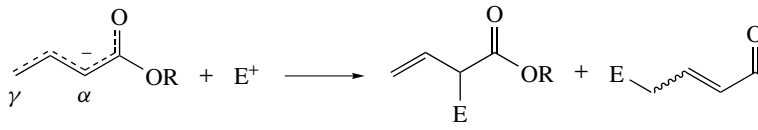

(97)

(190) α-adduct γ-adduct

In this section, reactions of zinc dienolates with carbonyl compounds, imines and conjugated enones will be considered; all of these reactions have been proved to be reversible, and, hence, conditions favouring either kinetic or thermodynamic control will drive the reaction towards the formation of different regioisomers. Generally, equilibrating conditions lead to attack at the γ position of **190**, as a thermodynamically more stable conjugated carbonyl or carboxylic compound is formed; on the other hand, kinetic control leads to attack at the electron richer α-position.

In the first reports on the use of esters of 4-bromo-2-butenoic acid (**191a** and **b**, crotonic acid) and of 4-bromo-3-methyl-2-butenoic acid (**191c**, senecioic acid), the corresponding Reformatsky reactions with benzaldehyde were performed with the old-fashioned procedure, which required heating the haloester, the aldehyde and granulated zinc in benzene/ether mixtures at reflux temperature.

Under these conditions γ-adducts and two downstream products, a dienoate and a lactone, were isolated in variable yields, also depending on the purification procedure adopted (distillation *vs* crystallization) (equation 98)[191].

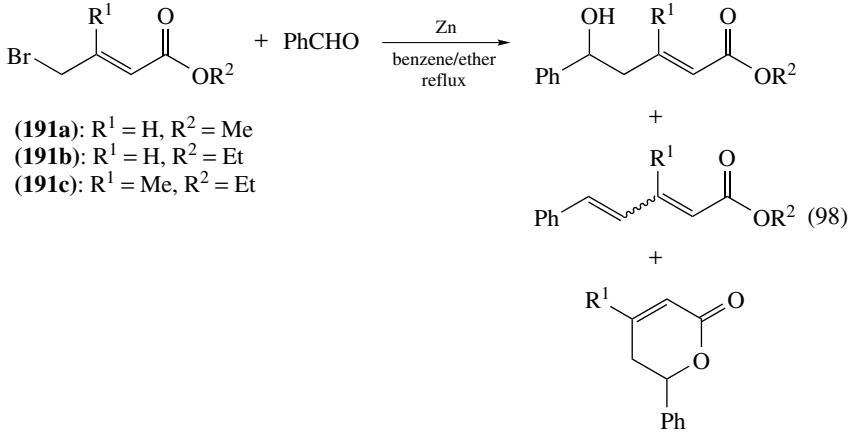

(**191a**): $R^1 = H$, $R^2 = Me$
(**191b**): $R^1 = H$, $R^2 = Et$
(**191c**): $R^1 = Me$, $R^2 = Et$

(98)

In the 1980s Gaudemar brought evidence, in a number of synthetic and mechanistic studies, that α/γ ratios must be interpreted in terms of solvent, temperature and substituent effects[192].

When **191a** was used in a vinylogous Reformatsky reaction with the 3-ulose derivative **192** in refluxing ether, a 2:1 α/γ adduct ratio was obtained (equation 99). The facial selectivity ensured by the rigid bicyclic framework of **192** was accompanied by a complete simple diastereoselectivity in the formation of the α-adduct[193].

An example of the directing effect on the regiochemical course of a substituent on the dienolate skeleton is outlined in equation 100. The ethoxy substituent in **193b** likely increases the electron density on carbon-4 and completely reverses regioselectivity in favour of the γ-adduct[194], with respect to **193a**[195]. Evidence of retroaldolization is given by the remarkable $E \rightarrow Z$ isomerization upon prolonged heating, which transforms the E-configured γ-adduct into 5,5-difluoro-5,6-dihydro-4-ethoxy-6-phenylpyran-2-one. This reaction works with aromatic or conjugated aldehydes only, while aliphatic aldehydes quench the Reformatsky reagent by protonation.

The chromium(II) version of the Reformatsky reaction of **191** with ketones also generates α-adducts, thus giving access to adjacent quaternary centres. Reactions are carried out using the $CrCl_2$/LiI system[65] at room temperature in a variety of polar solvents. The

amount of the minor γ-regioisomer was found to mainly depend on the steric bulk of ketone substituents[196].

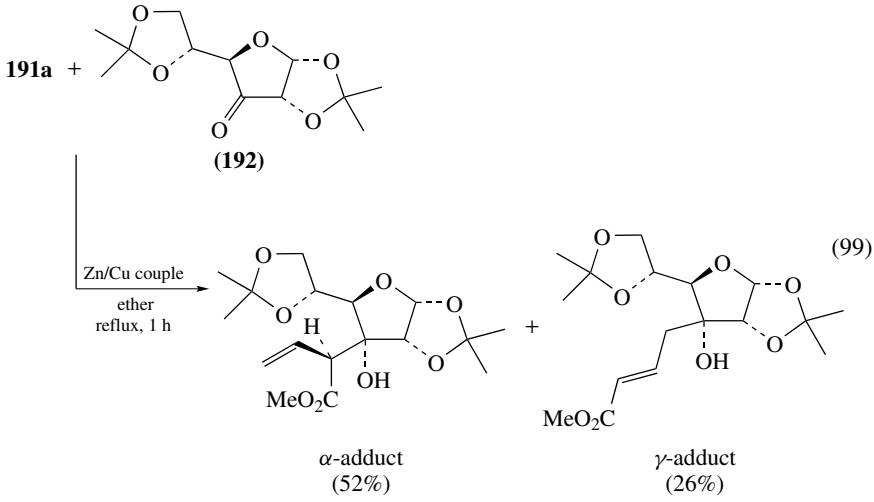

(99)

(193a): R = H
(193b): R = OEt (3 h)
(193b): R = OEt (8 h)

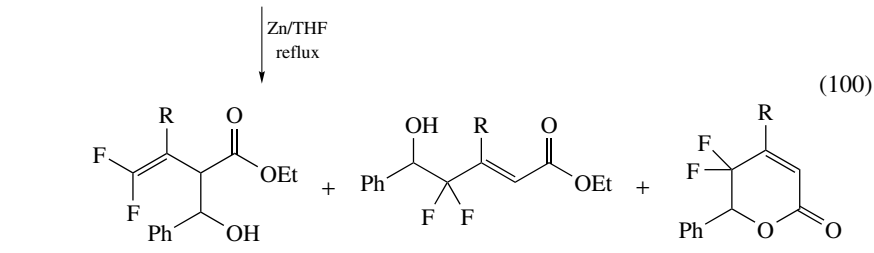

(100)

	α-adduct	γ-adducts	
(193a):	81% (*syn*/*anti* 1:1)	0	0
(193b):	0	80	0
(193b):	0	0	65

The joint effect of substituents and of temperature is clearly evident in imino-Reformatsky reactions of zinc dienolates[197]. At −78 °C, imines **194a–d** react with crotonate derived zinc-dienolate **195**, affording the products listed in Table 4. Imine substituents play a fundamental role in controlling the reaction regiochemistry.

Moving from **195** to senecioate enolate **196**, the introduction of a methyl group leads to strong regiochemical effects: only γ-adducts are obtained at −78 °C with **194a**

TABLE 4. Nucleophilic addition of crotonate zinc dienolate **195** to imines **194a–d** in THF at −78 °C

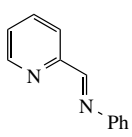

(194a)

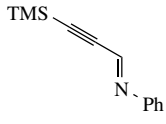

(194b)

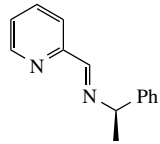

(194c)

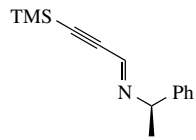

(194d)

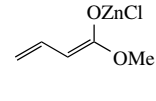

(195)

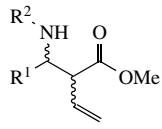

α-adduct

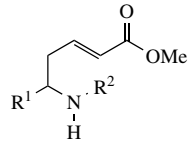

γ-adduct

	α-adduct, Yield(%)	*syn/anti*	γ-adduct, Yield(%)	d.e. (%)
194a	60	30:70	40	—
194b	>98	20:80	0	—
194c	0	—	>98	92
194d	0	—	>98	15

(equation 101), while the role of thermodynamic equilibration when the temperature is raised from −78 to 20 °C is apparent in equation 102.

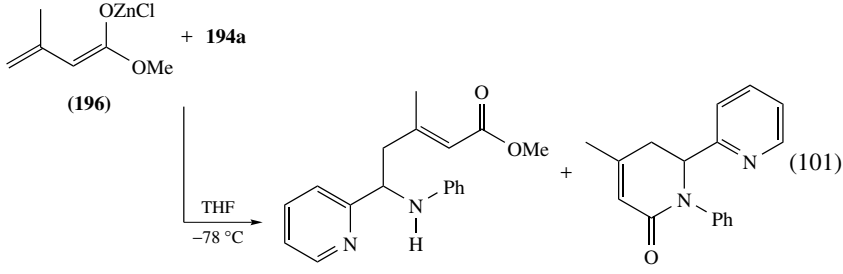

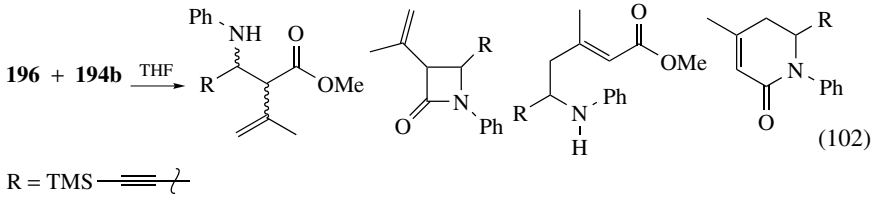

$T = -78$ °C	100	0	0	0
$T = -20$ °C	4	19	25	52

Again, the use of the homochiral imine **194c** ensures a good level of asymmetric induction (equation 103).

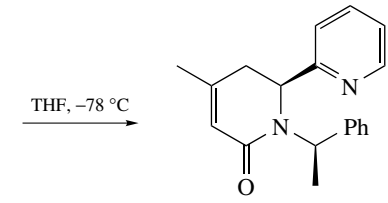

100%, 77% d.e. (103)

Fully aromatic Schiff bases react with zinc dienolates, derived from trimethylsilyl 3-butenoate (**197a**) and trimethylsilyl 3-methyl-3-butenoate (**197b**), at −70 °C in a perfect regio- and diastereoselective way to *anti*-α-adducts only (equation 104)[198]. The same authors previously devised a complementary route to γ-adducts by exploiting $ZnCl_2$ as Lewis acid in a Mukaiyama reaction between silyl dienolates **198** and aromatic Schiff bases (equation 105)[199]. Even though very few reports are present in the literature, zinc dienolates may also react with α,β-unsaturated carbonyl compounds. The challenge of this reaction is to control the double regiochemical issue, since four adducts are possible, labelled as 1,2-α,1,2-γ, 1,4-α and 1,4-γ (Table 5). It should also be noted that adducts 1,2-α and 1,2-γ could in principle be converted into 1,4-γ and 1,4-α, respectively, via [3,3]-oxy-Cope rearrangements.

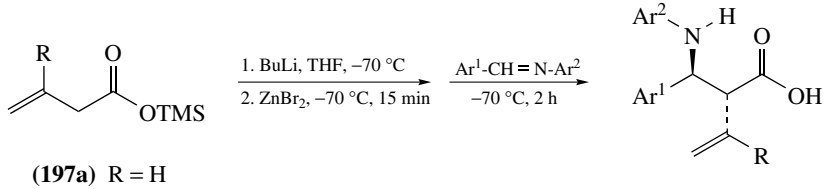

(197a) R = H
(197b) R = Me

55–74% (104)

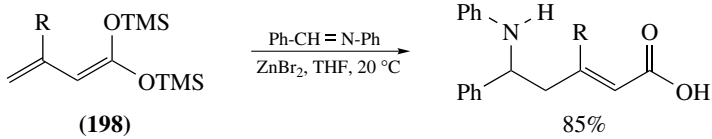

(198) 85% (105)

Table 5 collects results obtained with **191b** and benzalacetone in different solvents at their reflux temperature[200].

The first two entries show that, after 1 minute, the 1,2-α is the sole product, but after 1 h the equilibrium is shifted towards the formation of 1,4-γ. Evidence is given for the combined effect of retroaldolization and of oxy-Cope rearrangement to the equilibration process. The latter process is estimated to contribute about 20% of final 1,4-γ adduct. The thermodynamic most stable regioisomer 1,4-γ dominates in refluxing THF, while the 1,2-γ adduct prevails in less polar solvent (benzene). Finally, the 1,4-α adduct is never observed in all the conditions examined, even though it is interesting to underline that it represents the major adduct when the lithium dienolate deriving from ethyl crotonate is condensed with conjugated enones at −78 °C.

A further example stressing the effect on regiochemistry exerted by the presence of a methyl group on the dienolate moiety is given by ketone **199** in the reaction with pure

TABLE 5. Reformatsky reaction of 4-bromocrotonate **191b** with benzalacetone

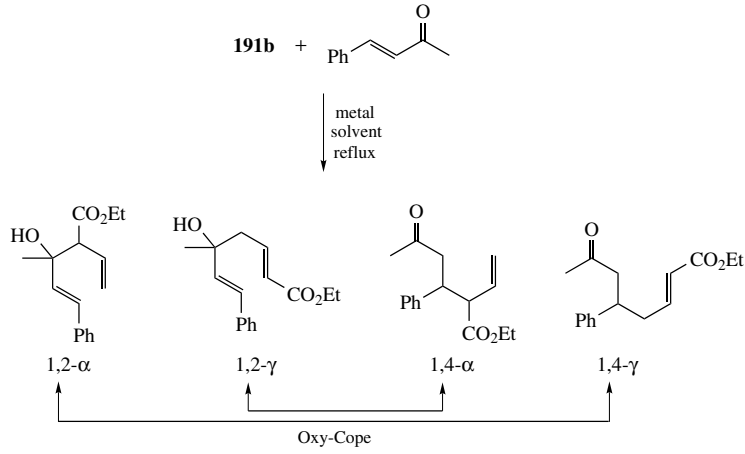

	Products distribution			
	1,2-α	**1,2-γ**	**1,4-α**	**1,4-γ**
Zn/Cu-$(AcOH)_{traces}$-ether-1 min	100	0	0	0
Zn/Cu-$(AcOH)_{traces}$-ether-1 h	16	26	0	58
Zn-benzene	15	60	0	25
Zn-THF-2h	traces	traces	0	>90

(*E*)- or (*Z*)-**191b** and **191c** under classical Reformatsky conditions (Zn, THF, reflux) (equations 106 and 107). It must be noted that **199** is denoted by a very poor reactivity, as testified by the impossibility to force it to react with simple Reformatsky reagents deriving from bromoacetates. In these examples, the starting configuration of the vinylogous bromoester has no effect on the product composition, both **191b** and **191c** react at the γ-position, but a perfect shift from 1,4-addition to 1,2-addition is obtained by simply moving from crotonate to senecioate[201]. Thus, both pure (*E*)-**191b** and (*Z*)-**191b** afforded moderate yields of mixtures of γ-1,4-adduct **200** and of lactone **201**, the latter derived from intramolecular hetero-Michael addition of the enolised ketone to the enoate group in **200** in a 6-*exo-trig* mode (equation 106). On the other hand, both (*E*)-**191c** and (*Z*)-**191c** converge to give trienoic acid **202** as single addition product; its likely origin is depicted in equation 107. The initially formed α-1,4-adduct, after isomerization to the (*Z*)-configured adduct and lactonization, could undergo base-catalysed elimination promoted by EtOZnBr, with formation of **202**.

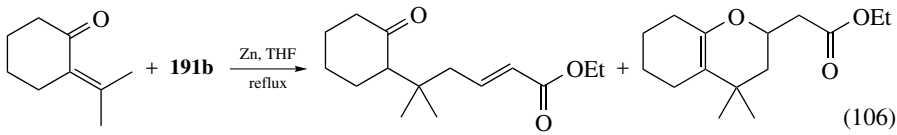

(106)

(199) **(200)** **(201)**

(*E*)-**191b**: 42% overall, **200/201** = 1:1
(*Z*)-**191b**: 49% overall, **200/201** = 4:6

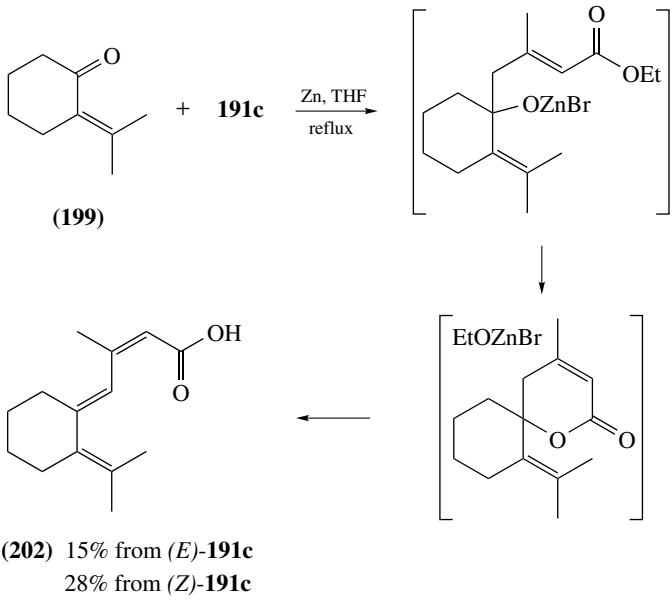

(107)

(202) 15% from *(E)*-**191c**
28% from *(Z)*-**191c**

In conclusion, the regiochemical outcome of a vinylogous Reformatsky reaction can be modified by checking the following variables: (i) the way the enolate is produced, (ii) the solvent, (iii) the temperature and (iv) the reaction time, if equilibration is supposed to be in action.

VII. CONCLUSIONS

Historically, Reformatsky reaction allowed the first efficient generation of an ester enolate, thus opening an efficient route to β-hydroxy esters. However, weak points affecting this reaction in the original experimental protocols, particularly a low level of stereochemical control and the occurrence of side products, limited the applications of zinc enolates, particularly when stereodefined aldol products were required. In this chapter, recent applications which outline the present status of the art have been presented, and a number of modern synthetic methods which ensured the renaissance of Reformatsky reaction in the last three decades have been reviewed. Just to remember a few remarkable issues, the insertion of different metals into α-haloesters produces metal enolates which compete favourably with zinc enolates in stereochemical terms; a variety of protocols for zinc activation proved to be precious for fast and quantitative zinc insertion; alternative routes to zinc enolates have been devised and exploited in unprecedented applications. Among recent efforts to introduce enantiocontrol on Reformatsky reactions, worthy of note is the design of chiral ligands (e.g. enantiopure aminoalcohols in Table 2), but the most challenging goal, the development of catalytic asymmetric protocols similar to those developed for other organozinc reagents, has not yet been attained.

VIII. REFERENCES

1. W. R. Vaughan and H. P. Knoess, *J. Org. Chem.*, **35**, 2394 (1970).
2. (a) F. Orsini, F. Pelizzoni and G. Ricca, *Tetrahedron Lett.*, **23**, 3945 (1982).
   (b) F. Orsini, F. Pelizzoni and G. Ricca, *Tetrahedron*, **40**, 2781 (1984).

(c) D. J. Burton and J. C. Easdon, *J. Fluorine Chem.*, **38**, 125 (1988).
(d) D. Pini, G. Uccello-Barretta, A. Mastantuono and P. Salvadori, *Tetrahedron*, **53**, 6065 (1997).
3. W. Hörner and H. Bertagnolli, *J. Organomet. Chem.*, **649**, 128 (2002).
4. J. Dekker, J. Boersma and G. J. M. van der Kerk, *J. Chem. Soc., Chem. Commun.*, 553 (1983).
5. J. Dekker, A. Schouten, P. H. M. Budzelaar, J. Boersma, G. J. M. van der Kerk, A. L. Spek and A. J. M. Duisenberg, *J. Organomet. Chem.*, **320**, 1 (1987).
6. M. J. S. Dewar and K. M. Merz, Jr., *J. Am. Chem. Soc.*, **109**, 6553 (1987).
7. J. Maiz, A. Arrieta, X. Lopez, J. M. Ugalde, F. P. Cossío and B. Lecea, *Tetrahedron Lett.*, **34**, 6111 (1993).
8. P. B. Chock, J. Halpern and F. E. Paulik, *Inorg. Synth.*, **14**, 90 (1973).
9. (a) W. C. Zeise, *Poggendorff Ann.*, **9**, 632 (1827).
(b) W. C. Zeise, *Magazine Pharm.*, **35**, 105 (1830).
10. E. Frankland, *Liebigs Ann. Chem.*, **71**, 171 (1848).
11. S. N. Reformatsky, *Ber. Dtsch. Chem. Ges.*, **20**, 1210 (1887).
12. (a) R. L. Shriner, *Org. React.*, **1**, 1 (1942).
(b) D. G. M. Diaper and A. Kuksis, *Chem. Rev.*, **59**, 89 (1959).
(c) M. Gaudemar, *Organomet. Chem. Rev. (A)*, **8**, 183 (1972).
(d) M. W. Rathke, *Org. React.*, **22**, 423 (1975).
(e) A. Fürstner, *Synthesis*, 571 (1989).
(f) E. Tagliavini, C. Trombini and A. Umani-Ronchi, *Adv. Carbanion Chem.*, **2**, 111 (1996).
(g) A. Fürstner, in *Organozinc Reagents* (Eds. P. Knochel and P. Jones), Oxford University Press, Oxford, 1999, p. 287.
(h) R. Ocampo and W. R. Dolbier, Jr., *Tetrahedron*, **60**, 9325 (2004).
13. H. Gilman and M. Speeter, *J. Am. Chem. Soc.*, **65**, 2255 (1943).
14. E. C. Kornfeld, E. J. Fornefeld, G. B. Kline, M. J. Mann, D. E. Morrison, R. G. Jones and R. B. Woodward, *J. Am. Chem. Soc.*, **78**, 3087 (1956).
15. M. S. Newman, *J. Am. Chem. Soc.*, **64**, 2131 (1942).
16. M. Bellassoued, M. Gaudemar, A. El Borgi and B. Baccar, *J. Organomet. Chem.*, **280**, 165 (1985).
17. C. R. Hauser, *Org. Synth. Coll. Vol.* **3**, 408 (1955).
18. W. R. Vaughan, S. C. Bernstein and M. E. Lorber, *J. Org. Chem.*, **30**, 1790 (1965).
19. (a) R. D. Rieke, *Acc. Chem. Res.*, **10**, 301 (1977).
(b) E. Erdik, *Tetrahedron*, **43**, 2203 (1987).
(c) R. D. Rieke, *Science*, **246**, 1260 (1989).
(c) A. Fürstner, *Angew. Chem., Int. Ed. Engl.*, **32**, 164 (1993).
(d) R. D. Rieke and M. V. Hanson, *Tetrahedron*, **53**, 1925 (1997).
20. F. W. Lichtenthaler, M. Lergenmüller and S. Schwidetzky, *Eur. J. Org. Chem.*, 3094 (2003).
21. (a) C. Palomo, J. M. Aizpurua, M. C. López and N. Aurrekoetxea, *Tetrahedron Lett.*, **31**, 2205 (1990).
(b) I. Izquierdo, M. T. Plaza, J. A. Tamayo and A. J. Mota, *Synthesis*, 1083 (2004).
22. A. S. Demir, C. Tanyeli, A. S. Mahasneh and H. Aksoy, *Synthesis*, 155 (1994).
23. J. F. Ruppert and J. D. White, *J. Org. Chem.*, **39**, 269 (1974).
24. K. Tanaka and F. Toda, *Chem. Rev.*, **100**, 1025 (2000).
25. T. Kitazume and K. Kasai, *Green Chem.*, **3**, 30 (2001).
26. L. W. Bieber, I. Malvestiti and E. C. Storch, *J. Org. Chem.*, **62**, 9061 (1997).
27. K. Takai, T. Kakiuchi and K. Utimoto, *J. Org. Chem.*, **59**, 2671 (1994).
28. G. Picotin and P. Miginiac, *J. Org. Chem.*, **52**, 4796 (1987).
29. P. Gomes, C. Gosmini and J. Périchon, *Synthesis*, 1909 (2003).
30. A. Chattopadhyay and A. Salaskar, *Synthesis*, 561 (2000).
31. K. Tanaka, S. Kishigami and F. Toda, *J. Org. Chem.*, **56**, 4333 (1991).
32. E. Santaniello and A. Manzocchi, *Synthesis*, 698 (1977).
33. M. Bortolussi and J. Seyden-Penne, *Synth. Commun.*, **19**, 2355 (1989).
34. K. S. Suslick and S. J. Doktycz, *J. Am. Chem. Soc.*, **111**, 2342 (1989).
35. B.-H. Han and P. Boudjouk, *J. Org. Chem.*, **47**, 5030 (1982).
36. N. A. Ross and R. A. Bartsch, *J. Org. Chem.*, **68**, 360 (2003).
37. N. A. Ross, R. A. Bartsch and A. P. Marchand, *ARKIVOC*, 27 (2003); available on the web at: http://www.arkat-usa.org/ark/journal/2003/I12_Shine/HS-766J/HS-766J.asp.

38. N. A. Ross and R. A. Bartsch, *J. Heterocycl. Chem.*, **38**, 1255 (2001).
39. N. A. Ross, R. R. MacGregor and R. A. Bartsch, *Tetrahedron*, **60**, 2035 (2004).
40. (a) S. Caddick, *Tetrahedron*, **51**, 10403 (1995).
    (b) C. Gabriel, S. Gabriel, E. H. Grant, B. S. J. Halstead and D. M. P. Mingos, *Chem. Soc. Rev.*, **27**, 213 (1998).
41. A. G. Whittaker and D. M. P. Mingos, *J. Chem. Soc., Dalton Trans.*, 2751 (1992).
42. A. R. Gholap and A. P. Chavan, *J. Chem. Res. (S)*, 374 (2003).
43. (a) R. D. Rieke, S. J. Uhm and P. M. Hundall, *J. Chem. Soc., Chem. Commun.*, 269 (1973).
    (b) R. D. Rieke and S. J. Uhm, *Synthesis*, 452 (1975).
44. D. Savoia, C. Trombini and A. Umani-Ronchi, *Pure Appl. Chem.*, **57**, 1887 (1985).
45. G. P. Boldrini, D. Savoia, E. Tagliavini, C. Trombini and A. Umani-Ronchi, *J. Org. Chem.*, **48**, 4108 (1983).
46. (a) R. Csuk, A. Fürstner and H. Weidmann, *J. Chem. Soc., Chem. Commun.*, 775 (1986).
    (b) R. Csuk, B. I. Glänzer and A. Fürstner, *Adv. Organomet. Chem.*, **28**, 85 (1988).
47. R. T. Arnold and S. T. Kulenovic, *Synth. Commun.*, **7**, 223 (1977).
48. (a) R. D. Rieke, P. T.-J. Li, T. P. Burns and S. T. Uhm, *J. Org. Chem.*, **46**, 4323 (1981).
    (b) M. V. Hanson, J. D. Brown, R. D. Rieke and Q. J. Niu, *Tetrahedron Lett.*, **35**, 7205 (1994).
49. M. Makosza, K. Grela and W. Fabianowski, *Tetrahedron*, **52**, 9575 (1996).
50. M. Makosza, P. Nieczypor and K. Grela, *Tetrahedron*, **54**, 10827 (1998).
51. M. V. Hanson and R. D. Rieke, *Synth. Commun.*, **25**, 101 (1995).
52. P. Boudjouk, D. P. Thompson, W. H. Ohrbom and B.-H. Han, *Organometallics*, **5**, 1257 (1986).
53. Y. Rollin, C. Gebehenne, S. Derien, E. Duñach and J. Périchon, *J. Organomet. Chem.*, **461**, 9 (1993).
54. (a) A. Durant, J.-L. Delplancke, R. Winand and J. Reisse, *Tetrahedron Lett.*, **36**, 4257 (1995).
    (b) A. Durant, J.-L. Delplancke, V. Libert and J. Reisse, *Eur. J. Org. Chem.*, 2845 (1999).
55. J. Chaussard, J.-C. Folest, J.-Y. Nedelec, J. Périchon, S. Sibille and M. Troupel, *Synthesis*, 369 (1990).
56. (a) K.-H. Schwarz, K. Kleiner, R. Ludwig and H. Schick, *J. Org. Chem.*, **57**, 4013 (1992).
    (b) K.-H. Schwarz, K. Kleiner, R. Ludwig and H. Schick, *Chem. Ber.*, **126**, 1247 (1993).
57. A. Conan, S. Sibille and J. Périchon, *J. Org. Chem.*, **56**, 2018 (1991).
58. J. C. Adrian, Jr. and M. L. Snapper, *J. Org. Chem.*, **68**, 2143 (2003).
59. H. Schick, R. Ludwig, K.-H. Schwarz, K. Kleiner and A. Kunath, *J. Org. Chem.*, **59**, 3161 (1994).
60. F. Orsinic and G. Sello, *Curr. Org. Synthesis*, **1**, 111 (2004).
61. Y. Yokoyama, T. Tsuchikawa, M. Hiramatsu and K. Mochida, *Main Group Metal Chem.*, **23**, 691 (2000).
62. (a) A. Kagayama, K. Igarashi, I. Shiina and T. Mukaiyama, *Bull. Chem. Soc. Jpn.*, **73**, 2579 (2000).
    (b) T. Mukaiyama, A. Kagayama, K. Igarashi and I. Shiina, *Chem. Lett.*, 1157 (1999).
63. J. D. Parrish, D. R. Shelton and R. D. Little, *Org. Lett.*, **5**, 3615 (2003).
64. Y. Kataoka, I. Makihira, T. Yamagata and K. Tani, *Organometallics*, **16**, 4788 (1997).
65. (a) L. Wessjohann and T. Gabriel, *J. Org. Chem.*, **62**, 3772 (1997).
    (b) T. Gabriel and L. Wessjohann, *Tetrahedron Lett.*, **38**, 1363 (1997).
    (c) T. Gabriel and L. Wessjohann, *Tetrahedron Lett.*, **38**, 4387 (1997).
    (d) R. Wittenberg, C. Beier, G. Dräger, G. Jas, C. Jasper, H. Monenschein and A. Kirschning, *Tetrahedron Lett.*, **45**, 4457 (2004).
66. K. Takai, T. Ueda, T. Hayashi and T. Moriwake, *Tetrahedron Lett.*, **37**, 7049 (1996).
67. G. Cahiez and P.-Y. Chavant, *Tetrahedron Lett.*, **30**, 7373 (1989).
68. H. Kakiya, S. Nishimae, H. Shinokubo and K. Oshima, *Tetrahedron*, **57**, 8807 (2001).
69. Y. S. Suh and R. D. Rieke, *Tetrahedron Lett.*, **45**, 1807 (2004).
70. M. Durandetti, C. Meignein and J. Périchon, *Org. Lett.*, **5**, 317 (2003).
71. (a) F. Orsini and C. Leccioli, *Tetrahedron: Asymmetry*, **8**, 4011 (1997).
    (b) F. Orsini, *Tetrahedron Lett.*, **39**, 1425 (1998).
    (c) F. Orsini, *J. Org. Chem.*, **62**, 1159 (1997).
    (d) J. J. Duffield and G. R. Pettit, *J. Nat. Prod.*, **64**, 472 (2001).

(e) G. R. Pettit and M. P. Grealish, *J. Org. Chem.*, **66**, 8640 (2001).
(f) F. Orsini and E. Di Teodoro, *Tetrahedron: Asymmetry*, **14**, 2521 (2003).
72. H. Kagoshima, Y. Hashimoto, D. Oguro and K. Saigo, *J. Org. Chem.*, **63**, 691 (1998).
73. J. Podlech and T. C. Maier, *Synthesis*, 633 (2003).
74. A. Yanagisawa, H. Takahashi and T. Arai, *Chem. Commun.*, 580 (2004).
75. Y. Aoyagi, W. Tanaka and A. Ohta, *J. Chem. Soc., Chem. Commun.*, 1225 (1994).
76. Z. Shen, J. Zhang, H. Zou and M. Yang, *Tetrahedron Lett.*, **38**, 2733 (1997).
77. (a) S. Fukuzawa, M. Tatsuzawa and K. Hirano, *Tetrahedron Lett.*, **39**, 6899 (1998).
(b) S. Fukuzawa, H. Matsuzawa and S. Yoshimitsu, *J. Org. Chem.*, **65**, 1702 (2000).
78. M. Obringer, F. Colobert, B. Neugnot and G. Solladié, *Org. Lett.*, **5**, 629 (2003).
79. (a) I. Shiina, K. Uoto, N. Mori, T. Kosugi and T. Mukaiyama, *Chem. Lett.*, 181 (1995).
(b) S. Ichikawa, S. Shuto, N. Minakawa and A. Matsuda, *J. Org. Chem.*, **62**, 1368 (1997).
(c) T. Nagamitsu, D. Takano, T. Fukuda, K. Otoguro, I. Kuwajima, Y. Harigaya and S. Omura, *Org. Lett.*, **6**, 1865 (2004).
(d) M. Inoue, M. Sasaki and K. Tachibana, *J. Org. Chem.*, **64**, 9416 (1999).
(e) H. Kigoshi, M. Kita, S. Ogawa, M. Itoh and D. Uemura, *Org. Lett.*, **5**, 957 (2003).
80. M.-I. Lannou, F. Hélion and J.-L Namy, *Tetrahedron*, **59**, 10551 (2003).
81. M. Shimizu, F. Kobayashi and R. Hayakawa, *Tetrahedron*, **57**, 9591 (2001).
82. I. Shibata, T. Suwa, H. Sakakibara and A. Baba, *Org. Lett.*, **4**, 301 (2002).
83. H. Kagoshima, Y. Hashimoto and K. Saigo, *Tetrahedron Lett.*, **39**, 8465 (1998).
84. Y. Hashimoto and S. Kikuchi, *Chem. Lett.*, 126 (2002).
85. V. V. Shchepin and N. F. Kirillov, *Chem. Heterocycl. Compds.*, **36**, 1110 (2001).
86. V. V. Shchepin, D. V. Fotin, A. N. Nedugov and V. V. Fotin, *Russ. J. Org. Chem.*, **38**, 256 (2002).
87. R. Filler, Y. Kobayashi and L. M. Yagupolskii (Eds.), *Organofluorine Compounds in Medicinal Chemistry and Biomedical Applications*, Elsevier, Amsterdam, 1993.
88. M. J. Tozer and T. F. Herpin, *Tetrahedron*, **52**, 8619 (1996).
89. S. Watanabe, T. Fujita, M. Sakamoto, H. Takeda, T. Kitazume and T. Yamazaki, *J. Fluorine Chem.*, **82**, 1 (1997).
90. H. Fukuda and T. Kitazume, *J. Fluorine Chem.*, **74**, 171 (1995).
91. R. Ocampo, W. R. Dolbier, Jr. and R. Paredes, *J. Fluorine Chem.*, **88**, 41 (1998).
92. Y. Wang and S. Zhu, *Tetrahedron Lett.*, **42**, 5741 (2001).
93. T. R. Johnson and R. B. Silverman, *Bioorg. Med. Chem.*, **7**, 1625 (1999).
94. P. L. Coe, M. Markou and J. C. Tatlow, *J. Fluorine Chem.*, **89**, 183 (1998).
95. (a) R. Noyori and M. Kitamura, *Angew. Chem., Int. Ed. Engl.*, **30**, 49 (1991).
(b) L. Pu and H.-B. Yu, *Chem. Rev.*, **101**, 757 (2001).
(c) B. Fu, D.-M. Du and J. Wang, *Tetrahedron*, **15**, 119 (2004).
96. (a) D. Pini, A. Mastantuono and P. Salvadori, *Tetrahedron: Asymmetry*, **5**, 1875 (1994); A. Mastantuono, D. Pini, C. Rolfini and P. Salvadori, *Chirality*, **7**, 499 (1995).
(b) A. Mi, Z. Wang, Z. Chen, Y. Jiang, A. S. C. Chan and T.-K. Yang, *Tetrahedron: Asymmetry*, **6**, 2641 (1995).
(c) M. Braun, A. Vonderhagen and D. Waldmüller, *Liebigs Ann.*, 1447 (1995).
(d) K. Soai, A. Oshio and T. Saito, *J. Chem. Soc., Chem. Commun.*, 811 (1993).
(e) J. M. Andrés, M. A. Martínez, R. Pedrosa and A. Pérez-Encabo, *Synthesis*, 1070 (1996); J. M. Andrés, Y. Martín, R. Pedrosa and A. Pérez-Encabo, *Tetrahedron*, **53**, 3787 (1997); J. M. Andrés, R. Pedrosa and A. Pérez-Encabo, *Tetrahedron*, **56**, 1217 (2000).
(f) Y. Zhang and W. Wu, *Tetrahedron: Asymmetry*, **8**, 3575 (1997).
(g) A. Ojida, T. Yamano, N. Taya and A. Tasaka, *Org. Lett.*, **4**, 3051 (2002).
(h) C. M. R. Ribeiro, E. de S. Santos, A. H. de O. Jardim, M. P. Maia, F. C. da Silva, A. P. D. Moreira and V. F. Ferreira, *Tetrahedron: Asymmetry*, **13**, 1703 (2002).
(i) Y. Fujiwara, T. Katagiri and K. Uneyama, *Tetrahedron Lett.*, **44**, 6161 (2003).
97. E. Ohki, S. Oida, A. Yoshida, T. Hayashi and S. Sugawara, U.S. Patent US4395418, July 26, 1983 (Derwent WPI 81-95037D).
98. A. H. Berks, *Tetrahedron*, **52**, 331 (1996).
99. J. Jurczak, S. Pikul and T. Bauer, *Tetrahedron*, **42**, 447 (1986).
100. (a) L. P. Kotra, Y. Xiang, M. G. Newton, R. F. Schinazi, Y.-C. Cheng and C. K. Chu, *J. Med. Chem.*, **40**, 3635 (1997).
(b) L. P. Kotra, M. G. Newton and C. K. Chu, *Carbohydrate Res.*, **306**, 69 (1998).

101. C. Crey, P. Dumy, J. Lhomme and M. Kotera, *Nucleosides Nucleotides Nucleic Acids*, **22**, 1093 (2003).
102. I. Izquierdo, M. T. Plaza, R. Robles and A. Mota, *Tetrahedron: Asymmetry*, **8**, 2597 (1997).
103. A. P. Rauter, O. Oliveira, T. Canda, E. Leroi, H. Ferreira, M. J. Ferreira and J. A. Ascenso, *J. Carbohydrate Chem.*, **21**, 257 (2002).
104. Y. Ding, J. Wang, K. A. Abboud, Y. Xu, W. R. Dolbier, Jr. and N. G. J. Richards, *J. Org. Chem.*, **66**, 6381 (2001).
105. (a) A. Presser, I. Pötschger, E. Haslinger and A. Hüfner, *Monatsh. Chem.*, **133**, 231 (2002).
(b) A. Presser, E. Haslinger, R. Weis and A. Hüfner, *Monatsh. Chem.*, **129**, 921 (1998).
106. A. R. McKinney and D. D. Ridley, *Aust. J. Chem.*, **54**, 757 (2001).
107. E. Vedejs and S. M. Duncan, *J. Org. Chem.*, **65**, 6073 (2000).
108. M. Sánchez and F. Bermejo, *Tetrahedron Lett.*, **38**, 5057 (1997).
109. (a) T. Basile, E. Tagliavini, C. Trombini and A. Umani-Ronchi, *J. Chem. Soc., Chem. Commun.*, 596 (1989).
(b) T. Basile, E. Tagliavini, C. Trombini and A. Umani-Ronchi, *Synthesis*, 305 (1990).
110. M. Hayashi, M. Sugiyama, T. Toba and N. Oguni, *J. Chem. Soc., Chem. Commun.*, 767 (1990).
111. (a) N. A. Ross, R. R. MacGregor and R. A. Bartsch, *Tetrahedron*, **60**, 2035 (2004).
(b) J. C. Adrian, Jr., J. L. Barkin and L. Hassib, *Tetrahedron Lett.*, **40**, 2457 (1999).
(c) S. Mohan, P. S. Sethi and A. L. Kapoor, *J. Indian Chem. Soc.*, **48**, 685 (1971).
112. F. Dardoize, J.-L. Moreau and M. Gaudemar, *Bull. Soc. Chim. Fr.*, 3841 (1972).
113. H. L. van Maanen, H. Kleijn, J. T. B. H. Jastrzebski and G. van Koten, *Recl. Trav. Chim. Pays-Bas*, **113**, 567 (1994).
114. T. Mecozzi and M. Petrini, *Tetrahedron Lett.*, **41**, 2709 (2000).
115. M. Petrini, R. Profeta and P. Righi, *J. Org. Chem.*, **67**, 4530 (2002).
116. N. Giri, M. Petrini and R. Profeta, *J. Org. Chem.*, **69**, 7303 (2004).
117. F. A. Davis, R. T. Reddy and R. E. Reddy, *J. Org. Chem.*, **57**, 6387 (1992).
118. D. D. Staas, K. L. Savage, C. F. Homnick, N. N. Tsou and R. G. Ball, *J. Org. Chem.*, **67**, 8276 (2002).
119. (a) V. A. Soloshonok, H. Ohkura, A. Sorochinsky, N. Voloshin, A. Markovsky, M. Belik and T. Yamazaki, *Tetrahedron Lett.*, **43**, 5445 (2002).
(b) A. Sorochinsky, N. Voloshin, A. Markovsky, M. Belik, N. Yasuda, H. Uekusa, T. Ono, D. O. Berbasov and V. A. Soloshonok, *J. Org. Chem.*, **68**, 7448 (2003).
120. A. Vidal, A. Nefzi and R. A. Houghten, *J. Org. Chem.*, **66**, 8268 (2001).
121. (a) A. R. Katritzky, Q. Hong and Z. Yang, *J. Org. Chem.*, **60**, 3405 (1995).
(b) A. R. Katritzky, D. A. Nichols and M. Qi, *Tetrahedron Lett.*, **39**, 7063 (1998).
122. (a) S. Lacroix, A. Cheguillaume, S. Gérard and J. Marchand-Brynaert, *Synthesis*, 2483 (2003).
(b) A. Cheguillaume, S. Lacroix and J. Marchand-Brynaert, *Tetrahedron Lett.*, **44**, 2375 (2003).
123. Y. Wang and S. Zhu, *Synthesis*, 1813 (2002).
124. J. D. Clark, G. A. Weisenburger, D. K. Anderson, P.-J. Colson, A. D. Edney, D. J. Gallagher, H. P. Kleine, C. M. Knable, M. K. Lantz, C. M. V. Moore, J. B. Murphy, T. E. Rogers, P. G. Ruminski, A. S. Shah, N. Storer and B. E. Wise, *Org. Proc. Res. Develop.*, **8**, 51 (2004).
125. (a) J. T. Kuethe and D. L. Comins, *Org. Lett.*, **2**, 855 (2000).
(b) D. L. Comins, J. T. Kuethe, H. Hong and F. J. Lakner, *J. Am. Chem. Soc.*, **121**, 2651 (1999).
126. B. B. Shankar, M. P. Kirkup, S. W. McCombie, J. W. Clader and A. K. Ganguly, *Tetrahedron Lett.*, **37**, 4095 (1996).
127. C. Baldoli, P. Del Buttero, E. Licandro and A. Papagni, *Tetrahedron*, **52**, 4849 (1996).
128. H. L. van Maanen, H. Kleijn, J. T. B. H. Jastrzebski, J. Verweij, A. P. G. Kieboom and G. van Koten, *J. Org. Chem.*, **60**, 4331 (1995).
129. L. Chen, G. Zhao and Y. Ding, *Tetrahedron Lett.*, **44**, 2611 (2003).
130. T. Nishiyama, H. Kishi, K. Kitano and F. Yamada, *Bull. Chem. Soc. Jpn.*, **67**, 1765 (1994).
131. (a) V. Gouge, P. Jubault and J.-C. Quirion, *Tetrahedron Lett.*, **45**, 773 (2004).
(b) S. Marcotte, X. Pannecoucke, C. Feasson and J.-C. Quirion, *J. Org. Chem.*, **64**, 8461 (1999).
132. (a) Y. Kobayashi, Y. Ito and S. Terashima, *Tetrahedron*, **48**, 55 (1992).

(b) K. Kondo, M. Seki, T. Kuroda, T. Yamanaka and T. Iwasaki, *J. Org. Chem.*, **60**, 1096 (1995). M. Seki, K. Kondo and T. Iwasaki, *J. Chem. Soc., Perkin Trans. 1*, 2851 (1996). K. Kondo, M. Seki, T. Kuroda, T. Yamanaka and T. Iwasaki, *J. Org. Chem.*, **62**, 2877 (1997). X. Lu, Z. Xu, G. Yang and R. Fan, *Org. Proc. Res. Develop.*, **5**, 186 (2001).
(c) Y. Ito, A. Sasaki, K. Tamoto, M. Sunagawa and S. Terashima, *Tetrahedron*, **47**, 2801 (1991).
(d) D. K. Pyun, W. J. Jeong, H. J. Jung, J. H. Kim, J. S. Lee, C. H. Lee and B. J. Kim, *Synlett*, 1950 (2001).
133. C. Dartiguelongue, S. Payan, O. Duval, L. M. Gomès and R. D. Waigh, *Bull. Soc. Chim. Fr.*, **134**, 769 (1997).
134. M. Lombardo and C. Trombini, *Synthesis*, 759 (2000).
135. H. Stamm and H. Steudle, *Tetrahedron*, **35**, 647 (1979).
136. R. Csuk, U. Franke, Z. Hu and C. Krieger, *Tetrahedron*, **59**, 7887 (2003).
137. M.-X. Wang, Y. Liu, H.-Y. Gao, Y. Zhang, C.-Y. Yu, Z.-T. Huang and G. W. J. Fleet, *J. Org. Chem.*, **68**, 3281 (2003).
138. R. J. Atkins, G. F. Breen, L. P. Crawford, T. J. Grinter, M. A. Harris, J. F. Hayes, C. J. Moores, R. N. Saunders, A. C. Share, T. C. Walsgrove and C. Wicks, *Org. Proc. Res. Develop.*, **1**, 185 (1997).
139. S. M. Hannick and Y. Kishi, *J. Org. Chem.*, **48**, 3833 (1983).
140. F. Effenberger, *Angew. Chem., Int. Ed. Engl.*, **33**, 1555 (1994).
141. J. J. Duffield and A. C. Regan, *Tetrahedron: Asymmetry*, **7**, 663 (1996).
142. J. Syed, S. Förster and F. Effenberger, *Tetrahedron: Asymmetry*, **9**, 805 (1998).
143. H. K. Lee, J. Kim and C. S. Pak, *Tetrahedron Lett.*, **40**, 2173 (1999).
144. H. K. Lee, J. Kim and C. S. Pak, *Tetrahedron Lett.*, **40**, 6267 (1999).
145. (a) J. P. Michael, C. B. de Koning and T. V. Stanbury, *Tetrahedron Lett.*, **37**, 9403 (1996).
(b) J. P. Michael, C. B. de Koning, G. D. Hosken and T. V. Stanbury, *Tetrahedron*, **57**, 9635 (2001).
146. J. P. Michael, C. B. de Koning, R. L. Petersen and T. V. Stanbury, *Tetrahedron Lett.*, **42**, 7513 (2001).
147. A. G. Brewster, S. Broady, M. Hughes, M. G. Moloney and G. Woods, *Org. Biomol. Chem.*, **2**, 1800 (2004).
148. J. Dyer, S. Keeling and M. G. Moloney, *Tetrahedron Lett.*, **37**, 4573 (1996).
149. Y. Ding, Z. Zhao and C. Zhou, *Tetrahedron*, **53**, 2899 (1997).
150. R. Menicagli and S. Samaritani, *Tetrahedron*, **52**, 1425 (1996).
151. K. Fuji, T. Kawabata, Y. Naniwa, T. Ohmori and M. Node, *Chem. Pharm. Bull.*, **42**, 999 (1994).
152. X. Yang and R. Wang, *Tetrahedron: Asymmetry*, **8**, 3275 (1997).
153. G.-W. Wang, Y. Murata, K. Komatsu and T. S. M. Wan, *Chem. Comman.*, 2059 (1996).
154. P. Kielbasiński and M. Mikolajczyk, *Synthesis*, 144 (1995).
155. D. J. Dellinger, D. M. Sheehan, N. K. Christensen, J. G. Lindberg and M. H. Caruthers, *J. Am. Chem. Soc.*, **125**, 940 (2003).
156. E. Erdik, *Tetrahedron*, **48**, 9577 (1992).
157. J. F. Fauvarque and A. Jutand, *J. Organomet. Chem.*, **209**, 109 (1981).
158. F. Orsini and F. Pelizzoni, *Synth. Commun.*, **17**, 1389 (1987).
159. E. Bentz, M. G. Moloney and S. M. Westaway, *Tetrahedron Lett.*, **45**, 7395 (2004).
160. T. Hama, X. Liu, D. A. Culkin and J. F. Hartwig, *J. Am. Chem. Soc.*, **125**, 11176 (2003).
161. (a) M. Cantin, R. Schütz and C. J. Leumann, *Tetrahedron Lett.*, **38**, 4211 (1997).
(b) C. D. Roberts, R. Schütz and C. J. Leumann, *Synlett*, 819 (1999).
162. M. Gaudemar, *Tetrahedron Lett.*, **24**, 2749 (1983).
163. G. P. Boldrini, M. Mengoli, E. Tagliavini, C. Trombini and A. Umani-Ronchi, *Tetrahedron Lett.*, **27**, 4223 (1986).
164. K. Fuji, N. Kinoshita and K. Tanaka, *Chem. Commun.*, 1895 (1999).
165. (a) U. Kazmaier and F. L. Zumpe, *Angew. Chem., Int. Ed.*, **39**, 802 (2000).
(b) U. Kazmaier and F. L. Zumpe, *Angew. Chem., Int. Ed.*, **38**, 1468 (1999).
166. T. Takahashi, N. Nakao and T. Koizumi, *Tetrahedron: Asymmetry*, **8**, 3293 (1997).

167. (a) H. J. M. Gijsen and C.-H. Wong, *J. Am. Chem. Soc.*, **117**, 2947 (1995).
(b) H. J. M. Gijsen and C.-H. Wong, *J. Am. Chem. Soc.*, **117**, 7585 (1995).
168. M. Schmittel and M. K. Ghorai, *Synlett*, 1992 (2001).
169. M. Okue, H. Watanabe and T. Kitahara, *Tetrahedron*, **57**, 4107 (2001).
170. N. J. Hovestad, A. Ford, J. T. B. H. Jastrzebski and G. van Koten, *J. Org. Chem.*, **65**, 6338 (2000).
171. U. Kazmaier, *Synlett*, 1138 (1995).
172. (a) K. Kubota and F. Nakamura, *Angew. Chem., Int. Ed. Engl.*, **36**, 2491 (1997).
(b) E. Nakamura, K. Kubota and G. Sakata, *J. Am. Chem. Soc.*, **119**, 5457 (1997).
173. E. Nakamura and K. Kubota, *Tetrahedron Lett.*, **38**, 7099 (1997).
174. E. Nakamura, G. Sakata and K. Kubota, *Tetrahedron Lett.*, **39**, 2157 (1998).
175. (a) P. Karoyan and G. Chassaing, *Tetrahedron Lett.*, **38**, 85 (1997).
(b) P. Karoyan and G. Chassaing, *Tetrahedron: Asymmetry*, **8**, 2025 (1997).
(c) P. Karoyan, A. Triolo, R. Nannicini, D. Giannotti, M. Altamura, G. Chassaing and E. Perrotta, *Tetrahedron Lett.*, **40**, 71 (1999).
(d) P. Karoyan and G. Chassaing, *Tetrahedron Lett.*, **43**, 253 (2002).
(e) J. Quancard, A. Labonne, Y. Jacquot, G. Chassaing, S. Lavielle and P. Karoyan, *J. Org. Chem.*, **69**, 7940 (2004).
176. (a) E. Lorthiois, I. Marek and J.-F. Normant, *Tetrahedron Lett.*, **38**, 89 (1997).
(b) E. Lorthiois, I. Marek and J.-F. Normant, *J. Org. Chem.*, **63**, 566 (1998).
(c) E. Lorthiois, I. Marek and J.-F. Normant, *J. Org. Chem.*, **63**, 2442 (1998).
177. B. M. Trost and H. Ito, *J. Am. Chem. Soc.*, **122**, 12003 (2000).
178. (a) M. D. Ronsheim and C. K. Zercher, *J. Org. Chem.*, **68**, 4535 (2003).
(b) S. Lai, C. K. Zercher, J. P. Jasinski, S. N. Reid and R. J. Staples, *Org. Lett.*, **3**, 4169 (2001).
179. Y. Aoki, K. Oshima and K. Utimoto, *Chem. Lett.*, 463 (1995).
180. I. Sato, Y. Takizawa and K. Soai, *Bull. Chem. Soc. Jpn.*, **73**, 2825 (2000).
181. S. Ito, H. Shinokubo and K. Oshima, *Tetrahedron Lett.*, **39**, 5253 (1998).
182. (a) Y. Ukaji, S. Takenaka, Y. Horita and K. Inomata, *Chem. Lett.*, 254 (2001).
(b) Y. Ukaji, Y. Yoshida and K. Inomata, *Tetrahedron: Asymmetry*, **11**, 733 (2000).
183. K. Kanai, H. Wakabayashi and T. Honda, *Org. Lett.*, **2**, 2549 (2000).
184. (a) K. Kanai, H. Wakabayashi and T. Honda, *Heterocycles*, **58**, 47 (2002).
(b) T. Honda, H. Wakabayashi and K. Kanai, *Chem. Pharm. Bull.*, **50**, 307 (2002).
185. K. Sato, A. Tarui, T. Kita, Y. Ishida, H. Tamura, M. Omote, A. Ando and I. Kumadaki, *Tetrahedron Lett.*, **45**, 5735 (2004).
186. M. Kitamura, T. Miki, K. Nakano and R. Noyori, *Bull. Chem. Soc. Jpn.*, **73**, 999 (2000).
187. A. Alexakis, *Pure Appl. Chem.*, **74**, 37 (2002).
188. (a) B. L. Feringa, M. Pineschi, L. A. Arnold, R. Imbos and A. H. M. de Vries, *Angew. Chem., Int. Ed. Engl.*, **36**, 2620 (1997).
(b) B. L. Feringa, *Acc. Chem. Res.*, **33**, 346 (2000).
189. A. Alexakis, G. P. Trevitt and G. Bernardinelli, *J. Am. Chem. Soc.*, **123**, 4358 (2001).
190. (a) S. J. Degrado, H. Mizutani and A. H. Hoveyda, *J. Am. Chem. Soc.*, **123**, 755 (2001).
(b) S. J. Degrado, H. Mizutani and A. H. Hoveyda, *J. Am. Chem. Soc.*, **124**, 13362 (2002).
191. (a) R. Kuhn and M. Hoffer, *Chem. Ber.*, **65**, 651 (1932).
(b) R. C. Fuson, R. T. Arnold and H. G. Cooke, Jr., *J. Am. Chem. Soc.*, **60**, 2272 (1938).
(c) K. Ziegler, W. Schumann and E. Winkelmann, *Ann. Chem.*, **551**, 120 (1942).
(d) R. C. Fuson and P. L. Southwick, *J. Am. Chem. Soc.*, **66**, 679 (1944).
192. (a) R. Couffignal and M. Gaudemar, *J. Organomet. Chem.*, **60**, 209 (1973).
(b) M. Bellassoued, F. Dardoize, Y. Frangin and M. Gaudemar, *J. Organomet. Chem.*, **219**, C1 (1981).
(c) M. Bellassoued, F. Habbachi and M. Gaudemar, *Tetrahedron*, **41**, 1299 (1985).
(d) M. Bellassoued, F. Habbachi and M. Gaudemar, *Tetrahedron*, **43**, 1785 (1987).
193. M. K. Gurjar, D. S. Reddy, M. M. Bhadbhade and R. G. Gonnade, *Tetrahedron*, **60**, 10269 (2004).
194. Q.-S. Hu and C.-M. Hu, *J. Fluorine Chem.*, **83**, 87 (1997).
195. T. Tsukamoto and T. Kitazume, *Synlett*, 977 (1992).
196. (a) L. Wessjohann and H. Wild, *Synthesis*, 512 (1997).
(b) L. Wessjohann and H. Wild, *Synthesis*, 731 (1997).

197. H. L. van Maanen, H. Kleijn, J. T. B. H. Jastrzebski, M. T. Lakin, A. L. Spek and G. van Koten, *J. Org. Chem.*, **59**, 7839 (1994).
198. (a) M. Bellassoued, J. Grugier and N. Lensen, *J. Organomet. Chem.*, **662**, 172 (2002).
(b) M. Bellassoued, J. Grugier, N. Lensen and A. Catheline, *J. Org. Chem.*, **67**, 5611 (2002).
199. M. Bellassoued, R. Ennigrou, R. Gil and N. Lensen, *Synth. Commun.*, **28**, 3955 (1998).
200. T. Hudlicky, M. G. Natchus, L. D. Kwart and B. L. Colwell, *J. Org. Chem.*, **50**, 4300 (1985).
201. C. Y. Robinson, W. J. Brouillette and D. D. Muccio, *J. Org. Chem.*, **54**, 1992 (1989).

CHAPTER **19**

Carbozincation of alkenes and alkynes

EDWIGE LORTHIOIS

Novartis Pharma AG, Novartis Institutes for Biomedical Research, Protease Platform WKL-122-3-27, Klybeckstrasse 144, CH-4002 Basel, Switzerland
Fax: +41 61 696 1163; e-mail: edwige.lorthiois@novartis.com

and

CHRISTOPHE MEYER

Laboratoire de Chimie Organique, associé au CNRS, ESPCI, 10 rue Vauquelin, F-75231, Paris Cedex 05, France
Fax: +33 14 079 4660; e-mail: christophe.meyer@espci.fr

The chemistry of organozinc compounds
Edited by Z. Rappoport and I. Marek

I. INTRODUCTION

Carbozincations are reactions that involve the addition of the carbon–zinc bond of an organozinc reagent **1** across a carbon–carbon multiple bond **2**, leading to a new organozinc species **3** (equation 1).

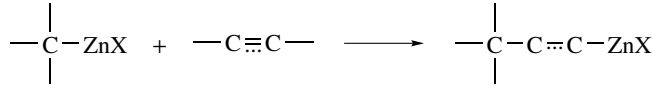

(1) **(2)** **(3)** (1)

Carbozincations belong to the more general class of reactions known as carbometallations, to which several reviews and book chapters have already been devoted[1–9]. Addition of organozinc reagents to alkenes and alkynes activated by electron-withdrawing groups will not be covered by this chapter as they are best considered as conjugate additions. As the reactivity of organozinc reagents towards carbon−carbon multiple bonds critically depends on their structures, this chapter has been organized so that the following representative classes of reagents may be distinguished: alkyl and arylzincs which exhibit a low intrinsic reactivity, allylic and allenic organozinc reagents as well as zinc enolates or aza-enolates that display a unique behavior in carbozincations, not attained by any other metals in some peculiar reactions. One of the most unique features of organozinc reagents lies in their ability to undergo several transmetallation reactions with transition metal complexes[10,11]. This property which has been widely exploited to broaden the scope of functionalization of organozincs has also found some applications in the field of carbozincations, especially for the less reactive classes of reagents (alkyl and arylzincs). Thus, transition metal-promoted or catalyzed additions to alkenes and alkynes have also been included in this chapter as they are still in agreement with the general definition of carbozincations (equation 1), even though the active species itself is not an organozinc reagent. Related metal-catalyzed multi-component reactions also involving organozinc reagents as partners will be mentioned for comparison, though they do not actually involve any carbozincation process.

Whereas the carbometallation reactions of alkynes generate alkenylmetal compounds which are less reactive compared to the parent organometallic species, carbozincation of alkenes raises the issue of chemoselectivity as the newly formed organozinc species **3** could in principle compete with **1** towards the addition to the double bond of **2**. This problem, usually observed with more reactive classes of organometallic reagents, will be in general of little concern with organozinc reagents when unactivated alkenes are considered as substrates, due to the low reactivity of the alkylzinc reagents generated. Exceptions can be encountered in a minority of reactions involving additions to 1,3-dienes or styrenes, where an allylic or a benzylic organozinc species displaying higher reactivity may be produced.

For each class of organozinc reagents, the corresponding possible substrates will be indicated and the issues concerning regioselectivity, either with respect to the substrate or the reagent, diastereoselectivity and in some cases enantioselectivity will be discussed.

II. REACTIVITY OF ALKYL AND ARYL ORGANOZINC REAGENTS

Arylzinc reagents are completely inert towards alkenes and alkynes in the absence of any added catalyst, whereas the reported examples of uncatalyzed intermolecular carbozincations involving alkylzincs appear to be restricted to the more nucleophilic di(*tert*-butyl)zinc.

A. Uncatalyzed Intermolecular Carbozincations

1. Intermolecular additions to alkynes

Di(*tert*-butyl)zinc reacts with a variety of terminal alkynes in refluxing THF (but not disubstituted ones), including those bearing functional groups such as alcohols, ethers, acetals or amines[12]. These additions are completely regioselective as the bulky *tert*-butyl group is delivered to the less substituted carbon, presumably for steric reasons. However,

the reaction is not stereoselective and affords mixtures of geometric isomers, with a ratio depending on the alkyne substituent (equation 2). Unfortunately, quenching with other electrophiles than water was not carried out by the authors.

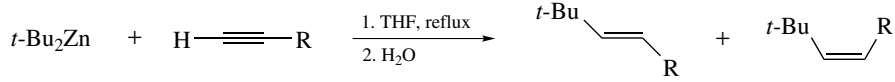

R = Bu, $(CH_2)_nOH$ (n = 1–3), CH_2OBu, CH_2OTHP, CH_2NHEt, CH_2NEt_2 $(E)/(Z)$ = 35/65 to 88/12 20–65% (2)

Phenylacetylene, in which the triple bond is conjugated with the aromatic ring, displayed a higher reactivity and readily underwent a stereoselective addition of t-Bu_2Zn in refluxing ether, leading to the (Z)-alkene **4** through an apparent *anti* addition process[13]. A variety of conjugated terminal enynes also reacted chemoselectively under the same conditions to afford stereoselectively 1,3-dienes **5**, whatever the substitution pattern of the double bond[14, 15] (equation 3). These reactions were not stereoselective when carried out in refluxing THF due to the isomerization of the initial adduct which is sterically crowded.

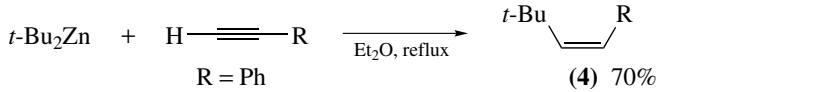

R = Ph **(4)** 70%

R = $(R^1)C{=}CHR^2$ **(5)** 30–55% (3)

R^1 = H, R^2 = Bu, CH_2OH, CH_2OBu, NHEt, NEt_2

$R^1R^2 = -(CH_2)_4-$

2. Intermolecular additions to alkenes

Uncatalyzed additions of alkylzincs to alkenes do not generally occur except with the more reactive di(*tert*-butyl)zinc[16]. Carbozincation of ethylene was performed under pressure in benzene at 50–75 °C and afforded the primary dialkylzinc **6** that was hydrolyzed to the corresponding hydrocarbon. Reaction also occurred with the less reactive monosubstituted olefins such as propene or 1-octene and the steric bulk of the organozinc favored the addition of the t-Bu group to the less substituted carbon of the alkene, leading with high regioselectivity ($\geqslant 98/\leqslant 2$) to the corresponding secondary dialkylzincs **7** and **8** respectively. The primary and the secondary organozincs **6** and **7** did not add further to the parent olefin but, at higher temperatures, the dialkylzinc **8** further reacted with 1-octene and led to **9**, as shown by the formation of a small amount of the alkane by-product **10** (equation 4)[16].

1,3-Butadiene displayed a much higher reactivity towards t-Bu_2Zn and the reaction initially generated an allylic diorganozinc species **11**, in equilibrium with its allylic counterpart **12** (or any of the mixed metallotropic forms). Under carefully controlled conditions, the reaction stopped at the monoaddition stage and a mixture of regio- and stereoisomeric hydrocarbons was obtained after hydrolysis (equation 5). At higher temperatures, the allylic organozincs **11** and **12** were able to further add to 1,3-butadiene (see Section III.A.1)[16].

Monoaddition of t-Bu_2Zn to styrene occurred if the reaction was conducted at 15 °C and led to the benzylic diorganozinc species **13** (equation 6)[16]. At higher temperatures, addition proceeded further and led to higher homologs as well as to polystyrene after demetallation.

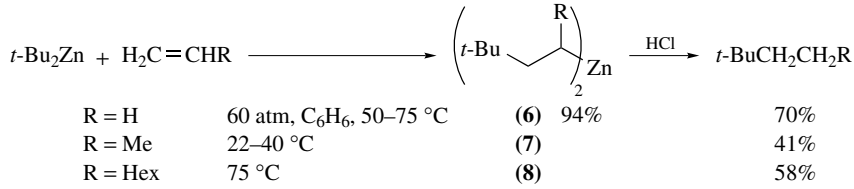

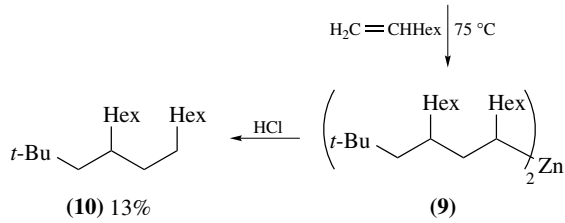

(4)

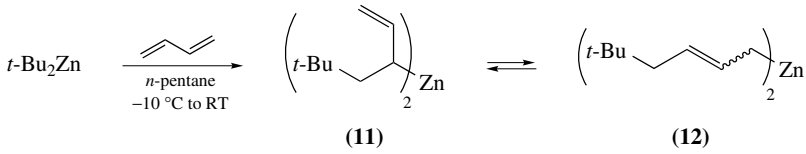

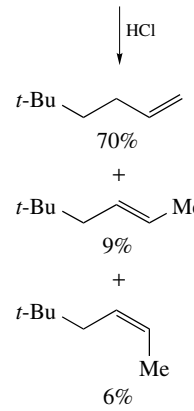

(5)

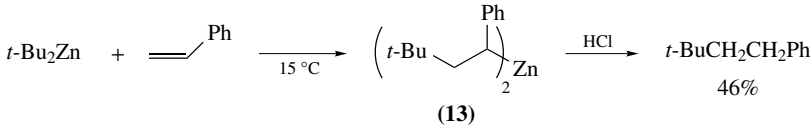

(6)

B. Uncatalyzed Intramolecular Carbozincations

1. Intramolecular carbozincation of alkynes

Whereas the propensity of several main-group organometallic reagents, especially those of 5-hexyn-1-yl type, to achieve the intramolecular carbometallation of alkynes has been clearly demonstrated[2–9, 17, 18], the comparative reactivity of organozinc reagents in this field appears significantly lower. Indeed, when 1-iododec-5-yne (**14**) was treated with zinc in THF, the corresponding organozinc iodide **15** remained unchanged for several hours at 35 °C. By contrast, addition of $Me_2Cu(CN)Li_2$ induced its transmetallation to a more reactive organocopper species **16** that effected the intramolecular carbocupration of the triple bond and the resulting alkenylcopper species could be functionalized by reaction with various electrophiles (equation 7)[19]. This efficient cyclization process based on a zinc to copper transmetallation was found to be applicable to several primary and secondary alkyl iodides.

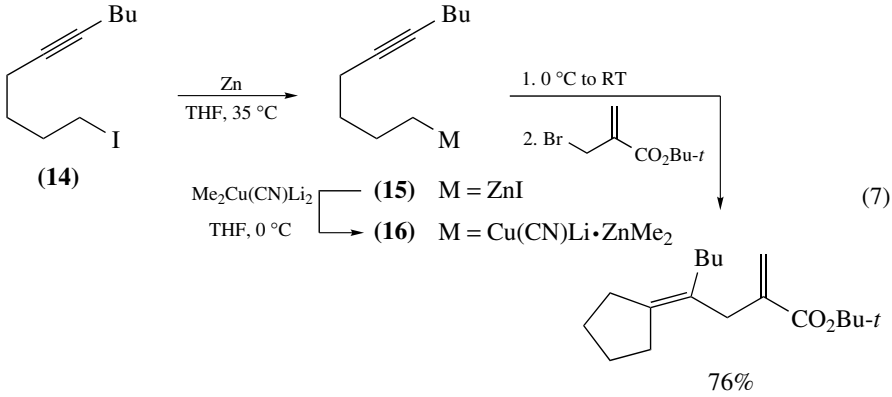

(7)

It was also reported that treatment of δ-alkynyl iodides **17** and **18**, having a triple bond activated by conjugation either with an aromatic ring or a double bond, with zinc dust in THF resulted in the formation of the cyclic products **19** and **20** respectively (equation 8)[20]. However, their formation was ascribed to a zinc-induced radical cyclization process due to the failure to detect any open-chain organozinc species prior to cyclization as well as unsuccessful attempts to efficiently functionalize any alkenylzinc species that would have been normally expected from an anionic pathway[20].

A more comprehensive study on the behavior of δ-acetylenic iodides in the presence of zinc was later reported[21] and clearly revealed that when iodide **14** was treated with acid-washed zinc (pre-treated with MeI for activation and removal of traces of moisture) in a mixture of benzene and DMF, the acyclic organozinc iodide **21** and the cyclic vinyl iodide **22** were both produced. The amount of **22** increased significantly when the reaction mixture was sonicated rather than stirred or if a zinc–copper couple was used. The accumulation of compound **22** was consistent with its inability to be converted to an alkenyl organozinc species by reaction with metallic zinc under these conditions. However, no substantial cyclization of the open-chain organozinc **21** was observed. The formation of the five-membered ring compound **22** was attributed to a free-radical process

as the reaction of iodide **14** at the zinc surface could produce the acyclic radical **23** by single-electron transfer. Some of these radicals could diffuse into the solution and undergo a 5-exo-Dig cyclization leading to the alkenyl radical **24**. Alternatively, further reduction of **23** prior to leaving or upon back-diffusion to the metal surface would produce the open-chain organozinc reagent **21**. Although the alkenyl radical **24** could in principle have been reduced to an alkenylzinc reagent, it rather propagated the radical chain by an iodine atom-transfer from **14** accounting for the formation of the cyclic alkenyl iodide **22** (equation 9).

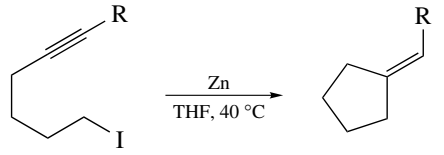

(8)

(17) R = **(19)** 73%

(18) R = Ph **(20)** 70%

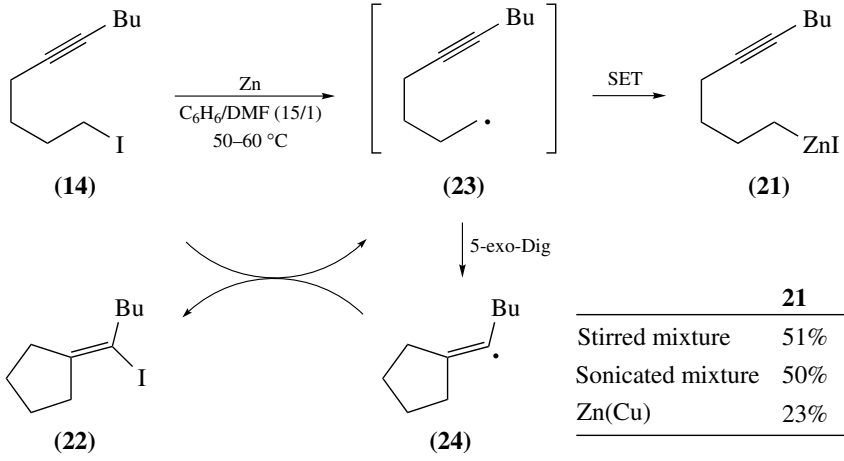

(14) **(23)** **(21)** **(22)** **(24)**

(9)

	21	**22**
Stirred mixture	51%	23%
Sonicated mixture	50%	39%
Zn(Cu)	23%	53%

By contrast, for iodide **18** having the triple bond activated by a phenyl group, conversion to the cyclic organozinc species **25** occurred effectively and the latter could be efficiently functionalized, provided that traces of moisture were excluded by pre-treatment of zinc powder with MeI. The substituted benzylidene cyclopentanes **26** and **27** were respectively obtained after iodinolysis and palladium-catalyzed cross-coupling reaction with benzoyl chloride (equation 10). However, it could not be assessed whether the formation of organozinc **25** was attributable to an anionic or a radical cyclization pathway (or both) as, had iodide **26** been produced by a radical iodine atom-transfer, it would have been converted to **25** by reaction with metallic zinc due to the presence of the activating phenyl group[21].

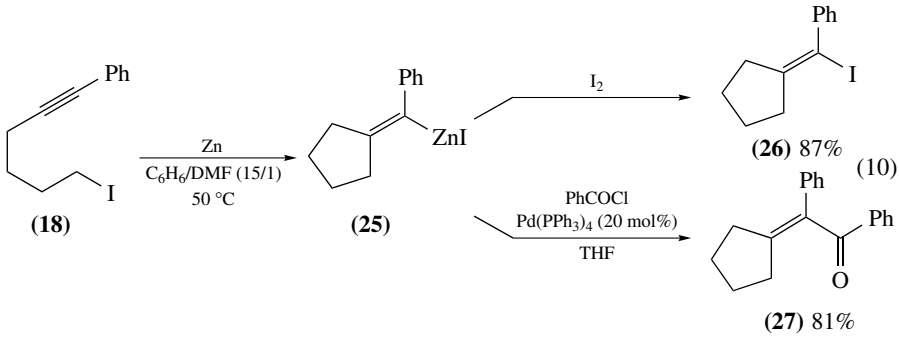

(10)

Intramolecular carbozincations of alkynes appeared relatively restricted in scope, at least under the conditions that were used to generate the open-chain organozinc species.

2. Intramolecular carbozincation of alkenes

Cyclization reactions of 5-hexenyl metals proceed with relative ease compared to the analogous intermolecular carbometallations and constitute an interesting entry to five-membered ring systems, potentially significant for synthetic purpose[4–9]. Reductive metal-exchange reactions applied to di(5-hexenyl)mercury were used to prepare various 5-hexenylmetals and their propensity to cyclize to the corresponding cyclopentylmethyl metals could be evaluated (equation 11)[22]. The observed order of reactivity, Al > Mg > Li > Zn ≫ Ga, In ≫ Hg = 0 (no cyclization) seemed to be affected by the polarity of the carbon–metal bond as well as the availability of a vacant orbital on the metal[23]. Thus, the zinc–mercury exchange (M = Zn, equation 11) at 120 °C for 24 h quantitatively led to a 90/10 mixture of open-chain and cyclized organozinc species. After a further 24 h, di(cyclopentylmethyl)zinc was found to be the major component (90%). By comparison, the rates of Hg/Mg exchange and cyclization (M = Mg, equation 11) were almost similar[23]. Di(4-pentenyl)zinc (**28**) could be prepared in the same manner but failed to cyclize to the corresponding four-membered ring organozinc species. However, examination of the ^{1}H NMR parameters of this compound suggested an intramolecular interaction between the double bond and zinc, resulting in a lower energy conformer[24,25]. Gas-electron diffraction studies also supported this result[26]. This weak dipole–dipole interaction arises from the inherent polarity of the carbon–zinc bond and the partial negative charge on the terminal olefinic carbon.

Whereas the interpretation of the NMR parameters of di(5-hexenyl)zinc do not suggest any metal–olefin interaction, probably because the chain length is not appropriate to accommodate the latter in the ground state, this interaction may play a crucial role in the reactive complex leading to the intramolecular carbozincation process. Conversely, the chain length is not sufficiently long in the case of di(4-pentenyl)zinc (**28**) to achieve the requisite conformation for addition to the double bond, but it is favorable for zinc–olefin interaction[24,25].

A related zinc–alkyne interaction was suggested on the basis of the ^{13}C and Raman spectra of di(4-hexynyl)zinc[27]. Interestingly, addition of coordinating additives such as pyridine prevented the formation of the latter interaction whereas weaker Lewis bases such as diethyl ether did not.

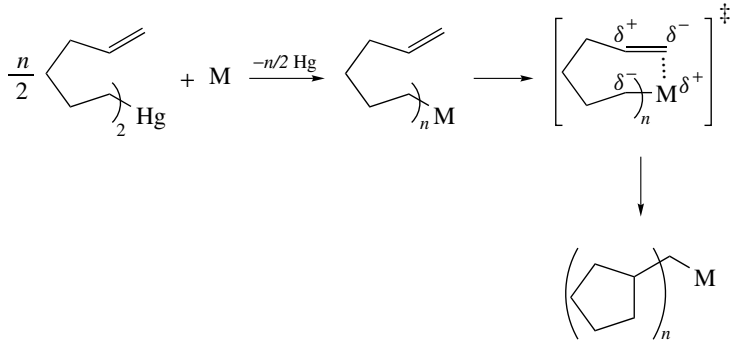

(11)

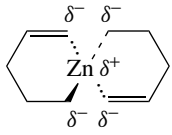

(28)

It is worth mentioning that the rates of the cyclization of di(5-hexenyl) metals were initially evaluated for the neat organometallic species but, in fact, it was observed that additives could exert a marked influence. Whereas the cyclization of 5-hexenyllithium (M = Li, equation 11) required several days at 25 °C, it was complete within 96 h in benzene or less than 1 h in ether[22], probably due to the stabilization of the polar transition state via the solvation of the metal which also resulted in an increase of the polarity of the carbon–metal bond. However, for more covalent organometallic species having a carbon–metal bond of lower intrinsic polarity (M = Al, Zn), a too strongly Lewis basic solvent would be detrimental to the success of the intramolecular carbometallation as it would compete with the double bond for coordination of the metal. Unfortunately, highly coordinating solvents such as DMF or THF are generally required for the generation of organozinc reagents from alkyl iodides and the metal[10, 11]. This problem was solved by using the highly reactive zinc powder (Zn*) prepared according to the method of Rieke, by reduction of $ZnBr_2$ with lithium naphthalenide[28], which allowed the preparation of some organozincs in ether. Thus, treatment of the alkyl iodide **29** with highly reactive zinc in ether rapidly led to the cyclic organozinc iodide **30** and iodinolysis afforded the disubstituted cyclopentane **31** (*trans*/*cis* = 93/7) (equation 12)[29]. A chair-like cyclic transition state in which the zinc is coordinated by the alkene and the methyl group preferentially occupies a pseudo-equatorial position can explain the observed high diastereoselectivity, as in the cyclization of the organolithium reagent derived from **29** by iodine–lithium exchange with *t*-BuLi[30].

The most unique advantage of organozincs compared to organolithium reagents lies in their tolerance towards a variety of functional groups, and the functionalized alkyl iodides of type **32** could indeed be converted to the corresponding cyclic organozinc compounds **33** by reaction with highly reactive zinc in ether. Hydrolysis, iodinolysis or transmetallation to an organozinc–copper species followed by acylation with acetyl chloride afforded the corresponding functionalized five-membered rings **34**–**36** in good

to excellent yields[29]. However, the diastereoselectivity was not as high as it was in the case of substrate **29** where a methyl group was present at the allylic position. This result was explained by the fact that an axial position for the allylic acyloxy substituents in the cyclic transition state was less disfavored than for the methyl group because of a favorable coordination of the zinc atom by the carbonyl group (equation 13).

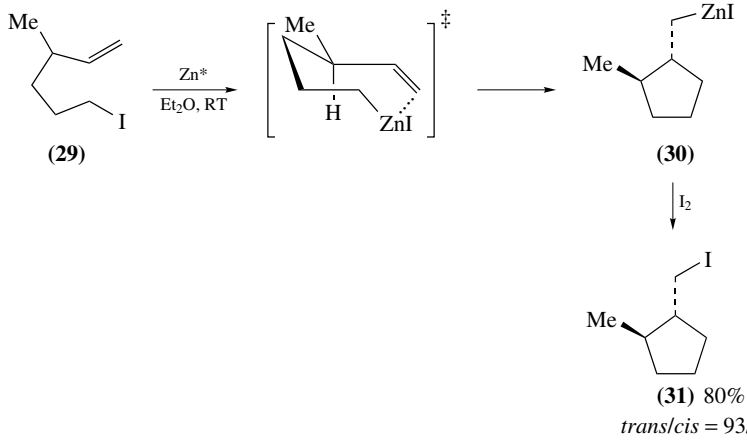

(29) **(30)** (12)

(31) 80%
trans/*cis* = 93/7

The formation of the cyclic organozinc compounds of type **33** was so rapid that it was not possible to detect more than 20% of open-chain organozinc species prior to complete cyclization. Although this result seemed to argue in favor of a radical cyclization process induced by metallic zinc, as described in the case of δ-acetylenic iodides (see Section II.B.1), the iodide **37** bearing an α,β-disubstituted double bond failed to undergo cyclization when treated with activated zinc. In this case, there was no obvious reason accounting for the unsuccessful cyclization of the radical **38**, if generated, and the formation of (*Z*)-5-decene (**39**) after hydrolysis ruled out a scenario that would have involved radical cyclization, subsequent reduction of **40** to the secondary organozinc **41** and ring-opening of the latter, as this would have unavoidably lead to scrambling of the double bond configuration (equation 14)[31].

It has also been reported that treatment of the alkyl iodide **42** with activated zinc led to the spirobicyclic ketone **43**. Due to the presence of an activated carbon–carbon bond, THF was a suitable solvent and kinetic studies strongly supported an anionic carbozincation process arising from an open-chain organozinc, although a small part of the cyclic product may derive from an initial radical pathway (equation 15)[32].

It is known that primary alkyl iodides undergo an iodine–zinc exchange when treated with excess diethylzinc (neat) to afford, after removal of EtI (and excess Et_2Zn), the corresponding dialkylzinc compounds[33]. When the functionalized iodide **32a** was treated with Et_2Zn in refluxing hexane, an iodine–zinc exchange also took place and afforded an open-chain organozinc compound formulated as **44**, and only a small amount of the cyclic organozinc **45** was produced. However, when hexane was removed and replaced by a slightly more polar solvent such as ether, the acyclic organozinc **44** did quantitatively cyclize to **45**[31]. Both the iodine–zinc exchange process and the cyclization could be run directly in ether albeit at a slower overall rate. The formation of the cyclic organozinc **45** was evidenced by reaction with several electrophiles (equation 16). It must be emphasized that this procedure turned out to be completely inefficient in the case of other 5-hexenyl-type iodides lacking oxygenated moieties at the allylic position, presumably because the latter may exert a beneficial influence on the iodine–zinc exchange process[34].

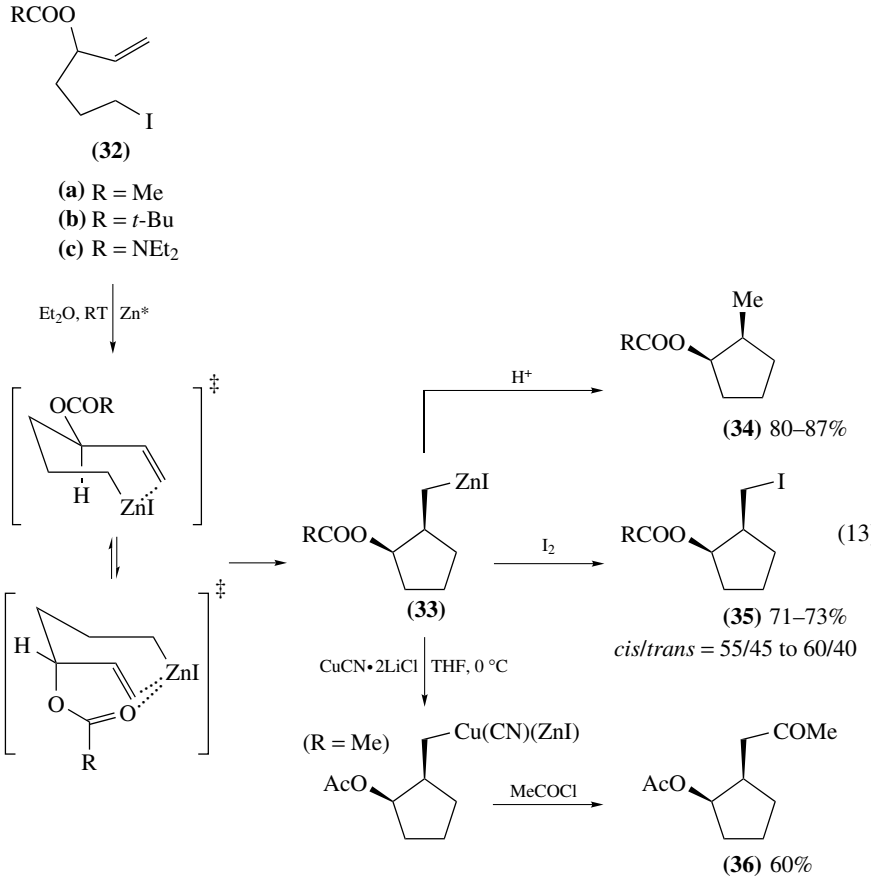
RCOO
I
(32)
(a) R = Me
(b) R = t-Bu
(c) R = NEt2
Et2O, RT
Zn*
OCOR
H
ZnI
‡
H+
Me
RCOO
(34) 80–87%
ZnI
RCOO
I2
I
RCOO
(33)
(35) 71–73%
cis/trans = 55/45 to 60/40
(13)
CuCN•2LiCl
THF, 0 °C
(R = Me)
Cu(CN)(ZnI)
AcO
MeCOCl
COMe
AcO
(36) 60%
Bu
I
(37)
Zn*
Et2O, RT
Bu
ZnI
HCl
Bu
Bu
(39) 62%
SET
(14)
Bu
(38)
Bu
(40)
SET
Bu
ZnI
(41)
Bu
ZnI

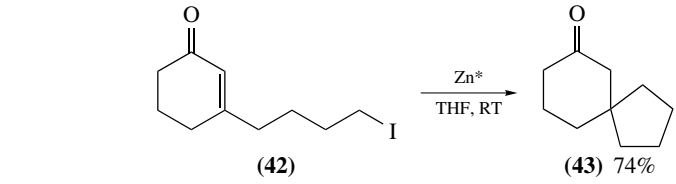

(42) (43) 74%

(15)

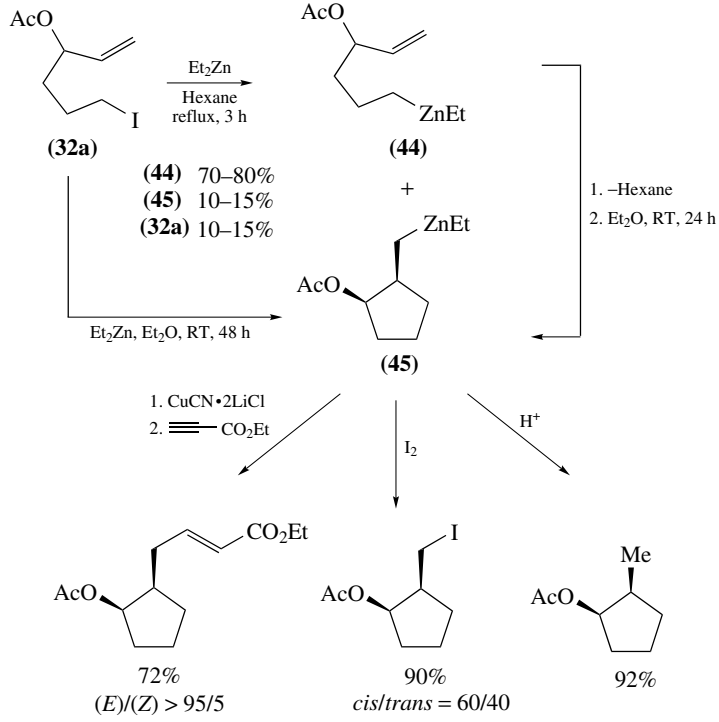

(16)

When the open-chain **44** was generated according to this protocol, it was observed that subsequent addition of lithium salts such as LiI or LiBr dramatically slowed down the rate of its cyclization to **45**[31]. It was postulated that halide ions may associate with the zinc atom and lead to the formation of a zincate-type species, thereby destroying the Lewis acidity of the metal and preventing its intramolecular coordination by the alkene. This assumption was later supported by the fact that halide ions can also promote the 1,2-metallate rearrangement of α-iodoorganozinc reagents[35]. This result could also explain that 5-hexenylzinc bromide, generated from **46** by iodine–lithium exchange with *tert*-butyllithium and subsequent transmetallation with $ZnBr_2$, failed to cyclize due to the presence of equimolar amounts of LiI and LiBr (equation 17)[31].

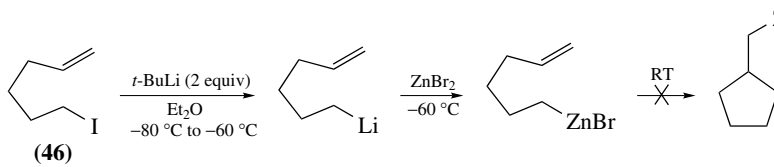

(46)

(17)

The use of Rieke zinc in ether turned out to be also satisfactory to convert a variety of secondary alkyl iodides of type **47** into the corresponding substituted cyclopentylmethylzinc species **48**[36]. Secondary alkyl iodides turned out to be much more reactive than the primary ones towards oxidative addition of zinc, and lowering the temperature to $-10\,^{\circ}C$ in the case of iodide **47a** enabled one to detect the corresponding open-chain organozinc species prior to its subsequent cyclization. The yields of the five-membered ring products **49**, obtained after protonation or iodinolysis, were generally good but the diastereomeric ratios were moderate with predominant formation of the *cis* diastereomers[36]. These results were explained by considering a rather early cyclic chair-like transition state wherein the secondary alkyl substituent (R^1) would preferentially occupy a pseudo-equatorial position. By comparison, related cyclizations of secondary organolithium or organomagnesium reagents, bearing more ionic carbon–metal bonds, led predominantly to the *trans* diastereomers, as a consequence of a rather product-like transition state[37]. Cyclization also occurred in the case of iodide **47f**, thereby demonstrating the possibility of achieving the intramolecular carbozincation of an α,β-disubstituted double with a more reactive secondary organozinc species, unlike for a primary one (equation 18).

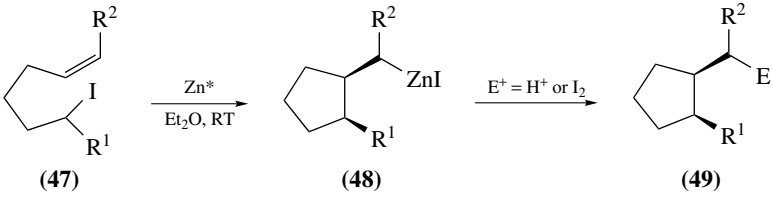

(47) **(48)** **(49)**

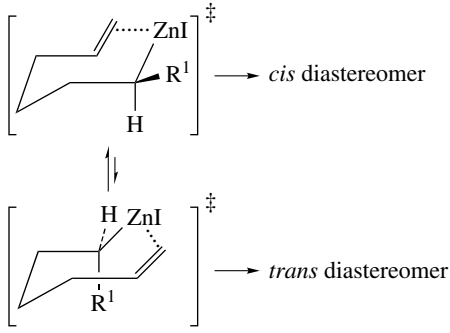

	R^1	R^2	E	Yield	*cis*/*trans*
(a)	Me	H	I	73%	81/19
(b)	Bu	H	I	68%	73/27
(c)	*i*-Pr	H	I	78%	73/27
(d)	*t*-Bu	H	I	60%	62/38
(e)	$SiMe_2Ph$	H	H	68%	66/34
(f)	Me	Pr	H	80%	68/32

(18)

The high chemoselectivity of organozinc reagents also allowed the use of the functionalized secondary α-acetoxy alkyl bromide **50** which was converted to **34a** (equation 19)[36], a product previously obtained by the cyclization of a δ-ethylenic primary iodide bearing the acetoxy group at the allylic position (equation 13).

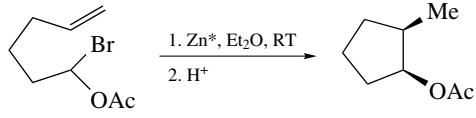

(50) **(34a)**
cis/*trans* = 86/14
50%

(19)

Thus, whereas intermolecular carbozincations of alkenes and alkynes appear restricted in scope and limited to the more reactive di(*tert*-butyl)zinc, the zinc-induced cyclization of δ-acetylenic or δ-ethylenic iodides by treatment with activated zinc constitutes a valuable strategy for the synthesis of functionalized five-membered rings. The success of these reactions relies on the use of the highly reactive Rieke zinc that allows the carbozincation to be carried out in ether.

From the experimental point of view, a particularly attractive procedure has been developed to produce cyclopentylmethylzinc species from primary or secondary halides, based on the use of diethylzinc and transition metal catalysts (see Section II.C.1)[34].

C. Transition Metal-catalyzed or promoted Carbozincations

1. Palladium- and nickel-catalyzed intramolecular carbozincations

It was reported that the iodine–zinc exchange process induced by treatment of alkyl iodides with Et_2Zn could be catalyzed by CuI, leading to shorter reaction times and reduction of the amount of Et_2Zn[38]. The use of palladium or nickel catalysts turned out to be also extremely efficient but produced an organozinc iodide instead of a dialkylzinc, with evolution of ethane and ethylene[34] (equation 20).

$$(RCH_2)_2Zn \xleftarrow[\text{neat, 50 °C}\\(-EtI)]{Et_2Zn\ (1.5\ equiv)\\CuI\ (0.3\ mol\%)} RCH_2I \xrightarrow[\text{THF, RT}\\(-C_2H_6, -C_2H_4)]{Et_2Zn\ (2\ equiv)\\PdCl_2(dppf)\ (1.5\ mol\%)} RCH_2ZnI \qquad (20)$$

dppf = 1,1′-bis(diphenylphosphino)ferrocene

When the Pd-catalyzed exchange protocol was applied to the δ-alkenyl iodides of type **51**, the cyclized organozinc reagents **52** were directly obtained and functionalized by allylation with ethyl 2-bromomethylacrylate after transmetallation with CuCN•2LiCl. The five-membered ring products **53** were obtained with high *trans* diastereoselectivity, irrespective of the nature of the allylic substituent (R = Ph or OBz) at the allylic position (equation 21)[34,39]. By contrast, the zinc-induced carbocyclizations were found to be moderately *cis* stereoselective when an acyloxy group was present at the allylic position (see Section II.B.2)[29].

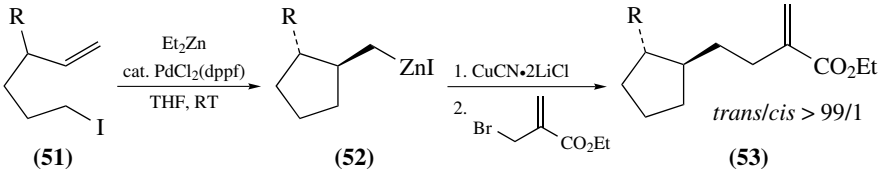

(51) **(52)** **(53)**

R = Ph R = Ph 73% (21)

R = OBz R = OBz 47%

Secondary alkyl iodides were even more reactive and underwent a smooth Pd-catalyzed carbozincation which proceeded with moderate *cis* diastereoselectivity (*cis*/*trans* = 70/30 to 81/19)[39,40]. Interestingly, **54** could be effectively cyclized to the organozinc species **55**, a result which seemed to rule out the involvement of an open-chain organozinc species

in the cyclization process, as the latter would have certainly triggered the β-elimination of the pivaloyloxy group (equation 22).

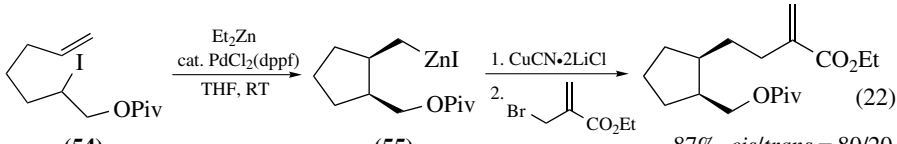

(22)

(54) (Piv = COBu-*t*) **(55)** 87% *cis*/*trans* = 80/20

Secondary alkyl iodides bearing an additional substituent at the allylic position underwent highly diastereoselective Pd-catalyzed carbozincations, as illustrated for **56** which led after allylation with ethyl 2-bromomethylacrylate to the trisubstituted cyclopentane **57** (C1-C2 *trans*/*cis* > 99/1, C2-C3 *cis*/*trans* = 95/5) (equation 23)[39,40].

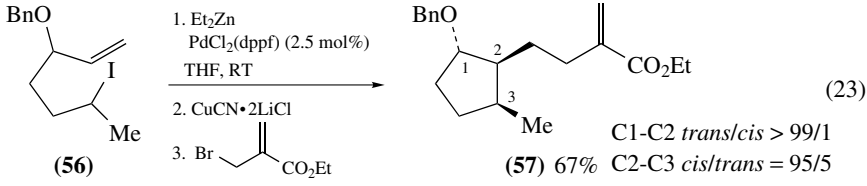

(23)

(56) **(57)** 67% C1-C2 *trans*/*cis* > 99/1 C2-C3 *cis*/*trans* = 95/5

Mechanistic studies supported a radical cyclization process initiated by the reaction of an *in situ* generated Pd^0 complex (reduction of $PdCl_2$(dppf) by Et_2Zn) with the alkyl halide **58**. This would produce a Pd^I complex and a δ-ethylenic radical **59** that would undergo a 5-exo-Trig cyclization to the corresponding cyclopentylmethyl radical **60**, the diastereoselectivity being in agreement with the proposed transition state model for such cyclizations. The radical **60** would then react with the Pd^I species to afford the Pd^{II} complex **61**, resulting from a formal 'cyclizing-oxidative addition' to **58**. Transmetallation of the Pd^{II} complex **61** with Et_2Zn would then deliver the corresponding cyclopentylmethylzinc iodide **62** and a diethylpalladium complex, which would undergo β-hydride elimination and reductive elimination to regenerate the active Pd^0 species with liberation of gaseous ethane and ethylene (equation 24).

The radical cyclization still proceeded for iodides bearing α,β-disubstituted double bonds, but trapping of the resulting secondary radical by a palladium or zinc species was no longer efficient as the reduced cyclized products were obtained[39]. However, attempts to extend the Pd-catalyzed carbozincations to the preparation of five-membered ring oxygen or nitrogen heterocycles were not efficient, but switching to $Ni(acac)_2$ provided excellent results[41]. Nickel-catalyzed intramolecular carbozincations have been applied to the synthesis of (+)-methyl *epi*-jasmonate[42], an essential component of jasmin oil, and to a formal synthetic approach of the antitumor antibiotic (−)-methylenelactocin[43].

Thus, the Pd- and Ni-catalyzed carbozincations of δ-ethylenic halides nicely exploit the high efficiency of radical cyclizations but the overall processes are advantageously leading to organozinc species that can be functionalized by reaction with a wide range of electrophiles. In this case, the unique mode of action of the transition metal catalyst is related to its ability to generate radicals during the oxidative addition process to alkyl halides. Transition metals have also found several interesting applications as catalysts or promotors for the addition of the organozinc reagents to unsaturated carbon−carbon bonds.

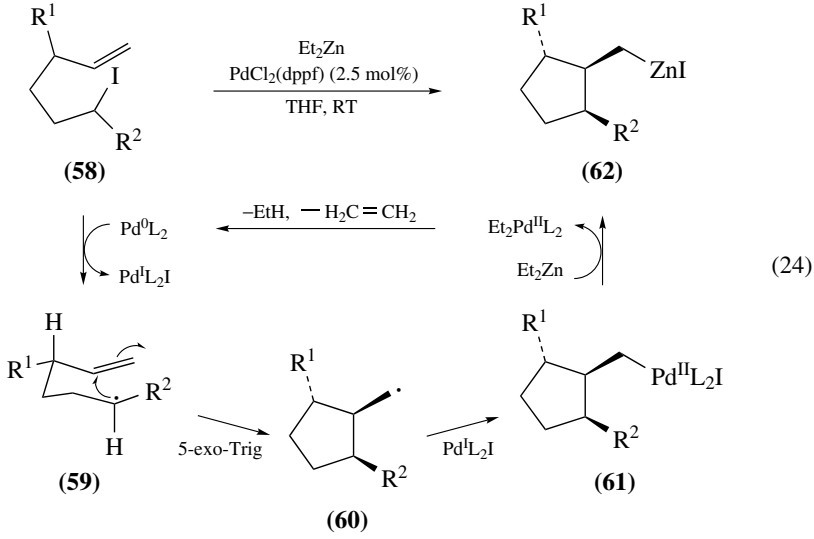

(24)

2. Transition metal-catalyzed/promoted intermolecular carbozincations of alkynes

a. Zirconium-promoted carbozincations. The first reported example of a transition metal-promoted carbozincation of alkynes involved the addition of dialkylzincs to alkynes in the presence of zirconocene dihalides[44]. Addition of Et_2Zn to 1-octyne in the presence of Cp_2ZrI_2 produced a 75/25 mixture of regioisomeric alkenylzincs **63** and **64**, with the ethyl group preferentially delivered to the most substituted carbon. The reaction was stereoselective (*syn* addition process) and protonation or iodinolysis afforded regioisomeric mixtures of alkenes or alkenyl iodides (equation 25). Et_2Zn could be replaced by EtZnCl without noticeable effects and other dialkylzincs, including those bearing β-hydrogen atoms, could be used leading to regioselectivities around 70–80%. Only the Zr-promoted methylzincation of 1-octyne proceeded with a substantially higher regioselectivity (95/5)[44].

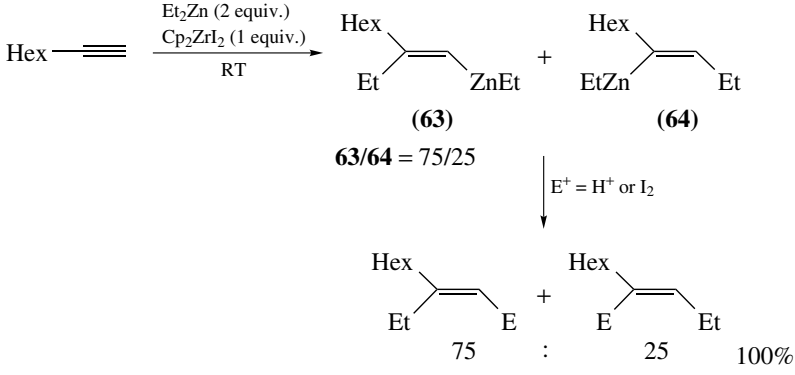

(25)

Zirconocene diiodide was found to be much more efficient than Cp_2ZrBr_2 or Cp_2ZrCl_2, the latter leading to considerably slower rates although the regioselectivity was much higher (**63**/**64** = 96/4). This high regioselectivity turned out to be a consequence of alkyne metallation as a competing side reaction when the ethylzincation was operating at a slow rate. Indeed, 1-octynylzinc chloride underwent a completely regioselective Zr-promoted ethylzincation leading to a sp^2 *gem*-diorganometallic species, as evidenced by deuteriolysis which afforded **65** (equation 26)[44].

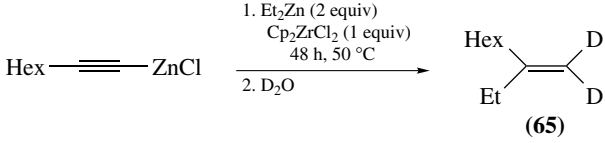

(65) (26)

Similarly, if 5-iodo-1-pentyne (**66**) was converted to the alkynylethylzinc reagent **67**, the subsequent Zr-promoted ethylzincation afforded the *gem*-diorganozinc **68** which was stable in dichloromethane. Replacement of the latter by a more basic solvent such as THF triggered a σ-type cyclization process leading to the cyclopentenylzinc **69**, as demonstrated by the formation of **70** after iodinolysis (equation 27)[45].

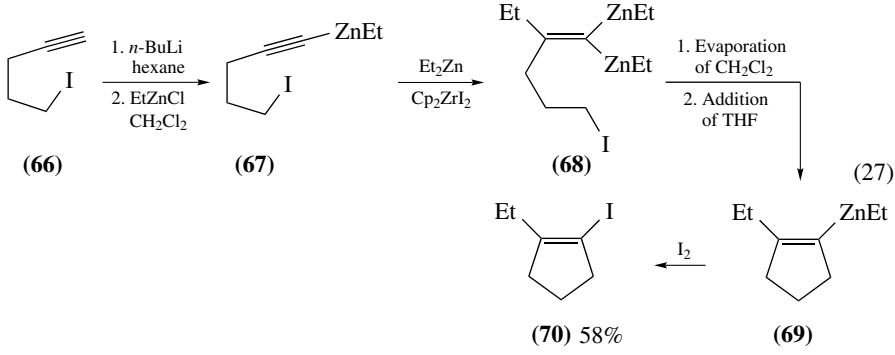

(66) **(67)** **(68)** (27)

(70) 58% **(69)**

Internal alkynes were also viable substrates as illustrated by the ethylzincation of 5-decyne which led to the tetrasubstituted alkenyl iodide **71** after iodinolysis, as a single geometric isomer (*syn* addition) (equation 28)[44].

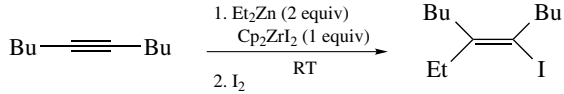

(71) 88% (28)

Mechanistic studies suggested that a full equivalent of Cp_2ZrI_2 was not required but the reaction proceeded rather sluggishly in the presence of a lesser amount. Moreover, addition of Et_2Zn to 1-octyne could be catalyzed by Cp_2ZrMeI and led to an exclusive ethylzincation process, suggesting that the addition of a carbon−zinc bond rather than a carbon−zirconium bond was involved.

b. Nickel-catalyzed carbozincations. The carbozincation of disubstituted arylacetylenes by diorganozincs can be catalyzed by $Ni(acac)_2$ in THF/NMP (NMP = *N*-methylpyrrolidinone). Under these conditions, reaction between Et_2Zn and diphenylacetylene led

to an intermediate tetrasubstituted alkenylzinc **72** resulting from a highly stereoselective *syn* addition process[46,47]. The latter was reacted with several electrophiles and afforded tri- or tetrasubstituted stilbenes of type **73** (equation 29). A small amount of (*Z*)-stilbene resulting from a hydrometallation process was generated as a by-product (2%).

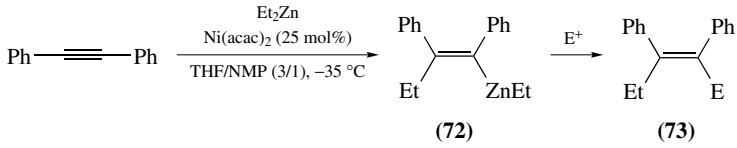

(72) **(73)**

(29)

E^+	E	Yield	
H^+	H	79%	(*Z*)/(*E*) > 98/2
I_2	I	73%	(*E*)/(*Z*) > 99/1
1. CuCN•2LiCl 2. AcCl	Ac	58%	(*E*)/(*Z*) > 99/1

In the case of arylacetylenes bearing an alkyl substituent, the regioselectivity was excellent as long as small alkyl groups (such as Me and Et) were present, but a lower regioselectivity was noticed for longer alkyl chains. Not only dialkylzincs but also diphenylzinc could be regioselectively added to the alkyne **74** and, after iodinolysis, the resulting (*Z*)-alkenyl iodide **75** was subjected to a Pd-catalyzed cross-coupling with the arylzinc bromide **76**. Acidification with HCl then afforded (*Z*)-tamoxifen hydrochloride **77**, an antiestrogenic anticancer drug (equation 30)[46,47].

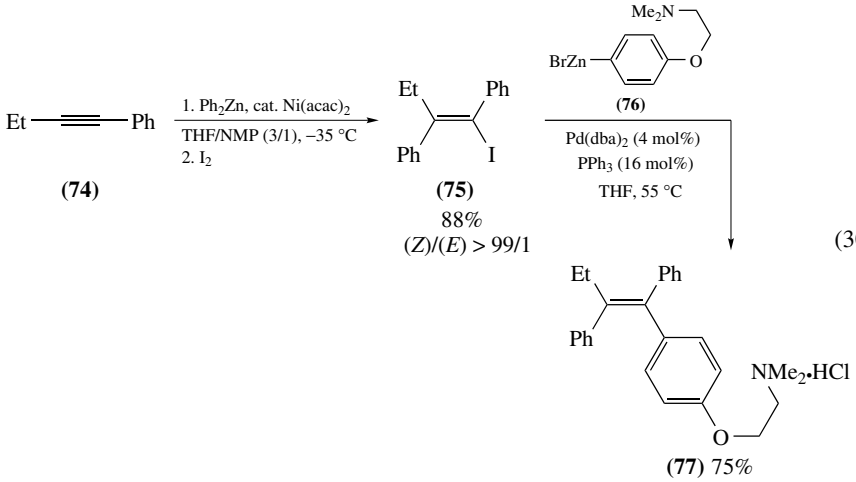

(74) **(75)** 88% (*Z*)/(*E*) > 99/1 **(76)** **(77)** 75%

(30)

In the case of silyl-substituted arylacetylenes, the regioselectivity was reversed and a stable α-silylalkenylzinc reagent was formed preferentially, the latter being configurationally stable under the reaction conditions (equation 31).

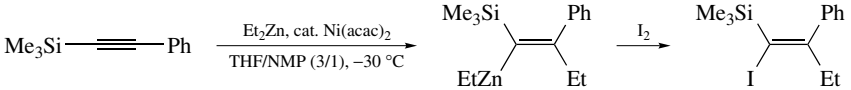

61% (31)

The reaction was not limited to arylacetylenes as a variety of disubstituted heteroarylalkynes bearing a 2-thienyl, a 5-pyrimidinyl or a 2-pyridyl group could also be used successfully[47].

The proposed mechanism involves an initial transmetallation of the dialkyl (or diphenyl) zinc with $Ni(acac)_2$ that generates an organonickel species. The latter then achieves the carbonickelation of the alkyne leading to an alkenylnickel(II) complex. Transmetallation with RZn(acac) then regenerates the Ni^{II} catalyst and affords the α-arylalkenylzinc compound (equation 32)[46,47].

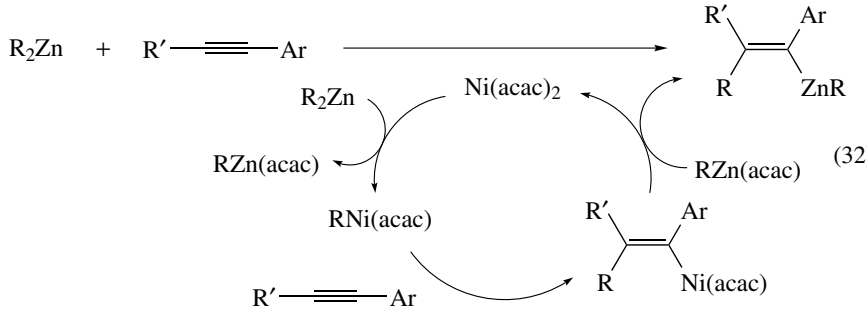

(32)

Thus, the catalytic activity of nickel is explained by the replacement of an unachievable carbozincation by a favorable carbonickelation process, and the catalytic cycle is sustained by two transmetallation reactions.

3. Transition metal-catalyzed intermolecular carbozincations of alkenes

a. Iron-catalyzed carbozincations. Iron salts are particularly attractive catalysts for many organometallic processes as they are non-toxic, cheap and environmentally benign[48]. The addition of several diorganozinc reagents such as Et_2Zn, Pen_2Zn or a zinc homoenolate species across the strained reactive double bond of the cyclopropenone ketal **78** could be catalyzed by $FeCl_3$ and the alkylated cyclopropanone ketals **79** were obtained in good yields after hydrolysis (equation 33)[49].

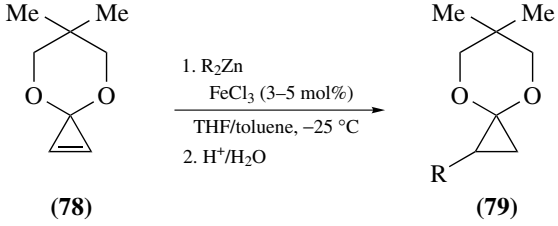

(78) **(79)**

(33)

(a) R = Et 73%
(b) R = Pen 91%
(c) R = $(CH_2)_2CO_2Pr$-*i* 76%

It was suggested that reduction of the Fe^{III} salt to a Fe^{I} catalyst may initially operate and lead to an alkyliron as the actual carbometallating species, followed by subsequent transmetallation of the resulting cyclopropyliron to a cyclopropylzinc reagent. Exploration of an enantioselective version led to the development of an original ternary catalytic system involving $FeCl_3$, a chiral diphosphine such as *p*-TolBINAP (**80**) and a bidentate achiral diamine such as TMEDA. The reaction was run in a toluene/tetrahydropyran

mixture as THF dramatically eroded the enantioselectivity. Although TMEDA slowed down the rate of the carbometallation, only a racemic product was obtained in its absence (equation 34)[49].

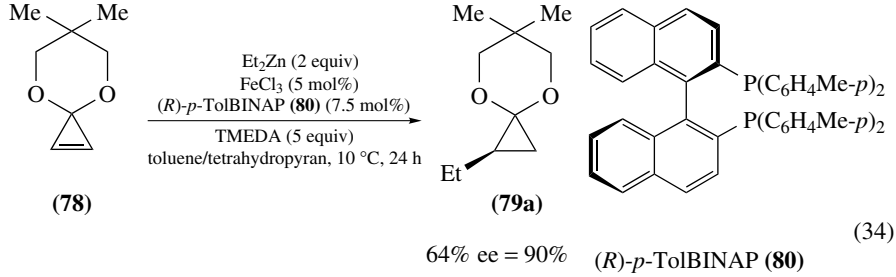

(78) **(79a)** 64% ee = 90% (*R*)-*p*-TolBINAP **(80)** (34)

However, extension of the iron-catalyzed carbozincation to other classes of alkenes has not been reported.

b. Palladium-catalyzed carbozincations. Oxabicyclic alkenes constitute an interesting class of compounds displaying high reactivity towards a variety of organometallic reagents. The alkylative ring-opening of such substrates provides an interesting strategy for the synthesis of cyclic and acyclic structures bearing multiple contiguous stereocenters[50,51]. Although such reactions may not be regarded as real carbometallations in the sense that they do not in general produce organometallic species, their formation was occasionally observed en route to the ring-opening process. As organozinc reagents are not reactive enough towards oxabicyclic alkenes, they offer the opportunity of developing transition metal-catalyzed reactions. Thus, the oxabenzonorbornene **81** underwent an alkylative ring-opening reaction with Et_2Zn in the presence of a palladium catalyst and the chiral ligand **80**, leading to the *syn*-dihydronaphthol **82** in high enantiomeric excess (equation 35)[52].

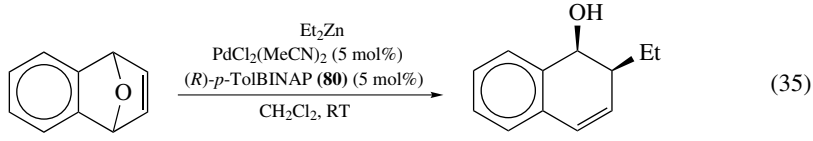

(81) **(82)** 98% ee = 96% (35)

A wide variety of diorganozinc reagents (provided that an adequate method for their preparation was followed) as well as the less reactive dimethylzinc led to excellent results in the enantioselective Pd-catalyzed alkylative ring-opening[52,53]. Recently, it was demonstrated that organozinc halides could also be used[54]. A complementary strategy relying on a copper-catalyzed alkylative ring-opening in the presence of a chiral phosphoramidite ligand has also been reported but led to the epimeric *anti*-dihydronaphthols, presumably by nucleophilic attack of the organozinc reagent to an intermediate π-allylcopper species[55].

Compared to oxabenzonorbornenes, oxabicyclo[2.2.1]heptenes or oxabicyclo[3.2.1] octenes are less reactive substrates, and the Pd-catalyzed alkylative ring-opening process with organozinc reagents generally required heating in 1,2-dichloroethane at reflux. The addition of $Zn(OTf)_2$ dramatically improved the rate of the reaction which could be carried out in CH_2Cl_2 at room temperature, as illustrated for the conversion of **83** to the

cycloheptenol **84**[56]. However, in the absence of $Zn(OTf)_2$, the reaction led to a mixture of **84** and the product **85** resulting from an enantioselective ethylzincation (equation 36)[53].

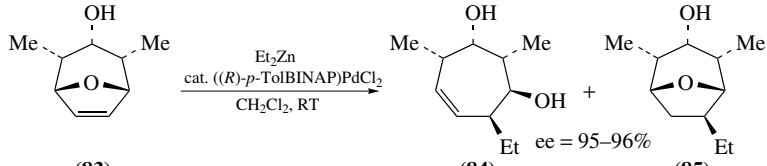

(36)

(83) **(84)** **(85)**

With added $Zn(OTf)_2$	87%	–
No additive	53%	28%

When the alcohol moiety was protected as a silyl ether, the resulting substrates such as **86** became even less reactive and the Pd-catalyzed process cleanly stopped at the carbozincation stage, even in the presence of $Zn(OTf)_2$. The resulting configurationally stable oxabicyclic organozinc reagent **87** could be protonated, iodinolyzed or alternatively transmetallated to an organozinc–copper reagent which reacted with allylbromide to afford the oxabicyclo[3.2.1] octenes of type **88**. The organozinc species **87** underwent ring-opening when heated at reflux in 1,2-dichloroethane (DCE) or if hard electrophiles such as benzoyl chloride or Me_3SiCl were added, probably due to the activation of the bridgehead oxygen. Alternatively, addition of EtMgBr induced the ring-opening of **87** presumably through the formation of a zincate species (equation 37)[53].

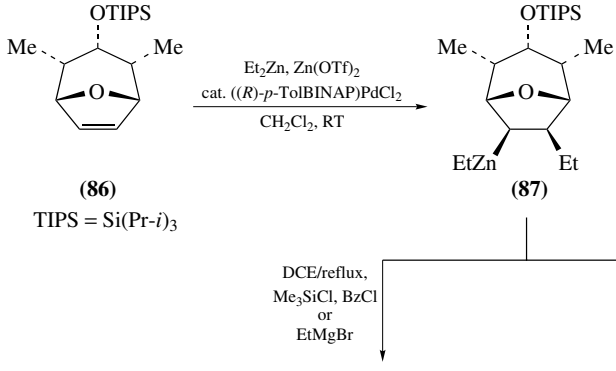

(86)
TIPS = Si(Pr-*i*)$_3$

(87)

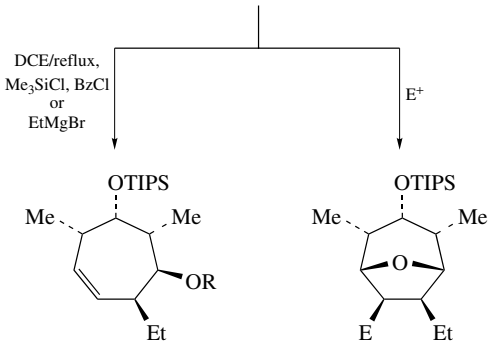

(37)

R = $SiMe_3$	65%
R = Bz	80%
R = H	84%

(88)

E^+	E	
H^+	H	83%
I_2	I	58%
1. CuCN·2LiCl 2. AllBr	All	64%

However, examples of Pd-catalyzed carbozincation appear to be limited so far to appropriately substituted oxabicyclic alkenes.

c. Zirconium-catalyzed ethylzincation. Addition of Et_2Zn to a variety of monosubstituted alkenes can be catalyzed by a combination of Cp_2ZrCl_2 (10 mol%) and EtMgBr (20 mol%) in THF to afford the corresponding ethyl-substituted dialkylzincs[57]. The reaction is reasonably general with respect to the alkene substituent, though allylbenzyl and allylphenyl ethers do not react. Under these conditions, 1-decene was converted to the diorganozinc **89** as demonstrated by iodinolysis, which afforded the primary alkyl iodide **90** in high yield. A palladium-catalyzed cross-coupling with iodobenzene leading to **91** could also be achieved, provided that THF was removed and replaced by a more polar solvent such as DMF (equation 38).

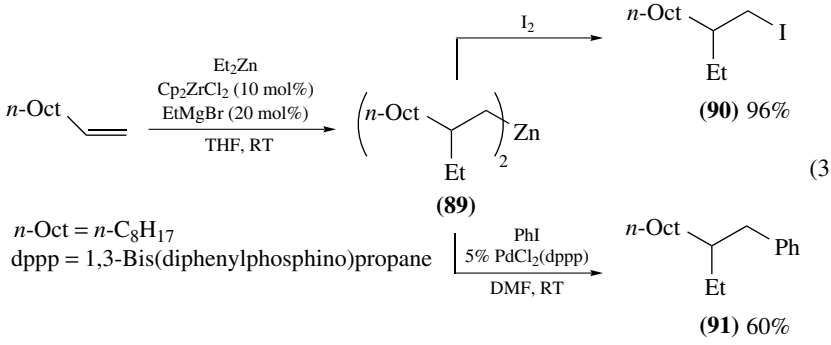

(38)

The proposed mechanism is based on the initial formation of ethylene–zirconocene complex, which upon oxidative coupling with the terminal alkene lead to a zirconacyclopentane. The latter would undergo a regioselective transmetallation with Et_2Zn producing a bimetallic species **92**, with the sterically hindered zirconocene moiety ending up at the less congested site. Chemoselective β-hydride elimination from the ethyl group, followed by reductive elimination, would then regenerate the catalytically active ethylene–zirconocene complex and deliver an ethylzincated compound which could enter a second catalytic cycle and ultimately lead to the ethyl-substituted dialkylzinc (equation 39).

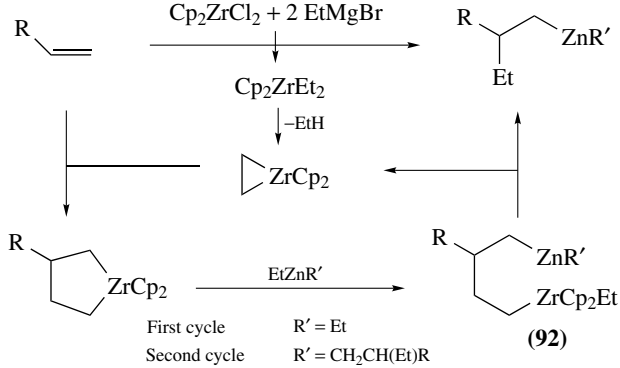

(39)

d. Titanium-catalyzed carbozincation of enynes. The cyclizing-carbozincation of 1,6- or 1,7-enynes of general formula **93** has been achieved by treatment with Et_2Zn in the

presence of a catalytic system consisting of a combination of $ClTi(OPr\text{-}i)_3$ and $EtMgBr$[58]. The reaction led to an organozinc species whose structure was tentatively formulated as **94**, based on the fact that a single equivalent of Et_2Zn per enyne appeared necessary (even though the latter was routinely used in excess). Hydrolysis (or deuteriolysis) afforded the alkylidene five- or six-membered rings **95**, whereas iodinolysis generated the corresponding diiodides **96**. Interestingly, reaction with (bromomethyl)methylether (MOMBr) afforded 1-alkenylbicyclo[n.1.0]alkenes ($n = 3$ or 4) **97**, presumably resulting from alkylation of the alkenylzinc moiety, subsequent homoallyl–cyclopropylcarbinyl rearrangement and β-elimination of the methoxy group (equation 40). The nature of the catalytic system suggests the intervention of a Ti^{II}–ethylene complex as the catalytically active species, which promotes the oxidative cyclization of enynes **93** leading to the titanabicycles **98**. Transmetallation of the two carbon–titanium bonds with Et_2Zn affords the cyclized diorganozinc species **94** and generates a diethyltitanium complex undergoing β-hydride elimination and reductive elimination of ethane to regenerate the catalytic species[58]. This extremely simple procedure appears therefore particularly attractive for achieving the cyclization of a variety of 1,6- or 1,7-enynes.

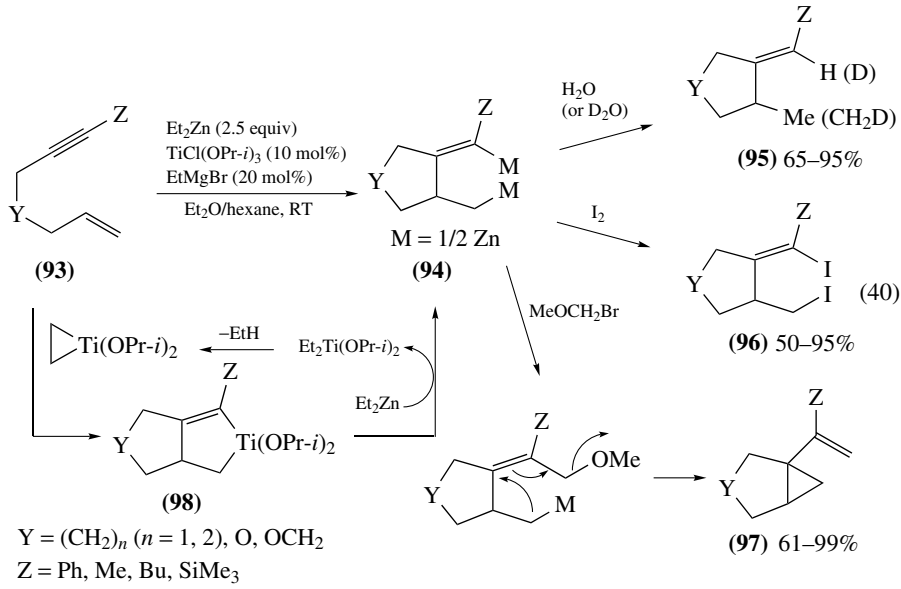

The key success of these metal-catalyzed processes lies in the replacement of an unachievable carbozincation by an alternative carbometallation involving the transition metal catalyst, or another pathway such as an alkene–alkene (or alkyne) oxidative coupling promoted by a group IV transition metal complex, followed by transmetallation. An organozinc is ultimately produced and the latter can be functionalized by reaction with electrophiles.

D. Multi-component Reactions involving Organozinc Reagents

The addition of diorganozincs to disubstituted arylacetylenes can be catalyzed by nickel complexes (see Section II.C.2). Under the same conditions, the terminal alkyne 6-iodo-3-phenylhex-1-yne (**99**) also reacted with Et_2Zn but the alkylidenecyclopentane **100** was

obtained. This product could appear as resulting from addition of Et_2Zn across the triple bond of **99** followed by intramolecular nucleophilic displacement of the iodide. However, the actual process followed an entirely different mechanism based on the oxidative addition of an *in situ* generated Ni^0 complex to the iodide **99** and subsequent intramolecular *syn* carbonickelation. Transmetallation with Et_2Zn would lead to an ethylalkenylnickel complex affording the final product **100** after reductive elimination. No carbozincation was thus involved (equation 41)[46,47].

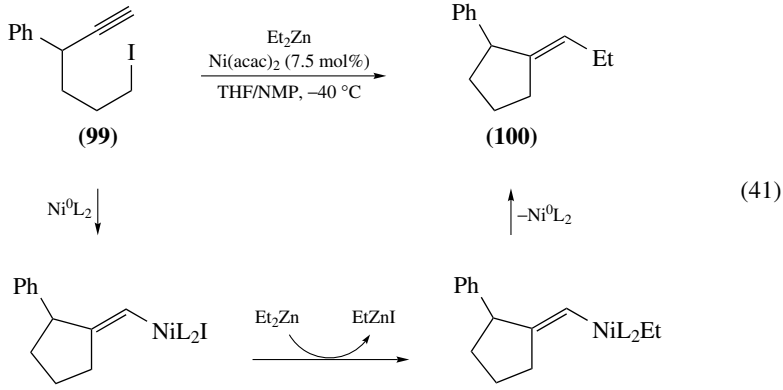

(41)

Indeed, organozinc reagents have been involved as partners in nickel-catalyzed/promoted multi-component reactions, involving an organic compound bearing a carbon−carbon multiple bond (alkenes, alkynes, 1,3-dienes, allenes) and another unsaturated compound acting as the formal electrophilic component, such as an α,β-unsaturated carbonyl compound or a carbonyl compound (aldehydes or ketones and even CO_2)[59,60]. These processes do not involve any carbozincation nor do they produce organozinc compounds as intermediates, but they have been included in this chapter for the sake of comparison and also for their high synthetic value.

The proposed mechanisms, in cases where an α,β-unsaturated ketone (equation 42) or a carbonyl compound (equation 43) are used as partners, involve an initial oxidative coupling of both unsaturated partners in the presence of a Ni^0 complex leading to a nickelacycle **101** or an oxanickelacycle **102**. Transmetallation with the organozinc species then delivers the Ni^{II} complexes **103** or **104** bearing either a zinc enolate or a zinc alkoxide. These complexes undergo reductive elimination to afford the products **105** or **106** resulting from the three-component coupling. However, in cases where the R substituent of the organozinc bears β-hydrogen atoms, β-hydride elimination may also compete with the direct reductive elimination and deliver a product incorporating a hydrogen instead of the R residue of the organozinc, leading to a formal reductive nickel-catalyzed coupling process.

Many elegant reactions that exploit such nickel-catalyzed three-component processes have been described[59,60] and some representative examples will be indicated.

Treatment of the alkynyl enones of type **107** with a variety of organozinc species ($RZnCl/R_2Zn$ from RLi and $ZnCl_2$) in the presence of a catalytic amount of $Ni(COD)_2$ (COD = 1,5-cyclooctadiene) afforded the functionalized alkylidenecyclopentanes **108** with complete control of the configuration of the exocyclic double bond. For organozinc possessing β-hydrogen atoms, these reactions were accompanied by variable amounts of by-products **109** resulting from a formal enone−alkyne reductive cyclization. The latter compounds were found to predominate when a phosphine such as PPh_3 was added (equation 44)[61–63].

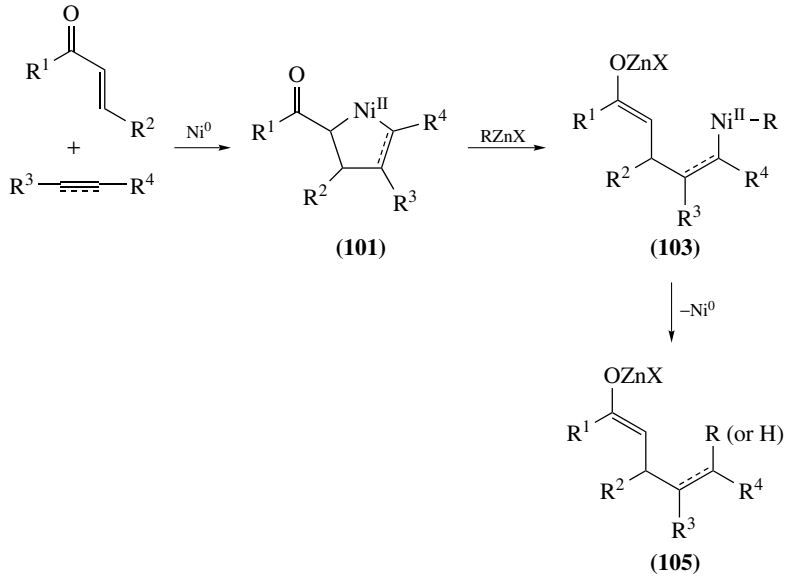

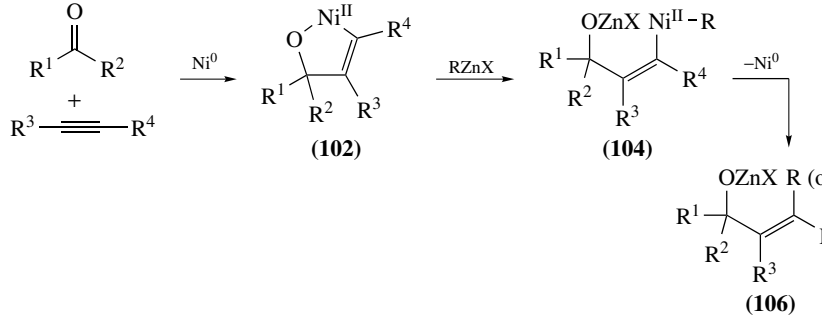

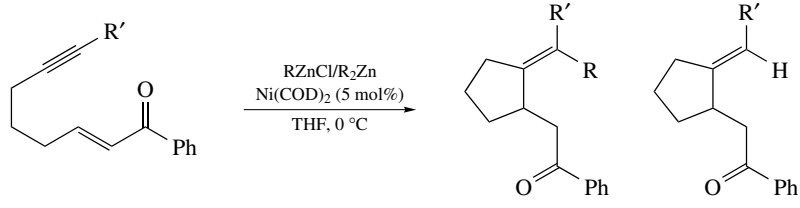

(107)
R′ = H, Ph, Bu

(108)
R = Me, Bu, Ph, Vinyl 38–82%
R = Bu and added PPh_3 (25 mol%) 47–92%

(109)

Besides enones, other successful partners include alkylidene malonates or acetoacetates and nitroalkenes[64]. Heteroatoms can also be included in the separating chain between the enone and the alkyne and this methodology was used as a key step in the synthesis of isodomoic acid G[65].

In the related intramolecular version, an alkyne, Me_2Zn and an α,β-unsaturated ketone were coupled in the presence of a catalytic amount of $Ni(acac)_2$ and Me_3SiCl to afford β-alkenylketones. The use of a chiral ligand such as **110** led to the development of an enantioselective version and ee's up to 81% could be obtained (equation 45)[66].

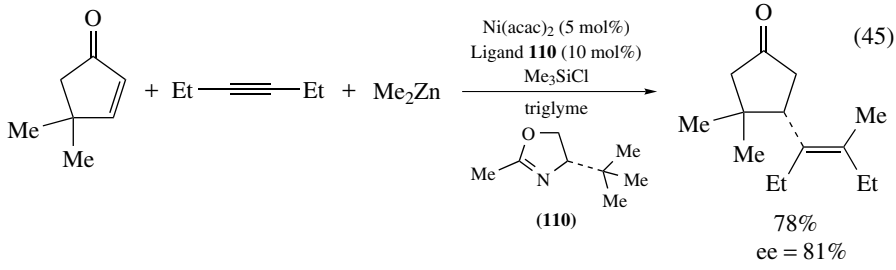

(45)

Aldehydes constitute useful electrophilic partners in such nickel-catalyzed reactions because the condensation between alkynes, aldehydes and diorganozinc compounds can afford stereodefined cyclic or acyclic allylic alcohols[67–69], as illustrated by the stereoselective cyclization of **111** to the corresponding 3-hydroxypyrrolidine (equation 46). Allenes or 1,3-dienes instead of alkynes also lead to similar reactivity[70].

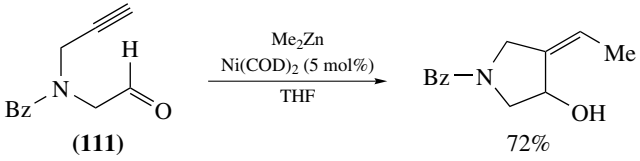

(46)

Other examples of intermolecular processes include the three-component coupling between 1,3-dienes, a diorganozinc species lacking β-hydrogen atoms (Me_2Zn or Ph_2Zn) and a carbonyl compound, catalyzed by $Ni(acac)_2$. This reaction provides a convenient strategy for the regio- and stereoselective synthesis of homoallylic alcohols[71–74]. The mechanism presumably involved the formation of a *syn* π-allylnickel complex **112** which underwent reductive elimination in such a way as to deliver the R group to the distal site, so that the coordination of Ni^0 with both the zinc alkoxide and the *trans* carbon–carbon double bond may be better maintained (equation 47). In the case of less reactive carbonyl compounds, the Ni^0 complex can promote the oxidative dimerization of the 1,3-diene prior to reaction with the carbonyl derivative, leading to homoallylic alcohols having incorporated two molecules of the diene. Contrary to initial reports, cyclic dienes that form *cis* complexes with Ni^0 can also participate in such reactions[74].

Carbon dioxide has also been used as partner in nickel-promoted three-component couplings involving an alkyne and an organozinc reagent. The reaction occurred under mild conditions, required DBU as an additive and allowed an efficient access to β,β-disubstituted acrylic acids (equation 48)[75]. The scope of this reaction is quite broad as *n*-alkyl, benzyl, aryl[75] and even alkynyl[76] organozinc reagents could be used successfully. However, in the case of Et_2Zn, β-hydride elimination preferentially occurred leading to a formal alkyne–CO_2 reductive coupling. Very recently, a catalytic version was achieved in the case of alkynylsilanes as substrates in the presence of an excess of DBU and afforded α-silyl-β,β-disubstituted acrylic acids with moderate to excellent regioselectivities[77].

Nickel-promoted couplings between 1,3-dienes, CO_2 and organozincs have also been reported[78]. Thus, 1,3-cyclohexadiene in the presence of $Ni(COD)_2$ and DBU, under an

atmospheric pressure of CO_2, generated an intermediate nickelacycle that was transmetallated with the organozinc reagent to afford the π-allylnickel complex **113**. If Me_2Zn was used, complex **113** (R = Me) did not rapidly undergo reductive elimination but reacted with CO_2 to afford the *trans*-dicarboxylic acid **114**. By contrast, if Ph_2Zn was added, the π-allylnickel complex **113** carrying an sp^2-hybridized substituent (R = Ph) underwent a more rapid reductive elimination leading to the *cis*-1,4-disubstituted carboxylic acid **115** (equation 49).

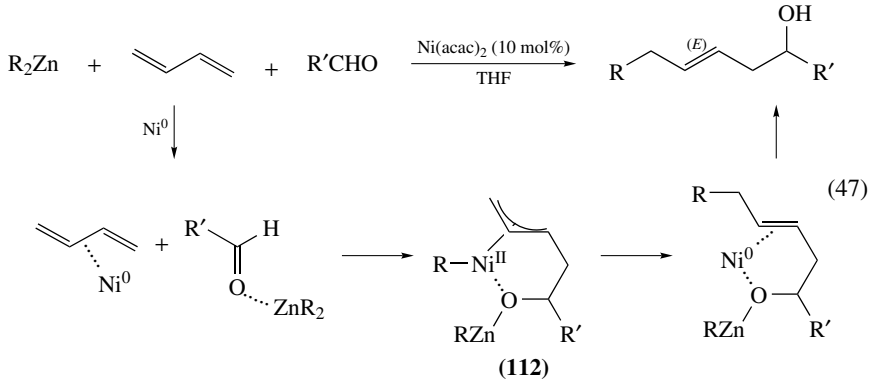

(47)

(112)

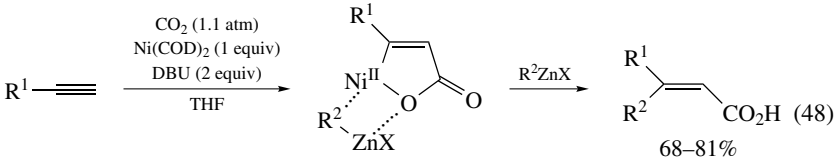

(48)

R = Ph, *p*-$MeOC_6H_4$, *p*-$CF_3C_6H_4$, $(CH_2)_2OBn$

R^2ZnX = PhZnCl, BnZnBr, BuZnI, $EtO_2C(CH_2)_nZnI$ (n = 3, 4).

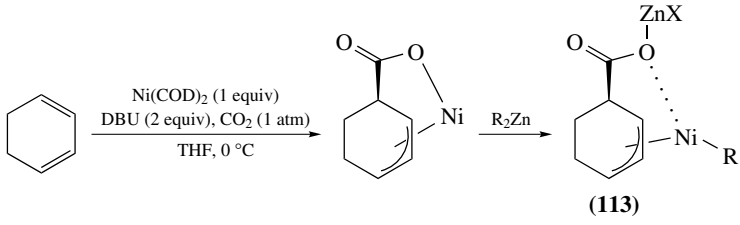

(113)

(49)

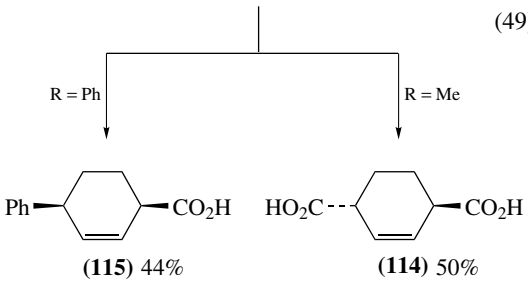

(115) 44% **(114)** 50%

Due to the low reactivity of alkyl and arylorganozinc reagents towards alkenes and alkynes, it appears clear that the carbozincation chemistry for this class of reagents is intimately associated with transition metal catalysts. Some of the metal-catalyzed/promoted reactions do indeed produce organozinc reagents as the final organometallic species that can further react with an appropriate electrophile, whereas other processes lead to highly functionalized products by an entirely different pathway.

E. Carbozincation of a 1,3-Dipolar Intermediate

Although this chapter is essentially devoted to the carbozincation of alkenes and alkynes, some noteworthy examples of addition of dialkylzincs to a 1,3-dipolar intermediate have been disclosed[79]. Heating a mixture of methylenecyclopropanone ketal **116**, Et_2Zn and cyclohexanone in toluene at 60 °C afforded the homoallylic alcohol **117** in good yield. It was suggested that thermolysis of **116** could generate a biradical species, also possessing some dipolar character, that could undergo addition of diethylzinc to produce an allylic organozinc reagent whose reaction with cyclohexanone led to **117** (equation 50).

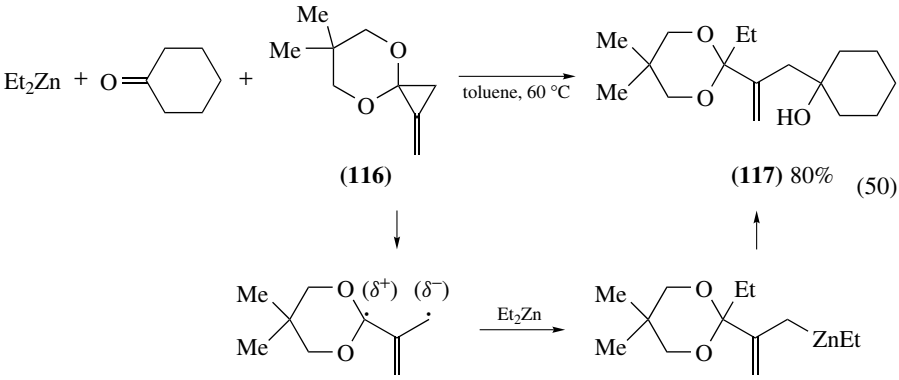

(50)

This is the first evidence of trapping of a diradical reactive intermediate with an organometallic reagent that opens new interesting synthetic possibilities.

III. REACTIVITY OF ALLYLIC ORGANOZINC REAGENTS

Allylic organozinc reagents are considerably more reactive towards unsaturated carbon–carbon bonds than alkylzincs. The use of allylic organometallic compounds is fortunately more attractive from the synthetic point of view as the allyl moiety can be converted to a variety of important functional groups. The carbozincation of alkenes and alkynes by allylic organozinc reagents has generally been considered as a metallo-ene process involving a six-centered transition state (equation 51)[5,6].

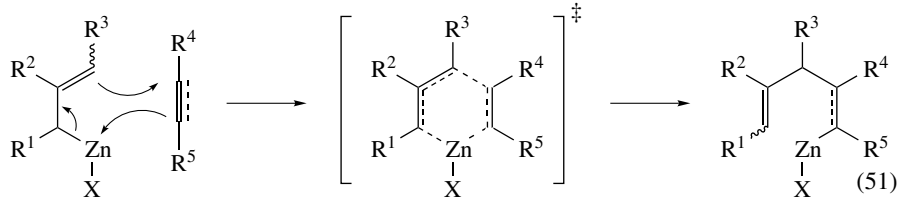

(51)

Besides the issues associated with the regioselectivity and stereoselectivity of these reactions, there is also one particular point of consideration in the case of substituted allylic organozinc reagents which deals with the metallotropic equilibrium of such species. Indeed, each regio- or stereoisomer of a substituted allylic organozinc can in principle give rise to a different carbometallation product.

A. Intermolecular Allylzincation of Alkenes

1. Uncatalyzed reactions

One of the first reports dealing with the carbozincation of alkenes by allylic organozinc reagents was the addition of allylzinc bromide to the homoallylic amine **118** which occurred in refluxing THF. A secondary organozinc **119** was regioselectively produced and provided the amine **120** after hydrolysis. A small amount of aminoalcohol **121**, resulting from oxidation of **119**, was also isolated when the reaction mixture was exposed to air (equation 52)[80,81].

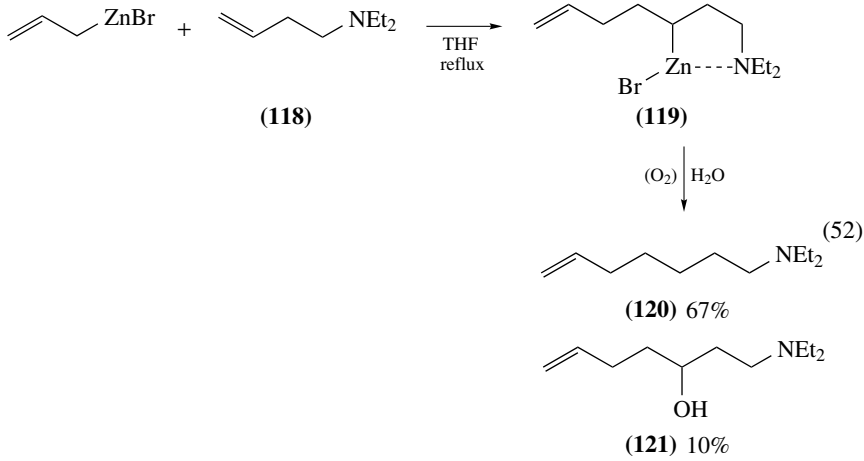

(52)

Interestingly, the allylzincation of the lower or higher homologs of the unsaturated amine **118** proceeded only to a small extent (3–10%) and afforded mixtures of regioisomers. Propyl or benzylzinc bromides did not react with **118**, neither did allylmagnesium bromide or allyllithium[82]. The allylzincation of other homoallylic amines critically depended on their substitution pattern. Thus, the yield dropped significantly when the double bond was α,β-disubstituted whereas α,α-disubstitution hampered the reaction. The efficiency of the addition as well as the regioselectivities were also affected by the steric hindrance around the nitrogen atom and its coordinating ability. Allylzincation of secondary homoallylic amines, which were deprotonated by allylzinc bromide, proceeded more efficiently even for sterically hindered substrates and without any incidence on the regioselectivity (equation 53)[82].

Whereas THF and DME were suitable solvents, Lewis basic additives such as HMPA, DMSO or TMEDA hampered the reaction.[82] These results point towards an intramolecular assistance of the zinc coordinated by the nitrogen atom. A related effect was evidenced in the additions of Grignard reagents to allylic alcohols[83–87]. Two mechanisms were proposed for the allylzincation of homoallylic amines involving formation of a complex with the

nitrogen substituent and delivery of the allyl group either through an intramolecular S_Ei reaction or through a bimolecular process (equation 54)[82].

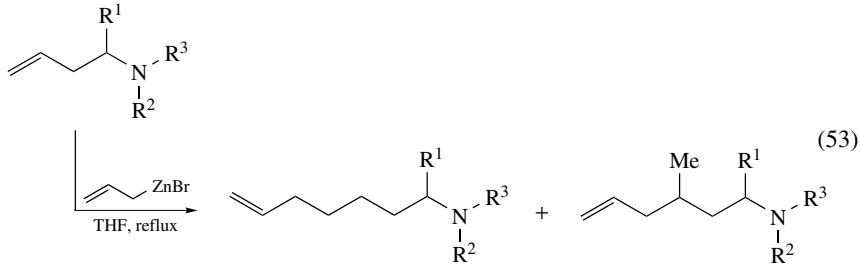

(53)

R^1 = Ph	R^2 = Et	R^3 = Et	20%	81	:	19
R^1 = *i*-Pr	R^2 = Et	R^3 = H	82%	100	:	0

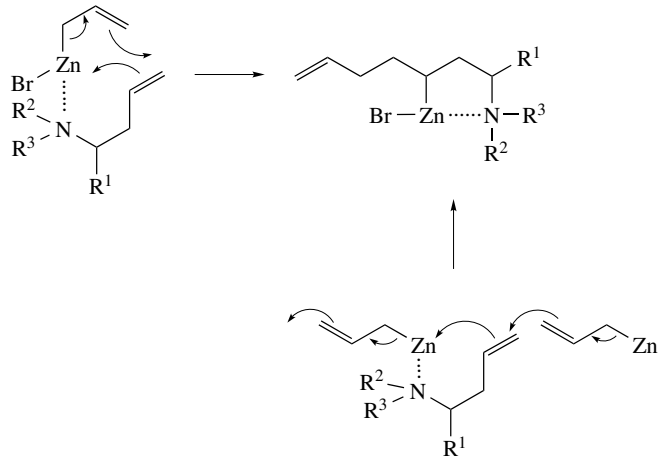

(54)

Failure for Grignard reagents to undergo similar additions to homoallylic amines may be explained by the greater stability of the complexes between an amine and zinc rather than magnesium. By contrast, addition of allylzinc bromide to allyl or homoallyl alcohols proceeded considerably less efficiently compared to amines and the regioselectivity was reversed (equation 55)[81].

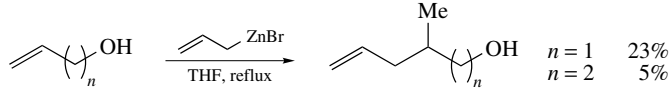

(55)

Successful allylzincations of the terminal double bond of α-allenic amines have also been reported (equation 56)[88].

Although the presence of an appropriately located heteroatom seemed to be required for the success of the allylzincation, it is in fact not necessary. Actually, one of the first reports of allylzincation of an unactivated olefin was related to an observed dimerization reaction when a solution of allylzinc bromide was heated at reflux (following its preparation from allyl bromide and metallic zinc in THF) or if reaction with an electrophile required

prolonged heating[89,90]. It was demonstrated that one molecule of allylzinc bromide could undergo allylzincation by another molecule of this reagent leading to a diorganozinc species **122**, whose formation was ascertained by hydrolysis, deuteriolysis or oxidation with oxygen. When **122** was treated with benzaldehyde, the first carbon–zinc bond reacted in the classical manner by nucleophilic attack, but the remaining one exerted a reduction of another equivalent of the aldehyde leading to the homoallylic alcohol **123** (equation 57).

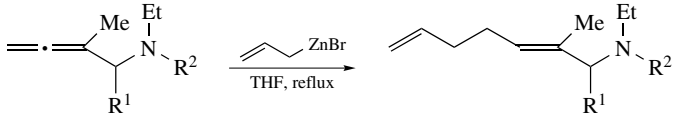

R^1 = H, Ph, *i*-Pr
R^2 = Et, H

32–72% (56)

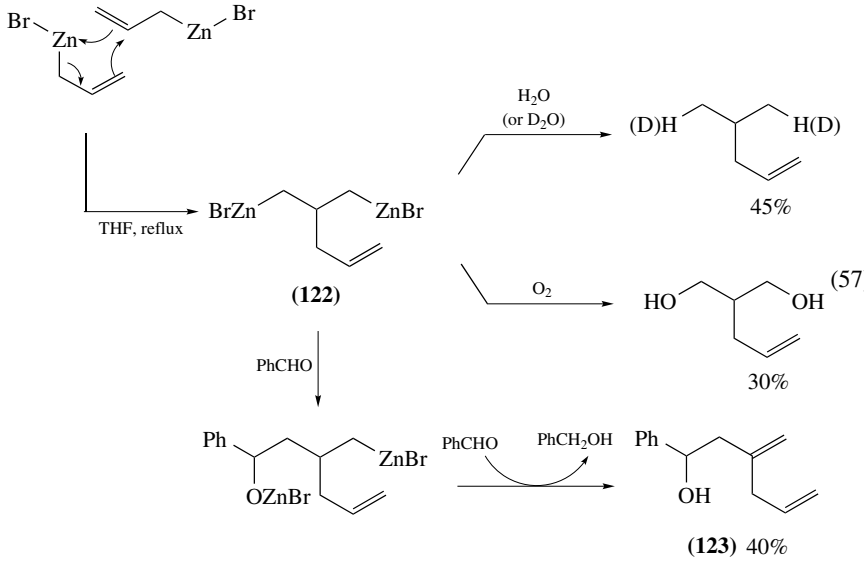

(57)

A similar oligomerization of diallylzinc was observed during its preparation from allylmagnesium bromide and $ZnCl_2$ followed by attempted purification by sublimation[91].

The propensity of various diallylic organozinc reagents to add to alkenes was further demonstrated[92–94]. Diallylzinc, dicrotylzinc, dimethallylzinc and diprenylzinc reacted with ethylene under pressure in toluene and in all cases the resulting dialkylzincs were obtained in high yields. It is also worth mentioning that allylic organozincs substituted at C3 reacted with complete allylic transposition (also referred to as S_E2' regioselectivity), although the ^{1}H NMR spectrum of dicrotylzinc indicated the 2-butenyl form to be predominant (equation 58).

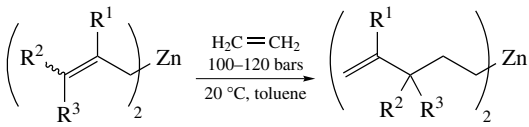

$R^1 = R^2 = R^3 = H$	91%
R^1 = Me, $R^2 = R^3 = H$	98%
$R^1 = R^3 = H$, R^2 = Me	91%
$R^1 = H$, $R^2 = R^3$ = Me	88%

(58)

Although monosubstituted alkenes were significantly less reactive than ethylene, dicrotylzinc could be added to 1-octene to produce the primary dialkylzinc **124**, that was hydrolyzed to the corresponding hydrocarbon (equation 59)[93]. The regioselectivity markedly differed from the one observed for the addition of t-Bu_2Zn to the same substrate (equation 4, Section II.A.2)[16] or addition of allylzinc bromide to the homoallylic amine **118** (equation 52), which both favored the formation of a secondary organozinc species presumably for steric reasons in the former case and due to nitrogen coordination in the latter. Related additions of crotylmagnesium chloride were found to be significantly less regioselective[93].

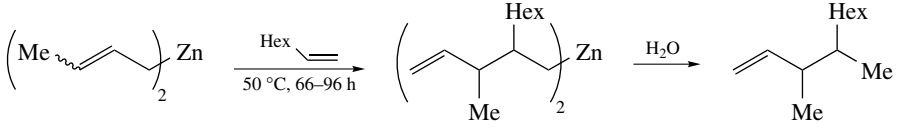

(124) 88% (59)

Addition of dicrotylzinc to styrene afforded a 2/1 mixture of the primary dialkylzinc **125** and the benzylic secondary diorganozinc **126** (equation 60)[93]. A Hammett correlation was found for the addition of di(methallyl)zinc to *para*- and *meta*-substituted styrenes with electron-donating substituents favoring the formation of a primary organozinc whereas electron-withdrawing ones favor the benzylic organozinc species[94,95]. In addition to these results, the regioselectivity of the addition of various crotylzinc species (crotylZnX) to styrene was evaluated and the ratio of regioisomers was correlated with the polar Taft constant σ^* of the X substituent. When X = OMe or Cl, the formation of the primary organozinc was particularly favored[94,96].

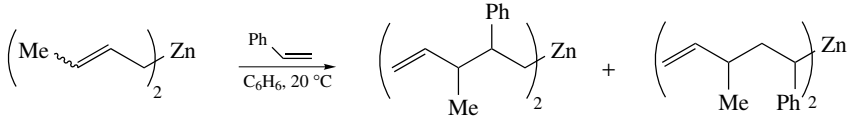

(125) **125/126** = 2/1 **(126)** (60)

Reaction of dicrotylzinc with 1,3-butadiene readily took place at 20 °C and addition competed between C2 and C1, leading respectively to a primary dialkylzinc **127** or a secondary allylic diorganozinc **128** (or any of the mixed metallotropic forms)[93]. Consequently, hydrolysis led to a mixture of three major hydrocarbons **129a–c** but the actual regioselectivity of the addition could not be accurately evaluated. Indeed, **129c** could also in principle arise from the addition of dicrotylzinc, without allylic transposition, to the $C_{(2)}$ atom of butadiene (equation 61).

As for additions of allylic Grignard reagents, the relative reactivity order of the olefins appears to be 1-alkenes < styrene < 1,3-butadiene < ethylene and α,α- or α,β-disubstituted alkenes do not react[94]. However, strained alkenes such as cyclopropenes constitute an exception. Indeed, dicrotylzinc smoothly reacted with 3,3-dimethylcyclopropene and afforded the dicyclopropylzinc reagent **130** resulting from a *syn* addition process (equation 62)[93].

The high reactivity of the strained double bond in cyclopropenes has led to several other more recent developments especially involving cyclopropenone ketals as substrates[97].

Alkoxyallylic organozinc reagents react with the cyclopropenone ketal **78** and the major regioisomer is always the one in which the γ-carbon linked to the alkoxy group becomes

attached to the three-membered ring (γ-adduct), whatever the substituents at the α and β positions. The diastereoselectivity for the newly formed carbon−carbon bond is excellent in all cases (>97%), while a (*Z*)-disubstituted double bond is formed in the relevant cases. By contrast, the regioselectivity in the case of the related alkoxyallylic organolithium reagents (α- vs γ-addition) depends on the substitution pattern, but the diastereoselectivity for the newly formed carbon−carbon bond always remains high (>97%) (equation 63)[98].

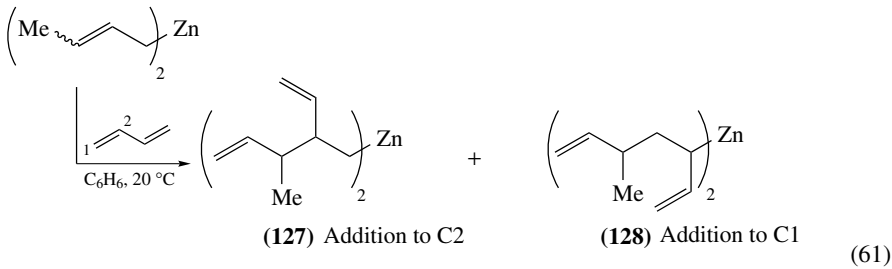

(127) Addition to C2 **(128)** Addition to C1 (61)

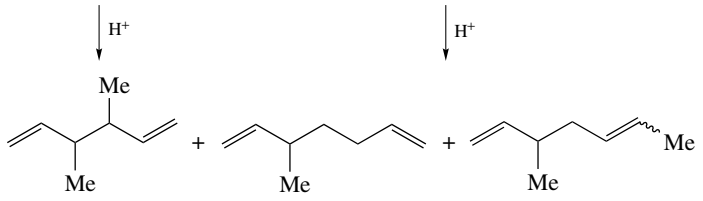

(129a) 56% **(129b)** 31% **(129c)** 10%

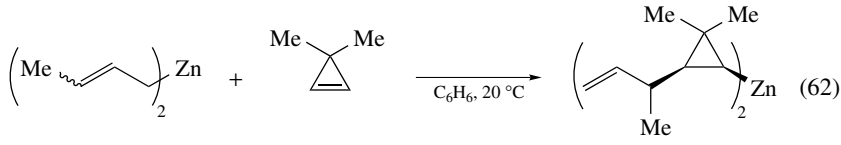

(62)

(130) 98%

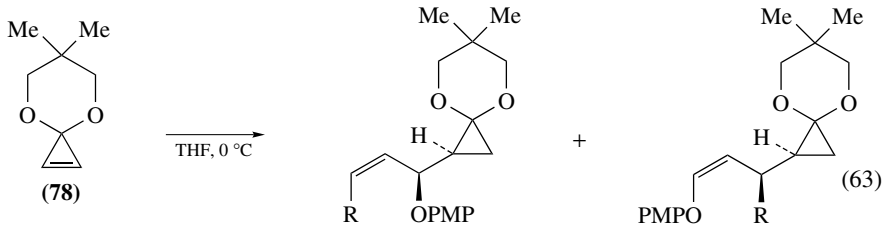

(63)

γ-adduct de > 97% α-adduct de > 97%

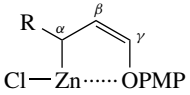

R = H	79%	> 97	:	< 3
R = Ph	90%	82	:	18

PMP = *p*-$MeOC_6H_4$

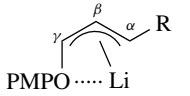

R = H	89%	91	:	9
R = Ph	81%	12	:	88

Theoretical studies using density functional theory (for a more simple hydroxyallylmetal model) revealed that the alkoxyallylzinc species is of σ-nature, due to the high covalent character of the carbon−zinc bond, and reacts with **78** via a single [4 + 2] type six-centered transition state to afford the γ-adduct selectively. By contrast, the related organolithium is of π-allylic nature and reacts with **78** via two different [2 + 2]-type four-centered transition states of similar energies leading to α- and/or γ-adducts[98].

The addition of other substituted allylic organozinc reagents to cyclopropenone ketals has been studied. Cinnamylzinc bromide reacted with **78** in THF to afford a 82/18 mixture of the two diastereomeric cyclopropanone ketals **131** and **132** respectively. It was found that the replacement of the bromide by a bulky electron-donating group such as *tert*-butyl or mesityl (acting as dummy ligands) not only accelerated the reaction but also improved the diastereoselectivity significantly (dr = 94.5/5.5) whereas addition of HMPA further enhanced it (dr = 98/2) (equation 64). The observed stereochemical outcome was supported by computational analysis for a simplified model (S_E2' addition of (*E*)-crotylZnCl(H_2O) to cyclopropene)[99,100].

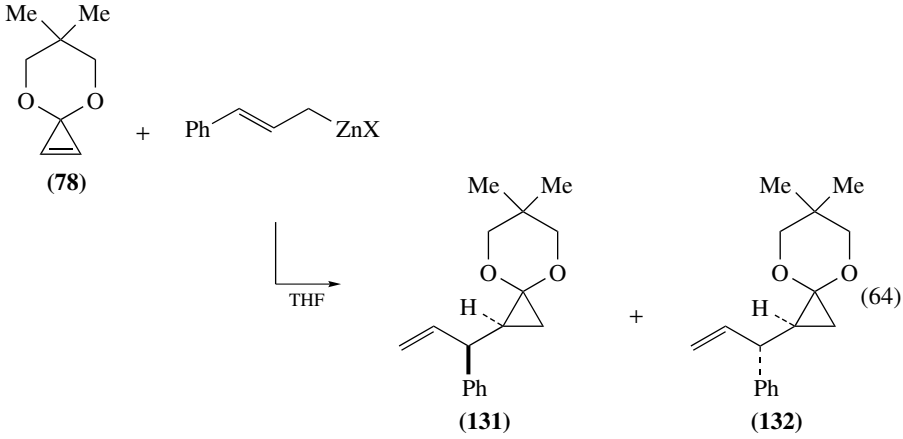

X = Br	THF, 0 °C	81%	82	:	18
X = Mes	THF, −23 °C	97%	94.5	:	5.5
X = Mes	THF/HMPA, −23 °C	70%	98	:	2

Mes = Mesityl = 2,4,6-trimethylphenyl

Addition of cinnamyl(mesityl)zinc to the C_2 symmetrical cyclopropenone ketal **133** led to excellent diastereoselectivities with respect to the newly formed carbon−carbon bond (de = 97%) and induction from the chiral ketal (de = 91%). Deuteriolysis afforded the cyclopropanone ketal **134** in which three stereocenters have been generated[99,100]. A product-like transition state model was proposed, in which the cyclopropene underwent considerable rehybridization and the zinc became preferentially attached to the less hindered equatorial olefinic carbon from the face opposite to the axial ketal methyl group (equation 65).

The first example of enantioselective allylzincation of an alkene was also reported for the cyclopropenone ketal **78** as substrate. The chiral allylzinc complex **135** was prepared from the corresponding bis-oxazoline derived from (*S*)-valine by deprotonation with *n*-BuLi and transmetallation with allylzinc bromide. This reagent reacted with **78** and afforded the allylated product **136** with high optical purity (ee = 99%) (equation 66)[101].

Allylzincation of the monosubstituted cyclopropenone ketal **137** with the chiral reagent **138** proceeded regioselectively so as to generate the less substituted secondary cyclopropylzinc species **139**. After hydrolysis, the resulting cyclopropanone ketal was obtained with high enantiomeric excess (ee = 99%). The reaction was very slow at 20 °C but was considerably accelerated under high pressure (1 GPa) (equation 67)[102].

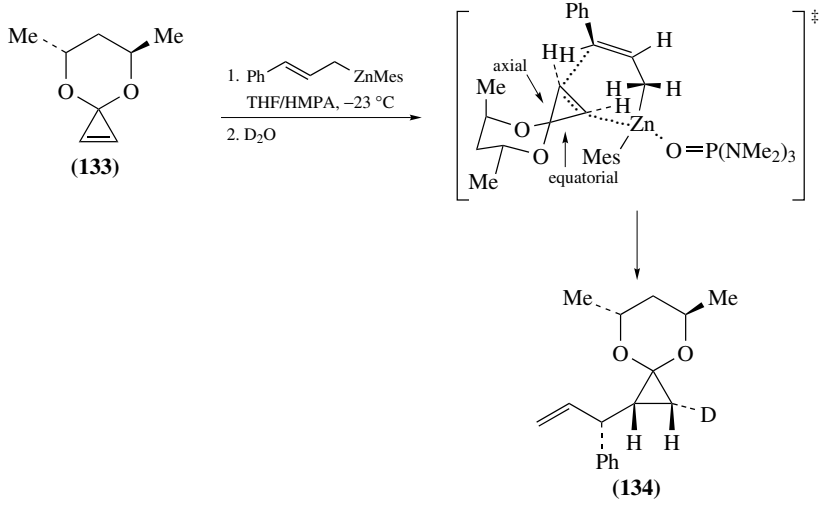

(65)

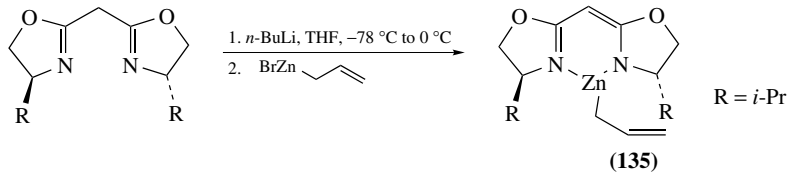

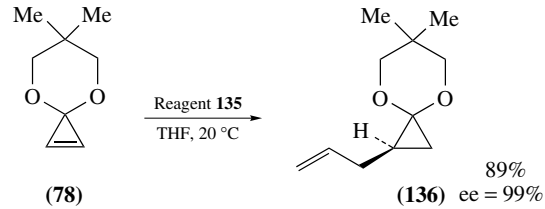

(66)

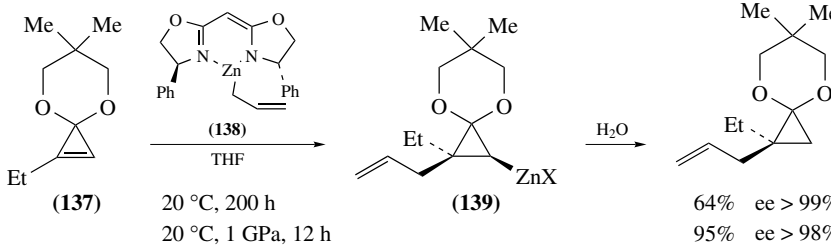

(67)

Unlike compound **137**, the cyclopropenone ketals of type **140** substituted by a group 14 metal (Si, Ge, Sn) reacted rapidly with allylzinc bromide and led after hydrolysis to the substituted three-membered rings **141**. The observed regioselectivities were consistent with the greater stabilization of the corresponding α-silyl-, α-germyl- or α-stannylcyclopropylzincs. Interestingly, when the allylzincation of **140** was performed with reagent **138**, the presence of the chiral ligand overwhelmed this latter favorable electronic factor and reversed the intrinsic regioselectivity of these substrates. After hydrolysis, the cyclopropanone ketals of type **142** were obtained with high optical purities and the regioselectivity became similar to the case of the ethyl-substituted substrate **137** (equation 68)[102].

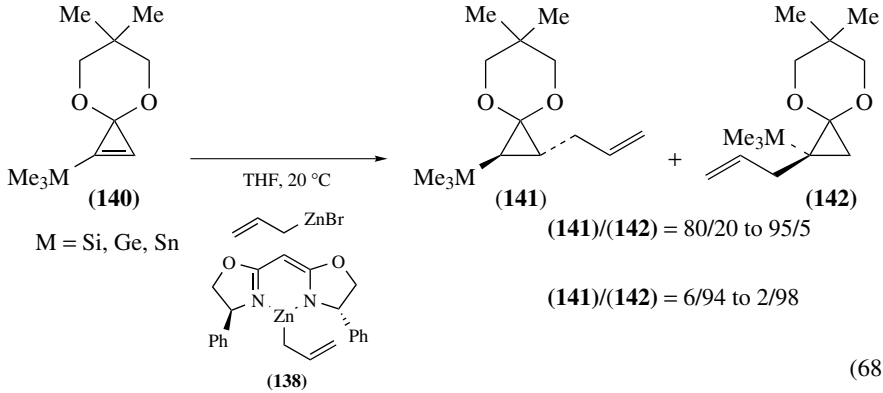

(68)

Unfortunately, additions to mono- or disubstituted alkenes other than the strained cyclopropenes cannot be so easily achieved due to their considerably lower reactivity.

2. Transition metal-catalyzed reactions

By comparison with the intermolecular additions of alkylzincs to alkenes, the use of transition metal catalysts for achieving allylzincations has not been widely investigated. Nevertheless, there is one report of a nickel-catalyzed process wherein a γ,γ-disubstituted allylic organozinc such as prenylzinc bromide was added to the acrolein acetal **143**[103]. Excellent regioselectivities were observed and the resulting primary organozinc bromide **144** could be functionalized by iodinolysis or allylation after transmetallation with copper salts (equation 69). Interestingly, the reaction occurred without allylic transposition, unlike in the uncatalyzed additions of substituted allylzincs to alkenes. However, the nickel catalyst was not successful at efficiently promoting the addition of allylzinc bromide itself to **143**.

B. Intermolecular Allylzincation of Alkynes

1. Uncatalyzed reactions

Terminal alkynes are usually deprotonated by allylic organozinc reagents but in such cases the triple bond becomes activated towards further addition. Such reactions will be treated in a separate section (see Section III.F).

Nevertheless, there is one report dealing with the addition of functionalized allylic organozinc reagents (bearing either an ester or a phosphonate moiety) to alkynes where deprotonation does not seem to operate based on the stoichiometry of the reagents and the yields. Thus, slow addition of the allylic bromide **145** to a sonicated mixture of

propargyl trimethylsilyl ether and zinc in THF led to the adduct **146** in excellent yield (equation 70)[104].

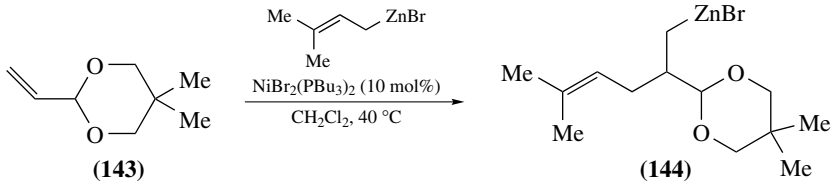

(143) **(144)**

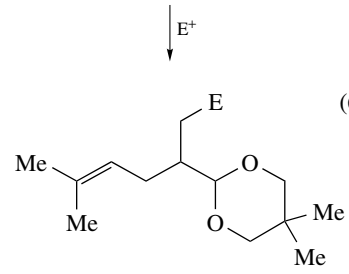

(69)

E^+	E	
I_2	I	60%
1. CuCN·2LiCl 2. AllI	All	45%

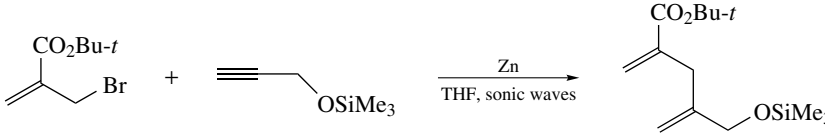

(70)

(145) **(146)** 81%

As a general rule, allylic organozinc reagents do not react with unactivated α,β-disubstituted alkynes. A few exceptions to this trend have been observed in the case of substrates bearing an appropriately located heteroatom such as the homopropargylic tertiary amine **147**. The latter reacted regioselectively with allylzinc bromide but led to a 67/33 mixture of two geometric isomers, apparently derived from *syn* and *anti* additions (equation 71)[82, 105].

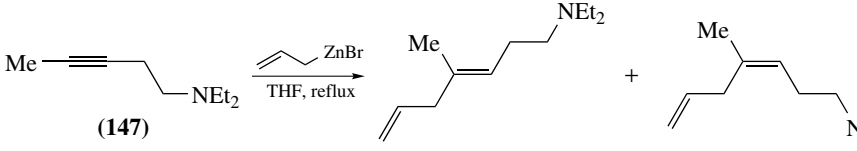

(71)

(147)

67 : 33

65%

Other additions to the triple bond of disubstituted conjugated enynols, bearing a propargylic alcohol moiety, were reported but proceeded in extremely low yields[15, 106].

By contrast with the low reactivity of disubstituted alkynes in general, alkynylsilanes **148** readily undergo addition of allylzinc bromide in THF at reflux[107, 108]. These reactions are highly regioselective leading to intermediate α-silylalkenylzinc reagents by an initial *syn* zinc–ene reaction. However, due to the configurational lability of α-silylalkenylmetals[109], subsequent isomerization can take place under the reaction conditions and finally afford mixtures of stereoisomeric alkenylsilanes **149** and **150**. The ratio depends on the steric bulk of the alkyne substituent as illustrated for substrate **148a** compared to **148b**. In the case of the conjugated enyne **148c**, the addition chemoselectively affected the triple bond (equation 72).

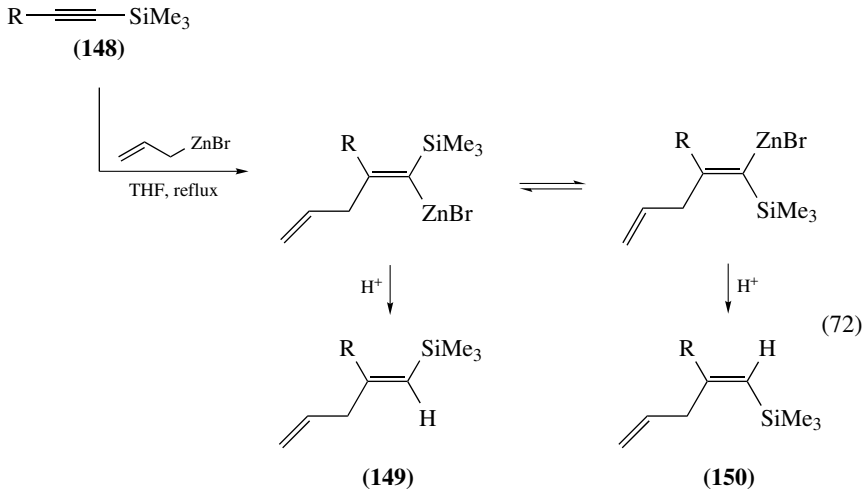

(72)

		149/150	Yield
(a)	R = *n*-Bu	85/15	70%
(b)	R = PrCH(OBn)	<5/>95	74%
(c)	R = $H_2C{=}C(CH_3)$	<5/>95	57%

Addition of the allylic organozinc halide **151**, possessing an additional allylic ether moiety, to the alkynylsilane **148a** led to the intermediate α-silylalkenylzinc **152**. Subsequent treatment with a catalytic amount of $Pd(PPh_3)_4$ generated a π-allylic palladium complex which underwent nucleophilic attack by the (Z) isomer of **152** and afforded the methylenecyclopentene **153**, the product of a formal [3 + 2] cycloaddition between the alkyne **148a** and trimethylenemethane[110]. Due to the configurational lability of **152**, the (*E*) geometric isomer also ultimately led to the same final product **153** (equation 73).

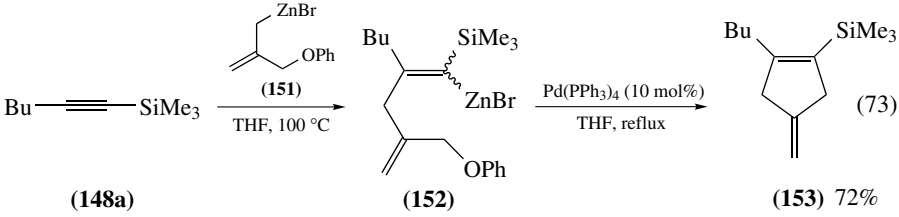

(73)

For other α,β-disubstituted alkynes lacking an activating group, transition metal catalysts or promotors could be used to achieve allylzincation.

2. Transition metal-promoted allylzincation of disubstituted alkynes

Zirconocene diiodide can promote the addition of diallylzinc to α,β-disubstituted unactivated alkynes. Thus, in the case of 5-decyne, a 94/6 mixture of the two isomeric alkenyl iodides (derived respectively from *syn* and *anti* additions to the triple bond) was obtained after iodinolysis (equation 74)[108]. However, the stereoselectivity was lower for 2-butyne (80/20) and the case of unsymmetrical alkynes was not mentioned.

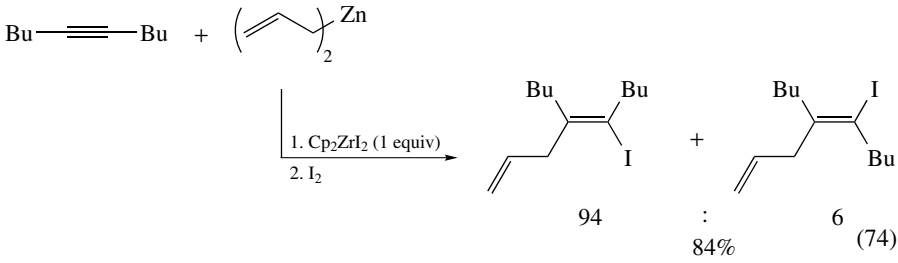

(74)

Interestingly, the Zr-promoted crotylzincation of 5-decyne occurred without allylic transposition (equation 75), presumably via a four-centered transition state, unlike the uncatalyzed addition of crotylzinc bromide to alkynylsilanes which proceeded with complete S_E2' regioselectivity[108].

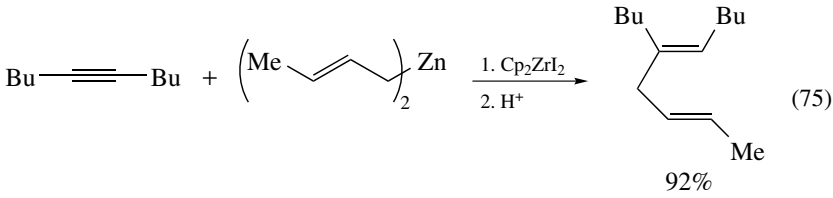

(75)

Recently, cobalt(II) chloride has been found to catalyze the allylzincation of a variety of 1-aryl-1-alkynes[111]. As illustrated for **154**, a *syn* addition to the triple bond occurred with high regioselectivity and afforded an intermediate α-arylzinc species that could be further functionalized (equation 76). Several tri- or tetrasubstituted styrenes have been prepared by this method.

Whereas the intermolecular uncatalyzed allylzincations of unactivated monosubstituted alkenes or disubstituted alkynes do not proceed readily, successful examples of intramolecular additions have been reported.

C. Intramolecular Zinc–Ene Reactions

Intramolecular metallo–ene reactions are thermodynamically favored and are thus more efficient than the intermolecular versions. The classical distinction of the cyclization modes, suggested by Oppolzer, depends on the carbon of the allylic organometallic (ene-component) to which the alkene or the alkyne (enophile) is linked (equation 77)[5,6].

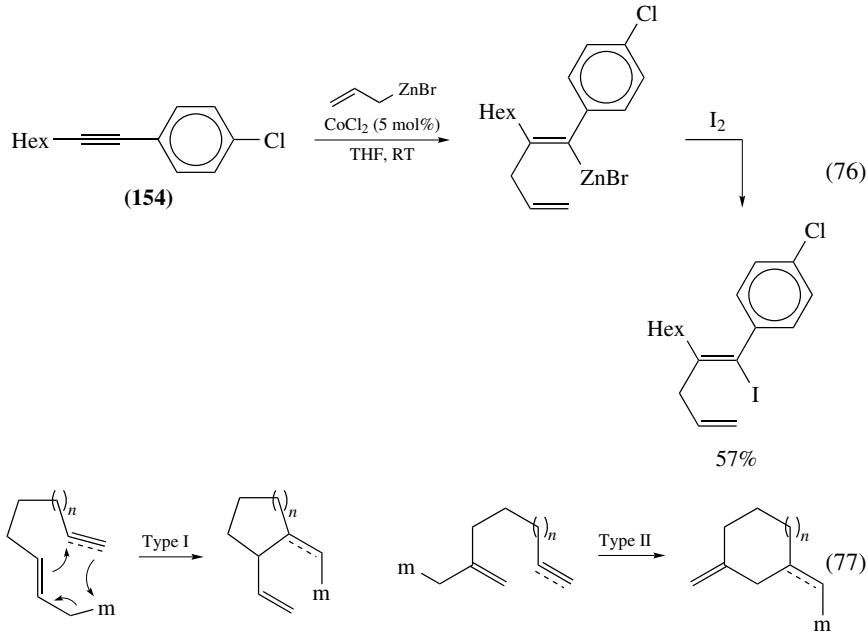

Type I cyclizations are generally restricted to the formation of five-membered rings, whereas formation of six-membered rings occurred more readily than that of five- or seven-membered rings in type II cyclizations. Examples of intramolecular zinc–ene reactions of both types have been reported.

1. Type I zinc–ene reactions

The first reported examples of type I intramolecular zinc–ene reactions involved alkynes as enophiles. Thus, treatment of the mixture of allylic bromides **155a** and **155b** with zinc powder in THF at 20–40 °C led after hydrolysis to 2-vinylmethylenecyclopentane (**156**). Deuteriolysis confirmed the formation of an alkenylzinc species arising from an intramolecular carbozincation. Despite the presence of a terminal alkyne, no competitive (intermolecular) metallation seemed to occur. Whereas unactivated α,β-disubstituted alkynes are reluctant to undergo intermolecular allylzincations, the intramolecular type I zinc–ene reaction proceeded efficiently when the mixture of allylic bromides **157a** and **157b** was treated with zinc in THF at reflux and afforded **158** as a single geometric isomer. Its (*E*) olefinic configuration confirmed that a *syn* addition took place (equation 78)[112]. By comparison, the analogous organomagnesium or organolithium reagents provided little (10–15%) or none of the cyclized products respectively.

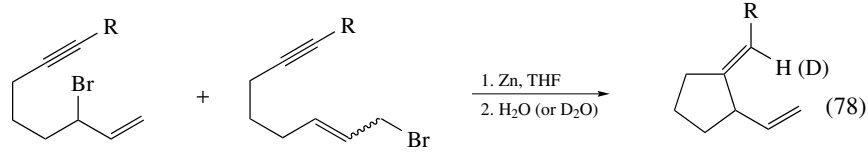

R = H	**(155a)**	**(155b)**	20–40 °C	43%	R = H **(156)**
R = Me	**(157a)**	**(157b)**	reflux	50%	R = Me **(158)**

These two reactions have remained the only reported type I zinc–ene processes for several years, before additional examples, still involving alkynes as enophiles, were disclosed.

The functionalized allylic organozinc reagents of type **159** (prepared by transmetallation of the corresponding Grignard reagents) underwent type I zinc–ene cyclizations with relative ease depending on the size of the ring formed. Formation of a five-membered ring from **159a** occurred at room temperature, whereas that of the six- or seven-membered rings from **159b** and **159c** respectively required heating in THF at reflux and led to lower yields. Formation of a five-membered ring also took place from **159d** having a triple bond substituted by an alkyl group. The corresponding alkenylzinc reagents **160** underwent subsequent ring-closure in the presence of a catalytic amount of a $Pd(PPh_3)_4$ to afford annelated methylenecyclopentenes of type **161** (equation 79)[113].

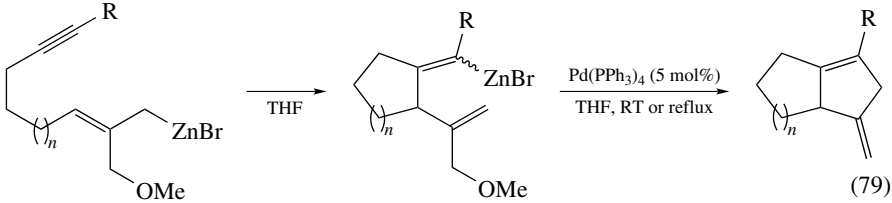

(159) **(160)** **(161)**

(a) R = $SiMe_3$	$n = 1$	THF, RT, 2 h	84%
(b) R = $SiMe_3$	$n = 2$	THF, reflux, 2 h	67%
(c) R = $SiMe_3$	$n = 3$	THF, reflux, 24 h	44%
(d) R = *n*-Bu	$n = 1$	THF, reflux, 24 h	75%

Type I zinc–ene reactions constitute a useful entry to alkylidenecyclopentanes. When alkenes instead of alkynes were considered as enophiles, the magnesium–ene reactions were considerably developed and elegantly applied to the synthesis of natural products[5,6]. However, the preparation of allylic organometallic species by reaction of allylic halides with the metal is not always a trivial task as by-products resulting from a Wurtz-type coupling may be generated. In order to overcome this limitation, practical zinc–ene reactions were reported in which the allylic organozinc reactive species was generated from readily available starting materials.

A palladium-catalyzed zinc–ene reaction was developed relying on the use of allylic alcohols derivatives (chlorides, esters, carbonates) as precursors[114]. Thus, when the allylic acetate **162** was treated with an excess of Et_2Zn in the presence of a catalytic amount of $Pd(PPh_3)_4$ in refluxing ether, cyclization took place leading to a cyclic organozinc species **163** which could be functionalized by reaction with various electrophiles. The reaction favored the formation of *cis*-1,2-disubstituted cyclopentanes as the major diastereomers with diastereoselectivities ranging from 83/17 to 98/2, depending on the substrates. Related processes with alkynylsilanes as intramolecular enophiles were also successful.

According to the proposed mechanism, an intermediate π-allyl palladium species was probably generated from the allylic acetate **162** and underwent transmetallation with Et_2Zn. The resulting ethylpalladium(II) complex would then undergo β-hydride elimination and reductive elimination of acetic acid (scavenged by excess Et_2Zn) in order to regenerate the Pd^0 catalyst, whereas the ethyl allylzinc reagent would in turn cyclize via a type I zinc–ene reaction leading to **163** (equation 80).

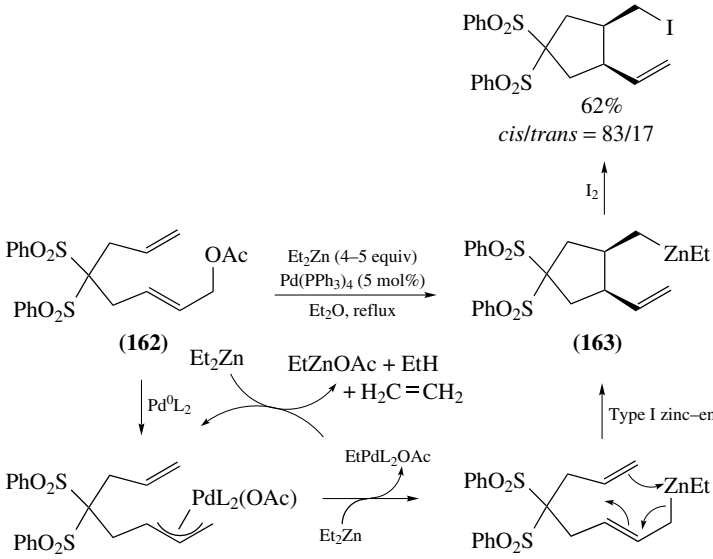

(80)

Although the fate of the zinc ligands was not unambiguously ascertained, it appeared clearly that palladium to zinc transmetallation occurred prior to cyclization. Indeed, palladium–ene reactions are known but generally require higher temperatures and, when run in association with a subsequent Stille cross-coupling, *trans*-1,2-disubstituted cyclopentanes were generated (equation 81)[115, 116].

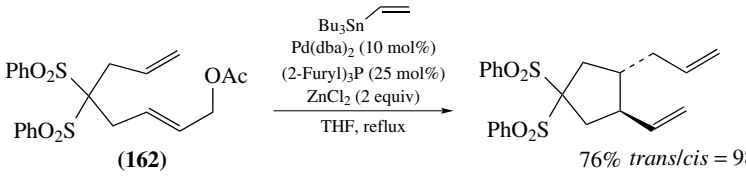

(81)

A Pd-catalyzed type I zinc–ene reaction was used to construct the spirobicyclic core of the sesquiterpenoid (−)-erythrodiene **164**[117, 118]. Thus, the allylic acetate **165** was treated with Et_2Zn in the presence of a catalytic amount of $Pd(OAc)_2$ and PBu_3 as the ligand to afford, after iodinolysis, the spirobicycle **166** with high diastereoselectivity (equation 82).

The use of an organozinc possessing β-hydrogen atoms was a firm requirement in order to regenerate the zero-valent palladium catalyst but it was found that Et_2Zn could be replaced by ethylzinc triflate (EtZnOTf). Rather surprisingly, a reversal of diastereoselectivity was observed and the Pd-catalyzed zinc–ene cyclization of **162** led to the *trans*-disubstituted cyclopentane **167** (equation 83)[119]. Although a reversible zinc–ene reaction could have explained the accumulation of the thermodynamically more stable *trans* diastereomer, it was unlikely due to the rather low temperature at which the reaction took place. The authors suggested that a radical cyclization could operate though the overall pathway ultimately produced an organozinc species. However, this assumption remained to be firmly established (equation 83).

Another interesting example of a practical zinc–ene reaction was reported, that exploited the reversibility of the addition of allylic organozinc reagents to carbonyl compounds[120]. Indeed, successive treatment of the β,γ-unsaturated ketone **168** with *n*-BuLi and $ZnCl_2$

generated the corresponding sterically hindered tertiary homoallylic zinc alkoxide **169**. The latter underwent fragmentation to *tert*-butylbutylketone and the resulting allylic organozinc species **170** produced in turn the spirobicyclic organozinc intermediate **171** by a smooth type I zinc–ene reaction, proceeding in a highly diastereoselective fashion. Transmetallation with copper salts and allylation with ethyl 2-bromomethylacrylate afforded **172** (equation 84)[120].

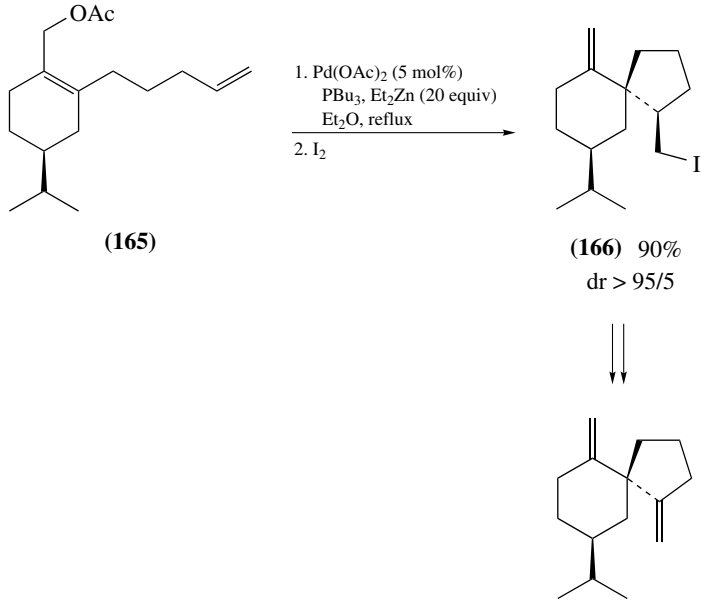

(165) **(166)** 90%
dr > 95/5

(82)

(164)

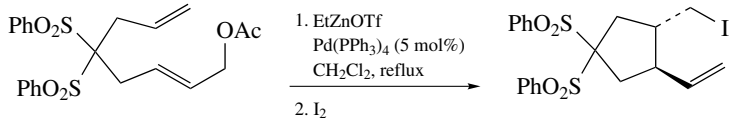

(162) **(167)**
trans/*cis* > 98/2
70%

(83)

2. Type II zinc–ene reactions

The first reports concerning the possibility of achieving type II zinc–ene reactions were carried out in the case of substrates having the allylmetal and the enophile interconnected through a chain containing a heteroatom. Whereas attempts to produce oxygen heterocycles from various Grignard reagents of type **173** at 100–130 °C in THF were mostly unsuccessful, transmetallation with $ZnBr_2$ led to the corresponding allylic organozinc reagents which underwent intramolecular type II zinc–ene reactions. The cyclization took place even in the case of substrates **173c** and **173d** possessing α,α- or α,β-disubstituted double bonds, although prolonged heating as well as higher temperatures were required. No cyclization was observed for **173e** in which the double bond was part of a cyclohexene

ring. The resulting cyclized organozinc reagents **174** were either hydrolyzed or treated with Me_3SnCl. Although satisfactory yields of substituted 3-methylene tetrahydropyrans **175** were obtained, quenching with Me_3SnCl was not efficient for the neopentyl-type organozinc **174c** and afforded a mixture of protonated and stannylated products, whereas the secondary organozinc **174d** failed to be stannylated (equation 85)[121].

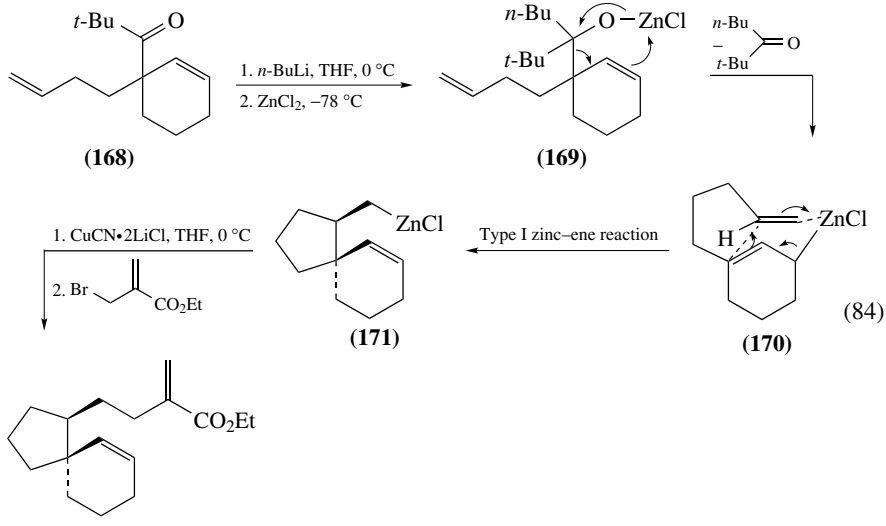

(84)

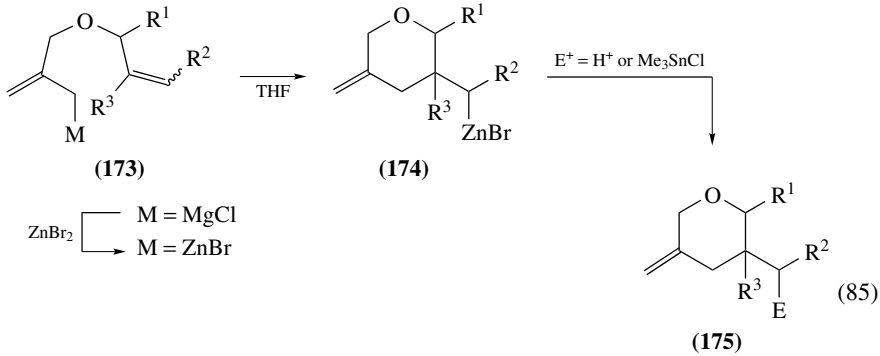

(85)

	R^1	R^2	R^3	Conditions	E^+	E in **175**	Yield	
(a)	H	H	H	80 °C	Me_3SnCl	$SnMe_3$	57%	
(b)	Ph	H	H	80 °C	H^+/H_2O	H	76%	*trans*/*cis* = 2/1
(c)	H	H	Me	80 °C	Me_3SnCl	$SnMe_3$	31%	+ E = H 18%
(d)	H	Me	H	130 °C	H^+/H_2O	H	50%	
(e)	$-(CH_2)_3-$		H	130 °C	–			

A seven-membered ring oxygen heterocycle **176** could also be generated by type II intramolecular metallo–ene reactions and the zinc–ene process appeared by far more efficient than the magnesium–ene. However, in the nitrogen series, type II zinc–and magnesium–ene reactions exhibited similar efficiencies and afforded the substituted 3-methylene piperidine **177** in comparable yields (equation 86)[121].

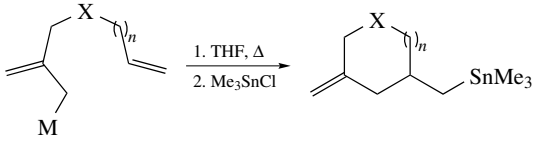

X = O $n = 2$ **(176)**
X = NMe $n = 1$ **(177)**

	Conditions	Yield
M = MgCl	100–130 °C	15%
M = ZnBr	80 °C	62%
M = MgCl	100 °C	76%
M = ZnBr	80 °C	64%

(86)

Type II zinc–ene reactions are conformationally more demanding than type I reactions and the difficulties for achieving cyclization became particularly important when alkynes were involved as enophiles. Indeed, it was not possible to obtain five-membered rings according to this strategy and the organozinc reagent **178a** provided only a small amount of the six-membered ring **179**, the allene **180** resulting from an S_N2' displacement being obtained as the major product. Only in the case of **178b** did a regioselective cyclization take place leading to **179b**, with C-C bond formation occurring at the most substituted terminus of the allylzinc reagent (equation 87)[122]. The formation of a seven-membered ring was observed under harsh conditions, with complete lack of stereoselectivity, and was attributed to a non-concerted radical process.

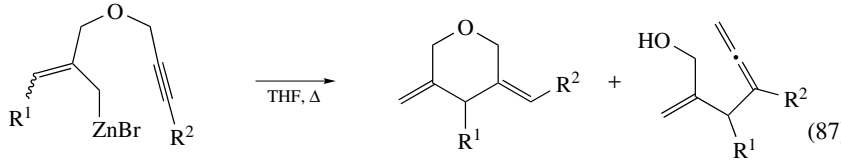

(87)

(178) **(179)** **(180)**

(a)	$R^1 = H$ $R^2 = Me$	75 °C	4%	83%
(b)	$R^1 = Et$ $R^2 = SiMe_3$	100 °C	74%	–

Additionally, some Pd-catalyzed type II zinc–ene cyclizations have been described. When the allylic acetate **181** was treated with Et_2Zn in the presence of a catalytic amount of $Pd(PPh_3)_4$, its slow conversion to a cyclic organozinc species by a type II zinc–ene reaction was observed and iodinolysis afforded the six-membered ring **182** in relatively low yield. The regioselectivity was noteworthy as C-C bond formation occurred at the most substituted terminus of the allylmetal. By contrast, the type II palladium–ene cyclization of the allylic acetate **181**, in conjunction with a β-elimination process, proceeded with opposite regioselectivity and led to the six-membered ring **183** (equation 88)[114].

Type II zinc–ene reactions seem to be more difficult to achieve compared to type I cyclizations even though successful examples of six- or seven-membered ring formations have been reported. Nevertheless, type I reactions constitute a particularly attractive strategy for the formation of five-membered rings that proceed smoothly compared to intermolecular additions to monosubstituted alkenes. However, allylic organozincs are able to add to substituted alkenylmetals under extremely mild conditions.

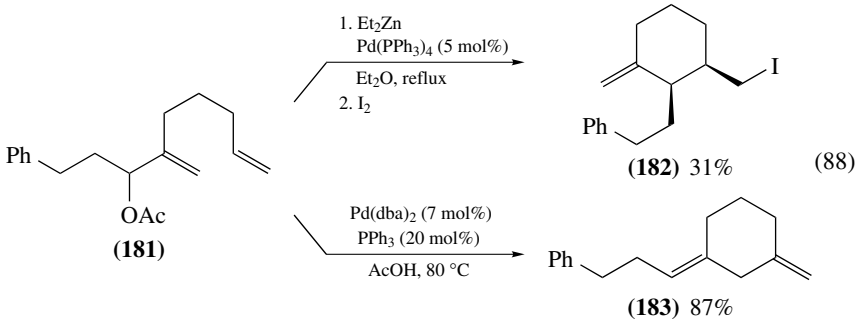

(88)

D. Allylzincation of Alkenylmetals

1. Synthesis and reactivity of gem-diorganometallic species

Allylzinc bromide is able to add to a variety of alkenyl Grignard reagents in THF at 35 °C[123]. The structure of the hydrocarbons **184**, obtained in moderate yields after hydrolysis (due to their volatility), suggested that 1,1-dimetallic species tentatively formulated as **185** were regioselectively formed (equation 89). Additional examples were subsequently reported but the scope of this intriguing reaction remained rather unexplored and the reactivity of **185** towards various electrophiles was not investigated[124, 125].

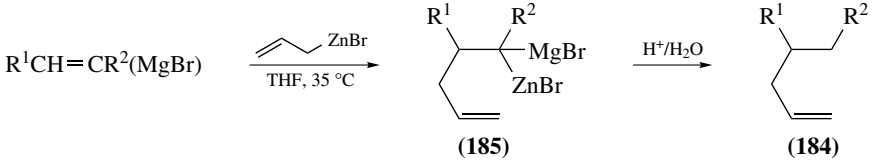

R^1	R^2	Yield
Me	H	24%
Pr	H	58%
H	Me	26%
H	Pr	36%

(89)

It was later demonstrated that this straightforward access to sp^3 *gem*-diorganometallic species[126] was in fact a general reaction as allyl, methallyl and crotylzinc bromides were able to add to a variety of alkenylmetals including organomagnesium and organoaluminum reagents in THF at 35 °C, or alkenyllithium reagents in THF at 5 °C. An inferior temperature was required in the latter case because the resulting dimetallic species suffered from lower stabilities[127]. The hydrocarbons resulting from the hydrolysis of the organometallic species formulated as **186a–c**, for the only purpose of representing the reagents from which they have been generated, were obtained in high yields and deuteriolysis also unambiguously confirmed the presence of two carbon–metal bonds. (equation 90)[127]. Other combinations of alkenyl and allylic organometallic species were successful provided that zinc (or cadmium) salts were present[128].

Preliminary studies demonstrated that, under the above conditions, the more substituted the alkenylmetal, the less reactive it was towards addition of allylzinc bromide. Disubstitution at the β position significantly retarded the addition[127]. The reaction still occurred efficiently in THF at 35 °C if silyl or aryl groups were present at the α-position

of the alkenylmetal, as illustrated by the allylzincation of the Grignard reagent derived from α-bromostyrene with the alkoxy-substituted allylzinc bromide **187**, which led after hydrolysis to the ketone **188**, the product resulting from a formal addition of acetone enolate to styrene (equation 91)[129].

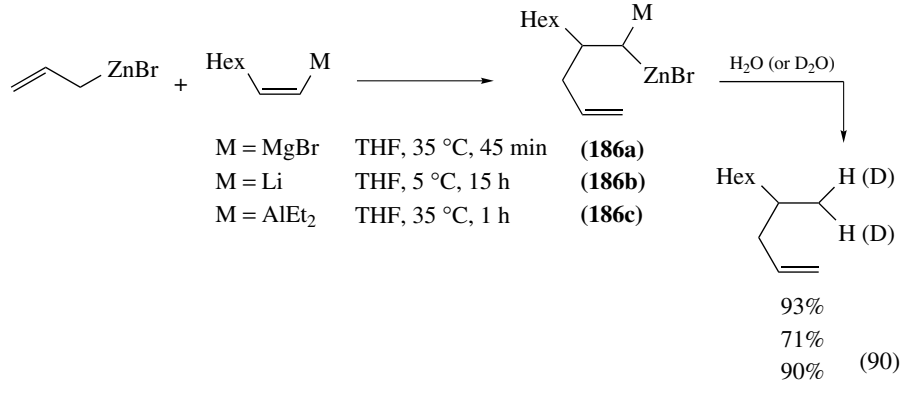

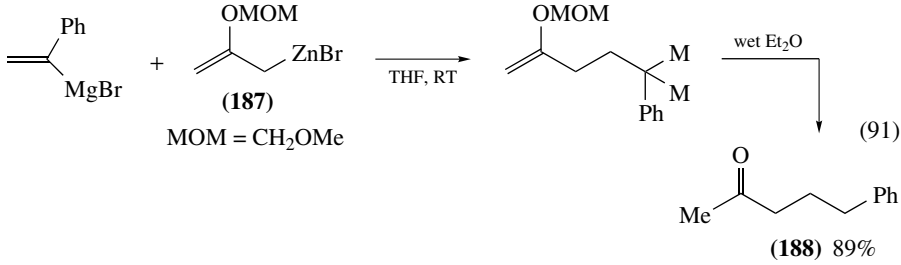

The reactivity of the dimetallic compounds **186a** and **186b** was then investigated and these species were less reactive than their formulas would lead to predict, as no reaction occurred with ketones, esters, Michael acceptors or trimethylsilyl chloride. In the presence of $BF_3{\bullet}OEt_2$, addition occurred to aldehydes and led after β-elimination to the corresponding olefination products **189** with good to excellent (*E*) stereoselectivity (equation 92)[127].

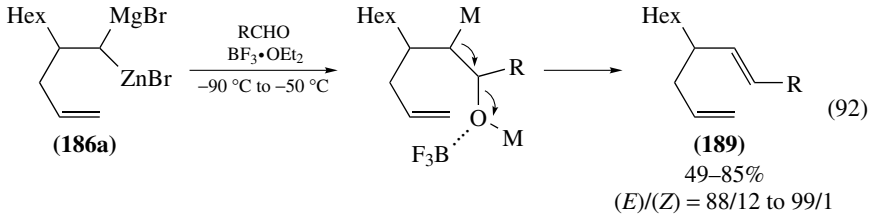

An alternative complementary olefination procedure involving alkylidene malonates was also developed that produces (*Z*) olefins as major stereoisomers when the R substituent is aliphatic (equation 93)[130]. The stereoselectivity depends on the bimetallic compounds and may be improved by bulky ester substituents (such as menthyl groups)[131].

This olefination protocol was applied to a short and efficient synthesis of (*Z*)-dodec-7-enyl acetate, the cabbage looper moth pheromone[131].

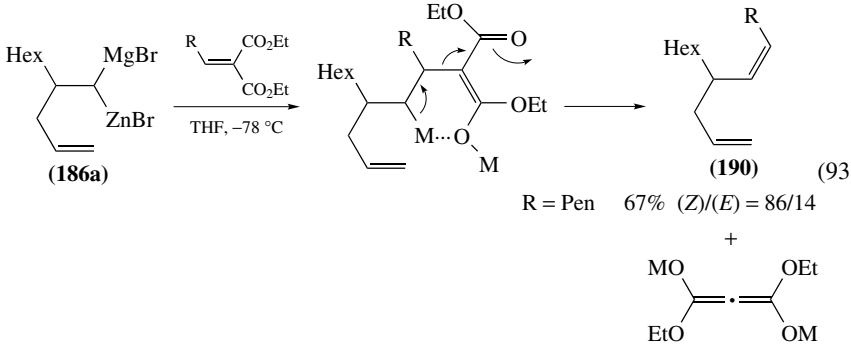

(93)

The ability of reagents **186a** and **186b** to act as multi-coupling agents was demonstrated by consecutive additions of two different electrophiles. Due to the low reactivity of **186a**, reactive electrophiles had to be used, such as a proton, a deuteron, iodine, trimethyltin chloride or dimethyl disulfide[130]. Interestingly, tosyl cyanide could be used to introduce the cyano group[132]. As second electrophiles, a proton, a deuteron or iodine could be used successfully[130], as well as oxygen to promote the oxidation of the remaining carbon–metal bond[133]. If excess dimethyl disulfide was used directly, an intermediate thioketal was generated and its subsequent acidic hydrolysis afforded the corresponding aldehyde. The latter was also obtained after stannylation of **186a** with Me_3SnCl and subsequent oxidation with dry air in the presence of Me_3SiCl, as the intermediate (β-trimethylstannyl)peroxysilane evolved by β-elimination of the trimethylsilyloxy group[134] (equation 94).

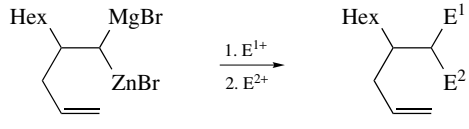

E^{1+}	E^{2+}	E^1	E^2	Yield
AcOH	I_2	H	I	61%
I_2	AcOH	I	H	60%
Me_3SnCl	H_2O	$SnMe_3$	H	88%
Me_3SnCl	D_2O	$SnMe_3$	D	94%
Me_3SnCl	I_2	$SnMe_3$	I	75%
i-PrOH	O_2	H	OH	63%
MeOD	O_2	D	OH	57%
TosCN	H_2O	CN	H	93%
MeSSMe (excess) then HCl		=O		63%
Me_3SnCl	dry air, Me_3SiCl	=O		81%

(94)

Transmetallation of the dimetallic species **186a** or **186b** with CuCN led to a new organometallic species formulated as **191** which displayed remarkable thermal stability. Addition of reactive alkylating agents such as allyl bromide to **191** directly produced compound **192**. Indeed, once the first alkylation occurred, the copper salts present in

solution could catalyze the alkylation of the second carbon–metal bond[135]. Interestingly, addition of acetyl chloride led to an α-acyl organometallic species in equilibrium with the metal enolate, and the latter underwent O-acylation by a second equivalent of the acid chloride to afford the enol acetate **193** (equation 95).

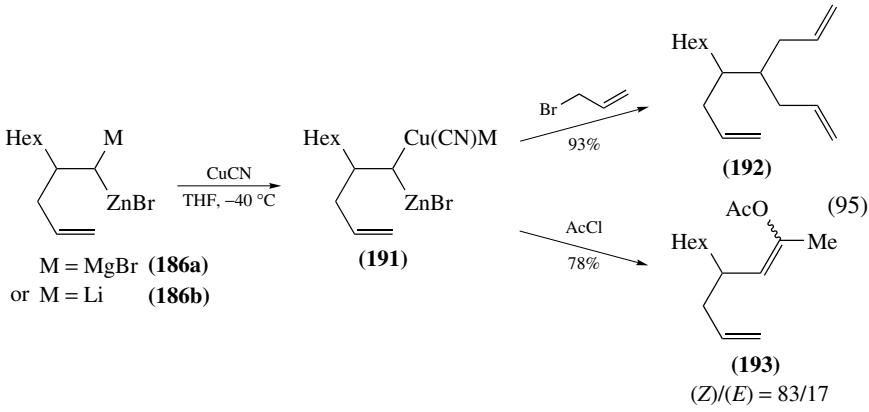

(95)

It was discovered that the bimetallic reagent **186b** displayed a higher reactivity compared to **186a** and its use as a multi-coupling agent allowed the use of a broader range of electrophiles[136]. A proton, a deuteron or trimethyltin chloride could be used as first electrophiles and the second carbon–metal bond underwent allylation after transmetallation to an organocopper species or could be involved in a Pd-catalyzed cross-coupling with acid chlorides, chloroformates or alkenyl iodides. After protonation, transmetallation of the resulting monometallic species with $ClTi(OPr\text{-}i)_3$ also enabled subsequent addition to benzaldehyde. Compound **186b** also underwent 1,4-addition reactions to Michael acceptors such as chalcone or β-nitrostyrene. Finally, addition of excess methyl iodide to **186b** led to a monomethylated product (equation 96)[136].

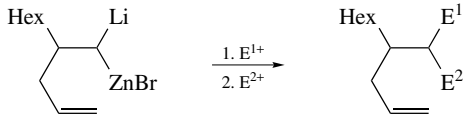

E^{1+}	E^{2+}	E^1	E^2	Yield
MeOH	I_2	H	I	73%
MeOD	CuCN, AllBr	D	All	76%
Me_3SnCl	CuCN, AllBr	$SnMe_3$	All	79%
t-BuSH	CuI, MeI	H	Me	78%
i-BuOH	RCOCl, cat. $Pd(PPh_3)_4$	H	COR	84–89%
i-BuOH	$ClCO_2Et$, cat. $Pd(PPh_3)_4$	H	CO_2Et	66%
i-BuOH	PhI, cat. $Pd(PPh_3)_4$	H	Ph	73%
i-BuOH	EtCH=CHI, cat. $Pd(PPh_3)_4$	H	CH=CHEt	64%
i-BuOH	$ClTi(OPr\text{-}i)_3$, PhCHO	H	CHOHPh	56%
PhCH=CHCOPh	H_2O	$CHPhCH_2COPh$	H	63%
$PhCH=CHNO_2$	H_2O	$CHPhCH_2NO_2$	H	65%
MeI (excess)	H_2O	Me	H	56%

(96)

Due to the rather restricted scope of the monoalkylation procedure of **186b**, an alternative strategy was developed relying on a 1,2-metallate rearrangement[137]. When the bimetallic species **194** was treated with benzenesulfonyl chloride, monochlorination took place leading to an α-chloroorganozinc sulfinate formulated as **195**. The latter carbenoid species was so poorly nucleophilic that it did not even react with iodine at a temperature below its limit of stability ($-20\,^{\circ}C$ in THF/ether mixtures) and underwent instead α-elimination and rearrangement to the diene **196**. Addition of one equivalent of an organometallic reagent such as *n*-BuLi led to the more reactive α-chlorozincate species **197** which could be successfully iodinolyzed. Addition of two equivalents of an organolithium or an organomagnesium reagent to **195** led to the ate-complex **198** that underwent a 1,2-metallate rearrangement producing a secondary organozinc **199**. The latter reacted with iodine to afford secondary alkyl iodides **200** and, in one case, oxidation was performed with dry air in the presence of HMPA in order to obtain the secondary alcohol **201**[138]. Primary, secondary, tertiary alkyl as well as allyl groups could be introduced by this strategy but the reaction was less efficient for MeMgBr or MeLi (*ca* 20% yield) (equation 97)[137].

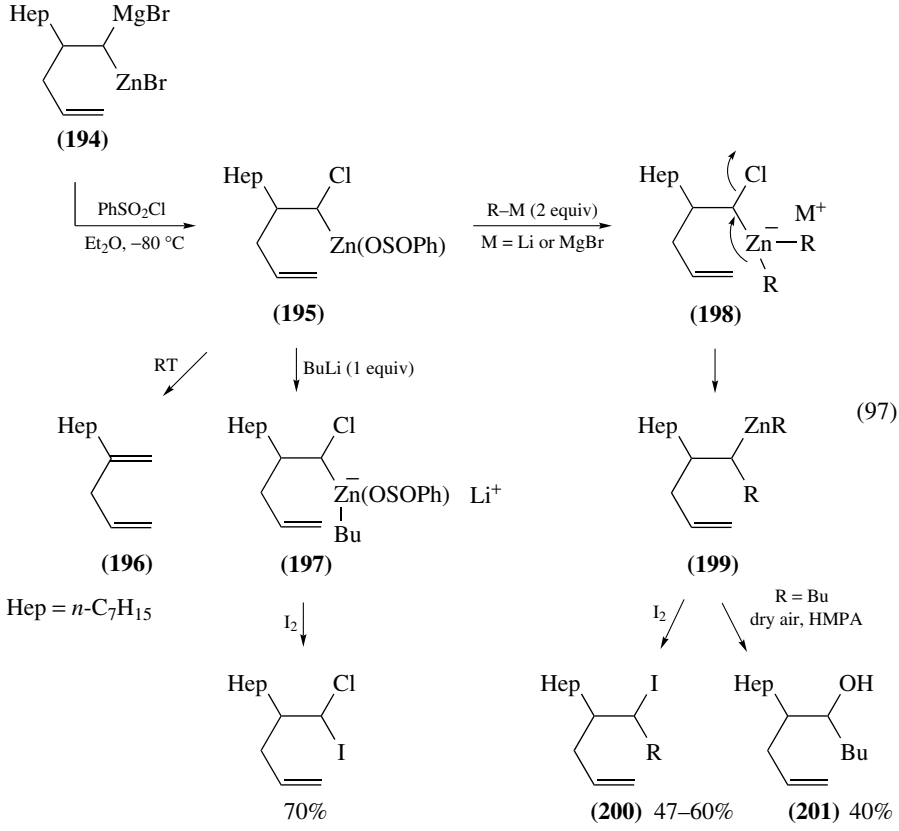

(97)

The allylzincation of alkenyllithium or alkenyl Grignard reagents therefore constitutes a straightforward access to sp^3 *gem*-diorganometallic species that can react subsequently with a variety of electrophiles and be regarded as multi-coupling reagents[126]. Although

unambiguously experimentally demonstrated, the feasibility of these processes which in fact formally involve the coupling of an allyl anion with a vinyl anion remained puzzling and, in particular, their considerable efficiencies compared to the allylzincation of substituted olefins was quite intriguing. The subsequent studies concerning the use of these reactions for stereoselective synthesis were actually carried out in the absence of any supporting theoretical calculations. Nevertheless, clever assumptions were made with respect to the possible mechanisms of such reactions as well as concerning the nature of the carbon–metal bonds in the dimetallic species[127, 128, 139].

2. Theoretical studies

Recently, theoretical calculations have been independently conducted by two groups and led to similar conclusions[140–142]. Whereas the computed potential energy surface for the addition of allylzinc bromide to ethylene reveals that the formation of the initial complex is endothermic with no favorable pre-organization of the reactants, allylzinc bromide and vinyllithium (or vinylmagnesium bromide) form a rather strong complex bringing the reactants in close contact through the square planar arrangement of the Li-C-Zn-Br or Mg-C-Zn-Br atoms. This initial pre-complexation is strongly exothermic. Due to an initial rapid transmetallation, starting from vinyllithium (or vinylmagnesium bromide) and allylzinc bromide, or the reversed combination of vinylzinc bromide and allyllithium (or allylmagnesium bromide), leads to the same complex that constitutes the key step of the reaction, as the metallated carbon of the vinylmetal is already attached to zinc[140]. The calculated activation barriers for allylzincation of vinyllithium and vinylmagnesium bromide are respectively 24.9 kcal mol^{-1} and 15.9 kcal mol^{-1}, the latter being inferior due to a less exothermic initial pre-complexation (Scheme 1). These results are in perfect agreement with the experimental observation that allylzincation of alkenyl Grignard reagents is a much faster reaction compared to that of alkenyllithium reagents[127].

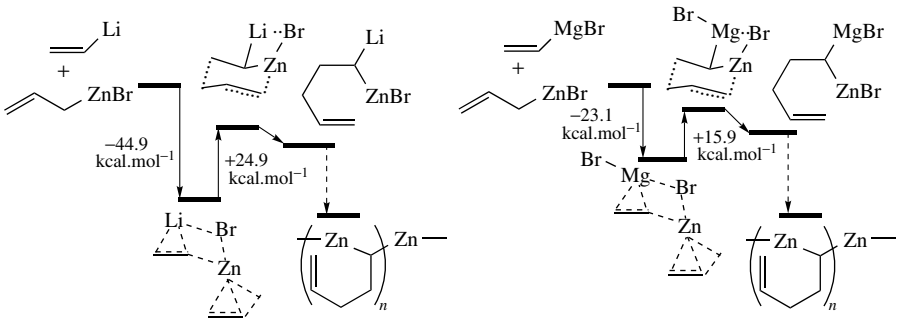

SCHEME 1

Whereas the formation of the initial heterodimetallic species products appears to be endothermic, the overall driving force of the reaction is gained by their degeneration to linear or cyclic 1,1-dizincio oligomers, presumably trimers or tetramers, that display considerable stabilization due to the formation of stable carbon–zinc bonds[141, 142]. Although a [3,3] sigmatropic rearrangement of an allyl alkenylzinc species, initially generated by rapid transmetallation, is a chemically unlikely and energetically unfavorable process as it would generate a zinc alkylidene carbene, theoretical calculations indicate that placing a molecule of $MgCl_2$ nearby the metallated carbon in an allyl vinylzinc species resulted in a dramatic drop of the activation energy. This is due to the stabilization of the developing

negative charge on this carbon by the magnesium atom. The addition proceeds through a late six-centered chair-like transition state (fused to a four-centered μ-halo bridge) and is conveniently described as a magnesium-assisted metalla-Claisen rearrangement[142], as was remarkably suggested before any theoretical calculations were carried out[127]. There is also some similarity with a metallo–ene reaction between an allylic organozinc and an alkenylmetal. In fact, as the carbon–metal bond of the vinylmetal becomes more ionic, the rate of the reaction should increase at such a point that, for a carbon–magnesium bond, transmetallation to an allyl alkenylzinc species occurs and a magnesium-assisted metalla-Claisen rearrangement may then operate. These two initially different processes lead to the same regioselectivity and may be in fact indistinguishable at the transition state stage (equation 98)[142].

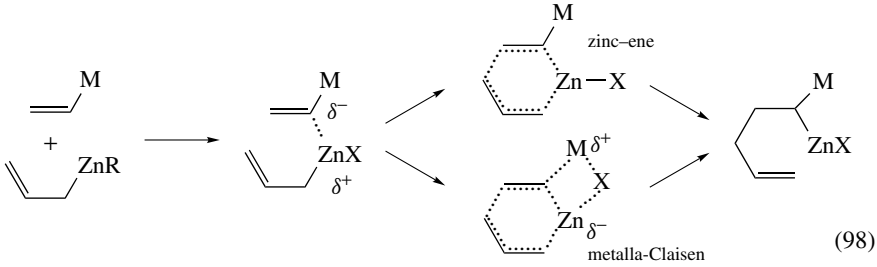

(98)

For comparison, one can also consider the addition of allylic organozinc reagents to alkenylboranes. Thus, the vinylboronate **202** derived from the sterically hindered pinacol, which shields the boron atom and prevents the formation of an ate-complex, reacted with methallyl butylzinc in a regioselective fashion and led to the α-borylorganozinc **203**. It was observed that an allyl butylzinc species was considerably more reactive towards **202** than the corresponding allylic organozinc bromide itself. A related countercation effect will be also seen in the addition of zinc aza-enolates to alkenes (see Section V.B). After conversion of **203** to an organozinc bromide by addition of $ZnBr_2$, transmetallation with copper salts, allylation and subsequent oxidation of the carbon–boron bond afforded the secondary alcohol **204** (equation 99)[143].

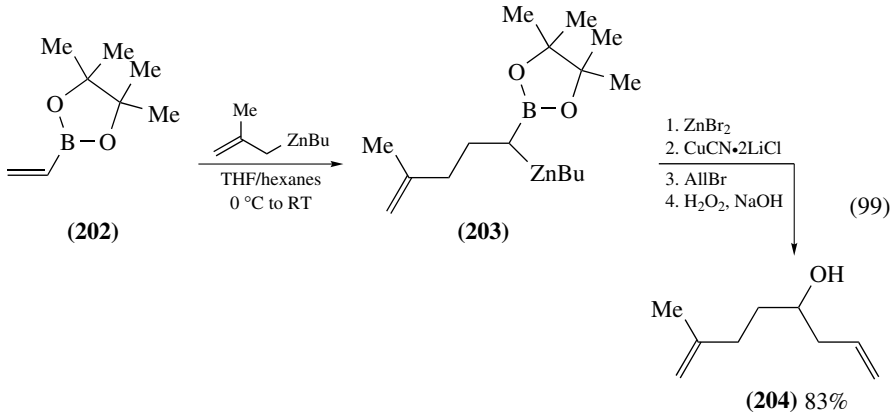

(**202**) (**203**) (**204**) 83%

(99)

Thus, in the case of alkenylboronates which possess a more covalent carbon–boron bond, it was established that allylzincation followed a classical zinc–ene process[143]. By

comparison, a metalla-Claisen pathway is favored for the more ionic alkenyllithium or alkenyl Grignard reagents. As in the other sigmatropic rearrangements proceeding through a cyclic transition state, the possibility of achieving acyclic diastereoselection has been examined.

3. Diastereoselective allylzincations of alkenylmetals

a. Mutual diastereoselection. Whereas the synthesis of an alkenylmetal partner of well-defined configuration is a trivial task, the problem of mutual diastereoselection in the reaction with a substituted allylic organozinc reagent seemed to be a rather complex issue due to the metallotropic equilibrium (equation 100). In principle, each form could potentially react with the alkenylmetal which would result in mixtures of regio- and/or diastereomers

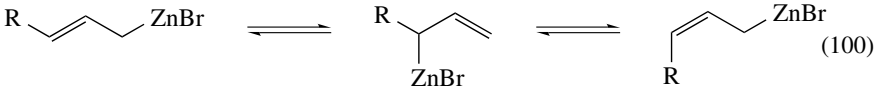

(100)

Despite these apparent problems, preliminary investigations led to the disclosure of a few diastereoselective additions of substituted allylic organozincs to alkenyllithium reagents in THF[144], but generalization to other organozincs such as crotylzinc bromide were much less successful[128]. It was later discovered that replacement of THF by a less Lewis basic solvent such as diethyl ether led to a considerable acceleration of the rate of the allylzincation. In fact, this result is consistent with a Lewis acid-assisted metalla-Claisen rearrangement[142]. However, the preparation of allylic organozinc compounds from the corresponding allylic bromides and metallic zinc requires THF as the solvent. Therefore, an alternative procedure was developed in which an alkenyllithium, generated by metal–halogen exchange from an alkenyl iodide using *tert*-butyllithium in ether at $-80\,^{\circ}C$, was treated successively with an ethereal solution of an allylic Grignard reagent and $ZnBr_2$. Under these conditions, the allylzincation proceeded at as low as $-50\,^{\circ}C$[145]. The presence of magnesium salts was also beneficial for these reactions, the Lewis acidity of Mg^{II} being considerably improved in ether compared to THF.

Thus, the alkenyllithium reagent derived from the (*Z*)-γ-iodo allylic ether **205** underwent addition of crotylzinc bromide in ether at $-50\,^{\circ}C$ and, after hydrolysis of the resulting dimetallic reagent, compound **206** was obtained with high diastereoselectivity (*anti*/*syn* = 93/7) (equation 101)[146].

Starting from the (*E*)-alkenyl iodide **207** reversed the diastereomeric ratio and afforded **208** (*syn*/*anti* = 92/8) (equation 102)[146].

The observed stereochemical outcome suggested that a cisoid configuration of the crotyl metal was kinetically favored in the cyclic transition state. Indeed, recent calculations supported that transition structures with cisoid crotylmetals are more stable whatever the olefinic configuration of the alkenyl metal[142].

It is worth mentioning that the crotylzincation is a reversible reaction as, after addition, prolonged stirring at room temperature or heating at reflux for a few hours resulted in the formation of an equilibrium mixture of diastereomers and regioisomers (equation 103)[128, 139].

High diastereoselection could therefore only be achieved if the reactions were conducted at low temperatures, which highlighted the tremendous importance of ether as a less coordinating solvent.

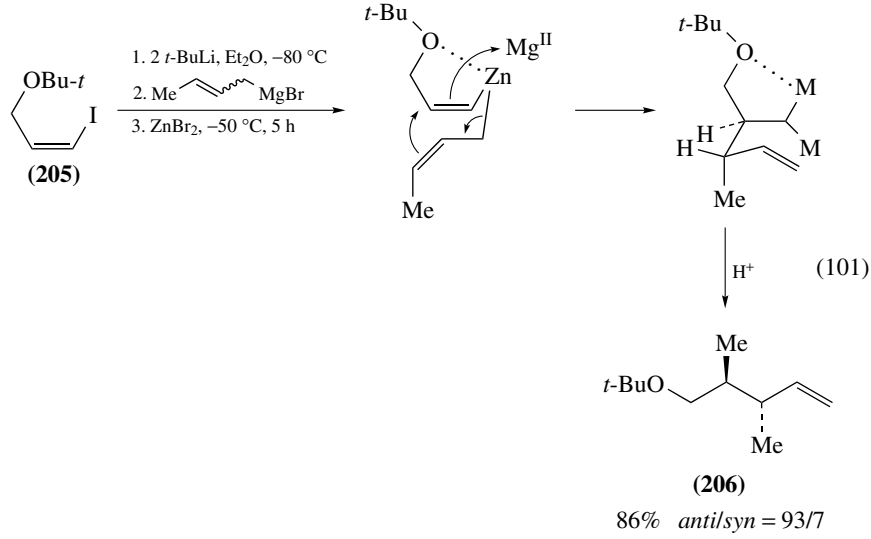
OBu-t
I
(205)
1. 2 t-BuLi, Et2O, −80 °C
2. Me MgBr
3. ZnBr2, −50 °C, 5 h
t-Bu
O
MgII
Zn
Me
t-Bu
O
M
H
H
M
Me
H+
(101)
Me
t-BuO
Me
(206)
86% anti/syn = 93/7

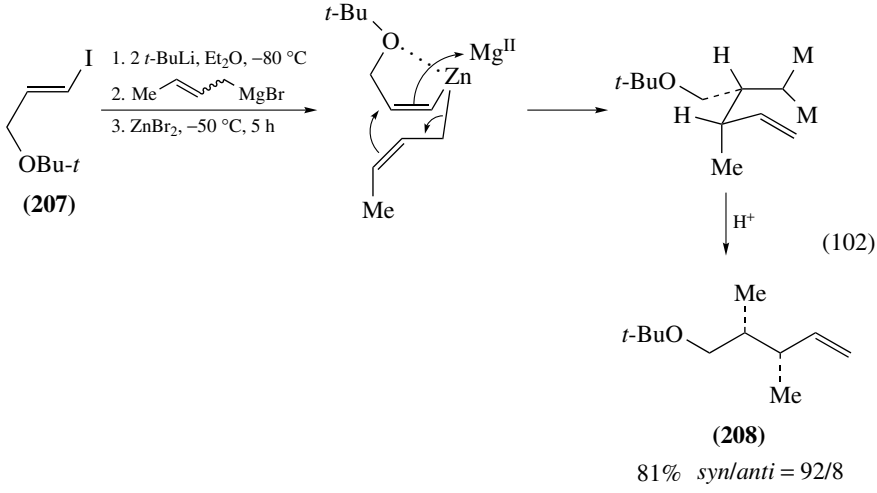
I
OBu-t
(207)
1. 2 t-BuLi, Et2O, −80 °C
2. Me MgBr
3. ZnBr2, −50 °C, 5 h
t-Bu
O
MgII
Zn
Me
H
M
t-BuO
H
M
Me
H+
(102)
Me
t-BuO
Me
(208)
81% syn/anti = 92/8

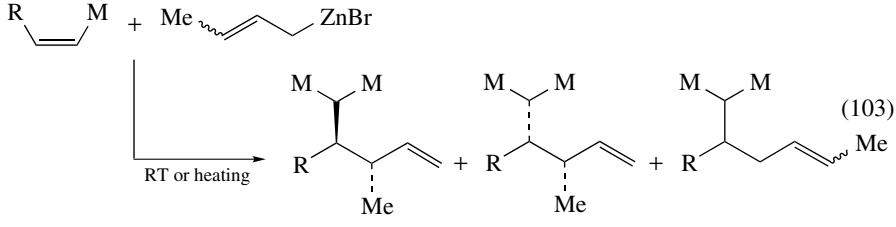
R
M
+
Me
ZnBr
RT or heating
M
M
R
Me
+
M
M
R
Me
+
M
M
R
Me
(103)

b. Substrate-induced diastereoselection. In light of the efficient chelation of the metal in γ-heterosubstituted organozinc reagents[147], secondary (*Z*)-γ-iodo allylic ethers were selected as starting materials in order to achieve substrate-induced diastereoselection. Indeed, addition of allylmagnesium bromide and $ZnBr_2$ to the alkenyllithium generated from **209** led to the bimetallic species **210**. After hydrolysis, the secondary ether **211** was obtained with high diastereoselectivity, whereas olefination with benzaldehyde provided the 1,5-diene **212** (equation 104)[145]. The observed stereochemical outcome could be rationalized by considering that the addition of the allyl moiety has occurred to the less hindered face (*anti* to the propyl substituent) of the chelated allyl alkenylzinc species **213**.

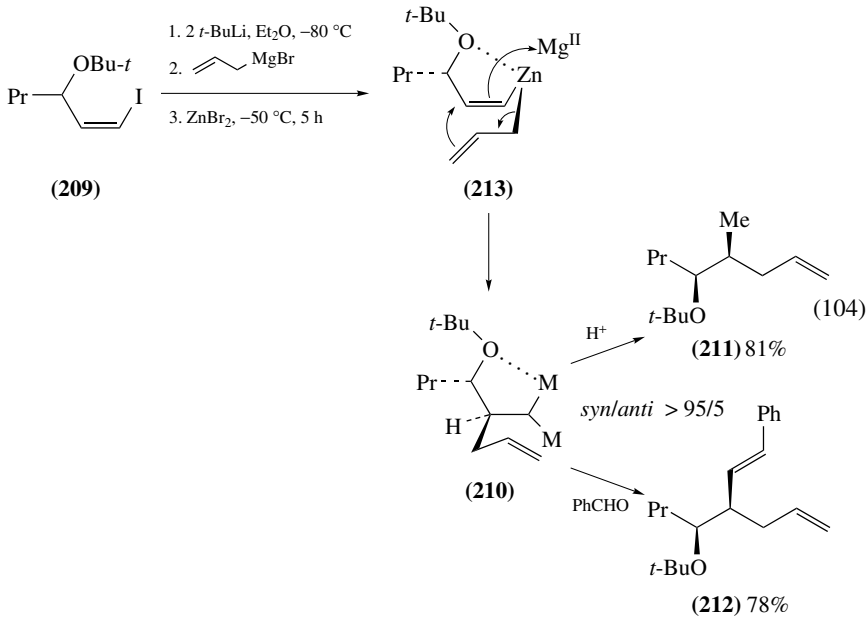

The *tert*-butyl ether turned out to be an efficient chelating group for the purpose of substrate-induced diastereoselection. A methoxymethyl ether (MOM) led to an even stronger coordination of the metal which slowed down the rate of the allylzincation. Slightly higher temperatures (typically $-20\,^{\circ}C$) were thus required but the diastereoselectivity remained constantly high. The secondary alcohol moiety could also be left unprotected as illustrated by the titanium-catalyzed hydromagnesiation reaction of the propargylic alcohol **214** which produced the chelated alkenylmagnesium species **215**. The latter underwent a highly diastereoselective allylzincation in ether at $-20\,^{\circ}C$, leading to an organometallic reagent bearing three carbon–metal bonds, which was hydrolyzed to **216** (dr > 95/5) (equation 105).

Combining substrate-induced diastereoselection and mutual diastereoselectivity, as illustrated for the crotylzincation of the alkenyllithium derived from **209**, led to excellent results as the *gem*-dimetallic species **217** was obtained in a highly stereoselective fashion. The stereochemical outcome was explained by the addition of the kinetically reactive cisoid metallotropic form of the crotylzinc reagent *anti* to the propyl group in the chelated allyl alkenylzinc intermediate. After hydrolysis, compound **218** was obtained as a single diastereomer (equation 106)[148,149].

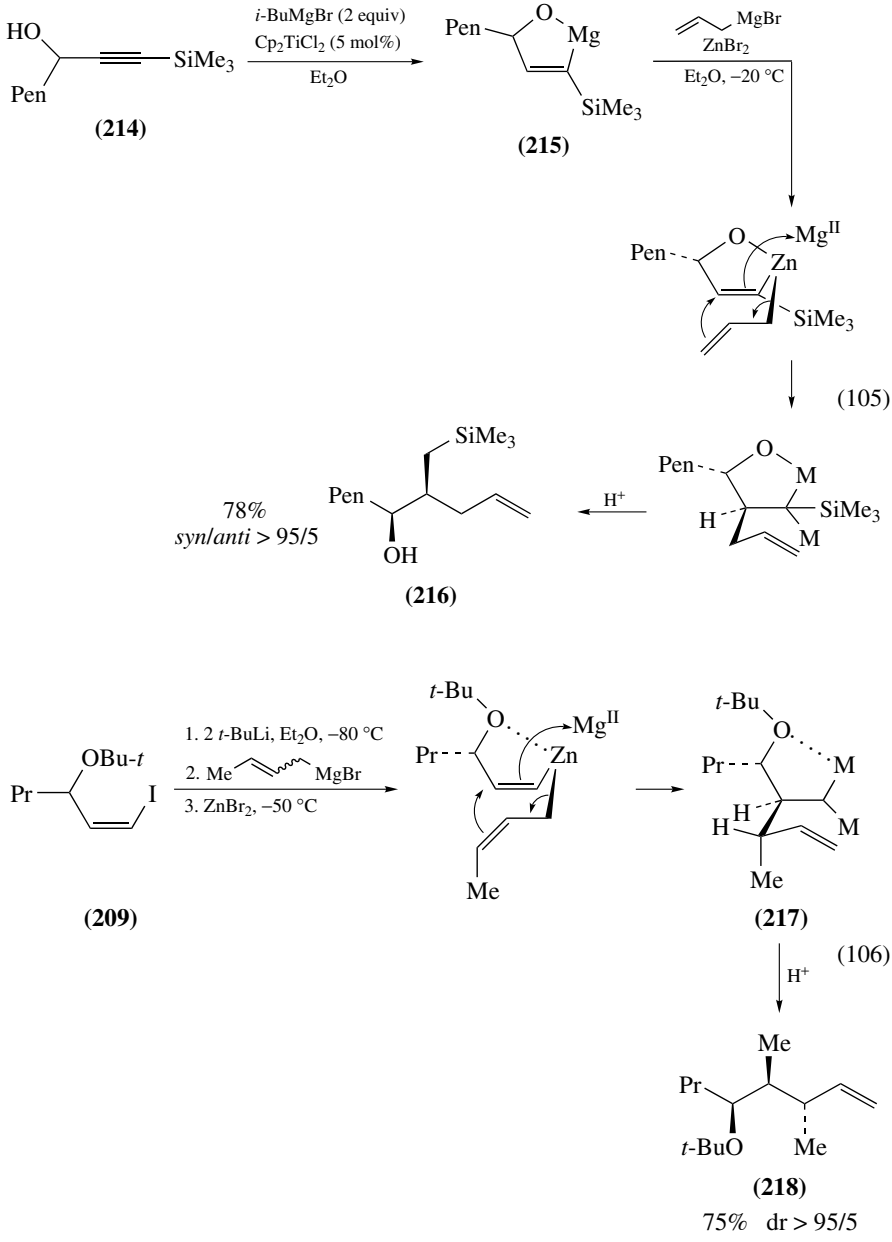

In the case of the alkenyllithium derived from the secondary (*E*)-γ-iodo allylic ether **219**, in which chelation of the metal by the alkoxy group could no longer operate, the allylzincation led after hydrolysis to **220** as a 76/24 mixture of *anti* and *syn* diastereomers. The stereochemical outcome was rationalized by assuming that the conformational

arrangement **221** was preferred due to minimization of $A^{1,3}$ strain and that the allylic moiety was delivered *anti* to the pentyl group in this reactive conformer (equation 107)[149].

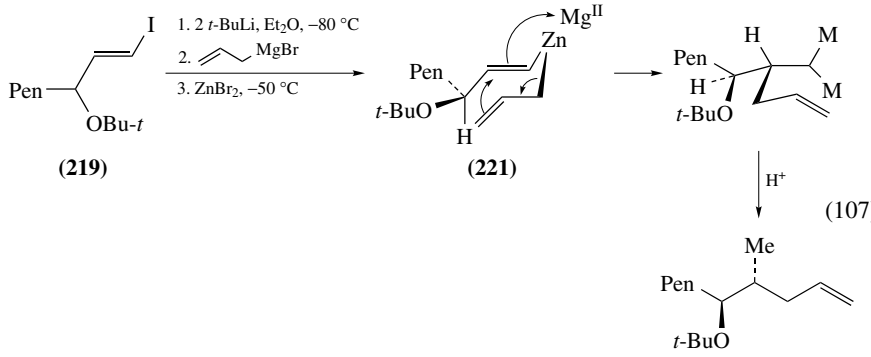

(219) (221) (107)

(220) 78%
anti/*syn* = 76/24

Besides crotylzinc bromide, the use of other substituted allylic organozinc species was considered. Allyltrimethylsilane can be metallated with *sec*-butyllithium in ether in the presence of TMEDA, but addition to the alkenyllithium derived from **209** in the presence of $ZnBr_2$ proceeded slowly and required warming to room temperature. After hydrolysis, the alkenylsilane **222** was obtained (rather than a regioisomeric allylsilane) with moderate diastereoselectivity (*syn*/*anti* = 73/27) but high olefinic stereoselection ((*E*)/(*Z*) > 95/5), presumably due to the preferential pseudo-equatorial positioning of the $SiMe_3$ group in the cyclic transition state. The sluggish reaction was attributed to the presence of the Lewis basic TMEDA required for the metallation of allyltrimethylsilane in ether[145]. Interestingly, the problem of lower diastereoselection was solved recently by carrying out the reaction in the presence of an excess of $ZnBr_2$ and $MgBr_2$ which both speed-up the reaction. Under these optimized conditions, compound **222** was obtained with high diastereoselectivity (equation 108)[150].

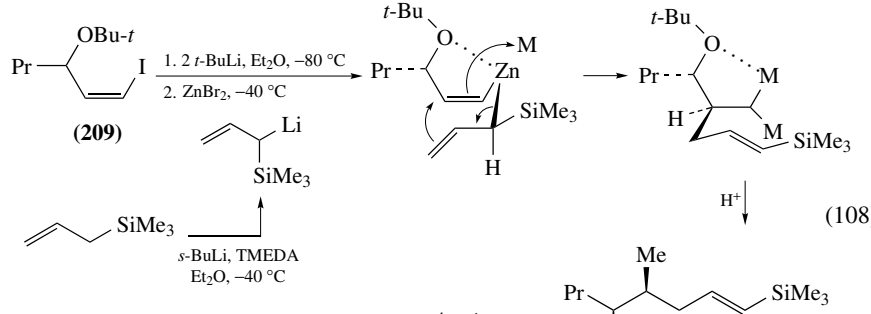

(209) (108)

		syn/*anti*
$ZnBr_2$, 92 h, RT	78%	73/27
$ZnBr_2$ and $MgBr_2$ (3 equiv) 0 °C, 24 h and RT, 24 h	64%	95/5

(*E*)/(*Z*) > 95/5

(222)

If chelation of the metal was more efficient, by switching from a *tert*-butyl ether to a methoxymethyl ether, the use of an excess of $ZnBr_2$ was efficient at accelerating

the reaction, as demonstrated in the case of substrate **223**. The presence of $MgBr_2$ has to be avoided since it is able to promote the γ-elimination of the OMOM group (see Section III.D.4). Under these conditions, the alkenylsilane **224** was obtained with complete diastereoselection. The latter, upon deprotection of the OMOM group and subsequent oxidation with peracetic acid, afforded lactone **225** (*cis*/*trans* = 92/8), a known intermediate in the synthesis of (±)-serricornin (equation 109)[150].

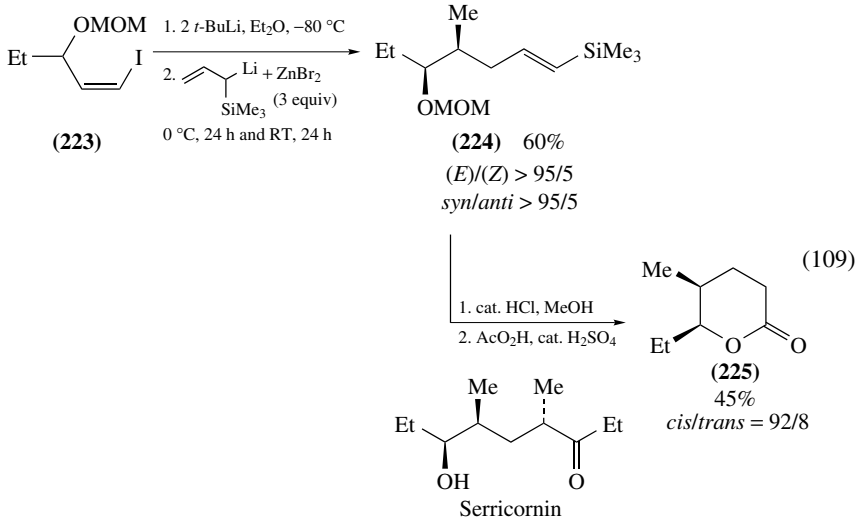

(109)

Metallated allylic ethers can also be used as partners in allylzincations of alkenylmetals[144]. Allyl methyl ether could be metallated with *s*-BuLi in ether provided that TMEDA was present and, after transmetallation with $ZnBr_2$, addition to the alkenyllithium derived from **205** proceeded slowly at room temperature. Nevertheless, after hydrolysis the corresponding allylic ether **227** was obtained with high diastereoselectivity (equation 110)[146].

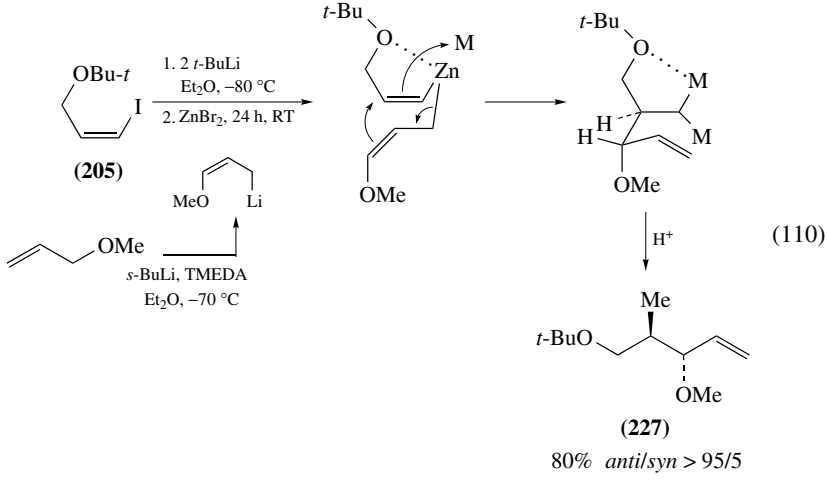

(110)

The mutual diastereoselection between the alkenyllithium and the zincated allylic ether turned out to be the same as for a crotylzinc species, and could be rationalized by kinetic addition of a cisoid γ-alkoxyallylic organozinc compound.

The slow carbozincation, attributed to the presence of TMEDA, was more problematic when substrate-induced diastereoselection was also involved. Thus, addition of zincated allyl ethyl ether to the alkenyllithium derived from the secondary γ-iodo allylic ether **209** afforded a 65/35 mixture of the diastereomers **228** and **229** in low yield after hydrolysis. The erosion of diastereoselectivity was not a consequence of a less efficient substrate-induced diastereoselection but rather of the fact that both the (*E*) and (*Z*) isomers of the zincated allyl ethyl ether had reacted. Although the use of a catalytic amount of TMEDA (10 mol%) in the metallation step substantially improved the yield, the diastereoselectivity remained low (equation 111)[151].

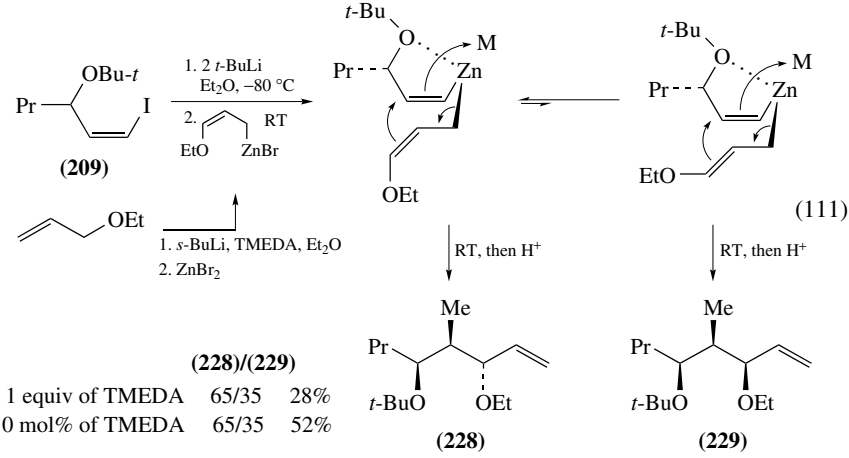

Substrate-induced diastereoselection has also been achieved in the case of alkenyllithium reagents derived from (*Z*)-δ-iodo homoallylic ethers[152, 153]. Thus, the allylzincation of the alkenyllithium derived from **230** proceeded efficiently in ether at $-20\,^{\circ}C$ and led after hydrolysis to **231** as a single diastereomer (equation 112).

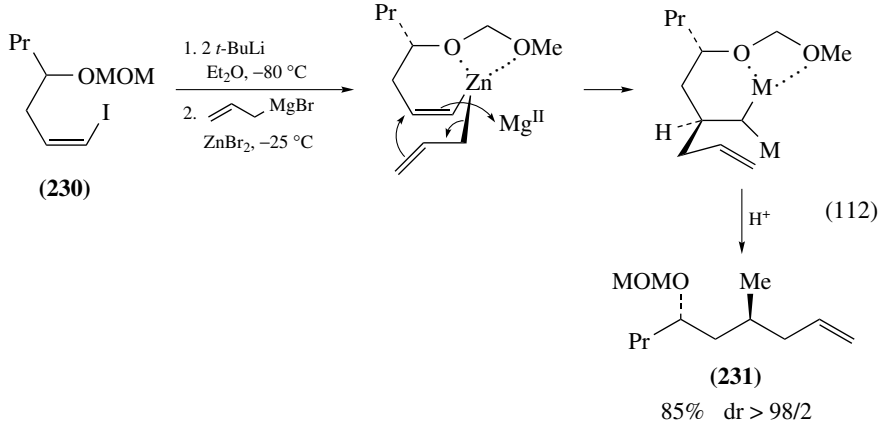

The stereochemical outcome was in agreement with the formation of a chelated allyl alkenylzinc compound that underwent a metalla-Claisen rearrangement with delivery of the allyl moiety *anti* to the homoallylic substituent. Although the stereocenter was more remote from the alkenylmetal, excellent induction was still observed[152, 153].

For alkenylmetals bearing two stereocenters at both the allylic and homoallylic positions, two situations have to be distinguished depending on their relative influence (matched or mismatched) with respect to the stereochemical outcome of the allylzincation. Not surprisingly, in the matched case, as illustrated for substrate **232**, the diastereoselectivity was excellent and **233** was obtained as a single diastereomer. The allyl moiety was delivered *anti* to both the allylic and homoallylic substituents in the chelated allyl alkenylzinc species (equation 113).

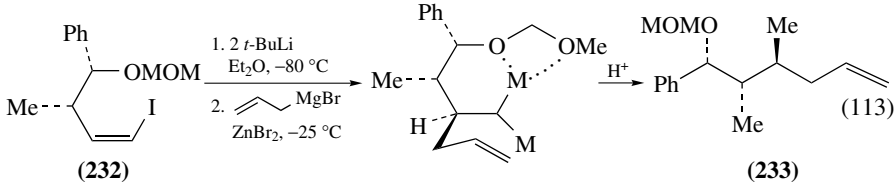

(113)

(232) **(233)**

60% dr > 95/5

Interestingly, in the mismatched manifold, the diastereoselectivity seemed to be controlled by the more remote homoallylic stereocenter. The allyl moiety was apparently delivered *syn* to the allylic substituent, as illustrated for the allylzincation of the organolithium derived from **234** which led to **235** with high diastereoselectivity (equation 114).

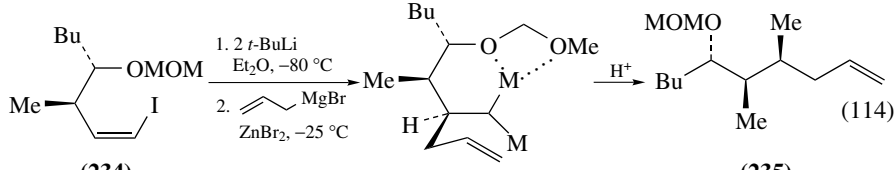

(114)

(234) **(235)**

80% dr = 96/4

A uniform explanation for the observed stereochemical outcome was provided[153]. An early transition state was considered, in which a kinetically controlled allylzincation, directed by coordination with the oxygen atom, occurred to the energetically most favored conformer of the six-membered ring chelated alkenylmetal. In the matched case, addition of the allyl moiety should preferentially operate on conformer **236b** having the allylic substituent (R^1) in a pseudo-equatorial position and the homoallylic substituent (R^2) in a pseudo-axial position, as the other arrangement **236a** would be destabilized by a steric interaction between the allyl moiety and the R^1 substituent (equation 115).

In the mismatched case, a severe gauche interaction should destabilize the conformer **237a** bearing both the allylic and homoallylic substituents in pseudo-equatorial positions and thus addition may preferentially occur on the pseudo-diaxial conformer **237b** as long as the R^1 substituent is not too bulky (equation 116). In agreement with this suggestion, it was experimentally observed that the allylzincation failed in this series when R^1 was an isopropyl group.

This transition state model also accounted well for the observed diastereoselectivities when the allyl and homoallyl substituents were both part of a six-membered ring[153].

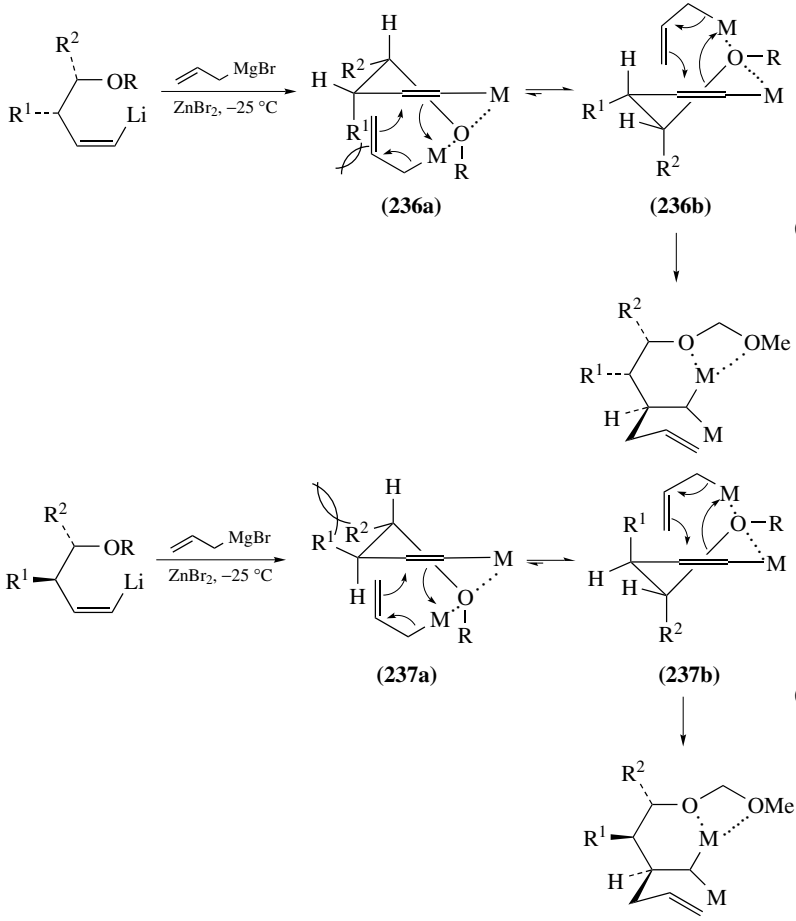

Although substrate-induced diastereoselection can be conveniently achieved when the alkenylmetal was coordinated by an oxygen atom, other heteroatoms such as sulfur and nitrogen resulted in high inductions as illustrated by the crotylzincation of the organolithium reagents derived from the allylic sulfide **238** or the tertiary amine **239** (equation 117)[154].

A nitrogen substituent, which was expected to induce a stronger chelation[147], did not slow down the rate of the allylzincation and this result opened the opportunity for achieving substrate-induced diastereoselection by using chiral amines or their derivatives. Thus, the chiral C_2 symmetric aminal **240** underwent iodine–lithium exchange and allylzincation in ether at $-30\,^{\circ}C$. After hydrolysis of the resulting *gem*-dimetallic species, the corresponding aminal **241** was obtained as a single diastereomer and was converted to the optically pure alcohol **242** (equation 118)[155]. The stereochemical outcome was consistent with the fact that the alkenylmetal should occupy an equatorial position on the imidazolidine ring and the metal should be coordinated by the axial lone pair of N1 resulting in the shielding of its *Re* face by the methyl substituent of N2.

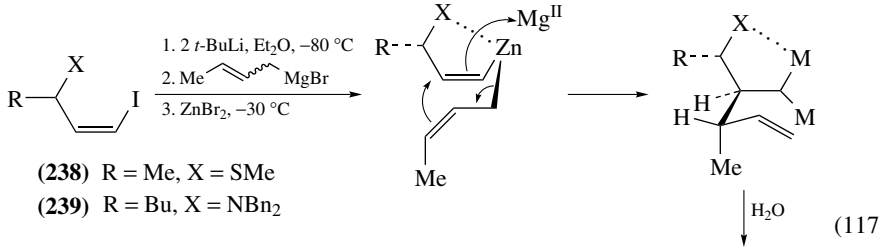

(238) R = Me, X = SMe
(239) R = Bu, X = NBn_2

(117)

R = Me, X = SMe 72% dr > 95/5
R = Bu, X = NBn_2 62% dr > 95/5

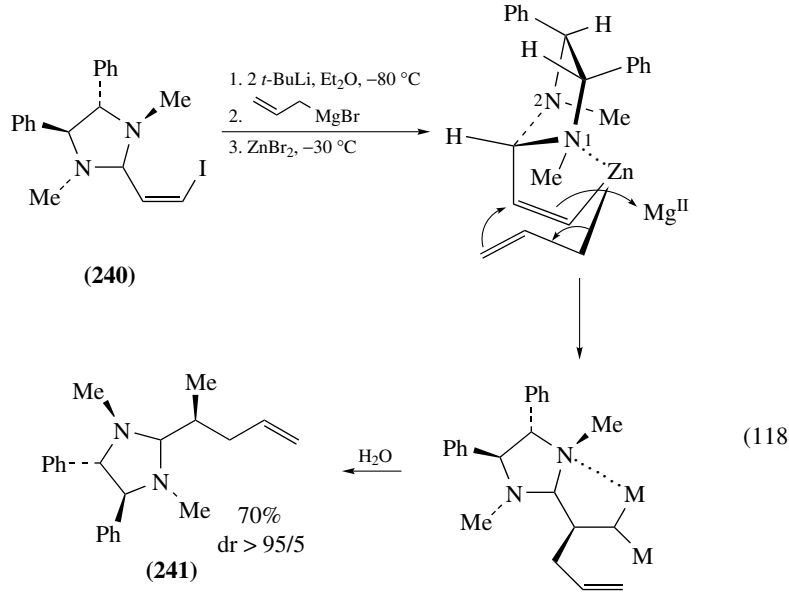

(240)

(241)

(118)

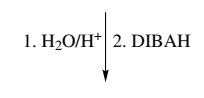

(242)

The organolithium reagents derived from the chiral (*Z*)-γ-iodo allylic amines of type **243** have also been considered as substrates for achieving diastereoselective allylzincations. The stereochemical induction was only moderate in the case of amine **243a** substituted by a phenyl group but a cyclohexyl substituent in **243b** resulted in no diastereoselection, whereas a 1-naphthyl group in substrate **243c** greatly improved it. These results seem to indicate the intervention of an arene–zinc π-interaction (π-stacking), as depicted in **244**, as a key control element of the diastereoselectivity (equation 119)[156].

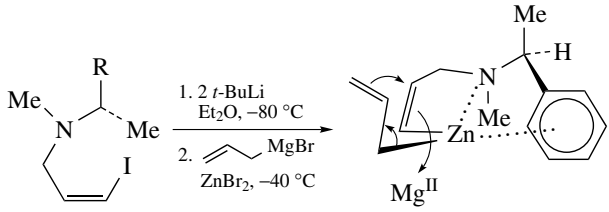

(243) **(244)**

(a) R = Ph
(b) R = *c*-Hex
(c) R = 1-Naphthyl

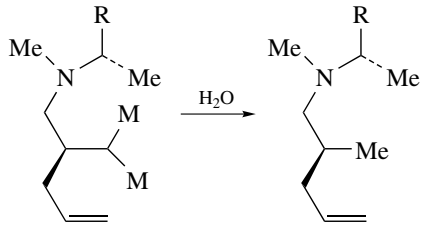

(119)

R = Ph	70%	dr = 80/20
R = *c*-Hex	72%	dr = 50/50
R = 1-Naphthyl	76%	dr = 96/4

The readily available γ-iodo allylic amines of type **245**, derived from (1*R*,2*S*)-ephedrine or nor-ephedrine, were also subjected to allylzincation after deprotonation with MeLi and lithium–iodine exchange with *t*-BuLi. The observed stereochemical outcome was in agreement with the formation of the bicyclic chelate **246** in which the allylzincation reaction preferentially occurred on the *Si* face of the chelated alkenylmetal opposite to the nitrogen substituent. In agreement with this model, the diastereomeric ratio of the resulting aminoalcohol **247** increased by switching the nitrogen substituent (R group) from a methyl group (dr = 88/12) to an isopropyl group (dr = 98/2), whereas complete erosion was observed in the case of a secondary amine (equation 120)[156].

Substrate-induced diastereoselective allylzincations essentially rely on coordination of the alkenylmetal by an appropriately located heteroatom, but a zinc–alkene π-interaction[23–27] can also exert a remarkable stereodirecting effect. Indeed, the alkenyllithium derived from **248**, bearing an appropriately located carbon–carbon double bond, underwent highly diastereoselective allyl- and crotylzincations which led after hydrolysis to the corresponding 1,6-dienes **249** and **250**. The stereochemical outcome

was rationalized by the addition of the allyl or crotyl moieties to the less hindered face of the alkenylmetal coordinated by the alkene. Indeed, replacement of the vinyl group by an ethyl group resulted in no diastereoselection (equation 121)[157].

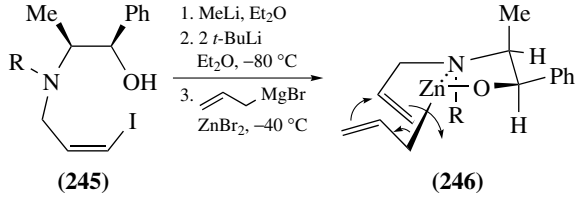

(245) **(246)**

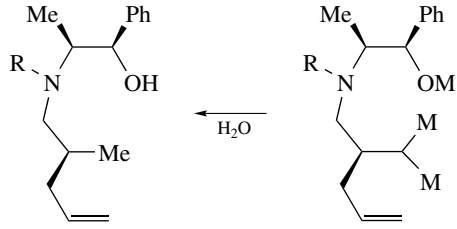

(120)

(247)

R = Me 70% dr = 88/12
R = *i*-Pr 60% dr = 98/2
R = H 55% dr = 60/40

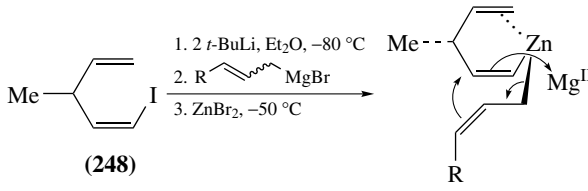

(248)

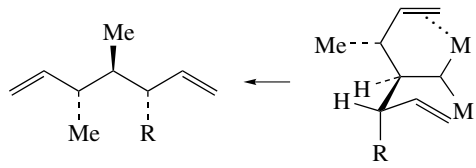

(121)

(249) R = H 67% dr = 90/10
(250) R = Me 77% dr > 95/5

Thus, the weak interaction between the zinc and a double bond was remarkably efficient at promoting the differentiation of the two pro-stereogenic faces of the alkenylmetal during the allylzincation process. Nevertheless, recent results have demonstrated that π-interactions with arenes or alkenes are less powerful in magnitude than the coordination by an alkoxy group such as a MOM ether, when both can exert a role on the stereochemical outcome[158].

As mutual face selectivity between an alkenylmetal and a substituted allylic organozinc reagent, combined with the alkenylmetal-induced diastereoselection, enabled the creation of two stereocenters, turning the sp^3 dimetallated carbon into an additional asymmetric carbon has also been examined.

4. Transformation of the sp^3 dimetallated carbon into a stereocenter

Two strategies have been used in order to convert the sp^3 dimetallated carbon, created by the allylzincation of alkenylmetals, into an additional stereocenter. The first approach relies on the use of an internal electrophilic trap consisting of an ether moiety (OMOM) acting as a leaving group in a 1,3-elimination process. Thus, the alkenyllithium derived from **251** underwent a diastereoselective allylzincation reaction in ether at $-20\,^{\circ}C$ leading to the dimetallic species **252**. The latter turned out to be thermally labile and, upon warming to room temperature, a 1,3-elimination of the OMOM group, probably assisted by the presence of magnesium salts, led to the cyclopropylzinc species **253**. Hydrolysis afforded the 1,2-disubstituted cyclopropane **254**, whereas trapping with electrophiles such as iodine or ethyl propiolate (after transmetallation with $Me_2Cu(CN)Li_2$) produced the trisubstituted cyclopropanes **255** and **256** as single diastereomers (equation 122)[159].

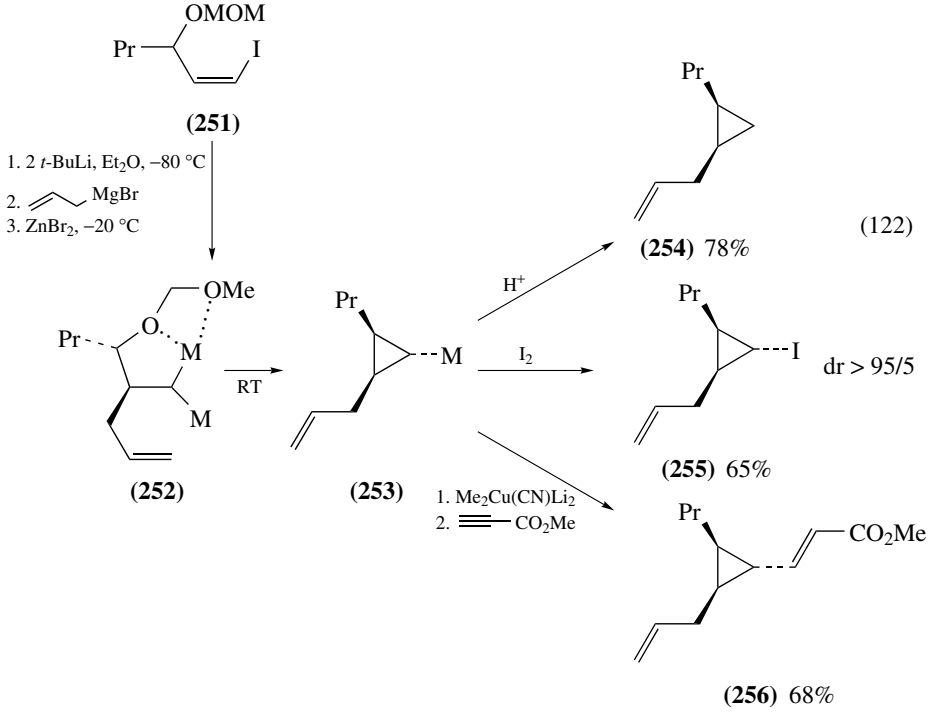

The *cis* stereochemical relationship between the propyl and the allyl groups in cyclopropanes **254**–**256** indicated that the 1,3-elimination has occurred with inversion of configuration at the carbon bearing the OMOM group and also that coordination of the metal has to be broken in order for the reaction to proceed. Moreover, cyclopropylzincs are known to be configurationally stable and the relative configuration of **253** could be explained by a 1,3-elimination involving a double inversion mechanism at both reacting centers probably proceeding on the most stable W-shaped conformer **257**. Indeed, the other possible arrangement **258** was disfavored by a steric interaction between the carbon–metal bond and the propyl group (equation 123)[159].

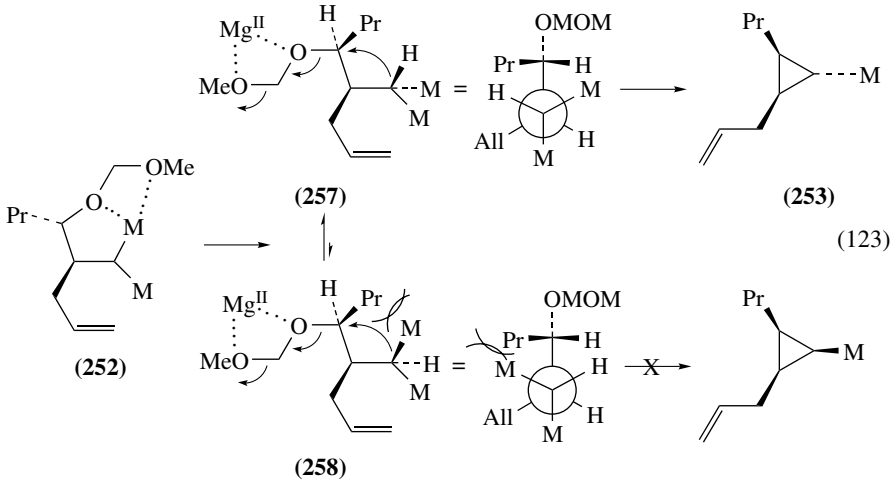

The organolithium reagents generated from the γ-iodo allylic ethers of type **259** bearing a trisubstituted double bond also underwent the allylzincation reaction in ether at $-20\,^{\circ}C$, and subsequent warming to room temperature afforded the cyclopropylzinc species **260** in which the metal and the allyl group now lay on the same face of the cyclopropane. Assuming that 1,3-elimination still proceeded on a W-shaped conformer, it is plausible that the steric interactions developed between the R^2 substituent and both the R^1 and allyl groups may be more destabilizing than similar interactions with the carbon–metal bond (equation 124)[159, 160].

By taking advantage of the propensity of the methoxymethyl ether moiety to act as a leaving group, other cyclopropylzinc compounds were synthesized. Thus, the organolithium derived from the alkenyl bromides of type **261** underwent a remarkably efficient allylzincation in ether at $-20\,^{\circ}C$, despite the α,α-disubstitution of the double bond. Upon warming to room temperature, two cyclopropylzinc compounds **262a** and **262b** could in principle result from the 1,3-elimination of the OMOM group. It was found that the stereochemical outcome of this reaction depended on the nature of the R substituent. When R was a butyl or an isopropyl group, the cyclopropane **262a**, possessing an *anti* relationship between the R substituent and the metal, was exclusively obtained, suggesting that the 1,3-elimination may proceed through the W-shaped conformer **263a**. Interestingly, when R was a phenyl group, the allylzincation proceeded at $-45\,^{\circ}C$ and was immediately followed by the 1,3-elimination of the benzylic OMOM group. In this case, a complete reversal of the diastereoselectivity was observed and the cyclopropylzinc **262b**, in which the metal and the phenyl group lay on the same face of the three-membered ring, was

exclusively formed[160,161]. This result was explained by the stabilization of the alternative W-shaped conformer **263b** by a π-interaction between the aromatic ring and the zinc. A similar reversal of diastereoselectivity was also noticed when R was a 1-propenyl group (due to an alkene–zinc π-interaction), but a trimethylsilyl ethynyl or an allyl group did not manage to reverse the diastereoselectivity in favor of **262b**. A pentafluorophenyl substituent decreased the efficiency of the π-stacking and led to an equimolar amount of the two diastereomeric cyclopropylzincs. A *p*-fluorophenyl substituent was slightly less efficient for coordinating the zinc compared to a phenyl group and, in the case of this substrate, the reaction could be also carried out in THF (0 °C to 35 °C) leading to a reversed diastereomeric ratio in favor of **262a**. Indeed, the more Lewis basic THF may compete with the intramolecular zinc–arene π-interaction (equation 125)[160].

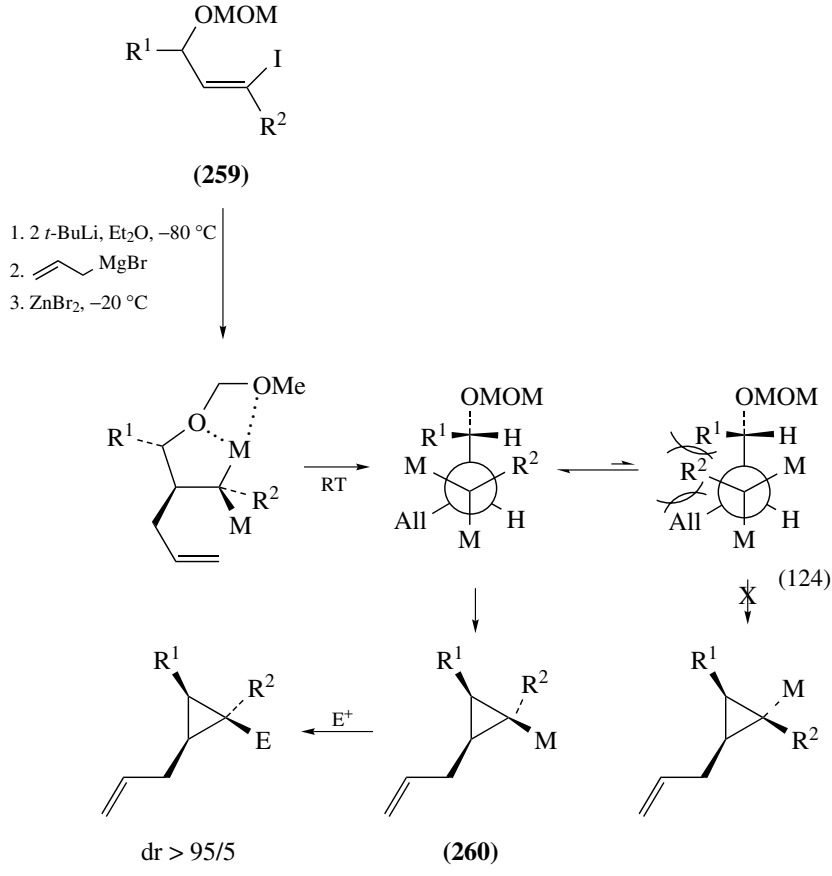

	E^+	E	Yield
(a) $R^1 = H$ $R^2 = Me$	CO_2Me	CO_2Me	62%
(b) $R^1 = H$ $R^2 = SiMe_3$	H^+	H	70%
(c) $R^1 = Pr$ $R^2 = SiMe_3$	H^+	H	68%

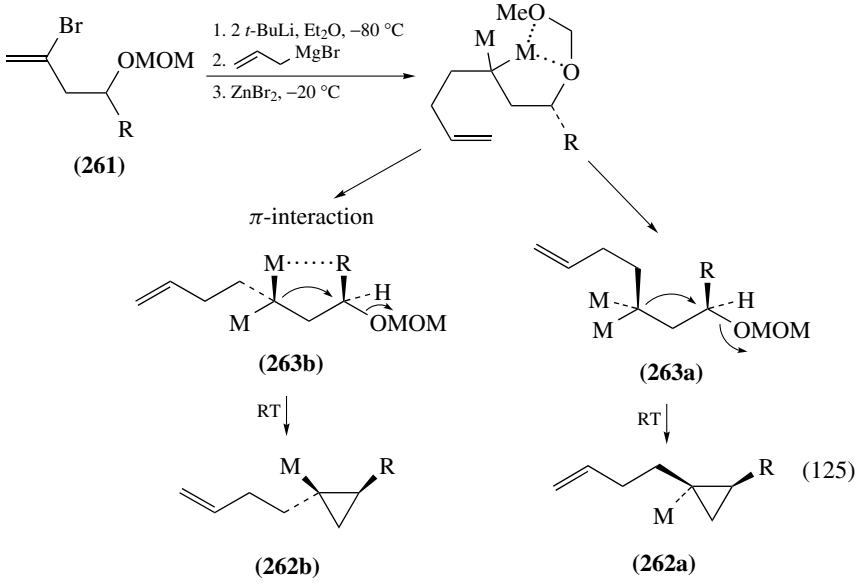

R	262a/262b	Yield (after hydrolysis)
Bu	> 95/5	80%
i-Pr	> 95/5	76%
Ph	> 5/95	90%
CH=CHMe	10/90	78%
≡—SiMe$_3$	70/30	67%
All	90/10	52%
C_6F_5	50/50	67%
p-FC_6H_4	10/90	79%
p-FC_6H_4	66/34 (in THF)	70%

Another way to generate a cyclopropylzinc species is to include the oxygenated leaving group as a substituent of the allylic organozinc partner. Thus, the γ-alkoxyallylic organozinc **264**, resulting from lithiation of allyl methoxymethyl ether with *sec*-butyllithium in the presence of TMEDA in ether and transmetallation with $ZnBr_2$, was added to the alkenyllithium derived from **209**. The reaction proceeded at an appreciable rate at room temperature provided that a catalytic amount of TMEDA was used in the metallation step and excess $MgBr_2$ was also added. This Lewis acid additive not only accelerated the allylzincation but promoted the 1,3-elimination of the OMOM group in the dimetallic species **265** leading to the *trans*-vinylcyclopropylcarbinyl ether **266** (after hydrolysis) with high diastereoselectivity (equation 126)[151].

In these 1,3-elimination reactions, the dimetallated carbon has been converted to a stereogenic center and the carbon bearing the OMOM group has played the role of an internal electrophilic site. The resulting configurationally stable cyclopropylzincs have been reacted in some cases with a second electrophile.

If two different external electrophiles are to be added to the dimetallic species, diastereoselectivity can only be achieved if the two carbon–metal bonds are properly discriminated against the reaction with a first electrophile. Moreover, the resulting monometallic species has to exhibit significant configurational stability. Coordination by a heteroatom, which turned out to be essential for achieving substrate-induced diastereoselection, also nicely served these purposes.

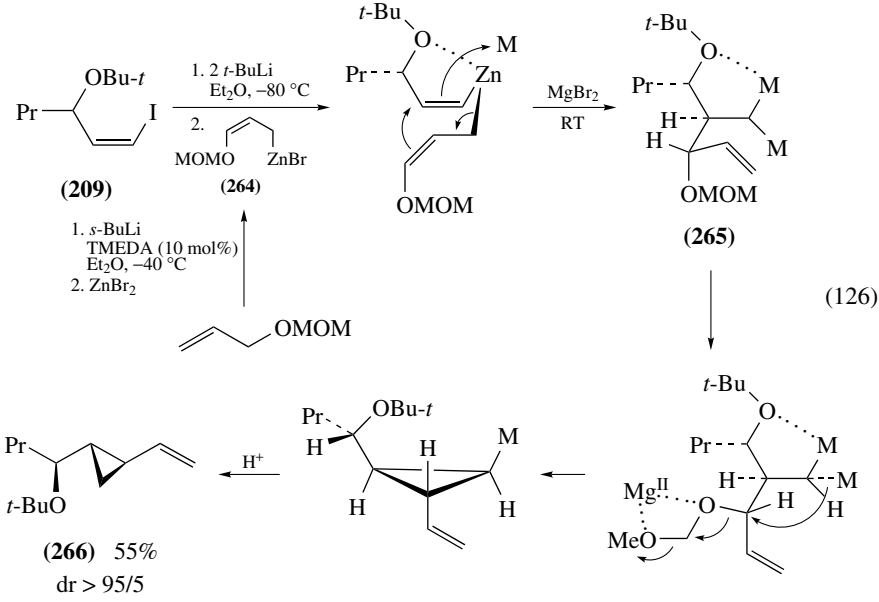

When the dimetallic species **210** was first deuteriated with MeOD and then subjected to iodinolysis, a 60/40 mixture of the two diastereomeric α-deuteriated iodides **267a** and **267b** was obtained. Although the use of a first small electrophile such as a MeOD did not enable efficient differentiation of the two carbon–metal bonds, a reversal of diastereoselectivity was observed when the α-deuteriated dimetallic species **268** was first protonated with MeOH and then reacted with iodine. This result points towards the configurational stability of the resulting monoorganozinc species generated after reaction with a first electrophile, presumably due to the coordination by *tert*-butyl ether moiety (equation 127)[162].

By contrast, when the more bulky tributyltin chloride was used as the first electrophile and iodine as the second one, the α-iodoorganostannane **269** was obtained with high diastereoselectivity. Elucidation of the stereochemical outcome indicated that the non-chelated carbon–metal bond reacted with the first electrophile (Bu_3SnCl) and that the resulting chelated α-stannylorganozinc reagent **270** displayed a high configurational stability, despite a *syn* stereochemical relationship between the tributylstannyl and allyl groups in the five-membered ring chelate (equation 128)[162].

Allylzincation of alkenylmetals provides a useful entry to the diastereoselective synthesis of sp^3 *gem*-dimetallic species that can react with two different electrophiles in a one-pot protocol, leading to elaborated acyclic structures with control of the configuration of up to three adjacent stereocenters, as well as to cyclopropanes bearing various substitution patterns[126, 163].

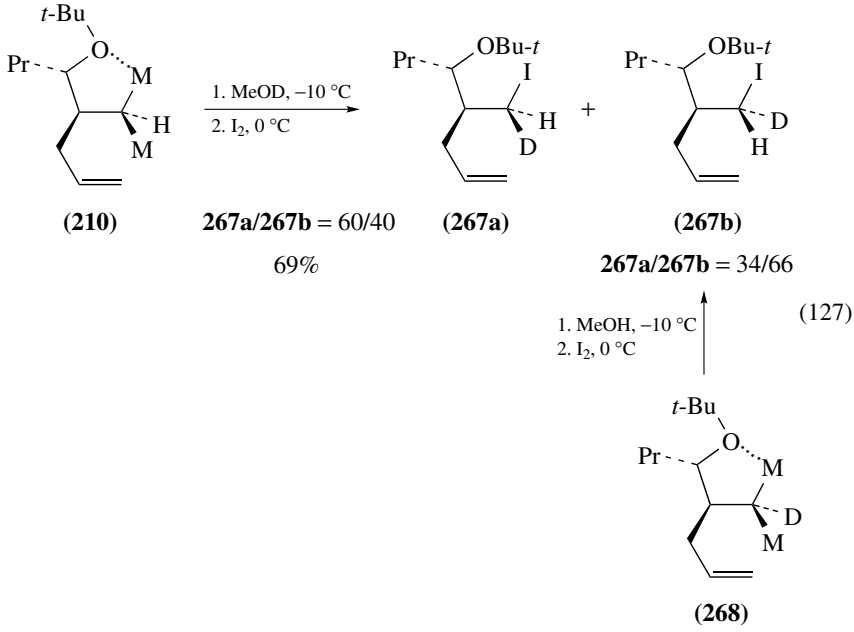

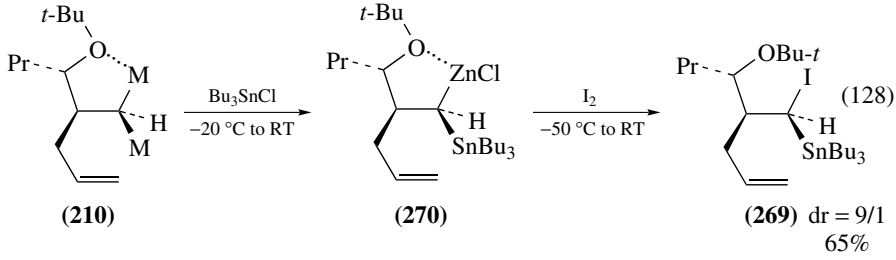

Allylic 1,1-diorganometallic species have also been prepared by allylzincation of allenylmetals.

E. Allylzincation of Allenylmetals

Allenic organometallics are accessible by different methods including metallation of allenes or of disubstituted alkynes at the propargylic position. Metallation of the α-silyl allenic ether **271** with *n*-butyllithium followed by addition of allylzinc bromide and heating in refluxing THF led to the allylic 1,1-dimetallic reagent **272** (presumably a diorganozinc species). The reaction could be regarded either as a zinc−ene reaction or a Lewis acid-assisted metalla-Claisen rearrangement, by analogy with the allylzincation of alkenylmetals (see Section III.D.2). In spite of the allylic metallotropic equilibrium, deuterolysis of the dimetallic species **272** exclusively afforded the 1,3-dideuterated allylic ether **273** as a single regio- and stereoisomer. This result was explained by deuteration of the non-chelated allylic carbon−metal bond in **272** with formation of a

chelated alkenylorganometallic species **274** which, in turn, was protonated stereoselectively (equation 129)[164].

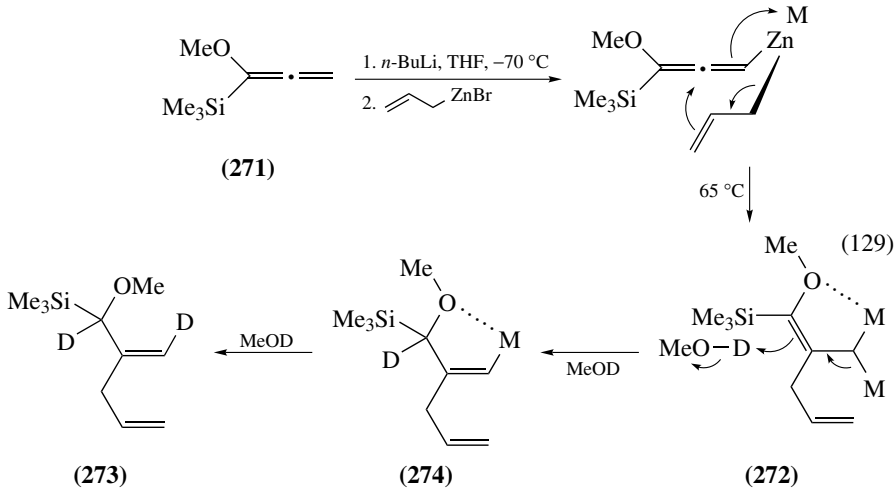

(129)

Due to the propargyl–allenyl metallotropy, it is also possible to generate the allenyllithium species from a propargylic ether[164]. Thus, compound **275** could be easily metallated at the propargylic position and, after addition of allylzinc bromide, the allenylmetal underwent allylzincation and led to the dimetallic reagent **276**. The propensity of such allylic 1,1-dimetallic species to act as multi-coupling agents has been investigated[165]. Not surprisingly, as the reaction of an allylic organometallic species was first involved, a wide range of electrophiles could be used successfully such as aldehydes, ketones, esters, acid chlorides, chloroformates, isocyanates, benzyl bromide or allyl bromide as well as *gem*-aminoethers. These reactions occurred regioselectively via a S_E2' process and consequently generated a chelated alkenylmetal compound which displayed considerably lower reactivity. When the latter was protonated, the functionalized products of type **277** bearing an (*E*)-alkenylsilane moiety were obtained (equation 130)[165].

When the first electrophile was not a ketone or an aldehyde, as illustrated for the reaction of **276** with crotonyl chloride, the intermediate chelated alkenylmetal **278** could also be subjected to iodinolysis or palladium-catalyzed cross-coupling reactions with aryl and alkenyl iodides in the presence of a stoichiometric amount of CuBr as a promotor as well as a polar cosolvent such as *N*,*N*-dimethylacetamide (DMA) (equation 131)[165,166].

By contrast, when the first electrophile was an aldehyde as illustrated for the reaction of **276** with benzaldehyde, the resulting alkenylmetal presumably became part of a six-membered ring alkoxide **279** and hence so poorly reactive that it did not even react with iodine. However, treatment with Me_3SiCl resulted in the silylation of the secondary zinc alkoxide and allowed iodinolysis to subsequently proceed, affording the (*Z*)-alkenyl iodide **280** (equation 132)[165]. Unfortunately, this protocol was not efficient for tertiary alkoxides generated by initial reaction of **276** with ketones.

Another option for the preparation of allenyllithium reagents involves the carbolithiation of activated conjugated enynes[15]. Thus, addition of BuLi to the enyne **281** led to an allenyllithium compound **282** (in metallotropic equilibrium with its propargylic counterpart). Subsequent addition of allylzinc bromide generated the allylic 1,1-dimetallic species

283 which was deuteriated regioselectively but not fully stereoselectively, as the alkenyl thioether **284** was obtained as a 88/12 mixture of geometric isomers (equation 133)[164].

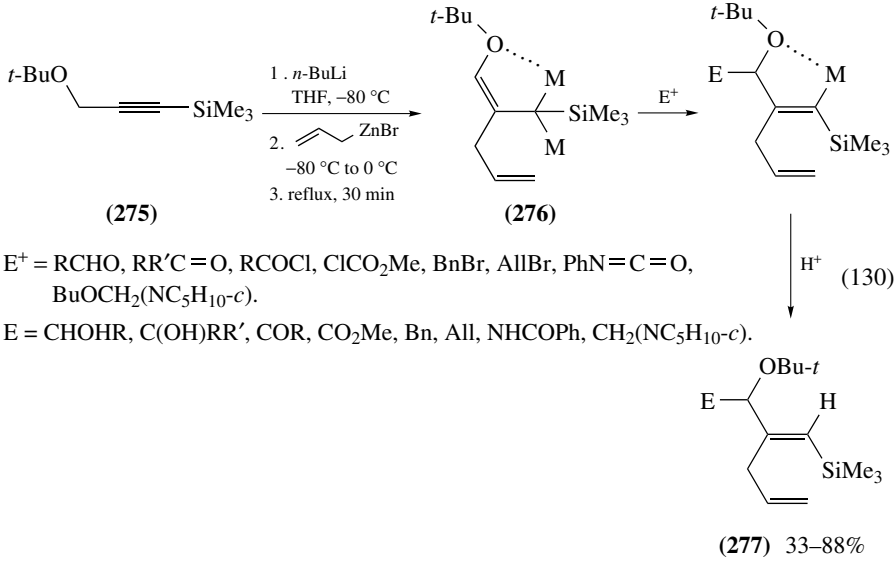

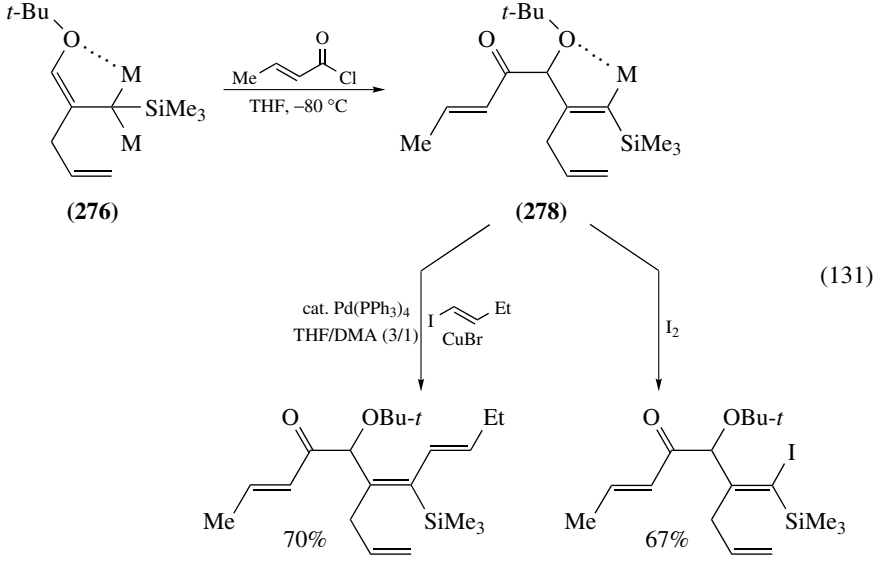

The presence of heteroatoms, not only for the regio- and stereoselective functionalization of the allylic 1,1-diorganometallic species, and/or silyl substituents was found to exert a dramatic influence on the course of the allylzincation of allenyllithium reagents. Indeed, when 1,2-decadiene (**285**) was metallated and treated with allylzinc bromide, the reaction followed a different course and led after hydrolysis to the bis(*exo*-methylene)cyclohexane

286 (90/10 mixture of stereoisomers) wherein two molecules of the allene have been incorporated (equation 134)[167].

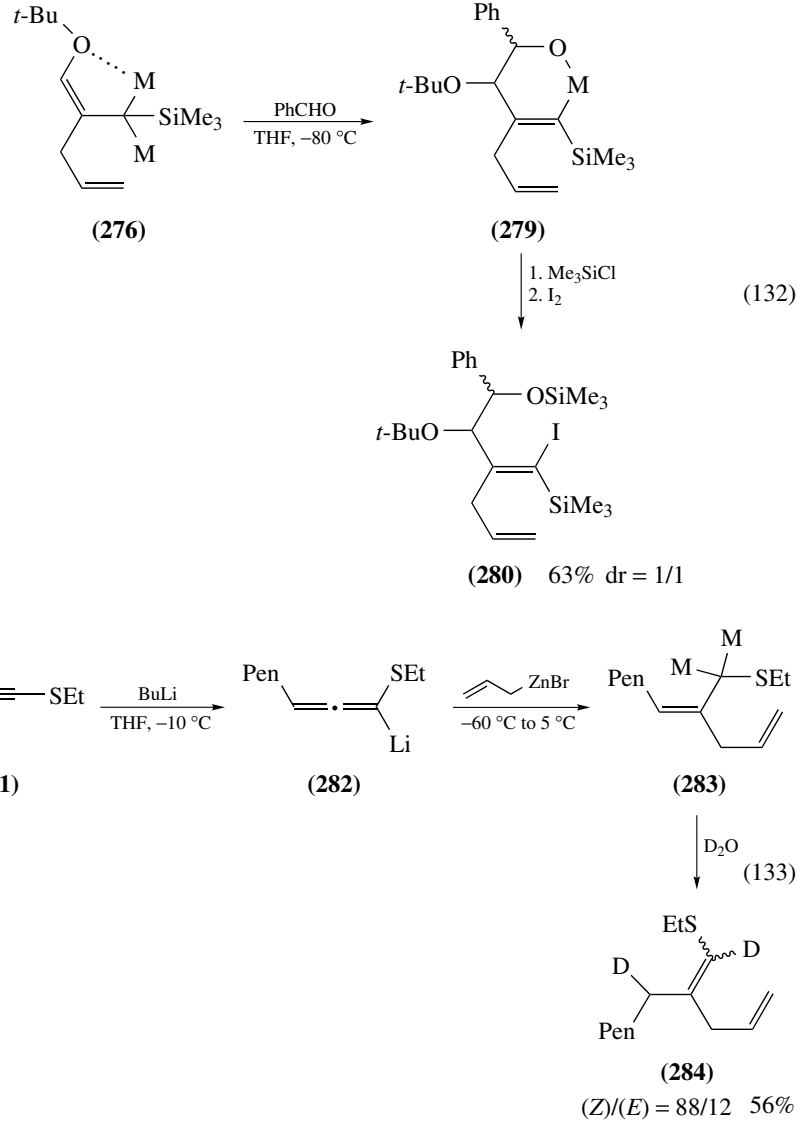

The formation of **286** was rationalized by considering that the initially generated allylic 1,1-dimetallic species **287**, which was presumably less stabilized in the absence of appropriately located heteroatoms and/or silyl groups, reacted with another molecule of allenymetal to produce a new allylic dimetallic species **288**. This process could in principle happen again and induce polymerization but instead, compound **288** underwent a type II

zinc–ene cyclization leading to the trismetallated species **289** bearing two alkenylmetals and one alkylmetal. The type II zinc–ene reaction of **288** occurred regioselectively with carbon–carbon bond formation at the most substituted teminus of the allyl dimetallic species.

This intriguing process was not restricted to 1,2-decadiene **(285)** and was also observed for methyl (3-phenylprop-2-ynyl) ether[167].

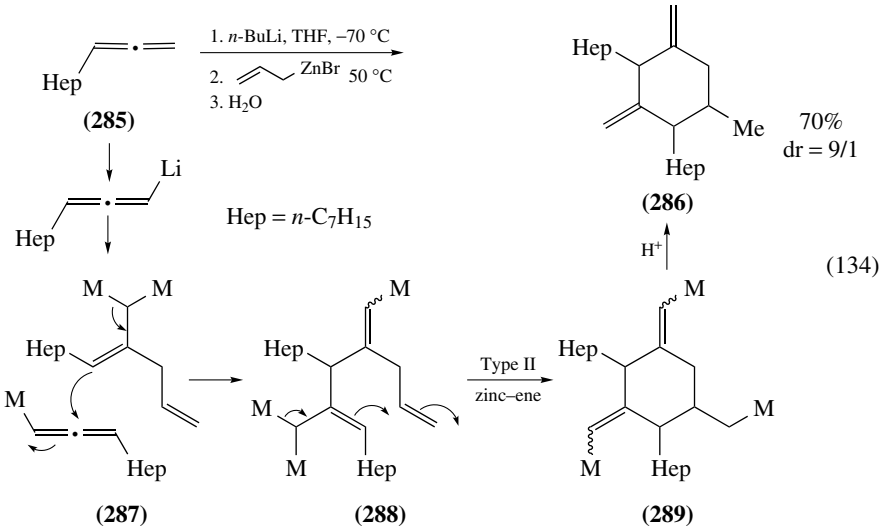

F. Allylzincation of Alkynylmetals

1. Reactivity of allylic organozinc reagents towards metallated alkynes

The ability of allylzinc bromide to add to terminal alkynes was first observed with acetylenic amines as substrates. Thus, the propargylic amine **290** underwent addition of allylzinc bromide in refluxing THF and afforded after hydrolysis the allylic amine **291**. This reaction occurred much more easily compared to the case of ethylenic amines (see Section III.A) and the regioselectivity was also noteworthy as a branched product was obtained predominantly[82,105]. It was suggested that metallation of the terminal alkyne was responsible for the observed regioselectivity. Indeed, the formation of an alkenyl 1,1-dimetallic species tentatively formulated as **292** was ascertained by deuteriolysis, which led to the *gem*-dideuteriated compound **293**, or by reaction with benzaldehyde which produced the allenic amine **294** (equation 135). For comparison, it is also worth mentioning that addition of an excess of allylmagnesium bromide to **290** in refluxing THF led to **291** in only 8% yield.

It was demonstrated that a variety of terminal alkynes, including propargylic alcohols or ethers, could also react with allylzinc bromide in THF. These reactions afforded mixtures of mono- and bis-addition products **295** and **296** respectively, presumably arising from 1,1-dimetallic or 1,1,1-trimetallic species (equation 136)[123–125,168,169]. Acetylene itself reacted twice but, for substrates more hindered at the propargylic position, monoaddition predominated. Interestingly, in some cases, the addition of magnesium salts was found to accelerate the reaction and significantly improved the proportion of the bis-addition product[170].

Addition of excess allylzinc bromide to the conjugated enynol **297** chemoselectively affected the triple bond and afforded a mixture of monoaddition and bis-addition products. The formation of di- and trimetallic species was unambiguously ascertained by deuteriolysis (equation 137)[171].

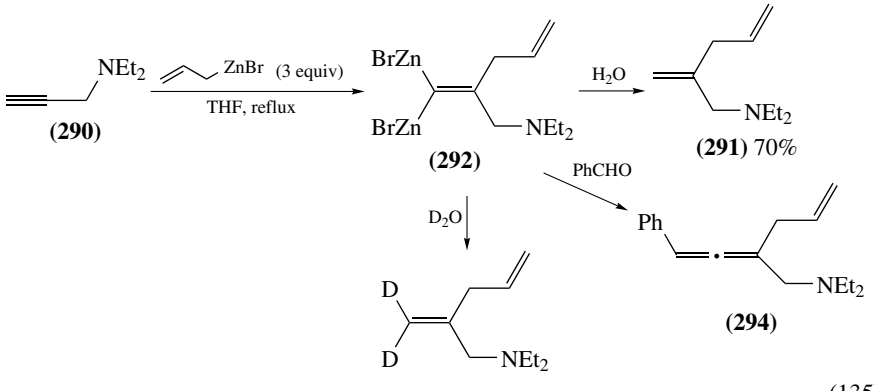

(135)

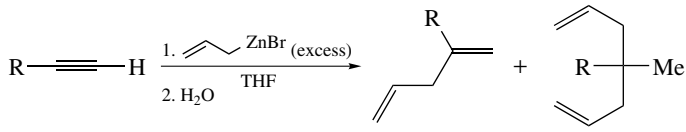

		(295)	(296)
R = H	35 °C	–	45%
R = Ph	35 °C	67%	6%
R = Bu	25 °C	52%	14%
R = CH(OH)Me	40 °C	79%	0%
	+ $MgBr_2$ (8 equiv)	13%	41%
R = CH(Et)Me	40 °C	50%	–

(136)

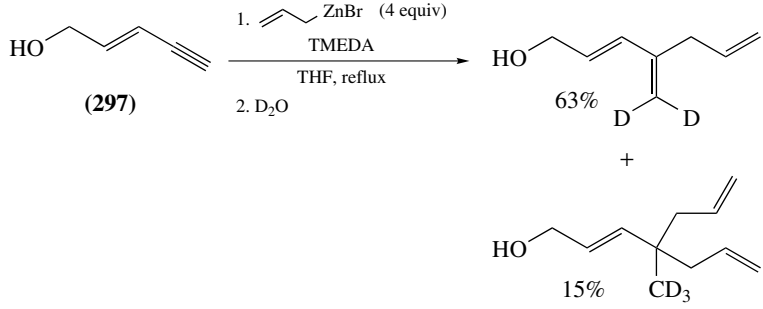

(137)

Other conjugated terminal enynes reacted in a similar fashion but the more substituted the double bond, the less efficient the allylzincation reaction[168, 172, 173]. By comparison, organolithium reagents and allylmagnesium bromide underwent conjugate addition to terminal enynes with nucleophilic attack of the double bond[168, 171, 172].

As 1,2-disubstituted triple bonds do not generally react with allylic organozinc reagents, conjugated terminal diynes underwent chemoselective allylzincation at the terminal alkyne moiety leading to allyl-substituted conjugated enynes (equation 138)[173].

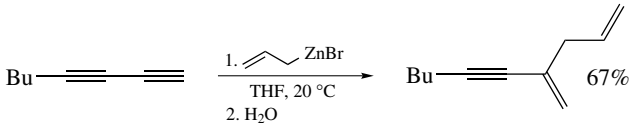

(138)

Allylic organozinc reagents substituted at C2 or C3 also add to terminal alkynes, but in general monoaddition predominates. In the case of crotylzinc bromide, the reaction could lead to two different regioisomers, either a branched one incorporating the 1-methylallyl moiety and resulting from reaction with allylic transposition (S_E2' regioselectivity), or a linear one incorporating the 2-butenyl moiety (S_E2 regioselectivity). Whereas the former is kinetically favored, extended reaction times or heating in refluxing THF increased the proportion of the latter which is thermodynamically favored, thereby demonstrating the reversibility of the allylzincation of terminal alkynes (equation 139)[168, 169, 172, 173].

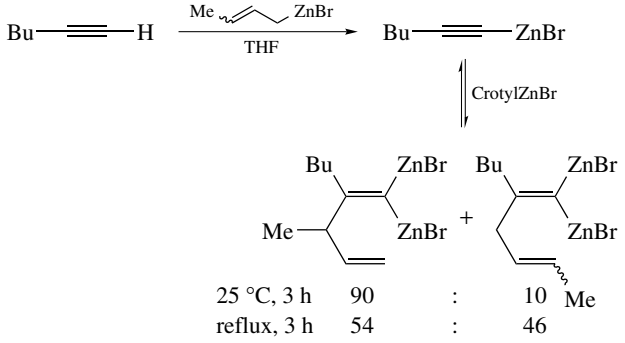

(139)

Cinnamyl- or 2,4-pentadienylzinc bromides led predominantly to the more stable adducts possessing α,β-disubstituted double bonds conjugated with the aromatic ring or the vinyl group respectively[174]. Bis-addition of crotylzinc bromide to terminal alkynes can occur under more forcing conditions and both groups incorporated in the final product exclusively possess the linear 2-butenyl structure[169, 175].

It was observed that the metallation of terminal alkynes by organomagnesium (or organolithium) reagents considerably accelerated the rate of the subsequent addition of allylzinc bromide. The products resulting from a bis-addition predominate even in the case of sterically more demanding alkynes (equation 140).

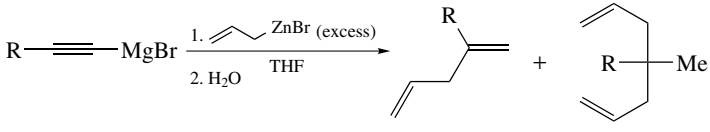

(140)

		(295)	(296)
R = Ph	35 °C	22%	65%
R = CH(Et)Me	65 °C	7%	71%

Crotylzinc bromide can also add twice to alkynyl Grignard reagents and the resulting bis-adducts exclusively incorporate two 2-butenyl groups (equation 141)[169, 170].

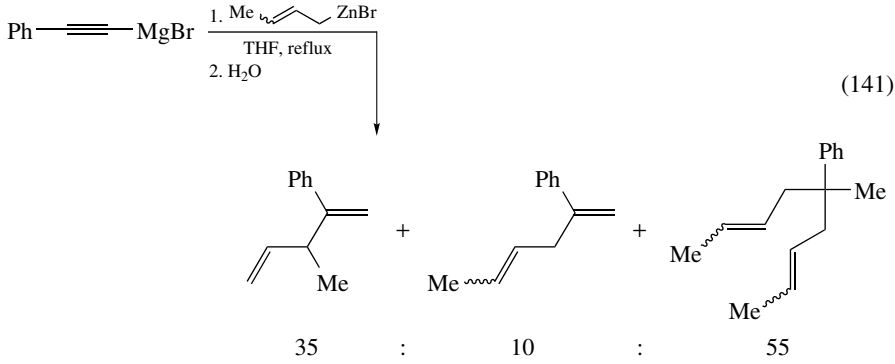

(141)

For terminal alkynes bearing a leaving group at the propargylic position (halogens, phenoxy or alkoxy groups), the organometallic species resulting from bis-addition across the carbon−carbon triple bond underwent a subsequent 1,3-elimination reaction leading to substituted cyclopropanes. Thus, treatment of the Grignard reagent **298** with excess crotylzinc bromide in THF at reflux afforded 1,1-di(2-butenyl)cyclopropane **(299)** (equation 142)[176].

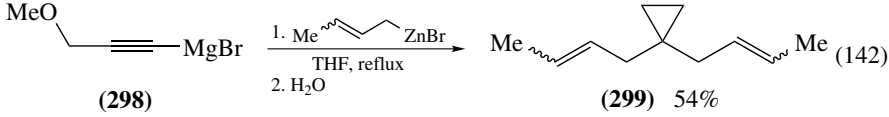

(298) **(299)** 54%

(142)

It is also possible to achieve the formation of five-membered rings by coupling the allylzincation of a metallated alkyne with an intramolecular nucleophilic substitution. Thus, allylzincation of the ethylzinc alkynylide generated from 5-iodo-1-pentyne (**66**)[45], or direct treatment of the latter with excess crotylzinc chloride[177], led to the alkenyl 1,1-dimetallic species of type **300** which underwent σ-type cyclizations, with nucleophilic displacement of the iodide, that produced the substituted cyclopentenylzincs **301** (equation 143).

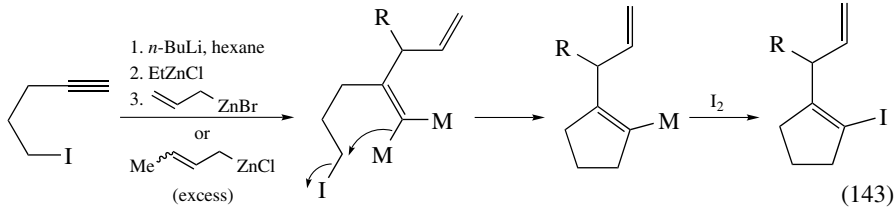

(143)

(66) **(300)** **(301)** R = H 86%
R = Me 75%

Although the exact structures of the alkenyl 1,1-dimetallic or the alkyl 1,1,1-trimetallic species generated by addition of allylzinc bromide to alkynes and/or alkynyl Grignard reagents were not established with certainty, it was observed that almost all the magnesium, the bromide, but only a small fraction of zinc, constituted the elements of a solid mineral phase thereby suggesting that only carbon–zinc bonds were present in such organometallic species[169]. Indeed, the latter are probably diorganozinc or triorganozinc oligomeric structures respectively (see Section III.D.2)[141,142].

The scope of the allylzincation of terminal alkynes was initially investigated in terms of substrates that could be conveniently used as well as the parameters which governed mono- or bis-addition. Although these reactions constituted a straightforward access to alkenyl 1,1-dimetallic species[178], the functionalization of the latter remained essentially unexplored.

2. Functionalization of the alkenyl 1,1-diorganometallic reagents

In the case of the sp^3 1,1-diorganometallic species prepared by allylzincation of alkenylmetals, coordination by a heteroatom allowed for the discrimination of the two carbon–metal bonds. A similar effect could be anticipated for the sp^2 1,1-diorganometallic species resulting from the allylzincation of the alkynyllithium reagents derived from propargylic ethers. Whereas THF had been invariably used as the solvent in the early investigations, its replacement by diethyl ether considerably accelerated the rate of the allylzincation and allowed the reaction to proceed at much lower temperatures (typically $-10\,^{\circ}C$)[179]. In ether, allylic organozinc reagents were replaced by the combination of the corresponding allylic Grignard reagents and $ZnBr_2$, the presence of magnesium salts being also probably responsible for the observed rate acceleration. It is worth mentioning that under these mild conditions, bis-addition of allylic organozinc to metallated alkynes was not observed.

Thus, the alkynyllithium derived from the propargylic ether **302** underwent allylzincation under the above-mentioned conditions and led to the dimetallic species **303**. Whereas treatment with NBS resulted in the formation of the dibromoolefin **304**, reaction of **303** with the less reactive benzenesulfonyl chloride produced an α-chlorozinc sulfinate **305**. The latter could in turn react with different electrophiles and afforded the corresponding tri- or tetra-substituted olefins of type **306** as single geometric isomers (equation 144)[179].

Indeed, the non-chelated carbon–metal bond reacted exclusively with $PhSO_2Cl$ as the first electrophile. It was checked that, in the absence of an appropriately located heteroatom, the monochlorination of alkenyl 1,1-dimetallic species was not stereoselective[179]. Monobromination could also be successfully achieved with TosBr whereas cyanation with TosCN produced the α-cyano organozinc compound **307**. In order to improve the reactivity of the remaining carbon–metal bond in this species, transmetallation to an organocopper reagent was carried out and subsequent allylation provided the tetrasubstituted α,β-unsaturated nitrile **308** as a single geometric isomer (equation 144)[180].

When **303** was directly treated with $Me_2Cu(CN)Li_2$, the transmetallation failed to discriminate between the two carbon–metal bonds. By contrast, the allylzincation of the alkynyllithium derived from the propargylic alcohol **309** produced the alkenyl 1,1-dimetallic species **310**, in which the two carbon–metal bonds exhibit different reactivities due to the presence of a metal-alkoxide. Indeed, transmetallation with $Me_2Cu(CN)Li_2$ led to the alkenyl copper–zinc species **311**, which was relatively poorly reactive towards electrophiles but underwent successful 1,4-addition to ethyl propiolate leading to **312** in satisfactory overall yield (equation 145)[180].

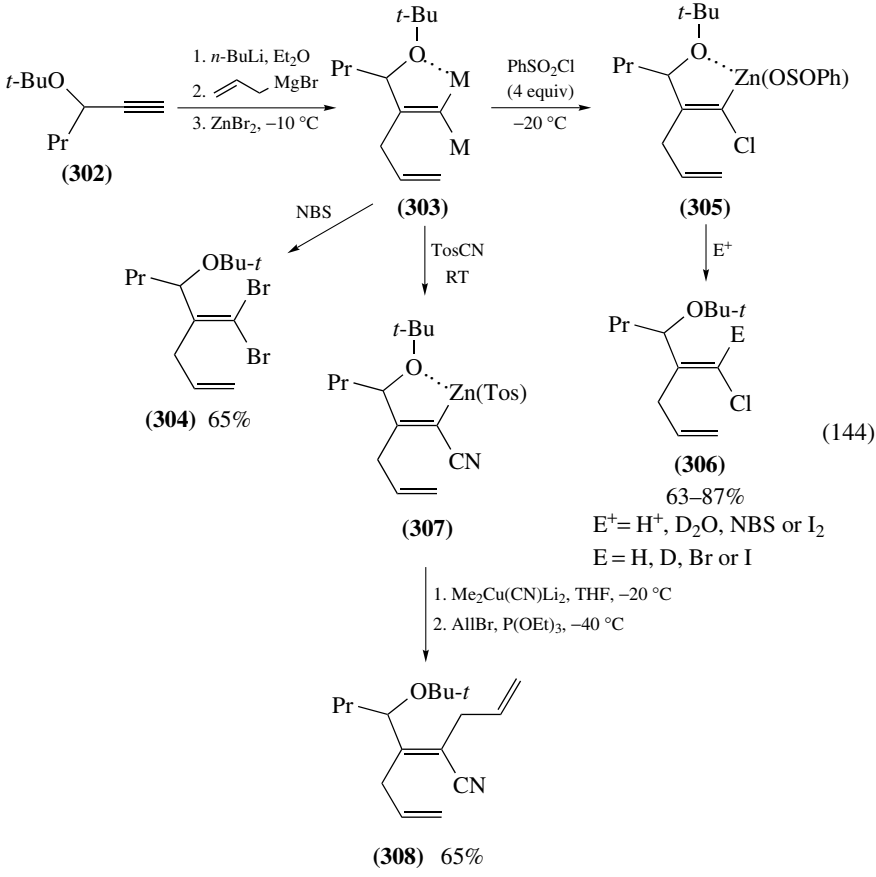
t-BuO
Pr
(302)
1. n-BuLi, Et2O
2. MgBr
3. ZnBr2, –10 °C
t-Bu
O
Pr
M
M
(303)
PhSO2Cl
(4 equiv)
–20 °C
t-Bu
O
Pr
Zn(OSOPh)
Cl
(305)
NBS
TosCN
RT
E+
Pr
OBu-t
Br
Br
(304) 65%
t-Bu
O
Pr
Zn(Tos)
CN
(307)
Pr
OBu-t
E
Cl
(306)
63–87%
E+= H+, D2O, NBS or I2
E = H, D, Br or I
(144)
1. Me2Cu(CN)Li2, THF, –20 °C
2. AllBr, P(OEt)3, –40 °C
Pr
OBu-t
CN
(308) 65%

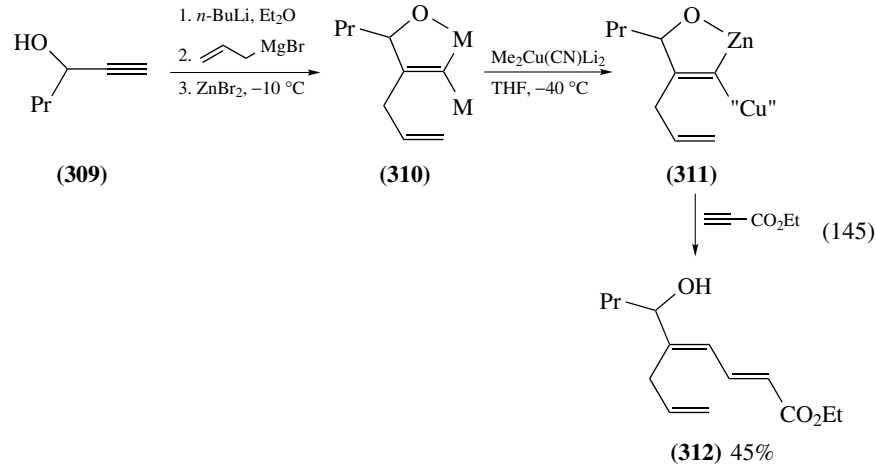
HO
Pr
(309)
1. n-BuLi, Et2O
2. MgBr
3. ZnBr2, –10 °C
Pr
O
M
M
(310)
Me2Cu(CN)Li2
THF, –40 °C
Pr
O
Zn
"Cu"
(311)
CO2Et
(145)
Pr
OH
CO2Et
(312) 45%

The reactivity of the α-chloro alkenylzinc species **305** as a zinc carbenoid was also exploited. Addition of *n*-BuLi (2 equiv) to **305** led to the organozincate **313**, which underwent a 1,2-metallate rearrangement and produced the α-alkylated alkenylzinc species **314** with predominant, but not exclusive, inversion of configuration. The latter was subjected to iodinolysis and afforded the tetrasubstituted alkenyl iodide **315** as a 92/8 mixture of (*E*)/(*Z*) geometric isomers[179]. On the other hand, the α-chloro zinc carbenoid **305** turned out to be stable up to $-20\,^{\circ}C$, but warming to room temperature resulted in its clean transformation to the disubstituted alkyne **316** (equation 146). This latter transformation, known as the Fritsch–Buttenberg–Wiechell (F.B.W.) rearrangement, was unprecedented for zinc carbenoids. Moreover, the behavior of **305** was interesting as the migration of an alkyl group in the F.B.W. rearrangement of alkylidene carbenoids is not particularly favored. Also relevant was the comparison with the related lithium carbenoid which led to a complex mixture of products containing less than 10% of the disubstituted alkyne **316**[181].

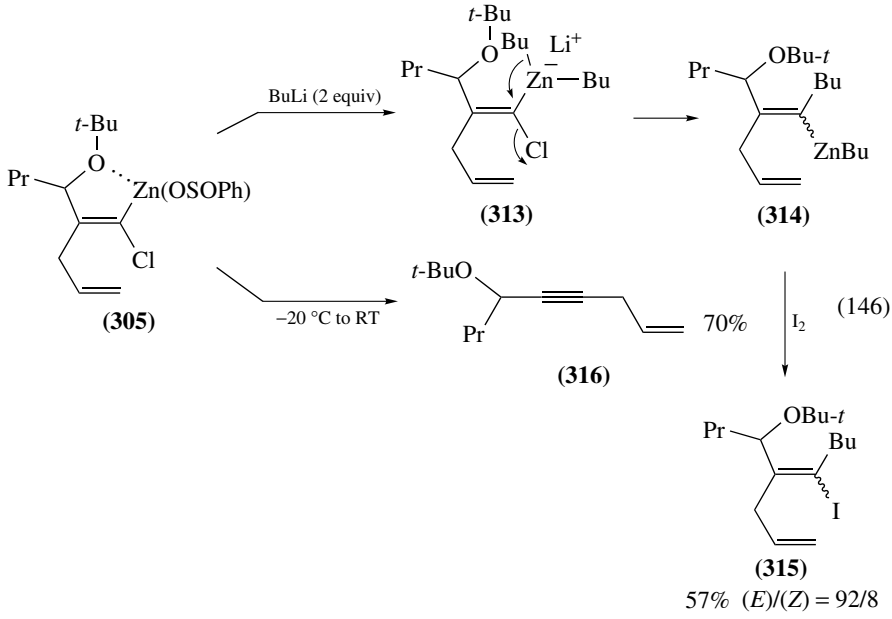

The diastereoselective crotylzincation of propargylic ethers was then investigated with the aim of achieving a chirality transfer through the use of the F.B.W. rearrangement. Crotylzincation of the alkynyllithium derived from the propargylic ethers **302** or **317** led to the alkenyl 1,1-dimetallic species of type **318**. Monochlorination with $PhSO_2Cl$ generated the α-chlorocarbenoids **319**, which could be protonated at $-20\,^{\circ}C$ to afford the (*E*)-alkenyl chlorides of type **320**. It was observed that the crotylzincation of the *tert*-butyl ether **302** proceeded with moderate diastereoselectivity (dr = 70/30) whereas the (methoxy)ethoxymethyl ether (MEM) led to a substantially higher diastereomeric ratio (dr = 92/8). Upon warning to room temperature, the α-chloro zinc carbenoids **319** underwent the F.B.W. rearrangement and led to the disubstituted alkynes **321** with a diastereomeric ratio similar to the carbenoid reagents **319** from which they arose. It was

observed that the more coordinated the metal (MEM ether compared to the *tert*-butyl ether), the slower the F.B.W. rearrangement (equation 147)[181].

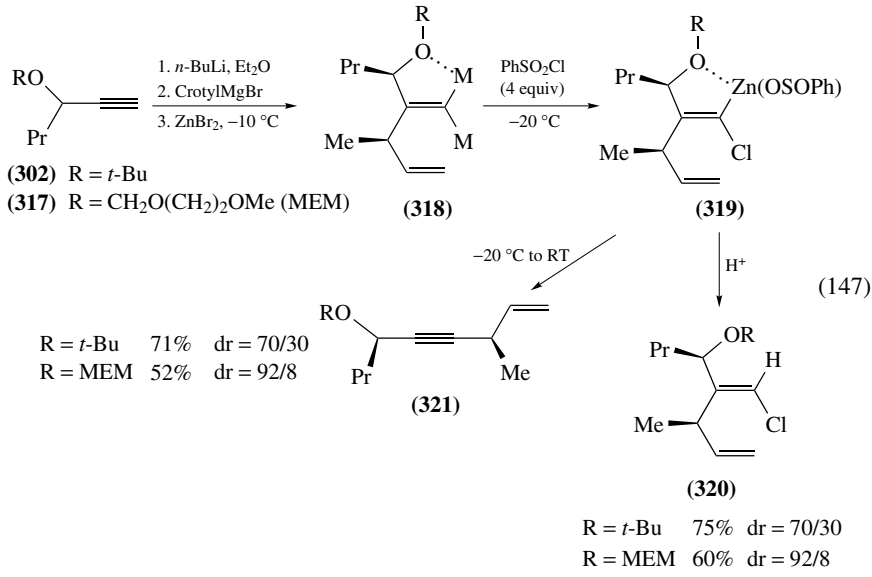

(147)

It was also demonstrated that the F.B.W. rearrangement proceeded with retention of configuration of the migrating group although its identity was initially unknown[181]. In order to address this issue, a series of ^{13}C labeled lithium alkynilides **322** was subjected to an allyl or a crotylzincation. The resulting alkenyl 1,1-dimetallic species **323** were monochlorinated with $PhSO_2Cl$ to afford the α-chlorozinc carbenoids of type **324**. The latter were generally obtained as mixtures of geometric isomers and the ratio was determined after hydrolysis to the corresponding alkenyl chlorides **325**. The reaction was stereoselective only when R^1 was an alkoxymethine group, as illustrated previously in the case of the 1,1-dimetallic species **303** (equation 144), due to the discrimination of the two carbon–metal bonds by coordination with the ether moiety. Upon warming to room temperature, the α-chlorozinc carbenoids **324** underwent the F.B.W. rearrangement and the ratio of the resulting disubstituted ^{13}C labeled alkynes **326** (preferential migration of R^1) and **327** (preferential migration of allyl or 1-methylallyl groups) was used to gain some insight on the stereochemical requirements as well as the migrating abilities of the different substituents (equation 148)[182].

From these experiments, it could be concluded that an exclusive migration of the alkoxymethine group (R^1 = C(OBu-*t*)Hep) located *trans* to the chlorine atom took place in the F.B.W. rearrangement of the α-chlorozinc carbenoids of type **324**. In the other cases, the migratory aptitudes of two groups depend on their degree of substitution, whatever the olefinic configuration of the α-chlorozinc carbenoid. The relative migratory aptitude order appeared to be: Alkoxymethine > allyl > cyclohexyl and alkoxymethine > 1-methylallyl > cyclohexyl as well as *n*-octyl > 1-methylallyl.

The behavior of propargylic amines has also been investigated as the use of a chiral amine would potentially enable one to control the absolute configuration of the newly formed stereocenter upon addition of a substituted allylic organozinc reagent to the corresponding alkynylmetal. Thus, the optically pure propargylic amine **328** underwent a

diastereoselective crotylzincation (under optimized conditions) leading, after hydrolysis of the intermediate dimetallic species **329**, to the allylic amine **330** as a 88/12 mixture of diastereomers[183]. However, the α-chlorozinc carbenoid **331**, generated by treatment of **329** with $PhSO_2Cl$, turned out to be stable even at room temperature and failed to undergo the F.B.W. rearrangement. Subsequent hydrolysis only afforded the (*E*)-alkenyl chloride **332**. The strong coordination of zinc by the amino group in the zinc alkylidene carbenoid **331** may prevent its rearrangement. Attempts to form a zincate species from **331**, to perform a transmetallation or to use Lewis acid additives had no beneficial effects. Although the α-iodozinc carbenoid **333**, generated from **329** by treatment with NIS, was more prone to undergo the F.B.W. rearrangement, the yield of the disubstituted alkyne **334** was extremely low (equation 149)[183].

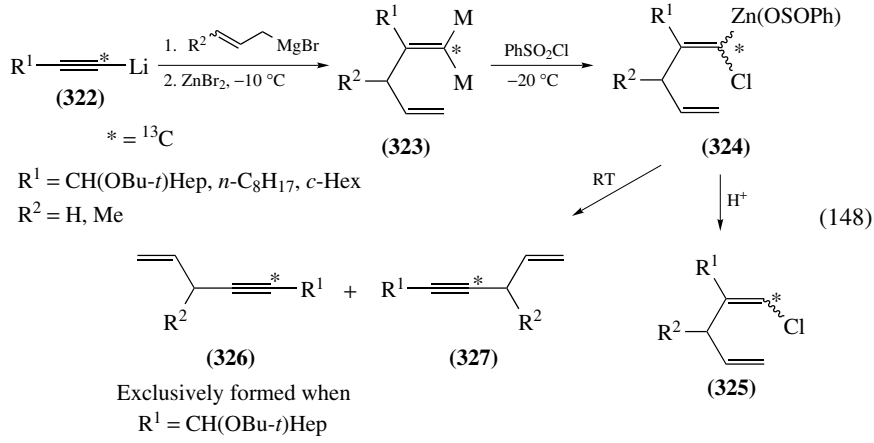

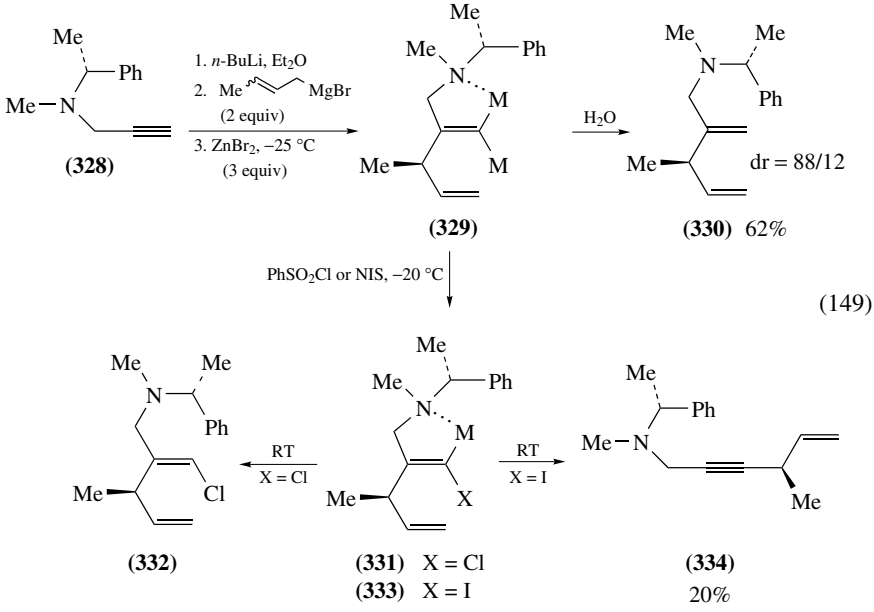

Nevertheless, chiral propargylic amines remain interesting substrates for achieving the diastereoselective addition of substituted allylic organozinc compounds to metallated alkynes. Besides crotylzincation, one example of diastereoselective addition of zincated allyl ethyl ether to **328** has also been reported[183].

Allylic organozinc reagents display a unique reactivity towards alkenyl-, allenyl- and alkynylmetals. Allenic organozinc reagents which are in metallotropic equilibrium with their propargylic counterparts (equation 150) also share some similarities with allylic organozinc reagents in their behavior towards alkenes and alkynes.

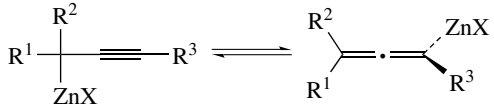

(150)

IV. REACTIVITY OF ALLENYLZINC REAGENTS

A. Intermolecular Carbozincations of Alkynes and Alkenes

Examples of intermolecular addition of allenylzinc reagents to carbon−carbon double and triple bonds appear to be restricted to the more reactive alkenyl and alkynyl organometallic species.

1. Addition to alkynylmetals

The organozinc reagent **335**, prepared from the propargylic bromide **336** by reaction with metallic zinc in THF, was able to add to a variety of terminal alkynes (but not disubstituted ones). As in the case of allylic organozinc reagents, metallation of the alkyne always occurred prior to addition and the reaction led to intermediate alkenyl 1,1-dimetallic species **337**. After hydrolysis, the 1,4-enynes **338** were obtained in moderate to good yields. Despite the allenyl−propargyl metallotropic equilibrium, only adducts possessing a propargyl moiety were formed with no trace of any isomeric allenic structure. The addition presumably involves a six-centered transition state (by analogy with the allylzincation of metallated alkynes or related zinc−ene reactions) wherein the allenic form of the organozinc reagent selectively reacts (equation 151)[184].

In general, monoaddition was observed when a terminal alkyne was directly treated with an excess of the allenylzinc reagent itself. However, starting from an alkynyl Grignard reagent predominantly led to bis-addition compounds (equation 152)[185].

For alkynes bearing a leaving group at the propargylic position, bis-addition also took place and subsequent 1,3-elimination afforded disubstituted cyclopropanes (equation 153)[176].

The organozinc prepared from propargyl bromide did not react with terminal alkynes because, under the reaction conditions, abstraction of the acidic terminal acetylenic hydrogen from the propargylic metallotropic form presumably occurred (equation 154)[185].

However, the organozinc **339** derived from trimethylsilyl propargyl bromide could be used as a substitute of allenylzinc bromide. This reagent underwent regioselective monoaddition to a variety of functionalized alkynes such as primary, secondary (but not tertiary) propargylic alcohols and ethers. Thus, addition of an excess of **339** to the secondary alcohol **340** provided the 1,4-enyne **341**, in which the trimethylsilyl group could be removed by treatment under alkaline conditions to afford **342** (equation 155). However, the presence of the trimethylsilyl group seemed to decrease the reactivity of **339** as no addition was observed to phenylacetylene or 1-octyne, even if such terminal alkynes were metallated with BuLi or EtMgBr prior to the reaction[186].

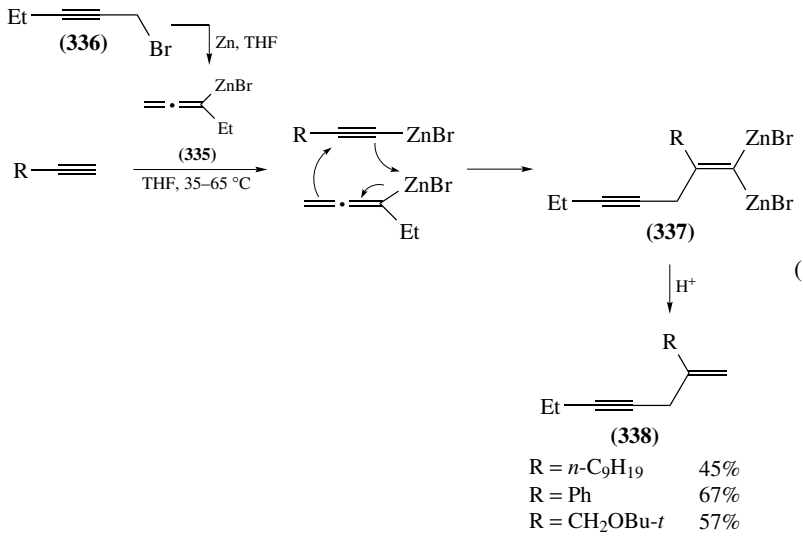

(151)

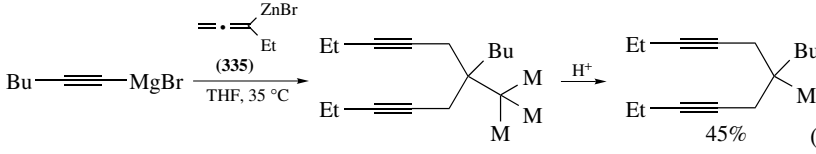

(152)

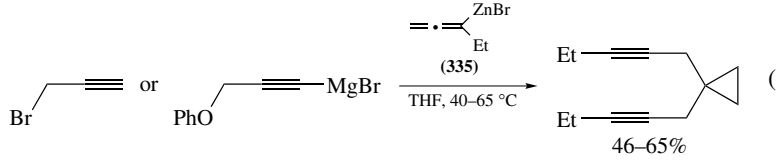

(153)

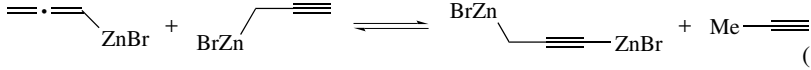

(154)

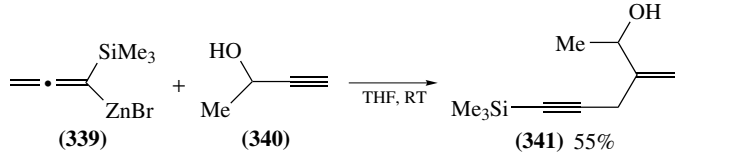

(155)

2. Addition to alkenylmetals

It was initially reported that an organozinc species generated from a propargylic bromide was not able to add to vinylmagnesium bromide in THF[184]. However, more recent investigations demonstrated that such reactions were indeed feasible in the less coordinating diethyl ether[154]. Thus, treatment of 1-trimethylsilyl-1-butyne (**343**) with *s*-BuLi in ether afforded the corresponding propargylmetal **344** in metallotropic equilibrium with its allenic counterpart **345**. In fact, protonation of the reaction mixture afforded a 60/40 mixture of **343** and the corresponding isomeric allenylsilane **346**. Interestingly, after transmetallation with $ZnBr_2$, the position of the metallotropic equilibrium seemed to be modified as

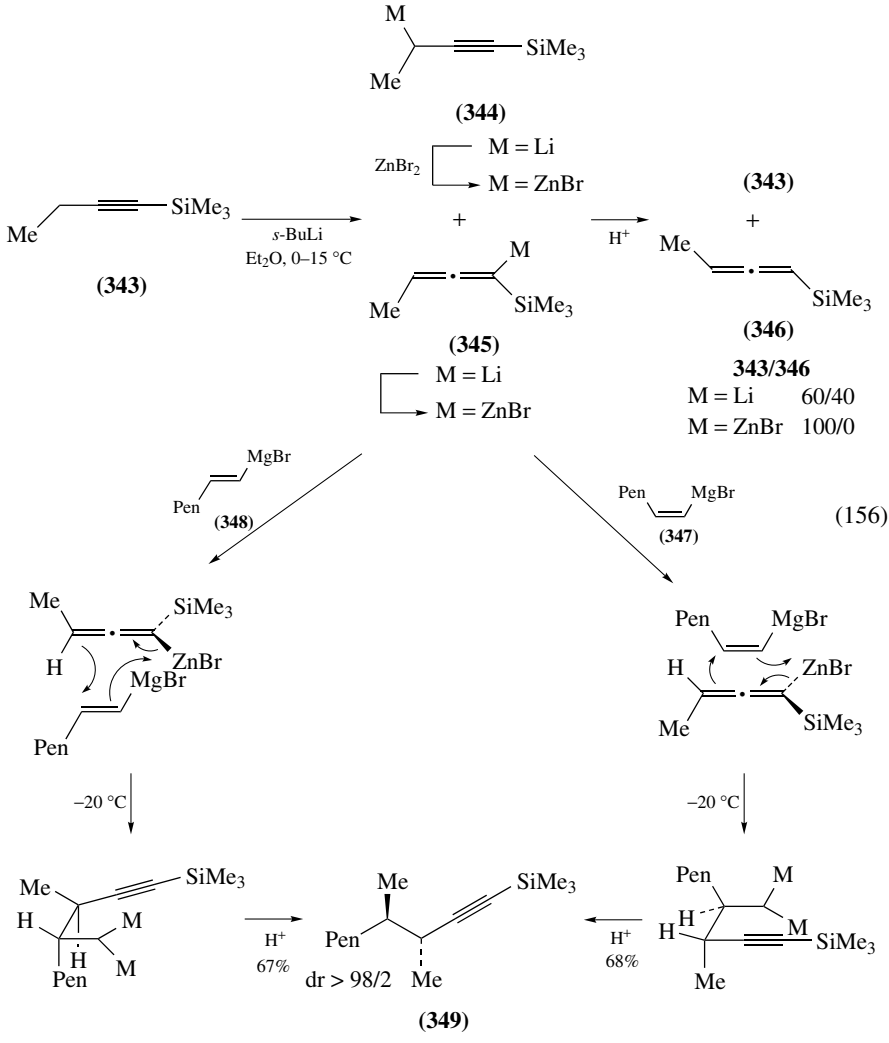

the alkyne **343** was exclusively recovered after protonation. This observation, as well as additional literature results[187], support an allenic structure **345** (M = ZnBr) for the organozinc species which underwent protonation with S_E2' regioselectivity. Addition of the allenylzinc **345** to the (*Z*)-alkenyl Grignard reagent **347**, or its (*E*) geometric isomer **348**, smoothly occurred in ether at −20 °C and, after hydrolysis of the intermediate dimetallic species, both reactions led to the same alkynylsilane **349** as a single diastereomer (equation 156)[154]. This result was explained by considering a cyclic transition state in which the allenylzinc reagent selected the face of attack of the alkenylmetal so as to avoid an unfavorable steric interaction between the pentyl substituent and the allenic methyl group. Consequently, the same diastereomer **349** possessing an *anti* relative configuration was obtained, whatever the olefinic configuration of the Grignard reagent.

Although no intermolecular additions of allenylzinc reagents to unactivated alkenes or alkynes have been apparently reported, the related intramolecular processes led to the development of synthetically useful routes towards five-membered rings.

B. Intramolecular Carbozincations of Alkynes and Alkenes

By analogy with allylic organometallic compounds (see Section III.C), the possibility of achieving intramolecular related zinc–ene reactions involving allenylzinc species acting as ene-components has been investigated. Such reactions benefit from favorable thermodynamics and were thus expected to proceed more readily than the related intermolecular additions of allenylzincs to alkynes or alkenes.

1. Intramolecular carbozincations of alkynes

Metallation of the symmetrical diyne **350** with *sec*-butyllithium in THF led to a propargyl-allenyllithium that was transmetallated to the corresponding allenylzinc **351**. Upon warming to room temperature, a smooth cyclization took place leading to the alkenylzinc species **352**. The latter resulted from a *syn* addition across the silylated alkyne and appeared to be configurationally stable under the reaction conditions. Subsequent electrophilic trapping with a proton, iodine or allyl bromide in the presence of CuCN or an alkenyl iodide in the presence of a catalytic amount of $Pd(PPh_3)_4$ afforded the corresponding functionalized five-membered ring products of type **353** (equation 157)[188]. In the case of substrate **354**, metallation occurred regioselectively at the propargylic position of the alkynylsilane moiety. However, after transmetallation with $ZnBr_2$, the resulting allenylzinc **351** (R = Et) did not cyclize to the α,β-disubstituted unactivated triple bond. This result highlights the greater reactivity of alkynylsilanes as enophiles in zinc–ene reactions (see Section III.C).

The behavior of propargylic ethers of type **355** was also investigated[188]. Metallation of the diyne **355a** with *s*-BuLi could be carried out in THF at −80 °C and selectively took place at the propargylic ether position. After addition of $ZnBr_2$, the resulting allenylzinc **356a** cyclized to the alkynylsilane moiety to afford after hydrolysis the corresponding five-membered ring product **358a**, as a single stereoisomer. By contrast, in the case of substrate **355b** possessing a bulky thexyldimethylsilyl ether (TDMS), kinetic deprotonation with *s*-BuLi in THF at −45 °C preferentially occurred at the less congested propargylic site, although not exclusively. After transmetallation with $ZnBr_2$, the two allenylzinc species **356b** and **357b** were generated and both cyclized to the alkynylsilane moiety to afford, after hydrolysis, a 14/86 mixture of the two five-membered rings **358b** and **359b** as single diastereomers. The high diastereoselectivity observed in the cyclization of **357b**, which

induced the formation of two stereocenters in the final product **359**, was particularly noteworthy (equation 158).

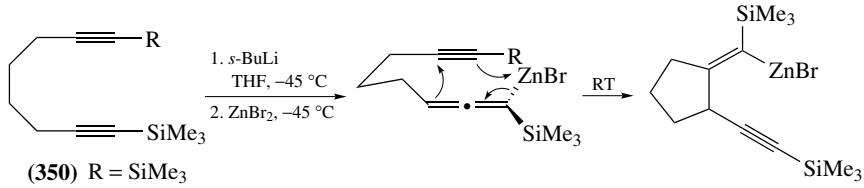

(350) R = $SiMe_3$
(354) R = Et

(351) **(352)**

E^+ (157)

E^+	E	Yield
H^+	H	85%
I_2	I	78%
AllBr, CuCN	All	67%
EtCH=CHI cat. $Pd(PPh_3)_4$	CH=CHEt	65%

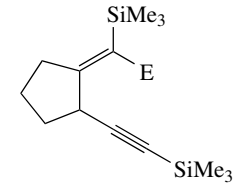

(353)

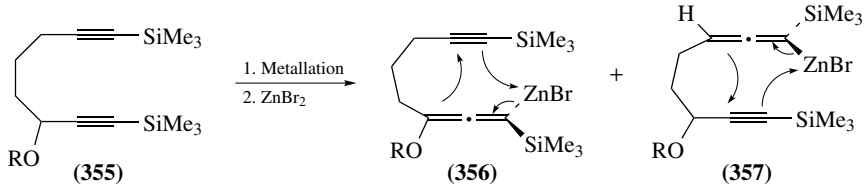

(355) **(356)** **(357)**

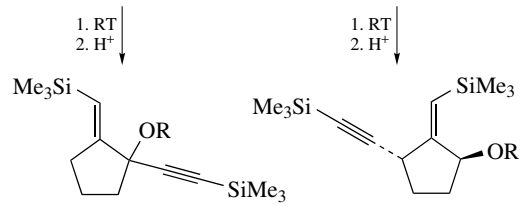

(358) **(359)**

	R	Metallation	**358/359**	Yield
(a)	Me	*s*-BuLi, THF, –80 °C	100/0	89%
(b)	TDMS	*s*-BuLi, THF, –45 °C	14/86	61%

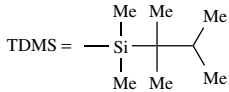

(158)

Although the cyclization of allenylzincs to alkynylsilanes proceeded quite efficiently, it was demonstrated that a metallated alkyne was an even much higher reactive enophilic partner. Treatment of the diyne **360** with *s*-BuLi in ether at room temperature resulted in

double deprotonation, first of the terminal alkyne and then at the less congested propargylic position. Subsequent addition of $ZnBr_2$ at room temperature resulted in an immediate cyclization of the allenylzinc **361** to the metallated triple bond, which occurred with virtually no diastereoselection. However, it was observed that this reaction could proceed as low as $-50\,^{\circ}C$ and with high diastereoselectivity. Deuteriolysis led to the five-membered ring **362** and confirmed that the cyclization had generated an alkenyl 1,1-dimetallic species (equation 159)[189].

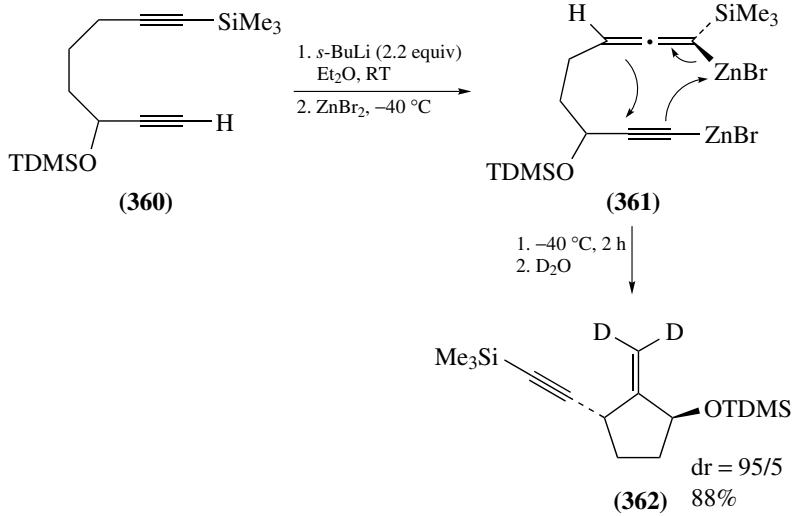

(360) **(361)** **(362)** (159)

2. Intramolecular carbozincations of alkenes

Intramolecular zinc–ene reactions involving allenylzinc reagents as ene components and alkenes as enophiles have been investigated. Interestingly, a thermal ene-reaction in which an allene played the role of the ene-component was postulated to interpret the formation of the five-membered ring product **363** in the flash pyrolysis of 1,2,7-octatriene (**364**) (equation 160)[190]. Although another related example was also disclosed[191], this thermal ene–allene reaction has received no subsequent attention in organic synthesis.

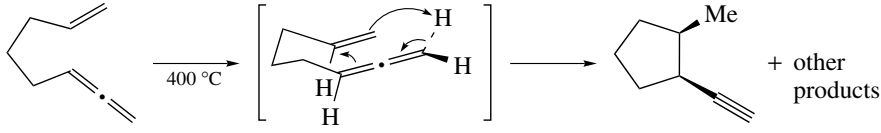

(364) **(363)** 53% (160)

When the 1,7-enyne **365** was metallated with *s*-BuLi in THF at $-45\,^{\circ}C$, the resulting propargyl-allenyl lithium failed to cyclize to the double bond upon warming to room temperature. The same result was observed after transmetallation with $MgBr_2$. However, transmetallation with $ZnBr_2$ led to the allenylzinc **366** that subsequently underwent a smooth cyclization to the double bond at room temperature. This process was ascribed to

a zinc–ene reaction in which the allenylzinc behaved as the ene-component and was subsequently referred to as the 'zinc–ene–allene' reaction. The latter occurred under mild conditions compared to the thermal ene process but with similar *cis*-1,2 -diastereoselectivity, as a consequence of a six-centered transition state. The cyclic organozinc species **367** reacted with several electrophiles (H^+, I_2) and could be involved in a copper-promoted allylation and a palladium-catalyzed cross-coupling with vinyl iodide, leading to the functionalized five-membered ring products **368**–**371** as single diastereomers (equation 161)[192].

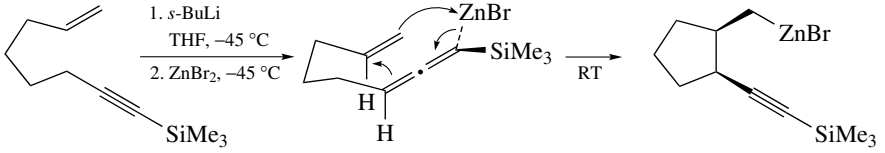

(365) **(366)** **(367)**

E^+	E		Yield
H^+	H	**(368)**	80%
I_2	I	**(369)**	75%
AllBr, CuCN	All	**(370)**	72%
$H_2C{=}CHI$ cat. $Pd(PPh_3)_4$	$CH{=}CH_2$	**(371)**	63%

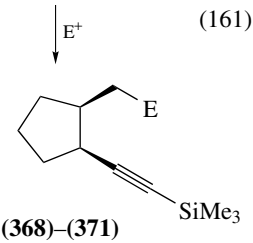

(368)–(371) (161)

The same zinc–ene–allene reaction was investigated for a variety of 1,7-enynes of type **372** bearing substituents at different positions. In all cases, the products obtained after metallation with an organolithium, transmetallation with $ZnBr_2$, cyclization at room temperature and quenching with an electrophile were obtained in good yields and as single diastereomers. The observed diastereoselectivities were consistent with a zinc–ene–allene cyclic transition state leading to an invariable *cis* stereochemical relationship between the trimethylsilylethynyl and the methylzinc groups, whereas substituents on the chain (R^2) would preferentially occupy a pseudo-equatorial position. The cyclization proceeded at a slightly lower rate for an enyne bearing an α,α-disubstituted double bond ($R^3 = Me$) (equation 162)[192, 193]. However, no cyclization could be achieved for enynes bearing an unactivated α,β-disubstituted double bond.

An alternative strategy for the generation of propargyl-allenyl lithium reagents involves the carbolithiation of conjugated enynes[15]. In particular, the presence of a trimethylsilyl substituent on the triple bond was found to facilitate the addition of organolithium reagents to such substrates[194, 195]. Thus, addition of *n*-BuLi or *t*-BuLi to the conjugated trimethylsilyl-substituted enyne **373** took place in THF at $-20\,^{\circ}C$ and transmetallation with $ZnBr_2$ allowed the subsequent cyclization of the allenylzinc **374** to proceed at room temperature. The resulting organozinc reagents were subjected to iodinolysis and afforded the five-membered rings **375**, bearing a quaternary carbon, as single diastereomers. Their relative configuration was in agreement with the zinc–ene–allene transition state (equation 163)[195, 7].

The same sequence proceeded equally well starting from the conjugated enyne **376** bearing an α,β-disubstituted double bond. After hydrolysis, the five-membered ring products **377** bearing three stereocenters were obtained as single diastereomers. The stereochemical outcome was likely a consequence of the preferential pseudo-equatorial positioning of the R group in the cyclic zinc–ene–allene transition state (equation 164).

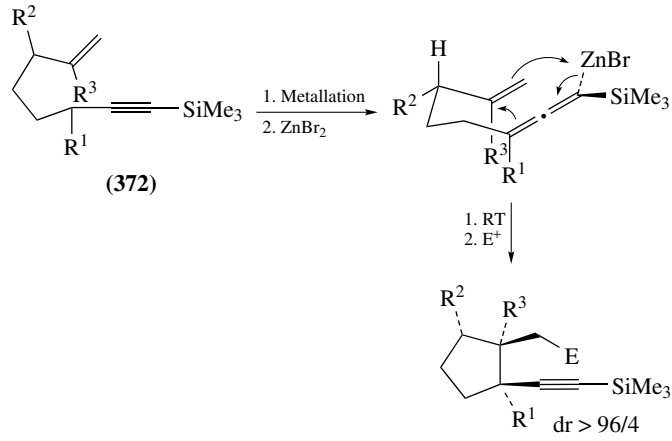

(372)

(162)

	R^1	R^2	R^3	Metallation conditions	E^+	E	Yield
(a)	OMe	H	H	*s*-BuLi, THF, −80 °C	H^+	H	81%
(b)	OMEM	H	H	*n*-BuLi, THF, −10 °C	H^+	H	80%
(c)	OTDMS	H	H	*n*-BuLi, THF, −10 °C	H^+	H	80%
(d)	H	Me	H	*s*-BuLi, THF, −80 °C	I_2	I	88%
(e)	H	H	Me	*s*-BuLi, THF, −80 °C	I_2	I	78%

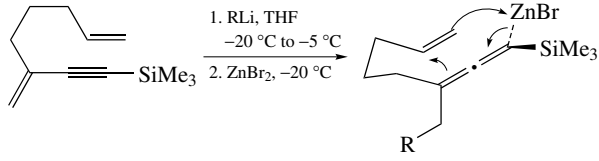

(373) (374)

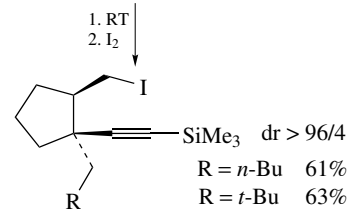

(375)

(163)

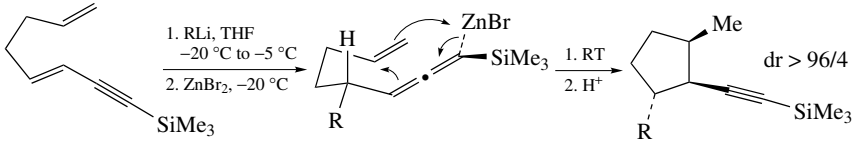

(376)

(377) R = *n*-Bu 69%
R = *t*-Bu 62%

(164)

The synthetic interest of the zinc–ene–allene cyclization was highlighted by its application to the elaboration of the frameworks of linear and angular triquinanes, in conjunction with the cyclization of 1,6-enynes induced by zirconocene complexes[196]. Thus, a first zinc–ene–allene reaction applied to enyne **372e**, followed by palladium-catalyzed cross-coupling with vinyl iodide, afforded the 1,6-enyne **378**. The latter, upon treatment with Cp_2Zr(1-butene) complex (generated by treatment of Cp_2ZrCl_2 with two equivalents of *n*-BuLi[197]), led to a zirconatricycle which underwent carbonylation with CO. The tricyclic enone **379** was obtained as a single diastereomer (equation 165)[196].

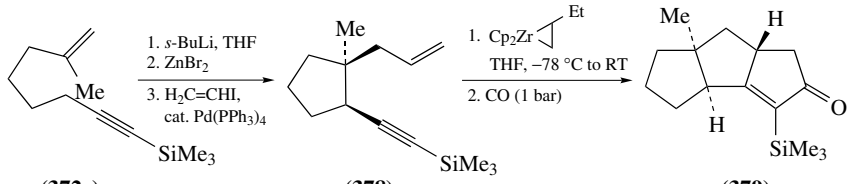

(372e) **(378)** 65% **(379)** 61% (165)

The synthesis of a prototype angular triquinane was achieved from the 1,7-enyne **370**, already prepared by a first zinc–ene–allene reaction applied to enyne **365** (see equation 161). Metallation of **370** at the propargylic position could be carried out with *s*-BuLi in THF at 0 °C and subsequent transmetallation with $ZnBr_2$ triggered the zinc–ene–allene cyclization which provided, after cross-coupling with vinyl iodide, the bicyclic 1,6-enyne **380** as a single diastereomer. Treatment of **380** with Cp_2Zr(1-butene) complex afforded a zirconatetracycle which was protonated and led to **381** (mixture of diastereomers). Subsequent treatment with *p*-toluenesulfonic acid in acetonitrile induced the desilylation of the alkenylsilane and concomitant migration of the double bond in the tetrasubstituted position to afford **382** (equation 166)[196].

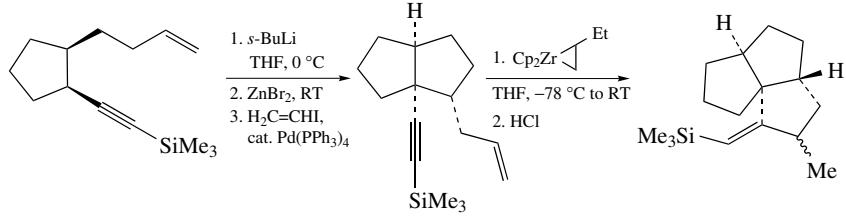

(370) **(380)** 68% **(381)** 61%

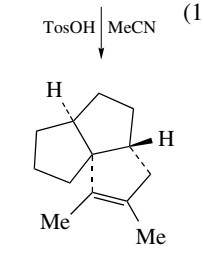

(382) 100% (166)

The zinc–ene–allene reaction has also been applied to the synthesis of heterocycles[198]. Metallation of the propargylic ether **383** with *s*-BuLi in ether at −70 °C and transmetallation with $ZnBr_2$ resulted in an extremely rapid intramolecular zinc–ene–allene reaction occurring as low as −40 °C. The resulting organozinc **384** was then reacted with iodine or allylated with methallyl bromide to afford the tetrahydrofurans **385** and **386** respectively as single diastereomers. The high rate observed for the cyclization of **383** was attributed to the *gem*-dialkyl effect exerted by the cyclohexyl group. Compound **386**, incorporating a 1,7-enyne unit, was subjected to another zinc–ene–allene cyclization and afforded the tricyclic product **387**, possessing two adjacent quaternary centers, as a single diastereomer. A *cis* stereochemical relationship was invariably observed between the CH_2ZnBr and the trimethylsilyl ethynyl groups in the oxygen heterocycles resulting from the zinc–ene–allene cyclizations (equation 167)[198, 199].

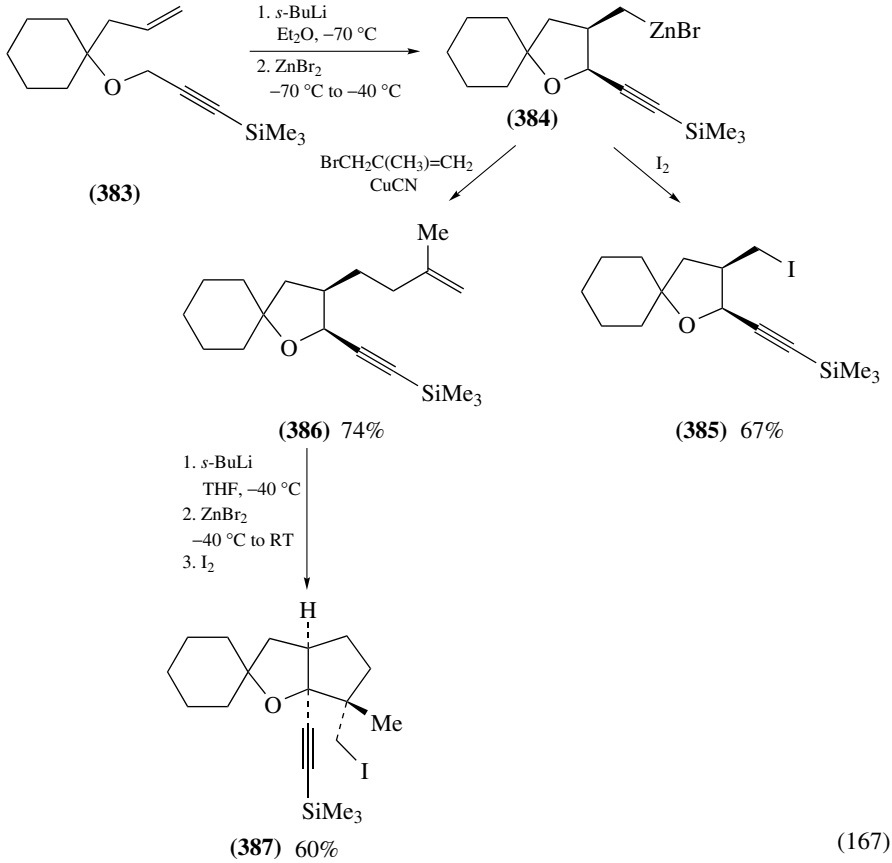

(167)

Ether was a better solvent in cases where the propargylic position was unsubstituted (methylene group) since, in THF, a competitive [1,2]-Wittig rearrangement took place and led to diminished yields. When applied to the secondary homoallylic propargyl ethers **388**, the zinc–ene–allene cyclization afforded the *cis*-2,3,5-trisubstituted tetrahydrofurans **389** with moderate to satisfactory levels of diastereoselectivity, which could be rationalized by the preferential pseudo-equatorial positioning of the homoallylic substituent in the cyclic

transition state. The minor diastereomeric tetrahydrofuran was indeed the epimer at C5 (equation 168).

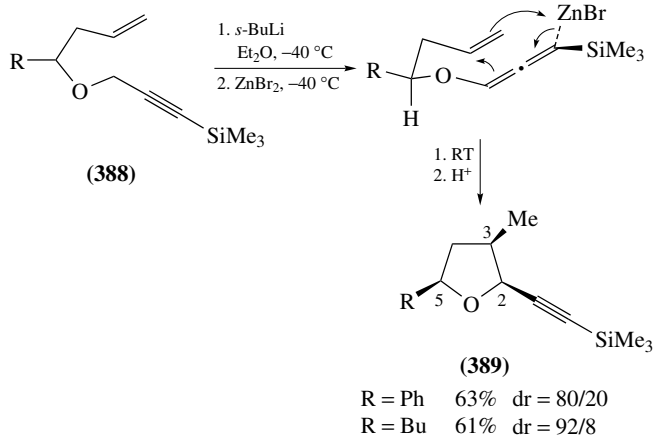

(168)

An extension of this strategy to the preparation of pyrrolidines has been reported[199,200]. The tertiary amine **390** could be metallated with *t*-BuLi in ether and, after transmetallation with $ZnBr_2$, the zinc–ene–allene took place leading, after hydrolysis or iodinolysis, to the disubstituted pyrrolidines of type **391** as single diastereomers (equation 169).

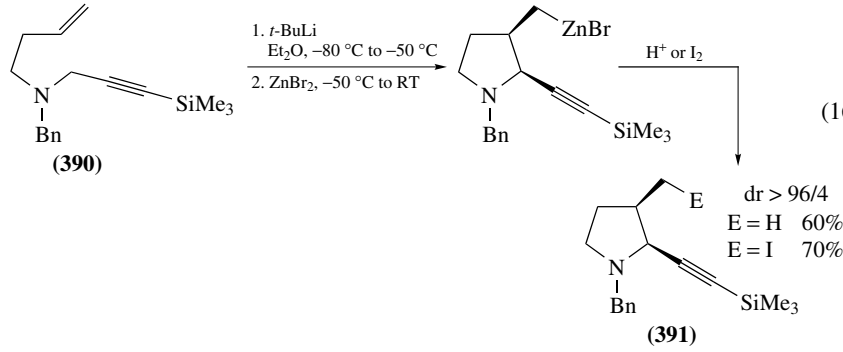

(169)

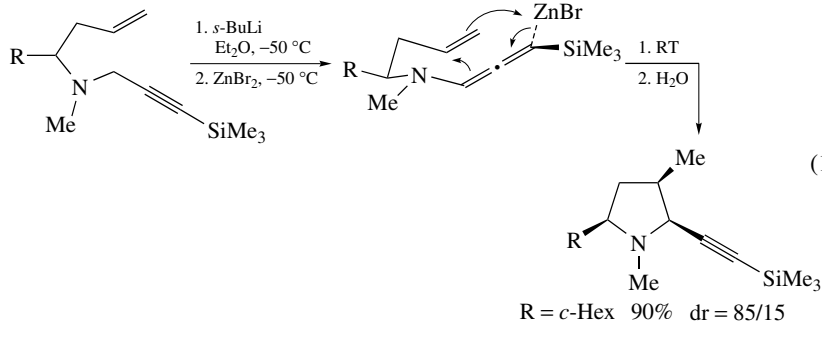

(170)

By analogy with the synthesis of oxygen heterocycles, the zinc–ene–allene cyclization was applied to the synthesis of 2,3,5-trisubstituted pyrrolidines with moderate diastereoselectivity (equation 170)[199,200].

However, an even more efficient access to functionalized pyrrolidines was developed relying on a zinc enolate cyclization (see Section V.B).

Zinc enolates or aza-enolates constitute a particular class of organozinc reagents that also display a unique reactivity in carbometallation reactions.

V. REACTIVITY OF ZINC ENOLATES AND AZA-ENOLATES

Despite the extensive investigation of the carbometallation of alkenes and alkynes[1–9], the addition of stabilized enolate-type organometallic species to unactivated carbon–carbon double or triple bonds has been the subject of only few reports[201–212]. The reason may be that the conversion of a stabilized enolate-type anion into an unstabilized sp^3 or sp^2 carbanion would suffer from unfavorable thermodynamics. Nevertheless, there are reports dealing with additions of enolates to unsaturated carbon–carbon bonds carried out with the assistance of a transition metal catalyst such as gold[213–215], cobalt[216,217], copper[218–220], iron[221–225], mercury[226], molybdenum[227–230] or palladium[231–241]. Other examples involve Lewis acids such as $TiCl_4$[242], $SnCl_4$[243–245], $GaCl_3$[246,247], $AlCl_3$[248] or $In(OTf)_3$[249]. Among the different metal enolates, the zinc derivatives have emerged as a promising alternative, allowing inter- and intramolecular carbometallation reactions to proceed with unactivated alkenes or alkynes and offering the opportunity to functionalize the resulting organozinc species with a wide range of electrophiles.

A. Addition of Zinc Enolates to Alkynes

One of the first examples of addition of a zinc enolate to an alkyne was a report dealing with the zinc or cadmium stearate-catalyzed addition of substituted malonates to acetylene under pressure[250]. Later, Schultze described the intermolecular nucleophilic addition of the zinc enolate derived from diethyl bromomalonate to phenylacetylene in refluxing xylene leading to the alkylidene malonate **392** (equation 171)[251].

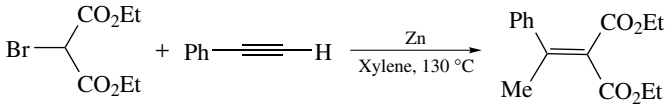

(171)

(392) 52%

Inspired by these results, Miginiac and coworkers explored the addition of preformed organozinc enolates[252] to a variety of alkynes[253]. Thus, the organozinc reagent prepared from diethyl methylbromomalonate reacted with functionalized propargylic[254] and homopropargylic alcohols, ethers and amines[255] under mild conditions and afforded the corresponding carbometallation products in moderate yields. The reaction was generally regioselective and afforded the branched isomer of type **393**, as usually observed in other carbozincations of monosubstituted alkynes[82]. In the case of propargyl and homopropargyl alcohols as substrates, the adducts of type **393** evolved to the corresponding lactones (while secondary amines provided lactams). However, when the steric hindrance became more important at the propargylic position, as in the case of propargylic ethers or substituted amines, the formation of an increased amount of the linear regioisomer **394** was observed. The (*Z*)-configuration of the latter suggested an *anti* addition mechanism

(equation 172). By contrast, no carbometallation reaction was observed in the case of disubstituted acetylenic compounds.

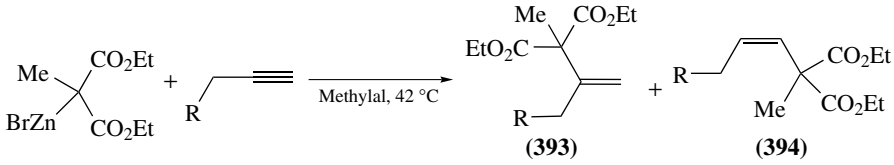

R	R′	Time	Yield	**393/394**
OH	H	4 h	42%	100*/0
OBu	H	23 h	59%	67/33
NEt_2	H	23 h	50%	48/52
CH_2OH	H	4 h	38%	100*/0
CH_2OEt	H	23 h	56%	100/0
CH_2NEt_2	H	23 h	40%	100/0

*Obtained as the corresponding lactone

(172)

Recently, Nakamura and coworkers described a related reaction of the zinc enolates derived from β-aminocrotonamides of type **395**[256]. In the presence of a stoichiometric amount of Et_2Zn, the latter underwent smooth addition to terminal alkynes upon heating in hexane and afforded the corresponding tetrasubstituted 2-alkylidene acetoacetamides **396** (after acidic hydrolysis of the imine) with high (*Z*)-stereoselectivity (equation 173).

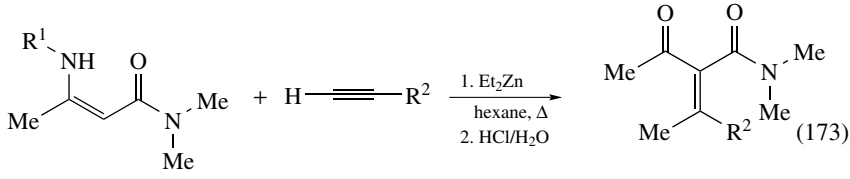

(395) 5 equiv (396)

R^1 = All, Bu, 2-methoxyethyl R^2 = Aryl, Alkyl

92–98%

(*Z*)/(*E*) = 95/5

(173)

A mechanism for this reaction was tentatively proposed by the authors based on deuterium labeling experiments. The carbometallation reaction could also be performed, albeit with decreased stereoselectivity ((*E*)/(*Z*) = 1/1), using the combination of a stoichiometric amount of $Zn(OTf)_2$ or $In(OTf)_3$ and triethylamine, but no addition was observed for the lithium or magnesium enolates derived from **395**.

An intramolecular version of this reaction was reported by Taguchi and coworkers, who demonstrated that treatment of the pent-4-ynyl substituted malonate **397** with $ZnCl_2$ and Et_3N in CH_2Cl_2 gave the five-membered ring product **398** in high yield (equation 174)[242]. However, the authors could not demonstrate the formation of an alkenylzinc intermediate **399** by quenching with an electrophile such as iodine, thereby suggesting that the latter was rapidly protonated *in situ* by Et_3N•HCl to afford **398**. By contrast, treatment of **397** with $TiCl_4$ and Et_3N resulted in an intramolecular carbotitanation of the triple bond involving the *syn* addition of a trichlorotitanium enolate. In this case, the resulting alkenyltitanium

intermediate could be further functionalized by reaction with various electrophiles, despite the presence of $Et_3N{\bullet}HCl$[242].

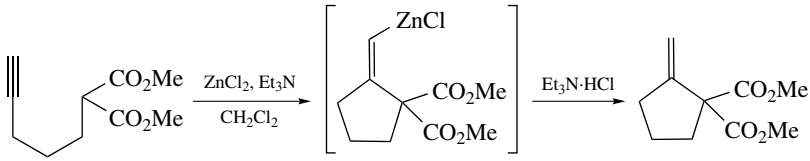

(397) **(399)** **(398)** 88% (174)

More recently, a zinc-catalyzed tandem 1,4-addition/carbocyclization, involving propargyl alcohol and 2-alkylidene-1,3-dicarbonyl compounds of type **400** as partners, was reported[257]. These compounds were stirred in the presence of $Zn(OTf)_2$ and Et_3N and afforded the 3-methylene tetrahydrofurans **401** in excellent yields (equation 175)[258].

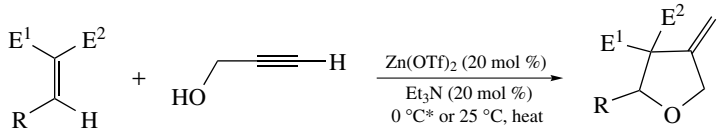

(400) 5 equiv **(401)** 70–94% (175)

E^1, E^2 = CO_2Me, COMe * Reaction performed at 0 °C when $E^1 = E^2 = CO_2Me$
R = substituted aryl, alkyl

The use of $Zn(OTf)_2$ was essential for the success of the reaction as other zinc salts ($ZnCl_2$, $ZnBr_2$, ZnI_2) or Et_2Zn resulted in low yields or no reaction. The authors postulated a mechanism involving the initial formation of the zinc alkoxide **402** and its conjugate addition to the Michael acceptor **400**. The resulting zinc enolate intermediate **403** should in turn promote the intramolecular carbometallation of the triple bond and deliver an alkenylzinc intermediate **404**, which is then protonated by the *in situ* generated triethylammonium salt to afford the final product **401** (equation 176).

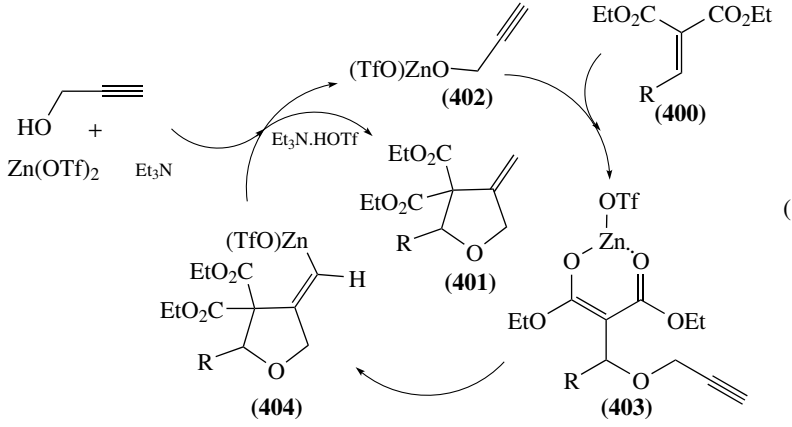

(176)

B. Addition of Zinc Enolates to Alkenes

1. Intramolecular reactions

Alkenes are less reactive than alkynes with respect to the addition of an enolate, because the generation of an alkylmetal rather than an alkenylmetal at the expense of a stabilized nucleophile is much less favorable. However, several recent publications have revealed remarkable new possibilities in the chemistry of zinc enolates. Indeed, Marek and Normant[200] as well as Karoyan and coworkers[259] developed the intramolecular carbometallation of unactivated olefins of α-amino zinc enolates as an efficient and stereoselective route towards substituted pyrrolidines. As a representative example, the enolization of the α-amino ester **405** was performed with LDA in Et_2O at $-40\,^{\circ}C$. The resulting lithium enolate failed to cyclize to the double bond upon warming to room temperature, but transmetallation to the corresponding α-amino zinc enolate by addition of $ZnBr_2$ resulted in a highly regioselective 5-exo-Trig cyclization, which generated the alkylzinc bromide **406**. The latter could then react with several electrophiles and afford the corresponding *cis*-2,3-disubstituted pyrrolidines **407** as single diastereomers (equation 177). The relative configuration of the two newly formed stereogenic centers was attributed to a chair-like transition state wherein the double bond of the (*Z*)-α-amino zinc enolate is eclipsing the terminal olefinic residue[260]. The (*Z*)-configuration of the enolate is imposed by an intramolecular Zn-N chelation, which has been observed both in solution or in the solid state for analogous α-aminoester zinc enolates[261–263]. Chemla, Normant and coworkers also proposed an alternative transition state wherein the C-metallated enolate was considered as the reacting species[264].

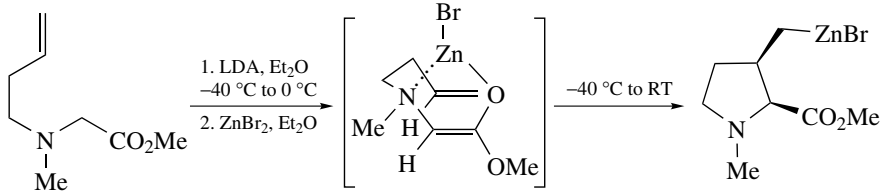

(405) **(406)**

E^+	E	Yield
H^+	H	70%
I_2/THF	I	64%
AllBr/CuCN	All	55%

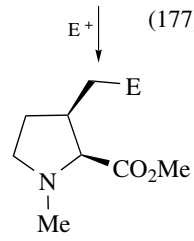

(407) (177)

This new methodology was successfully applied to the diastereoselective synthesis of polysubstituted pyrrolidines[260]. Moreover, the introduction of a chiral appendage on the nitrogen atom led to the development of an enantioselective version[200, 259, 260]. Thus, the optically pure α-aminoester **408** derived from (*S*)-α-methylbenzylamine was subjected to the one-pot metallation–transmetallation–cyclization procedure described above and, after hydrolysis of the intermediate organozinc **409**, the pyrrolidine **410** was obtained in excellent yield and with high stereochemical induction (dr = 98/2). Its configuration could

be assigned after conversion to the known (2*S*,3*R*)-β-methylproline **(411)** (ee = 96%)[259] (equation 178).

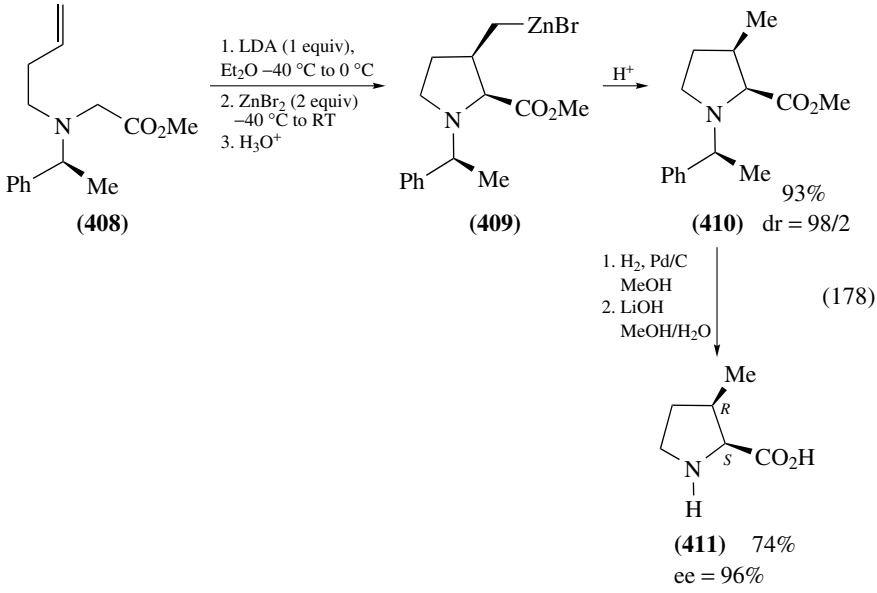

(408) **(409)** **(410)** dr = 98/2

(411) 74%
ee = 96%

(178)

The choice of α-methylbenzylamine[265,266] as a chiral auxiliary was found to be crucial. When performing the same sequence with the α-aminoester derived from (*R*)-1-(cyclohexyl)ethylamine, a dramatic drop of the stereochemical induction was observed (dr = 59/41). Moreover, the use of two equivalents of $ZnBr_2$ in the transmetallation step was also mandatory to reach an excellent level of diastereoselectivity. A single equivalent of zinc salt led to a 75/25 mixture of the two *cis* diastereomers of **410**. In view of these results, a π-chelation between the aromatic ring and the amino zinc enolate in the transition state was postulated[200,260]. The second equivalent of $ZnBr_2$ would probably act as a coordinating relay between the phenyl group and the zinc enolate, leading to a conformationally locked chelated structure. In this hypothetical transition state the chiral inductor should adopt a position and a conformation around the C−N bond leading to minimization of the eclipsing strain with the two hydrogens at the α-position of the nitrogen atom (Figure 1).

The zinc–enolate carbocyclization reaction was applied to the synthesis of diverse 3-substituted proline chimeras. To this end, the stable cyclic organozinc intermediate

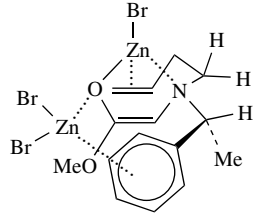

FIGURE 1

409 was functionalized with various electrophiles such as TosCN[267], $H_2C{=}CHNO_2$[268] or $MeSSO_2Me$[269] after transmetallation to an organocopper reagent[270] and provided advanced intermediates **412**–**414** towards the synthesis of enantiomerically pure 3-prolino glutamic acid, arginine and methionine respectively. Additionally, a cross-coupling reaction with iodobenzene catalyzed by Pd_2dba_3/P(Tol-*o*)$_3$ led to **415**, a precursor of 3-prolino phenylalanine[271] (equation 179).

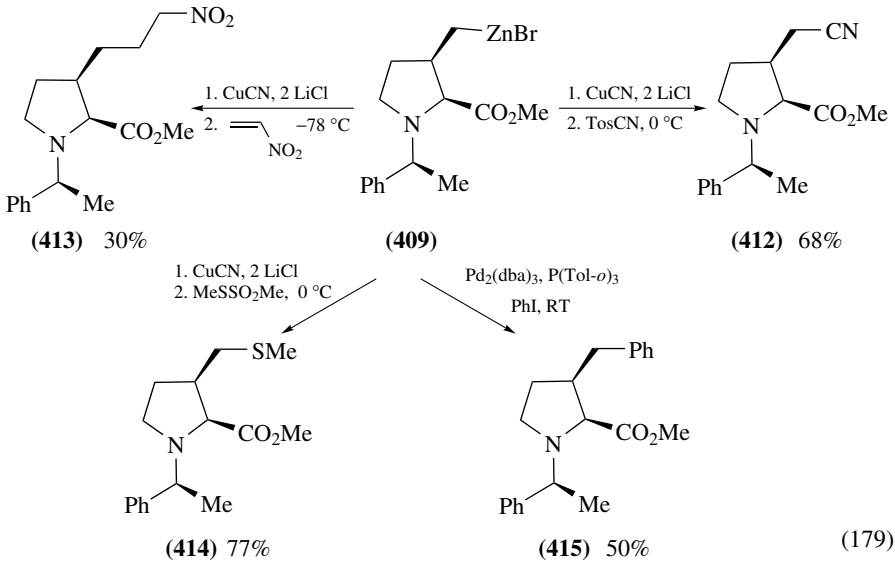

(179)

One limitation of this zinc–enolate cyclization is its restriction to unsubstituted terminal double bonds, as for the related carbozincation of alkenes by primary alkylzincs (see Section II.B), allylzincs (Section III.C) and allenylzincs (Section IV.B). Indeed, the conversion of a stabilized enolate to a secondary or tertiary unstabilized sp^3 carbanion was expected to be strongly endothermic. However, a recent report has demonstrated that alkylidene cyclopropanes could be used successfully, presumably due to the release in angle strain of the cyclopropylidene unit upon cyclization[272]. Thus, the α-aminoester **416** underwent a smooth zinc–enolate carbocyclization but, in sharp contrast with the preceding examples, the cyclization afforded the *trans*-2,3-disubstituted proline derivative **417** as a single diastereomer (equation 180). The unexpected *trans* relative configuration was explained by a product-like transition state involving a perpendicular approach of the enolate moiety and the cyclopropylidene unit. The chiral inductor adopts a position in which the methyl group led to a lower steric hindrance with the hydrogens at the α-position.

The zinc–enolate cyclization of α-aminoesters was also extended to the synthesis of polysubstituted piperidines[273]. When the α-aminoester **418** was metallated with LDA in Et_2O and transmetallated with $ZnBr_2$, a slow carbocyclization reaction took place and led to the corresponding cyclized organozinc bromide **419**, which could subsequently react with electrophiles to deliver the *cis*-β-methylpipecolic acid derivatives **420** in good yields and as single diastereomers (equation 181). The *cis* relative configuration of the pipecolic acid derivatives **420** was explained by the (*Z*)-configuration of the zinc enolate derived from the α-aminoester **418** and a chair-like transition state in which the electrophilic double bond occupies a pseudo-axial position allowing zinc coordination. The zinc–enolate

carbocyclization appears to be a promising route for the synthesis of six-membered ring nitrogen heterocycles. This result is quite noteworthy in light of the difficulties normally associated with the 6-exo-Trig cyclizations of 6-heptenyl metals to the corresponding cyclohexylmethyl metals[274], which proceed at a considerably slower rate compared to the analogous 5-exo-Trig cyclizations.

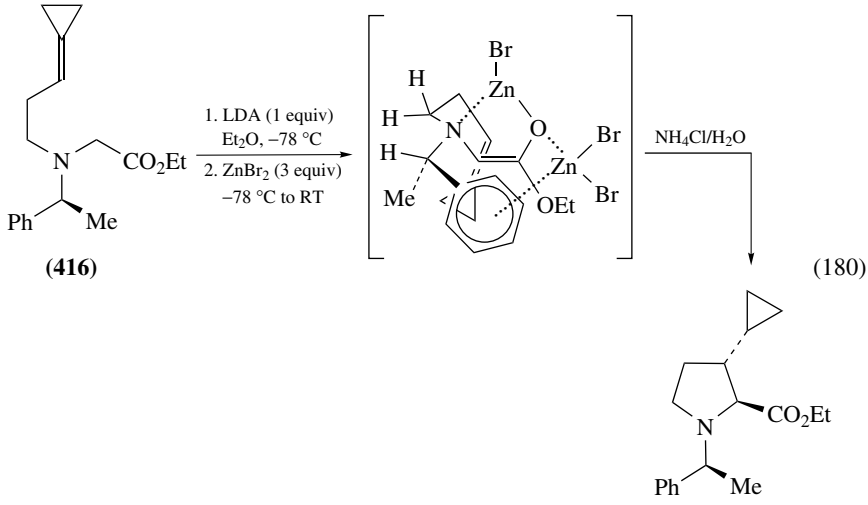

(180)

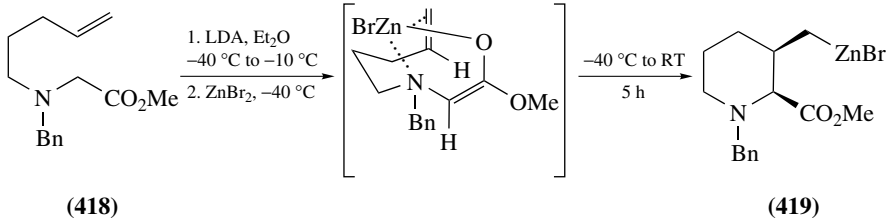

(181)

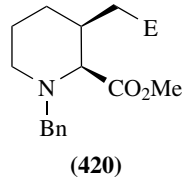

E^+	E	Yield
H^+	H	66%
I_2/THF	I	81%
AllBr/CuCN	All	65%

It is also worth mentioning that such cyclizations could be achieved for α-aminoesters bearing the amino group located outside of the chain. Indeed, Chemla and coworkers recently reported that the α-aminoester **421** successfully underwent a zinc–enolate cyclization, according to the standard conditions, and afforded after hydrolysis the five-membered ring tertiary amine **422** as a 80/20 mixture of diastereomers (equation 182)[264].

The *cis* relative configuration of the major diastereomer was explained by a transition state involving a chelated C-metallated enolate.

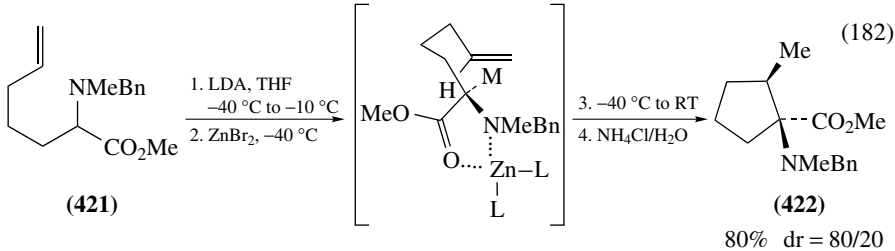

(182)

(421) **(422)**

80% dr = 80/20

The zinc–enolate cyclizations are not restricted to α-aminoesters as β-aminoesters have also been successfully involved in such reactions[275]. The preformed lithium enolate generated by treatment of the β-aminoester **423** with LDA had to be added dropwise to an ethereal solution of $ZnBr_2$ in order to avoid a competing β-elimination reaction induced by the zinc enolate. If this 'reverse addition' protocol was respected, a smooth carbocyclization reaction occurred and provided, after hydrolysis, the substituted 3-carbomethoxypyrrolidine **424** as a 87/13 mixture of diastereomers (equation 183).

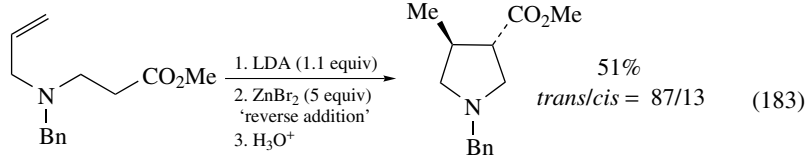

(183)

(423) **(424)**

When an additional substituent was present at the α-position of the ester moiety, the 'reverse addition' was no longer necessary in order to avoid the β-elimination as a side reaction since the corresponding zinc enolate displayed a substantially higher reactivity towards the double bond. Thus, addition of $ZnBr_2$ to the lithium enolate derived from the α-methyl-β-aminoester **425** in ether triggered a smooth carbocyclization reaction and subsequent deuteriolysis of the resulting cyclized organozinc species provided the pyrrolidine **426** bearing a quaternary center at position 3 and as a single *trans* diastereomer (equation 184). The authors explained the observed diastereoselectivity by a C-centered zinc enolate intermediate analogous to a C-metallated Reformatsky reagent[276–279]. In this transition state, the carbomethoxy group should occupy a pseudo-axial position on the basis of steric hindrance and of a possible chelation with an external zinc species which could be indeed coordinated by the nitrogen lone pair and the oxygen of the carbomethoxy group[264, 280].

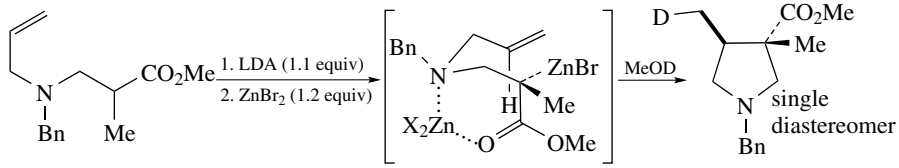

(184)

(425) **(426)** 70%

Chemla, Normant and coworkers also reported a one-pot 1,4-addition/carbocyclization domino sequence as a new access to 3-carbomethoxypyrrolidines. Conjugate addition of the mixed organocopper–zinc reagent *n*-BuCu(CN)ZnBr•LiBr to the Michael acceptor **427** in ether at room temperature directly led after hydrolysis to the 3-carbomethoxypyrrolidine **428** as a 84/16 diastereomeric mixture, the *trans* disubstituted isomer being predominant (equation 185). A similar explanation as described above was proposed for the stereochemical outcome[264].

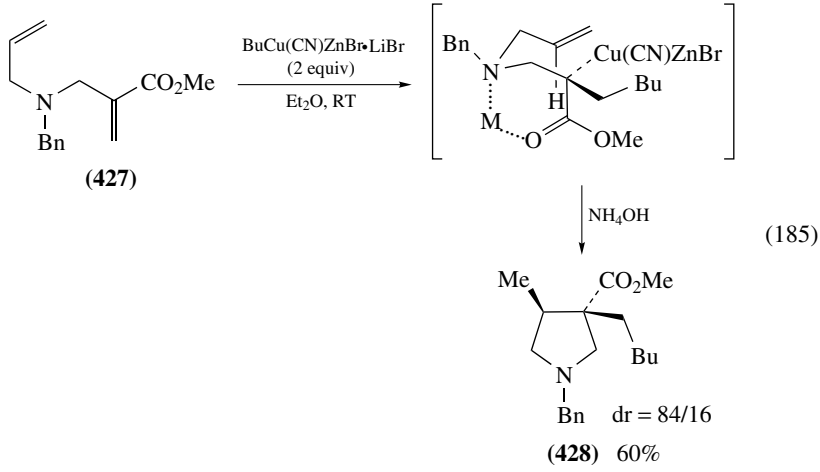

(185)

The feasibility of intramolecular carbometallation of double bonds is not restricted to the zinc enolates derived from α- and β-aminoesters. Nakamura and coworkers demonstrated that zincated hydrazones also exhibit a high reactivity[281]. Thus, the olefinic *N*,*N*-dimethylhydrazone **429** was metallated with *t*-BuLi and, after transmetallation with $ZnBr_2$, the corresponding aza-enolate bearing a $BrZn^{II}$ countercation cyclized very slowly to give the cyclic hydrazone **430** as a single *trans* diastereomer albeit in low yield (15% after 25 h). Changing the countercation to $BuZn^{II}$ (by addition of *n*-BuLi) enhanced the reactivity and allowed the 5-exo and 6-exo-Trig cyclizations of the metallated hydrazones derived from **429** and **431** to proceed. The 1,2-disubstituted cyclopentane and cyclohexane derivatives bearing a hydrazone moiety, **430** and **432** respectively, were obtained with reasonably high *cis* diastereoselectivity. Functionalization of the cyclized organozinc intermediate **433** has also been accomplished by allylation after transmetallation with CuCN[282], and provided the *cis*-disubstituted cyclopentane **434**. This result indicated that the γ-zincio hydrazones, resulting from the intramolecular carbozincation, were stable and that no shift of the metal that would have regenerated a more stable α-zincated hydrazone took place, due to the low basicity of organozincs (equation 186).

2. Intermolecular additions of zinc enolates to alkenes

Compared to the intramolecular reactions that benefit, at least for a small part, from a favorable thermodynamic component due to the formation of a cyclic product, intermolecular additions of enolates to alkenes are rather challenging and constitute the so-called 'olefinic version of the aldol condensation'[281].

Based on the observation that alkenylmetals were highly reactive partners in carbozincations involving allylic organozinc reagents (see Section III.D), Nakamura and

coworkers demonstrated that the zincated hydrazone derived from **435** readily reacted with vinylmagnesium bromide in ether at 0 °C to generate the dimetallic species **436**. Indeed, deuteriolysis resulted in exclusive dideuteriation at the terminal methyl group and afforded **437** in high yield[283]. Alternatively, trapping of **436** with two different electrophiles could also be achieved. One equivalent of *t*-BuOH was used to protonate one of the two anionic sites and subsequent treatment with allyl bromide led to the monoallylated product **438**. Successive treatment of **436** with a mixture of MeSSMe and allyl bromide afforded the four-component coupling product **439** (equation 187).

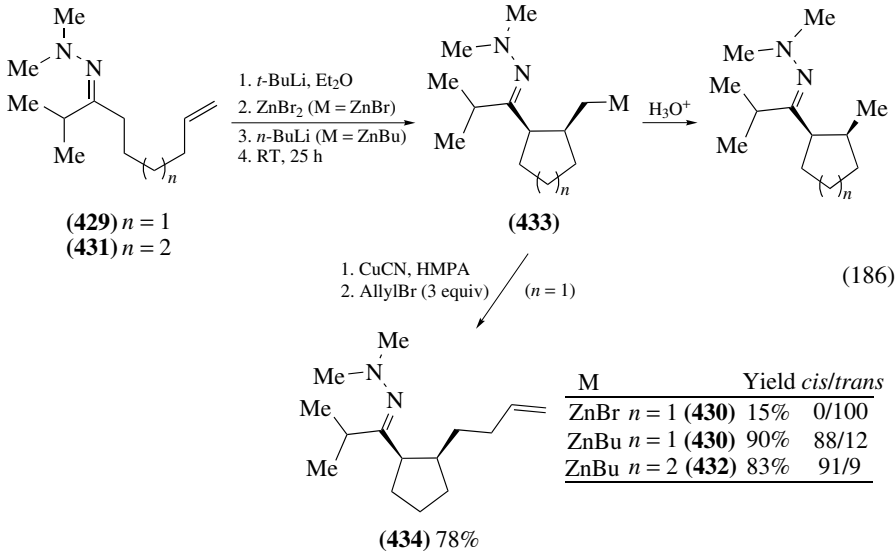

(429) $n = 1$
(431) $n = 2$

(433)

(186)

M		Yield	*cis*/*trans*
ZnBr	$n = 1$ **(430)**	15%	0/100
ZnBu	$n = 1$ **(430)**	90%	88/12
ZnBu	$n = 2$ **(432)**	83%	91/9

(434) 78%

Interestingly, the lithiated hydrazone derived from **435** or the zincated derivative bearing a $BuZn^{II}$ countercation were found to be unreactive towards vinylmagnesium bromide. This latter result is in sharp contrast with the observed countercation effect for the intramolecular carbozincations of *N*,*N*-dimethylhydrazones **429** and **431** (equation 186). Based on these observations, the authors speculated that the reaction probably involved a metalla-aza-Claisen rearrangement of a neutral aza-allyl vinylzinc intermediate such as **440** (equation 188), by analogy with the magnesium-assisted metalla-Claisen rearrangement of allyl alkenylzincs[142] (see Section III.D), rather than a simple carbometallation reaction of the vinyl Grignard reagent.

Other vinylmetals such as silanes and stannanes, although more covalent than vinylmagnesium bromide itself, were also viable partners for the addition of zincated hydrazones, due to the ability of Si and Sn to stabilize an adjacent organozinc species. For such substrates, the mechanism of addition was clearly different from the case of vinylmagnesium bromide and presumably involved a carbozincation, as a $BuZn^{II}$ countercation (rather than $BrZn^{II}$) for the metallated hydrazones was mandatory. Thus, the addition of the $BuZn^{II}$ aza-enolate derived from hydrazone **441** to vinyltrimethylsilane[284] proceeded slowly at 25–35 °C and led to the γ-silylated-γ-zincated hydrazone intermediate **442**. Upon treatment with iodine and removal of the hydrazone moiety by ozonolysis, the γ-iodo-γ-trimethylsilyl ketone **443** was obtained in good yield (equation 189).

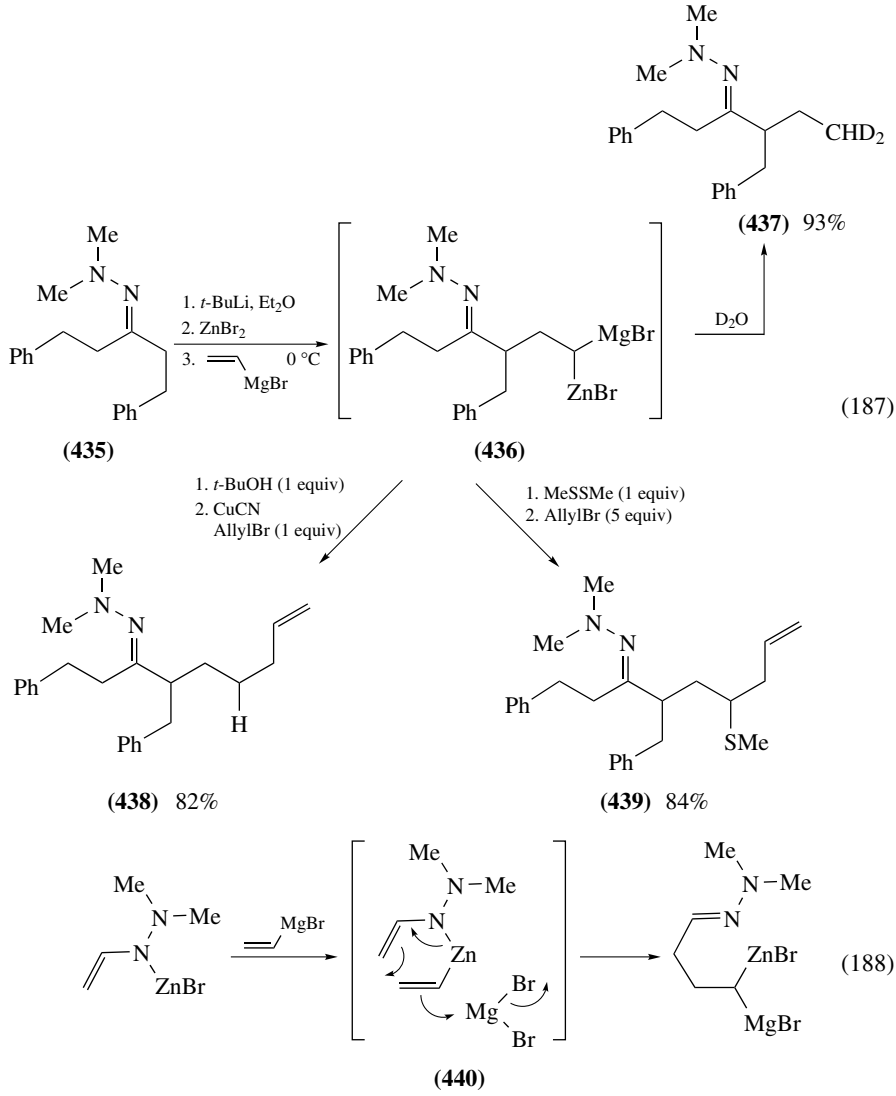

This reaction was successfully applied to various hydrazones derived from acyclic or cyclic ketones and extended to a variety of unsubstituted vinylsilanes as acceptors (trialkyl, triphenyl and alkoxy vinylsilanes). In all cases, the regioselectivity of the addition reaction was consistent with the formation of a silicon-stabilized organozinc reagent.

Application of this methodology to vinylstannane[285] led to the discovery of a one-pot preparation of pyrroles. Indeed, the aza-enolate derived from hydrazone **435** smoothly reacted with vinyltrimethylstannane at 30 °C to afford exclusively the *gem*-Zn/Sn dimetallated adduct **444**, which upon hydrolysis delivered the corresponding γ-stannylhydrazone **445**. Alternatively, exposure of **444** to oxygen afforded the 2,3-disubstituted-1-(dimethylamino)-1*H*-pyrrole **446** (equation 190).

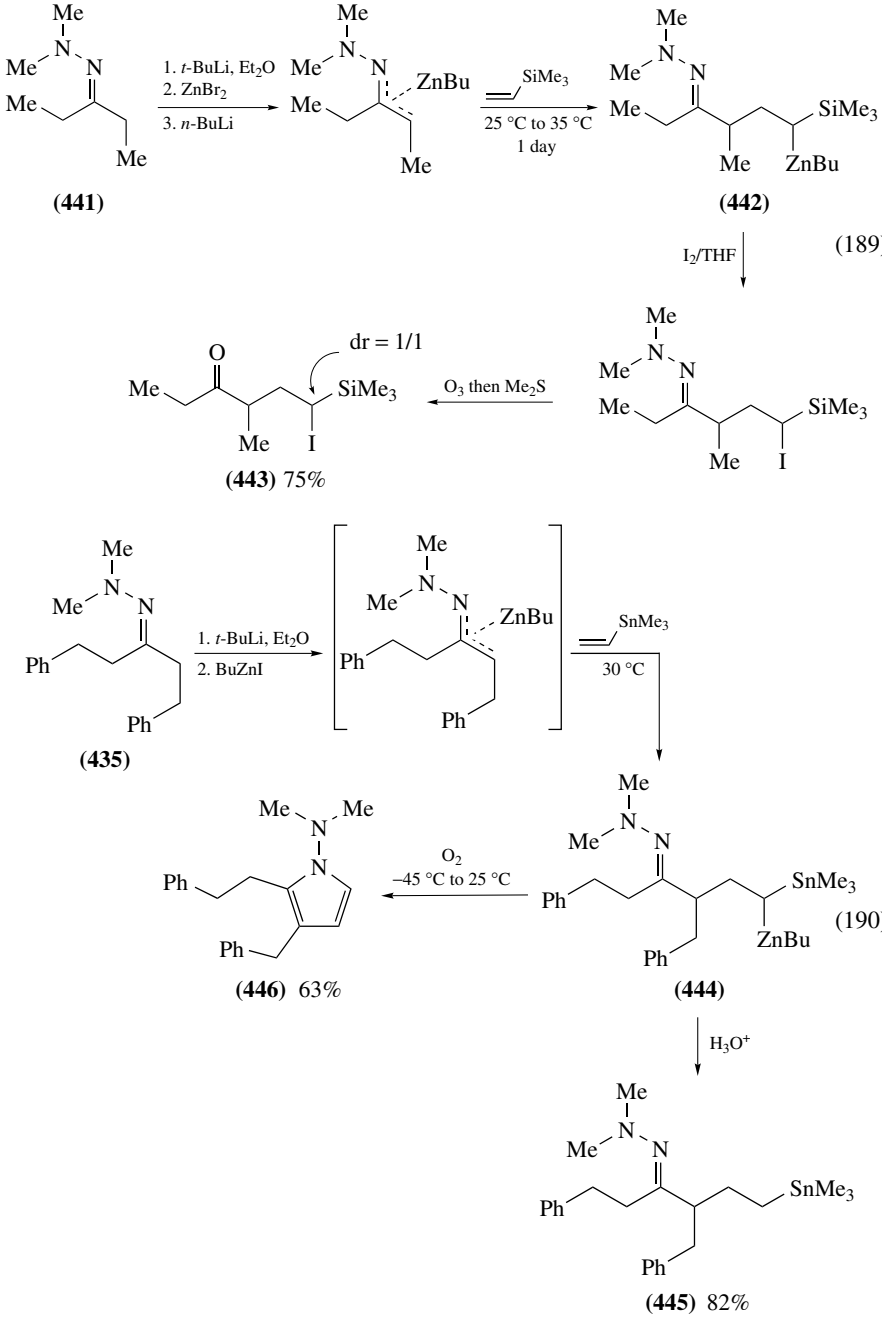
1. t-BuLi, Et2O
2. ZnBr2
3. n-BuLi
SiMe3
25 °C to 35 °C
1 day
(441)
(442)
I2/THF
(189)
dr = 1/1
O3 then Me2S
(443) 75%
1. t-BuLi, Et2O
2. BuZnI
SnMe3
30 °C
(435)
O2
–45 °C to 25 °C
(446) 63%
(444)
(190)
H3O+
(445) 82%

Besides the activation of the olefinic partner by a metal, the unfavorable thermodynamics associated with the addition of an enolate to a carbon−carbon multiple bond could be overwhelmed by using a strained alkene such as a cyclopropene derivative[286]. Indeed, Nakamura and coworkers demonstrated that the butylzinc enolate derived from *N*-methyl-*δ*-valerolactam (**447**) smoothly reacted with the cyclopropenone ketal **78** and subsequent deuterolysis led to the *cis*-substituted cyclopropanone ketal **448**, indicating that the carbometallation involved a *syn* addition process. Moreover, a high level of diastereoselectivity at the newly formed carbon−carbon bond was observed (de = 97%) (equation 191). The butylzinc enolates derived from other amides, lactams, esters and hydrazones also add successfully to the strained cyclopropenone ketal **78**. Moreover, the cyclopropylzincs generated are stable and no rearrangements to the more stable zinc enolates occur after the addition.

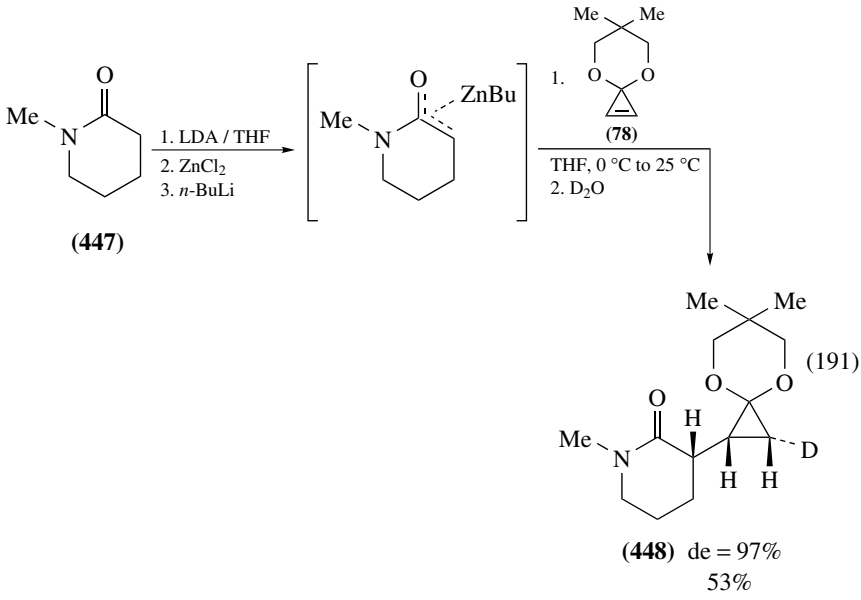

(447)

(448) de = 97%
53%

(191)

The reaction with optically active hydrazones provided an access to optically active ketones. The butylzinc aza-enolate generated from the hydrazone **449** (derived from 4-heptanone and (*S*)-1-amino-2-(methoxymethyl)pyrrolidine (SAMP)) reacted with the cyclopropenone ketal **78** and led to **450** after hydrolysis. The reaction proceeded with 100% of 1,2-diastereoselectivity at the newly formed carbon−carbon bond (mutual diastereoselection) and 78% of substrate-induced diastereoselectivity (with respect to the chiral induction from the SAMP hydrazone). The latter level of diastereoselection was improved to 87% by the use of the ZnCl enolate derived from **449**, at the expense of a slight decrease in yield. Finally, the resulting cyclopropanone ketal **450** could be transformed to the polyfunctional open-chain dicarbonyl compound **451** by removal of the hydrazone moiety and oxymercuration of the three-membered ring (equation 192).

By contrast with the above examples which involve activated olefins, the addition of zinc enolates to unactivated alkenes is much more difficult to achieve. Although ethylene seems to be an acceptable partner for such additions, the reactions have to be carried out under pressure and require relatively long reaction times. Thus, the butylzinc aza-enolate generated from the SAMP hydrazone of cyclohexanone **452** reacted slowly with ethylene

under pressure and provided the carbometallated product **453** in moderate yield and with a satisfactory level of diastereoselection (dr = 88/12) (equation 193)[287].

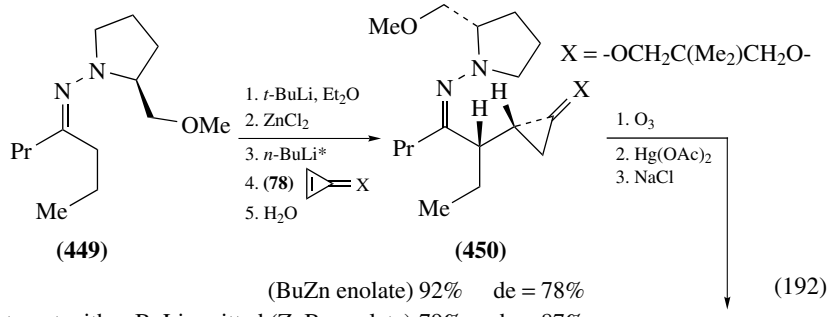

(449) **(450)**

(BuZn enolate) 92% de = 78%

*Treatment with *n*-BuLi omitted (ZnBr enolate) 79% de = 87%

(192)

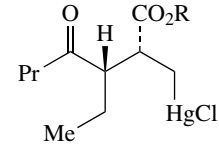

(451) 92%

R = $OCH_2C(Me_2)CH_2OH$

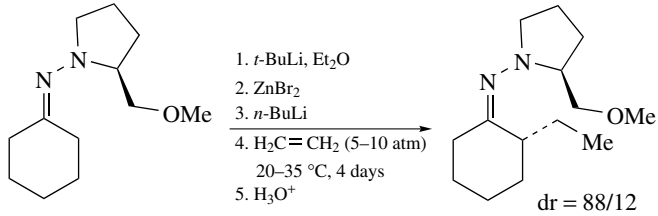

dr = 88/12

(452) **(453)** 42%

(193)

After extensive investigation, Nakamura and coworkers reported an improved enantioselective synthesis of α-substituted ketones through the three-component coupling of an optically active zinc enamide derived from (*S*)-*tert*-leucinol, an unactivated alkene and an electrophile[288]. Thus, the methylzinc enamide generated from imine **454** reacted with ethylene under high pressure in hexanes and provided, after protonation of the carbon–metal bond in the γ-zincio imine intermediate **455** and acidic hydrolysis of imine, the ethylated ketone **456** with high enantiomeric excess (ee = 97.7%). The observed sense of induction was explained by a six-centered transition state, in which the ethylene approached the chelated zinc enamide from its less hindered face. The γ-zincio imine **455** was found to be very stable under the reaction conditions, likely because of its chelate structure, but could also be allylated with ethyl 2-(bromomethyl)acrylate in the presence of copper salts to give compound **457** in high enantiomeric purity (ee = 96.8%) (equation 194).

The scope of the reaction is reasonably general in terms of the cyclic ketones that could be used, but an acyclic substrate such as 3-pentanone led to a lower enantioselectivity. Besides ethylene, other olefinic partners such as propene and styrene also took part in the reaction. Addition to propene occurred with a lower yield and the adduct incorporating an isopropyl group was obtained, indicating that the addition took place regioselectively

to generate a primary alkylzinc intermediate. In the case of styrene, the formation of a benzylic organozinc was favored[288].

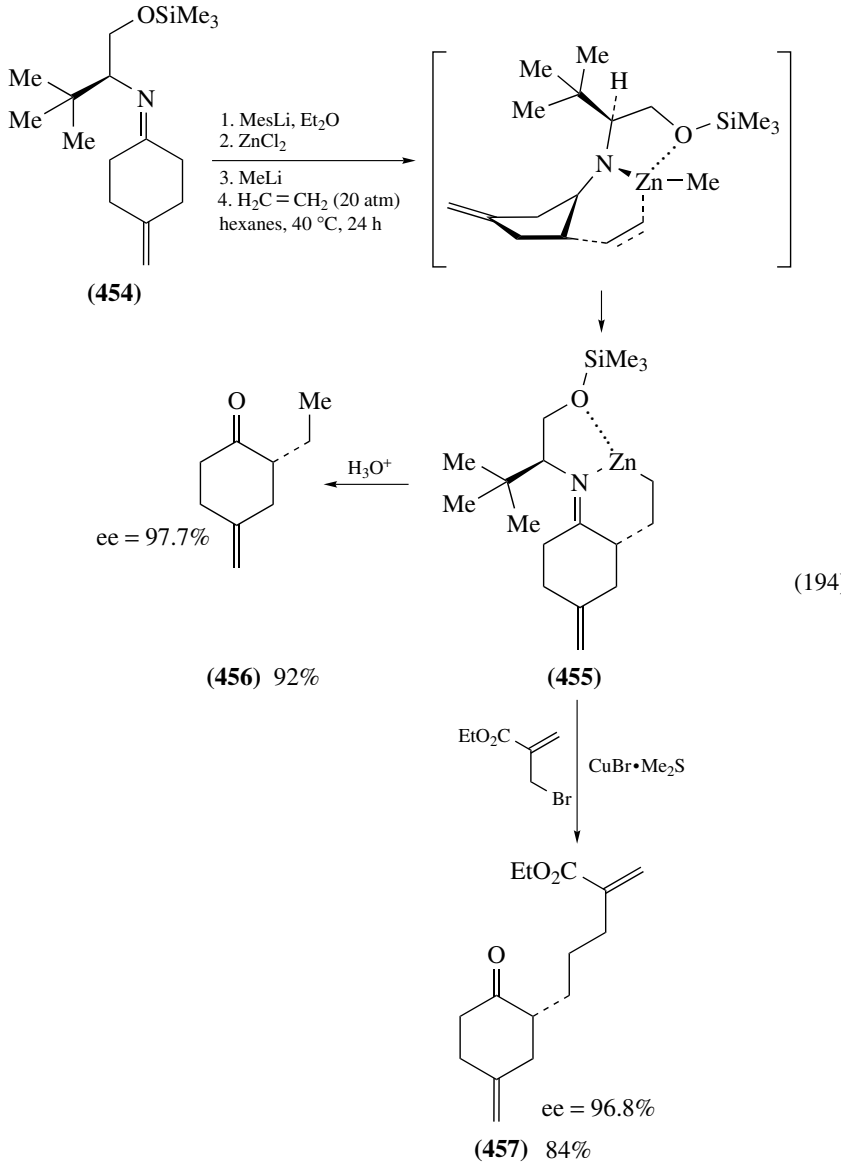

(194)

An extension of the carbozincation of unactivated olefins by zinc enamides was recently reported and opened a new efficient entry to α-alkylated ketones, especially those bearing an α-secondary or tertiary alkyl group[289]. Indeed, such substrates are difficult to obtain by the conventional method relying on the alkylation of metal enamides or enolates

with secondary or tertiary halides. In this report, the *N*-aryl-butylzinc enamide **458**, derived from 2,4-dimethylaniline, was reacted with various olefins. The high reactivity of **458** was already apparent in the addition to ethylene, where an atmospheric pressure was only required to generate the γ-zincio imine of type **459**. Under these conditions, 2-ethyl-3-pentanone (**460**) was then obtained in 94% yield after acidic hydrolysis of the imine. Remarkably, a variety of monosubstituted olefins could be used (propene, 1-octene, styrene) all of them leading to the same regioselectivities in favor of the formation of a primary organozinc species. The reversal of regioselectivity for styrene was attributed to a subtle steric effect that may overwhelm the electronic effect of this substrate. The addition of **458** could even be performed with isobutene (4–5 atm) and, after acidic hydrolysis of the resulting γ-zincio imine **461**, 2-*tert*-butyl-3-pentanone (**462**) was obtained in 85% yield. Alternatively, trapping **461** with allyl bromide was successful even in the absence of additives and provided the α-substituted ketone **463** after hydrolysis of the imine (equation 195).

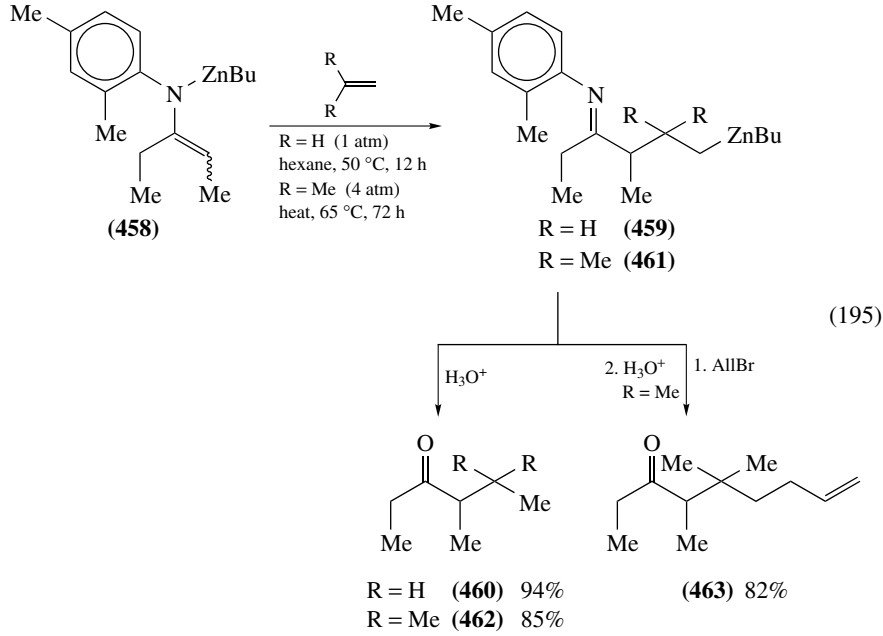

(195)

A significant decrease in reactivity was observed when the *N*-aryl zinc enamide generated from 4-methylaniline was used. It was suggested that this 2-methyl effect on reactivity may arise from a steric effect contributing to the conformational stabilization of the transition state. These recent results have thus greatly expanded the scope of the so-called 'olefinic aldol condensation' as the experimental procedure is quite simple and applicable to a variety of monosubstituted or α,α-disubstituted alkenes.

VI. CONCLUSION

Carbozincations constitute undoubtedly one of the most fascinating fields of organozinc chemistry. Whereas alkenes and alkynes are not traditionally considered as electrophiles in polar organometallic chemistry, carbometallation reactions offer many synthetically

useful possibilities and fine tuning of the reactivity can often be achieved by proper choice of the organometallic reagent. There are several processes that one could have considered chemically unlikely, such as the addition of an allylmetal to an alkenylmetal, an allenylmetal or an alkynylmetal, as well as the addition of a stabilized enolate to an unactivated alkene, that are in fact achievable with organozinc reagents under mild conditions.

It can be anticipated that many other reactions will be discovered in the rapidly expanding field of carbometallation where organozincs occupy a prominent position, and that they will serve not only to complement the fundamental knowledge on these reagents, but also stimulate some applications to the synthesis of biologically active compounds that have not been so widely developed until now.

VII. REFERENCES

1. E. Negishi, *Pure Appl. Chem.*, **53**, 2333 (1981).
2. J. F. Normant and A. Alexakis, *Synthesis*, 841 (1981).
3. J. V. N. Vara Prasad and C. N. Pillai, *J. Organomet. Chem.*, **259**, 1 (1983).
4. P. Knochel, in *Comprehensive Organic Synthesis* (Eds. B. Trost and I. Fleming), Vol. 4, Pergamon, Oxford, 1991, pp. 865–911.
5. W. Oppolzer, *Angew. Chem., Int. Ed. Engl.*, **28**, 38 (1989).
6. W. Oppolzer, in *Comprehensive Organic Synthesis* (Eds. B. Trost and I. Fleming), Vol. 5, Pergamon, Oxford, 1991, pp. 29–61.
7. I. Marek and J. F. Normant, in *Metal-Catalyzed Cross-Coupling Reactions* (Eds. F. Diederich and P. J. Stang), 1st edn., Wiley, Weinheim, 1998, pp. 271–337.
8. I. Marek, *J. Chem. Soc., Perkin Trans. 1*, 535 (1999).
9. I. Marek, N. Chinkov and D. Banon-Tenne, in *Metal-Catalyzed Cross-Coupling Reactions* (Eds. A. de Mejere and F. Diederich), 2nd edn., Wiley, Weinheim, 2004, pp. 395–478.
10. P. Knochel and R. D. Singer, *Chem. Rev.*, **93**, 2117 (1993).
11. P. Knochel, in *Metal-Catalyzed Cross-Coupling Reactions* (Eds. F. Diederich and P. J. Stang), 1st edn., Wiley, Weinheim, 1998, pp. 387–419.
12. G. Courtois and L. Miginiac, *C. R. Acad. Sci. Paris, Ser. C*, **285**, 207 (1977).
13. J. Auger, G. Courtois and L. Miginiac *J. Organomet. Chem.*, **133**, 285 (1977).
14. G. Courtois and L. Miginiac, *J. Organomet. Chem.*, **195**, 13 (1980).
15. L. Miginiac, *J. Organomet. Chem.*, **238**, 235 (1982).
16. H. Lehmkuhl and O. Olbrysch, *Justus Liebigs Ann. Chem.*, 1162 (1975).
17. W. F. Bailey and T. V. Ovaska, *J. Am. Chem. Soc.*, **115**, 3080 (1993).
18. G. Wu, F. E. Cederbaum and E. Negishi, *Tetrahedron Lett.*, **30**, 3901 (1989).
19. S. Achyutha Rao and P. Knochel, *J. Am. Chem. Soc.*, **113**, 5735 (1991).
20. M. C. P. Yeh and P. Knochel, *Tetrahedron Lett.*, **30**, 4799 (1989).
21. J. K. Crandall and T. A. Ayers, *Organometallics*, **11**, 473 (1992).
22. J. St Denis, T. Dolzine and J. P. Oliver, *J. Am. Chem. Soc.*, **94**, 8260 (1972).
23. J. St Denis, J. P. Oliver, T. W. Dolzine and J. B. Smart, *J. Organomet. Chem.*, **71**, 315 (1974).
24. J. St Denis, J. P. Oliver and J. B. Smart, *J. Organomet. Chem.*, **44**, C32 (1972).
25. M. J. Albright, J. N. St Denis and J. P. Oliver, *J. Organomet. Chem.*, **125**, 1 (1977).
26. A. Haaland, H. Lehmkuhl and H. Nehl, *Acta Chem. Scand. A*, **38**, 547 (1984).
27. E. Okninska and K. B. Starowieyski, *J. Organomet. Chem.*, **376**, 7 (1989).
28. L. Zhu, R. M. Wehmeyer and R. D. Rieke, *J. Org. Chem.*, **56**, 1445 (1991).
29. C. Meyer, I. Marek, G. Courtemanche and J. F. Normant, *Synlett*, 266 (1993).
30. W. F. Bailey, A. D. Khanolkar, K. Gavaskar, T. V. Ovaska, K. Rossi, Y. Thiel and K. B. Wiberg, *J. Am. Chem. Soc.*, **113**, 5720 (1991).
31. C. Meyer, I. Marek, G. Courtemanche and J. F. Normant, *Tetrahedron*, **50**, 11665 (1994).
32. B. S. Bronk, S. J. Lippard and R. L. Danheiser, *Organometallics*, **12**, 3340 (1993).
33. M. J. Rozema, S. AchyuthaRao and P. Knochel, *J. Org. Chem.*, **57**, 1956 (1992).
34. H. Stadtmüller, R. Lentz, C. E. Tucker, T. Stüdemann, W. Dörner and P. Knochel, *J. Am. Chem. Soc.*, **115**, 7027 (1993).

35. A. Shibli, J. P. Varghese, P. Knochel and I. Marek, *Synlett*, 818 (2001).
36. C. Meyer, I. Marek, G. Courtemanche and J. F. Normant, *Tetrahedron Lett.*, **34**, 6053 (1993).
37. E. A. Hill, *J. Organomet. Chem.*, **91**, 123 (1975).
38. M. J. Rozema, C. Eisenberg, H. Lütjens, K. Belyk and P. Knochel, *Tetrahedron Lett.*, **34**, 3115 (1993).
39. H. Stadtmüller, A. Vaupel, C. E. Tucker, T. Stüdemann and P. Knochel, *Chem. Eur. J.*, **2**, 1204 (1996).
40. H. Stadtmüller, C. E. Tucker, A. Vaupel and P. Knochel, *Tetrahedron Lett.*, **34**, 7911 (1993).
41. A. Vaupel and P. Knochel, *Tetrahedron Lett.*, **35**, 8349 (1994).
42. H. Stadtmüller and P. Knochel, *Synlett*, 463 (1995).
43. A. Vaupel and P. Knochel, *Tetrahedron Lett.*, **36**, 231 (1995).
44. E. Negishi, D. E. Van Horn, T. Yoshida and C. L. Rand, *Organometallics*, **2**, 563 (1983).
45. E. Negishi, H. Sawada, J. M. Tour and Y. Wei, *J. Org. Chem.*, **53**, 913 (1988).
46. T. Stüdemann and P. Knochel, *Angew. Chem., Int. Ed. Engl.*, **36**, 93 (1997).
47. T. Stüdemann, M. Ibrahim-Ouali and P. Knochel, *Tetrahedron*, **54**, 1299 (1998).
48. C. Bolm, J. Legros, J. Le Paih and L. Zani, *Chem. Rev.*, **104**, 6217 (2004).
49. M. Nakamura, A. Hirai and E. Nakamura, *J. Am. Chem. Soc.*, **122**, 978 (2000).
50. M. Lautens, *Synlett*, 177 (1993).
51. P. Chiu and M. Lautens, *Top. Curr. Chem.*, **190**, 1 (1997).
52. M. Lautens, J.-L. Renaud and S. Hiebert, *J. Am. Chem. Soc.*, **122**, 1804 (2000).
53. M. Lautens and S. Hiebert, *J. Am. Chem. Soc.*, **126**, 1437 (2004).
54. M. Li, X.-X.; Yan, W. Hong, X.-Z. Zhu, B.-X. Cao, J. Sun and X.-L. Hou, *Org. Lett.*, **6**, 2833 (2004).
55. F. Bertozzi, M. Pineschi, F. Macchia, L. A. Arnold, A. J. Minnaard and B. L. Feringa, *Org. Lett.*, **4**, 2703 (2002).
56. M. Lautens, S. Hiebert and J.-L. Renaud, *Org. Lett.*, **2**, 1971 (2000).
57. S. Gagneur, J.-L. Montchamp and E. Negishi, *Organometallics*, **19**, 2417 (2000).
58. J.-L. Montchamp and E. Negishi, *J. Am. Chem. Soc.*, **120**, 5345 (1998).
59. S.-I. Ikeda, *Acc. Chem. Res.*, **33**, 511 (2000).
60. J. Montgomery, *Angew. Chem., Int. Ed.*, **43**, 3890 (2004).
61. J. Montgomery and A. V. Sachenko, *J. Am. Chem. Soc.*, **118**, 2099 (1996).
62. J. Montgomery, J. Seo and H. M. P. Chui, *Tetrahedron Lett.*, **37**, 6839 (1996).
63. J. Montgomery and J. Seo, *Tetrahedron*, **54**, 1131 (1998).
64. J. Montgomery, E. Oblinger and A. V. Savchenko, *J. Am. Chem. Soc.*, **119**, 4911 (1997).
65. Y. Ni, K. K. D. Amarasinghe, B. Ksebati and J. Montgomery, *Org. Lett.*, **5**, 3771 (2003).
66. S.-I. Ikeda, D.-M. Cui and Y. Sato, *J. Am. Chem. Soc.*, **121**, 4712 (1999).
67. E. Oblinger and J. Montgomery, *J. Am. Chem. Soc.*, **119**, 9065 (1997).
68. X. Qi and J. Montgomery, *J. Org. Chem.*, **64**, 9310 (1999).
69. M. Lozanov and J. Montgomery, *Tetrahedron Lett.*, **42**, 3259 (2001).
70. J. Montgomery and M. Song, *Org. Lett.*, **4**, 4009 (2002).
71. M. Kimura, S. Matsuo, K. Shibata and Y. Tamaru, *Angew. Chem., Int. Ed.*, **38**, 3386 (1999).
72. M. Kimura, H. Fujimatsu, A. Ezoe, K. Shibata, M. Shimizu, S. Matsumoto and Y. Tamaru, *Angew. Chem., Int. Ed.*, **38**, 397 (1999).
73. K. Shibata, M. Kimura, K. Kojima, S. Tanaka and Y. Tamaru, *J. Organomet. Chem.*, **624**, 348 (2001).
74. T.-P. Loh, H.-Y. Song and Y. Zhou, *Org. Lett.*, **4**, 2715 (2002).
75. M. Takimoto, K. Shimizu and M. Mori, *Org. Lett.*, **3**, 3345 (2001).
76. K. Shimizu, M. Takimoto and M. Mori, *Org. Lett.*, **5**, 2323 (2003).
77. K. Shimizu, M. Takimoto, Y. Sato and M. Mori, *Org. Lett.*, **7**, 195 (2005).
78. M. Takimoto and M. Mori, *J. Am. Chem. Soc.*, **123**, 2895 (2001).
79. M. Nakamura, N. Yoshikai and E. Nakamura, *Chem. Lett.*, 146 (2002).
80. L. Miginiac and B. Mauzé, *Bull. Soc. Chim. Fr.*, 462 (1968).
81. B. Mauzé, G. Courtois and L. Miginiac, *C. R. Acad. Sci. Paris, Ser. C*, **269**, 1225 (1969).
82. B. Mauzé, C. Nivert and L. Miginiac, *J. Organomet. Chem.*, **44**, 69 (1972).
83. J. J. Eisch and G. R. Husk, *J. Am. Chem. Soc.*, **87**, 4194 (1965).
84. J. J. Eisch and J. H. Merkley, *J. Organomet. Chem.*, **20**, P27 (1969).
85. M. Chérest, H. Felkin, C. Frajerman, C. Lion, G. Roussi and G. Swierczewski, *Tetrahedron Lett.*, 875 (1966).

86. J. J. Eisch, J. H. Merkley and J. E. Galle, *J. Org. Chem.*, **44**, 587 (1979)
87. H. G. Richey, Jr. and C. W. Wilkins, Jr., *J. Org. Chem.*, **45**, 5027 (1980).
88. C. Nivert and L. Miginiac, *C. R. Acad. Sci. Paris, Ser. C*, **272**, 1996 (1971).
89. G. Courtois and L. Miginiac, *Bull. Soc. Chim. Fr.*, 3330 (1969).
90. G. Courtois and L. Miginiac, *J. Organomet. Chem.*, **52**, 241 (1973).
91. H. Lehmkuhl, I. Döring, R. McLane and H. Nehl, *J. Organomet. Chem.*, **221**, 1 (1981).
92. H. Lehmkuhl, I. Döring and H. Nehl, *J. Organomet. Chem.*, **221**, 123 (1981).
93. H. Lehmkuhl and H. Nehl, *J. Organomet. Chem.*, **60**, 1 (1973).
94. H. Lehmkuhl, *Bull. Soc. Chim. Fr.*, 87 (1981).
95. H. Lehmkuhl and R. McLane, *Justus Liebigs Ann. Chem.*, 736 (1980).
96. H. Lehmkuhl and H. Nehl, *J. Organomet. Chem.*, **221**, 131 (1981).
97. M. Nakamura, H. Isobe and E. Nakamura, *Chem. Rev.*, **103**, 1295 (2003).
98. K. Kubota, S. Mori, M. Nakamura and E. Nakamura, *J. Am. Chem. Soc.*, **120**, 13334 (1998).
99. K. Kubota, M. Nakamura, M. Isaka and E. Nakamura, *J. Am. Chem. Soc.*, **115**, 5867 (1993).
100. E. Nakamura, *Pure Appl. Chem.*, **68**, 123 (1996).
101. M. Nakamura, M. Arai and E. Nakamura, *J. Am. Chem. Soc.*, **117**, 1179 (1995).
102. M. Nakamura, T. Inoue, A. Sato and E. Nakamura, *Org. Lett.*, **2**, 2193 (2000).
103. A. Yanagisawa, S. Habaue and H. Yamamoto, *J. Am. Chem. Soc.*, **111**, 366 (1989).
104. P. Knochel and J. F. Normant, *Tetrahedron Lett.*, **25**, 1475 (1984).
105. C. Nivert, B. Mauzé and L. Miginiac, *C. R. Acad. Sci. Paris, Ser. C*, **271**, 698 (1970).
106. J. P. Charpentier, D. Mesnard and L. Miginiac, *J. Organomet. Chem.*, **214**, 135 (1981).
107. G. A. Molander, *J. Org. Chem.*, **48**, 5409 (1983).
108. E. Negishi and J. A. Miller, *J. Am. Chem. Soc.*, **105**, 6761 (1983).
109. E. Negishi and T. Takahashi, *J. Am. Chem. Soc.*, **108**, 3402 (1986).
110. J. van der Louw, J. L. van der Baan, F. Bickelhaupt and G. W. Klumpp, *Tetrahedron Lett.* **28**, 2889 (1987).
111. T. Nishikawa, H. Yorimitsu and K. Oshima, *Synlett*, 1573 (2004).
112. G. Courtois, A. Masson and L. Miginiac, *C. R. Acad. Sci. Paris, Ser. C*, **286**, 265 (1978).
113. J. van der Louw, C. M. D. Komen, A. Knol, F. J. J. de Kanter, J. L. van der Baan, F. Bickelhaupt and G. W. Klumpp, *Tetrahedron Lett.*, **30**, 4453 (1989).
114. W. Oppolzer and F. Schröder, *Tetrahedron Lett.*, **35**, 7939 (1994).
115. W. Oppolzer, *Pure Appl. Chem.*, **62**, 1941 (1990).
116. W. Oppolzer and J. Ruiz-Montes, *Helv. Chim. Acta*, **76**, 1266 (1993).
117. W. Oppolzer and F. Flachsmann, *Tetrahedron Lett.*, **39**, 5019 (1998).
118. W. Oppolzer and F. Flachsmann, *Helv. Chim. Acta*, **84**, 416 (2001).
119. W. Oppolzer, F. Schröder and S. Kahl, *Helv. Chim. Acta*, **80**, 2047 (1997).
120. N. Millot and P. Knochel, *Tetrahedron Lett.*, **40**, 7779 (1999).
121. J. van der Louw, J. L. van der Baan, H. Stieltjes, F. Bickelhaupt and G. W. Klumpp, *Tetrahedron Lett.*, **28**, 5929 (1987).
122. J. van der Louw, J. L. van der Baan, C. M. D. Komen, A. Knol, F. J. J. de Kanter, F. Bickelhaupt and G. W. Klumpp, *Tetrahedron*, **48**, 6105 (1992).
123. M. Gaudemar, *C. R. Acad. Sci. Paris, Ser. C*, **273**, 1669 (1971).
124. Y. Frangin and M. Gaudemar, *C. R. Acad. Sci. Paris, Ser. C*, **278**, 885 (1974).
125. M. Bellasoued, Y. Frangin and M. Gaudemar, *Synthesis*, 205 (1977).
126. I. Marek and J. F. Normant, *Chem. Rev.*, **96**, 3241 (1996).
127. P. Knochel and J. F. Normant, *Tetrahedron Lett.*, **27**, 1039 (1986).
128. I. Marek, J.-M. Lefrançois and J. F. Normant, *J. Org. Chem.*, **59**, 4154 (1994).
129. P. Knochel, M. C. P. Yeh and C. Xiao, *Organometallics*, **8**, 2831 (1989).
130. P. Knochel and J. F. Normant, *Tetrahedron Lett.*, **27**, 1043 (1986).
131. C. E. Tucker and P. Knochel, *Synlett*, 530 (1993).
132. I. Klement, K. Lennick, C. E. Tucker and P. Knochel, *Tetrahedron Lett.*, **34**, 4623 (1993).
133. I. Klement, H. Lütjens and P. Knochel, *Tetrahedron*, **53**, 9135 (1997).
134. P. Knochel, C. Xiao and M. C. P. Yeh, *Tetrahedron Lett.*, **29**, 6697 (1988).
135. P. Knochel and J. F. Normant, *Tetrahedron Lett.*, **27**, 4427 (1986).
136. P. Knochel and J. F. Normant, *Tetrahedron Lett.*, **27**, 4431 (1986).
137. F. Chemla, I. Marek and J. F. Normant, *Synlett*, 665 (1993).
138. F. Chemla and J. Normant, *Tetrahedron Lett.*, **36**, 3157 (1995).

139. J. F. Normant, I. Marek and J.-M. Lefrançois, *Pure Appl. Chem.*, **64**, 1857 (1992).
140. I. Marek, P. R. Schreiner and J. F. Normant, *Org. Lett.*, **1**, 929 (1999).
141. A. Hirai, M. Nakamura and E. Nakamura, *J. Am. Chem. Soc.*, **121**, 8665 (1999).
142. A. Hirai, M. Nakamura and E. Nakamura, *J. Am. Chem. Soc.*, **122**, 11791 (2000).
143. M. Nakamura, K. Hara, T. Hatakeyama and E. Nakamura, *Org. Lett.*, **3**, 3137 (2001).
144. P. Knochel and J. F. Normant, *Tetrahedron Lett.*, **27**, 5727 (1986).
145. I. Marek, J.-M. Lefrançois and J. F. Normant, *Tetrahedron Lett.*, **32**, 5069 (1991).
146. I. Marek, J.-M. Lefrançois and J. F. Normant, *Synlett*, 633 (1992).
147. H. K. Hoftsee, J. Boersma, J. D. Van der Meulen and G. J. M. Van der Kerk, *J. Organomet. Chem.*, **153**, 245 (1978).
148. I. Marek and J. F. Normant, *Tetrahedron Lett.*, **32**, 5973 (1991).
149. I. Marek, J. M. Lefrançois and J. F. Normant, *Bull. Soc. Chim. Fr.*, 910 (1994).
150. F. Ferreira and J. F. Normant, *Eur. J. Org. Chem.*, 3581 (2000).
151. F. Ferreira, C. Herse, E. Riguet and J. F. Normant, *Tetrahedron Lett.*, **41**, 1733 (2000).
152. A. Bähr, I. Marek and J. F. Normant, *Tetrahedron Lett.*, **37**, 5873 (1996).
153. N. Bernard, F. Chemla, F. Ferreira, N. Mosetefai and J. F. Normant, *Chem. Eur. J.*, **8**, 3139 (2002).
154. D. Brasseur, I. Marek and J. F. Normant, *Tetrahedron*, **52**, 7235 (1996).
155. D. Brasseur, H. Rezaei, A. Fuxa, A. Alexakis, P. Mangeney, I. Marek and J. F. Normant, *Tetrahedron Lett.*, **39**, 4821 (1998).
156. D. Brasseur, I. Marek and J. F. Normant, *C. R. Acd. Sci. Paris, Ser. II C*, **1**, 621 (1998).
157. I. Marek, D. Beruben and J. F. Normant, *Tetrahedron Lett.*, **36**, 3695 (1995).
158. S. Cheramy, F. Ferreira and J. F. Normant, *Tetrahedron Lett.*, **45**, 4549 (2004).
159. D. Beruben, I. Marek, J. F. Normant and N. Platzer, *Tetrahedron Lett.*, **34**, 7575 (1993).
160. D. Beruben, I. Marek, J. F. Normant and N. Platzer, *J. Org. Chem.*, **60**, 2488 (1995).
161. D. Beruben, I. Marek, L. Labaudinière and J. F. Normant, *Tetrahedron Lett.*, **34**, 2303 (1993).
162. F. Wang, J. Tang, L. Labaudinière, I. Marek and J. F. Normant, *Synlett*, 723 (1995).
163. J. F. Normant, *Acc. Chem. Res.*, **34**, 640 (2001).
164. J. F. Normant, J. C. Quirion, A. Alexakis and Y. Masuda, *Tetrahedron Lett.*, **30**, 3955 (1989).
165. L. Labaudinière, J. Hanaïzi and J. F. Normant, *J. Org. Chem.*, **57**, 6903 (1992).
166. L. Labaudinière and J. F. Normant, *Tetrahedron Lett.*, **33**, 6139 (1992).
167. J. F. Normant and J. C. Quirion, *Tetrahedron Lett.*, **30**, 3959 (1989).
168. F. Bernadou, B. Mauzé and L. Miginiac, *C. R. Acad. Sci. Paris, Ser. C*, **276**, 1645 (1973).
169. Y. Frangin and M. Gaudemar, *Bull. Soc. Chim. Fr.*, 1173 (1976).
170. Y. Frangin and M. Gaudemar, *J. Organomet. Chem.*, **142**, 9 (1977).
171. B. Mauzé, G. Courtois and L. Miginiac, *C. R. Acad. Sci. Paris, Ser. C*, **274**, 658 (1972).
172. D. Mesnard and L. Miginiac, *J. Organomet. Chem.*, **117**, 99 (1976).
173. B. Mauzé, *J. Organomet. Chem.*, **131**, 321 (1977).
174. F. Bernadou and L. Miginiac, *C. R. Acad. Sci. Paris, Ser. C*, **280**, 1473 (1975).
175. F. Bernadou and L. Miginiac, *Tetrahedron Lett.*, 3083 (1976).
176. M. Bellasoued and Y. Frangin, *Synthesis*, 838 (1978)
177. Y.-Y. Wei, *Gaodeng Xuexia Huaxue Xuebao*, **15**, 1497 (1994); *Chem. Abstr.*, **122**, 132635 (1995).
178. I. Marek, *Chem. Rev.*, **100**, 2887 (2000).
179. I. Creton, I. Marek and J. F. Normant, *Tetrahedron Lett.*, **36**, 7451 (1995).
180. I. Creton, I. Marek and J. F. Normant, *Synthesis*, 1499 (1996).
181. I. Creton, H. Rezaeï, I. Marek and J. F. Normant, *Tetrahedron Lett.*, **40**, 1899 (1999).
182. H. Rezaei, S. Yamanoi, F. Chemla and J. F. Normant, *Org. Lett.*, **2**, 419 (2000).
183. H. Rezaeï, I. Marek and J. F. Normant, *Tetrahedron*, **57**, 2477 (2001).
184. Y. Frangin, E. Favre and M. Gaudemar, *C. R. Acad. Sci. Paris, Ser. C*, **282**, 277 (1976).
185. M. Bellasoued, Y. Frangin and M. Gaudemar, *J. Organomet. Chem.*, **166**, 1 (1979).
186. D. Mesnard and L. Miginiac, *J. Organomet. Chem.*, **420**, 163 (1991).
187. G. Zweifel and G. Hahn, *J. Org. Chem.*, **49**, 4565 (1984).
188. C. Meyer, I. Marek, J. F. Normant and N. Platzer, *Tetrahedron Lett.*, **35**, 5645 (1994).
189. C. Meyer, I. Marek and J. F. Normant, unpublished results.
190. W. D. H. Hunstmann, Y. J. Li and V. Giannamore, *Isr. J. Chem.*, **26**, 88 (1985).

191. L. Skattebøl and Y. Stenstrøm, *Tetrahedron Lett.*, **24**, 3021 (1983).
192. C. Meyer, I. Marek, G. Courtemanche and J. F. Normant, *J. Org. Chem.*, **60**, 863 (1995).
193. G. Courtemanche and J. F. Normant, *Tetrahedron Lett.*, **32**, 5317 (1991).
194. V. A. Korner and A. A. Petrov, *Zh. Obshch. Khim.*, **30**, 216 (1960); *Chem. Abstr.*, **54**, 117422 (1960).
195. E. Lorthiois, I. Marek, C. Meyer and J. F. Normant, *Tetrahedron Lett.*, **37**, 6689 (1996).
196. C. Meyer, I. Marek and J. F. Normant, *Tetrahedron Lett.*, **37**, 857 (1996).
197. E. Negishi, S. J. Holmes, J. M. Tour, J. A. Miller, F. E. Cederbaum, D. R. Swanson and T. Takahashi, *J. Am. Chem. Soc.*, **111**, 336 (1989).
198. E. Lorthiois, I. Marek, C. Meyer and J. F. Normant, *Tetrahedron Lett.*, **36**, 1263 (1995).
199. E. Lorthiois, I. Marek and J. F. Normant, *Bull. Soc. Chim. Fr.*, **134**, 333 (1997).
200. E. Lorthiois, I. Marek and J. F. Normant, *Tetrahedron Lett.*, **38**, 89 (1997).
201. Na enolate: G. Eglington and M. C. Whinting, *J. Chem. Soc.*, 3052 (1953).
202. Na enolate: D. Curran and C. T. Chang, *J. Org. Chem.*, **54**, 3140 (1989).
203. Na enolate: J. Cossy and A. Thellend, *Tetrahedron Lett.*, **31**, 1427 (1990).
204. Na enolate: A. L. J. Beckwith and M. J. Tozer, *Tetrahedron Lett.*, **33**, 4975 (1992).
205. Na enolate: A. Archadi, S. Cacchi, G. Fabrizi and F. Marinelli, *Synlett*, 65 (1993).
206. Na enolate: A. Archadi, S. Cacchi, G. Fabrizi, F. Manna and P. Pace, *Synlett*, 446 (1998).
207. Li enolate: R. L. Funk, G. L. Bolton, K. M. Brummond, K. E. Ellestad and J. B. Stallman, *J. Am. Chem. Soc.*, **115**, 7023 (1993).
208. K enolate: K. H. Ehrhardt and H. Mildenberger, *Justus Liebigs Ann. Chem.*, 989 (1982).
209. Li enolate: O. Kitagawa, T. Suzuki, H. Fujiwara, M. Fujita and T. Taguchi, *Tetrahedron Lett.*, **40**, 4585 (1999).
210. Cs enolate: C. Koradin, A. Rodriguez and P. Knochel, *Synlett*, 1452 (2000).
211. $BnMe_3N^+$ enolate: M. Guillaume, E. Dumez, J. Rodriguez and J.-P. Dulcere, *Synlett*, 1883 (2002).
212. Re enolate: J. G. Stack, R. D. Simpson, F. J. Hollander, R. G. Bergman and C. H. Heathcock, *J. Am. Chem. Soc.*, **112**, 2716 (1990).
213. S. T. Staben, J. J. Kennedy-Smith and F. D. Toste, *J. Am. Chem. Soc.*, **126**, 4526 (2004).
214. S. T. Staben, J. J. Kennedy-Smith and F. D. Toste, *Angew. Chem., Int. Ed.*, **43**, 5350 (2004).
215. X. Yao and C. J. Li, *J. Am. Chem. Soc.*, **126**, 6884 (2004).
216. P. Cruciani, C. Aubert and M. Malacria, *Tetrahedron Lett.*, **35**, 6677 (1994).
217. P. Cruciani, R. Stammler, C. Aubert and M. Malacria, *J. Org. Chem.*, **61**, 3874 (1996).
218. D. Bouyssi, N. Monteiro and G. Balme, *Tetrahedron Lett.*, **40**, 1297 (1999).
219. B. Clique, N. Monteiro and G. Balme, *Tetrahedron Lett.*, **40**, 1301 (1999).
220. B. Clique, S. Vassiliou, N. Monteiro and G. Balme, *Eur. J. Org. Chem.*, 1493 (2002).
221. S. Raghu and M. Rosenblum, *J. Am. Chem. Soc.*, **95**, 3060 (1973).
222. P. Lennon, A. M. Rosan and M. Rosenblum, *J. Am. Chem. Soc.*, **99**, 8426 (1977).
223. M.-C. P. Yeh, B.-A. Shen, H.-W. Fu, S.-I. Tau and L.-W. Chuang, *J. Am. Chem. Soc.*, **115**, 5941 (1993).
224. M. L. Lai, S.-C. Chang, C.-C. Hwu and M.-C. P. Yeh, *Tetrahedron Lett.*, **37**, 6149 (1996).
225. M.-C. P. Yeh, L.-W. Chuang and C.-H. Ueng, *J. Org. Chem.*, **61**, 3874 (1996).
226. M. A. Boavantura, J. Drouin and J. M. Conia, *Synthesis*, 801 (1983).
227. A. J. Pearson, and Md. N. I. Khan, *J. Am. Chem. Soc.*, **106**, 1872 (1984).
228. A. J. Pearson, and Md. N. I. Khan, *Tetrahedron Lett.*, **26**, 1407 (1985).
229. A. J. Pearson, Md. N. I. Khan, J. C. Clardy and H. Cum-Heng, *J. Am. Chem. Soc.*, **107**, 2748 (1985).
230. F. E. McDonald and T. C. Olson, *Tetrahedron Lett.*, **38**, 7691 (1997).
231. Y. Ito, M. Nakatsuka, N. Kise and T. Saegusa, *Tetrahedron Lett.*, **21**, 2873 (1980).
232. G. Fournet, G. Balme, B. Van Hemelryck and J. Gore, *Tetrahedron Lett.*, **31**, 5147 (1990).
233. N. Monteiro, J. Gore and G. Balme, *Tetrahedron*, **48**, 10103 (1992) and references cited therein.
234. G. Balme, D. Bouyssi, R. Faure, J. Gore and B. Van Hemelryck, *Tetrahedron*, **48**, 3891 (1992).
235. X. Marat, N. Monteiro and G. Balme, *Synlett*, 845 (1997).
236. N. Tsukada and Y. Yamamoto, *Angew. Chem., Int. Ed. Engl.*, **36**, 2477 (1997) and references cited therein.
237. T. Pei and R. A. Widenhoefer, *J. Am. Chem. Soc.*, **123**, 11290 (2001).

238. X. Wang, T. Pei, X. Han and R. A. Widenhoefer, *Org. Lett.*, **5**, 2699 (2003).
239. X. Wang and R. A. Widenhoefer, *Chem. Commun.*, 660 (2004).
240. X. Han, X. Wang, T. Pei and R. A. Widenhoefer, *Chem. Eur. J.*, **10**, 6333 (2004).
241. C. Liu, X. Wang, T. Pei and R. A. Widenhoefer, *Chem. Eur. J.*, **10**, 6343 (2004).
242. O. Kitagawa, T. Suzuki, T. Inoue and T. Taguchi, *Tetrahedron Lett.*, **39**, 7357 (1998).
243. O. Kitagawa, T. Suzuki, H. Fujiwara and T. Taguchi, *Tetrahedron Lett.*, **40**, 2549 (1999).
244. O. Kitagawa, H. Fujiwara, T. Suzuki, T. Taguchi and M. Shiro, *J. Org. Chem.*, **65**, 6819 (2000).
245. M. Yamaguchi, A. Hayashi and M. Hirama, *J. Am. Chem. Soc.*, **115**, 3362 (1993).
246. M. Yamaguchi, T. Tsukagoshi and M. Arisawa, *J. Am. Chem. Soc.*, **121**, 4074 (1999).
247. M. Arisawa, K. Akamatsu and M. Yamaguchi, *Org. Lett.*, **3**, 789 (2001).
248. M. Bodajla, G. R. Jones and C. A. Ramsden, *Tetrahedron Lett.*, **38**, 2573 (1997).
249. M. Nakamura, K. Endo and E. Nakamura, *J. Am. Chem. Soc.*, **125**, 13002 (2003).
250. M. Seefelder, *Justus Liebigs Ann. Chem.*, **652**, 107 (1962).
251. K. E. Schultze, G. Rücker and J. Feldkamp, *Chem. Ber.*, **105**, 24 (1972).
252. M. Gaudemar, *Bull. Soc. Chim. Fr.*, 3113 (1966).
253. M. T. Bertrand, G. Courtois and L. Miginiac, *Tetrahedron Lett.*, 1945 (1974).
254. M. T. Bertrand, G. Courtois and L. Miginiac, *Tetrahedron Lett.*, 3147 (1975).
255. M. T. Bertrand, G. Courtois and L. Miginiac, *C. R. Acad. Sci. Paris, Ser. C,* **280**, 999 (1975).
256. M. Nakamura, T. Fujimoto, K. Endo and E. Nakamura, *Org. Lett.*, **6**, 4837 (2004).
257. M. Nakamura, C. Liang and E. Nakamura, *Org. Lett.*, **6**, 2015 (2004).
258. For a similar Li/Pd-mediated approach to functionalized 3-methylenetetrahydrofurans or pyrrolidines, see References 219 and 235.
259. P. Karoyan and G. Chassaing, *Tetrahedron Lett.*, **38**, 85 (1997).
260. E. Lorthiois, I. Marek and J. F. Normant, *J. Org. Chem.*, **63**, 2442 (1998).
261. F. H. Van Der Steen, H. Kleijn, G. J. P. Britovsek, J. T. B. H. Jastrzebski and G. Van Koten, *J. Org. Chem.*, **57**, 3906 (1992).
262. F. H. Van Der Steen, J. Boersma, A. L. Spek and G. Van Koten, *J. Organomet. Chem.*, **390**, C21 (1990).
263. F. H. Van Der Steen, J. Boersma, A. L. Spek and G. Van Koten, *Organometallics*, **10**, 2467 (1991).
264. E. Sliwinski, F. Prian, F. Denes, F. Chemla and J. F. Normant, *C.R. Chimie*, **6**, 67 (2003).
265. I. Coldham, R. Hufton and R. E. Rathmell, *Tetrahedron Lett.*, **38**, 7617 (1997).
266. For a review on the recent applications of α-methylbenzylamine in the preparation of enantiopure compounds, see: E. Juaristi, J. L. Leon-Romo, A. Reyes and J. Escalante, *Tetrahedron: Asymmetry*, **10**, 2441 (1999).
267. P. Karoyan and G. Chassaing, *Tetrahedron Lett.*, **43**, 253 (2002).
268. J. Quancard, A. Labonne, Y. Jacquot, G. Chassaing, S. Lavielle and P. Karoyan, *J. Org. Chem.*, **69**, 7940 (2004).
269. P. Karoyan and G. Chassaing, *Tetrahedron: Asymmetry*, **8**, 2025 (1997).
270. P. Knochel, J. J. A. Perea and P. Jones, *Tetrahedron*, **54**, 8275 (1998).
271. J. Quancard, H. Magellan, S. Lavielle, G. Chassaing and P. Karoyan, *Tetrahedron Lett.*, **45**, 2185 (2004).
272. P. Karoyan, J. Quancard, J. Vaissermann and G. Chassaing, *J. Org. Chem.*, **68**, 2256 (2003).
273. E. Lorthiois, I. Marek and J. F. Normant, *J. Org. Chem.*, **63**, 566 (1998).
274. W. F. Bailey, T. T. Nurmi, J. J. Patricia and W. Wang, *J. Am. Chem. Soc.*, **109**, 2442 (1987).
275. F. Denes, F. Chemla and J. F. Normant, *Synlett*, 919 (2002).
276. F. Orsini, F. Pelizzoni and G. Ricca, *Tetrahedron Lett.*, **23**, 3945 (1982).
277. F. Orsini, F. Pelizzoni and G. Ricca, *Tetrahedron*, **40**, 2781 (1984).
278. J. Boersma, J. Dekker and G. J. M. Van Der Kerck, *J. Chem. Soc., Chem. Commun.*, 553 (1983).
279. J. Boersma, P. H. M. Budzelaar, J. Dekker and G. J. M. Van Der Kerck, *Organometallics*, **3**, 1403 (1984).
280. F. Denes, F. Chemla and J. F. Normant, *Eur. J. Org. Chem.*, 3536 (2002).
281. E. Nakamura, G. Sakata and K. Kubota, *Tetrahedron Lett.*, **39**, 2157 (1998).
282. E. Nakamura, S. Aoki, K. Sekiya, H. Oshimo and I. Kuwajima, *J Am. Chem. Soc.*, **109**, 8056 (1987).
283. E. Nakamura, K. Kubota and G. Sakata, *J. Am. Chem. Soc.*, **119**, 5457 (1997).

284. E. Nakamura and K. Kubota, *Tetrahedron Lett.*, **38**, 7099 (1997).
285. M. Nakamura, K. Hara, G. Sakata and E. Nakamura, *Org. Lett.*, **1**, 1505 (1999).
286. E. Nakamura and K. Kubota, *J. Org. Chem.*, **62**, 792 (1997).
287. K. Kubota and E. Nakamura, *Angew. Chem., Int. Ed. Engl.*, **36**, 2491 (1997).
288. M. Nakamura, T. Hatakeyama, K. Hara and E. Nakamura, *J. Am. Chem. Soc.*, **125**, 6362 (2003).
289. M. Nakamura, T. Hatakeyama and E. Nakamura, *J. Am. Chem. Soc.*, **126**, 11820 (2004).

Author Index

This author index is designed to enable the reader to locate an author's name and work with the aid of the reference numbers appearing in the text. The page numbers are printed in normal type in ascending numerical order, followed by the reference numbers in parentheses. The numbers in italics refer to the pages on which the references are actually listed.

With kind thanks to Paul Nash for creation of this index.

Subject Index

Entries are in letter-by-letter alphabetical order ignoring spaces and punctuation marks. Page numbers in *italic* refer to Figures and Tables not included in the relevant page ranges.

The chemistry of organozinc compounds
Edited by Z. Rappoport and I. Marek

With kind thanks to Caroline Barlow for creation of this index.